Institute of Organic Chemistry
Polish Academy of Sciences

Photochemical Methods for the Synthesis of Protected Amines

Kitti Franciska Szabó M.Sc.

A monothematic series of publications, with commentary, submitted to the Scientific Council of the Institute of Organic Chemistry, Polish Academy of Sciences for the purpose of obtaining a doctoral degree

Supervisor: Prof. Dorota Gryko

Warsaw 2025

Doctoral thesis completed as part of the project:

„Red light - a tool for organic and bioorthogonal chemistry”

Grant number: NCN MAESTRO 2020/38/A/ST4/00185

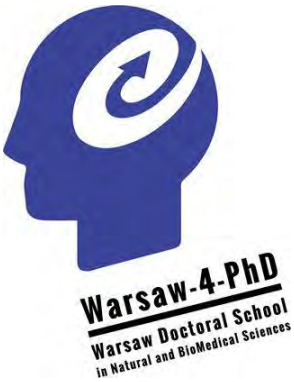

Acknowledgements

I sincerely appreciate the support and encouragement I received along the way:

Prof. Dorota Gryko - for her support and guidance during my PhD studies and for giving me the opportunity to work in her research group,

dr. João Victor Santiago, dr. Katarzyna Rybicka-Jasińska, dr. Mateusz Woźny, dr. Piotr Banachowicz, dr. Tomasz Wdowik- for their invaluable guidance and assistance in the laboratory,

Group XV - for their help, support and friendship that developed along the way:

Adam, Antek, Asia, Basia, Joe, Kacper, Kasia O., Klaudia, Krzysztof D., Krzysztof G., Krzysztof M., Kuba D., Kuba P., Łukasz, Magda, Marianna, Marzena, Michał O., Mohad, Monica, Ola P., Ola,Wierzba, Ola Wincenciuk, Piotrek K., Shantanu, Souvik, Szymon, Wojtek,

Deepshika, Gana and Prachi - for their kind support and companionship outside the lab over the years,

Arturo and Jacqueline - thank you for becoming my family here in Poland,

My Family - to my parents for their unconditional love, support and encouragement during this journey and I am deeply grateful to my sister, who is my best friend - her caring nature and constant presence in my life have been my greatest strength.

Abstract in English

Constructing C-N bond remains highly relevant in modern organic synthesis, as it enables the introduction of ubiquitous nitrogen-containing heterocycles. Owing to their basicity, nucleophilicity, and dipole character, these structures are valuable in pharmaceutical and agrochemical industries. The synthesis of amines is essential because they occur in several biologically important processes. In classical chemistry, transition metal-catalysis is a well-established strategy to furnish C-N bonds. However, such approaches often do not meet sustainable requirements.

Along this line, photochemistry enables to perform reactions with the use of light source and open new synthetic routes to the compounds that are unavailable under thermal conditions. Along this line, *N*-Aminopyridinium salts recently gained more attention as amination reagents which can easily generate an electrophilic nitrogen-centered radical precursors by reductive cleavage of the N-N bond. The resulting radicals offer broad synthetic potential.

The main goal of my PhD dissertation was to investigate novel reactivity of photochemically generated nitrogen-centered radicals and aziridines for the formation of C-N and C-C bonds, leading to amines and their derivatives.

Three publications are included as part of my doctoral thesis. The first publication reports photochemical γ-amidation of α,β-unsaturated carbonyl compounds using amidyl radicals derived from *N*−aminopyridinium salt. The robustness of this method was demonstrated with a broad substrate scope, generally high yields, and successful application to biologically relevant compounds.

The second paper further describes the utility of amidyl radicals from *N*-aminopyridinium salts to functionalize pyridine moieties. It shows the use of *N*-aminopyridinium salts and Zincke imine intermediates to peripheral editing of pyridine at C3-position under photochemical conditions. The new C-N bond occurs predominantly at C3 position, however, changing substituent at C2 position (aryl to alkyl) changes the regioselectivity. These experimental observations are supported by DFT calculations.

The final publication discusses photochemical ring-opening of epoxides and aziridines using native vitamin B_{12} in micellar medium, yielding alcohol and amines in moderate to high yields and with high regioselectivity.

In conclusion, I have developed new methods for C-N bond-forming reactions via generation of reactive radical intermediates under photochemical conditions, contributing with novel approaches towards more sustainable and efficient amine synthesis.

Streszczenie w języku polskim

Tworzenie wiązań C-N pozostaje niezwykle istotnym zagadnieniem w nowoczesnej syntezie organicznej, ponieważ umożliwia dalsze wprowadzenie powszechnie występującego ugrupowania aminowego. Ze względu na swoją zasadowość, nukleofilowość i charakter dipolowy, aminy te są cenne w przemyśle farmaceutycznym i agrochemicznym. Synteza amin jest niezbędna, ponieważ często wystepuja one w naturze. W klasycznej chemii, kataliza metalami przejściowymi jest dobrze ugruntowanas strategią tworzenia wiązań C-N, jednak takie metody często nie spełniają wymagań zrównoważonej chemii.

Odpowiedzią na te wymagania jest fotochemia, która umożliwia prowadzanie reakcji z wykorzystaniem energii światła i otwiera nowy drogi syntezy, które są niedostępne w warunkach termicznych. Sole *N*-aminopirydyniowe zyskali na znaczenią jako odczynniki aminowania, które mogą łatwo generować elektrofilowe prekursory rodników azotowych poprzez redukcyjne rozerwanie wiązania N-N. Powstałe rodniki moją ogromny potencjał syntetyczny.

Głównym celem mojej rozprawy doktorskiej było zbadanie nowej reaktywności fotochemicznie generowanych rodników azotowych i azirydyn w celu tworzenia wiązań C-N i C-C, prowadzących do amin i ich pochodnych.

Badania zawarte w przedłożonej pracy doktorskiej zostały opisane w trzech publikacjach. W pierwszej publikacji opisuję fotochemiczne γ-amidowanie α,β-nienasyconych związków karbonylowych przy użyciu rodników amidylowych pochodzących z soli *N*-aminopirydyniowych. Zakres stosowalności tej metody został wykazany przy zastosowaniu szerokim zakresiem substratów, ogólnie wysokimi wydajnościami i pomyślnym w syntezie związków biologicz zna czemu.

W drugiej pracy opisałam użyteczność rodników amidylowy generowanych z soli *N*-aminopirydyniowej do funkcjonalizacji ugrupowań pirydynowych. Przedstawiłam w niej zastosowanie soli *N*-aminopirydyniowych i imin Zincke do C-H funkcjonalizacji pirydyny w pozycji C3 w warunkach fotochemicznych. Nowe wiązanie C-N występuje głównie w pozycji C3, jednak zmiana podstawnika w pozycji C2 (z arylowego na alkilowy) zmienia regioselektywność. Te obserwacje eksperymentalne są poparte obliczeniami DFT.

W ostatniej publikacji omawiam fotochemiczne otwieranie pierścieni epoksydów i azirydyn przy użyciu witaminy B_{12} w środowisku micelarnym, otrzymując alkohole i aminy z umiarkowaną wydajnością, ale wysokon regioselektywnością.

Podsumowując, opracowałam nowe metody tworzenia wiązania C-N poprzez generowanie reaktywnych pośrednich rodników w warunkach fotochemicznych i wnosząc nowe podejścia do bardziej zrównoważonej i wydajnej syntezy amin.

Table of Contents

List of Publications in the Doctoral Thesis

1. *Site-Selective, Photocatalytic Vinylogous Amidation of Enones*

Szabó, K. F.; Goliszewska, K.; Szurmak, J.; Rybicka-Jasińska, K.; Gryko, D. *Org. Lett.* **2022**, *24*, 8120−8124.

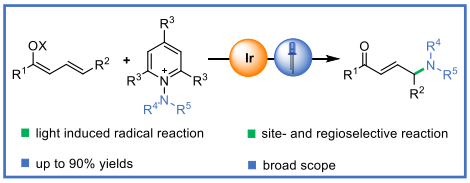

2. *Photochemical C3-amination of pyridines via Zincke Imine intermediates*

Szabó, K. F.; Banachowicz, P.; Powała, A.; Lunic, D.; Ardoiz, I. F.; Gryko, D. *Nat. Commun.* **2025**, accepted, doi:10.26434/chemrxiv-2024-3dj94.

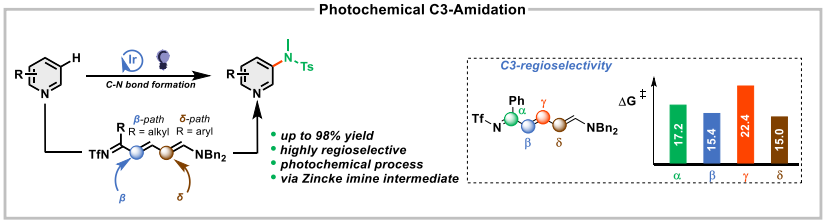

3. *Vitamin B_{12} and Micellar Solution Enable Regioselective Ring Opening of Epoxides and Aziridines with Electrophilic Olefins*

Szabó, K. F.; Wdowik, T.; Krzeszewska, A.; Mazurek, K.; Andersson, M. P.; Gryko, D. *Org. Lett.*, **2025**, doi.org/10.1021/acs.orglett.5c01376.

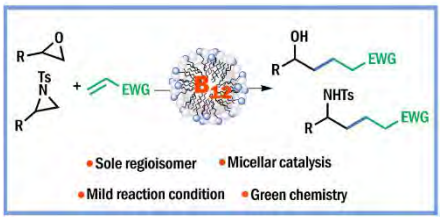

Gryko, Dorota <dorota.gryko@icho.edu.pl>

From: jamal.malik@nature.com
Date: Fri, May 2, 2025 at 11:17 AM
Subject: Acceptance of NCOMMS-24-63500B
To: dorota.gryko@icho.edu.pl

Dear Professor Gryko,

We are delighted to accept your manuscript entitled "Photochemical C3-Amination of Pyridines via Zincke Imine Intermediates" for publication in Nature Communications. Thank you for choosing to publish your interesting work with us.

Licence to Publish and Article-processing Charge

- In approximately 7-10 business days you will receive an email with a link to choose the grant of rights necessary for publishing your paper and - if applicable - to provide payment information for your article-processing charge (APC), either via credit card or by requesting an invoice.

  If needed, our Author Services team will be in touch regarding any additional information that may be required.

  In order to avoid any delays, please ensure that you have emails from Springer Nature whitelisted in your mail system. Please note that production will not continue until the Licence to Publish and Article-Processing Charge steps are completed and your proof corrections are submitted.

  If you have any questions about our Open Access requirements, or our legal forms, costs, please contact ORsupport@springernature.com.

In recognition of the time and expertise our reviewers provide to Nature Communications's editorial process, as of November, 2018, we formally acknowledge their contribution to the external peer review of

articles published in the journal. All peer-reviewed content will carry an anonymous statement of peer reviewer acknowledgement, and for those reviewers who give their consent, we will publish their names alongside the published article. For more information, please refer to our FAQ page: https://www.nature.com/documents/ncomms-reviewer-information.pdf

We will edit your manuscript to ensure that it conforms with our house style and send you a link to an online eProof for checking in a separate email to the publishing agreements. Please read your proof with great care to ensure that the sense has not been altered. We also suggest you discuss the proof with your co-authors, but please ensure that only one author communicates with us and that only one set of corrections is returned via the online correction in the eProof. The corresponding (or nominated) author is responsible on behalf of all co-authors for the accuracy of all content, including spelling of names and current affiliations.

To ensure prompt publication, we request that proofs are returned within two working days. If there is any period within the next four weeks in which you won't be available, please nominate a co-author with whom we can correspond, and let us know their email address as soon as possible.

Please note that your Supplementary Information files may have been edited for style and are now finalized. They will be uploaded directly to the Nature Communications website in preparation for publication of the Article. Any requests to make changes will only be considered in exceptional circumstances and will result in a delay to publication.

Acceptance of your manuscript is conditional on all authors' agreement with our publication policies (see www.nature.com/nature/authors/policy/index.html). In particular, your manuscript must not be published elsewhere and there must be no announcement of the work in the media until the publication date.

At this stage, you may wish to make your institution's press office aware of the forthcoming publication, if you wish to bring your work to the media's attention, so that they can start preparing any publicity. Please note that the paper is still under embargo until it is published in the journal. Further details of our embargo policy can be found here http://www.nature.com/authors/policies/embargo.html.

Publication is typically within two to three weeks of acceptance. Please note there will be no further correspondence about your publication date. When your article is published, you will receive a notification email. **If you are planning an embargoed press release or require a specific publication date, please complete our scheduling requests form, or contact NatureCommunicationsProduction@springernature.com, as soon as possible after acceptance and we will endeavour to accommodate your request.** For further information on the journey of your article from acceptance to publication, please see our Author FAQs.

If you have not already done so, we would welcome the submission of material for the 'Featured Image' section on the Nature Communications home page. Images should relate to the content of your manuscript, but need not be contained within the paper. Suggestions should be sent by email to naturecommunications@nature.com. Please provide 1200x675-pixel RGB images. Unfortunately, we cannot promise that your suggestions will be used.

A form to order reprints of your Article is available

at http://www.nature.com/reprints/author-reprints.html#options

If you have any questions about open-access invoicing or payment, please contact authororders@nature.com

You can now use a single sign-on for all your accounts, view the status of all your manuscript submissions and reviews, access usage statistics for your published articles and download a record of your refereeing activity for the Nature journals.

We look forward to publishing your paper.

Best regards,

Dr. Jamal A. Malik
Senior Editor
Nature Communications

** See Nature Portfolio's author and referees' website at www.nature.com/authors for information about policies, services and author benefits

** Visit the Springer Nature Editorial and Publishing website at www.springernature.com/editorial-and-publishing-jobs for more information about our career opportunities. If you have any questions please click here**

This email has been sent through the Springer Nature Tracking System NY-610A-NPG&MTS

Participation in Conferences and Seminars

1. IX Ciamician Photochemistry School, 6-9 June, 2022, Bologna, Italy

2. International Symposium on Synthesis and Catalysis (ISySyCat 2023), 5-8 September, 2023, Évora, Portugal
   Poster presentation, title: "*Application of N-Aminopyridinium salts in photochemistry*"

3. Organic Synthesis under Non-Classical Conditions, 2-6 September, 2024, Warsaw, Poland
   Oral presentation, title: "*Application of N-Aminopyridinium salts in photochemistry*"

List of abbreviations

Boc - *tert*-Butoxycarbonyl group

Cbz - Benzyloxycarbonyl

CMC - Critical Micellar Concentrations

DTAC - Dodecyltrimethylammonium chloride

EDA - Electron Donor-Acceptor

EDG - Electron-donating group

EWG - Electron-withdrawing group

E*n*T - Energy Transfer

DFT - Density Functional Theory

DMPO - (5,5-dimethyl-1-pyrroline N-oxide)

HAT - Hydrogen Atom Transfer

HME - Heptamethyl cobyrinate

HRMS - High Resolution Mass Spectrometry

h*ν* - Light

***i*PrOH** - isopropanol

LEDs - Light-Emitting Diodes

NCS - *N*-chlorosuccinimide

NHC - *N*-heterocyclic carbene

NMP - N-methyl-2-pyrrolidone

PCET - proton-coupled electron transfer

SET - Single-Electron Transfer

TEMPO - 2,2,6,6-Tetramethylpiperidine 1-oxyl

TRIP thiol - 2,4,6-triisopropylbenzenethiol

Ts - Tosyl group, *p*-toluenesulfonyl

UV - Ultraviolet

1. Aims and Objectives

Amines are ubiquitous functional groups in both organic and medicinal chemistry, and therefore methods for the formation of new C-N bonds are highly desired. Particularly, there is considerable interest in developing more environmentally friendly protocols for their synthesis. With their wide importance, a vast number of transformations are known and accessible. In the context of the C–N bond formation, nitrogen precursors can be classified according to their philicity.[1] Nucleophilic amine precursors are often used, including sulfonamides, carboxamides, aryl and alkylamines performing amination with suitable electrophilic partners such as azides, hydroxylamines or nitro compounds. Employing nucleophilic amines often require prefunctionalized substrates such as halide or pseudohalide groups.[2] On the other hand, electrophilic and radical precursors can also be applied to amination processes in the presence of nucleophilic precursors, including olefins and organometallic reagents.[3] Along this line, *N*-aminopyridinium salts are bifunctional reagents, which contain a pyridinium moiety that, upon accepting an electron, enable single-electron transfer, as well as an amino group that can generate nitrogen-centered radicals under light irradiation.[4] The key goal in organic synthesis is to find innovative approaches for chemical transformations that require lower energy inputs. In the last few decades, visible light photoredox catalysis has arised as one of the most effective alternatives to traditional catalysis. With this in mind:

The main goal of my PhD dissertation was to investigate novel reactivity of photochemically generated nitrogen-centered radicals and aziridines for the formation of C-N and C-C bonds, leading to amines and their derivatives.

Therefore, in the first part of my PhD, I explored photocatalyzed processes for amine synthesis with *N*-aminopyridinium salts, which were prompted by the unique reactivity of their electrophilic N-centered radicals.

One of the key challenge was this area, is regioselective electrophilic N-centered radical addition to α,β-unsaturated carbonyl compounds at the distal γ-position. Previous work has shown that α-amido carbonyls can be accessed via N-centered radical addition. However, photoredox vinylogous transformations have typically utilized substrates bearing leaving groups at the site of functionalization.[5] Thus, use of unsaturated enolate substrates offers a better strategy for γ-functionalization with electrophilic N-centered radicals.

Recognizing the versatility of *N*-aminopyridinium salts, I further investigated the applicability of N-centered radicals under photochemical conditions. More particularly, I discovered that these

[1] Wolfe, J. P.; Wagaw, S.; Marcoux, J.-F.; Buchwald, S. L. *Acc. Chem. Res.,* **1998**, *31*, 805-818.
[2] Surry, D. S.; Buchwald, S. L. *Angew. Chem. Int. Ed.* **2008**, *47*, 6338-6361.
[3] Zhou, Z.; Kurti, L. *Synlett*, **2019**, *30*, 1525-1535.
[4] (a) Xu, J.; Chen, D.; Liu, C. *Org. Biomol. Chem.* **2022**, *20*, 8353-8365. (b) Roychowdhury, P.; Samanta, S.; Tan, H.; Powers, D. C. *Org. Chem. Front.* **2023**, *10*, 2563-2580.
[5] (a) Yang, W.; Hu, W.; Dong, X.; Li, X.; Sun, J. *Angew. Chem., Int. Ed.* **2016**, *55*, 15783−15786. (b) Dai, L.; Xia, Z. H.; Gao, Y. Y.; Gao, Z. H.; Ye, S. *Angew. Chem., Int. Ed.* **2019**, *58*, 18124−18130.

electrophilic radicals could functionalize pyridine analogues at the C3 position, a position that previously hold several synthetic challenges.[6]

In the latter part of my PhD, I focused on developing a green catalytic route to synthesize alcohols and amines derived from epoxides and aziridines. This was achieved by using native vitamin B_{12} as a catalyst in micellar media, adhering to sustainable chemistry principles.

In conclusion, this work summarizes sustainable and innovative strategies for new C-N bond formation under photochemical conditions, allowing an easier access to synthetically relevant compounds.

[6] Ziegler, T. *Organic Nitro Chemistry Series*, **1990**, p. *84* (VCH, Weinheim).

2. Introduction

2.1 Photochemistry

Photochemistry is considered one of the sustainable methodologies in green chemistry, implementing light as an energy source, to perform a variety of reactions that are inaccessible under classical thermal conditions.[7]

Photochemistry driven by sunlight has existed on Earth for billions of years. However, from a chemical perspective, the evolution of photochemistry began at the end of the 19th century with pioneering scientists such as Liebermann[8] and Perkin.[9] The formal establishment of photochemistry within organic chemistry is connected to the work of Ciamician and Silber in the early 20th century.[10]

In recent years, photochemistry has gained increased attention, particularly **photoredox catalysis** with the recognition of the unique potential of transition metal complexes and organic dyes. These complexes exhibit broad absorption in the visible range, enabling single-electron transfer (SET) processes under mild reaction conditions.[11] Several transition-metal complexes have been investigated over the years; among the most extensively studied are iridium complexes (**Scheme 1, A**), which produce long-lived excited states. Since common organic molecules do not absorb visible light, irradiation in this range allows for selective excitation of the photoredox catalyst. These excited photoredox catalysts can undergo SET oxidation and/or reduction, offering a unique activation mode to generate highly reactive neutral or ionic radicals in a controlled manner (**Scheme 1, B**).[12] Photocatalysis can also convert light into chemical energy through different mechanisms, such as **energy transfer** (E*n*T)[13] or **atom transfer**[14] reactions. All these methods require the use of a photocatalyst. In recent years, an alternative, photocatalyst-free approach has gained attention: **electron donor-acceptor** (EDA) concept, consisting of electron-rich donors such as amines, anisole or thiophenes, and electron-poor acceptors including nitrobenzenes, aryl halides, and pyridinium salts. Upon complex formation they are able to absorb visible light, triggering intramolecular SET to generate radicals.[15] In contrast, **photolysis** occurs with certain organic molecules-for example diazo reagents-that directly absorb visible light, become electronically excited, and yield highly reactive intermediates known as carbenes.[16]

[7] Albini, A.; Fagnoni, M. *Green Chem.* **2004**, *6*, 1–6.
[8] Liebermann, C. *Ber. Dtsch. Chem. Ges*. **1895**, *28*, 143-1448.
[9] Perkin, W. H. *J. Chem. Soc*. **1881**, *39*, 409-452.
[10] Roth, H. D. *Angew. Chem. Int. Ed. Engl.* **1989**, *28*, 1193-1207.
[11] Nicholls, T. P.; Leonori, D.; Bissember, A. C. *Nat. Prod. Rep*. **2016**, *33*, 1248-1254.
[12] Shaw, M. H.; Twilton, J.; MacMillan, D. W. C. *J. Org. Chem.* **2016**, *81*, 6898-6925.
[13] Dutta, S.; Erchinger, J. E.; Strieth-Kalthoff, F.; Kleinmans, R.; Glorius, F. *Chem. Soc. Rev.* **2024**, *53*, 1068-1089.
[14] Capaldo, L.; Ravelli, D. *Eur. J. Org. Chem.* **2017**, 2056-2071.
[15] Crisenza, G. E. M.; Mazzarella, D.; Melchiorre, P. *J. Am. Chem. Soc.* **2020**, *142*, 5461-5476.
[16] Gallo, R. D. C.; Cariello, G.; Goulart, T. A. C.; Jurberg, I. D. *Chem. Commun.* **2023**, *59*, 7346-7360.

In this literature part, a selection of distinct examples will be discussed, focusing on visible-light mediated novel C-N bond formation reactions, followed by a description of my own research.

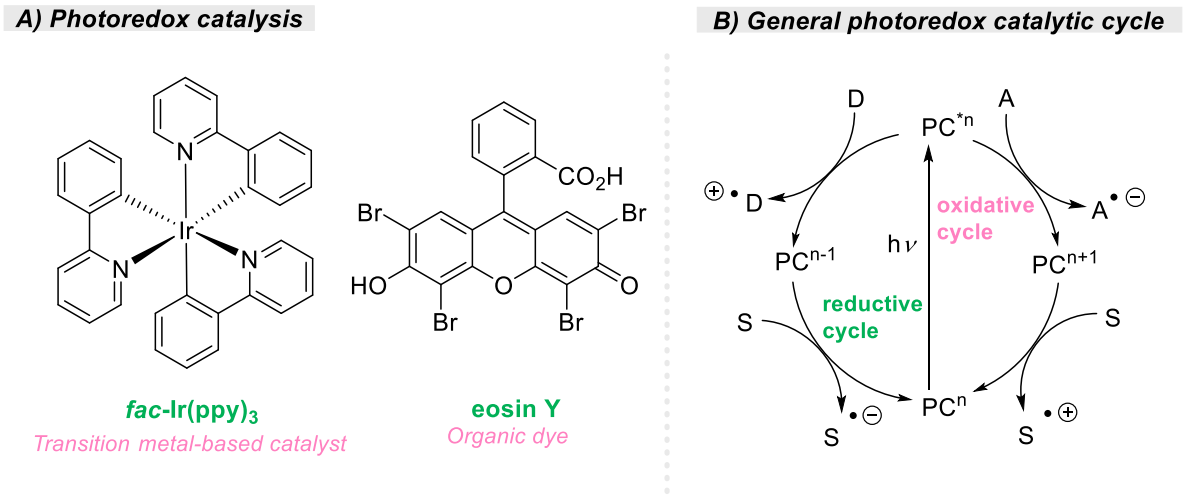

Scheme 1. A) Examples of photoredox catalysis, B) General mechanism of photoredox catalysis.

2.2 Importance of amines in organic chemistry

Amine functional groups represent a significant class of compounds in organic chemistry and act as essential building blocks in biological systems (**Scheme 2**).[17] Their significance is clear; naturally occurring amines are found in amino acids, various vitamins, hormones and nucleobases in DNA. In particular, secondary and tertiary amines are key precursors to both synthetic and naturally occurring compounds in the pharmaceutical,[18] agricultural,[19] and polymer[20] industries. Furthermore, their importance is due to the fact that most drugs contain either amine or nitrogen moieties, according to the U.S. FDA reports.

Over decades, the synthesis of amine derivatives under classical conditions such as reductive amination or transition metal-catalyzed approaches, like Pd-catalyzed Buchwald-Hartwig amination[21], and copper catalyzed Ullmann type[22] and Chan-Evans-Lam coupling,[23] have become a robust tool for the new C-N bond formation. However, these methods still have limitations, such as the requirement for ligands or directing groups, poor functional group tolerance, limited selectivity, harsh reaction conditions and above all, environmental concerns. Consequently, the development of new and more sustainable methods for the synthesis of amine derivatives is highly desirable for the pharmaceutical industry. The involvement of light as a driving force for new synthetic methodologies represents a unique activation mode for sustainable chemistry.

[17] J. McMurry *Organic Chemistry*, Brooks/Cole Cengage Learning, **2011**.
[18] Vitaku, E.; Smith, D. T.; Njardarson, J. T. *J. Med. Chem.* **2014**, *57* (24), 10257–10274.
[19] Wittcoff, H. A.; Reuben, B. G.; Plotkin, J. S. *Industrial Organic Chemicals*, Wiley, **2012**.
[20] Froidevaux, V.; Negrell, C.; Caillol, S.; Pascault, J.-P.; Boutevin, B. *Chem. Rev.* **2016**, *116* (22), 14181–14224.
[21] Heravi, M. M.; Kheilkordi, Z.; Zadsirjan, V.; Heydari, M.; Malmir, M. *J.Organomet. Chem.* **2018**, *861*, 17-104.
[22] Sambiagio, C.; Marsden, S. P.; Blacker, A. J.; McGowan, P. C. *Chem. Soc. Rev.* **2014**, *43*, 3525-3550.
[23] Bhunia, S.; Pawar, G. G.; Kumar, S. V.; Jiang, Y.; Ma, D. *Angew. Chem. Int. Ed.* **2017**, *56*, 16136-16179.

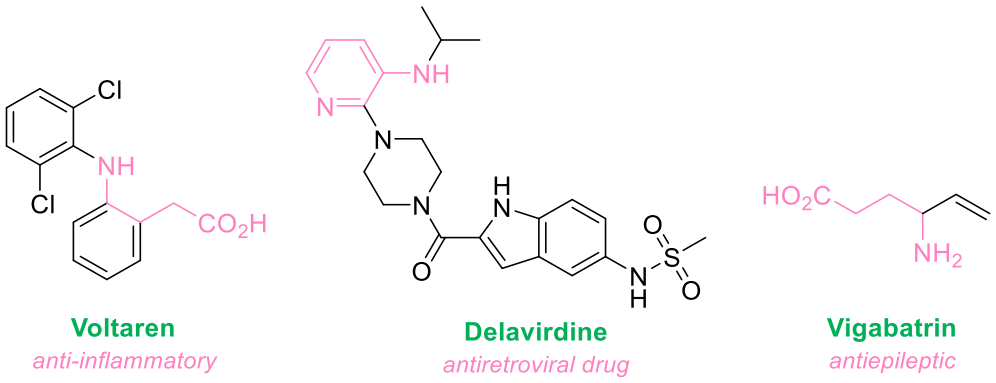

Scheme 2. Biologically active molecules containing amino groups.

2.3 Photochemical strategies for C-N bond formation

In recent years, photochemical strategies have gained increasing attention as a sustainable alternative to facilitate bond formation under mild conditions with excellent selectivity. These visible-light-mediated methods enable novel C-N bond formation via different mechanisms, including single-electron transfer, transition-metal-catalyzed coupling, energy transfer, and direct photoactivation of substrates. However, this literature section is dedicated to highlight recent advances in photochemical C-N bond-forming reactions generated via different N-centered radicals and emphasizing their mechanisms, scope, limitations, and potential applications.

2.3.1 Generation of N-centered radicals

The formation of N-centered radicals was limited for a long time, by their high and uncontrolled reactivity, which created significant challenges to the development of convenient, mild, and elegant synthetic methods.[24] From a retrosynthetic perspective, chemists traditionally created C-N bonds by coupling a nucleophilic amine with an electrophilic carbon center.[25] Therefore, it is not surprising, that amine-nucleophilicity-based strategies dominated in the early methodologies. Reversing the polarity of amines-so-called "umpolung" of nitrogen-offers a powerful alternative to overcome these limitations.[26] In this context, photoredox catalysis has emerged as a mild and highly selective platform for the generation of N-centered radicals. To expand the synthetic collection for C-H bond functionalization, four distinct classes of nitrogen radicals (**Figure 1**) aminyl, amidyl, hydrazonyl, and iminyl have been developed and employed.

[24] (a) Neale, R.S. *Synthesis* **1971**, 1-15. (b) Bowman, W. R.; Fletcher, A. J.; Potts, G. B. S. *J. Chem. Soc. Perkin Trans.* **2002**, *1*, 2747-2762.
[25] Ingold, C. K. *Chem. Rev.* **1934**, *15*, 225-274.
[26] Ganley, J. M.; Murray, P. R. D.; Knowles, R. R. *ACS Catal.* **2020**, *10*, 11712-11738.

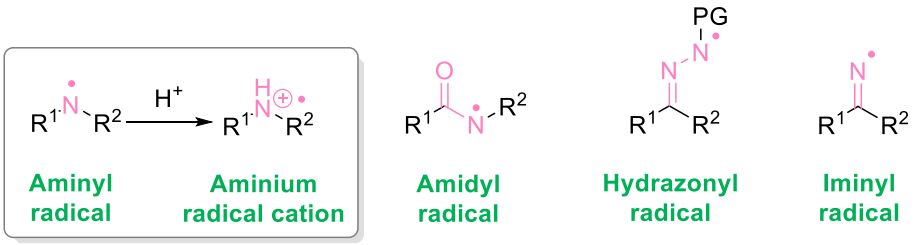

Figure 1. Types of N-centered radicals.

The first pioneering work on N-centered radicals was the Hofmann-Löffler-Freytag cyclization,[27] although its mechanism was proposed in 1950 by Wawzonek and Thelen (**Scheme 3**)[28]. Under UV irradiation, N-halogenated amines generate both aminyl and chlorine radicals. Protonation of the aminyl radical effects changes in the character and gives an electrophilic aminium radical cation **A**. This reactive intermediate then undergoes an intramolecular 1,5-hydrogen-atom transfer (HAT) to form a carbon-centered radical **B**, which is subsequently trapped by the chlorine atom to yield the γ−chlorinated amine **C**. Ionic cyclization of this species furnishes the desired heterocyclic product **2**.[29] Alternatively, in the absence of a hydrogen-atom, the nucleophilic aminyl radical can add to alkenes.[30]

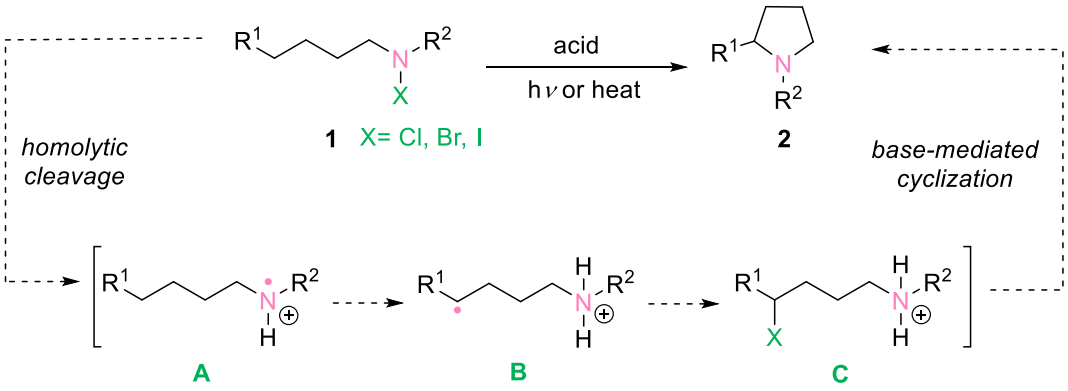

Scheme 3. Hofmann- Löffler-Freytag reaction mechanism.

2.3.2 Aminyl and aminium radicals

In the selection of N-centered radicals, both aminyl and aminium species have been explored as nucleophilic- and electrophilic radicals respectively, to furnish C-N bonds. However, neutral aminyl radicals have seen limited application compared to their protonated species due to their lower electrophilicity and reduced reactivity and selectivity.[31] Aminyl radicals can be generated

[27] (a) Hofmann, A. W. *Ber. Dtsch. Chem. Ges.* **1883**, *16*, 558-560. (b) Freytag, C.; Loffler, K. *Ber. Dtsch. Chem. Ges.* **1909**, *42*, 3427-3431.
[28] Wawzonek, S.; Thelen, P. J. *J. Am. Chem. Soc.* **1950**, *72*, 2118-2120.
[29] Wolff, M. E. *Chem. Rev.* **1963**, *63*, 55-64.
[30] Michejda, C. J.; Campbell, D. H. *J. Am. Chem. Soc.* **1979**, *101*, 7687-7693.
[31] Morris, A. A.; Wang, J.; Zheng, N. *Acc. Chem. Res.* **2016**, *49*, 1957-1968.

either by deprotonation of an aminium radical[32] or by N-Cl bond cleavage in *N*-chloroamines[33] via a photochemical pathway.

In 2012, Maity and Zheng developed a strategy for the intramolecular synthesis of *N*-aryl indoles via the addition of a diarylaminium radical cation generated from alkenes **3**.[34] *β*–Monosubstituted styrene derivatives afforded corresponding indoles **4** in good to excellent yields (**Scheme 4**, left). Notably, cyclopropane substituents were well tolerated under the reaction conditions and ring opening did not occur. When having *β,β*-disubstituted styrene substrates, first underwent 1,2-alkyl or aryl shift to furnish 2,3-disubstituted indoles **5** in moderate to good yields (**Scheme 4**, right). The proposed reaction mechanism involves the formation of a diarylaminium radical cation as a result of single-electron oxidation of the diarylamine by the Ru photocatalyst. This intermediate undergoes a 5-*endo*-trig cyclization to generate a distant aminium radical cation.[35] Subsequent deprotonation by superoxide leads to the formation of a carbocation, which then undergoes either a direct proton transfer or a 1,2-alkyl shift followed by proton transfer to furnish the desired indole derivative.

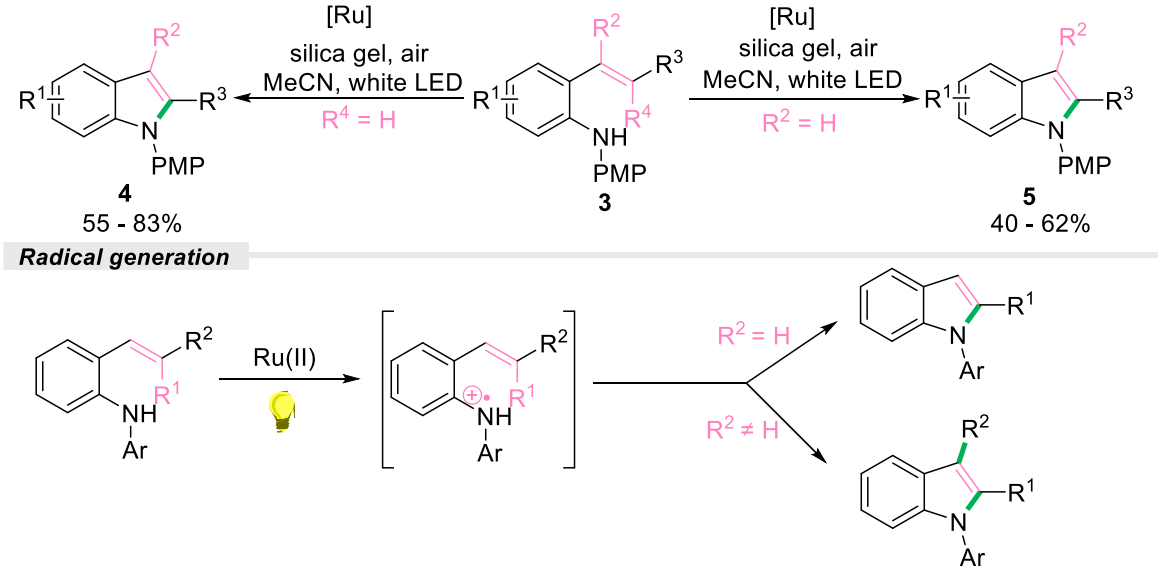

Scheme 4. Intramolecular cyclization of diarylaminium radicals for Indole synthesis.

Knowles and co-workers explored the intermolecular anti-Markovnikov hydroamination of unactivated alkenes **6** in the presence of secondary dialkylamines to afford acyclic tertiary alkylamines **7** (**Scheme 5**, left).[36] To align with the redox potential demands of the reaction, they used thiophenols as co-catalysts for the terminal hydrogen atom transfer (HAT) process, due to the

[32] Morozova, O. B.; Yurkovskaya, A. V. *J. Phys. Chem. B* **2008**, *112*, 12859-12862.
[33] Wolff, M. E. *Chemical Reviews*, **1963**, *63*, 55-64.
[34] Maity, S.; Zheng, N. *Angew. Chem. Int. Ed.* **2012**, *51*, 9562-9566.
[35] Yates, B. F.; Bouma, W. J.; Radom, L. *J. Am. Chem. Soc.* **1984**, *106*, 5805-5808.
[36] Musacchio, A. J.; Lainhart, B. C.; Zhang, X.; Naguib, S. G.; Sheerwood, T. C.; Knowles, R. R. *Science*, **2017**, *355*, 727-730.

weak S-H bond, which enables fast HAT to carbon-centered radicals.[37] Yields were high in most cases, regardless of whether mono-, di-, tri-, or tetrasubstituted alkenes as well as different cyclic amines were used. Acyclic amines were also compatible, though yields diminished due to their competing reactivity as coupling partners. The same group further broadened the scope of anti-Markovnikov hydroamination by having primary alkylamines, while simultaneously preventing over-alkylation (**Scheme 5**, right).[38] Compared to the previous protocol, they modified a few parameters, yet the reaction still provided the desired products **8** in moderate to good yields.

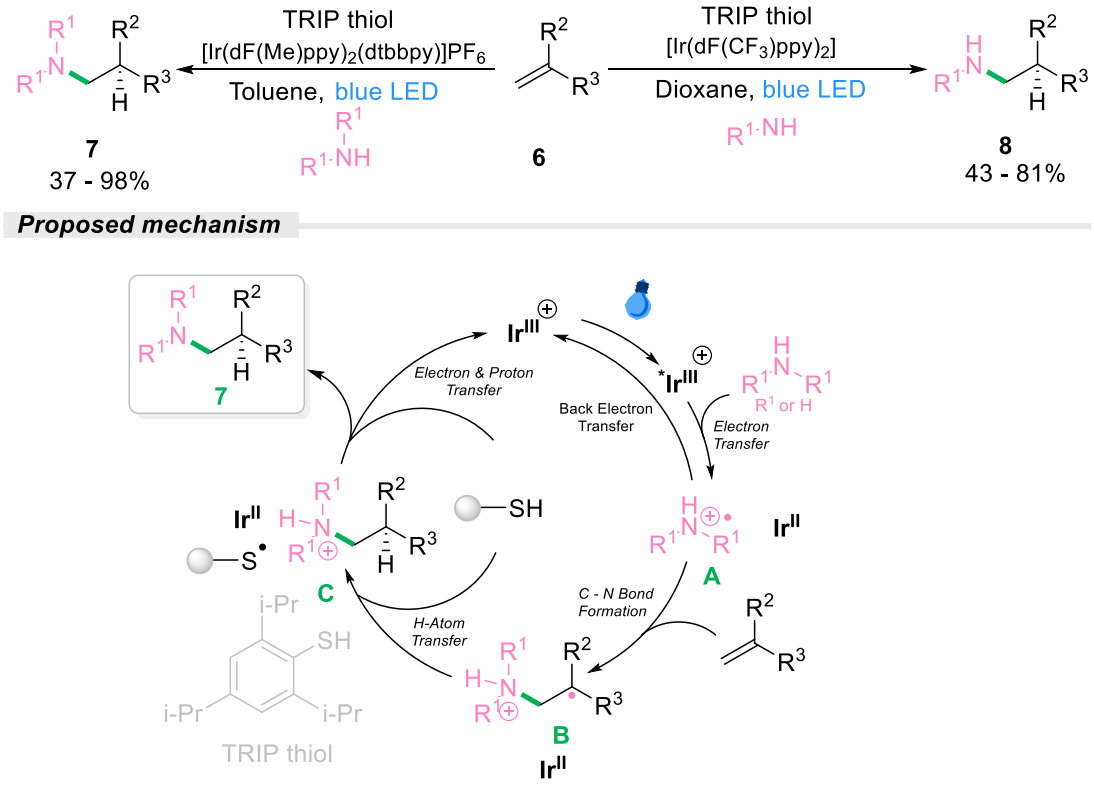

Scheme 5. Intermolecular anti-Markovnikov hydroamination of unactivated alkenes with secondary and primary amines with proposed reaction mechanism.

The proposed reaction mechanism in both cases involves SET from the photoexcited Ir catalyst to the amine generating an aminium radical cation **A**. Subsequent anti-Markovnikov addition of this radical cation to an alkene yielded a distant radical cation **B**. This intermediate is, then, quenched by a TRIP thiol affording an ammonium ion **C**, and a thiyl radical. Finally, deprotonation of the ammonium ion furnishes the desired amine product **7**, and reduction of the thiyl radical by Ir(II) regenerates the catalyst, completing the cycle.

[37] (a) Miller, D. C.; Choi, G. J.; Orbe, H. S.; Knowles, R. R. *J. Am. Chem. Soc.* **2015**, *137*, 13492-13495. (b) Nguyen, T. M.; Nicewicz, D. A. *J. Am. Chem. Soc.* **2013**, *135*, 9588-9591. (c) Guin, J.; Mück-Lichtenfeld, C.; Grimme, S.; Studer, A. *J. Am. Chem. Soc.* **2007**, *129*, 4498-4503.

[38] Miller, D. C.; Ganley, J. M.; Musacchio, A. J.; Sherwood, T. C.; Ewing, W. R.; Knowles, R. R. *J. Am. Chem. Soc.* **2019**, *141*, 16590-16594.

While studying arene trifluoromethoxylation, the Togni group unexpectedly identified, for the first time, the formation of pyridinium radical cation as a side product.[39] This radical added to an arene substrate, leading to arene pyridination and opening the door development of synthetic protocols for arene C–H pyridination.

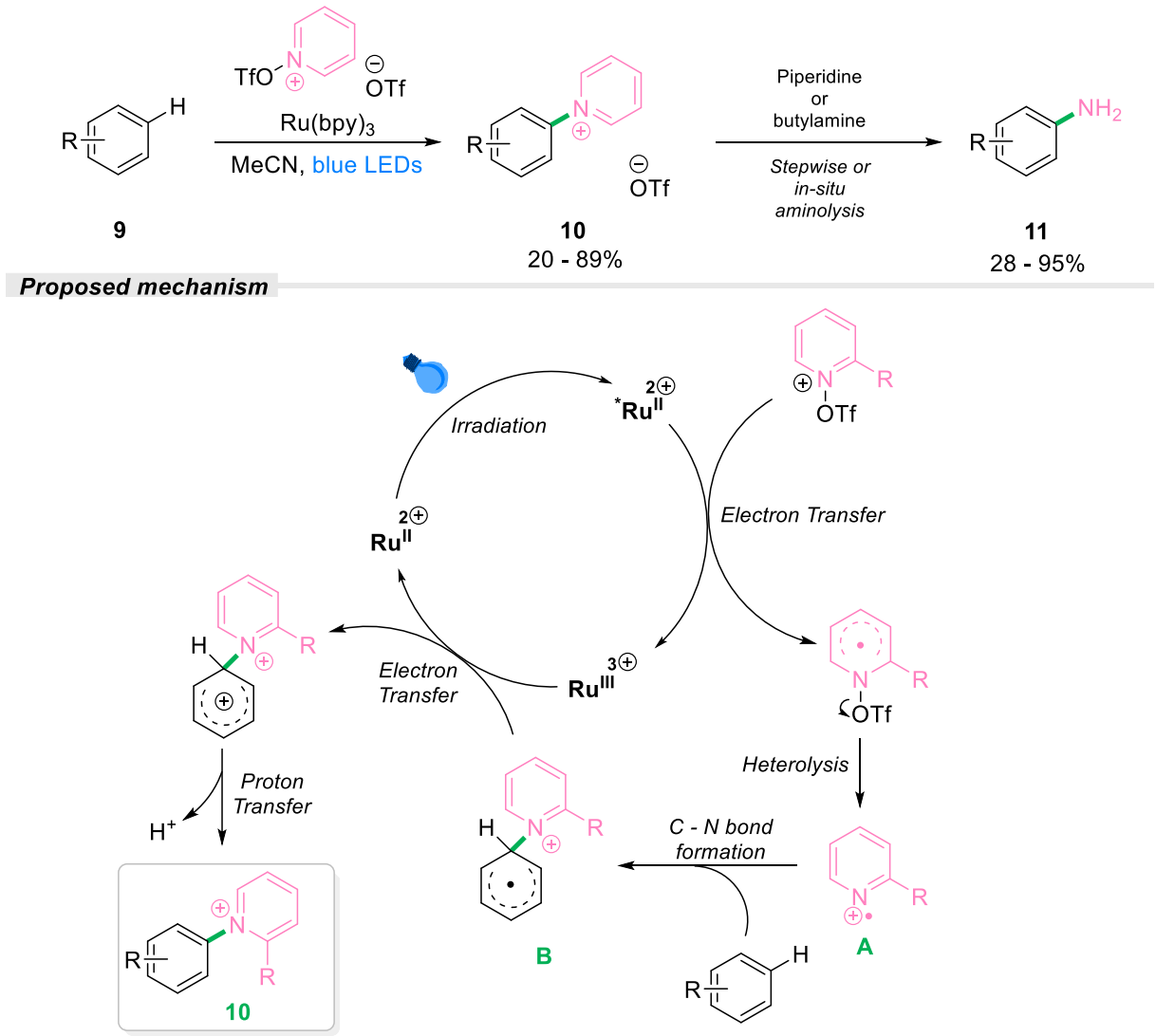

Scheme 6. (Hetero)arene C-H pyridination by visible-light-mediated generation of aminium radicals with proposed reaction mechanism.

Then, Carreira in collaboration with the Togni group and the Ritter group further investigated into arene C-H pyridination reactions. *N*-aryl pyridinium products can undergo aminolysis to mimic the behavior of primary anilines, reflecting the characteristic reactivity of Zincke salts.[40] In order to overcome the original homolysis pathway, they replaced pyridinium fluorides with pyridinium

[39] Jelier, B. J.; Tripet, P. F.; Pietrasiak, E.; Franzoni, I.; Jeschke, G.; Togni, A. *Angew. Chem. Int. Ed.* **2018**, *57*, 13784-13789.
[40] Zincke, T.; Heuser, G.; Möller, W. *Justus Liebigs Ann. Chem.* **1904**, *333*, 296–345.

triflates. Triflates are not only more straightforward to synthesize[41] but also furnish the anion leaving group that more effectively stabilizes the pyridinium radical cation. Using this approach, *N*-arylpyridinium products **10** were obtained in moderate to high isolated yields (**Scheme 6**). Furthermore, direct aminolysis of pyridinium triflate afforded primary anilines and piperidines **11**.[42] In terms of substrate scope, only electron-neutral and electron-rich functional groups were well tolerated; however, Leonori and co-workers demonstrated that electron-poor alkenes could also be employed, albeit with diminished regioselectivity.[43] The proposed mechanism proceeds through the following steps: under blue-light irradiation, a Ru photocatalyst is excited and reduces the *N*-pyridinium triflate in a single-electron transfer, causing N-O bond heterolysis to generate a pyridinium radical cation **A**. This radical then adds to the arene substrate to form intermediate **B**, and subsequent electron and proton transfers deliver the *N*-arylpyridinium product **10** while regenerating the photocatalyst and closing the catalytic cycle.

In summary, the generation of aminium radicals - either via oxidation of amines or reduction of *N*-functionalized amines - facilitates broad functionalization such as alkene hydroamination and arene C-H amination.

2.3.3 Amidyl radicals

Generation of amidyl radicals via visible light has enabled several challenging synthetic transformations and opened new application routes such as direct C-H bond functionalization. Along this line, the Knowles group has reported that hydroamination of olefins can be achieved using a proton-coupled electron transfer (PCET) system (**Scheme 7**, left).[44] The key components are a thiophenol hydrogen-atom donor, a Brønsted base, and a photocatalyst, which together enable intramolecular hydroamination of unactivated olefins **12**. In general, the hydroamination proceeds in high yield and with excellent diastereoselectivity for substituted olefins; however, they noted that intermolecular coupling remains a limitation of their method. Mechanistically, PCET generates an amidyl radical **A** from a hydroxamic acid derivative, which adds to the olefin to form a carboN-centeredradical **B**; this intermediate is then reduced by the thiophenol donor to furnish the desired product **13**. The same group later extended the PCET strategy to the intermolecular carboamination of olefins, delivering products **14** in moderate to excellent yields (**Scheme 7**, right).[45]

[41] Zhen-Chu, C.; Stang, P. J. *Tetrahedron Lett.* **1984**, *25*, 3923-3926.
[42] (a) Rössler, S. L.; Jelier, B. J.; Tripet, P. F.; Shemet, A.; Jeschke, G.; Togni, A.; Carreira, E. M. *Angew. Chem. Int. Ed.* **2019**, *58*, 526-531. (b) Ham, W. S.; Hillenbrand, J.; Jacq, J.; Genicot, C.; Ritter, T. *Angew. Chem. Int. Ed.* **2019**, *58*, 532-536. (c) Hillenbrand, J.; Ham, W. S.; Ritter, T. *Org. Lett.* **2019**, *21*, 5363-5367.
[43] Ruffoni, A.; Julia, F.; Svejstrup, T. D.; McMillan, A. J.; Douglas, J. J.; Leonori, D. *Nat. Chem.* **2019**, *11*, 426-433.
[44] Miller, D. C.; Choi, G. J.; Orbe, H. S.; Knowles, R. R. *J. Am. Chem. Soc*. **2015**, *137*, 13492−13495.
[45] Choi, G. J.; Knowles, R. R. *J. Am. Chem. Soc.* **2015**, *137*, 9226− 9229.

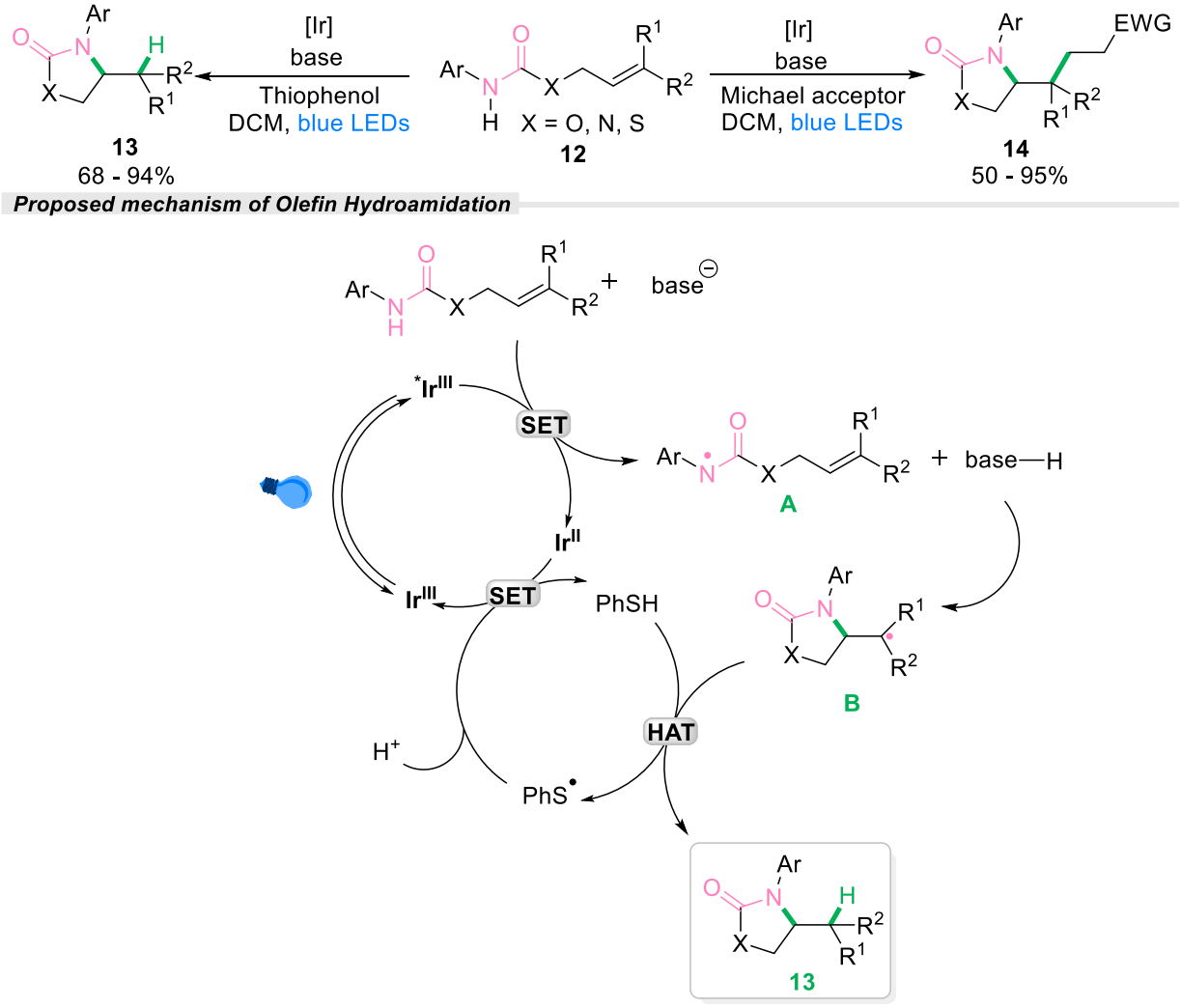

Scheme 7. Visible light-mediated alkene hydroamination and carboamination with proposed mechanism of the alkene hydroamination.

Under visible-light irradiation, Meggers and co-workers reported an enantioselective β-amination of α,β-unsaturated 2-acyl imidazole-substituted ketones using *N*-aryl carbamates (**Scheme 8**).[46] A chiral Rh catalyst is essential for enantioselectivity: it coordinates to the imidazole nitrogen and the ketone to form a rigid, electron-rich rhodium enolate. Upon generation of the amidyl radical from *N*-alkoxyamides and the rhodium enolate radical via an Ir photocatalyst, radical-radical cross-coupling furnishes the chiral product **17** with excellent enantiomeric excess.

As previously shown in **Scheme 7**, hydroamination was performed using Ir photocatalysis but hydroamination of aryloxy amides is also feasible under metal-free conditions using eosin Y as the photocatalyst, because aryloxy amides have a lower oxidation potential and allow efficient

[46] Zhou, Z.; Li, Y.; Han, B.; Gong, L.; Meggers, E. *Chem. Sci.* **2017**, *8*, 5757–5763.

generation of amidyl radicals.[47] In the same study, they developed an intermolecular *N*-arylation protocol employing aryloxy amides **18** and electron-rich arenes **19** in the presence of eosin Y, base, and green LEDs (**Scheme 9**).

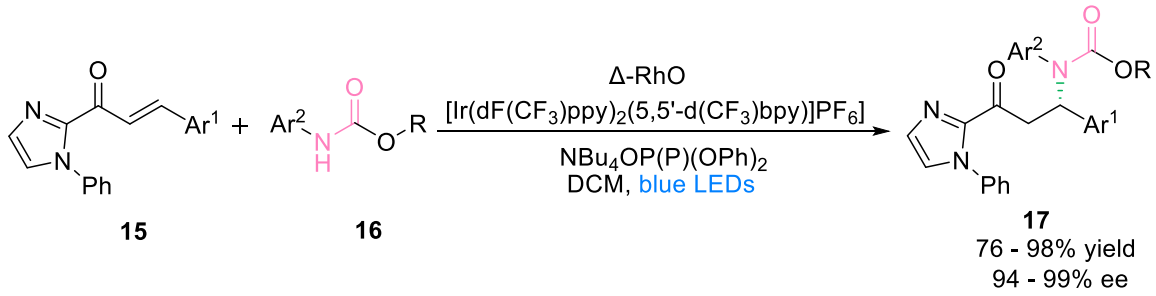

Scheme 8. Enantioselective β-amination of α,β-unsaturated 2-acyl imidazoles.

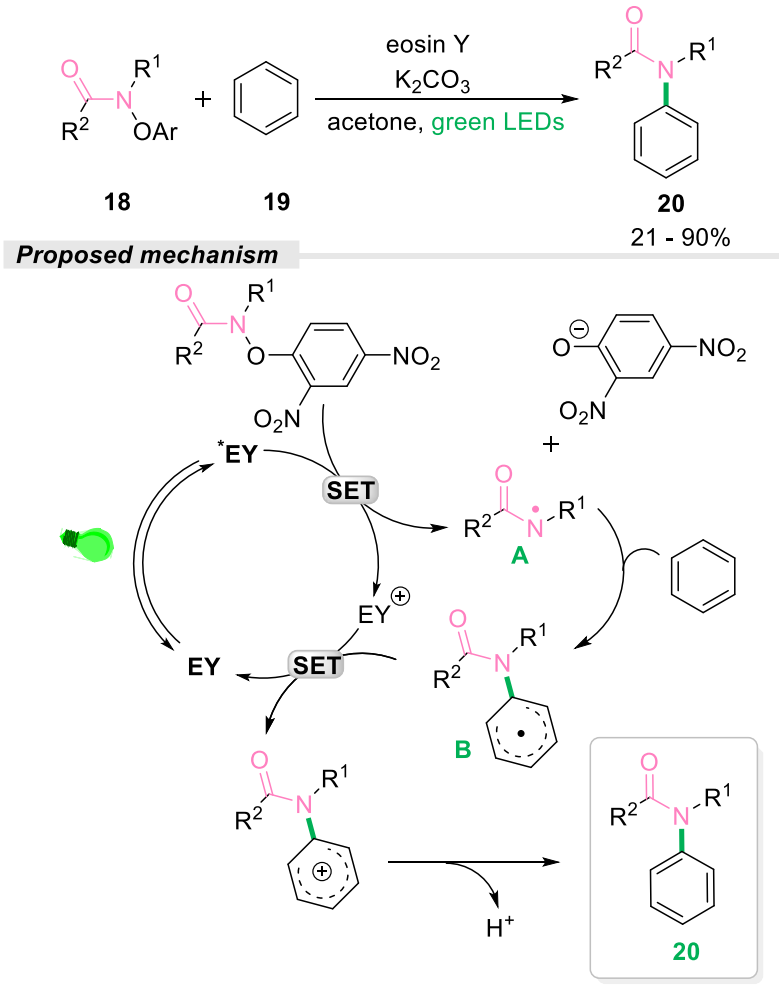

Scheme 9. *N*-Arylation of aryloxy amides with proposed mechanism.

[47] Davies, J.; Svejstrup, T. D.; Fernandez Reina, D.; Sheikh, N. S.; Leonori, D. *J. Am. Chem. Soc.* **2016**, *138*, 8092−8095.

A wide range of heteroaromatics were obtained, in yields from moderate to excellent. To demonstrate the method's robustness, several late-stage modifications of complex molecules-such as indole alkaloids-have been carried out. The proposed mechanism involves SET oxidation of the aryloxy amide to generate the amidyl radical **A**. Subsequent addition to the arene yields an *N*-arylated radical **B**, which undergoes oxidation and deprotonation to afford the final product **20**.

Amidyl radicals can also be produced by cleavage of *N*-aminopyridinium salts, releasing N-centered radicals. These amidyl radicals readily add to various indole derivatives.[48] Following this discovery, several groups have developed protocols that utilize sulfonamidyl radical precursors for C-H functionalization.[49] For example, the Gryko group reported a robust method for α-amidation of *O*–protected enolates **21** under blue LED irradiation using an Ir photocatalyst to afford N-protected amino carbonyl compounds **23** in excellent yields - even in the presence of an aldehyde functional group. Furthermore, preliminary studies demonstrated that ester and dihydropyran functionalities are compatible, although further optimization is required (**Scheme 10**).[50]

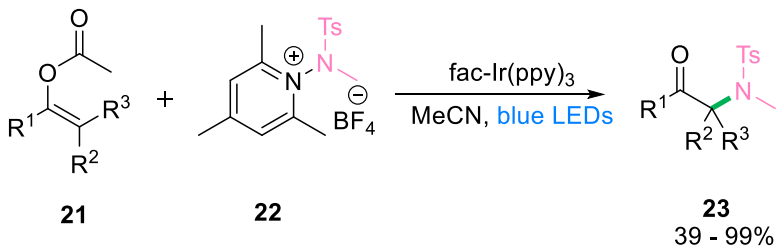

Scheme 10. α-Amidation of O-protected enolates to afford α-sulfamyl-containing carbonyl compounds.

In summary, amidyl radicals are useful and versatile intermediates that enable a wide range of transformations such as direct C-H functionalization, hydroamination, carboamination, aminoarylation, aziridination, and remote C-H activation via 1,5-hydrogen atom transfer (1,5–HAT).

2.3.4 Iminyl radicals

The formation of iminyl radicals via visible light opens new routes for the synthesis of heterocyclic compounds, which would otherwise require harsh reaction conditions.[51] The Studer group reported an efficient synthesis of pyrroline derivatives with iminyl radicals under visible-light irradiation (**Scheme 11**).[52] Using α-imino-oxy propionic acids **24** in the presence of Michael acceptors **25** afforded the desired products **26** in good to excellent yields. In their scope and limitations study,

[48] Greulich, T. W.; Daniliuc, C. G.; Studer, A. *Org. Lett.* **2015**, *17*, 254–257.
[49] (a) Tong, K.; Liu, X.; Zhang, Y.; Yu, S. *Chem.- Eur. J.* **2016**, *22*, 15669–15673. (b) Ito, E.; Fukushima, T.; Kawakami, T.; Murakami, K.; Itami, K. *Chem.* **2017**, *2*, 383–392.
[50] Goliszewska, K.; Rybicka-Jasińska, K.; Szurma, J.; Gryko, D. *J. Org. Chem.* **2019**, *84*, 15834-15844.
[51] McBurney, R. T.; Walton, J. C.; *J. Am. Chem. Soc.* **2013**, *135*, 7349-7354.
[52] Jiang, H.; Studer, A. *Angew. Chem. Int. Ed.* **2017**, *56*, 12273-12276.

they observed low diastereoselectivity with open-chain substrates, whereas rigid bicyclic systems provided excellent stereocontrol. Considering the reaction mechanism, visible-light excitation of the Ir photocatalyst triggers SET oxidation of the deprotonated α-imino-oxy acid **A**, generating a carboxyl radical **B**. Decarboxylation and elimination of an aldehyde then yields an iminyl radical **C**, which undergoes a 5-*exo*-trig cyclization. The resulting radical **D** is trapped by a Michael acceptor to form an adduct radical **E** that, upon SET reduction, closes the catalytic cycle by delivering an anion **F**. Finally, protonation furnishes the pyrroline product **26**.

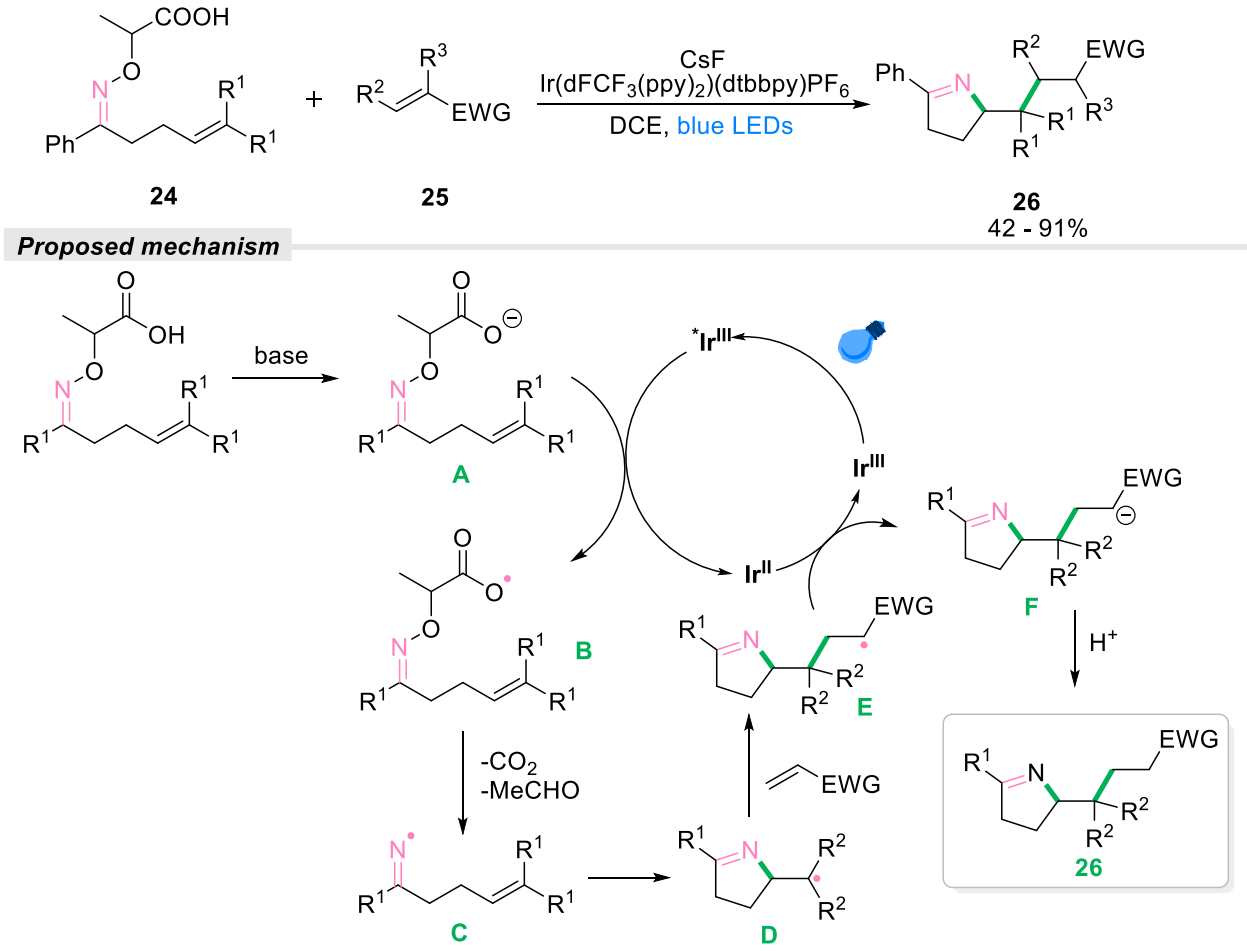

Scheme 11. Synthesis of pyrrolines under visible light with proposed mechanism.

The Studer group further extended the use of iminyl radicals to achieve remote γ-functionalization of ketones via α-aminooxypropionic acids **27**.[53] Under mild conditions, the reaction delivered γ−functionalized ketones in moderate to good yields with broad functional-group tolerance (**Scheme 12**). The necessary α-imino-oxy propionic acids are prepared by condensation of ketones with an α-aminoxy acid. Mechanistically, visible-light excitation of the Ir photocatalyst induces SET oxidation of the deprotonated α-aminooxypropionic acid, generating a carboxyl radical **A**. Decarboxylation and loss of an aldehyde then produce an iminyl radical **B**, which undergoes a

[53] Jiang, H.; Studer, A. *Angew. Chem. Int. Ed.* **2018**, *57*, 1692-1696.

1,5−HAT to form a γ-carbon radical **C**. This radical is intercepted by a Michael acceptor to make a new C-C bond, yielding an adduct radical **D**, that, upon SET reduction, closes the catalytic cycle. Finally, hydrolysis of the resulting imine **E** affording the γ-functionalized ketone **29**.

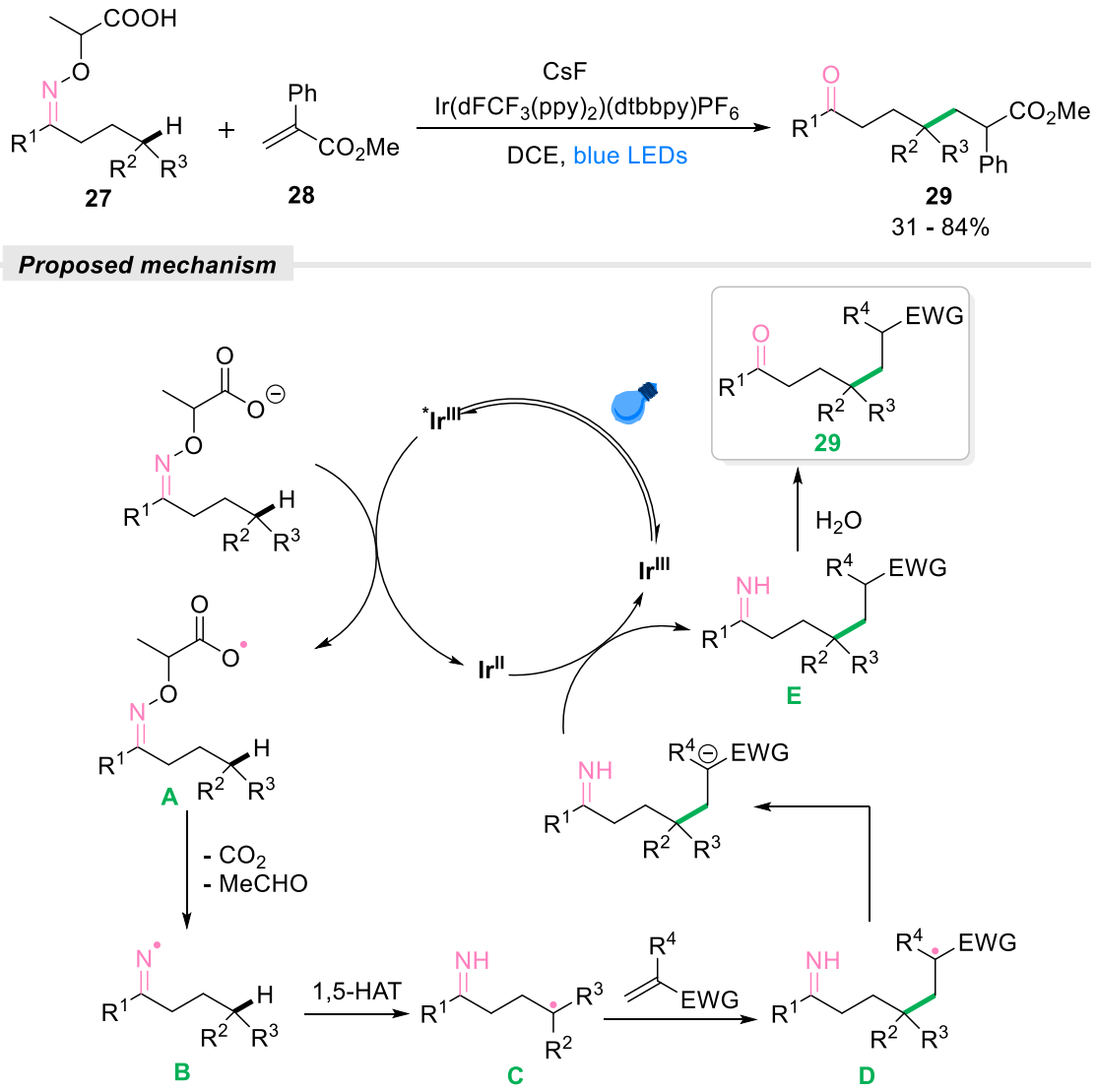

Scheme 12. Synthesis of γ-functionalized ketones with proposed mechanism.

Independently, the Leonori group also utilized α-amino-oxy acids **27** to achieve γ-functionalization of both ketones and nitriles (**Scheme 13**).[54] Condensation of a ketone with an α-amino-oxy acid furnishes the corresponding α-imino-oxy acid derivative, which is oxidized by a photoexcited organocatalyst. Subsequent decarboxylation and loss of acetone generates an iminyl radical. A 1,5−HAT produced a distal carbon radical, which was trapped with N-chlorosuccinimide (NCS) or Selectfluor to give, after imine hydrolysis, γ-chlorinated **30** or γ-fluorinated **31** ketones in moderate to high yields. Furthermore, cyclic ketones could undergo β-cleavage of the

[54] Dauncey, E. M.; Morcillo, S. P.; Douglas, J. J.; Sheikh, N. S.; Leonori, D. *Angew. Chem. Int. Ed.* **2018**, *57*, 744-748.

corresponding iminyl radical to effect ring opening and deliver a cyano-alkyl radical **33**. This species can then be intercepted by NCS, Selectfluor, or an azide donor to afford halogenated or azidated nitrile derivatives.

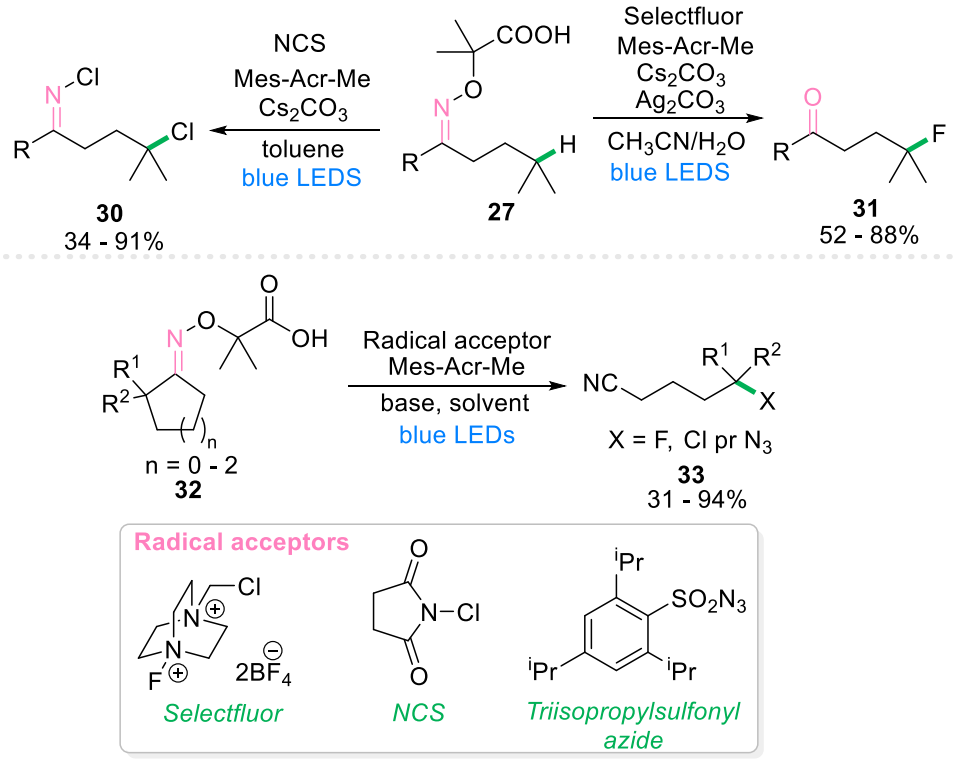

Scheme 13. Photoinduced remote functionalization via iminyl radical.

In summary, iminyl radicals serve as versatile intermediates that unlock diverse intra- and intermolecular functionalization strategies in organic synthesis, enabling the synthesis of nitrogen−containing heterocycles such as pyrrolines, pyrroles, isoquinolines, and quinolines, as well as aminated and aziridinated products.

2.3.5 Hydrazonyl radicals

The generation of hydrazonyl radicals via visible light has enabled several challenging synthetic transformations, opening new avenues such as direct C-H bond functionalization and the synthesis of nitrogen-rich heterocycles. The Xiao and Chen groups developed a new approach[55] to the well-established intramolecular hydroamination of alkenes.[56] They established a visible-light-mediated protocol in which β,γ-unsaturated hydrazones **34** are converted into hydrazonyl radicals to deliver both hydroaminated and oxyaminated derivatives (**Scheme 14**, left).

[55] Hu, X.-Q.; Chen, J.-R.; Wei, Q.; Liu, F.-L.; Deng, Q.-H.; Beauchemin, A. M.; Xiao, W.-J. *Angew. Chem., Int. Ed.* **2014**, *53*, 12163− 12167.
[56] (a) Patel, M.; Saunthwal, R. K.; Verma, A. K. *Acc. Chem. Res.* **2017**, *50*, 240−254. (b) Wang, Y.-F.; Chen, H.; Zhu, X.; Chiba, S. *J. Am. Chem. Soc.* **2012**, *134*, 11980−11983.

The influence of different aliphatic- or aromatic β,γ-unsaturated hydrazones were examined, and the desired products were obtained in moderate to good yields. Mechanistically, the hydrazone is first deprotonated by a base to generate a hydrazonyl anion **A**, which undergoes SET oxidation by the photoexcited Ru catalyst to form the hydrazonyl radical **B**. This radical then cyclizes via a 5-*exo*-trig pathway to give an alkyl radical intermediate **C**. HAT from $CHCl_3$ to this radical intermediate delivers the desired product **35** and simultaneously generates a trichloromethyl radical. A final SET reduction of the trichloromethyl radical regenerates the Ru catalyst, thus closing the catalytic cycle. Additionally, when a stoichiometric amount of TEMPO is present, the alkyl radical intermediate is trapped by TEMPO to furnish oxyaminated products **36** in good to excellent yields (**Scheme 14**, right). Subsequently, the methodology was extended to cascade reactions, yielding dihydropyrazole-fused benzosultams under cooperative Ru-Co catalysis.[57]

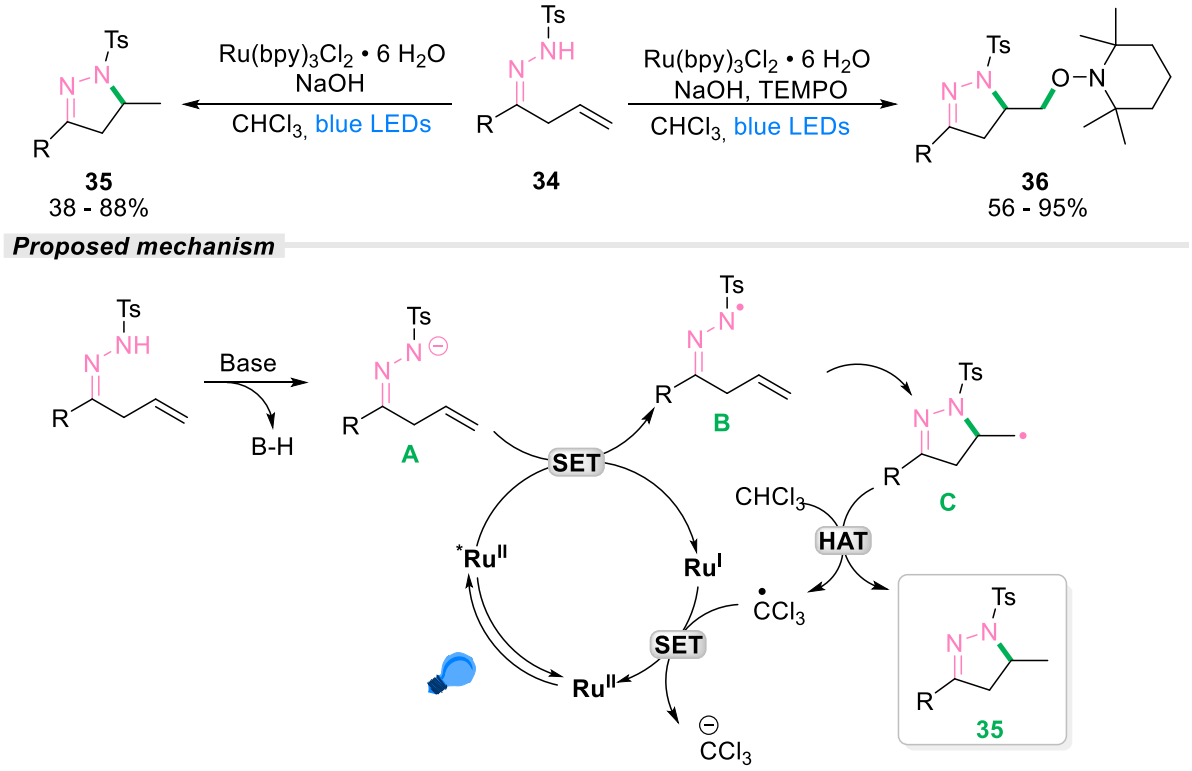

Scheme 14. Synthesis of Hydro- and Oxypyrazoles with proposed mechanism.

The Chen group further expanded these cyclization strategies to promote an *endo*-type pathway for synthesizing 1,6-dihydropyridazines **38** under visible-light irradiation in the presence of TEMPO (**Scheme 15**).[58] Under the previously optimized conditions, substrates bearing electronically activating aryl substituents on the alkene prefers to undergo 6-*endo* cyclization over the 5-*exo* mode. In this protocol, TEMPO has a distinct mechanistic role, serving as a hydrogen-atom acceptor to the azaallylic radical intermediate **C** to deliver the final product **38**.

[57] Zhao, Q.-Q.; Hu, X.-Q.; Yang, M.-N.; Chen, J.-R.; Xiao, W.-J. *Chem. Commun.* **2016**, *52*, 12749−12752.
[58] Hu,X.-Q.; Qi, X.; Chen, J.-R.; Zhao, Q.-Q.; Wei, Q.; Lan, Y.; Xiao, W.-J. *Nat. Commun.* **2016**, *7*, 11188.

Yields were not significantly affected by the presence of either electron-donating or electron-withdrawing groups, and the methodology proved applicable to aliphatic β,γ-unsaturated hydrazones, affording the corresponding products in good to high yields.

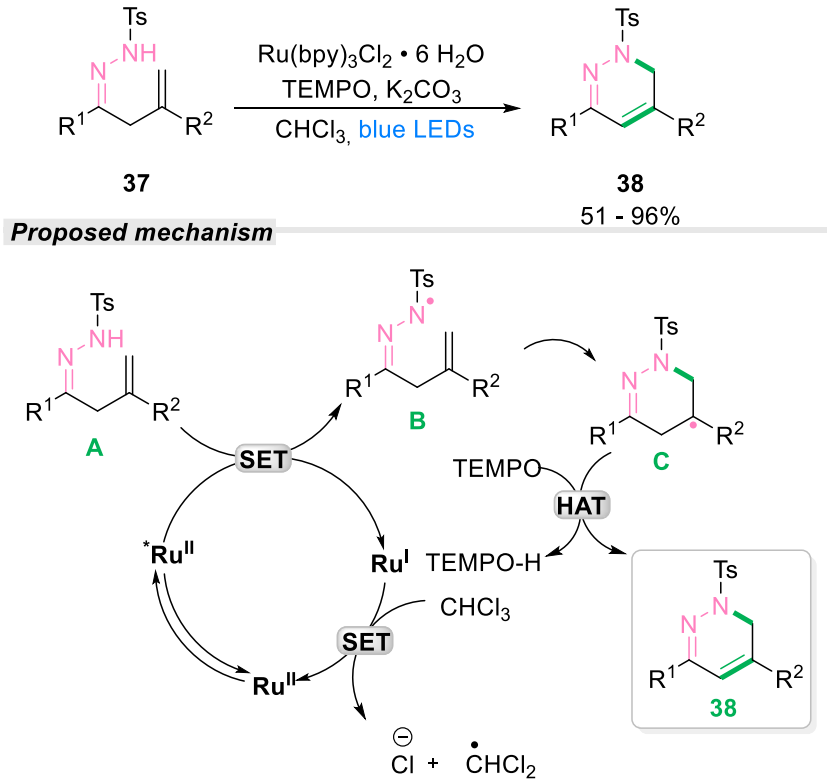

Scheme 15. Synthesis of 1,6-Dihydropyridazines with proposed mechanism.

The Belmont group reported a visible-light-mediated Smiles rearrangement method for the synthesis of phthalazine derivatives **40** involving hydrazonyl radicals (**Scheme 16**).[59] Most of the reactions provided products in good to high yields, although for the sterically hindered xylene substrate the yield diminished to 30 %. The one-pot protocol afforded yields comparable to those of the two-step sequence.

The proposed mechanism begins with excitation of the Ru photocatalyst, which oxidizes the deprotonated hydrazone to form a hydrazonyl radical **A**. A consecutive intramolecular 6-*exo*-dig cyclization then generates a vinylic radical **B**, which undergoes a radical Smiles rearrangement at the ipso position with the removal of SO_2. Finally, the reduction of the benzylic radical **C** followed by protonation furnishes the desired product **40** while regenerating the Ru photocatalyst.

[59] Brachet, E.; Marzo, L.; Selkti, M.; König, B.; Belmont, P. *Chem. Sci.* **2016**, *7*, 5002−5006.

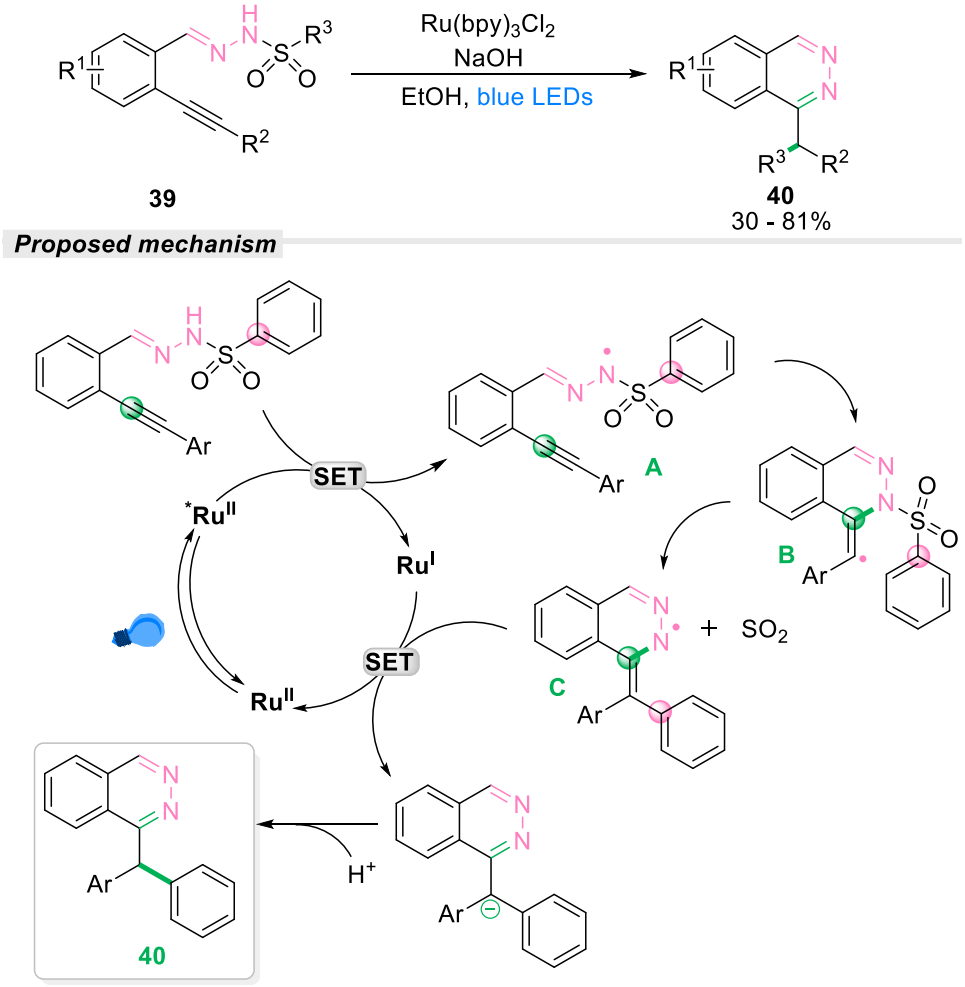

Scheme 16. Synthesis of phthalazine derivatives by visible light with proposed mechanism.

In summary, the generation of hydrazonyl radicals enables a broad range of synthetic approaches for intramolecular hydroamination reactions, as well as for the synthesis of nitrogen-containing heterocycles, C-H functionalization, aziridination, and radical cyclization processes.

2.4 Summary

N-Centered radicals have emerged as versatile intermediates for visible-light-mediated amidation of arenes and olefins. Historically, they were generated by homolysis of N-halogen bonds under harsh conditions, which limited functional-group tolerance. Over the past decade, photocatalytic methods have revolutionized their generation, allowing milder, more selective access to N-centered radicals. [60]

Photocatalytic oxidation of amides or reduction of *N*-functionalized amines furnishes aminium radical cations, which exhibit electrophilic reactivity and anti-Markovnikov selectivity in olefin addition.[26] Most described protocols rely on SET oxidation using transition-metal photoredox catalysts, but organic dyes can also achieve such transformations.[47] PCET strategies-exemplified by Knowles and co-workers-enable direct oxidation of N-H bonds in amides and sulfonamides to generate the corresponding amidyl radicals.[44,45] Likewise, α-aminooxy-acid auxiliaries afford iminyl radicals via SET oxidation.[52,53,54]

Whether amidyl, sulfonamidyl, hydrazonyl, or iminyl, these visible-light generated radicals participate in a broad range of intra- and intermolecular olefin and arene functionalization-including remote C-H functionalization. Radical adducts formed with diverse trapping reagents are readily reduced to the final products, closing the photoredox cycle in a redox-neutral manner. Despite these advances, challenges remain, expanding asymmetric variants and developing even more sustainable, metal-free protocols are important goals for future work.

[60] (a) Karkas, M. D. *ACS Catal.* **2017**, *7*, 4999-5022. (b) Jiang, H.; Studer, A. *CCS Chem.* **2019**, *1*, 38-49.

3. Results and Discussion

The main goal of my PhD dissertation was to investigate novel reactivity of photochemically generated nitrogen-centered radicals and aziridines for the formation of C-N and C-C bonds, leading to amines and their derivatives.

3.1 Site-Selective, Photocatalytic Vinylogous Amidation of Enones

Remote functionalization, or vinylogy, transmits the electronic influence of a functional group across a conjugated π-system.[61] This approach is particularly valuable for the challenging γ−functionalization of α,β-unsaturated carbonyl compounds. Vinylogy was pioneered by Mukaiyama, who performed remote aldol reactions to access δ-α,β-unsaturated aldehydes.[62] In recent years, various activation strategies-iminium/enamine catalysis, N-heterocyclic carbene (NHC) catalysis, cooperative organo/metal catalysis, and photocatalysis-have emerged.[63] However, these methods often require a branched α-substituent to block the α-position and enforce site-selectivity or pre-γ-functionalization is necessary.[64] Only few electrophilic partners have been explored, among them Jørgensen's [4+2] cycloaddition using azodicarboxylates remains the sole example of γ-C(sp^3)-N bond formation.[63a]

To overcome these limitations, we envisioned generating N-centered radicals from *N*−aminopyridinium salts (**Figure 2**) under blue LED irradiation and selectively adding them to the γ-position of silylated dienol ethers. Despite the widespread use of nitrogen-centered radicals in photochemistry,[50] their vinylogous functionalization is underexplored. We reported the first site−selective photocatalytic γ-amidation of α,β-unsaturated enones using *N*-aminopyridinium salts and *fac*-Ir(ppy)$_3$ as a photocatalyst (**Scheme 17**).

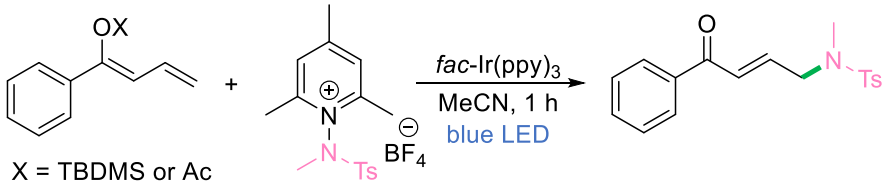

Scheme 17. Model reaction of γ-amidation of α,β-unsaturated carbonyl compounds.

[61] Fuson, C. R. *Chem. Rev.* **1935**, *16*, 1− 27.
[62] Mukaiyama, T.; Ishida, A. *Chem. Lett.*, **1975**, 319.
[63] (a) Bertelsen, S.; Marigo, M.; Brandes, S.; Dinér, P.; Jørgensen, K. A. *J. Am. Chem. Soc.* **2006**, *128*, 12973−12980. (b) Bencivenni, G.; Galzerano, P.; Mazzanti, A.; Bartoli, G.; Melchiorre, P. *Proc. Natl. Acad. Sci. U. S. A.* **2010**, *107*, 20642−20647. (c) Yin, Y.; Jiang, Z. *ChemCatChem.* **2017**, *9*, 4306−4318. (d) Chen, X. Y.; Liu, Q.; Chauhan, P.; Enders, D. *Angew. Chem., Int. Ed.* **2018**, *57*, 3862−3873. (e) Chen, Z.; Yu, X.; Wu, J. *Chem. Commun.* **2010**, *46*, 6356− 6358. (f) Mondal, S.; Reddy Yetra, S.; Mukherjee, S.; Biju, A. T. *Acc. Chem. Res.* **2019**, *52*, 425−436. (g) Romano, C.; Fiorito, D.; Mazet, C. *J. Am. Chem. Soc.* **2019**, *141*, 16983−16990. (h) Dai, L.; Xia, Z. H.; Gao, Y. Y.; Gao, Z. H.; Ye, S. *Angew. Chem., Int. Ed.* **2019**, *58*, 18124−18130.
[64] (a) Bergonzini, G.; Vera, S.; Melchiorre, P. *Angew. Chem., Int. Ed.,* **2010**, *49*, 9685. (b) Stiller, J.; Marques-Lopez, E.; Herrera, R. P.; Frohlich, R.; Strohmann, C.; Christmann, M. *Org. Lett.,* **2011**, *13*, 70.

The synthetic utility of vinylogy lies in its ability to create additional reactive sites in π-extended enolizable carbonyl systems.[65] In our case, the nitrogen-centered radical selectively adds to the γ-position of the silyl dienol ether, forming allylic radical intermediate **A** rather than radical **B**, as **A** is resonance-stabilized and thus represents the more stable intermediate (**Scheme 18**).

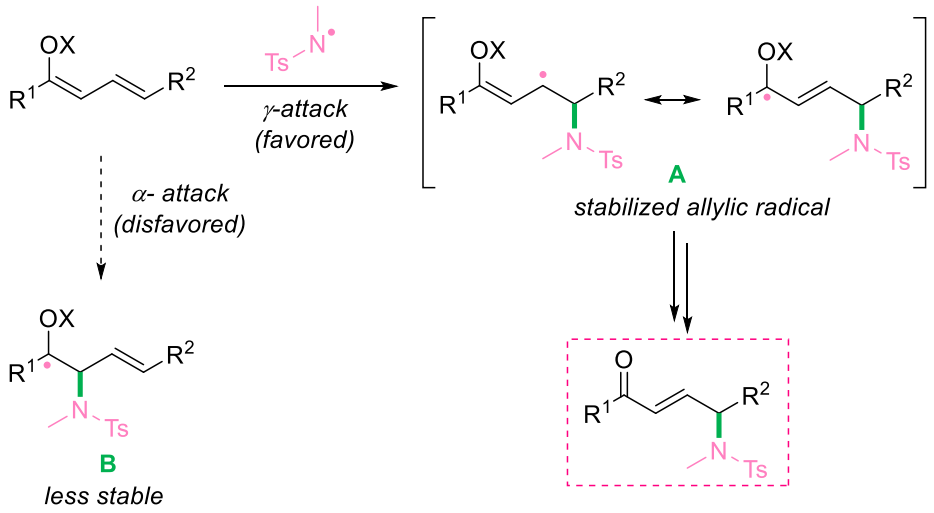

Scheme 18. Remote radical γ-amidation in π-extended silyl dienol ether.

During the optimization of the silyl dienol ether reaction, Katarzyna Goliszewska identified the ideal catalyst loading, solvent, and reaction time (1 h), obtaining exclusively the *E*-isomer. A slight increase in salt loading further improved the yield to 90%. The photocatalyst of choice, *fac*–Ir(ppy)$_3$, was selected based on the redox potentials of the *N*-aminopyridinium salts.[66]

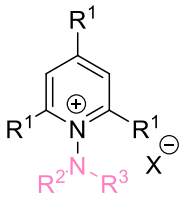

Figure 2. General structure of *N*-Aminopyridinium salt.

My work focused on expanding scope with respect to *N*-aminopyridinium salts and worked on the scope of α,β-unsaturated carbonyl compounds. I found that both *N*-mono- and *N*,*N*-disubstituted aminopyridinium salts were compatible, affording the γ-product in high yields and with excellent *E*-selectivity. However, the nature of the protecting group on the amidyl radical had an influence on the diastereoselectivity. For example, bulky Boc-protected salts led to *E*/*Z* mixtures (~6:5), while Cbz- and Ts-protected salts delivered the γ-amidated product with complete site- and stereoselectivity (**Table 1**).

[65] Curti, C.; Battistini, L.; Sartori, A.; Zanardi, F. *Chem. Rev.* **2020**, *120*, 2448–2612.
[66] Goliszewska, K.; Rybicka-Jasinska, K.; Szurmak, J.; Gryko, D. *J. Org. Chem.* **2019**, *84*, 15834–15844.

Table 1. Scope of *N*-Aminopyridinium salts.

Entry	R^1	R^2	R^3	X^-	*E*:*Z*	Isolated yield [%]
1	Me	Me	Ts	BF_4	*E*	90
2	Me	Me	Boc	BF_4	*6:5*	76
3	Me	Me	Cbz	BF_4	*E*	46
4	Ph	Me	Boc	BF_4	*6:5*	74
5	H	H	COC_6F_5	OTf	*E*	48
6	Me	H	Ts	BF_4	*E*	74

In the next step, I evaluated the scope of enones. The methodology also proved highly effective for various enone substrates. Aryl-substituted enones bearing either electron-donating (EDG) or electron-withdrawing groups (EWG) afforded products **51-58** in high to excellent yields with full site−selectivity. Other substrates, such as cyclic enones **59-60**, also performed well. Even extended conjugated systems **63-64** were tolerated, although yields were lower. Importantly, I demonstrated that this approach could be applied to late-stage functionalization. Biologically relevant molecules furnished the desired γ-amidated products exclusively **65-68** (**Scheme 20**). Interestingly, a few cases highlighted how α/γ selectivity is influenced by the electronic nature of the terminal aryl ring. Substrates containing EDG groups on both aryl rings consistently gave γ-products **44-47**, whereas electron-deficient systems favored α-amidation, yielding *Z*−configured products **48-50** (**Scheme 19**).

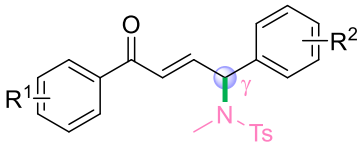

44 R_1,R_2(p-OMe) 71%
45 R_1,R_2(m-OMe) 62%
46 R_1,R_2(o-OMe) 60%
47 R_1(p-CF_3),R_2(p-OMe) 44%

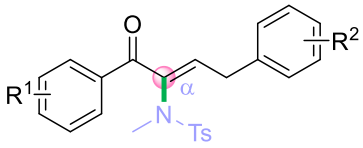

48 R_1,R_2(p-CN) 58%
49 R_1,R_2(p-CF_3) 64%
50 R_1(p-OMe),R_2(p-CF_3) 60%, *Z*/*E* 12:1

Scheme 19. Competition between α and γ amidation of α,β-unsaturated carbonyl compounds.

Additionally, to support our mechanistic proposal, I carried out radical-trapping experiments. The addition of DMPO (5,5-dimethyl-1-pyrroline N-oxide), a spin-trapping reagent confirmed the formation of N-centered radical, as evidenced by the corresponding adduct detected via high-resolution mass spectrometry (HR-MS). To further confirm the radical nature of the reaction, the addition of TEMPO completely suppressed the reaction.

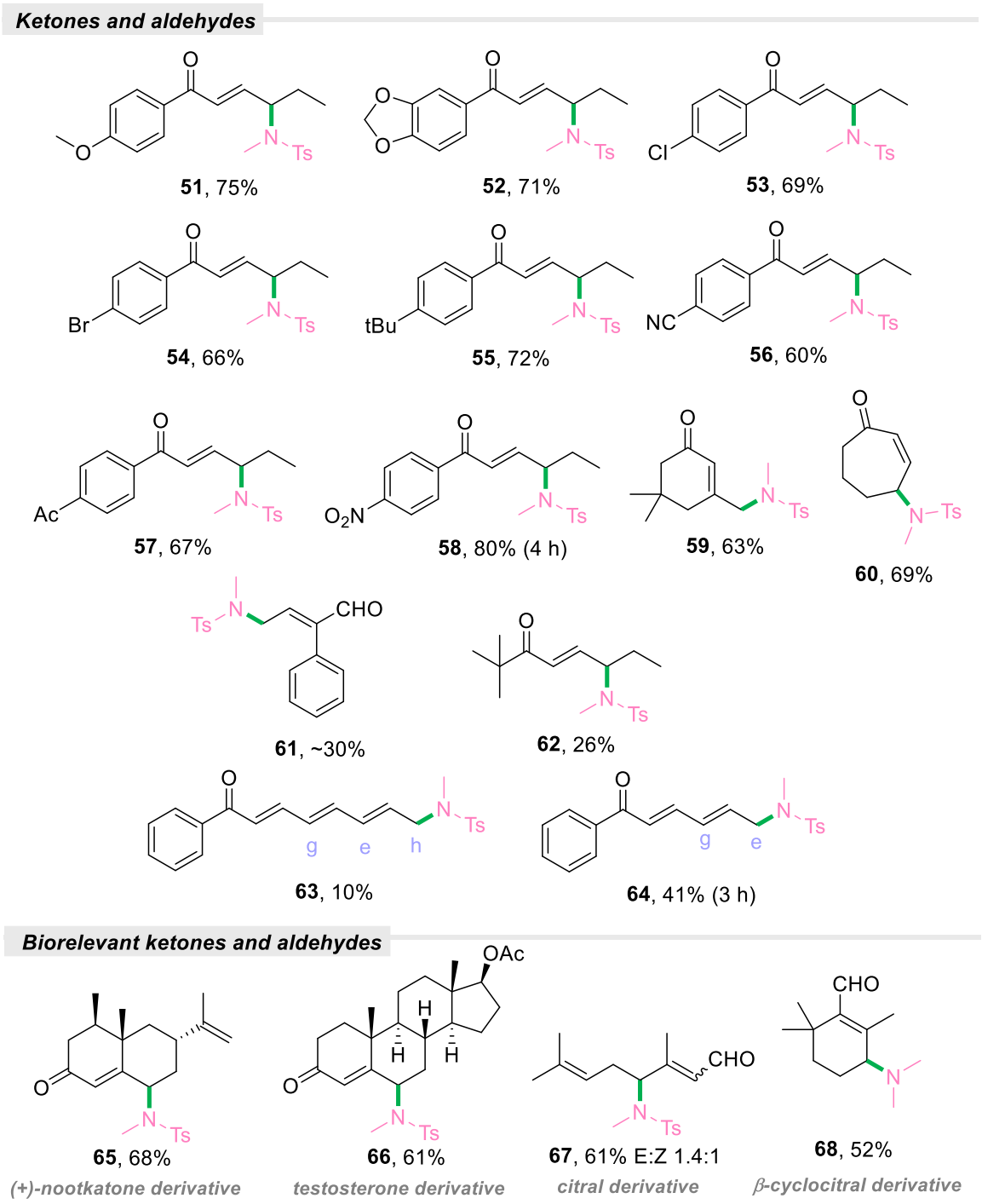

Scheme 20. Investigation of the scope of amidation of α,β-unsaturated carbonyl compounds that I synthesized.

In summary, we reported, for the first time, a site-selective, photocatalytic γ-amidation of α,β−unsaturated enones using *N*-protected aminopyridinium salts. This strategy, enabled by vinylogous activation, offers a powerful method for remote C-N bond formation. Key features of

this methodology include mild conditions, high site- and stereoselectivity, broad substrate scope, and applicability to biologically important molecules.

The results of this study were published in a scientific journal:[67]

[P1] Site-Selective, Photocatalytic Vinylogous Amidation of Enones, **Szabó, K. F.**; Goliszewska, K.; Szurmak, J.; Rybicka-Jasińska, K.; Gryko, D. *Org. Lett.* **2022**, *24*, 8120-8124.

[67] Szabó, K. F.; Goliszewska, K.; Szurmak, J.; Rybicka-Jasińska, K.; Gryko, D. *Org. Lett.* **2022**, *24*, 8120-8124.

3.2 Photochemical C3-Amination of Pyridines via Zincke Imine Intermediates

Pyridine is among the most prevalent heterocyclic scaffolds in approved drugs, and its biological activity is strongly influenced by substituent positions on the ring.[68] The ring's nitrogen atom makes the C2 and C4 positions more electron-deficient, so C2- and C4-functionalization methods-using these electronic biases-are well established. In contrast, C3-functionalization of pyridine remains a significant challenge. Classical approaches, such as electrophilic aromatic nitration, often require harsh conditions, large excesses of pyridine, and still deliver poor regioselectivity.[69] Consequently, there is a high demand for selective C3-functionalization strategies.

Recently, peripheral editing of pyridines has emerged as a powerful strategy for meta-selective functionalization.[70] Some significant protocols showed below that employ dearomatization-rearomatization sequences to achieve C3-functionalized pyridines (**Scheme 21**).

Wang and co-workers reported a borane-catalyzed hydroboration of pyridines to generate nucleophilic 1,4-dihydropyridines, which subsequently react with electrophiles. Reoxidation then delivers C3-substituted pyridines.[71] Using this strategy, they successfully installed pharmaceutically relevant functional groups such as trifluoromethylthio (SCF_3), difluoromethylthio (SCF_2H), cyano, and allyl groups (**Scheme 21, top**).[72] Studer and McNally's groups independently developed efficient redox-neutral C3-functionalization strategies for pyridines via peripheral editing.[73] The Studer group designed a method to synthesize an oxazinopyridine intermediate, which reacts with electrophiles or radicals through a dienamine pathway.[74] They later extended this approach to C4-selective functionalization under acidic conditions (**Scheme 21, middle**).[75] Meanwhile, McNally and co-workers reported C3-halogenation of pyridines by modifying the Zincke reaction to generate Zincke salts (**Scheme 21, bottom**).[40,76] They further expanded this work to prepare *N*-(heteroaryl) pyridinium salts,

[68] (a) Vitaku, E.; Smith, D. T.; Njardarson, J. T. *J. Med. Chem.* **2014**, *57*, 10257–10274. (b) Bhutani, P.; Joshi, G.; Raja, N.; Bachhav, N.; Rajanna, P. K.; Bhutani, H.; Paul, A. T.; Kumar, R. *J. Med. Chem.* **2021**, *64*, 2339–2381.
[69] (a) Ziegler, T. *Angew. Chem.* **1990**, *102*, 848. (b) Joule, J. A. *Heterocyclic Chemistry*, CRC Press, **2020**.
[70] Cao, H.; Cheng, Q.; Studer, A. *Angew. Chem. Int. Ed.* **2023**, *62*, e202302941.
[71] Fan, X.; Zheng, J.; Li, Z. H.; Wang, H. *J. Am. Chem. Soc.* **2015**, *137*,4916 – 4919.
[72] (a) Zhou, X.-Y.; Zhang, M.; Liu, Z.; He, J.-H.; Wang, X.-C. *J. Am. Chem. Soc.* **2022**, *144*, 14463–14470. (b) Liu, Z.; He, J.-H.; Zhang, M.; Shi, Z.-J.; Tang, H.; Zhou, X.-Y.; Tian, J.-J.; Wang, X.-C. *J. Am. Chem. Soc.* **2022**, *144*, 4810–4818. (c) Tian, J.-J.; Li, R.-R.; Tian, G.-X.; Wang, X.-C. *Angew. Chem. Int. Ed.* **2023**, *62*, e202307697. (d) Liu, Z.; Shi, Z.-J.; Liu, L.; Zhang, M.; Zhang, M.-C.; Guo, H.-Y.; Wang, X.-C. *J. Am. Chem. Soc.* **2023**, *145*, 11789–11797. (e) Zhang, M.; Zhou, Q.; Luo, H.; Tang, Z.-L.; Xu, X.; Wang, X.-C. *Angew. Chem. Int. Ed.* **2023**, *62*, e202216894.
[73] Chakraborty, S.; Biju, A. T. *Angew. Chem. Int. Ed.* **2023**, *62*, e202300049.
[74] Cao, H.; Cheng, Q.; Studer, A. *Science* **2022**, *378*, 779–785.
[75] (a) Cao, H.; Bhattacharya, D.; Cheng, Q.; Studer, A. *J. Am. Chem. Soc.* **2023**, *145*, 15581–15588. (b) Xu, P.; Wang, Z.; Guo, S.-M.; Studer, A. *Nat. Commun.* **2024**, *15*, 4121. (c) Cheng, Q.; Bhattacharya, D.; Haring, M.; Cao, H.; Mück-Lichtenfeld, C.; Studer, A. *Nat. Chem.* **2024**, *16*, 741–748.
[76] Boyle, B. T.; Levy, J. N.; de Lescure, L.; Paton, R. S.; McNally, A. *Science* **2022**, *378*, 773–779.

incorporate stable radioisotope ^{15}N atom into pyridine ring, and demonstrate C3-selective fluorination of pyridines.[77]

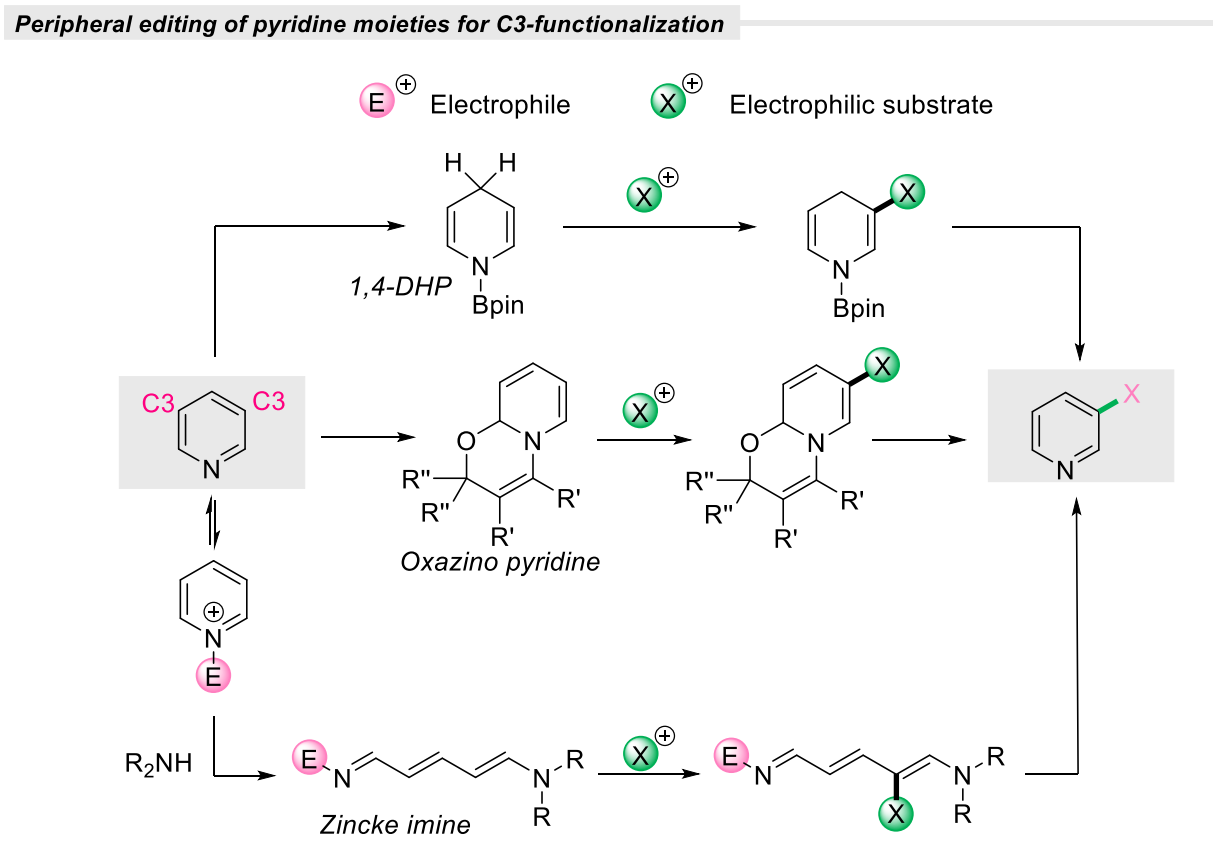

Scheme 21. Strategies enabling C-H functionalization of pyridines at C3-position.

Inspired by these studies, especially the McNally's work and recent reports on peripheral editing of pyridines via Zincke imine formation,[78] I investigated a photochemical reaction of *N*–methyl–*N*–tosyl aminopyridinium salt **42** with 2-phenyl Zincke imine **69** to form a new C-N bond (**Scheme 22**). Although *N*-aminopyridinium salts have been employed in a variety of photocatalyzed transformations, their application in direct C3-functionalization of pyridines has not been previously reported.

[77] (a) Selingo, J. D.; Greenwood, J. W.; Andrews, M. K.; Patel, C.; Neel, A. J.; Pio, B.; Shevlin, M.; Phillips, E. M.; Maddess, M. L.; McNally, A. *J. Am. Chem. Soc.* **2024**, *146*, 936–945. (b) Nguyen, H. M. H.; Thomas, D. C.; Hart, M. A.; Steenback, K. R.; Levy, J. N.; McNally, A. *J. Am. Chem. Soc.* **2024**, *146*, 2944–2949. (c) Hart, M. A.; Uhlenbruck, B. J. H.; Levy, J. N.; McNally, A. *J. Am. Chem. Soc.* **2025**, doi.org/10.1021/jacs.5c03091.

[78] (a) Feng, M.; Norlöff, M.; Guichard, B.; Kealey, S.; Thuéry, P.; Gee, A.; Feuillastre, S.; Audisio, D. *Nat. Commun.*, **2024**, *15*, 6063. (b) Tolchin, Z. A.; Smith, J. M. *J. Am. Chem. Soc.* **2024**, *146*, 2939–2943. (c) Wang, H.; Greaney, M. F. *Angew. Chem. Int. Ed.* **2024**, *63*, e202315418. (d) Conboy, A.; Greaney, M. F. *Chem* **2024**, *10*, 1940–1949. (e) Bartholomew, G. L.; Kraus, S. L.; Karas, L. J.; Carpaneto, F.; Bennett, R.; Sigman, M. S.; Yeung, C. S.; Sarpong, R. *J. Am. Chem. Soc.* **2024**, *146*, 2950–2958.

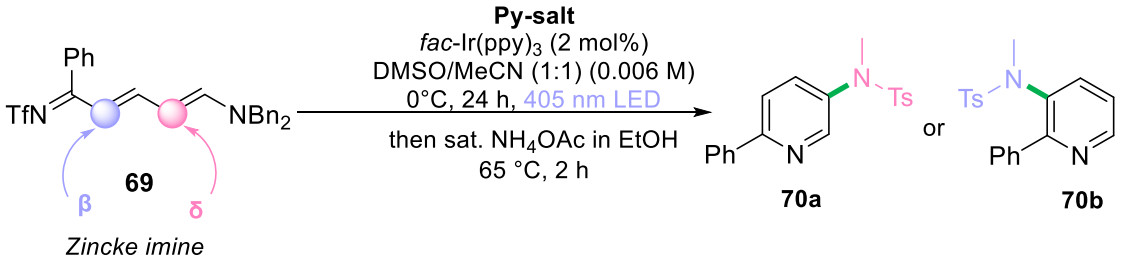

Scheme 22. Model reaction of 2Ph-Zincke imine with *N*-aminopyridinium salt.

Although prior work showed that photoexcited Ir(III) catalysts can reduce *N*-aminopyridinium salts via single-electron transfer to generate N-centered radicals,[79] yields were only 16% under standard 450 nm blue light-likely due to strong absorption of the 2-phenyl-Zincke imine **69** (**Figure 3**). We found that switching to 405 nm irradiation was crucial for the efficient Ir-catalyst excitation and the amidyl radical formation. Further optimization with Piotr Banachowicz established the ideal catalyst loading, solvent, and reaction time, ultimately delivering the desired product in 99% yield with a 5:1 regioisomeric ratio.

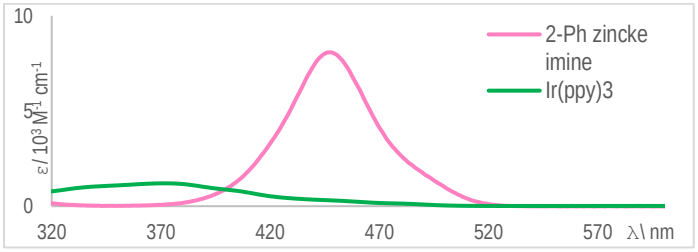

Figure 3. UV-Vis spectrum of 2Ph-Zincke Imine and $Ir(ppy)_3$ in MeCN.

The preparation of Zincke imine derivatives was divided between Piotr, Antoni, and me. After synthesizing them, I investigated the substrate scope. I explored various 2-substituted pyridines bearing EDG or EWG, which afforded the desired products **71-80** in high yields and good regioselectivity. However, steric hindrance at both *ortho* positions of the 2-phenyl-substituted pyridine ring **75** was found to reduce yields, requiring harsher conditions to promote ring closure. Interestingly, in the case of alkyl-substituted pyridines **85-90**, adjustments to the reaction conditions were necessary to achieve improved yields. Surprisingly, regioselectivity shifted: the amidyl radical attacked the Zincke imine at the β-position, resulting in the pyridine products having substituents at the C2 and C3 positions rather than the typical C3 and C5 (**Scheme 23**).

Additionally, I tested various mono- and di-protected *N*-aminopyridinium salts under our optimal conditions; however, they proved to be less effective than *N*-methyl-*N*-tosyl protected aminopyridinium salt **42**. To determine whether regioselectivity is influenced by the amine group on the Zincke imine derivative, I synthesized additional Zincke imines bearing amines different from the model substrate, such as *N*-benzyl-*N*-phenyl and morpholine derivatives. Only the *N*–benzylaniline derivative afforded the desired product, albeit with a significant drop in both yield

[79] Greulich, T. W.; Daniliuc, C. G.; Studer, A. *Org. Lett.* **2015**, *17*, 254–257.

(26%) and regioselectivity (2:1 ratio). The morpholine derivative remained unreacted and did not provide the desired product.

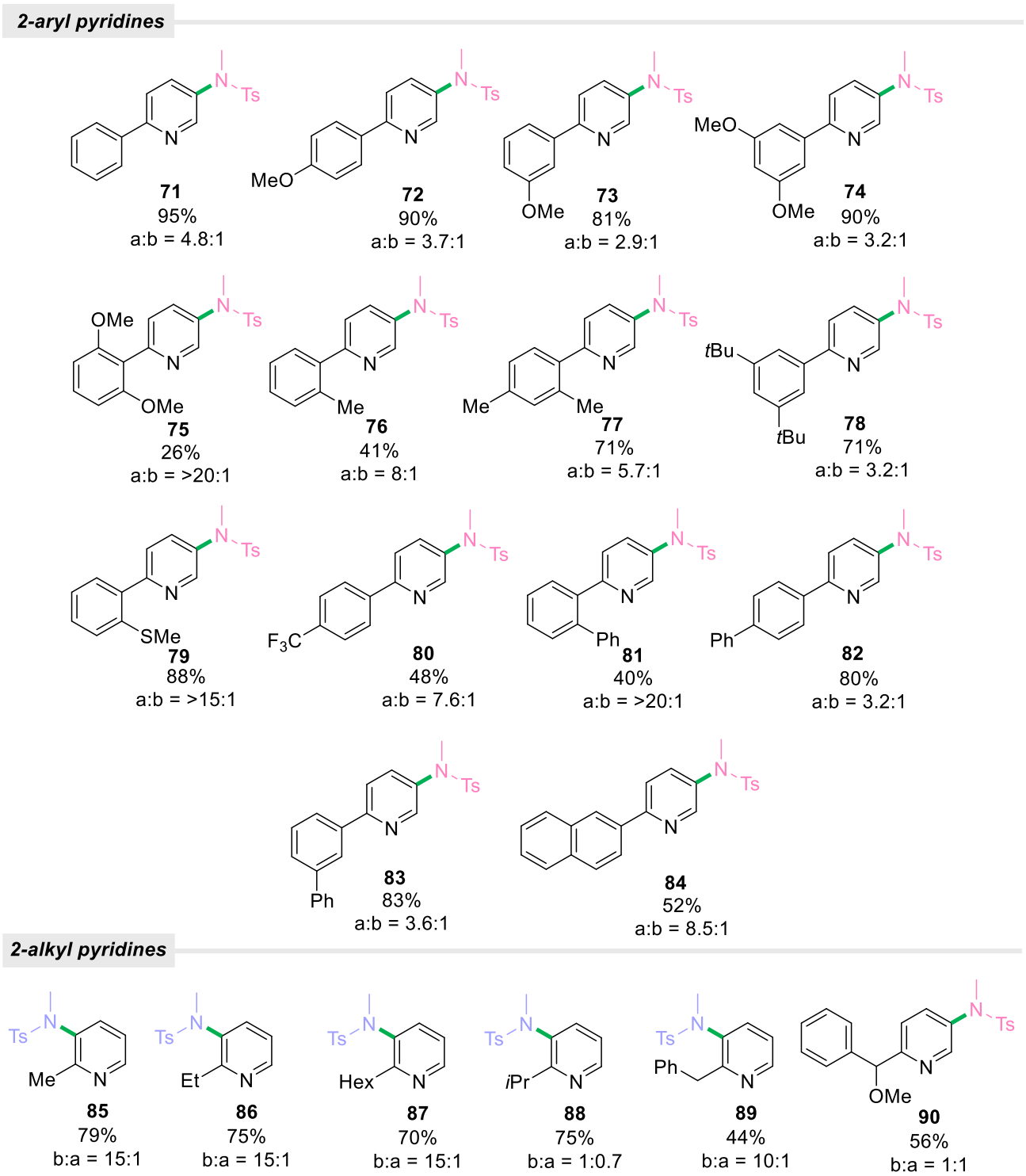

Scheme 23. Investigation of the scope for C3-amination of pyridines that I synthesized.

Although DFT calculations indicated that C-N bond formation at the δ-position of the 2-phenyl Zincke imine **69** is favored over α, β, and γ positions, the β-position can be competitive, as observed experimentally. The transition state energy at the γ-position is significantly higher, and while the α-position has a similar energy to β, the resulting radical leads to an unproductive intermediate thus unable to complete the catalytic cycle (**Figure 4**).

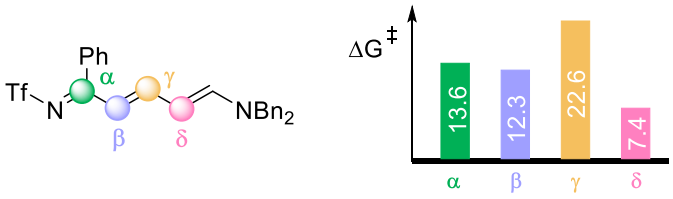

Figure 4. DFT calculations of transition state energies.

In conclusion, we developed a photocatalytic C3-amidation strategy for pyridines via Zincke imine functionalization using an electrophilic N-centered radical. The reaction proceeds under mild conditions, using pyridine as the limiting reagent, and demonstrates a broad substrate scope with good to excellent yields and excellent regioselectivity, showcasing the robustness of the protocol.

The above results were published in a scientific article:[80]

[P2] Photochemical C3-amination of pyridines via Zincke Imine intermediates, **Szabó, K. F.**; Banachowicz, P.; Powała, A.; Lunic, D.; Funes, A. I.; Gryko, D. *Nat. Commun.* **2025**, accepted, doi:10.26434/chemrxiv-2024-3dj94.

[80] Szabó, K. F.; Banachowicz, P.; Powała, A.; Lunic, D.; Funes, A. I.; Gryko, D. *Nat. Commun.* **2025**, doi:10.26434/chemrxiv-2024-3dj94.

3.3 Vitamin B_{12} and Micellar Solution Enable Regioselective Ring Opening of Epoxides and Aziridines with Electrophilic Olefins

Identification of new methods of organic molecule synthesis with a greener protocol is highly desirable to reduce chemical waste. In the chemical industry, over 60 % of organic solvents are considered waste by mass.[81] Water as a solvent offers a better alternative for organic reactions, relative to other solvents because it follows the principles of green chemistry.[82] On the other hand, the poor water solubility of most organic molecules limits the number of reactions in this solvent.

Epoxides and aziridines are three-membered strained molecules and possess high value in organic synthesis due to their high reactivity and the potential further functionalization. These ring-opening reactions have been conventionally carried out under general conditions using acid or base catalysts,[83] transition metal complexes,[84] or organocatalysts.[85] However, these conventional protocols are subjected to harsh reaction conditions and generate low yields along with poor regioselectivity. To address these problems, photochemical methods over the recent past have developed as more environmentally options.[86] Typically, these transformations are performed in solvents such as *N*-methyl-2-pyrrolidone (NMP), which are organic in nature and pose both environmental and safety concerns.[87] Using water as a medium of the reaction can help to be a solution but the solubility of the organic compounds in water is a major challenge. This can be circumvented by utilizing surfactants.

Surfactants consist of a hydrophilic head, which is commonly charged and situated at the micelle−water interface, and a hydrophobic tail, within the micelle core, thus creating a microenvironment efficient for organic reactions in water (**Figure 5**). Above the critical micelle concentration (CMC), surfactants spontaneously self-assemble into micelles, which act as nanoreactors and significantly enhance the aqueous solubility of organic compounds.[88] Micelles

[81] Gallou, F.; Isley, N. A.; Ganic, A.; Onken, U.; Parmentier, M. *Green Chem.* **2016**, *18*, 14-19.
[82] Anastas, P.T.; Warner, J. C. *Green Chemistry: Theory and Practice*, **1998**, Oxford University Press.
[83] (a) Bonollo, S.; Lanari, D.; Vaccaro, L. *Eur. J. Org. Chem.* **2011**, *2011*, 2587–2598. (b) Thirumalaikumar, M. *Org. Prep. Proced. Int.* **2022**, *54*, 1–39. (c) Lu, P. *Tetrahedron* **2010**, *66*, 2549–2560.
[84] (a) Wang, C.; Luo, L.; Yamamoto, H. *Acc. Chem. Res.* **2016**, *49*, 193–204. (b) Bera, P. S.; Mirza, Y. K.; Sachdeva, T.; Bera, M. *Compounds* **2024**, *4*, 626–649.
[85] Meninno, S.; Lattanzi, A. *ACS Org. Inorg. Au* **2022**, *2*, 289–305.
[86] (a) Furniel, L. G.; Corrêa, A. G. *ChemPhotoChem* **2024**, *8*, e202400120. (b) Steiman, T. J.; Liu, J.; Mengiste, A.; Doyle, A. G. *J. Am. Chem. Soc.* **2020**, *142*, 7598–7605. (c) Parasram, M.; Shields, B. J.; Ahmad, O.; Knauber, T.; Doyle, A. G. *ACS Catal.* **2020**, *10*, 5821–5827. (d) Lau, S. H.; Borden, M. A.; Steiman, T. J.; Wang, L. S.; Parasram, M.; Doyle, A. G. *J. Am. Chem. Soc.* **2021**, *143*, 15873–15881. (e) Dongbang, S.; Doyle, A. G. *J. Am. Chem. Soc.* **2022**, *144*, 20067–20077. (f) Potrząsaj, A.; Musiejuk, M.; Chaładaj, W.; Giedyk, M.; Gryko, D. *J. Am. Chem. Soc.* **2021**, *143*, 9368–9376. (g) Funk, B. E.; Pauze, M.; Lu, Y.-C.; Moser, A. J.; Wolf, G.; West, J. G. *Cell Rep. Phys. Sci.* **2023**, *4*, 101372.
[87] German, L.; Cuevas, J. M.; Cobos, R.; Perez-Alvarez, L.; Vilas-Vilela, J. L. *RSC Adv.*, **2021**, *11*, 19070-19075.
[88] (a) Lorenzetto, T.; Berton, G.; Fabris, F.; Scarso, A. *Catal. Sci. Technol.* **2020**, *10*, 4492-4502. (b) Borrego, E.; Caballero, A.; Perez, P. J. *Organometallics* **2022**, *41*, 3084-3098. (c) Lipshutz, B. H. *Green Chem.* **2024**, *26*, 739-752.

not only increase water solubility but may also improve regioselectivity and extend the lifetimes of highly reactive intermediates, such as radicals.[89]

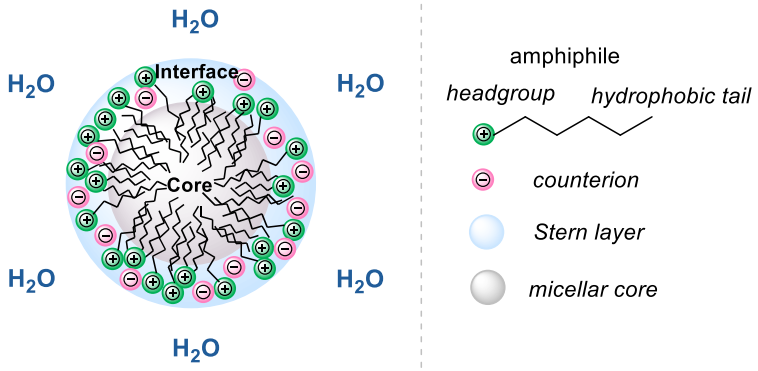

Figure 5. General representation of a micellar system.

Along this line, vitamin B_{12}, a water-soluble molecule, that has proved as an effective cobalt-based catalyst for C-C bond formation over recent decades, is perfectly suited for applications in aqueous system. Hydrophobic derivatives of vitamin B_{12} (HME) have been shown to catalyze various radical transformations in organic solvents, generating alkyl and acyl radicals from substrates such as organic halides, diazo compounds, and strained molecules.[90] To enhance sustainability, there is growing interest in adapting these transformations to aqueous systems using native vitamin B_{12} under micellar conditions. Motivated by this, our research group aimed to develop more sustainable protocols by exploring the photochemical ring-opening of three-membered rings, specifically epoxides and aziridines, via vitamin B_{12} catalysis in micellar solutions.

In this study, we successfully demonstrated the regioselective ring-opening of aryl and alkyl epoxides, as well as alkyl aziridines, with Michael acceptors **92**, catalyzed by vitamin B_{12} under micellar conditions. Model reactions involving alkyl epoxides and alkyl aziridines with acrylonitrile yielded the desired products in high yields (**Scheme 24**).

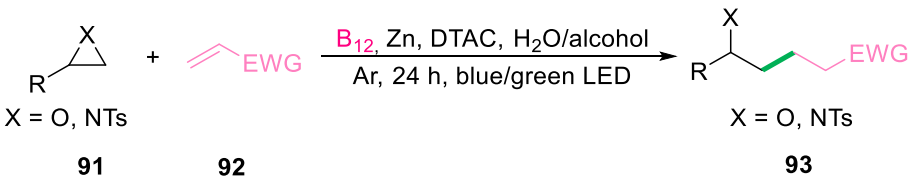

Scheme 24. Model reaction for the ring-opening of epoxides and aziridines in a micellar medium.

[89] (a) Sorella, G. L.; Strukul, G.; Scarso, A. *Green Chem.* **2015**, *17*, 644-683. (b) Lipschutz, B. H.; Ghorai, S.; Cortes-Clerget, M. *Chem. Eur. J.* **2018**, *24*, 6672-6695. (c) Cybularczyk-Cecotka, M.; Predygier, J.; Crespi, S.; Szczepanik, J.; Giedyk, M. *ACS Catal.* **2022**, *12*, 3543-3549. (d) Bruss, L.; Jeyaseelan, R.; Kurschner, J. C. G.; Utikal, M.; Næsborg, L. *ChemCatChem* **2023**, 15, e202201146.

[90] (a) Ociepa, M.; Wierzba, A. J.; Turkowska, J.; Gryko, D. *J. Am. Chem. Soc.* **2020**, *142*, 5355-5361. (b) Komeyama, K.; Michiyuki, T.; Teshima, Y.; Osaka, I. *RSC Adv.* **2021**, *11*, 3539-3546. (c) Wdowik, T.; Gryko, D. *ACS Catal.* **2022**, *12*, 6517-6531. (d) Giedyk, M.; Gryko, D. *Chem. Catal.* **2022**, *2*, 1534-1548. (e) Zhang, Z.; Chen, M.; Zheng, G. *RSC Adv.* **2024**, *14*, 29168-29173.

The optimization, scope and limitations of the epoxide reaction was conducted by A. Krzeszewska and K. Mazurek, who identified the optimal conditions to obtain the desired alcohol product in 85% yield. Notably, the use of dodecyltrimethylammonium chloride (DTAC) eliminated the need for NH_4Cl.

My work focused on optimizing reactions involving aziridine derivatives and expanding the scope with respect to both aziridines and epoxides, as well as various Michael acceptors (**Scheme 25**). I found that reducing the amount of DTAC and the catalytic amount of native vitamin B_{12}, along with the addition of isopropanol (*i*-PrOH) as a co-solvent, significantly improved the reaction yields. I further expanded the scope of the epoxide reaction; an aryl-substituted epoxide bearing a *para*-fluorine substituent gave the corresponding product **96** in good yield. Scaling up the model substrate phenoxymethyloxirane to a 1 mmol scale afforded the product **94** in 80% yield.

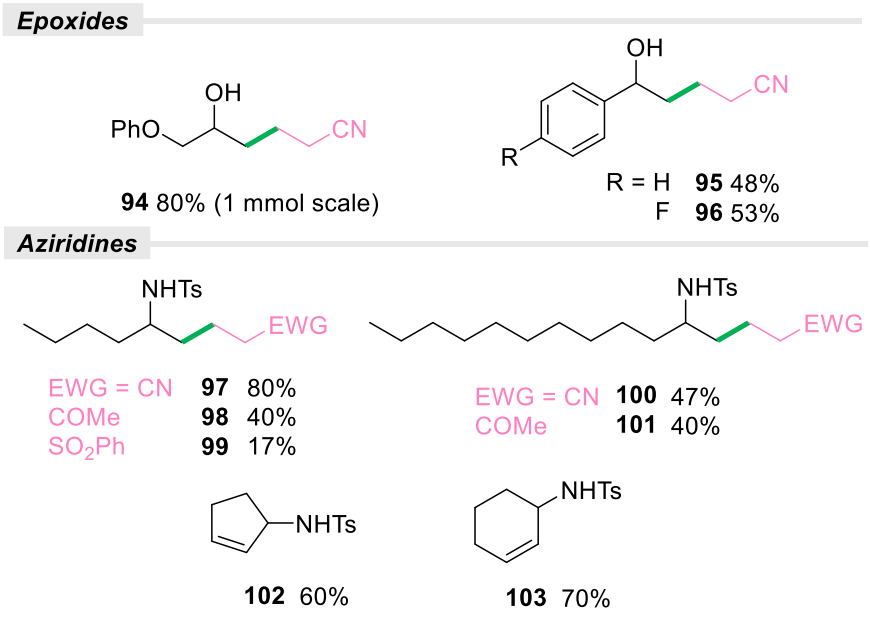

Scheme 25. Selected scope and limitations of ring-opening of epoxides and aziridines.

In the case of aziridine derivatives, increasing the alkyl chain length was generally tolerated **100-101**. However, several aryl aziridines with *N*-protecting groups such as *N*-methyl or *N*-dodecyl were unreactive, showing no conversion of the starting materials or formation of ring-opened products. Our hypothesis is based on previous studies showing that the reduced Co(I) species is localized in the Stern layer;[91] thus, the nitrogen atom must orient toward the micelle-water interface. Hydrophobic protecting groups may hinder this orientation, leading to poor reactivity. Moreover, several acrylates were tested but remained unreactive, likely due to their different polarity compared to typical organic media, causing them to reside deeper in the micelle and reducing their accessibility.

[91] Wincenciuk, A.; Cmoch, P.; Giedyk, M.; Andersson, M. P.; Gryko, D. *J. Am. Chem. Soc.* **2024**, *146*, 19828-19838.

Finally, I would like to highlight some interesting observations: azabicyclic derivatives yielded allylamines **102-103** in high yields, supporting an S_N2-like mechanism followed by elimination, as previously proposed by Scheffold and Zhang.[92]

I also investigated the possible generation of reaction intermediates to support our proposed mechanism (**Scheme 26**). A radical trapping experiment using the model epoxide substrate 2-(phenoxymethyl)oxirane confirmed the formation of the carbon-centered radical **D** via HR-MS detection of its TEMPO adduct, thereby validating the radical nature of the reaction. Additionally, both model substrates were tested to observe the formation of alkylcobalamin intermediates **B**. In both cases, HR-MS analysis confirmed the presence of the expected masses. Upon Zn-mediated reduction and blue/green-light irradiation, vitamin B_{12} is converted into a Co(I) species, which regioselectively opens the epoxide or aziridine ring at the less hindered site, forming a Co(III)-alkyl intermediate **B**. Light-induced homolysis then generates alkyl radical **C**, which is trapped by acrylonitrile to produce radical **D**. Protonation of this species leads to the formation of Markovnikov-type alcohol and amine derivatives.

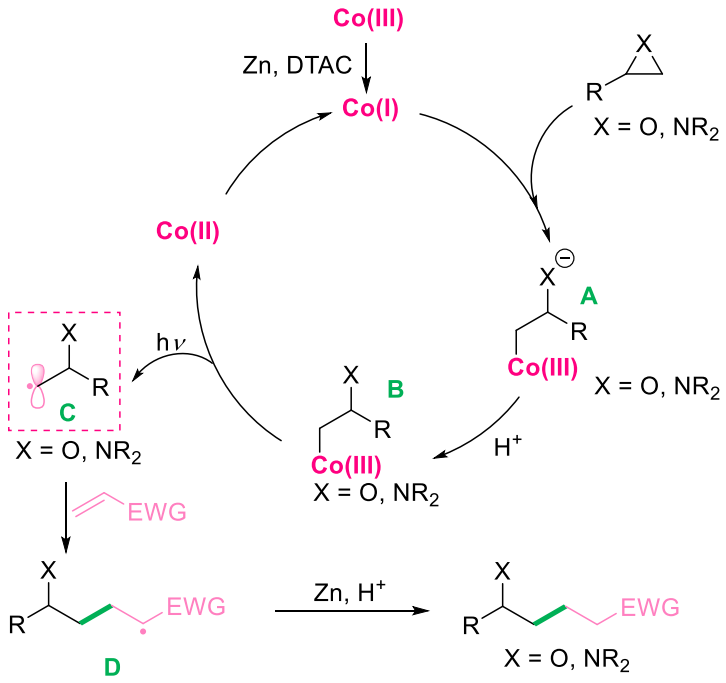

Scheme 26. Proposed reaction mechanism.

In conclusion, we developed a photochemical vitamin B_{12}-catalyzed ring-opening protocol for epoxide and aziridine compounds under micellar conditions. The reactions proceeded with moderate to good yields and exhibited complete regioselectivity, yielding aryl- and alkyl alcohol products. The method also showed compatibility with alkyl aziridines, although the resulting amine products were obtained in typically lower yields.

[92] Zhang, Z. D.; Scheffold, R. *Helv. Chim. Acta* **1993**, *76*, 2602−2615.

The results of this study were published in a scientific journal:[93]

[P3] Vitamin B_{12} and Micellar Solution Enable Regioselective Ring Opening of Epoxides and Aziridines with Electrophilic Olefins, **Szabó, K. F.**; Wdowik, T.; Krzeszewska, A.; Mazurek, K.; Andersson, M. P.; Gryko, D. *Org. Lett.*, **2025**, doi.org/10.1021/acs.orglett.5c01376.

[93] Szabó, K. F.; Wdowik, T.; Krzeszewska, A.; Mazurek, K.; Andersson, M. P.; Gryko, D. *Org. Lett.* **2025**, https://doi.org/10.1021/acs.orglett.5c01376.

4. Conclusions

The main goal of my PhD dissertation was to investigate novel reactivity of photochemically generated nitrogen-centered radicals and aziridines for the formation of C-N and C-C bonds, leading to amines and their derivatives. To this end, I accomplished the following:

1. **γ-Amidation of α,β-Unsaturated Carbonyls:** I expanded the scope of a highly site−selective γ-amidation using *N*-aminopyridinium salts. *N*, *N*-disubstituted pyridinium salts bearing a Ts protecting group gave the highest yields with exclusive *E*-diastereoselectivity. Various aryl ketone substrates afforded excellent yields and selectivity, and even extended remote functionalization's were successful. I also synthesized more complex, biologically relevant analogues in good to high yields, and demonstrated scalability of the model reaction to 1 mmol.

2. **Photochemical C3-Amination of Pyridines:** I reported the first photochemical C3−amination of pyridine derivatives using *N*-aminopyridinium salts and 2-phenyl Zincke imine to further expand the use of pyridiniums. Switching to violet LEDs was essential to achieve a 99% yield with a 5:1 regioisomeric ratio. DFT calculations revealed that the transition state energy at the δ-position on the Zincke imine was the lowest. However, competitive reactivity at the β-position was observed, as confirmed by our experimental findings showing that C2-alkyl-substituted pyridines shifted the regioselectivity. The robustness of the reaction was confirmed by a broad substrate scope and further derivatizations. A one-pot protocol also yielded the desired product, in only slightly diminished yield.

3. **Aziridine and Epoxide Ring-Opening with Native Vitamin B_{12}:** I discovered that native vitamin B_{12} catalyzes the ring-opening of alkyl aziridines in micellar media under visible light, minimizing the need for harmful organic solvents. Under Zn reduction in the presence of DTAC, vitamin B_{12} is converted to "supernucleophilic" Co(I), which attacks aziridines at the less hindered carbon to afford Markovnikov amine products in moderate to good yields. While the substrate scope was narrower than in organic media, the reactions proceeded with complete regioselectivity. I also demonstrated that the model epoxide could be scaled to 1 mmol with consistent yields.

In conclusion, these newly developed photochemical protocols significantly advance C-N bond-forming chemistry under mild, sustainable conditions. My work has mainly focused on *N*−aminopyridinium salt chemistry under visible light, contributing valuable improvements to this field.

5. Original Publications

OL Organic Letters

pubs.acs.org/OrgLett

Letter

Site-Selective, Photocatalytic Vinylogous Amidation of Enones

Kitti Franciska Szabó, Katarzyna Goliszewska, Jakub Szurmak, Katarzyna Rybicka-Jasińska,* and Dorota Gryko*

Cite This: *Org. Lett.* 2022, 24, 8120–8124

Read Online

ACCESS | Metrics & More | Article Recommendations | Supporting Information

ABSTRACT: Despite the broad interest in organic compounds possessing a γ-aminocarbonyl motif, limited strategies for their synthesis have been reported. Herein, we describe a mild and efficient method for the site-selective amidation of unsaturated enones with electrophilic N-centered radicals as a key intermediate. The photocatalytic vinylogous reaction of dienolates with *N*-amino pyridinium salts affords γ-amido carbonyl compounds. This process is high-yielding, scalable, and tolerates a broad range of unsaturated α,β-unsaturated carbonyls, including biologically relevant compounds, as starting materials.

The concept of vinylogy, established by Fuson in 1935,[1] postulates that the influence of a functional group can be propagated through a conjugated system of unsaturated bonds. This phenomenon is particularly important for the functionalization of α,β-unsaturated carbonyl compounds, which are versatile starting materials in organic synthesis.[2−15] Typically, in vinylogous reactions, π-extended carbonyl derivatives of type **I** are transformed into dienolates **II** that contain two nucleophilic sites (Scheme 1). Consequently, the addition of electrophiles can occur at either α-position (**III**) or more remote γ-position (**IV**).[1,7] The regio- and stereoselectivity of these transformations are affected by multiple factors, such as the presence of bulky substituents, a catalyst (if any), or the electron density at the nucleophilic carbon sites, and remain one of the most challenging issues that have to be addressed.[1−3,7−13]

Scheme 1. Concept of Vinylogy and Bioactive Molecules Containing a γ-Amino Group[16−18]

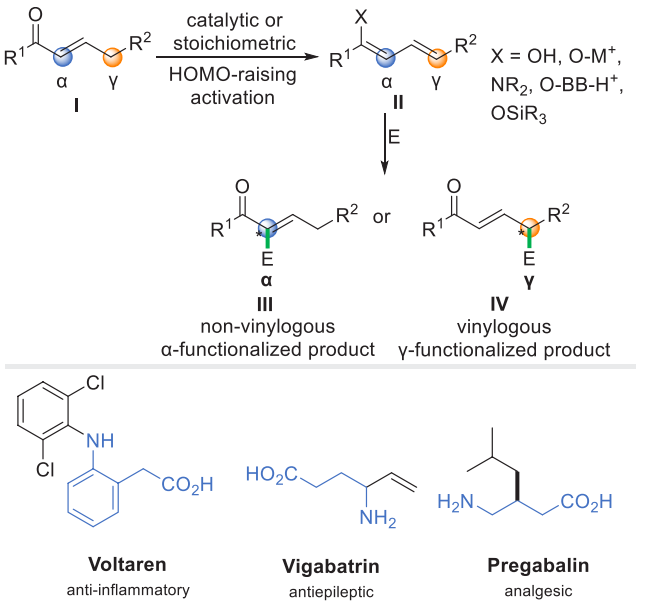

In recent years, in addition to the established use of preformed silyl enol ethers, novel activation strategies have been developed for vinylogous transformations.[19−25] These include iminium/enamine organocatalysis,[19,20,22,26−28] NHC organocatalysis,[23,24,26] cooperative organo/metal catalysis,[10,25] and photocatalysis.[29,30] Because the application of vinylogy creates an additional reaction site in enolizable π-extended carbonyl systems, it has been widely utilized in the synthesis of distantly substituted carbonyl derivatives.[8,15,31−33] Among them, γ-amination occupies a particular position as γ-aminocarbonyl motifs are quite ubiquitous in natural compounds, γ-aminobutyric acid (GABA), and bioactive molecules (Scheme 1).[16,34,35] Currently, the known methods for vinylogous amination mainly utilize tetraazodicarboxylates as a nitrogen source and are often limited in scope. Jørgensen et al. first introduced an organocatalytic approach for the enantioselective γ-amination of dienamines via [4+2] cycloaddition to azodicarboxylates.[19] Alternatively, dienolates were found to react site-selectively with the same electrophile in the presence of a base.[16]

Significant advances have been made in the field of photoredox catalysis, and a great deal of effort has been spent on expanding the utility of radicals in organic synthesis.[36−41] In

Received: September 16, 2022
Published: November 3, 2022

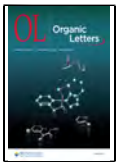

vinylogous transformations, substrates that bear a leaving group at the functionalized position have been mainly utilized.[29,30] However, despite the broad application of nitrogen-centered radicals in synthetic chemistry,[42−46] their reactivity in vinylogous reactions has rarely been explored.[44,46−49] We have recently reported that electrophilic nitrogen-centered radicals generated from *N*-aminopyridinium salts are trapped by enol equivalents to give α-amido carbonyl compounds in excellent yields.[50] On the basis of the vinylogy principle, we hypothesized that photocatalytic amidation at the γ-position of the enone system with electrophilic amidyl radicals should also be feasible.

Herein, we present the first example of a photocatalytic, vinylogous amidation of extended enolate derivatives. Under visible-light irradiation, silyl dienol ethers react with pyridinium salts in a highly selective manner via a radical mechanism. Our novel procedure opens doors for the site-selective synthesis of various γ-amido-α,β-unsaturated carbonyl compounds.

We initiated our studies by exploring the reactivity of α,β-unsaturated carbonyl compounds under previously developed conditions for the α-amidation.[50] The model reaction of silyl dienol ether **1a** with *N*-aminopyridinium salt **2a** in the presence of the *fac*-Ir(ppy)$_3$ catalyst, under blue-light irradiation, site-selectively gave the desired γ-amidated product **3a** in 65% yield as the only product (Table 1, entry 1). Background experiments

Table 1. Optimization of the Reaction Conditions[a]

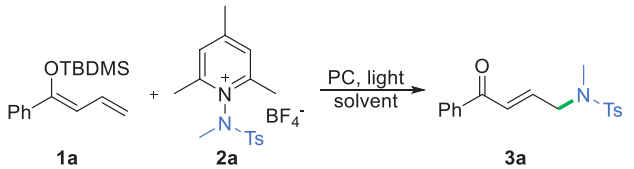

entry	catalyst	catalyst loading (mol %)	light	yield (%)[b]
1[c]	*fac*-Ir(ppy)$_3$	1.0	blue	65
2	none	none	blue	trace
3	*fac*-Ir(ppy)$_3$	1.0	none	trace
4	none	none	none	0
5	*fac*-Ir(ppy)$_3$	1.0	blue	84
6[d]	*fac*-Ir(ppy)$_3$	1.0	blue	90

[a]Reaction conditions: enol **1a** (0.25 mmol), salt **2a** (1.2 equiv), dry MeCN (c = 0.05 M), ambient temperature (20−22 °C), 1 h, under an Ar atmosphere, LED light source (446 nm, 6 W). TBDMS = *tert*-butyldimethylsilyl. [b]Isolated yield. [c]Reaction mixture irradiated for 16 h. [d]Salt **2a** (1.3 equiv).

confirmed that the desired transformation cannot take place without the Ir photocatalyst and a light source (entries 2−4). Subsequently, several reaction parameters [catalyst loading, substrate ratio, duration, and the power of the light (for details, see the Supporting Information)] were optimized. The yield substantially increased when the salt was used in a slight excess (1.3 equiv, entry 6); moreover, the reaction time was decreased to 1 h.

Gratifyingly, decreasing the catalyst loading to 0.75 mol % did not decrease the yield. Overall, irradiation of a solution of **1a** with **2a** (1:1.3 molar ratio) and *fac*-Ir(ppy)$_3$ (0.75 mol %) with blue LEDs at room temperature for 1 h gives the *E*-isomer as sole product **3a** in 90% yield.

With the optimized conditions in hand, we examined a set of *N*-aminopyridinium salts and various α,β-unsaturated compounds. Silyl dienol ether **1a** tolerates both *N*-mono- and *N,N*-disubstituted *N*-aminopyridinium salts **2**, giving the desired products in good to high yields [**3a**−**3f** (Table 2)]. Among N,N-disubstituted derivatives **2a**−**2d**, similarly to α-amidation

Table 2. Scope of *N*-Aminopyridinium Salts[a]

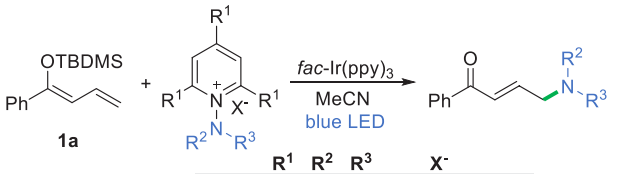

	R^1	R^2	R^3	X^-	
2a	Me	Me	Ts	BF_4	**3a**
2b	Me	Me	Boc	BF_4	**3b**
2c	Me	Me	Cbz	BF_4	**3c**
2d	Ph	Me	Boc	BF_4	**3d**
2e	H	H	COC_6F_5	OTf	**3e**
2f	Me	H	Ts	BF_4	**3f**

entry	salt	*E*:*Z*	product	yield (%)
1	**2a**	*E*	**3a**	90
2	**2b**	6:5	**3b**	76
3	**2c**	*E*	**3c**	46
4	**2d**	6:5	**3d**	74
5	**2e**	*E*	**3e**	48
6	**2f**	*E*	**3f**	74

[a]Reaction conditions: enol **1a** (0.25 mmol), salt **2a**−**2f** (1.3 equiv), dry MeCN (c = 0.05 M), ambient temperature (20−22 °C), 1 h, under an Ar atmosphere, LED light source (446 nm, 6 W). Times: 1 h for **2a**, **2b**, **2d**, and **2f**; 2 h for **2c**; and 16 h for **2e**.

reactions,[50] the most efficient salt **2a** with *N*-Me, *N*-Ts functionality gives the desired product in 90% yield in a site-selective manner, and only the *E*-alkene forms (entry 1). The stereoselectivity of the reaction is, however, affected by the substituents at the amidyl radical. For salts **2b** and **2d** (entries 1 and 4, respectively) with a bulky Boc protecting group, high yields are observed, but a mixture of diastereoisomeric *E*/*Z* dienes (~6:5 *E*:*Z*) was isolated (entries 2 and 4). With Cbz salt **2c**, the reaction is again fully site- and stereoselective (entries 3 and 5).

Various vinylogous substrates are well tolerated (Scheme 2). Aryl-substituted enones with various functional groups with both electron-withdrawing (CN, NO_2, COMe, and halides) and electron-donating (*tert*-butyl and OMe) groups at the *para* and *meta* positions give products **4**−**11** in good to excellent yields (60−90%). Principally, the use of silyl enol ether derivatives preferentially generates the γ-product over the α-product due to higher orbital coefficients and higher electrophilic susceptibility.[51] Furthermore, diphenylbuta-1,3-diene acetate and benzoate exclusively furnish γ-amidated products **12a** and **12b**, respectively, in a similar high yield. Interestingly, in the 1,4-diaryl α,β-unsaturated carbonyl compound series, the α,γ-siteselectivity of the amidation is strongly influenced by the electronic character of the phenyl ring present at the terminal double bond, while the nature of the chalcone phenyl substituent does not have an impact on the process. In particular, having the electron-donating methoxy group at the *para* (**13a**), *meta* (**13b**), or *ortho* (**13c**) position on both phenyl substituents does not alter the reaction outcome, and the desired γ-amidated products form site-selectively. Similarly, substrates with both electron-donating and electron-withdrawing substituents on the aryl rings give only the γ-product provided the methoxy group is in the R^2 position (**13d**). On the contrary, compounds bearing a phenyl substituent with electron-with-

https://doi.org/10.1021/acs.orglett.2c03161
Org. Lett. 2022, 24, 8120−8124

Scheme 2. Scope of the amidation of α,β-Unsaturated Carbonyl Compounds[a]

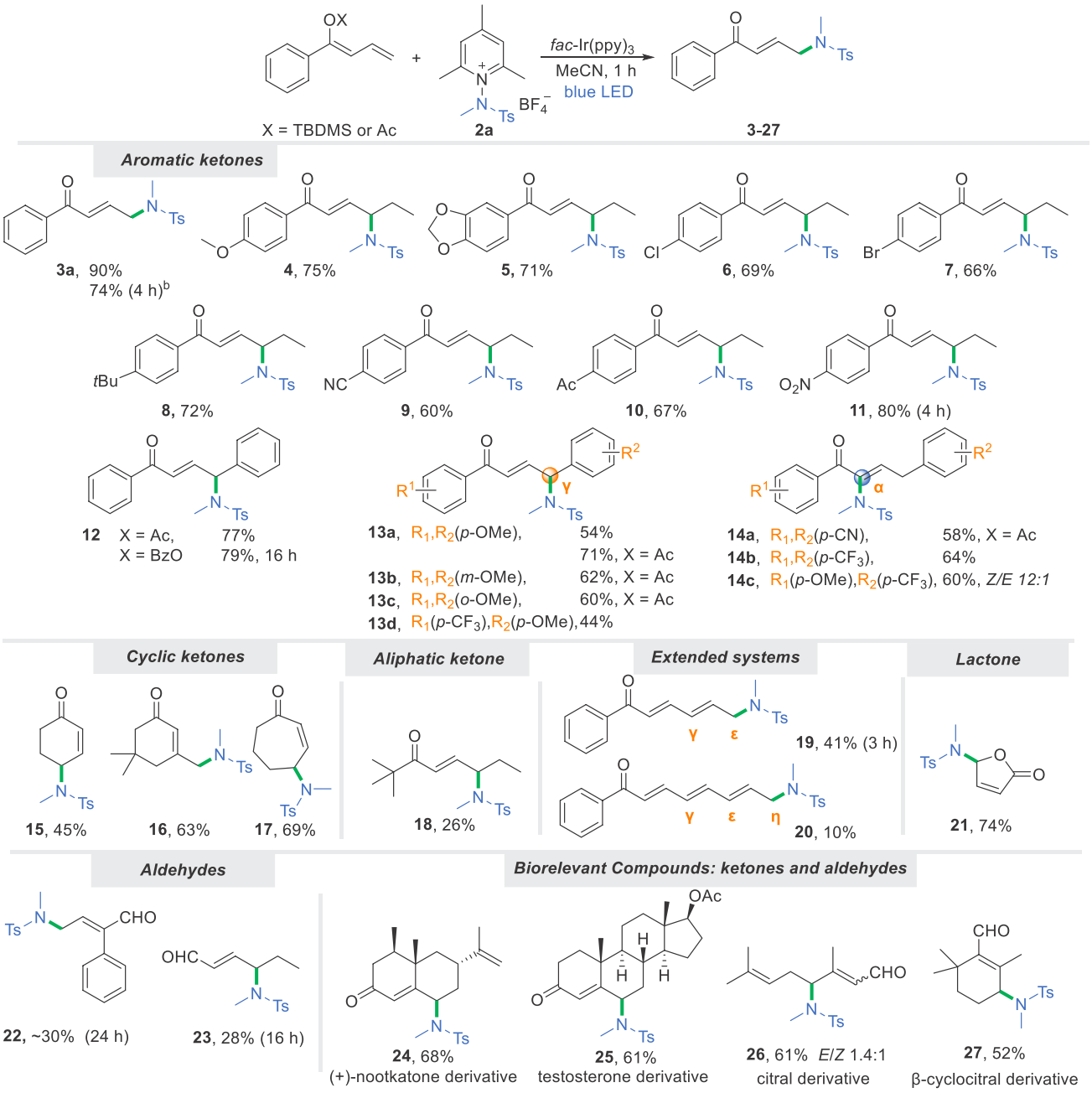

[a]Reaction conditions: enol **1a** (0.25 mmol), salt **2a** (1.3 equiv), dry MeCN (c = 0.05 M), ambient temperature (20−22 °C), 1 h, under an Ar atmosphere, LED light source (446 nm, 6 W). Unless otherwise noted, X = TBDMS. [b]Reaction performed on a 1 mmol scale.

drawing substituents (-CN or -CF_3) at the *para* position undergo selective α-amidation using either acetyl- or TBDMS-protected dienol ether derivatives, giving product **14a** or **14b**, respectively, as single *Z*-diastereoisomers in moderate yields. However, when the nucleophilicity of the carbonyl group decreases, the diastereoselectivity of the α-amidation decreases. Product **14c** forms as a mixture of *Z*/*E* diastereoisomers (12:1).

Furthermore, enols derived from cyclic ketones afford products **15**−**17** in good yields. Although, in general, the steric hindrance should affect product generation, here this is not the case. For a sterically hindered cyclohexenone derivative, the yield increases in comparison to that of the parent cyclohexenone presumably due to the electron-donating effect imposed by the methyl groups present at the reactive sites (**16**). Increasing the ring size effectively increases the yield. The γ-amidation of aliphatic enones is less effective (**18**, 26%).

Our methodology can be employed for functionalizations of enones with elongated systems of double bonds. Both substrates are compatible with the reaction conditions, although yields for ε and η functionalizations (**19** and **20**, respectively) are lower, due to the lower electron density at these positions. Furthermore, lactones and aldehydes are also suitable starting materials; the latter ones prove, however, to be challenging, with products **22** and **23** forming in lower yields. On the contrary, ester derivatives proved challenging, due to the hydrolysis of the starting dienolate (for details, see the Supporting Information).

https://doi.org/10.1021/acs.orglett.2c03161
Org. Lett. 2022, 24, 8120−8124

The utility and effectiveness of the developed method in late-stage functionalization are demonstrated on biologically active compounds such as (+)-nootkatone (**24**), testosterone (**25**), citral (**26**), and β-citral (**27**). In contrast to simple aldehyde dienolates, citral and β-cyclocitral provide products in satisfactory yields, highlighting the robustness of the methodology. We emphasize that in all these cases only the γ-amidated product is obtained, although a mixture of E/Z dienolate silyl ethers was used as the starting material.

With regard to the mechanism, the addition of TEMPO stops the reaction, thus confirming the radical nature of the reaction. Employing DMPO as a spin trap for N-centered radicals leads to the trapping product as HR-MS confirms (see Figure S3). These results clearly indicate that the developed reaction is radical in nature. Data from the literature,[50,52] along with the results of control experiments, allow us to propose a plausible light-induced radical reaction pathway for the γ-amidation that is similar to that reported for α-amidation (Scheme 3). The

Scheme 3. Mechanistic Proposal for the γ-Reactivity of Vinylogous Ketone with *N*-Aminopyridinium Salt

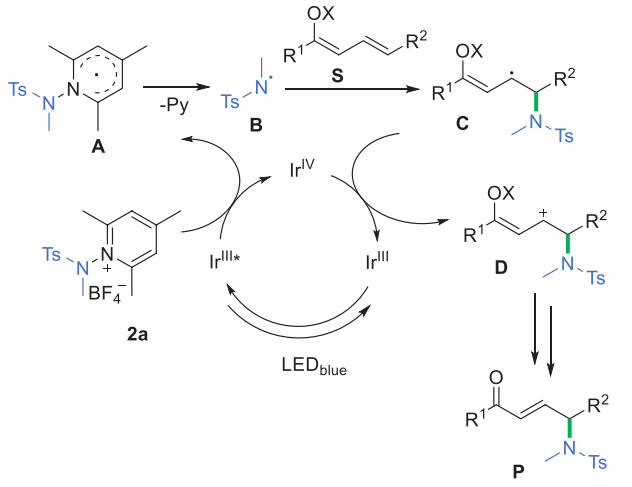

reduction of *N*-aminopyridinium salt **2a** ($E_{1/2}$ = −0.70 V vs Ag/AgCl) by Ir(III) in the excited state generates radical **A** via single-electron transfer (SET). Thus, the formed species, **A**, undergoes fragmentation to afford N-centered radical **B** and pyridine as a byproduct. The addition of N-centered radical **B** to dienolate **1a** generates allylic radical **C**, which is oxidized by the Ir(IV) catalyst to allylic cation **D** with the regeneration of the ground state of the Ir(III) catalyst. Removal of the acyl or silyl group affords γ-product **3a**.

In conclusion, on the basis of the vinylogy principle, we have developed a method for the site-selective amidation of α,β-unsaturated enones with *N*-protected aminopyridinium salts giving access to γ-amidocarbonyl compounds. The reaction of N-centered radical, generated via Ir photocatalysis, with a dienolate intermediate is the key step in this transformation. The advantages of this approach include mild reaction conditions, high site- and stereoselectivity and substrate tolerance, a simple setup, and scalability. In addition, it is suitable for functionalizations of biologically active derivatives.

We believe that the vinylogy strategy may find applications in the design of other radical transformations of α,β-unsaturated compounds.

■ ASSOCIATED CONTENT

Supporting Information

The Supporting Information is available free of charge at https://pubs.acs.org/doi/10.1021/acs.orglett.2c03161.

Optimization details, experimental procedures, and characterization data for all new compounds (PDF)

■ AUTHOR INFORMATION

Corresponding Authors

Katarzyna Rybicka-Jasińska − *Institute of Organic Chemistry, Polish Academy of Sciences, 01-224 Warsaw, Poland;* orcid.org/0000-0002-9018-7846; Email: krybicka-jasinska@icho.edu.pl

Dorota Gryko − *Institute of Organic Chemistry, Polish Academy of Sciences, 01-224 Warsaw, Poland;* orcid.org/0000-0002-5197-4222; Email: dorota.gryko@icho.edu.pl

Authors

Kitti Franciska Szabó − *Institute of Organic Chemistry, Polish Academy of Sciences, 01-224 Warsaw, Poland*

Katarzyna Goliszewska − *Institute of Organic Chemistry, Polish Academy of Sciences, 01-224 Warsaw, Poland*

Jakub Szurmak − *Institute of Organic Chemistry, Polish Academy of Sciences, 01-224 Warsaw, Poland*

Complete contact information is available at: https://pubs.acs.org/10.1021/acs.orglett.2c03161

Notes

The authors declare no competing financial interest.

■ ACKNOWLEDGMENTS

Financial support for this work was provided by the National Science Center (PL): MAESTRO UMO-2020/38/A/ST4/00185 to K.F.S. and D.G. and ETIUDA 7 UMO-2019/32/T/ST4/00303 to K.G.

■ REFERENCES

(1) Fuson, C. R. The Principle of Vinylogy. *Chem. Rev.* **1935**, *16*, 1−27.

(2) Casiraghi, G.; Battistini, L.; Curti, C.; Rassu, G.; Zanardi, F. The Vinylogous Aldol and Related Addition Reactions: Ten Years of Progress. *Chem. Rev.* **2011**, *111*, 3076−3154.

(3) Mao, B.; Fañanás-Mastral, M.; Feringa, B. L. Catalytic Asymmetric Synthesis of Butenolides and Butyrolactones. *Chem. Rev.* **2017**, *117*, 10502−10566.

(4) Casiraghi, G.; Zanardi, F.; Battistini, L.; Rassu, G. Advances in Exploring Heterocyclic Dienoxysilane Nucleophiles in Asymmetric Synthesis. *Synlett* **2009**, *2009*, 1525−1542.

(5) Hoppmann, L.; García Mancheño, O. Silyldienolates in Organocatalytic Enantioselective Vinylogous Mukaiyama-Type Reactions: A Review. *Molecules* **2021**, *26*, 6902−6923.

(6) Denmark, S. E.; Xie, M. Lewis Acid-Promoted Conjugate Addition of Dienol Silyl Ethers to Nitroalkenes: Synthesis of 3-Substituted Azepanes. *J. Org. Chem.* **2007**, *72*, 7050−7053.

(7) Curti, C.; Battistini, L.; Sartori, A.; Zanardi, F. New Developments of the Principle of Vinylogy as Applied to π-Extended Enolate-Type Donor Systems. *Chem. Rev.* **2020**, *120*, 2448−2612.

(8) Li, H.; Yin, L. Recent Progress on Direct Catalytic Asymmetric Vinylogous Reactions. *Tetrahedron Lett.* **2018**, *59*, 4121−4135.

(9) Denmark, S. E.; Heemstra, J. R.; Beutner, G. L. Catalytic, Enantioselective, Vinylogous Aldol Reactions. *Angew. Chem., Int. Ed.* **2005**, *44*, 4682−4698.

(10) Romano, C.; Fiorito, D.; Mazet, C. Remote Functionalization of α,β-Unsaturated Carbonyls by Multimetallic Sequential Catalysis. *J. Am. Chem. Soc.* **2019**, *141*, 16983−16990.
(11) Cordes, M.; Kalesse, M. Very Recent Advances in Vinylogous Mukaiyama Aldol Reactions and Their Applications to Synthesis. *Molecules* **2019**, *24*, 3040−3059.
(12) Hosokawa, S. Recent Development of Vinylogous Mukaiyama Aldol Reactions. *Tetrahedron Lett.* **2018**, *59*, 77−88.
(13) Schneider, C.; Abels, F. Catalytic, Enantioselective Vinylogous Michael Reactions. *Org. Biomol. Chem.* **2014**, *12*, 3531−3543.
(14) Casiraghi, G.; Zanardi, F.; Appendino, G.; Rassu, G. The Vinylogous Aldol Reaction: A Valuable, Yet Understated Carbon−Carbon Bond-Forming Maneuver. *Chem. Rev.* **2000**, *100*, 1929−1972.
(15) Oiarbide, M.; Palomo, C. Extended Enolates: Versatile Intermediates for Asymmetric C-H Functionalization via Noncovalent Catalysis. *Eur. J. Chem.* **2021**, *27*, 10226−10246.
(16) Chen, X.; Liu, X.; Mohr, J. T. Direct Regioselective γ-Amination of Enones. *Org. Lett.* **2016**, *18*, 716−719.
(17) Galisteo, A.; Jannus, F.; García-García, A.; Aheget, H.; Rojas, S.; Lupiañez, J. A.; Rodríguez-Diéguez, A.; Reyes-Zurita, F. J.; Quílez del Moral, J. F. Quílez Del Moral, Diclofenac N-Derivatives as Therapeutic Agents with Anti-Inflammatory and Anti-Cancer Effect. *Int. J. Mol. Sci.* **2021**, *22*, 5067−5090.
(18) Fukasawa, H.; Muratake, H.; Ito, A.; Suzuki, H.; Amano, Y.; Nagae, M.; Sugiyama, K.; Shudo, K. Silicon-Containing GABA Derivatives, Silagaba Compounds, as Orally Effective Agents for Treating Neuropathic Pain without Central-Nervous-System-Related Side Effects. *ACS Chem. Neurosci* **2014**, *5*, 525−532.
(19) Bertelsen, S.; Marigo, M.; Brandes, S.; Dinér, P.; Jørgensen, K. A. Dienamine Catalysis: Organocatalytic Asymmetric γ-Amination of α,β-Unsaturated Aldehydes. *J. Am. Chem. Soc.* **2006**, *128*, 12973−12980.
(20) Bencivenni, G.; Galzerano, P.; Mazzanti, A.; Bartoli, G.; Melchiorre, P. Direct Asymmetric Vinylogous Michael Addition of Cyclic Enones to Nitroalkenes via Dienamine Catalysis. *Proc. Natl. Acad. Sci. U. S. A.* **2010**, *107*, 20642−20647.
(21) Wang, J.; Chen, J.; Kee, C. W.; Tan, C. H. Enantiodivergent and γ-Selective Asymmetric Allylic Amination. *Angew. Chem., Int. Ed.* **2012**, *51*, 2382−2386.
(22) Yin, Y.; Jiang, Z. Organocatalytic Asymmetric Vinylogous Michael Reactions. *ChemCatChem.* **2017**, *9*, 4306−4318.
(23) Vora, H. U.; Wheeler, P.; Rovis, T. Exploiting Acyl and Enol Azolium Intermediates *via* N-Hetero-cyclic Carbene-Catalyzed Reactions of α-Reducible Aldehydes. *Adv. Synth. Catal.* **2012**, *354*, 1617−1639.
(24) Chen, X. Y.; Liu, Q.; Chauhan, P.; Enders, D. N-Heterocyclic Carbene Catalysis via Azolium Dienolates: An Efficient Strategy for Remote Enantioselective Functionalizations. *Angew. Chem., Int. Ed.* **2018**, *57*, 3862−3873.
(25) Chen, Z.; Yu, X.; Wu, J. Silver triflate and *N*-heterocyclic carbene Co-catalyzed reaction of *N*′-(2-alkynylbenzylidene)hydrazide, methanol with α,β-unsaturated aldehyde. *Chem. Commun.* **2010**, *46*, 6356−6358.
(26) Mondal, S.; Reddy Yetra, S.; Mukherjee, S.; Biju, A. T. NHC-Catalyzed Generation of α,β-Unsaturated Acylazoliums for the Enantioselective Synthesis of Heterocycles and Carbocycles. *Acc. Chem. Res.* **2019**, *52*, 425−436.
(27) Ho, X. H.; Jung, W. J.; Shyam, P. K.; Jang, H. Y. Copper-Dienamine Catalysis: γ-Oxyamination of α,β- Unsaturated Aldehydes. *Catal. Sci. Technol.* **2014**, *4*, 1914−1919.
(28) Salvador González, A.; Gómez Arrayás, R.; Rodríguez Rivero, M.; Carretero, J. C. Catalytic Asymmetric Vinylogous Mannich Reaction of *N*-(2-Thienyl) Sulfonylimines. *Org. Lett.* **2008**, *10*, 4335−4337.
(29) Yang, W.; Hu, W.; Dong, X.; Li, X.; Sun, J. N-Heterocyclic Carbene Catalyzed γ-Dihalomethylenation of Enals by Single-Electron Transfer. *Angew. Chem., Int. Ed.* **2016**, *55*, 15783−15786.
(30) Dai, L.; Xia, Z. H.; Gao, Y. Y.; Gao, Z. H.; Ye, S. Visible-Light-Driven N-Heterocyclic Carbene Catalyzed γ- and ϵ-Alkylation with Alkyl Radicals. *Angew. Chem., Int. Ed.* **2019**, *58*, 18124−18130.
(31) Saini, G.; Mondal, A.; Kapur, M. Palladium-Mediated Remote Functionalization in γ- And ϵ-Arylations and Alkenylations of Unblocked Cyclic Enones. *Org. Lett.* **2019**, *21*, 9071−9075.
(32) Hyde, A. M.; Buchwald, S. L. Palladium-Catalyzed γ-Arylation of β,γ-Unsaturated Ketones: Application to a One-Pot Synthesis of Tricyclic Indolines. *Angew. Chem., Int. Ed.* **2008**, *47*, 177−180.
(33) Liu, X.; Chen, X.; Mohr, J. T. Copper-Catalyzed γ-Sulfonylation of α,β-Unsaturated Carbonyl Compounds by Means of Silyl Dienol Ethers. *Org. Lett.* **2015**, *17*, 3572−3575.
(34) Sigel, E.; Steinmann, M. E. Structure, Function, and Modulation of $GABA_A$ Receptors. *J. Biol. Chem.* **2012**, *287*, 40224−40231.
(35) Chebib, M.; Johnston, G. A. R. The "ABC" of GABA Receptors: A Brief Review. *Clin. Exp. Pharmacol* **1999**, *26*, 937−940.
(36) König, B. *Chemical Photocatalysis*; De Gruyter, 2013.
(37) Albini, A.; Fagnoni, M. *Handbook of Synthetic Photochemistry*; Wiley, 2010.
(38) Shaw, M. H.; Twilton, J.; MacMillan, D. W. C. Photoredox Catalysis in Organic Chemistry. *J. Org. Chem.* **2016**, *81*, 6898−6926.
(39) Bach, T.; Hehn, J. P. Photochemical Reactions as Key Steps in Natural Product Synthesis. *Angew. Chem., Int. Ed.* **2011**, *50*, 1000−1045.
(40) Holmberg-Douglas, N.; Nicewicz, D. A. Photoredox-Catalyzed C−H Functionalization Reactions. *Chem. Rev.* **2022**, *122*, 1925−2016.
(41) Di Terlizzi, L.; Cola, I.; Raviola, C.; Fagnoni, M.; Protti, S. Dyedauxiliary Group Strategy for the α-Functionalization of Ketones and Esters. *ACS Org. Inorg. Au* **2021**, *1*, 68−71.
(42) Wang, P.; Zhao, Q.; Xiao, W.; Chen, J. Recent Advances in Visible-Light Photoredox-Catalyzed Nitrogen Radical Cyclization. *Green Synth. Catal.* **2020**, *1*, 42−51.
(43) Kärkäs, M. D. Photochemical Generation of Nitrogen-Centered Amidyl, Hydrazonyl, and Imidyl Radicals: Methodology Developments and Catalytic Applications. *ACS Catal.* **2017**, *7*, 4999−5022.
(44) Kumar, G.; Pradhan, S.; Chatterjee, I. N-Centered Radical Directed Remote C−H Bond Functionalization via Hydrogen Atom Transfer. *Asian J. Chem.* **2020**, *15*, 651−672.
(45) Luo, J.; Wei, W. T. Recent Advances in the Construction of C−N Bonds Through Coupling Reactions between Carbon Radicals and Nitrogen Radicals. *Adv. Synth. Catal.* **2018**, *360*, 2076−2086.
(46) Jiang, H.; Studer, A. Chemistry with N-Centered Radicals Generated by Single-Electron Transfer-Oxidation Using Photoredox Catalysis. *CCS Chem.* **2019**, *1*, 38−49.
(47) Mathi, G. R.; Jeong, Y.; Moon, Y.; Hong, S. Photochemical Carbopyridylation of Alkenes Using *N*-Alkenoxypyridinium Salts as Bifunctional Reagents. *Angew. Chem., Int. Ed.* **2020**, *59*, 2049−2054.
(48) Zheng, J.; Tang, N.; Xie, H.; Breit, B. Regio-, Diastereo-, and Enantioselective Decarboxylative Hydroaminoalkylation of Dienol Ethers Enabled by Dual Palladium/Photoredox Catalysis. *Angew. Chem., Int. Ed.* **2022**, *61*, No. e202200105.
(49) Im, H.; Choi, W.; Hong, S. Photocatalytic Vicinal Aminopyridylation of Methyl Ketones by a Double Umpolung Strategy. *Angew. Chem., Int. Ed.* **2020**, *59*, 17511−17516.
(50) Goliszewska, K.; Rybicka-Jasińska, K.; Szurmak, J.; Gryko, D. Visible-Light-Mediated Amination of π-Nucleophiles with *N*-Aminopyridinium Salts. *J. Org. Chem.* **2019**, *84*, 15834−15844.
(51) Deuri, S.; Phukan, P. A Density Functional Theory Study on π-Nucleophilicity and Electron-Transfer Oxidation of Silyl Enol Ethers and Ketene Silyl Acetals. *J. Mol. Struct.* **2010**, *945*, 64−70.
(52) Tcyrulnikov, S.; Cai, Q.; Twitty, J. C.; Xu, J.; Atifi, A.; Bercher, O. P.; Yap, G. P. A.; Rosenthal, J.; Watson, M. P.; Kozlowski, M. C. Dissection of Alkylpyridinium Structures to Understand Deamination Reactions. *ACS Catal.* **2021**, *11*, 8456−8466.

https://doi.org/10.1021/acs.orglett.2c03161
Org. Lett. 2022, 24, 8120−8124

nature communications

Article

https://doi.org/10.1038/s41467-025-59809-9

Photochemical C3-amination of pyridines via Zincke imine intermediates

Received: 2 October 2024

Accepted: 2 May 2025

Published online: xx xx 2025

Check for updates

Kitti Franciska Szabó[1,4], Piotr Banachowicz[1,4], Antoni Powała[1,2], Danijela Lunic[3], Ignacio Funes Ardoiz[3] ✉ & Dorota Gryko[1] ✉

Selective skeletal and peripheral editing of the pyridine moiety has broadly expanded the chemical space. While C-H functionalization at C2 and C4 positions are enabled by the inherent reactivity of this heteroarene, selective derivatization at the C3 position has long posed a significant challenge. Recently, based on a dearomatization-rearomatization sequence, involving Zincke imine intermediates, selective halogenation (-Br, -Cl, and -I) and isotopic labelling were accomplished. Here, we report a mild and regioselective method for C3 amination that relies on the photochemical reaction of Zincke imine with an amidyl radical generated from *N*-aminopyridinium salts. Mechanistic and theoretical studies indicate that radical intermediates are involved and explains the C3 regioselectivity of the reaction.

Heterocyclic scaffolds are present in numerous natural products, pharmaceuticals, agrochemicals, and have found their place in material science[1–3]. Among them, the pyridine moiety is, according to the US Food and Drug Administration, one of the most common motif in approved drugs (Fig. 1A)[4,5]. As biological activity can be fine-tuned by the substitution pattern at this core, methodologies for pyridine functionalizations are highly sought.

Q1 – Q5

Numerous strategies for the peripheral editing of pyridines have been developed but, due to their inherent reactivity functionalization at C2 and C4 positions of the heterocycle prevail[6–9], with chemical modification at the C3 position still presenting a significant challenge. Classical C3-halogenation or C3-nitration via electrophilic aromatic substitutions suffer from harsh reaction conditions, excessive use of the desired pyridine, and low regioselectivity (Fig. 1B)[10,11]. Over the last decades, peripheral editing methodologies have emerged as a powerful tool for the introduction of substituents at the C3 position, primarily employing non-directed transition-metal catalysis[12–17], directing groups[7], and most recently a dearomatization-aromatization strategy (Fig. 1B)[9]. In this approach, electron-deficient azines are transformed into electron-rich intermediates (enamine, dienamine) that react with electrophilic reagents. Subsequent rearomatization leads to C3-substituted pyridine derivatives. Along this line, Wang and coworkers reported a one-pot borane-catalysed pyridine hydroboration tandem reactions[18]. Herein, a nucleophilic 1,4-dihydropyridine (1,4-DHP) formed, reacts with electrophiles (imines, enol esters, SCF_3-, SCF_2H-, -CN reagents) and undergoes subsequent oxidation to afford C3-functionalized pyridines[19–23]. In 2022, Studer and coworkers developed an efficient C3 functionalizations of pyridines involving a bench-stable electron-rich oxazinopyridine generated from dimethyl acetylenedicarboxylate, methyl pyruvate and a pyridine[24,25]. This intermediate, as a dienamine, reacts with electrophilic reagents or radicals leading to, after rearomatization, C3 functionalized pyridines. By switching from an oxazino intermediate to a pyridinium salt, direct selective peripheral editing of pyridines at C4 was achieved[26–28]. The McNally group proposed another strategy for C3-halogenation of pyridines that proceeds via ring opening, halogenation, and ring-closure[29] for which they modified the classic Zincke reaction[30,31]. Furthermore, they expanded their methodology to synthesize *N*-(heteroaryl)pyridinium salts[32], and to incorporate stable radioisotope ^{15}N atom into the pyridine ring[33].

In recent years, significant advances have been made in photoredox catalysis and have expanded the toolbox of radical transformations available to synthetic chemists[34–36]. Recently, we and others have developed photochemical methods for site-selective amination of electron-rich double bonds using electrophilic *N*-centred radicals[37–40].

Based on reports concerning the functionalization of Zincke imines[41–47], and our studies on photochemical amination of dienol

[1]Institute of Organic Chemistry Polish Academy of Sciences, Warsaw, Poland. [2]Department of Chemistry, Warsaw University of Technology, Warsaw, Poland. [3]Complejo Científico-Tecnológico, Universidad de La Rioja, Madre de Dios, Logroño, La Rioja, Spain. [4]These authors contributed equally: Kitti Franciska Szabó, Piotr Banachowicz ✉e-mail: ignacio.funesa@unirioja.es; dorota.gryko@icho.edu.pl

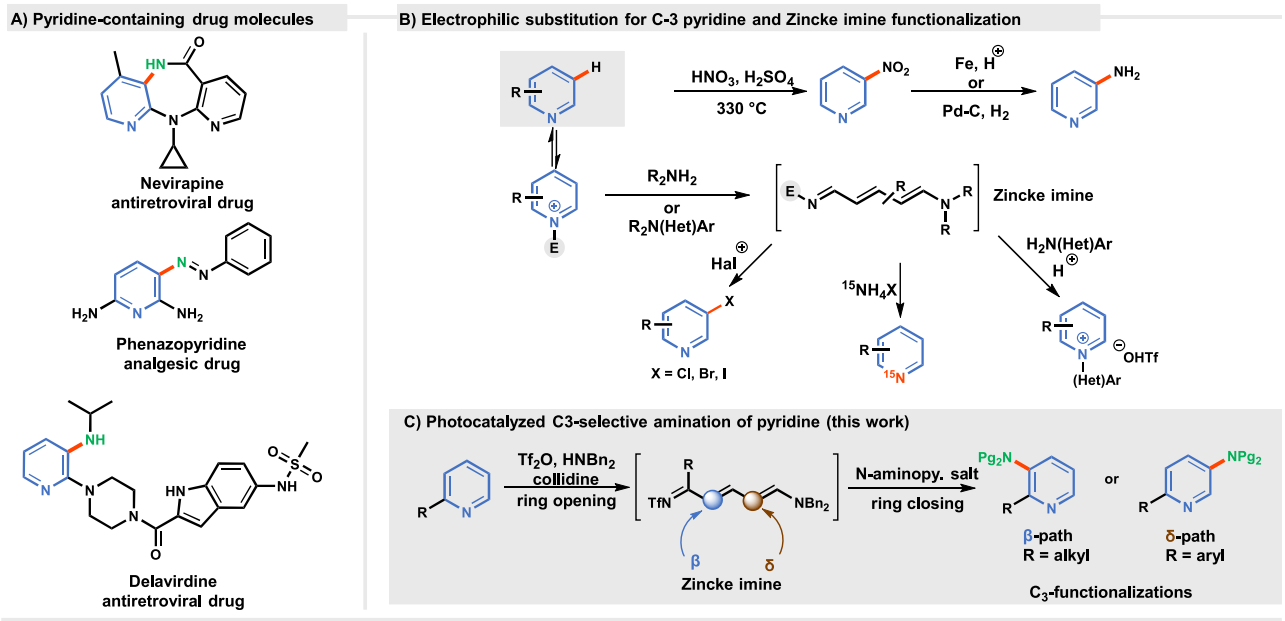

Fig. 1 | State-of-the-art in the synthesis of C-3 aminopyridines. A Representative drugs bearing the pyridine moiety and (**B**) Strategies enabling C-H functionalizations of pyridines at the C3-position. **C** This work – Photocatalyzed C-3-selective amination of pyridine.

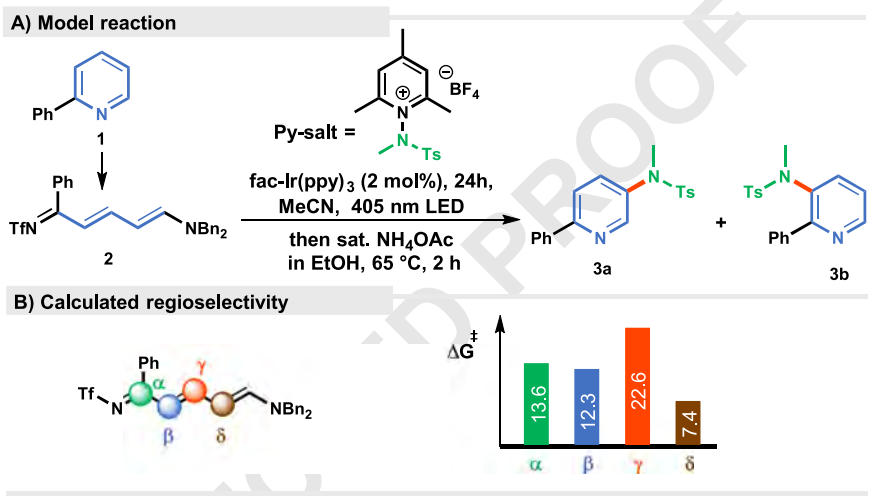

Fig. 2 | Photochemical amination of pyridines. A Model reaction of Zincke imine **2** with *N*-aminopyridinum salt. **B** Calculated Gibbs free energies for the regioselective reactions.

ethers, we hypothesized that selective C3- amination of pyridines could be achieved in a photocatalytic manner. Indeed, here we demonstrate that *N*- centred radicals, generated from *N*-aminopyridinum salts in a photochemical manner, react with Zincke imines to regioselectively produce, after rearomatization, C3-amino pyridines (Fig. 1C).

Results and discussion

Reaction development

Based on the reported data, in the initial phase of our study, a model 2-phenyl Zincke imine **2**, obtained from 2-phenylpyridine (**1**)[29], was reacted with an aminopyridinium salt in the presence of *fac*-Ir(ppy)$_3$ under blue light irradiation to give, after the consecutive ring closure, desired product **3** (for details, see SI), but in a low yield (Fig. 2A).

DFT calculations revealed that the formation of C-N bonds at the δ position should be predominant over the β position due to the lower transition state energy (Fig. 2B, *vide infra* for the full free energy profile). Thorough optimization studies enabled a significant improvement in yield (Table 1, entry 1). The optimal conditions are as follows: under an argon atmosphere, a mixture of 2-phenyl Zincke imine **2** (1 equiv.) and *N*-aminopyridinium salt (1.5 equiv.) in the presence of *fac*-Ir(ppy)$_3$ (2 mol%) in a MeCN/DMSO mixture (v/v 1:1) (0.006 M) was irradiated (LED, 405 nm) at 0 °C for 24 h. The subsequent treatment with saturated NH_4OAc in EtOH in a one-pot manner gave the desired rearomatized C3-amidopyridine **3** as a mixture of two regioisomers **3a** and **3b** in 99% yield (5:1, entry 1). Among other Zincke imines tested, only the *N*-benzylaniline derivative yielded the desired product, although a significant drop in both yield (26%) and regioselectivity to a 2:1 ratio was observed (for further information, see SI). The use of either sole DMSO or MeCN diminished the yield (entries 2 and 3). Previous studies have demonstrated that reduction of *N*- aminopyridinium salts to *N*-centred radicals by Ir(III) in the excited state involving single electron transfer (SET) can be performed under blue LED irradiation[38,48]. Intriguingly, in our case, the reaction yield decreased significantly to 16%, probably due to strong absorption around 450 nm in the UV-Vis

https://doi.org/10.1038/s41467-025-59809-9

Table. 1 | Conditions for selective *C3*-amination of pyridines via Zincke imine

Entry	Variation form optimal conditions[d]	Yield of 3a and 3b (%)[a]	3a:3b ratio[a]
1	None	>99; >95[b], 95[c]	4.8:1
2	MeCN	66	2.6:1
3	DMSO	48	5.2:1
4	Blue LED (455 nm)	16	n.d.
5	1.1 eq. of Py-	68	5.8:1
6	0.0125 M	61	3.1:1
7	No PC	6	n.d.
8	No light	Traces	n.d.
9	No light + no PC	0	n.d.

[a]Yields determined by GC-FID analysis of crude reaction mixtures.
[b]Yield determined by ^{1}H NMR analysis of the crude reaction mixture with CH_2Br_2 as internal standard.
[c]Isolated yield.
[d]Optimal conditions: 0.05 mmol scale (**2**, c = 0.006 M), 0.075 mmol (1.5 equiv. Py-salt), 2 mol% *fac*-Ir(ppy)$_3$, violet LED (405 nm), 24 h, 0 °C, DMSO/MeCN (v:v 1:1), then sat. NH_4OAc in EtOH, 65 °C, 2 h.

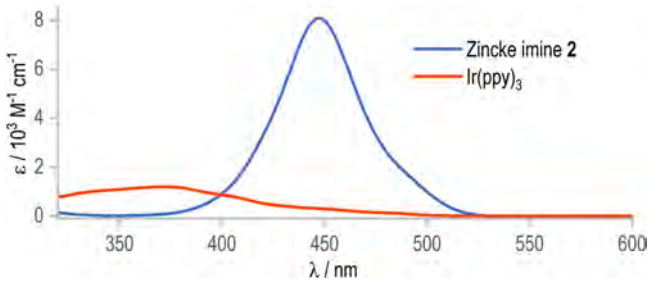

Fig. 3 | UV-Vis spectrum of Zincke Imine 2 and *fac*-Ir(ppy)$_3$. Spectra measured in (MeCN), blue line – Zincke imine 2, orange line – *fac*-Ir(ppy)$_3$.

spectrum of Zincke imine **2** (entry 4, Fig. 3). As a result, violet light (405 nm) irradiation proved a crucial factor for the excitation of the Ir-catalyst and thus the generation of amidyl radicals in the presence of Zincke imines. A lower excess of the pyridinium salt (1.1 equiv.) did not ensure a full conversion of the starting material (entry 5). Other mono- and di-protected *N*-aminopyridinium salts were less effective under the developed conditions (for further information, see SI). Dilute conditions were deemed necessary, as a significant decrease in the yield was observed in the case of concentrated solutions (entry 6). Control experiments, without the photocatalyst or light clearly indicated that the reaction is a photochemically induced process (entries 7–9).

Scope and limitations

The scope with respect to the pyridine was then examined (Fig. 4). Zincke Imines derived from 2- phenyl-substituted pyridines bearing electron-donating groups (EDG) (e.g., methoxy, methyl) on the phenyl ring are well tolerated giving products **4**–**12** in high yields, though the yield diminishes when substituents impose a steric hindrance around the newly forming bond, for example two methoxy groups at *ortho*-positions (**7a**). In these cases, harsher conditions are required for effective ring closure (using a microwave with higher temperature; for details, see SI). However, having only one substituent in the *ortho* position such as 2- methylthio-substituted (**8a**) pyridine, allowed for the synthesis the desired product in 88% yield and high regioselectivity. Other 2-aryl derivatives, such as biphenyls (**13**–**15**), phenanthrene (**17**), and pyrene (**18**) furnishes similar results, but we observed a reduced yield for the naphthalene derivative (**16**) due to incomplete conversion of the reaction. On the other hand, electron-withdrawing groups (e. g., -CN, NO_2) are not only well tolerated, but also have a beneficial impact on the regioselectivity of the reaction. For example, the reaction with 2-(4-nitrophenyl)pyridine affords exclusively product **20a** in 98% yield. 2-Heteroaryl substituted pyridines provide aminated products **24**–**29** in satisfactory yields (35–86%). The low yield for the substrate bearing the *N*-Boc-pyrrole moiety results from partial deprotection of the carbamate group under the acidic condition. Furthermore, the influence of alkyl groups at position 2 was examined. For a series of 2-alkylpyridines (methyl, ethyl, hexyl, and benzyl), decreased yields were observed under standard conditions. We fine-tuned the reaction conditions and found that the exclusive use of MeCN, alongside with a higher power of the light source, effectively increased the efficiency of the C3-amination reaction with 2-alkylsubstituents (for details, see SI). Interestingly, the regioselectivity switches, in this case an amidyl radical attacks Zincke imine preferentially at the β position therefore, the resultant pyridine bears substituents at positions C2 and C3 in contrast to 2- phenylpyridine, for which they occupy positions C3 and C5. An exception are isopropyl and methoxy-substituted benzyl derivatives that form aminated products **33** and **35** with almost no selectivity.

To further demonstrate the synthetic utility, the one-pot amination reaction involving three consecutive steps was attempted. The process is compatible with the model reaction, after three steps, the total yield equals 55% and the regioselectivity did not erode (Fig. 5).

Mechanistic studies

To gain a better understanding of the reaction developed, we conducted a series of control experiments. They indeed confirmed the relevance of both the light and the catalyst. The radical nature of the mechanism was confirmed by an experiment with the addition of TEMPO, which completely halted the reaction (Fig. 6A). DMPO, a radical spin trap was added to the reaction mixture, which formed an adduct with the radical generated from the *N*-aminopyridinium salt as confirmed by ESI-MS analysis (Fig. 6B). Furthermore, kinetic experiments revealed that amidated Zincke imine **2a** forms gradually over 12 h (Fig. 6C). Due to its instability, the isolated yield was only 15% but allowed us to confirm its structure by NMR spectroscopy and X-ray crystallography (Fig. 6D).

Based on data from our previous work and literature[49,50], along with our control experiments and DFT and DLPNO-CCSD(T) calculations (Fig. 7A, for more computational details, see SI), we propose a light-induced radical formation of *N*-aminopyridinium salt ($E_{1/2}$ = −0.70 V vs Ag/AgCl) via Single Electron Transfer (SET) from the excited [Ir(III)] photoredox catalyst (Fig. 7B). *N*-aminopyridinium salt is reduced and generates radical **A** (−24.4 kcal/mol). This radical undergoes fragmentation to form an N-centred radical **B** (−52.6 kcal/mol) and collidine as a byproduct through a low energy transition state (**TS-1**, 4.1 kcal/mol). The resulting electrophilic N-centred radical **B** reacts with the Zincke imine derivative at the δ-position ($\Delta G^{\ddagger}$ = 7.4 kcal/mol), leading to the formation of a C-N bond and the corresponding intermediate **C** (−52.0 kcal/mol).

Then, intermediate **C** can be easily oxidized by the Ir-(IV) catalyst to form cation derivative **D** (ΔG = −64.1 kJ/mol) with the regeneration of the ground state of the Ir-(III) catalyst. Finally, deprotonation of cation **D** with collidine affords product **E** ($\Delta G°$ = −106.7 kcal/mol). From this point, ring cyclization from product E to final product **3a** occurs via a deprotection/ring closure sequence with a barrier of 15.1 kcal/mol (see Supplementary Information and Supplementary Data 1 for details).

The reaction mechanism was also evaluated for the attack of the *N*- centred radical at position α, β and γ (Fig. 2B, see SI for the selectivity evaluation). At β, the reaction can be competitive, as demonstrated by

https://doi.org/10.1038/s41467-025-59809-9

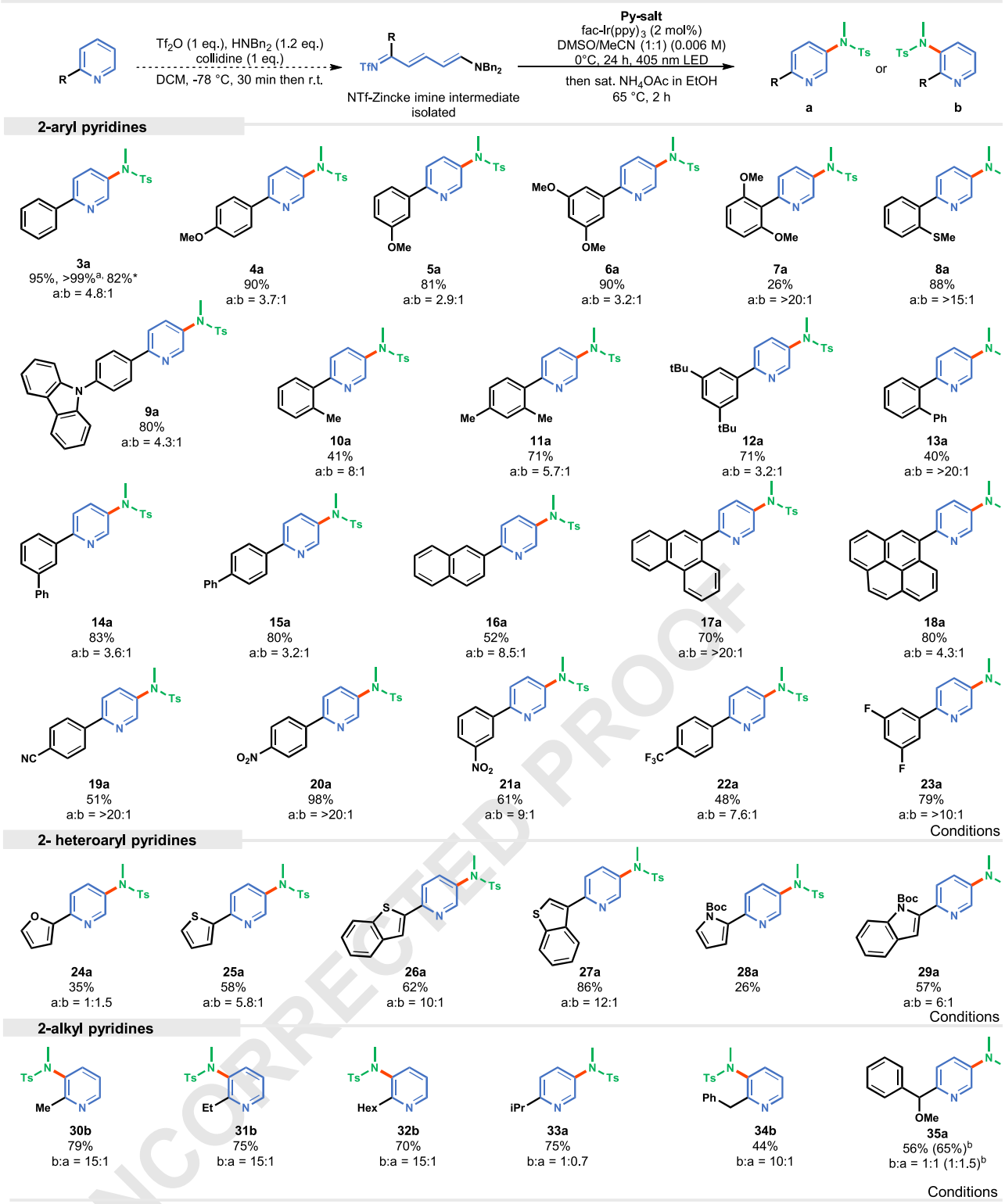

Fig. 4 | Scope of C3-amination of pyridines. The yields given are isolated unless otherwise stated. [a] Yield determined by GC-FID analysis of crude reaction mixtures; [b] Reaction was carried out under Conditions A; The ratio was determined by the GC-FID method or by ^{1}H NMR analysis of crude reaction mixtures; for each case a major isomer is drawn. Conditions A: 1) Zincke imine (0.05 mmol), *fac*-Ir(ppy)$_3$ (2 mol%), *N*-aminopyridinium salt (1.5 eq.), DMSO/MeCN (1:1), 0 °C, 24 h, 405 nm LED (2.4 W); 2) sat. NH_4OAc in EtOH, 65 °C, 2 h. Conditions B: 1) Zincke imine (0.05 mmol), *fac*-Ir(ppy)$_3$ (2 mol%), *N*-aminopyridinium salt (1.5 eq.), dry MeCN, 0 °C, 24 h, 405 nm LED (4.8 W); 2) sat. NH_4OAc in EtOH, 65 °C, 2 h. *Zincke imine (0.2 mmol) scale.

the experimental observation of the minor isomer. However, at *γ*, the radical attack is much higher in energy (22.6 kcal/mol) and at *α* the activation free energy is similar to β (13.6 kcal/mol), but the resulting radical cannot be oxidized, preventing the turnover of the catalytic cycle and resulting as a nonproductive reaction pathway.

In the final stage, further synthetic transformations of synthesized pyridines were then explored: the deprotection of the tosyl group and

https://doi.org/10.1038/s41467-025-59809-9

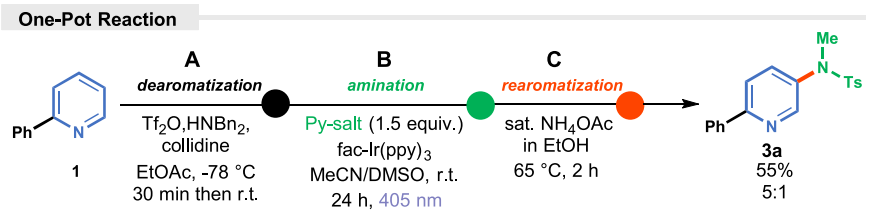

Fig. 5 | One-pot *meta*-amination of 2-phenylpyridine (1). **A** Dearomatization: Tf_2O, $HNBn_2$, EtOAc, −78 °C to rt); (**B**) Amination: Py-salt, *fac*-Ir(ppy)$_3$, MeCN/DMSO, rt, 24 h, 405 nm LEDs; (**C**) Rearomatization; sat. $NH_4OAc_{(EtOH)}$, 65 °C, 2 h).

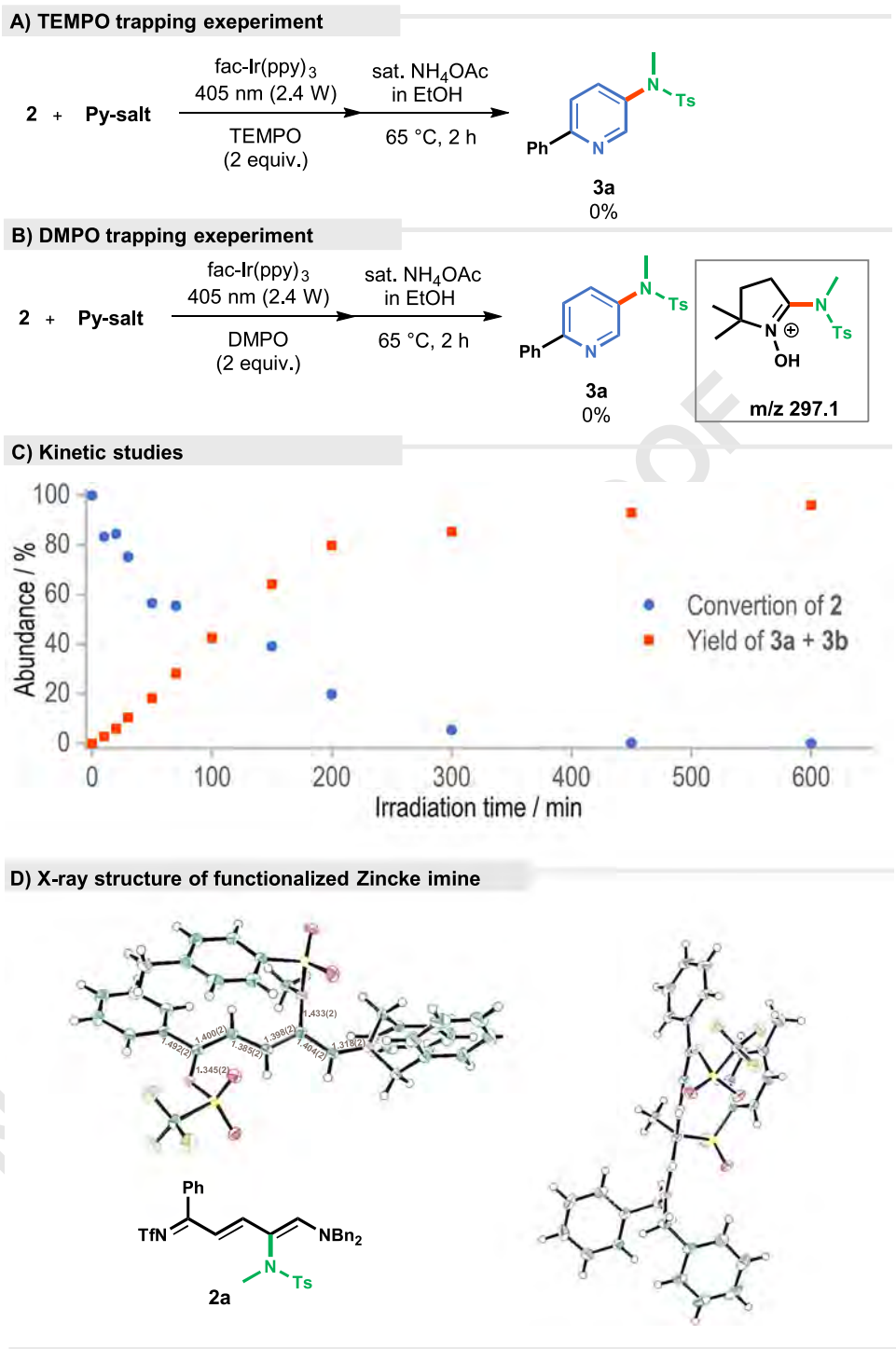

Fig. 6 | Mechanistic studies. **A** Radical trap experiment with TEMPO. **B** Radical trap experiment with DMPO. **C)** Kinetic reaction profile of the model reaction. **D** X-Ray structure of aminated Zincke imine **2a**.

https://doi.org/10.1038/s41467-025-59809-9

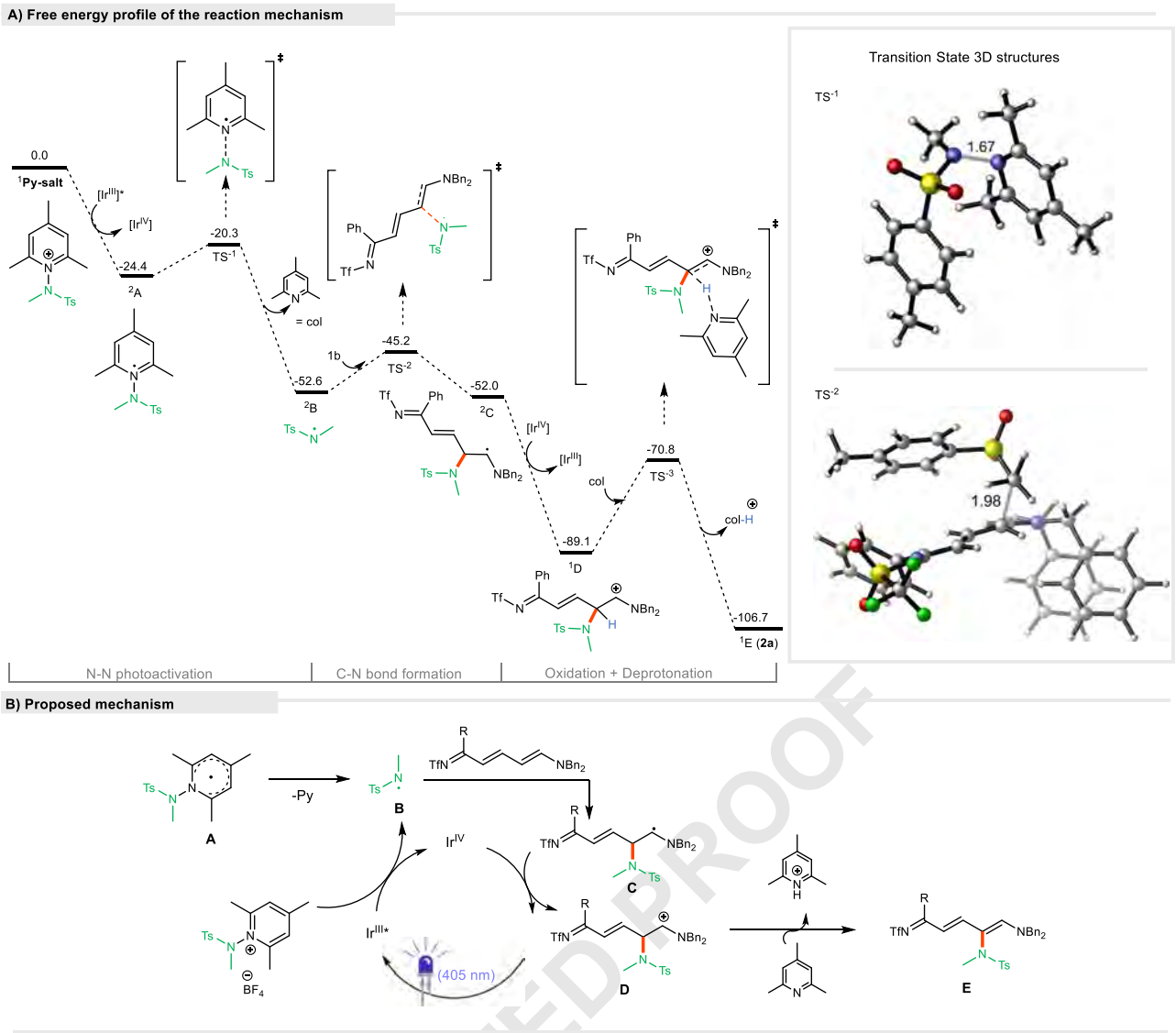

Fig. 7 | Theoretical studies. A Free energy profile of the reaction mechanism for the major product at SMD(MeCN) DLPNO-CCSD(T)/Def2TZVPP//ωB97xD/Def2SVP level of theory. Free energies in kcal/mol and bond distances in Å. Inset: Activation free energy barriers for C-N bond formation at the different reactive positions of the Zincke intermediates. **B** Proposed mechanism.

peripheral editing of the pyridine ring. Both regioisomers underwent tosyl group cleavage with high yields, providing free NH groups (**36** and **37**) (Fig. 8A).

The resulting pyridine derivative was then readily acylated with acyl halide, forming amide **38** in 80% yield (Fig. 8B). Furthermore, the synthesis of *N*-oxide (**39**) and *N*-methylpyridinium (**40**) derivatives was successfully achieved using *m*CPBA and MeI, respectively, in good yields (Fig. 8C, D). The sequential C3 and C5 difunctionalization of pyridine was also investigated using 2-phenyl Zincke imine. The resulting amidated intermediate underwent a subsequent functionalization through an ionic *meta*- bromination with *N*-bromosuccinimide, yielding regioselectively brominated pyridine **41a** in a 65% yield after the rearomatization (Fig. 8E).In summary, we have developed a photochemical methodology for the peripheral editing of the pyridine core that relies on a dearomatization/aromatization strategy. After activation of a pyridine as a Zincke imine intermediate, it reacts with an electrophilic *N*-centred radical generated from *N*-aminopyridinium salts in a photochemical manner. The amido-derivative formed, after aromatization, furnishes the desired product. Importantly, the C-N bond formation occurs predominantly at the C3 position. Depending on the nature of the C2-substituent (aryl versus alkyl) in the starting material, C3, C5 or C2, C3 functionalized pyridines are formed. The method is characterized by mild reaction conditions, scalability, pyridine as the limiting reagent, and excellent regioselectivity. Importantly, it can be performed in a one-pot fashion. DFT calculations confirms the preferential attack at the δ position, and the reaction mechanism consists of the following reaction steps: generation of *N*-centred radical via Ir-mediated reduction of the *N*-aminopyridinium salt, selective addition of *N*-radical and oxidation/deprotonation of the resulting radical species.

Our work opens new photochemical avenues in the peripheral editing of the pyridine scaffold via Zincke imine. Further work is currently undergoing in our laboratory.

Methods

Synthetic procedures and compound characterization

Photochemical reactions were carried out in the UOSlab Miniphoto photoreactor. Detailed synthetic procedures, including reaction conditions, yields, NMR spectra, high-resolution mass spectrometry, and X-ray crystallographic data, are given in the Supplementary Information.

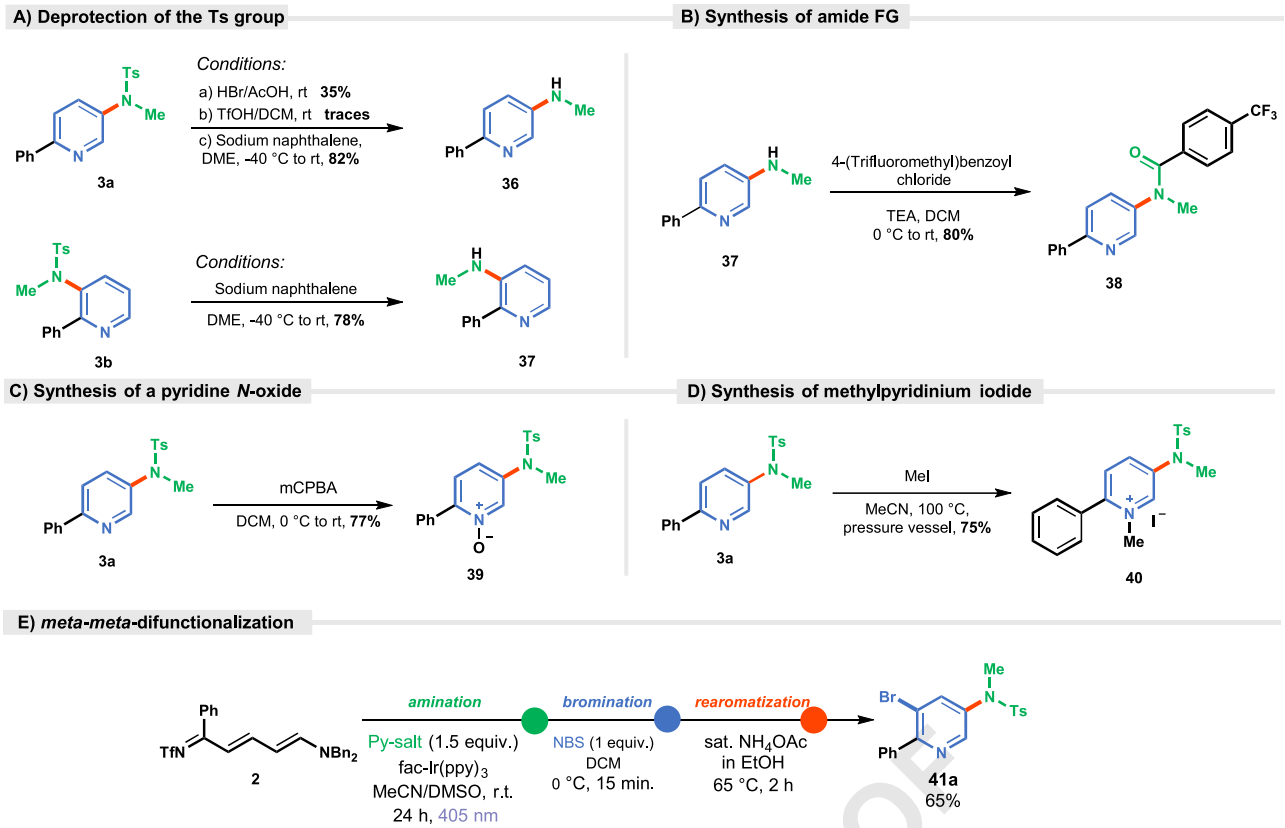

Fig. 8 | Synthetic applications. A Deprotection of the Ts group under different reaction conditions, (**B**) Synthesis of amide functional group, (**C**) Synthesis of a pyridine *N*-oxide, (**D**) Synthesis of methylpyridinium iodide, (**E**) Formation of *meta-meta*-difunctionalized 2-phenylpyridine via Zincke Imine.

General protocol for photoamination and closure of the 2-aryl Zincke imines

Zincke imine (0.05 mmol), Py-salt (0.075 mmol), *fac*-Ir(ppy)$_3$ (0.67 mg, ~10 µmol, 2 mol%) were placed in the closed-cup vial and MeCN (4 ml) and DMSO (4 ml) were added through the septum. The reaction mixture was placed in ultrasound bath and degassed by bubbling argon through the solution for 15 min. The vial was then moved to the photoreactor and irradiated with violet light (2.4 W) for 24 h maintaining temperature between 0 °C to 5 °C with a dedicated cooling system. After the indicated time, a saturated NH_4OAc solution was added in anhydrous ethanol (2 ml) and reaction was heated up to 65 °C for 2 h. DMSO and an excess of NH_4OAc were removed by extraction (AcOEt/ H_2O). The organic phase was dried over anhydrous sodium sulphate and evaporated with silica gel (dry load for the preparation of the sample for flash chromatography). The pure products were isolated by flash chromatography in the hexanes/AcOEt gradient.

General procedure for the functionalization of 2-alkyl Zincke imines

Zincke imine (0.05 mmol), Py-salt (0.075 mmol), *fac*-Ir(ppy)$_3$ (0.67 mg, ~10 µmol, 2 mol%) were placed in the closed-cup vial and MeCN (8 ml) were added through the septum. The reaction mixture was placed in ultrasound bath and degassed by bubbling argon through the solution for 15 min. The vial was then moved to the photoreactor and irradiated with violet light (4.8 W) for 24 h, maintaining a temperature between 0 °C and 5 °C. After the indicated time, the saturated NH_4OAc solution in anhydrous ethanol was added (2 ml) and the reaction mixture was heated up to 65 °C for 2 h. The excess of NH_4OAc was removed by extraction (AcOEt/ H_2O). The organic phase was dried over anhydrous sodium sulphate and evaporated with silica gel (dry load for the preparation of the sample for flash chromatography). The pure products were isolated by flash chromatography in hexanes/AcOEt gradient.

Computational details

DFT calculations were carried out using the G16 programme package using the ωB97xD functional. Geometry optimisations and frequency calculations were computed with the Def2SVP basis set without symmetry restrictions. The nature of all the stationary points was characterized by frequency calculations as minima (no imaginary frequencies) or transition states (one imaginary frequency). Transition states were relaxed to reactants and products, and IRC calculations were performed to further validate the connectivity. Additionally, the solvation energy was obtained from single-point calculations using ωB97xD/Def2TZVPP and the implicit solvent model (acetonitrile). The solvation free energy was then obtained by the difference between the energy calculated with the SMD model – the energy in gas phase. The standard state was corrected from 1 atm to 1 M by adding 1.89 kcal/mol when needed.

The potential energies were further refined using the DLPNO-CCSD(T) method in ORCA. Combination of Def2TZVPP and Ri-C auxiliary basis set (Def2-TZVPP/C) and RIJCOSX (Def2/J). The tightSCF option was also selected.

Data availability

The authors declare that the data supporting the findings of this study are available within the article and its Supplementary Information (experimental details, NMR spectroscopic data, X-ray crystal information), Supplementary Data 1 (Cartesian coordinates of DFT calculated geometries) or from the corresponding authors upon request. Crystallographic data for the aminated Zincke imine **2a** reported in this article has been deposited at the Cambridge Crystallographic Data Centre under deposition numbers CCDC 2369412. Copies of the data can be obtained free of charge via https://www.ccdc.cam.ac.uk/structures/.

References

1. McAteer, C. H., Murugan, R. & Yamamoto, J. H. *Comprehensive heterocyclic chemistry IV* pp. 217–242 (Elsevier, Oxford, 2022).
2. Altaf, A. A. et al. A Review on the medicinal importance of pyridine derivatives. *J. Drug Des. Med. Chem.* **1**, 1–11 (2015).
3. Kallitsis, J. K., Geormezi, M. & Neophytides, S. G. Polymer electrolyte membranes for high-temperature fuel cells based on aromatic polyethers bearing pyridine units. *Polym. Int.* **58**, 1226–1233 (2009).
4. Bhutani, P. et al. U.S. FDA approved drugs from 2015–June 2020: a perspective. *J. Med. Chem.* **64**, 2339–2381 (2021).
5. Vitaku, E., Smith, D. T. & Njardarson, J. T. Analysis of the structural diversity, substitution patterns, and frequency of nitrogen heterocycles among U.S. FDA approved pharmaceuticals. *J. Med. Chem.* **57**, 10257–10274 (2014).
6. Murakami, K., Yamada, S., Kaneda, T. & Itami, K. C–H Functionalization of azines. *Chem. Rev.* **117**, 9302–9332 (2017).
7. Zhou, F.-Y. & Jiao, L. Recent developments in transition-metal-free functionalization and derivatization reactions of pyridines. *Synlett* **32**, 159–178 (2020).
8. Maity, S., Bera, A., Bhattacharjya, A. & Maity, P. C–H functionalization of pyridines. *Org. Biomol. Chem.* **21**, 5671–5690 (2023).
9. Cao, H., Cheng, Q. & Studer, A. *meta*-Selective C–H Functionalization of Pyridines. *Angew. Chem. Int. Ed.* **62**, e202302941 (2023).
10. Ziegler, T. *Organic Nitro Chemistry Series*, p. 84 (VCH, Weinheim, 1990).
11. Joule, J. A. *Heterocyclic Chemistry* (CRC Press, 2020).
12. Das, R. & Kapur, M. Transition-metal-catalyzed C–H functionalization reactions of π-deficient heterocycles. *Asian J. Org. Chem.* **7**, 1217–1235 (2018).
13. Ye, M. et al. Ligand-promoted C3-selective arylation of pyridines with Pd catalysts: gram-scale synthesis of (±)-preclamol. *J. Am. Chem. Soc.* **133**, 19090–19093 (2011).
14. Ye, M., Gao, G.-L. & Yu, J.-Q. Ligand-promoted C-3 selective C H olefination of pyridines with Pd catalysts. *J. Am. Chem. Soc.* **133**, 6964–6967 (2011).
15. Cong, X., Tang, H., Wu, C. & Zeng, X. Role of mono-N-protected amino acid ligands in palladium(II)-catalyzed dehydrogenative heck reactions of electron-deficient (Hetero)arenes. *Exp. Computational Stud. Organomet.* **32**, 6565–6575 (2013).
16. Murphy, J. M., Liao, X. & Hartwig, J. F. Meta halogenation of 1,3-disubstituted arenes via iridium-catalyzed arene borylation. *J. Am. Chem. Soc.* **129**, 15434–15435 (2007).
17. Zhang, T. et al. A directive Ni catalyst overrides conventional site selectivity in pyridine C–H alkenylation. *Nat. Chem.* **13**, 1207–1213 (2021).
18. Park, S. & Chang, S. Catalytic dearomatization of N-heteroarenes with silicon and boron compounds. *Angew. Chem. Int. Ed.* **56**, 7720–7738 (2017).
19. Zhou, X.-Y., Zhang, M., Liu, Z., He, J.-H. & Wang, X.-C. C3-selective trifluoromethylthiolation and difluoromethylthiolation of pyridines and pyridine drugs via dihydropyridine intermediates. *J. Am. Chem. Soc.* **144**, 14463–14470 (2022).
20. Liu, Z. et al. Borane-catalyzed C3-alkylation of pyridines with imines, aldehydes, or ketones as electrophiles. *J. Am. Chem. Soc.* **144**, 4810–4818 (2022).
21. Tian, J.-J., Li, R.-R., Tian, G.-X. & Wang, X.-C. Enantioselective C3-allylation of pyridines via tandem borane and palladium catalysis. *Angew. Chem. Int. Ed.* **62**, e202307697 (2023).
22. Liu, Z. et al. Borane-catalyzed C3-alkylation of pyridines with imines, aldehydes, or ketones as electrophiles. *J. Am. Chem. Soc.* **145**, 11789–11797 (2023).
23. Zhang, M. et al. C3-cyanation of pyridines: constraints on electrophiles and determinants of regioselectivity. *Angew. Chem. Int. Ed.* **62**, e202216894 (2023).
24. Chakraborty, S. & Biju, A. T. Directing group-free regioselective *meta*-C–H functionalization of pyridines. *Angew. Chem. Int. Ed.* **62**, e202300049 (2023).
25. Cao, H., Cheng, Q. & Studer, A. Radical and ionic *meta*-C-H functionalization of pyridines, quinolines, and isoquinolines. *Science* **378**, 779–785 (2022).
26. Cao, H., Bhattacharya, D., Cheng, Q. & Studer, A. C–H functionalization of pyridines via oxazino pyridine intermediates: switching to *para*-selectivity under acidic conditions. *J. Am. Chem. Soc.* **145**, 15581–15588 (2023).
27. Xu, P., Wang, Z., Guo, S.-M. & Studer, A. Introduction of the difluoromethyl group at the meta- or para-position of pyridines through regioselectivity switch. *Nat. Commun.* **15**, 4121 (2024).
28. Cheng, Q. et al. Skeletal editing of pyridines through atom-pair swap from CN to CC. *Nat. Chem.* **16**, 741–748 (2024).
29. Boyle, B. T., Levy, J. N., Lescure, Lde, Paton, R. S. & McNally, A. Halogenation of the 3-position of pyridines through Zincke imine intermediates. *Science* **378**, 773–779 (2022).
30. Zincke, T., Heuser, G. & Möller, W. Ueber Dinitrophenylpyridiniumchlorid und dessen Umwandlungsproducte *Justus Liebigs. Ann. Chem.* **333**, 296–345 (1904).
31. Toscano, R. A. et al. Nucleophilic reactions on 1-trifluoromethanesulfonylpyridinium trifluoromethanesulfonate (triflylpyridinium triflate, TPT). Ring-opening and "unexpected" 1,4-dihydropyridine reaction products). *Chem. Pharm. Bull.* **45**, 957–961 (1997).
32. Selingo, J. D. et al. A general strategy for n-(hetero)arylpiperidine synthesis using Zincke imine intermediates. *J. Am. Chem. Soc.* **146**, 936–945 (2024).
33. Nguyen, H. M. H. et al. Synthesis of ^{15}N-pyridines and higher mass isotopologs via zincke imine intermediates. *J. Am. Chem. Soc.* **146**, 2944–2949 (2024).
34. Shaw, M. H., Twilton, J. & MacMillan, D. W. C. Photoredox catalysis in organic chemistry. *J. Org. Chem.* **81**, 6898–6926 (2016).
35. Bach, T. & Hehn, J. P. Photochemical reactions as key steps in natural product synthesis. *Angew. Chem. Int. Ed.* **50**, 1000–1045 (2011).
36. Holmberg-Douglas, N. & Nicewicz, D. A. Photoredox-catalyzed C–H functionalization reactions. *Chem. Rev.* **122**, 1925–2016 (2022).
37. Szabó, K. F., Goliszewska, K., Szurmak, J., Rybicka-Jasińska, K. & Gryko, D. Site-selective, photocatalytic vinylogous amidation of enones. *Org. Lett.* **24**, 8120–8124 (2022).
38. Greulich, T. W., Daniliuc, C. G. & Studer, A. *N*-Aminopyridinium salts as precursors for N-centered radicals – direct amidation of arenes and heteroarenes. *Org. Lett.* **17**, 254–257 (2015).
39. Banoun, C., Bourdreux, F. & Dagousset, G. Highly selective γ-alkoxylation, γ-amination and γ-alkylation of unbiased enals by means of photoredox catalysis. *Chem. Commun.* **59**, 760–763 (2023).
40. Briand, M. et al. Remote radical trifluoromethylation: a unified approach to the selective synthesis of γ-trifluoromethyl α,β-unsaturated carbonyl compounds. *Org. Lett.* **24**, 9375–9380 (2022).
41. Feng, M. et al. Pyridine-based strategy towards nitrogen isotope exchange. Preprint at https://chemrxiv.org/engage/chemrxiv/article-details/653f7120a8b423585a8f929f (2023). Q6
42. Tolchin, Z. A. & Smith, J. M. ^{15}NRORC: an azine labeling protocol. *J. Am. Chem. Soc.* **146**, 2939–2943 (2024).
43. Wang, H. & Greaney, M. F. Regiodivergent arylation of pyridines via Zincke intermediates. *Angew. Chem. Int. Ed.* **63**, e202315418 (2024).
44. Conboy, A. & Greaney, M. F. Synthesis of benzenes from pyridines via N to C switch. *Chem* **10**, 1940–1949 (2024).
45. Bartholomew, G. L. et al. ^{14}N to ^{15}N isotopic exchange of nitrogen heteroaromatics through skeletal editing. *J. Am. Chem. Soc.* **146**, 2950–2958 (2024).
46. Li, S. et al. C3 Selective chalcogenation and fluorination of pyridine using classic Zincke imine intermediates. *Nat. Commun.* **15**, 7420 (2024).

47. Szabó, K.F. et al. Photochemical C3-amidation of pyridines via Zincke imine intermediates. Preprint at https://chemrxiv.org/engage/chemrxiv/article-details/668e89795101a2ffa8fa35af (2024).
48. Goliszewska, K., Rybicka-Jasińska, K., Szurmak, J. & Gryko, D. Visible-light-mediated amination of π-nucleophiles with *N*-aminopyridinium salts. *J. Org. Chem.* **84**, 15834–15844 (2019).
49. Deuri, S. & Phukan, P. A density functional theory study on π-nucleophilicity and electron-transfer oxidation of silyl enol ethers and ketene silyl acetals. *J. Mol. Struct. Theochem.* **945**, 64–70 (2010).
50. Tcyrulnikov, S. et al. Dissection of alkylpyridinium structures to understand deamination reactions. *ACS Catal.* **11**, 8456–8466 (2021).

Acknowledgements

This work is supported by the National Science Centre, Poland (MAESTRO UMO-2020/38/A/ST4/00185, K.F. Sz., P.B., D.G.).

Author contributions

D.G. conceived the project and designed the initial experiments. K.F. Sz., P.B., A.P. developed methodology and performed experiments regarding the synthesis and characterization of all the compounds. I.F.A. designed the computational study and. D.L. performed the calculations. All authors analysed the data, discussed the results, and commented on the manuscript. K.F.Sz. and P.B. contributed equally to this work.

Competing interests

The authors declare no competing interests.

Additional information

Supplementary information The online version contains supplementary material available at https://doi.org/10.1038/s41467-025-59809-9.

Correspondence and requests for materials should be addressed to Ignacio Funes Ardoiz or Dorota Gryko.

Peer review information *Nature Communications* thanks Curtis Moore, Hai-Tao Qin, Sermadurai Selvakumar, and the other, anonymous, reviewer for their contribution to the peer review of this work. A peer review file is available.

OL Organic Letters

pubs.acs.org/OrgLett
Letter

Vitamin B_{12} and Micellar Solution Enable Regioselective Ring Opening of Epoxides and Aziridines with Electrophilic Olefins

Kitti Franciska Szabó, Tomasz Wdowik, Aleksandra Krzeszewska, Krzysztof Mazurek, Martin P. Andersson, and Dorota Gryko*

Cite This: https://doi.org/10.1021/acs.orglett.5c01376

ABSTRACT: Vitamin B_{12}, a water-soluble cobalt complex, is inherently predisposed to catalyze reactions under aqueous conditions. Despite its potential, adopting this strategy for transformations of hydrophobic reagents has been challenging, because of their low aqueous solubility. Here, we demonstrate that vitamin B_{12} promotes the reaction of epoxides and aziridines with electrophilic olefins in a micellar system. The desired products are obtained efficiently in a fully regioselective manner. This green catalytic approach further advances the use of vitamin B_{12} in sustainable catalysis providing a valuable method to synthesize important intermediates.

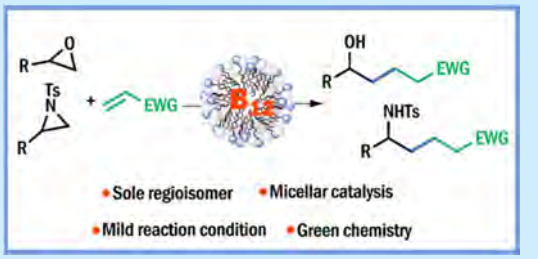

Three-membered heterocycles, epoxides, and aziridines, are versatile synthetic intermediates in organic synthesis, with broad applications ranging from polymer chemistry to chemical biology.[1−7] Along this line, the ring-opening reactions with nucleophiles that often enable further chemical transformations are highly prized. Classical methods for epoxide and aziridine ring-opening mostly rely on acid or base catalysis,[8−10] involve transition metal complexes[11,12] or organocatalysts.[13] These approaches, however, often suffer from harsh reaction conditions, poor selectivity or low yields. Thus, greener, selective methods for their transformations are highly desired.

In recent years, sustainable ring-opening protocols, including photochemical transformations, have attracted substantial attention.[5] For example, in 2020, Doyle et al. reported photocatalyzed cross-electrophile coupling of epoxides and aziridines with aryl iodides in the presence of 4-CzIPN/Ni.[14,15] Notably, both aliphatic and aromatic derivatives yielded phenylamine derivatives, but only for alkyl substituted aziridines, these reactions were fully regioselective. Side reactions such as homocoupling of aryl iodides and epoxide rearrangements represented a challenge and required careful ligand selection. Subsequent advances led to asymmetric variants allowing them to obtain linear products with moderate to high enantioselectivity.[16] Further improvements included a photocatalytic aziridine ring-opening reaction employing acetals as alkyl radical sources.[17] In 2021, our group developed a dual vitamin B_{12}/Ni catalytic system for the regioselective ring-opening of aryl and alkyl epoxides with aryl halides (Scheme 1A).[18] It is the vitamin that governs the regioselectivity of the ring-opening on the less hindered side of the epoxide. Subsequently, this methodology was extended to include the ring-opening of oxetane derivatives, which required the addition of a Lewis acid.[19] The West group

Scheme 1. (A) Photochemical Functionalizations of Epoxides and Aziridines; (B) Vitamin B_{12}-Catalyzed Radical Addition/1,2-aryl Migration Reaction in Micelles

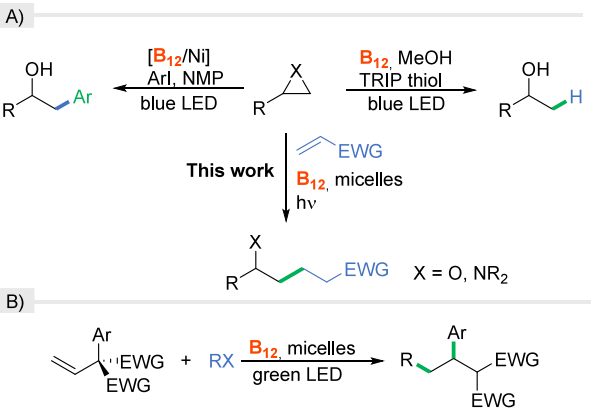

reported vitamin a B_{12}/HAT-catalyzed reduction of epoxides selectively yielding Markovnikov alcohols (Scheme 1A).[20] However, these photochemical transformations are typically conducted in organic solvents that pose environmental and safety concerns.[21] Therefore, we sought to use an alternative reaction medium, namely micellar solutions, which not only enhance solubilization but also may improve regioselectiv-

Received: April 7, 2025
Revised: May 14, 2025
Accepted: May 20, 2025

ity.[22−25] In this context, our group has recently demonstrated that micellar solutions are not only compatible with vitamin B_{12}-catalyzed radical addition/1,2-aryl migration reactions, but are also essential for achieving high yields of the desired product (Scheme 1B).[26]

Recognizing the potential of micellar systems to direct reactivity, we have strived to investigate whether they could facilitate the ring-opening of epoxides and aziridines (Scheme 1A). Given that these strained three-membered heterocycles are fundamental building blocks, exploring their regioselective transformations under micellar conditions aligns well with our goal of developing sustainable methodologies. What is more, the role of micellar solutions in vitamin B_{12}-catalyzed reactions remains underexplored.

Vitamin B_{12}, in its reduced Co(I) form, is known to open the epoxide[18,27] ring from the less hindered side due to its "supernucleophilicity" in organic solvents. Based on our previous studies, for our preliminary studies we selected the ring-opening of 2-(phenoxymethyl)oxirane (**1**) with acrylonitrile (**2**) as a model reaction. Initially, hydrophobic heptamethyl cobyrinate (HME) as catalyst, Zn/NH_4Cl as a reducing agent were used in acetonitrile under blue LED irradiation. The reaction afforded desired product **3** in 43% yield (Table 1, entry 1). Replacement of HME with native

Table 1. Optimization Studies of the Ring Opening of Epoxide (1) with Acrylonitrile (2)[a]

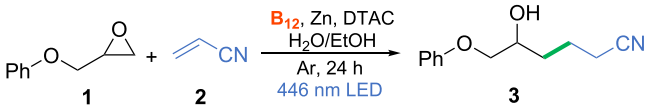

1 2 3

entry	deviation from standard conditions	yield **3** (%)[b]
1	HME, MeCN	43
2	2.5 equiv DTAC	59
3	2.5 mol% B_{12}	66
4	0.03 M	70
5	no additives	76
6	**none**	**85**
7	no light	n.d.
8	no B_{12}	n.d.
9	no Zn	n.d.

[a]Conditions: epoxide (**1**, 0.2 mmol), acrylonitrile (2, 1.5 equiv), B_{12} (5 mol %), Zn (3 equiv), DTAC (5 equiv), H_2O/EtOH (9:1, v/v, c = 0.04 M), blue LEDs (446 nm, 3 W), 24 h. [b]Yields determined by GC FID analysis, n.d. = not detected.

vitamin B_{12} and organic solvent with micellar solution (dodecyl trimethylammonium chloride, DTAC, as a surfactant) improved the yield up to 59% (entry 2). All tested cationic surfactants performed well, except for 1-hexadecylpyridinium bromide, which afforded only 31% of the desired product (see Supporting Information (SI) for more details). The use of DTAC eliminated also the need for NH_4Cl, which is typically required for B_{12}-catalyzed reactions.[28] On the contrary, anionic surfactants, such as potassium laurate and sodium lauryl sulfate (SLES), were less efficient in both reactions. Increasing the amount of the surfactant and vitamin B_{12} further improved yields (entries 2 and 3), while any changes in their concentrations decreased the efficacy of the reaction (entry 4). The addition of alcohol cosolvents significantly improved yields (entry 5), with ethanol proving the most effective (see SI). Alcohols are believed to integrate into the micellar interface, increasing its flexibility and enhancing the capacity of the hydrophobic microenvironment within the aqueous solution. This adjustment likely improves the permeability of the interface to organic compounds.[27] All other reaction parameters, including light source, light power, and substrate ratios, were also optimized (see SI). Under the optimized conditions—native vitamin B_{12}, Zn as a reductant, DTAC as a surfactant, and a H_2O/EtOH (9:1) solvent mixture, irradiated with blue light (446 nm)—the model reaction yielded the desired product in 85% yield (entry 6).

In parallel, the conditions for the aziridine ring-opening were optimized, building upon the selected parameters for epoxides (detailed optimization data can be found in the SI, with key differences highlighted in Table 2). Using 2-butyl-1-tosylazir-

Table 2. Optimization Studies of the Ring Opening of Aziridine (4) with Acrylonitrile (2)[a]

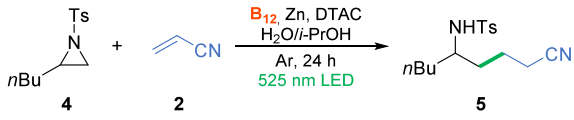

4 2 5

entry	deviation from standard conditions	yield **5** (%)[b]
1	3.5 equiv DTAC	57
2	2.5 mol% B_{12}	57
3	green LED (40 W)	61
4	***i*-PrOH**	**83, 80[c]**
5	no DTAC	29

[a]Conditions: aziridine (**4**, 0.2 mmol), acrylonitrile (2, 1.5 equiv), B_{12} (2.5 mol %), Zn (3 equiv), DTAC (3.5 equiv), H_2O/*i*PrOH (9:1, v/v, c = 0.04 M), green LEDs (525 nm, 40 W), 24 h. [b]Yields determined by GC FID analysis. [c]Isolated yield.

idine (**4**) and acrylonitrile (**2**) as model substrates, we found that reducing the amount of DTAC to 3.5 equiv and vitamin B_{12} to 2.5 mol % proved beneficial, enabling the synthesis of protected amine **5** in 57% (entries 1−2). Switching the light source from blue (446 nm) to green (525 nm) further improved the yield to 61% (entry 3).

Finally, the replacement of EtOH with *i*-PrOH as a cosolvent had the most significant impact (83%, entry 4). In this case, the model reaction proceeded even in the absence of DTAC, but given that both starting materials are liquids, it is plausible that this reaction partially occurs as an 'on-water' process (entry 5).

Vitamin B_{12} as a hydrophilic molecule should be found in the aqueous phase, but our theoretical studies indicate that in the Co(I)-form it is located at the micellar interface. Other and our studies clearly indicate that reactions in micellar solutions are strongly affected by the philicity of starting materials, in contrast to those performed in organic solvents.[26,29] For that reason, the alkyl chain length and functional groups that significantly influence the location of molecules within micellar solutions, affect the efficacy of the reaction. Consequently, we tested the behavior of structurally diverse epoxides but not tetra and three substituted, as for it has already been documented that these are not suitable substrates for vitamin B_{12}-catalyzed reactions (Scheme 2A).[18] These reactions yielded Markovnikov alcohol products in moderate to high yields (33−85%) in a fully regioselective manner. 2-(Phenoxymethyl)oxirane with (vinylsulfonyl)benzene as the acceptor afforded product **6** but in lower yields, while other ester-derived acceptors remained unreactive toward the

https://doi.org/10.1021/acs.orglett.5c01376
Org. Lett. XXXX, XXX, XXX−XXX

Scheme 2. Scope of the Giese Addition of Epoxides and Aziridines to Electrophilic Alkenes[a]

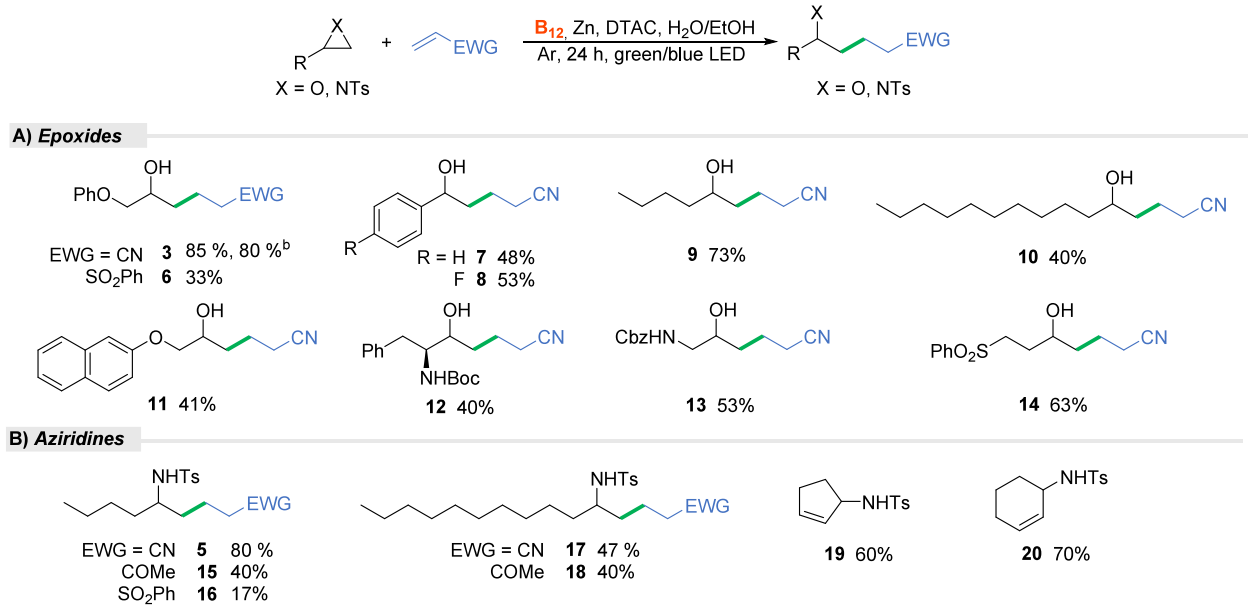

[a]Reaction conditions: A) epoxide (0.2 mmol), alkene (**2**, 1.5 equiv), B_{12} (5 mol %), Zn (3 equiv), DTAC (5 equiv), H_2O/EtOH (9:1, v/v) c = 0.04 M, blue LEDs (446 nm, 3 W), time 24 h. B) aziridine (0.2 mmol), alkene (1.5 equiv), B_{12} (2.5 mol %), Zn (3 equiv), DTAC (3.5 equiv), H_2O/*i*PrOH (9:1, v/v) c = 0.04 M, green LEDs (525 nm, 40 W), 24 h. [b]Reaction performed on a 1 mmol scale.

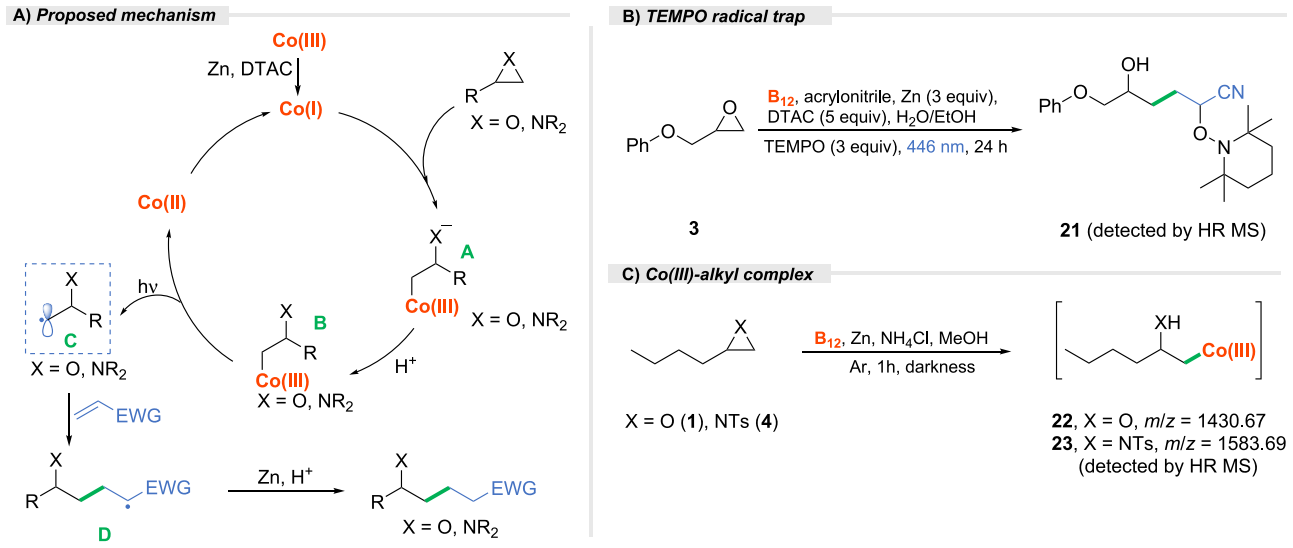

Figure 1. Mechanistic investigations: A) proposed reaction mechanism, B) detection of the product/TEMPO adduct, C) key mechanistic intermediates detected.

epoxide (see SI for details). These starting materials are less polar than acrylonitrile, and presumably they are buried deeper inside the micelle and become less accessible to the radical, presumably formed within the Stern layer. In such small molecules as Michael acceptors, philicity and, as a result, a location in the micelle is governed by an EWG group. For phenyloxirane, additional optimization was required, reducing the amount of surfactant and increasing acrylonitrile to 5 equiv was required to achieve a yield of 48% (**7**). A fluorine substituent in the *para* position of the aromatic ring (**8**) also afforded the desired product in 53% yield as a sole regioisomer. These both oxiranes are more hydrophobic substrates, therefore their contact with catalytically active vitamin B_{12} located at the interface is less favorable. Interestingly, the yield with *n*-butyl epoxide increased significantly to 73% (**9**), possibly because its shorter chain allows for greater mobility and facilitates proper orientation. The longer hydrophobic decyl derivative, provided nitrile **10** in 40% yield, probably due to the not optimal alignment of the starting materials within the micelle in contrast to reactions with arylbromides. Naphthalene and phenylethyl carbamate derivatives gave desired products **11**, **12** in lower yields of 41% and 40%, respectively. The benzylcarbamate and phenylsulfonyl derivatives were well tolerated as (**13** and **14** formed in good yields of 53% and 63%, respectively). Polar substituents present in these substrates have a stronger affinity for the interface, and as a result, the reaction occurs efficiently.

https://doi.org/10.1021/acs.orglett.5c01376
Org. Lett. XXXX, XXX, XXX−XXX

Furthermore, to prove the synthetic utility of the developed method, the model reaction was performed on a 1 mmol scale. The desired product was isolated in 80% yield.

Similar observations were made for the reaction of aziridines (Scheme 2B). The reaction of 2-butyl-1-tosylaziridine with a ketone-derived Michael acceptor afforded the desired product **15** in 40% yield, while for vinylsulfonylbenzene as the acceptor the yield substantially diminished (**16**). A broad range of other acrylates proved unreactive under these conditions (see SI). Therefore, the functional groups of acrylates have a substantial impact on their organization within the micelles. Increasing the alkyl chain length of the aziridines (**17**−**18**) gave comparable results regardless of the use of different Michael acceptors.

Further tests with various aziridines (see SI) revealed additional limitations of our method. Intriguingly, under the developed conditions, aryl aziridines and *N*-methyl- or *N*-dodecyl-substituted aziridines remained unreactive, with no conversion of starting materials nor the formation of ring-opened products observed. We hypothesize that the reaction occurs within the Stern layer, where the Co-catalyst's active form is located.[26] This requires the nitrogen atom to be oriented toward the interface, and hydrophobic protecting groups interfere with this necessary orientation within the micellar solution. Intriguingly, the azabicyclo derivatives, azabicyclohexane (**19**) and azabicycloheptane (**20**) led to allylamines of 60% and 70% in yields, respectively. Scheffold and Zhang reported the plausible mechanism for this process.[30] The aziridine ring is opened via the S_N2 mechanism to generate a Co(III)cycloalkyl derivative. Subsequent elimination occurs to yield the allylamine derivative.

Based on the mechanistic insights gained and prior reports, we propose the following reaction mechanism analogous to that observed in organic solvents (Figure 1A).[31−33] In the presence of Zn/DTAC, vitamin B_{12} is reduced to "super-nucleophilic" Co(I) species. The efficient reduction of Co(III) to Co(I) is indicated by a color change from pink to deep brown (see SI). This Co(I) species then attacks the less hindered side of the epoxide or aziridine ring, resulting in ring opening in a Markovnikov fashion and forming a Co(III)-alkyl anion intermediate **A**. Subsequently, protonation of intermediate **A** leads to the formation of alkylcobalamin intermediate **B**. Upon light irradiation, the homolytic cleavage of **B** generates a carbon-centered alkyl radical **C** and a Co(II) complex. The alkyl radical **C** is then captured by electron-deficient acrylonitrile to form radical intermediate **D**, which is further protonated to yield the final product.

Indeed, control experiments confirmed that light, vitamin B_{12}, and Zn are essential for the reaction to proceed (Table 1, entries 7−9; see SI). To further support the mechanistic pathway, a radical trap experiment with TEMPO was performed. It allowed to detect adduct **21** by HRMS analysis. (Figure 1B; see SI). This strongly suggests that a radical mechanism is at play and that radical **D** is an intermediate in the catalytic cycle. In the absence of acrylonitrile and light, ESI-MS analysis detected alkylcobalamin intermediates **22**−**23**, further proving the proposed mechanism (Figure 1C).

In summary, we have developed a regioselective epoxide- and aziridine ring-opening reaction catalyzed by vitamin B_{12} in the micellar system. This method successfully converted alkyl-/aryl epoxides and alkyl aziridines in the presence of acrylate derivatives to the desired products with moderate to good yields, forming a single regioisomer. Mechanistic studies support our proposed reaction pathway, which involves the initial ring-opening of strained molecules by the Co(I) species, followed by homolytic cleavage of the Co(III)−C bond to produce alkyl radicals.

Our work advances the use of vitamin B_{12} in catalysis, offering a sustainable strategy for the synthesis of important molecular structures and emphasizes the need for further insights into micellar catalysis which is now ongoing in our laboratory.

■ ASSOCIATED CONTENT

Data Availability Statement

The data underlying this study are available in the published article and the Supporting Information.

Supporting Information

The Supporting Information is available free of charge at https://pubs.acs.org/doi/10.1021/acs.orglett.5c01376.

Full description of optimization and mechanistic studies, general procedures, compound characterization (NMR, HRMS), and NMR spectra (PDF)

■ AUTHOR INFORMATION

Corresponding Author

Dorota Gryko − *Institute of Organic Chemistry, Polish Academy of Sciences, 01-224 Warsaw, Poland;* orcid.org/0000-0002-5197-4222; Email: dorota.gryko@icho.edu.pl

Authors

Kitti Franciska Szabó − *Institute of Organic Chemistry, Polish Academy of Sciences, 01-224 Warsaw, Poland;* orcid.org/0000-0001-6224-1342

Tomasz Wdowik − *Institute of Organic Chemistry, Polish Academy of Sciences, 01-224 Warsaw, Poland;* orcid.org/0000-0002-9840-1501

Aleksandra Krzeszewska − *Institute of Organic Chemistry, Polish Academy of Sciences, 01-224 Warsaw, Poland;* orcid.org/0000-0003-0549-7792

Krzysztof Mazurek − *Institute of Organic Chemistry, Polish Academy of Sciences, 01-224 Warsaw, Poland*

Martin P. Andersson − *Center for Integrative Petroleum Research, King Fahd University of Petroleum and Minerals, Dhahran 31261, Kingdom of Saudi Arabia;* orcid.org/0000-0002-4921-1461

Complete contact information is available at: https://pubs.acs.org/10.1021/acs.orglett.5c01376

Notes

The authors declare no competing financial interest.

■ ACKNOWLEDGMENTS

We thank National Science Centre, Poland (MAESTRO UMO-2020/38/A/ST4/00185) for funding this work.

■ REFERENCES

(1) Ferrier, R. C. J.; Pakhira, S.; Palmon, S. E.; Rodriguez, C. G.; Goldfeld, D. J.; Iyiola, O. O.; Chwatko, M.; Mendoza-Cortes, J. L.; Lynd, N. A. Demystifying the Mechanism of Regio- and Isoselective Epoxide Polymerization Using the Vandenberg Catalyst. *Macromolecules* **2018**, *51*, 1777−1786.

(2) Stewart, I. C.; Lee, C. C.; Bergman, R. G.; Toste, F. D. Living Ring-Opening Polymerization of *N*-Sulfonylaziridines: Synthesis of

High Molecular Weight Linear Polyamines. *J. Am. Chem. Soc.* **2005**, *127*, 17616−17617.
(3) Becker, D.; Kaczmarska, Z.; Arkona, C.; Schulz, R.; Tauber, C.; Wolber, G.; Hilgenfeld, R.; Coll, M.; Rademann, J. Irreversible Inhibitors of the 3C Protease of Coxsackie Virus through Templated Assembly of Protein-Binding Fragments. *Nat. Commun.* **2016**, *7*, 12761.
(4) McGregor, N. G. S.; Kuo, C.-L.; Beenakker, T. J. M.; Wong, C.-S.; Offen, W. A.; Armstrong, Z.; Florea, B. I.; Codée, J. D. C.; Overkleeft, H. S.; Aerts, J. M. F. G.; Davies, G. J. Synthesis of Broad-Specificity Activity-Based Probes for Exo-β-Mannosidases. *Org. Biomol. Chem.* **2022**, *20*, 877−886.
(5) Furniel, L. G.; Corrêa, A. G. Photochemical Synthesis and Ring-Opening of Aziridines and Epoxides: State-of-the-Art. *ChemPhotoChem.* **2024**, *8*, No. e202400120.
(6) Hansen, T.; Nin-Hill, A.; Codée, J. D. C.; Hamlin, T. A.; Rovira, C. Rational Tuning of the Reactivity of Three-Membered Heterocycle Ring Openings via SN2 Reactions. *Chem. − A Eur. J.* **2022**, *28*, No. e202201649.
(7) Xu, F.; Zeng, F.-W.; Luo, W.-J.; Zhang, S.-Y.; Huo, J.-Q.; Li, Y.-P. 2H-Azirines: Recent Progress in Synthesis and Applications. *Eur. J. Org. Chem.* **2024**, *27*, No. e202301292.
(8) Bonollo, S.; Lanari, D.; Vaccaro, L. Ring-Opening of Epoxides in Water. *Eur. J. Org. Chem.* **2011**, *2011*, 2587−2598.
(9) Thirumalaikumar, M. Ring Opening Reactions of Epoxides. A Review. *Org. Prep. Proced. Int.* **2022**, *54*, 1−39.
(10) Lu, P. Recent Developments in Regioselective Ring Opening of Aziridines. *Tetrahedron* **2010**, *66*, 2549−2560.
(11) Wang, C.; Luo, L.; Yamamoto, H. Metal-Catalyzed Directed Regio- and Enantioselective Ring-Opening of Epoxides. *Acc. Chem. Res.* **2016**, *49*, 193−204.
(12) Bera, P. S.; Mirza, Y. K.; Sachdeva, T.; Bera, M. Recent Advances in Transition Metal-Catalyzed Ring-Opening Reaction of Aziridine. *Compounds* **2024**, *4*, 626−649.
(13) Meninno, S.; Lattanzi, A. Epoxides: Small Rings to Play with under Asymmetric Organocatalysis. *ACS Org. Inorg. Au* **2022**, *2*, 289−305.
(14) Steiman, T. J.; Liu, J.; Mengiste, A.; Doyle, A. G. Synthesis of β-Phenethylamines via Ni/Photoredox Cross-Electrophile Coupling of Aliphatic Aziridines and Aryl Iodides. *J. Am. Chem. Soc.* **2020**, *142*, 7598−7605.
(15) Parasram, M.; Shields, B. J.; Ahmad, O.; Knauber, T.; Doyle, A. G. Regioselective Cross-Electrophile Coupling of Epoxides and (Hetero)Aryl Iodides via Ni/Ti/Photoredox Catalysis. *ACS Catal.* **2020**, *10*, 5821−5827.
(16) Lau, S. H.; Borden, M. A.; Steiman, T. J.; Wang, L. S.; Parasram, M.; Doyle, A. G. Ni/Photoredox-Catalyzed Enantioselective Cross-Electrophile Coupling of Styrene Oxides with Aryl Iodides. *J. Am. Chem. Soc.* **2021**, *143*, 15873−15881.
(17) Dongbang, S.; Doyle, A. G. Ni/Photoredox-Catalyzed $C(Sp_3)$−$C(Sp_3)$ Coupling between Aziridines and Acetals as Alcohol-Derived Alkyl Radical Precursors. *J. Am. Chem. Soc.* **2022**, *144*, 20067−20077.
(18) Potrząsaj, A.; Musiejuk, M.; Chaładaj, W.; Giedyk, M.; Gryko, D. Cobalt Catalyst Determines Regioselectivity in Ring Opening of Epoxides with Aryl Halides. *J. Am. Chem. Soc.* **2021**, *143*, 9368−9376.
(19) Potrząsaj, A.; Ociepa, M.; Chaładaj, W.; Gryko, D. Bioinspired Cobalt-Catalysis Enables Generation of Nucleophilic Radicals from Oxetanes. *Org. Lett.* **2022**, *24*, 2469−2473.
(20) Funk, B. E.; Pauze, M.; Lu, Y.-C.; Moser, A. J.; Wolf, G.; West, J. G. Vitamin B_{12} and Hydrogen Atom Transfer Cooperative Catalysis as a Hydride Nucleophile Mimic in Epoxide Ring Opening. *Cell Rep. Phys. Sci.* **2023**, *4*, 101372.
(21) Germán, L.; Cuevas, J. M.; Cobos, R.; Pérez-Alvarez, L.; Vilas-Vilela, J. L. Green Alternative Cosolvents to *N*-Methyl-2-Pyrrolidone in Water Polyurethane Dispersions. *RSC Adv.* **2021**, *11*, 19070−19075.
(22) La Sorella, G.; Strukul, G.; Scarso, A. Recent Advances in Catalysis in Micellar Media. *Green Chem.* **2015**, *17*, 644.
(23) Lipshutz, B. H.; Ghorai, S.; Cortes-Clerget, M. The Hydrophobic Effect Applied to Organic Synthesis: Recent Synthetic Chemistry "in Water.". *Chem. − Eur. J.* **2018**, *24*, 6672−6695.
(24) Brüss, L.; Jeyaseelan, R.; Kürschner, J. C. G.; Utikal, M.; Næsborg, L. Micellar Effects and Their Relevance in Photochemistry and Photocatalysis. *ChemCatChem.* **2023**, *15*, No. e202201146.
(25) Cybularczyk-Cecotka, M.; Predygier, J.; Crespi, S.; Szczepanik, J.; Giedyk, M. Photocatalysis in Aqueous Micellar Media Enables Divergent C−H Arylation and N-Dealkylation of Benzamides. *ACS Catal.* **2022**, *12*, 3543−3549.
(26) Wincenciuk, A.; Cmoch, P.; Giedyk, M.; Andersson, M. P.; Gryko, D. Aqueous Micellar Environment Impacts the Co-Catalyzed Phototransformation: A Case Study. *J. Am. Chem. Soc.* **2024**, *146*, 19828−19838.
(27) Su, H.; Walder, L.; Zhang, Z.; Scheffold, R.; Su et al., 1988. Asymmetric Catalysis by27. Vitamin B_{12}. The Isomerization of Achiral Epoxides to Optically Active Allylic Alcohols. *Helv. Chim. Acta* **1988**, *71*, 1073−1078.
(28) Peacock, H.; Blum, S. A. Single-Micelle and Single-Zinc-Particle Imaging Provides Insights into the Physical Processes Underpinning Organozinc Reactions in Water. *J. Am. Chem. Soc.* **2022**, *144*, 3285−3296.
(29) Milton, J. P.; Milanowski, A.; Andersson, M.; Gryko, D. Photochemical Cyclopropanation in Aqueous Micellar Media − Experimental and Theoretical Studies. *Chem. Commun.* **2024**, *60*, 4483−4486.
(30) Zhang, Z. Da; Scheffold, R. Asymmetric Catalysis by Vitamin B_{12}: The Isomerization of Achiral Aziridines to Optically Active Allylic Amines. *Helv. Chim. Acta* **1993**, *76*, 2602−2615.
(31) Ociepa, M.; Wierzba, A. J.; Turkowska, J.; Gryko, D. Polarity-Reversal Strategy for the Functionalization of Electrophilic Strained Molecules via Light-Driven Cobalt Catalysis. *J. Am. Chem. Soc.* **2020**, *142*, 5355−5361.
(32) Giedyk, M.; Gryko, D. Vitamin B_{12}: An Efficient Cobalt Catalyst for Sustainable Generation of Radical Species. *Chem. Catal* **2022**, *2*, 1534−1548.
(33) Wdowik, T.; Gryko, D. C−C Bond Forming Reactions Enabled by Vitamin B_{12}−Opportunities and Challenges. *ACS Catal.* **2022**, *12*, 6517−6531.

https://doi.org/10.1021/acs.orglett.5c01376
Org. Lett. XXXX, XXX, XXX−XXX

6. Supporting Information for the Original Publications

Note: NMR spectra are available online from the respective articles except for second publication.

Supporting Information

Site-selective, photocatalytic vinylogous amidation of enones

Kitti Franciska Szabó, Katarzyna Goliszewska, Jakub Szurmak, Katarzyna Rybicka-Jasińska*, Dorota Gryko*

*Institute of Organic Chemistry **P**olish Academy of Sciences*

Kasprzaka 44/52, 01-224 Warszaw, Poland

e-mail: dorota.gryko@icho.edu.pl

Table of Contents

General information

All solvents and commercially available reagents were purchased as reagent grade and were used without further purification, unless otherwise stated. Yields refer to spectroscopically (^{1}H NMR) homogeneous materials. Reactions were monitored by thin layer chromatography (TLC), using 0.20 mm Merck silica plates (60F-254) or 0.20 mm Merck aluminum oxide plates (60F-254) and visualized using UV-light or cerium molybdate and ninhydrin stain with heat as a developing agent. Colum chromatography was performed using Merck silica gel 60 (230-400 mesh) or Merck Al_2O_3 neutral (50-300 mesh) deactivated with 15 wt% of H_2O.

- NMR spectra were recorded on Bruker 400 MHz, Varian 500 or 600 MHz and calibrated using residual undeuterated solvent ($CHCl_3$ – 7.26 ppm ^{1}H NMR, 77.16 ppm ^{13}C NMR) or TMS as an internal reference.
- High-resolution mass spectra (HRMS) were recorded on a Waters AutoSpec Premier instrument using electron ionization (EI) or a Waters SYNAPT G2-S HDMS instrument using electrospray ionization (ESI) with time-of-flight detector (TOF).
- Elemental analysis (C, H, N, S) were performed using a PERKIN-ELMER 240 Elemental Analyzer.
- Melting points were recorded on a Marienfeld MPM-H2 melting point apparatus and are uncorrected.
- Preparative HPLC separations were performed using Knauer HPLC chromatograph with PDA detector and Preparative column chromatography Knauer EII 100-10 Si column (250 x 20 mm).
- Commercial reagents were purchased from Sigma-Aldrich, Alfa Aesar, TCI and AmBeed, and used as received unless otherwise noted.

1.2 Setup for photoreactions with aluminum cooling block

Photo-induced reactions were performed using a bottom plate irradiated vials in a specially constructed photoreactor with cooling by tap water and LED plate connected to constant current (0.7 A) power supply (Figure S1). The LED plates are commercially available radiators (Fischer Electronic part no. SK 105 100 SA) with 6 epoxy-glued star-cased 3 W LEDs connected in series. Reactions were carried out under blue light irradiation on a single diode (LT-2855 royal blue, λmax: 446 nm, 7W), distance from the reaction vessel: 6 mm.

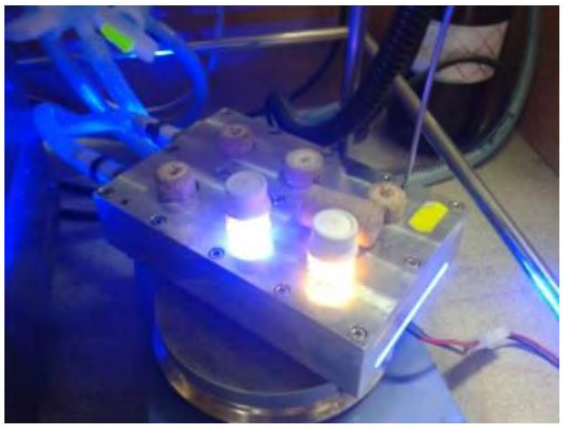

Figure S1.

1. General synthetic procedures

2.1. General synthetic procedure A - preparation of enol ethers

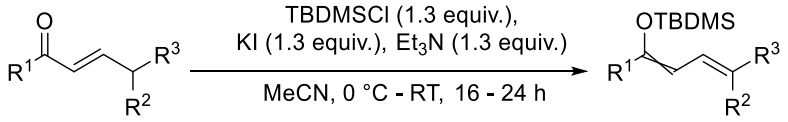

Scheme S1.

To a precooled to 0 °C solution of carbonyl compound (5.0 mmol, 1.0 equiv.) and KI (6.5 mmol, 1.3 equiv.) in anhydrous MeCN (0.5 M) under Ar atmosphere, Et_3N (6.5 mmol, 1.3 equiv) was added dropwise followed by the addition of TBDMSCl (6.5 mmol, 1.3 equiv. in one portion). The mixture was stirred for 16-24 h (determined by TLC) at room temperature. The reaction was quenched with $NaCl_{(sat.)}$ and then extracted with Et_2O. The organic solution was dried over Na_2SO_4, filtered, and concentrated in vacuo. The crude product was passed through deactivated the Al_2O_3 (neutral Al_2O_3 treated with 15 wt% of H_2O) plug using pentane as an eluent. The filtrate after evaporation was used for the next step without further purification.

2.2. General synthetic procedure B - preparation of enol ethers

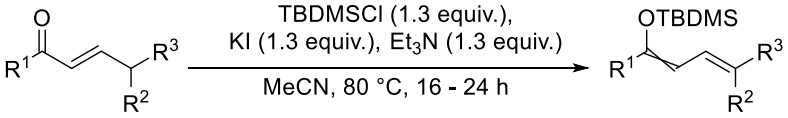

Scheme S2.

To a solution of carbonyl compound (5.0 mmol, 1.0 equiv.) and KI (6.5 mmol, 1.3 equiv.) in anhydrous MeCN (0.5 M) under Ar atmosphere, Et_3N (6.5 mmol, 1.3 equiv) was added dropwise followed by the addition of TBDMSCl (6.5 mmol, 1.3 equiv. in one portion). The reaction mixture was heated to 80 °C using a heating mantle and was stirred for 16-24 h (determined by TLC). The reaction was quenched with $NaCl_{(sat.)}$ and then extracted with Et_2O. The organic solution was dried over Na_2SO_4, filtered, and concentrated in vacuo. The crude product was passed through deactivated the Al_2O_3 (neutral Al_2O_3 treated with 15 wt% of H_2O) plug using pentane as an eluent. The filtrate after evaporation was used for the next step without further purification.

2.3. General synthetic procedure C - visible-light mediated amidation of enols

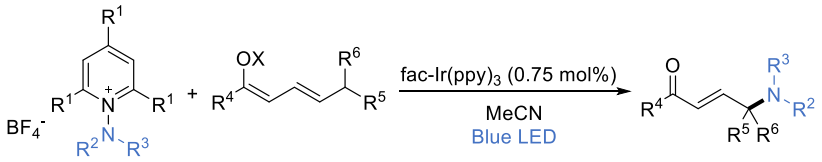

Scheme S3.

A glass vial equipped with a stirring bar and sealed with a septum was charged with an enol (if solid, 0.25 mmol, 1.0 equiv.), *fac*-Ir(ppy)$_3$ (0.01875 mmol, 0.75 mol%) and an *N*-aminopyridinium salt (0.33 mmol, 1.3 equiv.). Anhydrous MeCN (5 ml) was added, and the resulting mixture was degassed by argon bubbling for 20 minutes. Subsequently, (enol if liquid, 0.25 mmol, 1.0 equiv. was added) the reaction mixture was placed in a photoreactor and irradiated with blue LED for the time specified. Then, the mixture was transferred to a round-bottom flask and concentrated *in vacuo*. A crude product was purified by flash column chromatography using hexane/EtOAc mixture as an eluent.

2.4. General synthetic procedure D – preparation of enones

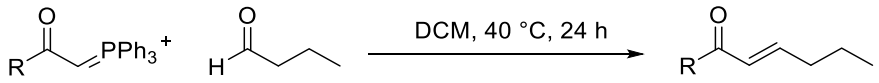

Scheme S4.

To a solution of phosphonium ylide (1.2 eq.) in dry DCM (15 ml) an aldehyde (1 eq.) was added dropwise. The mixture was refluxed (heating mantle as a heat source) until TLC showed full conversion (1-2 days). The solution was cooled, and the solvent was evaporated *in vacuo*. The product was purified by flash column chromatography using hexane, (pentane)/Et$_2$O mixture as eluent.

2.5 Procedure for 1 mmol-scale synthesis of (*E*)-N,4-dimethyl-*N*-(4-oxo-4-phenylbut-2-en-1-yl)benzenesulfonamide (P1)

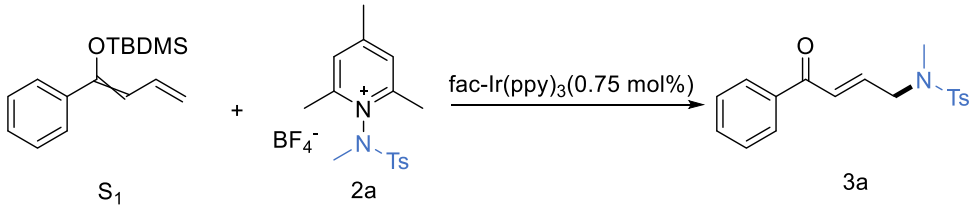

Scheme S5.

Following the general procedure **C** compound **3a** was obtained from tert-butyldimethyl((1-phenylbuta-1,3-dien-1-yl)oxy)silane (1 mmol) and 1-((*N*,4-dimethylphenyl)sulfonamido)-2,4,6-trimethylpyridinium tetrafluoroborate (1.3 mmol) (Figure S2) as yellow oil (245 mg) (**Yield = 74%**).

Figure S2.

2. Optimization details

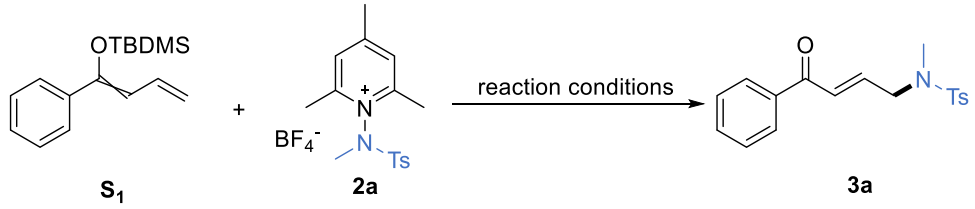

Scheme S5.

3.1 Table S1: Optimization of the substrate ratio[a]

Entry	Enol S1 [mmol]	Pyridinium salt 2a [mmol]	Ratio	Yield 3a[b] [%]
1	0.25	0.25	1:1	76
2	0.25	0.3	1:1.2	84
3	**0.325**	**0.25**	**1:1.3**	**90**
4	0.375	0.25	1:1.5	89

[a]Conditions: enol **S1** (0.25 mmol), salt **2a**, PC, MeCN (c = 0.05 M), ambient temperature (20-22 °C), 1 h under argon atmosphere, light source: blue LED diode (446 nm), [b]Isolated yield.

3.2 Table S2: Catalyst investigation and loading[a]

Entry	Catalyst	Catalyst loading [mol%]	Time [h]	Yield of 3a[b] [%]
1	$Ir(ppy)_3$	1	16	65
2	$Ir(ppy)_3$	1	1	84
3	$Ir(ppy)_3$	0.5	1	79
4	**$Ir(ppy)_3$**	**0.75**	**1**	**90**
5	$[Ir(dtbbpy)(ppy)_2PF_6$	1	1	20
6	$Ru(bpy)_3Cl_2•6H_2O$	1	1	5

[a]Conditions: enol **S1** (0.25 mmol), salt **2a**, PC, MeCN (c = 0.05 M), ambient temperature (20-22 °C), under argon atmosphere, light source: blue LED diode (446 nm), [b]Isolated yield.

3.3 Table S3: Influence of the light power[a]

Entry	Light Power [W]	Time [h]	Yield of 3a[b]
1	3	1	81
2	**6**	**1**	**90**
3	6	16	65
4	10	1	84

[a]Conditions: enol **S1** (0.25 mmol), salt **2a**, PC, MeCN (*c* = 0.05 M), ambient temperature (20-22 °C), under argon atmosphere, light source: blue LED diode (446 nm), [b]Isolated yield.

3.4 Table S4: Optimization of the reaction time[a]

Entry	Time [h]	Yield of 3a[b]
1	**1**	**90**
2	16	65

[a]Conditions: enol **S1** (0.25 mmol), salt **2a**, PC, MeCN (*c* = 0.05 M), ambient temperature (20-22 °C), under argon atmosphere, light source: blue LED diode (446 nm), [b]Isolated yield.

3. Mechanistic considerations

4.1 Proposed mechanism

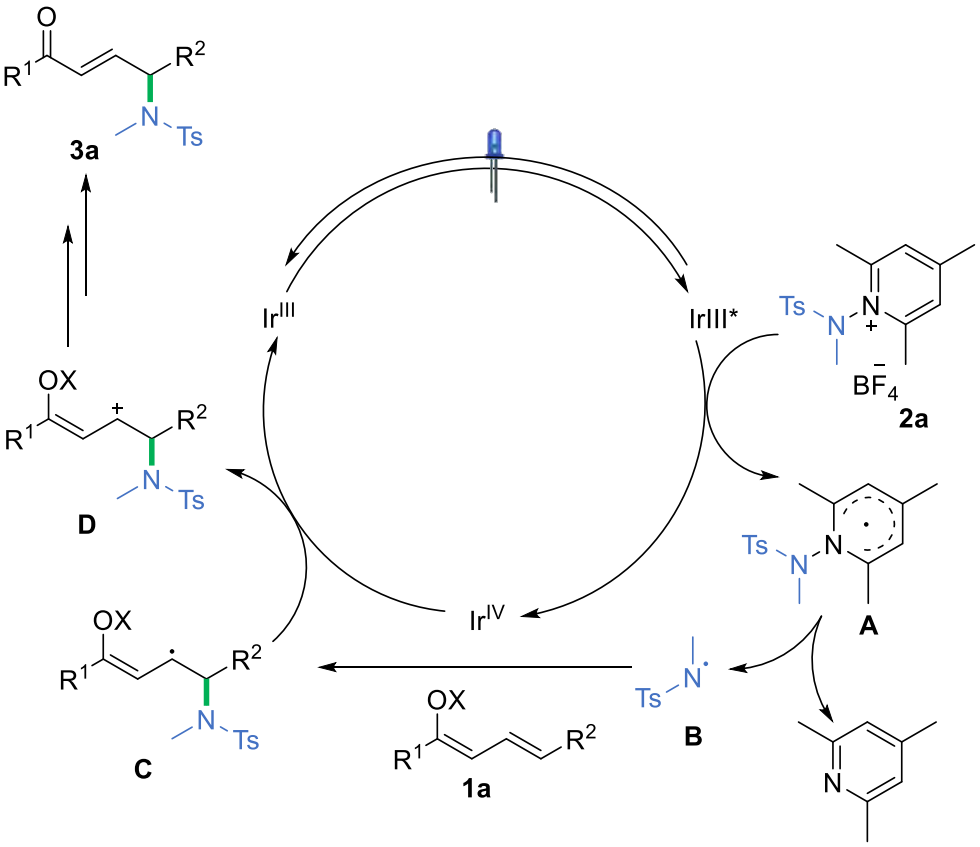

Scheme S6. Proposed reaction mechanism

4.2 Addition of 5,5-dimethyl-1-pyrroline *N*-oxide (DMPO)

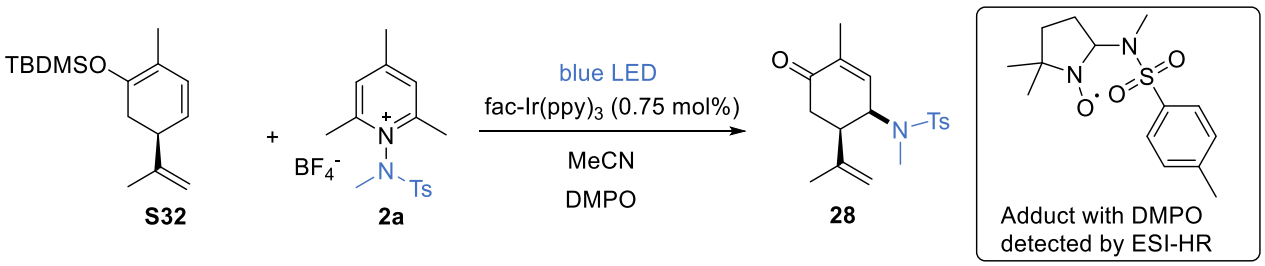

Scheme S7. Experiment with addition of DMPO[a]

[a]Reaction condition: Enol **S32** (0.25 mmol), salt **2a** (1.3 equiv.), $Ir(ppy)_3$ (0.75 mol%), DMPO (0.5 mmol), dry MeCN (c = 0.05 M), ambient temperature (20-22 °C), under Ar atmosphere was irradiated (blue LED, 446 nm)).

The assumed adduct formation with DMPO was confirmed by ESI-HRMS.

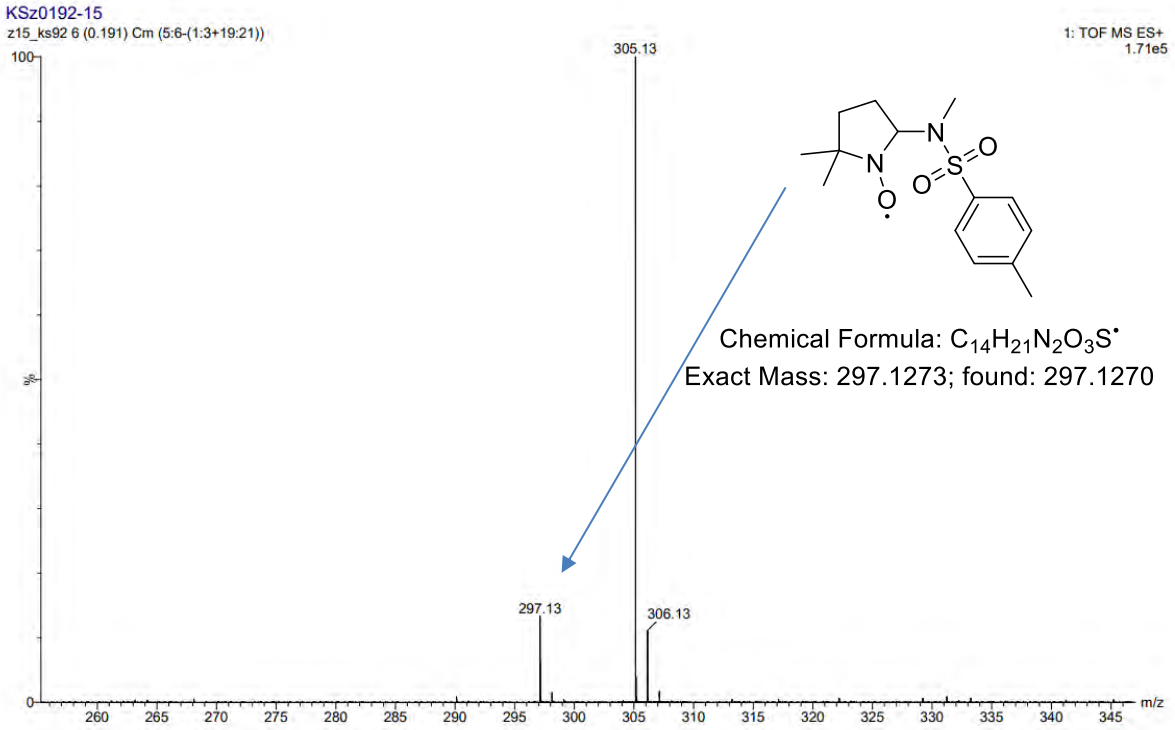

Figure S3. HRMS analysis of adduct form with DMPO

4.3 Addition of (2,2,6,6-tetramethylpiperidin-1-yl)oxyl (TEMPO)

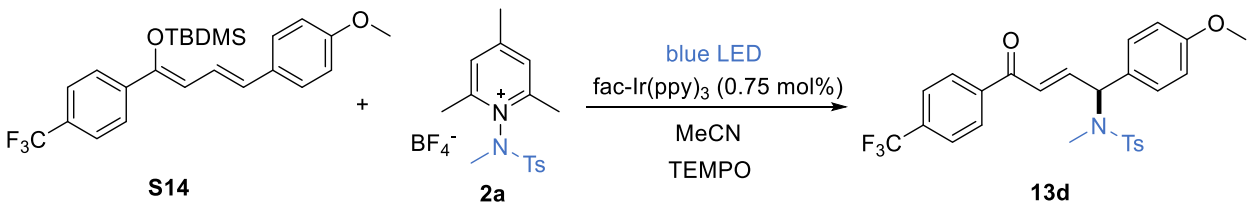

Scheme S8. Experiment with addition of TEMPO[a]

[a]Reaction condition: Enol **S14** (0.25 mmol), salt **2a** (1.3 equiv.), $Ir(ppy)_3$ (0.75 mol%), TEMPO (2 equiv.), dry MeCN (c = 0.05 M), ambient temperature (20-22 °C), under Ar atmosphere was irradiated (blue LED, 446 nm) for 1.5 hours. The reaction was checked by TLC- no product was observed - **reaction stopped**.

5. Scope and limitations, characterization of new compounds

5.1 Unsuccessful examples

ENTRY	SUBSTRATE	OUTCOME	PRODUCT
1	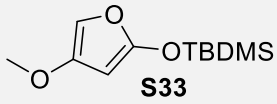 **S33**	**Hydrolysis to ketone**	-
2	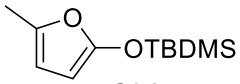 **S34**	**Hydrolysis to ketone**	-
3	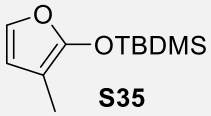 **S35**	**<5% of product**	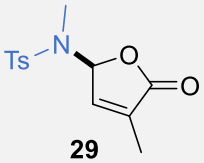 **29**
4	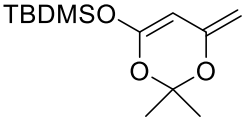 **S36**	**No conversion**	-
5	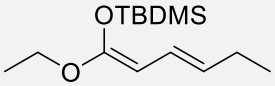 **S37**	**No conversion**	-
6	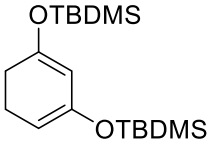 **S38**	**<1% of product**	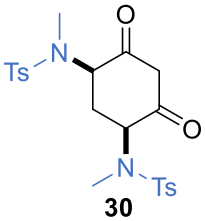 **30**
7	 **S39**	**<10% of product**	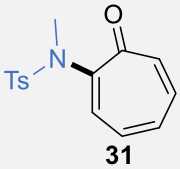 **31**
8	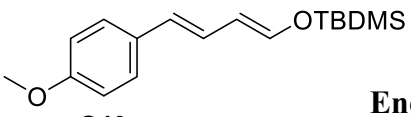 **S40**	**Enol degradation**	-

9	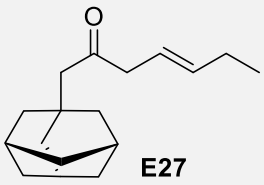 E27	No conversion	-
10	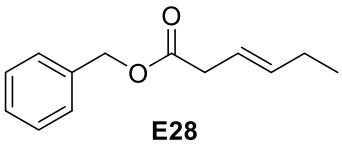 E28	No conversion	-
11	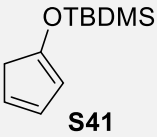 S41	Enol degradation	-
12	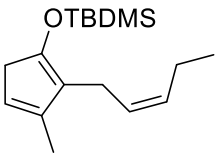 S42	Enol degradation	-
13	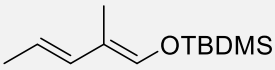 S43	<10% of product	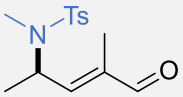 32
16	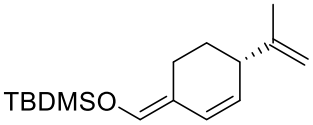 S44	<10% of product	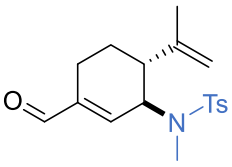 33
17	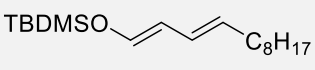 S45	18%	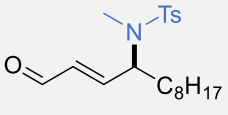 34

5.2 Enones

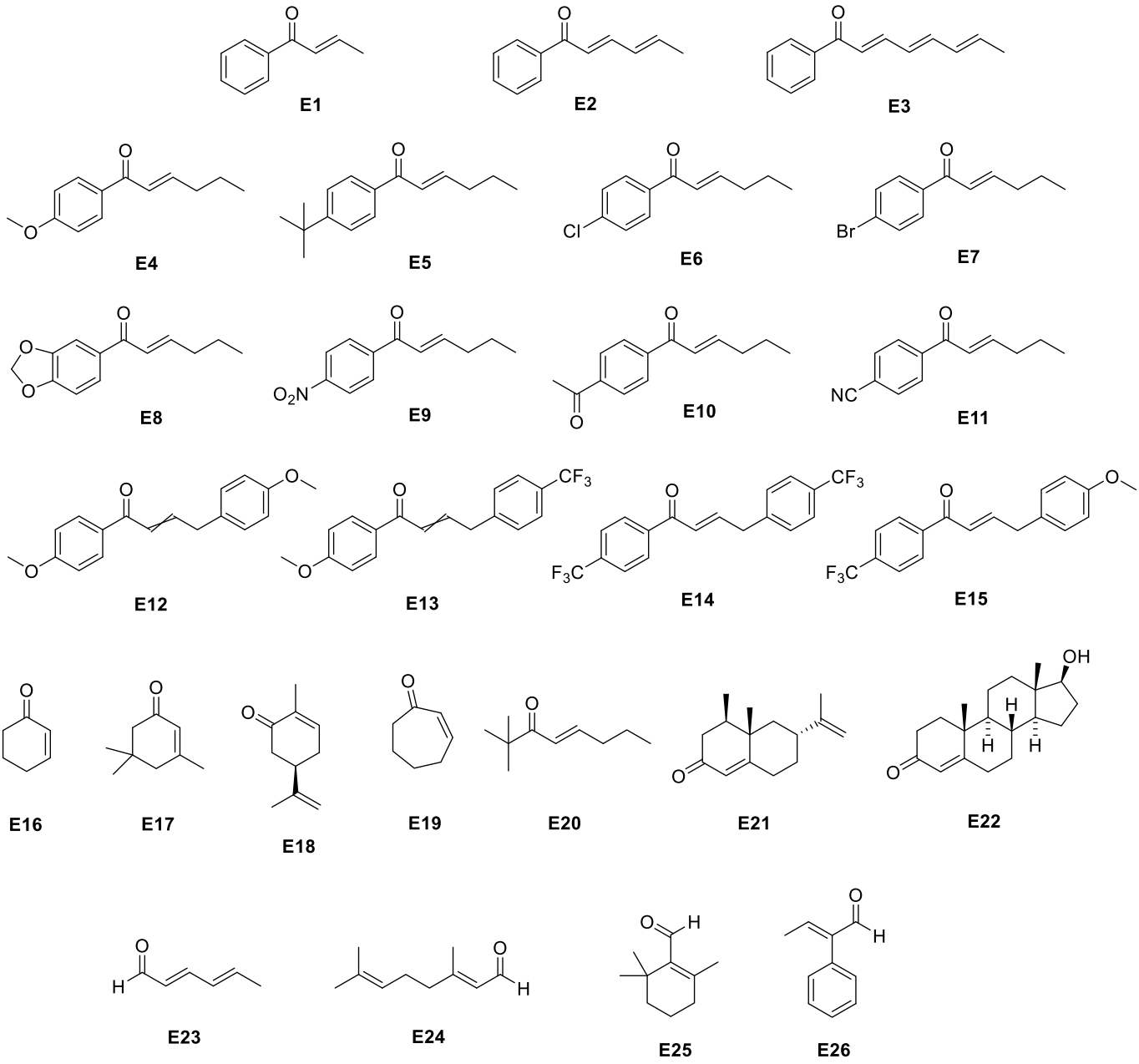

Compounds **E3**, **E9**, **E12**, **E13**, **E14**, **E15** and **E20** were prepared according to general procedure **D**. Compounds **E4**[1], **E5**[1], **E6**[1], **E7**[1], **E8**[1], **E10**[1] and **E11**[1] were prepared according to literature procedure.

Compounds **E1**, **E2**, **E16**, **E17**, **E18**, **E19**, **E21**, **E22**, **E23, E24, E25** and **E26** are commercially available reagents and were used without further purification.

5.2.1 (2*E*,4*E*,6*E*)-1-phenylocta-2,4,6-trien-1-one (E3)

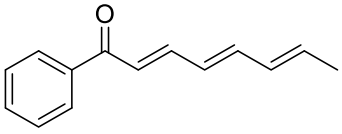

Following the general procedure **D** compound **E3** was obtained from 1-phenyl-2-(triphenyl-λ^5-phosphaneylidene)ethan-1-one (3.7 mmol) and (2*E*,4*E*)-hexa-2,4-dienal (18 mmol). The crude product was purified by column chromatography (5:95 AcOEt:Hex) to afford 0.37 g ketone (**E3**) as a white solid. (**Yield = 50%**).

NMR data matched those reported in the literature.[8]

^{1}H NMR (400 MHz, $CDCl_3$): δ 8.02 – 7.88 (m, 2H, Ph), 7.59 – 7.44 (m, 4H, COCH= and Ph), 6.96 – 5.74 (m, 5H, olefinic CH), 1.85 (d, *J* = 6.7 Hz, 3H, Me) ppm.

5.2.2 (*E*)-1-(4-methoxyphenyl)hex-2-en-1-one (E4)

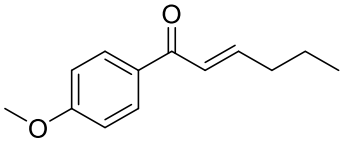

Following the literature procedure[1] compound **E4** was obtained from 1-(4-methoxyphenyl)ethan-1-one (7.5 mmol) and butyraldehyde (15 mmol). The crude product was purified by column chromatography (20:80 AcOEt:Hexane) to afford 0.23 g ketone (**E4**) as a colorless oil. (**Yield = 15% over 3 steps**).

NMR data matched those reported in the literature.[1]

^{1}H NMR (400 MHz, $CDCl_3$): δ 7.87 – 7.85 (m, 2H), 7.44 – 7.42 (m, 2H), 7.06 (dt, *J* = 15.3, 7.0 Hz, 1H), 6.82 (dt, *J* = 15.4, 1.4 Hz, 1H), 2.29 (qd, *J* = 7.3, 1.4 Hz, 2H), 1.56 (h, *J* = 7.4 Hz, 2H), 0.97 (t, *J* = 7.4 Hz, 3H) ppm.

5.2.3 (*E*)-1-(4-(*tert*-butyl)phenyl)hex-2-en-1-one (E5)

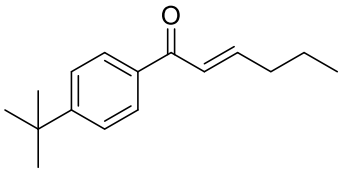

Following the literature procedure[1] compound **E5** was obtained from 1-(4-(tert-butyl)phenyl)ethan-1-one (7.5 mmol) and butyraldehyde (15 mmol). The crude product was purified by column chromatography (20:80 AcOEt:Hexane) to afford 0.95 g ketone (**E5**) as a yellow oil. (**Yield = 56% over 3 steps**).

^{1}H NMR (400 MHz, $CDCl_3$): δ 7.90 – 7.87 (m, 2H), 7.49 – 7.46 (m, 2H), 7.05 (dt, *J* = 15.4, 6.9 Hz, 1H), 6.88 (dt, *J* = 15.4, 1.4 Hz, 1H), 2.29 (qd, *J* = 7.2, 1.4 Hz, 2H), 1.56 (sext., *J* = 7.3 Hz, 2H), 1.35 (s, 9H), 0.97 (t, *J* = 7.4 Hz, 3H) ppm.

^{13}C NMR (126 MHz, $CDCl_3$): δ 190.5, 156.3, 149.2, 135.4, 128.5, 126.0, 125.4, 35.1, 34.8, 31.1, 21.5, 13.8 ppm.

HRMS (ESI) m/z: calcd. For $(C_{16}H_{22}O + Na)^+$: 253.1568, found: 253.1571.

Analytical HPLC:

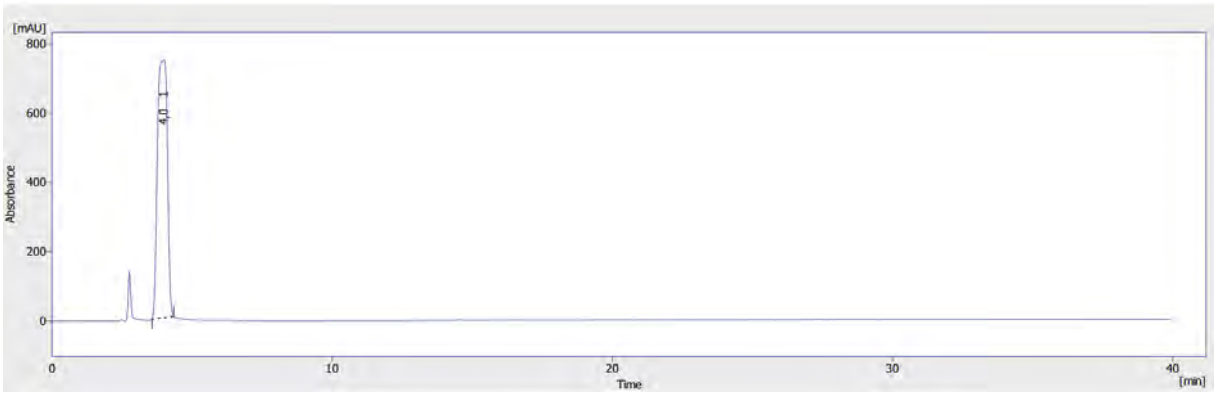

	Reten. Time [min]	Area [mAU.s]	Height [mAU]	Area [%]	Height [%]	W05 [min]	PDA Peak Purity	Compound Name	PDA Best Match Name	PDA Best Match
1	4,000	18330,178	745,353	100,0	100,0	0,42	922			
	Total	18330,178	745,353	100,0	100,0					

5.2.4 (*E*)-1-(4-chlorophenyl)hex-2-en-1-one (E6)

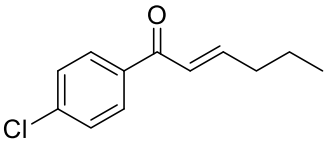

Following the literature procedure[1] compound **E6** was obtained from 1-(4-chlorophenyl)ethan-1-one (7.5 mmol) and butyraldehyde (15 mmol). The crude product was purified by column chromatography (10:90 AcOEt:Hexane) to afford 1.4 g ketone (**E6**) as a colorless oil. (**Yield = 89% over 3 steps**).

^{1}H NMR (500 MHz, $CDCl_3$): δ 7.89 – 7.84 (m, 2H), 7.46 – 7.40 (m, 2H), 7.06 (dt, *J* = 15.3, 7.0 Hz, 1H), 6.83 (dt, *J* = 15.4, 1.4 Hz, 1H), 2.29 (qd, *J* = 7.3, 1.4 Hz, 2H), 1.56 (sext., *J* = 7.4 Hz, 2H), 0.97 (t, *J* = 7.4 Hz, 3H) ppm.

^{13}C NMR (126 MHz, $CDCl_3$): δ 189.5, 150.4, 139.0, 136.3, 129.9, 128.8, 125.6, 34.9, 21.4, 13.7 ppm.

HRMS (ESI) m/z: calcd. for $(C_{12}H_{13}ClO + H)^+$: 209.0733, found: 209.0724.

Elemental analysis (%): calcd. for $C_{12}H_{13}ClO$: C 69.07, H 6.28; found: C 68.88, H 6.37.

5.2.5 (*E*)-1-(4-bromophenyl)hex-2-en-1-one (E7)

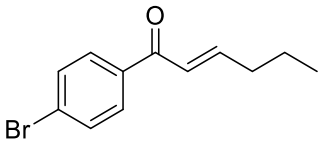

Following the literature procedure[1] compound **E7** was obtained from 1-(4-bromophenyl)ethan-1-one (7.5 mmol) and butyraldehyde (15 mmol). The crude product was purified by column chromatography (20:80 AcOEt:Hexane) to afford 0.74 g ketone (**E7**) as a yellow oil. (**Yield = 39% over 3 steps**).

^{1}H NMR (400 MHz, $CDCl_3$): δ 7.80 – 7.76 (m, 2H), 7.61 – 7.57 (m, 2H), 7.06 (dt, *J* = 15.4, 7.0 Hz, 1H), 6.82 (dt, *J* = 15.4, 1.5 Hz, 1H), 2.29 (qd, *J* = 7.2, 1.5 Hz, 2H), 1.55 (sext., *J* = 7.5 Hz, 2H), 0.97 (t, *J* = 7.4 Hz, 3H) ppm.

^{13}C NMR (126 MHz, $CDCl_3$): δ 189.7, 150.5, 136.7, 131.8, 130.0, 127.6, 125.5, 34.9, 21.4, 13.7 ppm.

HRMS (ESI) m/z: calcd. for $(C_{12}H_{13}BrO - H)^-$: 251.015, found: 251.0063.

Analytical HPLC:

	Reten. Time [min]	Area [mAU.s]	Height [mAU]	Area [%]	Height [%]	W05 [min]	PDA Peak Purity	Compound Name	PDA Best Match Name	PDA Best Match
1	4,217	21087,811	1374,941	100,0	100,0	0,27	882			
	Total	21087,811	1374,941	100,0	100,0					

5.2.6 (*E*)-1-(benzo[*d*][1,3]dioxol-5-yl)hex-2-en-1-one (E8)

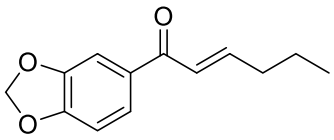

Following the literature procedure[1] compound **E8** was obtained from 1-(benzo[d][1,3]dioxol-5-yl)ethan-1-one (7.5 mmol) and butyraldehyde (15 mmol). The crude product was purified by column chromatography (5:95 Et_2O:Hexane) to afford 1.48 g ketone (**E8**) as a yellow oil. (**Yield = 90% over 3 steps**).

NMR data matched those reported in the literature.[1]

^{1}H NMR (400 MHz, $CDCl_3$): δ 7.54 (dd, *J* = 8.2, 1.7 Hz, 1H), 7.45 – 7.43 (m, 1H), 7.03 (dt, *J* = 15.3, 6.9 Hz, 1H), 6.87 – 6.79 (m, 2H), 6.03 (s, 2H), 2.28 (qd, *J* = 7.1, 1.5 Hz, 2H), 1.60 – 1.50 (m, 2H), 0.97 (t, *J* = 7.4 Hz, 3H) ppm.

5.2.8 (*E*)-1-(4-nitrophenyl)hex-2-en-1-one (E9)

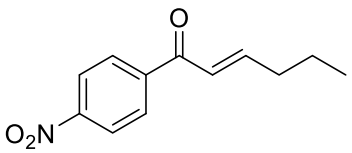

Following the general procedure **D** compound **E9** was obtained from 1-(4-nitrophenyl)-2-(triphenyl-λ^5-phosphaneylidene)ethan-1-one (3.3 mmol) and butyraldehyde (16.5 mmol). The crude product was purified by column chromatography (6:94 Et_2O:Hexane) to afford 0.51 g ketone (**E9**) as a yellow oil. (**Yield = 73% over 2 steps**).

^{1}H NMR (500 MHz, $CDCl_3$): δ 8.32 – 8.28 (m, 2H), 8.05 – 8.01 (m, 2H), 7.10 (dt, *J* = 15.4, 7.0 Hz, 1H), 6.83 (dt, *J* = 15.4, 1.5 Hz, 1H), 2.32 (qd, *J* = 7.2, 1.5 Hz, 2H), 1.56 (sext., *J* = 7.4 Hz, 2H), 0.98 (t, *J* = 7.4 Hz, 3H) ppm.

^{13}C NMR (126 MHz, $CDCl_3$): δ 189.4, 152.2, 150.0, 142.9, 129.4, 125.7, 123.7, 34.9, 21.3, 13.7 ppm.

HRMS (ESI) m/z: calcd. for $(C_{12}H_{13}NO_3 - H)^-$: 218.0895, found: 218.0819.

Analytical HPLC:

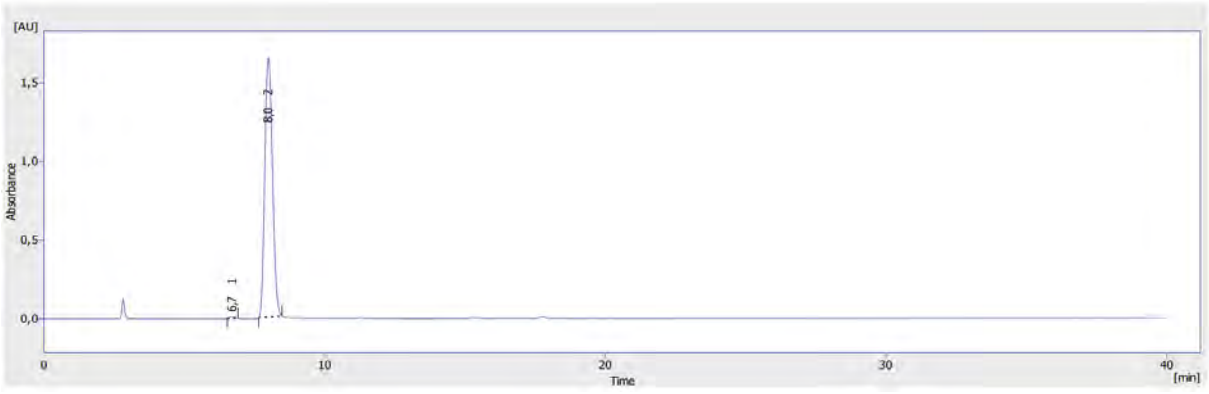

	Reten. Time [min]	Area [mAU.s]	Height [mAU]	Area [%]	Height [%]	W05 [min]	PDA Peak Purity	Compound Name	PDA Best Match Name	PDA Best Match
1	6,717	141,380	10,763	0,4	0,6	0,23	929			
2	8,000	31375,698	1648,726	99,6	99,4	0,32	915			
	Total	31517,077	1659,489	100,0	100,0					

5.2.9 (*E*)-1-(4-acetylphenyl)hex-2-en-1-one (E10)

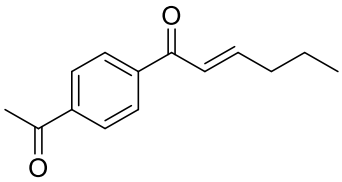

Following the literature procedure[1] compound **E10** was obtained from 1,1'-(1,4-phenylene)bis(ethan-1-one) (6.2 mmol) and butyraldehyde (12.3 mmol). The crude product was purified by column chromatography (20:80 AcOEt:Hexane) to afford 0.27 g ketone (**E10**) as a yellow oil in 20%.

^{1}H NMR (400 MHz, $CDCl_3$): δ 8.04 – 8.00 (m, 2H), 7.99 – 7.94 (m, 2H), 7.07 (dt, *J* = 15.4, 6.9 Hz, 1H), 6.85 (dt, *J* = 15.4, 1.5 Hz, 1H), 2.64 (s, 3H), 2.31 (qd, *J* = 7.3, 1.4 Hz, 2H), 1.56 (sext., *J* = 7.4 Hz, 2H), 0.98 (t, *J* = 7.4 Hz, 3H) ppm.
^{13}C NMR (101 MHz, $CDCl_3$): δ 190.5, 156.3, 149.2, 135.4, 128.5, 126.1, 125.4, 35.1, 34.8, 31.1, 21.5, 13.7 ppm.

HRMS (EI) m/z: calcd. for $C_{14}H_{16}O_2$: 216.1150, found: 216.1142.

Analytical HPLC:

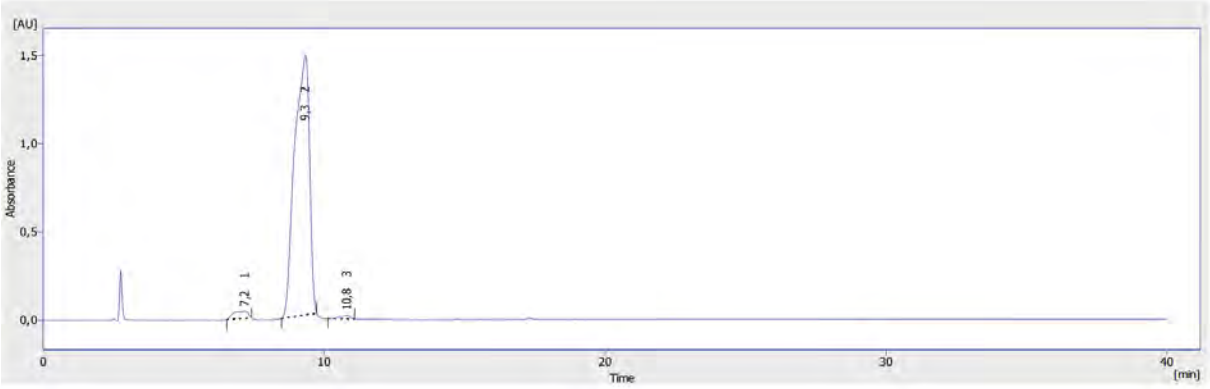

	Reten. Time [min]	Area [mAU.s]	Height [mAU]	Area [%]	Height [%]	W05 [min]	PDA Peak Purity	Compound Name	PDA Best Match Name	PDA Best Match
1	7,183	1465,306	39,317	2,6	2,6	0,63	922			
2	9,333	54118,134	1472,698	96,6	96,2	0,67	922			
3	10,817	433,641	19,324	0,8	1,3	0,43	998			
	Total	56017,081	1531,339	100,0	100,0					

5.2.10 (*E*)-4-(hex-2-enoyl)benzonitrile (E11)

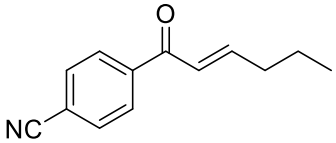

Following the literature procedure[1] compound **E11** was obtained from 4-acetylbenzonitrile (7.5 mmol) and butyraldehyde (15 mmol). The crude product was purified by column chromatography (20:80 AcOEt:Hexane) to afford 0.75 g ketone (**E11**) as a yellow oil. (**Yield = 50% over 3 steps**).

NMR data matched those reported in the literature.[1]

^{1}H NMR (400 MHz, $CDCl_3$): δ 8.00 – 7.95 (m, 2H), 7.78 – 7.74 (m, 2H), 7.09 (dt, *J* = 15.4, 7.0 Hz, 1H), 6.81 (dt, *J* = 15.4, 1.5 Hz, 1H), 2.31 (qd, *J* = 7.2, 1.5 Hz, 2H), 1.55 (sext., *J* = 7.4 Hz, 2H), 0.97 (t, *J* = 7.4 Hz, 3H) ppm.

5.2.11 1,4-bis(4-methoxyphenyl)but-2-en-1-one (*Z*/*E* mixture) (E12)

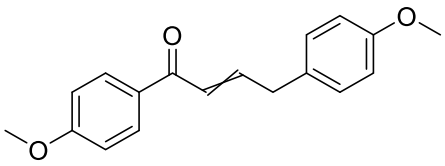

Following the general procedure **D** compound **E12** was obtained from 1-(4-methoxyphenyl)-2-(triphenyl-λ^5-phosphaneylidene)ethan-1-one (2.8 mmol) and 4-methoxybenzaldehyde (2.3 mmol). The crude product was purified by column chromatography (10:90 AcOEt:Hexane) to afford 0.55 g ketone (**E12**) as a white solid. (**Yield = 84% over 3 steps,** mixture of diastereoisomers ratio ~ 4:1).

^{1}H NMR (400 MHz, $CDCl_3$): (major) δ 7.91 (m, 2H), 7.13 (m, 2H), 6.88 (m, 6H), 6.82 3.86 (s, 3H), 3.80 (s, 3H), 3.57 (dd, *J* = 6.6, 1.2, 2H) ppm.

^{13}C NMR (400 MHz, $CDCl_3$): δ 189.0, 163.3, 158.4, 147.1, 132.27, 130.8, 130.6, 130.0, 129.8, 127.4, 126.2, 120.7, 114.1, 113.9, 113.8, 113.7, 55.4, 42.5, 38.1 ppm.

HRMS (ESI) m/z: calcd. for $(C_{18}H_{18}O_3 + Na)^+$: 305.1154, found: 305.1158.

Analytical HPLC:

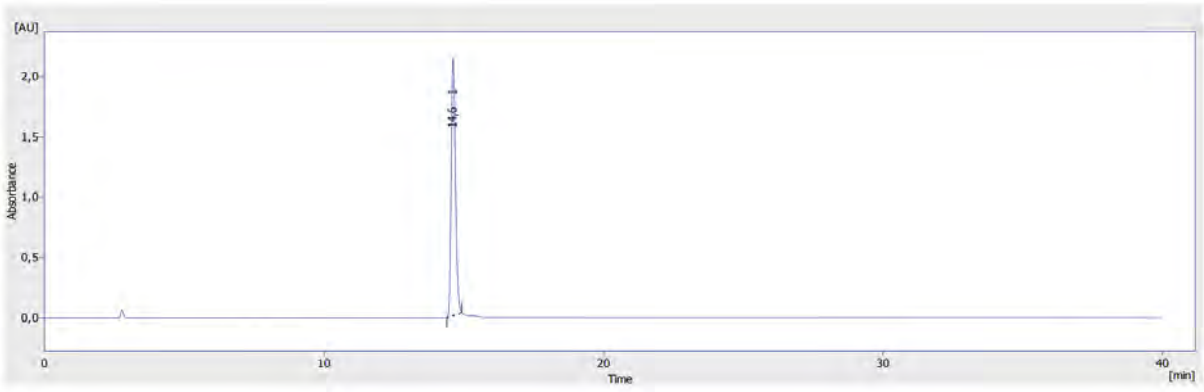

	Reten. Time [min]	Area [mAU.s]	Height [mAU]	Area [%]	Height [%]	W05 [min]	PDA Peak Purity	Compound Name	PDA Best Match Name	PDA Best Match
1	14,617	22597,238	2134,287	100,0	100,0	0,18	836			
	Total	22597,238	2134,287	100,0	100,0					

m.p.: 96-97 °C.

5.2.12 1-(4-methoxyphenyl)-4-(4-(trifluoromethyl)phenyl)but-2-en-1-one (*Z*/*E* mixture) (E13)

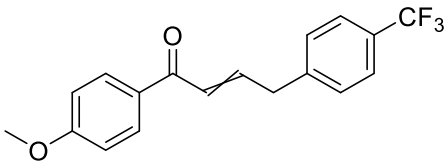

Following the general procedure **D** compound **E13** was obtained from 1-(4-methoxyphenyl)-2-(triphenyl-λ^5-phosphaneylidene)ethan-1-one (3.8 mmol) and 2-(4-(trifluoromethyl)phenyl)acetaldehyde (3.3 mmol). The crude product was purified by column chromatography (10:90 Et_2O:Hexane) to afford 0.58 g ketone (**E13**) as a colorless oil. (**Yield = 55% over 3 steps**, mixture diastereoisomers, ratio ~ 8:1).

^{1}H NMR (400 MHz, $CDCl_3$): (major) δ 7.98 (d, *J* = 8.9 Hz, 2H), 7.54 (d, *J* = 8.2 Hz, 2H), 7.46 (d, *J* = 8.1 Hz, 2H), 6.95 (d, *J* = 8.9 Hz, 2H), 6.58 (m, 2H), 3.88 (m, 5H) ppm.
^{13}C NMR (400 MHz, $CDCl_3$): (major) δ 196.04, 163.74, 140.50, 132.01, 130.60, 129.57, 126.41, 125.94, 125.51, 125.48, 125.45, 125.42, 113.90, 55.49, 42.23 ppm.
HRMS (ESI) m/z: calcd. For $(C_{18}H_{15}F_3O_2 + Na)^+$: 343.0922, found: 343.0921.
Analytical HPLC:

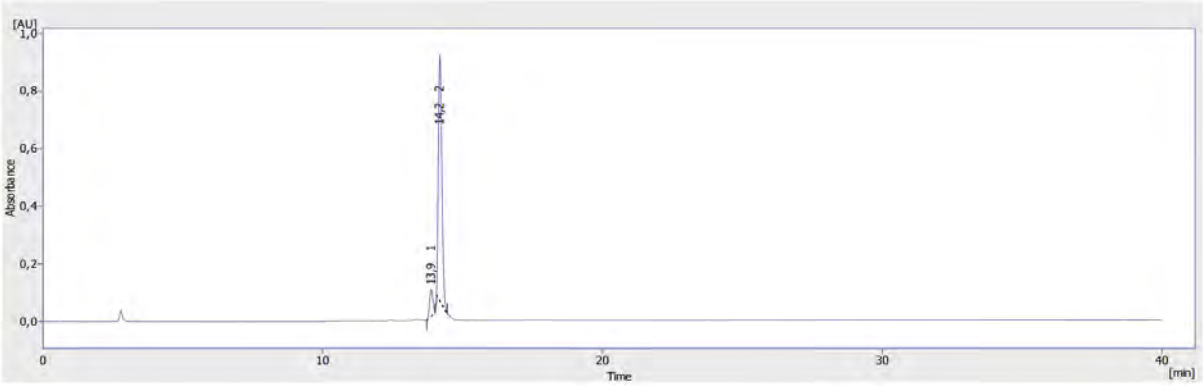

	Reten. Time [min]	Area [mAU.s]	Height [mAU]	Area [%]	Height [%]	W05 [min]	PDA Peak Purity	Compound Name	PDA Best Match Name	PDA Best Match
1	13,883	737,427	93,065	9,0	9,8	0,15	993			
2	14,183	7483,397	853,704	91,0	90,2	0,15	921			
	Total	8220,824	946,769	100,0	100,0					

5.2.13 (*E*)-1,4-bis(4-(trifluoromethyl)phenyl)but-2-en-1-one (E14)

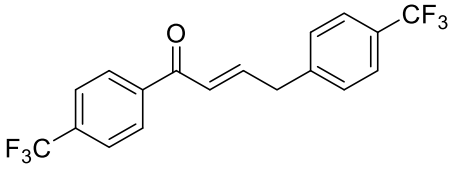

Following the general procedure **D** compound **E14** was obtained from 1-(4-(trifluoromethyl)phenyl)-2-(triphenyl-λ^5-phosphaneylidene)ethan-1-one (3.9 mmol) and 2-(4-(trifluoromethyl)phenyl)acetaldehyde (3.3

mmol). The crude product was purified by column chromatography (20:80 Et_2O:Hexane) to afford 0.27 g ketone (**E14**) as a yellow oil. (**Yield = 23% over 3 steps**).

^{1}H NMR (400 MHz, $CDCl_3$): δ 8.10 (d, *J* = 8.1 Hz, 2H), 7.76 (d, *J* = 8.4 Hz, 2H), 7.57 (d, *J* = 8.4 Hz, 2H), 7.48 (d, *J* = 8.2 Hz, 2H), 6.58 (m, 2H), 3.97 (d, *J* = 5.1 Hz, 2H) ppm.
^{13}C NMR (400 MHz, $CDCl_3$): δ 196.5, 140.2, 139.1, 134.9, 134.6, 132.8, 128.6, 126.5, 125.9, 125.8, 125.6, 125.5, 124.6,124.5, 42.7 ppm.
HRMS (ESI) m/z: calcd. for $(C_{18}H_{12}F_6O\text{-}H)^-$: 357.0792, found: 357.0711.
Analytical HPLC:

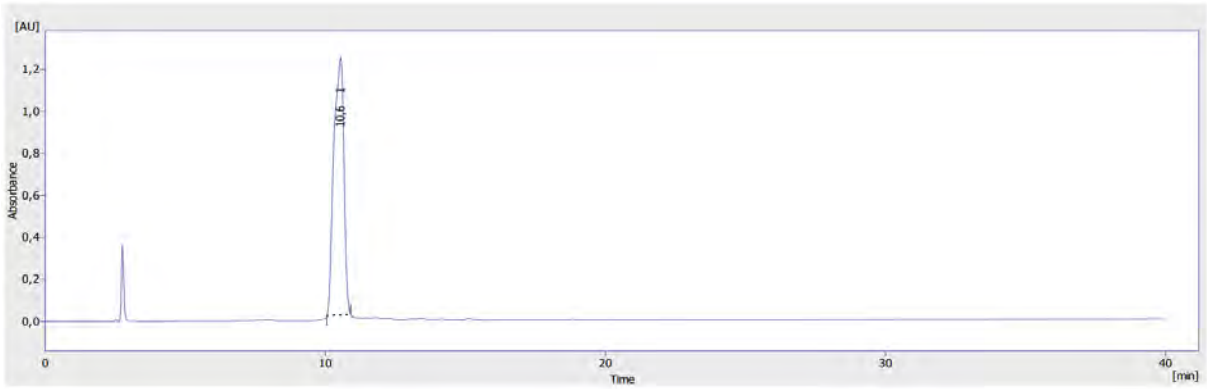

	Reten. Time [min]	Area [mAU.s]	Height [mAU]	Area [%]	Height [%]	W05 [min]	PDA Peak Purity	Compound Name	PDA Best Match Name	PDA Best Match
1	10,550	30631,966	1226,049	100,0	100,0	0,43	940			
	Total	30631,966	1226,049	100,0	100,0					

5.2.14 (*E*)-4-(4-methoxyphenyl)-1-(4-(trifluoromethyl)phenyl)but-2-en-1-one (E15)

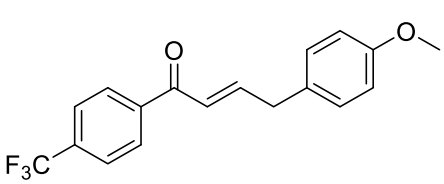

Following the general procedure **D** compound **E15** was obtained from 1-(4-(trifluoromethyl)phenyl)-2-(triphenyl-λ^5-phosphaneylidene)ethan-1-one (3.4 mmol) and 4-methoxybenzaldehyde (2.8 mmol). The crude product was purified by column chromatography (20:80 Et_2O:Hexane) to afford 0.16 g ketone (**E15**) as a yellow solid. (**Yield = 18% over 3 steps**).

^{1}H NMR (400 MHz, $CDCl_3$): δ 8.14 (d, *J* = 8.1 Hz, 1H), 8.00 (d, *J* = 8.1 Hz, 1H), 7.73 (dd, *J* = 16.5, 8.2 Hz, 2H), 7.31 (d, *J* = 8.7 Hz, 1H), 7.20 + 6.29 (dt, *J* = 15.4, 6.7 Hz, dt, *J* = 15.9, 6.84 1H), 7.13 (d, *J* = 8.6 Hz, 1H), 6.89 – 6.84 (m, 2H), 6.80 – 6.49 (m, 1H), 3.90 (dd, *J* = 6.8, 1.3 Hz, 1H), 3.80 (d, *J* = 2.4 Hz, 3H), 3.60 (dd, *J* = 6.5, 0.9 Hz, 1H) ppm.

^{13}C NMR (400 MHz, $CDCl_3$): δ 197.1, 190.0, 158.5, 149.7, 140.7, 139.3, 133.5, 129.8, 129.6, 129.4, 128.8, 128.7, 127.5, 126.2, 125.8, 125.7, 125.6, 125.5, 119.3, 114.2, 11 4.0, 55.3, 43.0, 38.2 ppm.

HRMS (ESI) m/z: calcd. for $(C_{18}H_{15}F_3O_2\text{-}H)^-$: 319.1024, found: 319.0945.

Analytical HPLC:

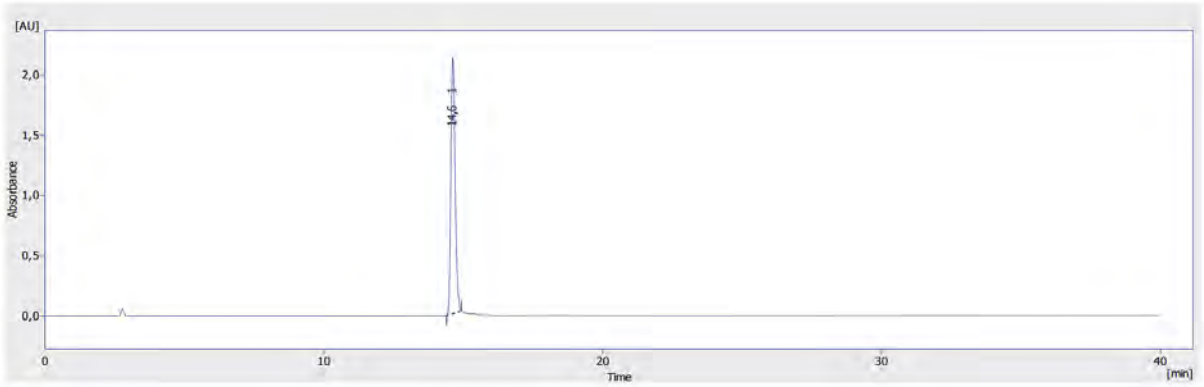

	Reten. Time [min]	Area [mAU.s]	Height [mAU]	Area [%]	Height [%]	W05 [min]	PDA Peak Purity	Compound Name	PDA Best Match Name	PDA Best Match
1	14,617	22597,238	2134,287	100,0	100,0	0,18	836			
	Total	22597,238	2134,287	100,0	100,0					

m.p.: 99-102 °C.

5.2.15 (*E*)-2,2-dimethyloct-4-en-3-one (E20)

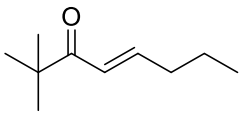

Following the general procedure **D** compound **E20** was obtained from 3,3-dimethyl-1-(triphenyl-λ^5-phosphaneylidene)butan-2-one (4.60 mmol) butyraldehyde (5.52 mmol). The crude product was purified by column chromatography (10:90 Et_2O:Pentane) to afford 0.39 g ketone (**E20**) as a yellow oil. (**Yield = 56% over 2 steps**).

NMR data matched those reported in the literature.[9]

^{1}H NMR (400 MHz, $CDCl_3$): major isomer δ 6.93 (dt, *J* = 15.2, 7.0 Hz, 1H), 6.49 (dt, *J* = 15.2, 1.5 Hz, 1H), 2.18 (qd, *J* = 7.2, 1.5 Hz, 2H), 1.49 (app sx, *J* = 7.4 Hz, 2H), 1.15 (s, 9H), 0.93 (t, *J* = 7.4 Hz, 3H) ppm.

5.3. Enols

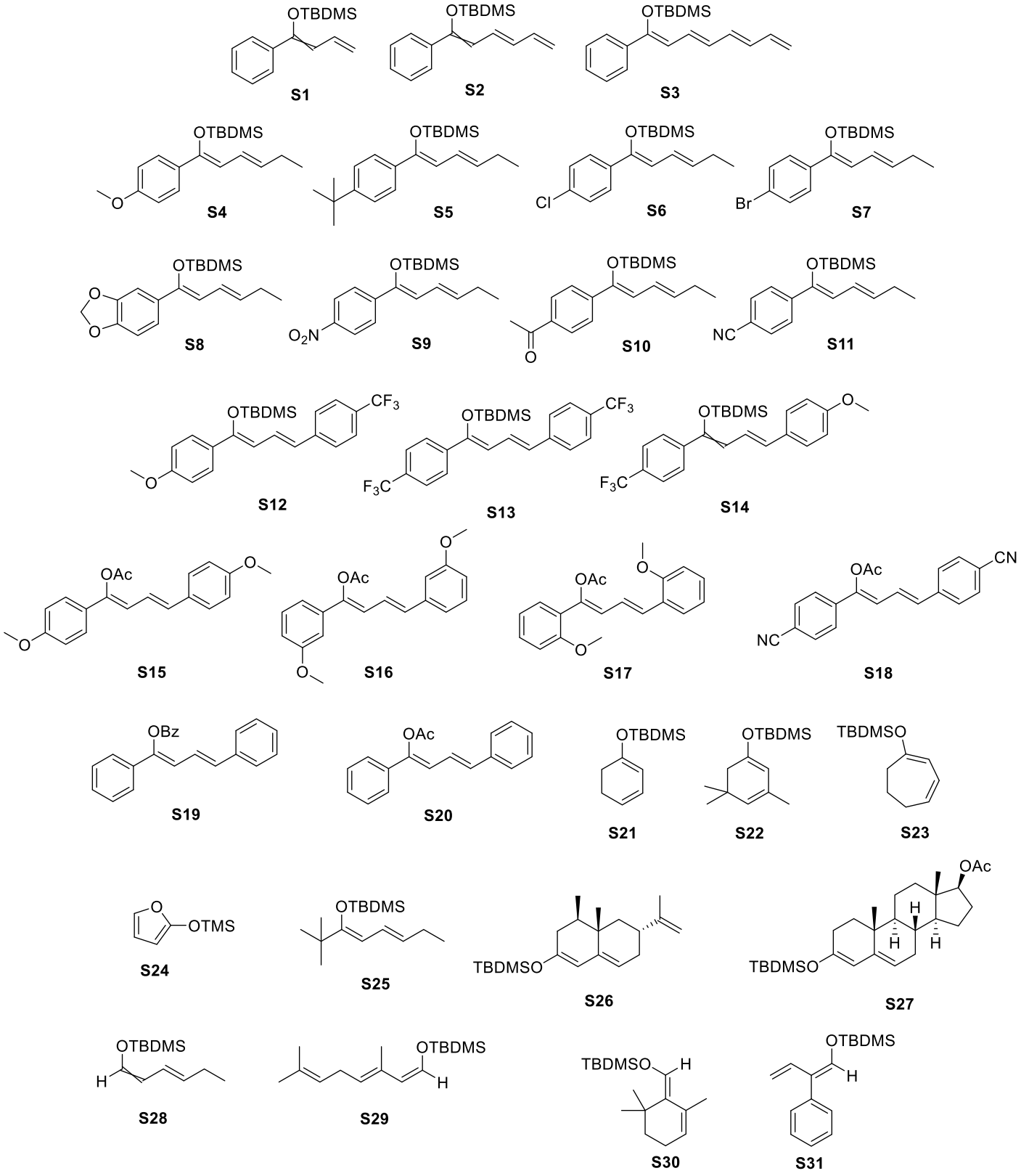
OTBDMS
S1
OTBDMS
S2
OTBDMS
S3
OTBDMS
O
S4
OTBDMS
S5
OTBDMS
Cl
S6
OTBDMS
Br
S7
OTBDMS
O
O
S8
OTBDMS
O_2N
S9
OTBDMS
O
S10
OTBDMS
NC
S11
OTBDMS
CF_3
O
S12
OTBDMS
CF_3
F_3C
S13
OTBDMS
O
F_3C
S14
OAc
O
O
S15
OAc
O
O
S16
OAc
O
O
S17
OAc
CN
NC
S18
OBz
S19
OAc
S20
OTBDMS
S21
OTBDMS
S22
TBDMSO
S23
O
OTMS
S24
OTBDMS
S25
TBDMSO
S26
OAc
H
H
H
TBDMSO
S27
OTBDMS
H
S28
OTBDMS
H
S29
TBDMSO
H
S30
OTBDMS
H
S31

Compounds **S1**, **S2**, **S3**, **S4**, **S5**, **S6**, **S7**, **S8**, **S10**, **S11**, **S12**, **S13**, **S14**, **S27** were prepared according to general procedure **B**.

Compounds **S23**, **S25**, **S28**, **S29**, **S30, S31** and **S32** were prepared according to general procedure **A**.

Compounds **S9**[7], **S15**[2], **S16**[2], **S17**[2], **S18**[2], **S19**[2], **S20**[2], **S21**[2], **S22**[3], **S26**[4] were prepared according to literature procedures.

Compound **S24** is commercially available and was used without further purification.

The crude product was passed through deactivated the Al_2O_3 (neutral Al_2O_3 treated with 15 wt% of H_2O) plug using pentane as an eluent. The filtrate after evaporation was used for the next step without further purification.

5.3.1 *tert*-butyldimethyl((1-phenylbuta-1,3-dien-1-yl)oxy)silane (*Z*/*E* mixture) (S1)

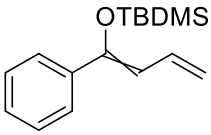

Following the general procedure **B** compound **S1** was obtained from 1-phenylbut-2-en-1-one (5.0 mmol). The reaction mixture was passed through a plug (deactivated, neutral Al_2O_3 treated with 15 wt% of H_2O) using hexane as an eluent. The crude product was used for the next step without further purification (1.18 g of compound **S1** as a colorless oil (**Yield = 91%**, 24 h, *Z*/*E* ratio ~ 1.1:1)).

^{1}H NMR (500 MHz, $CDCl_3$): δ 7.54–7.52 (m, 2H), 7.48–7.42 (m, 2H), 7.40–7.28 (m, 6H), 6.81 (dt, *J* = 17.1, 10.6 Hz, 1H), 6.51 (dt, *J* = 16.8, 10.6 Hz, 1H), 5.97 (d, *J* = 10.8 Hz, 1H), 5.82 (d, *J* = 11.1 Hz, 1H), 5.22 (dd, *J* = 17.1, 1.4 Hz, 1H), 5.13 (dd, *J* = 16.8, 1.5 Hz, 1H), 5.04 (dd, *J* = 10.3, 1.4 Hz, 1H), 4.88 (dd, *J* = 10.3, 1.5 Hz, 1H), 1.05 (s, 9H), 0.97 (s, 9H), 0.12 (s, 6H), 0.02 (s, 6H) ppm.

^{13}C NMR (125 MHz, $CDCl_3$): δ 153.3, 150.8, 138.9, 137.5, 133.7, 132.0, 128.8, 128.2, 128.0, 128.0, 127.9, 125.9, 114.2, 113.2, 112.7, 112.5, 25.9, 25.7, 18.4, 18.2, -4.0, -4.4 ppm.

HRMS (EI, *m/z*): calcd. for $C_{16}H_{24}OSi$: 260.1596; found: 260.1592.

5.3.2 *tert*-butyldimethyl(((3*E*)-1-phenylhexa-1,3,5-trien-1-yl)oxy)silane (*Z*/*E* mixture) (S2)

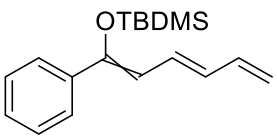

Following the general procedure **B** compound **S2** was obtained from 1-phenylhexa-2,4-dien-1-one (3.5 mmol, prepared according to literature procedure[4]). The reaction mixture was passed through a plug (deactivated, neutral Al_2O_3 treated with 15 wt% of H_2O) using hexane as an eluent. The crude product was used for the next step without further purification (0.68 g of compound **S2** as a yellow oil (**Yield = 68%**, 20 h, *Z*/*E* ratio ~ 1.5:1)).

^{1}H NMR (600 MHz, $CDCl_3$): δ 7.51 – 7.49 (m, 2H), 7.44 – 7.42 (m, 2H), 7.36 (t, *J* = 7.3 Hz, 1H), 7.33 – 7.29 (m, 2H + 1H), 7.26 (t, *J* = 7.3 Hz, 2H), 6.66 (ddd, *J* = 15.1, 11.1, 0.6 Hz, 1H), 6.48 – 6.37 (m, 1H + 1H), 6.34 – 6.15 (m, 1H + 2H), 5.99 (dd, *J* = 11.1, 0.5 Hz, 1H), 5.79 (d, *J* = 11.4 Hz, 1H), 5.20 (dt, *J* = 16.9, 1.8 Hz, 1H), 5.12 (dt, *J* = 16.8, 0.8 Hz, 1H), 5.04 (dt, *J* = 10.1, 0.7 Hz, 1H), 4.97 (dt, *J* = 10.1, 0.7 Hz, 1H), 1.03 (s, 9H), 0.94 (s, 9H), 0.09 (s, 6H), -0.00 (s, 6H) ppm.

^{13}C NMR (150 MHz, $CDCl_3$): δ 153.7, 151.4, 138.7, 137.8, 137.5, 137.4, 130.5, 130.2, 130.0, 128.73, 128.71, 128.3, 128.03, 127.96, 127.9, 125.7, 115.7, 114.8, 112.1, 111.8, 25.9, 25.7, 18.4, 18.2, -4.0, -4.4 ppm.

HRMS (EI, *m/z*): calcd. for $C_{18}H_{26}OSi$: 286.1753; found: 286.1758.

5.3.3 *tert*-butyldimethyl(((1*Z*,3*E*,5*E*)-1-phenylocta-1,3,5,7-tetraen-1-yl)oxy)silane (S3)

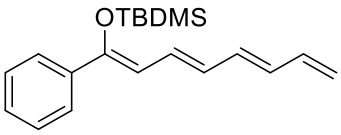

Following the general procedure **B** compound **S3** was obtained from (2*E*,4*E*,6*E*)-1-phenylocta-2,4,6-trien-1-one (2.5 mmol). The reaction mixture was passed through a plug (deactivated, neutral Al_2O_3 treated with 15 wt% of H_2O) using hexane as an eluent. The crude product was used for the next step without further purification (0.29 g of compound **S3** as a yellow oil (**Yield = 38%**)).

^{1}H NMR (400 MHz, $CDCl_3$): δ 7.58 – 7.17 (m, 6H), 6.94 – 4.94 (m, 7H), 1.07 – 0.99 (m, 9H), 0.02 – -0.02 (m, 6H) ppm.

^{13}C NMR (400 MHz, $CDCl_3$): δ 151.13, 138.7,137.3, 134.3, 132.1, 130.7, 130.6, 129.9, 129.1, 128.1, 128.0, 125.7, 116.5, 112.3, 25.9, 25.7, 18.5 ppm.

HRMS (APCI, *m/z*): calcd. for $(C_{20}H_{28}OSi + H)^+$: 313.1988; found: 313.1983.

5.3.4 *tert*-butyl(((1*Z*,3*E*)-1-(4-methoxyphenyl)hexa-1,3-dien-1-yl)oxy)dimethylsilane (S4)

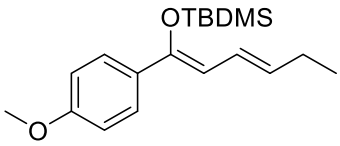

Following the general procedure **B** compound **S4** was obtained from (*E*)-1-(4-methoxyphenyl)hex-2-en-1-one (1.2 mmol). The reaction mixture was passed through a plug (deactivated, neutral Al_2O_3 treated with 15 wt% of H_2O) using hexane as an eluent. The crude product was used for the next step without further purification (0.27 g of compound **S4** as a yellow oil (**Yield = 70%**)).

^{1}H NMR (400 MHz, $CDCl_3$): δ 7.45 – 7.36 (m, 2H), 6.91 – 6.82 (m, 2H), 6.48 – 5.19 (m, 3H), 3.82 (dd, *J* = 7.1, 3.7 Hz, 3H), 2.25 – 2.02 (m, 2H), 1.06 – 1.01 (m, 9H), 0.95 – 0.92 (m, 3H), 0.10 (d, *J* = 15.4 Hz, 2H), 0.00 (d, *J* = 4.8 Hz, 4H) ppm.

^{13}C NMR (500 MHz, $CDCl_3$): δ 159.4, 159.2, 150.2, 148.4, 132.8, 132.4, 131.8, 131.0, 130.4, 130.01, 129.9, 126.9, 125.7, 124.4, 122.8, 113.4, 113.1, 111.5, 110.6, 106.8, 106.0, 55.2, 25.9, 25.7, 21.2, 18.4, 18.2, 14.3, 14.0, 13.6, -4.0, -4.4 ppm.

HRMS (EI, *m/z*): calcd. for $(C_{19}H_{30}O_2Si + H)^+$: 319.2093; found: 319.2078.

5.3.5 *tert*-butyl(((1*Z*,3*E*)-1-(4-(tert-butyl)phenyl)hexa-1,3-dien-1-yl)oxy)dimethylsilane (S5)

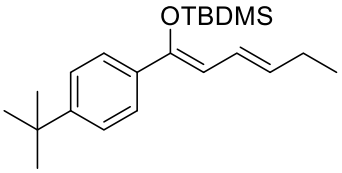

Following the general procedure **B** compound **S5** was obtained from (*E*)-1-(4-(tert-butyl)phenyl)hex-2-en-1-one (2.2 mmol). The reaction mixture was passed through a plug (deactivated, neutral Al_2O_3 treated with 15 wt% of H_2O) using hexane as an eluent. The crude product was used for the next step without further purification (0.35 g of compound **S5** as a yellow oil (**Yield = 47%**)).

^{1}H NMR (400 MHz, $CDCl_3$): δ 7.46 – 7.28 (m, 4H), 6.52 – 5.34 (m, 3H), 2.28 – 2.02 (m, 2H), 1.35 – 1.29 (m, 9H), 1.09 – 0.92 (m, 12H), 0.02 (d, *J* = 4.5 Hz, 6H) ppm.

^{13}C NMR (400 MHz, $CDCl_3$): δ 150.6, 148.6, 136.1, 133.2, 125.5, 125.3, 124.8, 124.5, 111.3, 34.5, 31.3, 25.9, 18.4, 13.6, -3.9 ppm.

HRMS (EI, *m/z*): calcd. for $(C_{22}H_{36}OSi + H)^+$: 345.2614; found: 345.2611.

5.3.6 *tert*-butyl(((1*Z*,3*E*)-1-(4-chlorophenyl)hexa-1,3-dien-1-yl)oxy)dimethylsilane (S6)

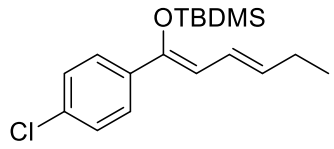

Following the general procedure **B** compound **S6** was obtained from (*E*)-1-(4-chlorophenyl)hex-2-en-1-one (0.96 mmol). The reaction mixture was passed through a plug (deactivated, neutral Al_2O_3 treated with 15 wt% of H_2O) using hexane as an eluent. The crude product was used for the next step without further purification (0.08 g of compound **S6** as a yellow oil (**Yield = 26%**)).

^{1}H NMR (400 MHz, $CDCl_3$): δ 7.45 – 7.27 (m, 4H), 6.55 – 6.31 (m, 1H), 6.15 – 5.95 (m, 1H), 5.81 – 5.59 (m, 1H), 2.25 – 2.03 (m, 2H), 1.09 – 0.78 (m, 12H), 0.14 – -0.06 (m, 6H) ppm.

^{13}C NMR (400 MHz, $CDCl_3$): δ 158.0, 151.1, 149.2, 147.4, 137.9, 137.7, 136.3, 134.4, 133.8, 133.6, 133.4, 133.2, 132.5, 132,2, 131.2, 130.1, 129.9, 129.7, 128.7, 128.2, 128.1, 128.0, 127.0, 126.8, 125.0, 124.5, 124.1, 123.7, 122.4, 112.8, 112.4, 108.0, 107.7, 106.2, 106.1, 25.8, 25.7, 21.5, 21.3, 21.1, 18.4, 18.1, 14.2, 13.9, 13.5, 12.2, -4.0, -4.4 ppm.

HRMS (EI, *m/z*): calcd. for $(C_{18}H_{27}ClOSi + H)^+$: 323.1598; found: 323.1588.

5.3.7 (((1*Z*,3*E*)-1-(4-bromophenyl)hexa-1,3-dien-1-yl)oxy)(tert-butyl)dimethylsilane (S7)

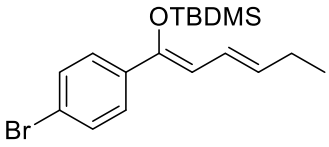

Following the general procedure **B** compound **S7** was obtained from (*E*)-1-(4-bromophenyl)hex-2-en-1-one (2.4 mmol). The reaction mixture was passed through a plug (deactivated, neutral Al_2O_3 treated with 15 wt% of H_2O) using hexane as an eluent. The crude product was used for the next step without further purification (0.73 g of compound **S7** as a yellow oil (**Yield = 83%**)).

^{1}H NMR (400 MHz, $CDCl_3$): δ 7.48 – 7.30 (m, 4H), 6.45 – 5.24 (m, 3H), 2.25 – 2.02 (m, 2H), 1.02 – 1.01 (m, 3H), 0.94 – 0.87 (m, 9H), 0.11 – 0.00 (m, 6H) ppm.

^{13}C NMR (400 MHz, $CDCl_3$): δ 136.8, 134.5, 133.8, 132.6, 131.2, 131.1, 131.0, 130.2, 127.3, 127.1, 125.0, 124.1, 123.7, 122.5, 121.3, 112.9, 112.5, 108.0, 107.8, 26.0, 25.9, 25.7, 21.3, 21.1, 18.4, 18.1, 13.5, -2.9, -4.0, -4.4 ppm.

HRMS (EI, *m/z*): calcd. for $(C_{18}H_{27}BrOSi + H)^+$: 367.1093; found: 367.1084.

5.3.8 (((1*Z*,3*E*)-1-(benzo[*d*][1,3]dioxol-5-yl)hexa-1,3-dien-1-yl)oxy)(tert-butyl)dimethyl silane (S8)

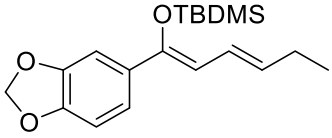

Following the general procedure **B** compound **S8** was obtained from (*E*)-1-(benzo[*d*][1,3]dioxol-5-yl)hex-2-en-1-one (3.2 mmol). The reaction mixture was passed through a plug (deactivated, neutral Al_2O_3 treated with 15 wt% of H_2O) using hexane as an eluent. The crude product was used for the next step without further purification (0.38 g of compound **S8** as a yellow oil (**Yield = 36%**)).

^{1}H NMR (400 MHz, $CDCl_3$): δ 7.05 – 6.90 (m, 2H), 6.81 – 6.71 (m, 1H), 6.48 – 5.17 (m, 5H), 2.26 – 1.99 (m, 2H), 1.10 – 0.87 (m, 12H), 0.12 – -0.01 (m, 6H) ppm.

^{13}C NMR (400 MHz, $CDCl_3$): δ 150.0, 147.4, 147.2, 133.9, 132.8, 131.4, 130.3, 125.5, 122.7, 119.8, 119.5, 111.8, 111.0, 109.0, 107.8, 106.5, 101.0, 25.9, 25.7, 21.2, 18.4, 14.3, -4.0, -4.4 ppm.

HRMS (APCI, *m/z*): calcd. for $(C_{19}H_{28}O_3Si + H)^+$: 333.1886; found: 333.1887.

5.3.9 *tert*-butyldimethyl(((1*Z*,3*E*)-1-(4-nitrophenyl)hexa-1,3-dien-1-yl)oxy)silane (S9)

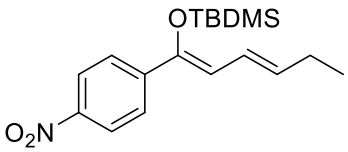

Following the general procedure **B** compound **S9** was obtained from (*E*)-1-(4-nitrocyclohexa-1,3-dien-1-yl)hex-2-en-1-one (1.6 mmol). The reaction mixture was passed through a plug (deactivated, neutral Al_2O_3 treated with 15 wt% of H_2O) using hexane as an eluent. The crude product was used for the next step without further purification (0.45 g of compound **S9** as a yellow oil (**Yield = 85%**)).

^{1}H NMR (400 MHz, $CDCl_3$): (major) δ 8.22 – 8.15 (m, 2H), 7.6 (dd, *J* = 8.8, 3.5 Hz, 2H), 6.16 – 6.01 (m, 2H), 5.92– 5.54 (m, 1H), 2.29 – 2.06 (m, 2H), 0.94 (d, *J* = 8.61 Hz, 9H), 0.12 (d, *J* = 16.12 Hz, 6H), 0.01 (d, *J* = 5.37 Hz, 3H) ppm.

^{13}C NMR (400 MHz, $CDCl_3$): δ 149.5, 147.8, 147.1, 144.4, 144.0, 137.1, 135.9, 134.9, 133.2, 129.4, 129.2, 126.0, 125.7, 124.2, 123.9, 123.5, 123.2, 122.9, 122.2, 115.8, 115.0, 110.8, 110.0, 26.1, 26.0, 25.8, 25.7, 25.6, 21.4, 21.2, 18.2, 18.1, 14.1, 13.7, 13.3, -3.9, -4.4 ppm.

HRMS (APCI, *m/z*): calcd. for $(C_{18}H_{27}NO_3Si + H)^+$: 334.1838; found: 334.1843.

5.3.10 1-(4-((1*Z*,3*E*)-1-((*tert*-butyldimethylsilyl)oxy)hexa-1,3-dien-1-yl)phenyl)ethan-1-one (S10)

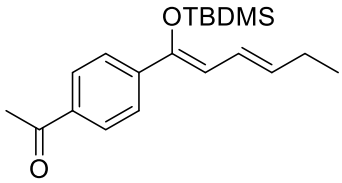

Following the general procedure **B** compound **S10** was obtained from (*E*)-1-(4-acetylphenyl)hex-2-en-1-one (1.3 mmol). The reaction mixture was passed through a plug (deactivated, neutral Al_2O_3 treated with 15 wt% of H_2O) using hexane as an eluent. The crude product was used for the next step without further purification (0.06 g compound **S10** as a yellow oil (**Yield = 15%**)).

^{1}H NMR (500 MHz, $CDCl_3$): δ 7.93 – 7.86 (m, 2H), 7.64 – 7.53 (m, 2H), 6.52 – 5.79 (m, 3H), 2.59 (d, *J* = 3.1 Hz, 3H), 2.29 – 2.09 (m, 2H), 1.10 – 0.99 (m, 12H), 0.01 – -0.02 (m, 6H) ppm.

^{13}C NMR (500 MHz, $CDCl_3$): δ 155.7, 150.1, 133.9,133.2, 132.0, 130.7, 128.5, 128.3, 125.5, 125.2, 124.9, 124.7, 124.4, 122.7, 112.7, 112.2, 107.5, 90.9, 30.3, 29.7, 25.9, 25.7, 18.1, 14.3, 13.5, -2.9, -4.4, -4.6 ppm.

HRMS (APCI, *m/z*): calcd. for $(C_{20}H_{30}O_2Si + H)^+$: 331.2093, found: 331.2099.

5.3.11 4-((1*Z*,3*E*)-1-((*tert*-butyldimethylsilyl)oxy)hexa-1,3-dien-1-yl)benzonitrile (S11)

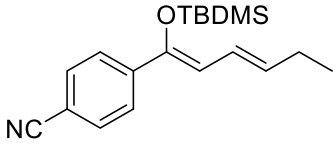

Following the general procedure **B** compound **S11** was obtained from (*E*)-1-(4-acetylphenyl)hex-2-en-1-one (2.5 mmol). The reaction mixture was passed through a plug (deactivated, neutral

Al_2O_3 treated with 15 wt% of H_2O) using hexane as an eluent. The crude product was used for the next step without further purification (0.30 g of compound **S11** as a yellow oil (**Yield = 38%**)).

^{1}H NMR (500 MHz, $CDCl_3$): δ 7.66 – 7.50 (m, 4H), 6.60 – 5.26 (m, 3H), 2.36 – 1.92 (m, 2H), 1.09 – 0.88 (m, 12H), 0.10 – -0.03 (m, 6H) ppm.

^{13}C NMR (500 MHz, $CDCl_3$): δ 143.5, 136.5, 131.9, 131.7, 129.0, 125.7, 123.9, 118.9, 115.0, 110.6, 25.8, 18.4, 13.3, -4.0, -4.4 ppm.

HRMS (APCI, *m/z*): calcd. for $(C_{19}H_{27}NOSi + H)^+$: 314.1940; found: 314.1943

5.3.12 *tert*-butyl(((1*Z*,3*E*)-1-(4-methoxyphenyl)-4-(4-(trifluoromethyl)phenyl)buta-1,3-dien-1-yl)oxy)dimethylsilane (S12)

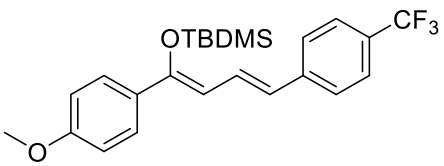

Following the general procedure **B** compound **S12** was obtained from (*E*)-1-(4-methoxyphenyl)-4-(4-(trifluoromethyl)phenyl)but-2-en-1-one (0.9 mmol). The reaction mixture was passed through a plug (deactivated, neutral Al_2O_3 treated with 15 wt% of H_2O) using hexane as an eluent. The crude product was used for the next step without further purification (0.18 g of compound **S12** as a yellow solid (**Yield = 46%**)).

^{1}H NMR (500 MHz, $CDCl_3$): δ 7.55 (d, *J* = 8.1 Hz, 2H), 7.49 – 7.45 (m, 4H), 7.34 (dd, *J* = 15.7, 10.9 Hz, 1H), 6.88 (d, *J* = 8.8 Hz, 2H), 6.50 (d, *J* = 15.8 Hz, 1H), 6.05 (d, *J* = 10.9 Hz, 1H), 3.84 (s, 3H), 1.08 (s, 9H), 0.05 (s, 6H) ppm.

^{13}C NMR (500 MHz, $CDCl_3$): δ 159.9, 152.8, 142.0, 131.0, 128.3, 128.1, 127.3, 127.1, 126.6, 125.8, 125.6, 125.5, 113.6, 113.5, 110.3, 55.3, 30.9, 25.9, 18.5, -4.0 ppm.

HRMS (APCI, *m/z*): calcd. for $(C_{24}H_{29}F_3O_2Si + H)^+$: 435.1967; found: 435.1965.

5.3.13 (((1*Z*,3*E*)-1,4-bis(4-(trifluoromethyl)phenyl)buta-1,3-dien-1-yl)oxy)(*tert*-butyl) dimethylsilane (S13)

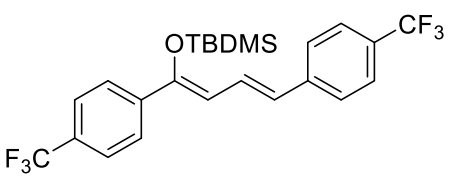

Following the general procedure **B** compound **S13** was obtained from (*E*)-1,4-bis(4-(trifluoromethyl)phenyl)but-2-en-1-one (0.75 mmol). The reaction mixture was passed through a plug (deactivated, neutral Al_2O_3 treated with 15 wt% of H_2O) using hexane as an eluent. The crude product was used for the next step without further purification (0.12 g of compound **S13** as a yellow oil (**Yield = 35%)**).

^{1}H NMR (500 MHz, $CDCl_3$): δ 7.66 (d, *J* = 8.4 Hz, 2H), 7.61 – 7.57 (m, 4H), 7.49 (d, *J* = 8.2 Hz, 2H), 7.32 (dd, *J* = 15.8, 10.9 Hz, 1H), 6.60 (d, *J* = 15.8 Hz, 1H), 6.22 (d, *J* = 10.9 Hz, 1H), 1.09 (s, 9H), 0.5 (s, 6H) ppm.

^{13}C NMR (500 MHz, $CDCl_3$): δ 151.1, 141.9, 141.3, 130.04, 130.02, 129.9,129.7, 129.0, 126.2, 126.1, 125.2, 123.1, 123.0, 113.4, 30.9, 25.8, 18.5, -4.0 ppm.

HRMS (EI, *m/z*): decomposition

5.3.14 *tert*-butyl(((1*Z*,3*E*)-4-(4-methoxyphenyl)-1-(4-(trifluoromethyl)phenyl)buta-1,3-dien-1-yl)oxy)dimethylsilane (*Z*/*E* mixture) (S14)

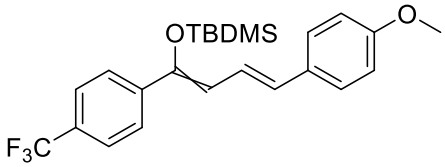

Following the general procedure **B** compound **S14** was obtained from (*E*)-1,4-bis(4-(trifluoromethyl)phenyl)but-2-en-1-one (0.75 mmol). The reaction mixture was passed through a plug (deactivated, neutral Al_2O_3 treated with 15 wt% of H_2O) using hexane as an eluent. The crude product was used for the next step without further purification (0.22 g of compound **S14** as a yellow solid (**Yield = 70 %**, *Z*/*E* mixture, ratio ~ 1:5)).

^{1}H NMR (500 MHz, $CDCl_3$δ 7.80 (d, *J* = 7.9 Hz, 2H), 7.69 (d, *J* = 8.4 Hz, 2H), 7.64 (d, *J* = 8.1 Hz, 2H), 7.67 (d, *J* = 8.4 Hz, 2H), 7.36 (d, *J* = 8.7 Hz, 2H), 7.24 (d, *J* = 8.9 Hz, 2H), 7.09 (dd, *J* = 15.8, 10.9 Hz, 1H), 6.96 (d, *J* = 8.8 Hz, 2H), 6.88 (d, *J* = 8.7 Hz, 2H), 6.84-6.82, (m, 1H), 6.75 (dd, *J* = 13.5, 11.0 Hz, 1H), 6.55 (d, *J* = 15.8 Hz, 1H), 6.20 (d, *J* = 10.9 Hz, 1H), 5.98 (d, *J* = 11.1 Hz, 1H), 3.86 (s, 3H), 3.82 (s, 3H), 1.08 (s, 9H), 0.96 (s, 9H), 0.13 (s, 6H), 0.05 (s, 6H) ppm.

^{13}C NMR (500 MHz, $CDCl_3$): δ 159.1, 148.6, 142.3, 130.7, 130.5, 129.5, 129.3, 128.9, 127.4, 125.5, 125.1, 123.4, 121.9, 114.2, 109.3, 105.9, 55.3, 30.9, 25.9, 18.5, -3.9 ppm.

HRMS (EI, *m/z*): calcd. for $(C_{24}H_{29}F_3O_2Si + H)^+$: 435.1967; found: 435.1969.

5.3.15 (1*Z*,3*E*)-1,4-bis(4-methoxyphenyl)buta-1,3-dien-1-yl acetate (S15)

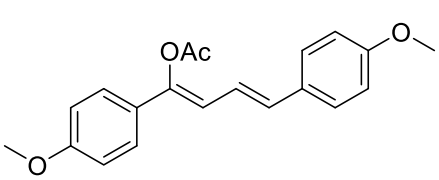

Compound **S15** was obtained from 1-ethynyl-4-methoxybenzene (2.5 mmol) according to literature procedure[2]. The crude was purified by column chromatography (20:80 AcOEt/Hexane) to afford 0.21 g compound **S15** as a colorless oil (**Yield = 52%**).

NMR data matched those reported in the literature.[2]

^{1}H NMR (400 MHz, $CDCl_3$): δ 7.43 – 7.39 (m, 2H), 7.30 – 7.27 (m, 2H), 6.95 – 6.92 (m, 2H), 6.85 – 6.78 (m, 3H), 6.59 (d, *J* = 15.6 Hz, 1H), 6.20 – 6.17 (m, 1H), 3.85 (s, 3H), 3.80 (s, 3H), 2.19 (s, 3H) ppm.

5.3.16 (1*Z*,3*E*)-1,4-bis(3-methoxyphenyl)buta-1,3-dien-1-yl acetate (S16)

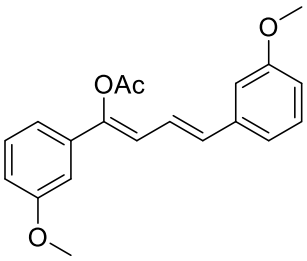

Compound **S16** was obtained from 1-ethynyl-3-methoxybenzene (2.5 mmol) according to literature procedure.[2] The crude was purified by column chromatography (20:80 AcOEt/Hexane) to afford 0.34 g compound **S16** as a yellow oil (**Yield = 83%**).

^{1}H NMR (500 MHz, $CDCl_3$): δ 7.34 (t, *J* = 8.0 Hz, 1H), 7.22 (t, *J* = 7.9 Hz, 1H), 7.09 (dt, *J* = 7.6, 1.0 Hz, 1H), 7.03 – 6.91 (m, 4H), 6.88 (t, *J* = 2.1 Hz, 1H), 6.78 (dd, *J* = 8.2, 0.8 Hz, 1H), 6.64 (d, *J* = 15.6 Hz, 1H), 6.27 (dd, *J* = 11.3, 0.7 Hz, 1H), 3.83 (s, 3H), 3.80 (s, 3H), 2.21 (s, 3H) ppm.

^{13}C NMR (500 MHz, $CDCl_3$): δ 206.8, 169.4, 159.8, 159.6, 148.2, 138.6, 135.8, 134.3, 129.5, 123.6, 121.0, 120.5, 119.1, 114.6, 113.8, 113.2, 112.0, 55.3, 30.9, 21.0 ppm.

HRMS (EI, *m/z*): calcd. for $(C_{20}H_{20}O_4 + Na)^+$: 347.1259; found: 347.1266.

5.3.17 (1*Z*,3*E*)-1,4-bis(2-methoxyphenyl)buta-1,3-dien-1-yl acetate (S17)

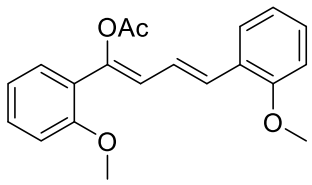

Compound **S17** was obtained from 1-ethynyl-2-methoxybenzene (2.5 mmol) according to literature procedure[2]. The crude was purified by column chromatography (20:80 AcOEt/Hexane) to afford 0.10 g compound **S17** as a yellow oil (**Yield = 23%**, *Z*/*E* ratio ~ 1:1).

^{1}H NMR (500 MHz, $CDCl_3$): δ 7.51 (dd, *J* = 7.7, 1.7 Hz, 1H), 7.41 (dd, *J* = 7.5, 1.8 Hz, 1H), 7.39 – 7.34 (m, 2H), 7.31 – 7.28 (m, 1H), 7.24 (t, *J* = 1.6 Hz, 1H), 7.24 – 7.15 (m, 2H), 7.07 – 6.92 (m, 8H), 6.89 – 6.82 (m, 4H), 6.68 (dd, *J* = 15.8, 11.2 Hz, 1H), 6.36 (dd, *J* = 11.2, 0.6 Hz, 1H), 3.91 (s, 3H), 3.87 (s, 3H), 3.85 (s, 3H), 3.81 (s, 3H), 2.33 (s, 3H), 2.15 (s, 3H) ppm.

^{13}C NMR (500 MHz, $CDCl_3$): δ 169.2, 168.7, 157.3, 157.0, 156.8, 156.7, 145.9, 143.5, 132.1, 130.4, 129.3, 128.8, 128.5, 128.1, 127.7, 126.7, 126.5, 124.4, 123.8, 123.2, 123.1, 122.4, 122.0, 120.7, 120.6, 120.3, 111.5, 111.3, 111.0, 110.9, 55.6, 55.5, 21.1 ppm.

HRMS (EI, *m/z*): calcd. for $(C_{20}H_{20}O_4 + Na)^+$: 347.1259; found: 347.1263.

5.3.18 (1*Z*,3*E*)-1,4-bis(4-cyanophenyl)buta-1,3-dien-1-yl acetate (S18)

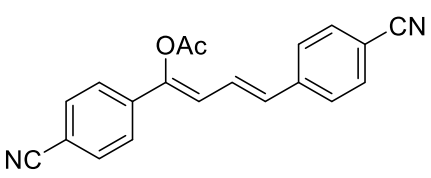

Compound **S18** was obtained from 4-ethynylbenzonitrile (2.5 mmol) according to literature procedure[2]. The crude was purified by column chromatography (30:70 AcOEt/Hexane) to afford 0.35 g compound **S18** as a yellow solid (**Yield = 88%**).

NMR data matched those reported in the literature. [2]

^{1}H NMR (400 MHz, $CDCl_3$): δ 7.73 (d, *J* = 8.5 Hz, 2H), 7.59 – 7.55 (m, 4H), 7.40 (d, *J* = 8.3 Hz, 2H), 6.93 (dd, *J* = 15.5, 11.3 Hz, 1H), 6.71 (d, *J* = 15.6 Hz, 1H), 6.39 (d, *J* = 11.2 Hz, 1H), 2.22 (s, 3H) ppm.

5.3.19 *tert*-butyl((5,5-dimethyl-3-methylenecyclohex-1-en-1-yl)oxy)dimethylsilane (S22)

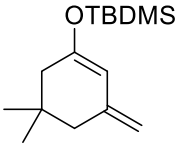

Following the general procedure **A** compound **S22** was obtained from 3,5,5-trimethylcyclohex-2-en-1-one (2.5 mmol). The reaction mixture was passed through a plug (deactivated, neutral Al_2O_3 treated with 15 wt% of H_2O) using hexane as an eluent. The crude product was used for the next step without further purification (0.39 g of compound **S22** as a colorless oil (**Yield = 61%**).

NMR data matched those reported in the literature.[3]

^{1}H NMR (400 MHz, $CDCl_3$): δ 5.47 (s, 1H), 4.61 (s, 1H), 4.56 (s, 1H), 2.00 (t, *J* = 1.3 Hz, 2H), 1.93 (s, 2H), 0.94 (s, 6H), 0.93 (s, 9H), 0.16 (s, 6H) ppm.

5.3.20 *tert*-butyl(cyclohepta-1,3-dien-1-yloxy)dimethylsilane (S23)

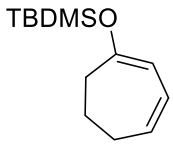

Following the general procedure **A** compound **S23** was obtained from cyclohept-2-en-1-one (5.0 mmol). The reaction mixture was passed through a plug (deactivated, neutral Al_2O_3 treated with 15 wt% of H_2O) using hexane as an eluent. The crude product was used for the next step without further purification (1.1 g of compound **S23** as a colorless oil (**Yield = 99%**)).

NMR data matched those reported in the literature.[10]

^{1}H NMR (400 MHz, $CDCl_3$): δ 5.79 (dt, 1H), 5.61 (dq, 1H), 5.17 (dt, 1H), 2.3 (q, *J* = 6.3 Hz, 2H), 2.2 (q, *J* = 5.9 Hz, 2H), 1.8 (p, *J* = 5.8 Hz, 2H), 0.9 (s, 9H), 0.1 (d, *J* = 14.3 Hz, 6H) ppm.

5.3.21 *tert*-butyl(((3*Z*,5*E*)-2,2-dimethylocta-3,5-dien-3-yl)oxy)dimethylsilane (S25)

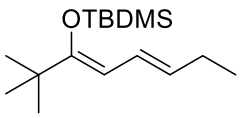

Following the general procedure, **A** compound **S25** was obtained from (*E*)-2,2-dimethyloct-4-en-3-one (1.61 mmol). The reaction mixture was passed through a plug (deactivated, neutral Al_2O_3 treated with 15 wt% of H_2O) using hexane as an eluent. The crude product was used for the next step without further purification (0.16 g of compound **S25** as a colorless oil (**Yield = 38%**)).

^{1}H NMR (400 MHz, $CDCl_3$): δ 6.48 – 6.15 (m, 1H), 5.57 – 5.49 (m, 1H), 5.39 – 5.12 (m, 1H), 2.15 – 2.06 (m, 2H), 1.10 (d, *J* = 10.7 Hz, 9H), 1.01 (dd, *J* = 8.1, 2.7 Hz, 9H), 0.95 (d, *J* = 7.0 Hz, 3H), 0.21 (d, *J* = 2.5 Hz, 3H), 0.19 (d, *J* = 5.9 Hz, 3H) ppm.

^{13}C NMR (126 MHz, $CDCl_3$): 160.5, 131.0, 129.2, 128.4, 124.7, 123.3, 104.8, 103.4, 100.2, 36.7, 29.8, 28.8, 26.0, 21.0, 14.2, 13.9 ppm.

HRMS (APCI, *m/z*): calcd. For $(C_{16}H_{32}OSi + H)^+$: 269.2301, found: 269.2303.

5.3.22 *tert*-butyl(((4*R*,4a*S*,6*R*)-4,4a-dimethyl-6-(prop-1-en-2-yl)-3,4,4a,5,6,7-hexahydronaphthalen-2-yl)oxy)dimethylsilane (S26)

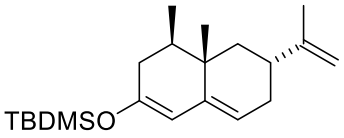

Following the general procedure **B** compound **S26** was obtained from (4*R*,4a*S*,6*R*)-4,4a-dimethyl-6-(prop-1-en-2-yl)-4,4a,5,6,7,8-hexahydronaphthalen-2(3H)-one (2.5 mmol). The reaction mixture was passed through a plug (deactivated, neutral Al_2O_3 treated with 15 wt% of H_2O) using hexane as an eluent. The crude product was used for the next step without further purification (0.80 of compound **S26** as a white solid (**Yield = 96%**)).

^{1}H NMR (400 MHz, $CDCl_3$): δ 5.37 – 5.20 (m, 2H), 4.73 – 4.70 (m, 2H), 2.44 – 2.12 (m, 2H), 2.03 – 1.85 (m, 3H), 1.74-1.71 (m, 3H), 1.68 (d, *J* = 12.3 Hz, 1H), 1.63 – 1.52 (m, 1H), 1.38 – 1.19 (m, 1H), 0.92 (s, 9H), 0.90-0.84 (m, 6H), 0.15 – 0.12 (m, 6H), ppm.

^{13}C NMR (126 MHz, $CDCl_3$): δ 150.8, 150.5, 141.6, 119.9, 118.3, 108.6, 108.5, 106.8, 45.6, 41.5, 40.2, 39.1, 37.4, 36.7, 35.9, 31.4, 31.2, 25.7, 20.9, 20.7, 18.0, 17.5, 14.6, 14.3, -4.2, -4.4 ppm.

HRMS (EI, *m/z*): calcd. for $(C_{21}H_{36}OSi + H)^+$: 333.2614; found: 333.2622.

5.3.23 (1*R*,8*R*,9*S*,13*S*,14*S*,17*S*)-3-((*tert*-butyldimethylsilyl)oxy)-1,13-dimethyl-2,7,8,9,10,11,12,13,14,15,16,17-dodecahydro-1H-cyclopenta[a]phenanthren-17-yl acetate (S27)

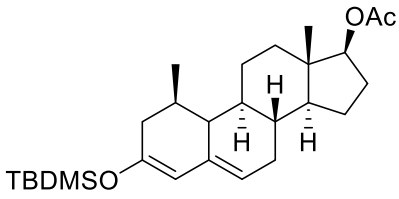

Following the general procedure **B** compound **S27** was obtained from (1*R*,8*R*,9*S*,13*S*,14*S*,17*S*)-1,13-dimethyl-3-oxo 2,3,6,7,8,9,10,11,12,13,14,15,16,17-tetradecahydro-1H-cyclopenta[*a*]phenanthren-17-yl acetate (1.7 mmol). The reaction mixture was passed through a plug (deactivated, neutral Al_2O_3 treated with 15 wt% of H_2O) using hexane as an eluent. The crude product was used for the next step without further purification (0.43 of compound **S27** as a white solid (**Yield = 57%**)).

^{1}H NMR (500 MHz, $CDCl_3$): δ 5.27 (d, *J* = 1.5 Hz, 1H), 5.17 – 5.16 (m, 1H), 4.63 – 4.59 (m, 1H), 2.23 – 2.12 (m, 3H), 2.04 (s, 3H), 1.81-1.75 (m, 2H), 1.66 – 1.00 (m, 12H), 0.97 (s, 3H), 0.93 (s, 9H), 0.83 (s, 3H), 0.15 (d, *J* = 5.0 Hz, 6H) ppm.

^{13}C NMR (126 MHz, $CDCl_3$): δ 171.2, 150.6, 141.3, 118.0, 108.8, 82.8, 51.3, 48.2, 42.5, 36.8, 34.9, 34.1, 31.7, 31.4, 27.6, 25.7, 23.5, 21.2, 20.7, 19.0, 18.0, 12.0, -4.2, -4.4 ppm.

HRMS (EI, *m/z*): calcd. for $(C_{27}H_{44}O_3Si + H)^+$: 445.3138; found: 445.3145.

5.3.24 *tert*-butyl((3*E*)-hexa-1,3-dien-1-yloxy)dimethylsilane (*Z*/*E* mixture) (S28)

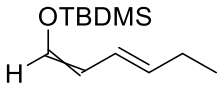

Following the general procedure **A** compound **S28** was obtained from hex-2-enal (5.0 mmol). The reaction mixture was passed through a plug (deactivated, neutral Al_2O_3 treated with 15 wt% of H_2O) using hexane as an eluent. The crude product was used for the next step without further purification (0.84 g of compound **S28** as a colorless oil (**Yield = 79%**, 16 h, *Z*/*E* ratio ~ 1.2:1)).

^{1}H NMR (400 MHz, $CDCl_3$): δ 6.53 (d, *J* = 11.5 Hz, 1H), 6.47 (d, *J* = 11.8 Hz, 1H), 5.97 – 5.78 (m, 2H + 1H), 5.68 (t, *J* = 11.3 Hz, 1H), 5.49 (dt, *J* = 15.2, 6.5 Hz, 1H), 5.19 (dt, *J* = 10.6, 7.4 Hz, 1H), 2.17 – 2.01 (m, 2H + 2H), 1.01 – 0.96 (m, 3H + 3H), 0.93 (s, 9H), 0.92 (s, 9H), 0.16 (s, 6H), 0.14 (s, 6H) ppm.

^{13}C NMR (100 MHz, $CDCl_3$): δ 144.6, 142.8, 131.0, 129.0, 124.9, 123.6, 113.6, 109.2, 25.8, 25.6, 21.0, 18.3, 14.3, 13.8, -5.3 ppm.

HRMS (EI, *m/z*): calcd. for $C_{12}H_{24}OSi$: 212.1596; found: 212.1602.

5.3.25 *tert*-butyl(((1*Z*,3*E*)-3,7-dimethylocta-1,3,6-trien-1-yl)oxy)dimethylsilane (S29)

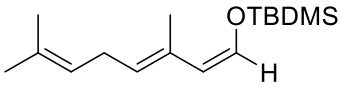

Following the general procedure **A** compound **S29** was obtained from (*E*)-3,7-dimethylocta-2,6-dienal (3.0 mmol). The reaction mixture was passed through a plug (deactivated, neutral Al_2O_3 treated with 15 wt% of H_2O) using hexane as an eluent. The crude product was used for the next step without further purification (0.79 g of compound **S29** as a colorless oil (**Yield = 100%**, 24 h).

^{1}H NMR (400 MHz, $CDCl_3$): δ 6.60 (d, *J* = 12.2 Hz, 1H), 5.74 (dd, *J* = 12.1, 4.7 Hz, 1H), 4.77 (d, *J* = 1.6 Hz, 1H), 4.69 (m, 1H), 2.16 – 2.14 (m, 2H), 1.76 – 1.69 (m, 6H), 1.62 (s, 3H), 0.93 (s, 9H), 0.16 (s, 6H) ppm.

^{13}C NMR (100 MHz, $CDCl_3$): δ 144.0, 142.2, 141.6, 139.8, 131.7, 129.3, 126.0, 125.0, 124.2, 123.1, 122.9, 118.3, 115.4, 112.4, 111.1, 110.4, 109.8, 33.0, 27.1, 26.6, 25.6, 20.6, 18.3, 17.7, -5.2 ppm.

HRMS (EI, *m/z*): decomposition

5.3.26 (*E*)-*tert*-butyldimethyl((2,6,6-trimethylcyclohex-2-en-1-ylidene)methoxy)silane (S30)

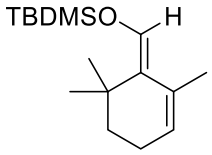

Following the general procedure **A** compound **S30** was obtained from 2,6,6-trimethylcyclohex-1-ene-1-carbaldehyde (3.0 mmol). The reaction mixture was passed through a plug (deactivated, neutral Al_2O_3 treated with 15 wt% of H_2O) using hexane as an eluent. The crude product was used for the next step without further purification (0.76 g of compound **S30** as a colorless oil (**Yield = 95%**, 24 h)).

^{1}H NMR (400 MHz, $CDCl_3$): δ 6.39 (s, 1H), 5.47 (t, *J* = 4.1 Hz, 1H), 2.09 (dt, *J* = 8.8, 4.2 Hz, 2H), 1.77 (m, 3H), 1.45 (t, *J* = 6.2 Hz, 2H), 1.26 (s, 6H), 0.99 (s, 9H), 0.21 (s, 6H).

^{13}C NMR (100 MHz, $CDCl_3$): δ 136.7, 131.0, 125.9, 123.3, 39.5, 33.2, 27.4, 25.7, 22.8, 20.6, 18.2, -5.4 ppm.

HRMS (EI, *m/z*): decomposition

5.3.27 (*E*)-*tert*-butyldimethyl((2-phenylbuta-1,3-dien-1-yl)oxy)silane (S31)

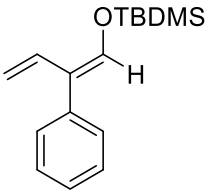

Following the general procedure **A** compound **S31** was obtained from 2-phenylbut-2-enal (3.0 mmol). The reaction mixture was passed through a plug (deactivated, neutral Al_2O_3 treated with 15 wt% of H_2O) using hexane as an eluent. The crude product was used for the next step without further purification (0.78 g of compound **S31** as a colorless oil (**Yield = 100%**, 24 h)).

^{1}H NMR (400 MHz, $CDCl_3$): δ 7.37 – 7.22 (m, 5H), 6.60 (s, 1H), 6.45 – 6.40 (m, 1H), 4.92 – 4.90 (m, 1H), 4.89-4.88 (m, 1H), 0.82 (s, 9H), 0.10 (s, 6H).

^{13}C NMR (100 MHz, $CDCl_3$): δ 141.7, 136.1, 135.2, 130.0, 127.7,126.4, 124.4, 111.0, 25.4, 18.1, -5.4 ppm.

HRMS (EI, *m/z*): calcd. for $C_{16}H_{24}OSi$: 260.1596; found: 260.1608.

5.4. *N*-aminopyridinium salts

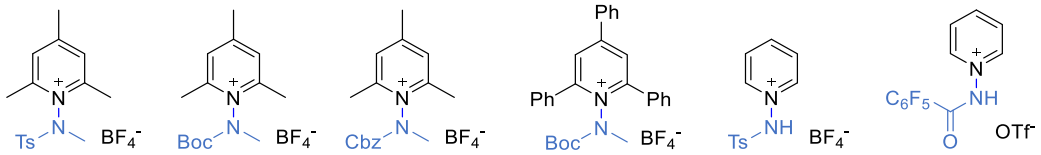

2a **2b** **2c** **2d** **2f** **2e**

Compounds were prepared following the procedures described previously.[6]

5.5. Scope of visible-light mediated amidation

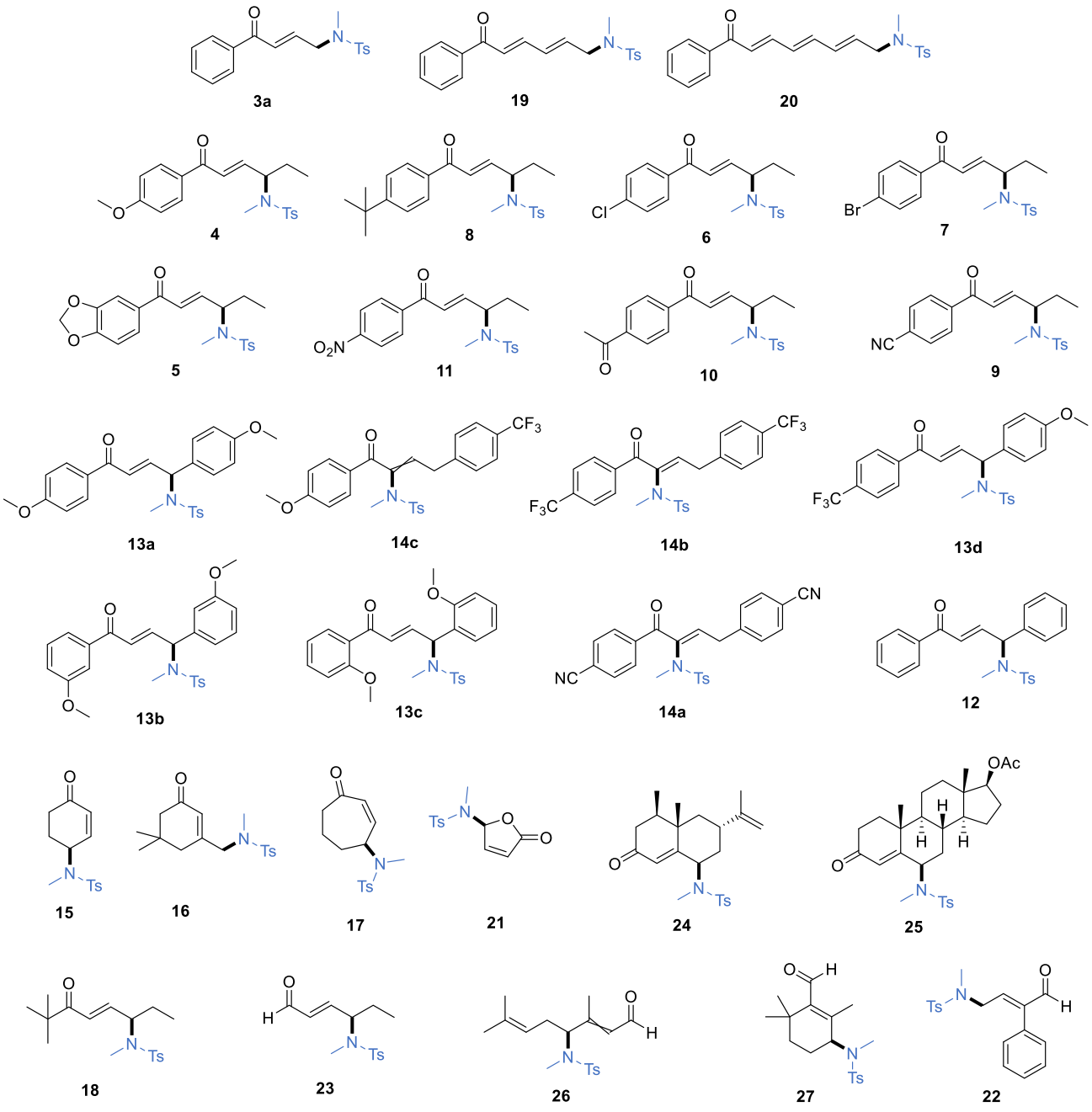

3a **19** **20**

4 **8** **6** **7**

5 **11** **10** **9**

13a **14c** **14b** **13d**

13b **13c** **14a** **12**

15 **16** **17** **21** **24** **25**

18 **23** **26** **27** **22**

5.5.1 (*E*)-*N*,4-dimethyl-*N*-(4-oxo-4-phenylbut-2-en-1-yl)benzenesulfonamide (3a)

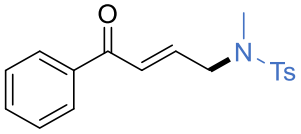

Following the general procedure **C** compound **3a** was obtained from enol **S1** (0.25 mmol) and *N*-aminopyridinium salt **2a** (0.33 mmol). The crude product was purified by column chromatography (20:80 AcOEt/Hexane) to afford 74 mg of compound **3a** as a colorless oil (**Yield = 90%**, 1 h).

^{1}H NMR (400 MHz, $CDCl_3$): δ 7.91 – 7.88 (m, 2H), 7.72 – 7.70 (m, 2H), 7.61 – 7.55 (m, 1H), 7.50 – 7.44 (m, 2H), 7.33 (d, *J* = 8.0 Hz, 2H), 7.05 (dt, *J* = 15.4, 1.7 Hz, 1H), 6.85 (dt, *J* = 15.4, 5.3 Hz, 1H), 3.93 (dd, *J* = 5.3, 1.6 Hz, 2H), 2.78 (s, 3H), 2.43 (s, 3H) ppm.

^{13}C NMR (100 MHz, $CDCl_3$): δ 189.8, 143.8, 141.8, 137.3, 134.4, 133.1, 129.9, 128.6, 128.6, 127.6, 127.4, 51.5, 35.2, 21.5 ppm.

HRMS (ESI, *m/z*): calcd. for $(C_{18}H_{19}NO_3S + Na)^+$: 352.0983; found: 352.0984.

Elemental analysis (%): calcd. for $C_{18}H_{19}NO_3S$: C 65.63, H 5.81, N 4.25, S 9.73; found: C 65.57, H 5.85, N 4.21, S 9.50.

5.5.2 *tert*-butyl methyl(4-oxo-4-phenylbut-2-en-1-yl)carbamate (*E*/*Z* mixture) (3b)

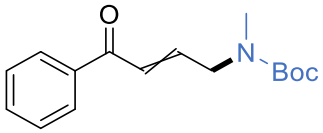

Following the general procedure **C** compound **3b** was obtained from enol **S1** (0.25 mmol) and *N*-aminopyridinium salt **2b** (0.33 mmol). The crude product was purified by column chromatography (20:80 AcOEt/Hexane) to afford 52 mg of compound **3b** as a colorless oil (**Yield = 76%**, 1 h, *E*/*Z* ratio ~ 1.2:1).

^{1}H NMR (500 MHz, $CDCl_3$): δ 7.92 (d, *J* = 7.5 Hz, 2H), 7.57 (t, *J* = 7.2 Hz, 1H), 7.47 (t, *J* = 7.6 Hz, 2H), 7.08 – 6.77 (m, 2H), 4.09 (s, 2H), 2.92 (s, 3H), 1.48 (s, 9H) ppm.

^{13}C NMR (125 MHz, $CDCl_3$): δ 190.5, 190.0, 155.5, 143.8, 137.5, 132.9, 128.6, 128.5, 128.3, 126.3, 125.2, 80.0, 50.5, 49.8, 34.5, 28.4 ppm.

HRMS (ESI, *m/z*): calcd. For $(C_{16}H_{21}NO_3 + Na)^+$: 298.1419; found: 298.1423.

Elemental analysis (%): calcd. For $C_{16}H_{21}NO_3$: C 69.79, H 7.69, N 5.09; found: C 69.65, H 7.70, N 5.18.

5.5.3 (*E*)-4-methyl-*N*-(4-oxo-4-phenylbut-2-en-1-yl)benzenesulfonamide (3f)

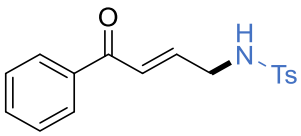

Following the general procedure **C** compound **3f** was obtained from enol **S1** (0.25 mmol) and *N*-aminopyridinium salt **2f** (0.33 mmol). The crude product was purified by column chromatography (20:80 AcOEt/Hexane) to afford 58 mg of compound **3f** as an off-white solid (**Yield = 74%**, 1 h).

^{1}H NMR (400 MHz, $CDCl_3$): δ 7.84 (d, *J* = 7.1 Hz, 2H), 7.78 (d, *J* = 8.3 Hz, 2H), 7.55 (t, *J* = 7.4 Hz, 1H), 7.42 (t, *J* = 7.7 Hz, 2H), 7.28 (d, *J* = 8.1 Hz, 2H), 7.01 (dt, *J* = 15.4, 1.8 Hz, 1H), 6.83 (dt, *J* = 15.4, 4.9 Hz, 1H), 5.30 (t, *J* = 6.3 Hz, 1H), 3.87 (ddd, *J* = 6.3, 4.9, 1.8 Hz, 2H), 2.37 (s, 3H) ppm.

^{13}C NMR (100 MHz, $CDCl_3$): δ 189.8, 143.9, 142.3, 137.2, 136.8, 133.1, 129.9, 128.6, 127.1, 126.4, 44.3, 21.5 ppm.

HRMS (ESI, *m/z*): calcd. for $(C_{17}H_{17}NO_3S + Na)^+$: 338.0827; found: 338.0825.

Elemental analysis (%): calcd. for $C_{17}H_{17}NO_3S$: C 64.74, H 5.43, N 4.44, S 10.17; found: C 65.50, H 5.48, N 4.48, S 10.27.

m.p.: 98-96 °C.

5.5.4 (*E*)-2,3,4,5,6-pentafluoro-*N*-(4-oxo-4-phenylbut-2-en-1-yl)benzamide (3e)

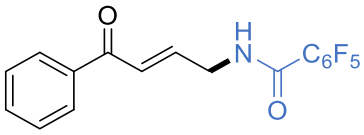

Following the general procedure **C** compound **3e** was obtained from enol **S1** (0.25 mmol) and *N*-aminopyridinium salt **2e** (0.33 mmol). The crude product was purified by column chromatography (20:80 AcOEt/Hexane) to afford 41 mg of compound **3e** as a white solid (**Yield = 46%**, 16 h).

^{1}H NMR (500 MHz, $CDCl_3$): δ 7.95 (d, *J* = 7.4 Hz, 2H), 7.66 (t, *J* = 7.4 Hz, 1H), 7.54 (t, *J* = 7.7 Hz, 2H), 7.15 (dt, *J* = 15.5, 2.0 Hz, 1H), 7.05 (dt, *J* = 15.5, 4.8 Hz, 1H), 6.83 (br s, 1H), 4.42 (t, *J* = 4.8 Hz, 2H) ppm.

^{13}C NMR (125 MHz, $CDCl_3$): 190.2, 157.5, 145.2 (m), 143.2 (m), 142.3, 141.4 (m), 138.7 (m), 137.1, 136.6 (m), 133.3, 128.7, 128.5, 126.3, 111.2 (m), 41.2 ppm.

^{19}F NMR (375 MHz, $CDCl_3$): δ -140.32–140.63 (m, 2F), -150.13 (tt, *J* = 20.8, 2.9 Hz, 1F), -159.55–159.84 (m, 2F).

HRMS (ESI, *m/z*): calcd. for $(C_{17}H_{10}NO_2F_5 + Na)^+$: 378.0529; found: 378.0526.

Elemental analysis (%) calcd. for $C_{17}H_{10}NO_2F_5$: C 57.47, H 2.84, N 3.94; found: C 57.75, H 2.85, N 3.87.

5.5.5 benzyl (*E*)-methyl(4-oxo-4-phenylbut-2-en-1-yl)carbamate (3c)

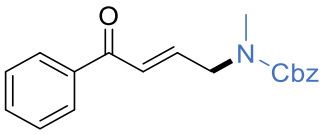

Following the general procedure **C** compound **3c** was obtained from enol **S1** (0.25 mmol) and *N*-aminopyridinium salt **2c** (0.33 mmol). The crude product was purified by column chromatography (20:80 AcOEt/Hexane) to afford 36 mg of compound **3c** as a colorless oil (**Yield = 46%**, 2 h).

^{1}H NMR (500 MHz, $CDCl_3$): δ 7.88 – 7.48 (m, 2H), 7.58 – 7.54 (m, 1H), 7.47 – 7.26 (m, 7H), 6.97 – 6.79 (m, 2H), 5.15 (s, 2H), 4.18 – 4.15 (m, 2H), 3.00 – 2.99 (m, 3H) ppm.

^{13}C NMR (125 MHz, $CDCl_3$): δ 143.0, 133.0, 132.9, 128.6, 128.5, 128.1, 128.0, 126.5, 125.7, 67.4, 50.4, 50.2, 36.4, 35.1, 34.3 ppm.

HRMS (ESI, *m/z*): calcd. for $(C_{19}H_{19}NO_3 + Na)^+$: 332.1263; found: 332.1268.

Analytical HPLC:

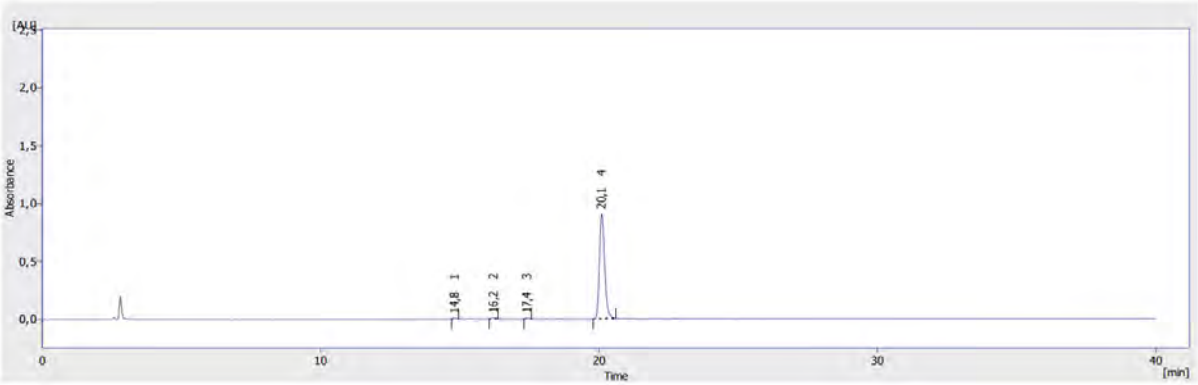

	Reten. Time [min]	Area [mAU.s]	Height [mAU]	Area [%]	Height [%]	W05 [min]	PDA Peak Purity	Compound Name	PDA Best Match Name	PDA Best Match
1	14,817	55,080	6,115	0,5	0,7	0,17	1000			
2	16,217	103,287	10,389	0,9	1,1	0,18	1000			
3	17,417	68,709	7,639	0,6	0,8	0,17	1000			
4	20,100	11794,221	907,218	98,1	97,4	0,22	879			
	Total	12021,296	931,362	100,0	100,0					

5.5.6 *N*,4-dimethyl-*N*-((2*E*,4*E*)-6-oxo-6-phenylhexa-2,4-dien-1-yl)benzenesulfonamide (19)

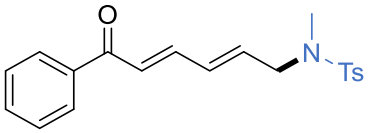

Following the general procedure **C** compound **19** was obtained from enol **S2** (0.25 mmol) and *N*-aminopyridinium salt **2a** (0.33 mmol). The crude product was purified by column chromatography (20:80 AcOEt/Hexane) to afford 36 mg of compound **19** as a yellow oil (**Yield = 41%**, 3 h).

^{1}H NMR (400 MHz, $CDCl_3$): δ 7.93 (d, *J* = 5.1 Hz, 2H), 7.69 (d, *J* = 8.3 Hz, 2H), 7.56 (t, *J* = 7.4 Hz, 1H), 7.47 (t, *J* = 7.5 Hz, 2H), 7.39 – 7.30 (m, 3H), 6.95 (d, *J* = 15.1 Hz, 1H), 6.44 (dd,

J = 14.9, 11.3 Hz, 1H), 6.04 (dt, *J* = 15.2, 6.2 Hz, 1H), 3.80 (d, *J* = 6.1 Hz, 2H), 2.71 (s, 3H), 2.44 (s, 3H) ppm.

^{13}C NMR (100 MHz, $CDCl_3$): δ 190.4, 143.7, 142.9, 137.0, 137.3, 134.5, 132.9, 131.9, 129.8, 128.6, 128.4, 127.4, 126.2, 51.9, 34.8, 21.5 ppm.

HRMS (ESI, *m/z*): calcd. For $(C_{20}H_{21}NO_3S + Na)^+$: 378.1140; found: 378.1136.

Elemental analysis (%) calcd. For $C_{20}H_{21}NO_3S$: C 67.58, H 5.95, N 3.94, S 9.02; found: C 67.35, H 5.94, N 4.05, S 8.99.

5.5.7 *N*,4-dimethyl-*N*-((2*E*,4*E*,6*E*)-8-oxo-8-phenylocta-2,4,6-trien-1-yl)benzenesulfonamide (20)

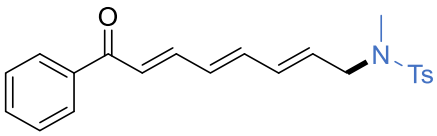

Following the general procedure **C** compound **20** was obtained from enol **S3** (0.25 mmol) and *N*-aminopyridinium salt **2a** (0.33 mmol). The crude product was purified by column chromatography (5:25:70 AcOEt/DCM/Hexane) to afford 8 mg of compound **20** as a yellow oil (**Yield = 10%**, 1 h).

^{1}H NMR (400 MHz, $CDCl_3$): δ 7.93-7.92 (m, 2H), 7.69 – 7.66 (m, 2H), 7.56 – 7.53 (m, 1H), 7.48-7.45 (m, 2H), 7.42 (ddd, *J* = 14.9, 11.3, 0.5 Hz, 1H), 7.33 – 7.31 (m, 2H), 6.97 (d, *J* = 14.9 Hz, 1H), 6.60 (dd, *J* = 14.8, 10.8 Hz, 1H), 6.41 (dd, *J* = 14.9, 11.3 Hz, 1H), 6.31 – 6.27 (m, 1H), 5.79 (dt, *J* = 15.11, 6.5 Hz, 1H), 3.73 (d, *J* = 6.4 Hz, 2H), 2.68 (s, 3H), 2.43 (s, 3H) ppm.

^{13}C NMR (100 MHz, $CDCl_3$): δ 190.4, 144.1, 143.5, 140.3, 138.1, 134.5, 133.2, 132.7, 132.3, 131.3, 129.7, 128.6, 128.3, 127.5, 127.3, 125.8, 52.0, 34.6, 21.5 ppm.

HRMS (ESI, *m/z*): calcd. for $(C_{22}H_{23}NO_3S + Na)^+$: 404.1296, found: 404.1295.

Analytical HPLC:

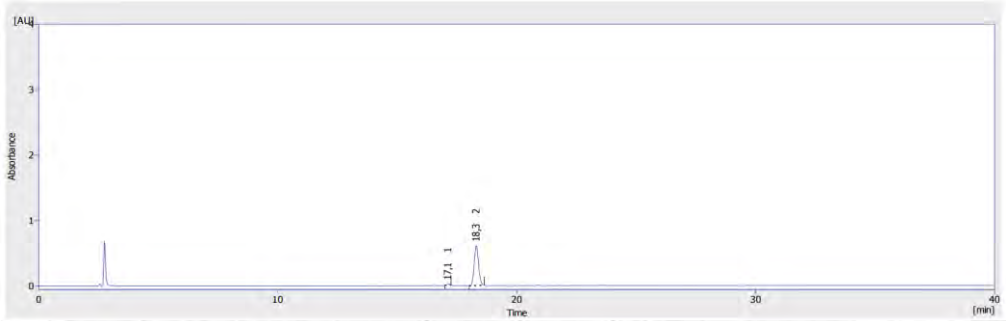

	Reten. Time [min]	Area [mAU.s]	Height [mAU]	Area [%]	Height [%]	W05 [min]	PDA Peak Purity	Compound Name	PDA Best Match Name	PDA Best Match
1	17,133	69,638	7,824	1,8	2,5	0,17	1000			
2	18,317	3851,998	304,984	98,2	97,5	0,22	760			
	Total	3921,636	312,808	100,0	100,0					

5.5.8 (*E*)-*N*-(6-(4-methoxyphenyl)-6-oxohex-4-en-3-yl)-*N*,4-dimethylbenzenesulfonamide (4)

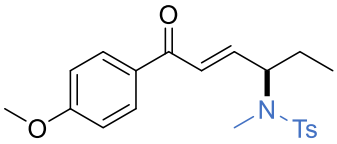

Following the general procedure **C** compound **4** was obtained from enol **S4** (0.25 mmol) and *N*-aminopyridinium salt **2a** (0.33 mmol). The crude product was purified by column chromatography (10:90 AcOEt/Hexane) to afford 73 mg of compound **4** as a colorless oil (**Yield = 75 %**, 1h).

^{1}H NMR (500 MHz, $CDCl_3$): δ 7.81 (d, *J* = 8.8 Hz, 2H), 7.71 (d, *J* = 8.1 Hz, 2H), 7.25 (d, *J* = 8.0 Hz, 2H), 6.93 (d, *J* = 8.8 Hz, 2H), 6.82-6.76 (dd, *J* = 15.7, 1.0 Hz, 1H), 6.66 (dd, *J* = 15.4, 5.9 Hz, 1H), 4.60 (q, *J* = 6.8 Hz, 1H), 3.88 (s, 3H), 2.76 (s, 3H), 2.34 (s, 3H), 1.60 (m, 2H), 0.94 (t, *J* = 7.3 Hz, 3H) ppm.

^{13}C NMR (100 MHz, $CDCl_3$): δ 187.9, 163.6, 143.3, 143.1, 136.9, 130.8, 130.2, 129.6, 127.2, 126.6, 113.8, 59.8, 55.5, 28.6, 24.8, 21.4, 10.8 ppm.

HRMS (ESI, *m/z*): calcd. for $(C_{21}H_{25}NO_4S + Na)^+$: 410.1402, found: 410.1407.

Analytical HPLC:

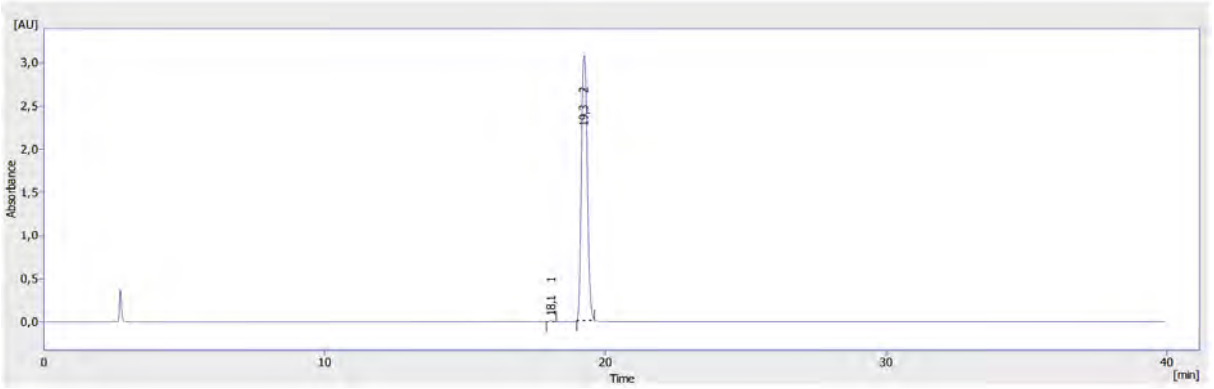

	Reten. Time [min]	Area [mAU.s]	Height [mAU]	Area [%]	Height [%]	W05 [min]	PDA Peak Purity	Compound Name	PDA Best Match Name	PDA Best Match
1	18,083	108,434	10,072	0,2	0,3	0,20	1000			
2	19,250	44875,850	3065,998	99,8	99,7	0,23	811			
	Total	44984,284	3076,070	100,0	100,0					

5.5.9 (*E*)-*N*-(6-(4-(*tert*-butyl)phenyl)-6-oxohex-4-en-3-yl)-*N*,4-dimethylbenzenesulfonamide (8)

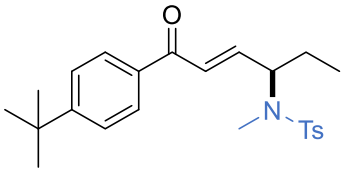

Following the general procedure **C** compound **8** was obtained from enol **S5** (0.25 mmol) and *N*-aminopyridinium salt **2a** (0.33 mmol). The crude product was purified by column chromatography (10:90 AcOEt/Hexane) to afford 74 mg of compound **8** as a colorless oil (Yield = 72 %, 1 h).

^{1}H NMR (400 MHz, $CDCl_3$): δ 7.75-7.68 (m, 4H), 7.49-7.42 (m, 2H), 7.26-7.22 (d, *J* = 8.7 Hz, 2H), 6.77 (dd, *J* = 15.5, 1.2 Hz, 1H), 6.66 (dd, *J* = 15.5, 5.8 Hz, 1H), 4.60 (m, 1H), 2.75 (s, 3H), 2.33 (s, 3H), 1.69-1.57 (m, 2H), 1.35 (s, 9H), 0.94 (t, *J* = 7.4 Hz, 3H) ppm.

^{13}C NMR (100 MHz, $CDCl_3$): δ 189.2, 156.9, 143.5, 143.3, 137.0, 134.7, 129.7, 128.5, 127.2, 126.9, 125.5, 59.8, 35.1, 31.1, 28.7, 24.9, 21.4, 10.8 ppm.

HRMS (ESI, *m/z*): calcd. for $(C_{24}H_{31}NO_3S + Na)^+$: 436.1922, found: 436.1934.

Analytical HPLC:

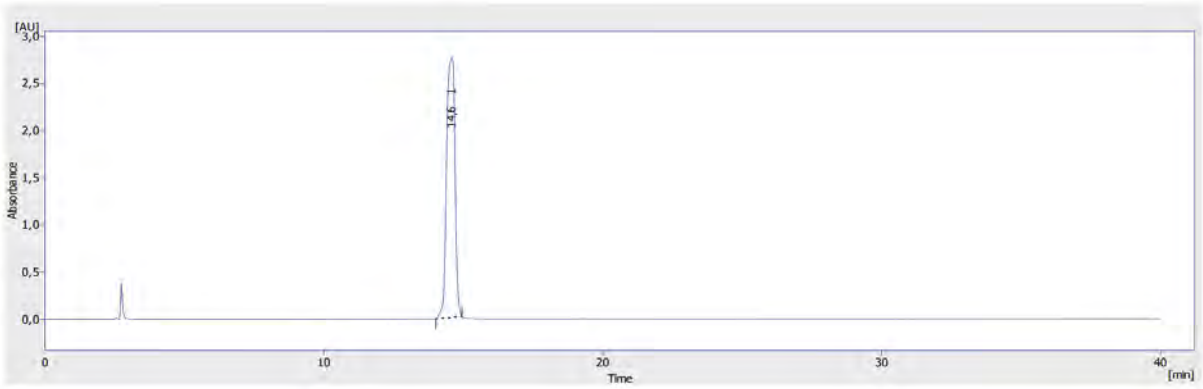

	Reten. Time [min]	Area [mAU.s]	Height [mAU]	Area [%]	Height [%]	W05 [min]	PDA Peak Purity	Compound Name	PDA Best Match Name	PDA Best Match
1	14,583	57649,301	2752,419	100,0	100,0	0,35	797			
	Total	57649,301	2752,419	100,0	100,0					

5.5.10 (*E*)-*N*-(6-(4-chlorophenyl)-6-oxohex-4-en-3-yl)-*N*,4-dimethylbenzenesulfonamide (6)

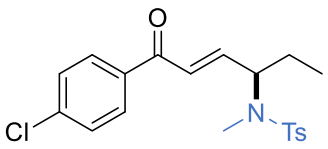

Following the general procedure **C** compound **6** was obtained from enol **S6** (0.25 mmol) and *N*-aminopyridinium salt **2a** (0.33 mmol). The crude product was purified by column chromatography (10:90 AcOEt/Hexane) to afford **68** mg of compound **6** as a yellow oil (**Yield = 69 %**, 1 h).

^{1}H NMR (400 MHz, $CDCl_3$): δ 7.75 – 7.67 (m, 4H), 7.44 – 7.39 (m, 2H), 7.26-7.24 (m 2H), 6.76 (dd, *J* = 15.5, 1.0 Hz, 1H), 6.69 (dd, *J* = 15.5, 5.3 Hz, 1H), 4.65 – 4.53 (m, 1H), 2.74 (s, 3H), 2.35 (s, 3H), 1.68 – 1.55 (m, 2H), 0.93 (t, *J* = 7.4 Hz, 3H) ppm.

^{13}C NMR (100 MHz, $CDCl_3$): δ 188.5, 144.8, 143.4, 139.6, 136.9, 135.6, 129.9, 129.7, 128.9, 127.2, 126.3, 59.7, 28.7, 24.7, 21.4, 10.8 ppm.

HRMS (ESI, *m/z*): calcd. for $(C_{20}H_{22}ClNO_3S + Na)^+$: 414.0907, found: 414.0913.

Analytical HPLC:

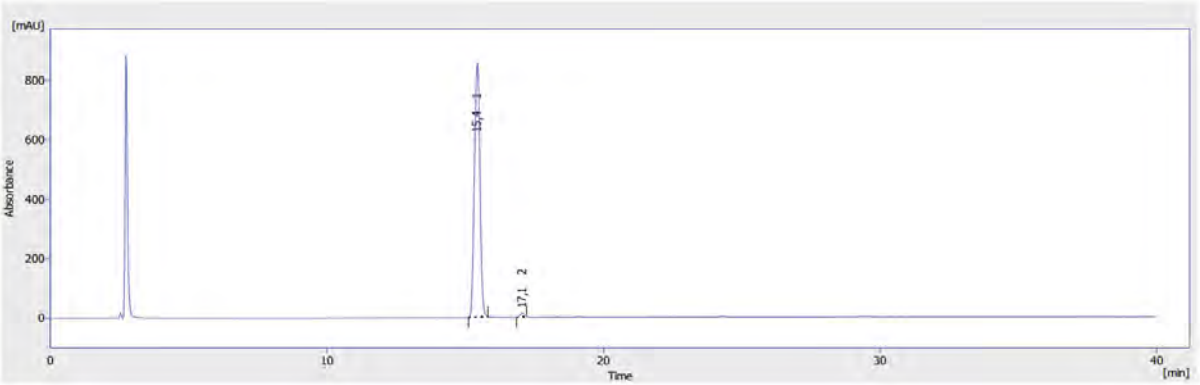

	Reten. Time [min]	Area [mAU.s]	Height [mAU]	Area [%]	Height [%]	W05 [min]	PDA Peak Purity	Compound Name	PDA Best Match Name	PDA Best Match
1	15,433	11935,971	855,053	98,9	98,5	0,25	896			
2	17,067	134,645	12,875	1,1	1,5	0,18	1000			
	Total	12070,616	867,929	100,0	100,0					

5.5.11 (*E*)-*N*-(6-(4-bromophenyl)-6-oxohex-4-en-3-yl)-*N*,4-dimethylbenzenesulfonamide (7)

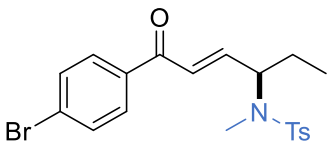

Following the general procedure **C** compound **7** was obtained from enol **S7** (0.25 mmol) and *N*-aminopyridinium salt **2a** (0.33 mmol). The crude product was purified by column chromatography (10:90 AcOEt/Hexane) to afford **72** mg of compound **7** as a yellow oil (**Yield = 66 %**, 1 h).

^{1}H NMR (400 MHz, $CDCl_3$): δ 7.73 – 7.67 (m, 2H), 7.67 – 7.62 (m, 2H), 7.61 – 7.56 (m, 2H), 7.26-7.24 (m, 2H), 6.78 – 6.72 (dd, *J* = 15.6, 0.6 Hz, 1H), 6.69 (dd, *J*= 15.5, 5.0 Hz, 1H), 4.65 – 4.55 (m, 1H), 2.74 (s, 3H), 2.35 (s, 3H), 1.67 – 1.56 (m, 2H), 0.93 (t, *J* = 7.0 Hz, 3H) ppm.

^{13}C NMR (100 MHz, $CDCl_3$): δ 188.7, 144.9, 143.4, 136.9, 136.0, 131.9, 130.0, 129.7, 128.2, 127.2, 126.3, 59.7, 28.7, 24.7, 21.4, 10.8 ppm.

HRMS (ESI, *m/z*): calcd. for $(C_{20}H_{22}BrNO_3S + H)^+$: 436.0582, found: 436.0591.

Analytical HPLC:

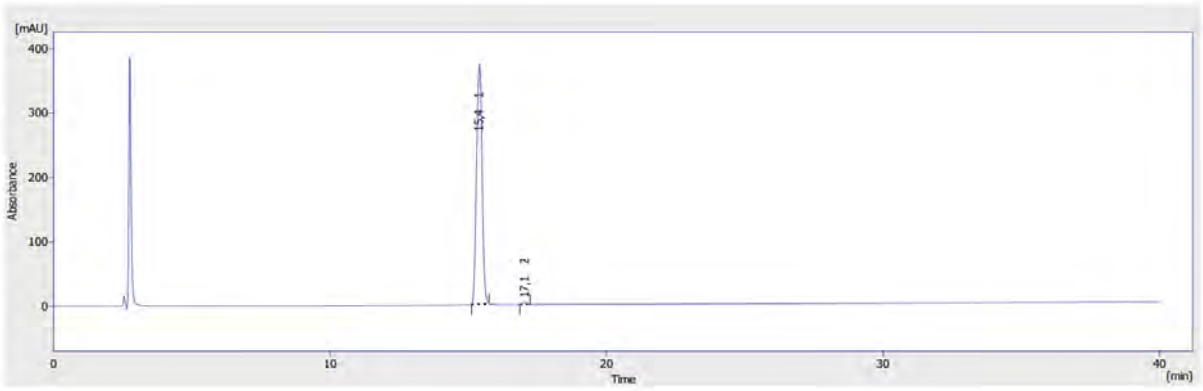

	Reten. Time [min]	Area [mAU.s]	Height [mAU]	Area [%]	Height [%]	W05 [min]	PDA Peak Purity	Compound Name	PDA Best Match Name	PDA Best Match
1	15,400	5163,452	372,508	99,3	99,2	0,23	948			
2	17,050	35,324	3,166	0,7	0,8	0,20	1000			
	Total	5198,776	375,674	100,0	100,0					

5.5.12 (*E*)-*N*-(6-(benzo[*d*][1,3]dioxol-5-yl)-6-oxohex-4-en-3-yl)-*N*,4-dimethylbenzenesulfonamide (5)

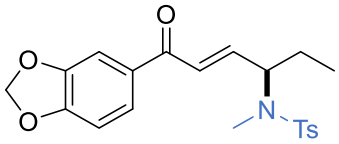

Following the general procedure **C** compound **5** was obtained from enol **S8** (0.25 mmol) and *N*-aminopyridinium salt **2a** (0.33 mmol). The crude product was purified by column chromatography (20:80 AcOEt/Hexane) to afford 71 mg of compound **5** as a colorless oil (**Yield = 71%**, 1 h).

^{1}H NMR (500 MHz, $CDCl_3$): δ 7.71 (d, *J* = 8.2 Hz, 2H), 7.38 (dd, *J* = 8.5, 1.4 Hz, 1H), 7.32 – 7.27 (m, 2H), 7.25 (s, 1H), 6.84 (d, *J* = 8.1 Hz, 1H), 6.73 (d, *J* = 15.1 Hz, 1H), 6.66 (dd, *J* = 15.5, 5.4 Hz, 1H), 6.06 (s, 2H), 4.64 – 4.55 (m, 1H), 2.75 (s, 3H), 2.36 (s, 3H), 1.66 – 1.54 (m, 2H), 0.94 (t, *J* = 7.5 Hz, 3H) ppm.

^{13}C NMR (100 MHz, $CDCl_3$): δ 187.5, 151.9, 148.3, 143.5, 137.0, 132.1, 129.7, 127.2, 126.5, 124.9, 108.3, 107.8, 101.9, 59.8, 28.7, 24.8, 21.4, 10.8 ppm.

HRMS (ESI, *m/z*): calcd. for $(C_{21}H_{23}NO_5S + Na)^+$: 424.1195, found: 424.1199.

Analytical HPLC:

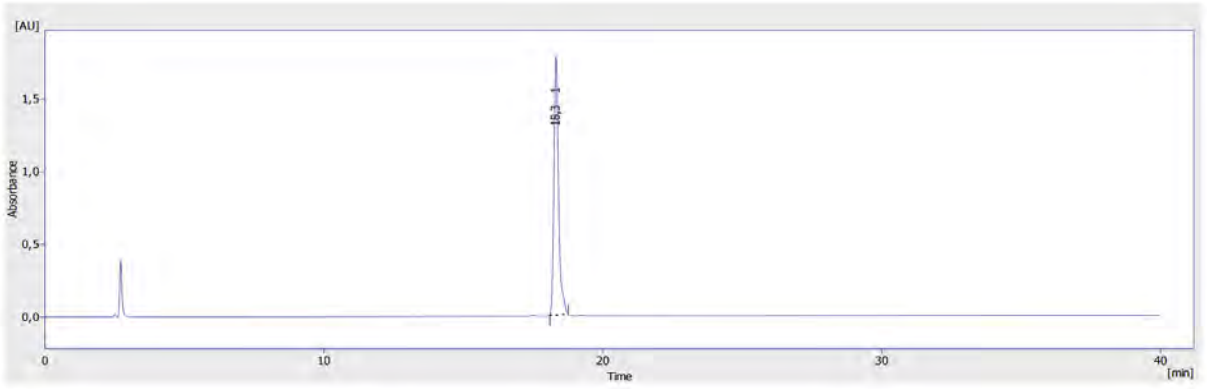

	Reten. Time [min]	Area [mAU.s]	Height [mAU]	Area [%]	Height [%]	W05 [min]	PDA Peak Purity	Compound Name	PDA Best Match Name	PDA Best Match
1	18,317	20529,150	1777,208	100,0	100,0	0,18	785			
	Total	20529,150	1777,208	100,0	100,0					

5.5.13 (*E*)-*N*,4-dimethyl-*N*-(6-(4-nitrophenyl)-6-oxohex-4-en-3-yl)benzenesulfonamide (11)

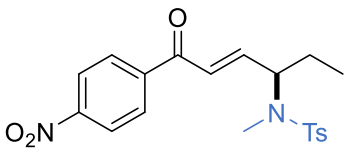

Following the general procedure **C** compound **11** was obtained from enol **S9** (0.25 mmol) and *N*-aminopyridinium salt **2a** (0.33 mmol). The crude product was purified by column chromatography (5:25:70 AcOEt/DCM/Hexane) to afford 81 mg of compound **11** as a yellow oil (**Yield = 80%**, 4 h).

^{1}H NMR (500 MHz, $CDCl_3$): δ 8.30 (d, *J* = 8.9 Hz, 2H), 7.95 (d, *J* = 8.9 Hz, 2H), 7.72 (d, *J* = 8.2 Hz, 2H), 7.29 (d, *J* = 7.9 Hz, 2H), 6.87 – 6.82 (dd, *J* = 15.6, 0.9 Hz, 1H), 6.79 (dd, *J* = 15.5, 5.0 Hz, 1H), 4.64 (dt, *J* = 8.2, 5.7 Hz, 1H), 2.76 (s, 3H), 2.38 (s, 3H), 1.66 (m, 2H), 0.92 (t, *J* = 7.4 Hz, 3H) ppm.

^{13}C NMR (100 MHz, $CDCl_3$): δ 188.3, 150.2, 146.7, 143.5, 142.0, 136.8, 129.7, 129.5, 127.2, 126.1, 123.8, 59.7, 28.7, 24.6, 21.5, 10.8 ppm.

HRMS (ESI, *m/z*): calcd. for $(C_{20}H_{22}N_2O_5S + Na)^+$: 425.1147, found: 425.1151.

Analytical HPLC:

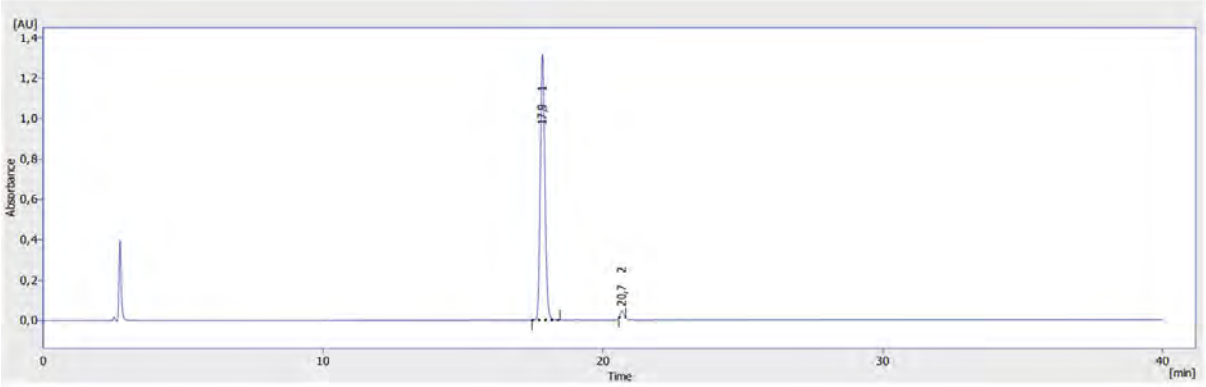

	Reten. Time [min]	Area [mAU.s]	Height [mAU]	Area [%]	Height [%]	W05 [min]	PDA Peak Purity	Compound Name	PDA Best Match Name	PDA Best Match
1	17,850	15011,773	1313,766	98,2	97,7	0,18	820			
2	20,683	270,156	31,579	1,8	2,3	0,17	1000			
	Total	15281,930	1345,345	100,0	100,0					

5.5.14 (*E*)-*N*-(6-(4-acetylphenyl)-6-oxohex-4-en-3-yl)-*N*,4-dimethylbenzenesulfonamide (10)

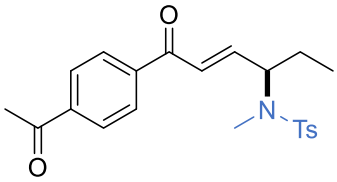

Following the general procedure **C** compound **10** was obtained from enol **S10** (0.15 mmol) and *N*-aminopyridinium salt **2a** (0.2 mmol). The crude product was purified by column chromatography (30:70 Et_2O/Hexane) to afford 34 mg of compound **10** as a yellow oil (**Yield = 67%**, 1 h).

^{1}H NMR (400 MHz, $CDCl_3$): δ 8.03 – 7.98 (m, 2H), 7.87 – 7.81 (m, 2H), 7.72 – 7.66 (m, 2H), 7.26 – 7.23 (m, 2H), 6.80 (dd, *J* = 15.5, 1.1 Hz, 1H), 6.71 (dd, *J* = 15.5, 5.4 Hz, 1H), 4.68 – 4.52 (m, 1H), 2.75 (s, 3H), 2.64 (s, 3H), 2.34 (s, 3H), 1.69 – 1.54 (m, 2H), 0.92 (t, *J* = 7.4 Hz, 3H) ppm.

^{13}C NMR (100 MHz, $CDCl_3$): δ 197.3, 189.3, 145.4, 143.4, 140.6, 140.1, 136.9, 129.7, 128.7, 128.4, 127.2, 126.6, 59.8, 28.7, 26.8, 24.7, 21.4, 10.8 ppm.

HRMS (ESI, *m/z*): calcd. for $(C_{22}H_{25}NO_4S + Na)^+$: 422.1402, found:422.1404.

Analytical HPLC:

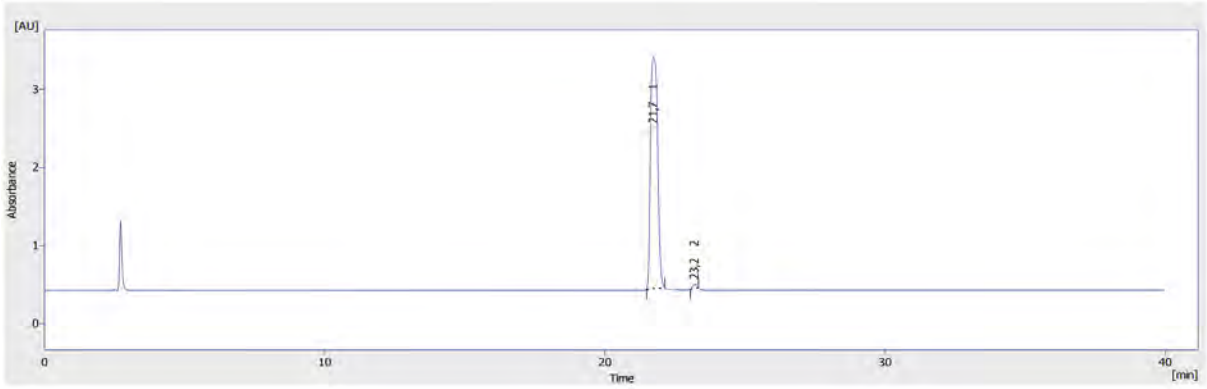

	Reten. Time [min]	Area [mAU.s]	Height [mAU]	Area [%]	Height [%]	W05 [min]	PDA Peak Purity	Compound Name	PDA Best Match Name	PDA Best Match
1	21,733	52725,117	2971,057	99,0	98,1	0,30	820			
2	23,200	522,094	56,156	1,0	1,9	0,18	999			
	Total	53247,211	3027,213	100,0	100,0					

5.5.15 (*E*)-*N*-(6-(4-cyanophenyl)-6-oxohex-4-en-3-yl)-*N*,4-dimethylbenzenesulfonamide (9)

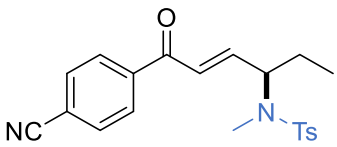

Following the general procedure **C** compound **9** was obtained from enol **S11** (0.25 mmol) and *N*-aminopyridinium salt **2a** (0.33 mmol). The crude product was purified by column chromatography (20:80 AcOEt/Hexane) to afford 58 mg of compound **9** as a colorless oil (**Yield = 60%**, 1 h).

^{1}H NMR (500 MHz, $CDCl_3$): δ 7.89 (d, *J* = 8.3 Hz, 2H), 7.76 (d, *J* = 8.3 Hz, 2H), 7.71 (d, *J* = 8.2 Hz, 2H), 7.28 (d, *J* = 7.8 Hz, 2H), 6.83 (d, *J* = 15.6 Hz, 1H), 6.77 (dd, *J* = 15.5, 5.0 Hz, 1H), 4.62 (q, *J* = 7.0, 6.1 Hz, 1H), 2.75 (s, 3H), 2.38 (s, 3H), 1.64 (m, 2H), 0.92 (t, *J* = 7.3 Hz, 3H) ppm.

^{13}C NMR (100 MHz, $CDCl_3$): δ 188.4, 146.4, 143.5, 140.5, 136.8, 132.4, 129.7, 128.9, 127.2, 126.0, 117.8, 116.3, 59.7, 28.6, 24.6, 21.4, 10.8 ppm.

HRMS (ESI, *m/z*): calcd. for $(C_{21}H_{22}N_2O_3S + Na)^+$: 405.1249, found: 405.1254.

Analytical HPLC:

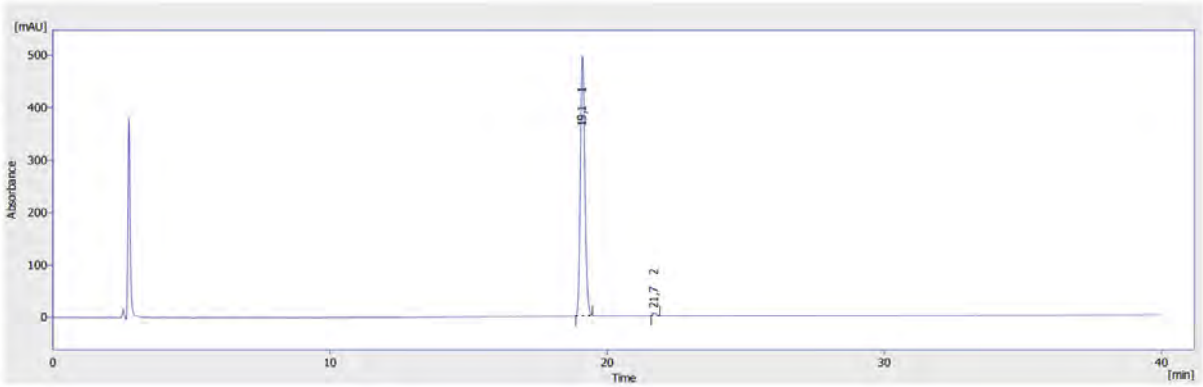

	Reten. Time [min]	Area [mAU.s]	Height [mAU]	Area [%]	Height [%]	W05 [min]	PDA Peak Purity	Compound Name	PDA Best Match Name	PDA Best Match
1	19,100	5559,421	493,409	99,2	99,1	0,18	941			
2	21,700	44,909	4,565	0,8	0,9	0,18	1000			
	Total	5604,331	497,975	100,0	100,0					

5.5.16 (*E*)-*N*-(1,4-bis(4-methoxyphenyl)-4-oxobut-2-en-1-yl)-N,4-dimethylbenzenesulfonamide (13a)

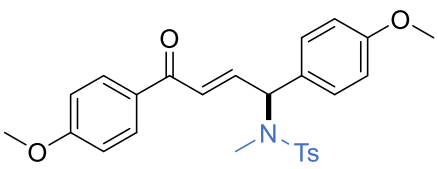

Following the general procedure **C** compound **13a** was obtained from enol **S15** (0.25 mmol) and *N*-aminopyridinium salt **2a** (0.33 mmol). The crude product was purified by column chromatography (15:20:65 AcOEt/DCM/Hexane) to afford 82 mg of compound **13a** as a colorless oil (**Yield = 71%**, 1 h).

^{1}H NMR (400 MHz, $CDCl_3$): δ 7.84 (d, *J* = 8.9 Hz, 2H), 7.72 (d, *J* = 8.2 Hz, 2H), 7.24 (d, *J* = 8.0 Hz, 2H), 7.15 (d, *J* = 8.5 Hz, 2H), 7.02 (dd, *J* = 15.4, 6.2 Hz, 1H), 6.95 (d, *J* = 8.9 Hz, 2H), 6.91 (dd, *J* = 15.4, 1.4 Hz, 1H), 6.84 (d, *J* = 8.8 Hz, 2H), 5.92 (d, *J* = 6.0 Hz, 1H), 3.89 (s, 3H), 3.80 (s, 3H), 2.65 (s, 3H), 2.33 (s, 3H) ppm.

^{13}C NMR (100 MHz, $CDCl_3$): δ 187.6, 163.7, 159.5, 143.4, 141.6, 136.8, 130.9, 130.2, 129.7, 129.5, 128.8, 127.9, 127.3, 114.1, 113.9, 61.0, 55.5, 55.3, 30.0, 21.4 ppm.

HRMS (ESI, *m/z*): calcd. For $(C_{26}H_{27}NO_5S + Na)^+$: 488.1508, found: 488.1511.

Analytical HPLC:

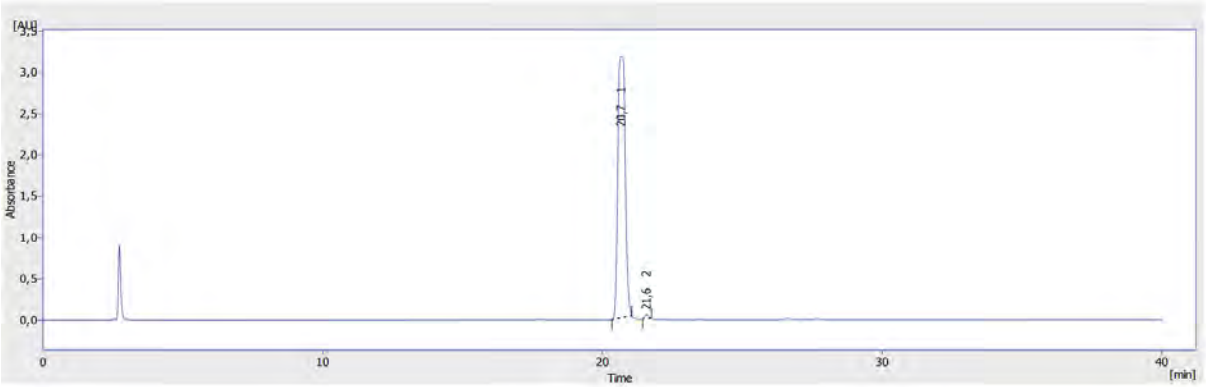

	Reten. Time [min]	Area [mAU.s]	Height [mAU]	Area [%]	Height [%]	W05 [min]	PDA Peak Purity	Compound Name	PDA Best Match Name	PDA Best Match
1	20,683	58010,912	3165,692	99,2	98,5	0,30	797			
2	21,583	486,591	47,542	0,8	1,5	0,18	997			
	Total	58497,503	3213,234	100,0	100,0					

5.5.17 (*Z*)-*N*-(1-(4-methoxyphenyl)-1-oxo-4-(4-(trifluoromethyl)phenyl)but-2-en-2-yl)-*N*,4-dimethylbenzenesulfonamide (14c)

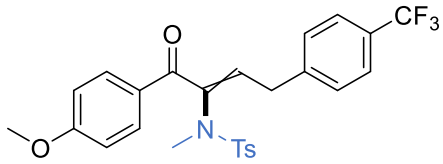

Following the general procedure **C** compound **14c** was obtained from enol **S12** (0.25 mmol) and *N*-aminopyridinium salt **2a** (0.33 mmol). The crude product was purified by column chromatography (5:25:70 AcOEt/DCM/Hexane) to afford 75 mg of compound **14c** as a yellow solid (**Yield = 60%**, *E/Z* ~1:12, 1 h). (Inseparable by column chromatography).

^{1}H NMR (400 MHz, $CDCl_3$): (major isomer) δ 7.86 (d, *J* = 8.8 Hz, 2H), 7.67 (d, *J* = 8.2 Hz, 2H), 7.49 (d, *J* = 8.2 Hz, 2H), 7.40 (d, *J* = 8.2 Hz, 2H), 7.24 (d, *J* = 8.0 Hz, 2H), 6.94 (d, *J* = 8.8 Hz, 2H), 6.64 (t, *J* = 6.9 Hz, 1H), 3.89 (s, 3H), 3.78 (d, *J* = 6.8 Hz, 2H), 3.14 (s, 3H), 2.36 (s, 3H) ppm.

^{13}C NMR (100 MHz, $CDCl_3$): (major isomer) δ 194.9, 163.8, 143.9, 140.6, 140.1, 136.7, 130.4, 129.7, 129.4, 127.4, 127.0, 126.6, 125.4, 125.3, 113.8, 55.5, 37.9, 37.6, 21.4 ppm.

HRMS (ESI, *m/z*): calcd. for $(C_{26}H_{24}F_3NO_4S + Na)^+$: 526.1276, found: 526.1271.

Analytical HPLC: major isomer

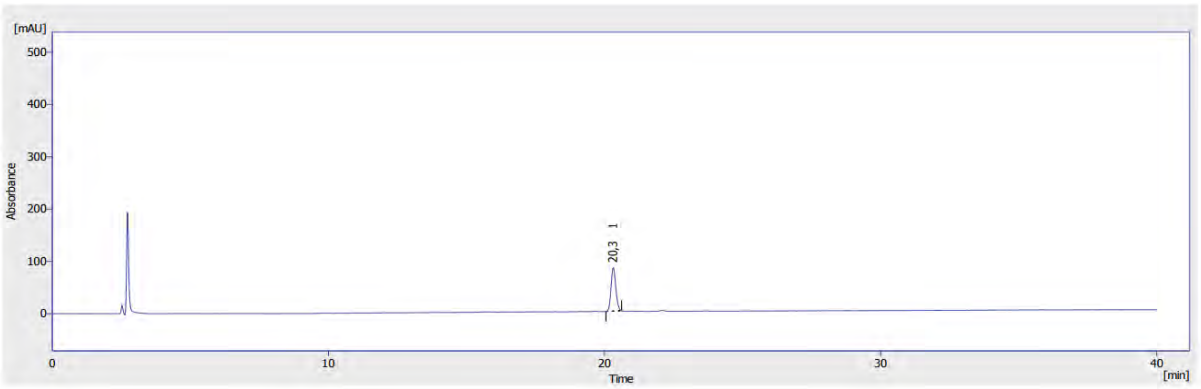

	Reten. Time [min]	Area [mAU.s]	Height [mAU]	Area [%]	Height [%]	W05 [min]	PDA Peak Purity	Compound Name	PDA Best Match Name	PDA Best Match
1	20,317	989,894	83,526	100,0	100,0	0,20	996			
	Total	989,894	83,526	100,0	100,0					

m.p.: 137-140 °C.

5.5.18 (*Z*)-*N*,4-dimethyl-*N*-(1-oxo-1,4-bis(4-(trifluoromethyl)phenyl)but-2-en-2-yl) benzenesulfonamide (14b)

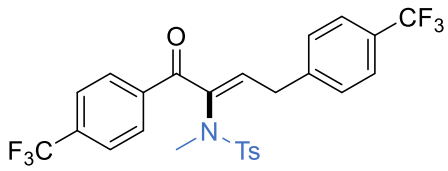

Following the general procedure **C** compound **14b** was obtained from enol **S13** (0.25 mmol) and *N*-aminopyridinium salt **2a** (0.33 mmol). The crude product was purified by column chromatography (20:80 AcOEt/Hexane) to afford 83 mg of compound **14b** as a yellow solid (**Yield = 64%**, 1h).

^{1}H NMR (400 MHz, $CDCl_3$): δ 8.02 (d, *J* = 8.1 Hz, 2H), 7.75 (d, *J* = 8.2 Hz, 2H), 7.67 (d, *J* = 8.2 Hz, 2H), 7.48 (d, *J* = 8.2 Hz, 2H), 7.34 (d, *J* = 8.2 Hz, 2H), 7.24 (d, *J* = 8.0 Hz, 2H), 6.63 (t, *J* = 6.8 Hz, 1H), 3.94 (d, *J* = 6.8 Hz, 2H), 3.12 (s, 3H), 2.35 (s, 3H) ppm.

^{13}C NMR (100 MHz, $CDCl_3$): δ 195.5, 144.0, 140.6, 140.1, 138.9, 136.5, 134.9, 134.7, 130.4, 129.8, 128.5, 127.4, 126.7, 125.8, 125.5, 125.4, 124.6, 122.9, 122.4, 38.6, 37.4, 21.4 ppm.

HRMS (ESI, *m/z*): calcd. for $(C_{26}H_{21}F_6NO_3S + H)^+$: 542.1225, found: 542.1226.

Analytical HPLC:

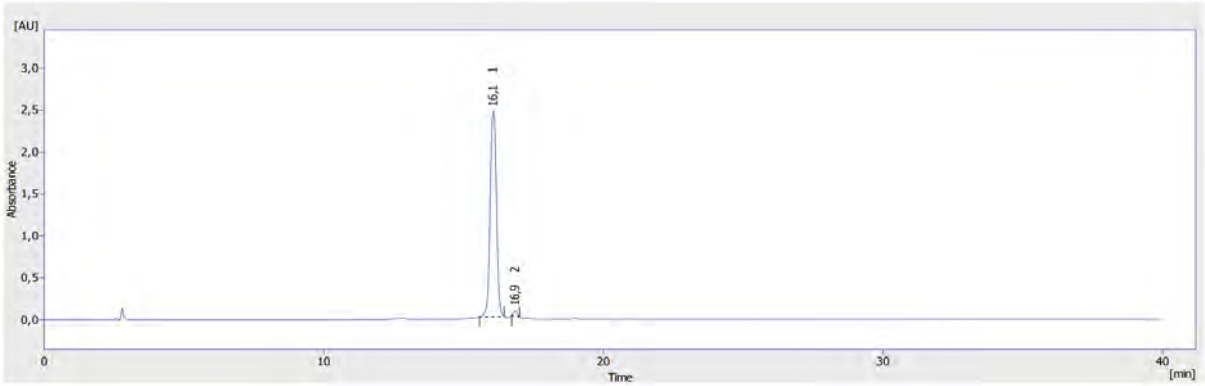

	Reten. Time [min]	Area [mAU.s]	Height [mAU]	Area [%]	Height [%]	W05 [min]	PDA Peak Purity	Compound Name	PDA Best Match Name	PDA Best Match
1	16,067	38288,818	2452,307	98,4	97,5	0,27	804			
2	16,850	625,174	63,251	1,6	2,5	0,18	998			
	Total	38913,992	2515,558	100,0	100,0					

m.p.: 144-146 °C.

5.5.19 (*Z*)-*N*-(1-(4-methoxyphenyl)-4-oxo-4-(4-(trifluoromethyl)phenyl)but-2-en-1-yl)-*N*,4-dimethylbenzenesulfonamide (13d)

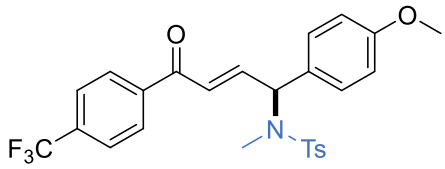

Following the general procedure **C** compound **13d** was obtained from enol **S14** (0.25 mmol) and *N*-aminopyridinium salt **2a** (0.33 mmol). The crude product was purified by column chromatography (20:80 AcOEt/Hexane) to afford 55 mg of compound **13d** as a yellow solid (**Yield = 44%**, 1h).

^{1}H NMR (400 MHz, $CDCl_3$): δ 7.93 (d, *J* = 8.1 Hz, 2H), 7.73 (d, *J* = 8.1 Hz, 4H), 7.27 (d, *J* = 7.8 Hz, 2H), 7.14 – 7.08 (m, 3H), 6.94 – 6.91 (m, 1H), 6.84 (d, *J* = 8.7 Hz, 2H), 5.93 (d, *J* = 5.7 Hz, 1H), 3.79 (s, 3H), 2.64 (s, 3H), 2.35 (s, 3H) ppm.

^{13}C NMR (100 MHz, $CDCl_3$): δ 188.6, 159.6, 144.5, 143.6, 140.0, 136.7, 134.8, 134.5, 134.3, 134.0, 129.7, 129.6, 128.9, 128.2, 127.3, 125.7, 125.6, 124.6, 122.5, 114.2, 61.1, 55.3, 30.1, 21.4 ppm.

HRMS (ESI, *m/z*): calcd. for $(C_{26}H_{24}F_3NO_4S + Na)^+$: 526.1276, found: 526.1278.

Analytical HPLC:

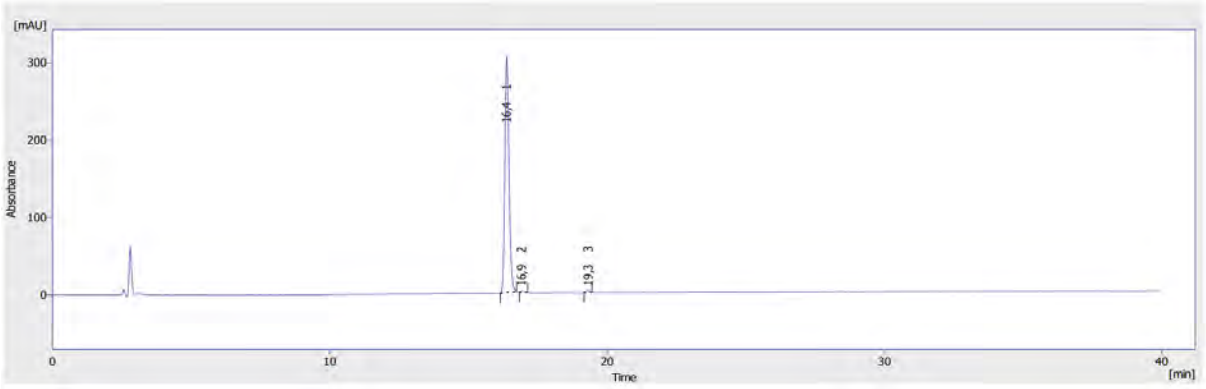

	Reten. Time [min]	Area [mAU.s]	Height [mAU]	Area [%]	Height [%]	W05 [min]	PDA Peak Purity	Compound Name	PDA Best Match Name	PDA Best Match
1	16,383	3174,496	305,962	99,0	98,8	0,17	955			
2	16,933	14,257	1,691	0,4	0,5	0,15	1000			
3	19,333	16,606	1,919	0,5	0,6	0,17	1000			
	Total	3205,358	309,572	100,0	100,0					

m.p.: 125-126 °C.

5.5.20 (*E*)-*N*-(1,4-bis(3-methoxyphenyl)-4-oxobut-2-en-1-yl)-*N*,4-dimethylbenzenesulfonamide (13b)

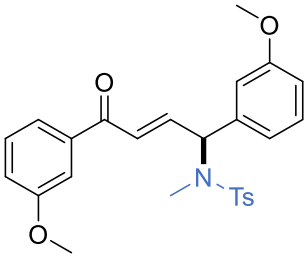

Following the general procedure **C** compound **13b** was obtained from enol **S16** (0.25 mmol) and *N*-aminopyridinium salt **2a** (0.33 mmol). The crude product was purified by column chromatography (30:70 AcOEt/Hexane) to afford 72 mg of compound **13b** as a yellow oil (**Yield = 62%**, 1 h).

^{1}H NMR (400 MHz, $CDCl_3$): δ 7.73 (d, *J* = 8.3 Hz, 2H), 7.42 – 7.39 (m, 1H), 7.38 – 7.34 (m, 2H), 7.26 (s, 1H), 7.23 (d, *J* = 7.8 Hz, 2H), 7.13 (dt, *J* = 6.5, 2.7 Hz, 1H), 7.04 (dd, *J* = 15.4, 6.4 Hz, 1H), 6.89 (dd, *J* = 15.4, 1.4 Hz, 1H), 6.86 – 6.79 (m, 2H), 6.74 (t, *J* = 1.9 Hz, 1H), 5.91 (d, *J* = 6.4 Hz, 1H), 3.87 (s, 3H), 3.75 (s, 3H), 2.68 (s, 3H), 2.33 (s, 3H) ppm.

^{13}C NMR (100 MHz, $CDCl_3$): δ 189.1, 159.9, 143.6, 142.0, 128.6, 138.3, 136.7, 129.7, 129.6, 128.4, 127.3, 121.1, 120.4, 119.7, 113.9, 113.8, 112.9, 61.5, 55.5, 55.2, 30.2, 21.4 ppm.

HRMS (ESI, *m/z*): calcd. for $(C_{26}H_{27}NO_5S + Na)^+$: 488.1508, found: 488.1514.

Analytical HPLC:

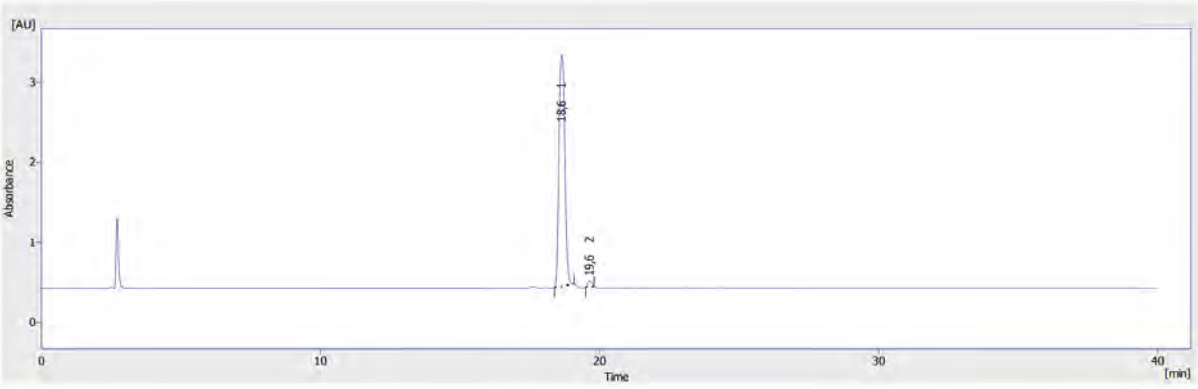

	Reten. Time [min]	Area [mAU.s]	Height [mAU]	Area [%]	Height [%]	W05 [min]	PDA Peak Purity	Compound Name	PDA Best Match Name	PDA Best Match
1	18,650	42171,853	2884,804	98,3	97,5	0,25	795			
2	19,650	714,954	73,826	1,7	2,5	0,18	998			
	Total	42886,807	2958,630	100,0	100,0					

5.5.21 (*Z*)-*N*-(1,4-bis(2-methoxyphenyl)-4-oxobut-2-en-1-yl)-*N*,4-dimethylbenzenesulfonamide (13c)

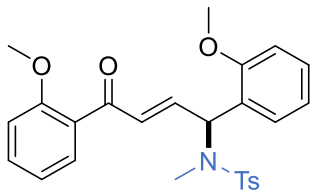

Following the general procedure **C** compound **13c** was obtained from enol **S17** (0.25 mmol) and *N*-aminopyridinium salt **2a** (0.33 mmol). The crude product was purified by column chromatography (30:70 AcOEt/Hexane) to afford 70 mg of compound **13c** as a yellow oil (**Yield = 60%**, 1 h).

^{1}H NMR (400 MHz, $CDCl_3$): δ 7.67 (d, *J* = 8.2 Hz, 2H), 7.59 (dd, *J* = 7.6, 1.7 Hz, 1H), 7.45 (ddd, *J* = 8.4, 7.4, 1.8 Hz, 1H), 7.28 (ddd, *J* = 8.4, 7.5, 1.8 Hz, 1H), 7.20 – 7.15 (m, 3H), 7.0 (td, *J* = 7.5, 0.8 Hz, 1H), 6.95 (d, *J* = 9.1 Hz, 3H), 6.90 (td, *J* = 7.5, 0.9 Hz, 1H), 6.8 (d, *J* = 8.2 Hz, 1H), 6.28 (s, 1H), 3.9 (s, 3H), 3.7 (s, 3H), 2.6 (s, 3H), 2.4 (s, 3H) ppm.

^{13}C NMR (100 MHz, $CDCl_3$): δ 192.0, 158.4, 157.1, 142.9, 142.8, 137.3, 133.2, 131.7, 130.5, 130.4, 129.8, 129.2, 128.6, 127.4, 125.0, 120.6, 120.2, 111.5, 110.8, 56.6, 55.6, 55.1, 30.9, 21.4 ppm.

HRMS (ESI, *m/z*): calcd. for $(C_{26}H_{27}NO_5S + Na)^+$: 488.1508, found: 488.1509.

Analytical HPLC:

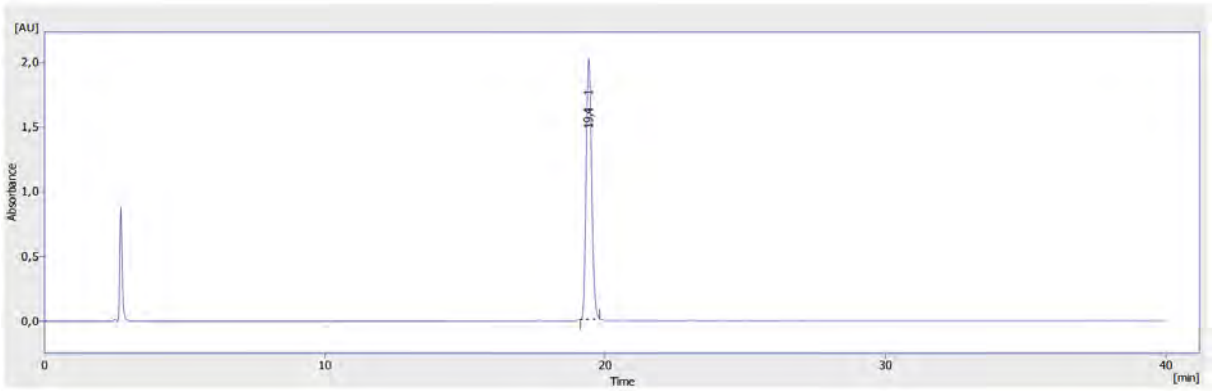

	Reten. Time [min]	Area [mAU.s]	Height [mAU]	Area [%]	Height [%]	W05 [min]	PDA Peak Purity	Compound Name	PDA Best Match Name	PDA Best Match
1	19,417	27359,927	2013,348	100,0	100,0	0,23	837			
	Total	27359,927	2013,348	100,0	100,0					

5.5.22 (*Z*)-*N*-(1,4-bis(4-cyanophenyl)-1-oxobut-2-en-2-yl)-*N*,4-dimethylbenzenesulfonamide (14a)

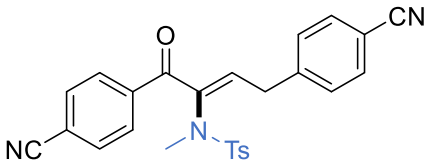

Following the general procedure **C** compound **14a** was obtained from enol **S18** (0.25 mmol) and *N*-aminopyridinium salt **2a** (0.33 mmol). The crude product was purified by column chromatography (30:70 AcOEt/Hexane) to afford 66 mg of compound **14a** as a yellow solid (**Yield = 58%**, 4 h).

^{1}H NMR (500 MHz, $CDCl_3$): δ 7.93 (d, *J* = 8.2 Hz, 2H), 7.71 (d, *J* = 8.2 Hz, 2H), 7.59 (d, *J* = 8.1 Hz, 2H), 7.45 (d, *J* = 8.2 Hz, 2H), 7.24 (d, *J* = 8.3 Hz, 2H), 7.19 (d, *J* = 8.7 Hz, 2H), 6.59 (t, *J* = 6.8 Hz, 1H), 3.86 (d, *J* = 6.8 Hz, 2H), 3.01 (s, 3H), 2.31 (s, 3H) ppm.

^{13}C NMR (100 MHz, $CDCl_3$): δ 195.0, 144.2, 141.0, 140.4, 139.1, 136.3, 132.6, 132.3, 129.8, 128.6, 127.4, 126.9, 126.6, 118.4, 117.7, 116.9, 111.9, 38.6, 37.3, 21.5 ppm.

HRMS (ESI, *m/z*): calcd. for $(C_{26}H_{21}N_3O_3S + Na)^+$: 478.1201, found: 478.1201.

Analytical HPLC: decomposition.

m.p.: 168-170 °C.

5.5.23 (*E*)-*N*,4-dimethyl-*N*-(4-oxo-1,4-diphenylbut-2-en-1-yl)benzenesulfonamide (12)

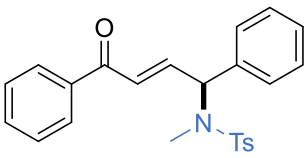

Following the general procedure **C** compound **12** was obtained from enol **S20** (0.25 mmol) and *N*-aminopyridinium salt **2a** (0.33 mmol). The crude product was purified by column chromatography (20:80 AcOEt/Hexane) to afford 80 mg of compound **12** as a yellow oil (**Yield = 79%**, 16 h).

^{1}H NMR (500 MHz, $CDCl_3$): δ 7.81 (d, *J* = 7.5 Hz, 2H), 7.72 (d, *J* = 8.1 Hz, 2H), 7.58 (t, *J* = 7.4 Hz, 1H), 7.46 (t, *J* = 7.7 Hz, 2H), 7.34 – 7.28 (m, 3H), 7.26 – 7.22 (m, 4H), 7.05 (dd, *J* = 15.5, 6.4 Hz, 1H), 6.90 (dd, *J* = 15.5, 0.9 Hz, 1H), 5.96 (d, *J* = 6.4 Hz, 1H), 2.66 (s, 3H), 2.31 (s, 3H) ppm.

^{13}C NMR (125 MHz, $CDCl_3$): δ 189.3, 143.6, 142.1, 137.2, 136.8, 136.7, 133.2, 129.7, 128.8, 128.7, 128.6, 128.3, 128.2, 127.3, 61.5, 30.2, 21.4 ppm.

HRMS (ESI, *m/z*): calcd. for $(C_{24}H_{23}NO_3S + Na)^+$: 428.1296; found: 428.1288.

Elemental analysis (%) calcd. for $C_{24}H_{23}NO_3S$: C 71.09, H 5.72, N 3.45, S 7.91; found: C 70.83, H 5.67, N 3.69, S 8.08.

5.5.24 *N*,4-dimethyl-*N*-(4-oxocyclohex-2-en-1-yl)benzenesulfonamide (15)

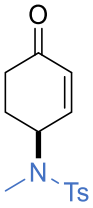

Following the general procedure **C** compound **15** was obtained from enol **S21** (0.25 mmol) and *N*-aminopyridinium salt **2a** (0.33 mmol). The crude product was purified by column chromatography (20:80 Et_2O/Pentane) to afford 31 mg of compound **15** as a white solid (**Yield = 45%**, 1 h).

^{1}H NMR (500 MHz, $CDCl_3$): δ 7.73 (d, *J* = 8.2 Hz, 2H), 7.34 (d, *J* = 8.1 Hz, 2H), 6.45 (dt, *J* = 10.3, 1.7 Hz, 1H), 6.01 (ddd, *J* = 10.3, 2.5, 0.8 Hz, 1H), 4.93 (ddd, *J* = 10.2, 5.4, 2.5 Hz, 1H), 2.76 (s, 3H), 2.59 – 2.37 (m, 5H), 2.08 – 1.95 (m, 2H) ppm.

^{13}C NMR (125 MHz, $CDCl_3$): δ 197.1, 150.2, 143.8, 136.3, 132.2, 130.0, 127.1, 54.5, 36.6, 29.8, 27.2, 21.5 ppm.

HRMS (ESI, *m/z*): calcd. for $(C_{14}H_{17}NO_3S + Na)^+$: 302.0827; found: 302.0818.

Elemental analysis (%) calcd. for $C_{14}H_{17}NO_3S$: C 60.19, H 6.13, N 5.01, S 11.48; found: C 60.13, H 6.11, N 5.22, S 11.56.

5.5.25 *N*-((5,5-dimethyl-3-oxocyclohex-1-en-1-yl)methyl)-*N*,4-dimethylbenzenesulfonamide (16)

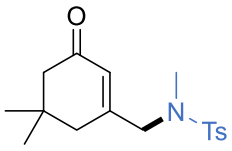

Following the general procedure **C** compound **16** was obtained from enol **S22** (0.25 mmol) and *N*-aminopyridinium salt **2a** (0.33 mmol). The crude product was purified by column chromatography (20:80 Et_2O/Pentane) to afford 51 mg of compound **16** as a yellow solid (**Yield = 63%**, 1 h).

^{1}H NMR (500 MHz, $CDCl_3$): δ 7.68 (d, *J* = 8.3 Hz, 2H), 7.35 (d, *J* = 8.0 Hz, 2H), 5.9 (s, 1H), 3.67 (s, 2H), 2.63 (s, 3H), 2.45 (s, 3H), 2.28 (s, 2H), 2.26 (s, 2H), 1.06 (s, 6H) ppm.

^{13}C NMR (125 MHz, $CDCl_3$): δ 199.4, 156.6, 143.8, 134.0, 129.9, 127.4, 126.8, 55.7, 51.3, 40.8, 34.8, 33.6, 28.2, 21.5 ppm.

HRMS (ESI, *m/z*): calcd. for $(C_{17}H_{23}NO_3S + Na)^+$: 344.1296, found: 344.1304.

Analytical HPLC:

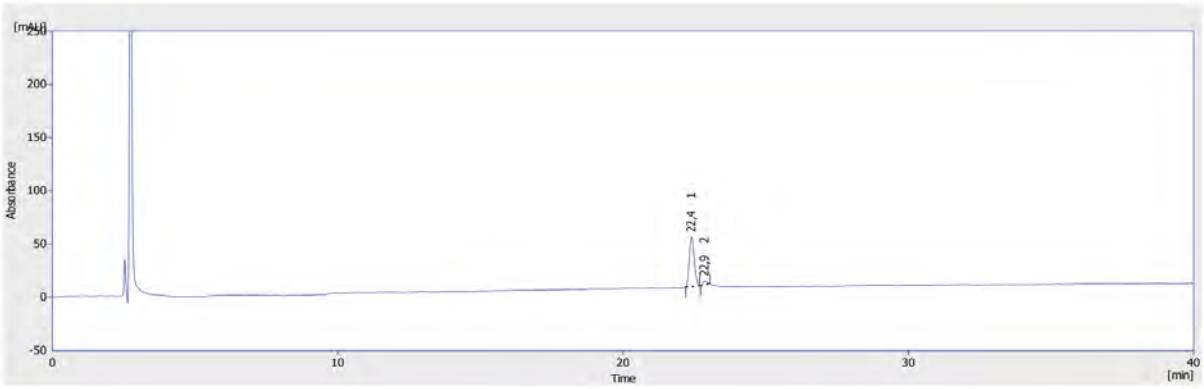

	Reten. Time [min]	Area [mAU.s]	Height [mAU]	Area [%]	Height [%]	W05 [min]	PDA Peak Purity	Compound Name	PDA Best Match Name	PDA Best Match
1	22,400	276,997	23,102	94,2	93,2	0,20	999			
2	22,867	17,185	1,686	5,8	6,8	0,22	1000			
	Total	294,182	24,789	100,0	100,0					

m.p.: 117-119 °C.

5.5.26 *N*,4-dimethyl-*N*-(4-oxocyclohept-2-en-1-yl)benzenesulfonamide (17)

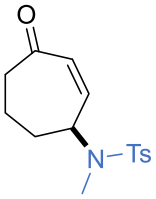

Following the general procedure **C** compound **17** was obtained from enol **S23** (0.25 mmol) and *N*-aminopyridinium salt **2a** (0.33 mmol). The crude product was purified by column chromatography (5:25:70 AcOEt/DCM/Hexane) to afford 50 mg of compound **17** as a yellow oil (**Yield = 69%**, 1 h).

^{1}H NMR (500 MHz, $CDCl_3$): δ 7.69 (d, *J* = 8.2 Hz, 2H), 7.28 (d, *J* = 8.1 Hz, 2H), 6.66 – 6.58 (m, 1H), 5.99 – 5.92 (m, 1H), 4.79 (dd, *J* = 10.6, 4.9 Hz, 1H), 2.83 (s, 3H), 2.55 – 2.43 (m, 2H), 2.42 (s, 3H), 2.05 – 1.79 (m, 4H) ppm.

^{13}C NMR (100 MHz, $CDCl_3$): δ 198.6, 146.4, 143.0, 136.6, 130.8, 129.4, 127.3, 65.7, 30.9, 29.3, 27.9, 23.6, 21.5 ppm.

HRMS (ESI, *m/z*): calcd. for $(C_{15}H_{19}NO_3S + Na)^+$: 316.0983, found: 316.0988.

Analytical HPLC:

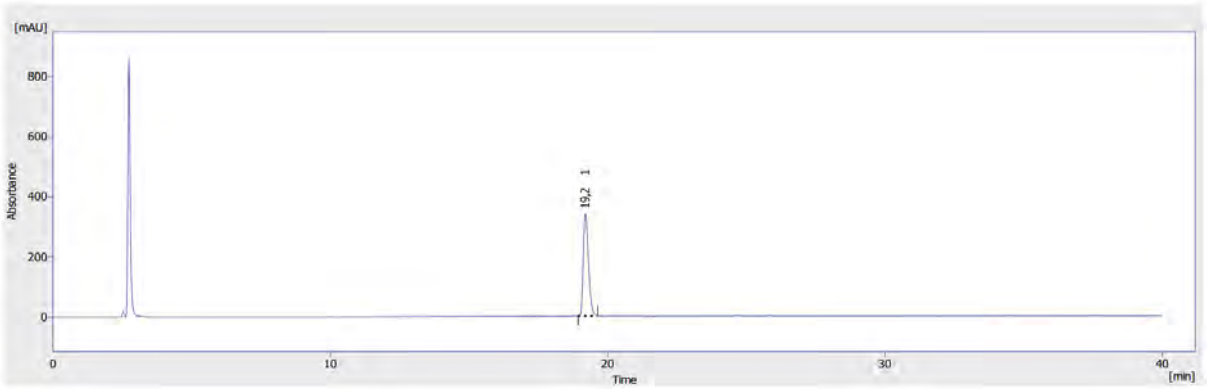

	Reten. Time [min]	Area [mAU.s]	Height [mAU]	Area [%]	Height [%]	W05 [min]	PDA Peak Purity	Compound Name	PDA Best Match Name	PDA Best Match
1	19,200	4400,738	340,387	100,0	100,0	0,22	944			
	Total	4400,738	340,387	100,0	100,0					

5.5.27 *N*,4-dimethyl-*N*-(5-oxo-2,5-dihydrofuran-2-yl)benzenesulfonamide (21)

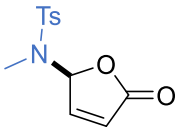

Following the general procedure **C** compound **21** was obtained from enol **S24** (0.25 mmol) and *N*-aminopyridinium salt **2a** (0.33 mmol). The crude product was purified by column chromatography (20:80 AcOEt/Hexane) to afford 50 mg of compound **21** as a white solid (**Yield = 74%**, 1 h).

^{1}H NMR (400 MHz, $CDCl_3$): δ 7.78 (d, *J* = 8.3 Hz, 2H), 7.35 (d, *J* = 8.1 Hz, 2H), 7.29 – 7.24 (m, 1H), 6.87 (t, *J* = 1.7 Hz, 1H), 6.30 (dd, *J* = 5.6, 1.9 Hz, 1H), 2.54 (s, 3H), 2.45 (s, 3H) ppm.
^{13}C NMR (100 MHz, $CDCl_3$): δ 170.0, 151.2, 144.5, 134.1, 129.9, 128.0, 125.7, 88.8, 28.3, 21.6 ppm.
HRMS (ESI, *m/z*): calcd. for $(C_{12}H_{13}NO_4S + Na)^+$: 290.0463; found: 290.0464.
Elemental analysis (%) calcd. for $C_{12}H_{13}NO_4S$: C 53.92, H 4.90, N 5.24, S 12.00; found: C 53.73, H 4.91, N 5.09, S 11.93.
m.p.: 89-92 °C.

5.5.28 *N*-((3*S*,4a*S*,5*R*)-4a,5-dimethyl-7-oxo-3-(prop-1-en-2-yl)-1,2,3,4,4a,5,6,7-octahydronaphthalen-1-yl)-*N*,4-dimethylbenzenesulfonamide (24)

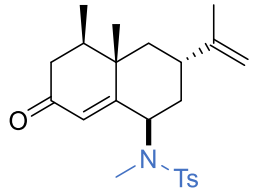

Following the general procedure **C** compound **24** was obtained from enol **S26** (0.25 mmol) and *N*-aminopyridinium salt **2a** (0.33 mmol). The crude product was purified by column chromatography (20:80 AcOEt/Hexane) to afford 68 mg of compound **24** as a white solid (**Yield = 68%**, 1h). Two diastereoisomers formed α/β = 1:7.

Two diastereoisomers: seperable by column chromatography, dr.r: α/β=1:7.

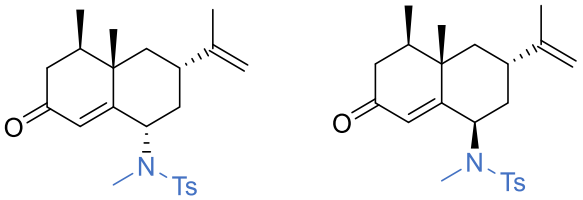

α β

^{1}H NMR (400 MHz, $CDCl_3$): (major diastereomer, β) δ 7.68 (d, *J* = 8.3 Hz, 2H), 7.29 (d, *J* = 8.1 Hz, 2H), 5.94 (d, *J* = 2.2 Hz, 1H), 4.83 (ddd, *J* = 13.4, 5.3, 2.1 Hz, 1H), 4.77 – 4.76 (m, 2H), 2.63 (s, 3H), 2.59 – 2.54 (m, 1H), 2.42 (s, 3H), 2.34 – 2.31 (m, 2H), 2.09 – 1.99 (m, 2H), 1.88 (dd, *J* = 13.7, 7.2 Hz, 1H), 1.70 (s, 3H), 1.39 – 1.29 (m, 2H), 1.09 (s, 3H), 0.95 (d, *J* = 6.7 Hz, 3H) ppm.

^{13}C NMR (100 MHz, $CDCl_3$): (major diastereomer, β) δ 198.8, 168.6, 148.2, 143.5, 136.4, 129.8, 127.1, 123.8, 109.8, 55.8, 42.2, 39.9, 39.2, 34.9, 34.3, 29.2, 26.0, 21.5, 20.6, 17.5, 15.0 ppm.

HRMS (ESI, *m/z*): calcd. for $(C_{23}H_{31}NO_3S + Na)^+$: 424.1922, found: 424.1931.

Analytical HPLC: (major diastereomer)

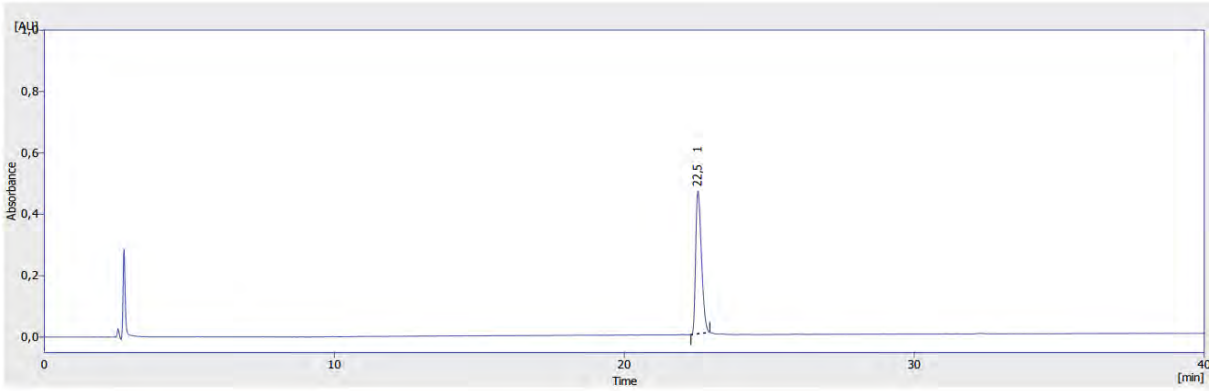

	Reten. Time [min]	Area [mAU.s]	Height [mAU]	Area [%]	Height [%]	W05 [min]	PDA Peak Purity	Compound Name	PDA Best Match Name	PDA Best Match
1	22,533	3221,411	232,495	100,0	100,0	0,23	957			
	Total	3221,411	232,495	100,0	100,0					

m.p.:151-153 °C.

5.5.29 (8*R*,9*S*,10*R*,13*S*,14*S*,17*S*)-6-((*N*,4-dimethylphenyl)sulfonamido)-10,13-dimethyl-3-oxo-2,3,6,7,8,9,10,11,12,13,14,15,16,17-tetradecahydro-1H-cyclopenta[*a*]phenanthren-17-yl acetate (25)

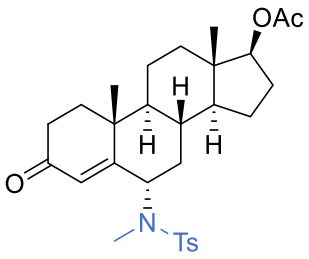

α

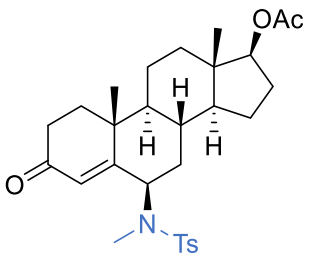

β

Following the general procedure **C** compound **25** was obtained from enol **S27** (0.25 mmol) and *N*-aminopyridinium salt **2a** (0.33 mmol). The crude product was purified by column chromatography (20:80 AcOEt/Hexane) to afford 68 mg of compound **25** as a white solid (**Yield = 61%**, 1h).

Two diastereoisomers: seperable by column chromatography, dr.r: α/β=1.73:1.

^{1}H NMR (400 MHz, $CDCl_3$): (major diastereomer, α) δ 7.67 (d, *J* = 8.2 Hz, 2H), 7.33 (d, *J* = 8.2 Hz, 2H), 5.90 (s, 1H), 4.62 (t, *J* = 8.5 Hz, 1H), 4.45 – 4.42 (m, 1H), 2.65 (s, 3H), 2.52 (ddd, *J* = 18.7, 13.5, 5.3 Hz, 1H), 2.43 (s, 4H), 2.21 – 2.13 (m, 1H), 2.04 (s, 3H), 2.00 – 1.93 (m, 2H), 1.86 (m, 1H), 1.79 (dt, *J* = 13.7, 3.4 Hz, 1H), 1.72 (dd, *J* = 13.3, 5.3 Hz, 1H), 1.60 – 1.56 (m, 2H), 1.51 – 1.46 (m, 1H), 1.42-1.38 (m, 1H), 1.43 – 1.31 (m, 1H), 1.27 – 1.22 (m, 2H), 1.19 (s, 3H), 1.12 – 1.07 (m, 2H), 0.8 (s, 3H) ppm.

^{13}C NMR (100 MHz, $CDCl_3$): (major diastereomer, α) δ 198.8, 171.1, 167.8, 143.7, 135.7, 129.8, 127.2, 124.9, 82.2, 57.0, 49.6, 48.8, 43.4, 38.5, 36.7, 35.3, 33.7, 31.4, 31.2, 27.4, 26.4, 23.1, 21.5, 21.1, 21.0, 18.5, 12.2 ppm.

HRMS (ESI, *m/z*): calcd. for $(C_{29}H_{39}NO_5S + Na)^+$: 536.2447, found: 536.2444.

Analytical HPLC: major diastereomer

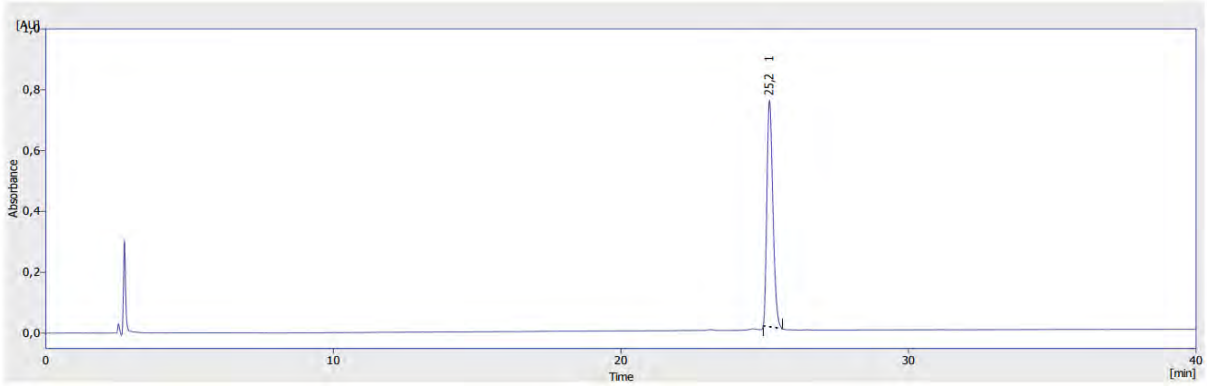

	Reten. Time [min]	Area [mAU.s]	Height [mAU]	Area [%]	Height [%]	W05 [min]	PDA Peak Purity	Compound Name	PDA Best Match Name	PDA Best Match
1	25,167	5394,776	372,341	100,0	100,0	0,25	940			
	Total	5394,776	372,341	100,0	100,0					

m.p.: 170-171 °C.

5.5.30 (*E*)-*N*-(7,7-dimethyl-6-oxooct-4-en-3-yl)-*N*,4-dimethylbenzenesulfonamide (18)

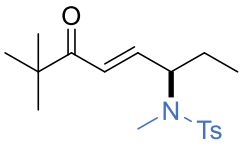

Following the general procedure **C** compound **18** was obtained from enol **S25** (0.25 mmol) and *N*-aminopyridinium salt **2a** (0.33 mmol). The crude product was purified by column chromatography (10:90 Et_2O/Pentane) to afford 22 mg of compound **18** as a colorless oil (**Yield = 26%**, 1 h).

^{1}H NMR (400 MHz, $CDCl_3$): δ 7.67 (d, *J* = 8.1 Hz, 2H), 7.26 (d, *J* = 8.0 Hz, 2H), 6.55 (dd, *J* = 15.4, 6.1 Hz, 1H), 6.39 – 6.33 (dd, *J* = 15.4, 0.9 Hz, 1H), 4.53 – 4.46 (q, *J* = 7.0 Hz, 1H), 2.69 (s, 3H), 2.39 (s, 3H), 1.60-1.52 (m, 2H), 1.06 (s, 9H), 0.91 (t, *J* = 7.3 Hz, 3H) ppm.
^{13}C NMR (100 MHz, $CDCl_3$): δ 203.6, 143.2, 142.3, 137.0, 129.6, 127.1, 125.5, 59.5, 43.0, 28.5, 25.9, 24.9, 21.4, 10.7 ppm.

HRMS (ESI, *m/z*): calcd. For $(C_{18}H_{27}NO_3S + Na)^+$: 360.1609, found: 360.1620.

Analytical HPLC:

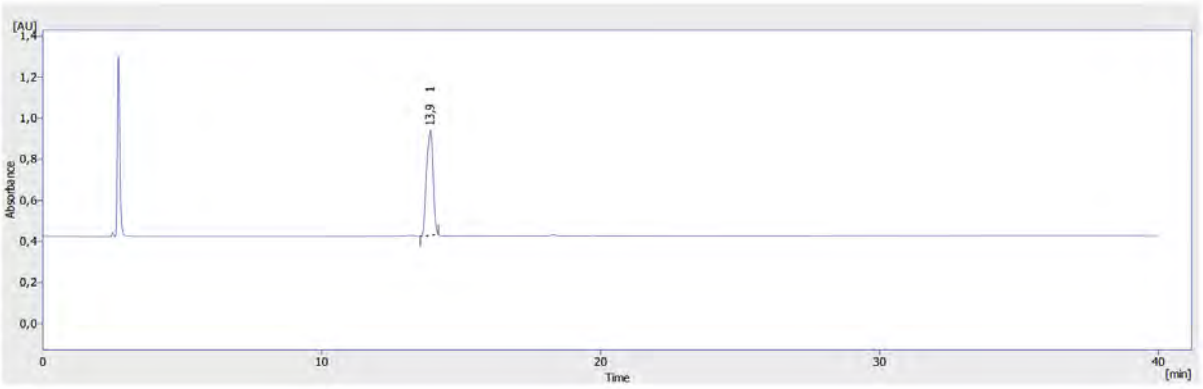

	Reten. Time [min]	Area [mAU.s]	Height [mAU]	Area [%]	Height [%]	W05 [min]	PDA Peak Purity	Compound Name	PDA Best Match Name	PDA Best Match
1	13,900	8333,381	509,664	100,0	100,0	0,30	924			
	Total	8333,381	509,664	100,0	100,0					

5.5.31 (*E*)-*N*,4-dimethyl-*N*-(6-oxohex-4-en-3-yl)benzenesulfonamide (23)

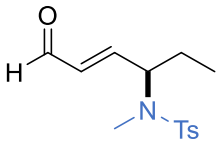

Following the general procedure **C** compound **23** was obtained from enol **S29** (0.25 mmol) and *N*-aminopyridinium salt **2a** (0.33 mmol). The crude product was purified by column chromatography (20:80 AcOEt/Pentane) to afford 20 mg of compound **23** as a colorless oil (**Yield = 28%**, 16 h).

^{1}H NMR (500 MHz, $CDCl_3$): δ 9.41 (d, *J* = 7.6 Hz, 1H), 7.69 (d, *J* = 8.2 Hz, 2H), 7.30 (d, *J* = 8.2 Hz, 2H), 6.48 (dd, *J* = 15.9, 5.4 Hz, 1H), 6.01 (ddd, *J* = 15.9, 7.6, 1.4 Hz, 1H), 4.61 (ddd, *J* = 10.5, 6.6, 1.3 Hz, 1H), 2.71 (s, 3H), 2.42 (s, 3H), 1.75 – 1.50 (m, 2H), 0.91 (t, *J* = 7.4 Hz, 3H) ppm.

^{13}C NMR (125 MHz, $CDCl_3$): δ 192.8, 153.0, 143.6, 136.6, 133.2, 129.7, 127.2, 59.2, 28.6, 24.1, 21.5, 10.7 ppm.

HRMS (ESI, *m/z*): calcd. for $(C_{14}H_{19}NO_3S + Na)^+$: 304.0983; found: 304.0980.

Elemental analysis (%) calcd. for $C_{14}H_{19}NO_3$: C 59.76, H 6.81, N 4.98, S 11.40; found: C 59.73, H 6.86, N 5.12, S 11.52.

5.5.32 *N*-(3,7-dimethyl-1-oxoocta-2,6-dien-4-yl)-*N*,4-dimethylbenzenesulfonamide (26)

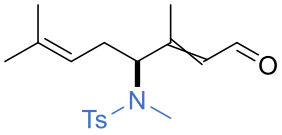

Following the general procedure **C** compound **26** was obtained from enol **S29** (0.25 mmol) and *N*-aminopyridinium salt **2a** (0.33 mmol). The crude product was purified by column chromatography (20:80 Et_2O/Pentane) to afford 51 mg of compound **26** as a colorless oil (**Yield = 61%**, *E*/*Z* ~ 1.38:1. 1 h).

^{1}H NMR (500 MHz, $CDCl_3$): (major) 9.96 (d, *J* = 7.9 Hz, 1H), 7.75-7.72 (m, 2H), 7.33-7.30 (m, 2H), 5.94 (dt, *J* = 7.7, 1.3 Hz, 1H), 5.09 (q, *J* = 7.4, 1.5 Hz, 1H), 4.37 – 4.36 (m, 1H), 3.69 (d, *J* = 1.4 Hz, 2H), 2.65 – 2.63 (m, 3H), 2.42 (6H), 1.68 (d, *J* = 1.3 Hz, 3H), 1.60 (d, *J* = 1.4 Hz, 3H) ppm.

^{13}C NMR (125 MHz, $CDCl_3$): δ 191.4, 190.5, 159.5, 158.7, 143.8, 143.5, 143.4, 136.8, 135.9, 134.7, 134.2, 134.0, 129.9, 129.7, 129.6, 128.8, 128.0, 127.4, 127.3, 122.0, 119.2, 62.6, 55.8, 35.0, 29.3, 29.0, 28.6, 27.6, 27.4, 25.7, 25.6, 21.5, 17.9, 17.8, 16.3 ppm.

HRMS (ESI, *m/z*): calcd. for $(C_{18}H_{25}NO_3S + Na)^+$: 358.1453, found: 358.1454.

Elemental analysis: decomposition.

5.5.33 *N*-(3-formyl-2,4,4-trimethylcyclohex-2-en-1-yl)-*N*,4-dimethylbenzenesulfonamide (27)

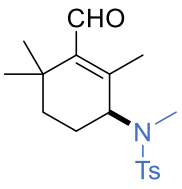

Following the general procedure **C** compound **27** was obtained from enol **S30** (0.25 mmol) and *N*-aminopyridinium salt **2a** (0.33 mmol). The crude product was purified by column chromatography (20:80 Et_2O/Pentane) to afford 43 mg of compound **27** as a colorless oil (**Yield = 52%**, 1 h).

^{1}H NMR (500 MHz, $CDCl_3$): δ 10.13 (s, 1H), 7.74 (d, *J* = 8.2 Hz, 2H), 7.34 (d, *J* = 7.9 Hz, 2H), 4.57 – 4.54 (m, 1H), 2.66 (s, 3H), 2.45 (s, 3H), 2.06 (s, 3H), 1.59 (ddd, *J* = 13.7, 9.8, 2.9 Hz, 1H), 1.49 – 1.41 (m, 3H), 1.18 (d, *J* = 1.3 Hz, 6H) ppm.

^{13}C NMR (125 MHz, $CDCl_3$): δ 192.8, 150.5, 145.0, 143.4, 136.9, 129.8, 127.0, 59.7, 37.6, 33.0, 29.6, 28.5, 26.7, 21.6, 15.0 ppm.

HRMS (EI, *m/z*): calcd. For $C_{18}H_{25}NO_3S$: 335.1555, found: 335.1553.

Analytical HPLC:

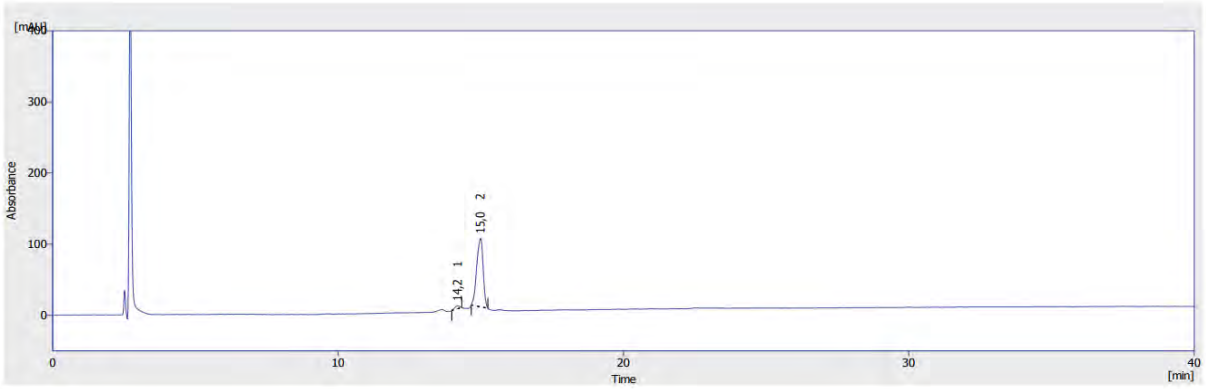

	Reten. Time [min]	Area [mAU.s]	Height [mAU]	Area [%]	Height [%]	W05 [min]	PDA Peak Purity	Compound Name	PDA Best Match Name	PDA Best Match
1	14,200	23,392	1,975	3,0	3,9	0,22	1000			
2	15,000	750,219	48,141	97,0	96,1	0,27	992			
	Total	773,611	50,117	100,0	100,0					

5.5.34 (*Z*)-*N*,4-dimethyl-*N*-(4-oxo-3-phenylbut-2-en-1-yl)benzenesulfonamide (22)

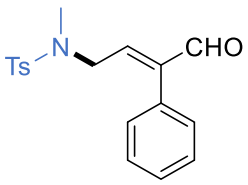

Following the general procedure **C** compound **22** was obtained from enol **S31** (0.25 mmol) and *N*-aminopyridinium salt **2a** (0.33 mmol). The crude product was purified by column chromatography (20:80 Et_2O/Pentane) to afford 36 mg of a mixture of compound **22** and Me-NH-Ts by-product which we were not able to separate flash column chromatography.

^{1}H NMR (500 MHz, $CDCl_3$): δ 9.62 (s, 1H), 7.62 (d, *J* = 8.1 Hz, 2H), 7.42 – 7.34 (m, 3H), 7.29 (d, *J* = 7.9 Hz, 2H), 7.11 – 7.08 (m, 2H), 6.64 (t, *J* = 6.4 Hz, 1H), 3.96 (d, *J* = 6.4 Hz, 2H), 2.69 (s, 3H), 2.42 (s, 3H) ppm.

^{13}C NMR (125 MHz, $CDCl_3$): δ 192.5, 148.4, 145.4, 143.8, 134.3, 131.2, 129.8, 129.7, 129.2, 128.6, 128.5, 127.4, 127.3, 48.7, 35.4, 21.5 ppm.

HRMS (ESI, *m/z*): calcd. for $(C_{18}H_{19}NO_3S + Na)^+$: 352.0983, found: 352.0987.

Analytical HPLC:

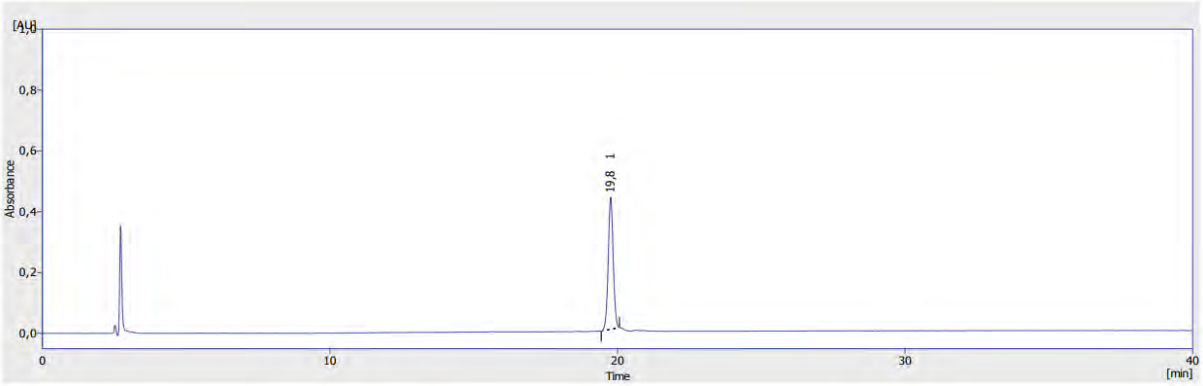

	Reten. Time [min]	Area [mAU.s]	Height [mAU]	Area [%]	Height [%]	W05 [min]	PDA Peak Purity	Compound Name	PDA Best Match Name	PDA Best Match
1	19,767	2606,011	216,766	100,0	100,0	0,20	977			
	Total	2606,011	216,766	100,0	100,0					

References

1. Cumbrias-Martin, J.; Perez-Aguilar M.C.; Mas-Balleste R.; Litta, A. D.; Lattanzi, A.; Sala, G.D.; Fernandez-Salas, J.A.; Aleman, J.; Enantioselective Conjugate Azidation of *α,β*-Unsaturated Ketones under Bifunctional Organocatalysis by Direct Activation of $TMSN_3$. *Adv. Synth. Catal.* **2019**, 361, 4790-4796.
2. Le Paih, J.; Monnier, F.; Dérien, S.; Dixneuf, P. H.; Clot, E.; Eisenstein, O.; Biscarbene-Ruthenium Complexes in Catalysis: Novel Stereoselective Synthesis of (1*E*,3*E*)-1,4-Disubstituted-1,3-dienes via Head-to-Head Coupling of Terminal Alkynes and Addition of Carboxylic Acids. *J. Am. Chem. Soc.* **2003**, *125*, 11964–11975.
3. Liu, X.; Chen, X.; Mohr, J. T.; Copper-Catalyzed γ-Sulfonylation of α,β-Unsaturated Carbonyl Compounds by Means of Silyl Dienol Ethers. *Org. Lett.* **2015**, *17*, 3572–3575.
4. Favara, D.; Omodei-Sale, A.; Consonni, P.; Depaoli, A.; A facile synthesis of trans (+)-4-carboxymethyl-3-ethylazetidin-2-one and its conversion into natural PS-5. *Tetrahedron Lett.* **1982**, *23*, 3105–3108.
5. Herscovici, J.; Boumaïza, L.; Antonakis, K.; Highly stereoselective preparation of conjugated dienones and dienoates via a new knoevnagel approach. *Tetrahedron Lett.* **1991**, *32*, 1791–1794.
6. Goliszewska, K.; Rybicka-Jasińska, K.; Szurmak, J.; Gryko. D.; Visible-Light-Mediated Amination of π-Nucleophiles with *N*-Aminopyridinium Salts. *J. Org. Chem.* **2019**, *84*, 15834–15844.
7. Lukas, R. J.; Muresan, A. Z.; Damaj, M. I.; Blough, B. E.; Huang, X.; Navarro, H. A.; Mascarella, S. W.; Eaton, J. B.; Marxer-Miller, S. K.; Carroll, F. I.; Synthesis and Characterization of in Vitro and in Vivo Profiles of Hydroxybupropion Analogues: Aids to Smoking Cessation. *J. Med. Chem.* **2010**, *53*, 4731-4748.
8. Fukuzawa S.; Tsuruta T.; Fujinami T.; Sakai S.; Reaction of α-halogeno ketones with carbonyl compounds promoted by CeI_3, $CeCl_3$-NaI, or $CeCl_3$-$SnCl_2$. *J. Chem. Soc.* **1987**, 1473-1477.
9. Pennel M. N., Unthank M. G., Turner P., Sheppard T. D., A General Procedure for the Synthesis of Enones via Gold-Catalyzed Meyer-Schuster Rearrangement of Propargylic Alcohols at Room Temperature. *J. Org. Chem.* **2011**, 76, 5, 1479-1482.
10. Zhang B., Davies H. M. L.; Rhodium-Catalyzed Enantioselective [4+2] Cycloadditions of Vinylcarbenes with Dienes. *Angew. Chem. Int. Ed.* **2020**, 59, 4937-4941.

Supplementary Information

Photochemical C3-Amination of Pyridines via Zincke Imine Intermediates

Kitti Franciska Szabó,[+[a]] Piotr Banachowicz,[+[a]] Antoni Powała,[[a,b]] Danijela Lunic,[[c]] Ignacio Funes Ardoiz,*[[c]] and Dorota Gryko*[[a]]

[a]*Institute of Organic Chemistry Polish Academy of Sciences; Kasprzaka 44/52, 01-224 Warsaw, Poland; correspondence: dorota.gryko@icho.edu.pl*

[b]*Department of Chemistry Warsaw University of Technology, Noakowskiego 3, 00-664 Warsaw, Poland*

[c]*Complejo Científico-Tecnológico Universidad de La Rioja, Madre de Dios, 53, 26004 Logroño, La Rioja, Spain; correspondence:ignacio.funesa@unirioja.es*

correspondence:

dorota.gryko@icho.edu.pl

ignacio.funesa@unirioja.es

Table of Contents

1. General information

All solvents and commercially available reagents were purchased as reagent grade and used without further purification, unless otherwise noted. Reactions were monitored by thin layer chromatography (TLC), using 0.20 mm Merck silica plates (60F-254) and visualized using UV-light or potassium permanganate stain with heat as a developing agent. GC yields were calibrated with dodecane as the internal standard.

NMR spectra were recorded on Bruker 400 MHz or Varian 600 MHz and calibrated using solvent residual peaks ($CHCl_3$ – 7.26 ppm ^{1}H NMR, 77.16 ppm ^{13}C NMR, D2O - 4.64 ppm ^{1}H NMR) or TMS as an internal reference. Chemical shifts are reported relatively in δ-scale as parts per million (ppm) referenced to the residual solvent peak. Coupling constants *J* are given in Hertz (Hz), and the following abbreviations were used to indicate signal multiplicity: ^{1}H NMR: s = singlet, d = doublet, t = triplet, q = quartet, m = multiplet, and the respective combinations.

Low-resolution mass spectra (LRMS) were recorded on an Applied Biosystems API 365 **mass spectrometer using an electrospray ionization (ESI)** technique. High resolution mass spectra (HRMS) were recorded on a Waters AutoSpec Premier instrument using electron ionization (EI) or a Waters SYNAPT G2-S HRMS instrument using electrospray ionization (ESI) or atmospheric-pressure chemical ionization (APCI) with a time-of-flight detector (TOF).

GC-FID analyses were performed using Shimadzu GCMS-QP2010 SE with helium as carrier gas chromatograph with FID detector and Zebron ZB 5MSi column (length: 30.0 m; thickness: 0.25 um, diameter: 0.25 mm).

GC programme: time: 19.39 min; pressure: 121.8 kPa; total flow: 30.3 mL/min; column flow: 1.30 mL/min; linear velocity: 33.1 cm/s; purge flow: 3.0 mL/min; split ratio: 20.0.

Flash column chromatography was performed on the CombiFlash NextGen 300 flash chromatography system. Colum chromatography was performed using Merck silica gel 60 (230-400 mesh).

Preparative HPLC separations were performed using a Knauer HPLC chromatograph with PDA detector and a Preparative column chromatography Knauer EII 100-10 Si column (250 x 20 mm), flow rate: 15 ml / min. Model reaction

1.1. Reaction set-up

Experiments (optimisation studies and scope) were carried out in the UOSlab Miniphoto photoreactor (**Supplementary Figure 1**). Violet light irradiation (emission maximum at 405 nm) was applied to each reaction vial with the use of 7 LUMINUS LED units (of overall 24 W intensity when 100% power applied). The ambient temperature of the LED block was maintained by cooling with Huber MiniChiller 600 ($T_{reaction}$ ~0-5 °C).

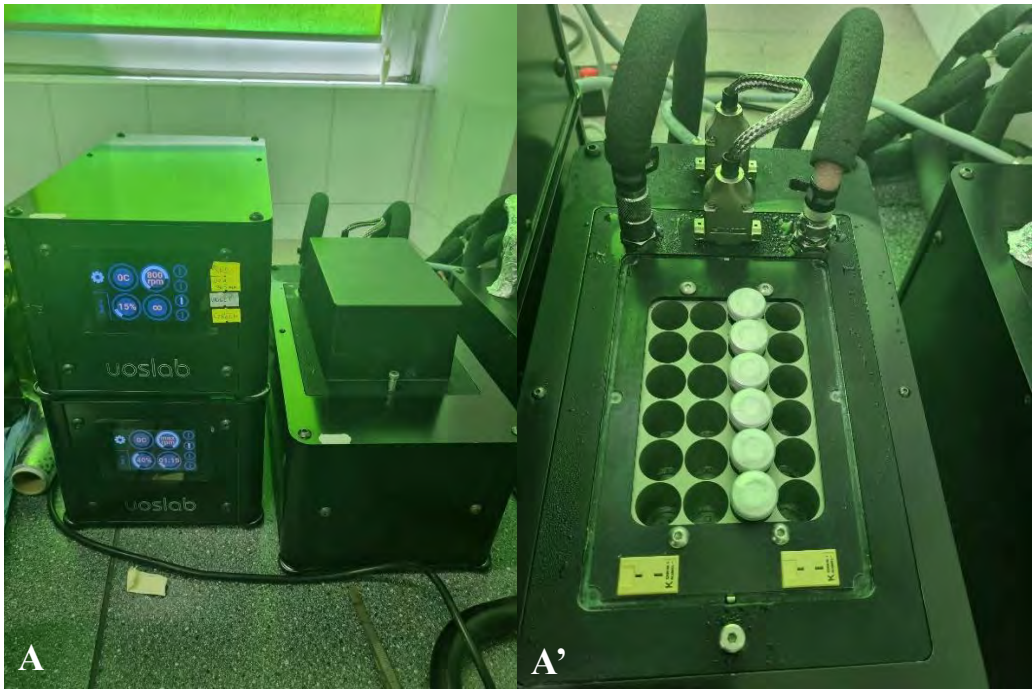

Supplementary Figure 1. *Photochemical reaction set-up: UOSlab Miniphoto photoreactor (A and A').*

1.2. Preparation of the model reaction system

Zincke imine as a starting material for the optimisation studies was prepared according to the modified McNally's protocol.[1]

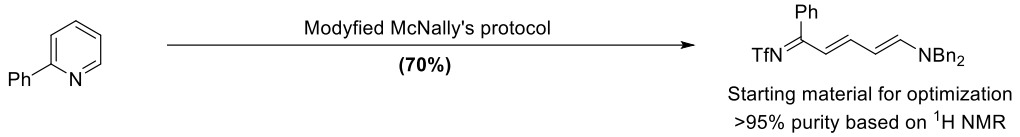

Supplementary Figure 2. *General scheme for the preparation of the starting material for optimisation studies.*

Zincke imines are rather stable compounds (if they are stored in pure form). In particular, 2-aryl Zincke imines can be stored in the presence of air and moisture at room temperature for a couple of days without significant decomposition.

Pyridinium salt (**Py-salt**) was prepared according to the Goliszewska's protocol.[2]

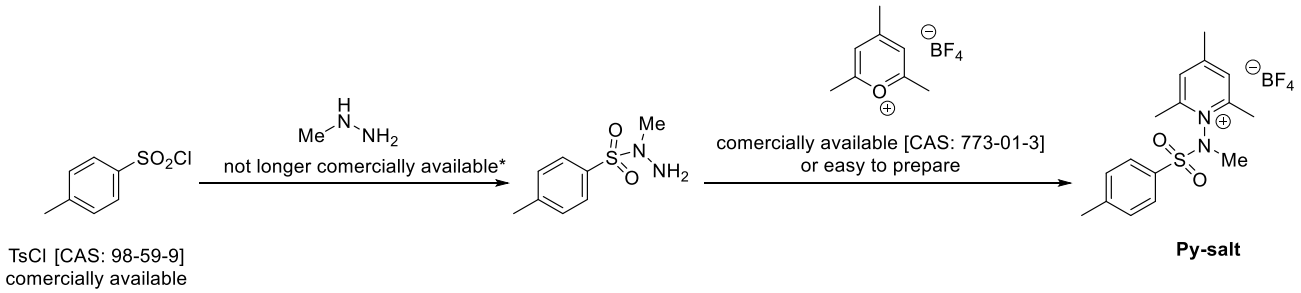

Supplementary Figure 3. *General scheme for the preparation of pyridinium salt **Py-salt**. (for details, see page 44); *could be replaced with methylhydrazine sulphate [CAS: 302-15-8] which is readily available and not expensive.*

The amount of 2-phenylpyridine in the reaction mixtures was monitored by the GC-FID calibration curve with dodecane as internal standard. The curve was validated using 5.4 mg of 2-phenylpyridine (**1**) in 10 ml of AcOEt solution. The average error of 3 measurements was lower than 2% (**Supplementary Figure 4**).

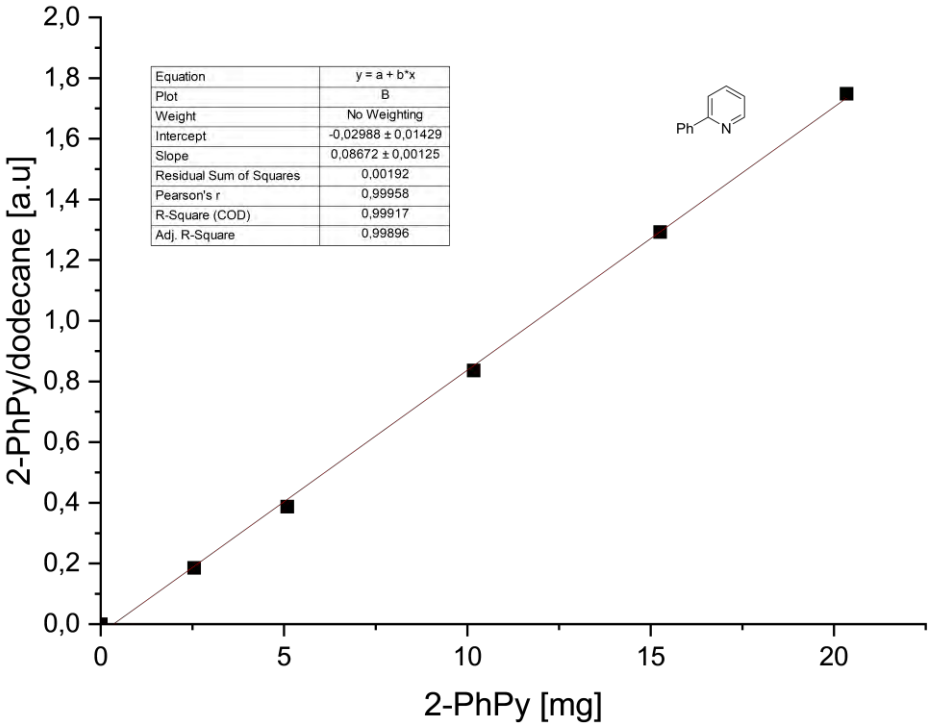

Supplementary Figure 4. GC-FID calibration curve for 2-phenylpyridine (**1**) with dodecane as internal standard.

Zincke imines were cyclized by heating with an excess of NH_4OAc. For simplification, saturated NH_4OAc solution was prepared in anhydrous ethanol (~24% w/w). The cyclization process is quantitative on GC-FID analysis of the reaction mixture.

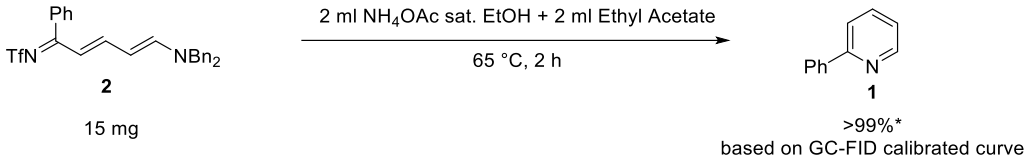

Supplementary Figure 5. *Recyclization process with the saturated* NH_4OAc *in the ethanol solution.*

*The reaction could be also performed in the DMSO/MeCN/EtOH or MeCN/EtOH mixture *In a DCM/EtOH mixture the reaction mixture was heated up to 45 °C typically for 4 h.

Procedure: Zincke imine **2** (0.031 mmol, 15 mg) was dissolved in AcOEt (2 ml) and a saturated solution of NH_4OAc in anhydrous EtOH (2 ml) was added. The reaction mixture was heated to 65 °C for 2 h. After the indicated time, dodecane as an internal standard was added (15 µl) and the mixture was diluted to 25 ml with AcOEt. The crude reaction mixture was then analysed with the GC-FID calibrated method indicating quantitative conversion of **2** to **1**.

1.3. Model reaction

The model reaction involves Zincke imine (**2**) prepared from 2-phenylpyridine (**1**) and *N*-methylpyridinium salt (**Py-salt**). Intermediate **2a** was not isolated in that process.

A general protocol for optimisation studies:

Zincke imine **2** (24 mg, 0.05 mmol), pyridinium salt **Py-salt** (x mmol), **cat.** (x mg, x μmol, <5 mol%) were placed in the closed cup vial and a solvent (x ml) and a co-solvent [if required] (x ml) were added through the septum. The reaction mixture was placed in ultrasound bath and degassed by bubbling argon through the solution for 15 min. The vial was then transferred to the photoreactor and irradiated with LED [wavelength] light (x W) for x h maintaining a temperature between 0 °C to 5 °C with the dedicated cooling system. The solution was then diluted with AcOEt (~15 ml) and dodecane was added as an internal standard (15 μl). The sample (2 ml) was filtered through cotton and subjected to GC-FID measurements.

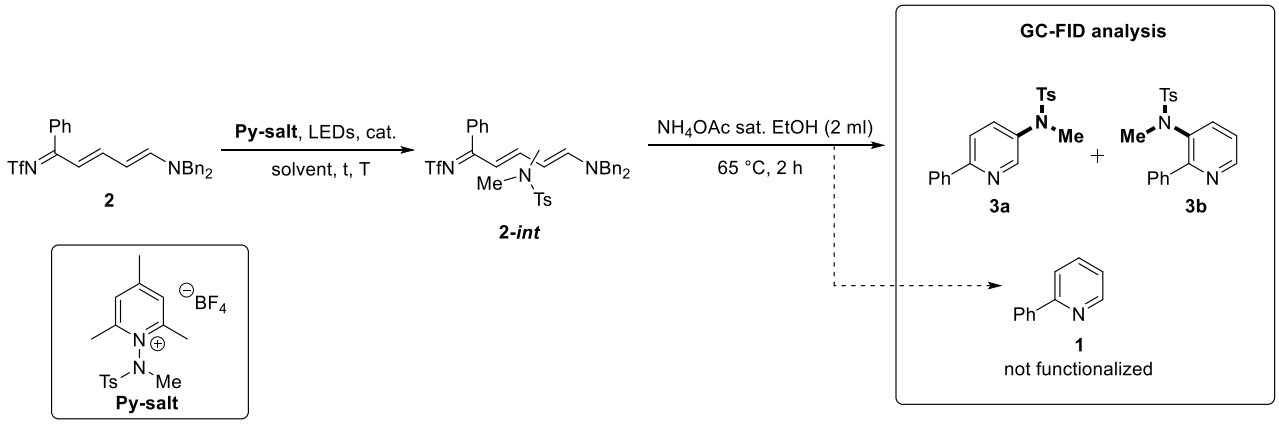

Supplementary Figure 6. *Model reaction system.*

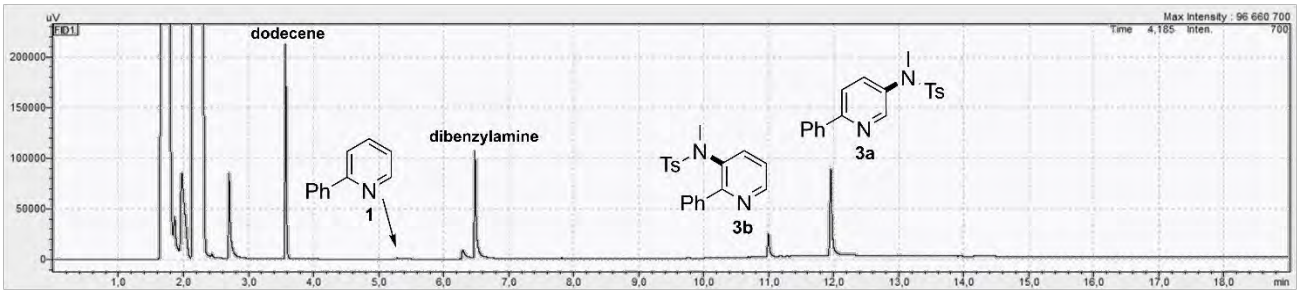

Supplementary Figure 7. *Typical GC-FID chromatogram of the crude reaction mixture (under optimised condition, >99% yield and >99 % conversion of the starting material)*

Based on the analytically pure sample of isolated product **3a** (50 mg), the GC-FID calibration curve with dodecane as an internal standard was prepared. The method curve was validated using **3a** (5.4 mg) in AcOEt (10 ml). The average error of 3 measurements was lower than 3%. Yields were directly calculated from the calibrated and validated curve (in optimal conditions confirmed also with ^{1}H NMR with CH_2Br_2 as internal standard).

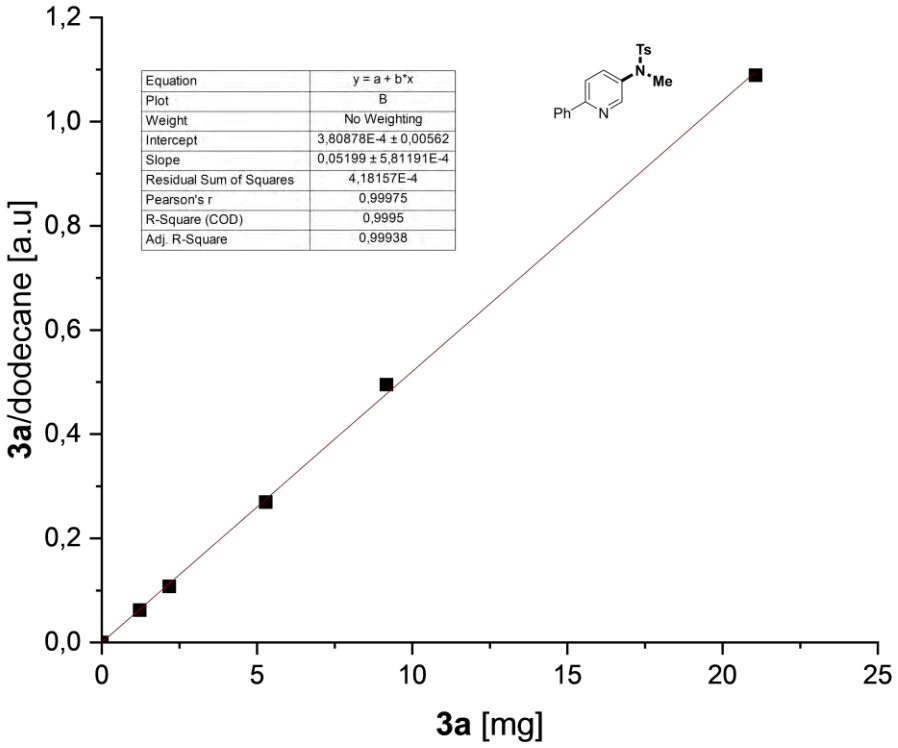

Supplementary Figure 8. *GC-FID calibration curve for product **3a** with dodecane as internal standard.*

1.4. Preliminary results

1.4.1 Photofunctionalization of the Zincke imine

Preliminary studies were initiated by testing our hypothesis that Zincke imine can undergo photofunctionalization with *N*-aminopyridinium salts. As a first, we have tested typical solvents and light sources for the pyridinium salt activation along with *fac*-Ir(ppy)$_3$, which has been already proven to act as effective photoredox catalyst compatible with different pyridinium salts.[2,3] Photochemical reactions were typically set up using a Zincke imine **2** 50 mg while maintaining the temperature between 0 and 5 °C with a dedicated cooling system.

Supplementary Table 1. Initial LED wavelength and solvent screening.

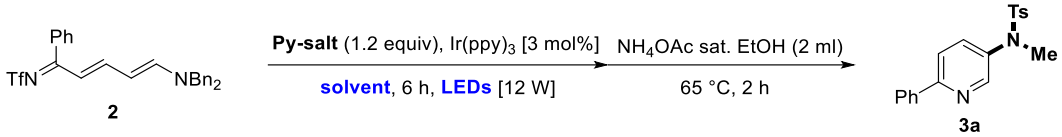

entry	solvent	light source	yield 3a [%][a]
1	MeCN	UV (365 nm)	<5%
2	MeCN	violet (405 nm)	20%
3	MeCN	blue (465 nm)	<5%
4	DCM	UV (365 nm)	<5%
5	DCM	violet (405 nm)	<5%
6	DCM	blue (465 nm)	<5%

[a]isolated yield

1.4.2 Control experiments

For the determination of photochemical nature of the reaction, control experiments were performed (no light, no catalyst etc.) and we also checked stability of starting material when exposed to catalyst or light.

Supplementary Table 2. Control experiments.

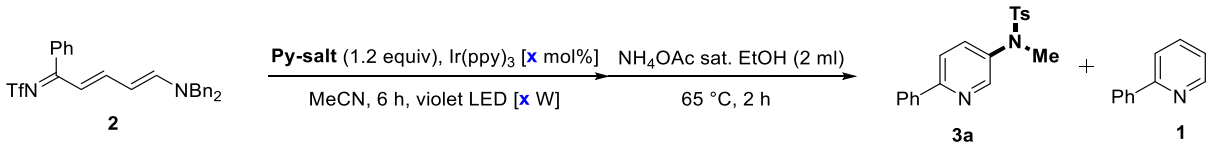

entry	modification	light source	yield 3a [%][a]	yield 1 [%][a]
1	none	violet (405 nm)	20	70
2	no light	no light	<1	87
3	no catalyst	violet (405 nm)	<5	76
4	no catalyst, no light	no light	0	>99

[a]GC-FID yield

Exposure of Zincke imine to light itself or the catalyst is responsible for unwanted reactivity (**entry 2** and **3**) only a combination of both the catalyst and light leads to the desired product (**entry 1**).

1.4.3. Initial conditions

Looking for a starting point for optimisation studies, several conditions were tested.

Supplementary Table 3. Initial conditions for the reaction set-up.

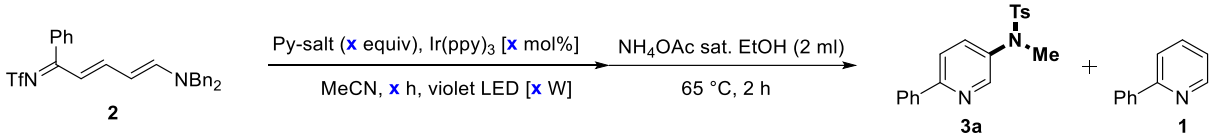

entry	concentration [mmol/ml]	irradiation power [W]	catalyst loading [mol%]	Py-salt [equiv.]	irradiation time [h]	yield 3a [%][a]	yield 1 [%][a]
1	0.05	24	1	2	8	41	14
2	0.025	12	3	3	12	36	20
3	0.0125	18	3	1.3	6	27	67
4	0.05	24	1	2	8	41	14
5	**0.05**	**24**	**3**	**2**	**8**	**46**	**9**
6	0.05	24	5	2	8	45	9
7	**0.05**	**24**	**3**	**2**	**2**	**43**	**17**
8	0.05	24	3	2	24	36	5

[a]*GC-FID yield*

The conditions presented in entry 7 were chosen as a promising starting point for our optimisation studies (*reaction time is the shortest and the yield is comparable to entry* 5).

1.4.3. Optimisation studies

Catalyst loading

Systematic studies were focused on optimisation of parameters such as the amount of catalyst and pyridinium salt **Py-salt**, the irradiation power, and the reaction time.

Supplementary Table 4. Optimisation of the catalyst loading.

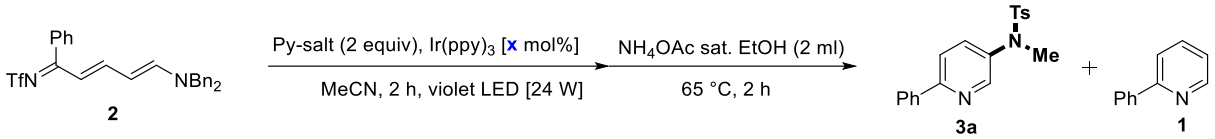

entry	catalyst loading [mol%]	yield 3a [%][a]	yield 1 [%][a]
1	0	5	66
2	0.2	22	44
3	0.5	35	27
4	**1.5**	**44**	**17**
5	2.5	44	14
8	4.5	40	13

[a]GC-FID yield

The conditions presented in **entry 4** were chosen because of the lowest catalyst loading giving satisfactory results.

Amount of pyridinium salt and its concentration

A detailed analysis of the reaction mixture showed that apart from pyridine **3a**, second regioisomer **3b** was also formed. Additional optimisation including concentration and an amount of the salt allows to increase efficacy outcome of the reaction.

Supplementary Table 5. Optimisation of the amount of the pyridinium salt and concentration.

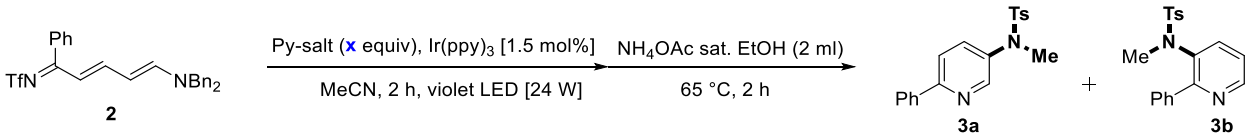

entry	Py-salt [equiv.]	concentration [mmol/ml]	yield 3a [%][a]	3a : 3b ratio	yield 1 [%][a]	total yield 3a & 3b [%][a]
0	2.0	0.05	44	2.1 : 1	17	65
1	1.1	0.05	38	2.1 : 1	35	55
2	1.5	0.05	39	2.0 : 1	22	59
3	5.0	0.05	31	2.6 : 1	10	43
4	2.0	0.1	34	nd	28	nd
5	**2.0**	**0.0125**	**48**	**2.6 : 1**	**8**	**66**

[a]GC-FID yield

Equivalents of pyridinium salt and concentration (under lower irradiation power [2.4 W])

Subsequent modifications, including decreasing the irradiation power (from 24 W to 2.4 W) improved selectivity and vastly eliminated side products (yield of **1** + **3a** + **3b** ~100%, **entry 5**).

Supplementary Table 6. Optimisation of the amount of the pyridinium salt and concentration under lower irradiation power [2.4W]

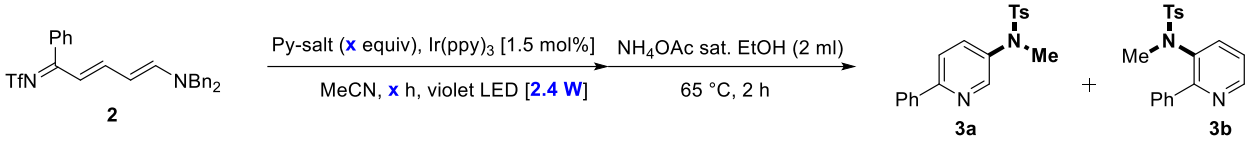

entry	Py-salt [equiv.]	concentration [mmol/ml]	t [h]	3a : 3b ratio	total yield 3a & 3b [%][a]	yield 1 [%][a]
1	1.3	0.025	12	4.0 : 1	21	59
2	1.3	0.025	2	2.0 : 1	6	80
3	1.5	0.025	12	3.6 : 1	29	51
4	2.0	0.025	12	3.6 : 1	36	40
5	**2.0**	**0.0125**	**12**	**3.1 : 1**	**66**	**33**

[a]GC-FID yield

The addition of 3 equivalents of salts gave better selectivity (**3a**:**3b** 4.8:1) (due to the faster consumption of isomer **3b** to form a disubstituted derivative (characterized by ^{1}H NMR, ^{13}C NMR, ^{1}H-^{1}H COSY and HRMS; for details, see pages 164-165).

Reaction time

Decreasing the concentration of along with the elongation of the irradiation time increased the yield (**entry 2**).

Supplementary Table 7. Fine tuning of the concentration of the reaction mixture.

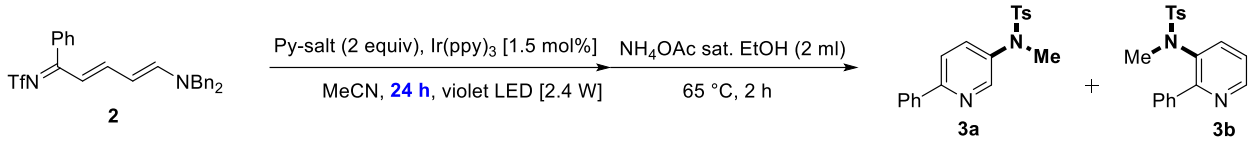

entry	concentration [mmol/ml]	3a : 3b ratio	total yield 3a & 3b [%][a]	yield 1 [%][a]
1	0.0125	3.1 : 1	76	17
2	**0.00625**	**3.1 : 0**	**83**	**13**

[a]GC-FID yield

Fine-tuning of the solvent (addition of the second solvent)

The addition of a co-solvent led to a further increase in the yield and regioselectivity of the reaction.

Supplementary Table 8. Fine tuning of the solvent.

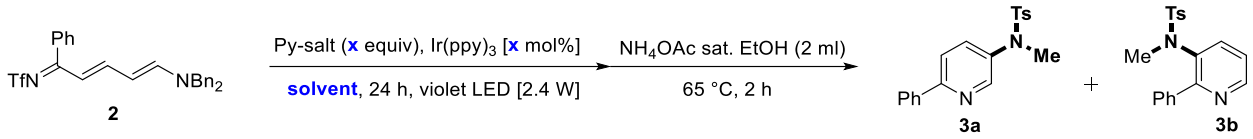

entry	Py-salt [equiv.]	solvent	t [h]	3a : 3b ratio	total yield 3a & 3b [%]	yield 1 [%][a]
1	2.0	MeCN/DMSO (v/v 1:1)	24	6.3 : 1	88	<5
2	1.8	MeCN/DMSO (v/v 1:1)	24	5.2 : 1	98	<5
3	**1.5**	MeCN/DMSO (v/v 1:1)	**24**	**5.5 : 1**	**98**	**<5**
4*	**1.5**	MeCN/DMSO (v/v 1:1)	**24**	**5.5 : 1**	**98**	**<5**
5*	**1.5**	AcOEt/DMSO (v/v 1:1)	**24**	**7.3 : 1**	**88**	**<5**
6*	**1.5**	DCM/DMSO (v/v 1:1)	**24**	**5.6 : 1**	**87**	**<5**

*[a]GC-FID yield, * 2 mol% of Ir(ppy)3*

*Reactions were set-up on a 25 mg scale of **2** (~6.25 mM).*

Increasing the amount of the catalyst to 2 mol% did not affect the yield, though it helped with the reproducibility of the reaction.

Reproducibility and robustness

To confirm reproducibility and robustness of the developed method the model reaction was set up independently by three authors.

Supplementary Table 9. Reproducibility and robustness of the optimised reaction.

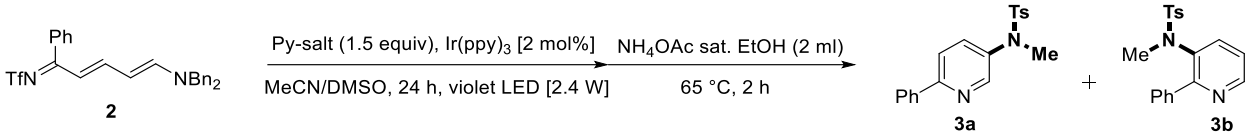

entry	3a : 3b ratio	total yield 3a & 3b [%][a]
1*	4.8 : 1	>99
2**	5.0 : 1	>99
3***	4.8 : 1	>99

*Piotr Banachowicz
**Kitti Szabó
***Antoni Powala
[a]GC-FID yield

*In addition, the reaction mixture from **entry 1** was worked out with the standard protocol (for details, see page **42**) leading to 95% isolated yield. The reaction mixture from **entry 2** was worked up only with the extraction step, and then ^1H NMR with CH_2Br_2 as an internal standard was measured gives >95% yield and ~5:1 regioisomers mixture.*

Other Zincke derivatives

Supplementary Table 10. Testing other Zincke Imines derivatives.

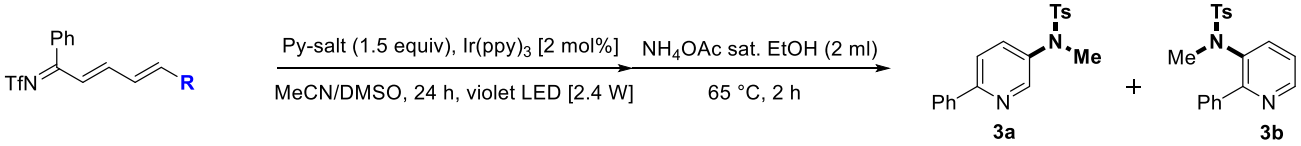

entry	Symbol of Zincke imine	R	3a : 3b ratio	total yield 3a & 3b [%][a]
1	**2**	NBn_2	4.8 : 1	>99
2	**S49b**	morpholine	NA	nd
3	**S50b**	NPhBn	26	1.9:1

NA – not assigned; nd – not detected

2. Mechanistic investigations

2.1.UV-VIS spectroscopy of the starting material

In general, Zincke imines are colourful derivatives that range from yellow to red and absorb light in the blue region. To explain why blue light irradiation does not give satisfactory results for the model reaction of Zincke imine **2** with Py-salt, UV-Vis spectra of both the photocatalyst and the Zincke imine were measured.

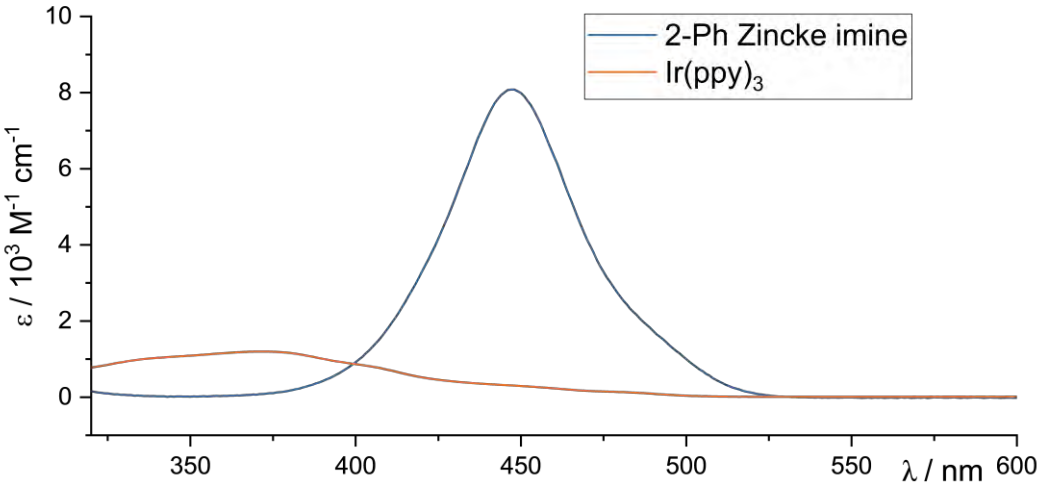

Supplementary Figure 9. *UV-VIS spectrum of 2-phenyl Zincke Imine (**2**) [solution in MeCN] and Ir(ppy)$_3$ [solution in MeCN].*

Conclusion: UV-VIS data clearly show that in the blue region Zincke imine **2** is a much stronger absorber than the catalyst. As a result, the Zincke imine is excited instead of the catalyst, thus, violet light (405 nm) was used to initiate the model reaction.

2.2.Kinetic studies

For kinetic studies, the model reaction under optimal conditions was set-up in one 10 ml closed-cup vial and in an indicated period, 100 µl aliquots were taken and treated with the saturated solution of NH_4OAc to convert intermediates **2** to pyridines (**3a**, **3b,** and **1**). After heating for the indicated time, the reaction mixture was diluted, and dodecane was added as an internal standard. The crude reaction mixtures were analysed using the calibrated GC-FID method.

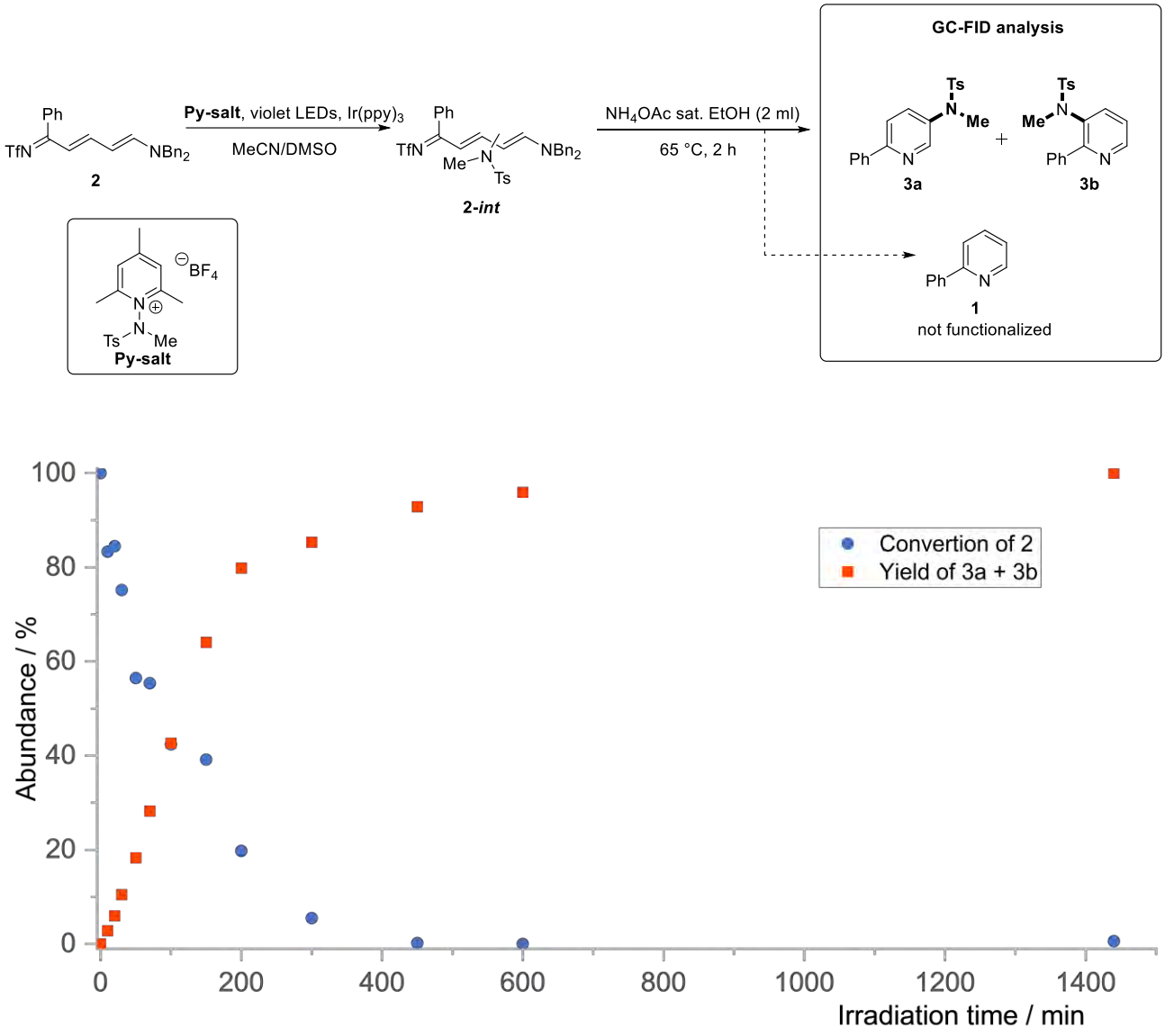

Supplementary Figure 10. *Total yield (**3a** + **3b**) and conversion of starting material **2**.*

The reaction profile indicates that the reaction is almost finished after 12 h (conversion of **2** >95%). For the scope and limitation studies reaction time were always extended to 24 h to assure full conversion of starting materials for a larger group of substrates.

2.3. Regioselectivity of the model reaction

According to the proposed reaction mechanism, two possible regioisomers can be formed. Based on a detailed analysis of ^{1}H, ^{1}H-^{1}H COSY spectra (for details, see pages 160), and the X-ray structure of main functionalized Zincke imine **2a** (**Supplementary Figure 12**), the regioselectivity of the photoamidation reaction was demonstrated univocally. In addition, the strongest shielded proton (which could be assigned as *CH* in 2 position of the pyridine moiety) has a very characteristic resonance and, in most cases, characteristic multiplicity.

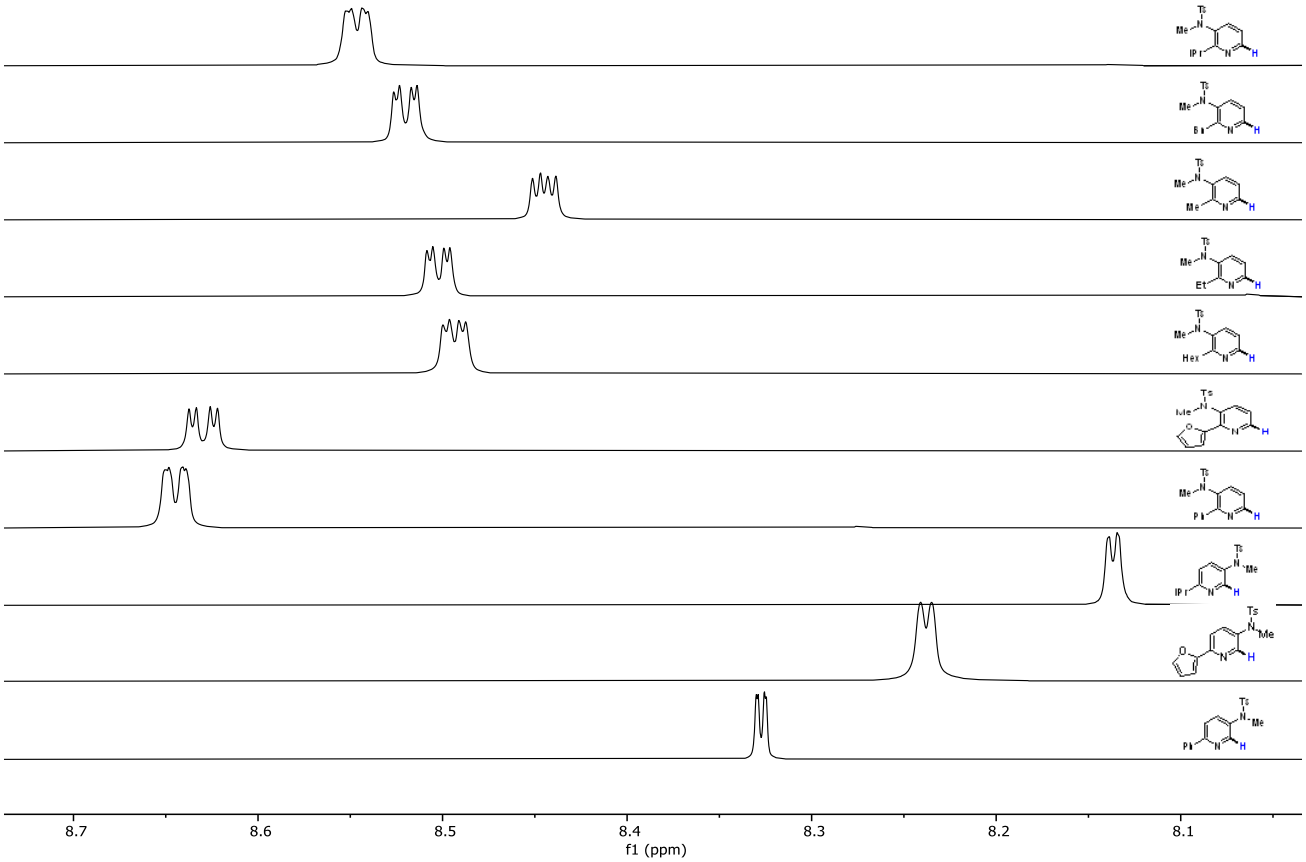

Supplementary Figure 11. *Examples of ^{1}H NMR spectra of products with assigned structure (zoom of the diagnostic region)*.

2.4. Characterization and reactivity of functionalized Zincke imine 2a

To isolate functionalized derivative **2a**, photochemical reactions were set-up (12 x 25 mg of **2**) without a subsequent ring closure step.

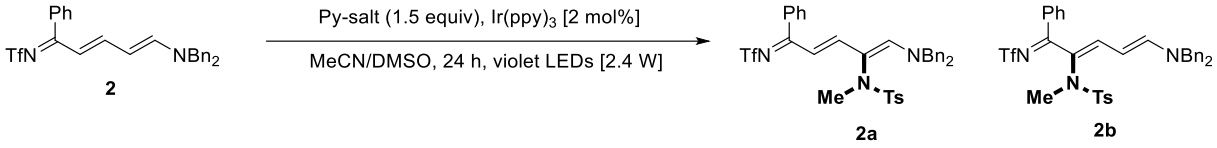

The reaction mixture after work-up was subjected to two consecutive columns chromatography in the hexanes/DCM/AcOEt (80:10:10) eluent system. It allowed to obtain ~ 100 mg of pure intermediate **2a** (most of compounds were disposed as mixed fractions). **^{1}H NMR** (500 MHz, $CDCl_3$) δ 7.77 (d, *J* = 7.9 Hz, 2H), 7.54 – 6.85 (m, 18H), 5.69 (s, 1H), 5.44 (s, 1H), 4.48 (d, *J* = 15.4 Hz, 4H), 2.86 (s, 3H), 2.35 (s, 3H); **^{13}C NMR** (126 MHz, $CDCl_3$) δ 178.0, 156.5, 156.1, 144.9, 137.5, 135.7, 134.9, 134.1, 131.5, 130.0, 129.3, 129.2, 128.6, 128.3, 127.5, 127.3, 126.9, 120.7, 118.1, 113.4, 111.3, 62.3, 51.7, 36.7, 21.5; **HRMS** (ESI) calcd. for $C_{34}H_{33}N_3O_4S_2$ [M+H] 668.1865; found 668.1863; Single crystal was obtained by diffuse *n*-hexane to the solution of **2a** in HPLC grade DCM.

^{1}H NMR, ^{1}H-^{1}H COSY spectra analysis along with X-ray analysis of a single crystal (obtained by diffusion of hexanes to DCM solution of intermediate **2a**) unambiguously confirmed the constitution of intermediate **2a**.

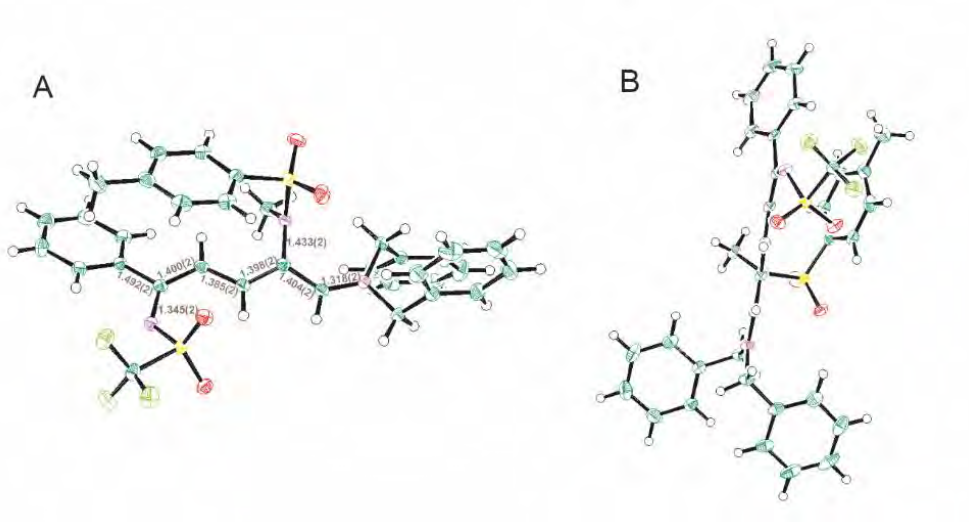

Supplementary Figure 12. *Crystal structure of compound **2a** (50% probability) A) top view, B) side view (solvent was omitted for clarity)*

In addition, the isolated pure sample of intermediate **2a** was subjected to the ring closure reaction under standard conditions. The crude reaction mixture was monitored using the calibrated GC-FID method, the analysis clearly indicated the formation of only one product (expected compound **3a**).

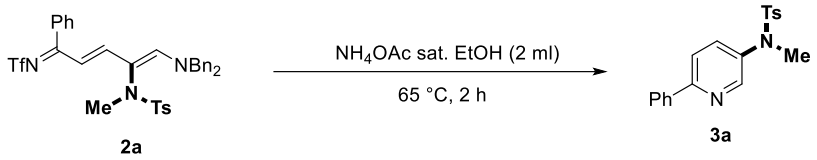

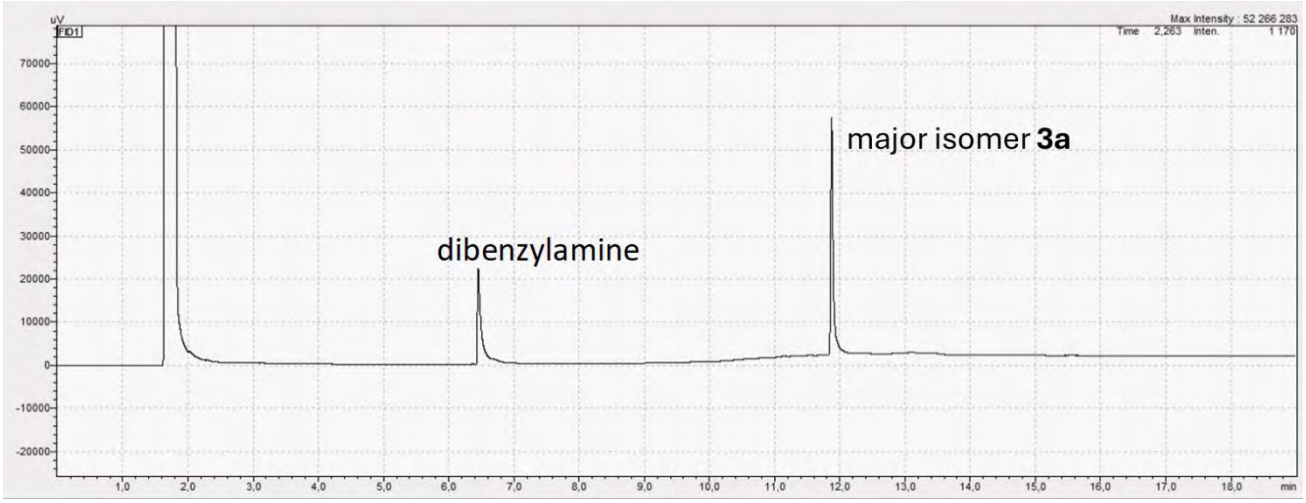

Supplementary Figure 13. *GC FID chromatogram from ring closing of pure isomer **2a**.*

3. Preparation of substrates

3.1. Preparation of substituted pyridines

Arylpyridines were prepared according to the **general procedure 1**.[4]

General Procedure 1. To a closed-cup vial 2-bromopyridine (250 mg, 1.59 mmol), arylboronic acid (2.23 mmol), Na_2CO_3 (1.35 g, 12.74 mmol), and $Pd(PPh_3)_4$ (5 mol%, 92.0 mg, 0.08 mmol) were added and the vial was closed under argon. Through the septum, toluene (3 ml) and H_2O: EtOH mixture (4 ml, 1:1 v/v) was added. The reaction mixture was heated at 100 °C for 18 h +/- 1h, while intensively stirred. After being cooled to room temperature, the vial was opened, and an upper layer was collected with Pasteur's pipette followed by the addition of 5 ml of AcOEt. The combined organic phases were dried over anhydrous sodium sulphate and then evaporated with silica gel (dry load for the preparation of samples for flash chromatography). Pure aryl pyridines were isolated by flash chromatography in the hexanes/AcOEt gradient.

Flash program: time: 25 min; column: silica 12 g; flow rate: 30 mL/min; automatic peak hold: on.

entry	time [min]	hexanes [%]	AcOEt [%]
1	0	100	0
2	25	85	15

2-(4-methoxyphenyl)pyridine (S2a)[5]

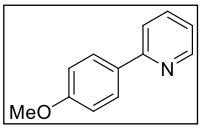

White solid (1.19 mmol, 221 mg, 75%); **^{1}H NMR** (400 MHz, $CDCl_3$) δ 8.68 – 8.62 (m, 1H), 7.98 – 7.93 (m, 2H), 7.74 – 7.65 (m, 2H), 7.20 – 7.14 (m, 1H), 7.03 – 6.96 (m, 2H), 3.87 (s, 3H).

2-(3-methoxyphenyl)pyridine (S3a)[6]

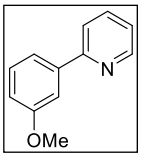

Colorless oil (1.35 mmol, 250 mg, 85%); **^{1}H NMR** (400 MHz, $CDCl_3$) δ 8.74 – 8.66 (m, 1H), 7.79 – 7.71 (m, 2H), 7.62 – 7.53 (m, 2H), 7.39 (t, *J* = 7.9 Hz, 1H), 7.27 – 7.22 (m, 1H), 6.98 (ddd, *J* = 8.2, 2.7, 1.0 Hz, 1H), 3.91 (s, 3H).

2-(3,5-dimethoxyphenyl)pyridine (S4a)[7]

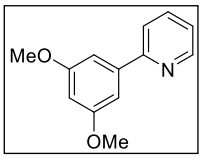

Colorless oil (1.51 mmol, 325 mg, 95%); **^{1}H NMR** (400 MHz, $CDCl_3$) δ 8.69 (ddd, *J* = 4.9, 1.8, 1.0 Hz, 1H), 7.77 – 7.72 (m, 1H), 7.70 (d, *J* = 7.9 Hz, 1H), 7.26 – 7.21 (m, 1H), 7.16 (d, *J* = 2.3 Hz, 2H), 6.54 (t, *J* = 2.3 Hz, 1H), 3.88 (s, 6H).

2-(2,6-dimethoxyphenyl)pyridine (S5a)[8]

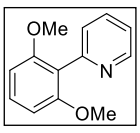

Colorless oil (0.97 mmol, 207 mg, 61%); **^{1}H NMR** (400 MHz, $CDCl_3$) δ 8.74 (ddd, *J* = 4.9, 1.9, 1.0 Hz, 1H), 7.76 – 7.69 (m, 1H), 7.36 – 7.29 (m, 2H), 7.23 (ddd, *J* = 7.6, 4.9, 1.2 Hz, 1H), 6.67 (s, 1H), 6.65 (s, 1H), 3.74 (s, 6H).

2-(2-(methylthio)phenyl)pyridine (S6a)[9]

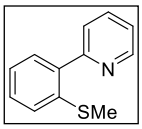

Colorless oil (0.92 mmol, 185 mg, 58%); **^{1}H NMR** (400 MHz, $CDCl_3$) δ 8.74 – 8.69 (m, 1H), 7.75 (td, *J* = 7.7, 1.8 Hz, 1H), 7.56 (dt, *J* = 7.9, 1.1 Hz, 1H), 7.46 – 7.41 (m, 1H), 7.40 – 7.33 (m, 2H), 7.29 – 7.21 (m, 2H), 2.39 (s, 3H).

2-(2-tolyl)pyridine (S7a)[6]

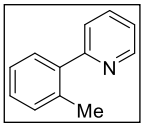

Colorless oil (1.03 mmol, 175 mg); **^{1}H NMR** (400 MHz, $CDCl_3$) δ 8.70 (d, *J* = 4.9 Hz, 1H), 7.74 (td, *J* = 7.7, 1.8 Hz, 1H), 7.40 (d, *J* = 7.8 Hz, 2H), 7.32 – 7.21 (m, 4H), 2.37 (s, 3H).

2-(2,4-dimethylphenyl)pyridine (S8a)[10]

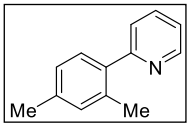

Colorless oil (1.40 mmol, 256 mg, 88%); **^{1}H NMR** (400 MHz, $CDCl_3$) δ 8.72 – 8.66 (m, 1H), 7.73 (td, *J* = 7.7, 1.8 Hz, 1H), 7.39 (dt, *J* = 7.8, 1.1 Hz, 1H), 7.32 (d, *J* = 7.6 Hz, 1H), 7.23 (ddd, *J* = 7.5, 4.9, 1.2 Hz, 1H), 7.10 (d, *J* = 8.3 Hz, 2H), 2.38 (s, 6H).

2-(3,5-di-*tert*-butylphenyl)pyridine (S9a)[11]

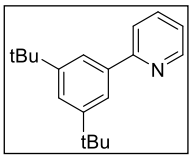

White solid (1.49 mmol, 397 mg, 93%); **^{1}H NMR** (400 MHz, $CDCl_3$) δ 8.70 (ddd, *J* = 4.9, 1.8, 1.1 Hz, 1H), 7.80 (d, *J* = 1.8 Hz, 2H), 7.76 – 7.68 (m, 2H), 7.50 (t, *J* = 1.8 Hz, 1H), 7.21 (ddd, *J* = 6.7, 4.8, 1.8 Hz, 1H), 1.39 (s, 18H).

2-(pyren-1-yl)pyridine (S10a)[5]

Off-White solid (1.28 mmol, 360 mg, 81%); **^{1}H NMR** (400 MHz, $CDCl_3$) δ 8.89 (ddd, *J* = 4.9, 1.9, 1.0 Hz, 1H), 8.40 (d, *J* = 9.3 Hz, 1H), 8.27 (d, *J* = 7.9 Hz, 1H), 8.24 – 8.16 (m, 3H), 8.12 (s, 2H), 8.09 (d, *J* = 9.3 Hz, 1H), 8.03 (t, *J* = 7.6 Hz, 1H), 7.90 (td, *J* = 7.7, 1.9 Hz, 1H), 7.75 (dt, *J*=7.8, 1.1, 1H), 7.39 (ddd, *J* = 7.6, 4.9, 1.2 Hz, 1H).

2-(phenanthren-9-yl)pyridine (S11a)[5]

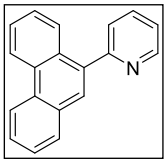

White solid (1.28 mmol, 309 mg, 80%) **^{1}H NMR** (400 MHz, $CDCl_3$) δ 8.83 (ddd, *J* = 4.9, 1.8, 1.0 Hz, 1H), 8.80 – 8.77 (m, 1H), 8.73 (dd, *J* = 8.2, 0.6 Hz, 1H), 8.08 (dd, *J* = 8.6, 1.3 Hz, 1H), 7.93 (dd, *J* = 7.9, 1.5 Hz, 1H), 7.89 – 7.83 (m, 2H), 7.72 – 7.55 (m, 5H), 7.40 – 7.35 (m, 1H).

9-(4-(pyridin-2-yl)phenyl)-9H-carbazole (S12a)[12]

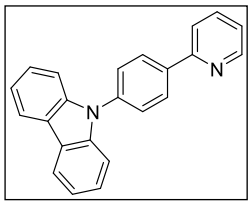

White solid (1.29 mmol, 413 mg, 81%); **^{1}H NMR** (400 MHz, $CDCl_3$) δ 8.77 (dt, *J* = 4.7, 1.4 Hz, 1H), 8.27 – 8.22 (m, 2H), 8.17 (d, *J* = 7.8 Hz, 2H), 7.85 – 7.79 (m, 2H), 7.73 – 7.68 (m, 2H), 7.50 (d, *J* = 9.2 Hz, 2H), 7.48 – 7.41 (m, 2H), 7.35 – 7.28 (m, 3H).

2-(naphthalen-2-yl)pyridine (S13a)[13]

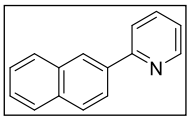

White solid (1.28 mmol, 261 mg, 80%); **^{1}H NMR** (400 MHz, $CDCl_3$) δ 8.77 (ddd, *J* = 4.8, 1.9, 0.9 Hz, 1H), 8.50 (d, *J* = 1.9 Hz, 1H), 8.16 (dd, *J* = 8.6, 1.8 Hz, 1H), 8.01 – 7.85 (m, 4H), 7.81 (td, *J* = 7.7, 1.9 Hz, 1H), 7.57 – 7.47 (m, 2H), 7.33 – 7.24 (m, 1 H).

2-([1,1'-biphenyl]-2-yl)pyridine (S14a)[14]

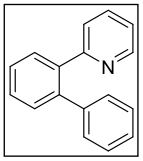

Colorless oil (1.27 mmol, 293 mg, 80%); **^{1}H NMR** (400 MHz, $CDCl_3$) δ 8.63 (ddd, *J* = 4.9, 1.9, 1.0 Hz, 1H), 7.73 – 7.67 (m, 1H), 7.50 – 7.42 (m, 3H), 7.41 – 7.35 (m, 1H), 7.25 – 7.21 (m, 3H), 7.18 – 7.14 (m, 2H), 7.12 – 7.07 (m, 1H), 6.88 (dt, *J* = 7.9, 1.1 Hz, 1H).

2-([1,1'-biphenyl]-3-yl)pyridine (S15a)[14]

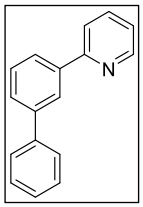

Colorless oil (1.56 mmol, 366 mg, 98%); **^{1}H NMR** (400 MHz, $CDCl_3$) δ 8.74 (dt, *J* = 4.7, 1.3 Hz, 1H), 8.25 (t, *J* = 1.8 Hz, 1H), 8.04 – 7.94 (m, 1H), 7.84 – 7.74 (m, 2H), 7.68 (ddt, *J* = 13.1, 7.5, 1.5 Hz, 2H), 7.56 (t, *J* = 7.7 Hz, 1H), 7.51 – 7.44 (m, 2H), 7.41 – 7.36 (m, 1H), 7.33 – 7.20 (m, 2H).

2-([1,1'-biphenyl]-4-yl)pyridine (S16a)[14]

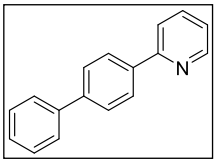

White solid (1.28 mmol, 298 mg, 81%); **^{1}H NMR** (400 MHz, $CDCl_3$) δ 8.72 (dt, *J* = 4.8, 1.4 Hz, 1H), 8.12 – 8.05 (m, 2H), 7.78 (dd, *J* = 6.3, 1.6 Hz, 2H), 7.74 – 7.70 (m, 2H), 7.67 (dd, *J* = 8.3, 1.3 Hz, 2H), 7.47 (t, *J* = 7.5 Hz, 2H), 7.40 – 7.34 (m, 1H), 7.26 – 7.22 (m, 1H).

4-(pyridin-2-yl)benzonitrile (S17a)[15]

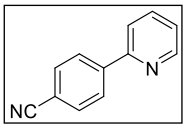

White solid (1.18 mmol, 212 mg, 74%); **^{1}H NMR** (400 MHz, $CDCl_3$) δ 8.74 (ddd, *J* = 4.8, 1.8, 1.0 Hz, 1H), 8.15 – 8.10 (m, 2H), 7.84 – 7.79 (m, 1H), 7.79 – 7.75 (m, 3H), 7.32 (ddd, *J* = 7.2, 4.8, 1.4 Hz, 1H).

2-(4-nitrophenyl)pyridine (S18a)[5]

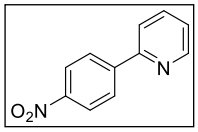

White solid (1.00 mmol, 200 mg, 63%); **^{1}H NMR** (400 MHz, $CDCl_3$) δ 8.77 (dt, *J* = 4.8, 1.4 Hz, 1H), 8.38 – 8.30 (m, 2H), 8.23 – 8.15 (m, 2H), 7.89 – 7.78 (m, 2H), 7.35 (ddd, *J* = 6.2, 4.8, 2.4 Hz, 1H).

2-(3-nitrophenyl)pyridine (S19a)[16]

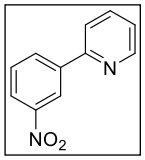

White solid (0.94 mmol, 187 mg, 59%); **^{1}H NMR** (400 MHz, $CDCl_3$) δ 8.88 (t, *J* = 2.0 Hz, 1H), 8.76 (dt, *J* = 4.9, 1.4 Hz, 1H), 8.39 (dt, *J* = 7.8, 1.4 Hz, 1H), 8.28 (ddd, *J* = 8.2, 2.3, 1.1 Hz, 1H), 7.89 – 7.79 (m, 2H), 7.67 (t, *J* = 8.0 Hz, 1H), 7.34 (ddd, *J* = 5.7, 4.8, 2.7 Hz, 1H).

2-(4-(trifluoromethyl)phenyl)pyridine (S20a)[17]

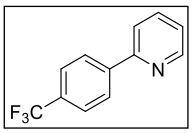

White solid (1.32 mmol, 294 mg, 83%); **^{1}H NMR** (400 MHz, $CDCl_3$) δ 8.73 (ddd, *J* = 4.8, 1.8, 1.1 Hz, 1H), 8.15 – 8.08 (m, 2H), 7.84 – 7.78 (m, 1H), 7.77 (dd, *J* = 1.6, 1.0 Hz, 1H), 7.76 – 7.69 (m, 2H), 7.29 (ddd, *J* = 6.7, 4.8, 1.7 Hz, 1H).

2-(3,5-difluorophenyl)pyridine (S21a)[7]

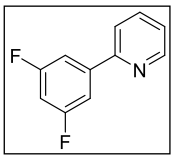

White solid (0.67 mmol, 128 mg, 42%); **^{1}H NMR** (400 MHz, $CDCl_3$) δ 8.70 (ddd, *J* = 4.9, 1.8, 1.0 Hz, 1H), 7.78 (td, *J* = 7.7, 1.8 Hz, 1H), 7.69 (d, *J* = 8.0 Hz, 1H), 7.59 – 7.51 (m, 2H), 7.31 – 7.27 (m, 1H), 6.85 (tt, *J* = 8.7, 2.4 Hz, 1H).

2-(furan-2-yl)pyridine (S22a)[17]

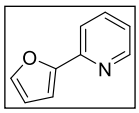

Colorless oil (0.74 mmol, 108 mg, 47%); **^{1}H NMR** (400 MHz, $CDCl_3$) δ 8.62 – 8.56 (m, 1H), 7.74 – 7.66 (m, 2H), 7.55 – 7.51 (m, 1H), 7.15 (ddd, *J* = 6.7, 4.9, 2.1 Hz, 1H), 7.05 (dd, *J* = 3.4, 0.8 Hz, 1H), 6.53 (dd, *J* = 3.4, 1.8 Hz, 1H).

2-(thiophen-2-yl)pyridine (S23a)[5]

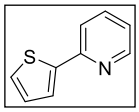

Off-white solid (1.13 mmol, 182 mg, 71%); **^{1}H NMR** (400 MHz, $CDCl_3$) δ 8.64 – 8.46 (m, 1H), 7.71 – 7.61 (m, 2H), 7.58 (td, *J* = 3.6, 1.2 Hz, 1H), 7.39 (ddt, *J* = 6.1, 4.1, 2.0 Hz, 1H), 7.12 (ddt, *J* = 12.0, 5.0, 3.4 Hz, 2H).

2-(benzo[b]thiophen-2-yl)pyridine (S24a)[17]

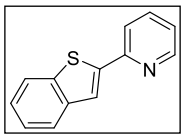

Tan solid (0.72 mmol, 151 mg, 45%); **^{1}H NMR** (400 MHz, $CDCl_3$) δ 8.79 – 8.72 (m, 1H), 8.47 (dd, *J* = 8.3, 1.1 Hz, 1H), 7.94 – 7.87 (m, 1H), 7.82 – 7.76 (m, 2H), 7.70 (dt, *J* = 7.9, 1.1 Hz, 1H), 7.47 – 7.43 (m, 1H), 7.40 (ddd, *J* = 8.2, 7.1, 1.4 Hz, 1H), 7.30 – 7.26 (m, 1H).

2-(benzo[b]thiophen-3-yl)pyridine (S25a)[17]

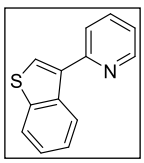

Pink oil (0.52 mmol, 111 mg, 33%); **^{1}H NMR** (400 MHz, $CDCl_3$) δ 8.76 (ddd, *J* = 4.9, 1.8, 1.0 Hz, 1H), 8.50 – 8.44 (m, 1H), 7.95 – 7.88 (m, 1H), 7.83 – 7.76 (m, 2H), 7.73 – 7.67 (m, 1H), 7.49 – 7.36 (m, 2H), 7.30 – 7.26 (m, 1H).

***tert*-butyl 2-(pyridin-2-yl)-1*H*-pyrrole-1-carboxylate (S26a)**[17]

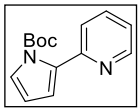

Colorless oil (0.57 mmol, 140 mg, 36%); **^{1}H NMR** (400 MHz, $CDCl_3$) δ 8.61 (ddd, *J* = 4.9, 1.8, 1.0 Hz, 1H), 7.71 – 7.64 (m, 1H), 7.39 (dt, *J* = 7.9, 1.1 Hz, 1H), 7.36 (dd, *J* = 3.3, 1.7 Hz, 1H), 7.19 (ddd, *J* = 7.5, 4.9, 1.2 Hz, 1H), 6.41 (dd, *J* = 3.3, 1.7 Hz, 1H), 6.24 (t, *J* = 3.3 Hz, 1H), 1.36 (s, 9H).

***tert*-butyl 2-(pyridin-2-yl)-1*H*-indole-1-carboxylate (S27a)**[17]

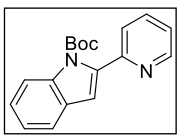

Colorless oil (1.05 mmol, 309 mg, 66%); **^{1}H NMR** (400 MHz, $CDCl_3$) δ 8.67 (ddd, *J* = 4.9, 1.9, 1.0 Hz, 1H), 8.19 (d, *J* = 8.3 Hz, 1H), 7.74 (td, *J* = 7.7, 1.8 Hz, 1H), 7.58 (d, *J* = 7.7 Hz, 1H), 7.51 (d, *J* = 7.9 Hz, 1H), 7.36 (ddd, *J* = 8.4, 7.2, 1.3 Hz, 1H), 7.29 – 7.22 (m, 2H), 6.77 (s, 1H), 1.34 (s, 9H).

2,5-diphenylpyridine (S28a)[18]

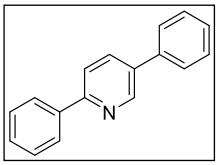

3 Equivalents of phenylboronic acid and 2,5-dibromopyridine (1.59 mmol) were used; white solid (0.97 mmol, 224 mg, 61%); **^{1}H NMR** (400 MHz, $CDCl_3$) δ 8.94 (dd, *J* = 2.4, 0.9 Hz, 1H), 8.09 – 8.01 (m, 2H), 7.96 (dd, *J* = 8.3, 2.4 Hz, 1H), 7.81 (dd, *J* = 8.3, 0.9 Hz, 1H), 7.68 – 7.60 (m, 2H), 7.54 – 7.49 (m, 3H), 7.49 – 7.37 (m, 3H).

***N*,*N*-dimethyl-4-(pyridin-2-yl)aniline (S29a)**[17]

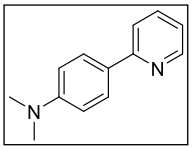

Off-white solid (0.91 mmol, 180 mg, 57%); **^{1}H NMR** (400 MHz, $CDCl_3$) δ 8.66 – 8.60 (m, 1H), 7.97 – 7.89 (m, 2H), 7.72 – 7.61 (m, 2H), 7.11 (ddd, *J* = 6.7, 4.9, 2.1 Hz, 1H), 6.85 – 6.77 (m, 2H), 3.03 (s, 6H).

2-(2-(trifluoromethyl)phenyl)pyridine (S30a)[14]

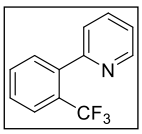

Colorless oil (0.97 mmol, 216 mg, 61%); **^{1}H NMR** (400 MHz, $CDCl_3$) δ 8.70 (dt, *J* = 4.9, 1.3 Hz, 1H), 7.81 – 7.70 (m, 2H), 7.63 (td, *J* = 7.6, 1.3 Hz, 1H), 7.58 – 7.48 (m, 2H), 7.44 (d, *J* = 7.8 Hz, 1H), 7.32 (ddd, *J* = 7.6, 4.9, 1.2 Hz, 1H).

Other pyridines

2-benzylpyridine (S31a); prepared according to the Seto's procedure.[19]

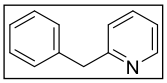

2 Steps; pale yellow oil (3.18 mmol, 538 mg, 43%), ~ 80% purity based on the ^{1}H NMR, the compound was used in this form for the preparation of the Zincke imine); ^{1}H NMR (400 MHz, $CDCl_3$) δ 8.57 – 8.53 (m, 1H), 7.57 (td, *J* = 7.7, 1.9 Hz, 1H), 7.34 – 7.18 (m, 5H), 7.13 – 7.07 (m, 2H), 4.16 (s, 2H).

2-(methoxy(phenyl)methyl)pyridine (S32a); prepared according to the Wong's procedure.[20]

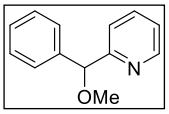

2 Steps; pale yellow oil (2.15 mmol, 428 mg, 84%); **^{1}H NMR** (400 MHz, $CDCl_3$) δ 8.58 – 8.52 (m, 1H), 7.68 (td, *J* = 7.7, 1.8 Hz, 1H), 7.50 (d, *J* = 7.8 Hz, 1H), 7.46 – 7.41 (m, 2H), 7.34 (dd, *J* = 8.4, 6.7 Hz, 2H), 7.30 – 7.22 (m, 1H), 7.16 (ddd, J = 7.5, 4.9, 1.2 Hz, 1H), 5.39 (s, 1H), 3.45 (s, 3H).

phenyl(pyridin-2-yl)methanol (S33a); prepared according to the Seto's procedure.[19]

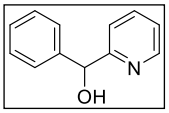

Pale yellow oil (7.95 mmol, 1.47 g, 97%); **^{1}H NMR** (400 MHz, $CDCl_3$) δ 8.57 (ddd, *J* = 4.9, 1.8, 1.0 Hz, 1H), 7.61 (td, J = 7.7, 1.7 Hz, 1H), 7.41 – 7.33 (m, 3H), 7.33 – 7.28 (m, 1H), 7.28 – 7.20 (m, 1H), 7.20 – 7.11 (m, 2H), 5.75 (d, *J* = 4.0 Hz, 1H), 5.23 (d, *J* = 4.3 Hz, 1H).

***N*,*N*-diphenylpyridin-2-amine (S34a) prepared according to the Verkade's procedure.**[21]

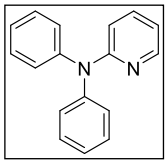

Off-white solid (1.27 mmol, 313 mg, 71%); ^{1}H NMR (400 MHz, $CDCl_3$) δ 8.23 (dd, *J* = 5.0, 1.2 Hz, 1H), 7.48 – 7.40 (m, 1H), 7.36 – 7.27 (m, 4H), 7.18 (d, *J* = 8.4 Hz, 4H), 7.16 – 7.09 (m, 2H), 6.81 – 6.72 (m, 2H).

2,5-diphenylpyridine (S35a) prepared according to the Wierks procedure.[22]

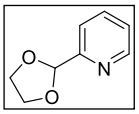

Pale yellow oil (15.9 mmol, 2.40 g, 80%); **^{1}H NMR** (400 MHz, $CDCl_3$) δ 8.62 (ddd, *J* = 4.8, 1.8, 0.9 Hz, 1H), 7.73 (td, *J* = 7.7, 1.8 Hz, 1H), 7.53 (dt, *J* = 7.8, 1.1 Hz, 1H), 7.31 – 7.24 (m, 1H), 5.86 (s, 1H), 4.23 – 4.02 (m, 4H).

3.2.Preparation of Zincke imines

Zincke imines were prepared according to **general procedure 2 (modified McNally's procedure)**. [1]

General Procedure 2. In a closed-cup vial, pyridine (0.1 mmol) was dissolved in anhydrous DCM (10 ml) and cooled to -78 °C (acetone/dry ice bath) followed by the addition of trifluoromethanesulfonic anhydride (1 mmol, 1.0 equiv.). The reaction mixture was stirred for 1 h at -78 ° C. After an indicated time, the solution of dibenzylamine (1.2 mmol, 1.2 equiv.) in anhydrous DCM (1 ml) was added dropwise and stirring was continued for another 30 min at -78 °C. The reaction mixture was removed from the cryogenic bath and allowed to reach room temperature. The crude reaction mixture was evaporated with silica gel (dry load for preparation of the sample for flash chromatography) and the pure product was isolated by flash chromatography in hexanes/DCM (85:15)/ AcOEt gradient.

Flash program: time: 25 min; column: silica 12 g; flow rate: 30 mL/min; automatic peak hold: on.

entry	time [min]	hexanes/DCM (85:10 v/v) [%]	AcOEt [%]
1	0	100	0
2	25	80	20

***N*-((1*E*,2*E*,4*E*)-5-(dibenzylamino)-1-phenylpenta-2,4-dien-1-ylidene)-1,1,1-trifluoromethanesulfonamide (2)**[1]

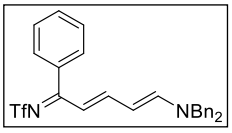

Orange solidified foam (0.7 mmol, 338 mg, 70%); **^{1}H NMR** (400 MHz, $CDCl_3$) δ 7.60 (dd, *J* = 6.9, 1.6 Hz, 2H), 7.54 – 7.48 (m, 1H), 7.47 – 7.36 (m, 8H), 7.34 – 7.25 (m, 2H), 7.16 (dd, *J* = 7.7, 1.8 Hz, 4H), 6.72 (d, *J* = 13.7 Hz, 1H), 5.84 (t, *J* = 12.2 Hz, 1H), 4.44 (s, 4H).

***N*-((1*Z*,2*E*,4*E*)-5-(dibenzylamino)-1-(4-methoxyphenyl)penta-2,4-dien-1-ylidene)-1,1,1-trifluoromethanesulfonamide (S2b)**

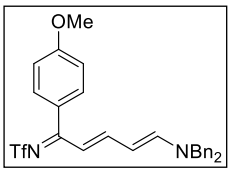

Yellow solid (0.48 mmol, 246 mg, 48%); **^{1}H NMR** (600 MHz, $CDCl_3$) δ 7.64 – 7.61 (m, 2H), 7.39 (tt, J = 8.8, 6.0 Hz, 7H), 7.29 (d, *J* = 12.4 Hz, 1H), 7.19 – 7.12 (m, 4H), 6.95 – 6.91 (m, 2H), 6.66 (d, *J* = 13.8 Hz, 1H), 5.81 (t, *J* = 12.2 Hz, 1H), 4.42 (s, 4H), 3.86 (s, 3H); **^{13}C NMR** (126 MHz, $CDCl_3$) δ 177.3, 162.6, 159.1, 156.9, 131.9, 130.3, 129.2, 128.7, 128.3, 127.7, 127.2, 120.8, 118.3, 114.3, 113.6, 102.3, 59.6, 55.4, 51.3; **HRMS** (ESI) calcd. for $C_{27}H_{26}F_3N_2O_3S$ [M+H] 515.1611; found 515.1616.

***N*-((1*Z*,2*E*,4*E*)-5-(dibenzylamino)-1-(3-methoxyphenyl)penta-2,4-dien-1-ylidene)-1,1,1-trifluoromethanesulfonamide (S3b)**

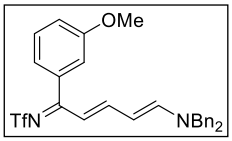

Orange solid (0.22 mmol, 113 mg, 22%); **^{1}H NMR** (500 MHz, $CDCl_3$) δ 7.38 (d, *J* = 7.2 Hz, 6H), 7.38 – 7.31 (m, 2H), 7.33 – 7.26 (m, 1H), 7.14 (ddd, *J* = 7.8, 6.1, 2.0 Hz, 6H), 7.03 (ddd, J = 8.3, 2.7, 1.0 Hz, 1H), 6.68 (d, *J* = 13.7 Hz, 1H), 5.83 (t, *J* = 12.1 Hz, 1H), 4.44 (s, *2*H), 4.42 (s, 2H), 3.83 (s, 3H); **^{13}C NMR** (126 MHz, $CDCl_3$) δ 177.9, 159.9, 159.3, 157.4, 139.3, 134.2, 133.7, 129.2, 129.1, 128.8, 128.4, 127.7, 127.2, 122.1, 118.2, 117.0, 114.7, 114.5, 102.6, 59.7, 55.4, 51.4, 30.9; **HRMS** (ESI) calcd. for $C_{27}H_{26}F_3N_2O_3S$ [M+H] 515.1611; found 515.1619.

***N*-((1*E*,2*E*,4*E*)-5-(dibenzylamino)-1-(3,5-dimethoxyphenyl)penta-2,4-dien-1-ylidene)-1,1,1-trifluoromethanesulfonamide (S4b)**

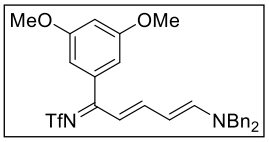

Yellow solid (0.81 mmol, 441 mg, 81%); **^{1}H NMR** (400 MHz, $CDCl_3$) δ 7.45 – 7.28 (m, 8H), 7.15 (dd, *J* = 7.6, 1.9 Hz, 4H), 6.73 (d, *J* = 2.3 Hz, 2H), 6.66 (d, *J* = 13.6 Hz, 1H), 6.57 (t, *J* = 2.3 Hz, 1H), 5.82 (t, *J* = 12.2 Hz, 1H), 4.43 (d, *J* = 7.1 Hz, 4H), 3.81 (s, 6H); **^{13}C NMR** (101 MHz, $CDCl_3$) δ 177.8, 160.4, 160.0, 157.6, 139.9, 134.2, 129.2, 128.8, 128.4, 127.8, 127.2, 121.1, 117.9, 114.4, 107.6, 103.0, 102.6, 59.8, 55.5, 51.9; **HRMS** (ESI) calcd. for $C_{28}H_{28}F_3N_2O_4S$ [M+H] 545.1722; found 545.1735.

***N*-((1*Z*,2*E*,4*E*)-5-(dibenzylamino)-1-(2,6-dimethoxyphenyl)penta-2,4-dien-1-ylidene)-1,1,1-trifluoromethanesulfonamide (S5b)**

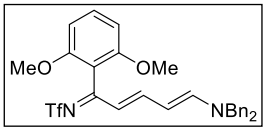

Yellow solid (0.48 mmol, 262 mg, 48%); **^{1}H NMR** (400 MHz, $CDCl_3$) δ 7.44 – 7.28 (m, 7H), 7.24 – 7.01 (m, 6H), 6.60 (s, 2H), 6.47 (s, 1H), 5.73 (t, *J* = 12.2 Hz, 1H), 4.37 (s, 4H), 3.81 (s, 6H); **^{13}C NMR** (101 MHz, $CDCl_3$) δ 157.2, 156.1, 130.9, 129.1, 128.3, 127.6, 118.4, 104.3, 101.9, 56.41; **HRMS** (ESI) calcd. for $C_{28}H_{28}F_3N_2O_4S$ [M+H] 545.1722; found 545.1727.

***N*-((1*Z*,2*E*,4*E*)-5-(dibenzylamino)-1-(2-(methylthio)phenyl)penta-2,4-dien-1-ylidene)-1,1,1-trifluoromethanesulfonamide (S6b)**

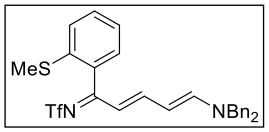

Yellow solid (0.32 mmol, 170 mg, 32%); **^{1}H NMR** (500 MHz, $CDCl_3$) δ 7.37 (d, *J* = 7.4 Hz, 8H), 7.25 – 7.17 (m, 3H), 7.13 (d, *J* = 7.6 Hz, 4H), 6.99 (d, *J* = 12.7 Hz, 1H), 6.67 (d, *J* = 13.5 Hz, 1H), 5.81 (t, *J* = 12.2 Hz, 1H), 4.39 (s, 4H), 2.46 (s, 3H); **^{13}C NMR** (126 MHz, $CDCl_3$) δ 180.9, 162.3, 160.1, 140.2, 139.8, 132.4, 131.9, 131.6, 131.5, 131.1, 130.4, 130.2, 129.9, 127.6, 118.6, 105.2, 62.3, 53.9, 19.7; **HRMS** (ESI) calcd. for $C_{38}H_{31}F_3N_3O_2S$ [M+H] 531.1388; found 531.1392.

***N*-((1*Z*,2*E*,4*E*)-5-(dibenzylamino)-1-(o-tolyl)penta-2,4-dien-1-ylidene)-1,1,1-trifluoromethanesulfonamide (S7b)**

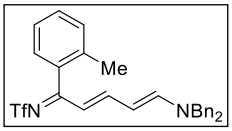

Yellow solid (0.32 mmol, 170 mg, 32%); **^{1}H NMR** (400 MHz, $CDCl_3$) δ 7.38 (s, 1H), 7.37 (d, *J* = 3.7 Hz, 1H), 7.36 – 7.27 (m, 5H), 7.27 – 7.08 (m, 8H), 6.93 (t, *J* = 12.8 Hz, 1H), 6.68 (d, *J* = 13.7 Hz, 1H), 5.78 (t, *J* = 12.2 Hz, 1H), 4.39 (s, 4H), 2.32 (s, 3H); **^{13}C NMR** (101 MHz, $CDCl_3$) δ 180.2, 159.5, 157.1, 137.2, 135.8, 130.4, 129.2, 129.2, 128.4, 127.7, 127.2, 125.2, 116.3, 102.1, 19.3; **HRMS** (ESI) calcd. for $C_{27}H_{26}F_3N_2O_2S$ [M+H] 499.1667; found 499.1665.

***N*-((1*Z*,2*E*,4*E*)-5-(dibenzylamino)-1-(2,4-dimethylphenyl)penta-2,4-dien-1-ylidene)-1,1,1-trifluoromethanesulfonamide (S8b)**

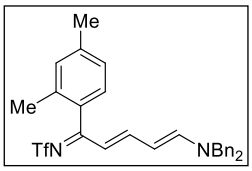

Yellow solid (0.79 mmol 405 mg, 79%); **^{1}H NMR** (500 MHz, $CDCl_3$) δ 7.37 (d, *J* = 7.3 Hz, 6H), 7.13 (d, *J* = 7.9 Hz, 6H), 7.08 – 7.01 (m, 2H), 6.96 (t, *J* = 12.8 Hz, 1H), 6.65 (d, *J* = 13.6 Hz, 1H), 5.77 (t, *J* = 12.2 Hz, 1H), 4.38 (s, 4H), 2.35 (s, 3H), 2.29 (s, 3H); **^{13}C NMR** (126 MHz, $CDCl_3$) δ 183.2, 162.1, 159.6, 141.9, 138.5, 137.0, 136.5, 133.9, 131.8, 131.4, 131.2, 131.0, 130.3, 129.9, 128.5, 123.3, 119.3, 104.6, 23.9, 22.0; **HRMS** (ESI) calcd. for $C_{28}H_{28}F_3N_2O_2S$ [M+H] 513.1824; found 513.1830.

***N*-((1*Z*,2*E*,4*E*)-1-(3,5-di-tert-butylphenyl)-5-(dibenzylamino)penta-2,4-dien-1-ylidene)-1,1,1-trifluoromethanesulfonamide (S9b)**

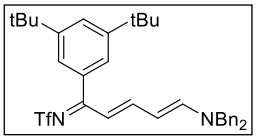

Yellow solid (0.56 mmol, 334,15 mg, 56%); **^{1}H NMR** (600 MHz, $CDCl_3$) δ 7.55 (t, *J* = 1.8 Hz, 1H), 7.44 (d, *J* = 1.8 Hz, 2H), 7.42 – 7.34 (m, 7H), 7.21 (d, *J* = 12.4 Hz, 1H), 7.19 – 7.12 (m, 4H), 6.70 (d, *J* = 13.7 Hz, 1H), 5.85 (t, *J* = 12.2 Hz, 1H), 4.43 (s, 4H), 1.34 (s, 18H); **^{13}C NMR** (151 MHz, $CDCl_3$) δ 179.2, 159.7, 156.7, 150.5, 137.2, 129.2, 127.8, 127.3, 125.4, 124.3, 114.7, 102.4, 34.9, 31.3; **HRMS** (ESI) calcd. for $C_{34}H_{39}F_3N_2O_2S$ [M+H] 597.2757; found 597.2757.

***N*-((1*Z*,2*E*,4*E*)-5-(dibenzylamino)-1-(pyren-4-yl)penta-2,4-dien-1-ylidene)-1,1,1-trifluoromethanesulfonamide (S10b)**

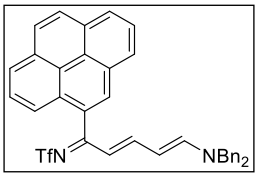

Red solid (0.59 mmol, 359 mg, 59%); **^{1}H NMR** (400 MHz, $CDCl_3$) δ 8.27 – 8.17 (m, 4H), 8.16 – 7.95 (m, 5H), 7.42 –7.27 (m, 6H), 7.16 – 6.77 (m, 7H), 5.83 (t, *J* = 12.0 Hz, 1H), 4.35 (s, 2H) 4.25 (s, 2H); **^{13}C NMR** (126 MHz, $CDCl_3$) δ 179.5, 157.8, 134.2, 133.8, 132.3, 131.4, 131.0, 129.4, 129.4, 129.2, 129.0, 128.7, 128.6, 127.9, 127.4, 127.4, 126.6, 126.5, 125.9, 125.8, 125.0, 124.8, 124.7, 124.3, 117.6, 102.8, 51.5; **HRMS** (ESI) calcd. for $C_{36}H_{28}F_3N_2O_2S$ [M+H] 609.1824; found 609.1821.

***N*-((1*Z*,2*E*,4*E*)-5-(dibenzylamino)-1-(phenanthren-9-yl)penta-2,4-dien-1-ylidene)-1,1,1-trifluoromethanesulfonamide (S11b)**

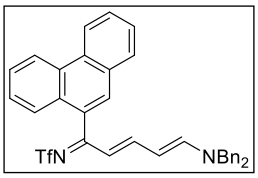

Yellow solid (0.49 mmol, 286 mg, 49%); **^{1}H NMR** (400 MHz, $CDCl_3$) δ 8.72 (t, *J* = 7.5 Hz, 2H), 8.04 (d, *J* = 8.1 Hz, 1H), 7.93 (d, *J* = 8.1 Hz, 1H), 7.77 – 7.59 (m, 5H), 7.36 (s, 6H), 7.17 – 6.85 (m, 7H), 5.82 (t, *J* = 12.1 Hz, 1H), 4.36 (s, 2H), 4.30 (s, 2H); **^{13}C NMR** (101 MHz, $CDCl_3$) δ 178.9, 160.2, 157.8, 134.0, 133.6, 130.7, 130.5, 130.3, 130.0, 129.2, 129.2, 128.8, 128.5, 127.8, 127.6, 127.4, 127.2, 127.2, 127.0, 126.7, 122.7, 122.6, 121.0, 117.8, 116.8, 102.4, 98.5, 77.2, 59.7, 51.3; **HRMS** (ESI) calcd. for $C_{34}H_{28}F_3N_2O_2S$ [M+H] 585.1824; found 585.1821.

***N*-((1*Z*,2*E*,4*E*)-1-(4-(9H-carbazol-9-yl)phenyl)-5-(dibenzylamino)penta-2,4-dien-1-ylidene)-1,1,1-trifluoromethanesulfonamide (S12b)**

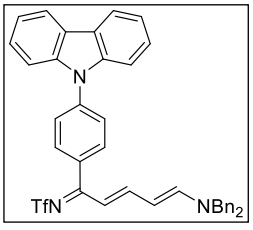

Red solid (0.29 mmol, 188 mg, 29%); **^{1}H NMR** (400 MHz, $CDCl_3$) δ 7.74 – 7.63 (m, 4H), 7.44 – 7.27 (m, 8H), 7.15 (d, *J* = 5.8 Hz, 4H) 6.67 (d, *J* = 13.6 Hz, 1H), 5.90 (t, *J* = 12.1 Hz, 1H), 4.47 (d, *J* = 11.1 Hz, 4H); **^{13}C NMR** (126 MHz, $CDCl_3$) δ 176.7, 160.1, 158.1, 140.8, 140.5, 136.9, 133.9, 131.6, 129.5, 129.1, 128.7, 128.0, 127.5, 126.5, 126.3, 123.9, 120.7, 120.6, 114.5, 110.0, 103.2, 60.1, 51.7; **HRMS** (ESI) calcd. for $C_{38}H_{31}F_3N_3O_2S$ [M+H] 650.2089; found 650.2084.

***N*-((1*Z*,2*E*,4*E*)-5-(dibenzylamino)-1-(naphthalen-1-yl)penta-2,4-dien-1-ylidene)-1,1,1-trifluoromethanesulfonamide (S13b)**

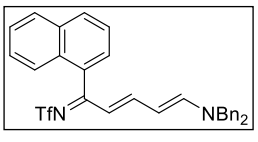

Red solid (0.51 mmol, 272 mg, 51%); **^{1}H NMR** (500 MHz, $CDCl_3$) δ 8.08 (s, 1H), 7.92 (d, *J* = 6.9 Hz, 1H), 7.88 (d, *J* = 8.7 Hz, 2H), 7.69 (dd, *J* = 8.5, 1.8 Hz, 1H), 7.59 – 7.52 (m, 2H), 7.44 – 7.32 (m, 7H), 7.24 (s, 1H), 7.15 (s, 4H), 6.81 (d, *J* = 13.7 Hz, 1H), 5.87 (t, *J* = 12.1 Hz, 1H), 4.42 (s, 4H); **^{13}C NMR** (126 MHz, $CDCl_3$) δ 178.1, 160.0, 157.4, 135.4, 134.5, 134.2, 133.7, 132.4, 130.1, 129.2, 128.9, 128.8,

128.4, 128.0, 127.8, 127.7, 127.6, 127.2, 126.6, 126.4, 120.8, 118.3, 114.8, 102.7, 59.7, 51.4; **HRMS** (ESI) calcd. for $C_{30}H_{26}F_3N_2O_2S$ [M+H] 535.1667; found 535.1663.

***N*-((1*Z*,2*E*,4*E*)-1-([1,1'-biphenyl]-2-yl)-5-(dibenzylamino)penta-2,4-dien-1-ylidene)-1,1,1-trifluoromethanesulfonamide (S14b)**

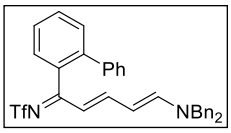

Yellow solid (0.31 mmol, 174 mg, 31%); **^{1}H NMR** (600 MHz, $CDCl_3$) δ 7.54 – 7.45 (m, 2H), 7.45 – 7.28 (m, 14H), 7.19 – 7.01 (m, 5H), 7.01-6.85 6.49-6.33 (s, 1H) 5.57 (t, *J* = 12.2 Hz, 1H), 4.39 (s, 2H), 4.32 (s, 2H); **^{13}C NMR** (151 MHz, $CDCl_3$) δ 179.6, 156.7, 140.5, 130.0, 129.8, 129.1, 128.6, 128.2, 127.6, 127.2, 127.0, 102.2, 51.3. **HRMS** (ESI) calcd. for $C_{32}H_{28}F_3N_2O_2S$ [M+H] 561.1824; found 561.1830. ^{1}H NMR (600 MHz, Chloroform-*d*) δ 7.54 – 7.45 (m, 2H), 7.45 – 7.28 (m, 13H), 7.19 – 7.01 (m, 5H), 5.57 (t, *J* = 12.2 Hz, 1H), 4.35 (d, *J* = 42.9 Hz, 4H).

***N*-((1*Z*,2*E*,4*E*)-1-([1,1'-biphenyl]-3-yl)-5-(dibenzylamino)penta-2,4-dien-1-ylidene)-1,1,1-trifluoromethanesulfonamide (S15b)**

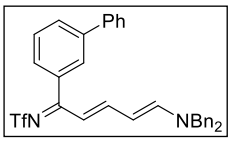

Yellow solid (0.48 mmol, 269 mg, 48%); **^{1}H NMR** (400 MHz, $CDCl_3$) δ 7.80 (s, 1H), 7.74 – 7.68 (m, 1H), 7.64 – 7.43 (m, 6H), 7.43 – 7.32 (m, 8H), 7.29 (d, *J* = 12.3 Hz, 1H), 7.15 (d, *J* = 7.4 Hz, 4H), 6.74 (d, *J* = 13.7 Hz, 1H), 5.84 (t, *J* = 12.2 Hz, 1H), 4.43 (s, 2H), 4.41 (s, 2H); **^{13}C NMR** (101 MHz, $CDCl_3$) δ 178.1, 160.0, 157.6, 141.2, 140.3, 138.6, 134.2, 133.7, 131.1, 129.7, 129.7, 129.2, 128.9, 128.8, 128.7, 128.5, 128.4, 128.2, 128.2, 127.8, 127.7, 127.2, 121.1, 117.9, 114.6, 102.7, 59.7, 51.4; **HRMS** (ESI) calcd. for $C_{32}H_{28}F_3N_2O_2S$ [M+H] 561.1824; found 561.1824.

***N*-((1*Z*,2*E*,4*E*)-1-([1,1'-biphenyl]-4-yl)-5-(dibenzylamino)penta-2,4-dien-1-ylidene)-1,1,1-trifluoromethanesulfonamide (S16b)**

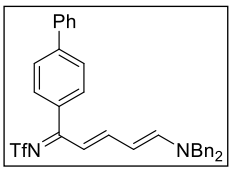

Yellow solid (0.40 mmol, 224 mg, 40%); **^{1}H NMR** (400 MHz, $CDCl_3$) δ 7.74 – 7.60 (m, 4H), 7.49 (d, *J* = 7.1 Hz, 1H), 7.50 – 7.41 (m, 1H), 7.45 – 7.33 (m, 4H), 7.32 (d, *J* = 12.3 Hz, 1H), 7.20 – 7.14 (m, 3H), 6.75 (d, *J* = 13.7 Hz, 1H), 5.87 (t, *J* = 12.1 Hz, 1H), 4.45 (s, 3H); **^{13}C NMR** (101 MHz, $CDCl_3$) δ 177.7, 159.6, 157.3, 144.1, 140.1, 136.8, 130.3, 129.2, 128.9, 128.0, 127.8, 127.2, 126.9, 114.6, 102.6, 51.4. **HRMS** (ESI) calcd. for $C_{32}H_{28}F_3N_2O_2S$ [M+H] 561.1824; found 561.1832.

***N*-((1*Z*,2*E*,4*E*)-1-(4-cyanophenyl)-5-(dibenzylamino)penta-2,4-dien-1-ylidene)-1,1,1-trifluoromethanesulfonamide (S17b)**

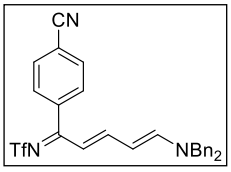

Yellow solid (0.75 mmol, 382 mg, 75%); **^{1}H NMR** (400 MHz, $CDCl_3$) δ 7.74 – 7.63 (m, 4H), 7.44 – 7.27 (m, 8H), 7.15 (d, *J* = 5.8 Hz, 4H), 6.67 (d, *J* = 13.6 Hz, 1H), 5.90 (t, *J* = 12.1 Hz, 1H), 4.48 (s, 2H), 4.45 (s, 2H);**^{13}C NMR** (126 MHz, $CDCl_3$) δ 175.2, 160.4, 158.9, 142.7, 133.9, 133.5, 132.2, 130.2, 129.6, 129.6, 129.3, 128.9, 128.1, 127.4, 121.0, 118.4, 114.4, 114.1, 103.8, 60.3, 51.9; **HRMS** (ESI) calcd. for $C_{27}H_{23}F_3N_3O_2S$ [M+H] 510.1457; found 510.1455.

***N*-((1*Z*,2*E*,4*E*)-5-(dibenzylamino)-1-(4-nitrophenyl)penta-2,4-dien-1-ylidene)-1,1,1-trifluoromethanesulfonamide (S18b)**

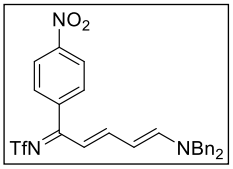

Red solid (0.33 mmol, 175 mg, 33%); **^{1}H NMR** (400 MHz, $CDCl_3$) δ 8.26 (d, *J* = 8.8 Hz, 2H), 7.72 (d, *J* = 8.7 Hz, 2H), 7.39 (d, *J* = 7.2 Hz, 7H), 7.31 (d, *J* = 12.9 Hz, 1H), 7.15 (dd, *J* = 7.2, 2.2 Hz, 4H), 6.69 (d, *J* = 13.6 Hz, 1H), 5.92 (t, *J* = 12.1 Hz, 1H), 4.49 (s, 2H), 4.46 (s, 2H); **^{13}C NMR** (101 MHz, $CDCl_3$) δ 174.5, 160.3, 158.9, 148.9, 144.3, 133.6, 133.2, 130.2, 129.4, 129.1, 128.7, 127.9, 127.2, 123.4, 121.1, 117.9, 114.0, 103.7, 60.1, 51.7; **HRMS** (ESI) calcd. for $C_{26}H_{23}F_3N_3O_4S$ [M+H] 530.1361; found 530.1366.

***N*-((1*Z*,2*E*,4*E*)-5-(dibenzylamino)-1-(3-nitrophenyl)penta-2,4-dien-1-ylidene)-1,1,1-trifluoromethanesulfonamide (S19b)**

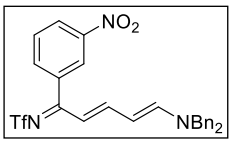

Red solid (0.27 mmol, 143 mg, 27%); **^{1}H NMR** (500 MHz, $CDCl_3$) δ 8.39 (s, 1H), 8.32 (d, *J* = 8.2 Hz, 1H), 7.93 (d, *J* = 7.8 Hz, 1H), 7.62 (t, *J* = 7.9 Hz, 1H), 7.39 (d, *J* = 5.8 Hz, 8H), 7.16 (d, *J* = 7.2 Hz, 4H), 6.70 (d, *J* = 13.5 Hz, 1H), 5.94 (t, *J* = 12.1 Hz, 1H), 4.49 (s, 2H), 4.46 (s, 2H); **^{13}C NMR** (126 MHz, $CDCl_3$) δ 160.3, 159.0, 147.8, 139.8, 135.3, 133.6, 133.2, 129.5, 129.3, 129.1, 128.6, 127.9, 127.2, 125.2, 124.1, 120.7, 118.2, 113.6, 103.8, 60.1, 51.6, 30.9; **HRMS** (ESI) calcd. for $C_{26}H_{23}F_3N_3O_4S$ [M+H] 530.1361; found 530.1366.

***N*-((1*Z*,2*E*,4*E*)-5-(dibenzylamino)-1-(4-(trifluoromethyl)phenyl)penta-2,4-dien-1-ylidene)-1,1,1-trifluoromethanesulfonamide (S20b)**

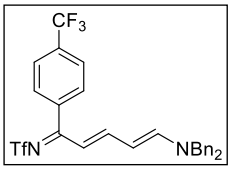

Red solid (0.14 mmol, 77 mg, 14%); **^{1}H NMR** (500 MHz, $CDCl_3$) δ 7.67 (d, *J* = 8.9 Hz, 4H), 7.38 (s, 8H), 7.15 (d, *J* = 6.0 Hz, 4H), 6.69 (d, J = 13.4 Hz, 1H), 5.88 (t, *J* = 12.4 Hz, 1H), 4.47 (s, 2H), 4.44 (s, 2H); **^{13}C NMR** (126 MHz, $CDCl_3$) δ 175.9, 160.2, 158.4, 141.5, 133.9, 133.4, 132.2, 129.9, 129.8, 129.7, 129.4, 129.3, 129.0, 128.6, 127.8, 127.2, 125.2, 125.2, 120.7, 114.2, 103.3, 59.9, 51.5, 50.0; **HRMS** (ESI) calcd. for $C_{27}H_{23}F_6N_2O_2S$ [M+H] 553.1384; found 553.1380.

***N*-((1*Z*,2*E*,4*E*)-5-(dibenzylamino)-1-(3,5-difluorophenyl)penta-2,4-dien-1-ylidene)-1,1,1-trifluoromethanesulfonamide (S21b)**

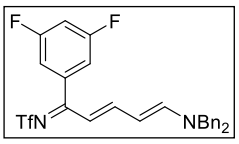

Red solid (0.44 mmol, 229 mg, 44%); **^{1}H NMR** (400 MHz, $CDCl_3$) δ 7.39 (q, *J* = 9.8, 8.2 Hz, 8H), 7.16 (s, 4H), 7.13 – 7.07 (m, 2H), 6.92 (tt, *J* = 8.7, 2.4 Hz, 1H), 6.64 (d, *J* = 13.6 Hz, 1H), 5.88 (t, *J* = 12.1 Hz, 1H), 4.49 (s, 2H), 4.45 (s, 2H); **^{13}C NMR** (101 MHz, $CDCl_3$) δ 174.3, 163.8, 163.7, 161.3, 161.2, 160.2, 158.7, 141.2, 141.1, 133.8, 133.3, 129.3, 129.0, 128.6, 127.9, 127.2, 124.2, 121.1, 117.9, 114.7, 113.4, 112.6, 112.6, 112.5, 112.4, 106.3, 106.0, 105.8, 103.4, 77.3, 77.0, 76.7, 60.0, 51.6; **HRMS** (ESI) calcd. for $C_{26}H_{22}F_5N_2O_2S$ [M+H] 521.1322; found 521.1326.

***N*-((1*E*,2*E*,4*E*)-5-(dibenzylamino)-1-(furan-2-yl)penta-2,4-dien-1-ylidene)-1,1,1-trifluoromethanesulfonamide (S22b)**[23]

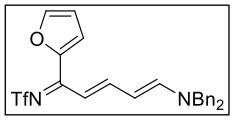

Yellow solid (0.68 mmol, 323 mg, 68%); **^{1}H NMR** (400 MHz, $CDCl_3$) δ 8.12 (t, *J* = 12.9 Hz, 1H), 7.67 – 7.56 (m, 2H), 7.46 – 7.30 (m, 7H), 7.19 (s, 4H), 6.65 (d, *J* = 13.6 Hz, 1H), 6.57 (dd, *J* = 3.7, 1.7 Hz, 1H), 5.95 (t, *J* = 12.1 Hz, 1H), 4.53 (s, 2H), 4.48 (s, 2H); **^{13}C NMR** (126 MHz, $CDCl_3$) δ

160.5, 158.9, 152.6, 146.7, 134.5, 133.9, 133.6, 133.5, 129.8, 128.9, 128.5, 127.9, 127.2, 121.2, 119.0, 118.3, 113.6, 111.8, 104.2, 60.0, 51.4.

***N*-((1*Z*,2*E*,4*E*)-5-(dibenzylamino)-1-(thiophen-2-yl)penta-2,4-dien-1-ylidene)-1,1,1-trifluoromethanesulfonamide (S23b)**

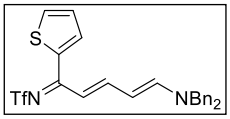

Orange solid (0.40 mmol, 196 mg, 40%); **^{1}H NMR** (400 MHz, $CDCl_3$) δ 7.94 – 7.77 (m, 1H), 7.71 – 7.46 (m, 3H), 7.39 (m, 6H), 7.14 (m, 5H), 6.66 (d, *J* = 13.6 Hz, 1H), 5.88 (t, J = 12.1 Hz, 1H), 4.49 (s, 2H), 4.45 (s, 2H); **^{13}C NMR** (101 MHz, $CDCl_3$) δ 167.3, 159.3, 158.6, 143.2, 134.1, 133.6, 132.8, 132.5, 129.2, 128.9, 128.4, 128.1, 128.0, 127.2, 124.6, 121.4, 118.2, 112.4, 103.5, 59.9, 51.5; **HRMS** (ESI) calcd. for $C_{24}H_{22}F_3N_2O_2S_2$ [M+H] 491.1075; found 491.1076.

***N*-((1*Z*,2*E*,4*E*)-1-(benzo[b]thiophen-2-yl)-5-(dibenzylamino)penta-2,4-dien-1-ylidene)-1,1,1-trifluoromethanesulfonamide (S24b)**

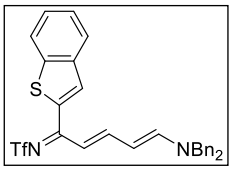

Orange solid (0.10 mmol, 54 mg, 10%); **^{1}H NMR** (600 MHz, $CDCl_3$) δ 7.94 – 7.89 (m, 1H), 7.88 (s, 1H), 7.83 (dd, J = 7.1, 4.9 Hz, 2H), 7.54 (d, J = 12.2 Hz, 1H), 7.44 – 7.35 (m, 8H), 7.18 (d, J = 7.1 Hz, 4H), 6.73 (d, J = 13.5 Hz, 1H), 5.95 (t, J = 12.1 Hz, 1H), 4.50 (s, 2H), 4.46 (s, 2H); **^{13}C NMR** (101 MHz, $CDCl_3$) δ 167.7, 159.3, 158.8, 143.1, 142.3, 139.3, 129.3, 129.2, 129.0, 128.5, 127.9, 127.3, 126.7, 125.2, 124.8, 122.5, 112.7, 103.8, 60.0, 51.5; **HRMS** (ESI) calcd. for $C_{28}H_{24}F_3N_2O_2S_2$ [M+H] 541.1231; found 541.1238.

***N*-((1*Z*,2*E*,4*E*)-1-(benzo[b]thiophen-3-yl)-5-(dibenzylamino)penta-2,4-dien-1-ylidene)-1,1,1-trifluoromethanesulfonamide (S25b)**

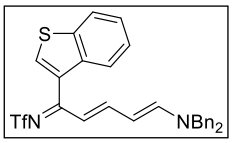

Orange solid (0.61 mmol, 330 mg, 61%); **^{1}H NMR** (500 MHz, $CDCl_3$) δ 8.13 (dd, *J* = 7.3, 1.4 Hz, 1H), 7.86 (d, *J* = 6.9 Hz, 1H), 7.76 (s, 1H), 7.45 – 7.33 (m, 9H), 7.24 (d, *J* = 12.3 Hz, 1H), 7.14 (s, 4H), 6.82 (d, *J* = 13.5 Hz, 1H), 5.83 (t, *J* = 12.2 Hz, 1H), 4.42 (s, 4H); **^{13}C NMR** (126 MHz, $CDCl_3$) δ 172.1, 159.0, 157.4, 140.0, 137.4, 134.2, 133.9, 133.7, 132.1, 129.2, 128.8, 128.4, 127.8, 127.2, 125.2, 125.0, 124.1, 122.4, 118.1, 115.8, 102.3, 59.7, 51.4; **HRMS** (ESI) calcd. for $C_{28}H_{24}F_3N_2O_2S_2$ [M+H] 541.1231; found 541.1238.

***tert*-butyl 2-((1*Z*,2*E*,4*E*)-5-(dibenzylamino)-1-(((trifluoromethyl)sulfonyl)imino)penta-2,4-dien-1-yl)-1H-pyrrole-1-carboxylate (S26b)**

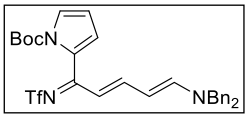

Orange solid (0.47 mmol, 270 mg, 47%); **^{1}H NMR** (500 MHz, $CDCl_3$) δ 7.43 – 7.31 (m, 8H), 7.28 – 7.23 (m, 1H), 7.15 (d, *J* = 7.0 Hz, 4H), 6.56 (d, *J* = 13.6 Hz, 1H), 6.49 (dd, *J* = 3.4, 1.7 Hz, 1H), 6.23 (t, *J* = 3.3 Hz, 1H), 5.75 (t, *J* = 12.2 Hz, 1H), 4.42 (s, 4H), 1.54 (s, 9H); **^{13}C NMR** (126 MHz, $CDCl_3$) δ 170.8, 157.8, 156.6, 148.2, 129.3, 129.2, 127.7, 127.2, 125.0, 120.6, 119.6, 117.1, 110.5, 101.9, 85.2, 30.9, 27.5; **HRMS** (ESI) calcd. for $C_{29}H_{30}F_3N_3O_4S$ [M+H] 574.1987; found 574.1985.

***tert*-butyl 2-((1*Z*,2*E*,4*E*)-5-(dibenzylamino)-1-(((trifluoromethyl)sulfonyl)imino)penta-2,4-dien-1-yl)-1H-indole-1-carboxylate (S27b)**

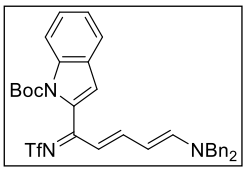

Orange solid (0.55 mmol, 343 mg, 55%); **^{1}H NMR** (400 MHz, $CDCl_3$) δ 8.19 (d, *J* = 7.4 Hz, 1H), 7.59 (d, *J* = 7.7 Hz, 1H), 7.42 – 7.31 (m, 8H), 7.30 – 7.21 (m, 2H), 7.14 (dd, *J* = 7.5, 2.0 Hz, 4H), 6.82 (s, 1H), 6.63 (d, *J* = 13.6 Hz, 1H), 5.78 (t, *J* = 12.2 Hz, 1H), 4.41 (s, 4H), 1.59 (s, 9H); **^{13}C NMR** (101 MHz, $CDCl_3$) δ 171.3, 157.0, 149.1, 137.3, 134.5, 129.2, 128.8, 128.2, 127.8, 127.2, 125.9, 123.2, 121.5, 116.8, 115.2, 113.8, 102.1, 85.1, 27.7; **HRMS** (ESI) calcd. for $C_{33}H_{33}F_3N_3O_4S$ [M+H] 624.2144; found 624.2142.

***N*-((2*E*,3*E*,5*E*)-6-(dibenzylamino)hexa-3,5-dien-2-ylidene)-1,1,1-trifluoromethanesulfonamide (S28b)**

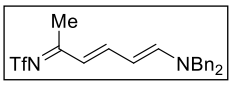

Yellow solid (0.32 mmol, 136 mg, 32%); **^{1}H NMR** (500 MHz, $CDCl_3$) δ 7.64 (s, 1H), 7.38 (d, *J* = 15.9 Hz, 7H), 7.17 (s, 4H), 6.10 (s, 1H), 5.67 (t, *J* = 12.2 Hz, 1H), 4.44 (s, 4H), 2.42 (s, 3H); **^{13}C NMR** (126 MHz, Chloroform-*d*) δ = 180.5, 156.8, 155.3, 129.2, 128.7, 128.4, 127.9, 127.2, 116.4, 101.3, 59.6, 51.4; **HRMS** (ESI) calcd. for $C_{21}H_{22}F_3N_2O_2S$ [M+H] 423.1354; found 423.1353.

***N*-((3*E*,4*E*,6*E*)-7-(dibenzylamino)hepta-4,6-dien-3-ylidene)-1,1,1-trifluoromethanesulfonamide (S29b)**

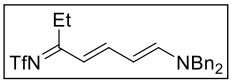

Yellow solid (0.60 mmol, 261 mg, 60%); **^{1}H NMR** (500 MHz, $CDCl_3$) δ 7.68 – 7.53 (m, 1H), 7.36 (d, *J* = 18.8 Hz, 7H), 7.17 (d, *J* = 7.9 Hz, 4H), 6.25 (d, *J* = 13.8 Hz, 1H), 5.68 (t, *J* = 12.1 Hz, 1H), 4.43 (s, 4H), 2.71 (q, *J* = 7.5 Hz, 2H), 1.23 (t, *J* = 7.5 Hz, 3H); **^{13}C NMR** (126 MHz, $CDCl_3$) δ 185.4, 156.9, 155.2, 129.7, 128.8, 128.3, 127.7, 121.1, 118.6, 115.0, 101.8, 60.0, 30.2, 13.1; **HRMS** (ESI) calcd. for $C_{22}H_{24}F_3N_2O_2S$ [M+H] 437.1511; found 437.1501.

***N*-((1*E*,3*E*,5*Z*)-1-(dibenzylamino)-6-oxoundeca-1,3-dien-5-ylidene)-1,1,1-trifluoromethanesulfonamide (S30b)**

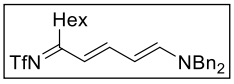

Yellow solid (0.58 mmol, 293 mg, 58%); **^{1}H NMR** (500 MHz, $CDCl_3$) δ 7.60 (t, *J* = 12.8 Hz, 1H), 7.36 (d, *J* = 12.4 Hz, 7H), 7.18 (s, 4H), 6.26 (d, *J* = 13.6 Hz, 1H), 5.67 (t, *J* = 12.1 Hz, 1H), 4.46 (s, 2H), 4.42 (s, 2H), 2.70 – 2.61 (m, 2H), 1.66 (p, *J* = 7.5 Hz, 2H), 1.36 (dt, *J* = 12.6, 7.0 Hz, 2H), 1.30 (d, *J* = 7.1 Hz, 2H), 0.88 (d, J = 13.8 Hz, 3H); **^{13}C NMR** (126 MHz, $CDCl_3$) δ 184.6, 157.0, 155.2, 129.7, 129.2, 128.8, 128.3, 127.7, 115.6, 101.9, 60.0, 51.8, 37.1, 32.0, 29.6, 29.1, 23.0, 14.5; **HRMS** (ESI) calcd. for $C_{26}H_{30}F_3N_2O_2S$ [M+H] 491.1982; found 491.1980.

***N*-((3*E*,4*E*,6*E*)-7-(dibenzylamino)-2-methylhepta-4,6-dien-3-ylidene)-1,1,1-trifluoromethanesulfonamide (S31b)**

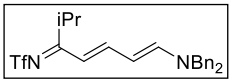

Yellow solid (0.47 mmol, 211 mg, 47%); **^{1}H NMR** (500 MHz, $CDCl_3$) δ 7.65 – 7.53 (m, 1H), 7.47 – 7.29 (m, 7H), 7.16 (s, 4H), 6.36 (d, *J* = 14.0 Hz, 1H), 5.70 (t, *J* = 12.1 Hz, 1H), 4.42 (s, 4H), 3.27 (p, *J* = 6.7 Hz, 1H), 1.18 (d, *J* = 6.6 Hz, 6H); **^{13}C NMR** (126 MHz, $CDCl_3$) δ 188.3, 156.4, 154.2, 134.9, 134.3, 129.4, 128.9, 128.6, 128.0, 127.4, 120.8, 118.3, 113.4, 101.7, 59.7, 51.6, 33.7, 21.6; **HRMS** (ESI) calcd. for $C_{23}H_{26}F_3N_2O_2S$ [M+H] 574.1987; found 574.1985.

***N*-((2*E*,3*E*,5*E*)-6-(dibenzylamino)-1-phenylhexa-3,5-dien-2-ylidene)-1,1,1-trifluoromethanesulfonamide (S32b)**

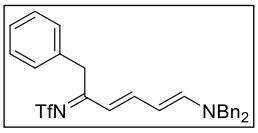

Yellow solid (0.42 mmol, 209 mg, 42%); **^{1}H NMR** (400 MHz, Chloroform-*d*) δ = 7.76 (d, *J*=12.6, 1H), 7.33 (d, *J*=23.0, 12H), 7.11 (s, 4H), 6.16 – 6.14 (m, 1H), 5.66 (t, *J*=12.2, 1H), 4.46 (s, 2H), 4.39 (s, 2H), 4.04 (s, 2H); **^{13}C NMR** (101 MHz, $CDCl_3$) δ 180.6, 157.5, 156.0, 136.7, 129.2, 129.0, 128.8, 128.6, 127.8, 127.2, 126.8, 121.0, 117.9, 114.7, 102.0, 67.0, 59.6, 51.3, 42.9; **HRMS** (ESI) calcd. for $C_{27}H_{26}F_3N_2O_2S$ [M+H] 499.1667; found 499.1670.

***N*-((2*Z*,3*E*,5*E*)-6-(dibenzylamino)-1-methoxy-1-phenylhexa-3,5-dien-2-ylidene)-1,1,1-trifluoromethanesulfonamide (S33b)**

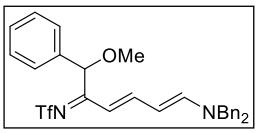

Yellow solid (0.23 mmol, 122 mg, 23%); **^{1}H NMR** (500 MHz, $CDCl_3$) δ 8.05 (dd, *J* = 13.7, 12.2 Hz, 1H), 7.53 – 7.48 (m, 2H), 7.42 (d, *J* = 12.3 Hz, 1H), 7.37 (d, *J* = 13.9 Hz, 6H), 7.33 (t, *J* = 7.5 Hz, 2H), 7.31 – 7.26 (m, 1H), 7.18 – 7.10 (m, 4H), 6.31 (d, *J* = 13.7 Hz, 1H), 5.75 (t, *J* = 12.2 Hz, 1H), 5.37 (s, 1H), 4.46 (s, 2H), 4.39 (s, 2H), 3.46 (s, 3H); **^{13}C NMR** (126 MHz, $CDCl_3$) δ 180.1, 158.5, 157.7, 138.5, 134.0, 133.5, 129.2, 128.9, 128.4, 128.0, 127.8, 127.2, 126.5, 111.0, 103.3, 85.4, 59.8, 57.5, 51.3; **HRMS** (ESI) calcd. for $C_{28}H_{228}F_3N_2O_3S$ [M+H] 529.1773; found 529.1782.

***N*-((1*Z*,2*E*,4*E*)-5-(dibenzylamino)-1-(2-(trifluoromethyl)phenyl)penta-2,4-dien-1-ylidene)-1,1,1-trifluoromethanesulfonamide (S34b)**

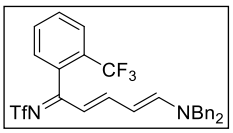

Yellow solid (0.53 mmol, 293 mg, 53%); **^{1}H NMR** (500 MHz, $CDCl_3$) δ 7.73 (d, *J* = 7.7 Hz, 1H), 7.57 (dt, *J* = 25.2, 7.2 Hz, 2H), 7.43 – 7.32 (m, 7H), 7.17 (s, 1H), 7.13 (d, *J* = 7.6 Hz, 4H), 6.75 (s, 2H), 5.81 (t, *J* = 11.8 Hz, 1H), 4.41 (s, 4H); **^{13}C NMR** (126 MHz, $CDCl_3$) δ 179.5, 159.1, 136.7, 136.1, 134.0, 132.6, 131.9, 131.5, 131.2, 130.4, 129.9, 129.2, 123.3, 120.7, 118.5, 105.2, 62.4, 54.0; **HRMS** (ESI) calcd. for $C_{27}H_{23}F_6N_2O_2S$ [M+H] 553.1384; found 553.1386.

***N*-((1*Z*,2*E*,4*E*)-5-(dibenzylamino)-1-(4-(dimethylamino)phenyl)penta-2,4-dien-1-ylidene)-1,1,1-trifluoromethanesulfonamide (S35b)**

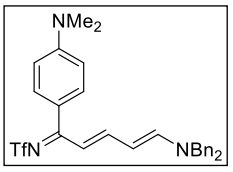

Red solid (0.20 mmol, 105 mg, 20%); **^{1}H NMR** (500 MHz, $CDCl_3$) δ 7.68 (d, *J* = 9.1 Hz, 2H), 7.50 (dd, *J* = 13.8, 11.8 Hz, 1H), 7.43 – 7.31 (m, 6H), 7.28 (d, *J* = 12.4 Hz, 1H), 7.16 (d, *J* = 6.5 Hz, 4H), 6.68 – 6.61 (m, 3H), 5.77 (t, *J* = 12.1 Hz, 1H), 4.41 (s, 4H), 3.06 (s, 6H); **^{13}C NMR** (126 MHz, $CDCl_3$) δ 179.3, 160.0, 158.5, 156.0, 135.1, 131.8, 131.0, 127.6, 123.8, 117.0, 113.5, 104.5, 42.7; **HRMS** (ESI) calcd. for $C_{27}H_{23}F_3N_3O_2S$ [M+H] 528.1933; found 528.1929.

(1*Z*,2*E*,4*E*)-5-(dibenzylamino)-*N*,*N*-diphenyl-*N*'-((trifluoromethyl)sulfonyl)penta-2,4-dienimidamide (S36b)

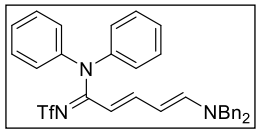

Yellow solid (0.11 mmol, 63 mg, 11%); **^{1}H NMR** (500 MHz, $CDCl_3$) δ 7.80 (dd, *J* = 14.1, 11.6 Hz, 1H), 7.38 – 7.27 (m, 12H), 7.25 – 7.20 (m, 5H), 7.13 (d, *J* = 7.2 Hz, 4H), 5.50 (d, *J* = 14.1 Hz, 1H), 5.38 (t, *J* = 12.1 Hz, 1H), 4.31 (s, 4H); **^{13}C NMR** (126 MHz, $CDCl_3$) δ 165.8, 154.6, 143.4, 129.3, 128.9, 127.5, 127.4, 107.8, 99.4; **HRMS** (ESI) calcd. for $C_{38}H_{31}F_3N_3O_2S$ [M+H] 576.1933; found 576.1926.

***N*-((1*E*,2*Z*,4*E*)-2-bromo-5-(dibenzylamino)-1-phenylpenta-2,4-dien-1-ylidene)-1,1,1-trifluoromethanesulfonamide (S37b)**[23]

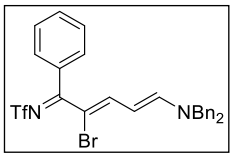

Yellow solid (0.30 mmol, 169 mg, 30%); **^{1}H NMR** (500 MHz, $CDCl_3$) δ 7.54 – 7.33 (m, 10H), 7.26 (s, 1H), 7.22 – 7.16 (m, 3H), 7.17 (s, 1H), 7.15 – 7.10 (m, 2H), 6.15 (t, *J* = 12.0 Hz, 1H), 4.46 (s, 2H), 4.42 (s, 2H); **^{13}C NMR** (126 MHz, $CDCl_3$) δ 176.4, 157.7, 156.7, 136.3, 133.9, 133.5, 130.5, 129.3, 129.2, 128.9, 128.6, 128.5, 128.2, 127.7, 127.6, 110.5, 103.2, 60.3, 59.7, 51.4, 21.0.

***N*-((1*E*,2*Z*,4*E*)-5-(dibenzylamino)-3-phenylpenta-2,4-dien-1-ylidene)-1,1,1-trifluoromethanesulfonamide (S38b)**[24]

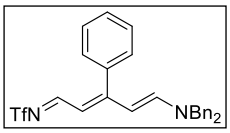

Yellow solid (0.10 mmol 48 mg, 10%); **^{1}H NMR** (400 MHz, $CDCl_3$) δ 8.00 (d, *J* = 11.2 Hz, 1H), 7.51 – 7.34 (m, 8H), 7.25 (s, 2H), 7.21 – 7.16 (m, 3H), 7.05 (s, 3H), 6.33 (d, *J* = 11.3 Hz, 1H), 5.96 (d, *J* = 12.6 Hz, 1H), 4.51 (s, 2H), 4.34 (s, 2H).

***N*-((1*E*,2*E*,4*E*)-5-(dibenzylamino)-2-phenylpenta-2,4-dien-1-ylidene)-1,1,1-trifluoromethanesulfonamide (S39b)**[1]

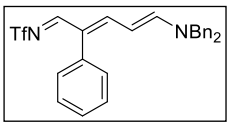

Yellow solid (0.80 mmol 387 mg, 80%); **^{1}H NMR** (400 MHz, $CDCl_3$) δ 8.39 (s, 1H), 7.52 (d, *J* = 12.2 Hz, 1H), 7.46 – 7.26 (m, 13H), 7.25 – 7.12 (m, 6H), 7.05 (s, 3H), 5.80 (t, *J* = 12.3 Hz, 1H), 4.53 (s, 3H), 4.30 (s, 3H).

***N*-((1*E*,2*E*,4*E*)-5-(dibenzylamino)penta-2,4-dien-1-ylidene)-1,1,1-trifluoromethanesulfonamide (S40b)**[24]

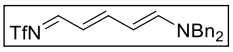

Yellow solid (0.50 mmol, 204 mg, 50%); **^{1}H NMR** (500 MHz, $CDCl_3$) δ 8.31 (d, *J* = 10.9 Hz, 1H), 7.54 (d, *J* = 12.2 Hz, 1H), 7.48 (d, *J* = 12.9 Hz, 1H), 7.46 – 7.34 (m, 6H), 7.18 (dd, *J* = 18.2, 7.2 Hz, 4H), 6.19 (dd, *J* = 13.4, 11.0 Hz, 1H), 5.87 (t, *J* = 12.2 Hz, 1H), 4.53 (s, 2H), 4.48 (s, 2H); **^{13}C NMR** (126 MHz, $CDCl_3$) δ 174.9, 165.8, 159.0, 133.7, 133.3, 129.3, 129.3, 129.0, 128.5, 128.1, 127.2, 121.1, 118.5, 115.8, 103.0, 59.9, 51.6.

***N*-((1*E*,2*E*,4*E*)-5-(dibenzylamino)-2-methylpenta-2,4-dien-1-ylidene)-1,1,1-trifluoromethanesulfonamide (S41b)**

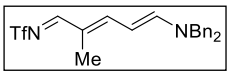

Yellow solid (0.60 mmol 253 mg, 60%); **^{1}H NMR** (500 MHz, $CDCl_3$) δ = 8.22 (s, 1H), 7.48 (d, *J* = 12.2, 1H), 7.39 (d, *J* = 11.3, 6H), 7.28 (d, *J* = 12.3, 1H), 7.19 (t, *J* = 8.4, 4H), 5.81 (t, *J* = 12.3, 1H), 4.53 (s, 2H), 4.49 (s, 2H), 1.86 (s, 3H); **^{13}C NMR** (126 MHz, $CDCl_3$) δ 175.4, 164.4, 157.8, 134.0, 133.6, 129.3, 129.2, 129.0, 128.5, 128.0, 127.3, 122.8, 121.1, 118.6, 100.1, 59.9, 51.7, 10.5; **HRMS** (ESI) calcd. for $C_{21}H_{22}F_3N_2O_3S$ [M+H] 423.1354; found 423.1356. **^{1}H NMR** (500 MHz, Chloroform-*d*) δ = 8.22 (s, 1H), 7.48 (d, *J*=12.2, 1H), 7.39 (d, *J*=11.3, 6H), 7.28 (d, *J*=12.3, 1H), 7.19 (t, *J*=8.4, 4H), 5.81 (t, *J*=12.3, 1H), 4.51 (d, *J*=17.9, 4H), 1.86 (s, 3H).

***N*-((1*Z*,2*E*,4*Z*)-5-(dibenzylamino)-1,4-diphenylpenta-2,4-dien-1-ylidene)-1,1,1-trifluoromethanesulfonamide (S42b)**

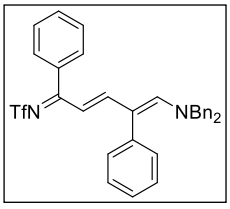

Yellow solid (0.18 mmol, 101 mg, 18%); **^{1}H NMR** (400 MHz, $CDCl_3$) δ 7.68 (d, *J* = 6.9 Hz, 2H), 7.61 (d, *J* = 11.3 Hz, 1H), 7.49 (t, *J* = 7.3 Hz, 4H), 7.33 (d, *J* = 17.5 Hz, 8H), 7.22 (s, 6H), 7.08 (m, 6H), 6.83 (d, *J* = 6.3 Hz, 1H), 6.48 (d, *J* = 6.1 Hz, 1H), 6.14 (s, 1H), 4.20 (s, 2H), 3.96 (s, 2H); **^{13}C NMR** (101 MHz, $CDCl_3$) δ 136.7, 136.5, 135.5, 134.7, 131.2, 130.3, 129.4, 129.4, 129.0, 128.8, 128.6, 128.4, 128.4, 128.3, 128.2, 128.1, 127.3, 127.1, 126.4, 121.3, 119.1, 113.5, 51.1, 30.8. **HRMS** (ESI) calcd. for $C_{32}H_{28}F_3N_2O_3S$ [M+H] 561.1824; found 561.1820.

methyl (1*Z*,2*E*,4*E*)-5-(dibenzylamino)-N-((trifluoromethyl)sulfonyl)penta-2,4-dienimidate (S43b)[25]

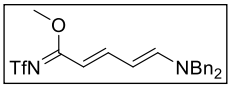

Yellow solid (0.29 mmol, 127 mg, 29%); **^{1}H NMR** (500 MHz, $CDCl_3$) δ 7.57 (dd, *J* = 14.0, 11.9 Hz, 1H), 7.42 – 7.30 (m, 6H), 7.17 (d, *J* = 3.1 Hz, 5H), 6.10 (d, *J* = 14.0 Hz, 1H), 5.57 (t, *J* = 12.2 Hz, 1H), 4.37 (s, 4H), 3.86 (s, 3H); **^{13}C NMR** (126 MHz, $CDCl_3$) δ 171.2, 154.5, 152.7, 129.1, 128.3, 127.4, 103.4, 99.4, 55.4; **HRMS** (ESI) calcd. for $C_{21}H_{21}F_3N_2O_3S$ [M+H] 461.1123; found 461.1122.

***N*-((1*Z*,2*Z*)-2-((*E*)-3-(dibenzylamino)allylidene)cyclohexylidene)-1,1,1-trifluoromethanesulfonamide (S44b)**[1]

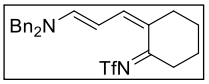

Yellow solid (0.48 mmol, 222 mg, 48%); **^{1}H NMR** (500 MHz, $CDCl_3$) δ 8.21 (d, *J* = 12.7 Hz, 1H), 7.52 (d, *J* = 12.1 Hz, 1H), 7.41 (s, 6H), 7.18 (s, 4H), 5.60 (d, *J* = 12.4 Hz, 1H), 4.50 (s, 2H), 4.45 (s, 2H), 3.01 (t, *J* = 6.2 Hz, 2H), 2.29 (d, *J* = 6.6 Hz, 2H), 1.78 – 1.59 (m, 4H); **^{13}C NMR** (126 MHz, $CDCl_3$) δ 182.1, 158.6, 152.5, 129.2, 128.8, 128.4, 127.9, 127.2, 120.2, 99.2, 59.9, 51.3, 34.2, 25.1, 22.0, 21.9.

***N*-((1*Z*,2*E*,4*E*)-5-(dibenzylamino)-1-(trimethylsilyl)penta-2,4-dien-1-ylidene)-1,1,1-trifluoromethanesulfonamide (S45b)**

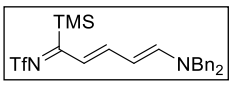

Yellow solid (0.56 mmol, 269 mg, 56%); **^{1}H NMR** (400 MHz, $CDCl_3$) δ 7.57 – 7.46 (m, 1H), 7.39 (s, 6H), 7.32 (d, *J* = 12.4 Hz, 1H), 7.18 (d, *J* = 7.4 Hz, 4H), 6.73 (d, *J* = 14.0 Hz, 1H), 5.73 (t, *J* = 12.1 Hz, 1H), 4.47 (s, 4H), 0.34 (s, 9H); **^{13}C NMR** (126 MHz, $CDCl_3$) δ 197.1, 156.8, 156.4, 129.2, 128.7, 128.3, 127.7, 127.2, 121.7, 120.0, 102.2, 60.2 51.2, 0.0; **HRMS** (ESI) calcd. for $C_{23}H_{28}F_3N_2O_2SSi$ [M+H] 481.1593; found 481.1594.

***N*-((1*Z*,2*E*,4*E*)-5-(dibenzylamino)-1-(1,3-dioxolan-2-yl)penta-2,4-dien-1-ylidene)-1,1,1-trifluoromethanesulfonamide (S46b)**[25]

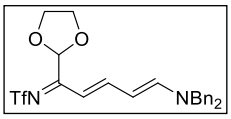

Yellow solid (0.14 mmol, 67 mg, 14%); **^{1}H NMR** (400 MHz, $CDCl_3$) δ 7.89 (t, *J* = 12.9 Hz, 1H), 7.55 – 7.34 (m, 7H), 7.14 (s, 4H), 6.35 (d, *J* = 13.8 Hz, 1H), 5.93 (s, 1H), 5.82 (t, *J* = 12.1 Hz, 1H), 4.51 (s, 2H), 4.46 (s, 2H), 4.20 – 3.96 (m, 4H).

***N*-((1*Z*,2*Z*)-2-((*E*)-3-(dibenzylamino)allylidene)cyclopentylidene)-1,1,1-trifluoromethanesulfonamide (S47b)**

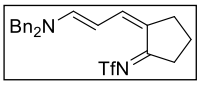

Yellow solid (0.40 mmol, 179 mg, 40%); **^{1}H NMR** (500 MHz, $CDCl_3$) δ 7.87 (d, *J* = 12.6 Hz, 1H), 7.47 (d, *J* = 12.2 Hz, 1H), 7.39 (s, 6H), 7.18 (d, *J* = 6.4 Hz, 4H), 5.51 (t, *J* = 12.4 Hz, 1H), 4.46 (s, 4H), 3.03 (t, *J* = 7.7 Hz, 2H), 2.48 – 2.37 (m, 2H), 1.94 (p, *J* = 7.6 Hz, 2H); **^{13}C NMR** (126 MHz, $CDCl_3$) δ 189.5, 157.8, 147.3, 134.3, 133.9, 129.2, 128.9, 128.3, 128.3, 127.9, 127.2, 125.7, 121.2, 118.6, 100.1, 59.7, 51.5, 37.1, 27.4, 21.7; **HRMS** (ESI) calcd. for $C_{23}H_{24}F_3N_2O_2S$ [M+H] 449.1511; found 449.1516.

***N*-((1*E*,2*Z*,4*E*)-2-bromo-5-(dibenzylamino)penta-2,4-dien-1-ylidene)-1,1,1-trifluoromethanesulfonamide (S48b)**[25]

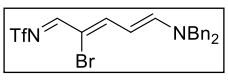

Red solid (0.45 mmol, 219 mg, 45%); **^{1}H NMR** (500 MHz, $CDCl_3$) δ 8.30 (s, 1H), 7.74 (s, 1H), 7.57 (d, *J* = 12.0 Hz, 1H), 7.48 – 7.35 (m, 6H), 7.22 (d, *J* = 7.1 Hz, 4H), 6.24 (t, *J* = 12.0 Hz, 1H), 4.59 (s, 2H), 4.57 (s, 2H); **^{13}C NMR** (126 MHz, $CDCl_3$) δ 169.6, 161.8, 160.3, 133.0, 132.8, 129.4, 129.4, 129.3, 128.9, 128.3, 127.6, 106.1, 103.8, 60.3, 52.2.

1,1,1-trifluoro-*N*-((1Z,2E,4E)-5-morpholino-1-phenylpenta-2,4-dien-1-ylidene)methanesulfonamide (S49b)[1]

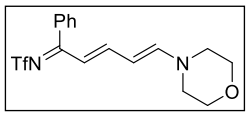

Red solid (0.30 mmol, 30%) **^{1}H NMR** (600 MHz, $CDCl_3$) δ 7.59 – 7.54 (m, 2H), 7.51 – 7.46 (m, 1H), 7.44 – 7.39 (m, 2H), 7.29 (dd, *J* = 13.7, 12.0 Hz, 1H), 6.96 (d, *J* = 12.2 Hz, 1H), 6.69 (d, *J* = 13.6 Hz, 1H), 5.69 (t, *J* = 12.2 Hz, 1H), 3.80 – 3.68 (m, 4H), 3.42 (t, J = 4.9 Hz, 4H).

***N*-((1Z,2E,4E)-5-(benzyl(phenyl)amino)-1-phenylpenta-2,4-dien-1-ylidene)-1,1,1-trifluoromethanesulfonamide (S50b)**[1]

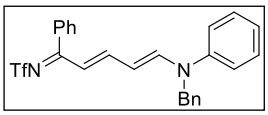

Red solid (0.70 mmol, 70%) **^{1}H NMR** (400 MHz, $CDCl_3$) δ 7.61 – 7.55 (m, 2H), 7.54 – 7.48 (m, 1H), 7.44 (dt, *J* = 7.9, 1.3 Hz, 2H), 7.37 (dddd, *J* = 13.6, 8.4, 6.5, 4.8 Hz, 6H), 7.27 – 7.23 (m, 3H), 7.22 – 7.18 (m, 2H), 7.18 – 7.12 (m, 2H), 6.70 (d, *J* = 13.9 Hz, 1H), 5.85 – 5.65 (m, 1H), 4.97 (d, *J* = 2.3 Hz, 2H).

3.3. Preparation of pyridinium salts

3.3.1. Preparation of *N*,4-dimethylbenzenesulfonohydrazide (from *N*-methylhydrazine)

To an ice-cold stirred solution of tosyl chloride (0.04 mol, 7.62 g) in THF (50 ml) *N*-methylhydrazine (4.4 ml, 0.08 mol) was added dropwise while the temperature was maintained between 0 and 5 ° C. After that, the mixture was stirred an additional 4 h. The solvent was evaporated under reduced pressure and 100 ml of cold water was added. The white solid was filtered, washed with water, and dried under high vacuum, producing the product as a white solid (26 mmol, 5.28 g, 66%).

3.3.2. Preparation of *N*,4-dimethylbenzenesulfonohydrazide (from *N*-methylhydrazine sulphate)

To an ice-cold stirred solution of tosyl chloride (0.04 mol, 7.62 g,) in THF/H_2O (50 ml + 50 ml) *N*- methylhydrazine sulphate (11.5 g, 0.08 mol) together with TEA (22.3 ml, 0.016 mol) were added while the temperature was maintained between 0 and 5 °C. After that, the mixture was stirred an additional 4 h. The solvent was evaporated under reduced pressure and 100 ml of cold water was added. The white solid was filtered, washed with water and dried under high vacuum, giving the product as a white solid (24.8 mmol, 4.96 g, 62%).

3.3.3. Preparation of *N*-Aminopirydinium salt (Py-salt)[2]

2,4,6-Trimethylpyrylium tetrafluoroborate (4.0 mmol, 1.0 equiv) was suspended in absolute EtOH (10 ml). Subsequently, *N*,4-dimethylbenzenesulfonohydrazide (4.8 mmol, 1.2 equiv) was added and the reaction mixture was stirred at room temperature for 16 h. After this time, Et_2O (20 ml) was added to the mixture. The resulting precipitate was filtered off, washed with Et_2O, and dried under vacuum. The crude salt was recrystallised from EtOH/Et_2O mixture to produce an off white solid (2.8 mmol, 1.08 g, 69% yield). **^{1}H NMR** (400 MHz, DMSO-d_6) δ 7.99 – 7.82 (m, 4H), 7.57 (d, J = 8.0 Hz, 2H), 3.57 (s, 3H), 2.47 – 2.58 (m, 12H).

3.4 Experiments with DMPO and TEMPO radical traps

3.4.1 DMPO radical trap

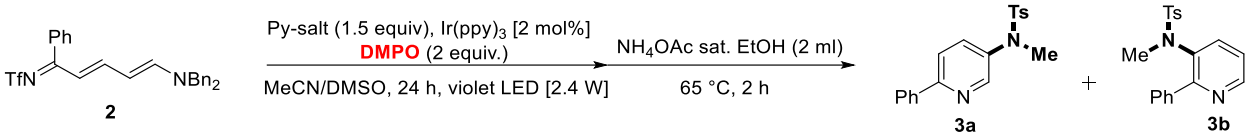

The reaction was set up following the general model reaction procedure (section 5.1) on a 0.05 mmol scale with the addition of DMPO (0.1 mmol, 2.0 equiv.) before irradiation. The reaction was irradiated for 24 hours and after that time, the crude reaction mixture was analysed by ESI MS.

The MS analysis of the crude reaction mixture revealed the presence of a peak at 297.13 m/z, corresponding to the DMPO amidyl radical adduct:

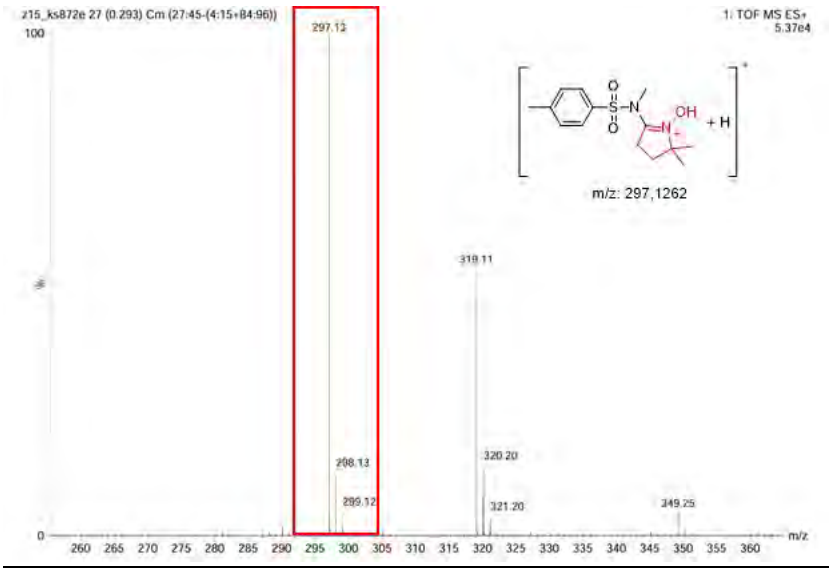

Conclusions No product formation was observed when DMPO was added prior irradiation. The result proves that the reaction is radical in nature. The presence of a peak in ESI MS spectra that corresponds to the adduct corroborates the formation of an amidyl radical.

3.4.2. TEMPO radical trap

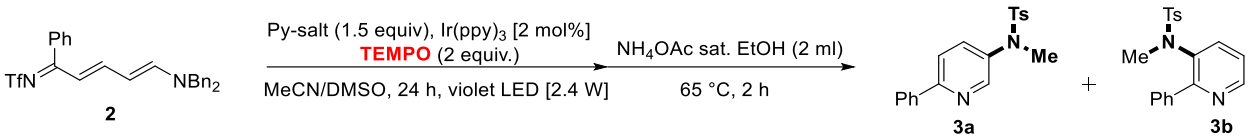

The reaction was set up following the general model reaction procedure (section 5.1) on a 0.05 mmol scale with the addition of TEMPO (0.1 mmol, 2.0 equiv.) before just irradiation or after 2 hours of irradiation of the reaction mixture. The irradiation in both experiments was maintained for 24 hours and after that time, crude reaction mixtures were analysed by ESI MS, TLC and ^{1}H NMR.

Conclusion: No product formation was observed when TEMPO was added prior to irradiation. TLC shows no conversion of the substrates and proves that the reaction is radical in nature. Furthermore, the crude ^{1}H NMR shows no conversion of the substrate.

4. Photocatalysed functionalization of Zincke imines

4.1. Isolation and characterization of reaction intermediate 2a/2b

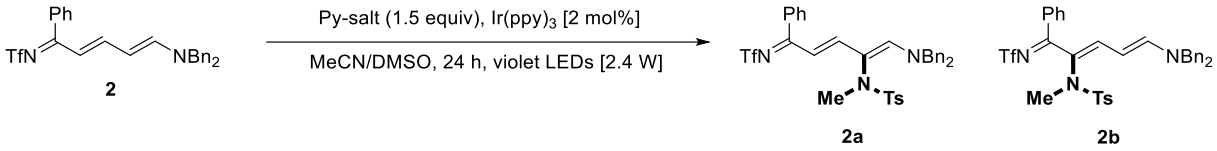

***N*-((1Z,3E,5Z)-1-(dibenzylamino)-5-phenyl-5-(((trifluoromethyl)sulfonyl)imino)penta-1,3-dien-2-yl)-*N*,4-dimethylbenzenesulfonamide (2c-*int*)**

(6 Reactions were set-up, each in 10 ml closed-cup vials) Zincke imine **2** (0.05 mmol), **Py-salt** (0.075 mmol), $Ir(ppy)_3$ (0.67 mg, ~10 μmol, 2 mol%) were placed in the closed-cup vial and MeCN (4 ml) and DMSO (4 ml) were added through the septum. The reaction mixture was placed in ultrasound bath and degassed by bubbling argon through the solution for 15 min. The vial was then placed in the photoreactor and irradiated with violet light (2.4 W) for 24 h, maintaining a temperature between 0 ° C and 5 °C. DMSO and excess of NH_4OAc were removed by extraction (AcOEt/ H_2O). The reaction mixtures were combined, and the organic phase was dried over anhydrous sodium sulphate and concentrated under reduced pressure. **2a** was isolated in a series of 2 chromatography in a mixture (80:10:10) as an orange-yellow amorphous solid; **^{1}H NMR** (500 MHz, $CDCl_3$) δ 7.77 (d, *J* = 7.9 Hz, 2H), 7.54 – 6.85 (m, 18H), 5.69 (s, 1H), 5.44 (s, 1H), 4.48 (d, *J* = 15.4 Hz, 4H), 2.86 (s, 3H), 2.35 (s, 3H); **^{13}C NMR** (126 MHz, $CDCl_3$) δ 178.0, 156.5, 156.1, 144.9, 137.5, 135.7, 134.9, 134.1, 131.5, 130.0, 129.3, 129.2, 128.6, 128.3, 127.5, 127.3, 126.9, 120.7, 118.1, 113.4, 111.3, 62.3, 51.7, 36.7, 30.9, 21.5; **HRMS** (ESI) calcd. for $C_{34}H_{33}N_3O_4S_2$ [M+H] 668.1865; found 668.1863. Single crystal was obtained by diffusing *n*-hexane to the solution of **2a** in HPLC grade DCM. The analytical sample (15 mg) of the isolated functionalized Zincke imine was subjected to a ring closure procedure with saturated NH_4OAc (1 ml) and heated up to 65 °C for 2 h yielding quantitatively (based on GC-FID) only a single isomer of closed, functionalized pyridines (without traces of parent pyridine (**1** or minor isomer **3b**).

4.2. General Protocol for photoamination and closure of the Zincke imine (General Procedure 3)

General Procedure 3. Zincke imine (0.05 mmol), **Py-salt** (0.075 mmol), $Ir(ppy)_3$ (0.67 mg, ~10 μmol, 2 mol%) were placed in the closed-cup vial and MeCN (4 ml) and DMSO (4 ml) were added through the septum. The reaction mixture was placed in ultrasound bath and degassed by bubbling argon through the solution for 15 min. The vial was then moved to the photoreactor and irradiated with violet light (2.4 W) for 24 h maintaining temperature between 0 °C to 5 °C with a dedicated cooling system. After the indicated time, a saturated NH_4OAc solution was added in anhydrous ethanol (2 ml) and reaction was heated up to 65 ° C for 2 h. DMSO and an excess of NH_4OAc were removed by extraction (AcOEt/ H_2O). The organic phase was dried over anhydrous sodium sulphate and evaporated with silica gel (dry load for the preparation of the sample for flash chromatography). The pure products were isolated by flash chromatography in the hexanes/AcOEt gradient.

Flash program: time: 25 min; column: silica 4 g; flow rate: 13 mL/min; automatic peak hold: on.

entry	time [min]	hexanes [%]	AcOEt [%]
1	0	95	5
2	25	75	25

Note:

- *Several products, especially minor regioisomers, were initially isolated by column or flash chromatography in a hexanes/AcOEt gradient, and due to some impurities from tailing N-methyltosylamide, further purification by semipreparative normal phase HPLC was necessary to obtain pure compounds.*

***N*,4-dimethyl-*N*-(6-phenylpyridin-3-yl)benzenesulfonamide (3a)**

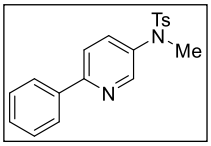

White solid (0.079 mmol, 26.6 mg, 79% yield); **^{1}H NMR** (600 MHz, $CDCl_3$) δ 8.33 (dd, *J* = 2.6, 0.8 Hz, 1H), 8.00 – 7.95 (m, 2H), 7.70 (dd, *J* = 8.5, 0.8 Hz, 1H), 7.62 (dd, *J* = 8.5, 2.6 Hz, 1H), 7.47 (t, *J* = 7.9 Hz, 4H), 7.44 – 7.40 (m, 1H), 7.27 (s, 2H), 3.23 (s, 3H), 2.42 (s, 3H); **^{13}C NMR** (151 MHz, $CDCl_3$) δ 155.9, 146.8, 144.2, 138.4, 136.9, 135.1, 133.2, 129.8, 129.3, 128.9, 127.9, 127.0, 120.2, 37.9, 21.6; **HRMS** (ESI) calcd. for $C_{19}H_{19}N_2O_2S$ [M+H] 339.1167; found 339.1174.

***N*,4-dimethyl-*N*-(2-phenylpyridin-3-yl)benzenesulfonamide (3b)**

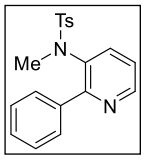

White solid (0.016 mmol, 5.5 mg, 16% yield); **^{1}H NMR** (500 MHz, $CDCl_3$) δ 8.64 (dd, *J* = 4.7, 1.6 Hz, 1H), 7.65 – 7.57 (m, 2H), 7.48 – 7.43 (m, 3H), 7.42 – 7.38 (m, 3H), 7.23 (d, *J* = 8.2 Hz, 3H), 3.04 (s, 3H), 2.43 (s, 3H); **^{13}C NMR** (126 MHz, $CDCl_3$) δ 158.9, 149.1, 144.0, 138.5, 136.2, 136.2, 135.2, 129.7, 128.9, 128.6, 128.3, 128.1, 122.7, 38.9, 21.6; **HRMS** (ESI) calcd. for $C_{19}H_{19}N_2O_2S$ [M+H] 339.1167; found 339.1162.

***N*,*N*'-(2-phenylpyridine-3,5-diyl)bis(N,4-dimethylbenzenesulfonamide) (3c)**

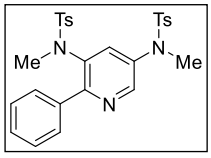

Off-white solid (side product – isolated by combining optimisation reaction mixtures); **^{1}H NMR** (600 MHz, $CDCl_3$) δ 8.27 (d, *J* = 2.4 Hz, 1H), 7.67 (dd, *J* = 6.8, 2.9 Hz, 2H), 7.49 (t, *J* = 8.1 Hz, 4H), 7.44 – 7.41 (m, 3H), 7.36 (d, *J* = 2.4 Hz, 1H), 7.30 (s, 2H), 7.28 – 7.24 (m, 2H), 3.17 (s, 3H), 2.98 (s, 3H), 2.44 (s, 3H), 2.43 (s, 3H); **^{13}C NMR** (151 MHz, $CDCl_3$) δ 157.0, 145.7, 144.5,

144.2, 137.7, 137.2, 136.0, 135.2, 134.2, 132.9, 129.9, 129.9, 129.0, 128.9, 128.4, 128.1, 127.9, 38.6, 37.8, 21.7; **HRMS** (ESI) calcd. for $C_{27}H_{28}N_3O_4S_2$ [M+H] 522.1521; found 522.1520.

***N*-(6-(4-methoxyphenyl)pyridin-3-yl)-*N*,4-dimethylbenzenesulfonamide (4a)**

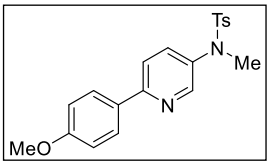

Purified by semi-preparative HPLC in hexanes/AcOEt gradient; white solid (0.071 mmol, 24.0 mg, 71% yield); **^{1}H NMR** (600 MHz, $CDCl_3$) δ 8.27 (d, *J* = 2.5 Hz, 1H), 7.96 – 7.91 (m, 2H), 7.64 (d, *J* = 8.5 Hz, 1H), 7.58 (dd, *J* = 8.5, 2.6 Hz, 1H), 7.47 (d, *J* = 8.2 Hz, 2H), 7.27 (d, *J* = 7.3 Hz, 2H), 7.02 – 6.97 (m, 2H), 3.87 (s, 3H), 3.22 (s, 3H), 2.42 (s, 3H); **^{13}C NMR** (151 MHz, $CDCl_3$) δ 160.6, 155.5, 146.6, 143.9, 136.1, 135.0, 133.1, 130.9, 129.6, 128.2, 127.7, 119.3, 114.1, 55.3, 37.8, 21.5; **HRMS** (ESI) calcd. for $C_{20}H_{21}N_2O_3S$ [M+H] 369.1273; found 369.1278.

***N*-(2-(4-methoxyphenyl)pyridin-3-yl)-N,4-dimethylbenzenesulfonamide (4b)**

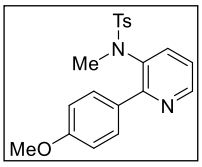

Purified by semi-preparative HPLC in hexanes/ AcOEt gradient; white solid (0.019 mmol, 6.5 mg, 19% yield); **^{1}H NMR** (500 MHz, $CDCl_3$) δ 8.62 (dd, *J* = 4.7, 1.6 Hz, 1H), 7.63 (d, *J* = 8.8 Hz, 2H), 7.51 (d, *J* = 8.3 Hz, 2H), 7.37 (dd, *J* = 8.0, 1.6 Hz, 1H), 7.25 (2H), 7.20 – 7.15 (m, 1H), 6.93 (d, *J* = 8.8 Hz, 2H), 3.86 (s, 3H), 3.06 (s, 3H), 2.44 (s, 3H); **^{13}C NMR** (126 MHz, $CDCl_3$) δ 159.9, 158.2, 148.9, 143.8, 136.0, 135.8, 135.3, 130.7, 130.2, 129.5, 127.9, 122.0, 113.6, 55.2, 38.7, 21.5.

***N*-(6-(3-methoxyphenyl)pyridin-3-yl)-*N*,4-dimethylbenzenesulfonamide (5a)**

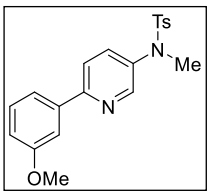

Purified by semi-preparative HPLC in hexanes/AcOEt gradient; white solid (0.060 mmol, 20.5 mg, 60% yield, ~5% MeNHTs); **^{1}H NMR** (500 MHz, $CDCl_3$) δ 8.33 (d, *J* = 1.9 Hz, 1H), 7.69 (d, *J* = 7.7 Hz, 1H), 7.61 (dd, *J* = 8.5, 2.6 Hz, 1H), 7.56 (d, *J* = 2.6 Hz, 1H), 7.52 (d, *J* = 8.2 Hz, 1H), 7.46 (d, *J* = 8.4 Hz, 2H), 7.38 (t, *J* = 7.9 Hz, 1H), 7.27 (d, *J* = 7.5 Hz, 2H), 6.97 (dd, *J* = 8.2, 2.6 Hz, 1H), 3.89 (s, 3H), 3.23 (s, 3H), 2.42 (s, 3H); **^{13}C NMR** (126 MHz, $CDCl_3$) δ 160.1, 155.5, 146.6, 144.0, 139.8, 136.9, 134.9, 133.0, 129.8, 129.7, 129.6, 127.7, 127.2, 120.3, 119.2, 115.3, 112.0, 55.3, 37.7, 21.5; **HRMS** (ESI) calcd. for $C_{20}H_{21}N_2O_3S$ [M+H] 369.1273; found 369.1271.

***N*-(2-(3-methoxyphenyl)pyridin-3-yl)-*N*,4-dimethylbenzenesulfonamide (5b)**

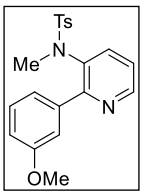

Purified by semi-preparative HPLC in hexanes/AcOEt gradient; white solid (0.021 mmol 7.1 mg, 21% yield); **^{1}H NMR** (500 MHz, $CDCl_3$) δ 8.64 (dd, *J* = 4.7, 1.6 Hz, 1H), 7.50 (d, *J* = 8.3 Hz, 2H), 7.46 – 7.42 (m, 1H), 7.30 (t, *J* = 7.9 Hz, 1H), 7.27 – 7.21 (m, 4H), 7.18 (d, *J* = 7.6 Hz, 1H), 6.96 (dd, *J* = 7.2, 2.7 Hz, 1H), 3.85 (s, 3H), 3.04 (s, 3H), 2.44 (s, 3H); **^{13}C NMR** (126 MHz, $CDCl_3$) δ 159.4, 158.5, 148.9, 143.8, 139.5, 136.1, 136.1, 135.4, 129.6, 129.1, 127.8, 122.6, 121.2, 114.9, 113.9, 55.3, 38.7, 21.5.

***N*-(6-(3,5-dimethoxyphenyl)pyridin-3-yl)-*N*,4-dimethylbenzenesulfonamide (6a)**

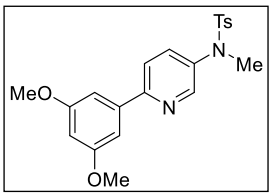

Purified by semi-preparative HPLC in hexanes/AcOEt gradient; off-white oil (0.069 mmol, 23.4 mg, 69% yield); **^{1}H NMR** (500 MHz, $CDCl_3$) δ 8.33 (d, *J* = 2.6 Hz, 1H), 7.67 (d, *J* = 8.6 Hz, 1H), 7.60 (dd, *J* = 8.5, 2.6 Hz, 1H), 7.46 (d, *J* = 8.3 Hz, 2H), 7.30 – 7.23 (m, 2H), 7.13 (d, *J* = 2.3 Hz, 2H), 6.54 (t, *J* = 2.3 Hz, 1H), 3.86 (s, 6H), 3.22 (s, 3H), 2.42 (s, 3H); **^{13}C NMR** (126 MHz, $CDCl_3$) δ 161.1, 155.4, 146.5, 144.0, 140.4, 137.0, 134.8, 133.0, 129.6, 127.7, 120.3, 104.9, 101.5, 55.5, 37.7, 21.0; **HRMS** (ESI) calcd. for $C_{21}H_{23}N_2O_4S$ [M+H]: 399.1379; found 399.1376.

***N*-(2-(3,5-dimethoxyphenyl)pyridin-3-yl)-*N*,4-dimethylbenzenesulfonamide (6b)**

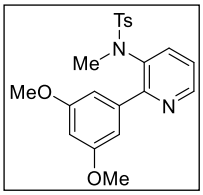

Purified by semi-preparative HPLC in hexanes/AcOEt gradient; off-white oil (0.021 mmol, 7.3 mg, 21% yield); **^{1}H NMR** (500 MHz, $CDCl_3$) δ 8.63 (dd, *J* = 4.7, 1.6 Hz, 1H), 7.54 (d, *J* = 8.3 Hz, 2H), 7.45 – 7.40 (m, 1H), 7.29 – 7.21 (m, 3H), 6.85 (d, *J* = 2.3 Hz, 2H), 6.52 (t, *J* = 2.3 Hz, 1H), 3.83 (s, 6H), 3.03 (s, 3H), 2.44 (s, 3H); **^{13}C NMR** (126 MHz, $CDCl_3$) δ 160.5, 158.4, 148.8, 143.8, 140.0, 136.1, 135.7, 129.6, 127.8, 122.7, 106.9, 101.4, 55.4, 38.8, 21.5.

***N*-(6-(2,6-dimethoxyphenyl)pyridin-3-yl)-*N*,4-dimethylbenzenesulfonamide (7a)**

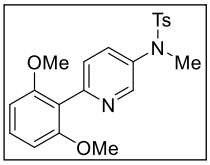

The ring closure reaction was performed in the microwave reactor (100 °C). Off-white solid (0.026 mmol, 8.9 mg, 26% yield); **^{1}H NMR** (400 MHz, $CDCl_3$) δ 8.29 (d, *J* = 1.9 Hz, 1H), 7.61 (dd, *J* = 8.4, 2.7 Hz, 1H), 7.49 (d, *J* = 8.3 Hz, 2H), 7.35 – 7.23 (m, 4H), 6.64 (d, *J* = 8.4 Hz, 2H), 3.73 (s, 6H), 3.23 (s, 3H), 2.41 (s, 3H); **^{13}C NMR** (126 MHz, $CDCl_3$) δ 158.0, 153.1, 146.1, 143.9, 136.2, 134.3, 133.2, 129.9, 129.5, 127.8, 126.2, 118.1, 104.1, 55.9, 37.8, 21.5; **HRMS** (ESI) calcd. for $C_{21}H_{23}N_2O_4S$ [M+H]: 399.1379; found 399.1381.

***N*,4-dimethyl-*N*-(6-(2-(methylthio)phenyl)pyridin-3-yl)benzenesulfonamide (8a)**

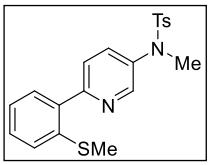

White solid (0.088 mmol, 30.2 mg, 88% yield); **^{1}H NMR** (600 MHz, $CDCl_3$) δ 8.30 (d, *J* = 2.0 Hz, 1H), 7.64 (dd, *J* = 8.4, 2.6 Hz, 1H), 7.55 (d, *J* = 8.4 Hz, 1H), 7.49 – 7.42 (m, 3H), 7.40 – 7.35 (m, 1H), 7.35 – 7.31 (m, 1H), 7.28 – 7.21 (m, 3H), 3.23 (s, 3H), 2.41 (s, 3H), 2.39 (s, 3H); **^{13}C NMR** (151 MHz, $CDCl_3$) δ 156.7, 145.9, 144.0, 138.5, 137.4, 136.7, 134.5, 133.0, 129.9, 129.6, 129.1, 127.7, 126.0, 124.9, 123.9, 37.8, 21.5, 16.4; **HRMS** (ESI) calcd. for $C_{20}H_{21}N_2O_2S_2$ [M+H]: 385.1044; found 385.1048.

***N*-(6-(4-(9H-carbazol-9-yl)phenyl)pyridin-3-yl)-*N*,4-dimethylbenzenesulfonamide (9a)**

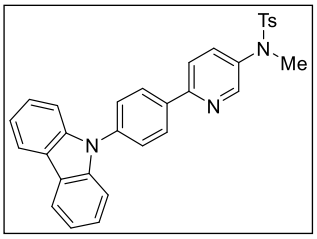

White solid (0.065 mmol, 32.7 mg, 65% yield); **^{1}H NMR** (400 MHz, $CDCl_3$) δ 8.40 (d, *J* = 2.6 Hz, 1H), 8.23 (d, *J* = 8.5 Hz, 2H), 8.16 (d, *J* = 7.8 Hz, 2H), 7.81 (d, *J* = 8.6 Hz, 1H), 7.70 (d, *J* = 8.5 Hz, 3H), 7.53 – 7.46 (m, 4H), 7.46 – 7.41 (m, 2H), 7.35 – 7.27 (m, 4H), 3.27 (s, 3H), 2.44 (s, 3H); **^{13}C NMR** (101 MHz, $CDCl_3$) δ 154.8, 146.9, 144.1, 140.7, 138.7, 137.3, 137.1, 135.0, 133.2, 129.7, 128.4, 127.8, 127.2, 126.0, 123.5, 120.3, 120.1, 120.1, 109.8, 37.8, 21.5; **HRMS** (ESI) calcd. for $C_{31}H_{26}N_3O_2S$ [M+H]: 504.1746; found 504.1749.

***N*-(2-(4-(9H-carbazol-9-yl)phenyl)pyridin-3-yl)-*N*,4-dimethylbenzenesulfonamide (9b)**

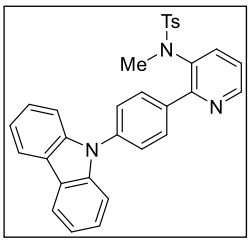

White solid (0.015 mmol, 7.6 mg, 15% yield); **^{1}H NMR** (400 MHz, $CDCl_3$) δ 8.71 (dd, *J* = 4.7, 1.6 Hz, 1H), 8.17 (d, *J* = 7.7 Hz, 2H), 7.90 (d, *J* = 8.4 Hz, 2H), 7.64 (d, *J* = 8.4 Hz, 2H), 7.59 – 7.49 (m, 5H), 7.48 – 7.41 (m, 2H), 7.37 – 7.27 (m, 5H), 3.17 (s, 3H), 2.41 (s, 3H); **^{13}C NMR** (101 MHz, $CDCl_3$) δ 149.1, 144.1, 140.7, 138.0, 137.4, 136.3, 130.5, 129.7, 128.1, 126.4, 126.0, 123.5, 122.9, 120.3, 120.1, 109.9, 38.9, 21.5; **HRMS** (ESI) calcd. for $C_{31}H_{26}N_3O_2S$ [M+H]: 504.1746; found 504.1750.

***N*,4-dimethyl-*N*-(6-(o-tolyl)pyridin-3-yl)benzenesulfonamide (10a)**

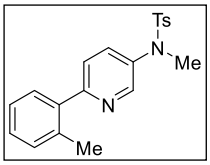

White solid (0.036 mmol, 12.8 mg, 36% yield); **^{1}H NMR** (500 MHz, CDCl3) δ 8.30 (d, *J* = 2.6 Hz, 1H), 7.63 (dd, *J* = 8.4, 2.7 Hz, 1H), 7.48 (d, *J* = 8.3 Hz, 2H), 7.42 – 7.37 (m, 2H), 7.34 – 7.23 (m, 5H), 3.24 (s, 3H), 2.42 (s, 3H), 2.37 (s, 3H); **^{13}C NMR** (126 MHz, $CDCl_3$) δ 158.5, 146.2, 144.1, 139.3, 136.4, 135.7, 134.5, 133.1, 130.8, 129.6, 129.6, 128.5, 127.7, 125.9, 123.8, 37.8, 21.5, 20.3; **HRMS** (ESI) calcd. for $C_{20}H_{21}N_2O_2S$ [M+H] 353.1324; found 353.1321.

***N*-(6-(2,4-dimethylphenyl)pyridin-3-yl)-*N*,4-dimethylbenzenesulfonamide (11a)**

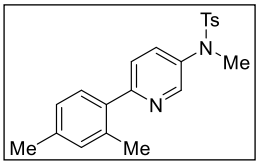

White solid (0.060 mmol, 22.0 mg, 60% yield); **^{1}H NMR** (500 MHz, $CDCl_3$) δ 8.29 (d, *J* = 2.6 Hz, 1H), 7.62 (dd, *J* = 8.4, 2.7 Hz, 1H), 7.48 (d, *J* = 8.4 Hz, 2H), 7.37 (d, *J* = 8.4 Hz, 1H), 7.33 – 7.25 (m, 3H), 7.09 (d, *J* = 8.8 Hz, 2H), 3.24 (s, 3H), 2.42 (s, 3H), 2.37 (s, 3H), 2.34 (s, 3H); **^{13}C NMR** (126 MHz, $CDCl_3$) δ 158.5, 146.2, 144.0, 138.3, 136.5, 136.1, 135.6, 134.5, 133.1, 131.6, 129.6, 127.7, 126.6, 123.8, 37.8, 21.5, 21.1, 20.3; **HRMS** (ESI) calcd. for $C_{21}H_{23}N_2O_2S$ [M+H] 367.1480; found 367.1483.

***N*-(6-(3,5-di-tert-butylphenyl)pyridin-3-yl)-*N*,4-dimethylbenzenesulfonamide (12a)**

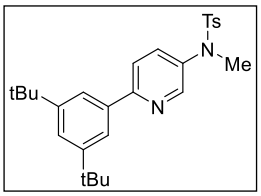

Purified by semi-preparative HPLC in hexanes/AcOEt gradient; pale yellow oil (0.054 mmol, 24.4 mg, 54% yield); **^{1}H NMR** (500 MHz, $CDCl_3$) δ 8.31 (d, *J* = 1.9 Hz, 1H), 7.79 (d, *J* = 1.8 Hz, 2H), 7.70 (d, J = 8.6 Hz, 1H), 7.63 (dd, *J* = 8.5, 2.6 Hz, 1H), 7.51 (t, *J* = 1.8 Hz, 1H), 7.47 (d, *J* = 8.3 Hz, 2H), 7.27 (d, *J* = 6.5 Hz, 2H), 3.23 (s, 3H), 2.42 (s, 3H), 1.39 (s, 18H); **^{13}C NMR** (126 MHz, $CDCl_3$) δ 157.0, 151.2, 146.5, 143.9, 137.8, 136.5, 135.0, 133.1, 129.6, 127.8, 123.5, 121.3, 120.5, 37.8, 35.0, 31.4, 21.5. **HRMS** (ESI) calcd. for $C_{27}H_{35}N_2O_2S$ [M+H] 451.2419; found 451.2415.

***N*-(2-(3,5-di-tert-butylphenyl)pyridin-3-yl)-*N*,4-dimethylbenzenesulfonamide (12b)**

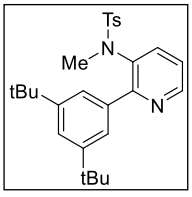

Purified by semi-preparative HPLC in hexanes/ AcOEt gradient; pale yellow oil (0.017 mmol, 7.6 mg, 17% yield); **^{1}H NMR** (500 MHz, $CDCl_3$) δ 8.66 (dd, *J* = 4.7, 1.6 Hz, 1H), 7.52 – 7.46 (m, 4H), 7.34 (d, *J* = 8.4 Hz, 2H), 7.23 (dd, *J* = 8.0, 4.7 Hz, 1H), 7.17 (d, *J* = 8.0 Hz, 2H), 3.03 (s, 3H), 2.40 (s, 3H), 1.34 (s, 18H); **^{13}C NMR** (126 MHz, $CDCl_3$) δ 160.3, 150.4, 148.9, 143.4, 137.5, 136.1, 136.0, 135.8, 129.5, 127.8, 123.1, 122.5, 122.3, 38.6, 34.9, 31.4, 21.5.

***N*-(6-([1,1'-biphenyl]-2-yl)pyridin-3-yl)-*N*,4-dimethylbenzenesulfonamide (13a)**

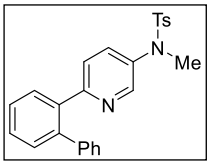

Purified by semi-preparative HPLC in hexanes/AcOEt gradient; white oil (0.040 mmol, 16.6 mg, 40% yield +~25% MeNHTs); ^{1}H NMR (500 MHz, $CDCl_3$) δ 8.27 (d, J = 2.7 Hz, 1H), 7.70 – 7.64 (m, 1H), 7.49 – 7.40 (m, 3H), 7.36 (d, *J* = 8.3 Hz, 2H), 7.27 – 7.21 (m, 5H), 7.18 (dd, *J* = 8.5, 2.6 Hz, 1H), 7.16 – 7.11 (m, 2H), 6.84 (d, *J* = 8.4 Hz, 1H), 3.14 (s, 3H), 2.40 (s, 3H); **^{13}C NMR** (126 MHz, $CDCl_3$) δ 157.8, 146.7, 144.0, 141.2, 140.6, 138.5, 136.0, 133.1, 132.8, 130.5, 130.3, 129.6, 129.6, 129.5, 128.7, 128.0, 127.7, 127.6, 127.2, 126.8, 125.0, 37.7, 21.5; **HRMS** (ESI) calcd. for $C_{25}H_{23}N_2O_2S$ [M+H]: 415.1480; found 415.1484.

***N*-(6-([1,1'-biphenyl]-3-yl)pyridin-3-yl)-*N*,4-dimethylbenzenesulfonamide (14a)**

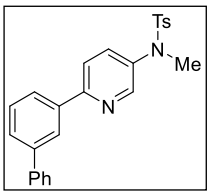

Purified by semi-preparative HPLC in hexanes/ AcOEt gradient; white solid (0.065 mmol, 26.9 mg, 65% yield); **^{1}H NMR** (500 MHz, $CDCl_3$) δ 8.34 (d, *J* = 2.6 Hz, 1H), 8.22 (s, 1H), 7.94 (d, *J* = 7.6 Hz, 1H), 7.77 (d, *J* = 8.6 Hz, 1H), 7.66 (t, *J* = 6.4 Hz, 4H), 7.55 (t, *J* = 7.7 Hz, 1H), 7.50 – 7.44 (m, 4H), 7.37 (t, *J* = 7.3 Hz, 1H), 7.27 (d, *J* = 8.0 Hz, 2H), 3.24 (s, 3H), 2.42 (s, 3H); **^{13}C NMR** (126 MHz, $CDCl_3$) δ 155.6, 146.7, 144.0, 141.8, 140.9, 138.8, 136.9, 135.0, 133.0, 129.6, 129.2, 128.8, 128.7, 128.0, 127.7, 127.4, 127.2, 125.8, 125.7, 120.2, 37.8, 21.5. **HRMS** (ESI) calcd. for $C_{25}H_{23}N_2O_2S$ [M+H]: 415.1480; found 415.1479.

***N*-(2-([1,1'-biphenyl]-3-yl)pyridin-3-yl)-*N*,4-dimethylbenzenesulfonamide (14b)**

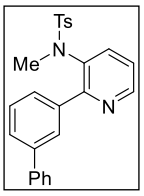

Purified by semi-preparative HPLC in hexanes/AcOEt gradient; white solid (0.018 mmol, 7.5 mg, 18% yield); **^{1}H NMR** (500 MHz, $CDCl_3$) δ 8.69 – 8.65 (m, 1H), 7.85 (s, 1H), 7.67 – 7.58 (m, 4H), 7.56 – 7.51 (m, 1H), 7.51 – 7.40 (m, 5H), 7.34 (t, *J* = 7.2 Hz, 1H), 7.27 (d, *J* = 13.6 Hz, 1H), 7.15 (d, *J* = 8.0 Hz, 2H), 3.09 (s, 3H), 2.34 (s, 3H); **^{13}C NMR** (126 MHz, $CDCl_3$) δ 158.7, 149.0, 143.8, 141.0, 140.9, 138.7, 136.3, 136.1, 135.0, 129.5, 128.7, 128.6, 127.9, 127.8, 127.7, 127.2, 127.2, 122.7, 38.8, 21.4.

***N*-(6-([1,1'-biphenyl]-4-yl)pyridin-3-yl)-*N*,4-dimethylbenzenesulfonamide (15a)**

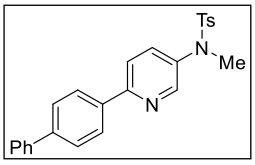

Purified by semi-preparative HPLC in hexanes/AcOEt gradient; white solid (0.061 mmol, 25.3 mg, 61% yield); **^{1}H NMR** (500 MHz, $CDCl_3$) δ 8.34 (d, *J* = 2.7 Hz, 1H), 8.06 (d, *J* = 8.4 Hz, 2H), 7.75 (d, *J* = 8.5 Hz, 1H), 7.72 (d, *J* = 8.5 Hz, 2H), 7.68 – 7.63 (m, 3H), 7.47 (t, *J* = 8.6 Hz, 4H), 7.38 (d, *J* = 8.7 Hz, 1H), 7.28 (d, *J* = 8.0 Hz, 2H), 3.22 (s, 3H), 2.42 (s, 3H); **^{13}C NMR** (126 MHz, $CDCl_3$) δ 155.3, 146.7, 144.0, 142.0, 140.4, 137.2, 136.8, 135.0, 133.0, 129.6, 128.8, 127.7, 127.6, 127.5, 127.2, 127.0, 120.0, 37.8, 30.9; **HRMS** (ESI) calcd. for $C_{25}H_{23}N_2O_2S$ [M+H]: 415.1480; found 415.1482.

***N*-(2-([1,1'-biphenyl]-4-yl)pyridin-3-yl)-*N*,4-dimethylbenzenesulfonamide (15b)**

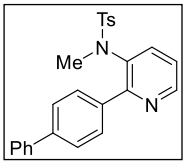

Purified by semi-preparative HPLC in hexanes/AcOEt gradient; white solid (0.019 mmol, 7.9 mg, 19% yield); **^{1}H NMR** (500 MHz, $CDCl_3$) δ 8.67 (dd, *J* = 4.7, 1.6 Hz, 1H), 7.72 (d, *J* = 8.4 Hz, 2H), 7.65 (dd, *J* = 12.8, 7.7 Hz, 4H), 7.51 – 7.44 (m, 5H), 7.41 – 7.31 (m, 1H), 7.25 – 7.20 (m, 3H), 3.11 (s, 3H), 2.41 (s, 3H); **^{13}C NMR** (126 MHz, $CDCl_3$) δ 158.3, 149.0, 143.8, 141.2, 140.7, 137.3, 136.2, 136.1, 135.1, 129.5, 129.3, 128.8, 127.9, 127.4, 127.1, 126.8, 122.6, 38.8, 21.5; **HRMS** (ESI) calcd. for $C_{25}H_{23}N_2O_2S$ [M+H]: 415.1480; found 415.1484.

_N_,4-dimethyl-_N_-(6-(naphthalen-2-yl)pyridin-3-yl)benzenesulfonamide (16a)

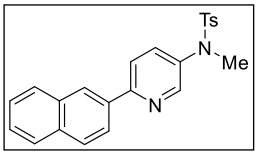

Off-white solid (0.047 mmol, 18.1 mg, 47% yield); **^{1}H NMR** (500 MHz, $CDCl_3$) δ 8.45 (s, 1H), 8.37 (d, *J* = 2.7 Hz, 1H), 8.10 (dd, *J* = 8.6, 1.8 Hz, 1H), 7.94 (d, *J* = 8.8 Hz, 2H), 7.90 – 7.84 (m, 2H), 7.70 – 7.66 (m, 1H), 7.52 (dt, J = 6.3, 3.4 Hz, 2H), 7.49 (d, *J* = 8.3 Hz, 2H), 7.28 (d, *J* = 9.3 Hz, 2H), 3.25 (s, 3H), 2.42 (s, 3H); **^{13}C NMR** (126 MHz, $CDCl_3$) δ 155.9, 147.0, 144.3, 137.1, 135.8, 135.4, 133.9, 133.7, 133.3, 129.9, 128.9, 128.8, 128.0, 127.9, 127.0, 126.7, 126.7, 124.6, 120.7, 38.0, 21.8; **HRMS** (ESI) calcd. for $C_{23}H_{21}N_2O_2S$ [M+H]: 389.1324; found 389.1327.

_N_,4-dimethyl-_N_-(6-(phenanthren-9-yl)pyridin-3-yl)benzenesulfonamide (17a)

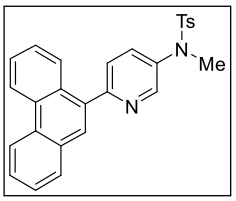

White solid (0.070 mmol, 30.7 mg, 70% yield); **^{1}H NMR** (400 MHz, $CDCl_3$) δ 8.76 (dd, J = 22.3, 7.9 Hz, 2H), 8.44 (d, *J* = 2.6 Hz, 1H), 8.08 (d, *J* = 7.8 Hz, 1H), 7.94 (d, *J* = 9.4 Hz, 1H), 7.87 (s, 1H), 7.78 – 7.67 (m, 3H), 7.64 (d, *J* = 8.3 Hz, 2H), 7.60 (d, *J* = 8.3 Hz, 1H), 7.56 (d, *J* = 8.3 Hz, 2H), 7.32 (d, *J* = 8.4 Hz, 2H), 3.31 (s, 3H), 2.44 (s, 3H); **^{13}C NMR** (101 MHz, $CDCl_3$) δ 157.8, 146.6, 144.2, 137.0, 136.1, 134.9, 133.3, 131.2, 130.8, 130.5, 130.0, 129.7, 129.7, 129.0, 128.8, 127.8, 127.2, 126.9, 126.7, 126.7, 126.3, 124.9, 123.0, 122.6, 37.9, 21.5; **HRMS** (ESI) calcd. for $C_{27}H_{23}N_2O_2S$ [M+H]: 439.1480; found 439.1484.

_N_,4-dimethyl-_N_-(6-(pyren-4-yl)pyridin-3-yl)benzenesulfonamide (18a)

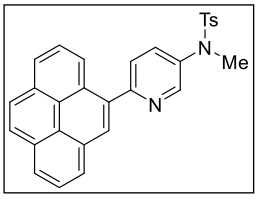

White solid (0.065 mmol, 30.0 mg, 65% yield); **^{1}H NMR** (400 MHz, $CDCl_3$) δ 8.52 (d, *J* = 2.3 Hz, 1H), 8.41 (d, *J* = 9.3 Hz, 1H), 8.30 – 8.15 (m, 4H), 8.15 – 8.09 (m, 3H), 8.05 (t, *J* = 7.6 Hz, 1H), 7.83 – 7.72 (m, 2H), 7.59 (d, *J* = 8.1 Hz, 2H), 7.34 (d, *J* = 7.9 Hz, 2H), 3.34 (s, 3H), 2.46 (s, 3H); **^{13}C NMR** (101 MHz, $CDCl_3$) δ 157.9, 146.8, 144.2, 136.7, 134.8, 134.5, 133.3, 131.6, 131.4, 130.8, 129.7, 129.7, 128.6, 128.2, 128.1, 127.8, 127.6, 127.3, 127.2, 126.1, 125.5, 125.4, 125.2, 125.1, 124.8, 124.5, 37.9, 21.5; **HRMS** (ESI) calcd. for $C_{29}H_{23}N_2O_2S$ [M+H]: 463.1480; found 463.1483.

***N*-(6-(4-cyanophenyl)pyridin-3-yl)-*N*,4-dimethylbenzenesulfonamide (19a)**

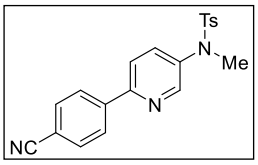

White solid (0.051 mmol, 18.5 mg, 51% yield); **^{1}H NMR** (500 MHz, $CDCl_3$) δ 8.40 (d, *J* = 1.9 Hz, 1H), 8.10 (d, *J* = 8.5 Hz, 2H), 7.75 (t, *J* = 8.8 Hz, 3H), 7.68 (dd, *J* = 8.5, 2.6 Hz, 1H), 7.47 (d, *J* = 8.3 Hz, 2H), 7.28 (d, *J* = 7.9 Hz, 2H), 3.24 (s, 3H), 2.43 (s, 3H); **^{13}C NMR** (126 MHz, $CDCl_3$) δ 153.7, 147.4, 144.7, 142.9, 138.5, 135.3, 133.5, 133.1, 130.2, 128.2, 127.9, 121.1, 119.2, 113.2, 38.1, 22.0; **HRMS** (ESI) calcd. for $C_{20}H_{18}N_3O_2S$ [M+H] 364.1120; found 522.1522.

_N_,4-dimethyl-_N_-(6-(4-nitrophenyl)pyridin-3-yl)benzenesulfonamide (20a)

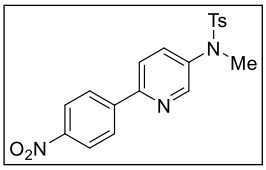

White solid (0.098 mmol, 37.6 mg, 98% yield); **^{1}H NMR** (500 MHz, $CDCl_3$) δ 8.43 (d, *J* = 2.6 Hz, 1H), 8.33 (d, *J* = 8.9 Hz, 2H), 8.17 (d, *J* = 8.9 Hz, 2H), 7.79 (d, *J* = 7.9 Hz, 1H), 7.70 (dd, *J* = 8.5, 2.6 Hz, 1H), 7.47 (d, *J* = 8.3 Hz, 2H), 7.28 (d, *J* = 8.0 Hz, 2H), 3.25 (s, 3H), 2.43 (s, 3H); **^{13}C NMR** (126 MHz, $CDCl_3$) δ 152.7, 148.2, 146.9, 144.3, 144.1, 138.1, 134.7, 133.0, 129.7, 127.7, 127.6, 124.0, 120.8, 37.6, 21.5; **HRMS** (ESI) calcd. for $C_{19}H_{18}N_3O_4S$ [M+H]: 384.1018; found 384.1021.

_N_,4-dimethyl-_N_-(6-(3-nitrophenyl)pyridin-3-yl)benzenesulfonamide (21a)

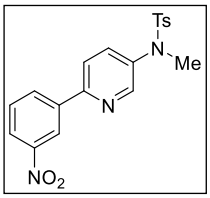

White solid (0.061 mmol, 21.0 mg, 61% yield); **^{1}H NMR** (400 MHz, $CDCl_3$) δ 8.75 (t, *J* = 2.0 Hz, 1H), 8.32 (dd, *J* = 2.7, 0.8 Hz, 1H), 8.25 (ddd, *J* = 7.8, 1.8, 1.0 Hz, 1H), 8.17 (ddd, *J* = 8.2, 2.3, 1.1 Hz, 1H), 7.74 – 7.67 (m, 1H), 7.61 – 7.53 (m, 2H), 7.40 – 7.35 (m, 2H), 7.23 – 7.16 (m, 2H), 3.15 (s, 3H), 2.33 (s, 3H). **^{13}C NMR** (101 MHz, $CDCl_3$) δ 152.8, 147.0, 144.3, 140.0, 138.0, 134.9, 133.0, 132.6, 129.8, 129.7, 129.7, 128.3, 127.7, 126.4, 123.7, 121.7, 120.2, 37.6, 21.5; **HRMS** (ESI) calcd. for $C_{19}H_{18}N_3O_4S$ [M+H]: 384.1018; found 384.1020.

_N_,4-dimethyl-_N_-(6-(4-(trifluoromethyl)phenyl)pyridin-3-yl)benzenesulfonamide (22a)

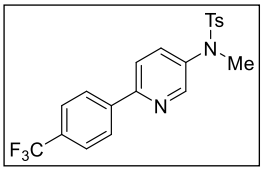

White solid (0.042 mmol, 17.2 mg, 42% yield); **^{1}H NMR** (500 MHz, $CDCl_3$) δ 8.38 (d, *J* = 1.9 Hz, 1H), 8.10 (d, *J* = 8.0 Hz, 2H), 7.74 (t, *J* = 8.3 Hz, 3H), 7.67 (dd, *J* = 8.5, 2.6 Hz, 1H), 7.47 (d, *J* = 8.3 Hz, 2H), 7.28 (d, *J* = 8.0 Hz, 2H), 3.24 (s, 3H), 2.40 (s, 3H); **^{13}C NMR** (126 MHz, $CDCl_3$) δ 153.9, 146.9, 144.2, 141.6, 137.6, 134.9, 133.0, 131.1, 130.9, 129.7, 127.7, 127.1, 125.8, 125.7, 125.7, 125.7, 125.1, 123.0, 120.4, 37.7, 21.5; **HRMS** (ESI) calcd. for $C_{20}H_{18}F_3N_2O_2S$ [M+H]: 407.1041; found 407.1043.

***N*-(6-(3,5-difluorophenyl)pyridin-3-yl)-*N*,4-dimethylbenzenesulfonamide (23a)**

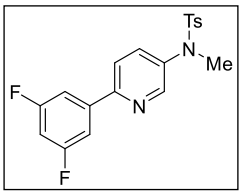

White solid (0.072 mmol, 26.9 mg, 72% yield); **^{1}H NMR** (400 MHz, $CDCl_3$) δ 8.35 (t, *J* = 1.7 Hz, 1H), 7.66 (d, *J* = 1.7 Hz, 2H), 7.56 – 7.49 (m, 2H), 7.46 (d, *J* = 8.3 Hz, 2H), 7.28 (d, *J* = 7.8 Hz, 2H), 6.90 – 6.82 (m, 1H), 3.23 (s, 3H), 2.43 (s, 3H); **^{13}C NMR** (101 MHz, $CDCl_3$) δ 164.7, 164.6, 162.2, 162.1, 146.7, 144.2, 137.8, 134.8, 133.1, 129.7, 127.7, 120.1, 109.8, 109.7, 109.6, 109.5, 104.6, 104.4, 104.1, 37.6, 21.5; **HRMS** (ESI) calcd. for $C_{19}H_{17}F_2N_2O_2S$ [M+H]: 375.0975; found 375.0983.

***N*-(6-(furan-2-yl)pyridin-3-yl)-*N*,4-dimethylbenzenesulfonamide (24a)**

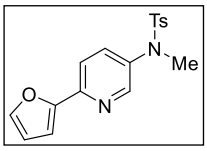

Purified by semi-preparative HPLC in the hexanes/AcOEt gradient (*N*-methyltosylamide is inseparable from the final product); white solid (0.014 mmol, 4.6 mg, 14% yield + TsNHMe); **^{1}H NMR** (400 MHz, $CDCl_3$) δ 8.24 (d, *J* = 2.6 Hz, 1H), 7.65 (d, *J* = 8.6 Hz, 1H), 7.58 (dd, *J* = 8.6, 2.6 Hz, 1H), 7.55 (s, 1H), 7.46 (d, *J* = 8.3 Hz, 2H), 7.30 – 7.25 (m, 2H), 7.04 (d, *J* = 3.4 Hz, 1H), 6.55 (s, 1H), 3.22 (s, 3H), 2.43 (s, 3H); **^{13}C NMR** (both for product and *N*-methyltosylamide) (101 MHz, $CDCl_3$) δ 147.7, 146.9, 144.0, 143.6, 143.5, 136.4, 134.9, 133.1, 129.7, 129.6, 127.7, 127.2, 118.3, 112.2, 109.2, 37.8, 29.3, 21.5, 21.5; **HRMS** (ESI) calcd. for $C_{17}H_{17}N_2O_3S$ [M+H]: 329.0960; found 329.0963.

***N*-(2-(furan-2-yl)pyridin-3-yl)-*N*,4-dimethylbenzenesulfonamide (24b)**

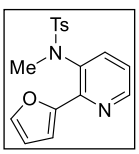

Purified by semi-preparative HPLC in hexanes/AcOEt gradient; white solid (0.021 mmol, 6.9 mg, 21% yield); **^{1}H NMR** (400 MHz, $CDCl_3$) δ 8.63 (dd, *J* = 4.6, 1.6 Hz, 1H), 7.64 (d, *J* = 8.3 Hz, 2H), 7.51 (dd, *J* = 1.8, 0.8 Hz, 1H), 7.34 – 7.29 (m, 3H), 7.24 (dd, *J* = 8.0, 1.6 Hz, 1H), 7.12 (dd, *J* = 8.0, 4.6 Hz, 1H), 6.53 (dd, *J* = 3.5, 1.8 Hz, 1H), 3.21 (s, 3H), 2.46 (s, 3H); **^{13}C NMR** (101 MHz, $CDCl_3$) δ 149.2, 143.9, 143.8, 136.6, 135.3, 133.7, 129.6, 128.0, 121.8, 113.5, 112.0, 38.4, 21.5; **HRMS** (ESI) calcd. for $C_{17}H_{17}N_2O_3S$ [M+H]: 329.0960; found 329.0962.

***N*,4-dimethyl-*N*-(6-(thiophen-2-yl)pyridin-3-yl)benzenesulfonamide (25a)**

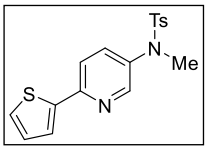

Off-white solid (0.049 mmol, 17.0 mg, 49% yield); **^{1}H NMR** (500 MHz, $CDCl_3$) δ 8.18 (dd, *J* = 2.5, 0.8 Hz, 1H), 7.62 (dd, *J* = 8.6, 0.9 Hz, 1H), 7.60 – 7.54 (m, 2H), 7.49 – 7.43 (m, 2H), 7.41 (dd, *J* = 5.0, 1.1 Hz, 1H), 7.27 (d, *J* = 8.2 Hz, 2H), 7.11 (dd, *J* = 5.0, 3.7 Hz, 1H), 3.20 (s, 3H), 2.42 (s, 3H); **^{13}C NMR** (126 MHz, $CDCl_3$) δ 151.3, 146.7, 144.3, 144.0, 136.7, 135.3, 133.2, 129.9, 128.4, 128.3, 128.0, 125.3, 118.7, 38.0, 21.8; **HRMS** (ESI) calcd. for $C_{17}H_{17}N_2O_2S_2$ [M+H]: 345.0731; found 345.0730.

***N*-(6-(benzo[b]thiophen-2-yl)pyridin-3-yl)-*N*,4-dimethylbenzenesulfonamide (26a)**

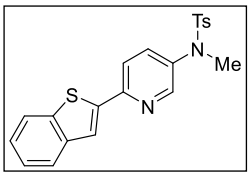

White solid (0.056 mmol, 22.2 mg, 56% yield); **^{1}H NMR** (400 MHz, $CDCl_3$) δ 8.25 (dd, *J* = 2.6, 0.7 Hz, 1H), 7.91 – 7.73 (m, 4H), 7.65 (dd, *J* = 8.6, 2.6 Hz, 1H), 7.52 – 7.45 (m, 2H), 7.42 – 7.33 (m, 2H), 7.28 (d, *J* = 7.9 Hz, 2H), 3.23 (s, 3H), 2.43 (s, 3H); **^{13}C NMR** (101 MHz, CDCl3) δ 150.9, 146.4, 144.1, 143.7, 140.8, 140.4, 137.1, 134.9, 133.0, 129.7, 127.7, 125.2, 124.6, 124.2, 122.5, 121.6, 119.3, 37.7, 21.5; **HRMS** (ESI) calcd. for $C_{21}H_{19}N_2O_2S_2$ [M+H]: 395.0888; found 395.0883.

***N*-(6-(benzo[b]thiophen-3-yl)pyridin-3-yl)-*N*,4-dimethylbenzenesulfonamide (27a)**

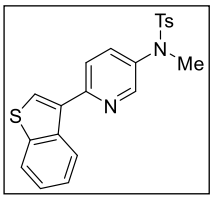

White solid (0.079 mmol, 31.3 mg, 79% yield); **^{1}H NMR** (500 MHz, $CDCl_3$) δ 8.50 – 8.45 (m, 1H), 8.37 (dt, *J* = 1.9, 0.9 Hz, 1H), 7.90 (dt, *J* = 7.9, 1.0 Hz, 1H), 7.81 (s, 1H), 7.70 – 7.62 (m, 2H), 7.51 – 7.30 (m, 5H), 7.30 – 7.23 (m, 1H), 3.24 (d, *J* = 0.7 Hz, 3H), 2.41 (s, 3H); **^{13}C NMR** (126 MHz, $CDCl_3$) δ 153.0, 146.6, 144.1, 140.8, 136.9, 136.5, 135.5, 135.0, 133.1, 129.7, 128.3, 127.8, 126.9, 124.7, 124.7, 124.1, 122.7, 122.1, 37.8, 21.5; **HRMS** (ESI) calcd. for $C_{21}H_{19}N_2O_2S_2$ [M+H]: 395.0888; found 395.0883.

***tert-butyl* 2-(5-((*N*,4-dimethylphenyl)sulfonamido)pyridin-2-yl)-1*H*-pyrrole-1-carboxylate (28a)**

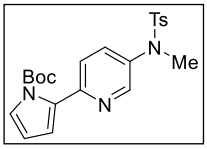

White solid (0.026 mmol, 11.1 mg, 26% yield); **^{1}H NMR** (400 MHz, $CDCl_3$) δ 8.29 – 8.23 (m, 1H), 7.58 – 7.46 (m, 3H), 7.41 – 7.34 (m, 2H), 7.29 (s, 2H), 6.46 (dt, *J* = 3.2, 1.5 Hz, 1H), 6.25 (td, *J* = 3.3, 1.3 Hz, 1H), 3.22 (d, *J* = 1.3 Hz, 3H), 2.43 (s, 3H), 1.42 (d, *J* = 1.3 Hz, 9H); **^{13}C NMR** (101 MHz, $CDCl_3$) δ 146.2, 144.3, 137.6, 136.6, 134.0, 133.3, 129.6, 127.8, 126.6, 125.1, 124.1, 123.0, 116.3, 110.6, 83.9, 37.9, 27.6, 21.5; **HRMS** (ESI) calcd. for $C_{22}H_{26}N_3O_4S$ [M+H]: 428.1644; found 428.1645.

***tert-butyl* 2-(5-((*N*,4-dimethylphenyl)sulfonamido)pyridin-2-yl)-1*H*-indole-1-carboxylate (29a)**

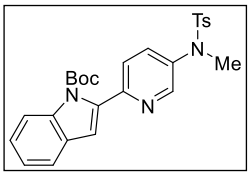

White solid (0.049 mmol, 23.3 mg, 49% yield); **^{1}H NMR** (500 MHz, $CDCl_3$) δ 8.32 (d, *J* = 2.3 Hz, 1H), 8.18 – 8.13 (m, 1H), 7.63 – 7.56 (m, 2H), 7.53 – 7.46 (m, 3H), 7.40 – 7.33 (m, 1H), 7.31 – 7.22 (m, 3H), 6.80 (d, *J* = 0.9 Hz, 1H), 3.24 (d, *J* = 1.0 Hz, 3H), 2.43 (s, 3H), 1.40 (d, *J* = 1.0 Hz, 9H); **^{13}C NMR** (126 MHz, $CDCl_3$) δ 151.8, 150.1, 146.6, 144.4, 138.6, 137.9, 137.1, 134.5, 133.6, 129.9, 129.0, 128.0, 125.4, 123.2, 123.1, 121.3, 115.2, 111.9, 83.9, 38.2, 27.9, 21.8; **HRMS** (ESI) calcd. for $C_{26}H_{28}N_3O_4S$ [M+H]: 478.1801; found 478.1803.

***N*-(6-(methoxy(phenyl)methyl)pyridin-3-yl)-*N*,4-dimethylbenzenesulfonamide (35a)**

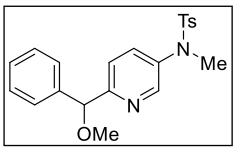

White solid (0.043 mmol, 14.9 mg, 43% yield); **^{1}H NMR** (500 MHz, $CDCl_3$) δ 8.17 (d, *J* = 2.5 Hz, 1H), 7.53 (dd, *J* = 8.5, 2.6 Hz, 1H), 7.46 (d, *J* = 8.5 Hz, 1H), 7.40 (dd, *J* = 7.6, 4.0 Hz, 4H), 7.34 (t, *J* = 7.5 Hz, 2H), 7.28 (d, *J* = 7.3 Hz, 1H), 7.23 (d, *J* = 8.0 Hz, 2H), 5.35 (s, 1H), 3.42 (s, 3H), 3.15 (s, 3H), 2.41 (s, 3H); **^{13}C NMR** (126 MHz, $CDCl_3$) δ 160.1, 146.3, 144.0, 140.3, 136.9, 135.0, 133.1, 129.6, 128.5, 127.8, 127.7, 126.9, 120.3, 86.0, 57.1, 37.8, 21.5. **HRMS** (ESI) calcd. for $C_{21}H_{31}N_2O_3S$ [M+H]: 384.1429; found 384.1428.

4.3. General procedure for the functionalization of 2-alkyl Zincke imines (General procedure 4)

General Procedure 4. Zincke imine (0.05 mmol), **Py-salt** (0.075 mmol), $Ir(ppy)_3$ (0.67 mg, ~10 μmol, 2 mol%) were placed in the closed-cup vial and MeCN (8 ml) were added through the septum. The reaction mixture was placed in ultrasound bath and degassed by bubbling argon through the solution for 15 min. The vial was then moved to the photoreactor and irradiated with violet light (4.8 W) for 24 h, maintaining a temperature between 0 °C and 5 °C. After the indicated time, the saturated NH_4OAc solution in anhydrous ethanol was added (2 ml) and the reaction mixture was heated up to 65 °C for 2 h. The excess of NH_4OAc was removed by extraction (AcOEt/ H_2O). The organic phase was dried over anhydrous sodium sulphate and evaporated with silica gel (dry load for the preparation of the sample for flash chromatography). The pure products were isolated by flash chromatography in hexanes/AcOEt gradient.

Flash program: time: 25 min; column: silica 4 g; flow rate: 13 mL/min; automatic peak hold: on.

entry	time [min]	hexanes [%]	AcOEt [%]
1	0	90	10
2	25	50	50

Note:

- *Several products, especially minor regioisomers, were initially isolated by the column or flash chromatography in a* hexanes*/AcOEt gradient. Due to some impurities from tailing N-methyltosylamide, further purification by semi-preparative normal phase HPLC was necessary to obtain pure compounds.*

***N*,4-dimethyl-*N*-(2-methylpyridin-3-yl)benzenesulfonamide (30b)**

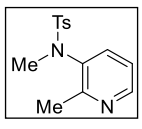

White solid (0.074 mmol, 20.4 mg, 74% yield); **^{1}H NMR** (400 MHz, $CDCl_3$) δ 8.45 (d, *J* = 3.0 Hz, 1H), 7.57 (d, *J* = 6.4 Hz, 2H), 7.31 (d, *J* = 8.1 Hz, 2H), 7.03 (d, *J* = 3.8 Hz, 2H), 3.13 (s, 3H), 2.54 (s, 3H), 2.45 (s, 3H); **^{13}C NMR** (101 MHz, $CDCl_3$) δ 159.6, 148.6, 143.9, 136.6, 135.1, 135.1, 134.8, 129.6, 127.9, 121.3, 38.6, 21.5, 21.3; **HRMS** (ESI) calcd. for $C_{14}H_{17}N_2O_2S$ [M+H]: 277.1013; found 277.1011.

***N*-(2-ethylpyridin-3-yl)-*N*,4-dimethylbenzenesulfonamide (31b)**

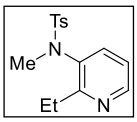

White solid (0.070 mmol, 20.4 mg, 70% yield); **^{1}H NMR** (500 MHz, $CDCl_3$) δ 8.50 (dd, *J* = 4.7, 1.7 Hz, 1H), 7.57 (d, *J* = 8.3 Hz, 2H), 7.31 (d, *J* = 7.7 Hz, 2H), 7.02 (dd, *J* = 8.0, 4.6 Hz, 1H), 6.97 (dd, *J* = 8.0, 1.7 Hz, 1H), 3.13 (s, 3H), 2.91 (s, 2H), 2.45 (s, 3H), 1.28 (t, *J* = 7.6 Hz, 3H); **^{13}C NMR** (126 MHz, $CDCl_3$) δ 164.2, 149.1, 144.1, 136.3, 135.1, 134.8, 129.9, 128.2, 121.4, 39.4, 26.8, 21.8, 13.1; **HRMS** (ESI) calcd. for $C_{15}H_{19}N_2O_2S$ [M+H]: 291.1167; found 291.1171.

***N*-(2-hexanoylpyridin-3-yl)-N,4-dimethylbenzenesulfonamide (32b)**

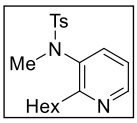

White solid (0.066 mmol, 23.6 mg, 66% yield); **^{1}H NMR** (500 MHz, $CDCl_3$) δ 8.49 (dd, *J* = 4.5, 1.9 Hz, 1H), 7.58 (d, *J* = 8.2 Hz, 2H), 7.31 (d, *J* = 8.5 Hz, 2H), 7.05 – 6.97 (m, 2H), 3.13 (s, 3H), 2.45 (s, 3H), 1.76 – 1.62 (m, 2H), 1.39 – 1.25 (m, 6H), 0.93 – 0.84 (m, 3H); **^{13}C NMR** (126 MHz, $CDCl_3$) δ 163.1, 148.8, 143.9, 136.2, 134.9, 134.6, 129.6, 128.0, 121.1, 39.2, 33.5, 31.7, 29.5, 28.8, 22.6, 21.5, 14.0; **HRMS** (ESI) calcd. for $C_{19}H_{27}N_2O_2S$ [M+H]: 347.1793; found 347.1790.

***N*-(6-isopropylpyridin-3-yl)-*N*,4-dimethylbenzenesulfonamide (33a)**

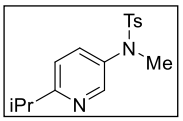

White solid (0.044 mmol, 13.4 mg, 44% yield); **^{1}H NMR** (500 MHz, $CDCl_3$) δ 8.14 (d, *J* = 1.9 Hz, 1H), 7.49 – 7.42 (m, 3H), 7.28 (s, 2H), 7.14 (d, *J* = 8.4 Hz, 1H), 3.17 (s, 3H), 3.06 (dt, *J* = 13.8, 6.9 Hz, 1H), 2.42 (s, 3H), 1.29 (d, *J* = 6.9 Hz, 6H); **^{13}C NMR** (126 MHz, $CDCl_3$) δ 166.1, 146.4, 143.9, 135.8, 135.1, 133.3, 129.6, 127.7, 120.5, 38.0, 35.9, 22.4, 21.5, **HRMS** (ESI) calcd. for $C_{16}H_{21}N_2O_2S$ [M+H]: 305.1324; found 305.1326.

***N*-(2-isopropylpyridin-3-yl)-*N*,4-dimethylbenzenesulfonamide (33b)**

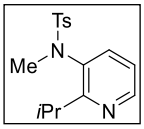

White solid (0.031 mmol, 9.4 mg, 31% yield); **^{1}H NMR** (500 MHz, $CDCl_3$) δ 8.55 (dd, J = 4.6, 1.9 Hz, 1H), 7.60 (d, J = 8.1 Hz, 2H), 7.32 (d, J = 7.3 Hz, 2H), 7.03 – 6.95 (m, 2H), 3.70 – 3.58 (m, 1H), 3.15 (s, 3H), 2.45 (s, 3H), 1.28 (d, J = 6.7 Hz, 3H), 1.19 (d, J = 6.8 Hz, 3H); **^{13}C NMR** (126 MHz, $CDCl_3$) δ 167.5, 149.1, 143.8, 135.2, 134.8, 134.8, 129.6, 128.0, 121.0, 77.2, 77.0, 76.7, 39.4, 29.6, 23.0, 21.3.

***N*-(6-benzylpyridin-3-yl)-*N*,4-dimethylbenzenesulfonamide (34b)**

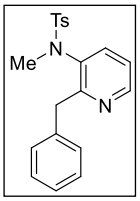

White solid (0.040 mmol, 14.1 mg, 40% yield); **^{1}H NMR** (500 MHz, $CDCl_3$) δ 8.52 (dd, *J* = 4.7, 1.6 Hz, 1H), 7.57 (d, *J* = 8.3 Hz, 2H), 7.32 (d, *J* = 8.7 Hz, 2H), 7.27 (d, *J* = 7.1 Hz, 4H), 7.17 (t, *J* = 6.5 Hz, 1H), 7.05 (dd, *J* = 8.0, 4.7 Hz, 1H), 6.86 (dd, *J* = 8.0, 1.6 Hz, 1H), 4.64 (s, 1H), 4.16 (s, 1H), 2.77 (s, 3H), 2.46 (s, 3H); **^{13}C NMR** (126 MHz, $CDCl_3$) δ 162.2, 148.8, 144.0, 139.2, 136.7, 134.9, 134.2, 129.6, 129.3, 128.3, 128.1, 126.1, 121.8, 40.8, 38.8, 21.5; **HRMS** (ESI) calcd. for $C_{20}H_{21}N_2O_2S$ [M+H]: 353.1324; found 353.1326.

***N*-(6-(methoxy(phenyl)methyl)pyridin-3-yl)-*N*,4-dimethylbenzenesulfonamide (35a)**

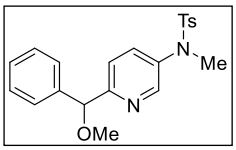

White solid (0.028 mmol, 10.7 mg, 28% yield); **^{1}H NMR** (500 MHz, $CDCl_3$) δ = 8.17 (d, *J* = 2.5, 1H), 7.53 (dd, *J* = 8.5, 2.6, 1H), 7.46 (d, *J* = 8.5, 1H), 7.40 (dd, *J* = 7.6, 4.0, 4H), 7.34 (t, *J* = 7.5, 2H), 7.28 (d, *J* = 7.3, 1H), 7.23 (d, *J* = 8.0, 2H), 5.35 (s, 1H), 3.42 (s, 3H), 3.15 (s, 3H), 2.41 (s, 3H); **^{13}C NMR** (126 MHz, $CDCl_3$) δ = 160.11, 146.38, 144.02, 140.37, 136.99, 135.08, 133.13, 129.62, 128.54, 127.89, 127.73, 126.99, 120.37, 86.03, 57.18, 37.81, 21.53. **HRMS** (ESI) calcd. for $C_{21}H_{23}N_2O_3S$ [M+H]: 383.1429; found 383.1428.

***N*-(2-(methoxy(phenyl)methyl)pyridin-3-yl)-*N*,4-dimethylbenzenesulfonamide (35b)**

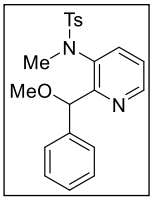

Purified by semi-preparative HPLC in hexanes/AcOEt gradient; white solid (0.28 mmol, 10.7 mg, 28% yield); **^{1}H NMR** (major rotamer) (400 MHz, $CDCl_3$) δ 8.70 (d, *J* = 4.6 Hz, 1H), 7.54 (dd, *J* = 32.6, 7.8 Hz, 5H), 7.32 (dd, *J* = 13.8, 7.6 Hz, 6H), 7.06 (dd, *J* = 8.0, 4.7 Hz, 1H), 6.72 (d, *J* = 7.9 Hz, 1H), 6.17 (s, 1H), 3.49 (s, 4H), 2.61 (s, 3H), 2.47 (s, 4H); **^{13}C NMR** (all signals are listed)(101 MHz, $CDCl_3$) δ 161.2, 149.4, 144.3, 140.1, 135.9, 134.6, 133.8, 129.8, 128.5, 128.3, 128.0, 122.4, 81.2, 80.5, 57.3, 53.5, 38.7, 21.7.

^{1}H NMR (major rotamer) (400 MHz, CD_3OD) δ 8.57 (d, *J* = 3.8 Hz, 1H), 7.57 (d, *J* = 8.0 Hz, 2H), 7.42 (dd, *J* = 11.6, 7.6 Hz, 5H), 7.36 – 7.29 (m, 2H), 7.30 – 7.25 (m, 1H), 7.25 – 7.18 (m, 1H), 6.90 (d, *J* = 8.0 Hz, 1H), 6.20 (s, 1H), 3.43 (s, 3H), 2.61 (s, 3H), 2.47 (s, 3H); **^{13}C NMR** (all signals are listed) (101 MHz, CD_3OD) δ 161.8, 149.6, 146.1, 141.1, 137.7, 136.9, 134.7, 131.0, 129.5, 129.4, 129.3, 129.2, 124.4, 82.3, 57.4, 39.0, 21.5, 21.5; **HRMS** (ESI) calcd. for $C_{21}H_{22}N_2O_3SNa$ [M+Na]: 405.1249; obtained 405.1250.

^{1}H NMR (500 MHz, DMSO-d_6, **353K**) δ 8.54 (d, *J* = 4.5 Hz, 1H), 7.67 – 7.60 (m, 2H), 7.47 (d, *J* = 8.1 Hz, 2H), 7.42 (d, *J* = 7.6 Hz, 2H), 7.32 (dd, *J* = 8.3, 6.7 Hz, 2H), 7.29 – 7.23 (m, 2H), 7.11 (d, *J* = 7.6 Hz, 1H), 5.98 (s, 1H), 3.32 (s, 3H), 3.05 (s, 3H), 2.45 (s, 3H), **^{13}C NMR** (126 MHz, DMSO-d_6, **353K**) δ 168.5, 157.8, 153.1, 149.0, 145.5, 144.2, 143.4, 138.9, 136.8, 136.3, 132.2, 89.1, 65.7, 48.1, 30.0.

4.4. Scale-up protocol

Reaction set-up

Photochemical reactions were irradiated with two Kessil lamps (maximum at 390 nm, 40 W when 100% power was applied), placed at opposite sites (**Supplementary Figure 14**) with cooling by fans ($T_{reaction}$ ~30°C).

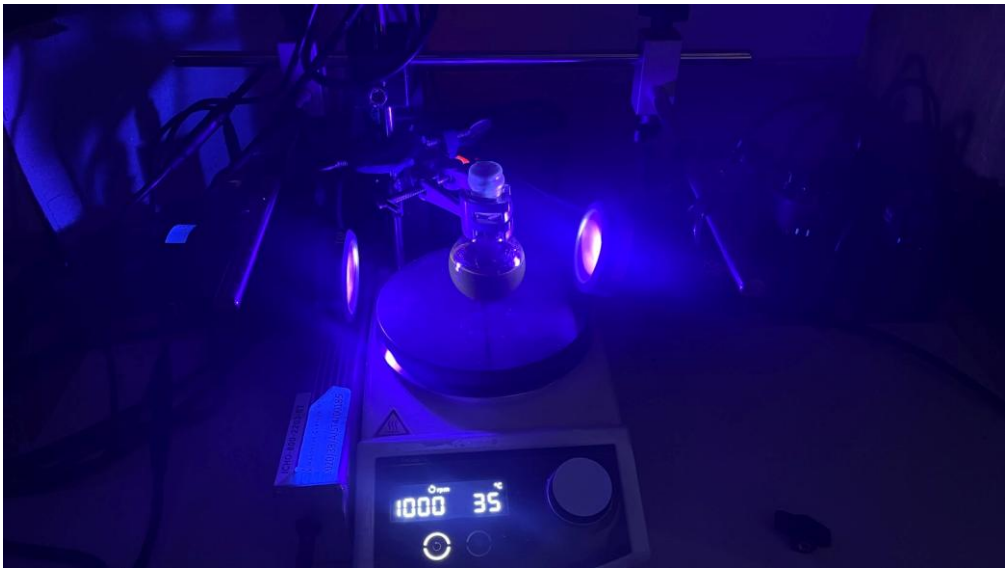

Supplementary Figure 14. *Photoreactor setup (390 nm, 20% power).*

Reaction protocol

Zincke imine **2** (0.25 mmol), **Py-salt** (0.375 mmol), $Ir(ppy)_3$ (3.4 mg, ~0.05 mmol, 2 mol%) were placed in a round bottom flask and MeCN (20 ml) and DMSO (20 ml) were added through the septum. The reaction mixture was placed in ultrasound bath and degassed by bubbling argon through the solution for 15 min. The flask was

then mounted to the photoreactor and irradiated with violet light (2 x 8 W) for 24 h maintaining a temperature of around 30 ° C with a dedicated cooling system. Then a saturated solution of NH_4OAc in anhydrous ethanol was added (10 ml) and the reaction was heated at to 65 °C for 2 h. DMSO and an excess of NH_4OAc were removed by extraction (AcOEt/ H_2O). The organic phase was dried over anhydrous sodium sulphate and evaporated with silica gel (dry load for the preparation of the sample for flash chromatography). The pure products were isolated by flash chromatography on hexanes/ AcOEt gradient (white solid, mixture of regioisomers ~5:1, 0.21 mmol, 69.3 mg, 82%).

4.5. One-pot procedure

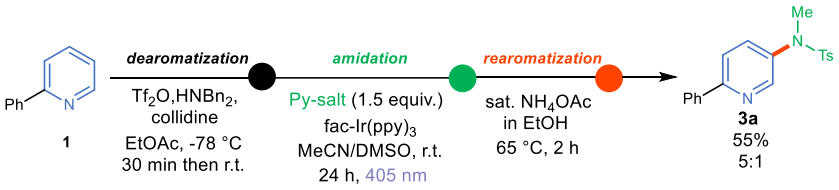

In the round bottom flask 2-phenylpyridine (**1**, 0.3 mmol) was dissolved in anhydrous AcOEt (3 ml) and cooled to -78 °C (acetone/dry ice bath) followed by the addition of trifluoromethanesulfonic anhydride (0.3 mmol) and stirred at -78 °C for 1 h. Then, a solution of dibenzylamine (0.36 mmol, 1.2 equiv.) in anhydrous AcOEt (0.5 ml) was added dropwise and stirring was continued for another 30 min at -78 °C. The reaction mixture was removed from the cryogenic bath and allowed to stir while the mixture was heated to room temperature.

To each of six 10 ml closed cup vials, **Py-salt** (0.075 mmol) and $Ir(ppy)_3$ (0.067 mg, ~10 µmol, 2 mol%) were added. The reaction mixture containing Zincke imine (from the previous step) was equally divided between six vials and to each DMSO (3 ml) and MeCN (4 ml) were added. The reaction mixture was placed in ultrasound bath and degassed by bubbling argon through the solution for 15 min. Vials were then transferred to the photoreactor and irradiated with violet light (2.4 W) for 24 h maintaining a temperature between 0 °C to 5 °C with a dedicated cooling system. After the indicated time, a saturated solution of NH_4OAc in anhydrous ethanol was added (2 ml) to each vial and the reactions were heated up to 65 °C for 2 h. An excess of NH_4OAc from the combined reaction mixtures was removed by extraction (AcOEt/ H_2O). The organic phase was dried over anhydrous sodium sulphate and evaporated with silica gel (dry load for the preparation of the sample for flash chromatography). The pure products were isolated by flash chromatography in a hexanes/AcOEt gradient (95:5 to 70:30) (white solid, mixture of regioisomers ~5:1, 0.165 mmol, 55.8 mg, 55% total yield).

4.6 Other functionalizations

General protocol for deprotection of the NTs (according to Rodríguez et al. protocol)[38]

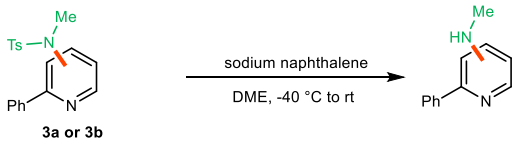

To the solution of compounds **3a** or **3b** (38 mg, 0.11 mmol) in anhydrous DME (2 ml), sodium naphthalene (0.8 ml; 0.5 M solution prepared from 516 mg of naphthalene and 71 mg of sodium in 6 ml of DME) was added dropwise at -40 °C. The reaction mixture was stirred for 2 h at this temperature and then for 30 min at room temperature. The reaction was quenched with water (5 ml) and extracted with AcOEt (3 x 5 ml). The combined organic phases were washed with water (10 ml) and brine (10 ml) and dried with anhydrous sodium sulphate. The desired product was purified by chromatography in a DCM / AcOEt gradient (from 0% AcOEt to 50% AcOEt) (easily identified a shiny spot on TLC under 365 nm irradiation).

***N*-methyl-6-phenylpyridin-3-amine (36)**

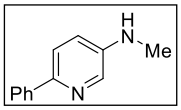

82% yield (17 mg, 0.092 mmol), white solid; **^{1}H NMR** (400 MHz, $CDCl_3$) δ 8.12 (dd, *J* = 2.9, 0.7 Hz, 1H), 7.94 – 7.86 (m, 2H), 7.58 (dd, *J* = 8.6, 0.7 Hz, 1H), 7.47 – 7.38 (m, 2H), 7.35 – 7.27 (m, 1H), 6.95 (dd, *J* = 8.6, 2.9 Hz, 1H), 3.83 (s, 1H), 2.91 (s, 3H); **^{13}C NMR** (101 MHz, $CDCl_3$) δ 146.6, 144.0, 139.6, 135.4, 128.5, 127.4, 125.8, 120.6, 118.8, 30.4; **HRMS** (ESI) calcd. for $C_{12}H_{13}N_2$ [M+H]: 185.1079; obtained 185.1078.

***N*-methyl-2-phenylpyridin-3-amine (37)**

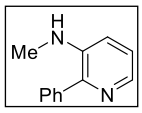

Reaction was started from 19 mg of **3b**; 78% yield (8.1 mg, 0.044 mmol), white solid; **^{1}H NMR** (400 MHz, $CDCl_3$) δ 8.05 (dd, *J* = 4.7, 1.4 Hz, 1H), 7.65 – 7.57 (m, 2H), 7.51 – 7.44 (m, 2H), 7.42 – 7.36 (m, 1H), 7.16 (dd, *J* = 8.2, 4.7 Hz, 1H), 6.96 (dd, *J* = 8.2, 1.4 Hz, 1H), 4.17 (s, 1H), 2.80 (d, *J* = 4.9 Hz, 3H); **^{13}C NMR** (101 MHz, $CDCl_3$) δ 142.8, 138.6, 137.8, 129.0, 128.8, 128.4, 123.3, 116.5, 30.50; **HRMS** (ESI) calcd. for $C_{12}H_{13}N_2$ [M+H] 185.1079; found 185.1083.

Preparation of the amide 38.

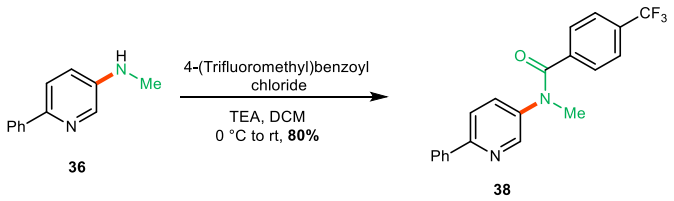

N-methyl-*N*-(6-phenylpyridin-3-yl)-4-(trifluoromethyl)benzamide (38)

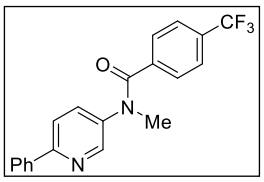

To the solution of compound **36** (17 mg, 0.092 mmol) in anhydrous DCM (0.5 ml), TEA (26 µl, 0.18 mmol) and *p*-CF_3 benzoyl chloride (14 µl, 0.092 mmol) were added at 0 °C. The reaction mixture was stirred for 30 min at 0 °C and then for 4 h at room temperature. The reaction mixture was quenched with water (5 ml) and extracted with AcOEt (3 x 5 ml). The combined organic phases were washed with water (10 ml) and brine (10 ml) and dried with anhydrous sodium sulphate. The desired product was purified by chromatography in a hexanes / AcOEt gradient (from 0% AcOEt to 20% AcOEt), yielding the product as a white solid (26.5 mg, 0.074 mmol, 80%). **^{1}H NMR** (500 MHz, $CDCl_3$) δ 8.39 (d, *J* = 2.7 Hz, 1H), 7.98 – 7.90 (m, 2H), 7.66 (d, *J* = 8.4 Hz, 1H), 7.53 – 7.39 (m, 8H), 3.56 (s, 3H); **^{13}C NMR** (126 MHz, $CDCl_3$) δ 169.3, 155.6, 147.7, 139.4, 138.8, 138.0, 134.5, (132.4, 132.1, 131.8, 131.6), 129.5, 129.1, 129.0, 126.9, (125.4, 125.4, 125.3, 125.3), 120.5, 38.57; **HRMS** (ESI) calcd. for $C_{20}H_{15}N_2O_3Na$ [M+Na] 379.1034; found 379.1031.

Preparation of *N*-oxide 39

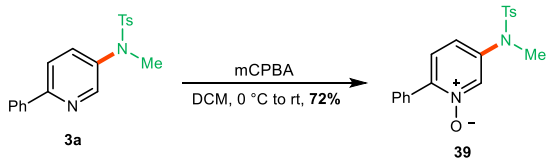

5-((*N*,4-dimethylphenyl)sulfonamido)-2-phenylpyridine 1-oxide (39)

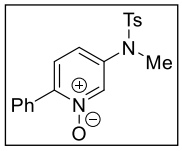

To the solution of **3a** (20 mg, 0.06 mmol) in anhydrous DCM (2 ml), mCPBA [≤77%, Sigma-Aldrich] (27 mg , ~0.12 mmol, ~2 equiv.) was added at 0 °C. The reaction mixture was stirred for 30 min at 0 °C and then for 18 h at room temperature. The reaction was directly transferred to the preprepared column (silica-gel/DCM). The product was eluted with 50% AcOEt-DCM mixture, yielding a white solid (16.2 mg, 0.046 mmol, 77%); **^{1}H NMR** (500 MHz, $CDCl_3$) δ 8.00 (d, *J* = 2.0 Hz, 1H), 7.84 – 7.77 (m, 2H), 7.57 – 7.51 (m, 2H), 7.47 (dddd, *J* = 8.8, 7.1, 5.8, 1.8 Hz, 3H), 7.43 – 7.37 (m, 2H), 7.31 (d, *J* = 8.0 Hz, 2H), 3.19 (s, 3H), 2.43 (s, 3H); **^{13}C NMR** (126 MHz, $CDCl_3$) δ 147.4, 144.9, 139.7, 137.0, 132.8, 131.9, 130.1, 129.9, 129.4, 128.5, 127.8, 126.6, 124.7, 37.6, 21.7; **HRMS** (ESI) calcd. for $C_{19}H_{19}N_2O_3S$ [M+H] 355.1116; found 355.1117.

Preparation of the methylpyridinium iodide 40

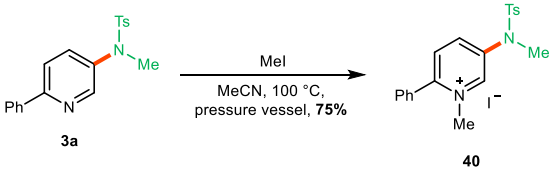

5-((*N*,4-dimethylphenyl)sulfonamido)-1-methyl-2-phenylpyridin-1-ium iodide (40)

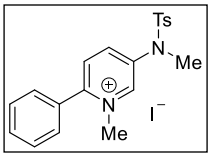

To the solution of **3a** (30 mg, 0.09 mmol) in anhydrous MeCN (1 ml) placed in a pressure vessel, MeI (110 µl, 1.77 mmol, 20 equiv.) was added. The reaction mixture was stirred for 8 h at 100 °C. After the indicated time, the reaction mixture was cooled down and solvent and an excess of methyl iodide were removed under reduced pressure. The semi-solid residue was then dissolved in the DCM / acetone mixture (2 ml, v/v 10:1) and transferred to the preprepared column (silica gel/DCM/10% acetone). The pure product was eluted with 40% acetone in the DCM mixture yielding a white solid (32 mg, 0.067 mmol, 75%); **^{1}H NMR** (600 MHz, DMSO-d_6) δ 9.21 (d, J = 2.4 Hz, 1H), 8.42 (dd, J = 8.7, 2.4 Hz, 1H), 8.04 (d, J = 8.7 Hz, 1H), 7.71 – 7.67 (m, 2H), 7.67 – 7.64 (m, 2H), 7.64 – 7.60 (m, 3H), 7.46 (d, J = 8.2 Hz, 2H), 4.12 (s, 3H), 3.21 (s, 3H), 2.41 (s, 3H); **^{13}C NMR** (151 MHz, DMSO-d_6) δ 153.0, 145.3, 143.9, 141.0, 140.2, 132.5, 131.6, 131.6, 130.7, 130.1, 129.8, 129.4, 128.3, 48.0, 37.2, 21.5; **HRMS** (ESI) for $C_{20}H_{21}N_2O_2S^+$ [M^+] 353.1324; found 353.1329.

4.7 Meta-meta (amination-bromination) difunctionalisation of Zincke imine

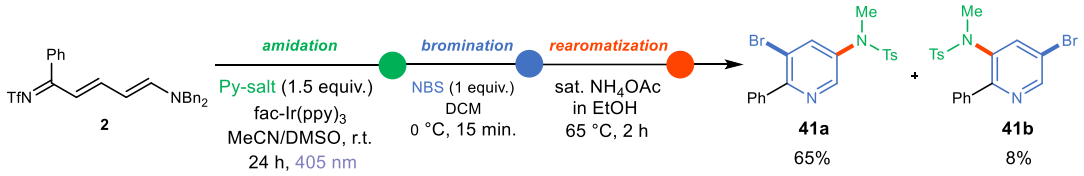

"One-pot" protocol

The reaction was carried out in 3 identical vials. For each: 2Ph-Zincke imine (**2a**) (25.07 mg, 0.05 mmol), **Py-salt** (0.075 mmol, 1.5 eq.), Ir(ppy)$_3$ (0.67 mg, ~10 µmol, 2 mol%) were placed in the closed cup vial and MeCN (4 ml) and DMSO (4 ml) were added through the septum. The reaction mixture was degassed by bubbling argon through the solution using an ultrasound bath for 15 min. The vial was transferred to the photoreaction and irradiated with violet light (2.4 W) for 24 h while maintaining a temperature between 0 °C and 5 °C with a dedicated cooling system. After the indicated time, the vial was placed in an ice bath and NBS (9.21 mg, 0.05 mol, 1.0 eq.) was added and then the ice bath was removed and the reaction was stirred at room temperature for 2 h. The saturated ammonium acetate solution in anhydrous ethanol was then added (2 ml) and the reaction was heated to 65 °C for 2 h. All vials were combined and DMSO and excess of ammonium acetate were removed by extraction (ethyl acetate/ water). The organic phase was dried over anhydrous sodium sulphate and evaporated with silica gel (dry load for the preparation of the sample for flash chromatography). Pure products were isolated by flash chromatography in the hexanes / AcOEt gradient (0-10% AcOEt).

***N*-(5-bromo-6-phenylpyridin-3-yl)-*N*,4-dimethylbenzenesulfonamide (41a)**

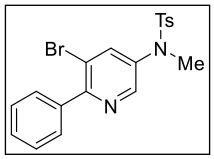

White solid (42 mg, 0.10 mmol, 65%); **^{1}H NMR** (500 MHz, $CDCl_3$) δ 8.31 (d, J = 2.3 Hz, 1H), 7.87 (d, J = 2.3 Hz, 1H), 7.71 – 7.65 (m, 2H), 7.55 – 7.50 (m, 2H), 7.49 – 7.43 (m, 3H), 7.34 – 7.28 (m, 2H), 3.21 (s, 3H), 2.44 (s, 3H); **^{13}C NMR** (126 MHz, $CDCl_3$) δ 156.4, 145.1,

144.5, 139.0, 138.8, 137.5, 133.1, 129.9, 129.4, 129.1, 128.1, 127.9, 118.8, 37.9, 21.7; **HRMS** (ESI) calcd. for $C_{19}H_{17}N_2O_2BrSNa$ [M+Na] 439.0092; found 439.0088.

***N*-(5-bromo-2-phenylpyridin-3-yl)-*N*,4-dimethylbenzenesulfonamide (41b)**

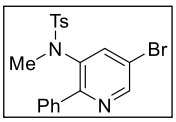

White solid (5.2 mg, 0.012 mmol, 8%; **^{1}H NMR** (400 MHz, $CDCl_3$) δ 8.70 (d, *J* = 2.1 Hz, 1H), 7.63 – 7.54 (m, 3H), 7.47 (d, *J* = 8.3 Hz, 2H), 7.41 (dd, *J* = 5.1, 2.0 Hz, 3H), 7.28 (s, 2H), 3.02 (s, 3H), 2.45 (s, 3H); **^{13}C NMR** (101 MHz, $CDCl_3$) δ 157.3, 150.1, 144.4, 138.9, 137.6, 136.8, 134.7, 129.8, 129.0, 128.9, 128.4, 128.1, 118.4, 38.8, 21.7; **HRMS** (ESI) calcd. for $C_{19}H_{17}N_2O_2BrSNa$ [M+Na] 439.0092; found 439.0093.

4.8 Unsuccessful functionalisation of Zincke imines

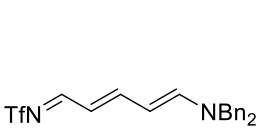

S40b

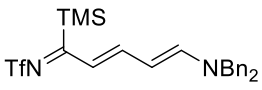

S45b

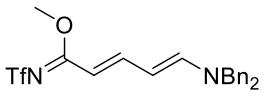

S43b

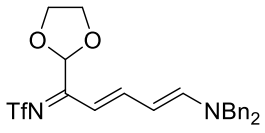

S46b

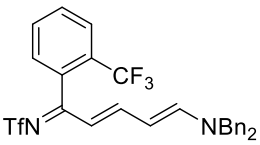

S34b

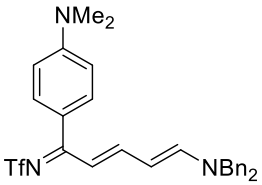

S35b

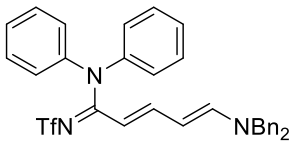

S36b

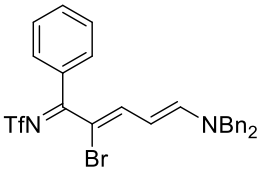

S37b

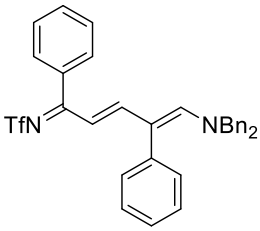

S42b

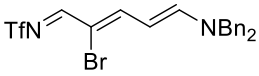

S48b

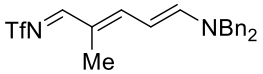

S41b

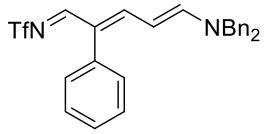

S39b

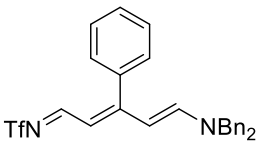

S38b

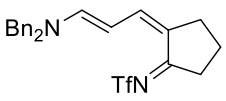

S47b

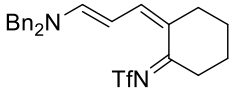

S44b

4.9 *N*-aminopyridinium salts scope

Supplementary Table 11. Scope of the *N*-aminopyridinium salts.

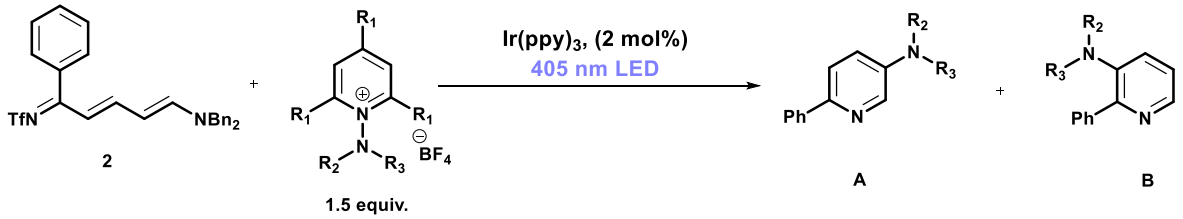

entry	R1	R2	R3	solvent	concentration [mmol/ml]	irradiation power [W]	irradiation time [h]	yield A+B [%]	ratio A to B
1	Me	Me	Ts	MeCN/DMSO (1:1)	0.006	2.4	24	99	4.8:1
2	Me	Me	Cbz	MeCN/DMSO (1:1)	0.006	2.4	24	nd	nd
3	Me	Me	Boc	MeCN/DMSO (1:1)	0.006	2.4	24	<10**	nd
4	Me	H	Ts	MeCN/DMSO (1:1)	0.006	2.4	24	nd	nd
5	H	H	Ts	MeCN/DMSO (1:1)	0.006	2.4	24	nd	nd
6	H	Me	Ts	MeCN/DMSO (1:1)	0.006	2.4	24	34%	8:1
7	H	Me	$COCF_3$	MeCN/DMSO (1:1)	0.006	2.4	24	nd	nd
8	Me	H	Boc	MeCN/DMSO (1:1)	0.006	2.4	24	nd	nd

*Entry 1-8 optimized conditions for the model reaction

**Based on ^{1}H NMR spectra of the crude reaction mixture with 2,4,6-trimethoxybenzene as an internal standard; These results should be treated as a preliminary data.

***Other variations, including solvents, concentrations, and irradiation power did not improve results

5. DFT Calculations

5.1. Computational Details

DFT calculations were carried out using the G16 programme package[26] using the ωB97xD functional[27]. Geometry optimisations and frequency calculations were computed with the Def2SVP basis set without symmetry restrictions[28,29]. The nature of all the stationary points was characterised by frequency calculations as minima (no imaginary frequencies) or transition states (one imaginary frequency). Transition states were relaxed to reactants and products, and IRC calculations were performed to further validate the connectivity. Additionally, the solvation energy was obtained from single-point calculations using ωB97xD/Def2TZVPP and the implicit solvent model (acetonitrile)[30]. The solvation free energy was then obtained by the difference between the energy calculated with the SMD model – the energy in gas phase. The standard state was corrected from 1atm to 1M by adding 1.89 kcal/mol when needed.

The potential energies were further refined using the DLPNO-CCSD(T)[31,32] method in ORCA[33-35]. Combination of Def2TZVPP and Ri-C auxiliary basis set (Def2-TZVPP/C) and RIJCOSX (Def2/J)[28,36]. The tightSCF option was also selected.

ORCA input:

```
! DLPNO-CCSD(T) Def2-TZVPP Def2-TZVPP/C Def2/J RIJCOSX GRIDX5 TightSCF
%maxcore 5000
%pal
nprocs 24
end
%scf
maxiter 2000
end
%mdci
UseFullLMP2Guess false
end
* xyz charge multiplicity structure.xyz*
```

3D representations were created using the CylView 1.0 program[37].

5.2. Comparison of free energy profiles for the regioselective addition of the N-centred radical

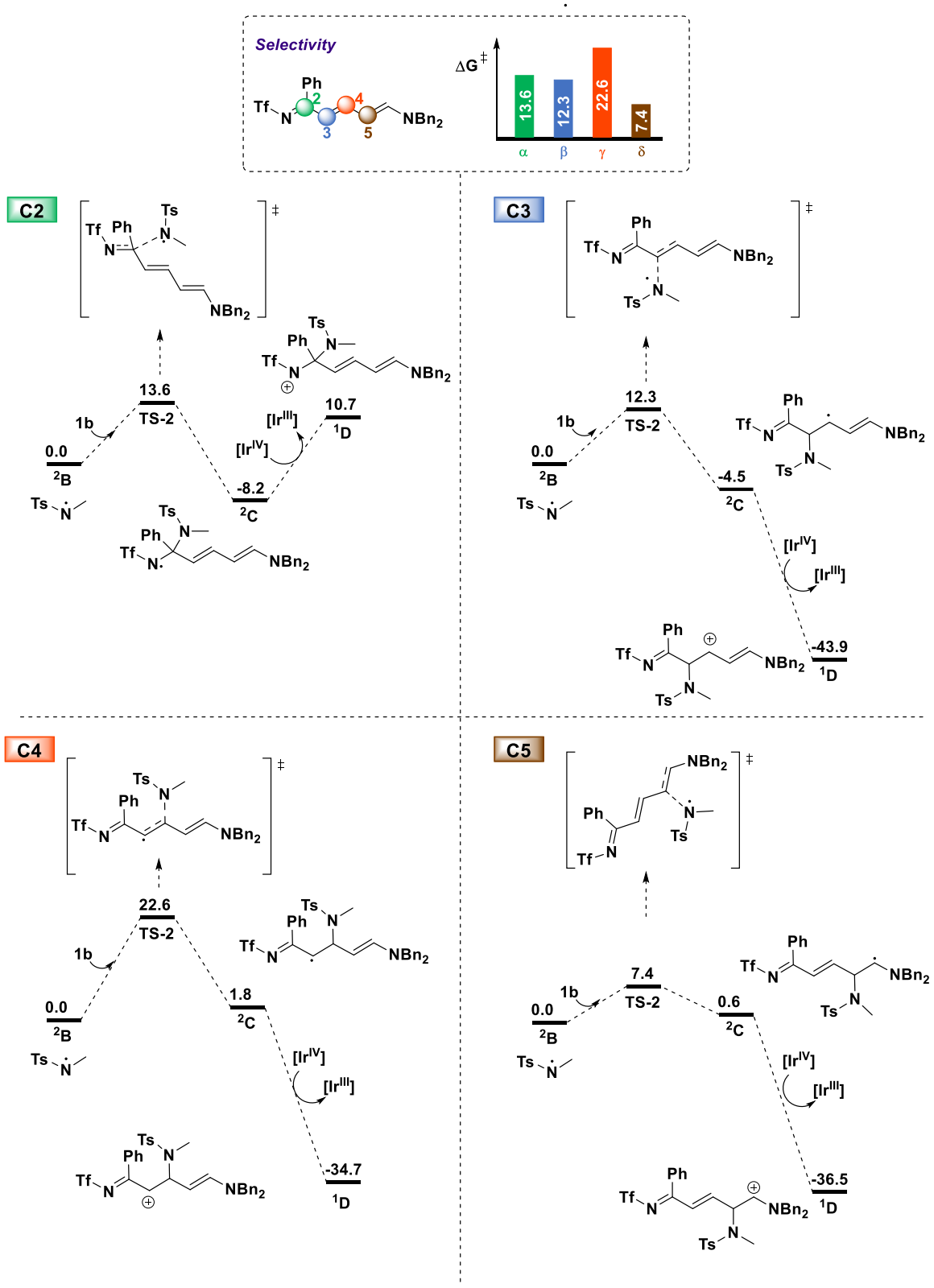

Supplementary Figure 15. *Selective radical addition and Ir-mediated oxidation for C2, C3, C4, and C5 of the Zincke intermediate. Energies in kcal/mol.*

5.3. Ring closing mechanism

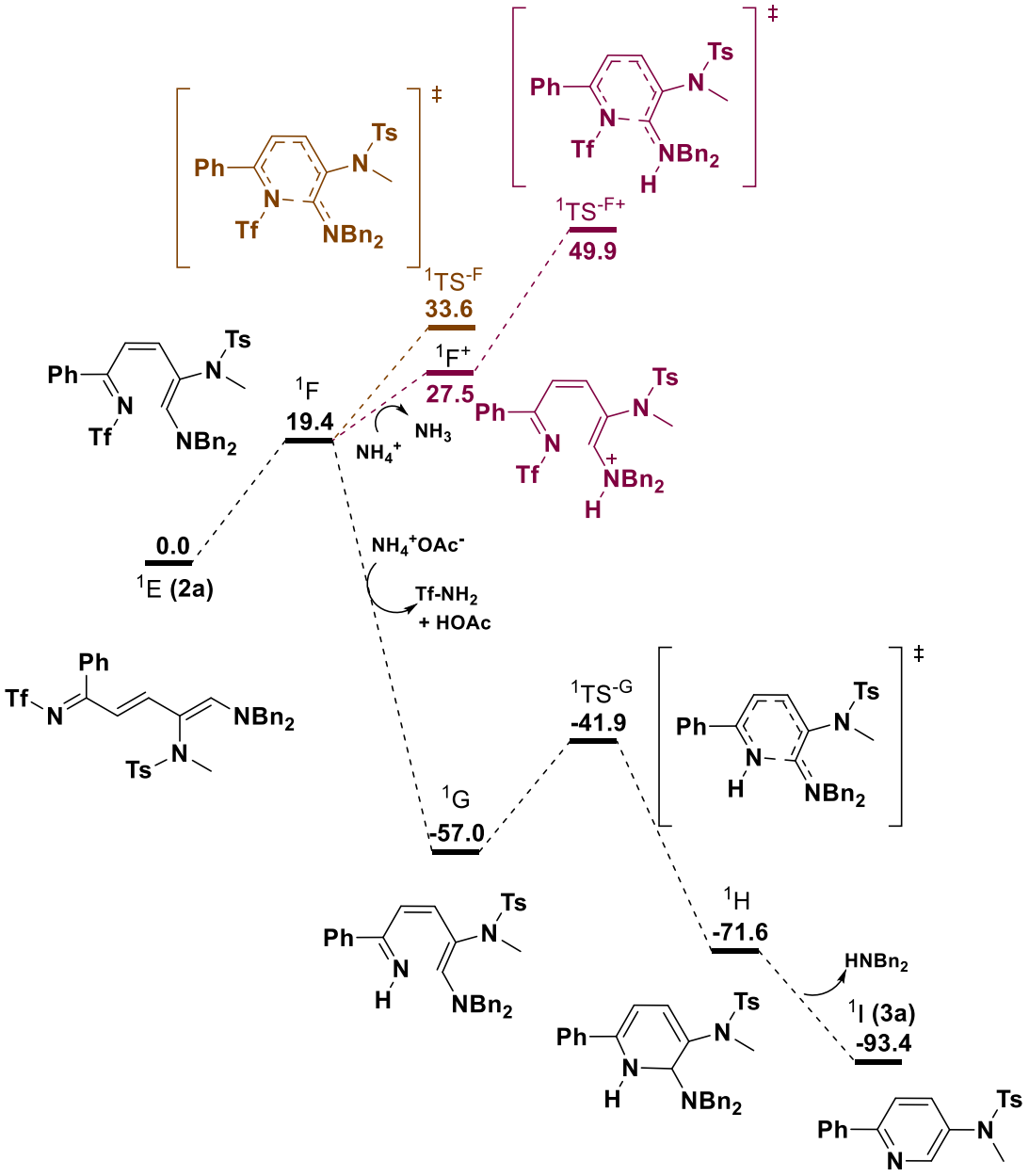

Supplementary Figure 16. *Ring closing free energy profile from 2a to 3a. Energies in kcal/mol.*

5.4. Alkyl vs Aryl selectivity

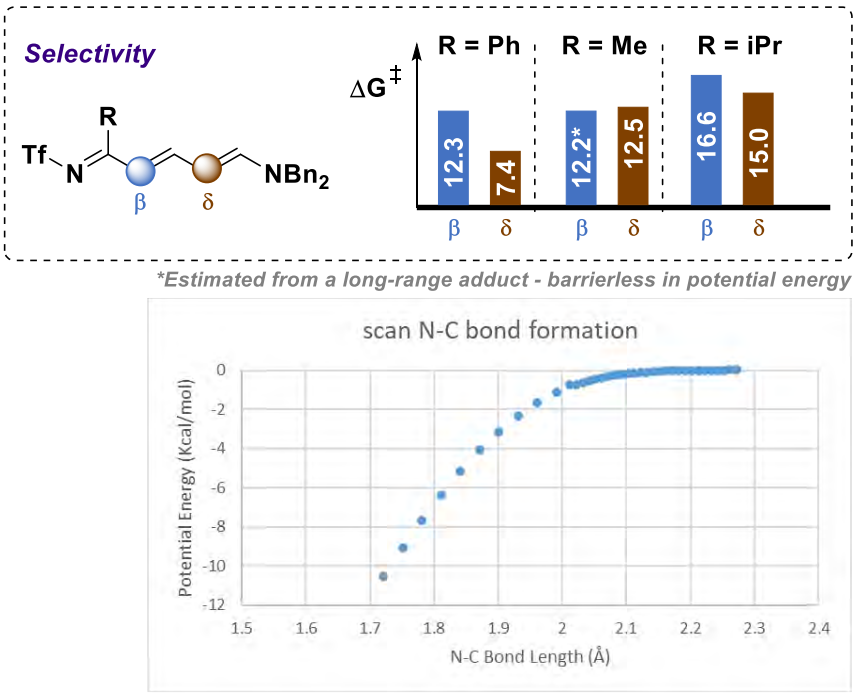

Supplementary Figure 17. *Selectivity of C3 vs C5 of Ph, Me and iPr substituted Zincke imines (top). Relaxed scan of the C-N bond for the C3 functionalization of Me-substituted Zincke imine.*

6. ^{1}H and ^{13}C NMR spectra

6.1. Pyridines

^{1}H NMR spectrum of pyridine S2a ($CDCl_3$, 298 K)

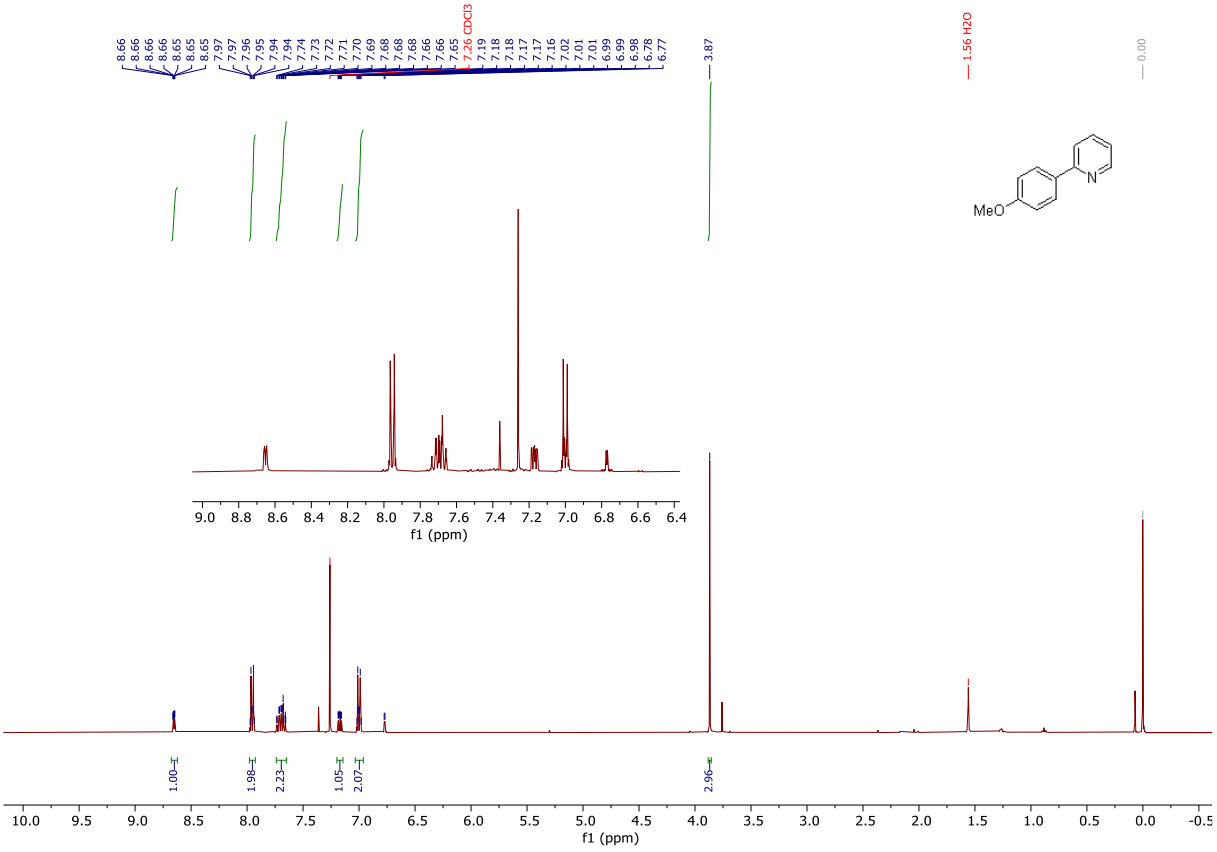

^{1}H NMR spectrum of pyridine S3a ($CDCl_3$, 298 K)

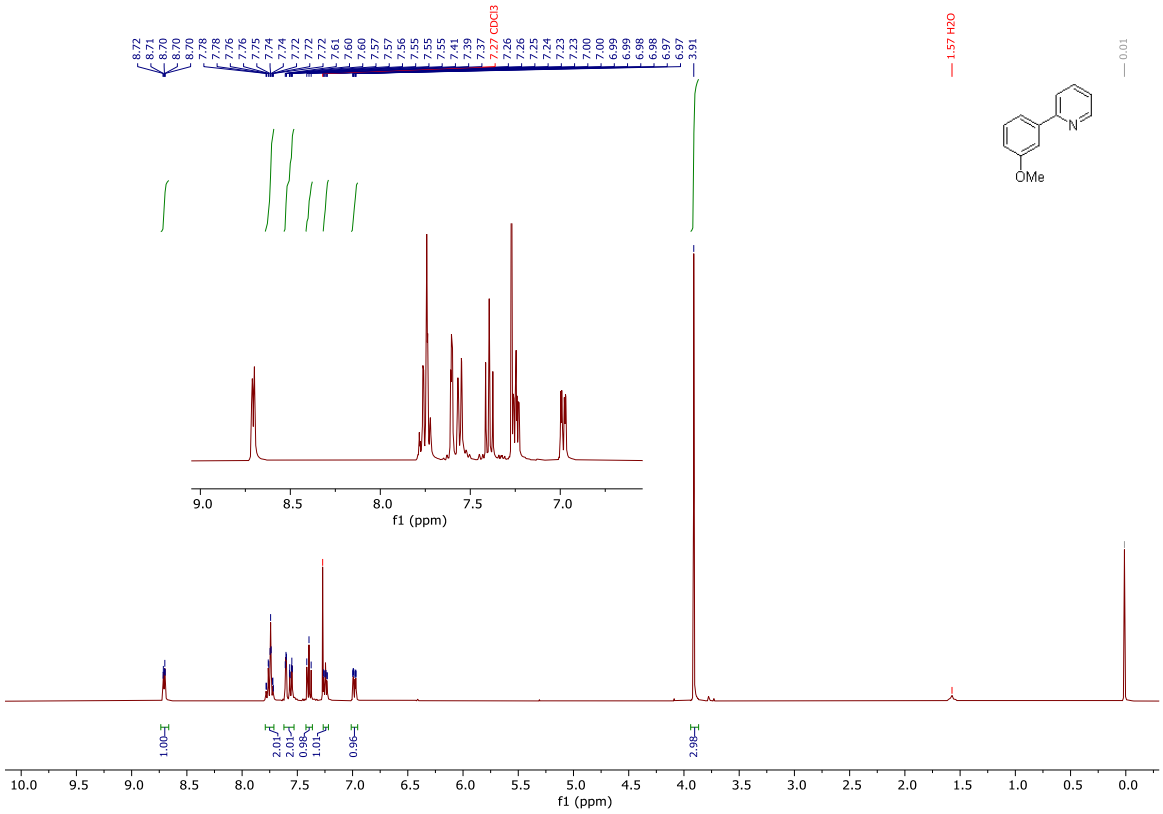

^{1}H NMR spectrum of pyridine S4a ($CDCl_3$, 298 K)

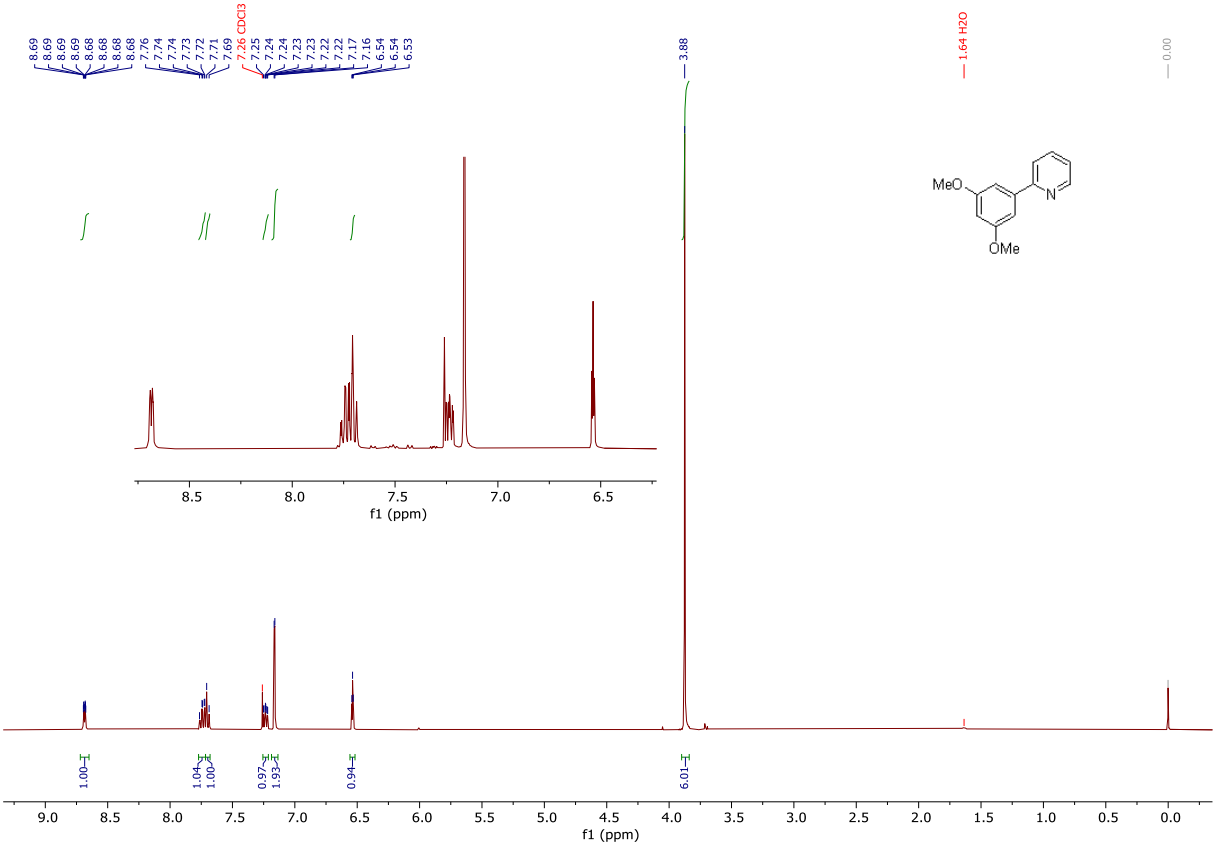

^{1}H NMR spectrum of pyridine S5a ($CDCl_3$, 298 K)

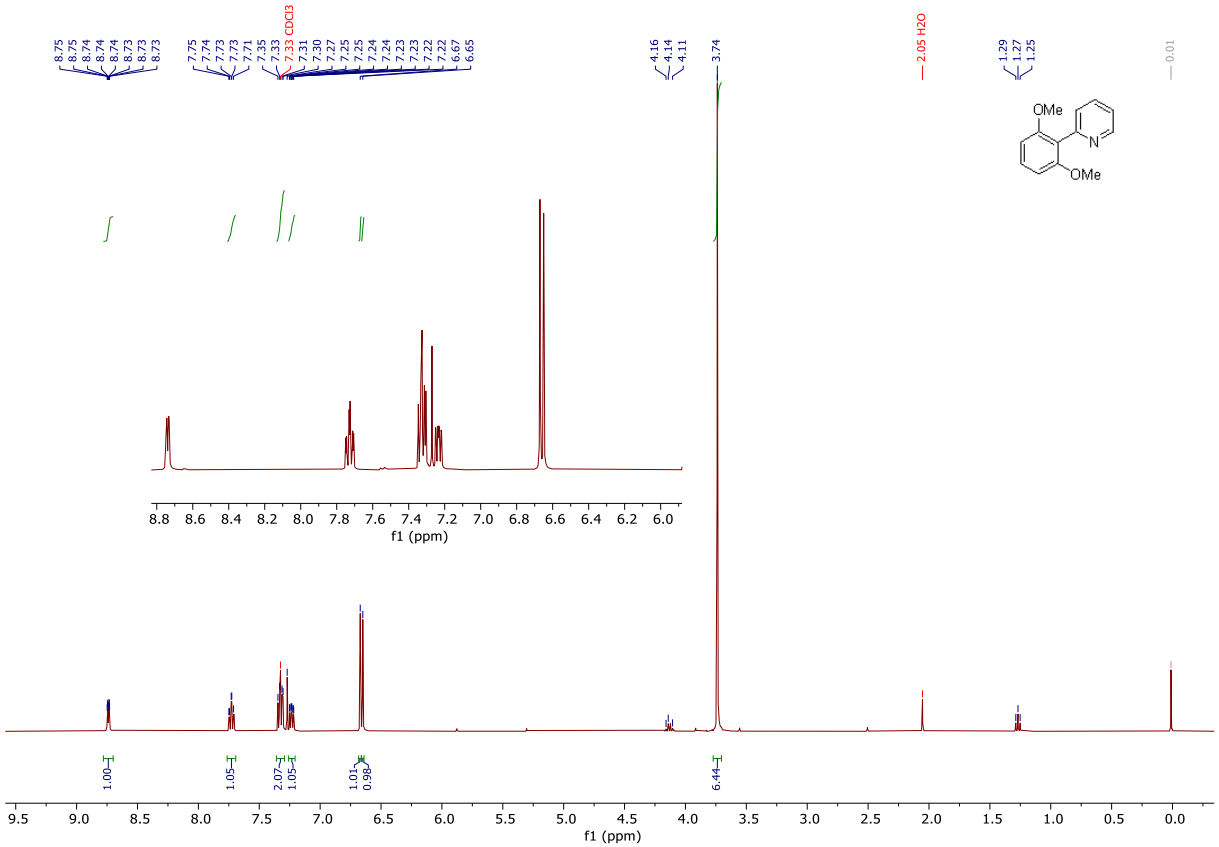

^{1}H NMR spectrum of pyridine S6a ($CDCl_3$, 298 K)

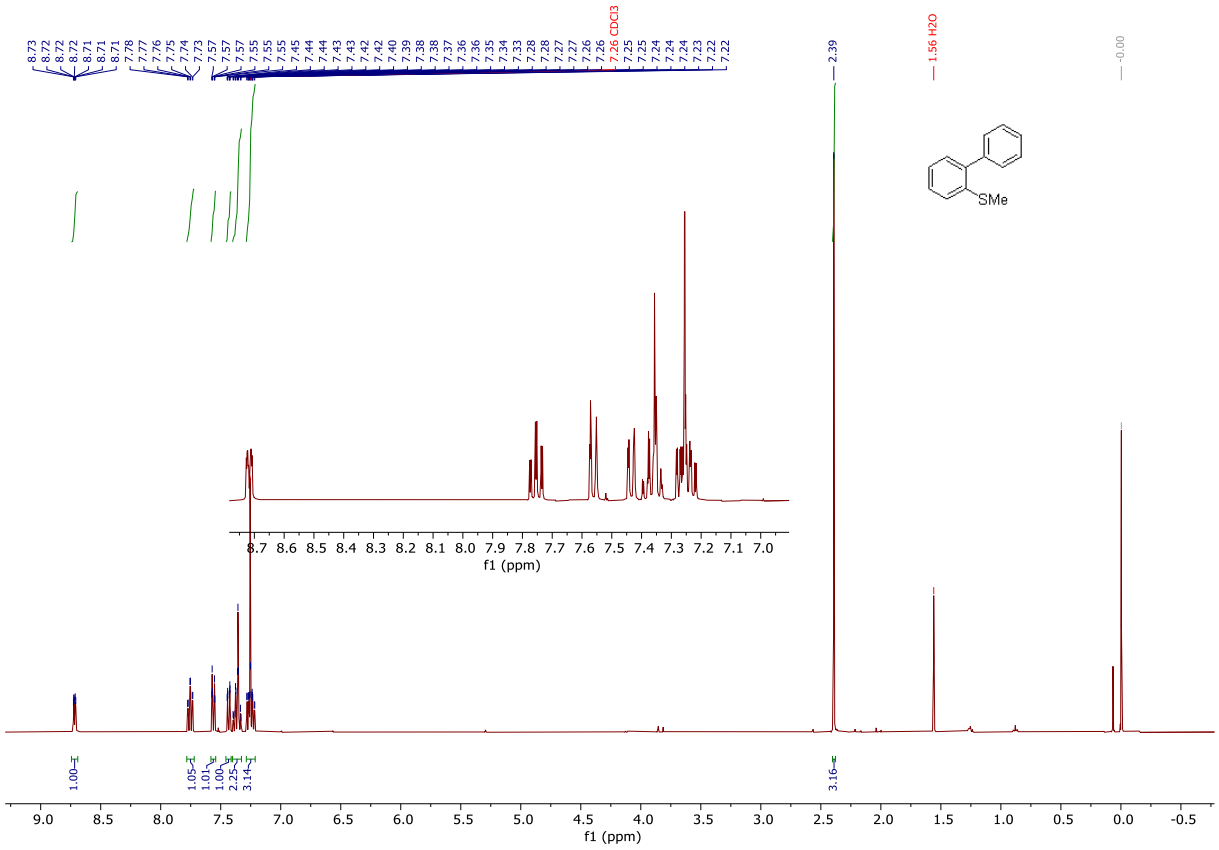

^{1}H NMR spectrum of pyridine S7a ($CDCl_3$, 298 K)

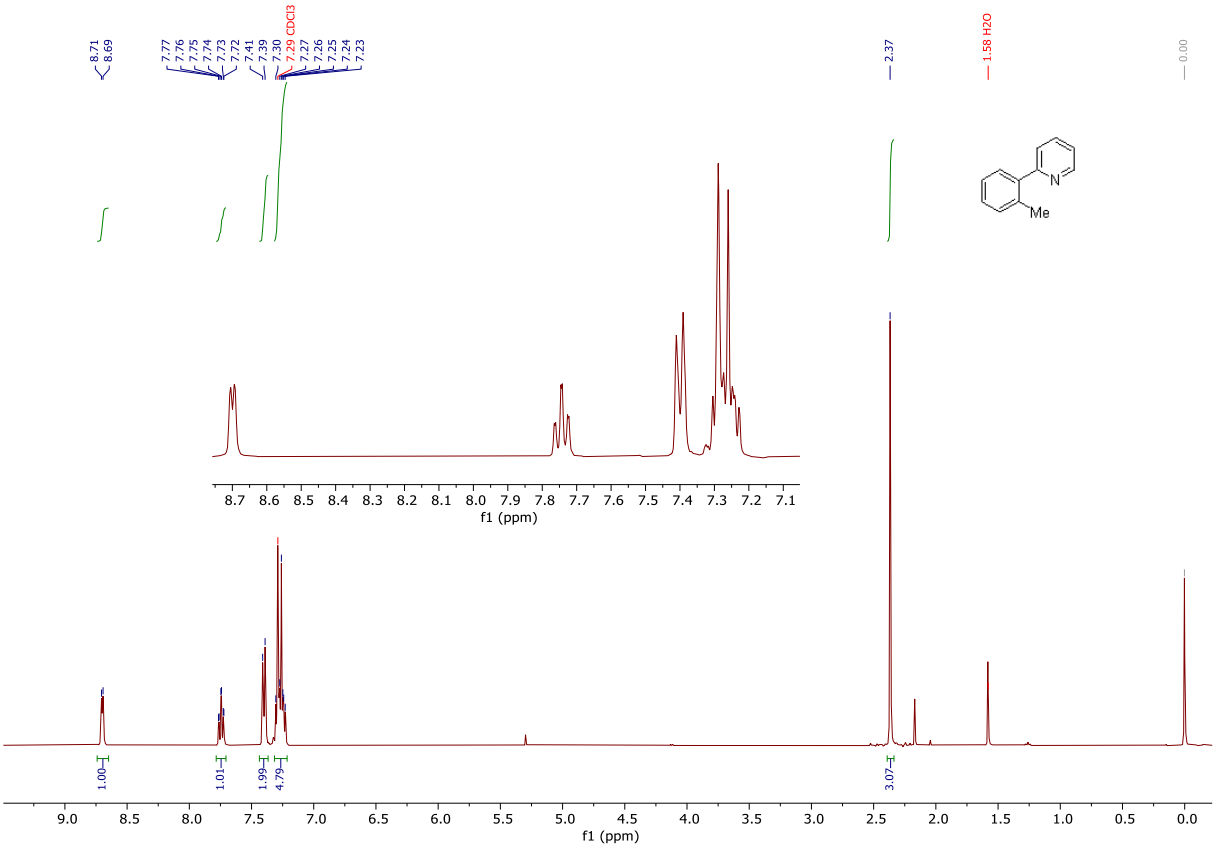

^{1}H NMR spectrum of pyridine S8a ($CDCl_3$, 298 K)

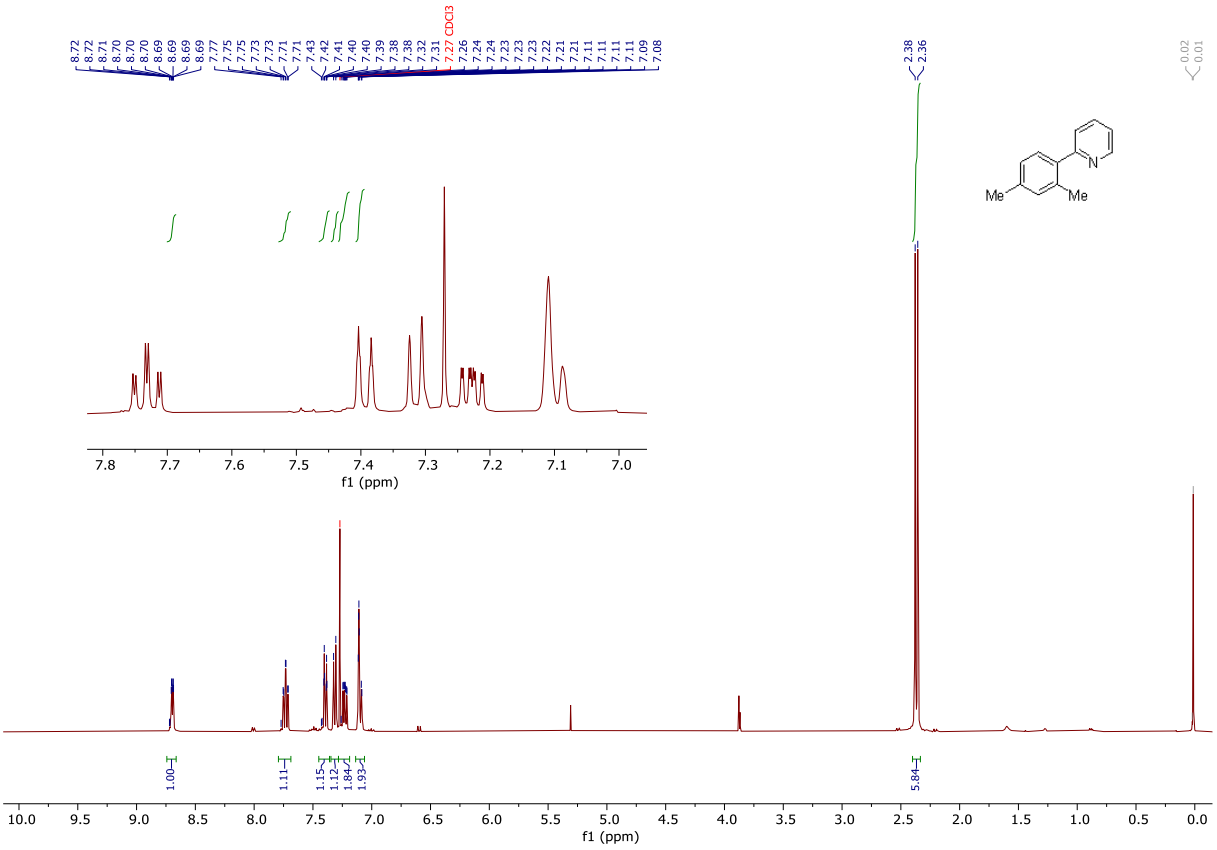

^{1}H NMR spectrum of pyridine S9a ($CDCl_3$, 298 K)

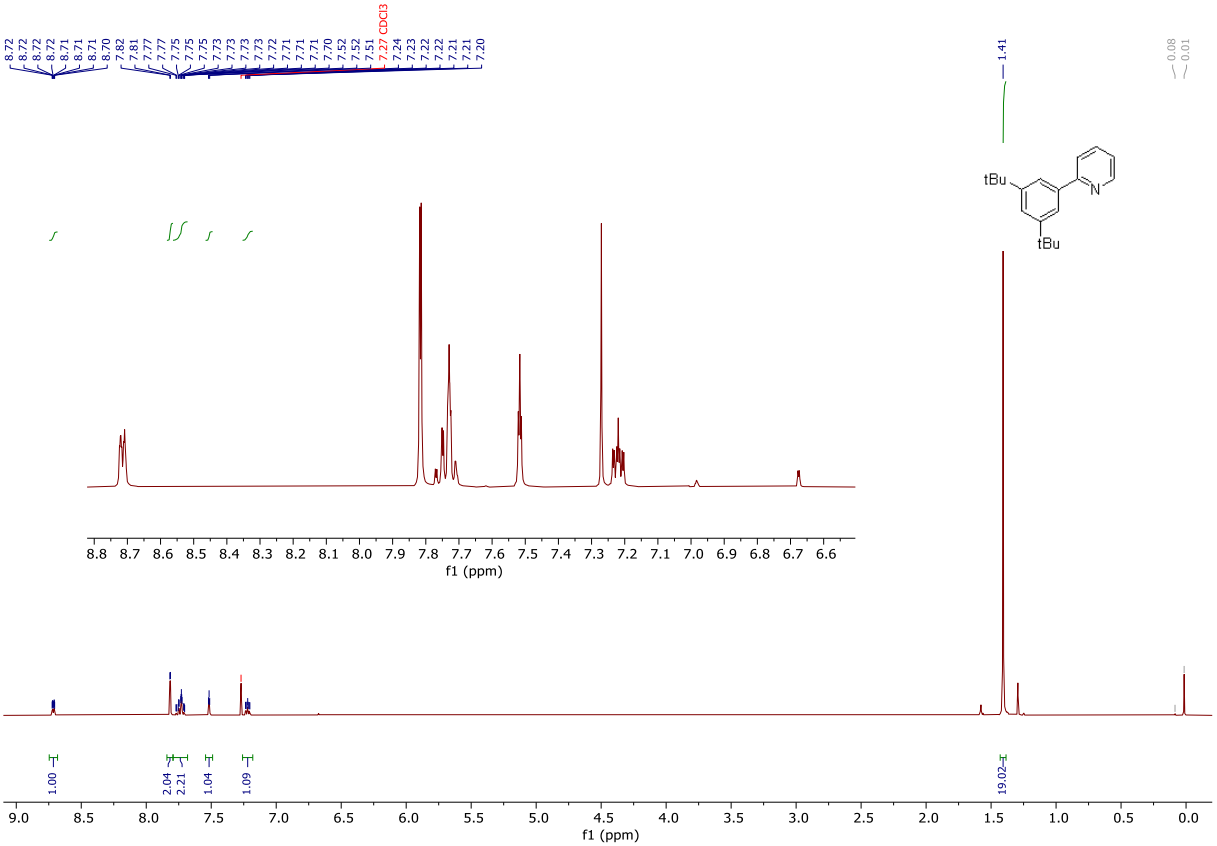

^{1}H NMR spectrum of pyridine S10a ($CDCl_3$, 298 K)

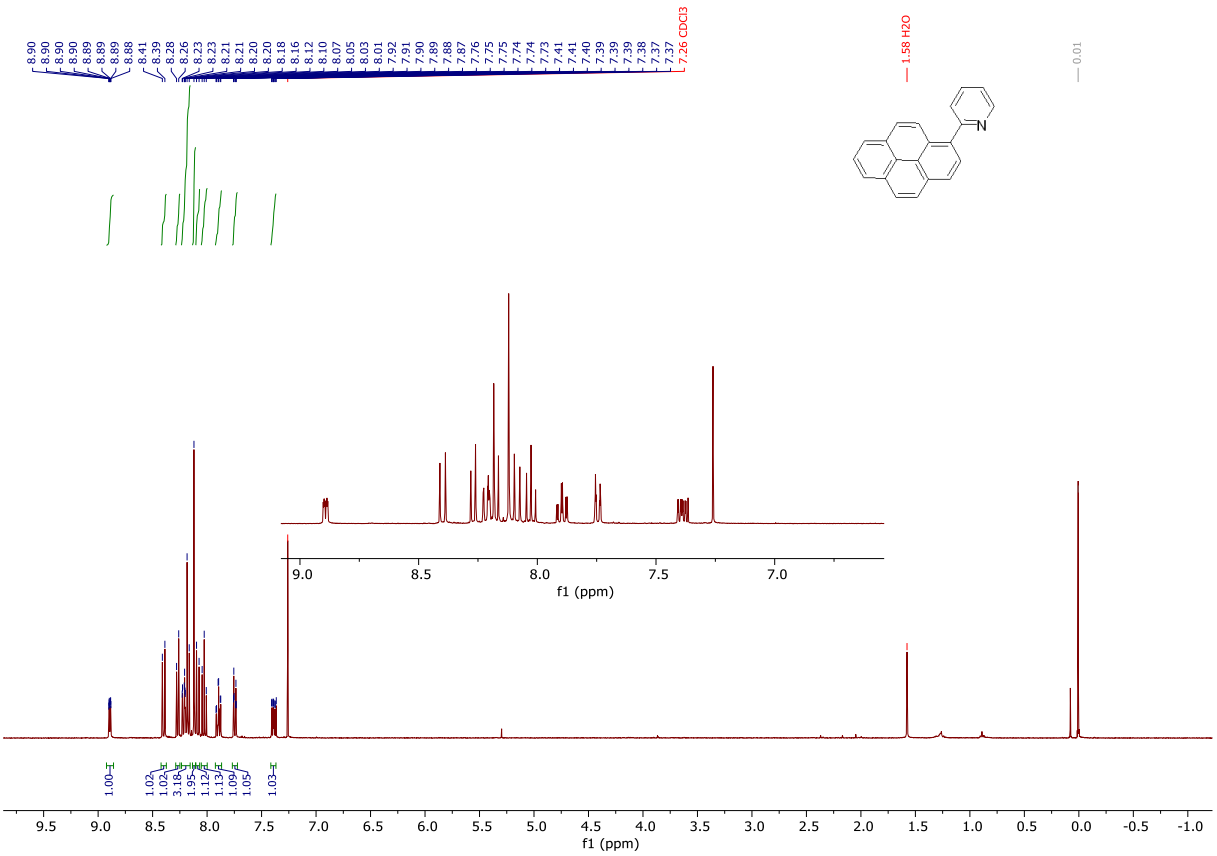

^{1}H NMR spectrum of pyridine S11a ($CDCl_3$, 298 K)

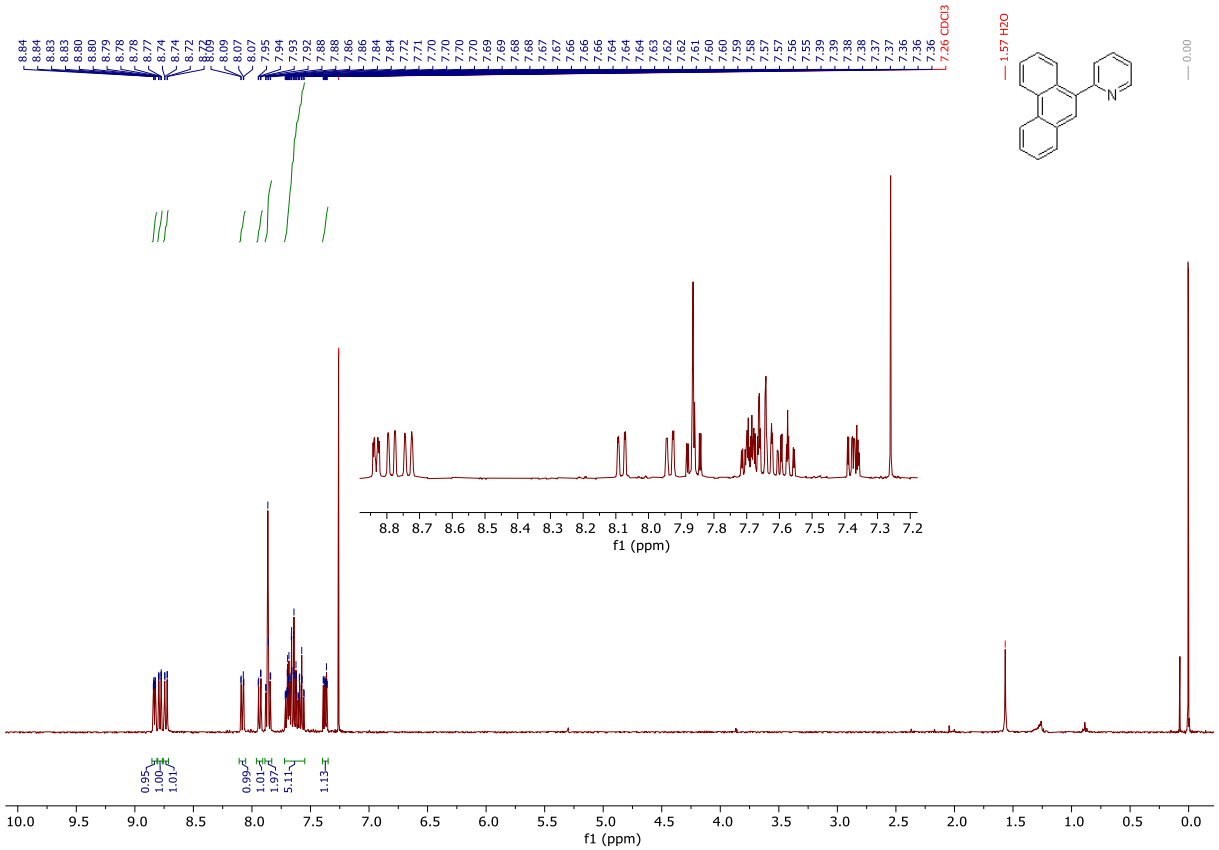

^{1}H NMR spectrum of pyridine S12a ($CDCl_3$, 298 K)

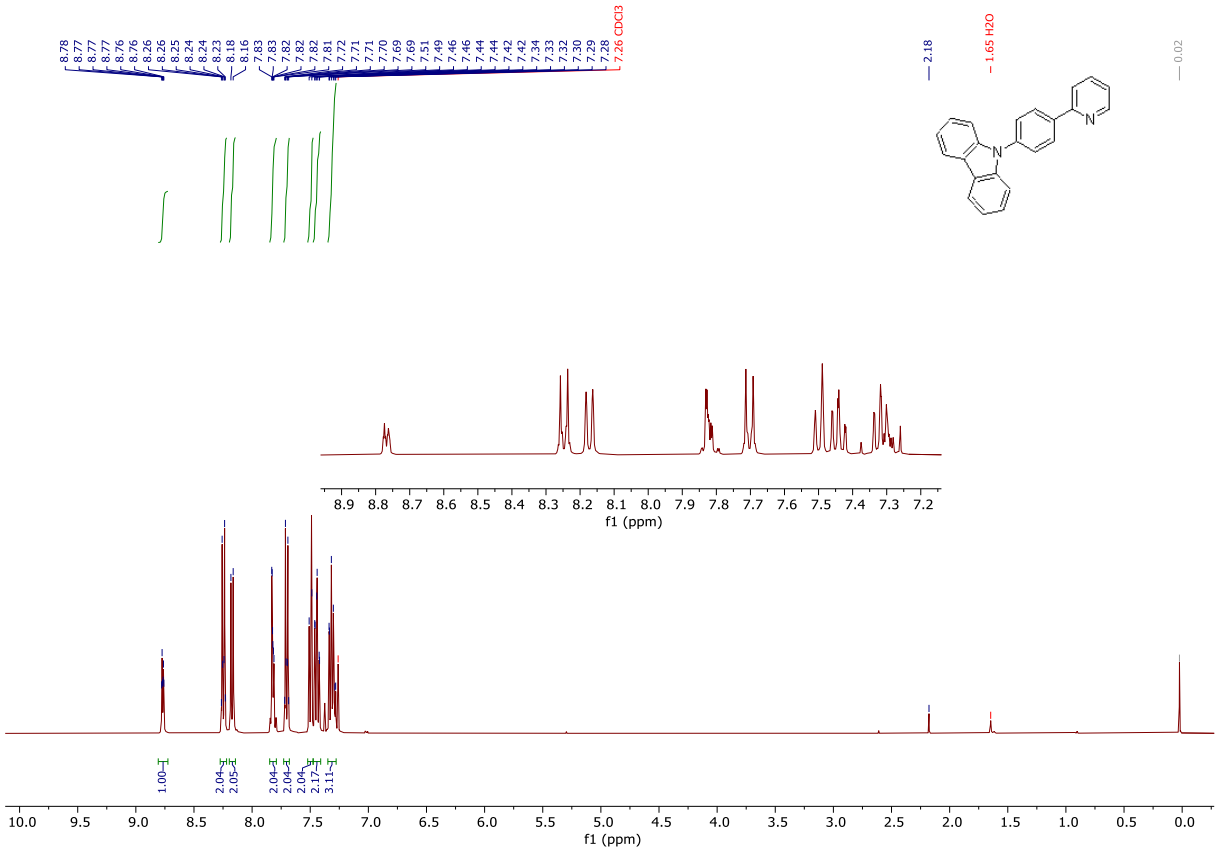

^{1}H NMR spectrum of pyridine S13a ($CDCl_3$, 298 K)

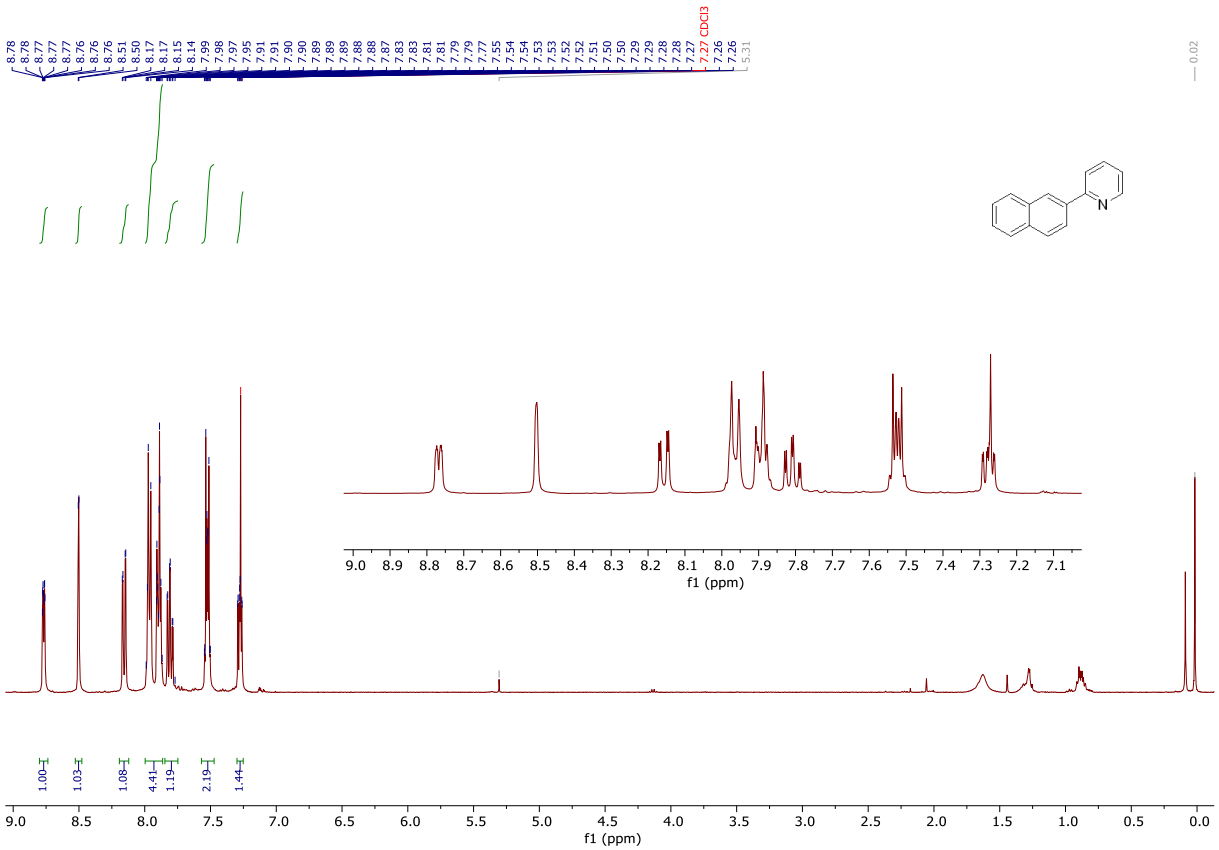

^{1}H NMR spectrum of pyridine S14a ($CDCl_3$, 298 K)

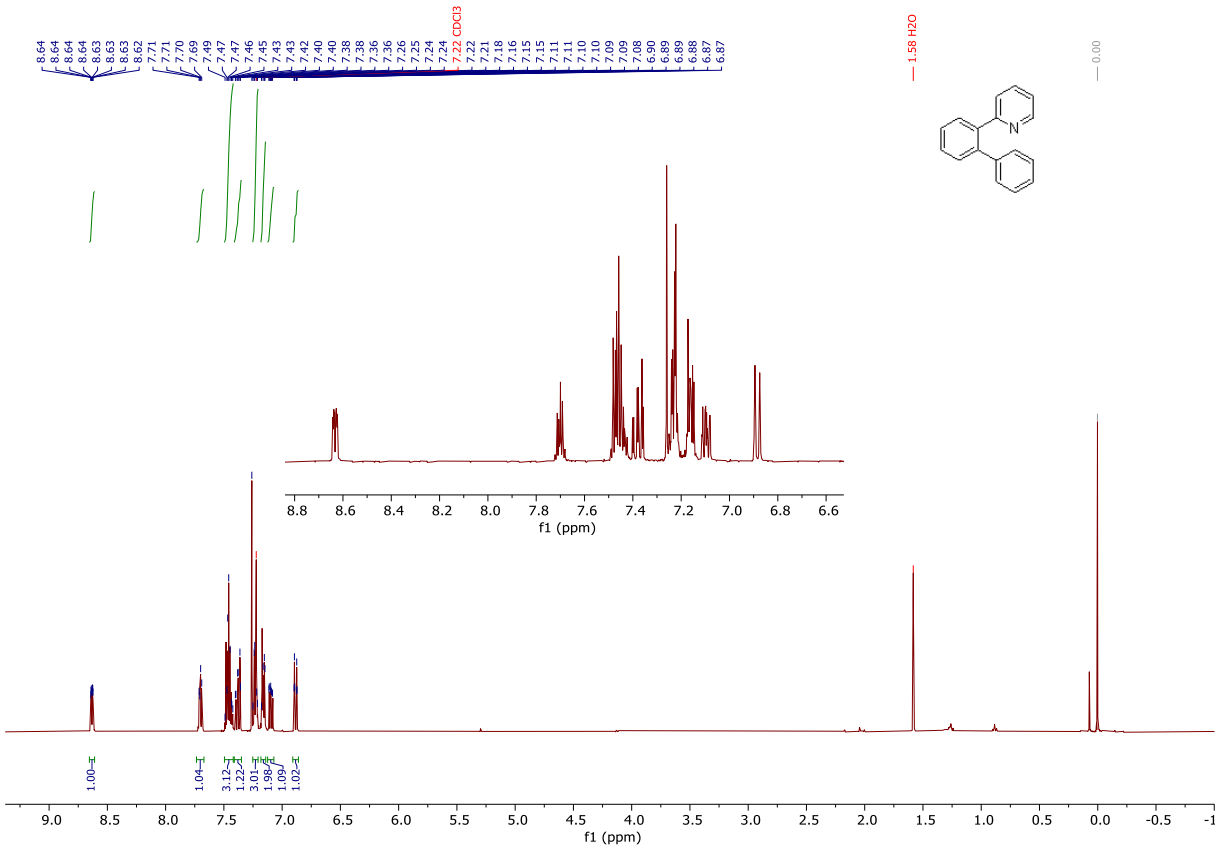

^{1}H NMR spectrum of pyridine S15a ($CDCl_3$, 298 K)

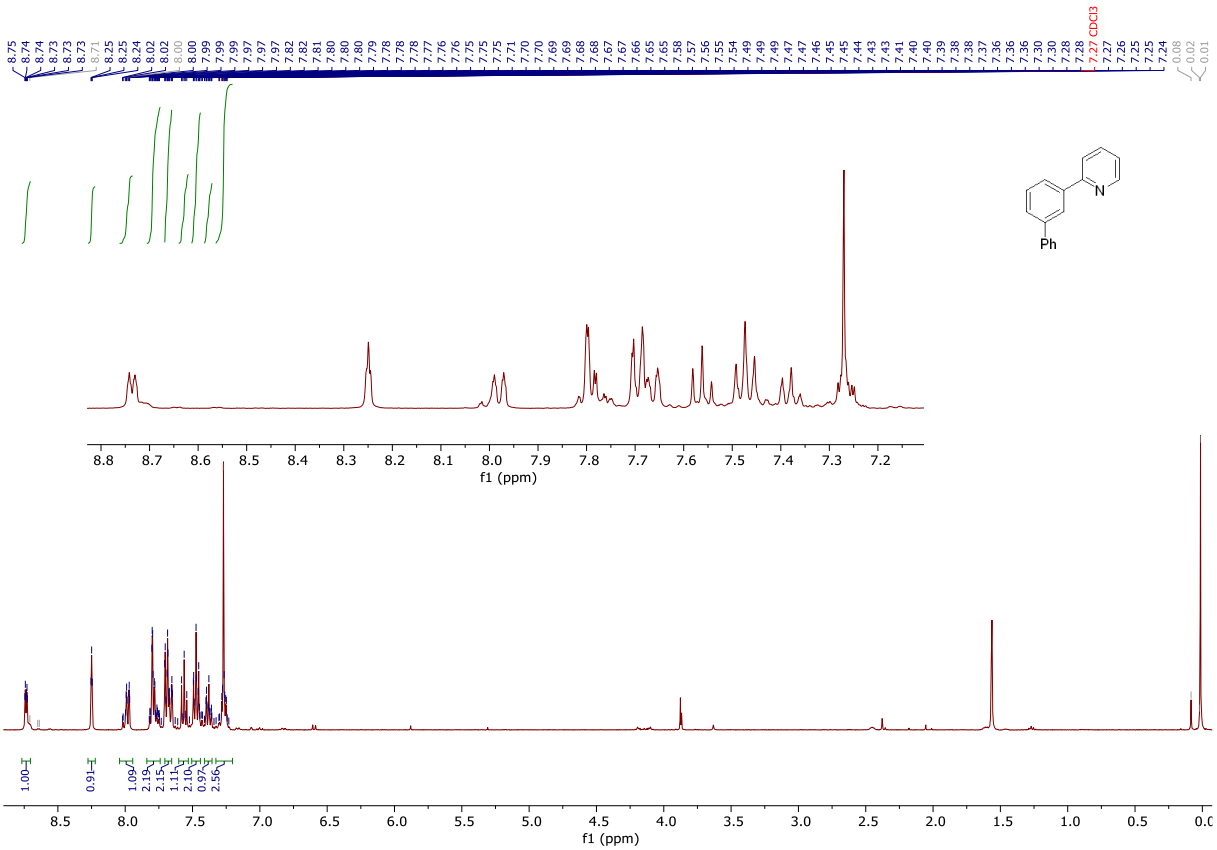

^{1}H NMR spectrum of pyridine S16a ($CDCl_3$, 298 K)

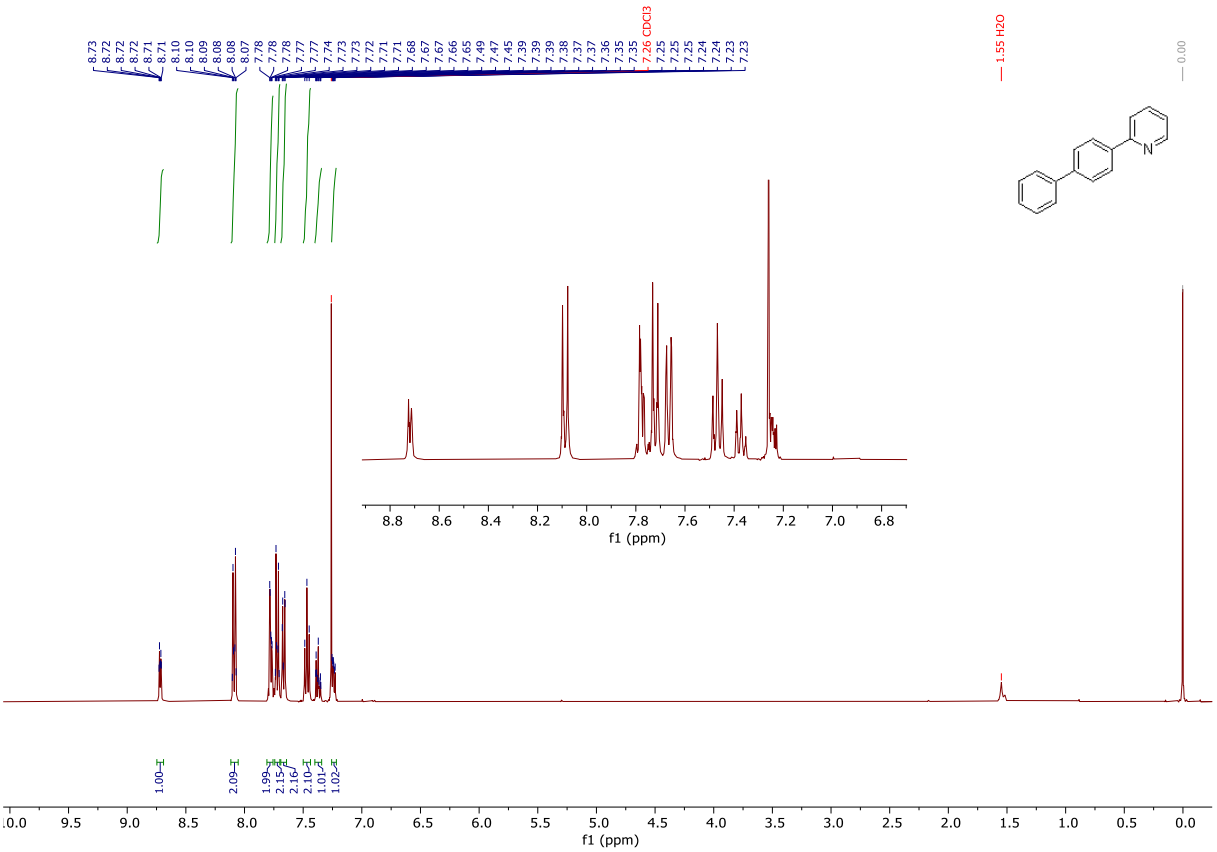

^{1}H NMR spectrum of pyridine S17a ($CDCl_3$, 298 K)

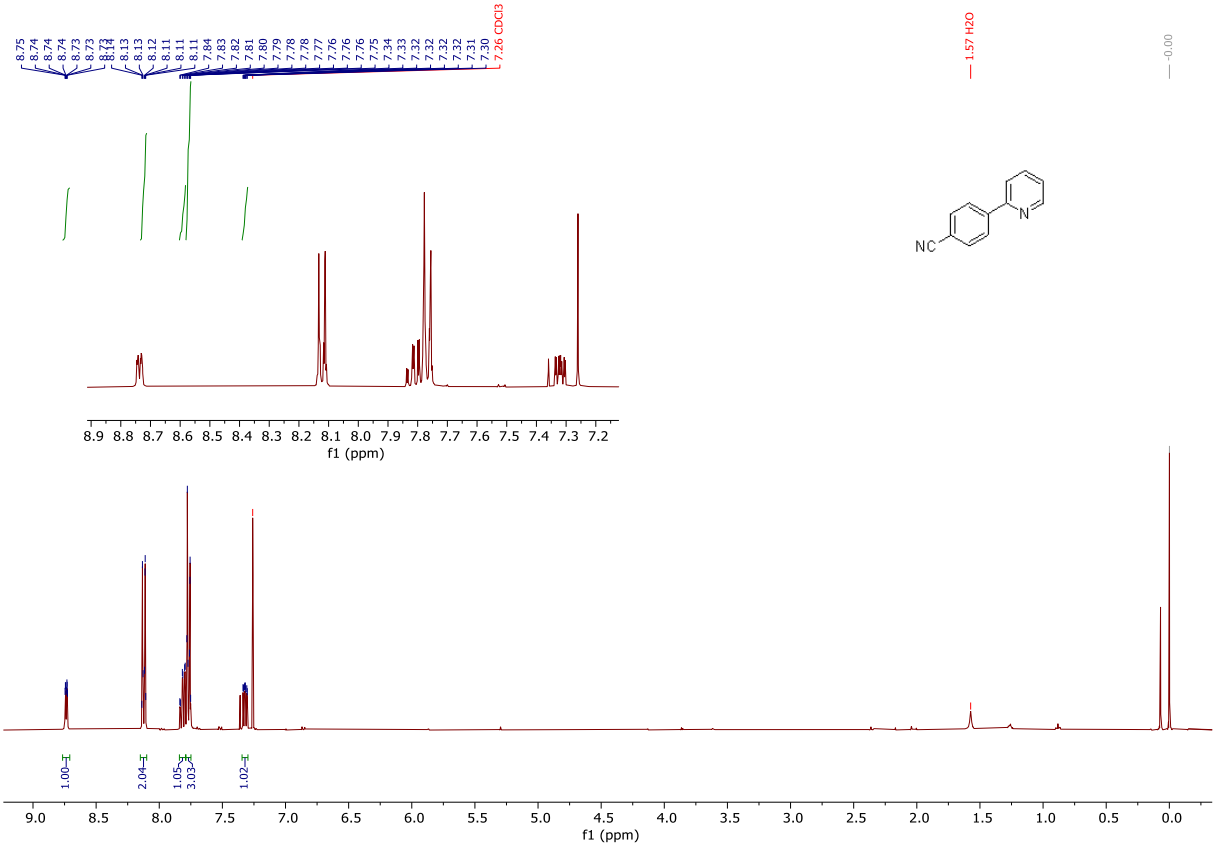

^{1}H NMR spectrum of pyridine S18a ($CDCl_3$, 298 K)

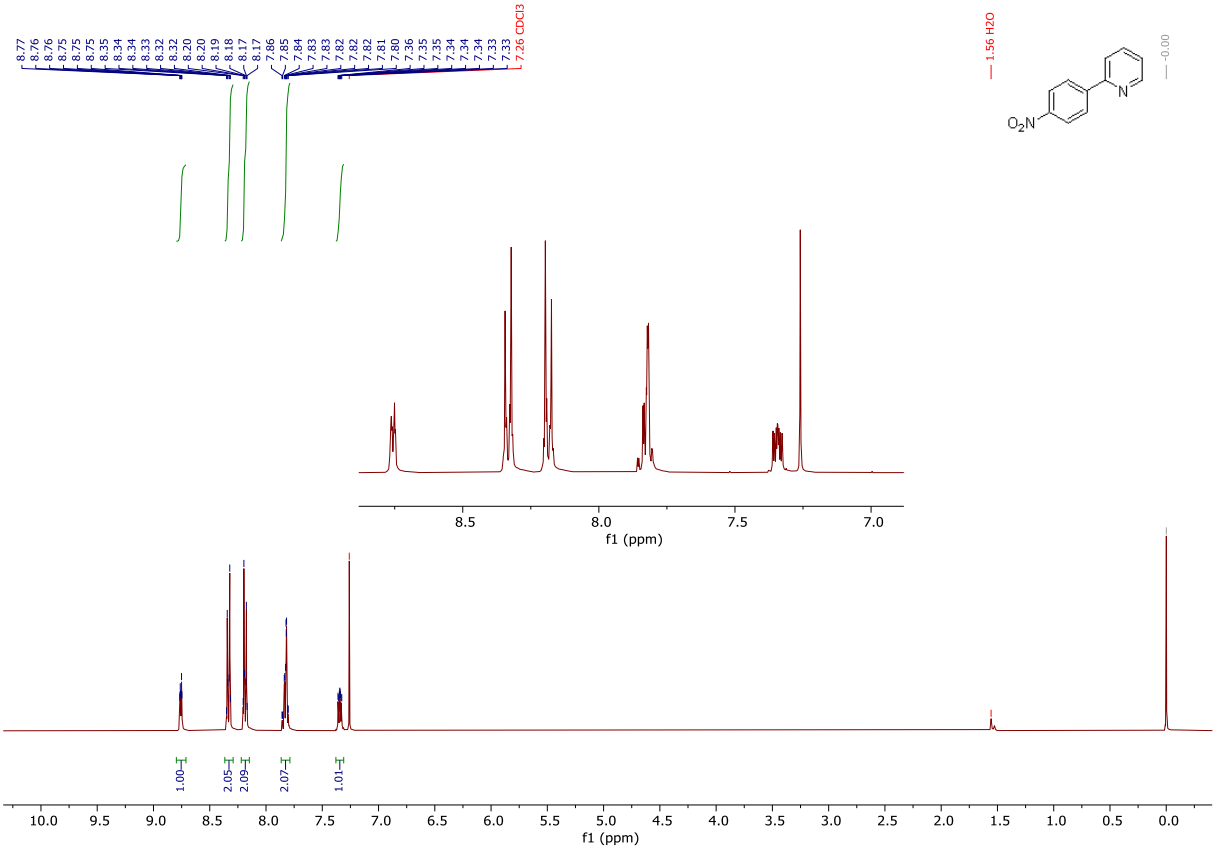

^{1}H NMR spectrum of pyridine S19a ($CDCl_3$, 298 K)

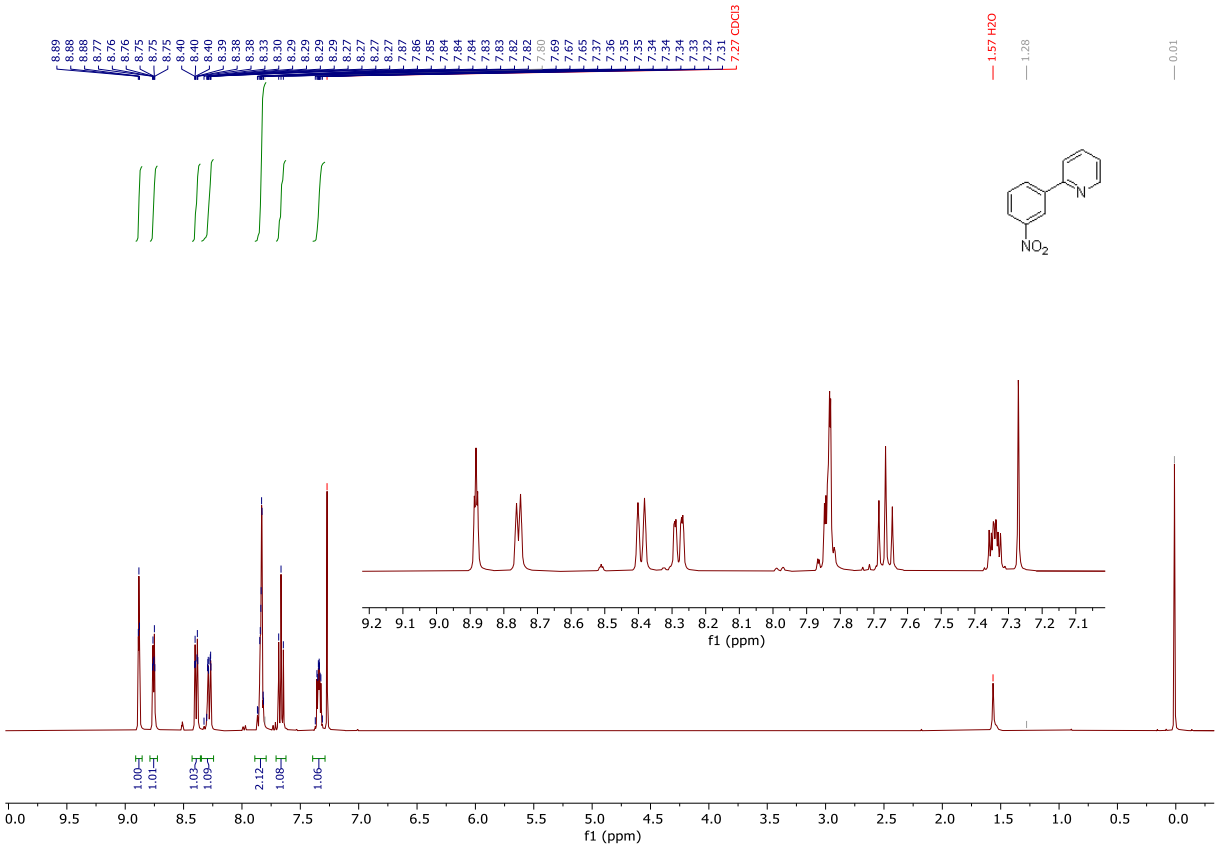

^{1}H NMR spectrum of pyridine S20a ($CDCl_3$, 298 K)

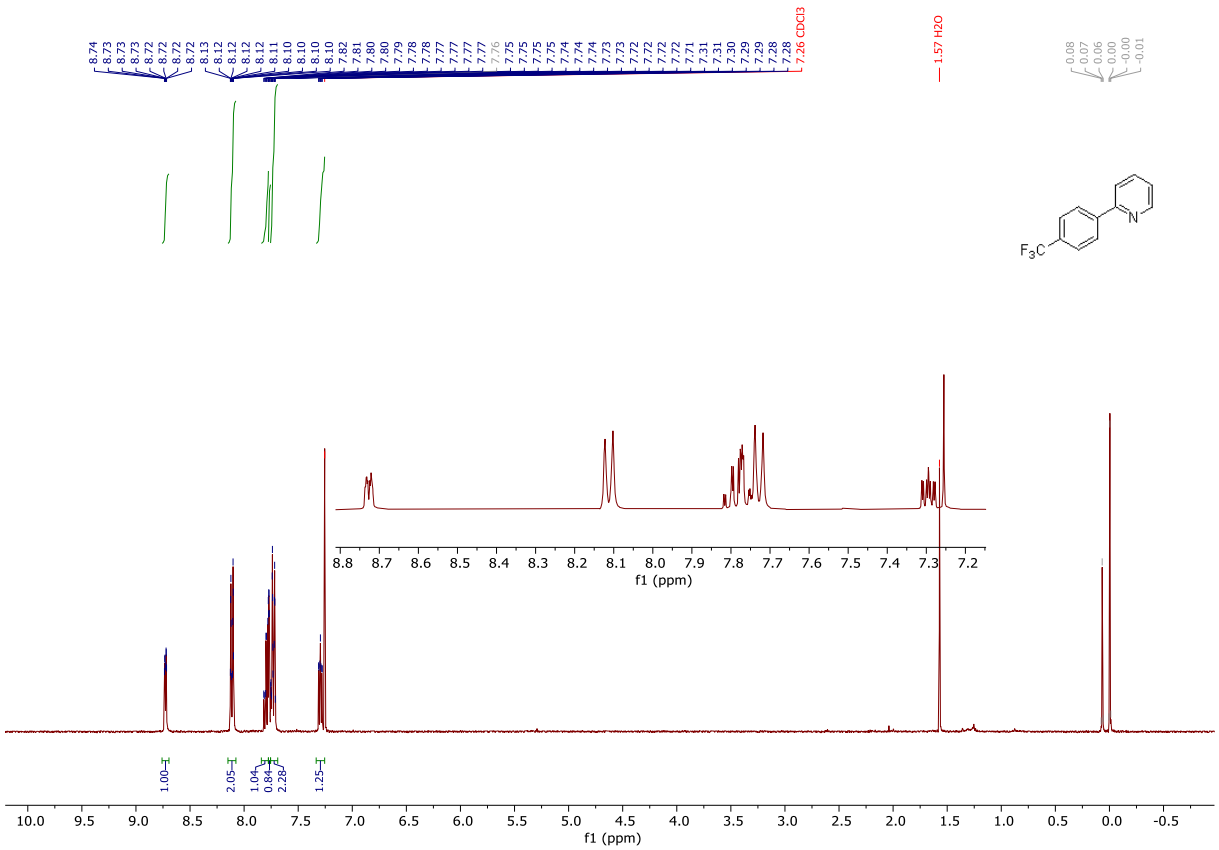

^{1}H NMR spectrum of pyridine S21a ($CDCl_3$, 298 K)

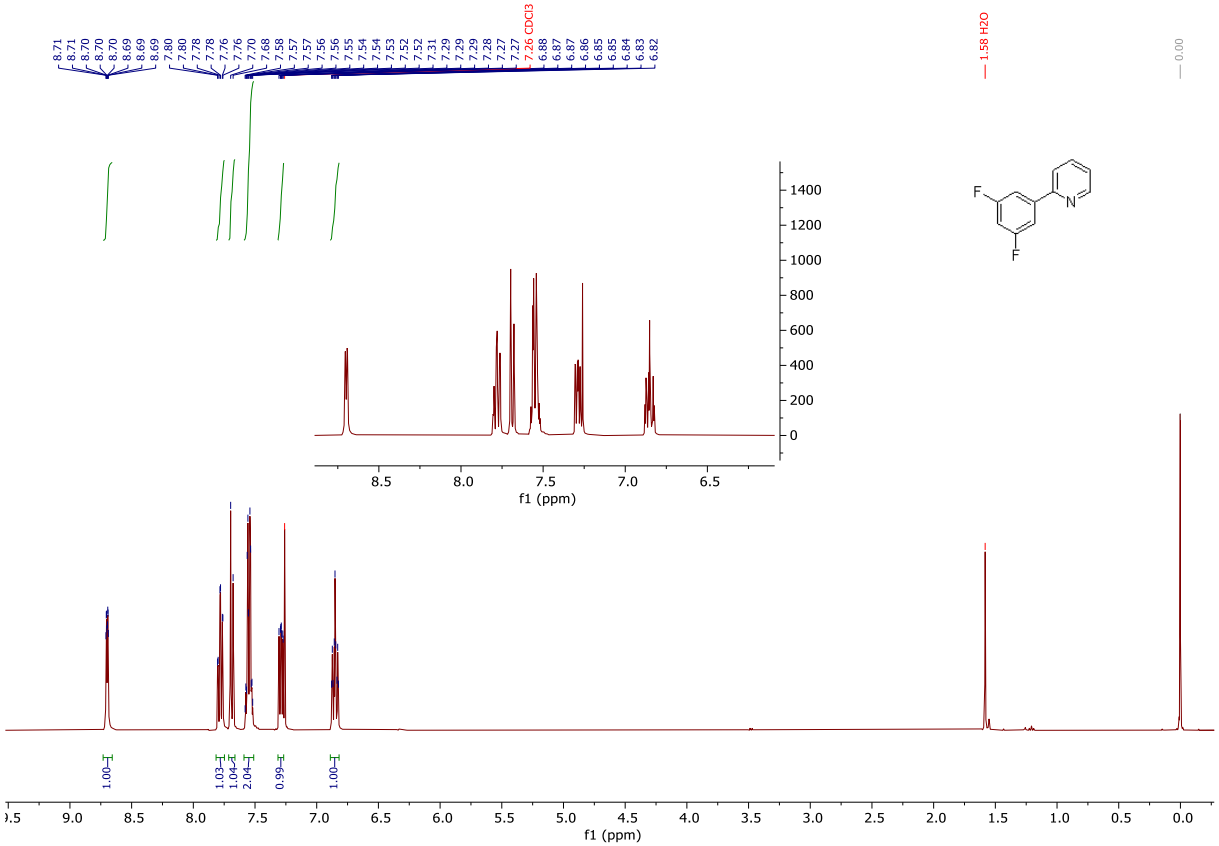

^{1}H NMR spectrum of pyridine S22a ($CDCl_3$, 298 K)

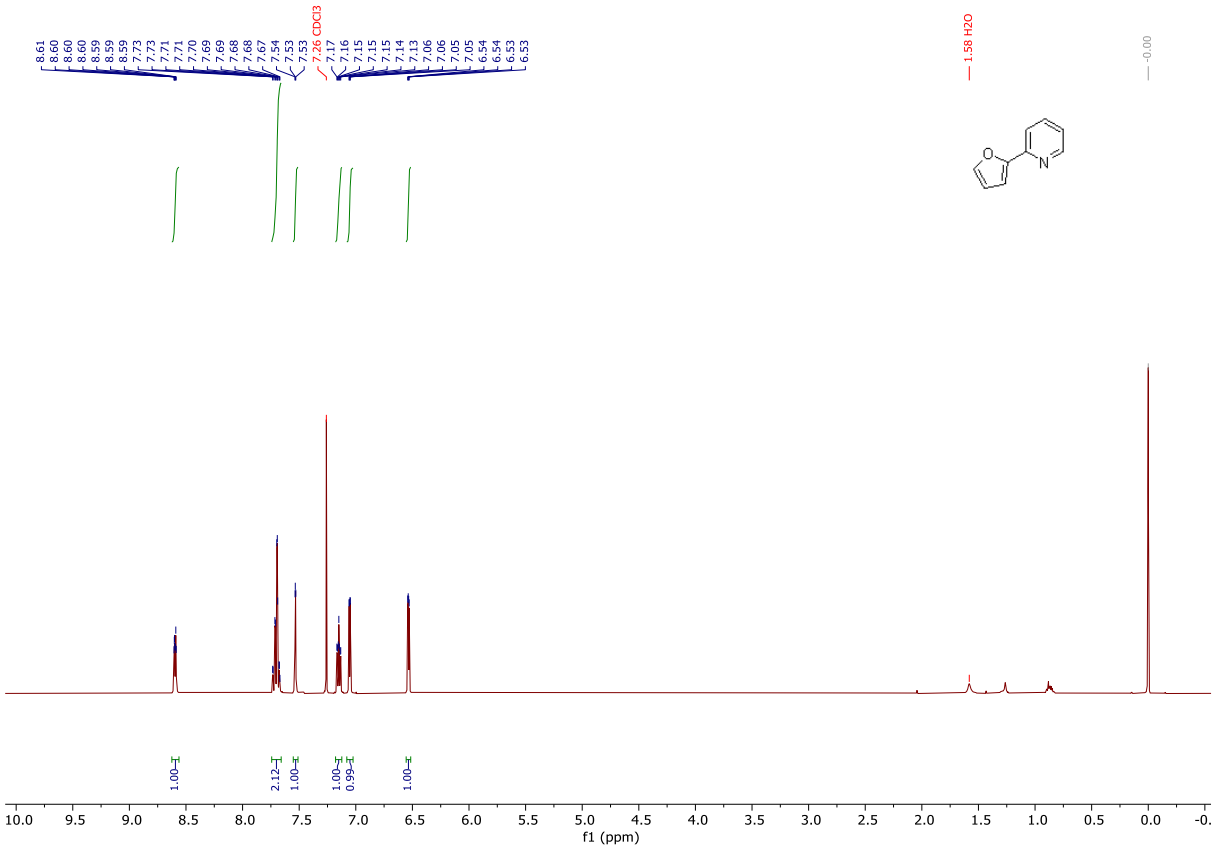

^{1}H NMR spectrum of pyridine S23a ($CDCl_3$, 298 K)

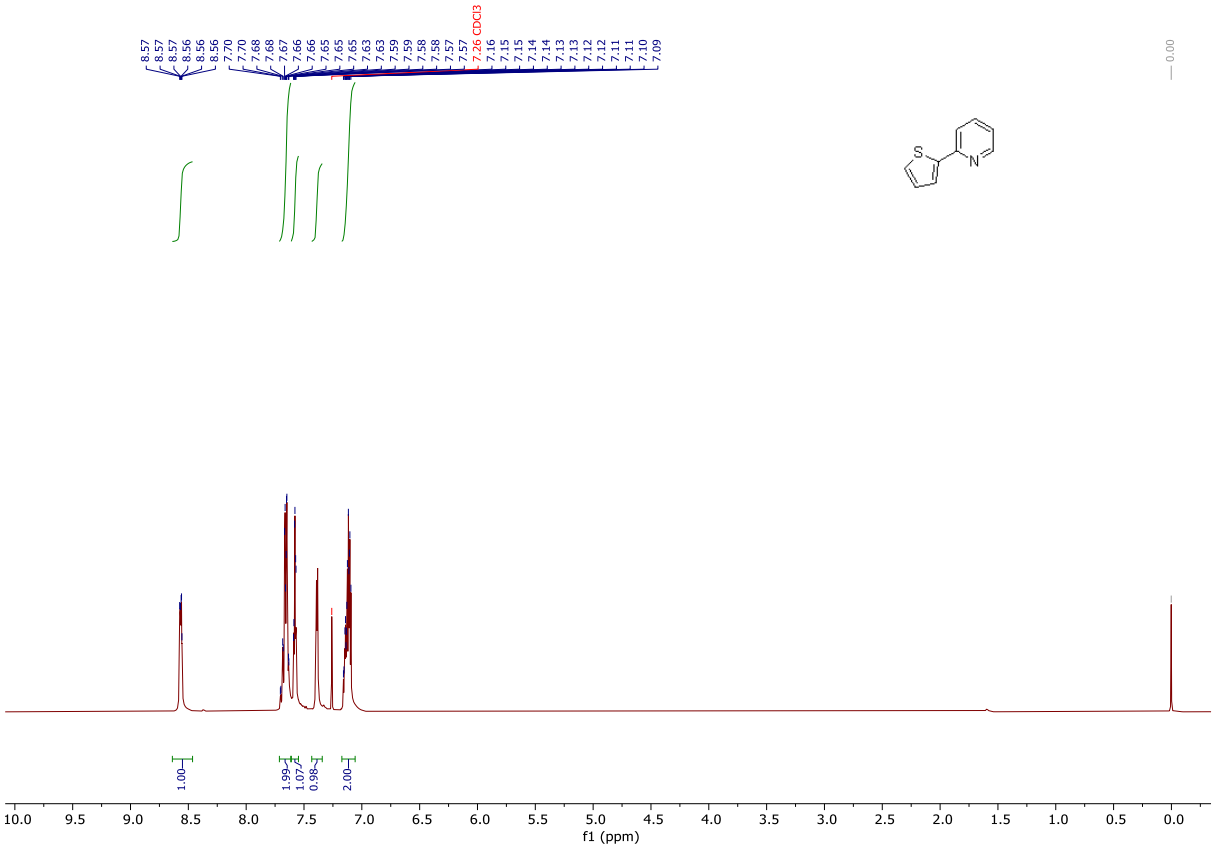

^{1}H NMR spectrum of pyridine S24a ($CDCl_3$, 298 K)

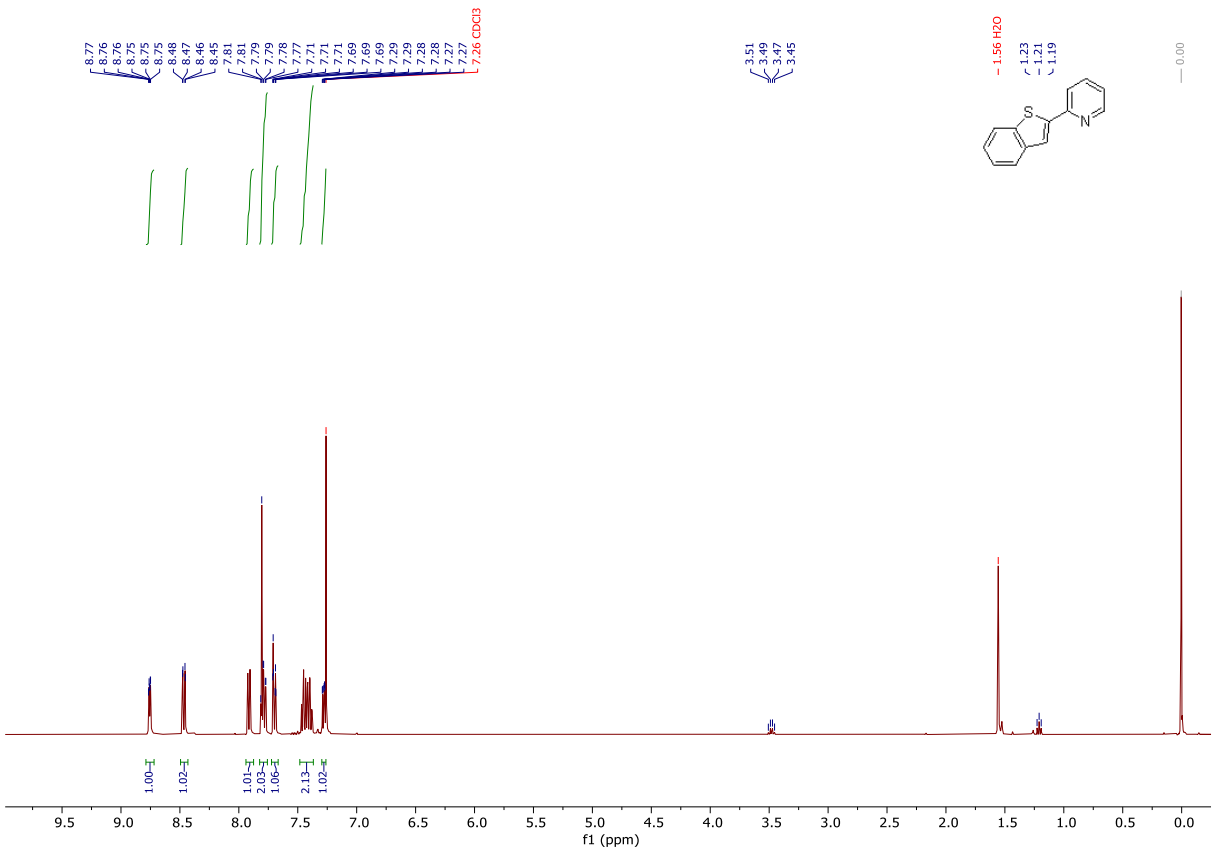

^{1}H NMR spectrum of pyridine S25a ($CDCl_3$, 298 K)

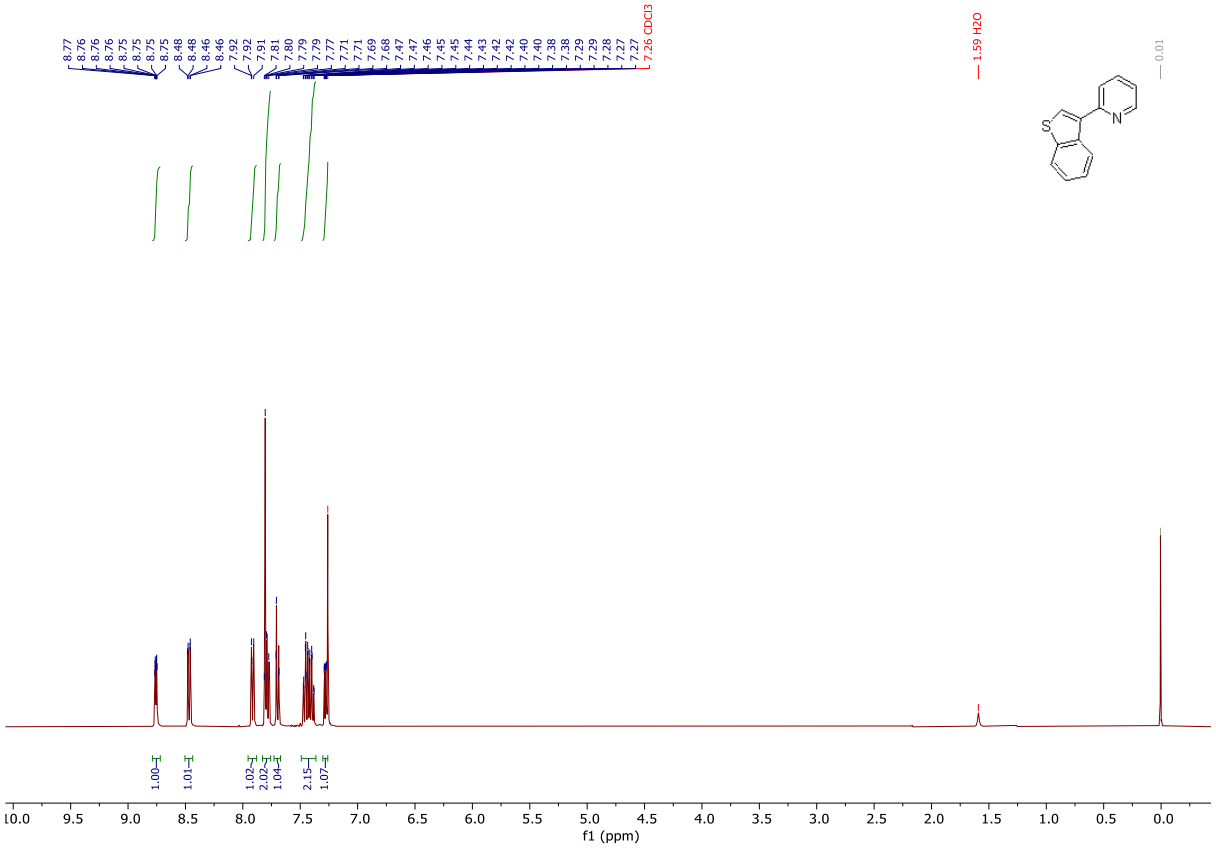

^{1}H NMR spectrum of pyridine S26a ($CDCl_3$, 298 K)

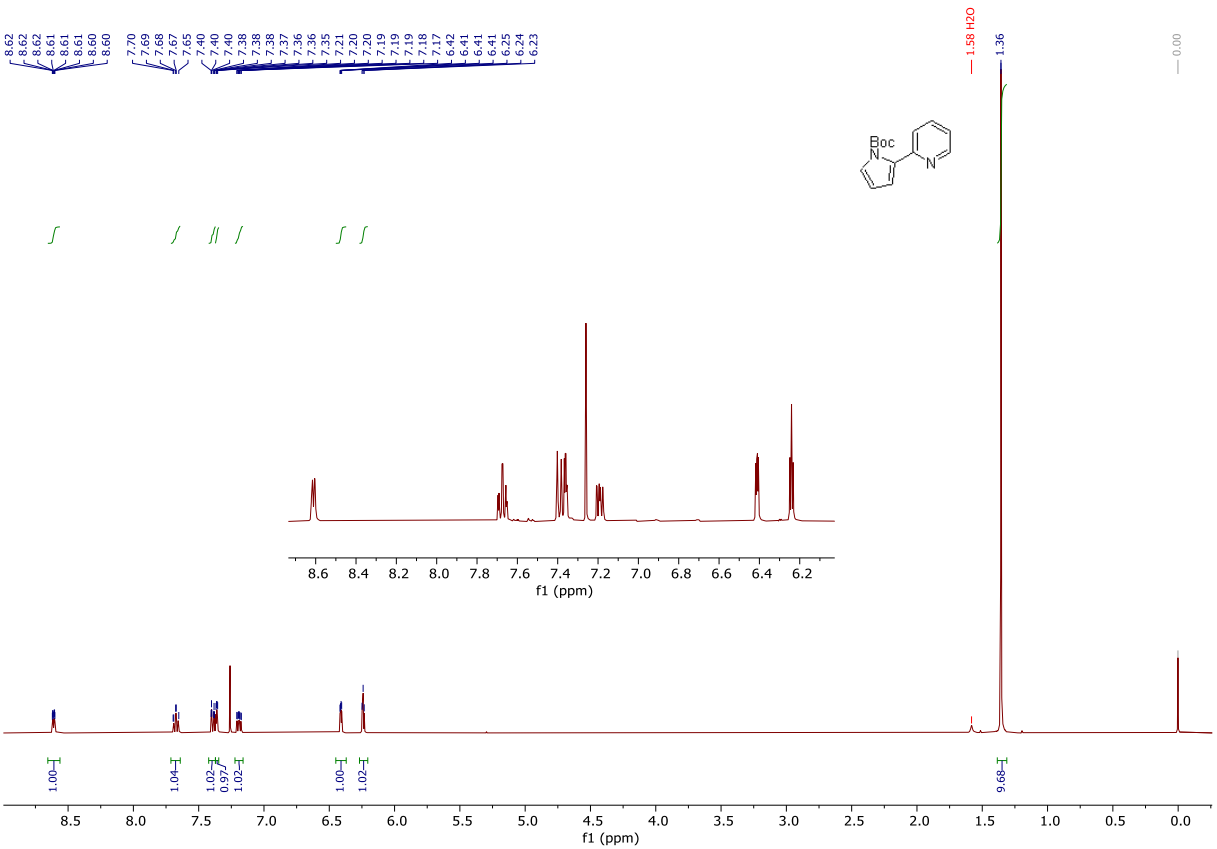

^{1}H NMR spectrum of pyridine S27a ($CDCl_3$, 298 K)

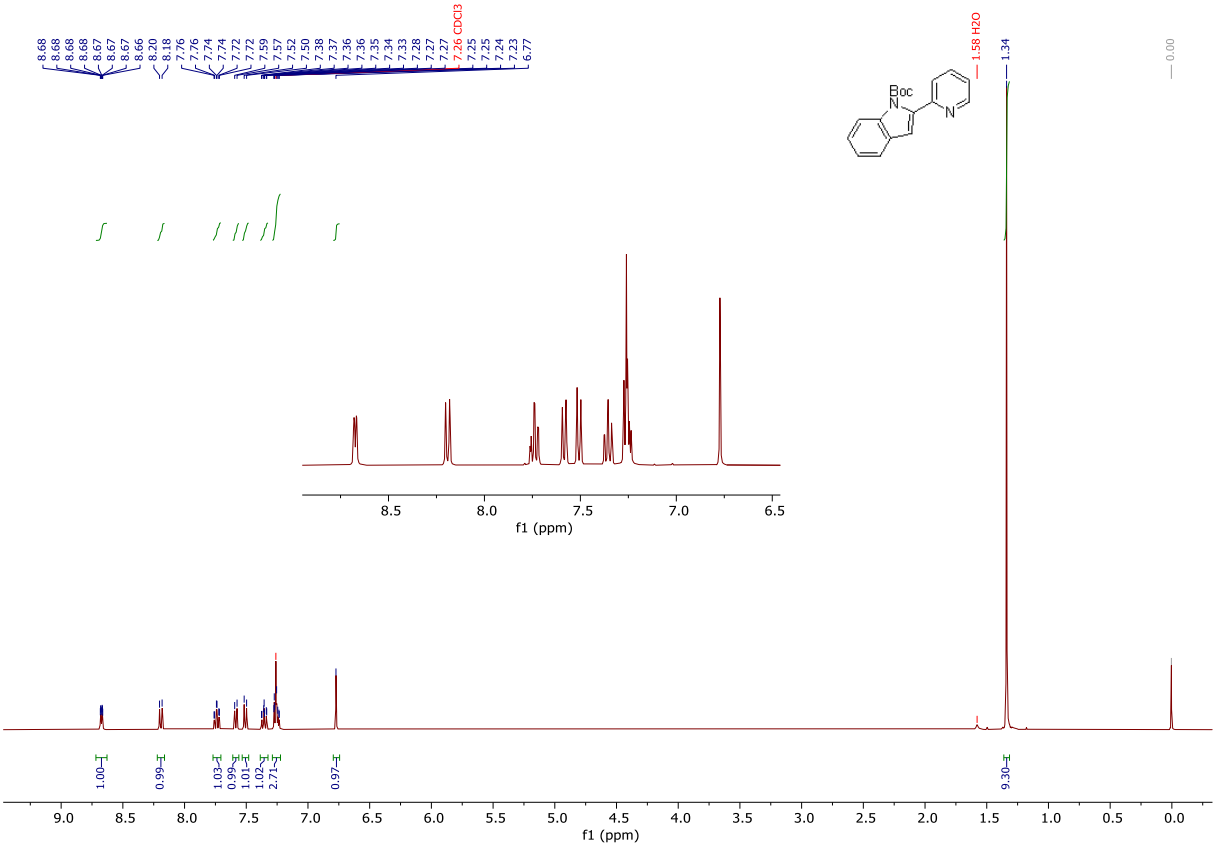

^{1}H NMR spectrum of pyridine S28a ($CDCl_3$, 298 K)

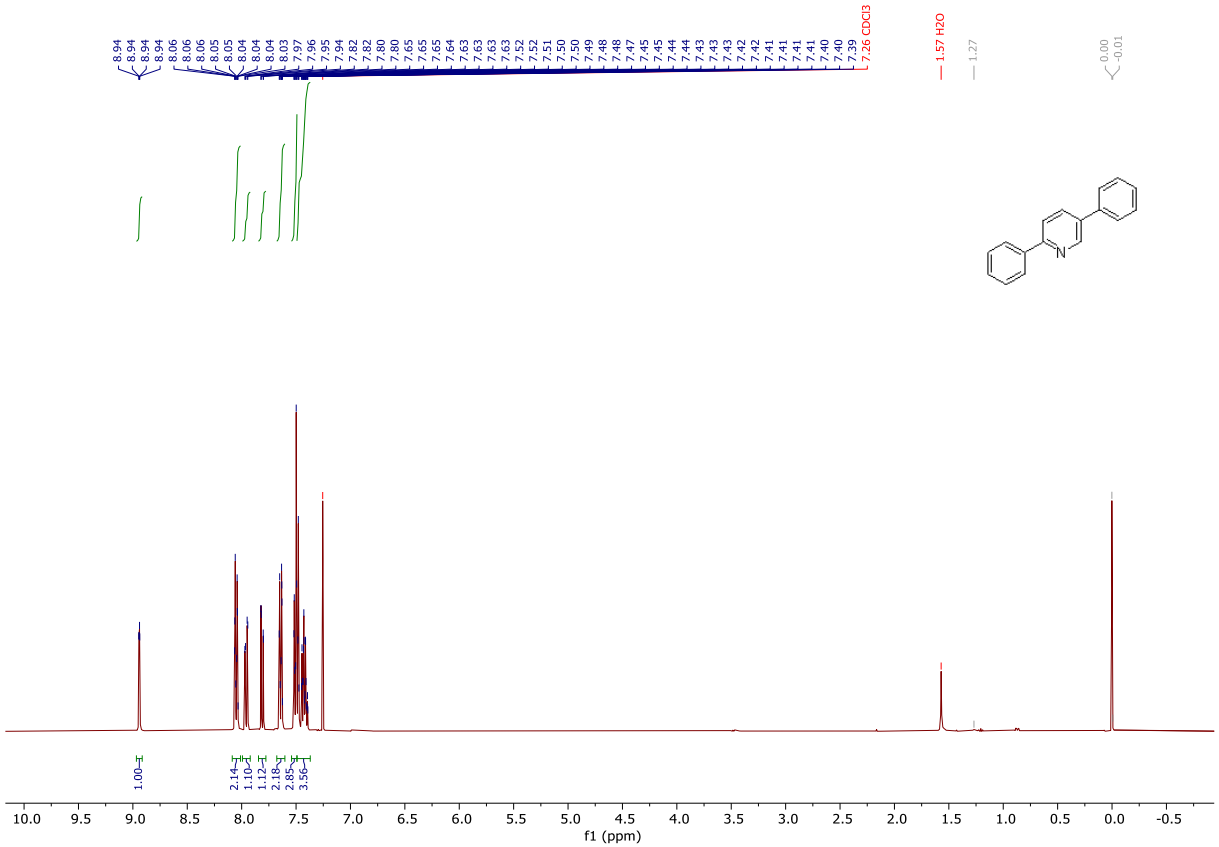

^{1}H NMR spectrum of pyridine S29a ($CDCl_3$, 298 K)

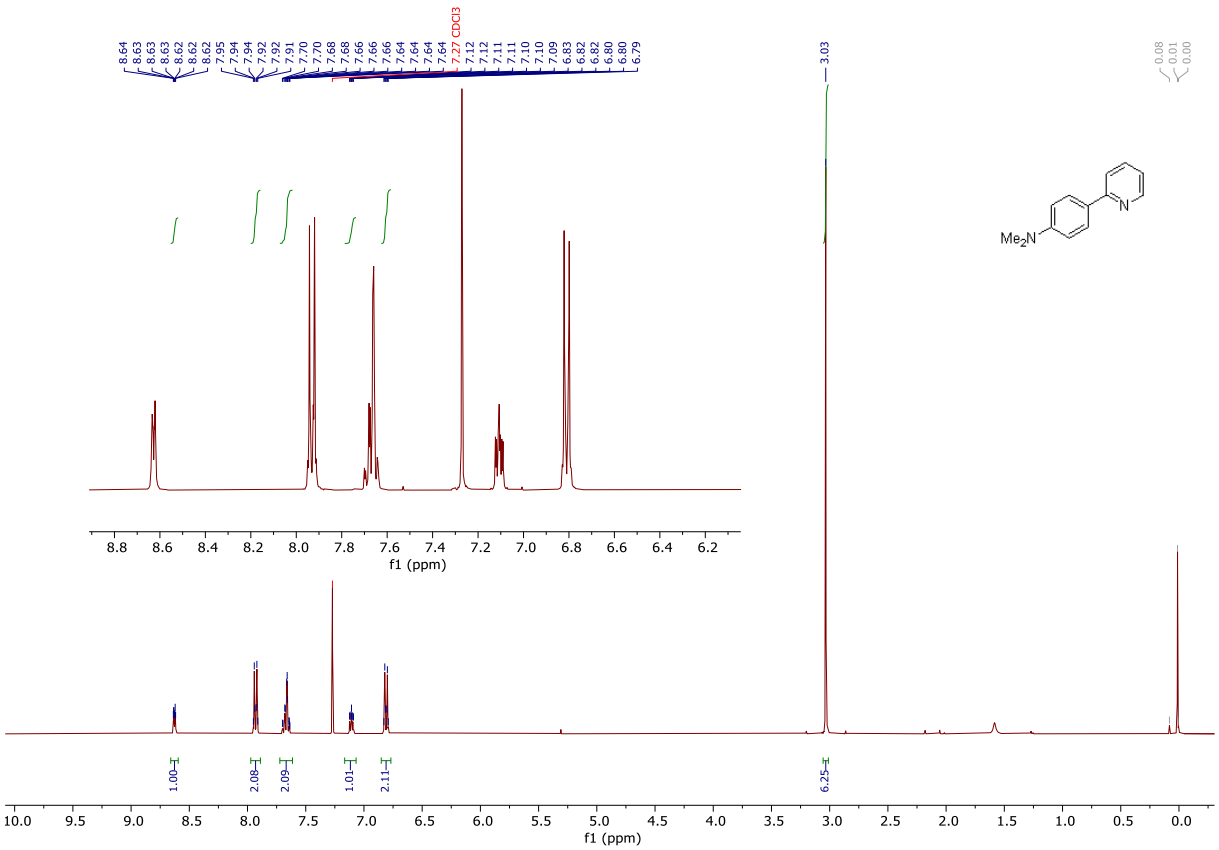

^{1}H NMR spectrum of pyridine S30a ($CDCl_3$, 298 K)

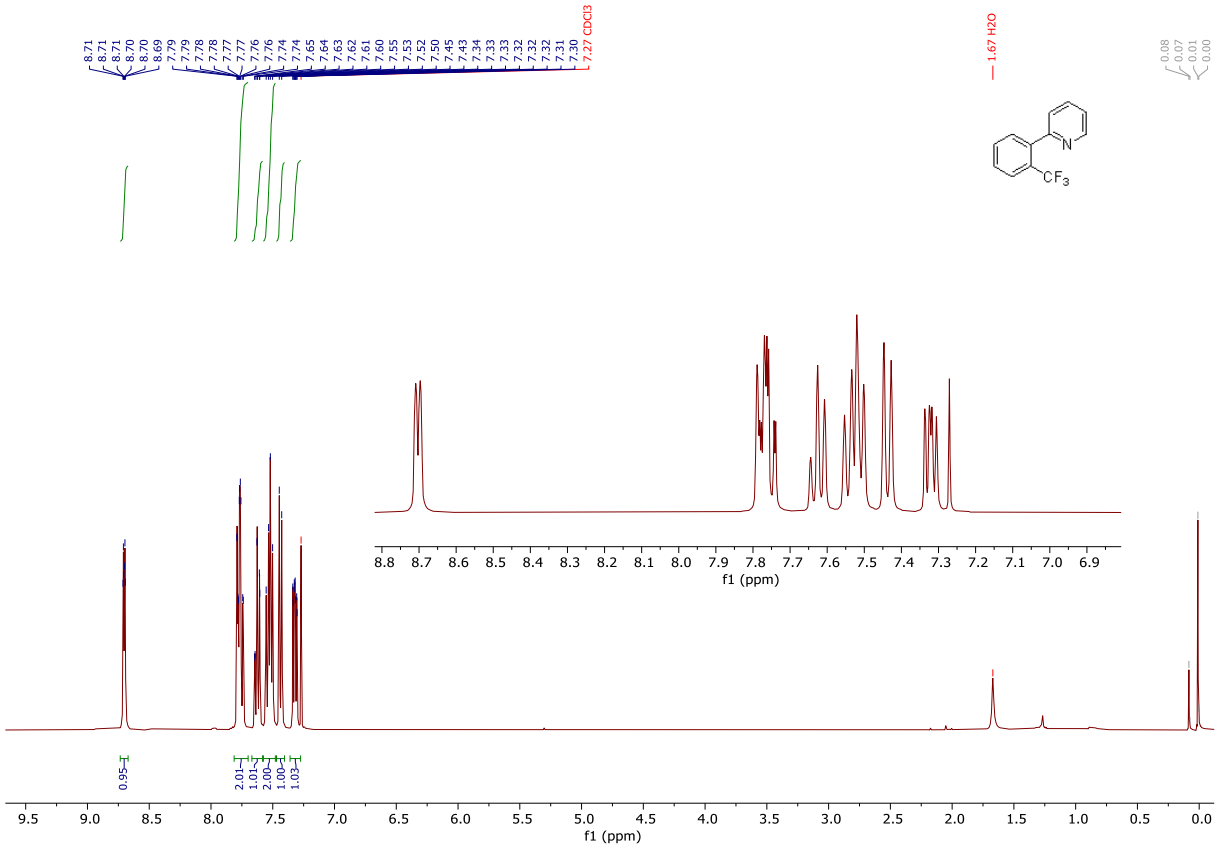

^{1}H NMR spectrum of pyridine S31a ($CDCl_3$, 298 K)

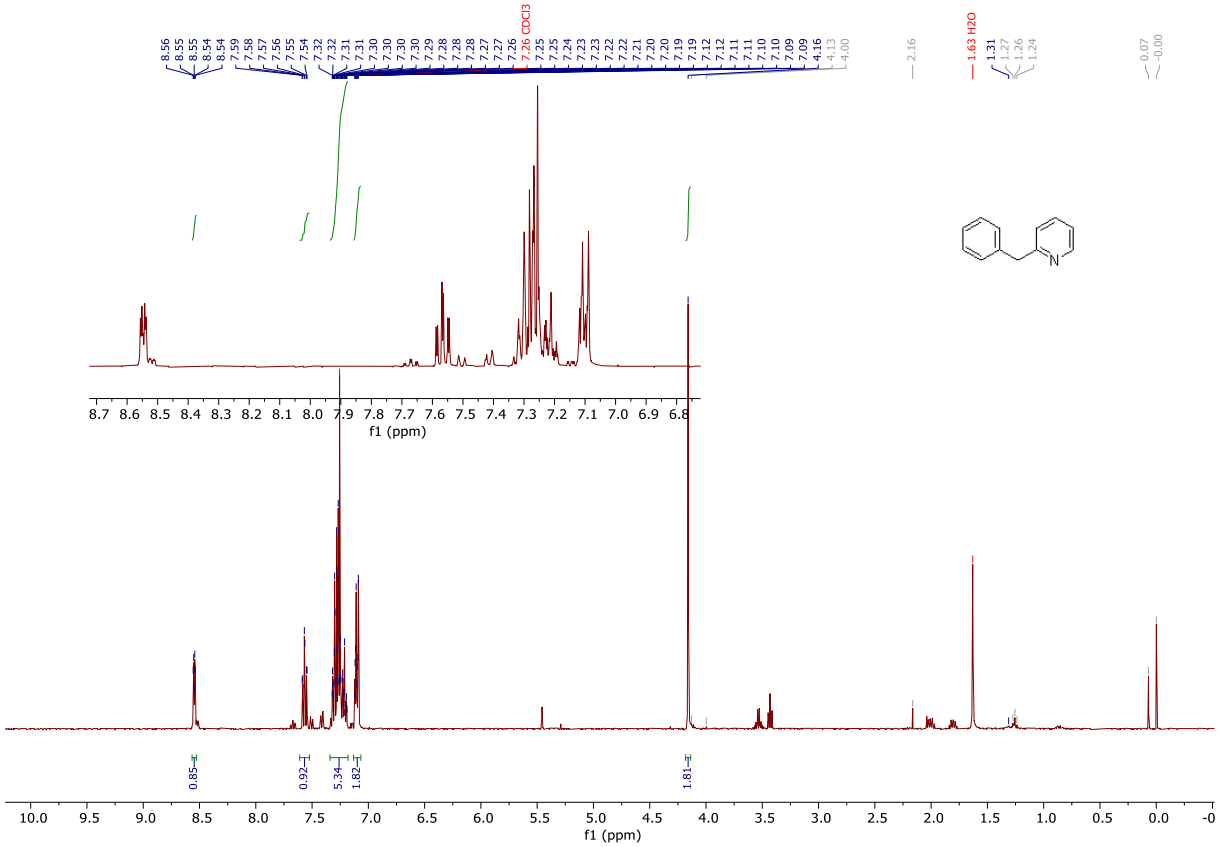

^{1}H NMR spectrum of pyridine S32a ($CDCl_3$, 298 K)

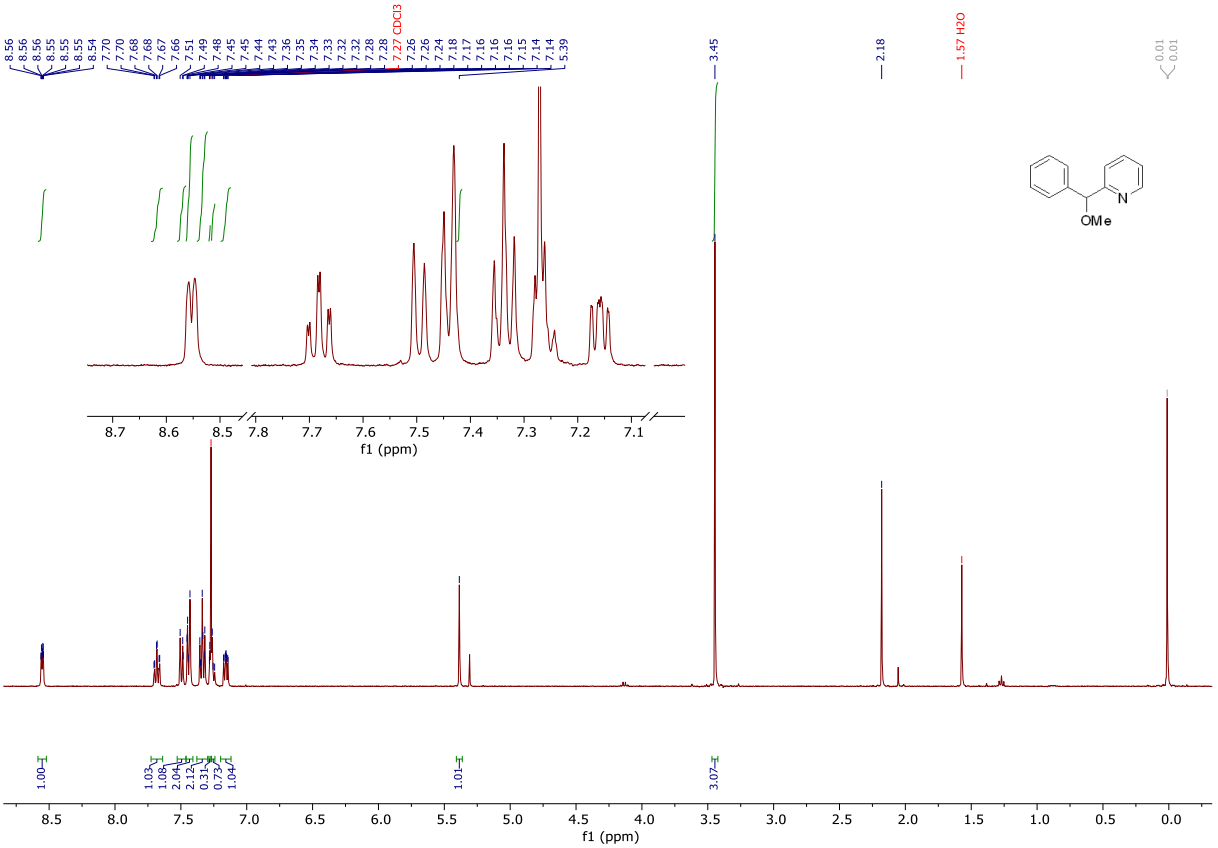

^{1}H NMR spectrum of pyridine S33a ($CDCl_3$, 298 K)

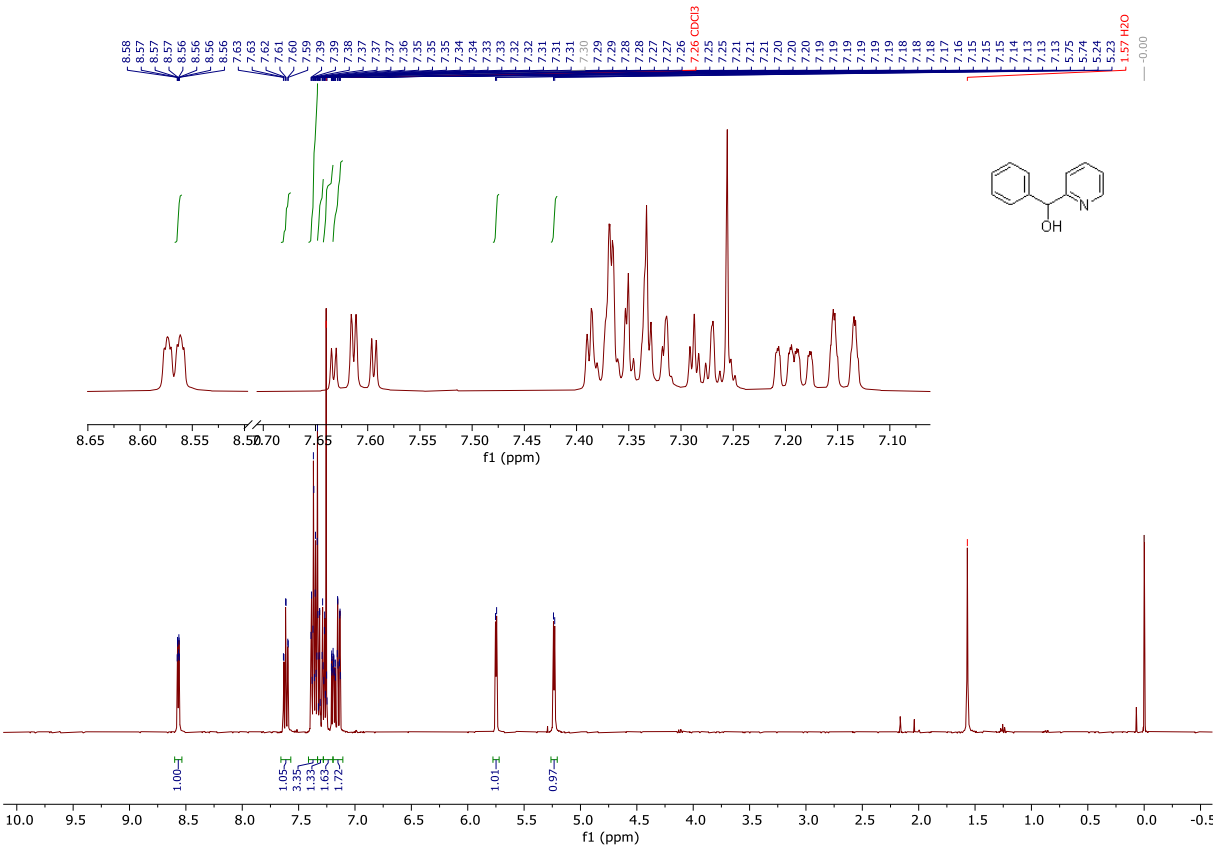

^{1}H NMR spectrum of pyridine S34a ($CDCl_3$, 298 K)

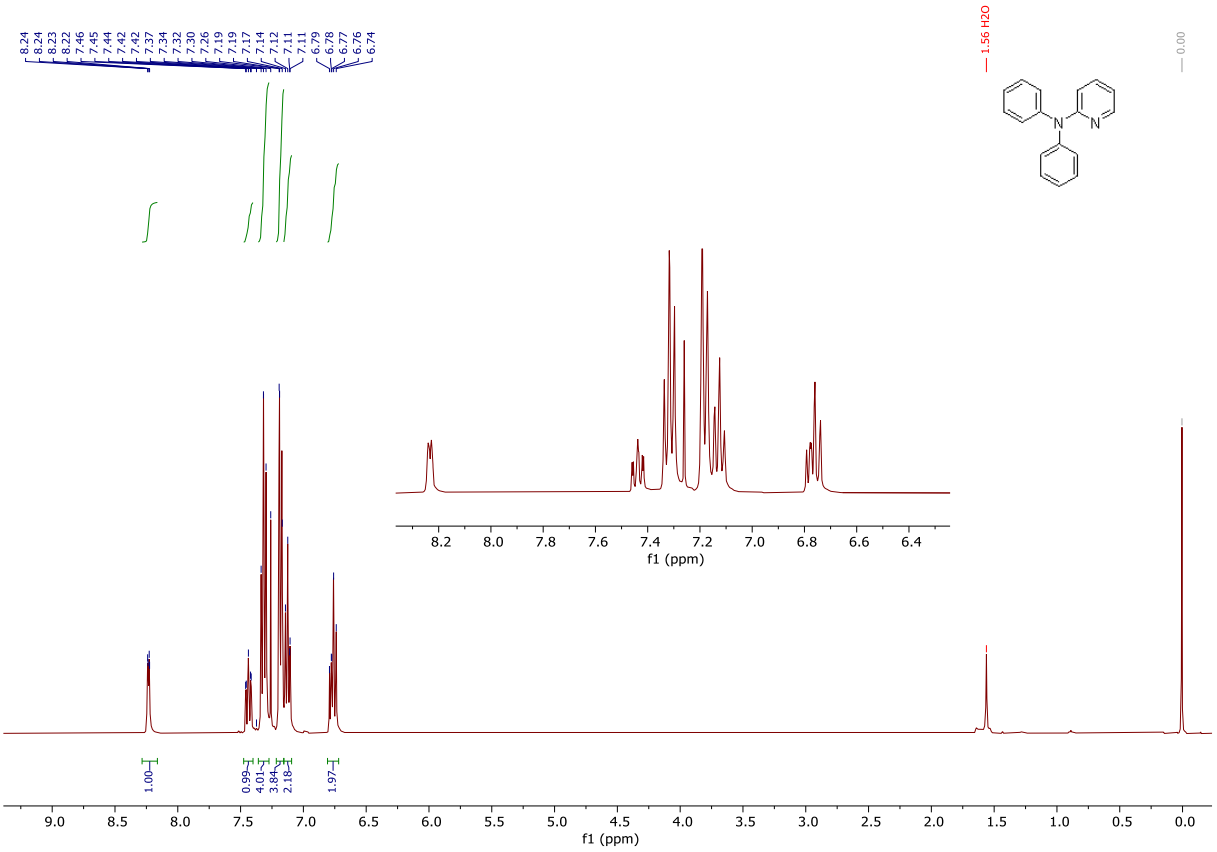

^{1}H NMR spectrum of pyridine S35a ($CDCl_3$, 298 K)

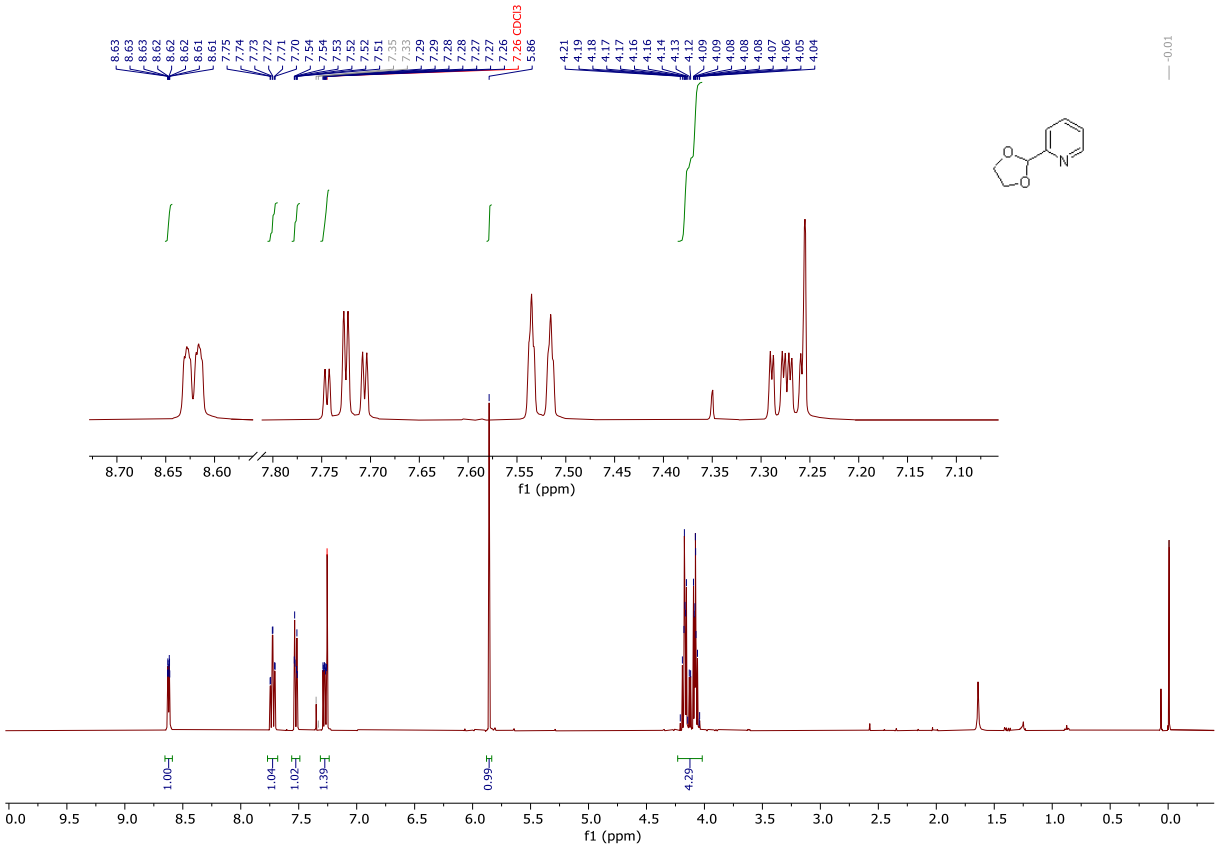

6.2. Zincke imines

^{1}H NMR spectrum of Zincke imine 2 ($CDCl_3$, 298 K)

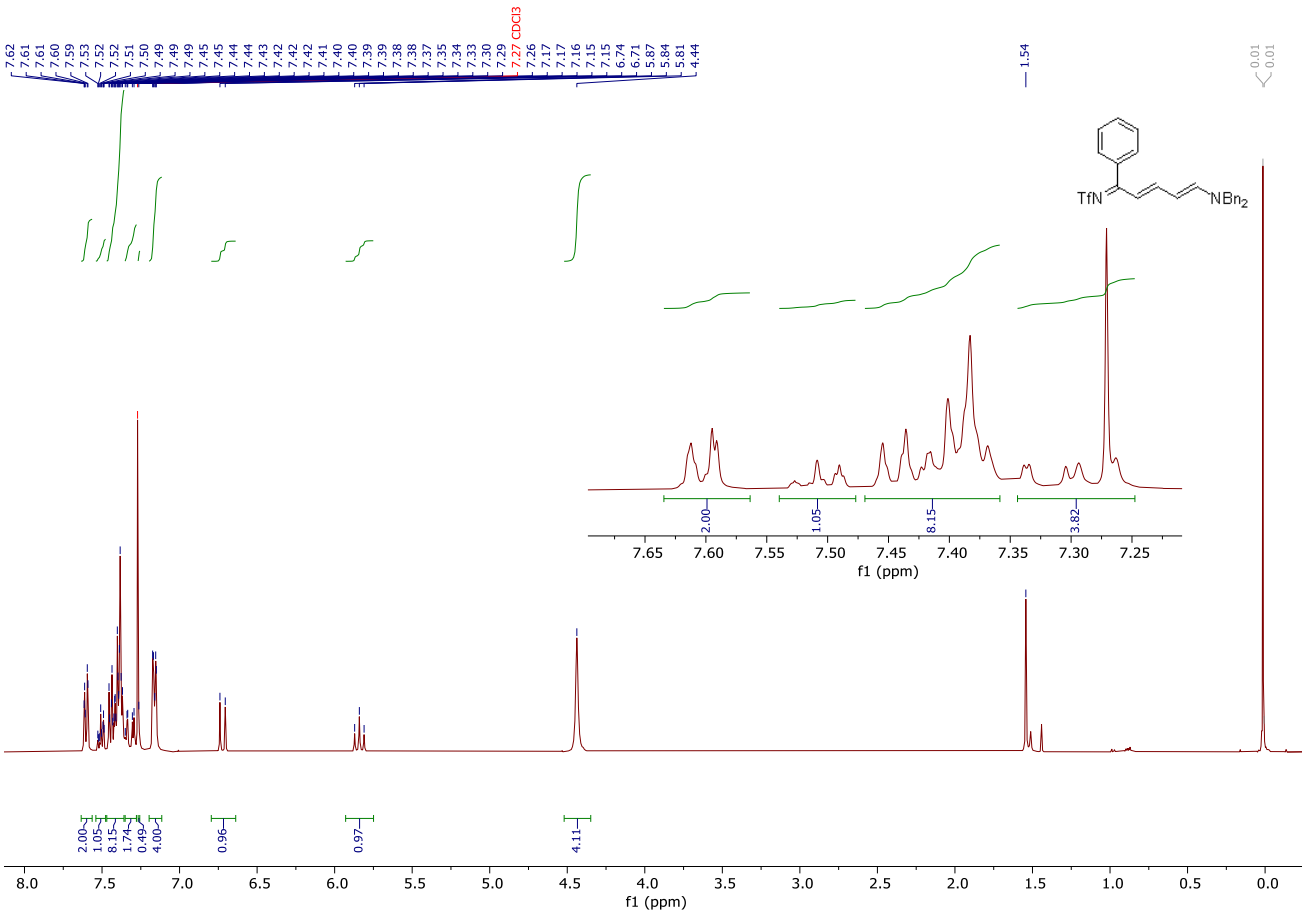

^{1}H NMR spectrum of Zincke imine S2b ($CDCl_3$, 298 K)

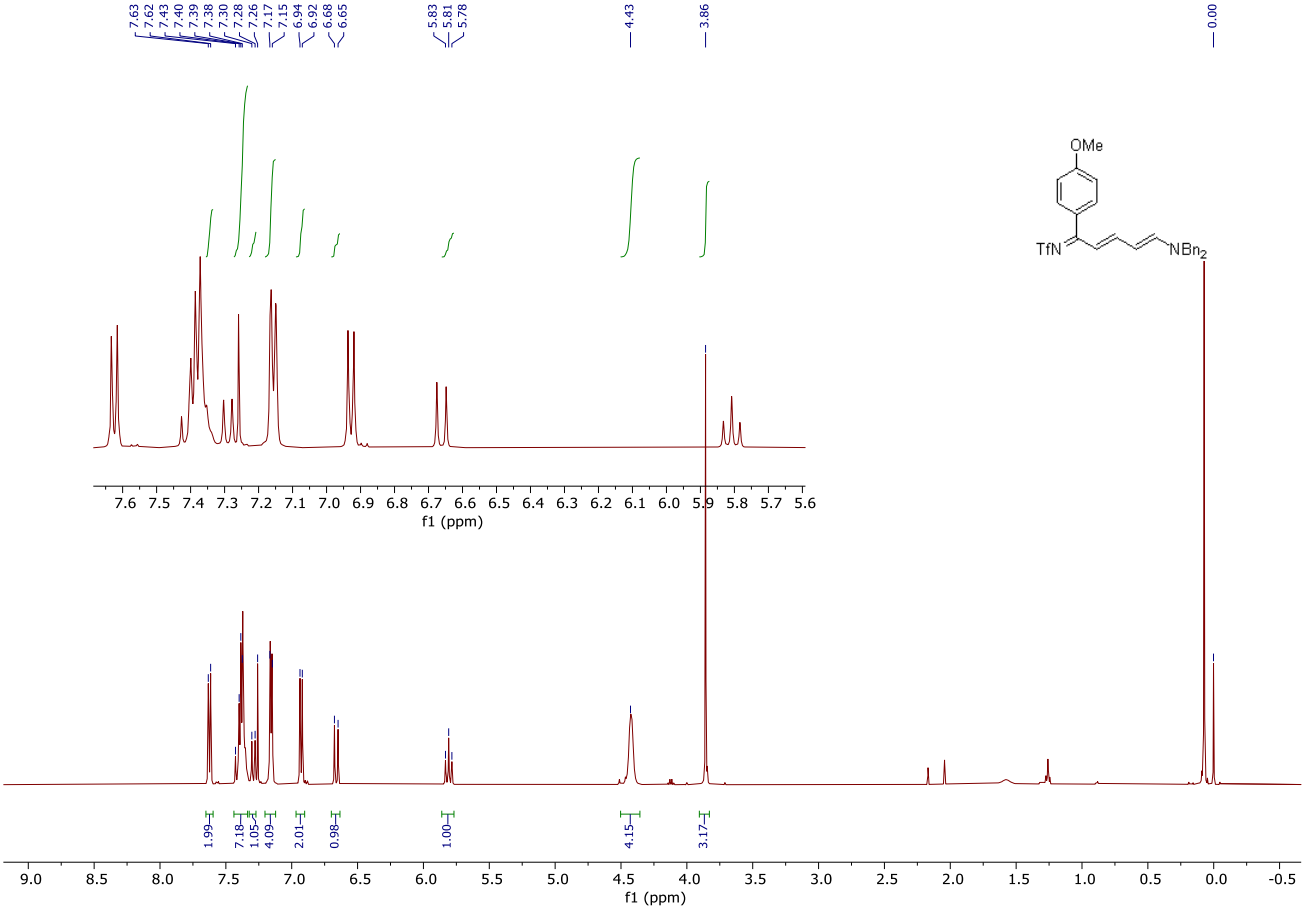

^{13}C NMR spectrum of Zincke imine S2b ($CDCl_3$, 298 K)

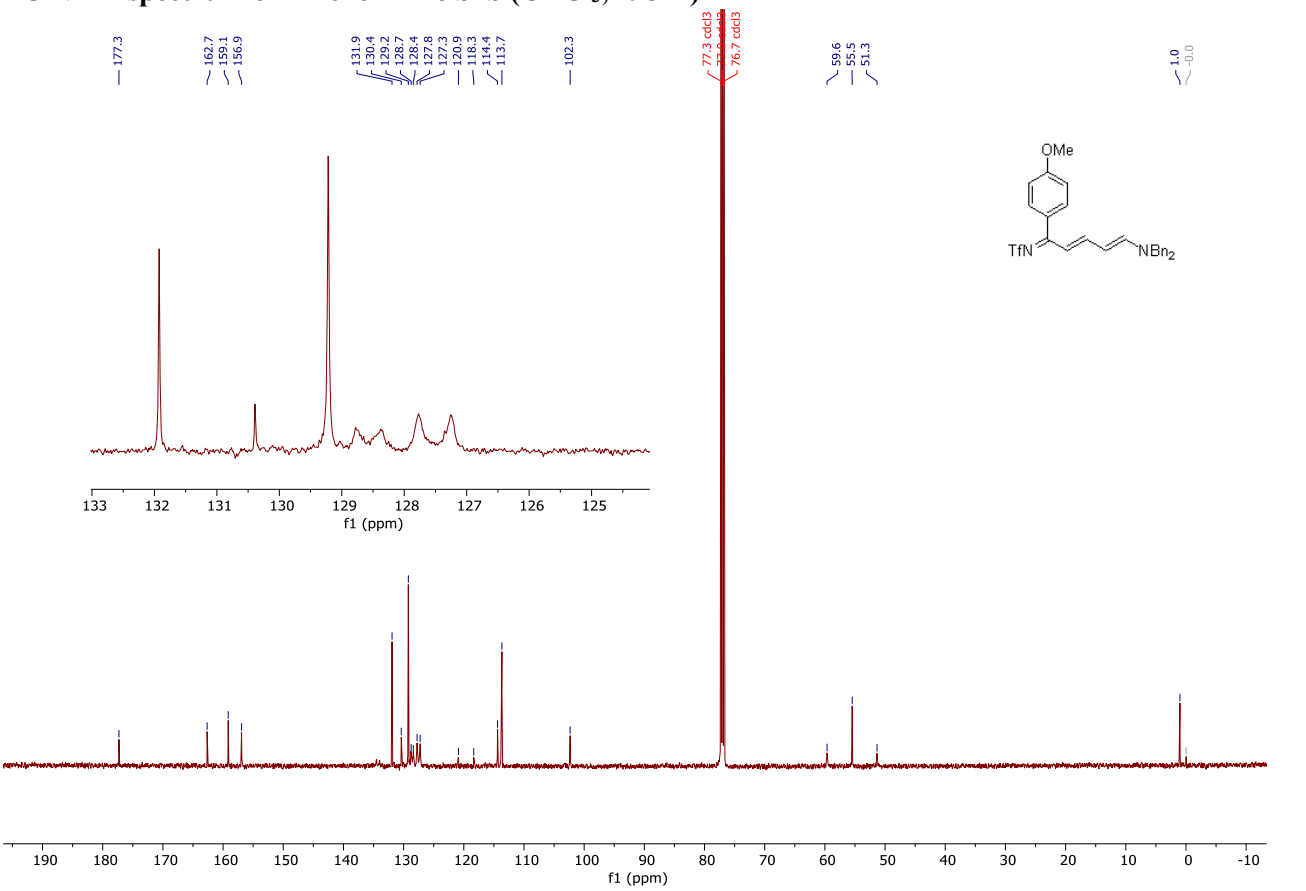

^{1}H NMR spectrum of Zincke imine S3b ($CDCl_3$, 298 K)

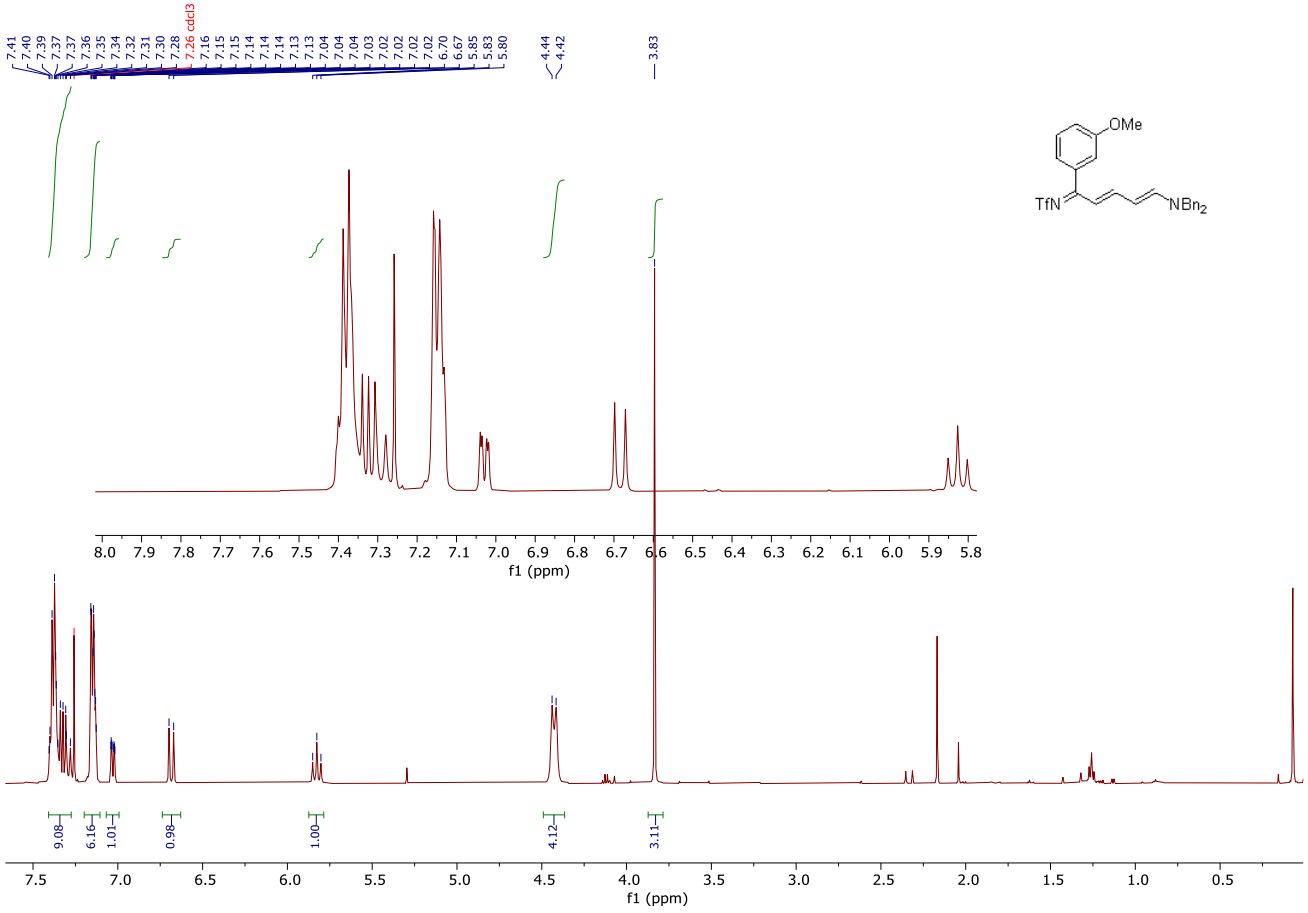

^{13}C NMR spectrum of Zincke imine S3b ($CDCl_3$, 298 K)

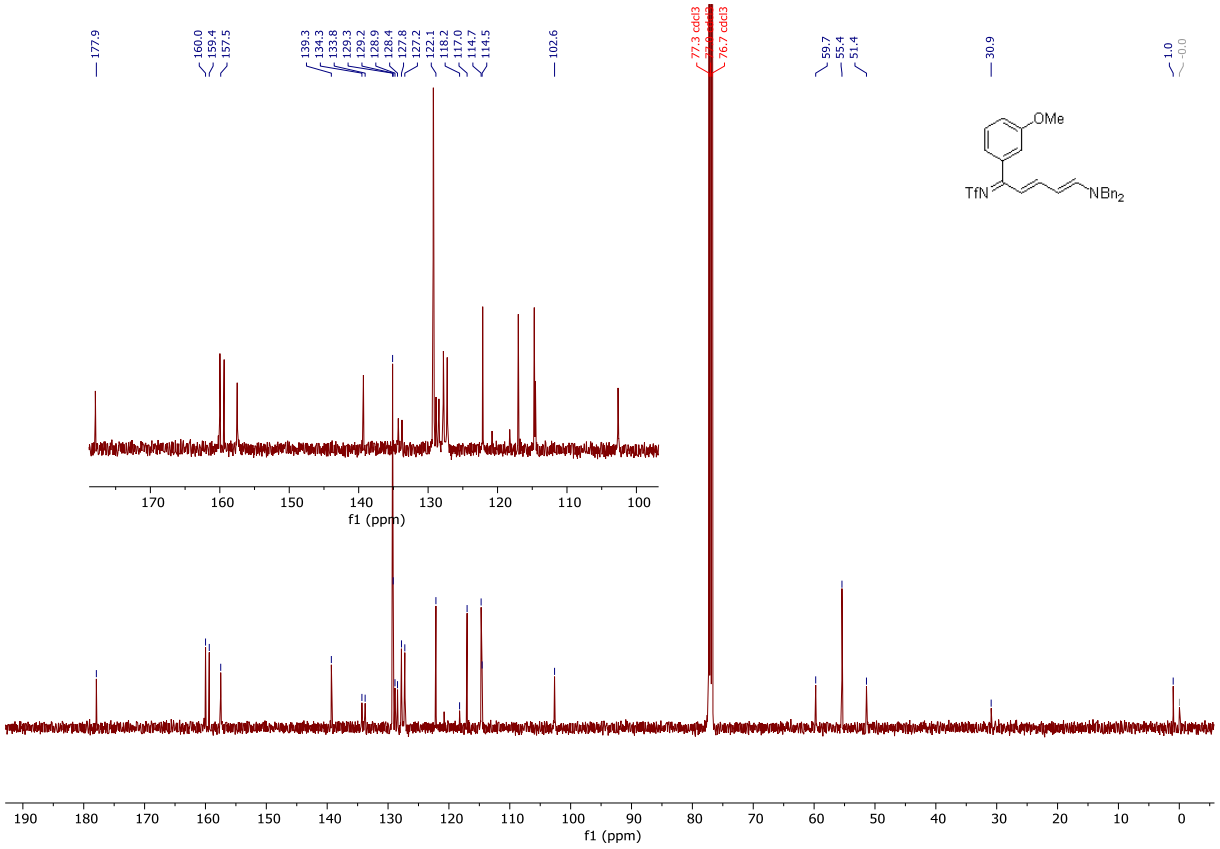

^{1}H NMR spectrum of Zincke imine S4b ($CDCl_3$, 298 K)

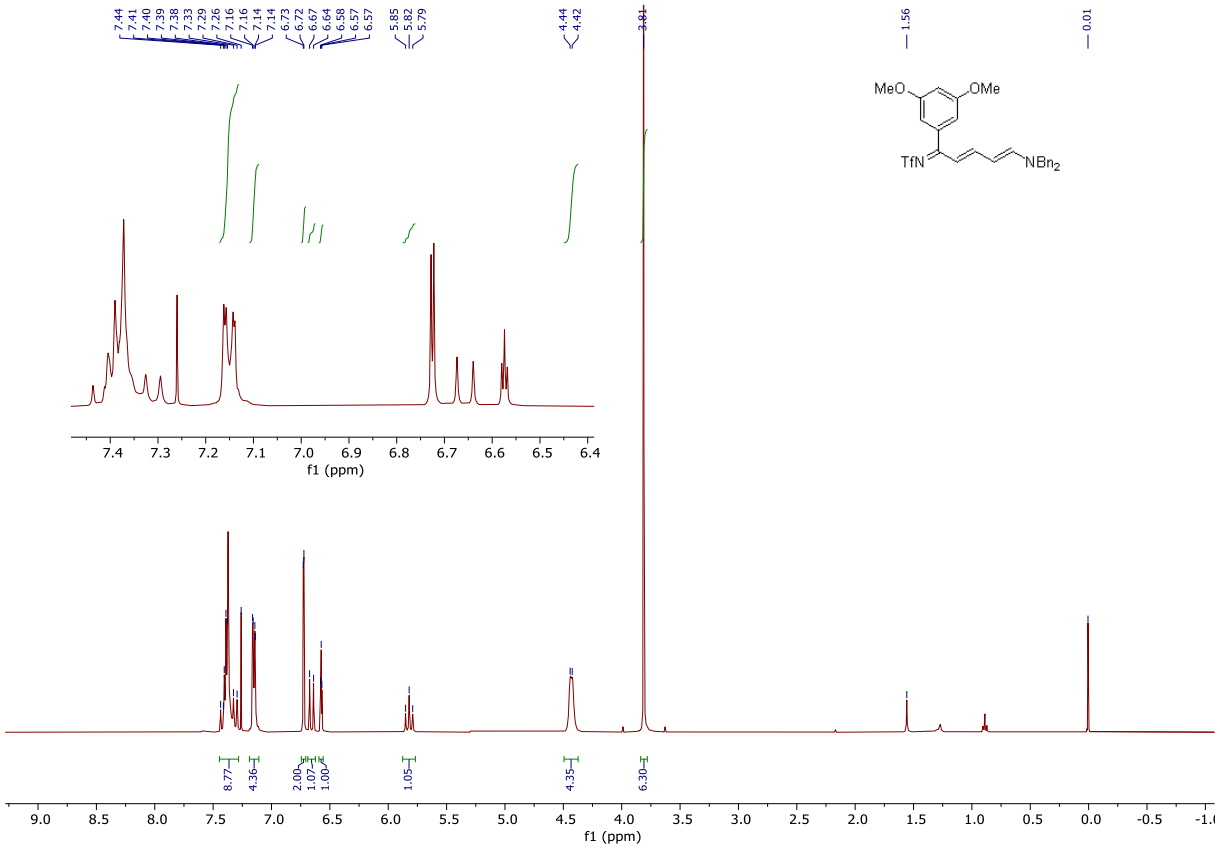

^{13}C NMR spectrum of Zincke imine S4b ($CDCl_3$, 298 K)

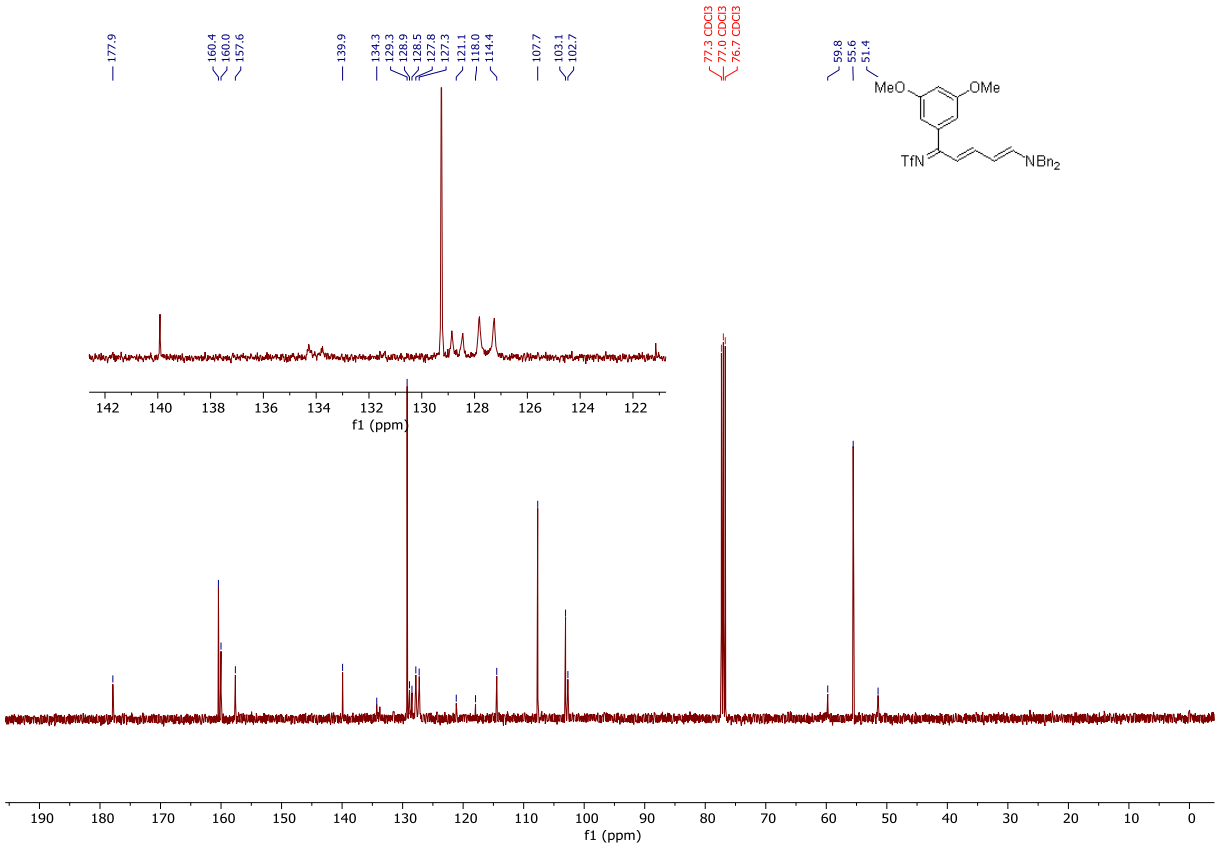

^{1}H NMR spectrum of Zincke imine S5b ($CDCl_3$, 298 K)

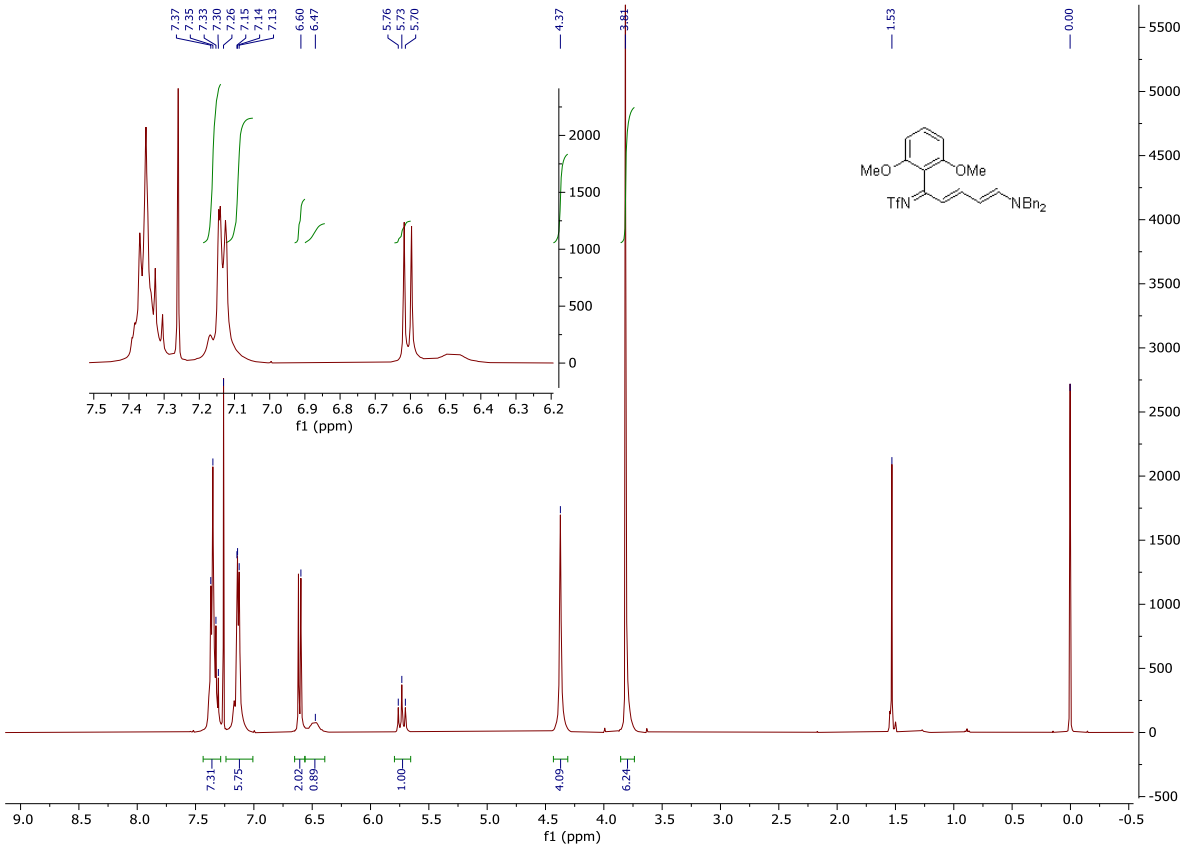

^{13}C NMR spectrum of Zincke imine S5b ($CDCl_3$, 298 K)

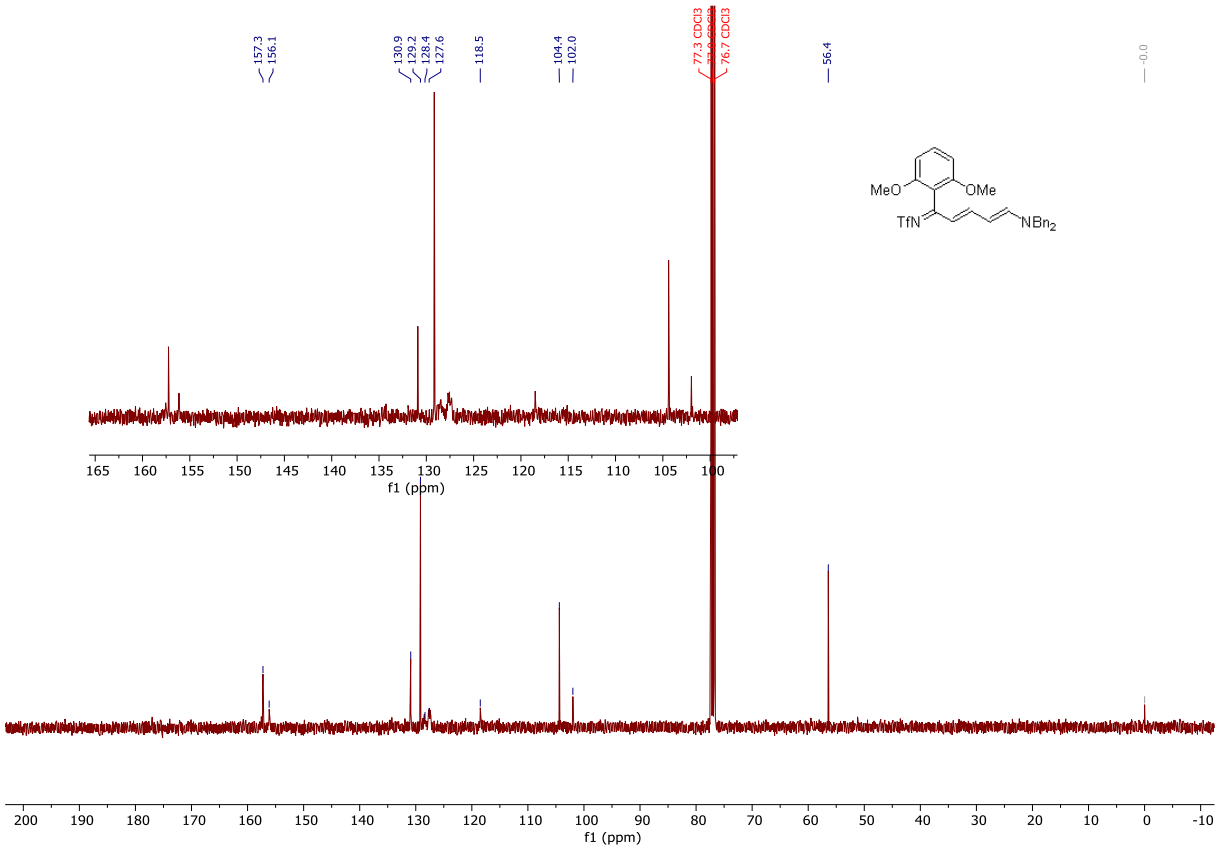

^{1}H NMR spectrum of Zincke imine S6b ($CDCl_3$, 298 K)

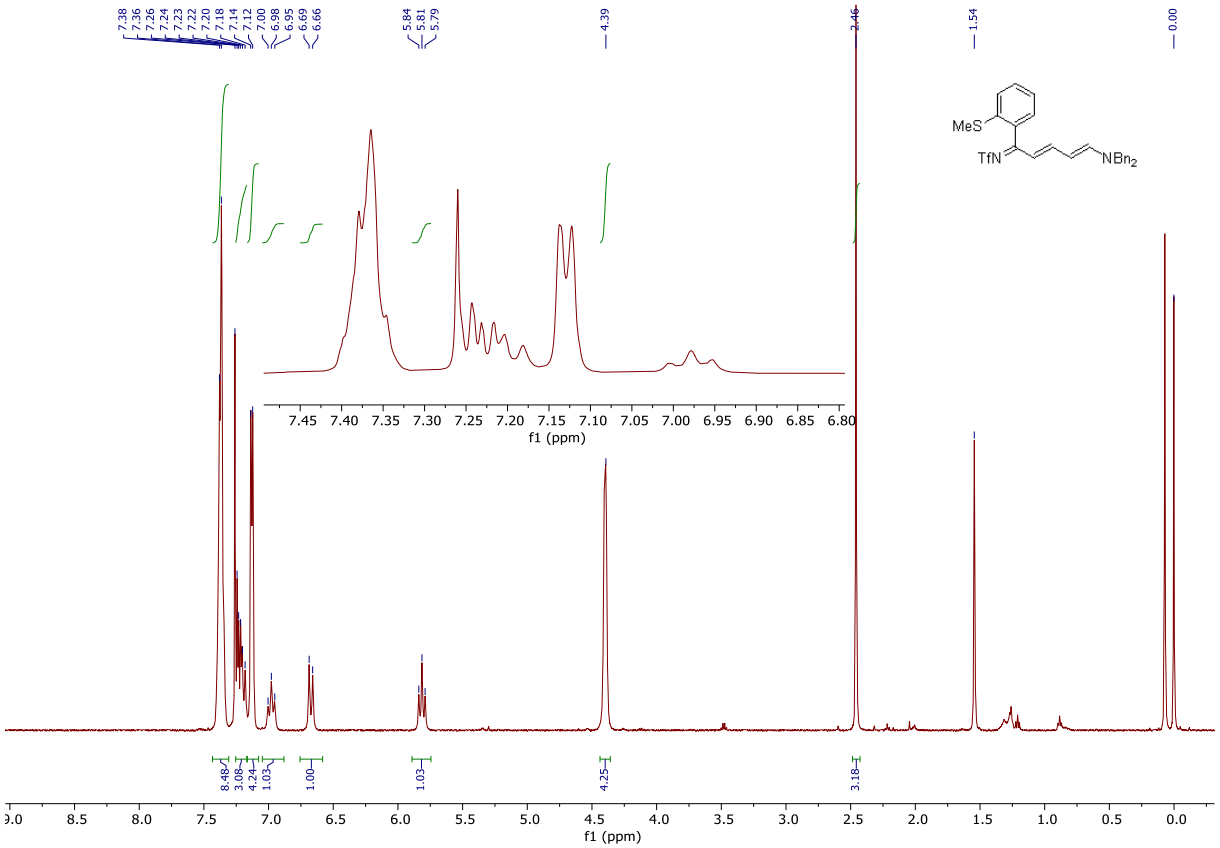

^{13}C NMR spectrum of Zincke imine S6b ($CDCl_3$, 298 K)

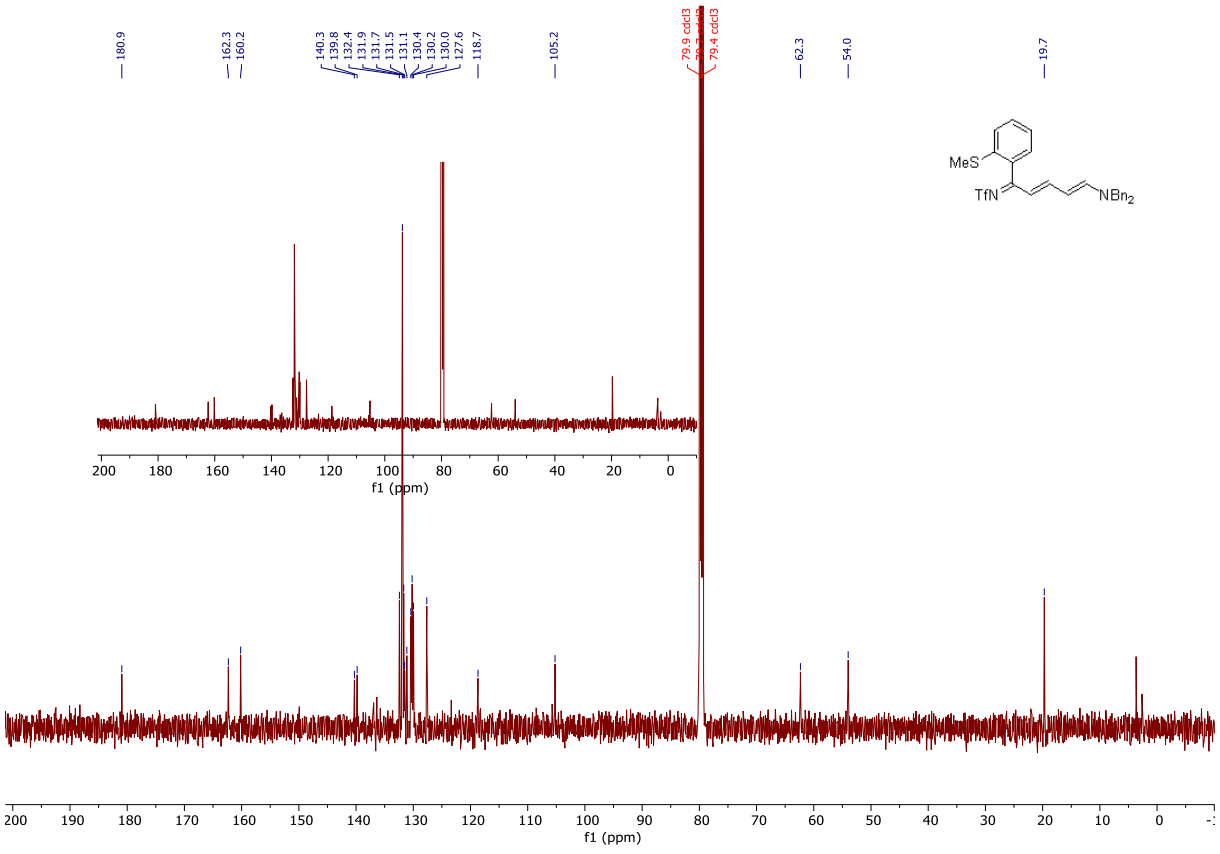

^{1}H NMR spectrum of Zincke imine S7b ($CDCl_3$, 298 K)

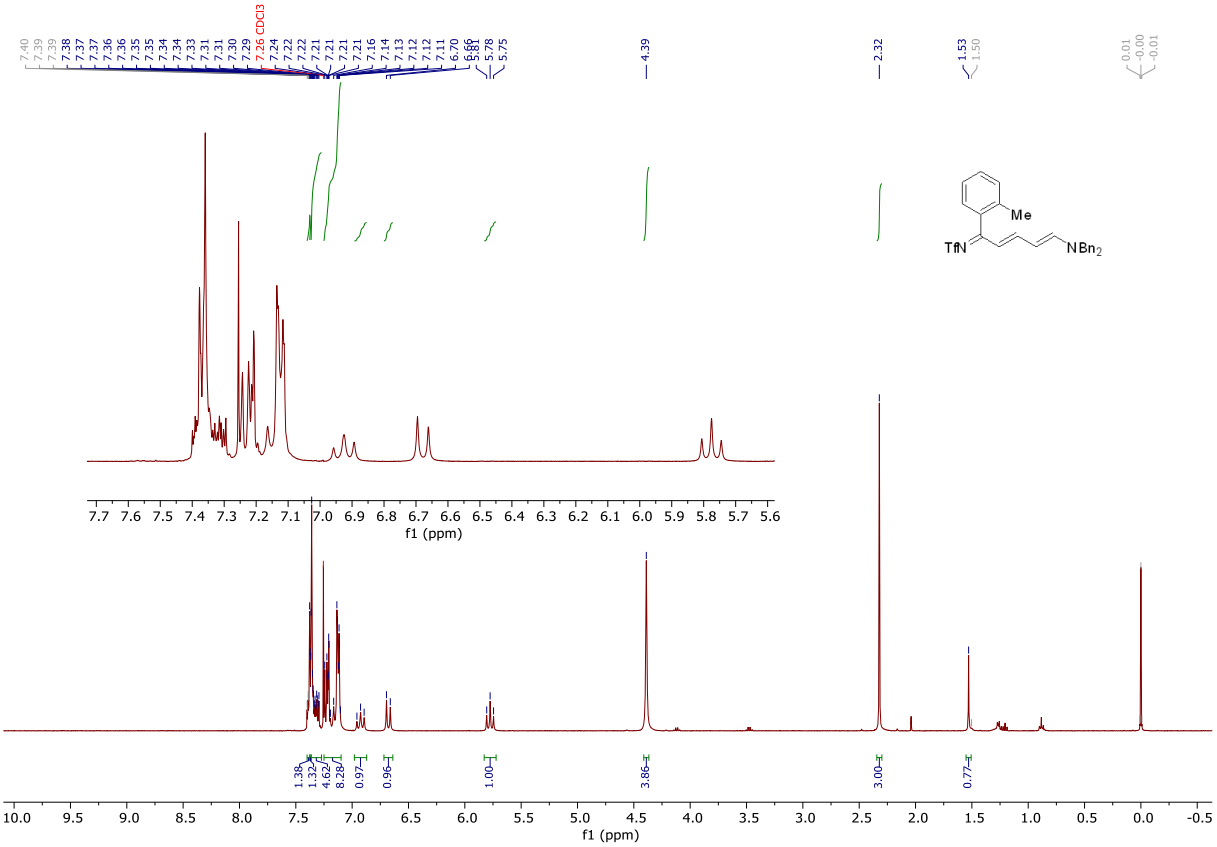

^{13}C NMR spectrum of Zincke imine S7b ($CDCl_3$, 298 K)

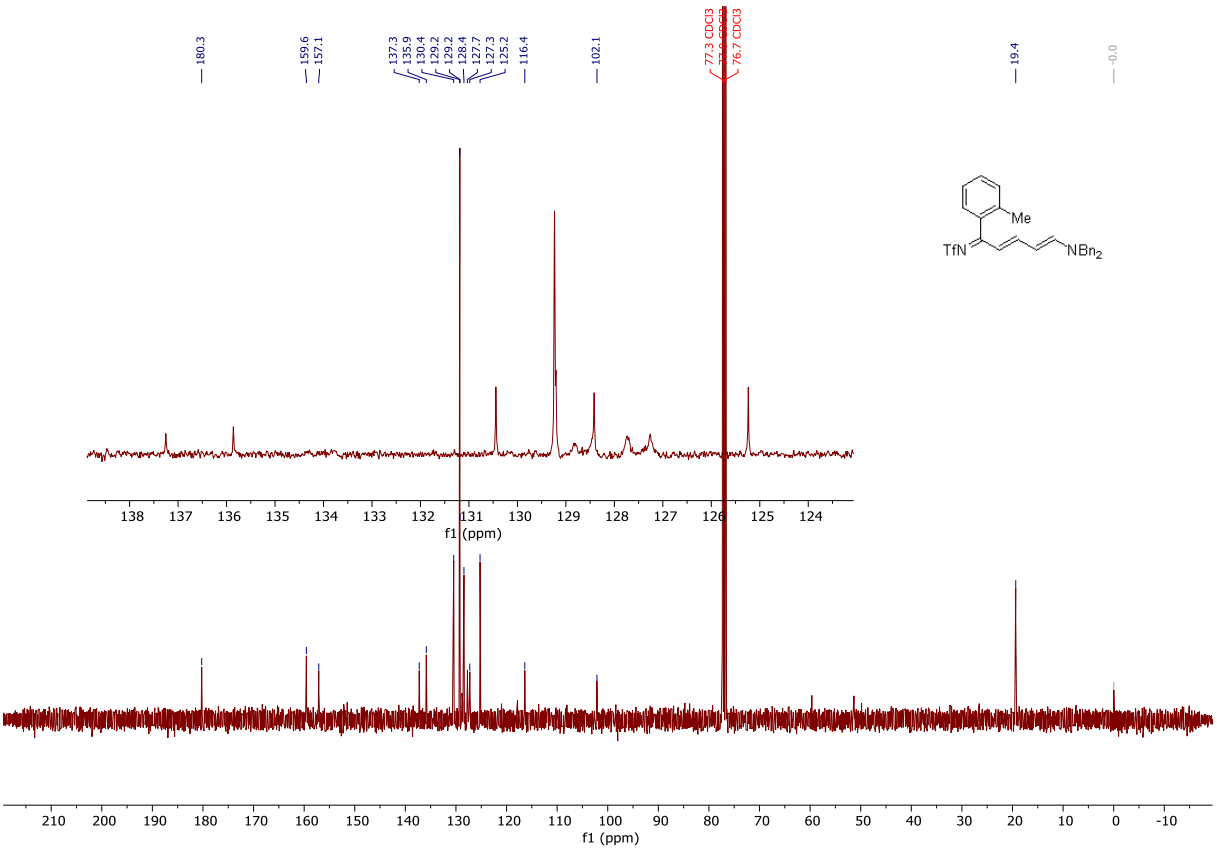

^{1}H NMR spectrum of Zincke imine S8b ($CDCl_3$, 298 K)

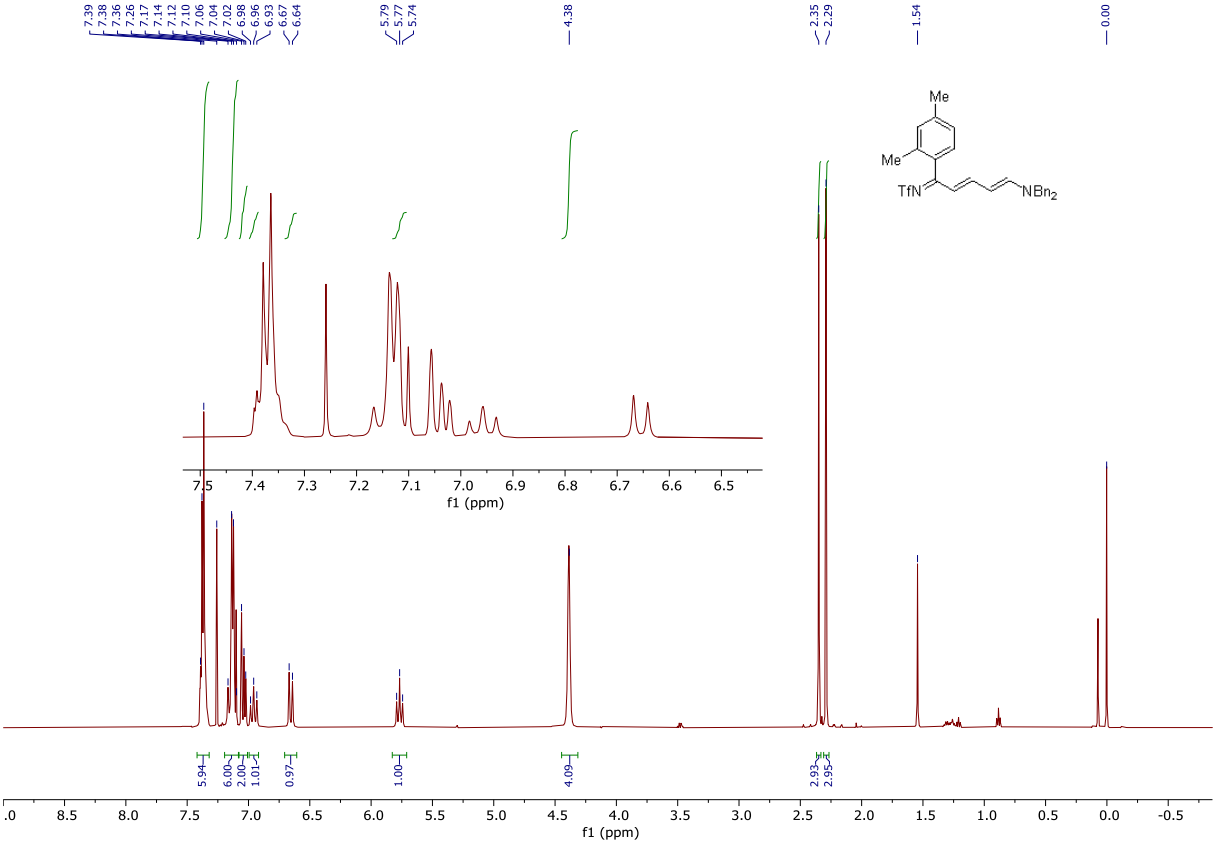

^{13}C NMR spectrum of Zincke imine S8b ($CDCl_3$, 298 K)

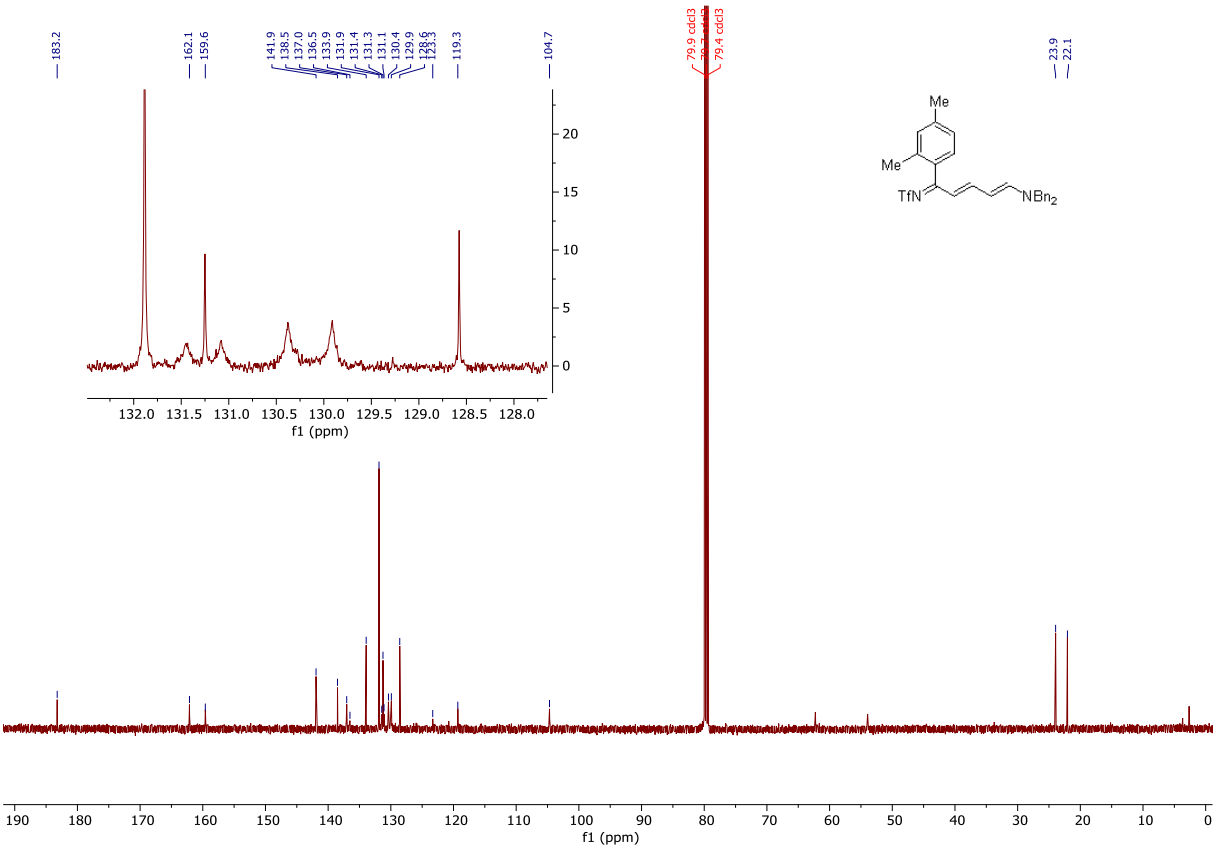

^{1}H NMR spectrum of Zincke imine S9b ($CDCl_3$, 298 K)

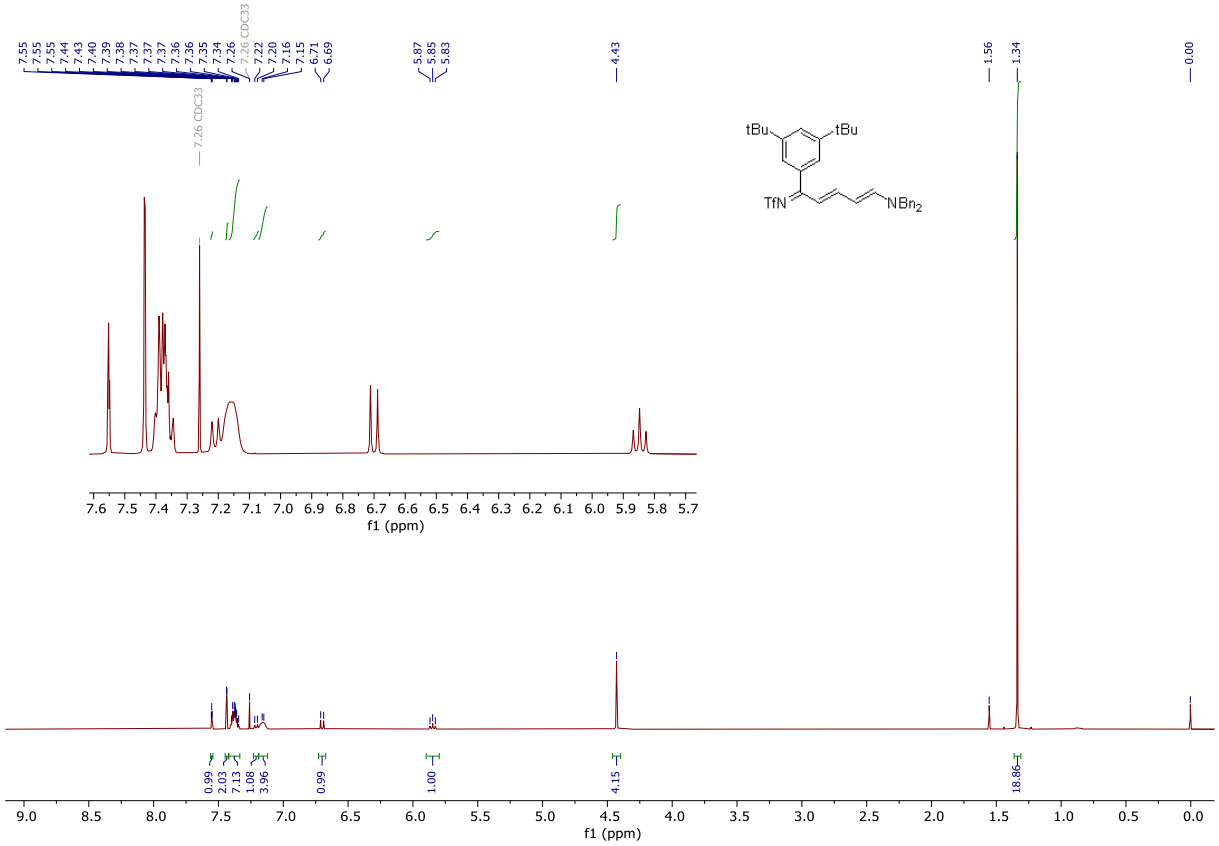

^{13}C NMR spectrum of Zincke imine S9b ($CDCl_3$, 298 K)

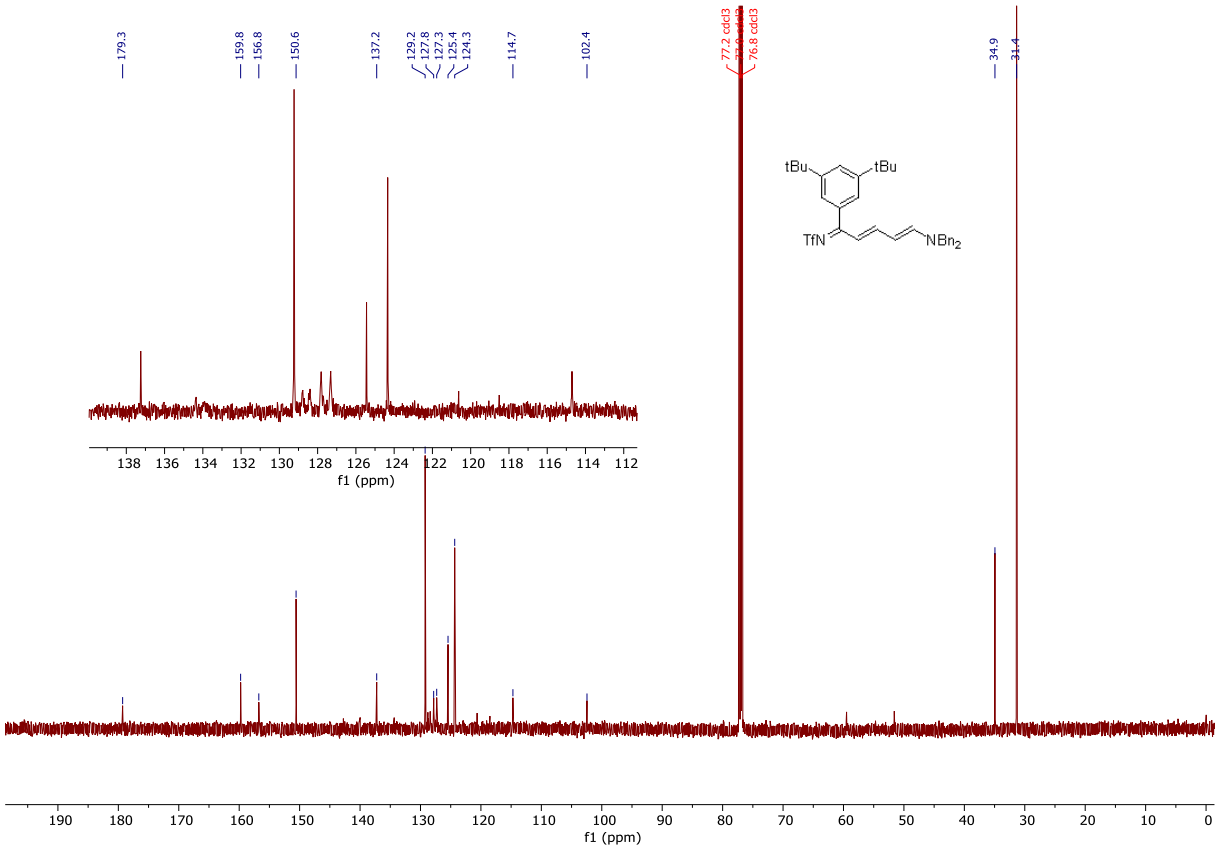

^{1}H NMR spectrum of Zincke imine S10b ($CDCl_3$, 298 K)

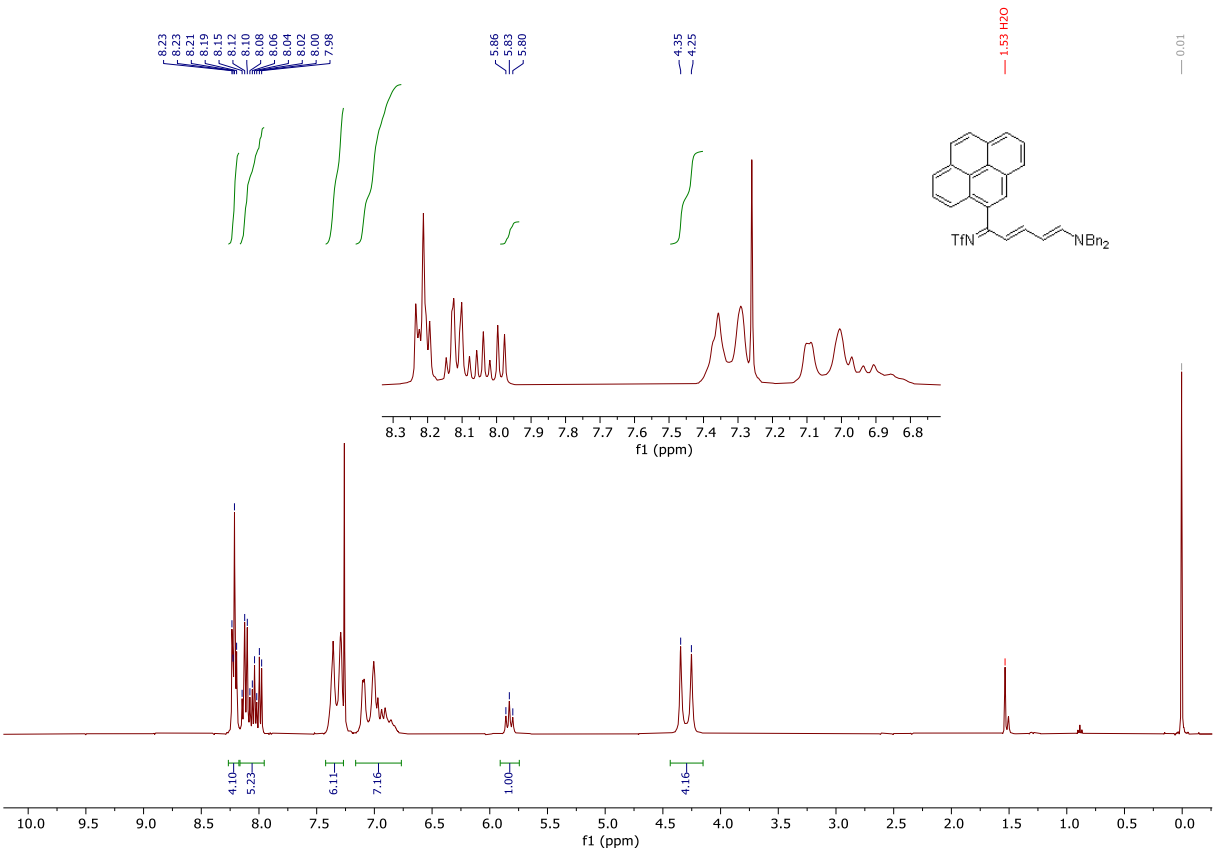

^{13}C NMR spectrum of Zincke imine S10b ($CDCl_3$, 298 K)

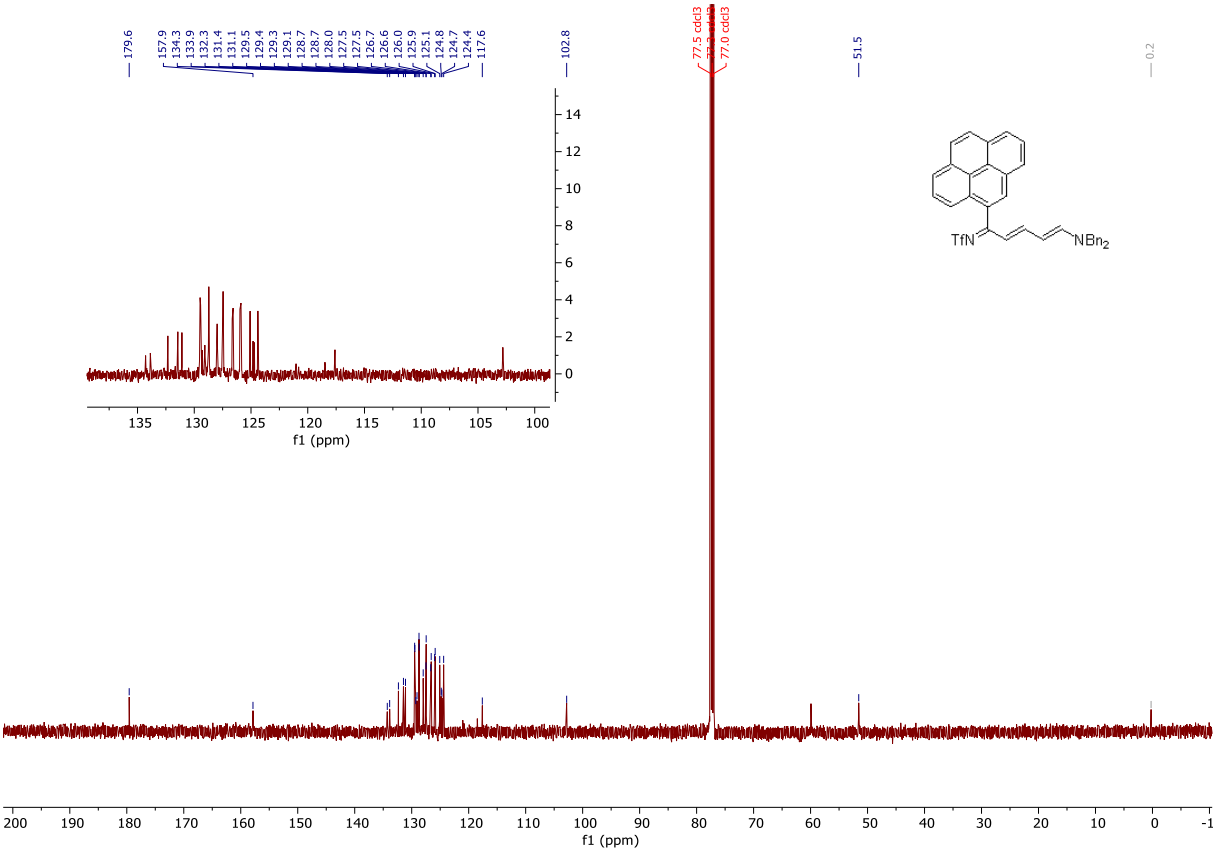

^{1}H NMR spectrum of Zincke imine S11b ($CDCl_3$, 298 K)

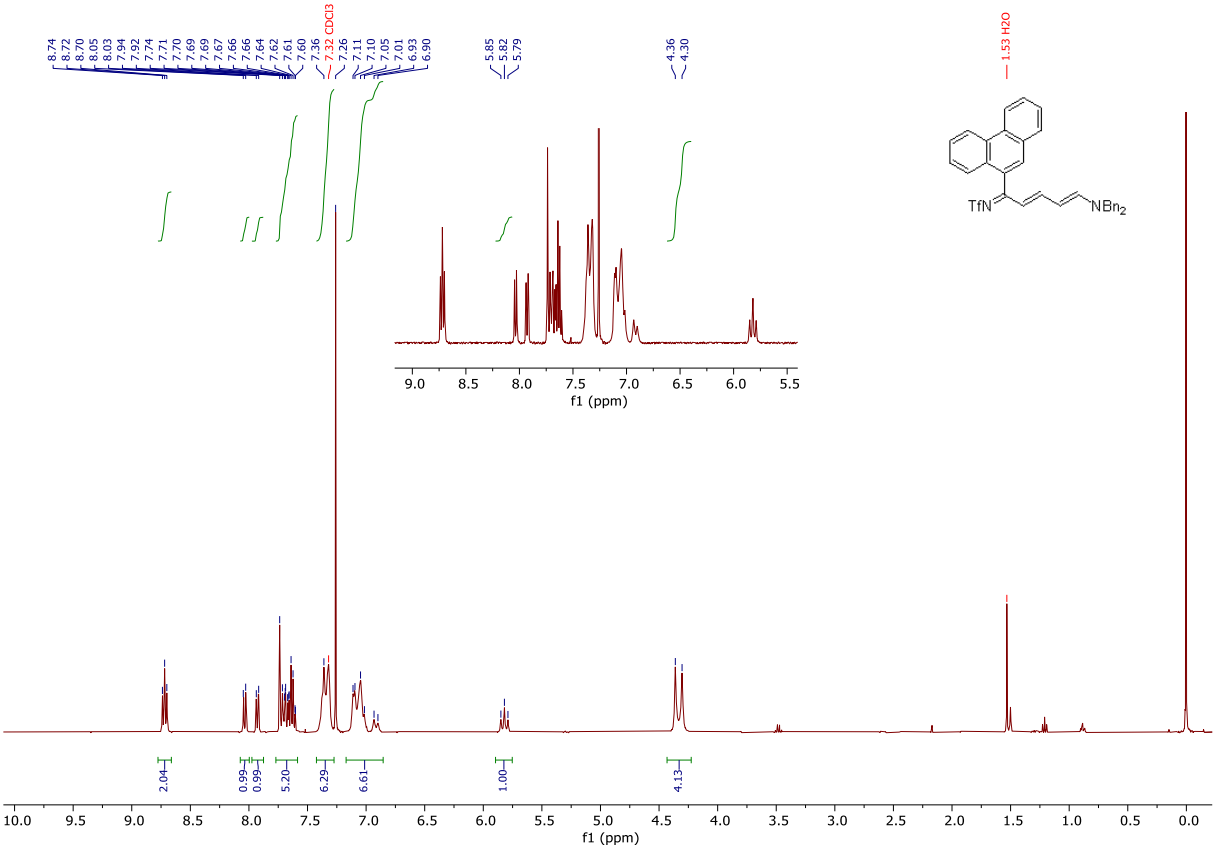

^{13}C NMR spectrum of Zincke imine S11b ($CDCl_3$, 298 K)

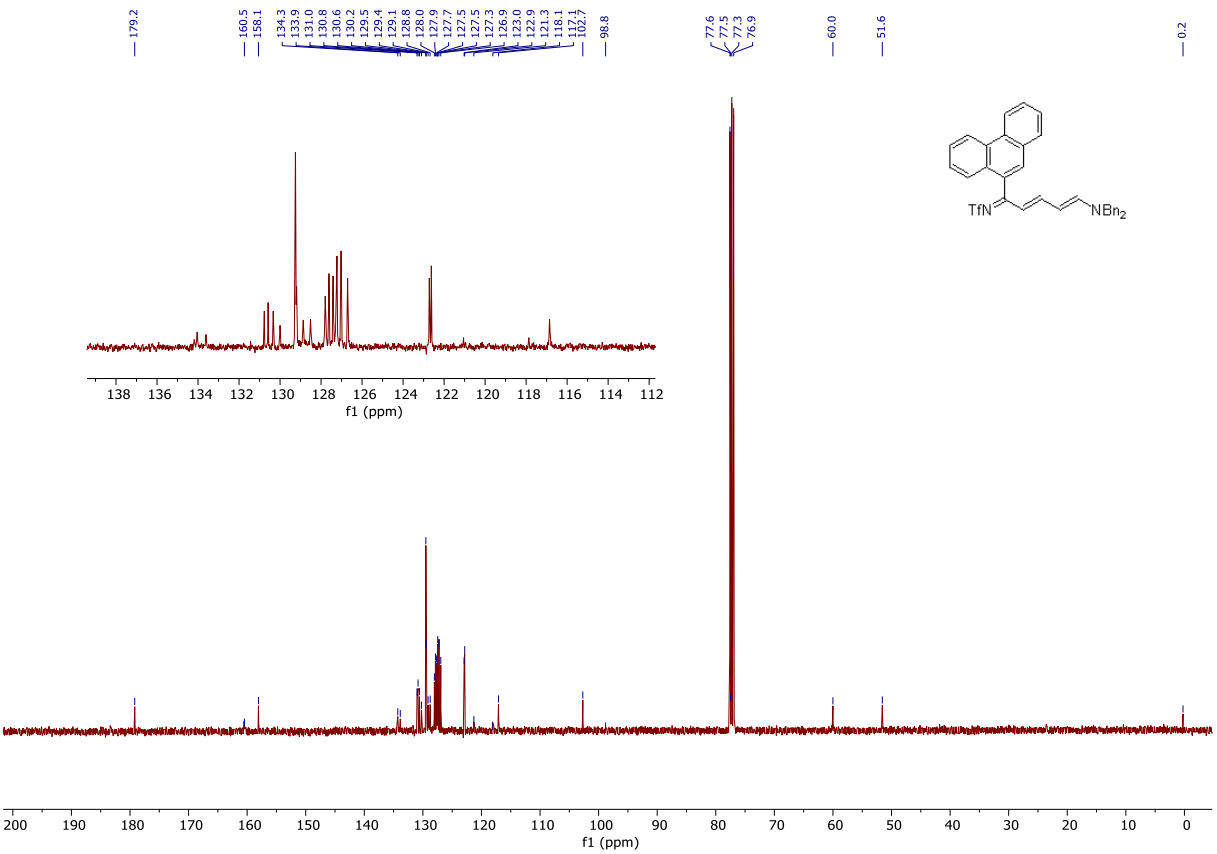

^{1}H NMR spectrum of Zincke imie S12b ($CDCl_3$, 298 K)

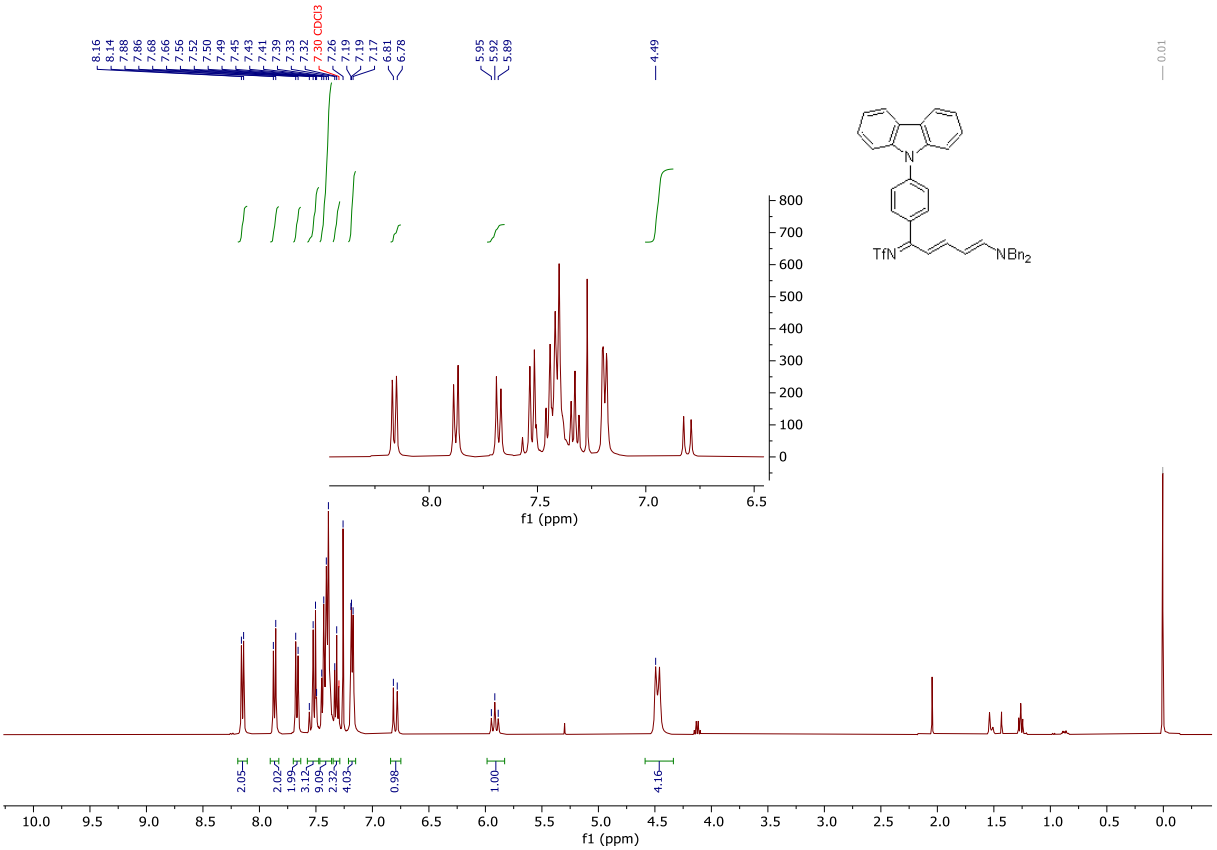

^{13}C NMR spectrum of Zincke imine S12b ($CDCl_3$, 298 K)

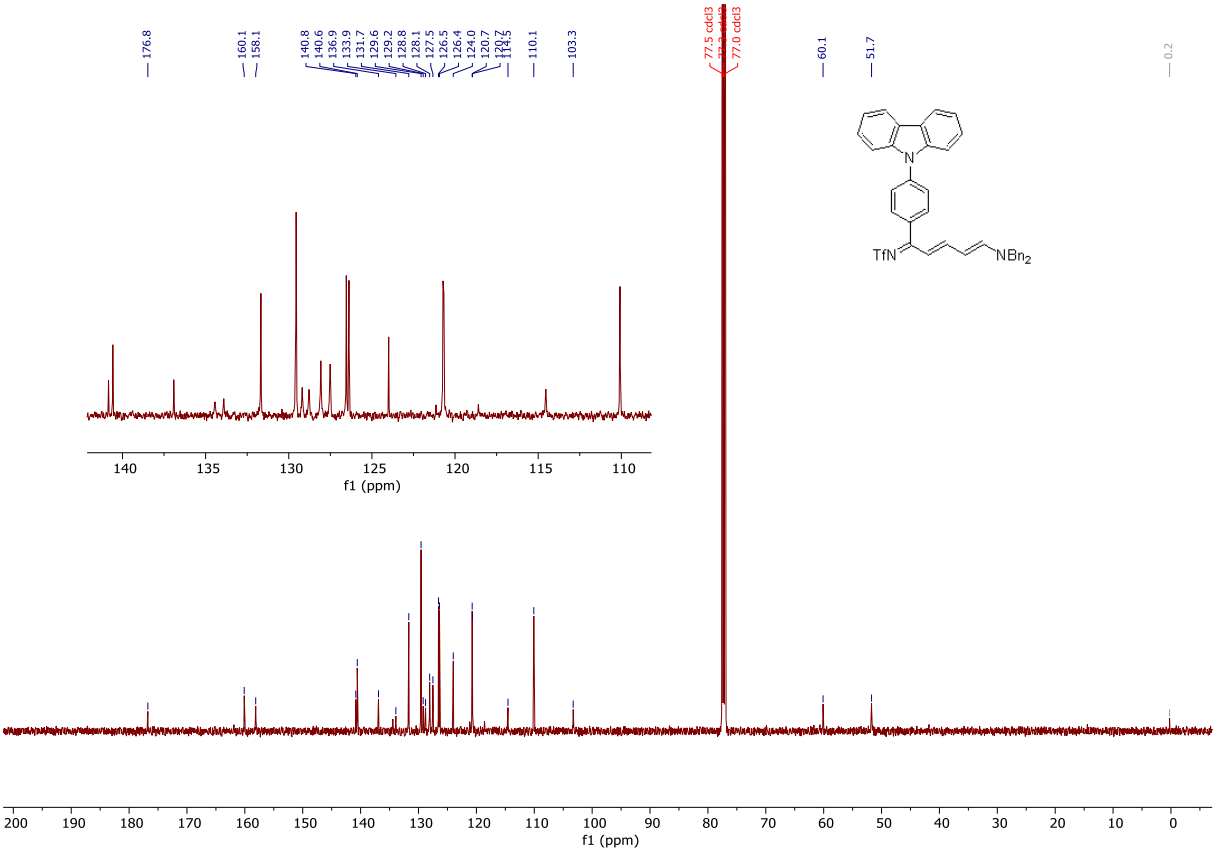

^{1}H NMR spectrum of Zincke imine S13b ($CDCl_3$, 298 K)

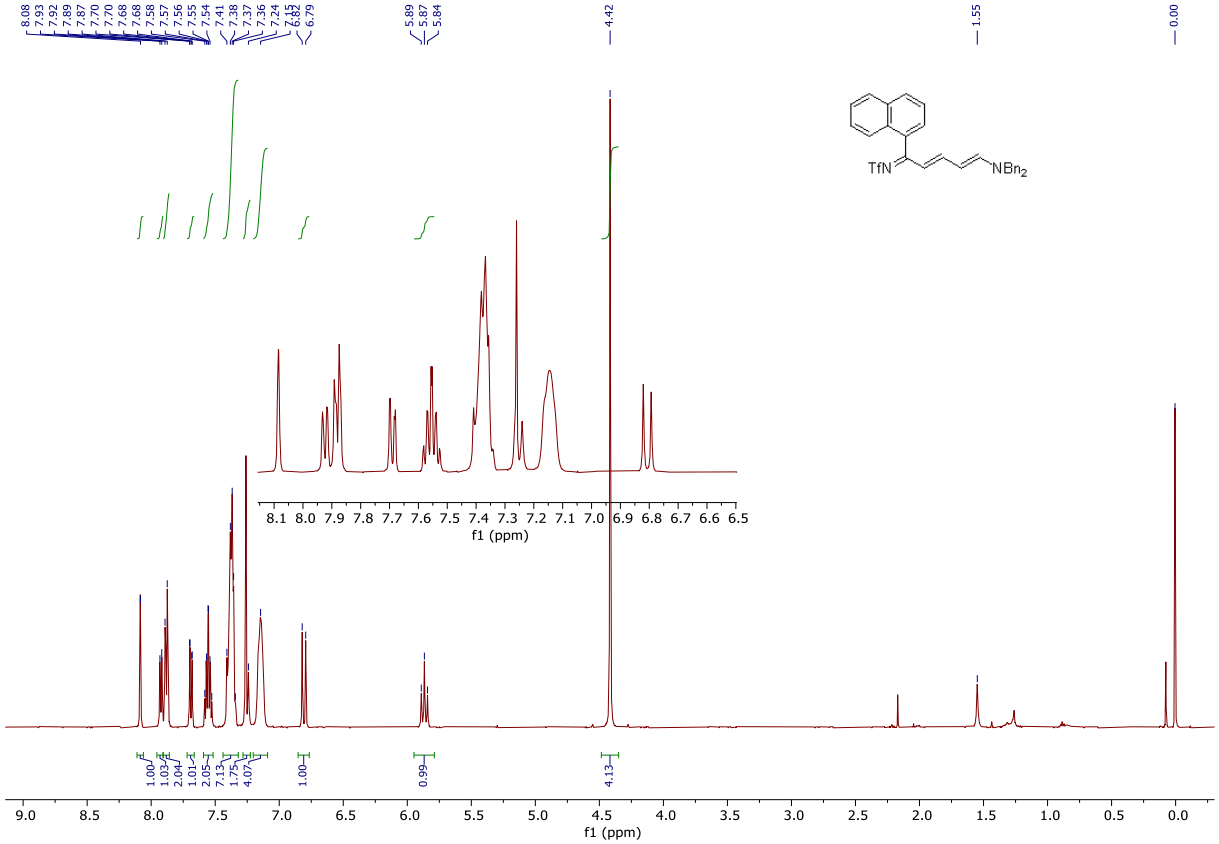

^{13}C NMR spectrum of Zincke imine S13b ($CDCl_3$, 298 K)

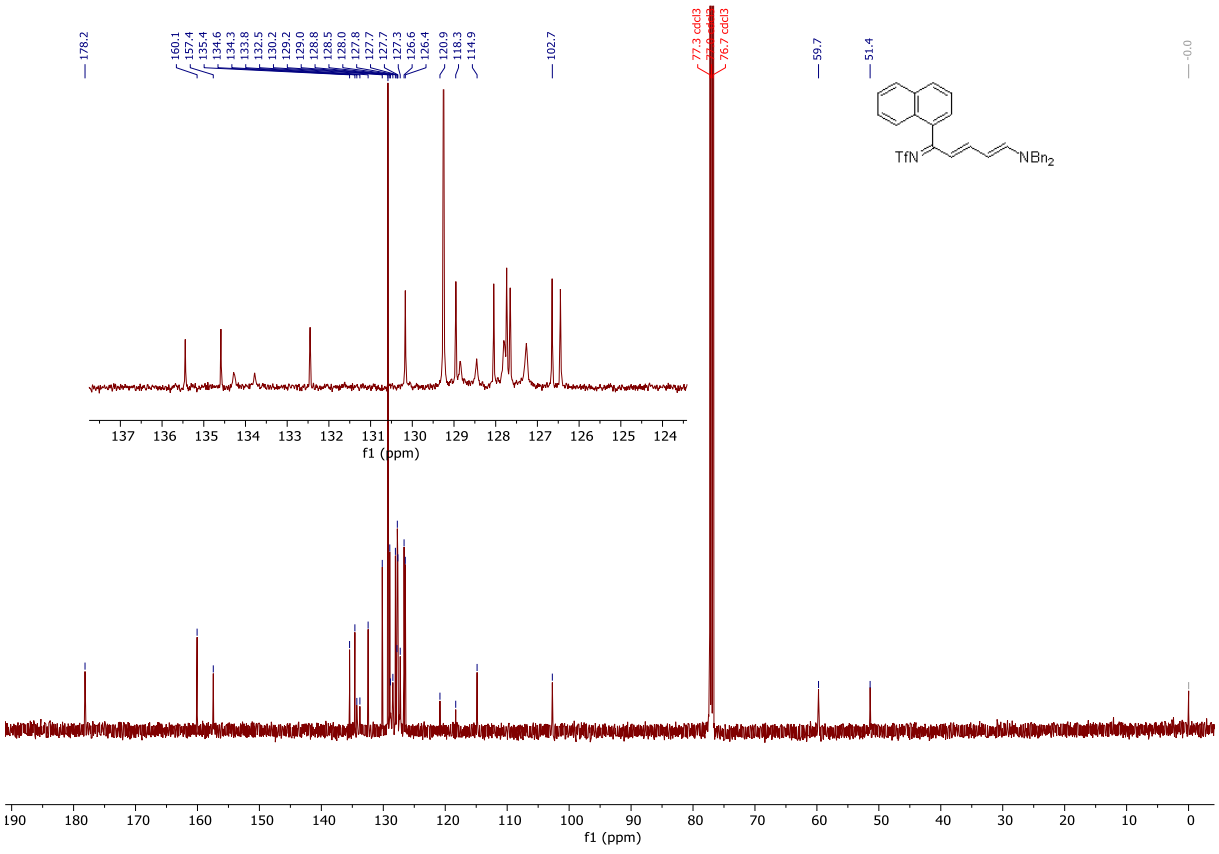

^{1}H NMR spectrum of Zincke imine S14b ($CDCl_3$, 298 K)

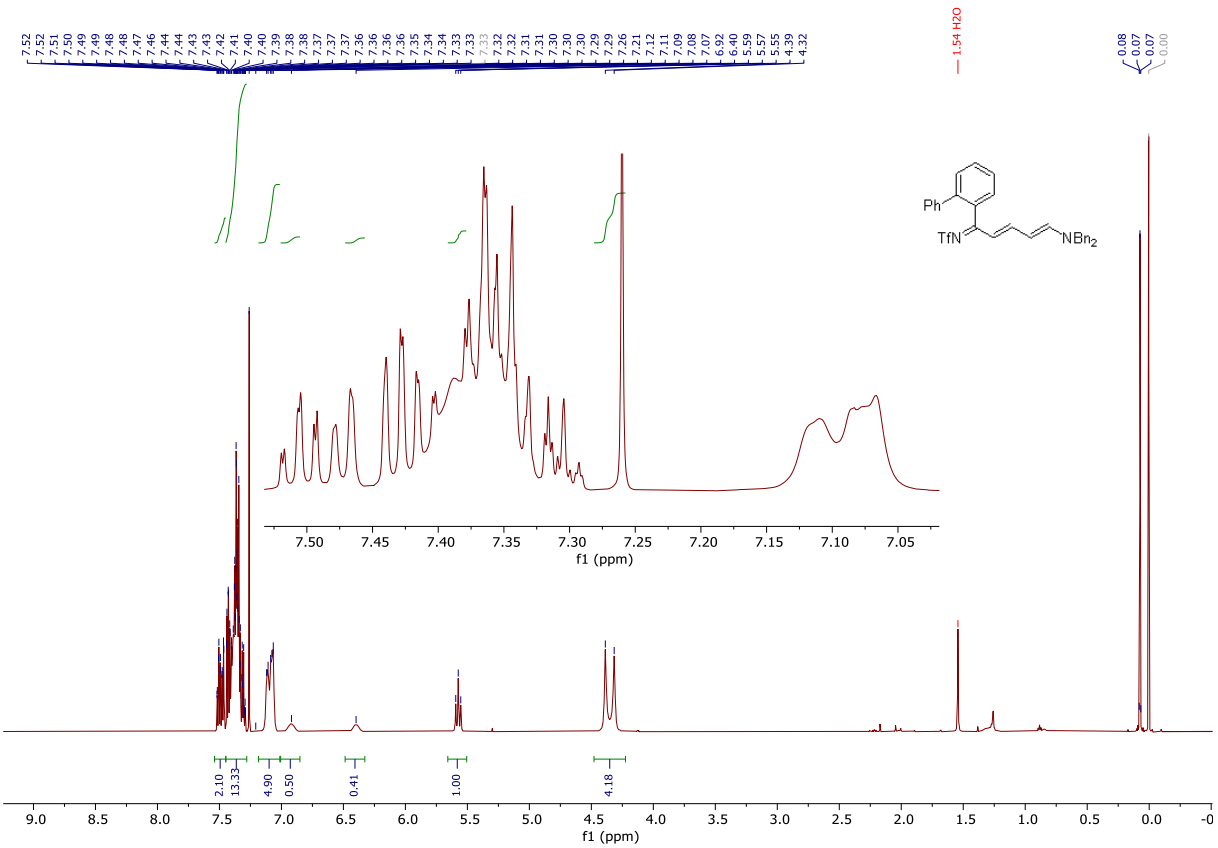

^{13}C NMR spectrum of Zincke imine S14b ($CDCl_3$, 298 K)

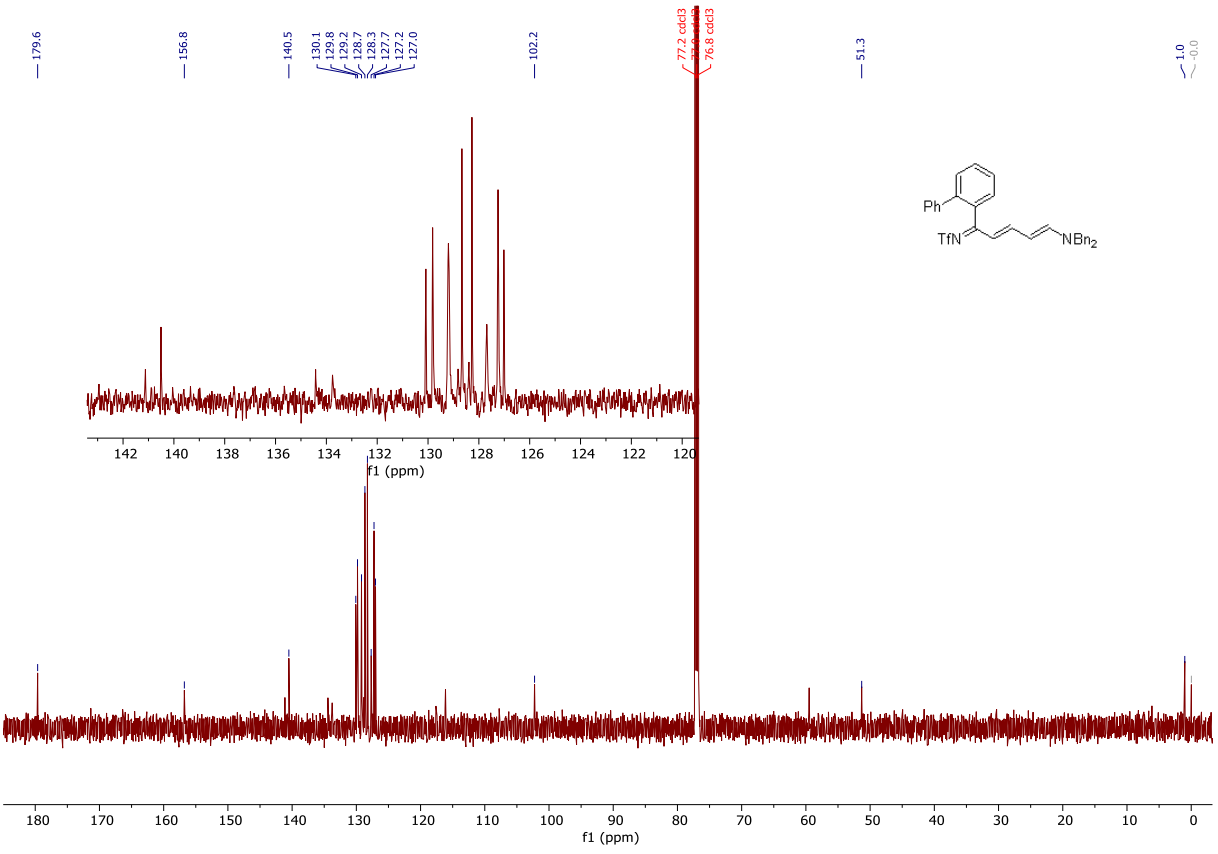

^{1}H NMR spectrum of Zincke imine S15b ($CDCl_3$, 298 K)

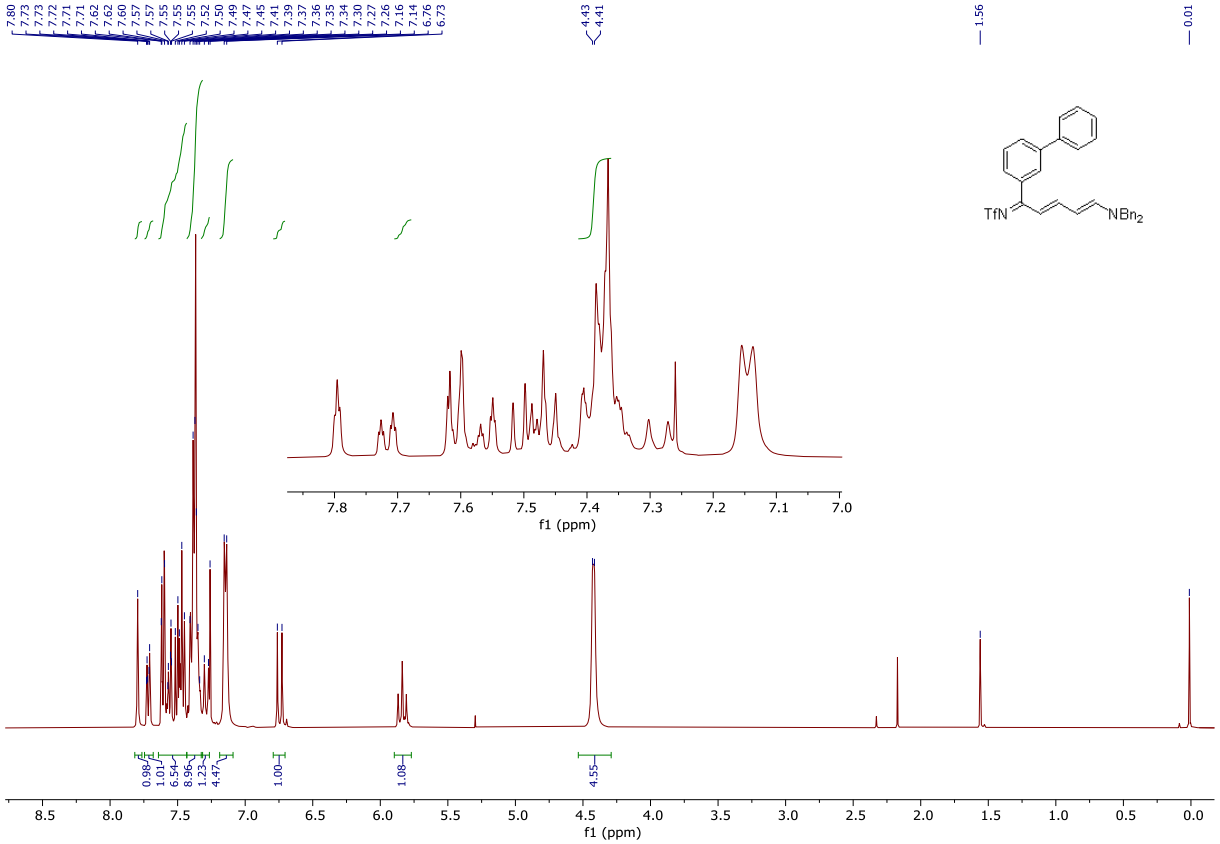

^{13}C NMR spectrum of Zincke imine S15b ($CDCl_3$, 298 K)

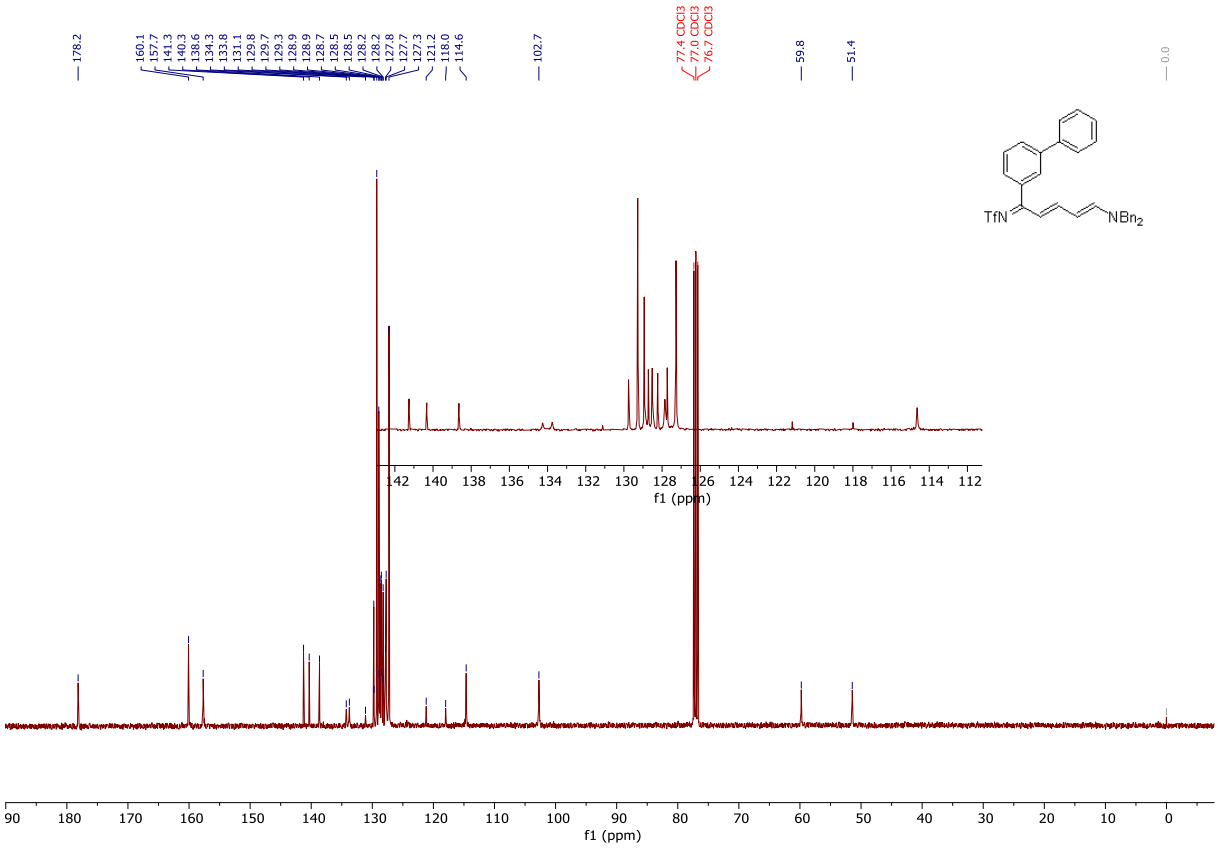

^{1}H NMR spectrum of Zincke imine S16b ($CDCl_3$, 298 K)

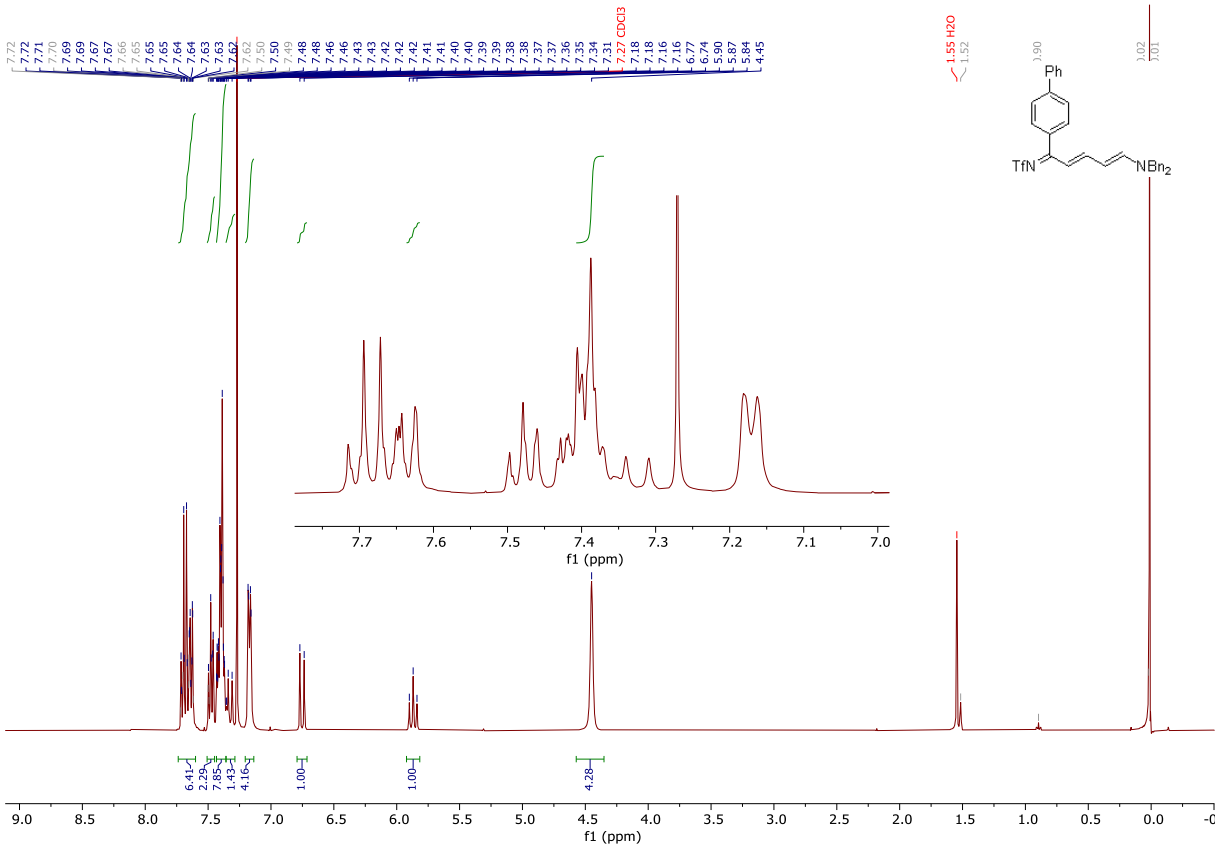

^{13}C NMR spectrum of Zincke imine S16b ($CDCl_3$, 298 K)

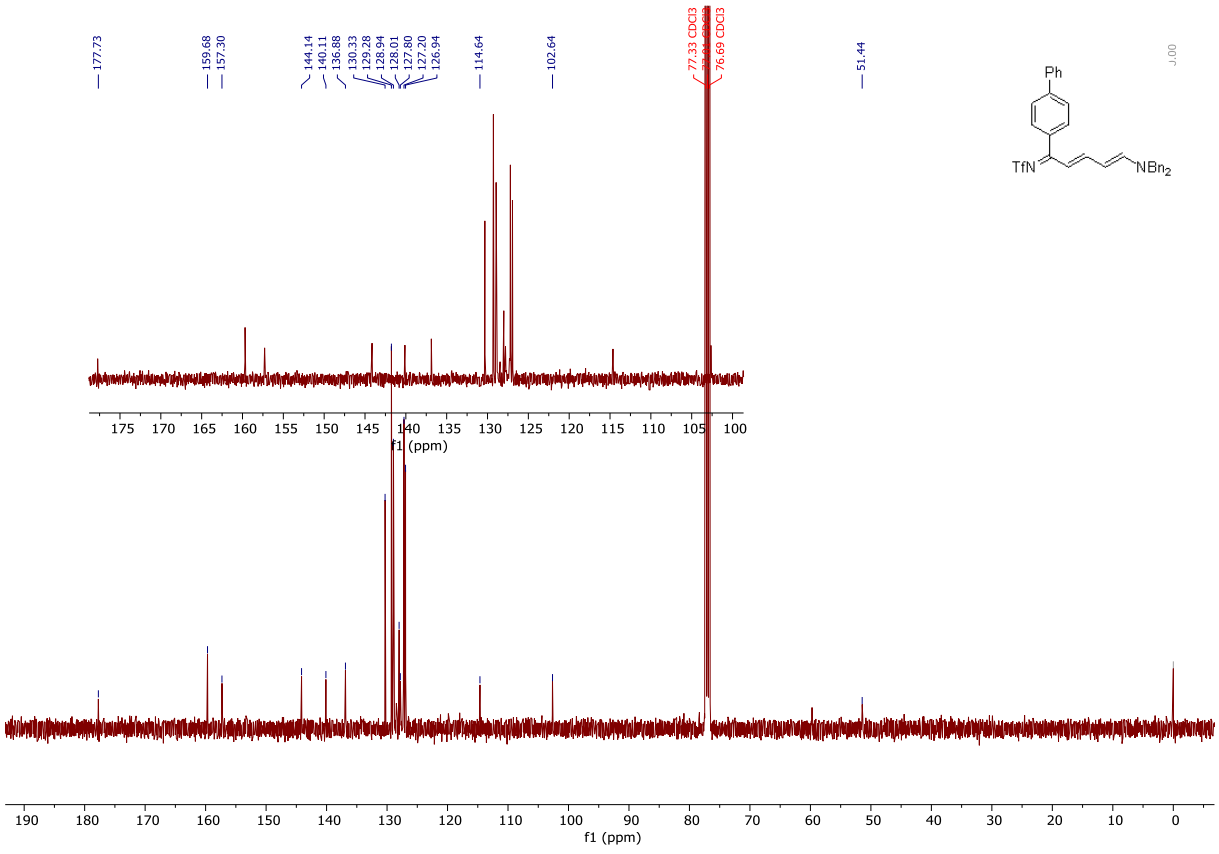

^{1}H NMR spectrum of Zincke imine S17b ($CDCl_3$, 298 K)

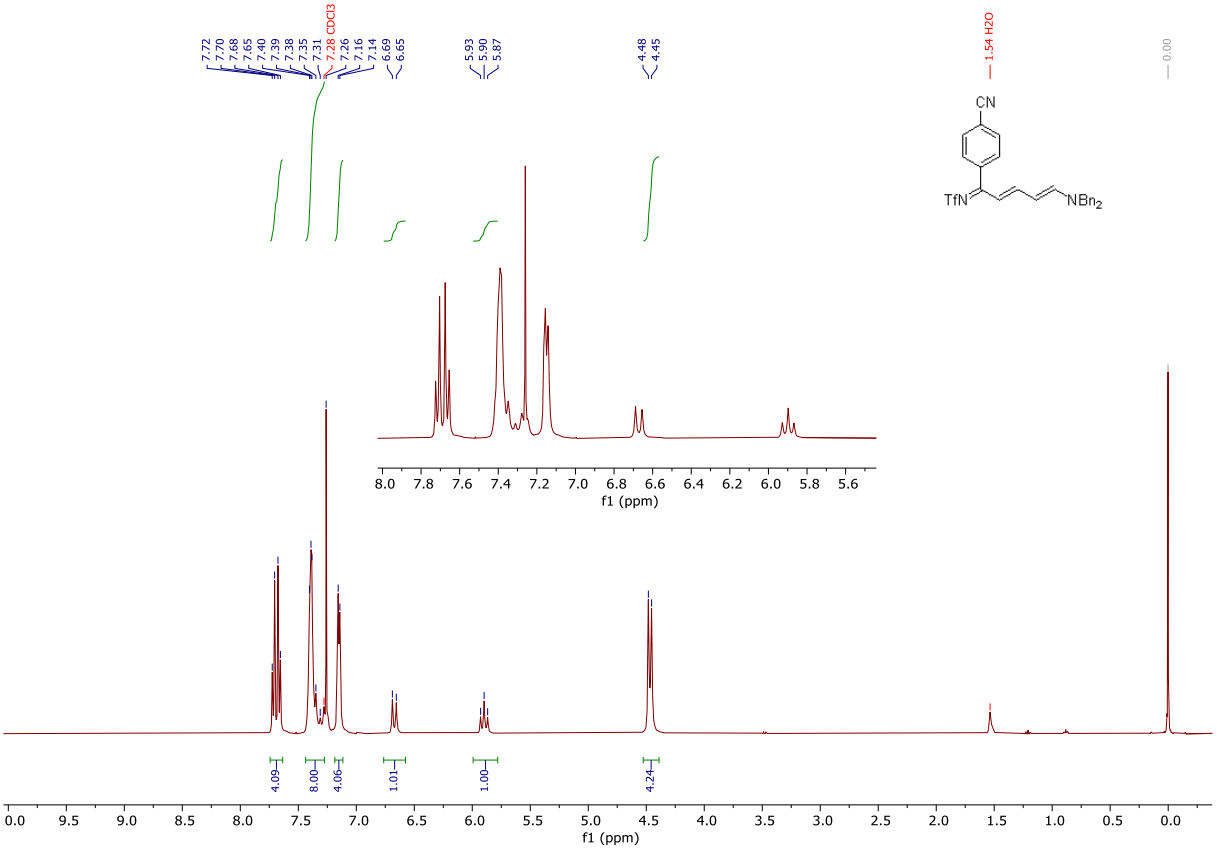

^{13}C NMR spectrum of Zincke imine S17b ($CDCl_3$, 298 K)

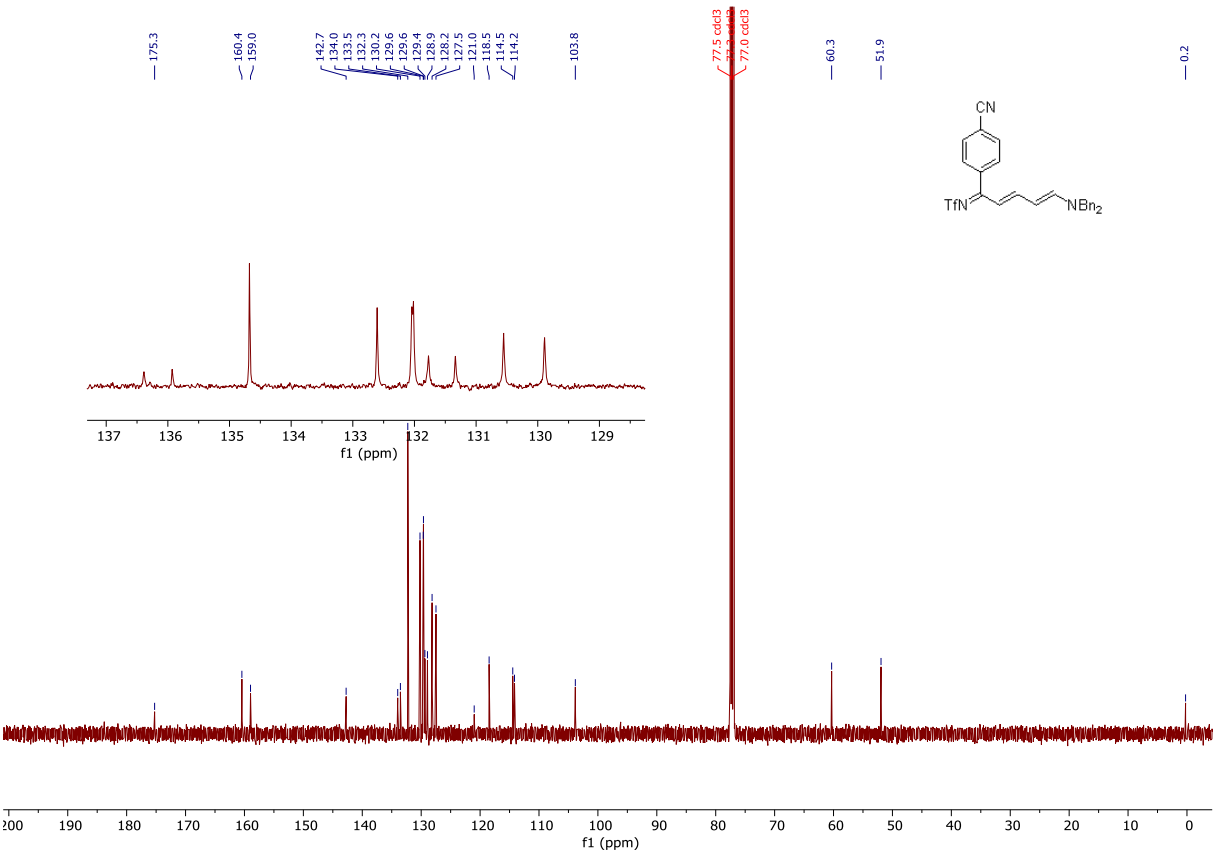

^{1}H NMR spectrum of Zincke imine S18b ($CDCl_3$, 298 K)

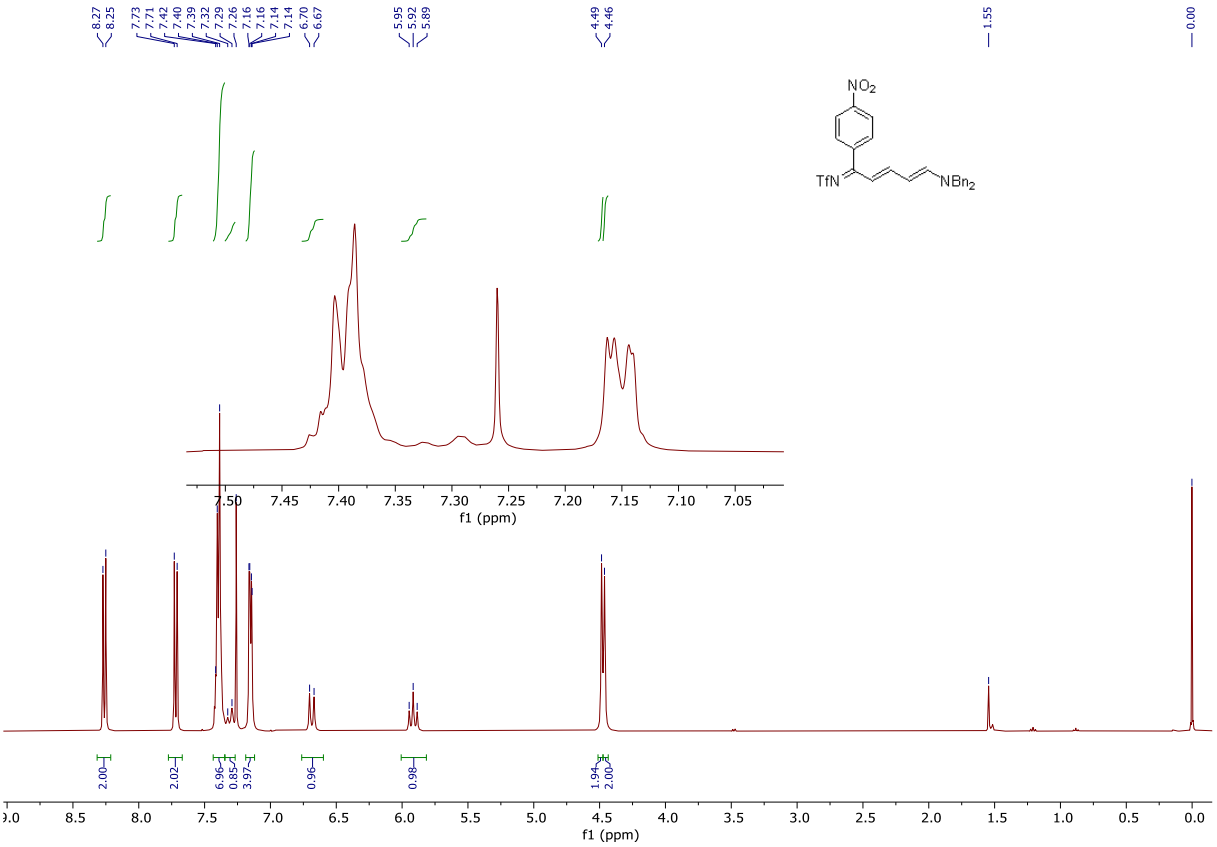

^{13}C NMR spectrum of Zincke imine S18b ($CDCl_3$, 298 K)

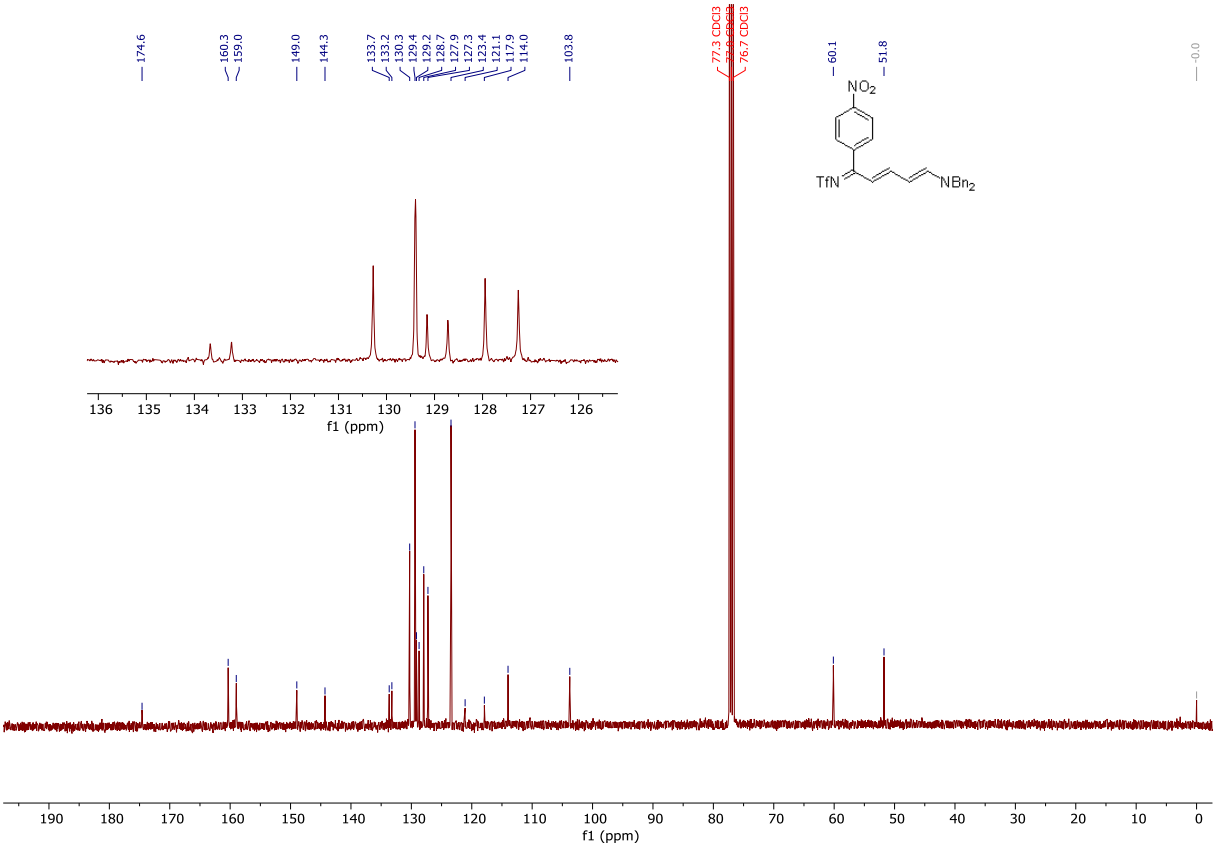

^{1}H NMR spectrum of Zincke imine S19b ($CDCl_3$, 298 K)

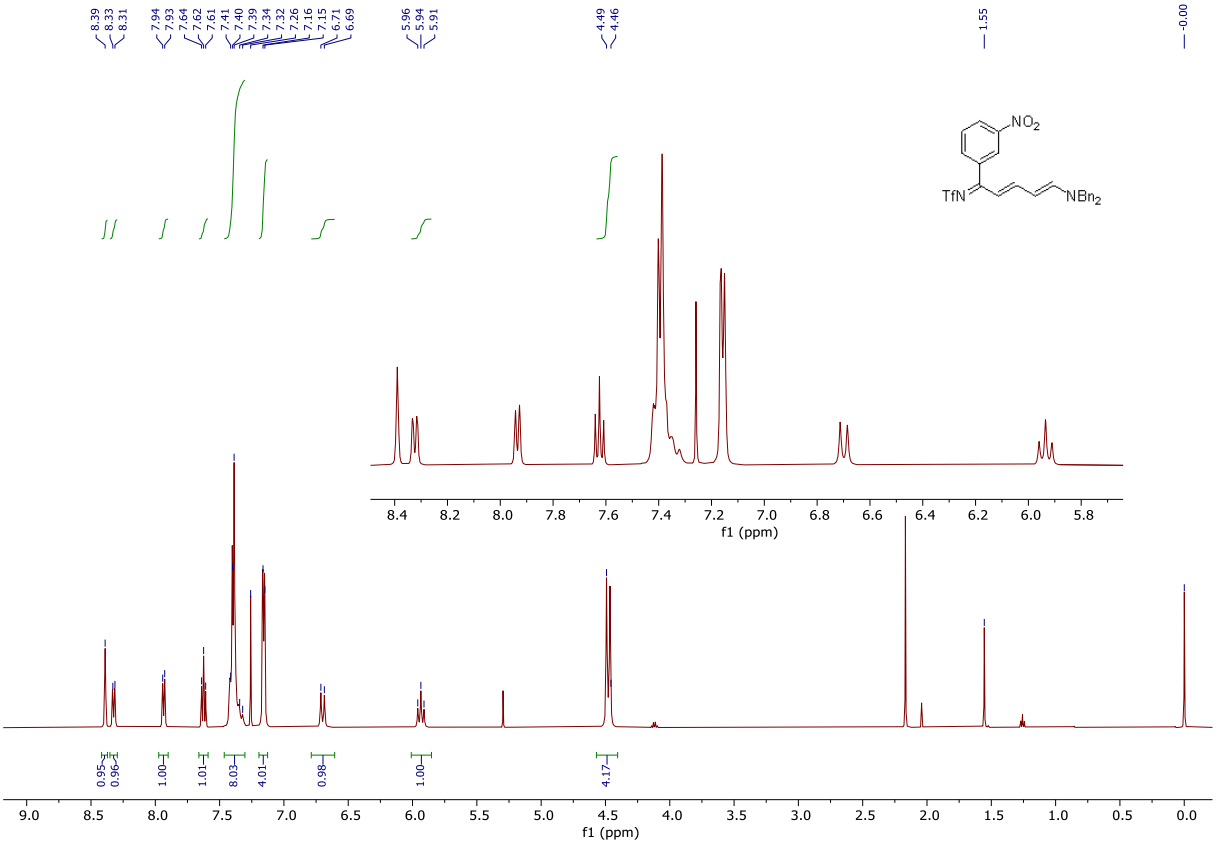

^{13}C NMR spectrum of Zincke imine S19b ($CDCl_3$, 298 K)

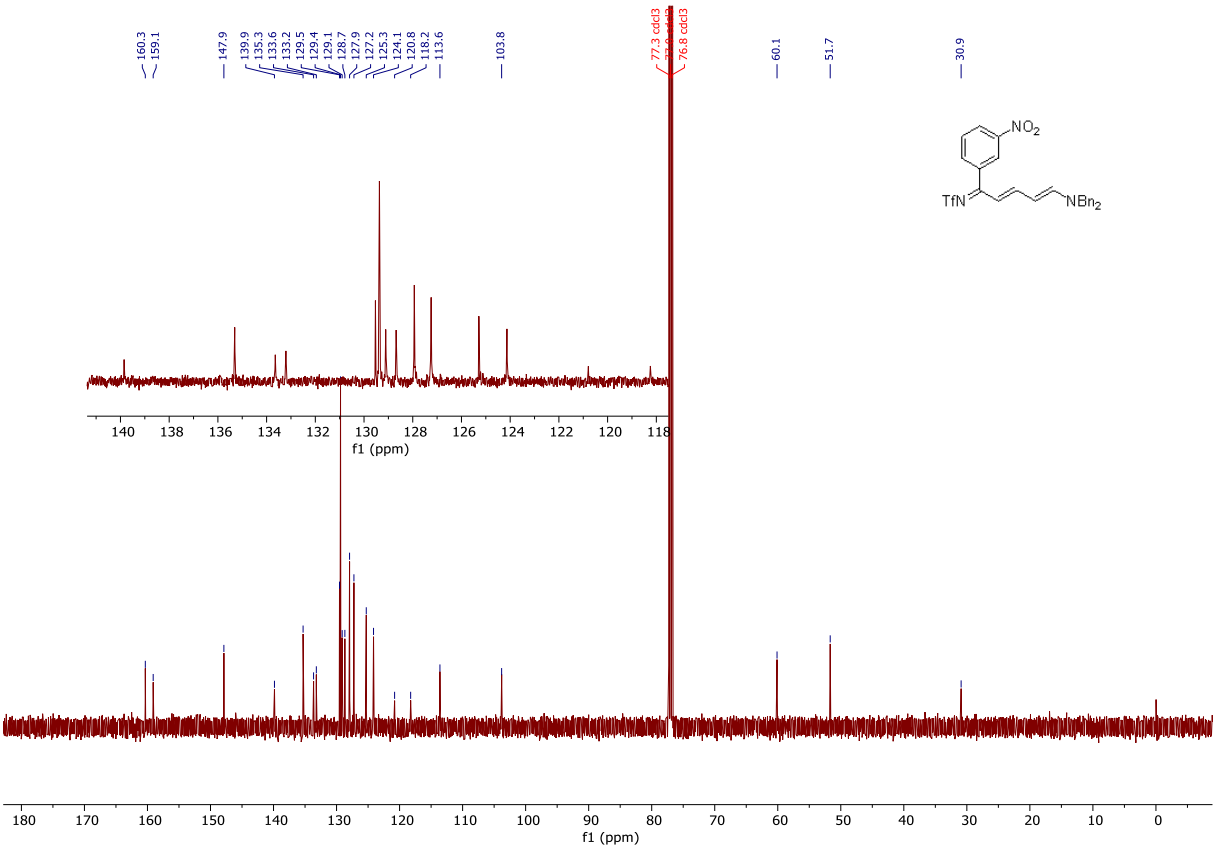

^{1}H NMR spectrum of Zincke imine S20b ($CDCl_3$, 298 K)

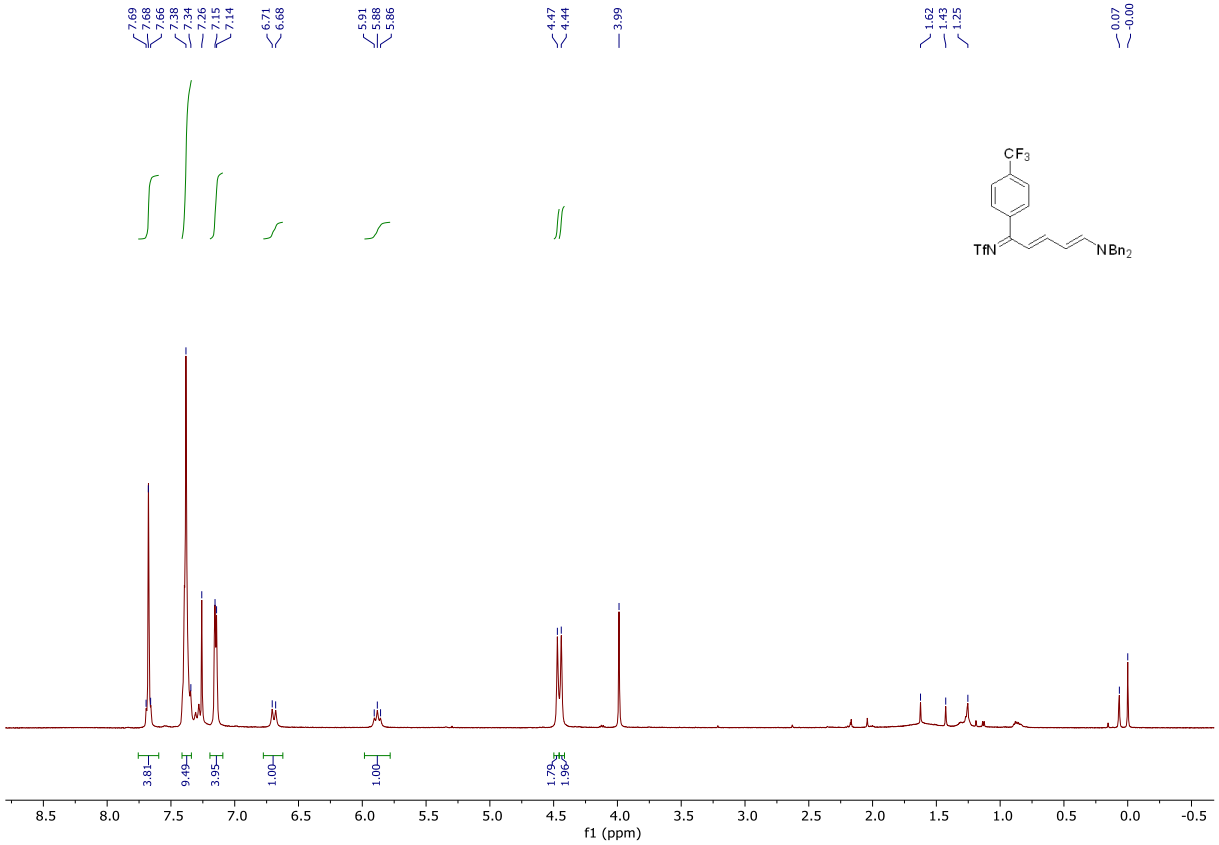

^{13}C NMR spectrum of Zincke imine S20b ($CDCl_3$, 298 K)

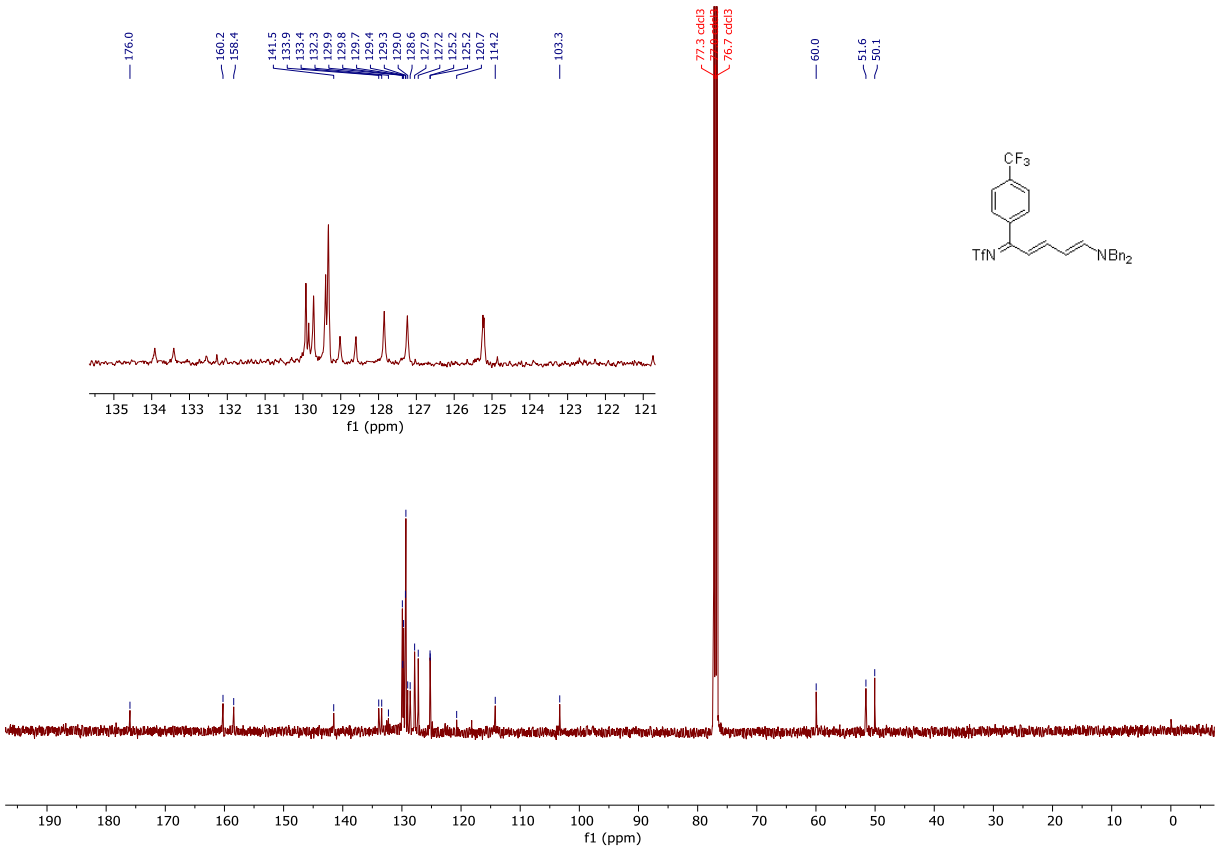

^{1}H NMR spectrum of Zincke imine S21b ($CDCl_3$, 298 K)

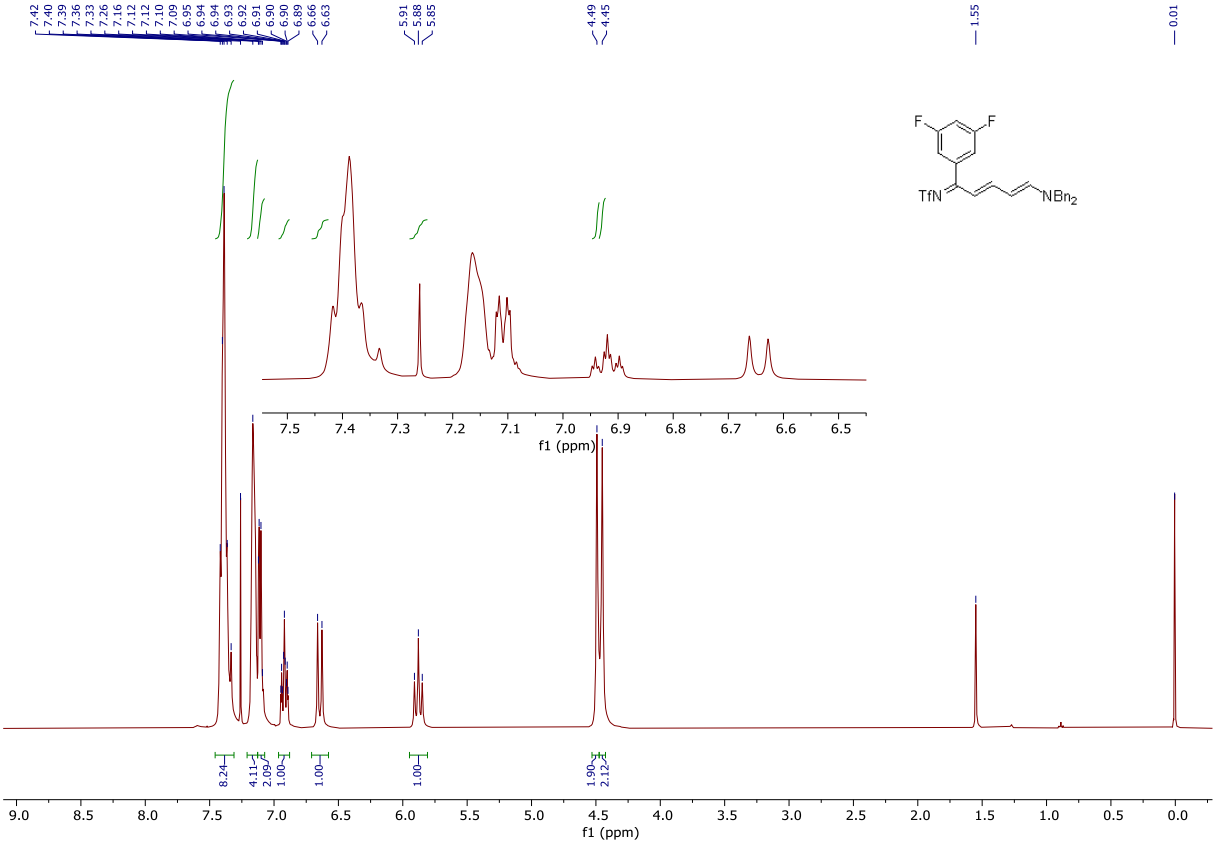

^{13}C NMR spectrum of Zincke imine S21b ($CDCl_3$, 298 K)

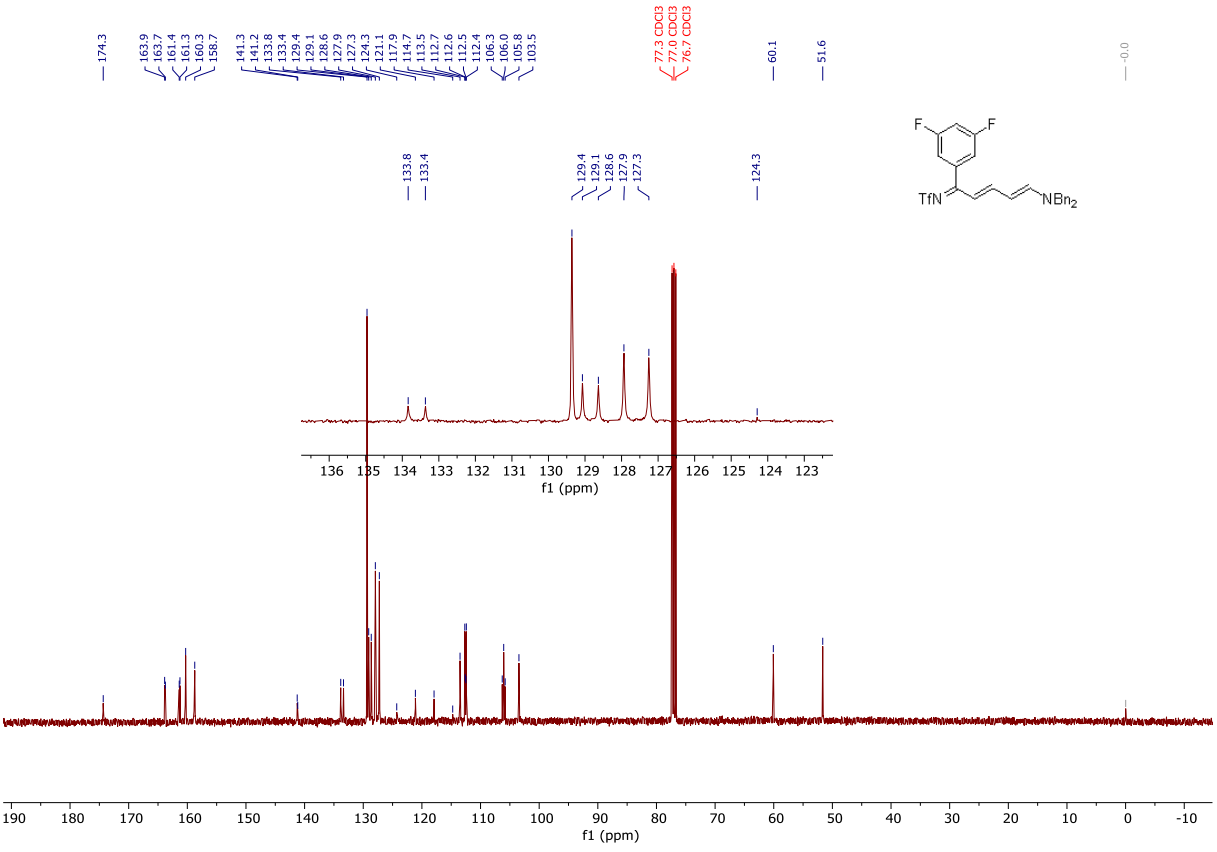

^{1}H NMR spectrum of Zincke imine S22b ($CDCl_3$, 298 K)

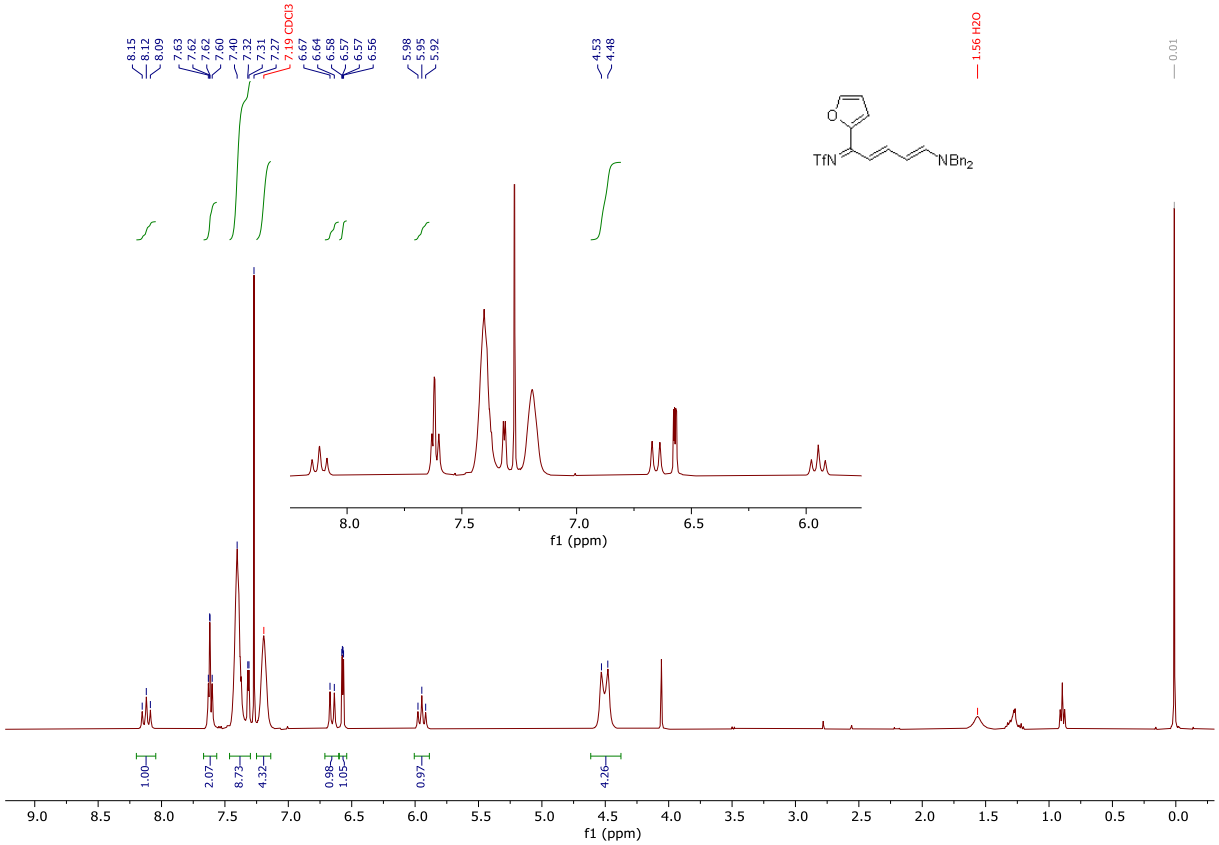

^{13}C NMR spectrum of Zincke imine S22b ($CDCl_3$, 298 K)

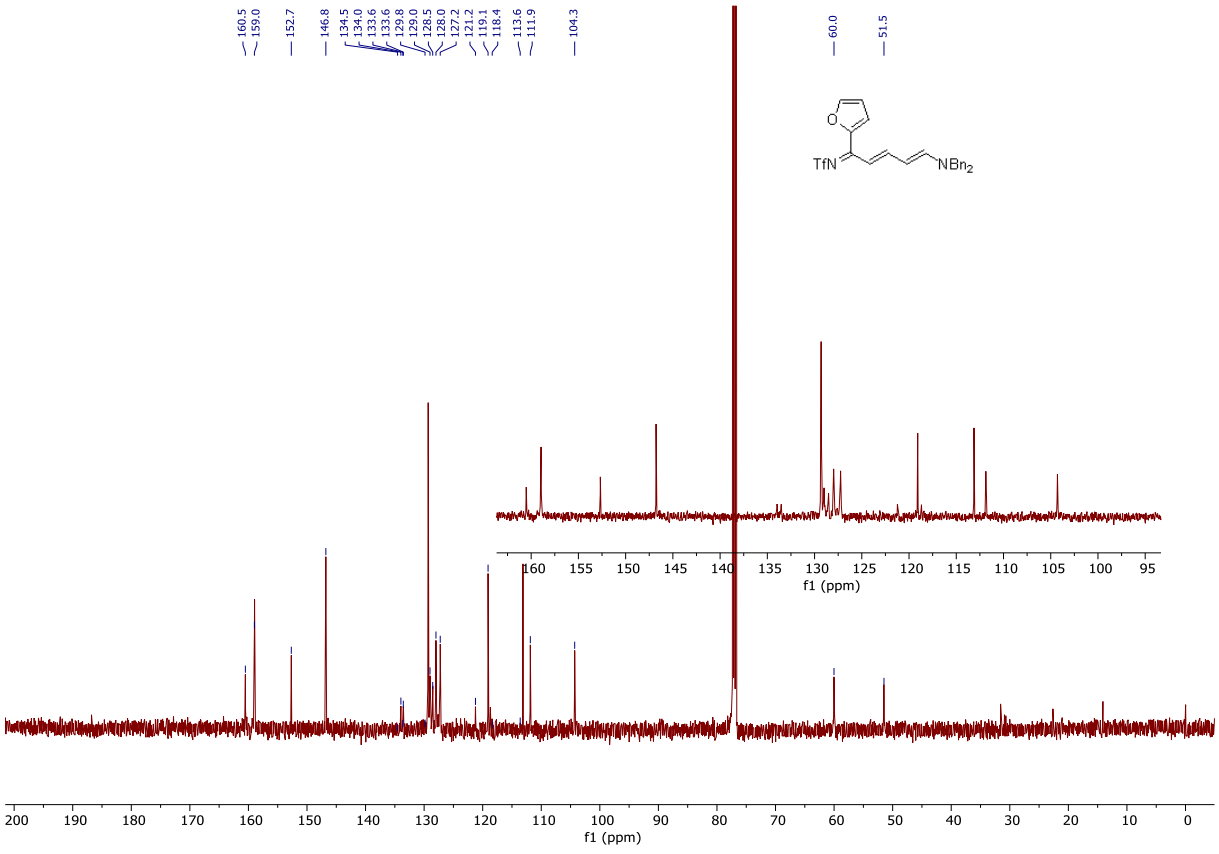

^{1}H NMR spectrum of Zincke imine S23b ($CDCl_3$, 298 K)

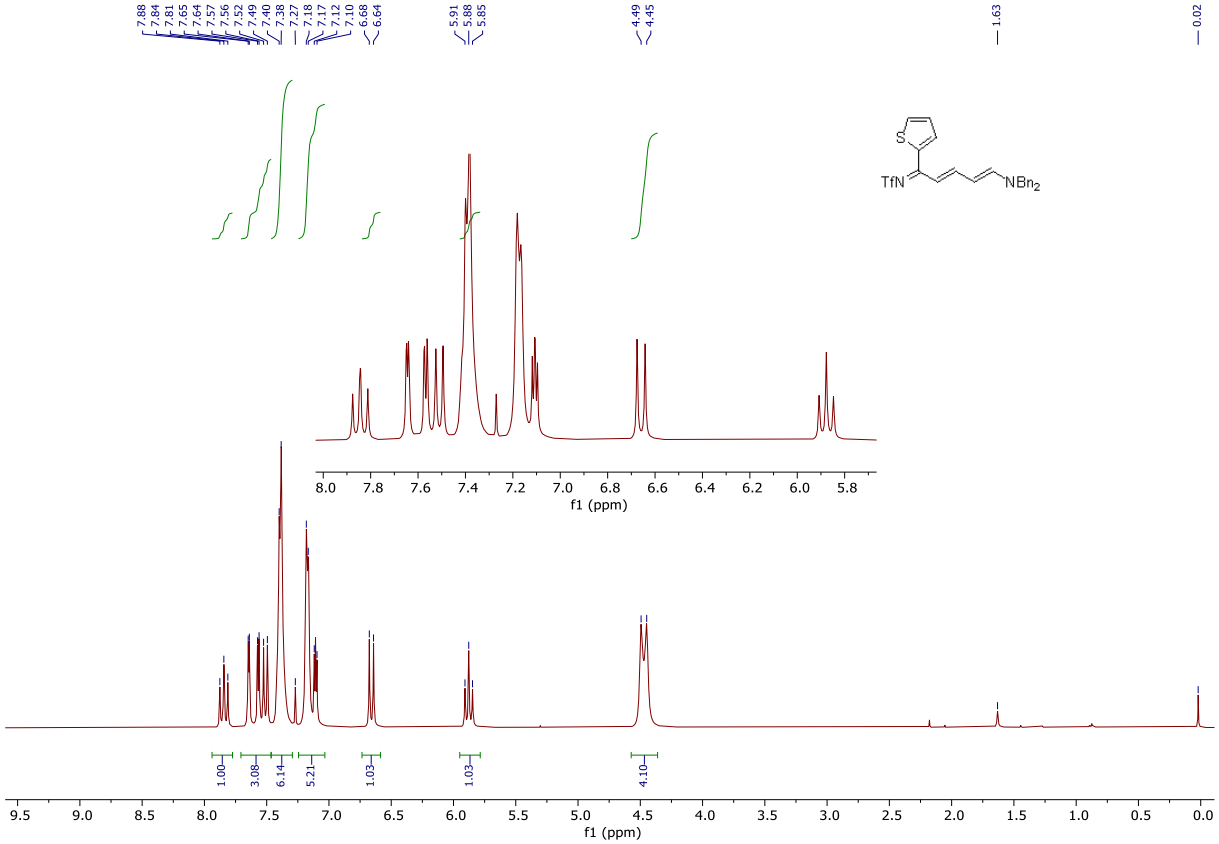

^{13}C NMR spectrum of Zincke imine S23b ($CDCl_3$, 298 K)

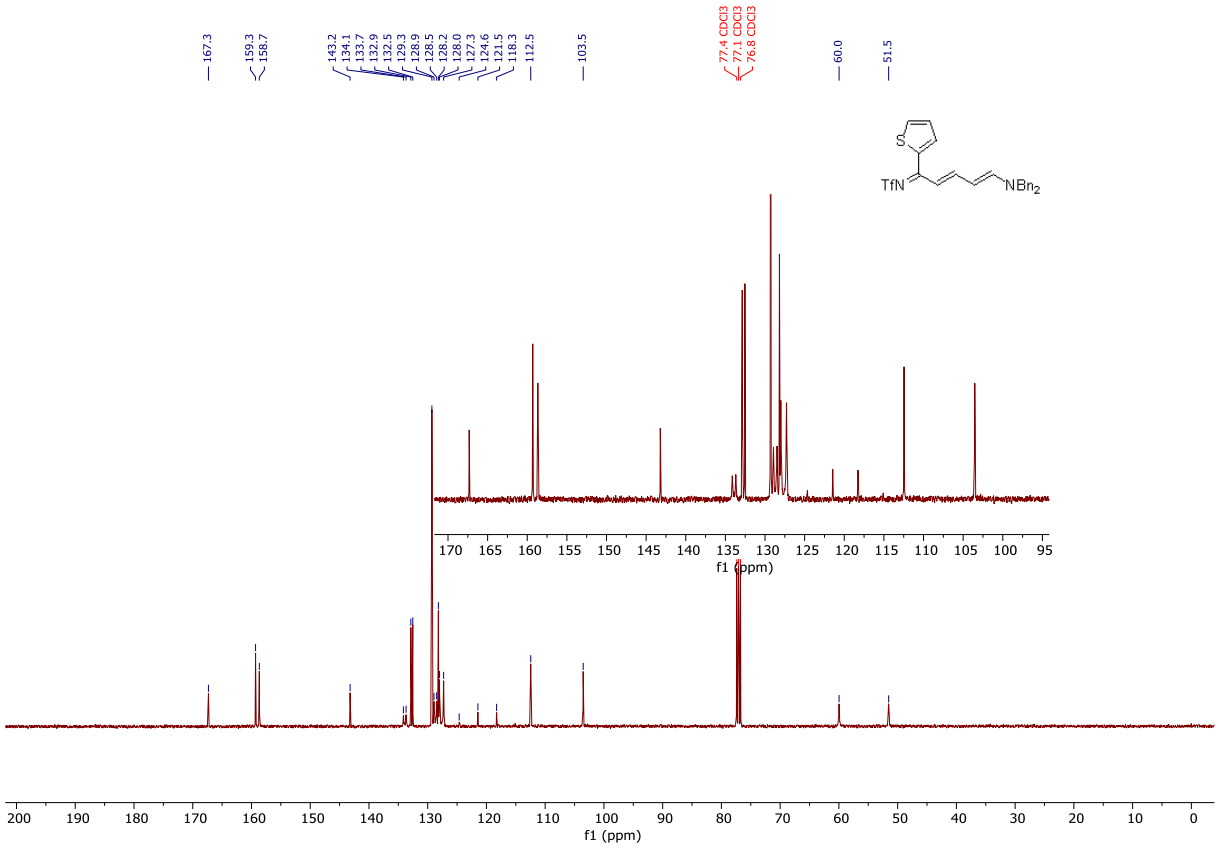

^{1}H NMR spectrum of Zincke imine S24b ($CDCl_3$, 298 K)

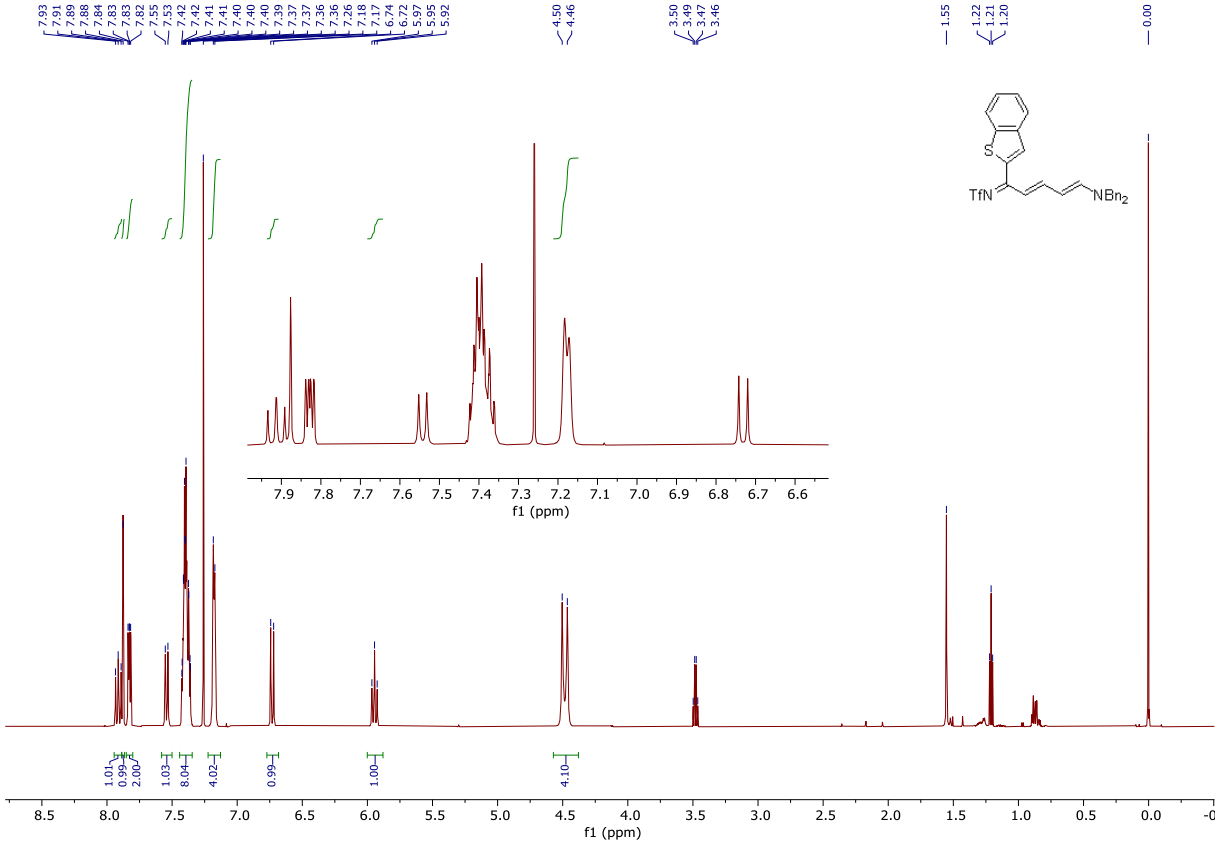

^{13}C NMR spectrum of Zincke imine S24b ($CDCl_3$, 298 K)

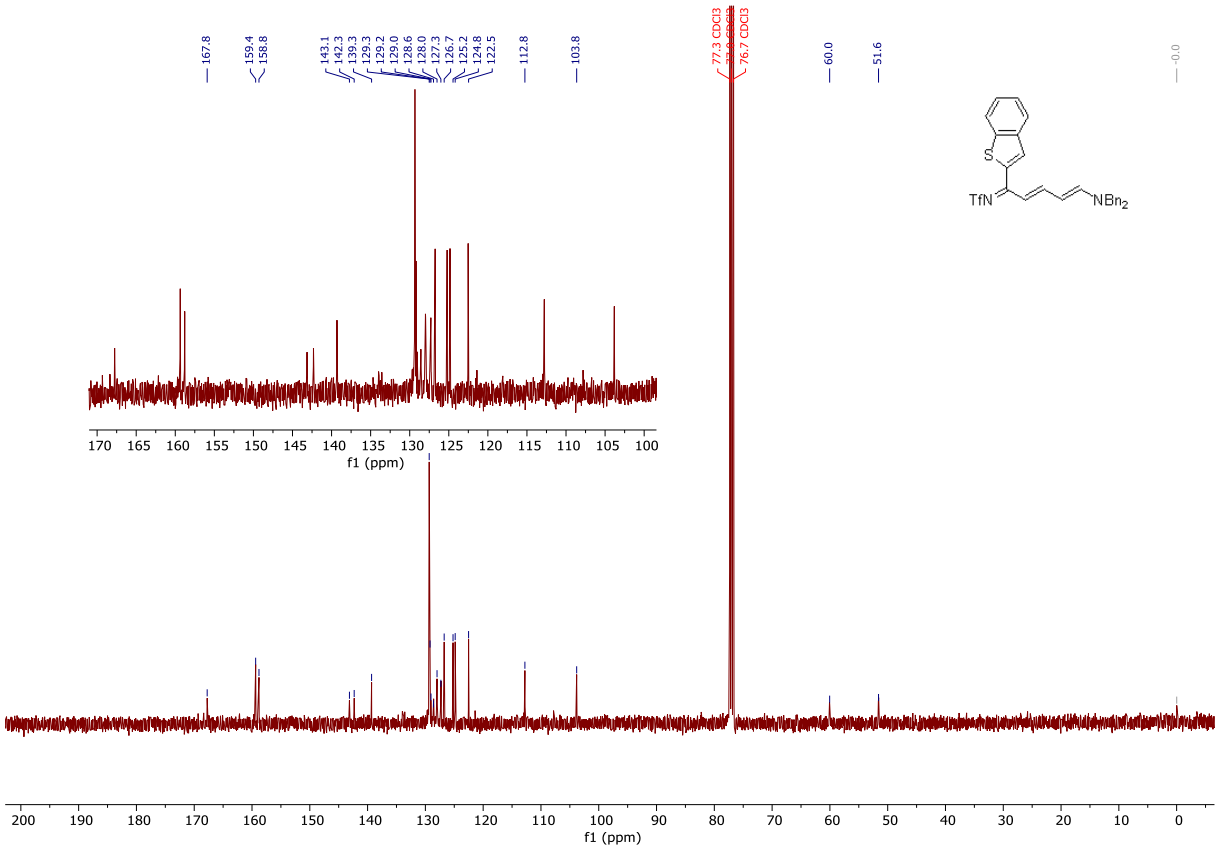

^{1}H NMR spectrum of Zincke imine S25b ($CDCl_3$, 298 K)

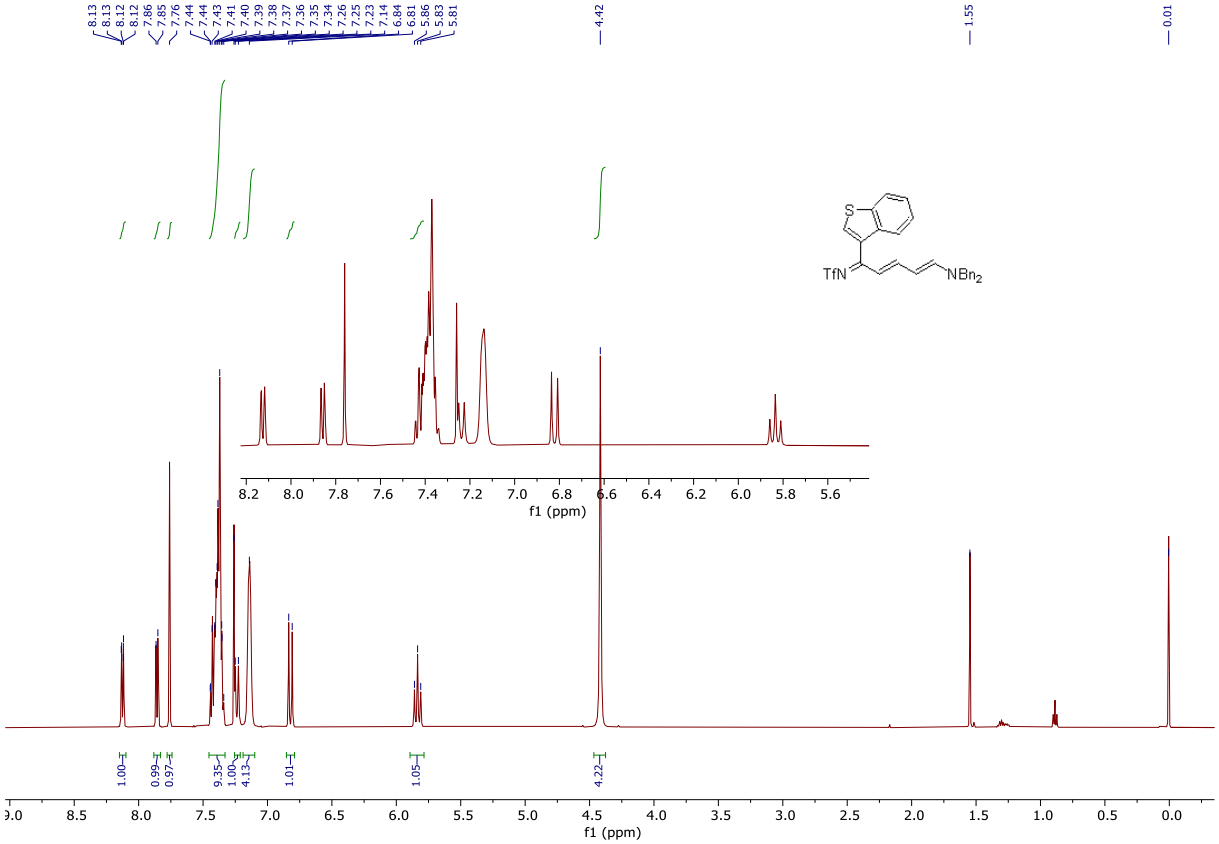

^{13}C NMR spectrum of Zincke imine S25b ($CDCl_3$, 298 K)

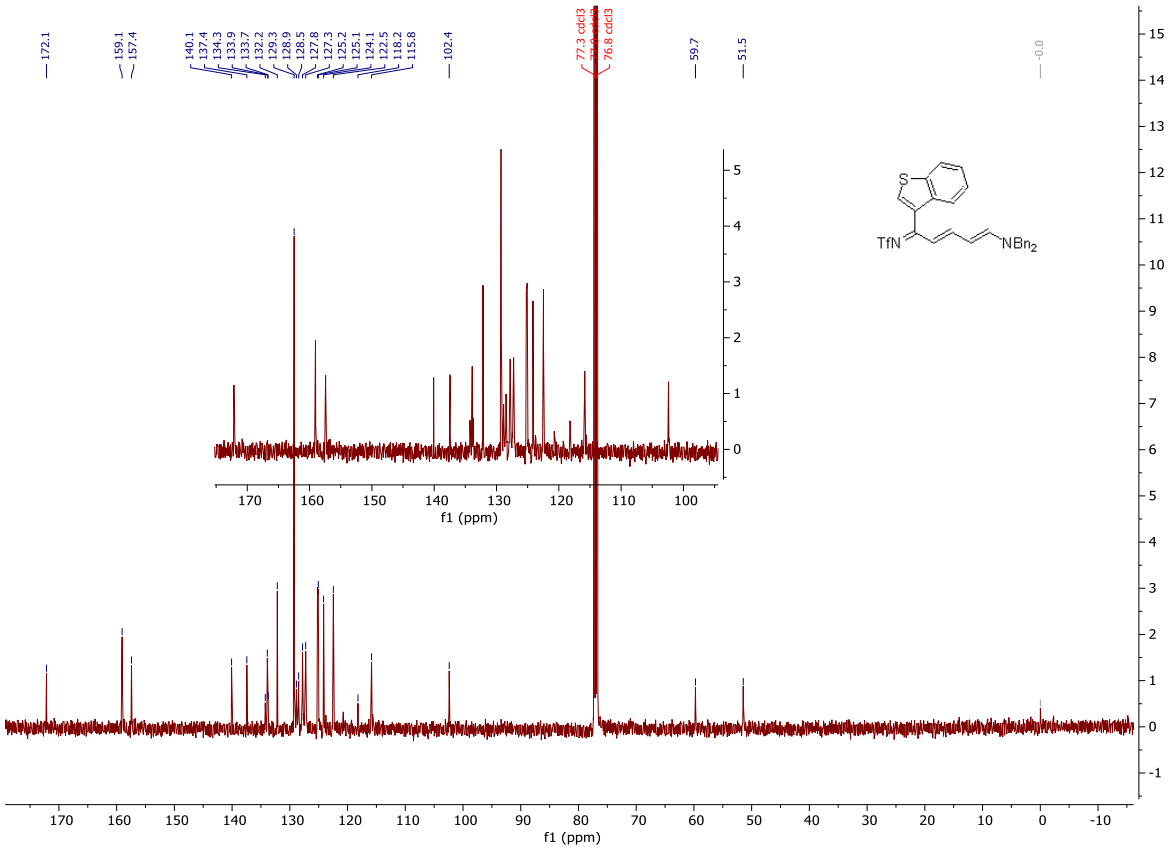

^{1}H NMR spectrum of Zincke imine S26b ($CDCl_3$, 298 K)

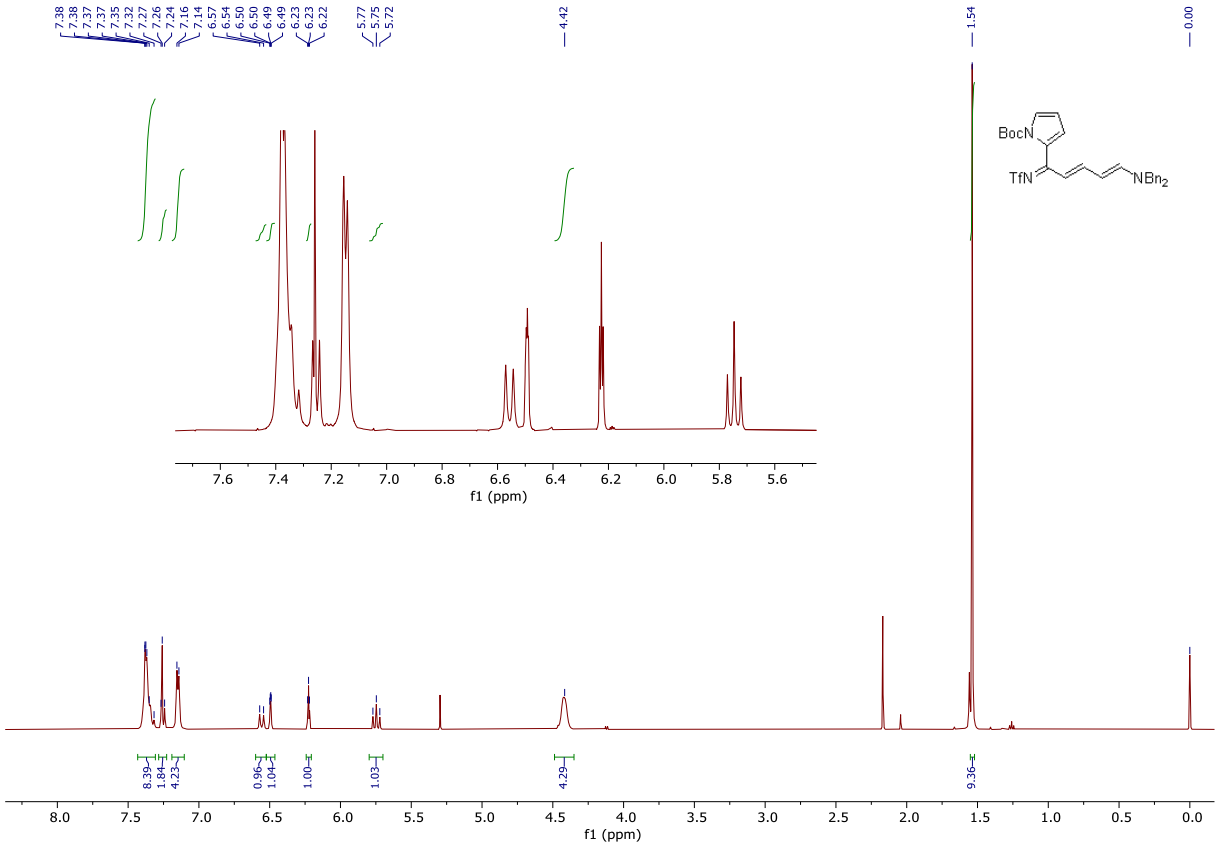

^{13}C NMR spectrum of Zincke imine S26b ($CDCl_3$, 298 K)

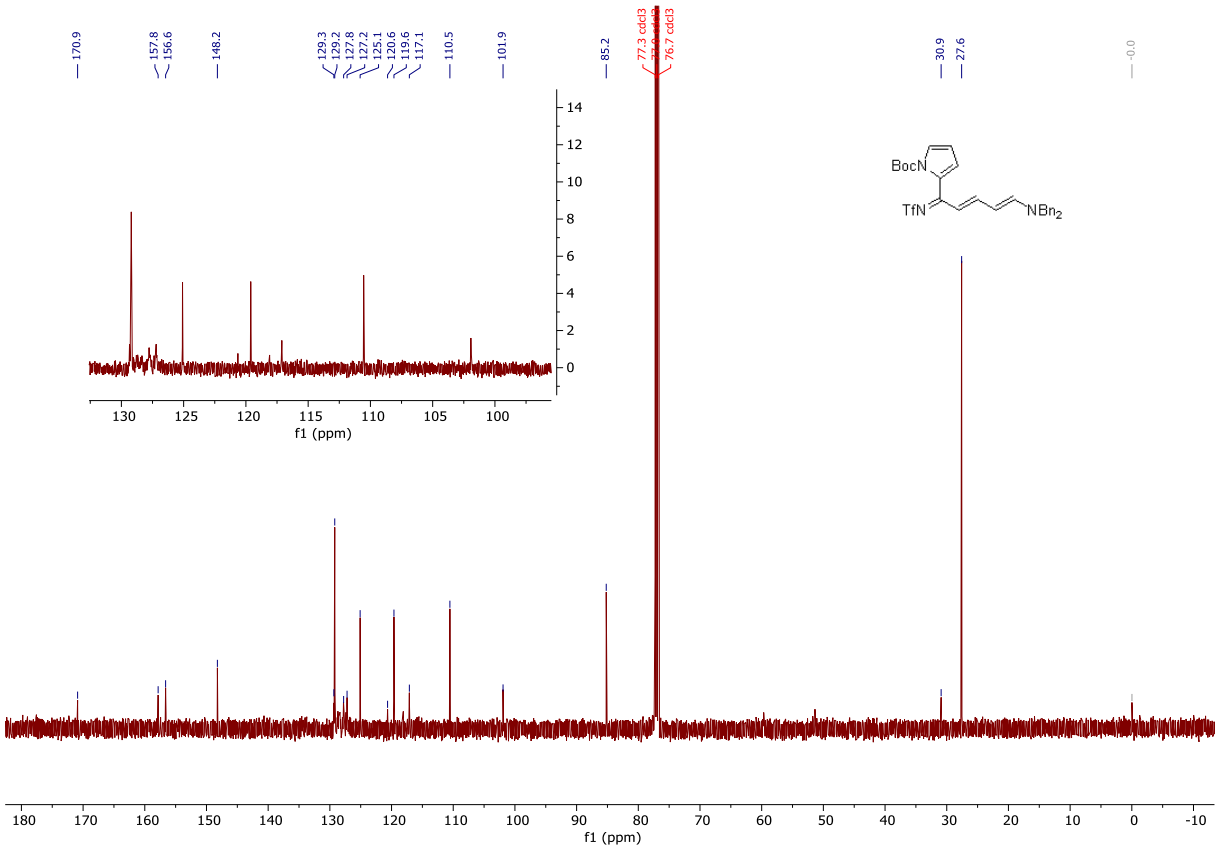

^{1}H NMR spectrum of Zincke imine S27b ($CDCl_3$, 298 K)

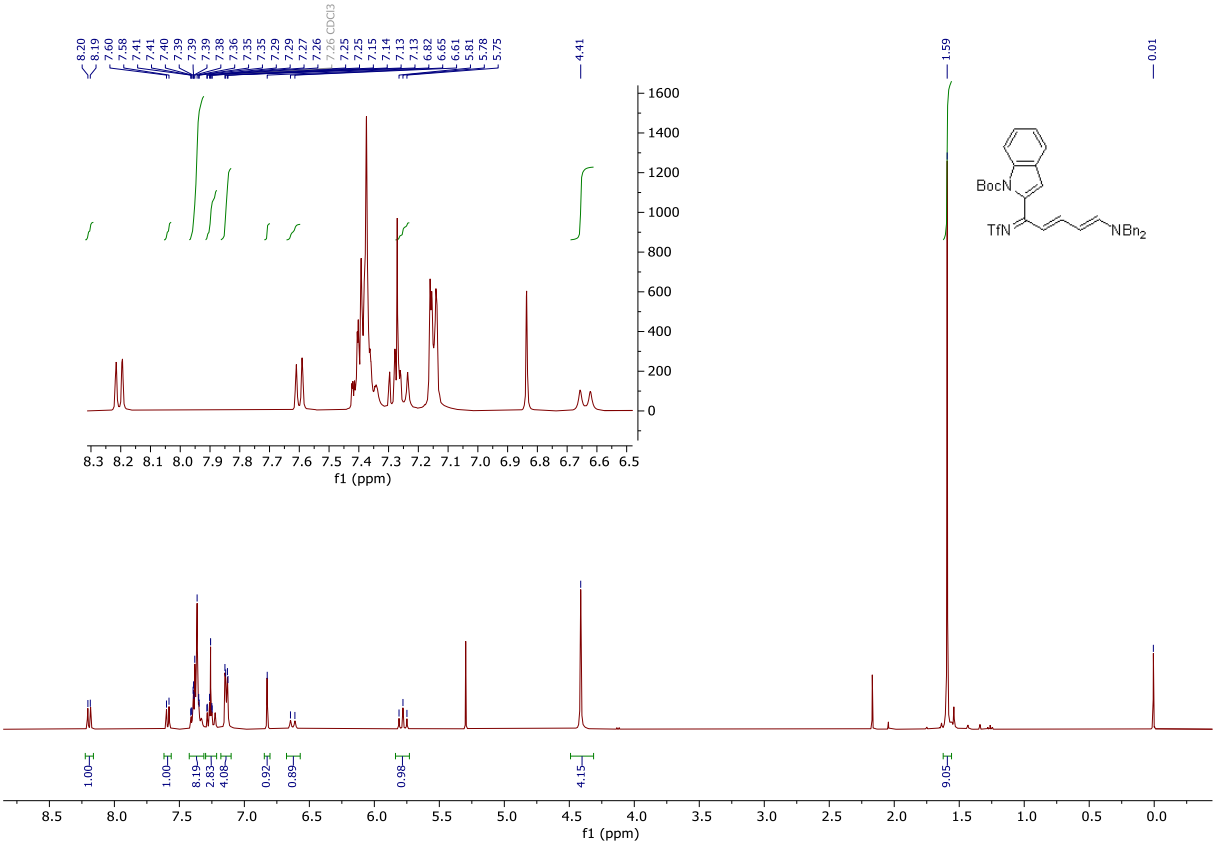

^{13}C NMR spectrum of Zincke imine S27b ($CDCl_3$, 298 K)

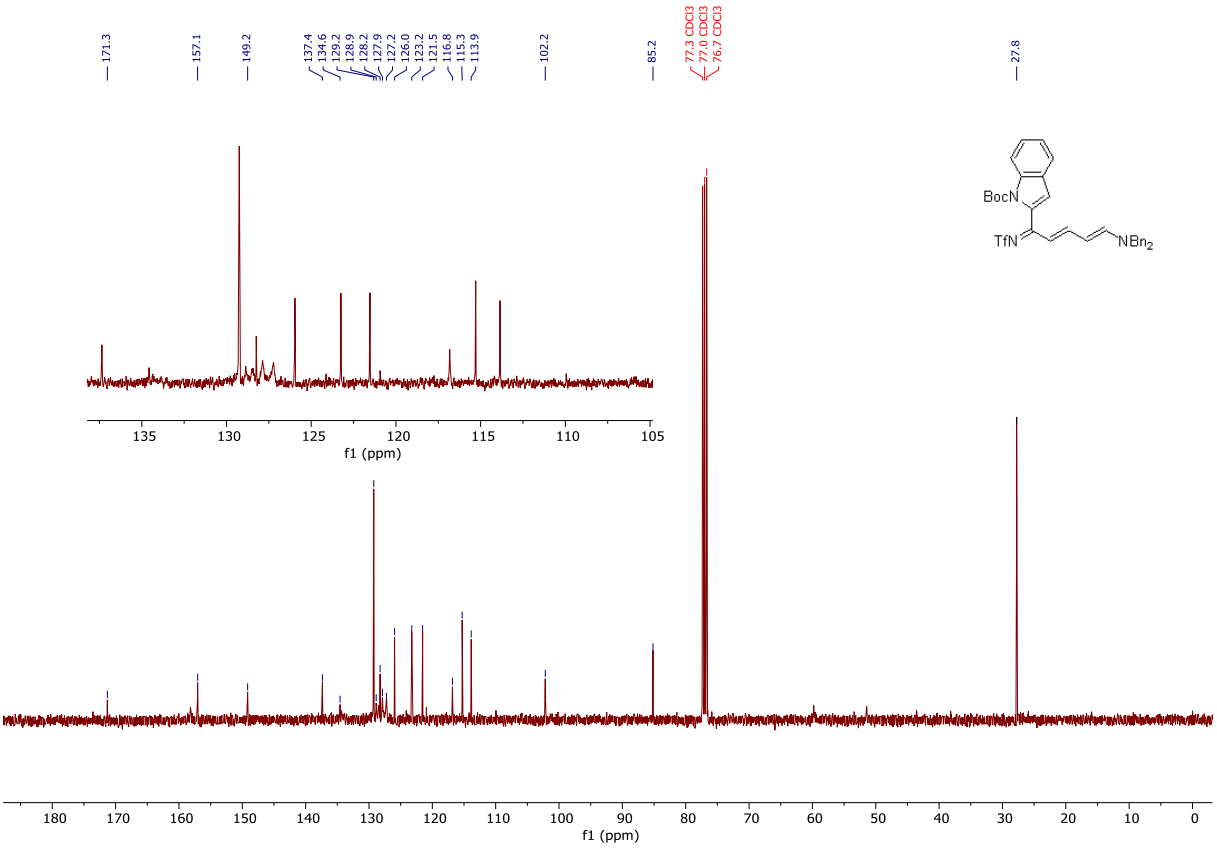

^{1}H NMR spectrum of Zincke imine S28b ($CDCl_3$, 298 K)

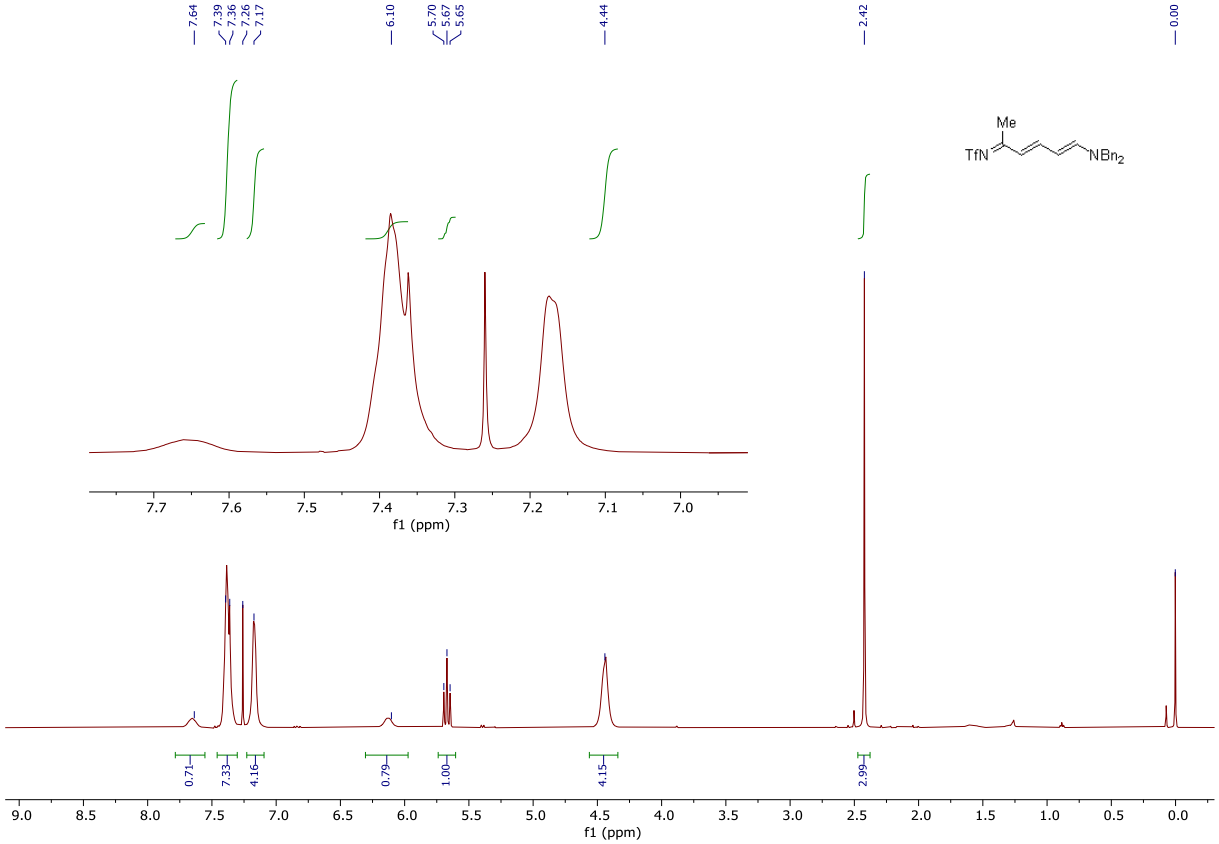

^{13}C NMR spectrum of Zincke imine S28b ($CDCl_3$, 298 K)

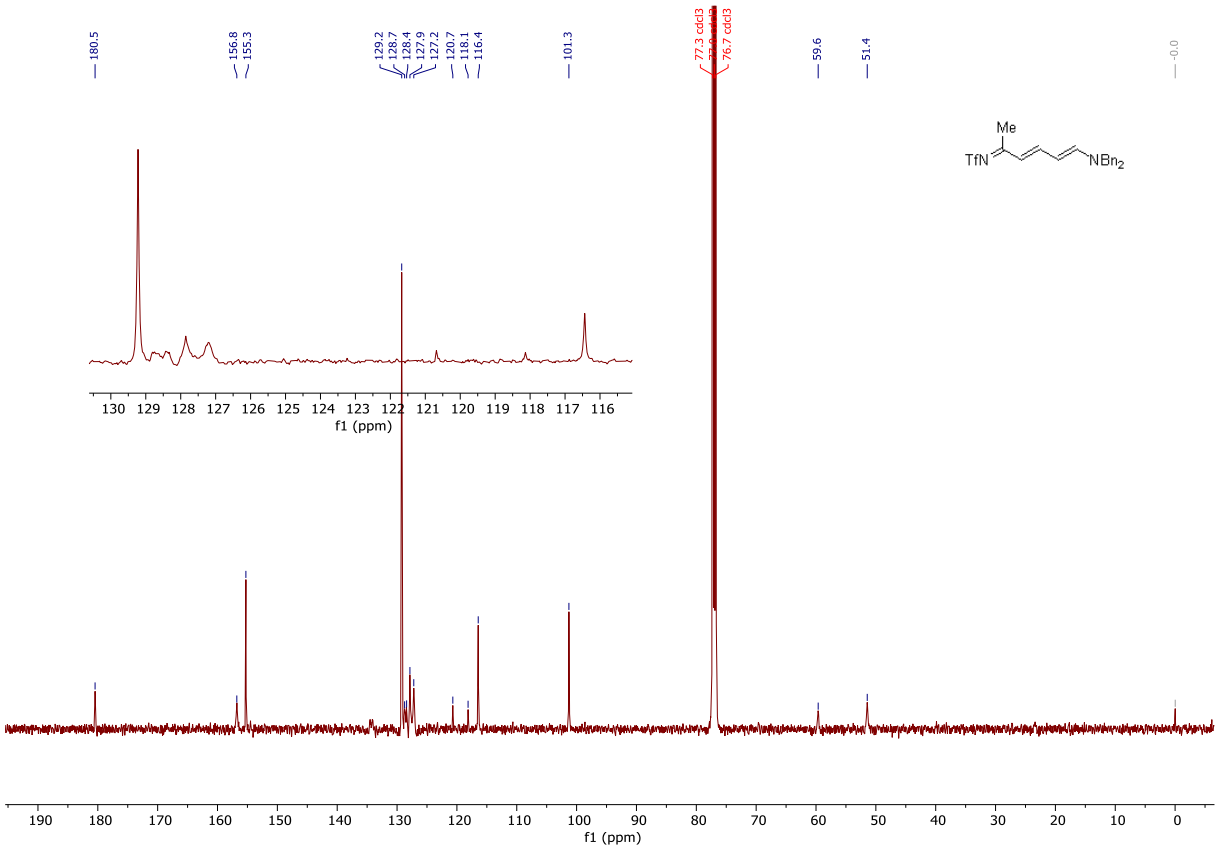

^{1}H NMR spectrum of Zincke imine S29b ($CDCl_3$, 298 K)

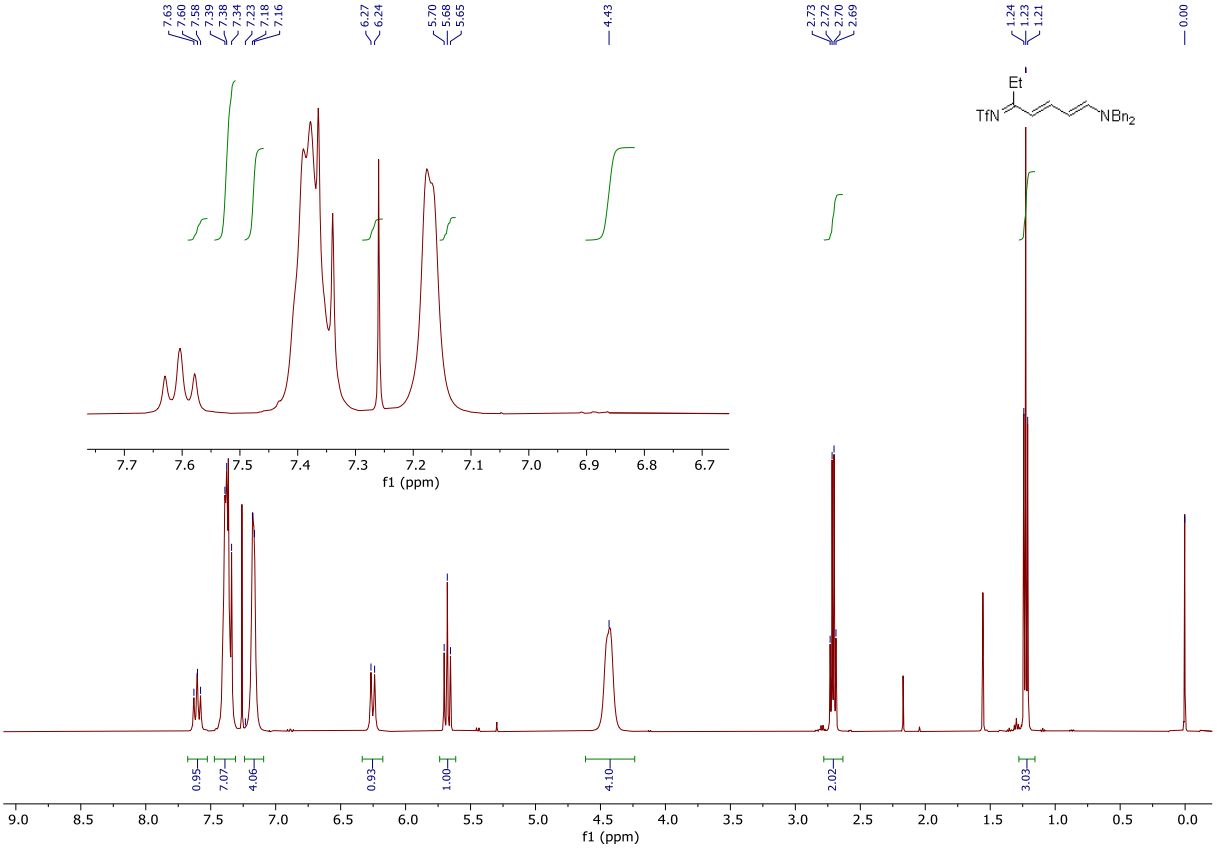

^{13}C NMR spectrum of Zincke imine S29b ($CDCl_3$, 298 K)

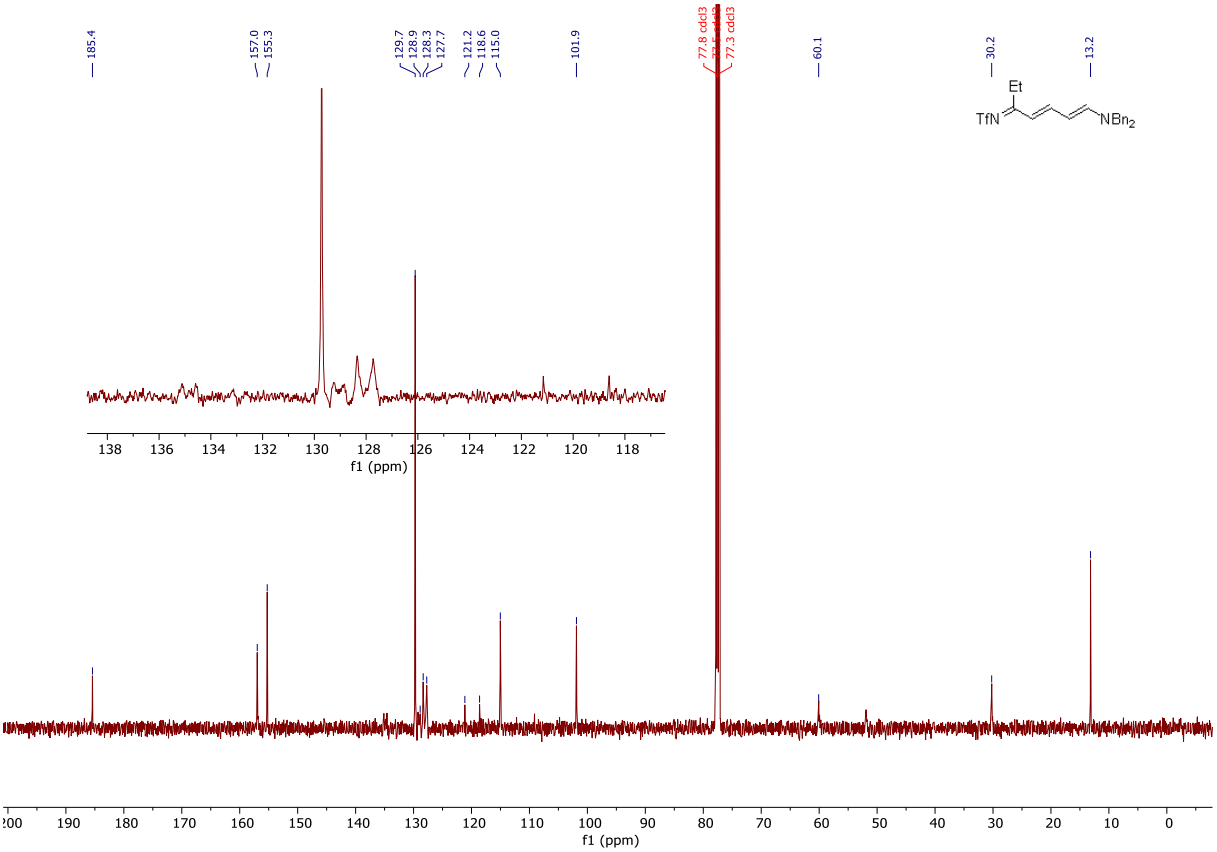

^{1}H NMR spectrum of Zincke imine S30b ($CDCl_3$, 298 K)

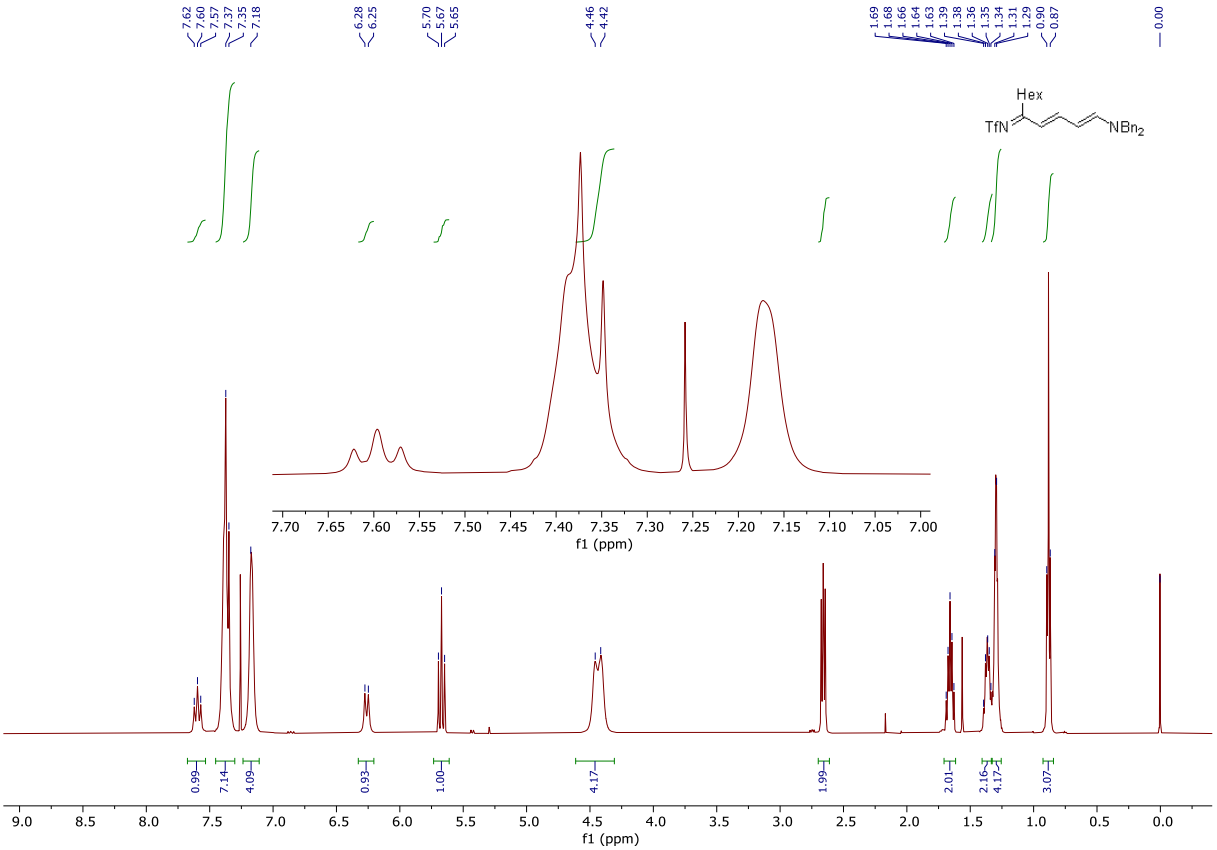

^{13}C NMR spectrum of Zincke imine S30b ($CDCl_3$, 298 K)

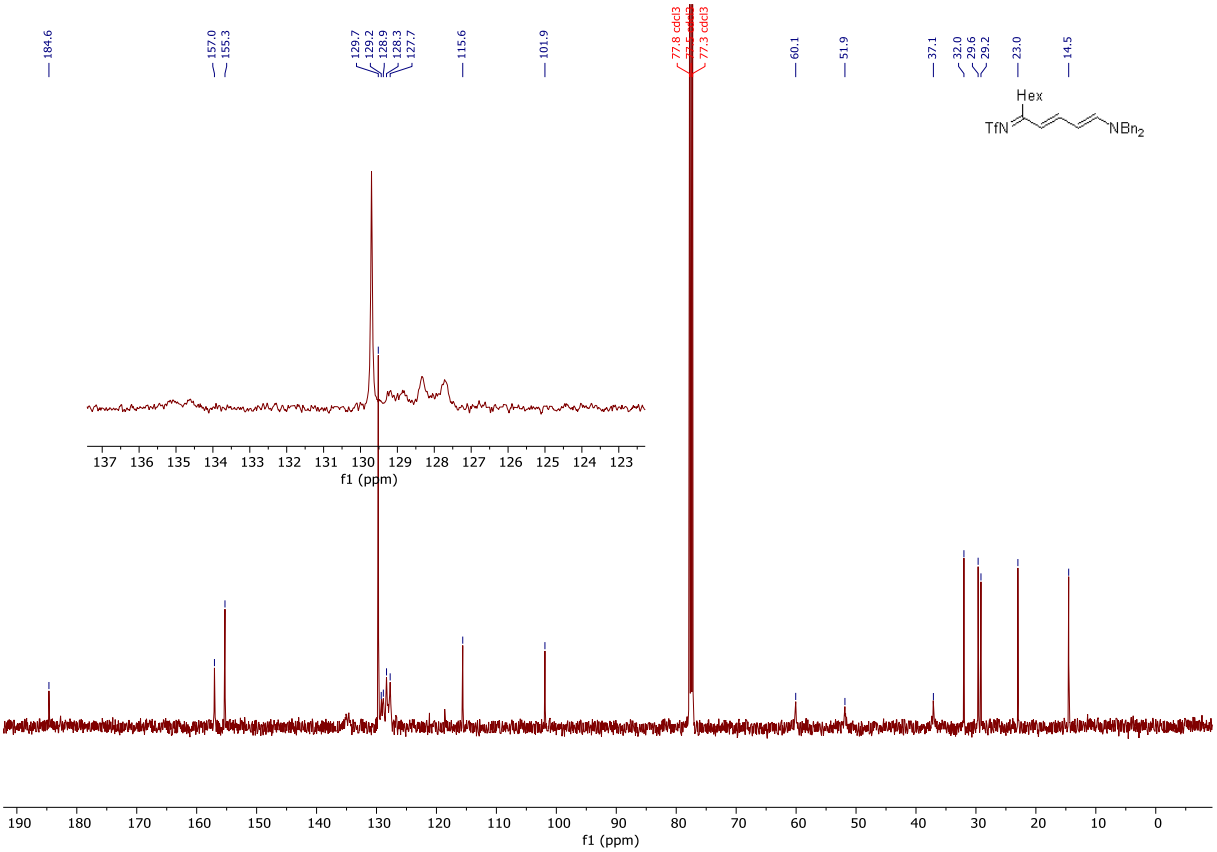

^{1}H NMR spectrum of Zincke imine S31b ($CDCl_3$, 298 K)

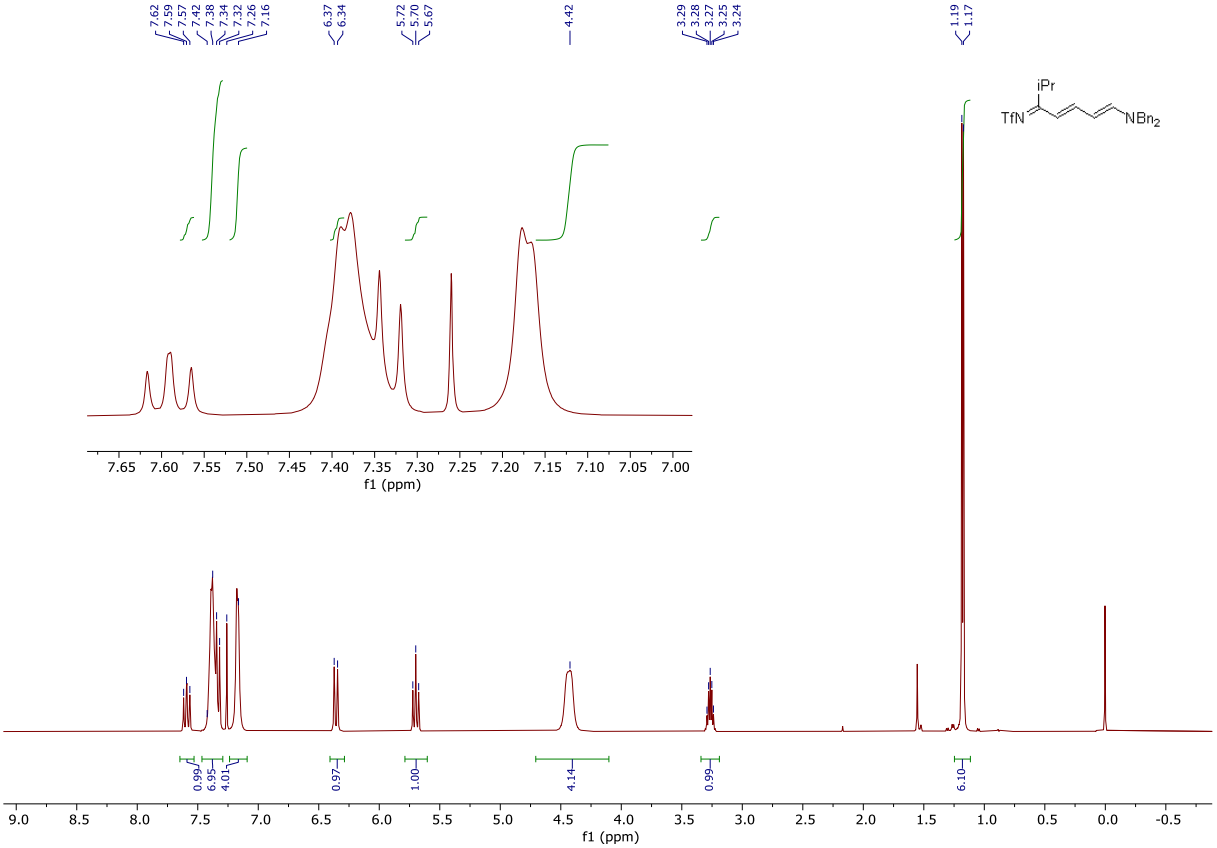

^{13}C NMR spectrum of Zincke imine S31b ($CDCl_3$, 298 K)

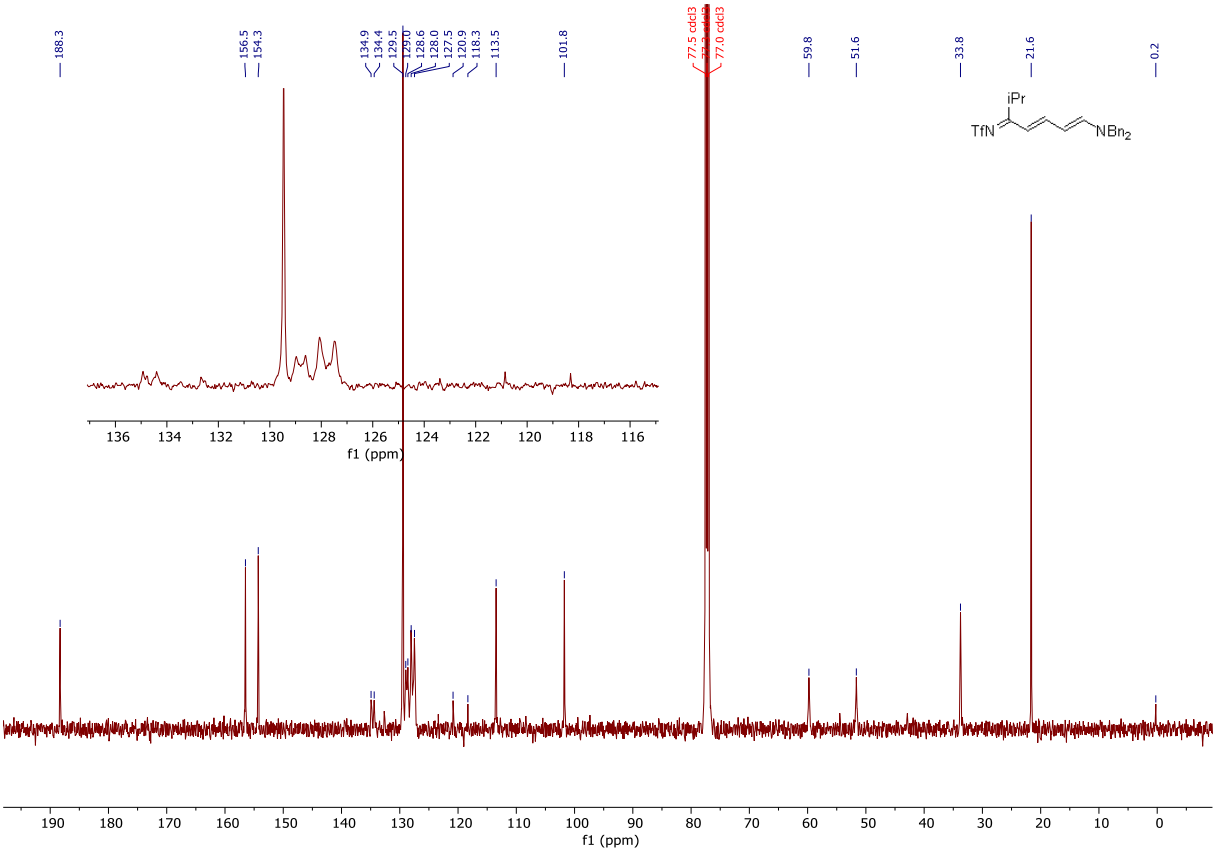

^{1}H NMR spectrum of Zincke imine S32b ($CDCl_3$, 298 K)

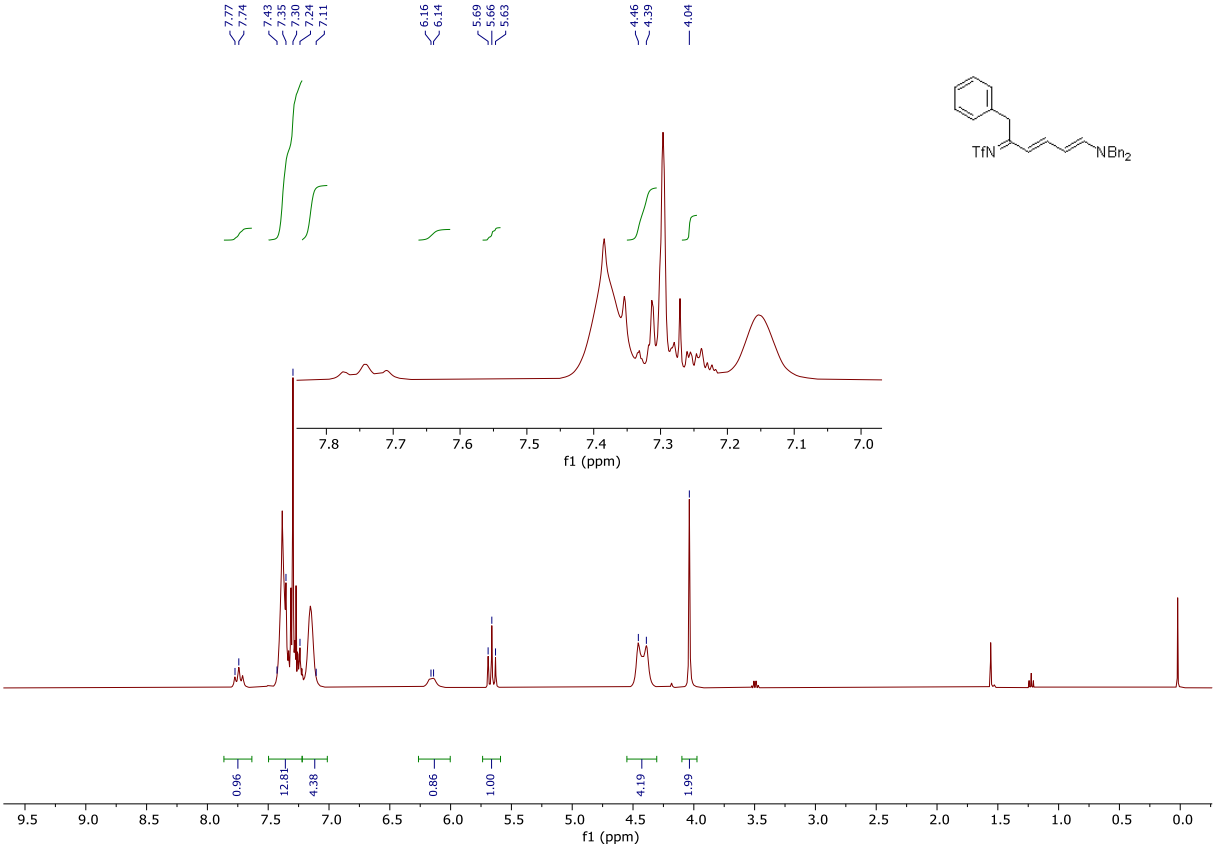

^{13}C NMR spectrum of Zincke imine S32b ($CDCl_3$, 298 K)

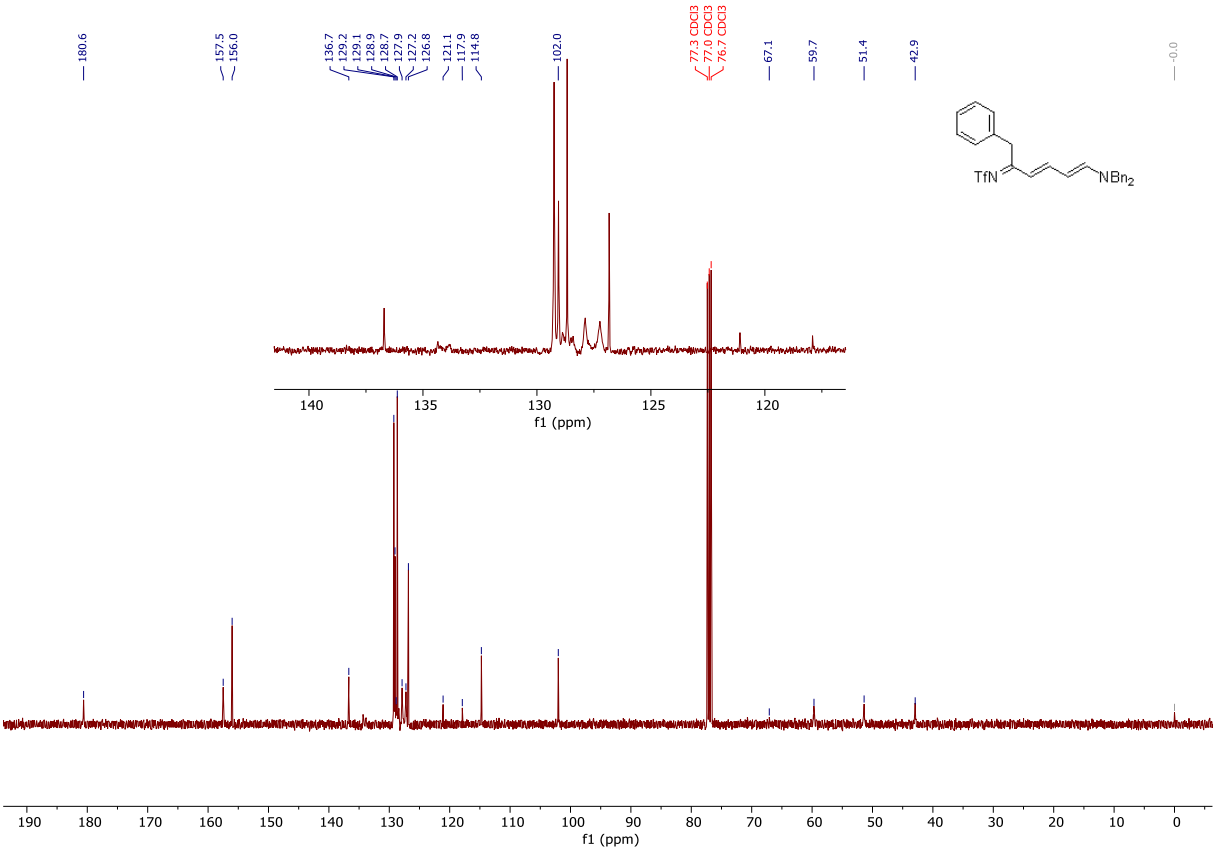

^{1}H NMR spectrum of Zincke imine S33b ($CDCl_3$, 298 K)

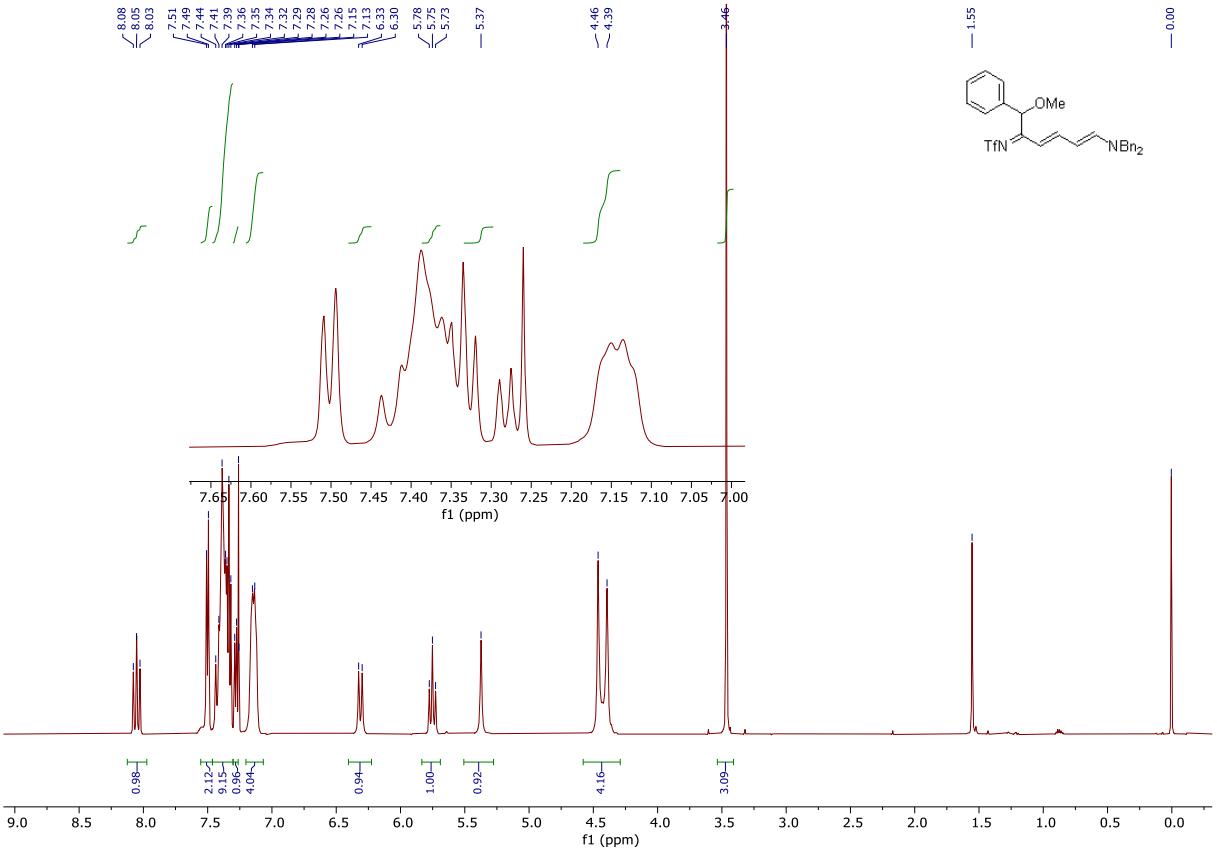

^{13}C NMR spectrum of Zincke imine S33b ($CDCl_3$, 298 K)

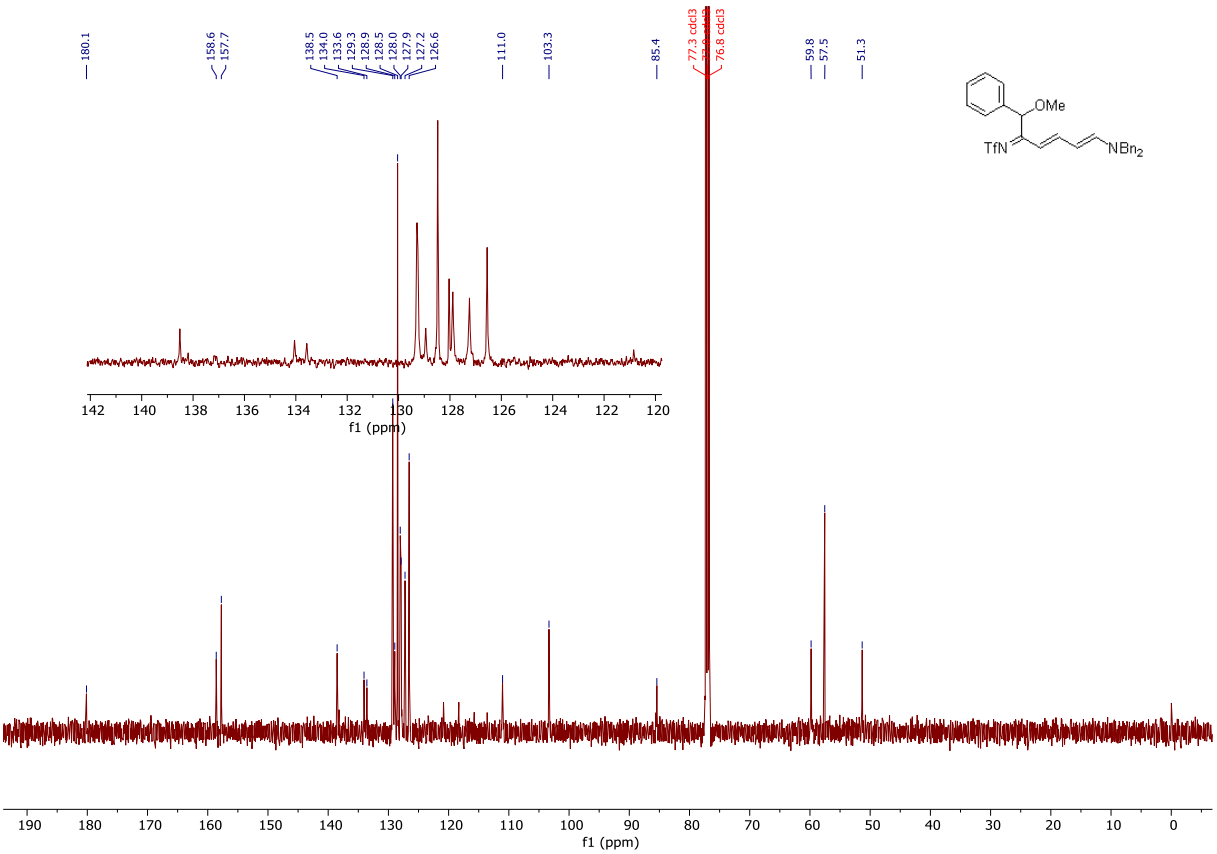

^{1}H NMR spectrum of Zincke imine S34b ($CDCl_3$, 298 K)

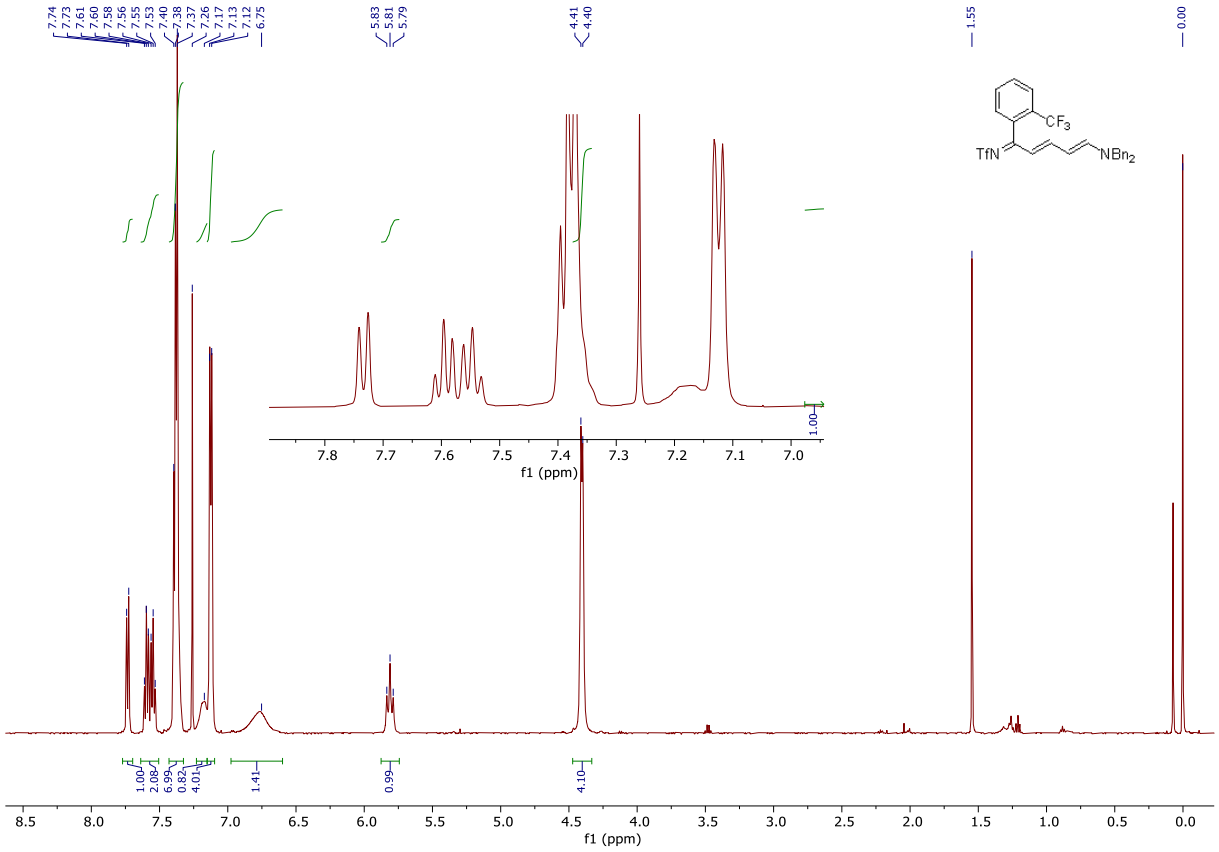

^{13}C NMR spectrum of Zincke imine S34b ($CDCl_3$, 298 K)

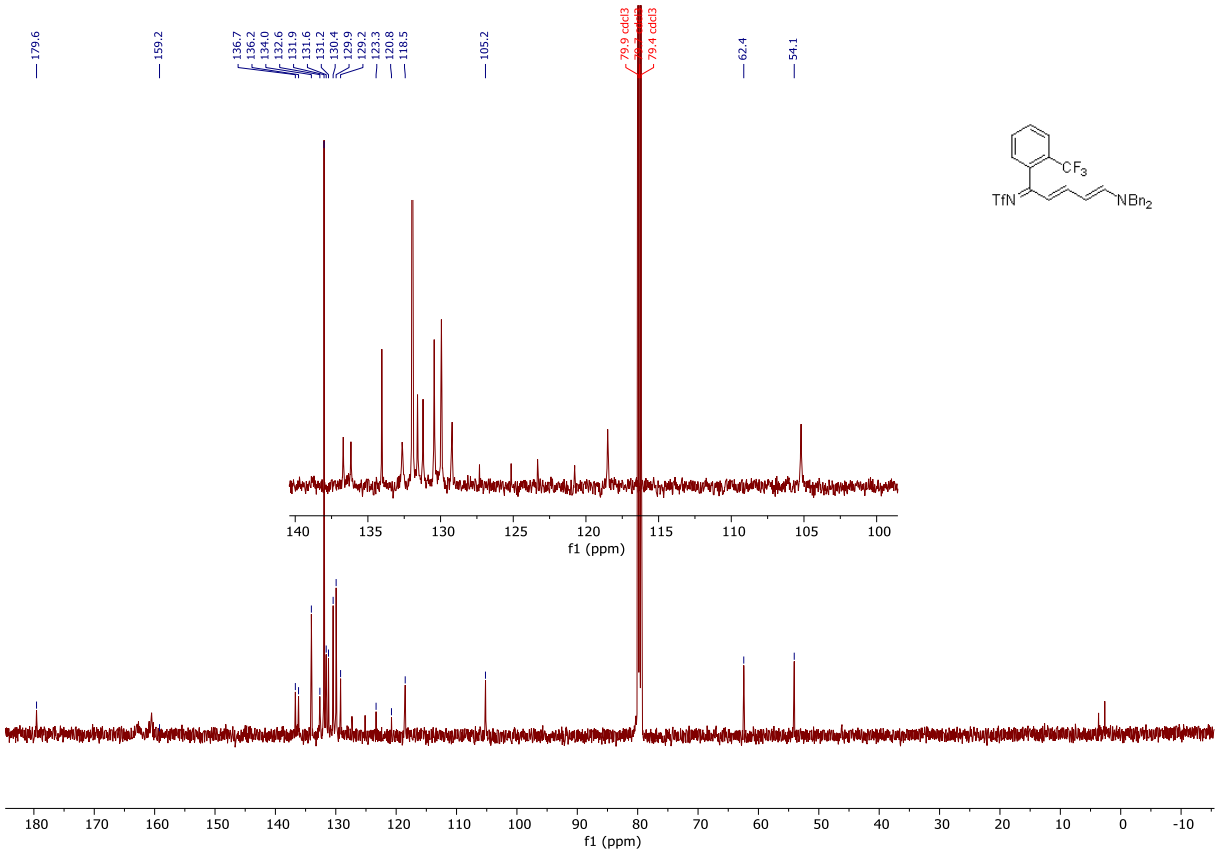

^{1}H NMR spectrum of Zincke imine S35b ($CDCl_3$, 298 K)

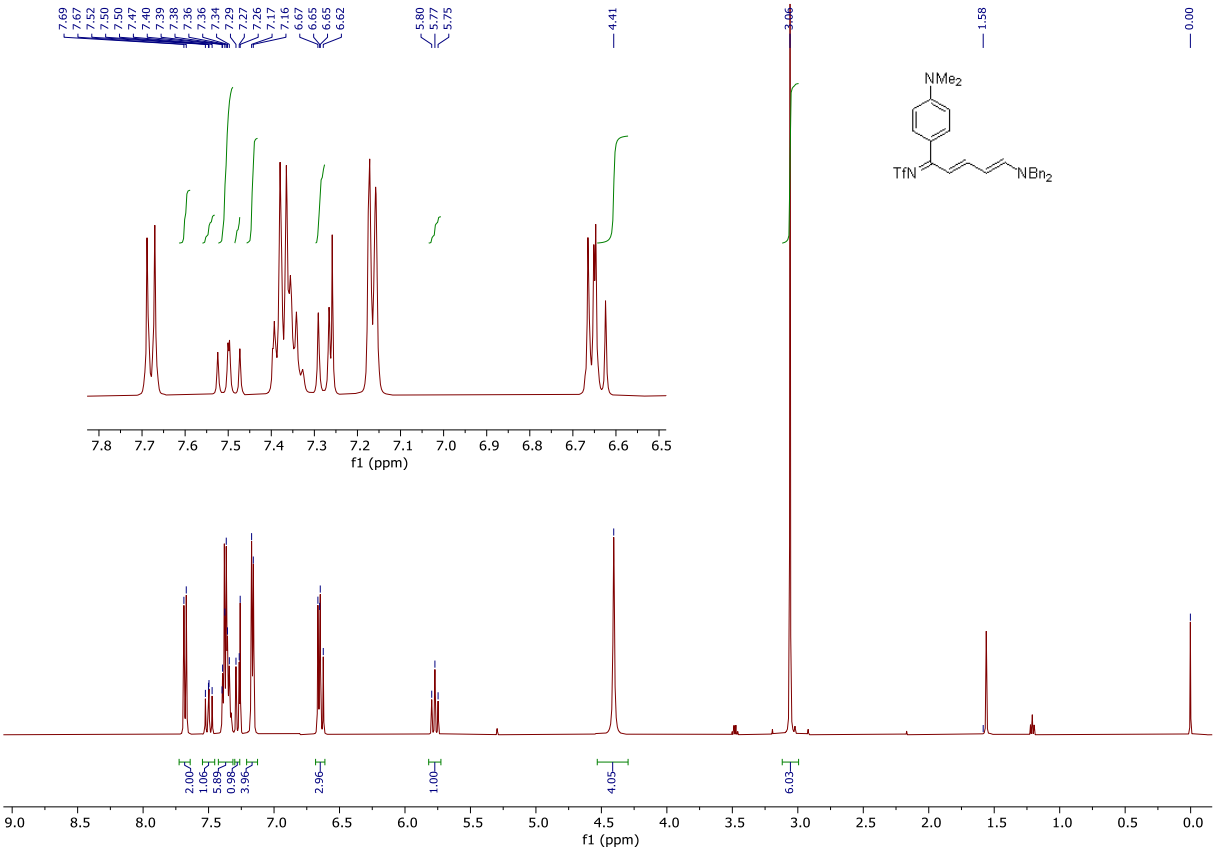

^{13}C NMR spectrum of Zincke imine S35b ($CDCl_3$, 298 K)

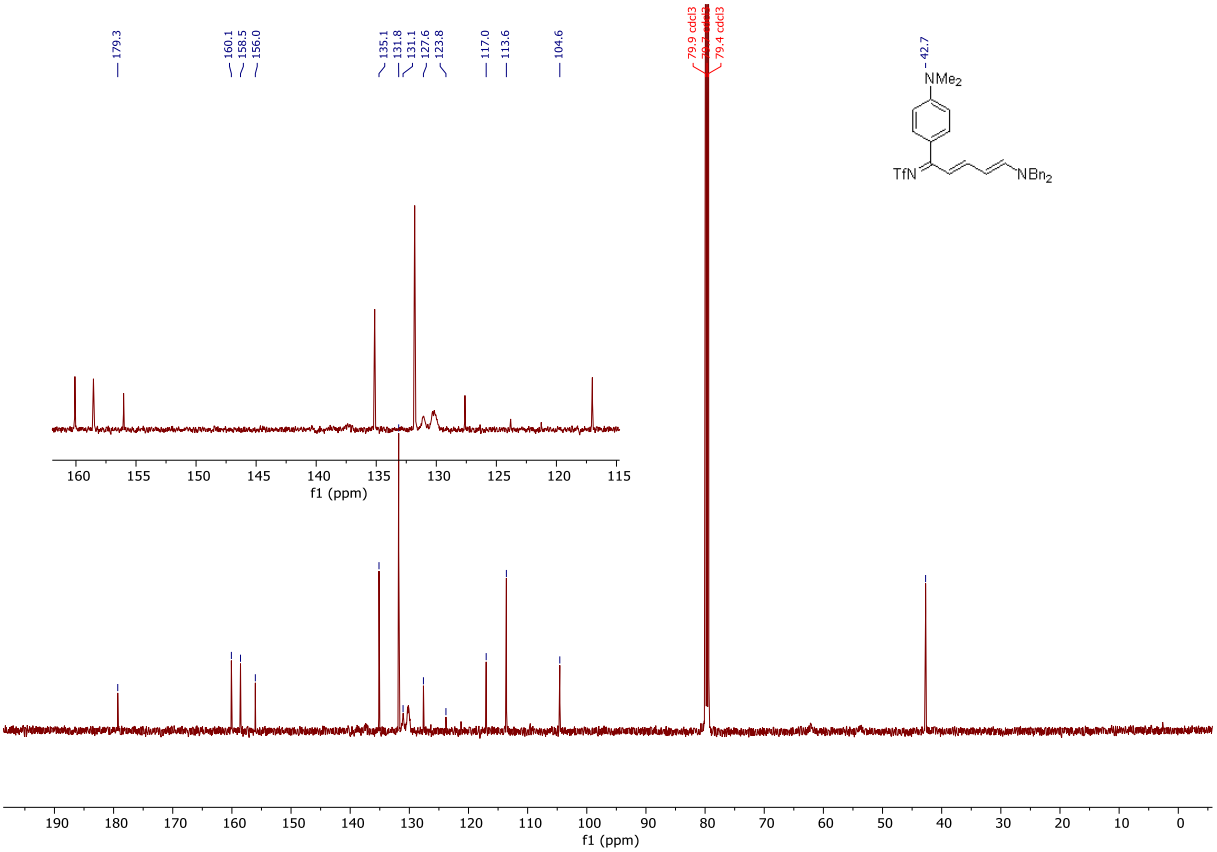

^{1}H NMR spectrum of Zincke imine S36b ($CDCl_3$, 298 K)

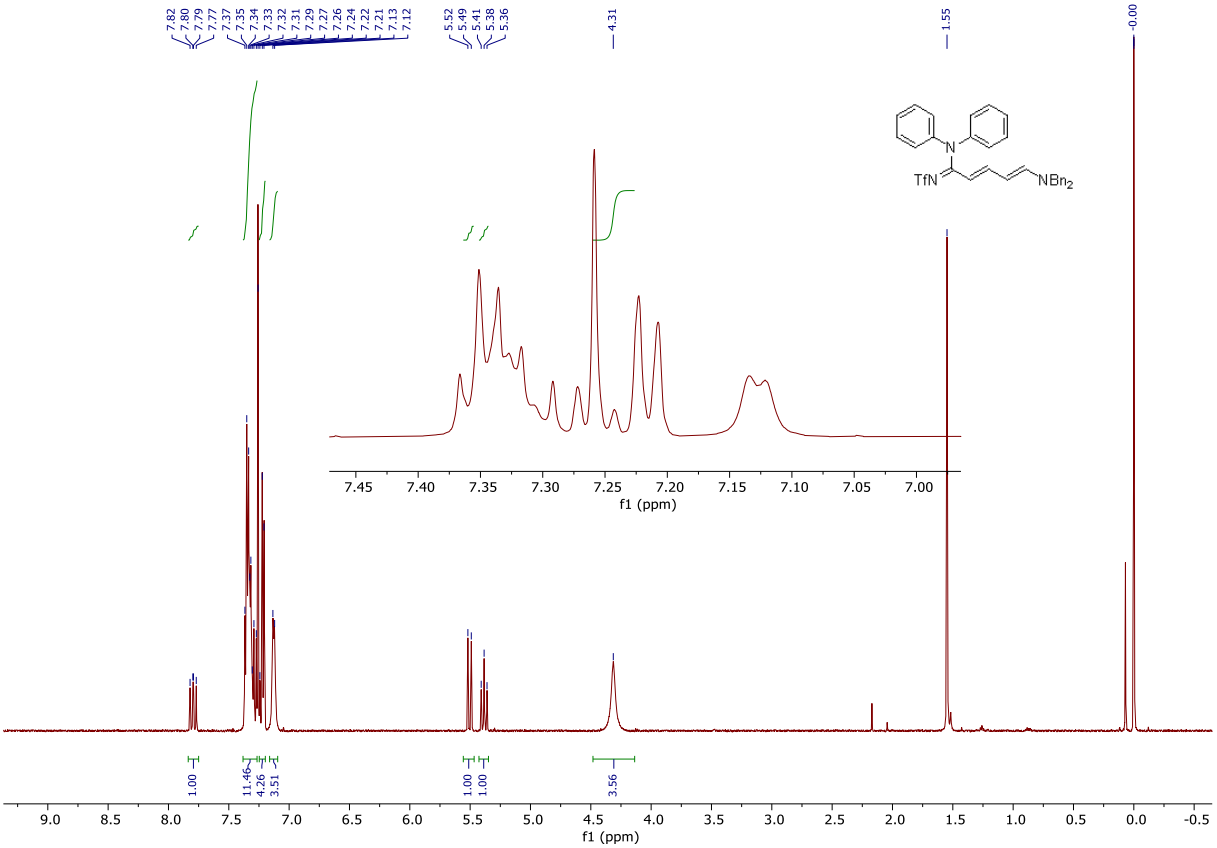

^{13}C NMR spectrum of Zincke imine S36b ($CDCl_3$, 298 K)

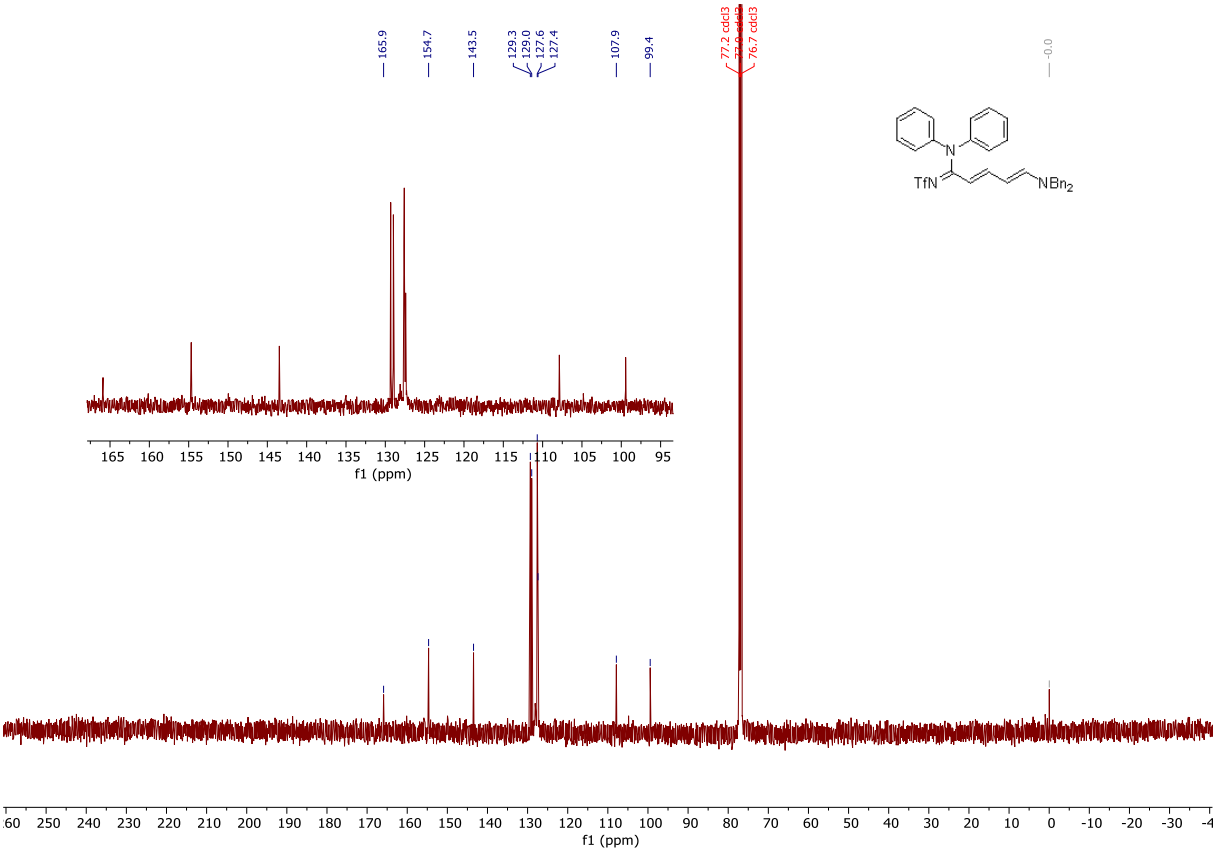

^{1}H NMR spectrum of Zincke imine S37b ($CDCl_3$, 298 K)

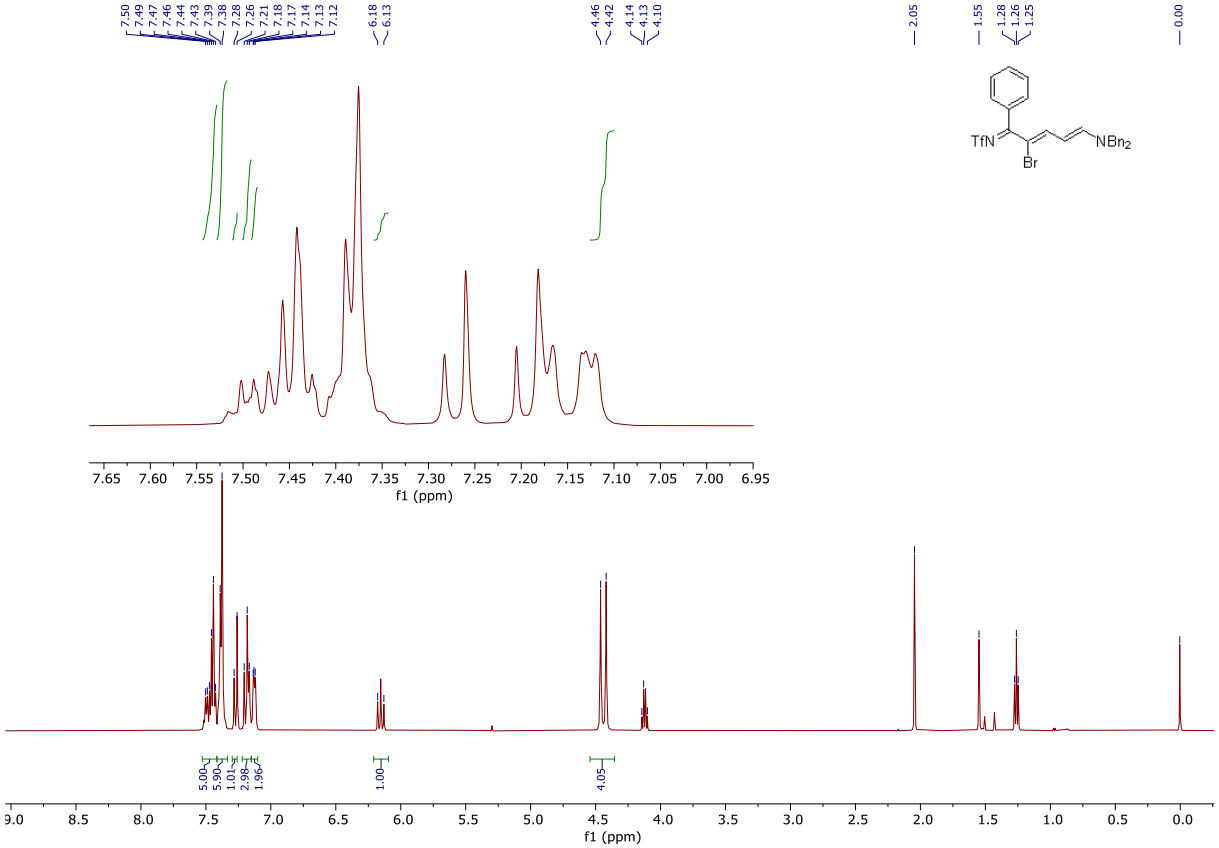

^{13}C NMR spectrum of Zincke imine S37b ($CDCl_3$, 298 K)

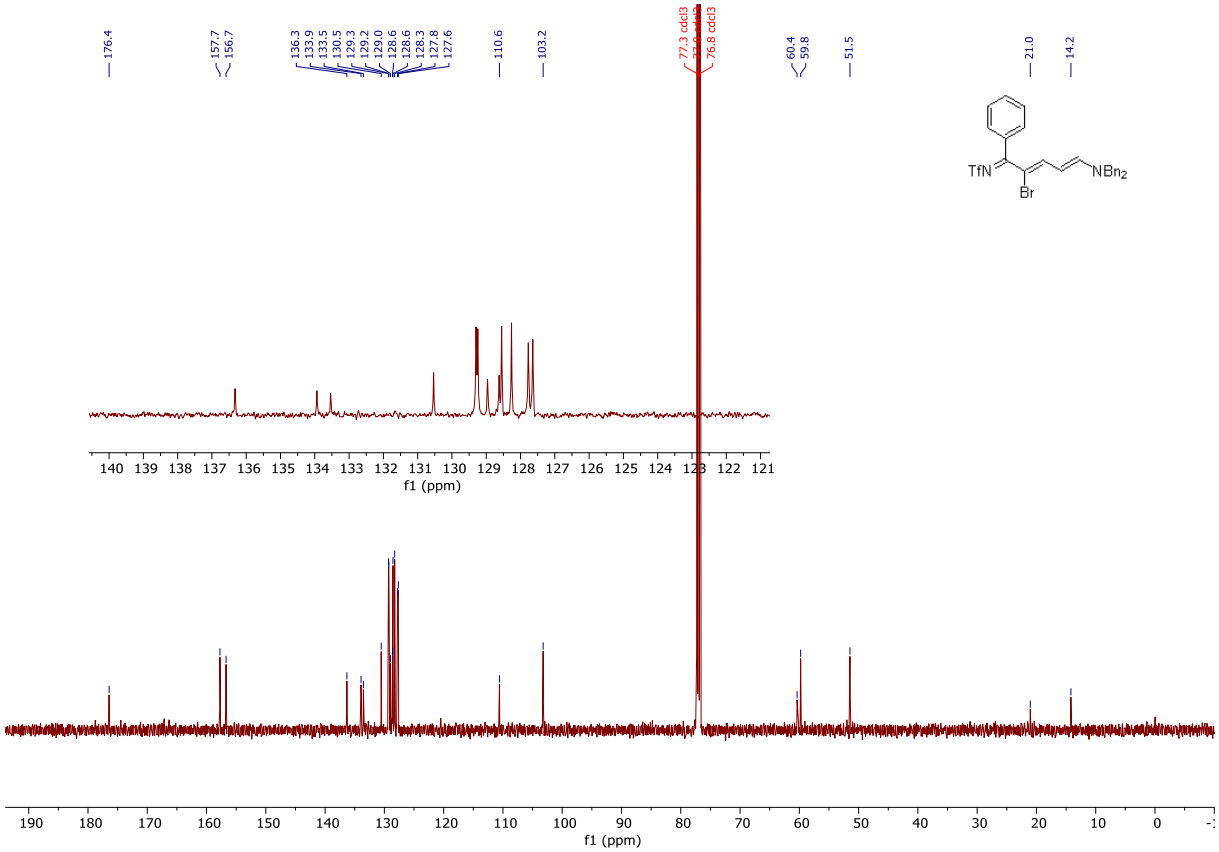

^{1}H NMR spectrum of Zincke imine S38b ($CDCl_3$, 298 K)

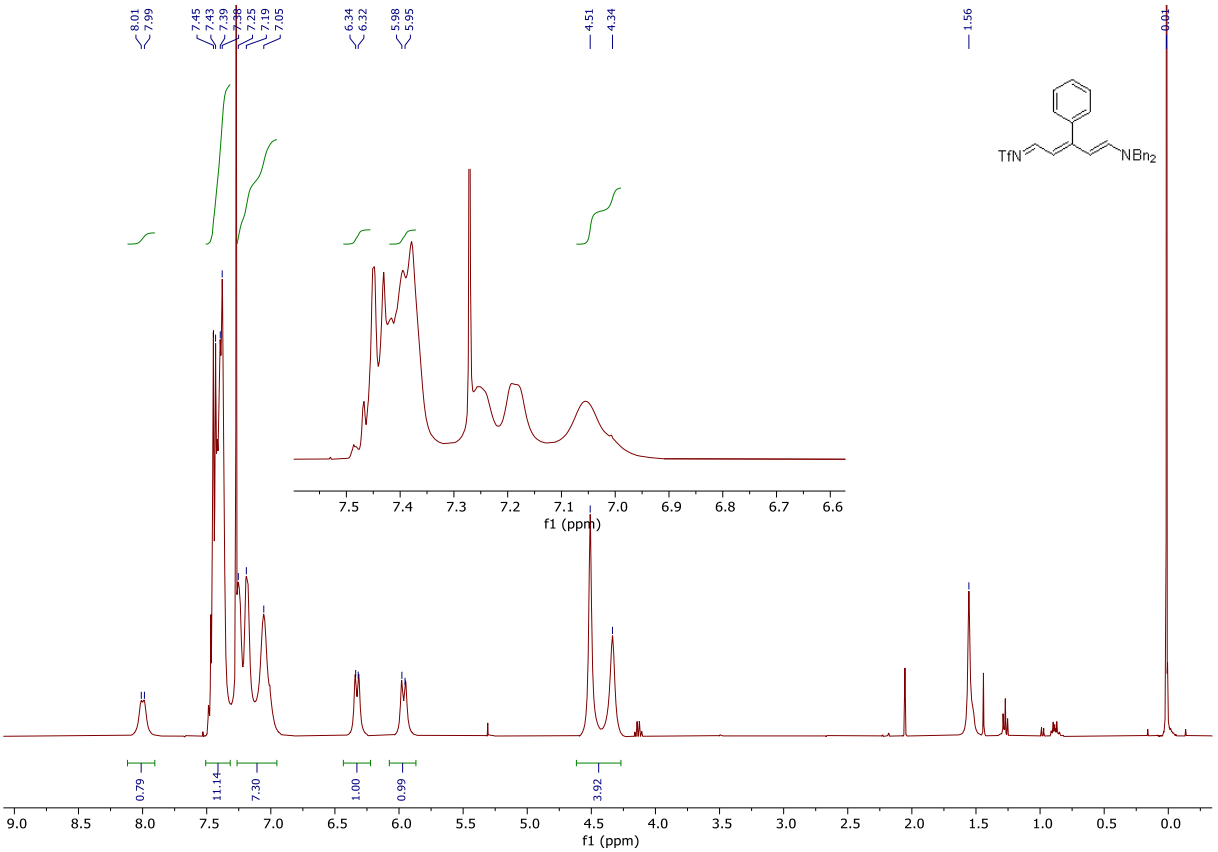

^{1}H NMR spectrum of Zincke imine S39b ($CDCl_3$, 298 K)

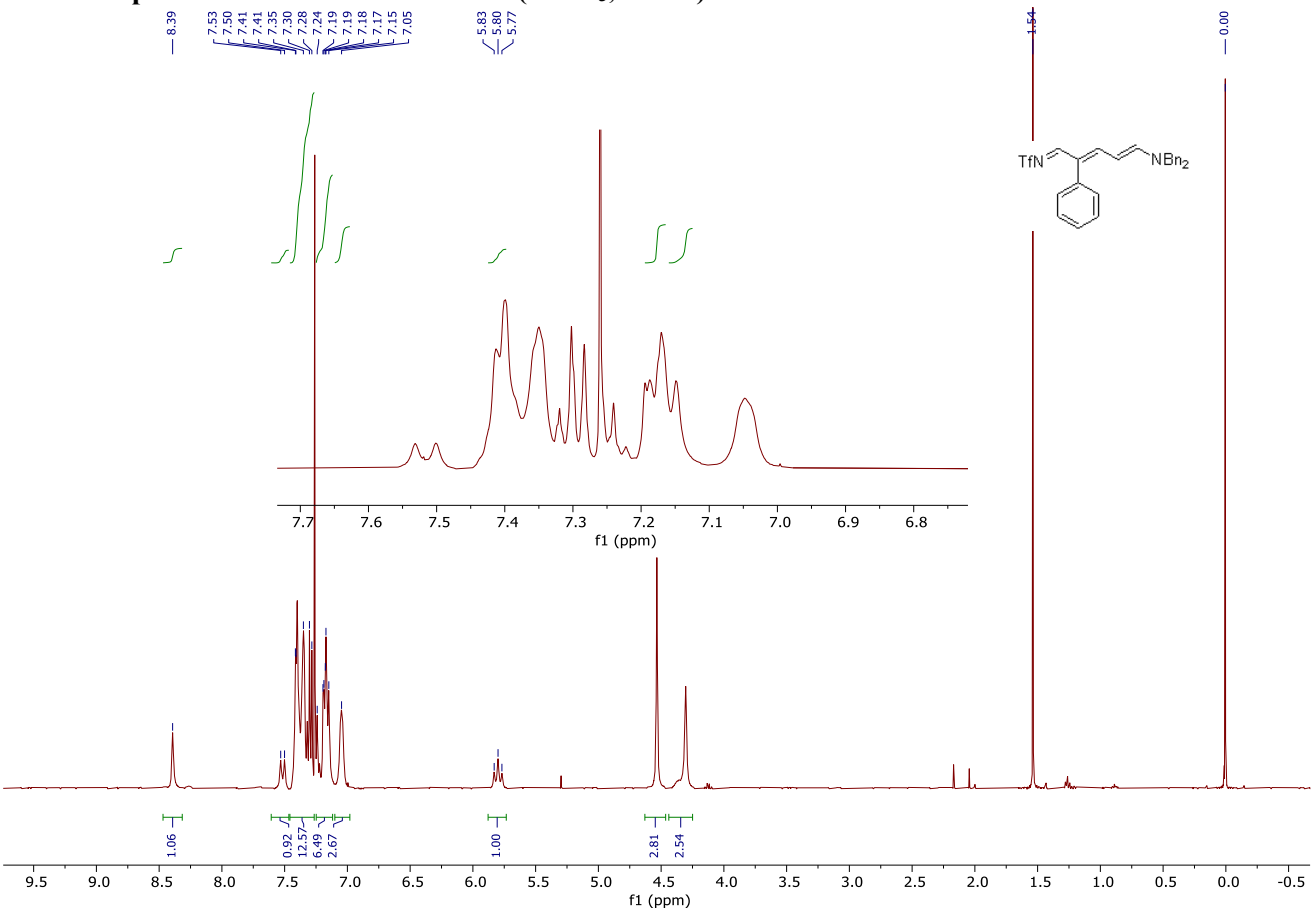

^{1}H NMR spectrum of Zincke imine S40b ($CDCl_3$, 298 K)

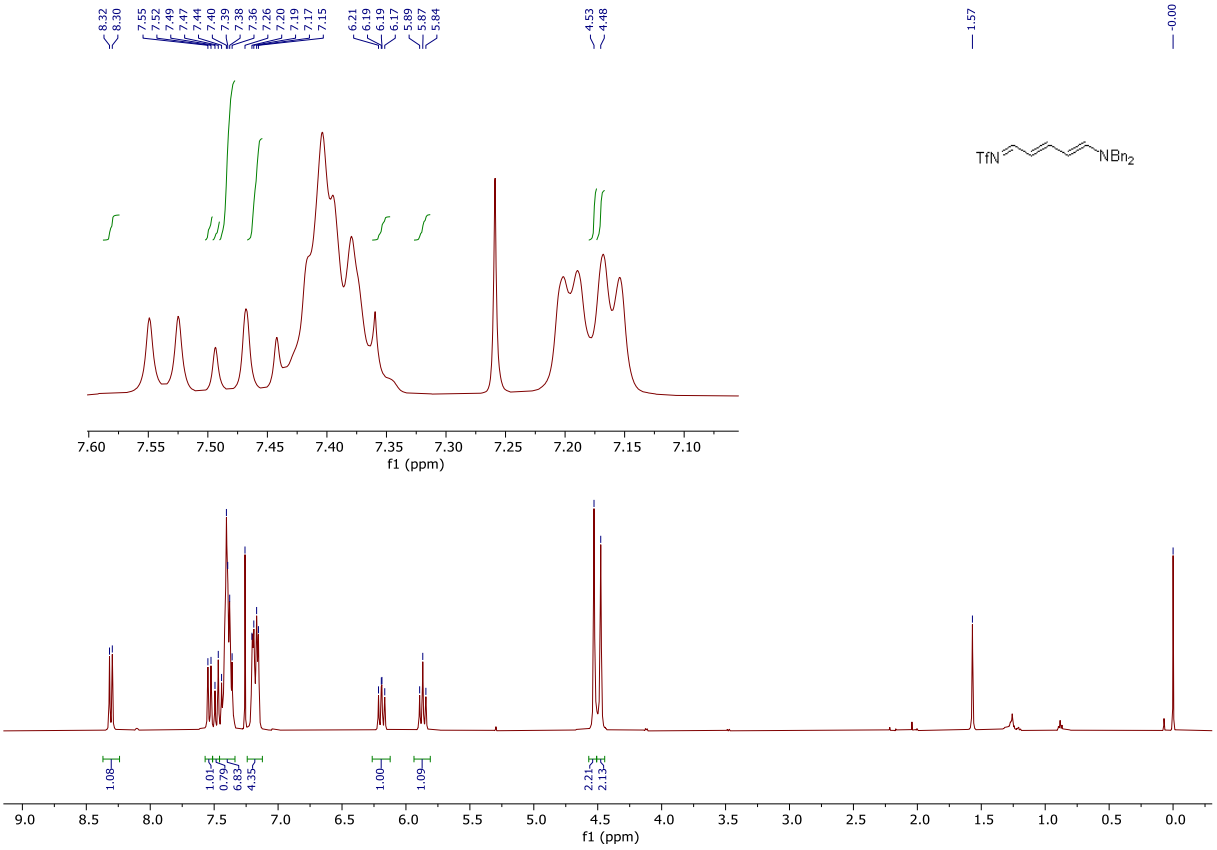

^{13}C NMR spectrum of Zincke imine S40b ($CDCl_3$, 298 K)

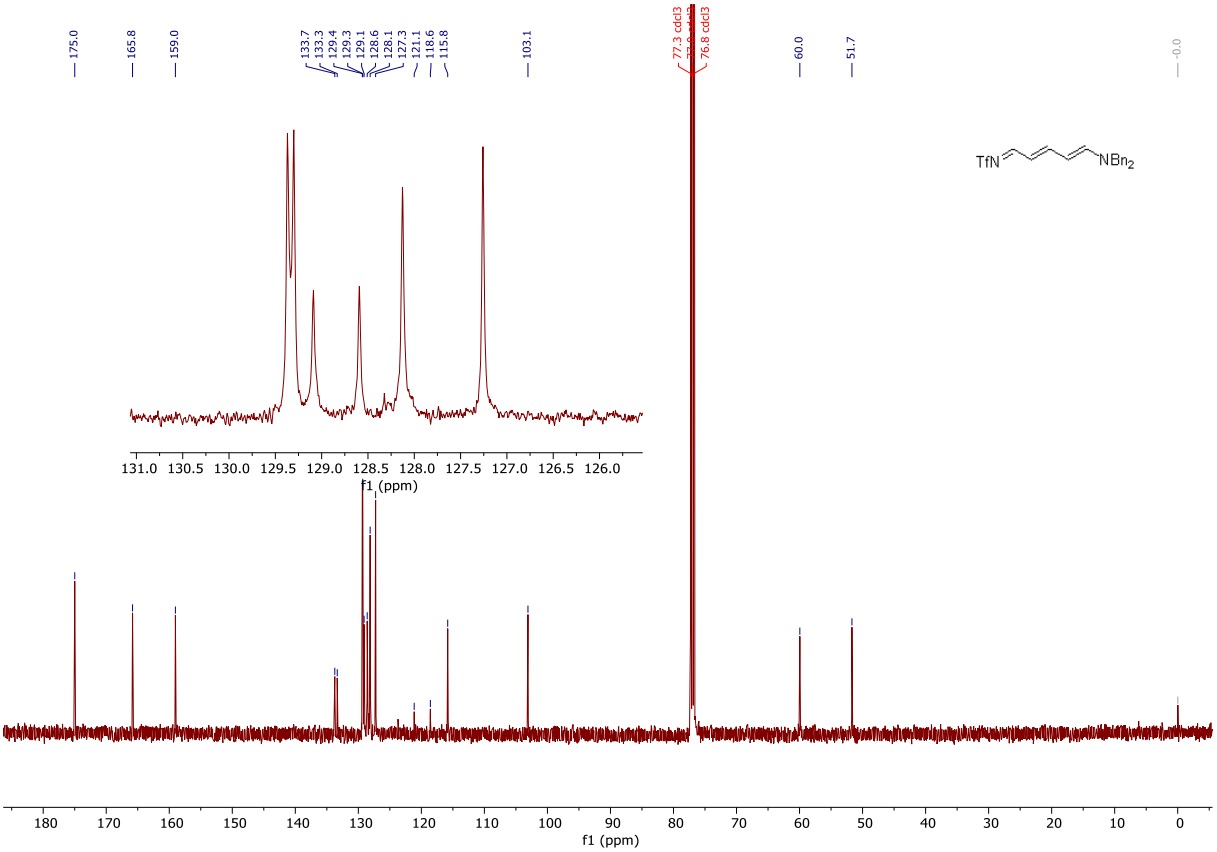

^{1}H NMR spectrum of Zincke imine S41b ($CDCl_3$, 298 K)

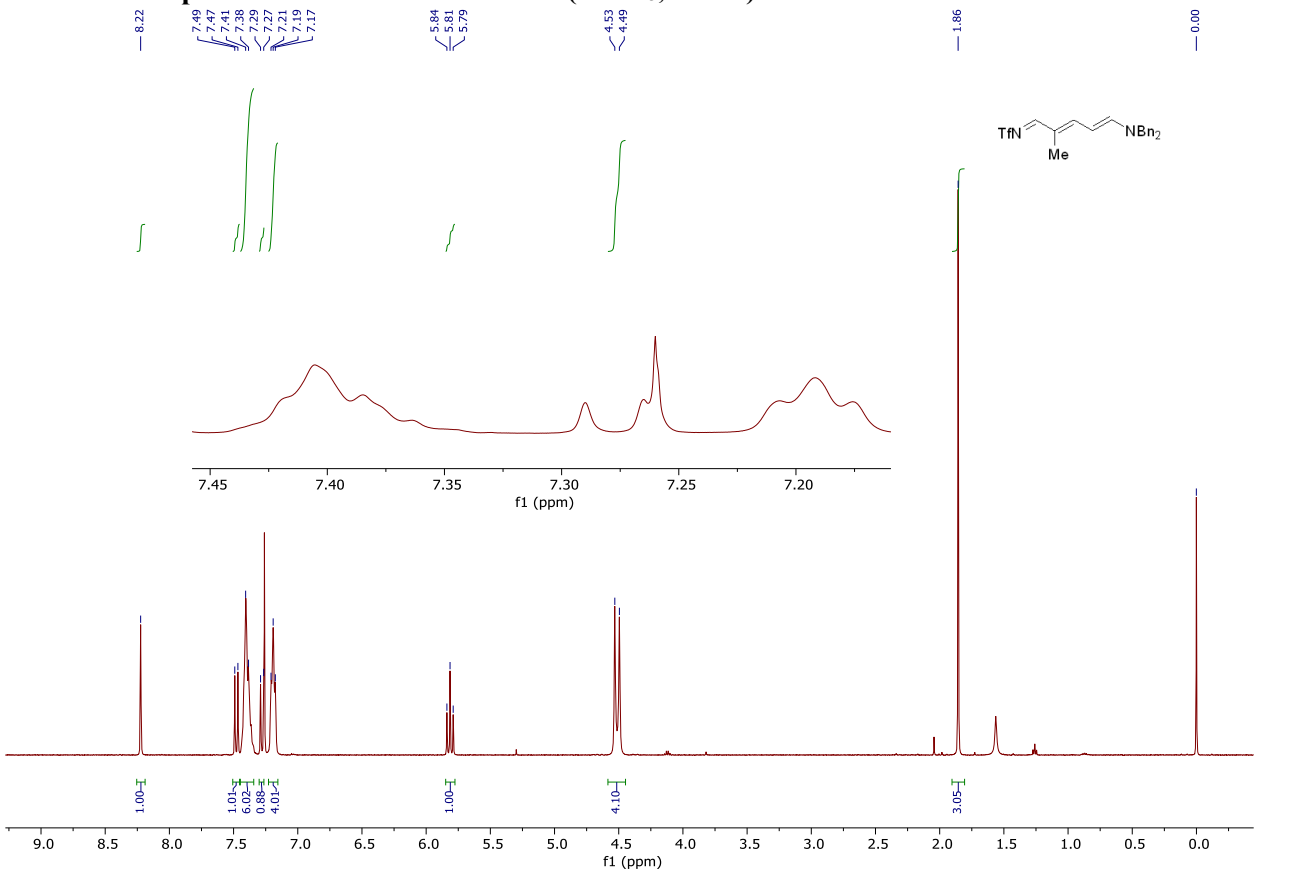

^{13}C NMR spectrum of Zincke imine S41b ($CDCl_3$, 298 K)

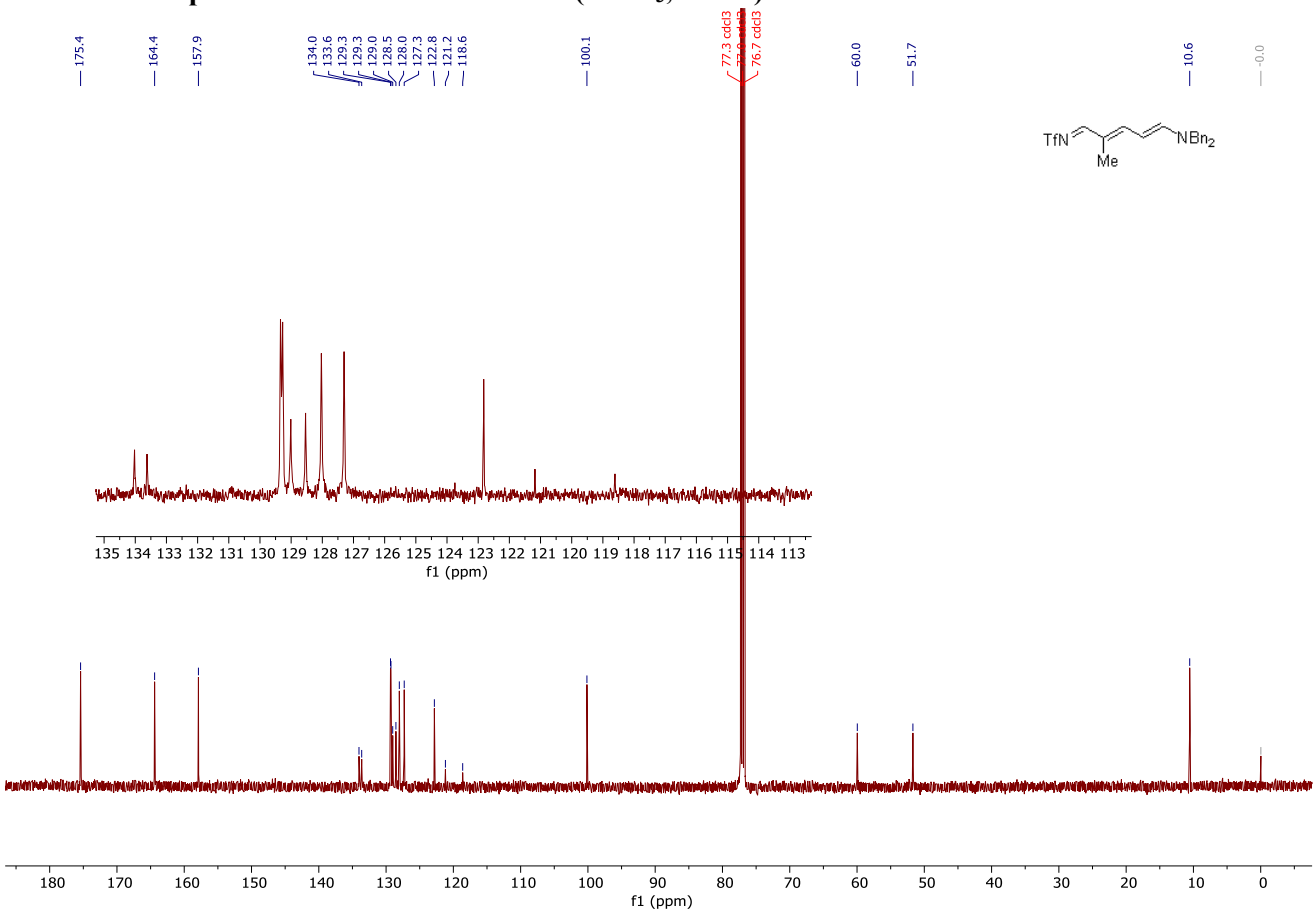

^{1}H NMR spectrum of Zincke imine S42b ($CDCl_3$, 298 K)

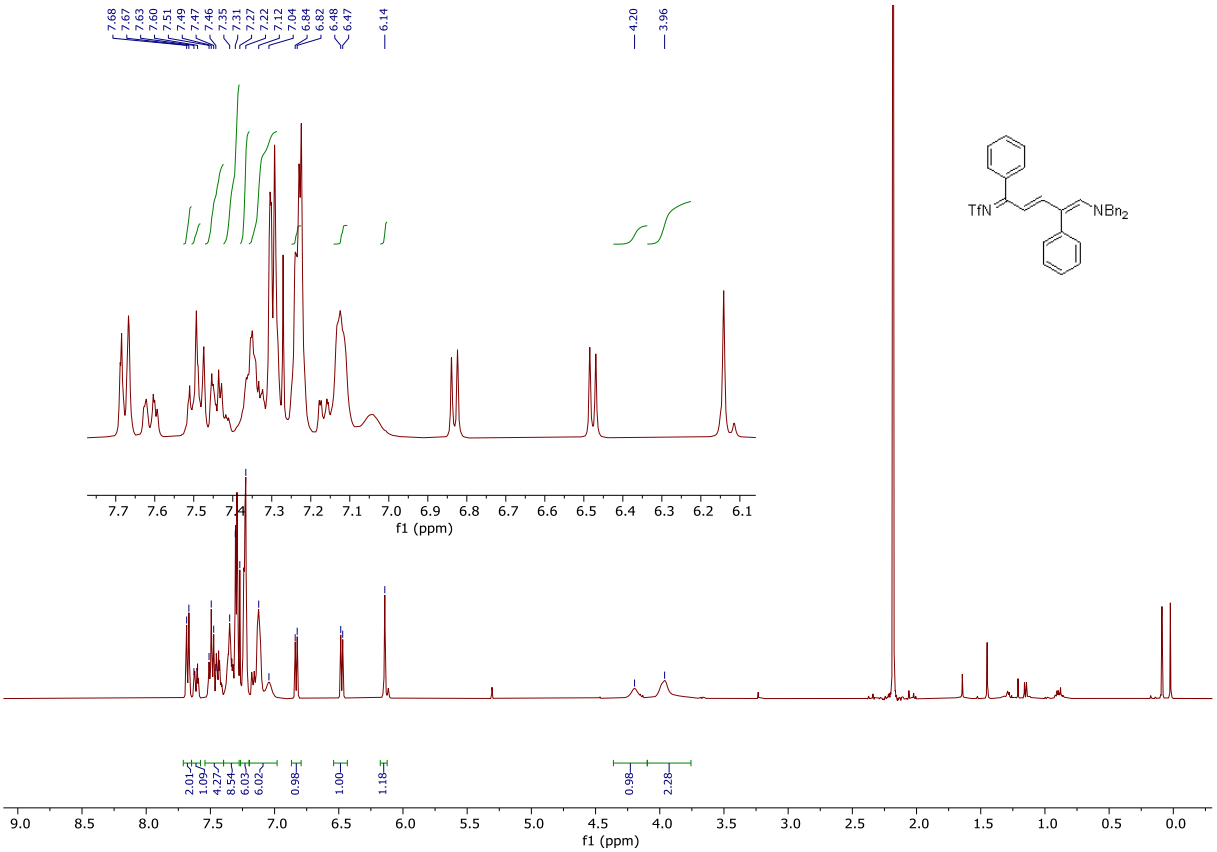

^{13}C NMR spectrum of Zincke imine S42b ($CDCl_3$, 298 K)

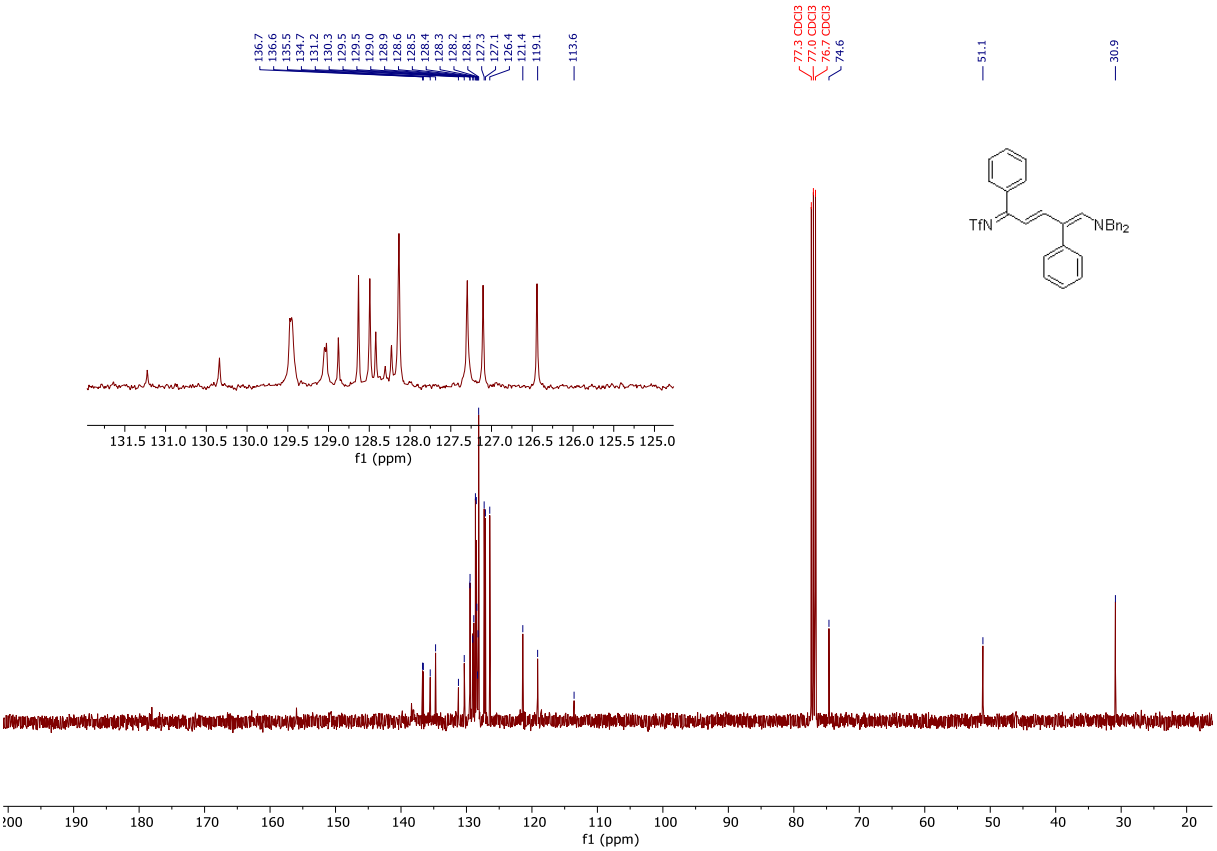

^{1}H NMR spectrum of Zincke imine S43b ($CDCl_3$, 298 K)

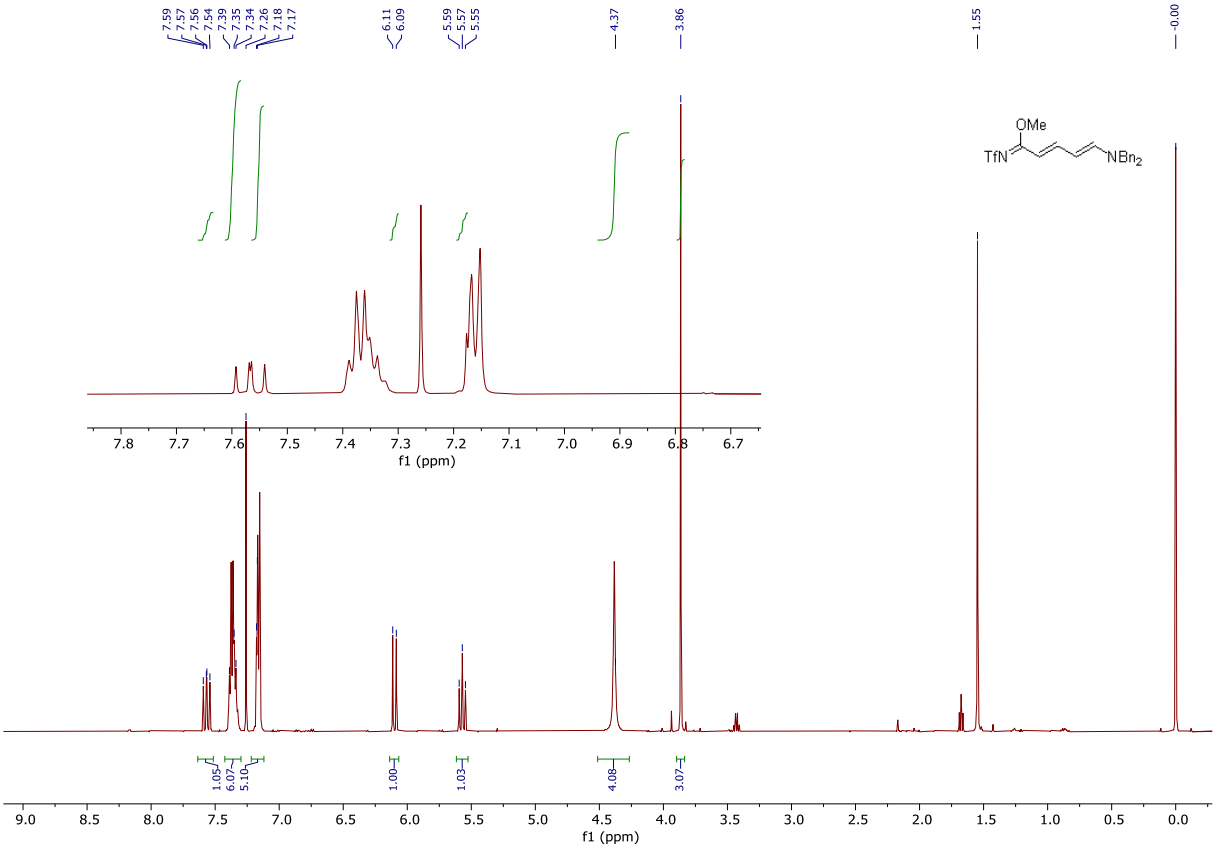

^{13}C NMR spectrum of Zincke imine S43b ($CDCl_3$, 298 K)

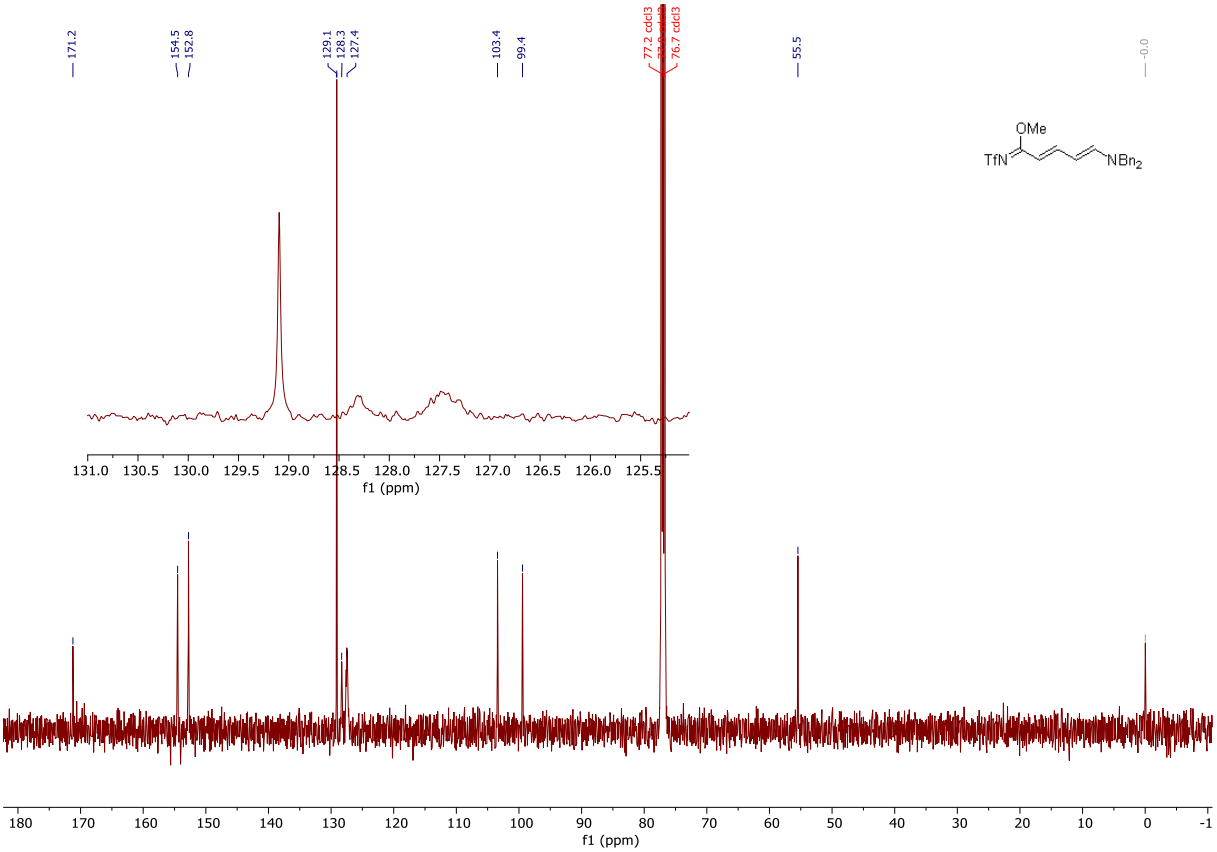

^{1}H NMR spectrum of Zincke imine S44b ($CDCl_3$, 298 K)

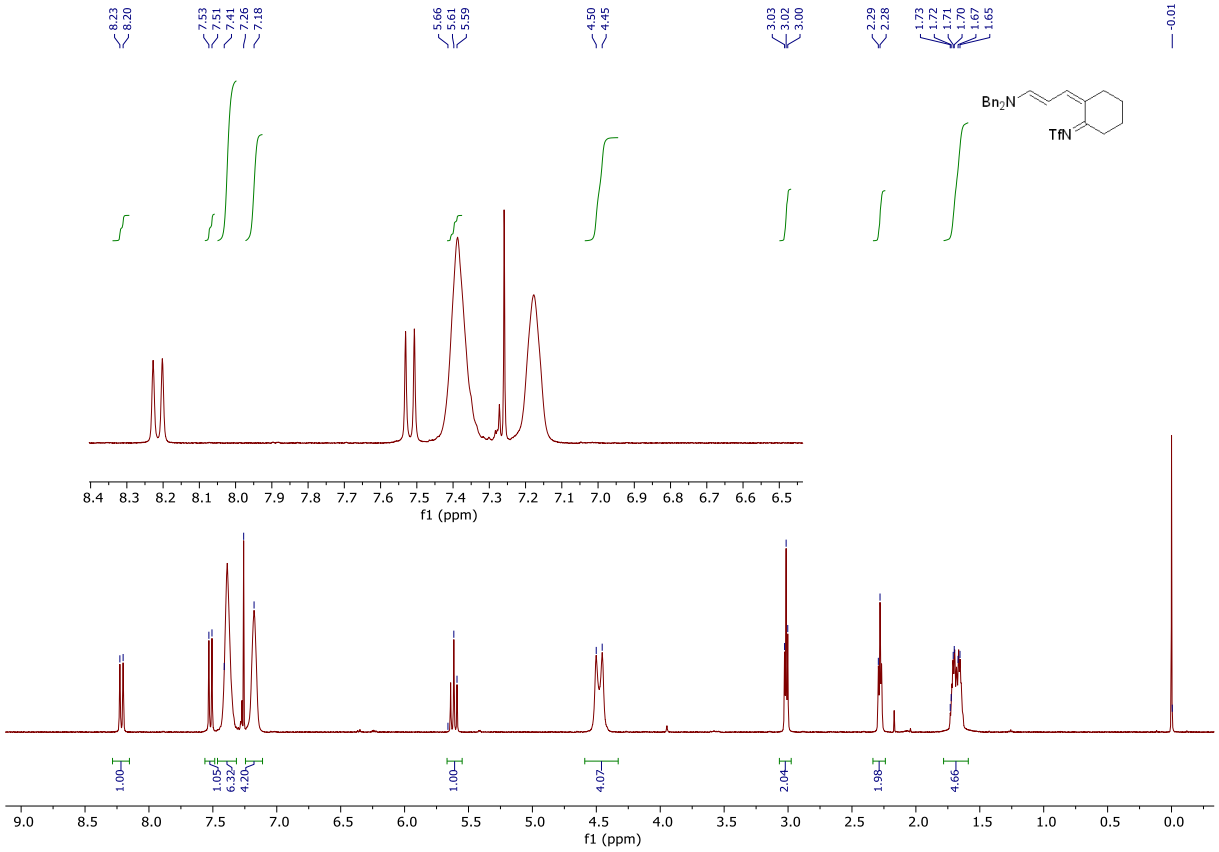

^{13}C NMR spectrum of Zincke imine S44b ($CDCl_3$, 298 K)

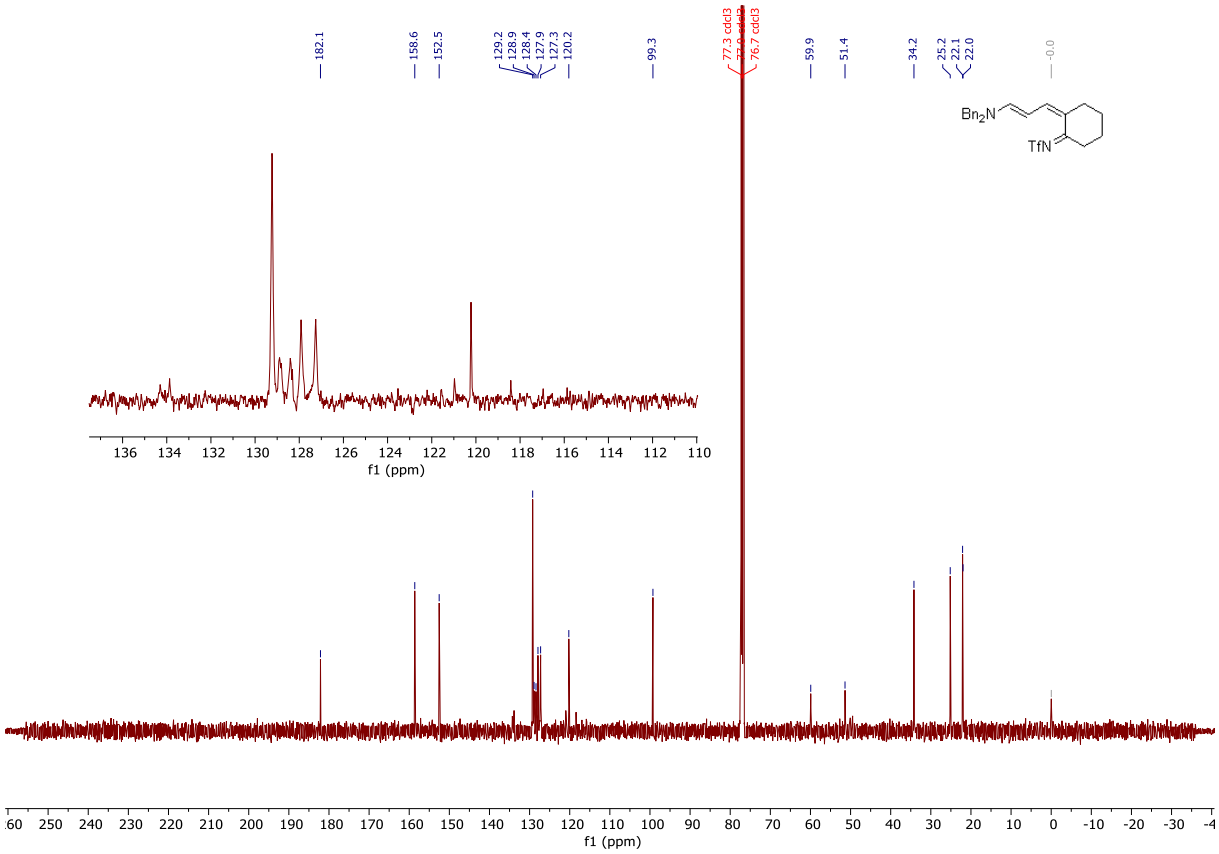

^{1}H NMR spectrum of Zincke imine S45b ($CDCl_3$, 298 K)

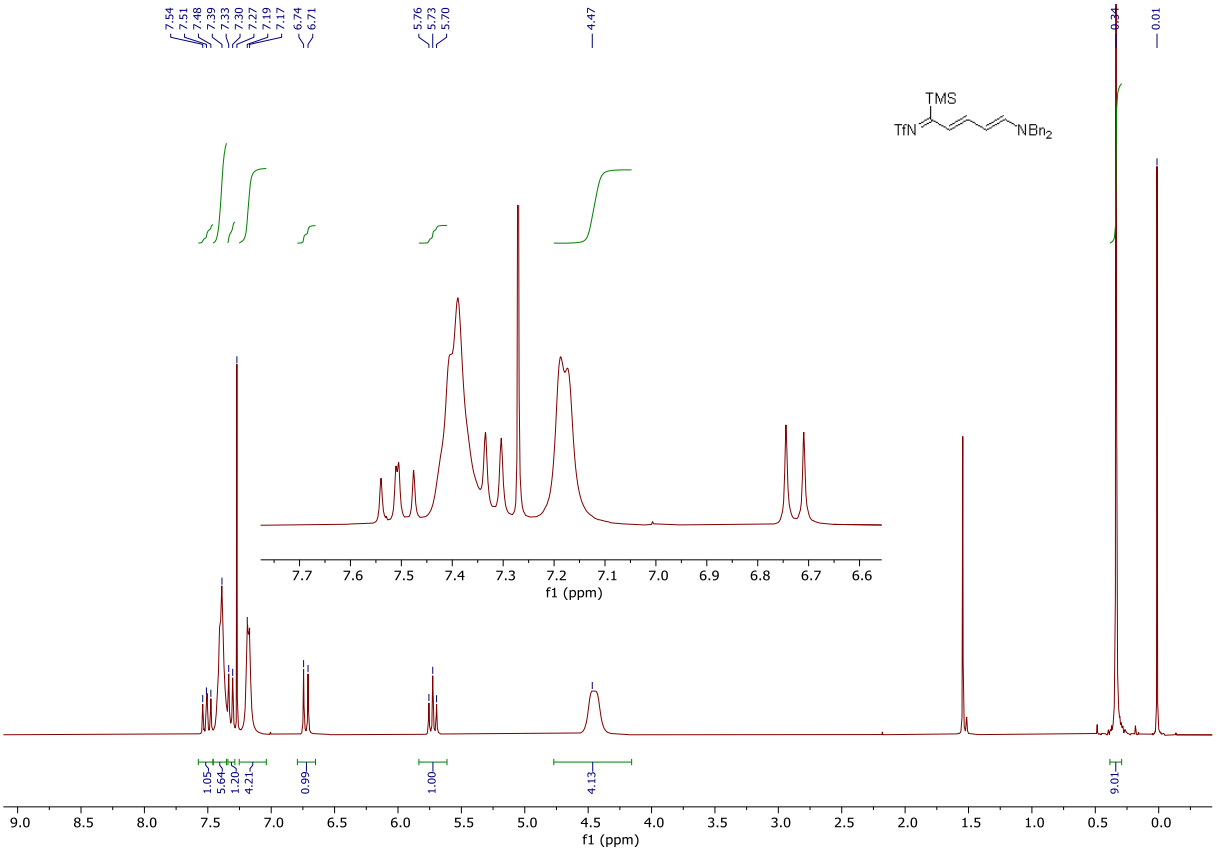

^{13}C NMR spectrum of Zincke imine S45b ($CDCl_3$, 298 K)

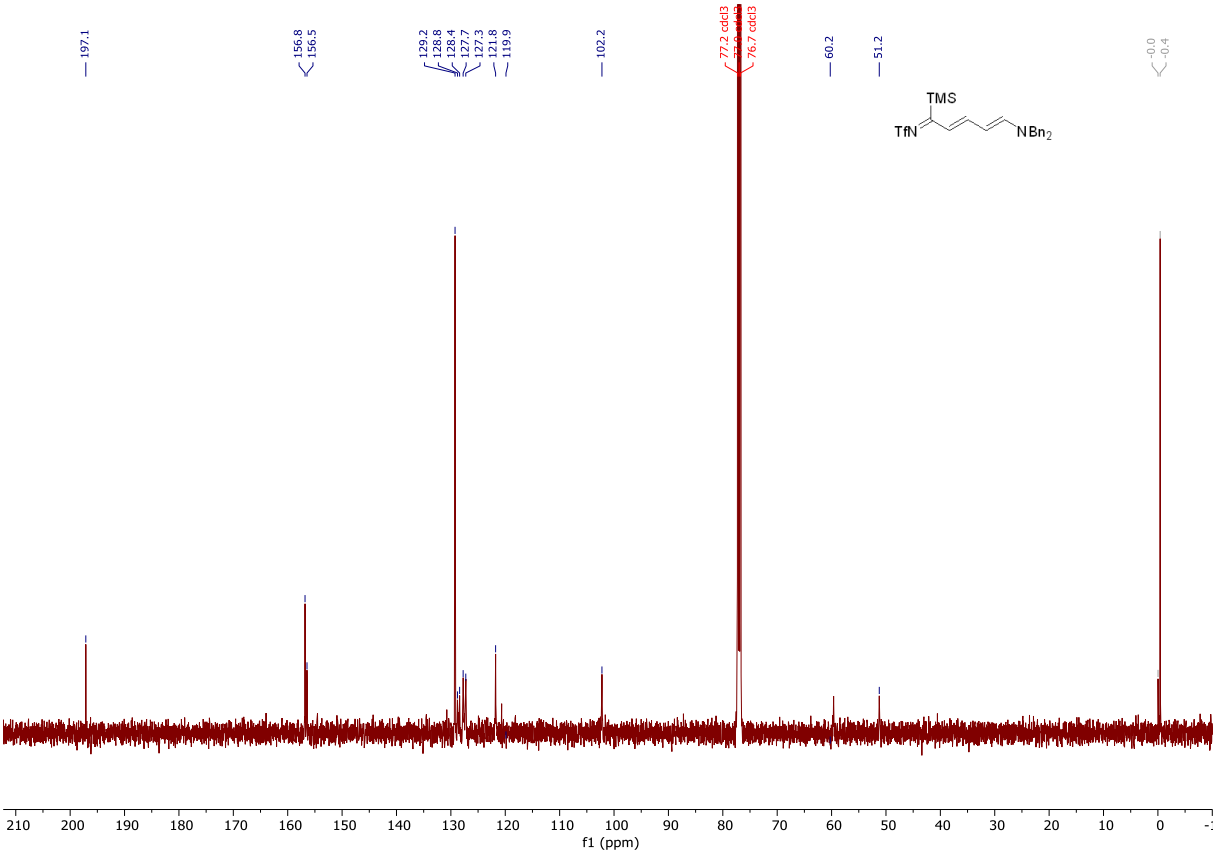

^{1}H NMR spectrum of Zincke imine S46b ($CDCl_3$, 298 K)

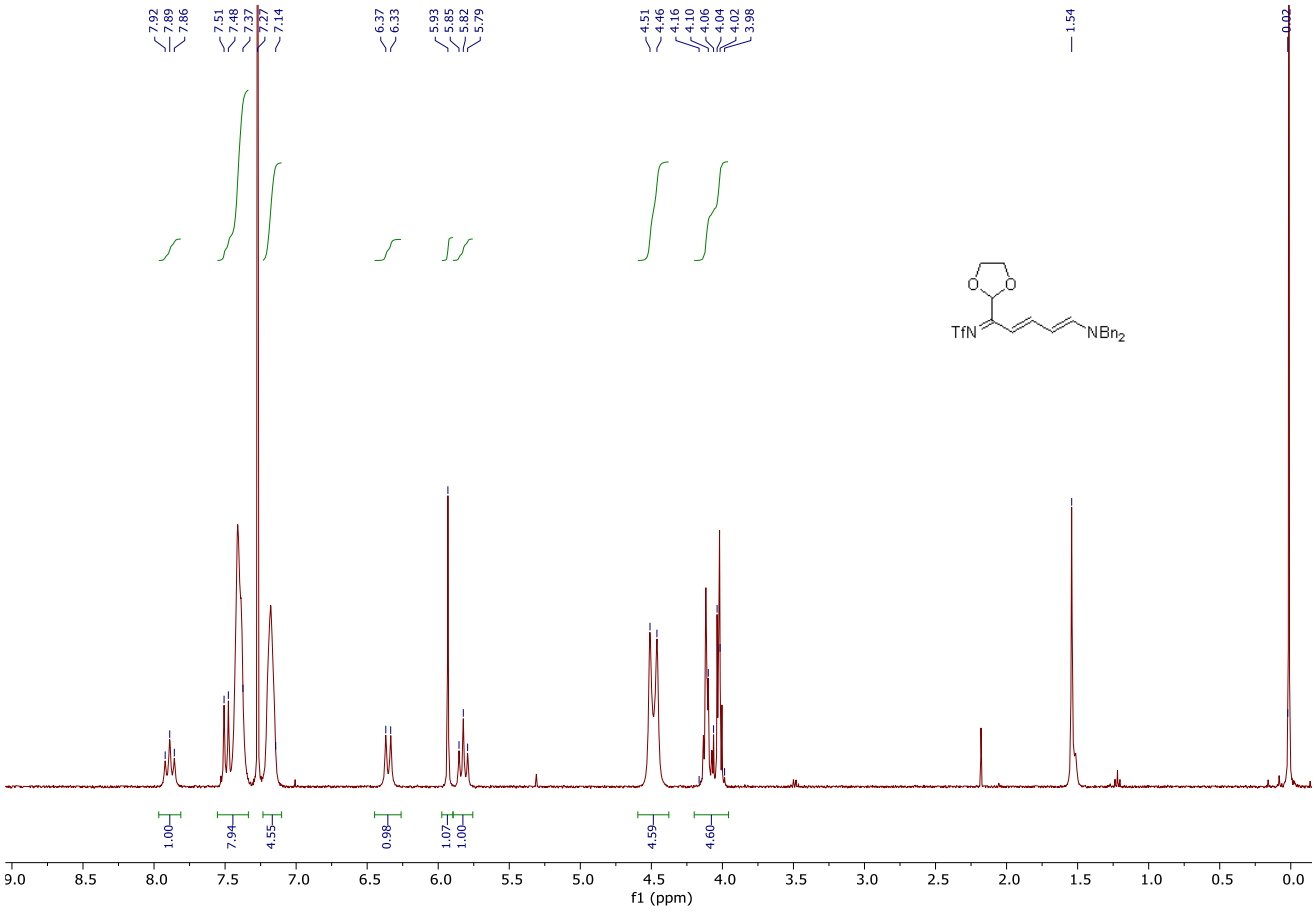

^{1}H NMR spectrum of Zincke imine S47b ($CDCl_3$, 298 K)

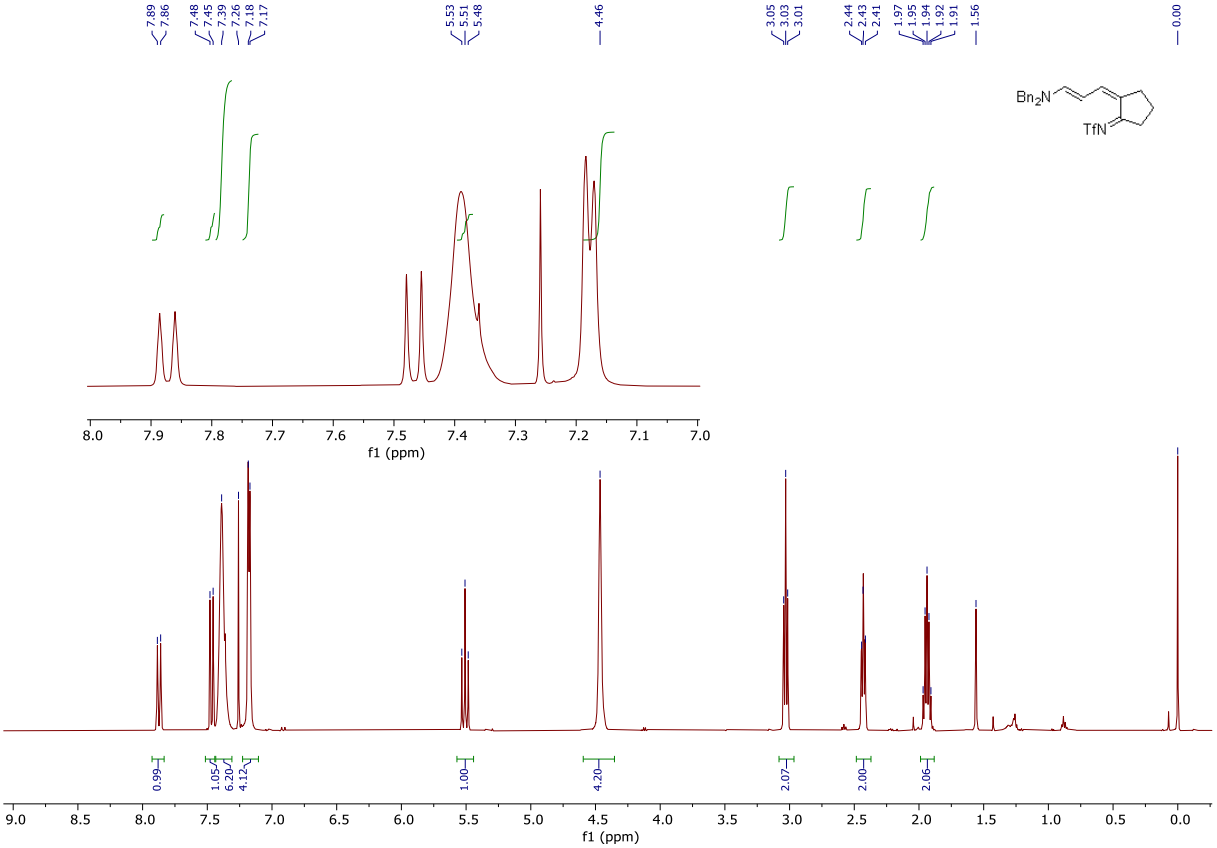

^{13}C NMR spectrum of Zincke imine S47b ($CDCl_3$, 298 K)

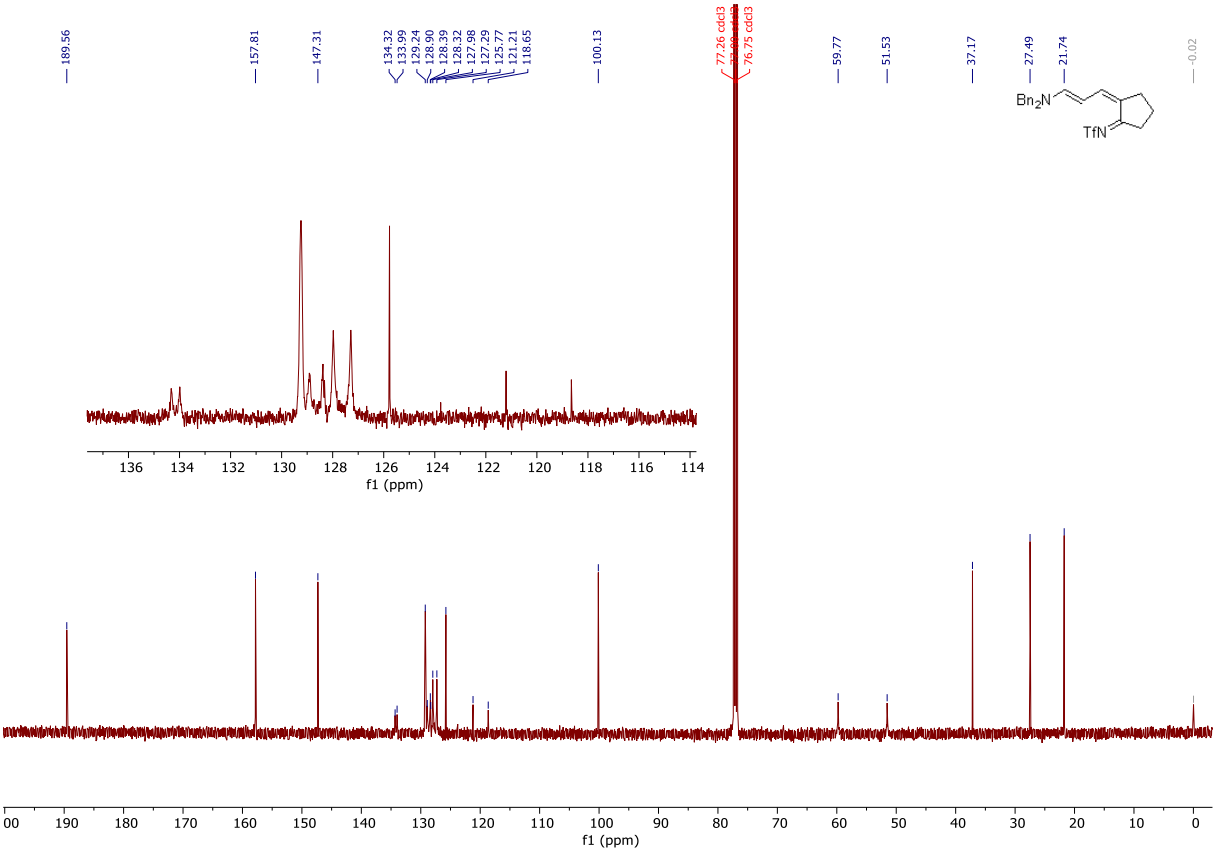

^{1}H NMR spectrum of Zincke imine S48b ($CDCl_3$, 298 K)

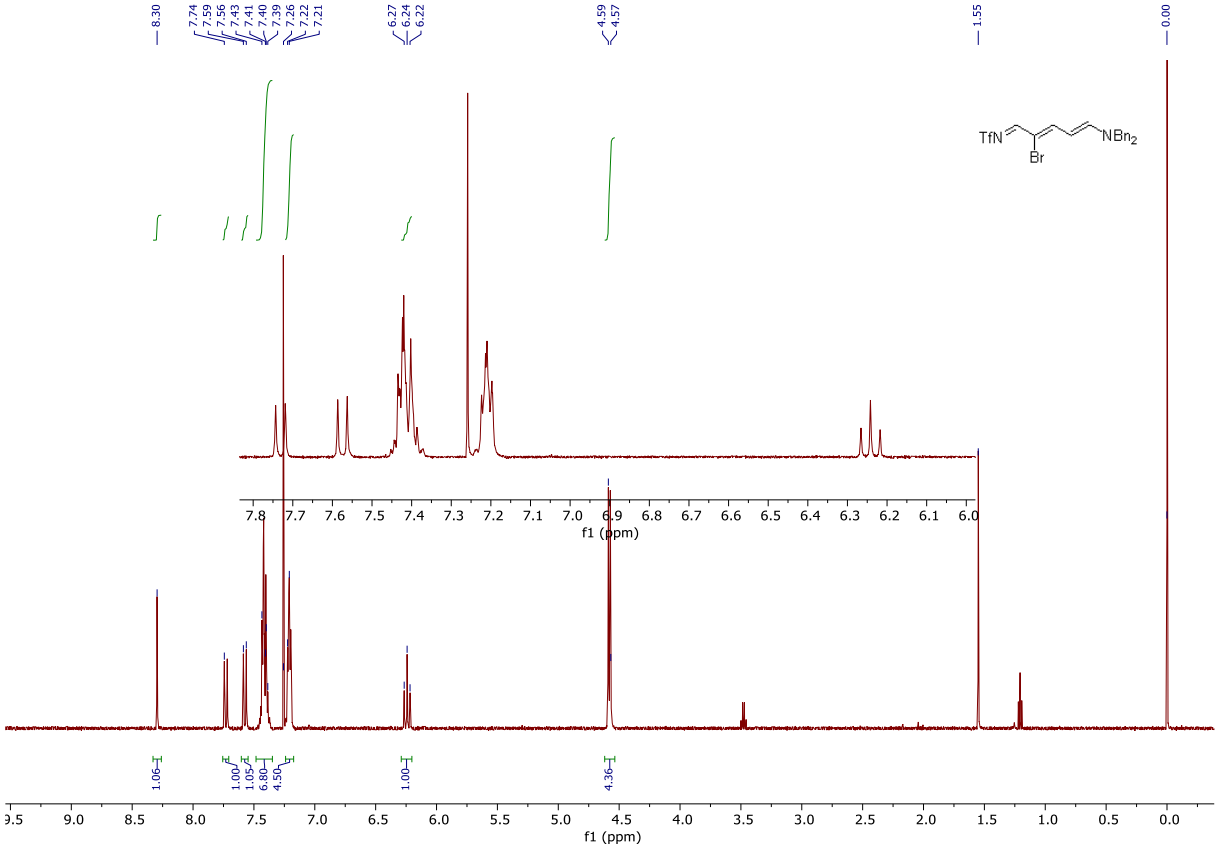

^{13}C NMR spectrum of Zincke imine S48b ($CDCl_3$, 298 K)

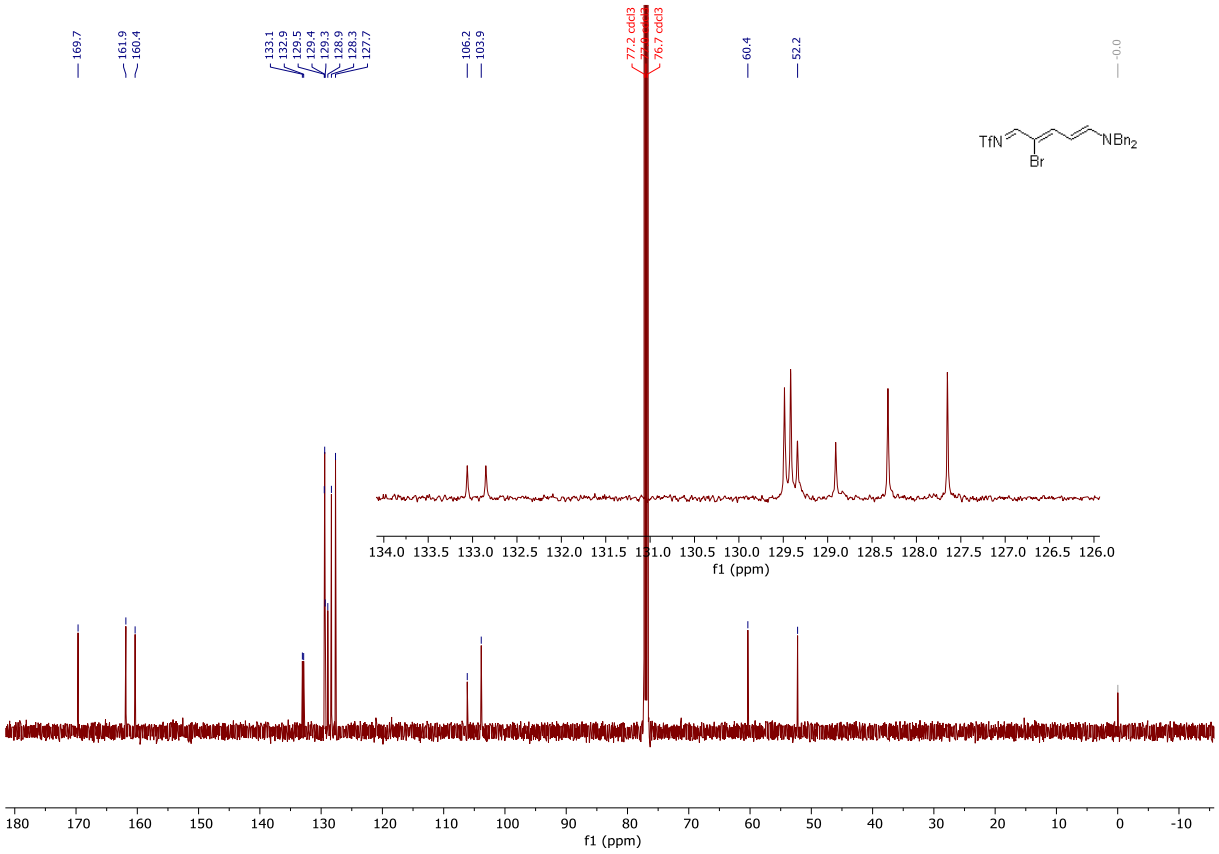

^{1}H NMR spectrum of compound S49b ($CDCl_3$, 298 K)

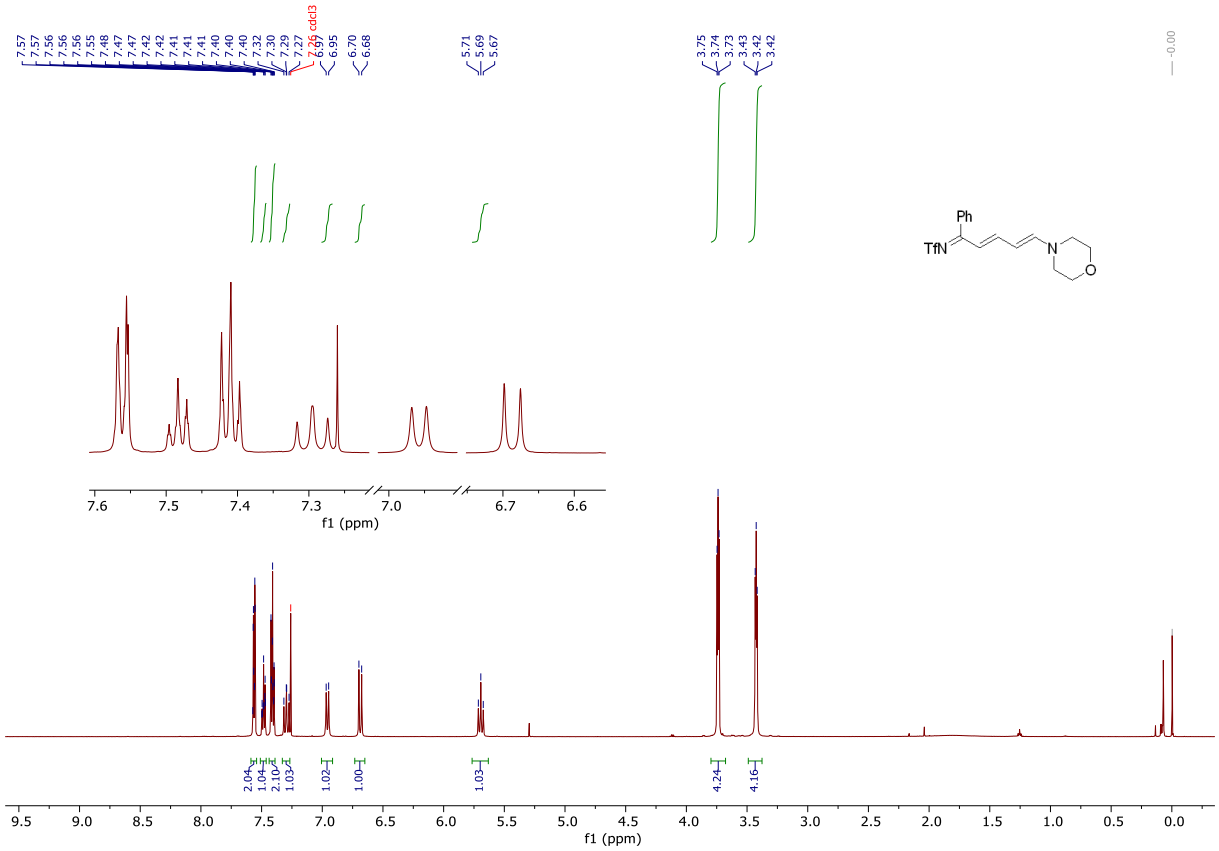

^{1}H NMR spectrum of compound S50b ($CDCl_3$, 298 K)

6.3. Functionalised pyridines

^{1}H NMR spectrum of compound 3a ($CDCl_3$, 298 K)

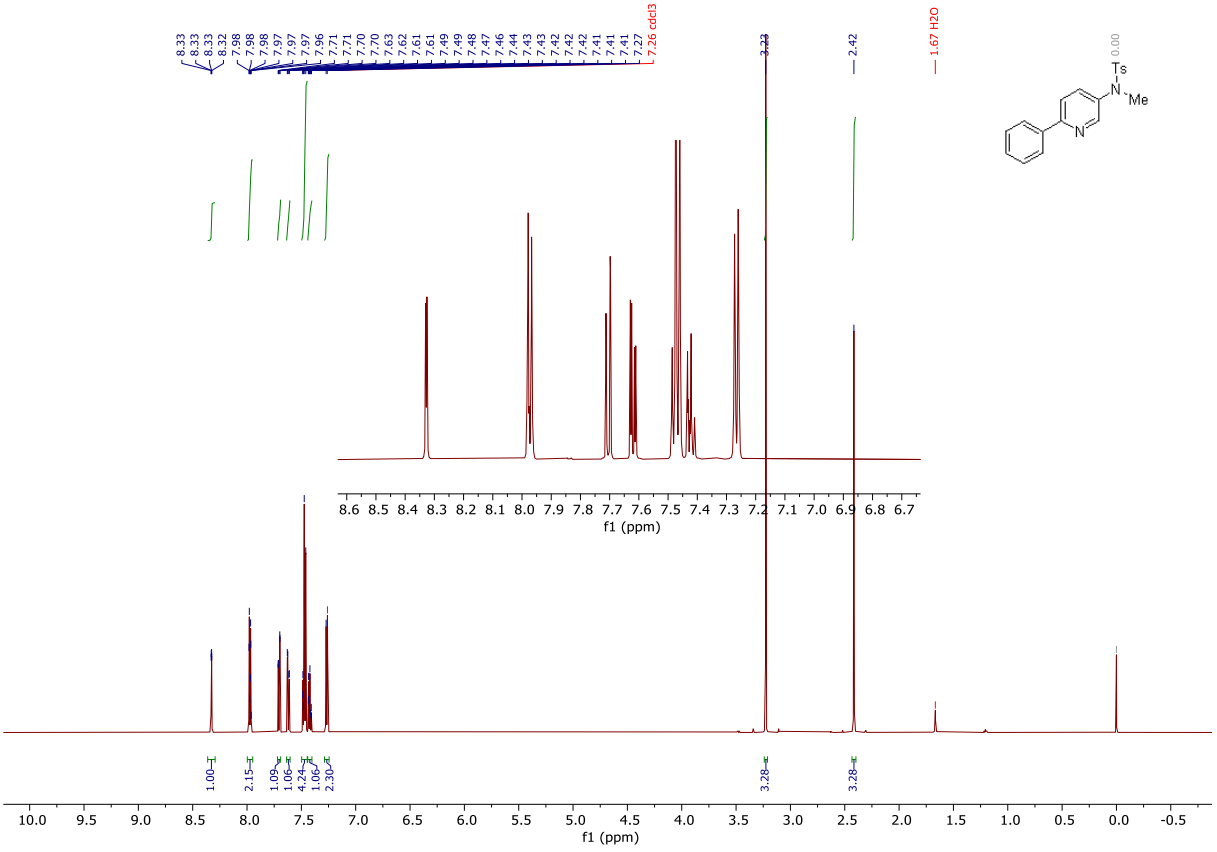

^{1}H-^{1}H COSY spectrum of compound 3a ($CDCl_3$, 298 K)

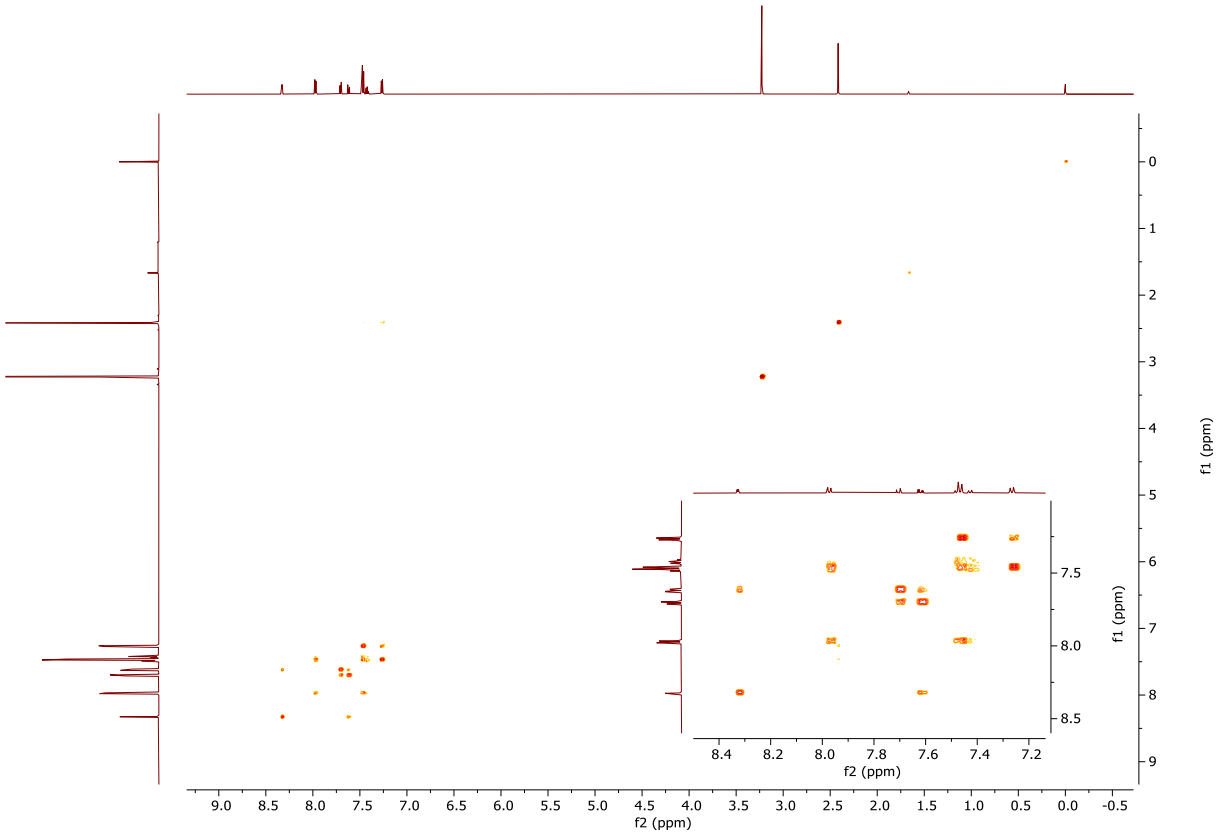

^{13}C NMR spectrum of compound 3a ($CDCl_3$, 298 K)

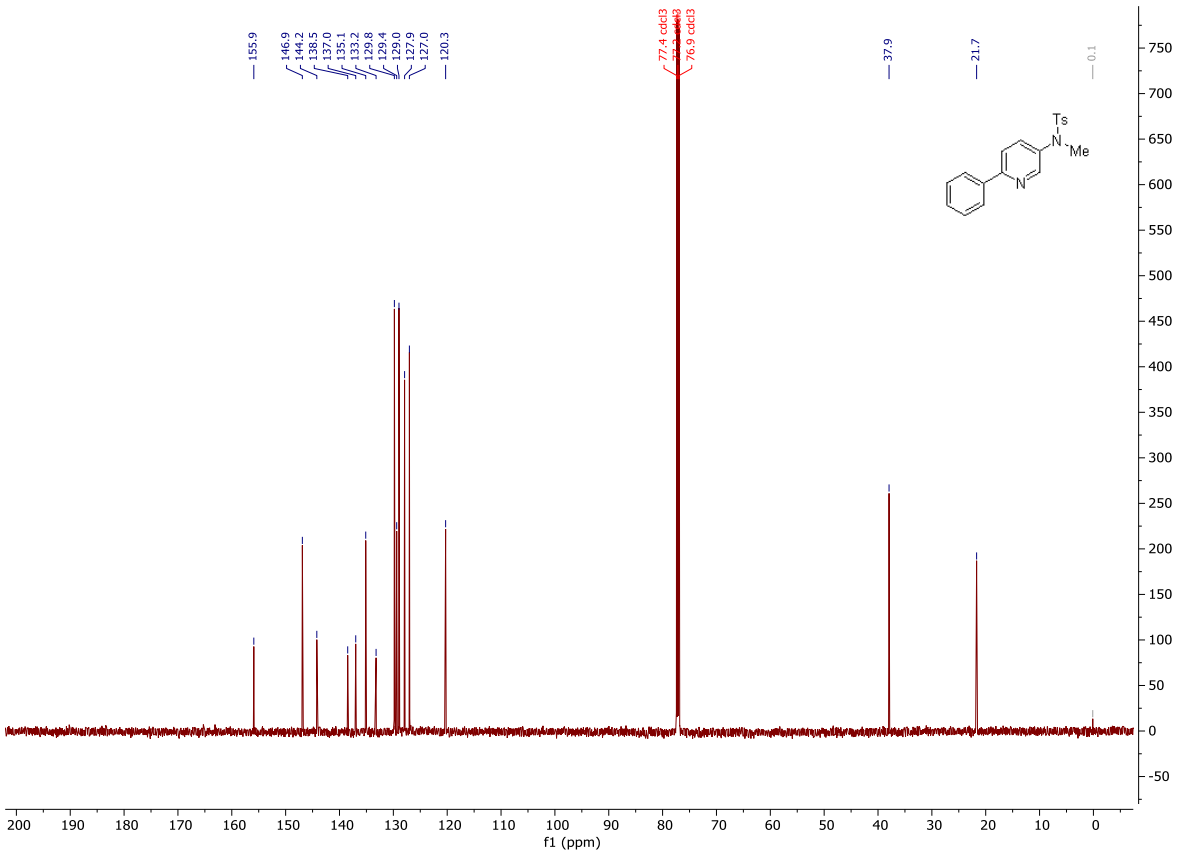

^{1}H NMR spectrum of compound 3b ($CDCl_3$, 298 K)

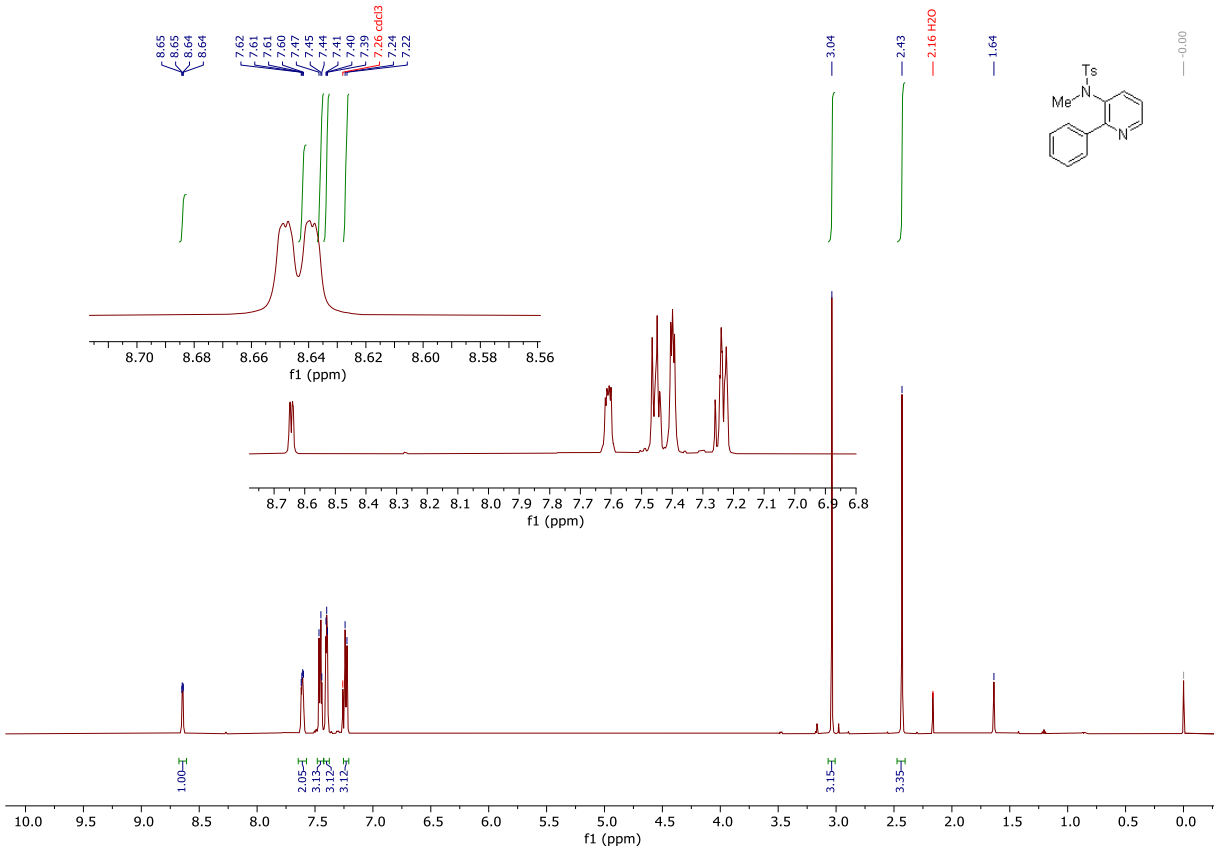

^{1}H-^{1}H COSY spectrum of compound 3b ($CDCl_3$, 298 K)

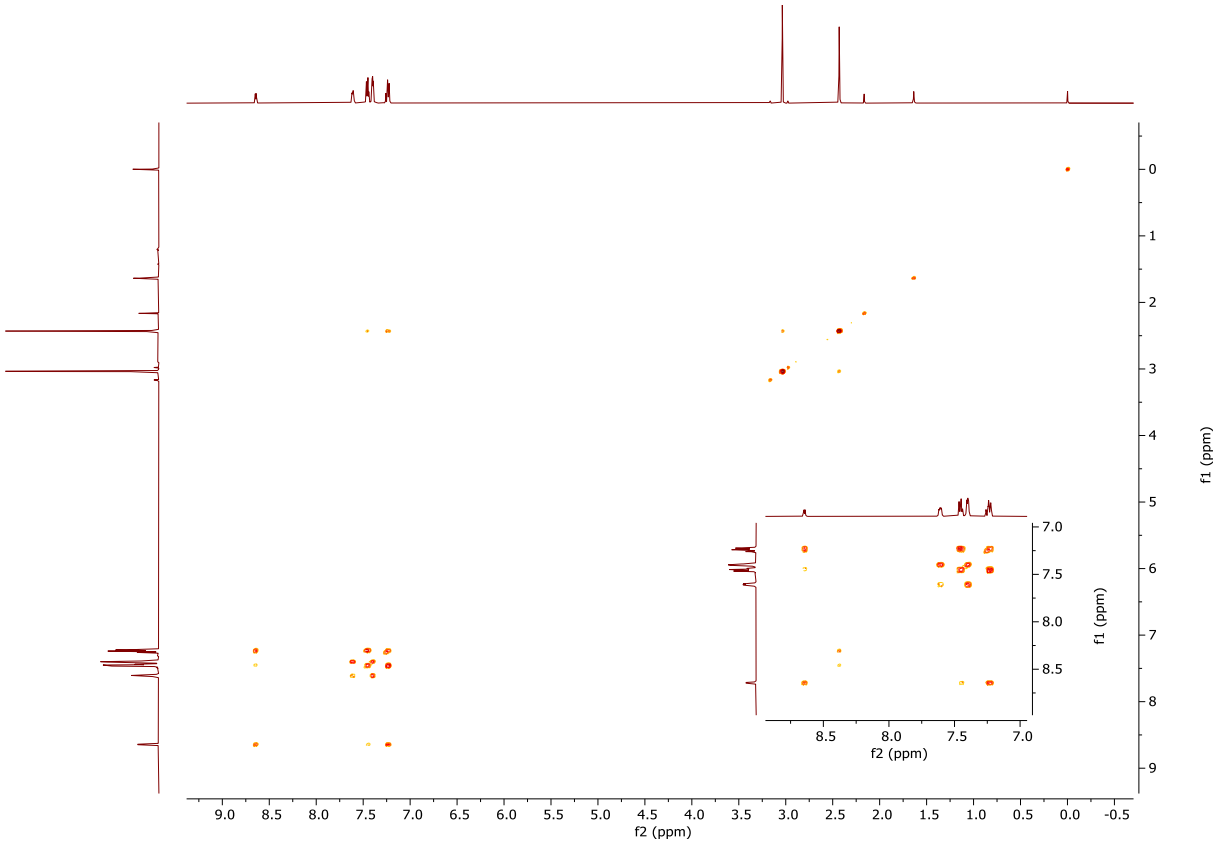

^{13}C NMR spectrum of compound 3b ($CDCl_3$, 298 K)

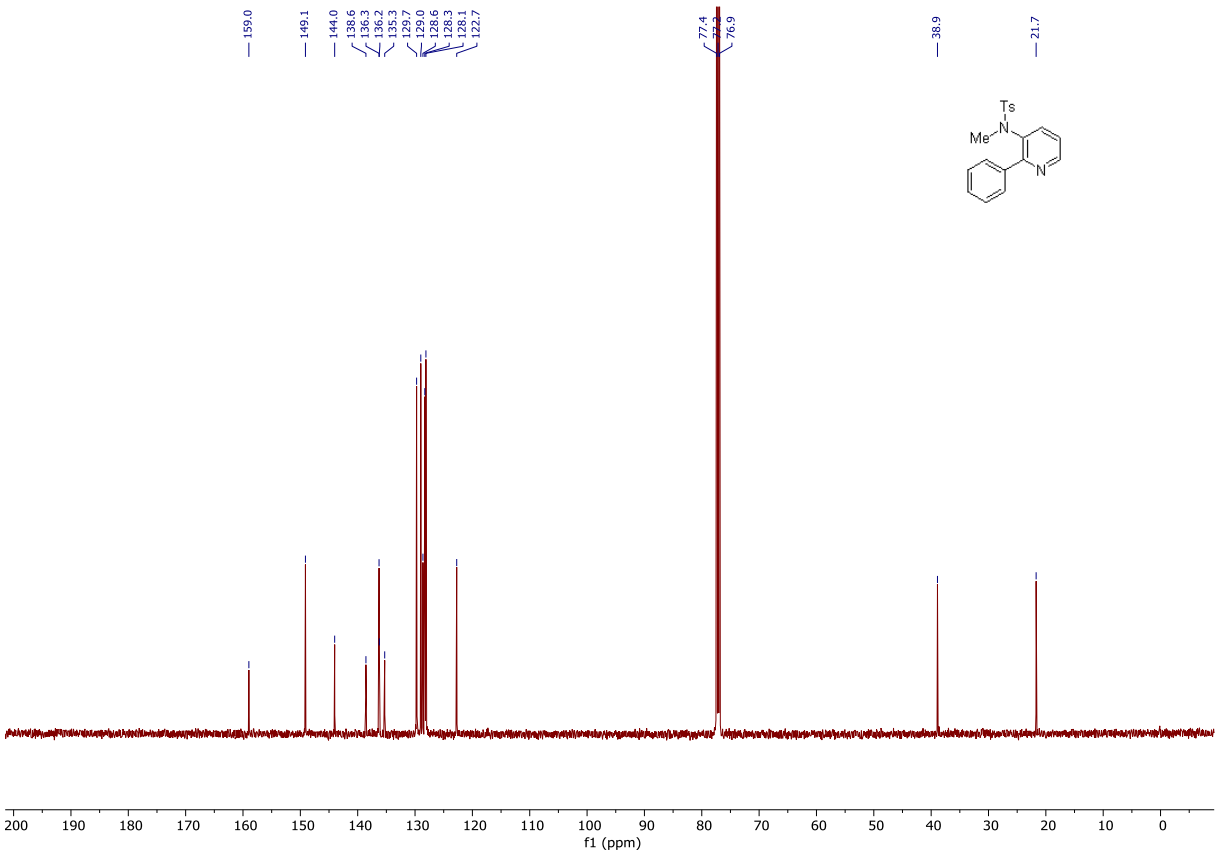

^{1}H NMR spectrum of compound 3c ($CDCl_3$, 298 K)

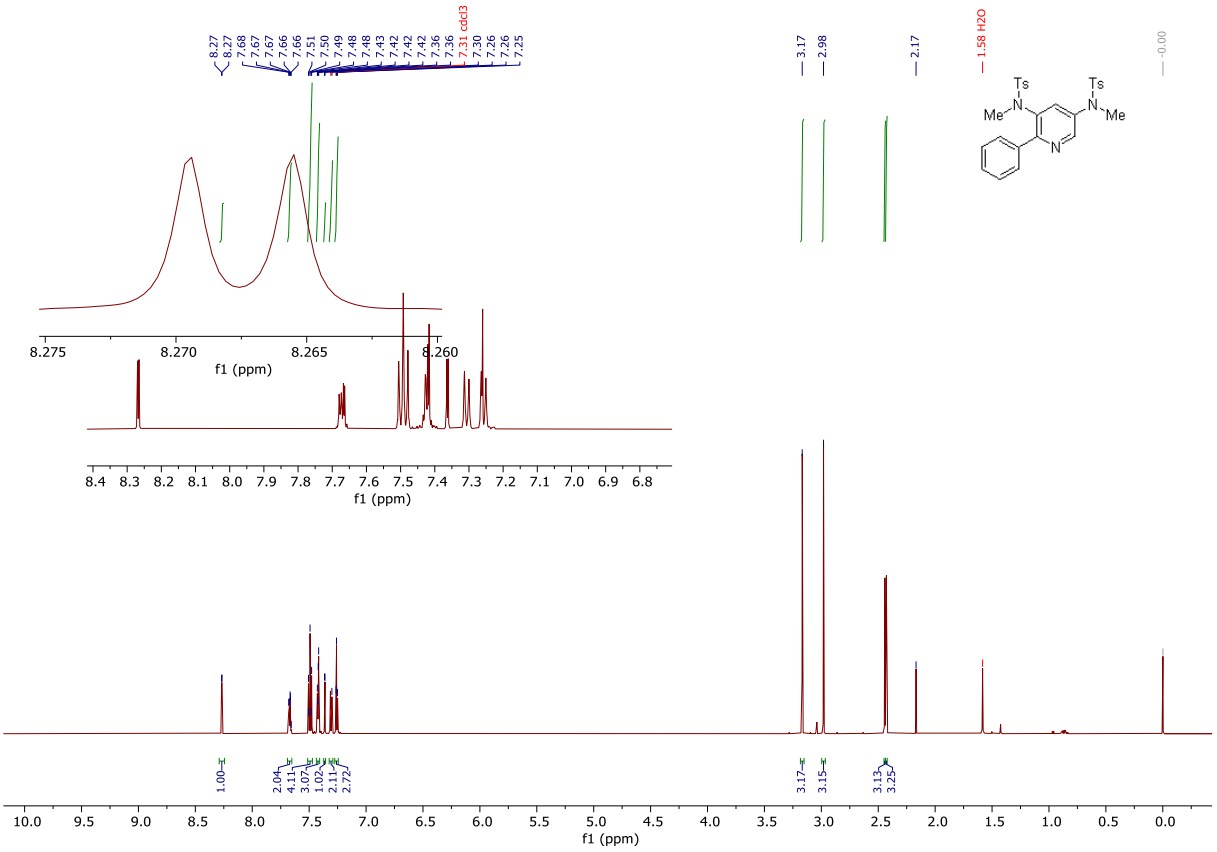

^{1}H-^{1}H COSY spectrum of compound 3c ($CDCl_3$, 298 K)

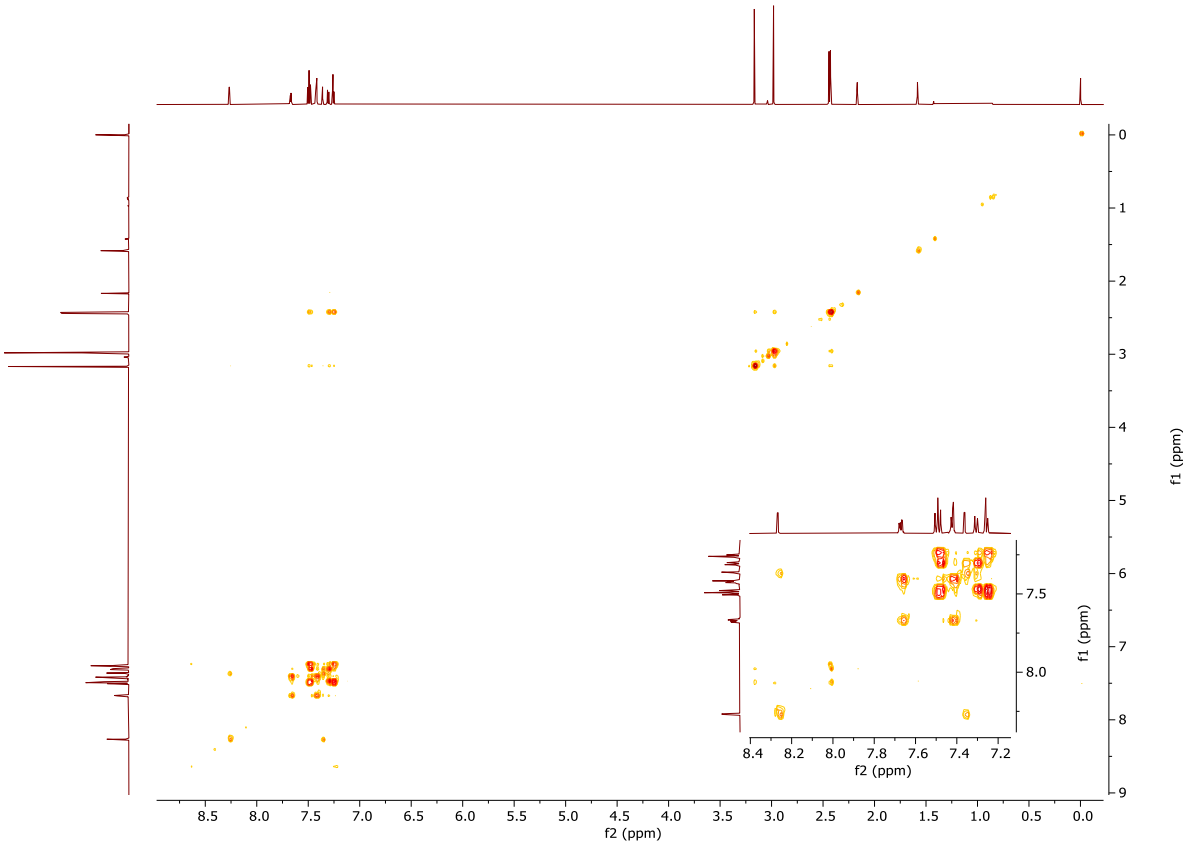

^{13}C NMR spectrum of compound 3c ($CDCl_3$, 298 K)

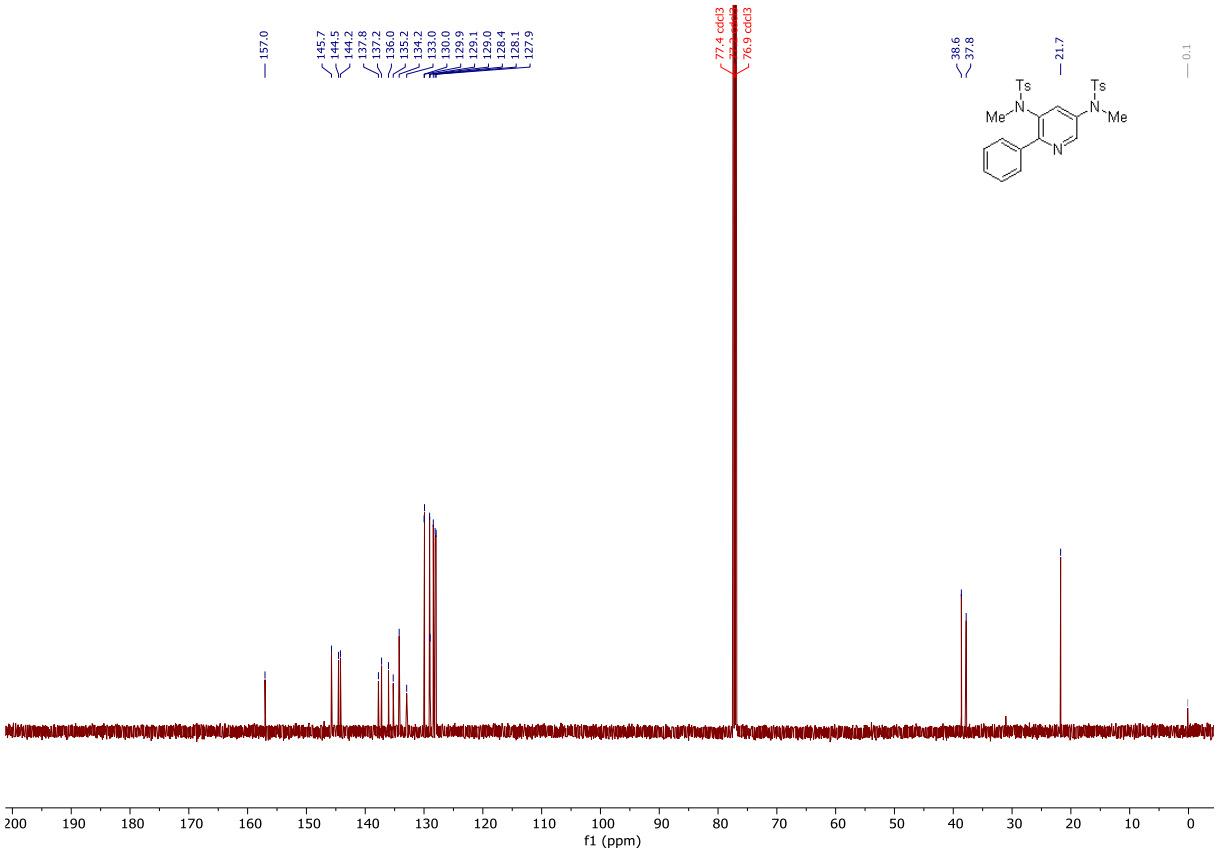

^{1}H NMR spectrum of compound 2a ($CDCl_3$, 298 K)

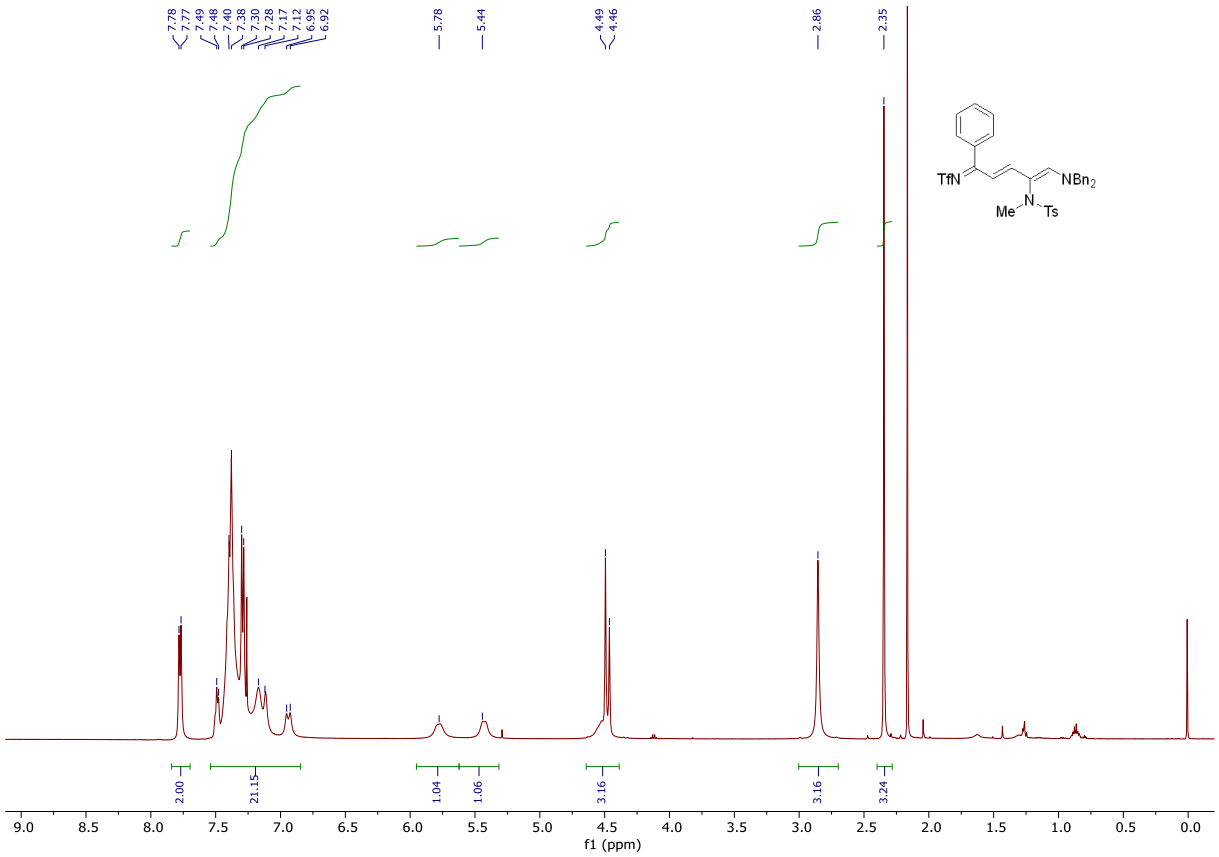

^{13}C NMR spectrum of compound 2a ($CDCl_3$, 298 K)

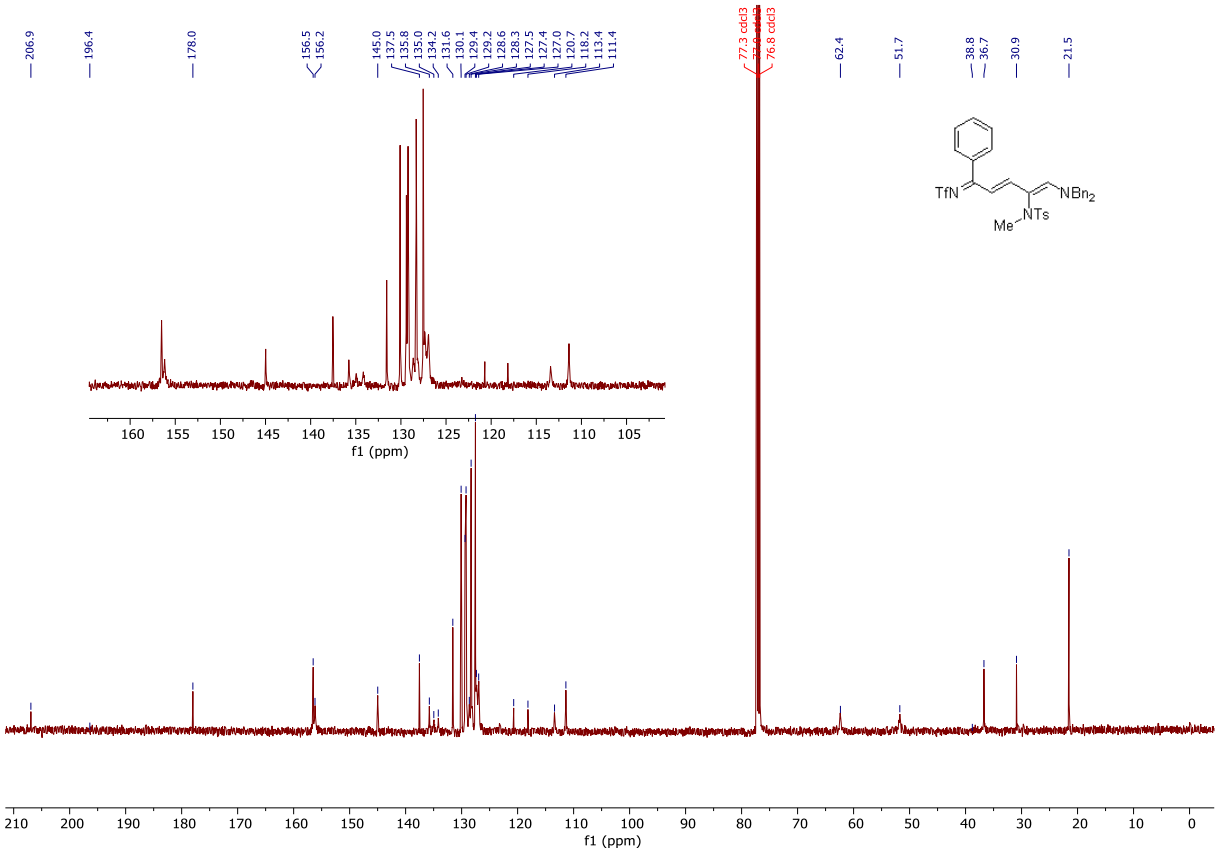

^{1}H-^{1}H COSY spectrum of compound 2a ($CDCl_3$, 298 K)

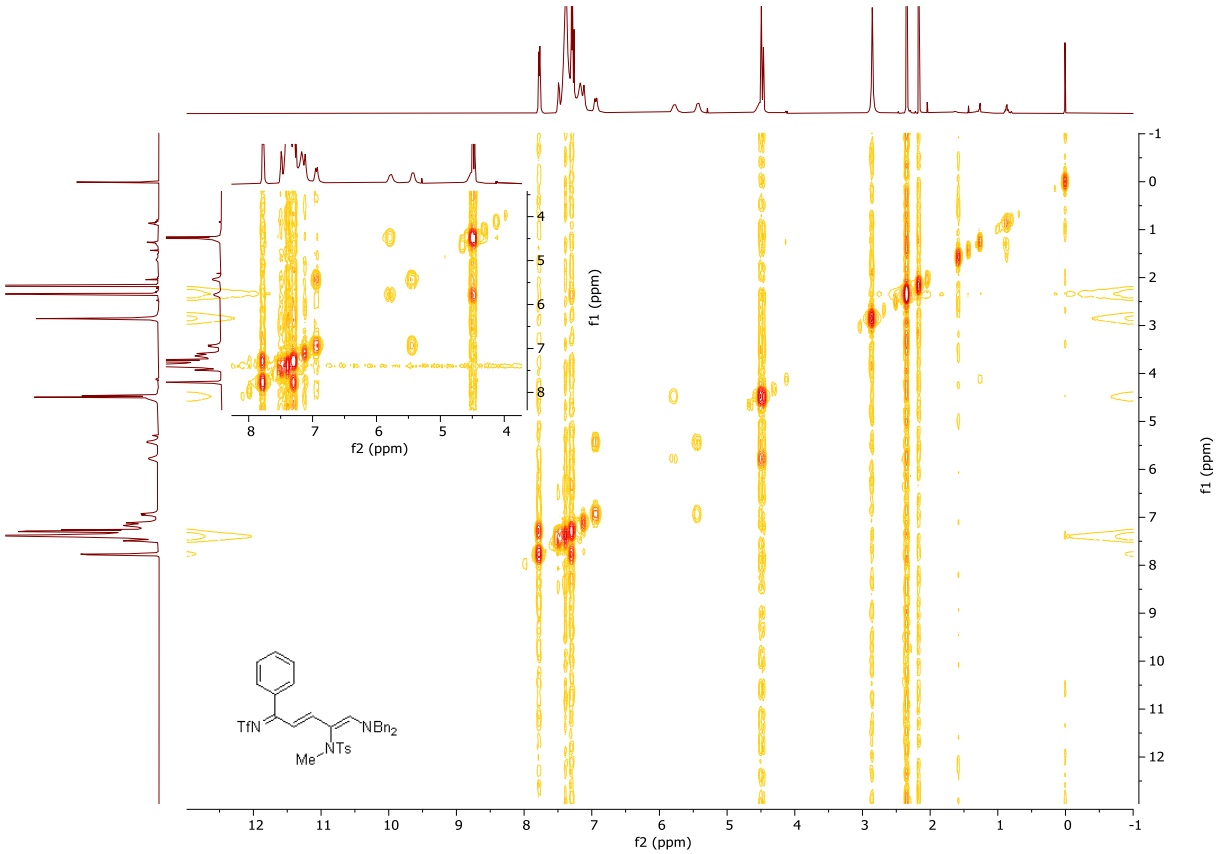

^{1}H NMR spectrum of compound 4a ($CDCl_3$, 298 K)

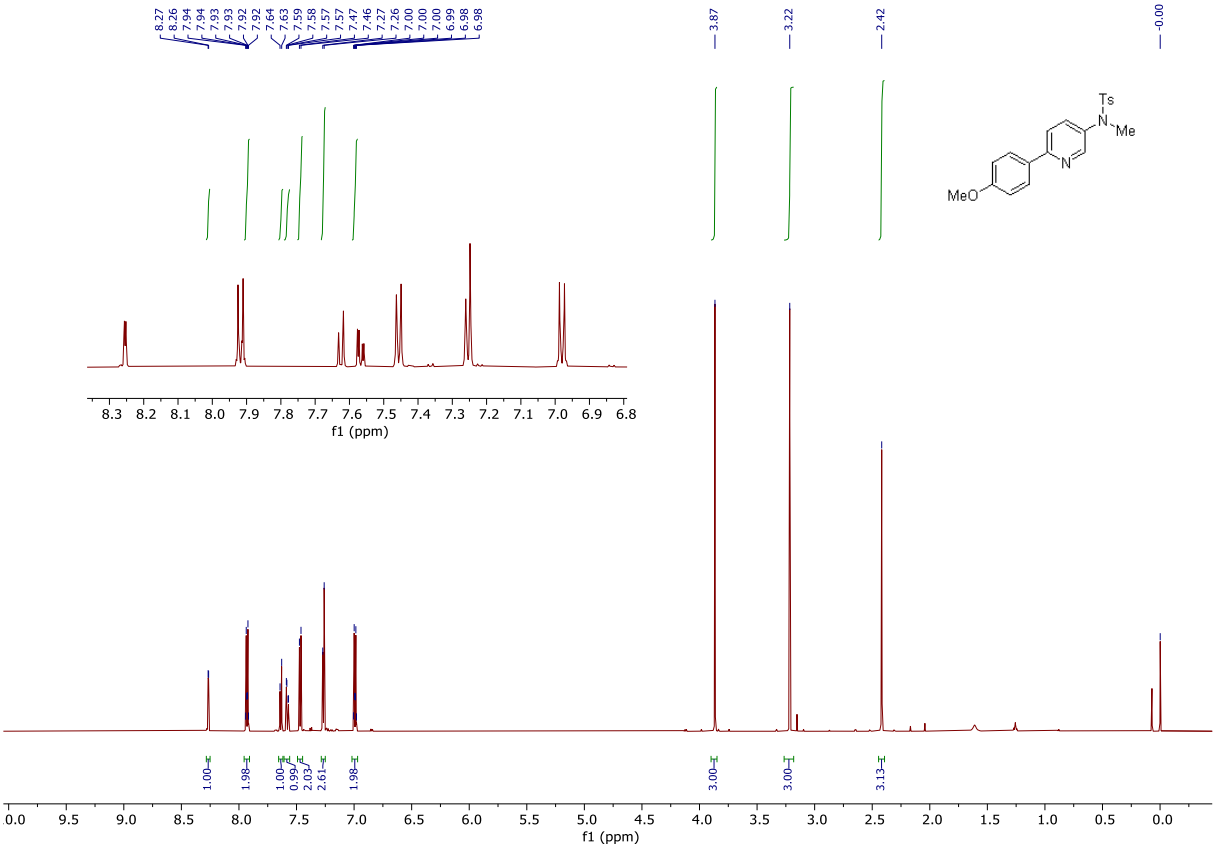

^{13}C NMR spectrum of compound 4a ($CDCl_3$, 298 K)

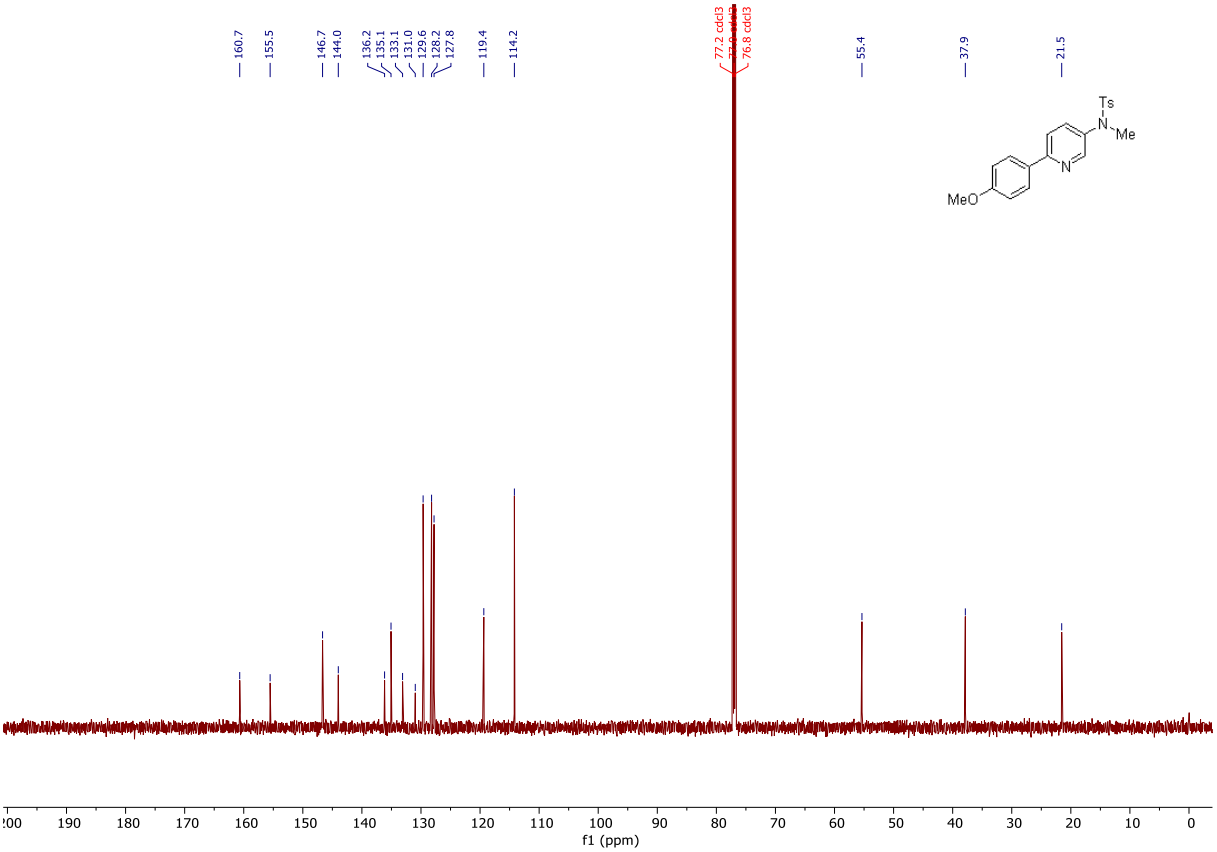

^{1}H NMR spectrum of compound 4b ($CDCl_3$, 298 K)

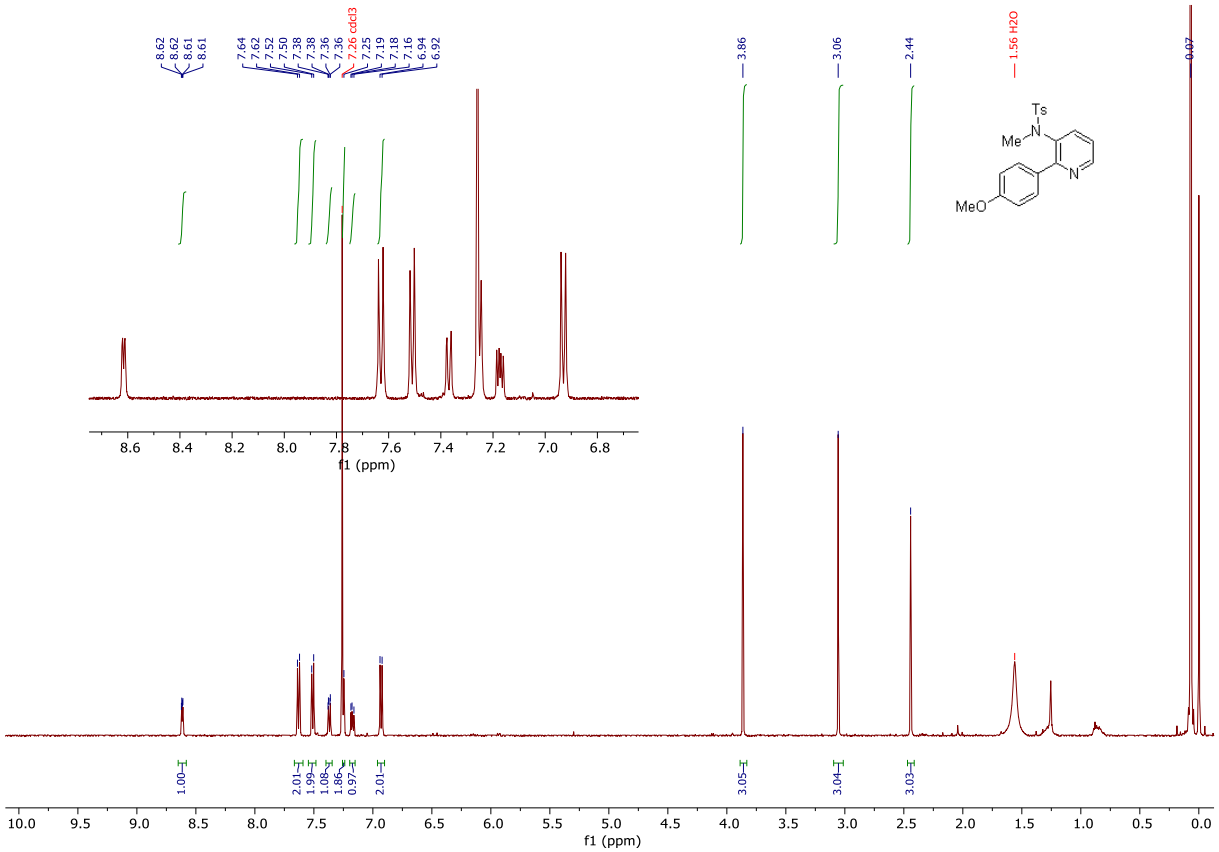

^{13}C NMR spectrum of compound 4b ($CDCl_3$, 298 K)

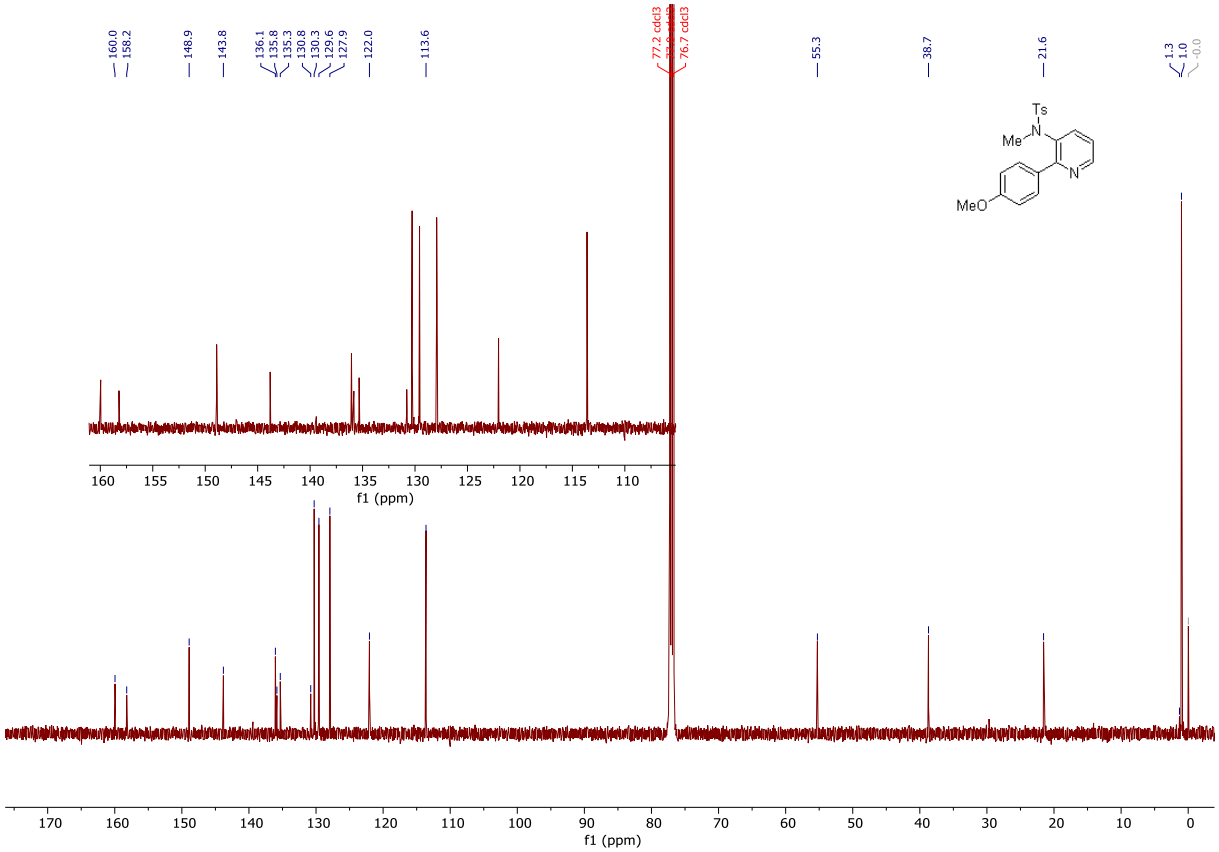

^{1}H NMR spectrum of compound 5a ($CDCl_3$, 298 K)

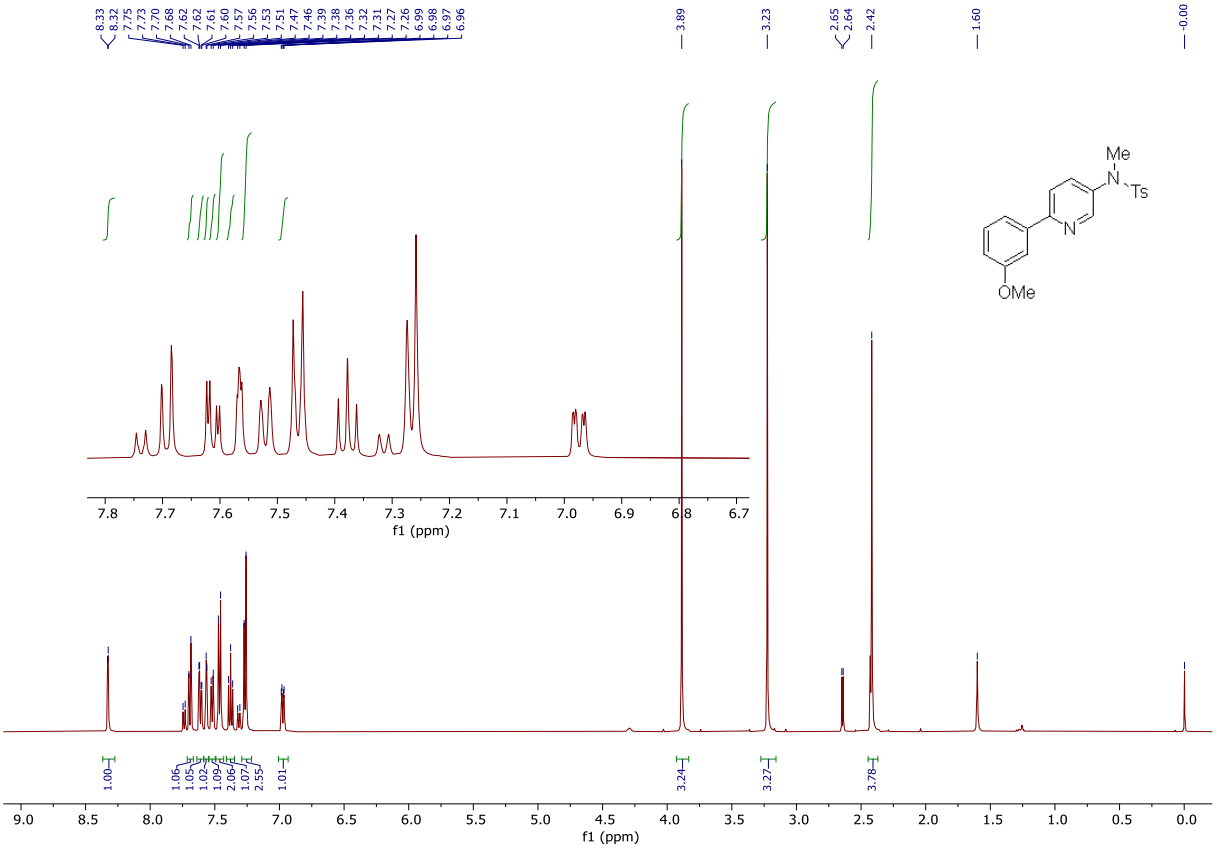

^{13}C NMR spectrum of compound 5a ($CDCl_3$, 298 K)

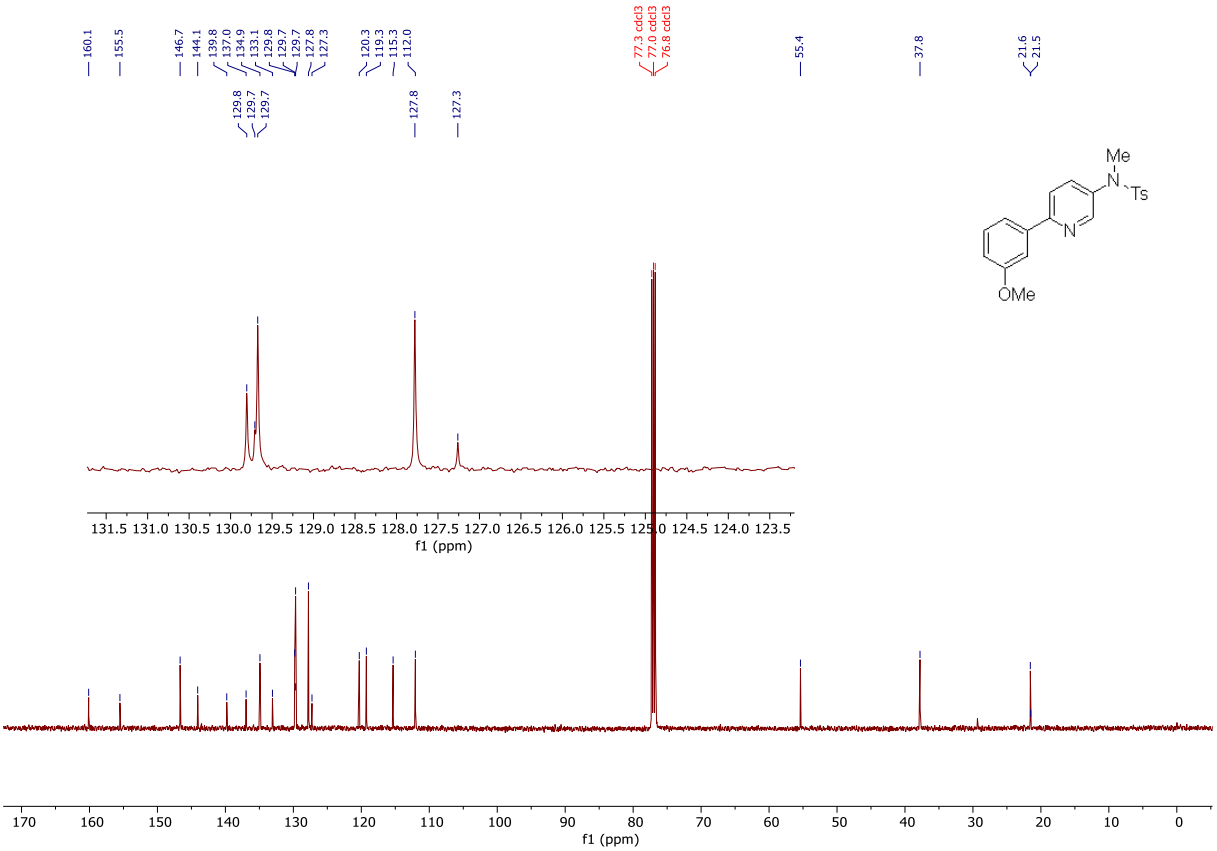

^{1}H NMR spectrum of compound 5b ($CDCl_3$, 298 K)

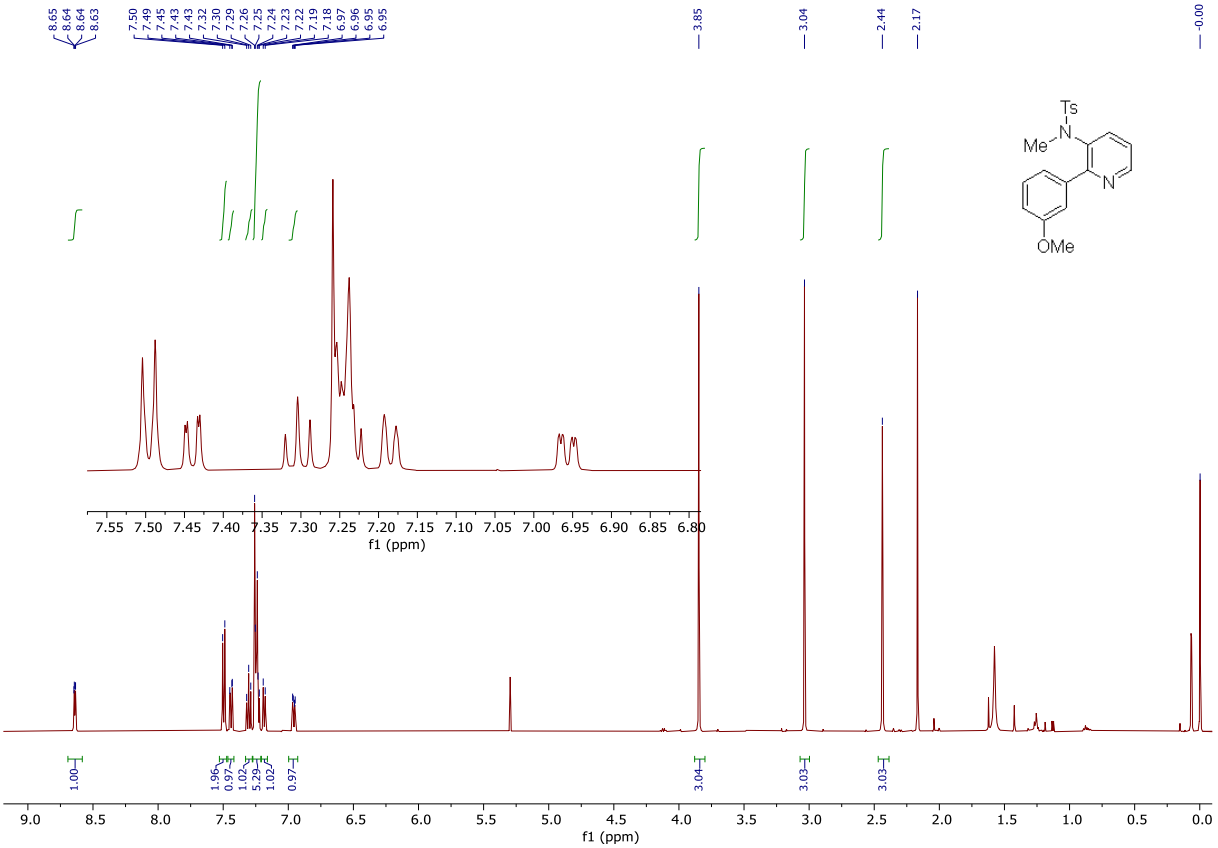

^{13}C NMR spectrum of compound 5b ($CDCl_3$, 298 K)

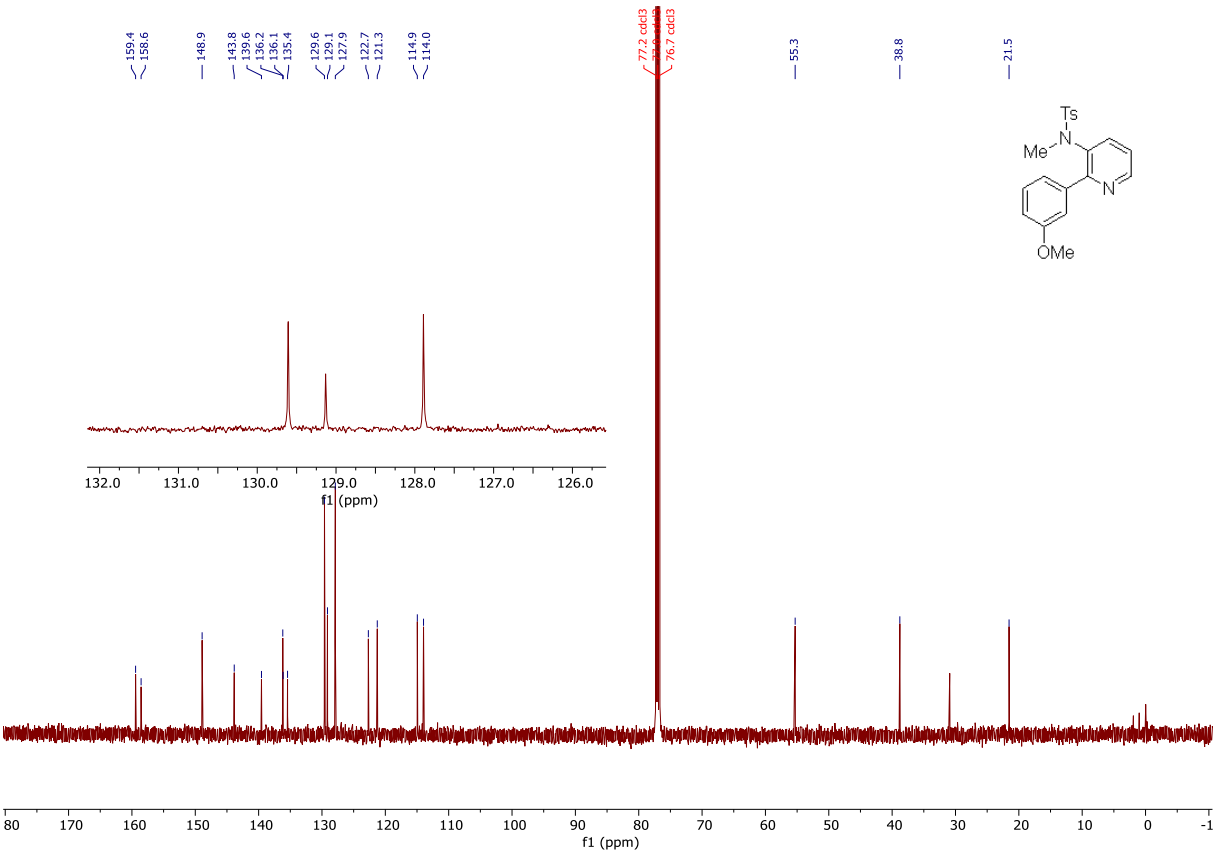

^{1}H NMR spectrum of compound 6a ($CDCl_3$, 298 K)

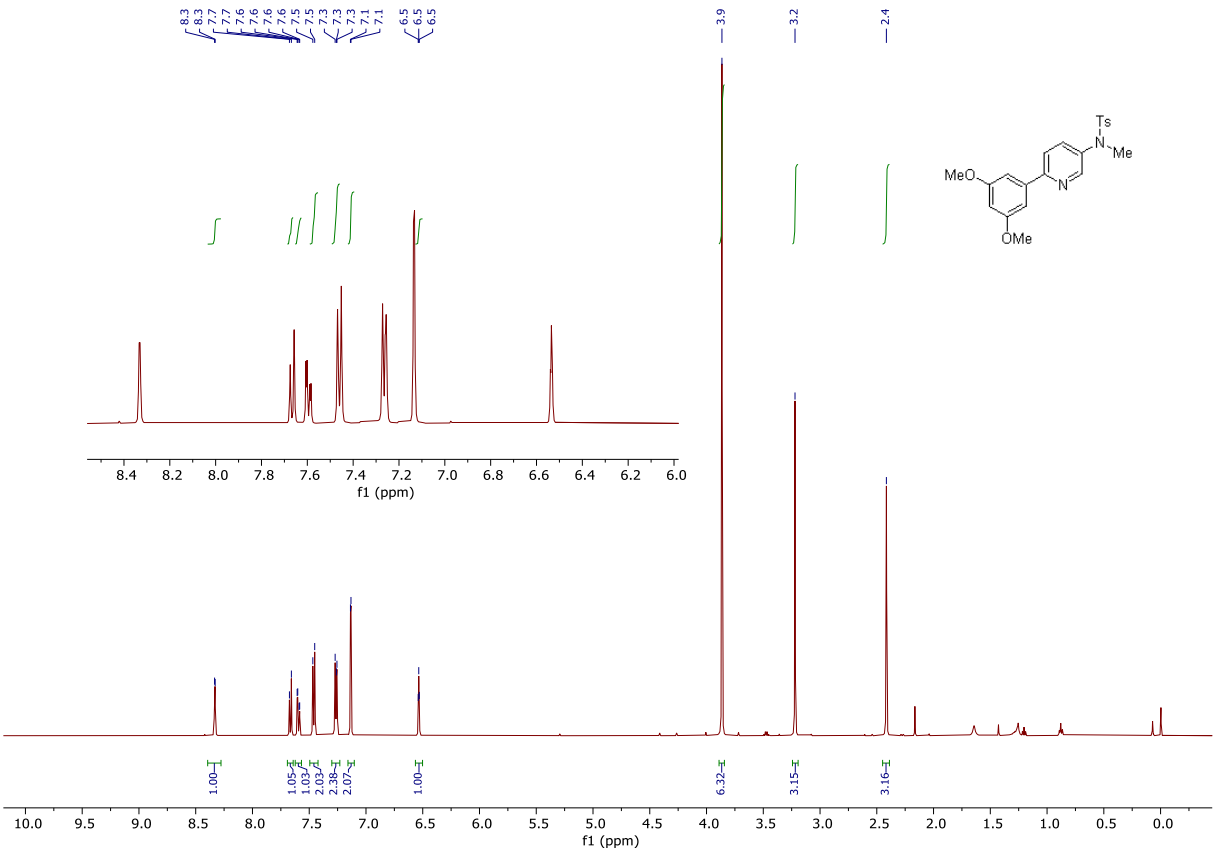

^{13}C NMR spectrum of compound 6a ($CDCl_3$, 298 K)

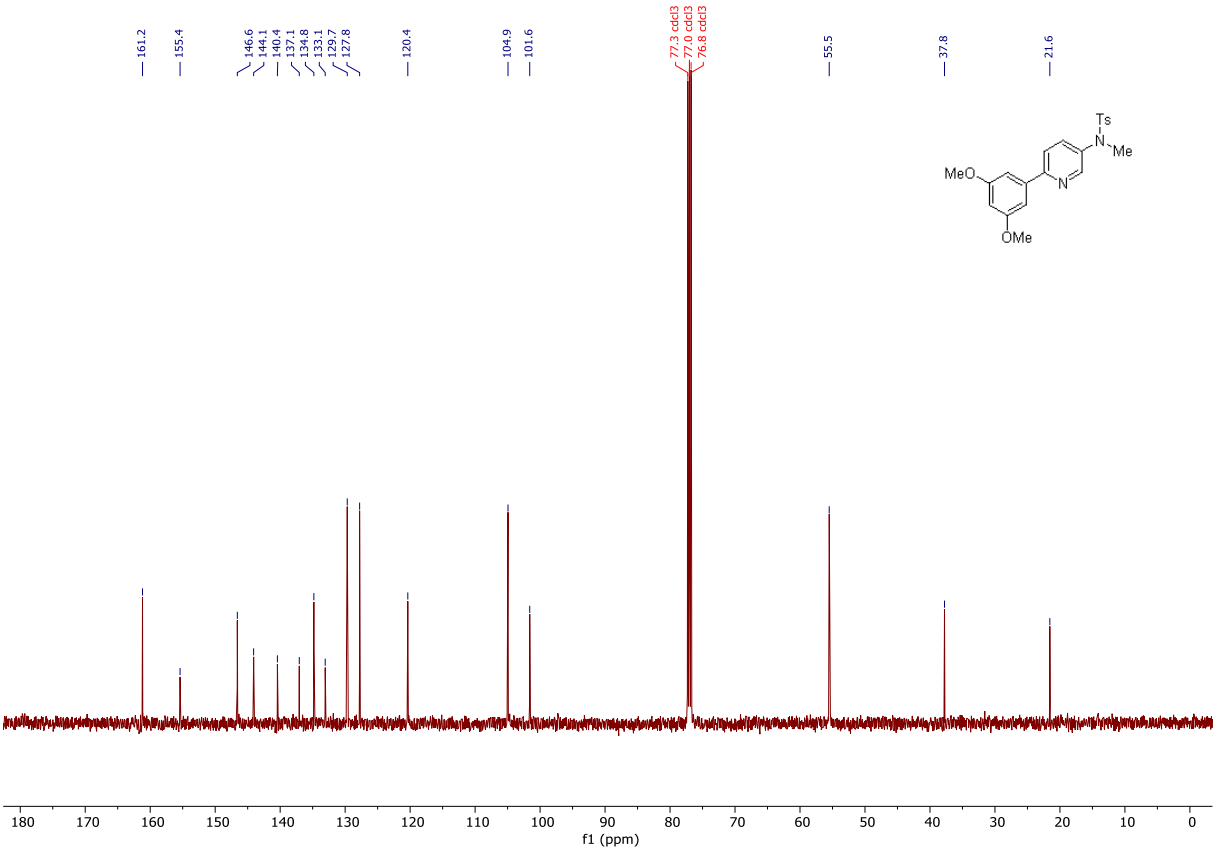

^{1}H NMR spectrum of compound 6b ($CDCl_3$, 298 K)

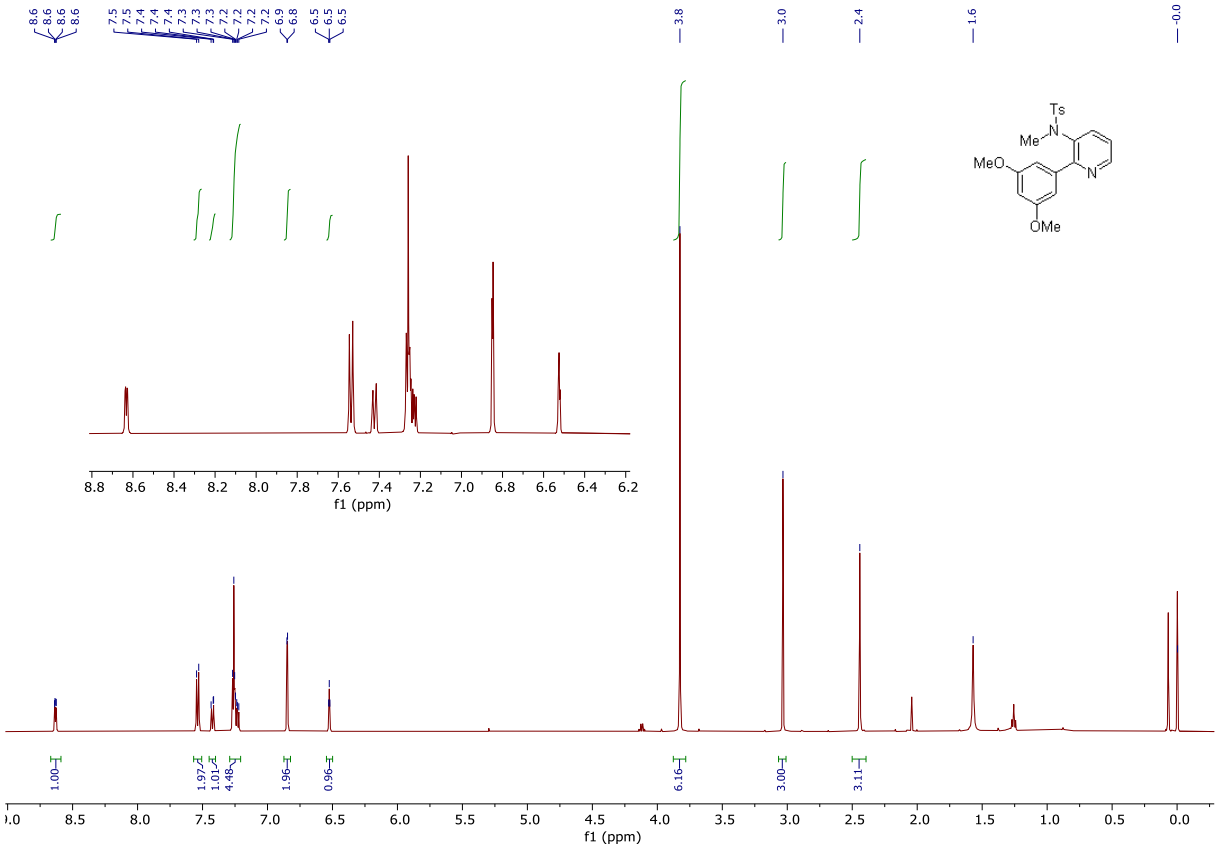

^{13}C NMR spectrum of compound 6b ($CDCl_3$, 298 K)

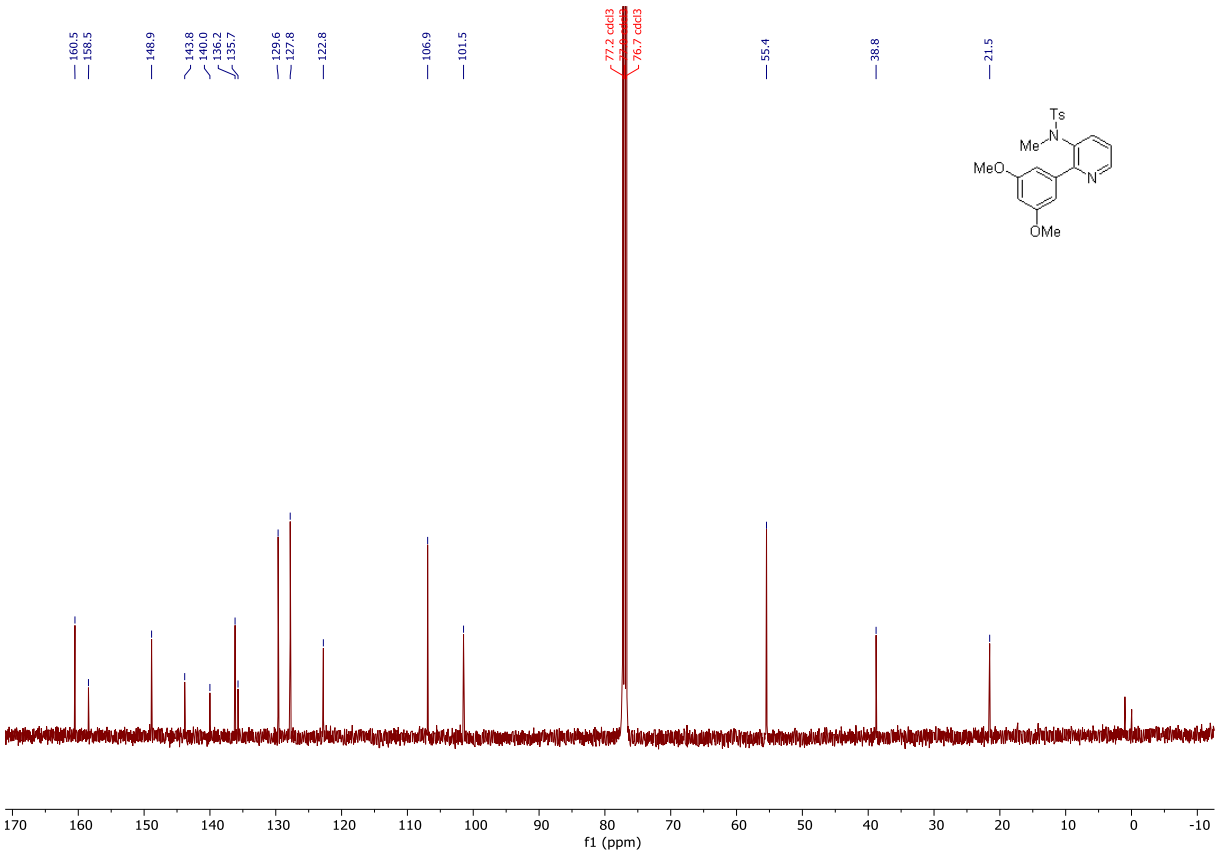

^{1}H NMR spectrum of compound 7a ($CDCl_3$, 298 K)

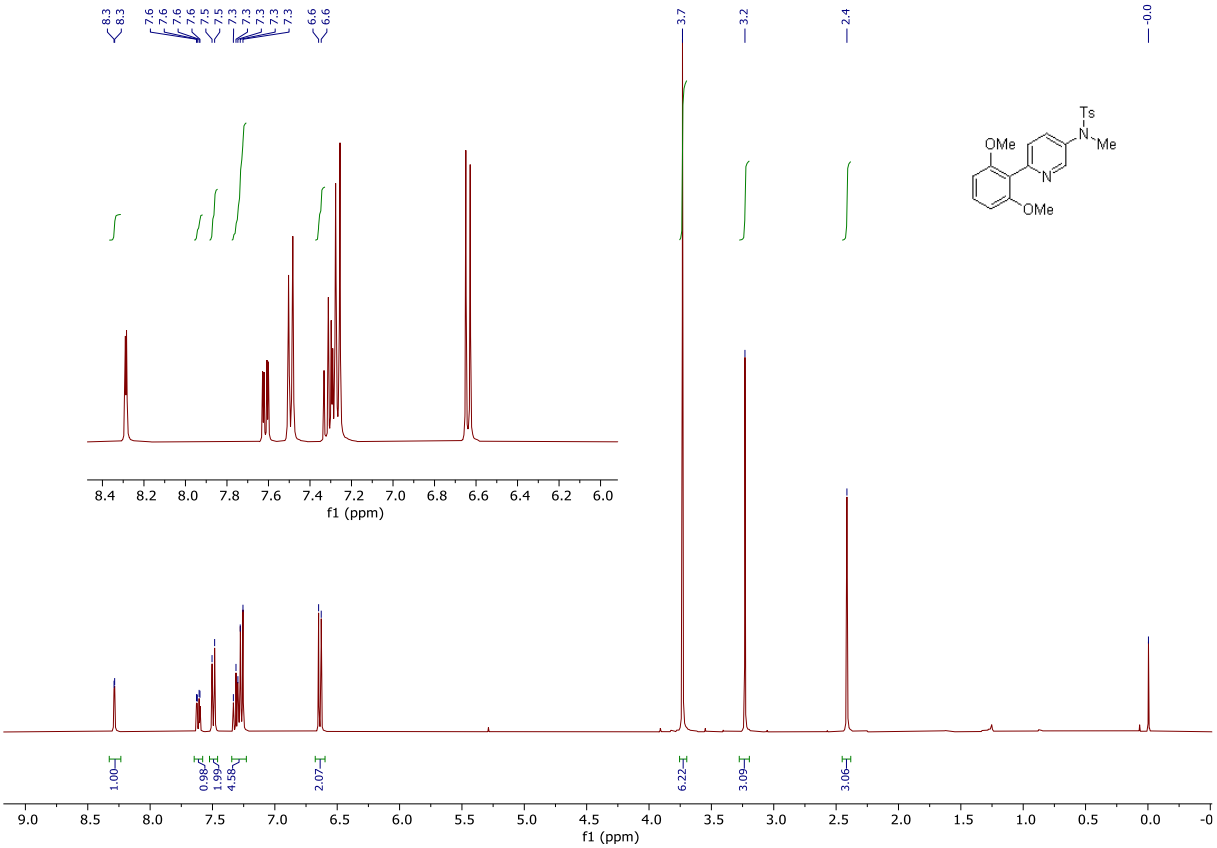

^{13}C NMR spectrum of compound 7a ($CDCl_3$, 298 K)

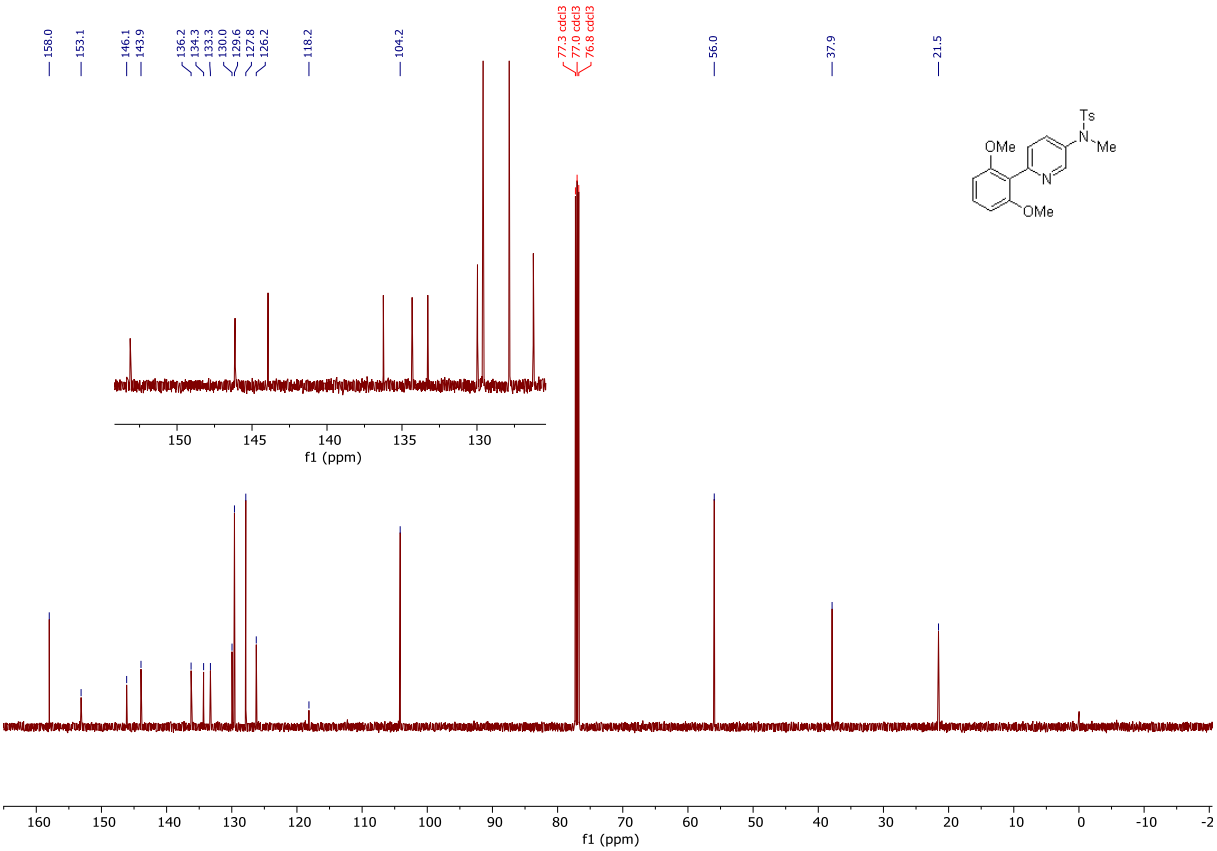

^{1}H NMR spectrum of compound 8a ($CDCl_3$, 298 K)

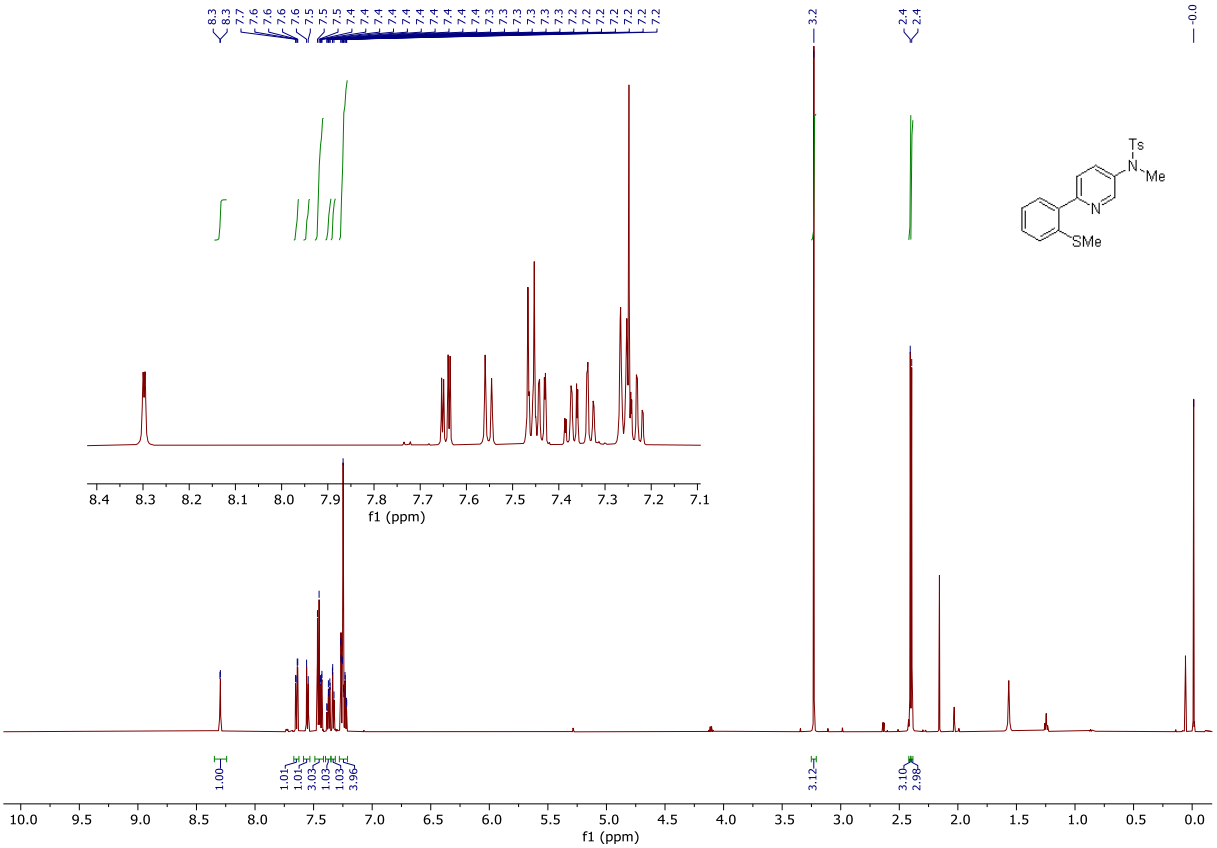

^{13}C NMR spectrum of compound 8a ($CDCl_3$, 298 K)

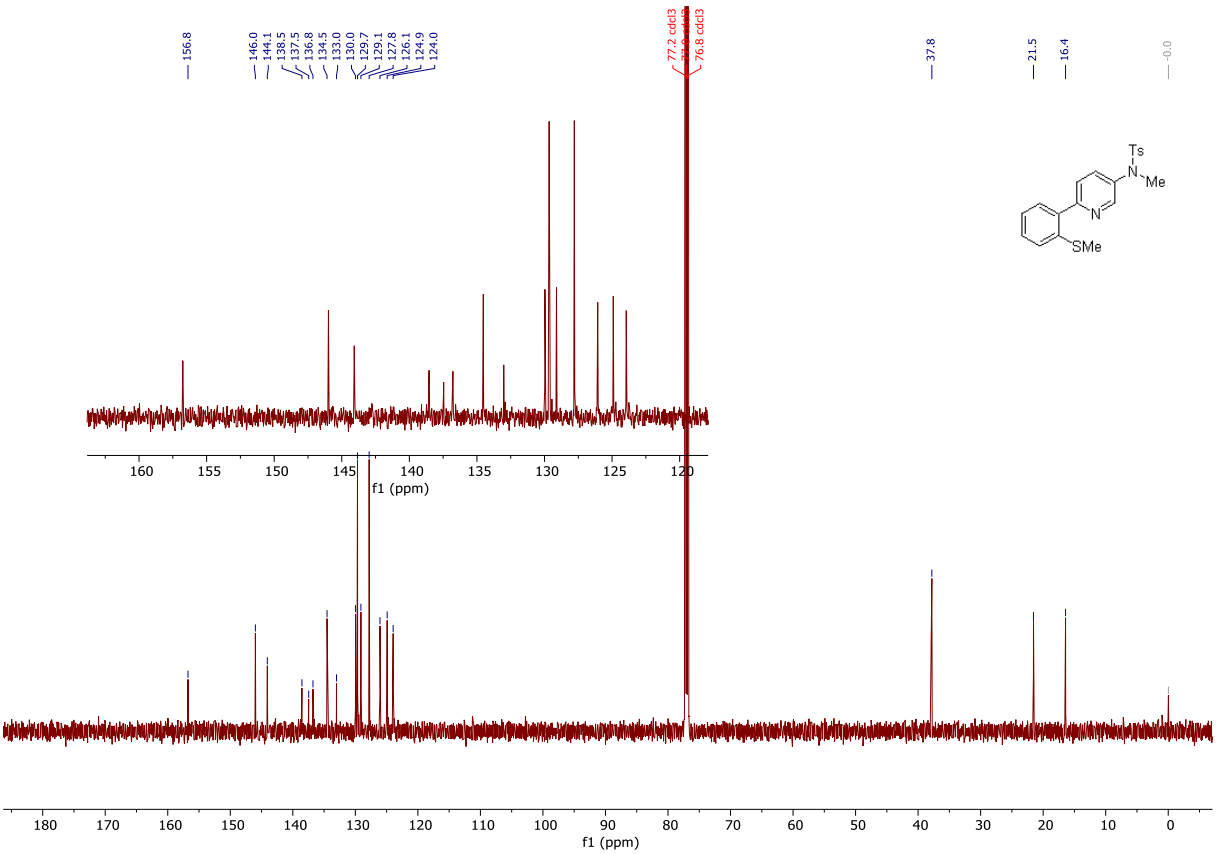

^{1}H NMR spectrum of compound 9a ($CDCl_3$, 298 K)

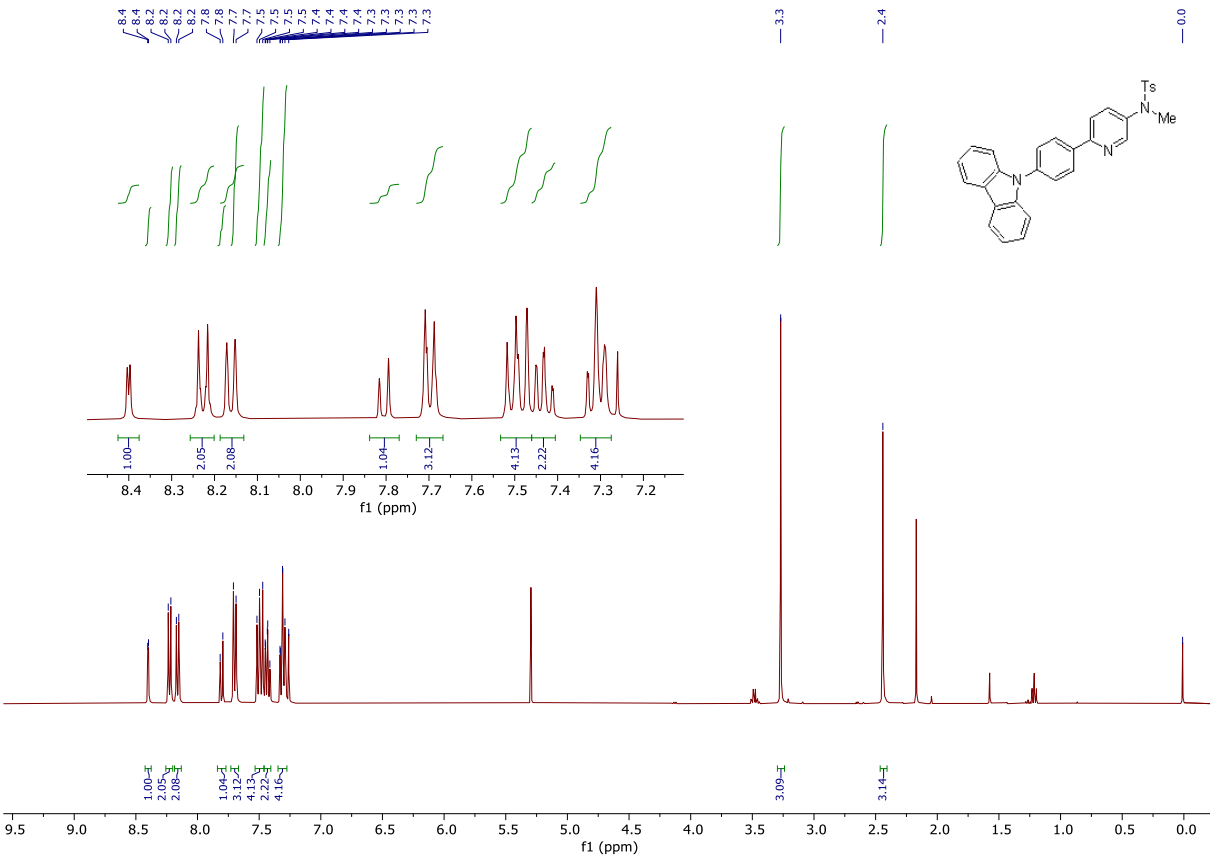

^{13}C NMR spectrum of compound 9a ($CDCl_3$, 298 K)

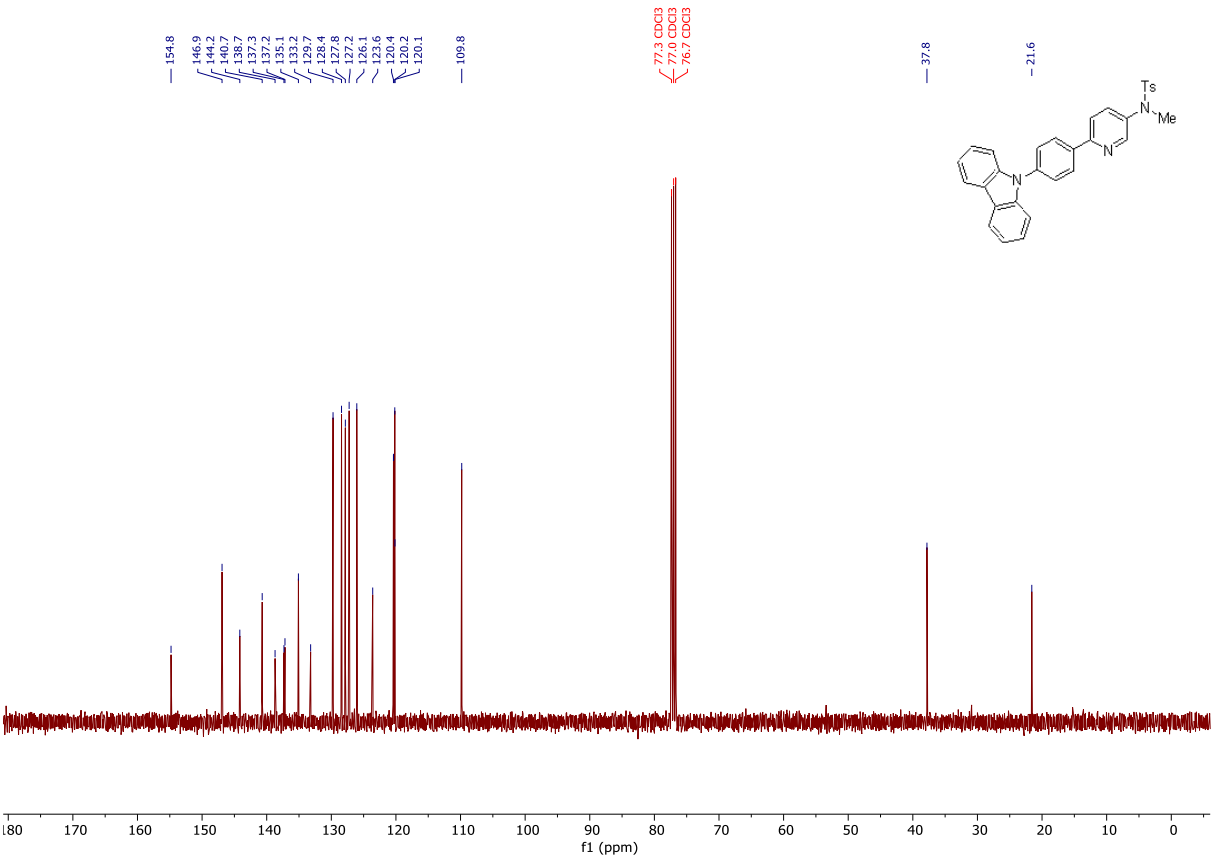

^{1}H NMR spectrum of compound 9b ($CDCl_3$, 298 K)

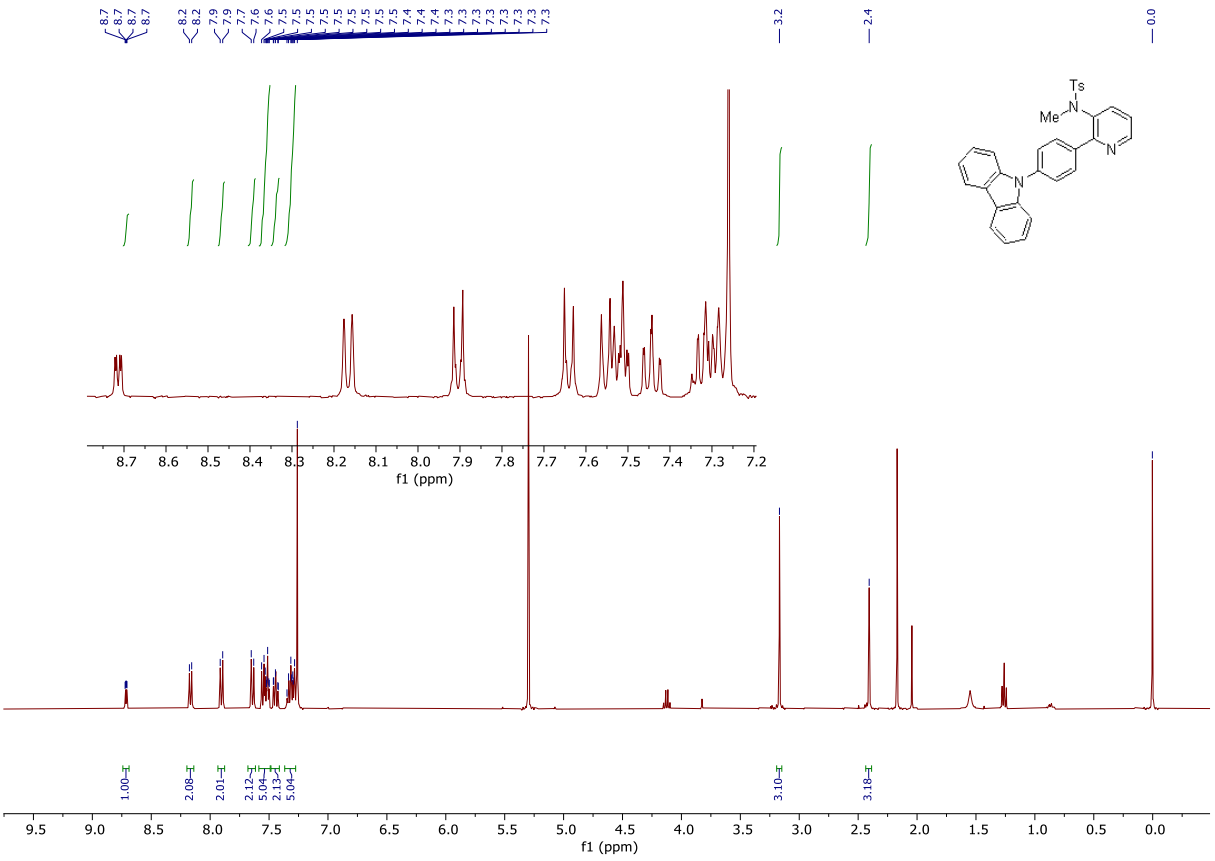

^{13}C NMR spectrum of compound 9b ($CDCl_3$, 298 K)

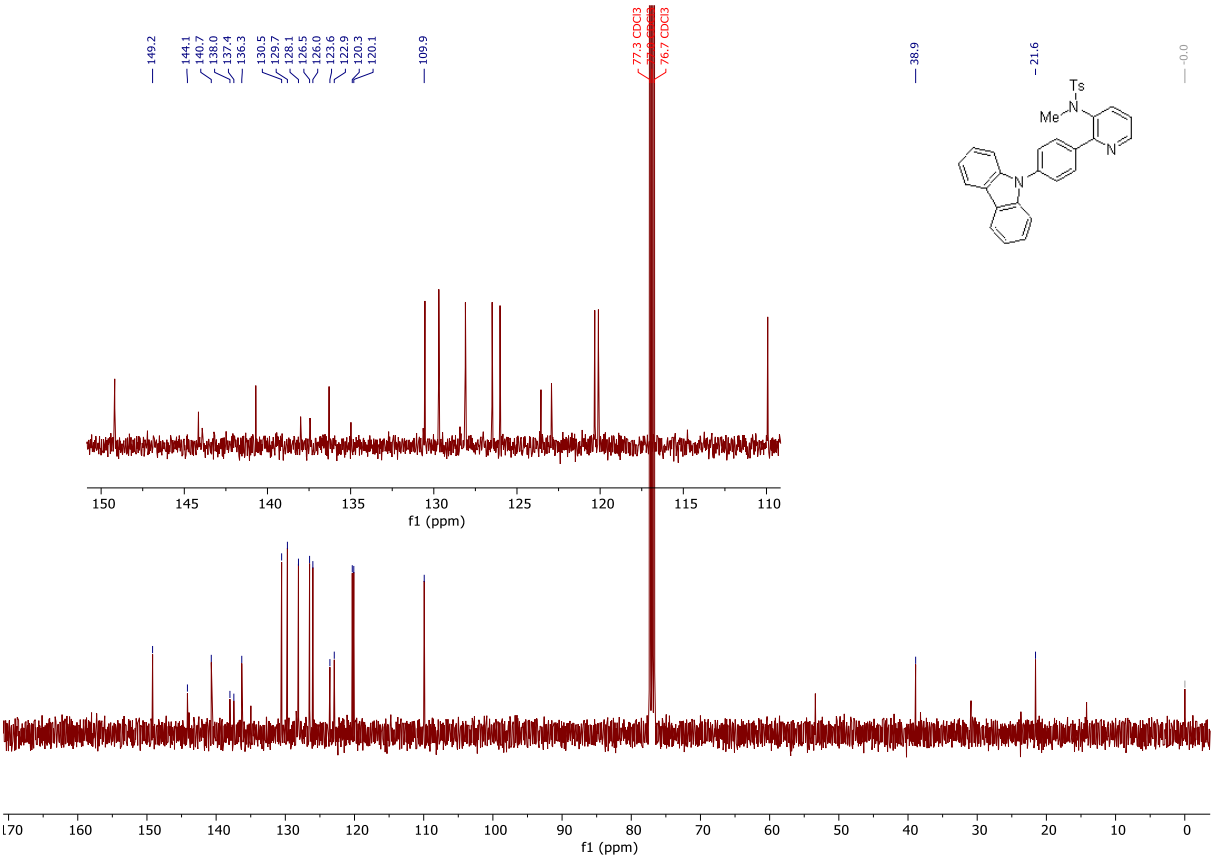

^{1}H NMR spectrum of compound 10a ($CDCl_3$, 298 K)

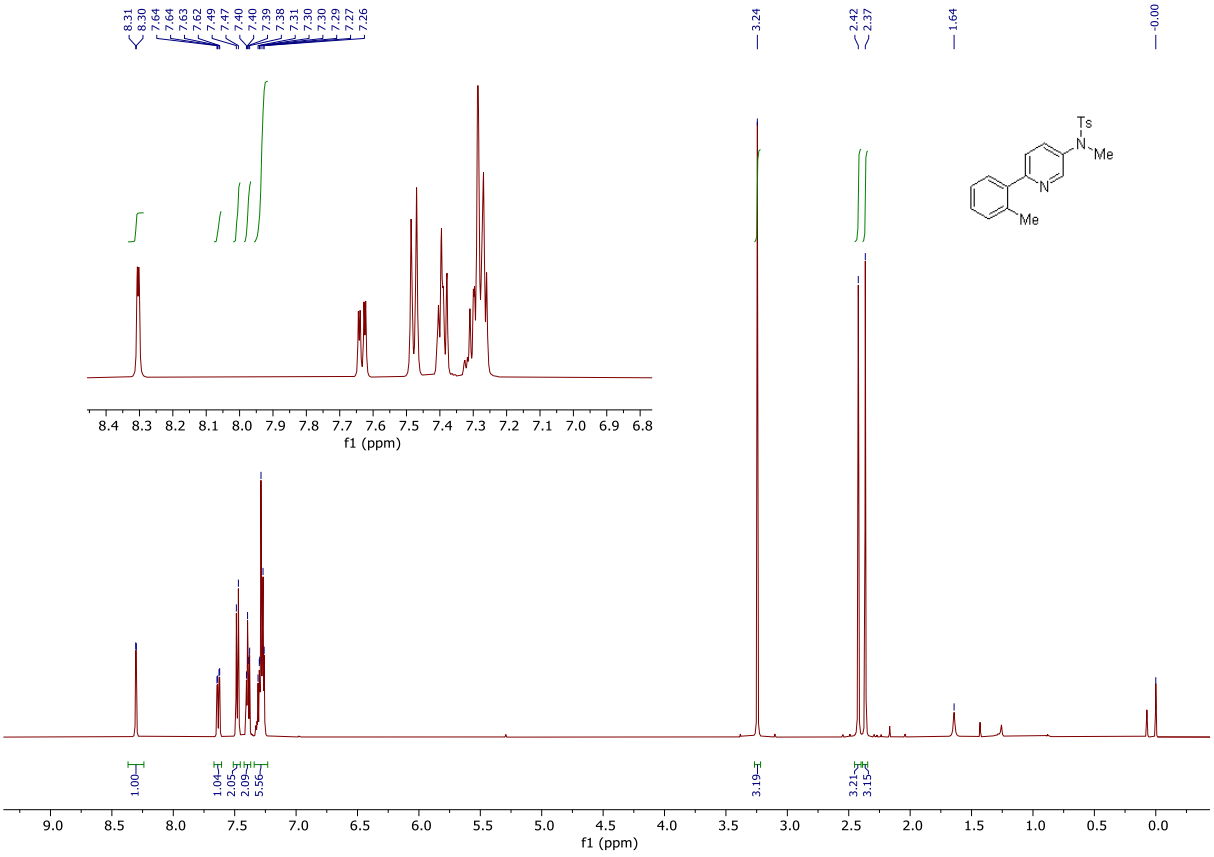

^{13}C NMR spectrum of compound 10a ($CDCl_3$, 298 K)

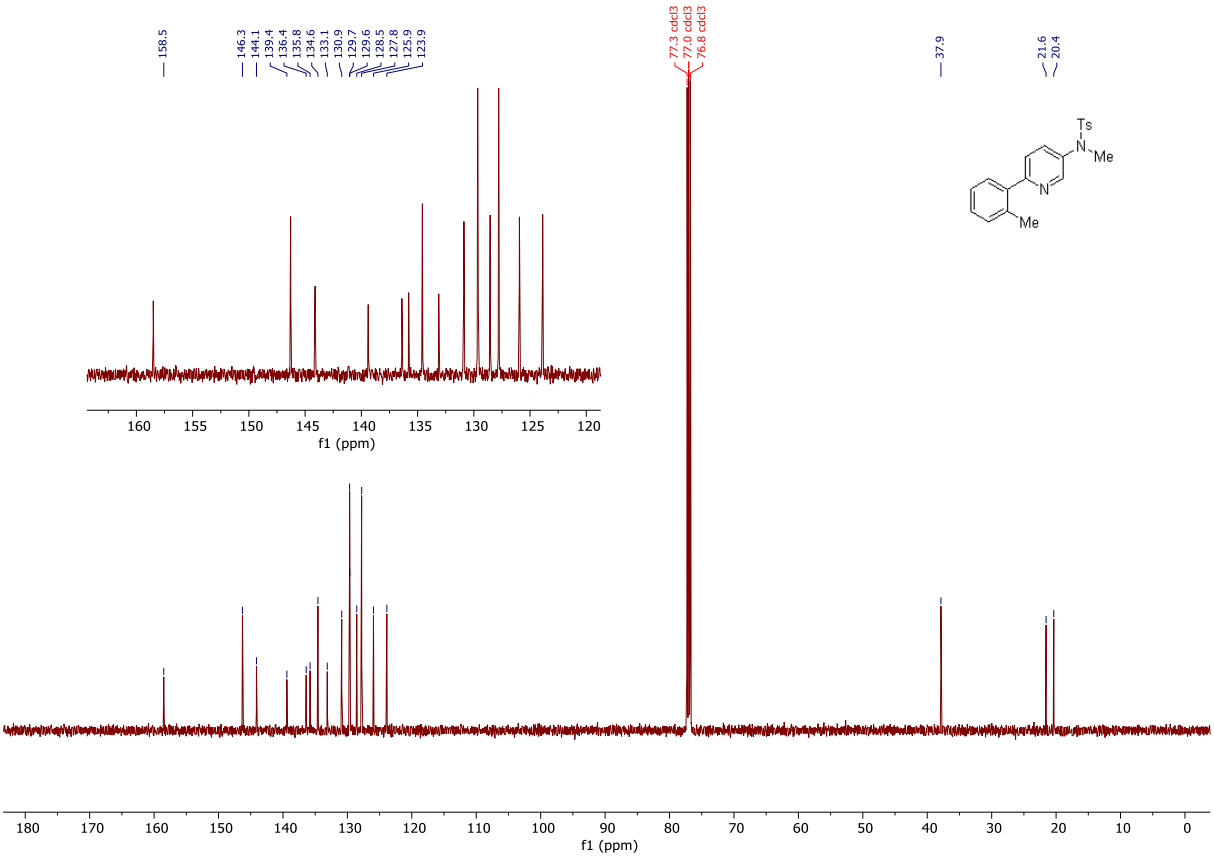

^{1}H NMR spectrum of compound 11a ($CDCl_3$, 298 K)

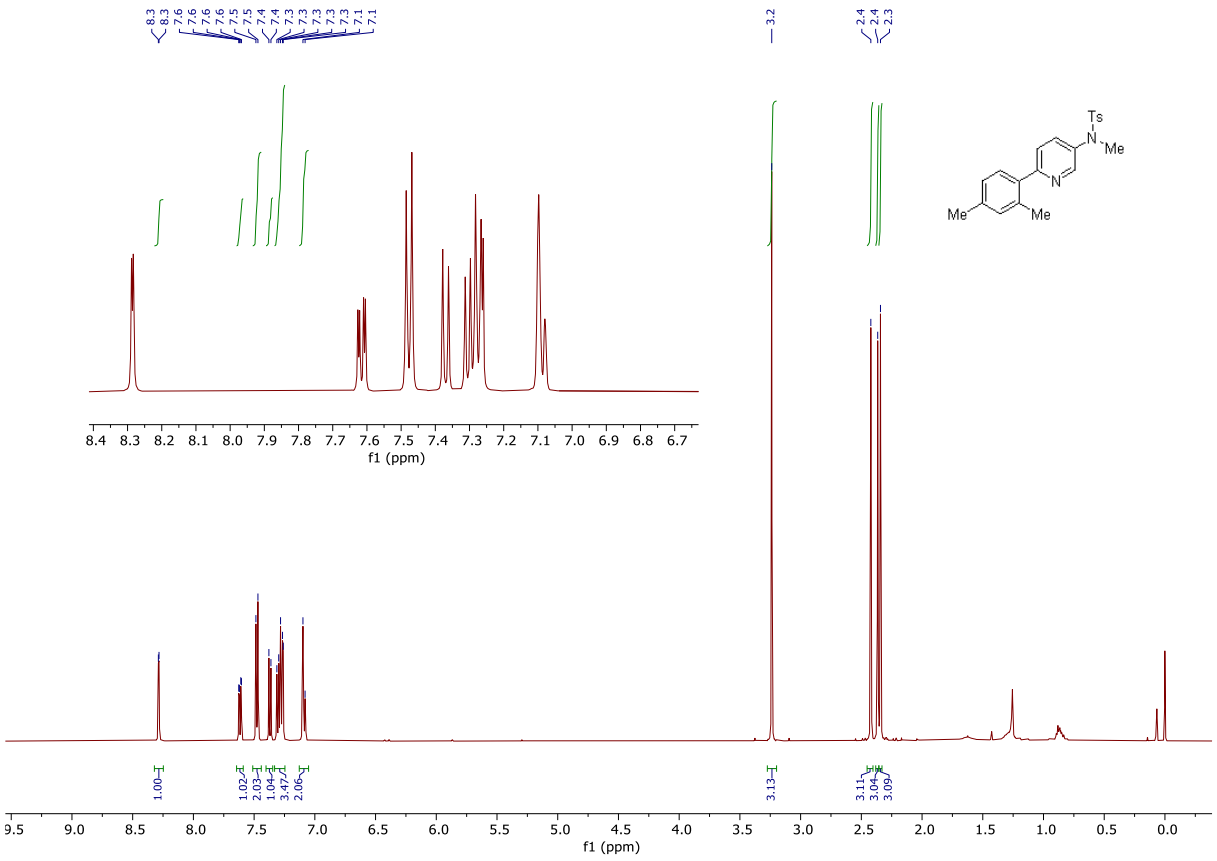

^{13}C NMR spectrum of compound 11a ($CDCl_3$, 298 K)

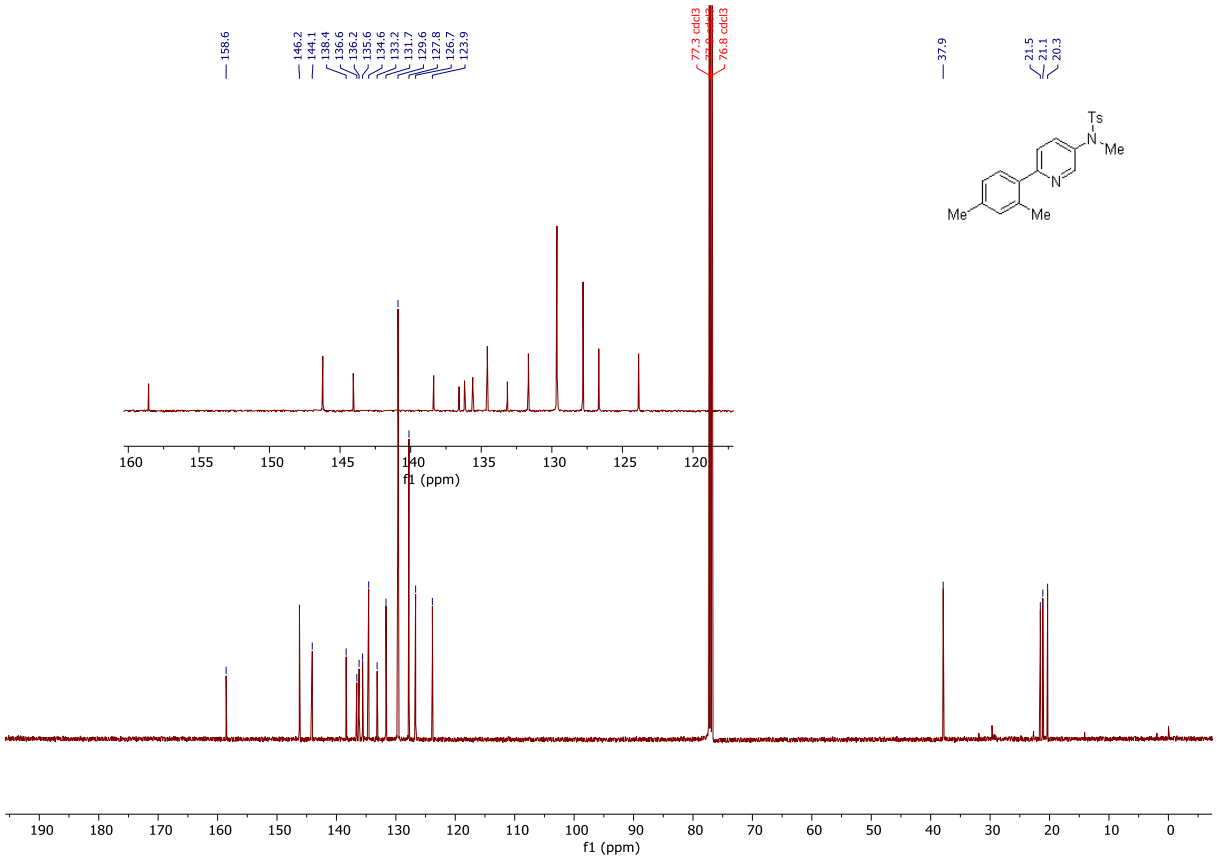

^{1}H NMR spectrum of compound 12a ($CDCl_3$, 298 K)

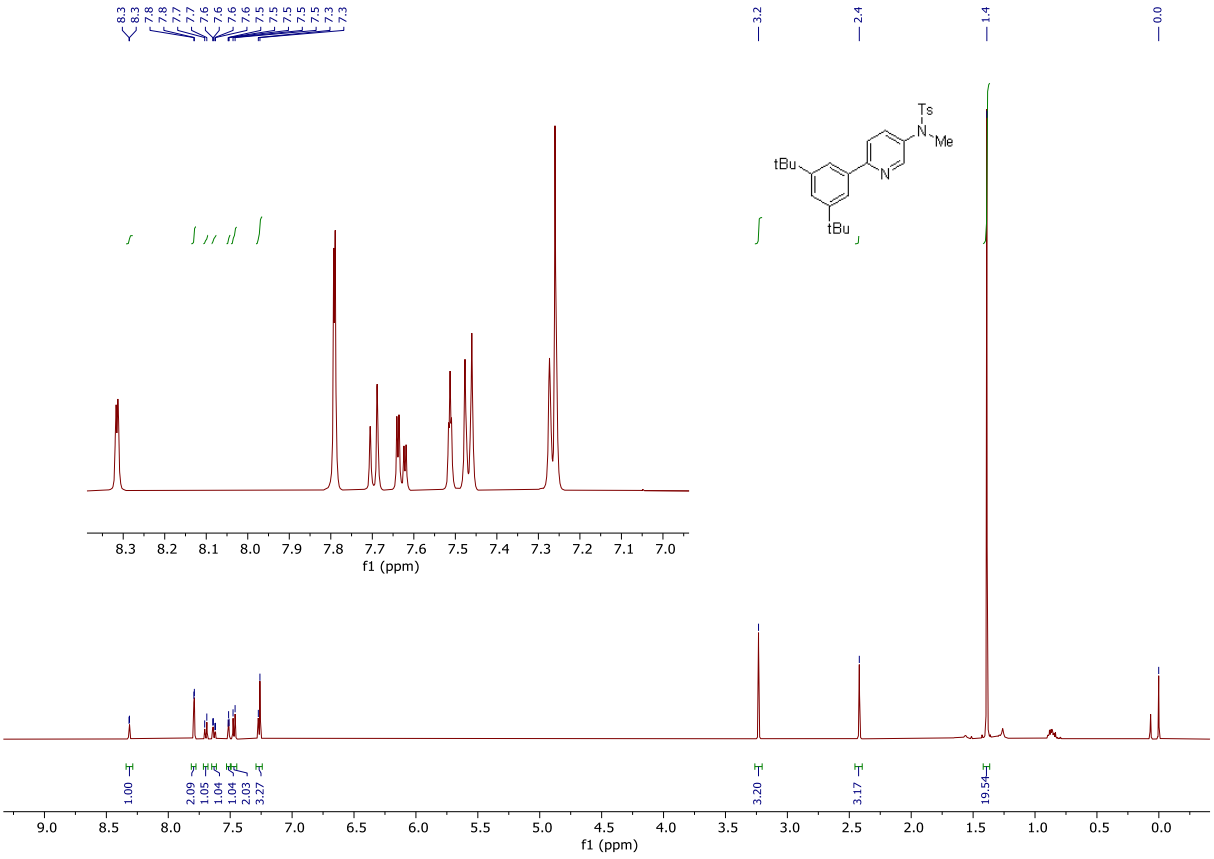

^{13}C NMR spectrum of compound 12a ($CDCl_3$, 298 K)

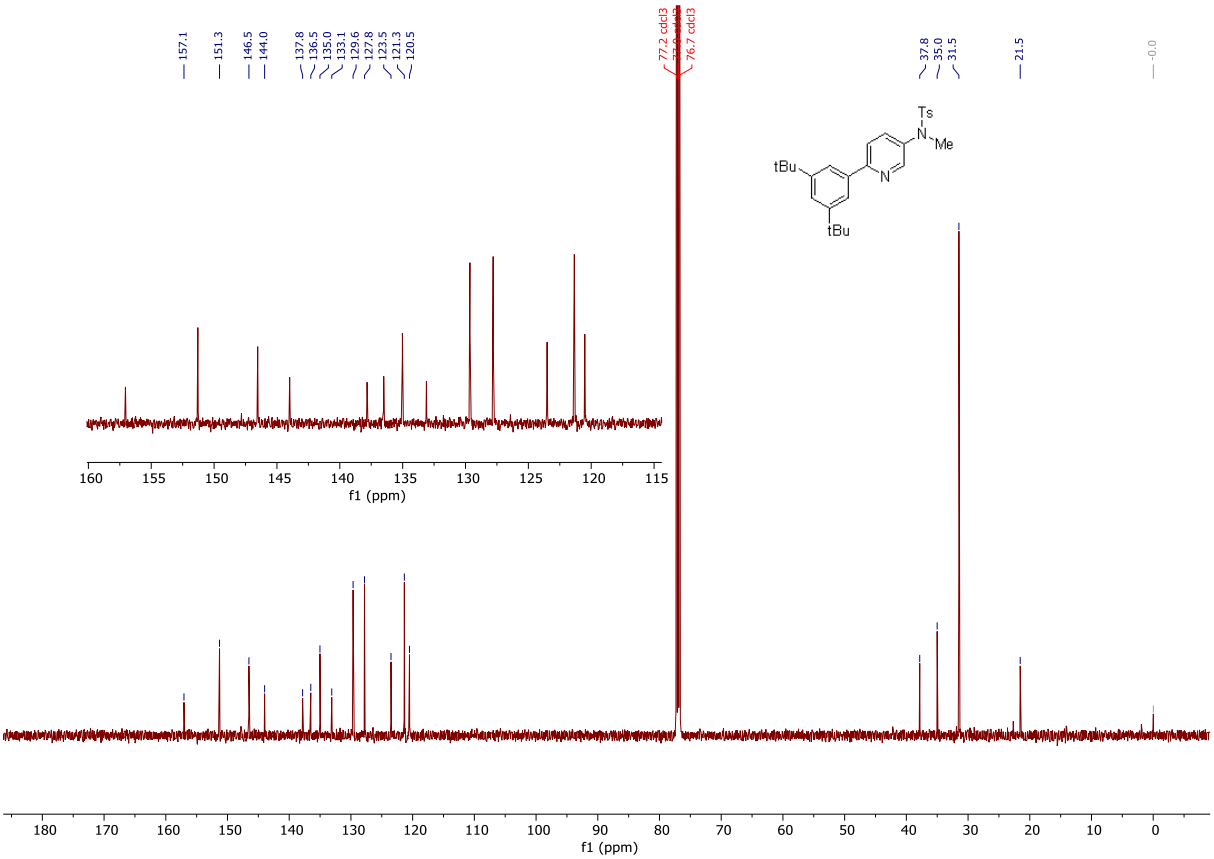

^{1}H NMR spectrum of compound 12b ($CDCl_3$, 298 K)

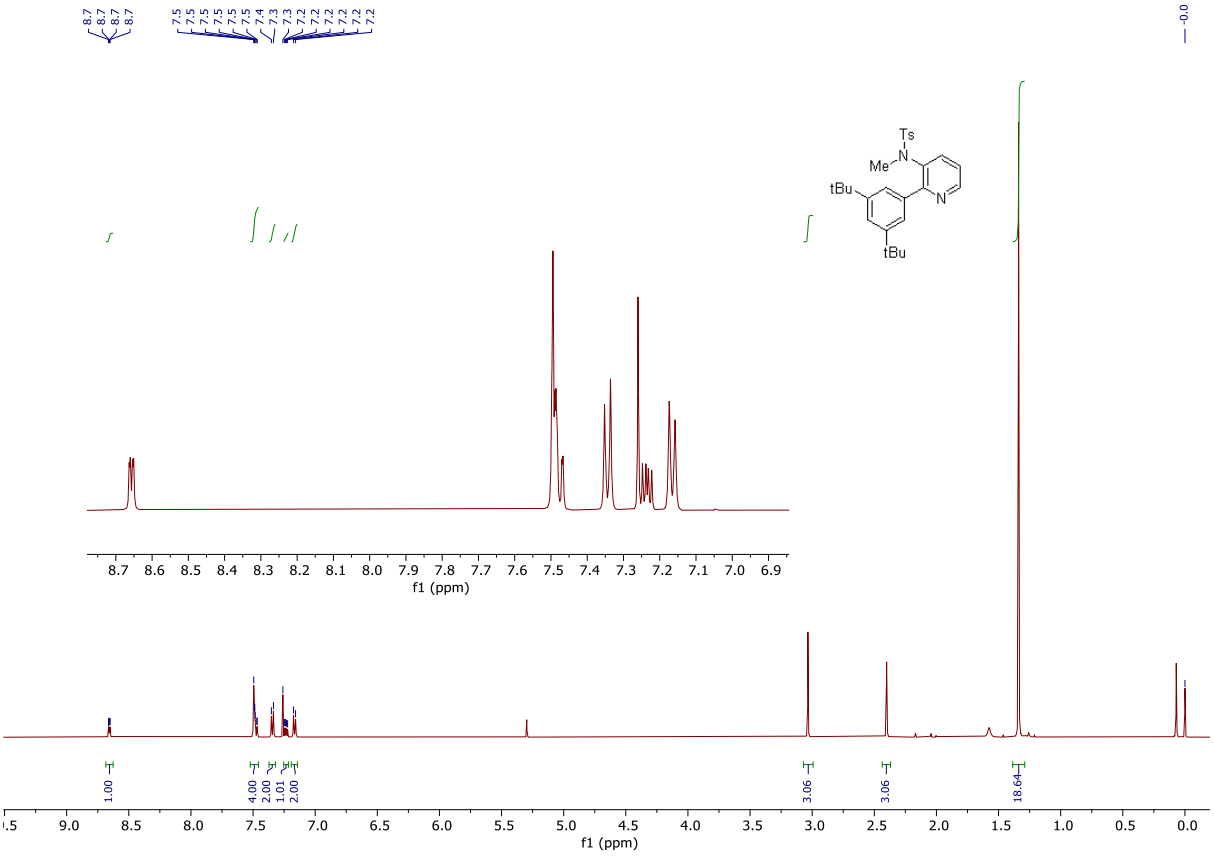

^{13}C NMR spectrum of compound 12b ($CDCl_3$, 298 K)

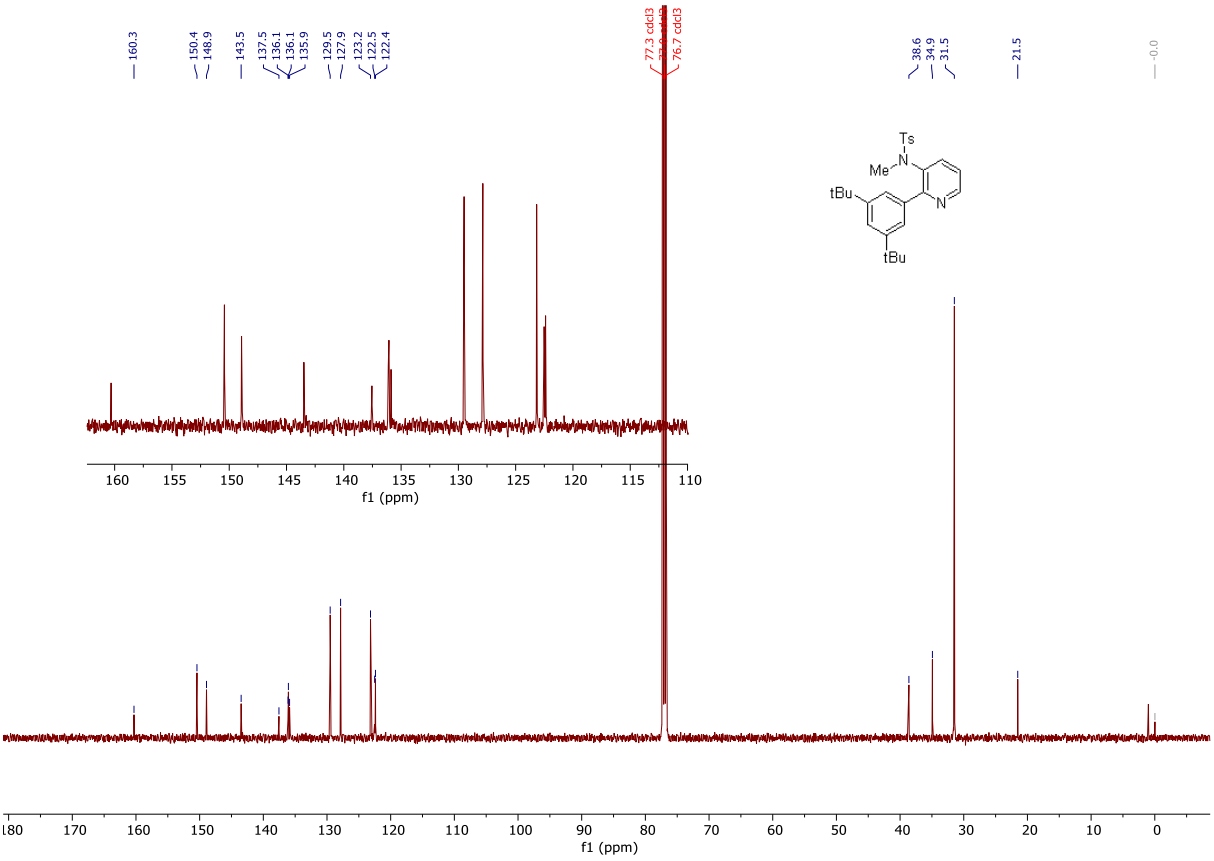

^{1}H NMR spectrum of compound 13a ($CDCl_3$, 298 K)

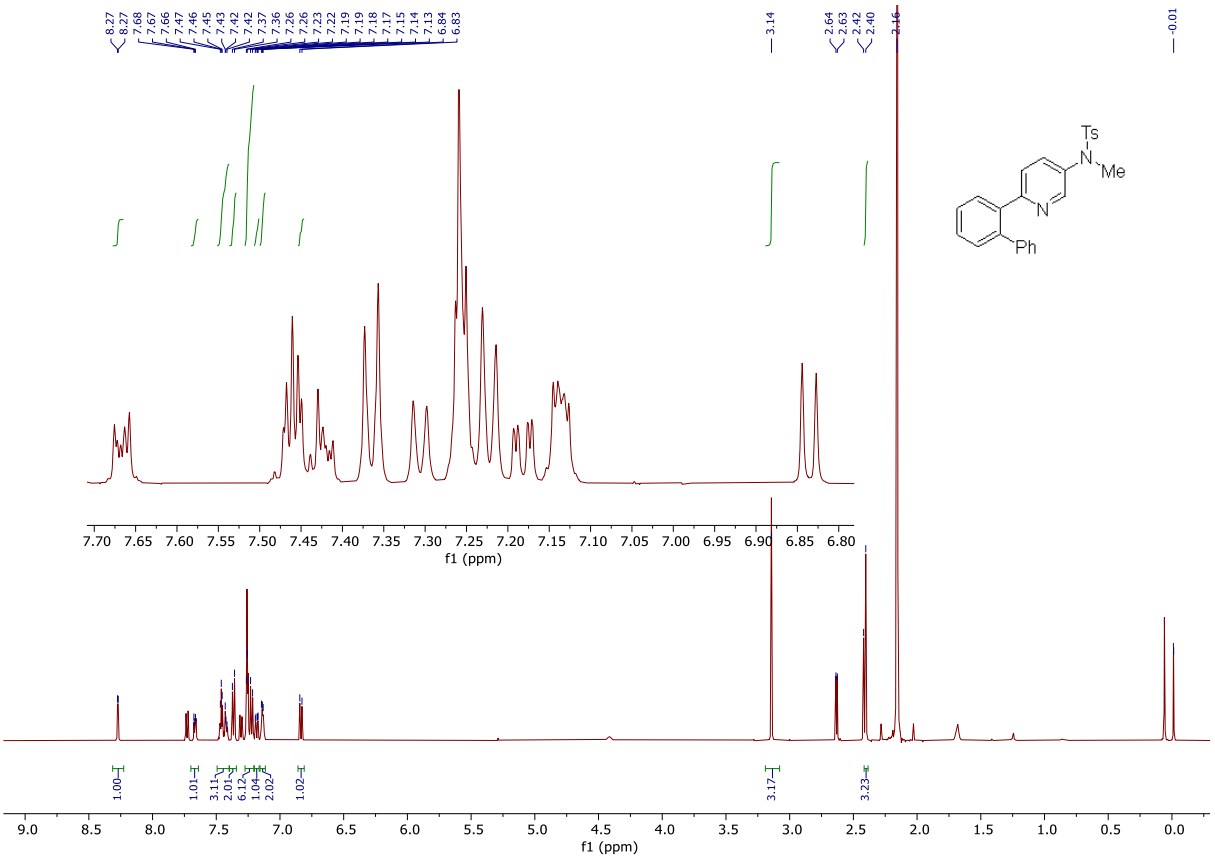

^{13}C NMR spectrum of compound 13a ($CDCl_3$, 298 K)

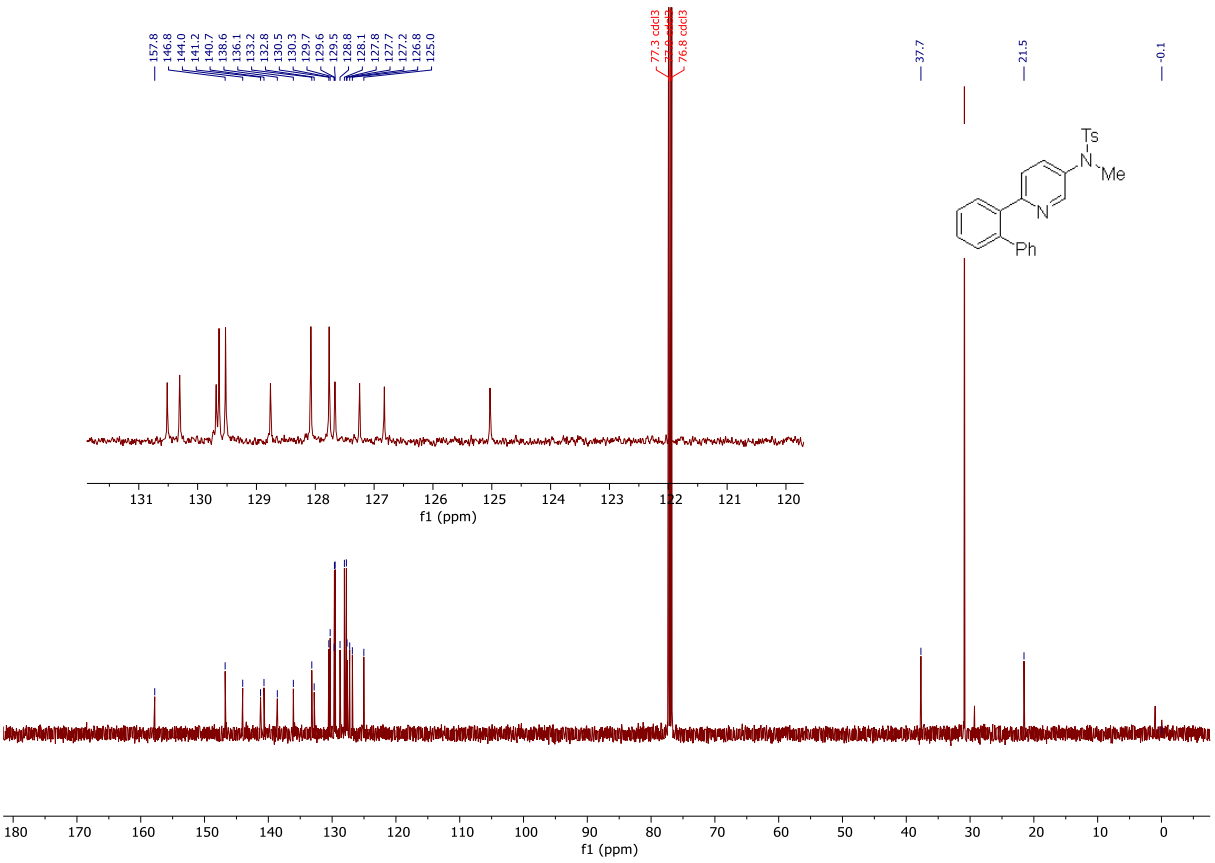

^{1}H NMR spectrum of compound 14a ($CDCl_3$, 298 K)

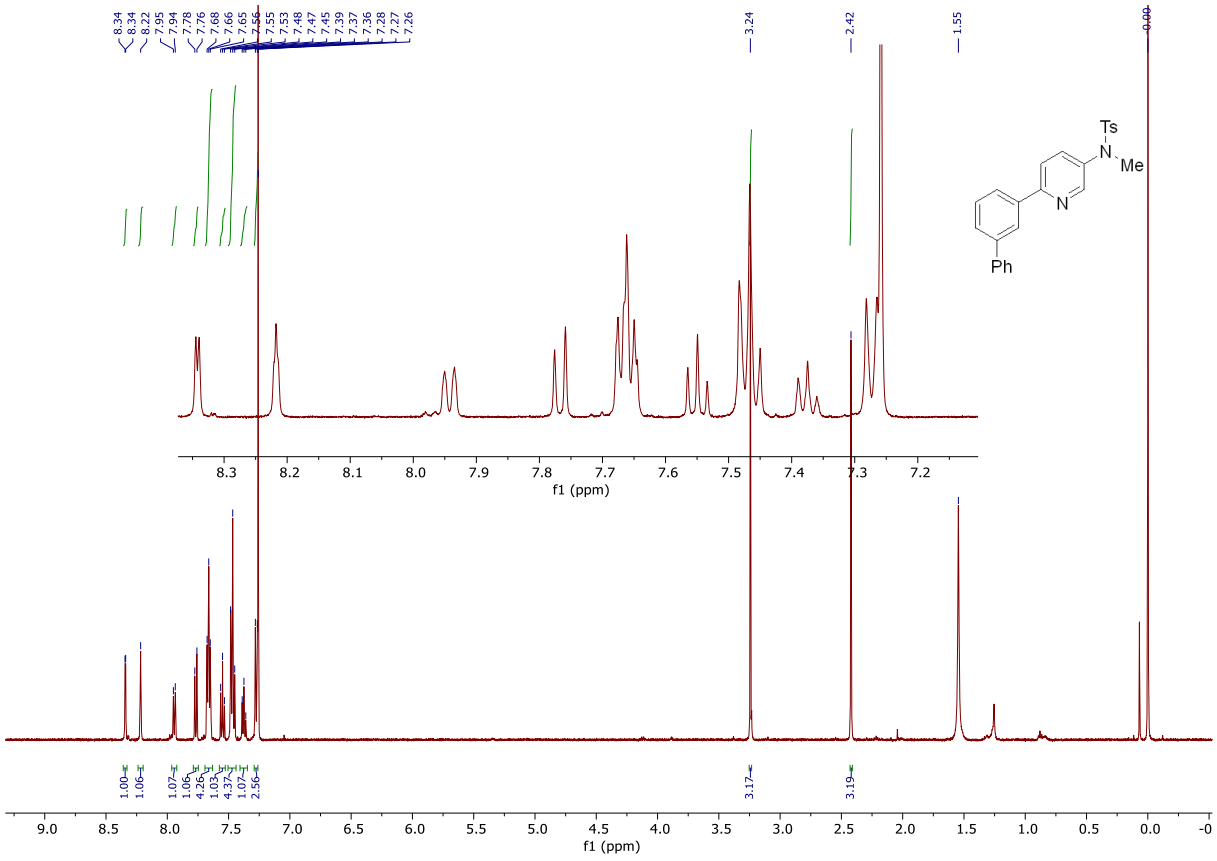

^{13}C NMR spectrum of compound 14a ($CDCl_3$, 298 K)

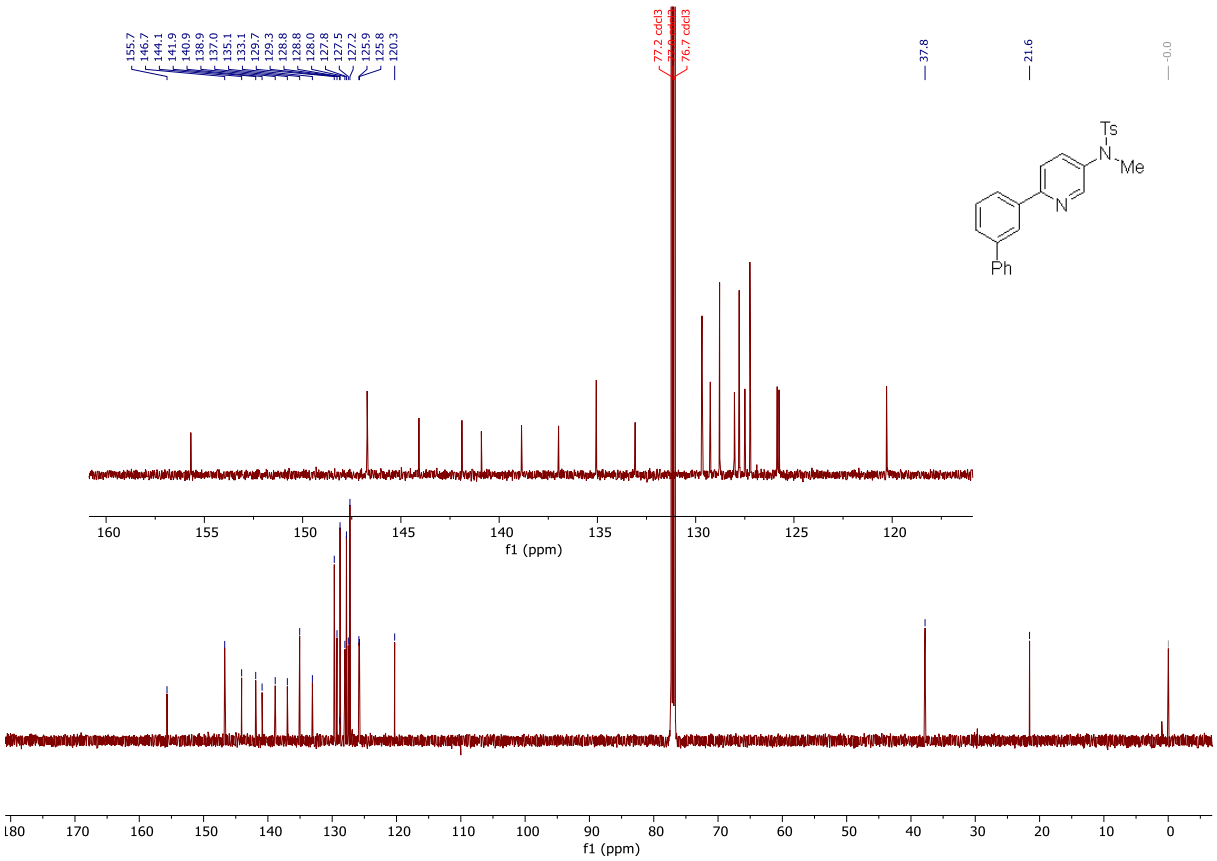

^{1}H NMR spectrum of compound 14b ($CDCl_3$, 298 K)

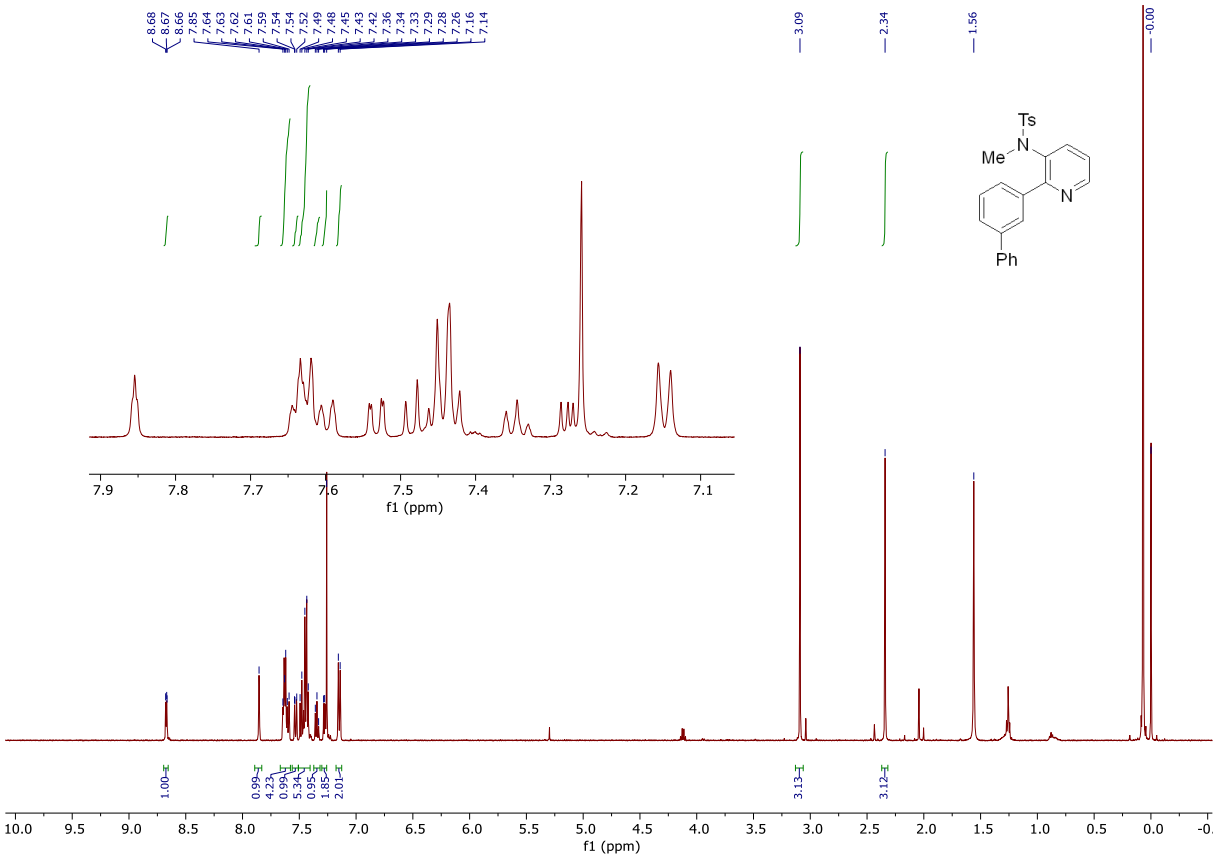

^{13}C NMR spectrum of compound 14b ($CDCl_3$, 298 K)

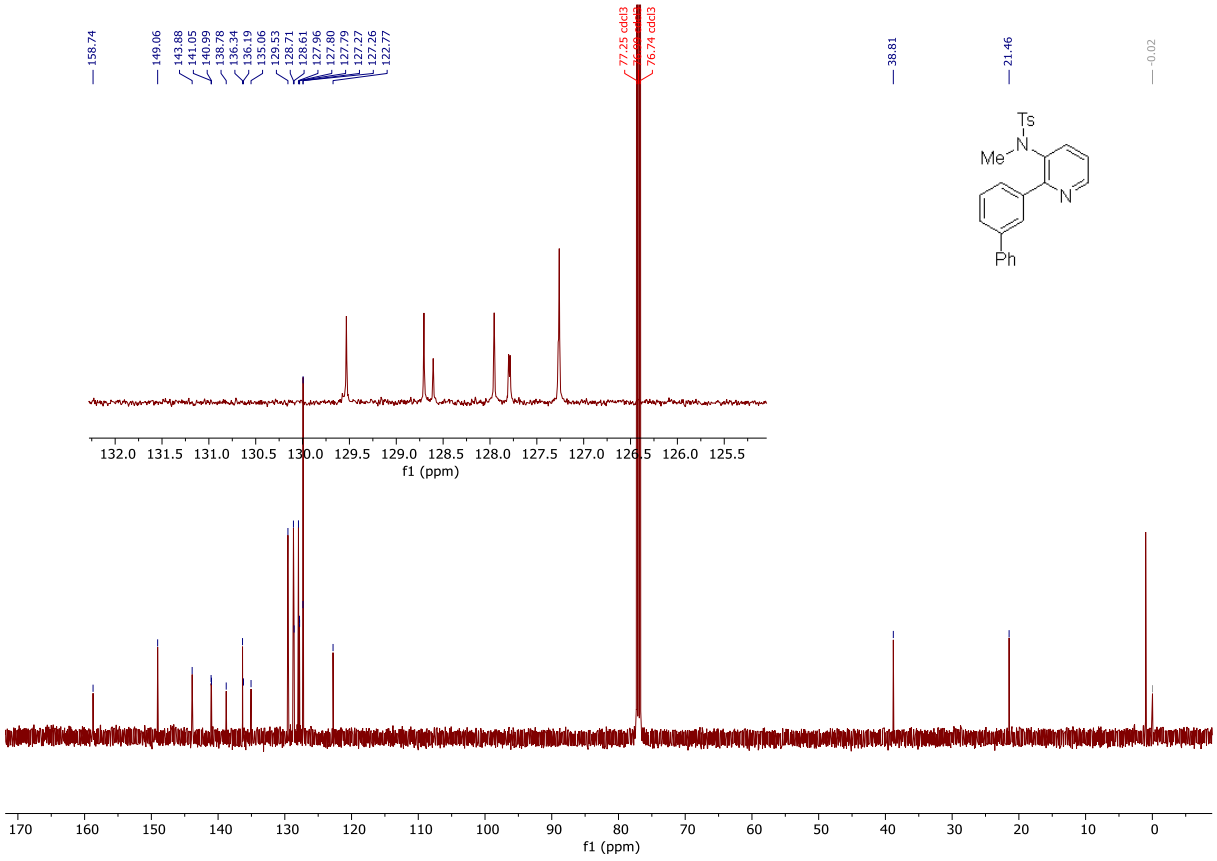

^{1}H NMR spectrum of compound 15a ($CDCl_3$, 298 K)

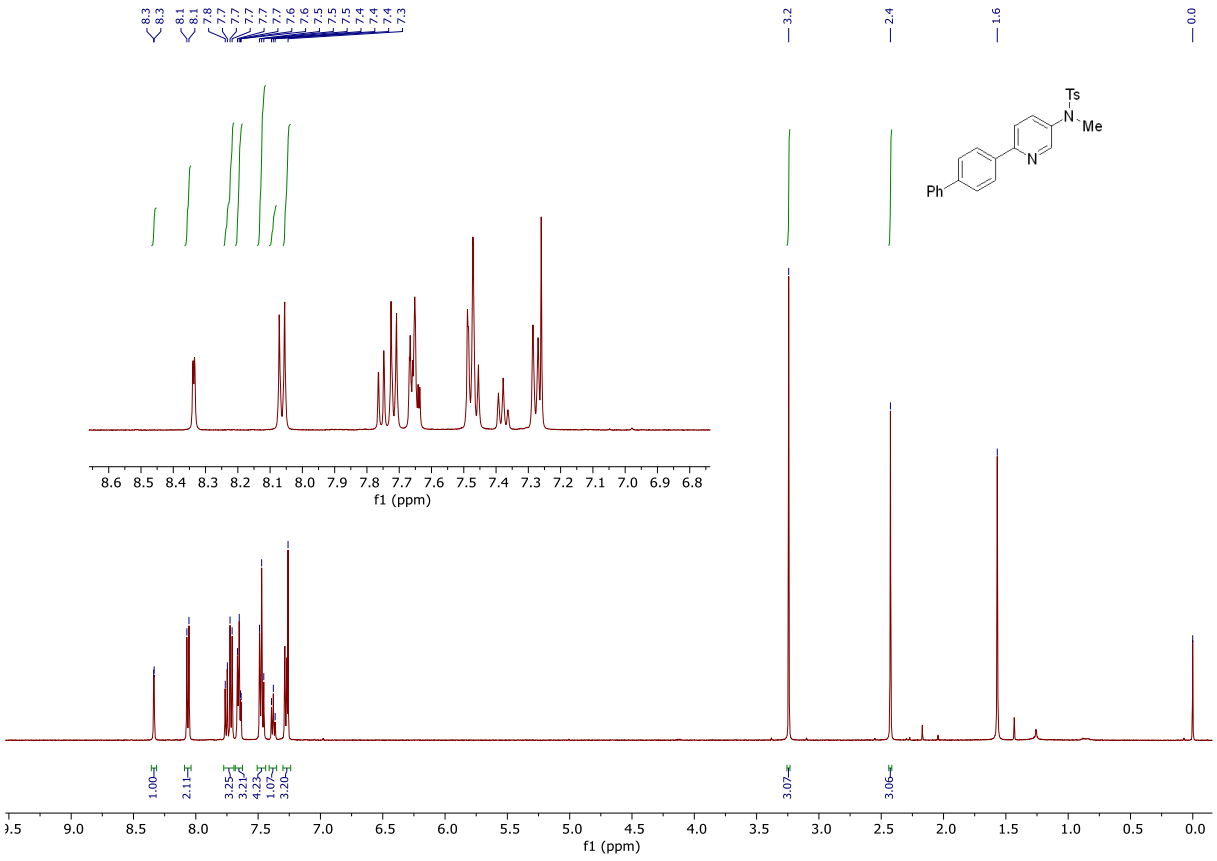

^{13}C NMR spectrum of compound 15a ($CDCl_3$, 298 K)

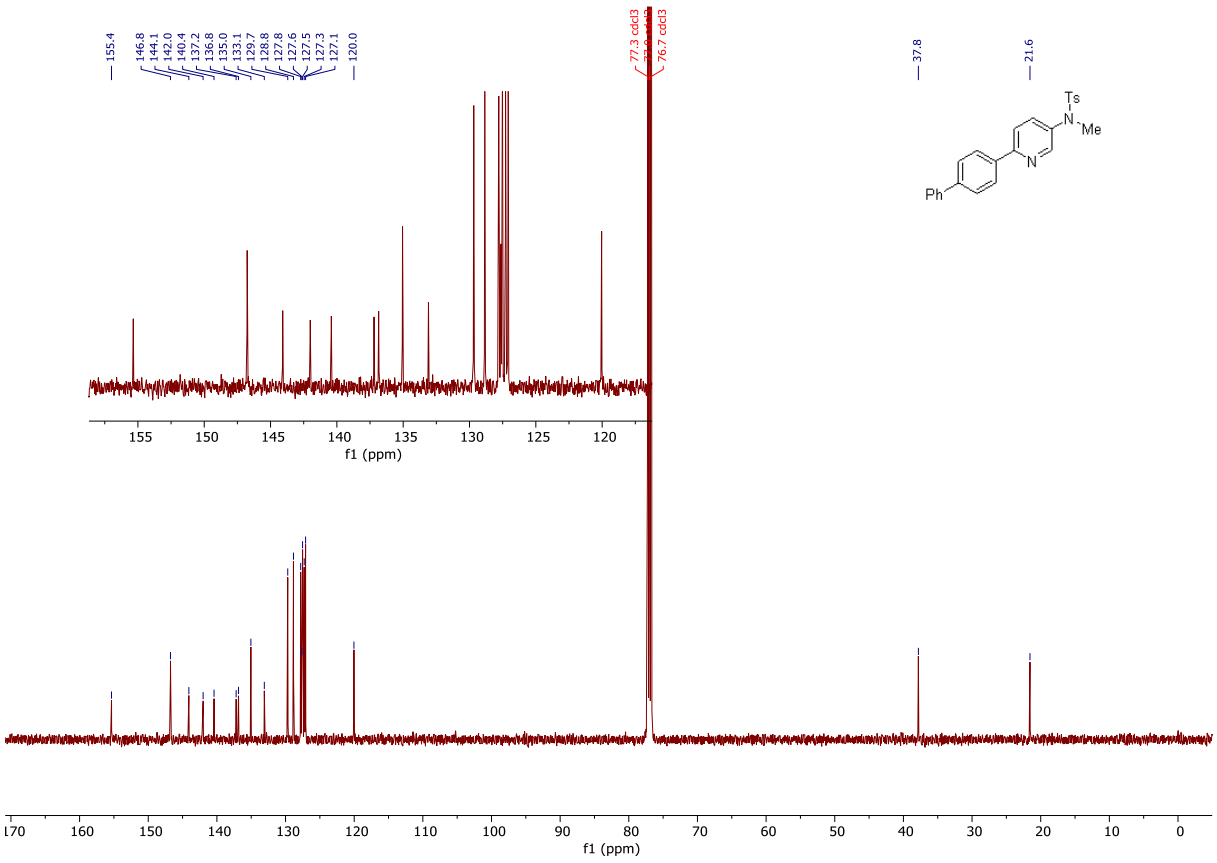

^{1}H NMR spectrum of compound 15b ($CDCl_3$, 298 K)

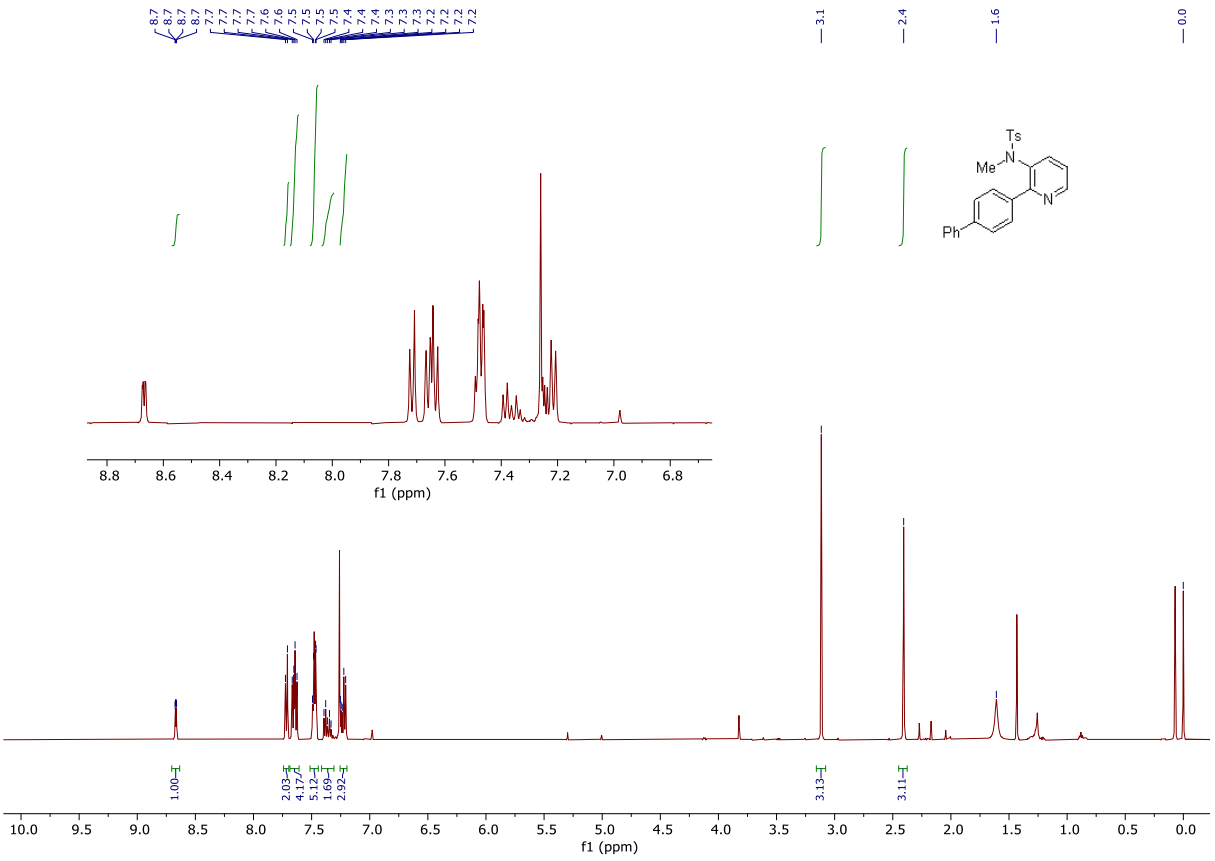

^{13}C NMR spectrum of compound 15b ($CDCl_3$, 298 K)

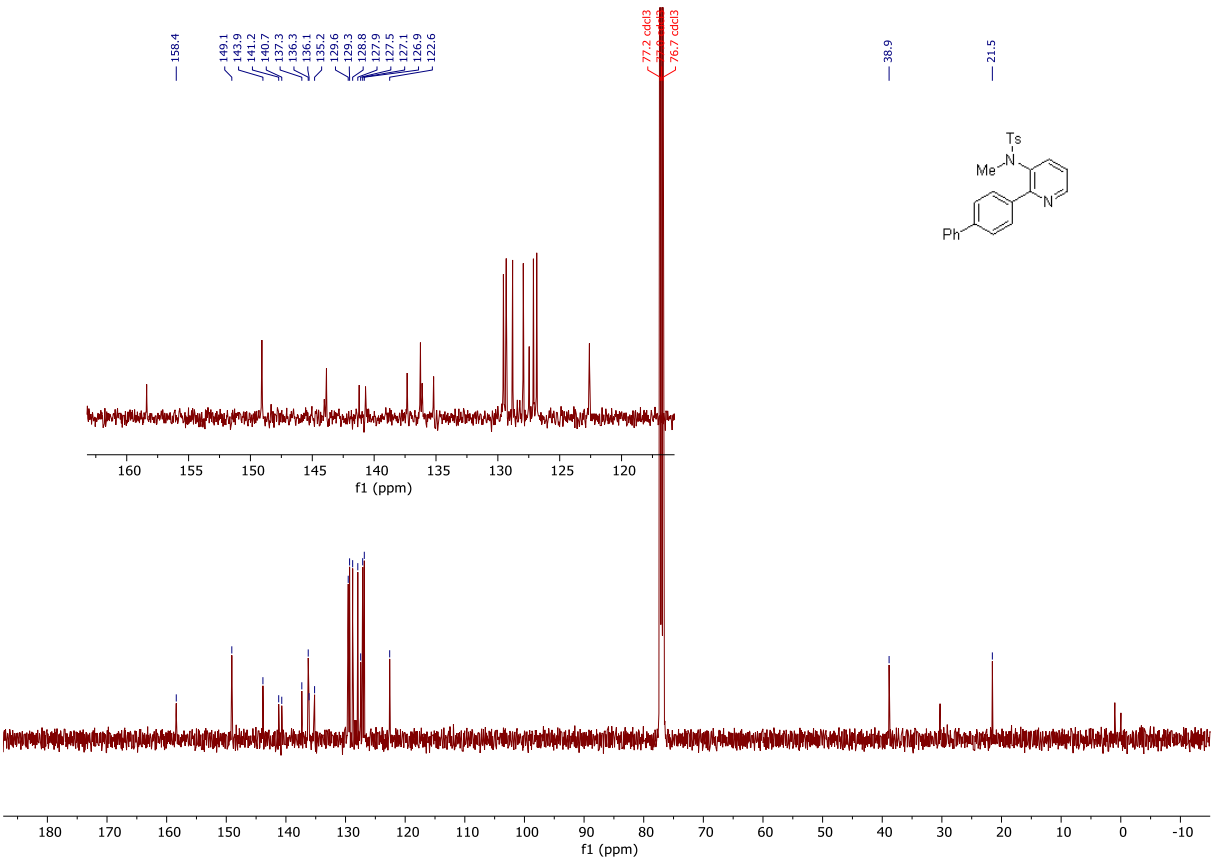

^{1}H NMR spectrum of compound 16a ($CDCl_3$, 298 K)

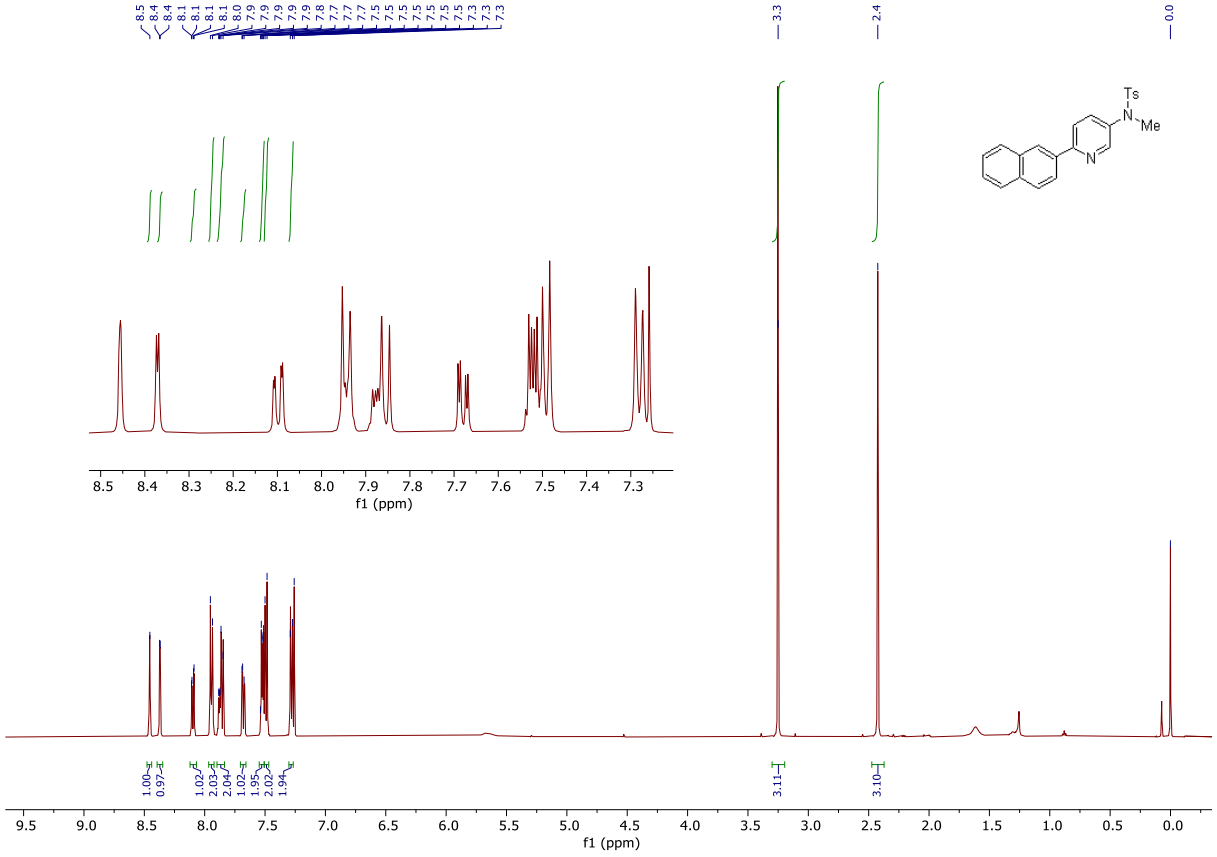

^{13}C NMR spectrum of compound 16a ($CDCl_3$, 298 K)

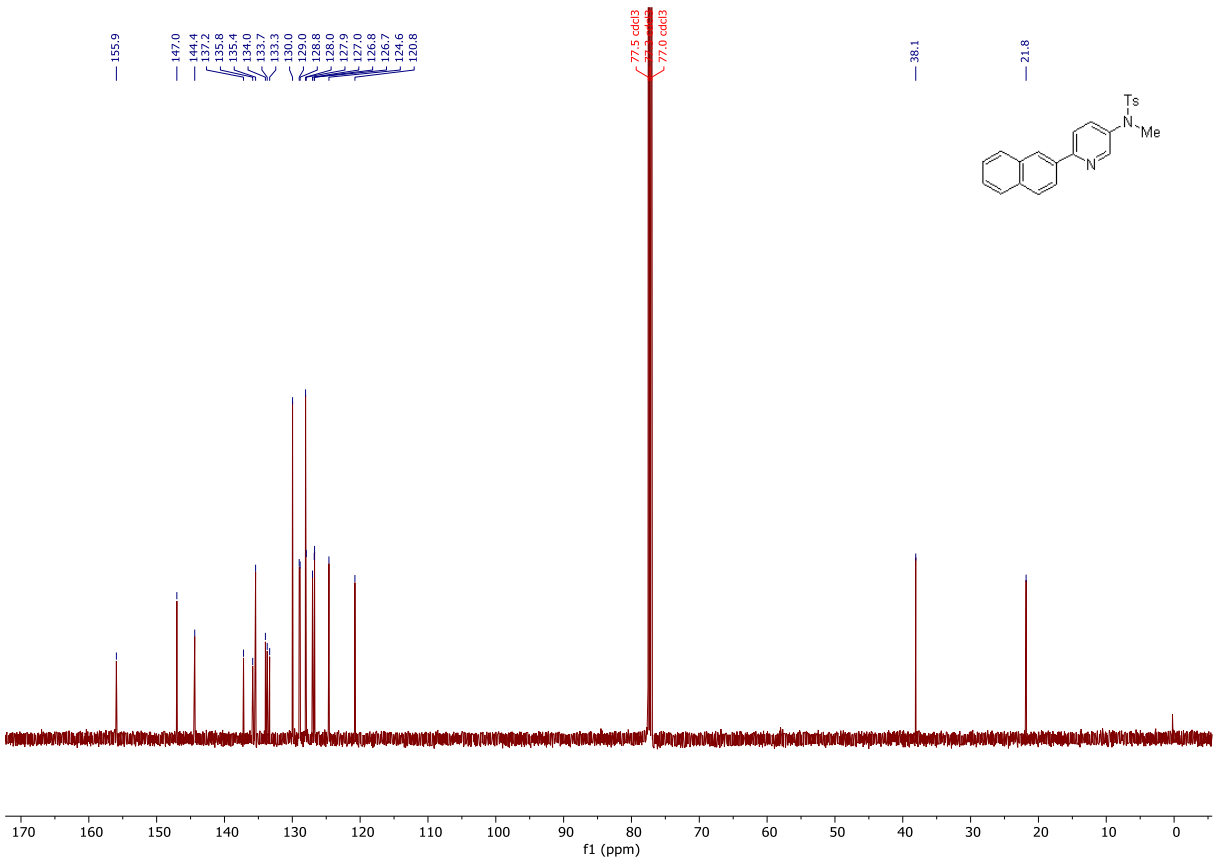

^{1}H NMR spectrum of compound 17a ($CDCl_3$, 298 K)

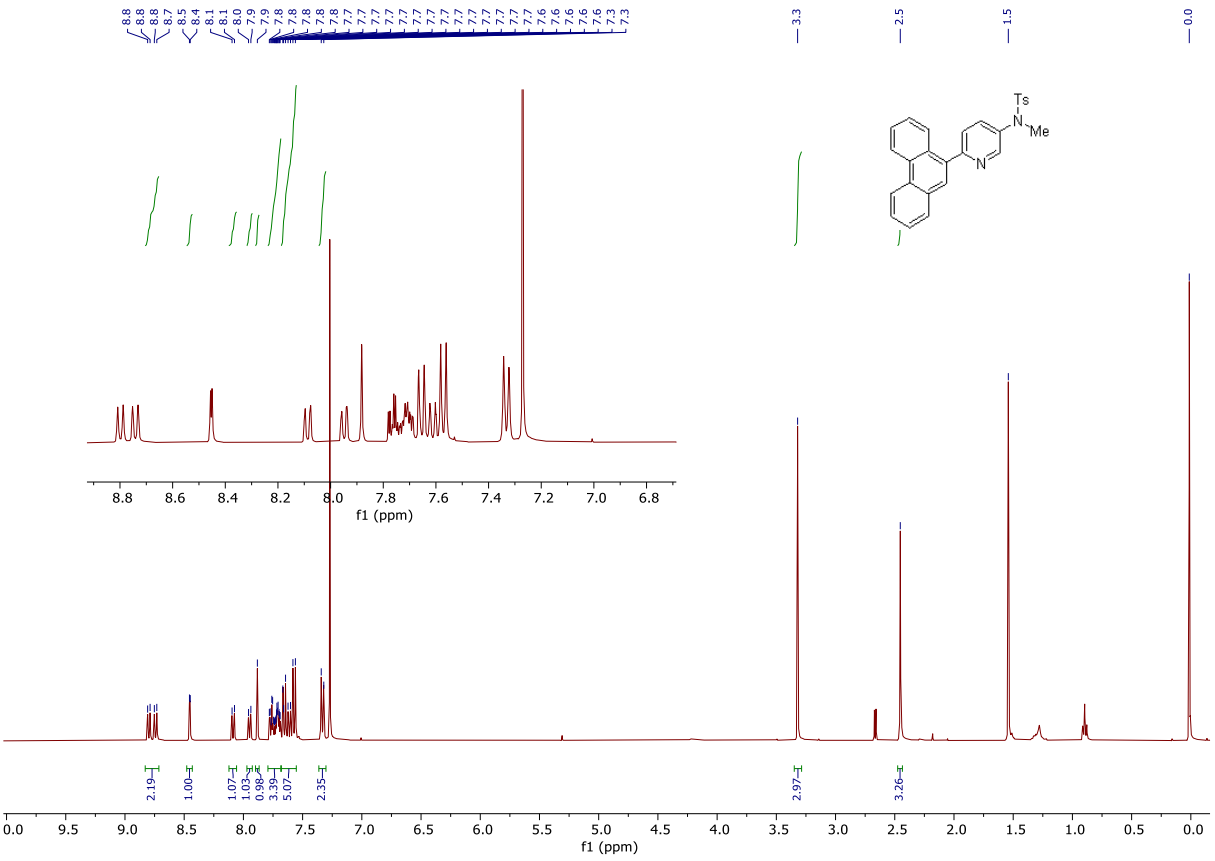

^{13}C NMR spectrum of compound 17a ($CDCl_3$, 298 K)

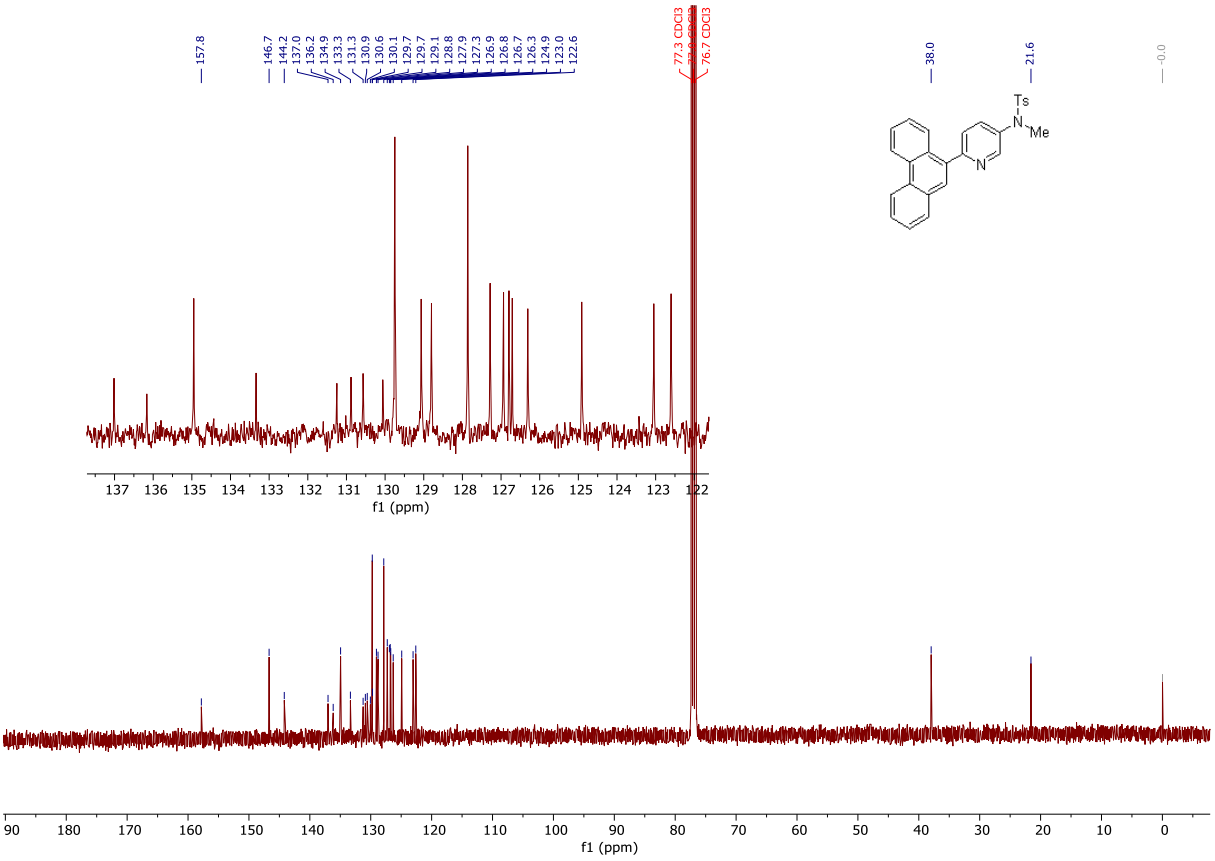

^{1}H NMR spectrum of compound 18a ($CDCl_3$, 298 K)

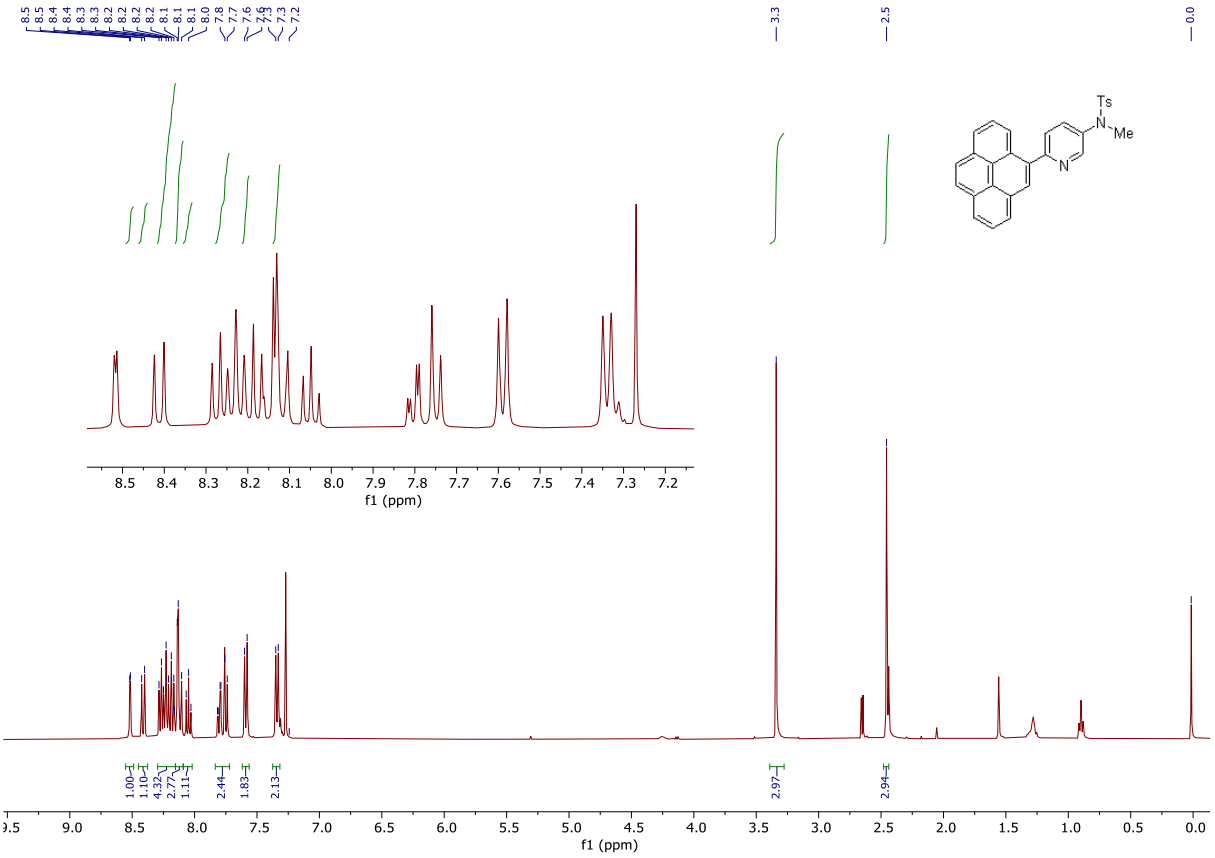

^{13}C NMR spectrum of compound 18a ($CDCl_3$, 298 K)

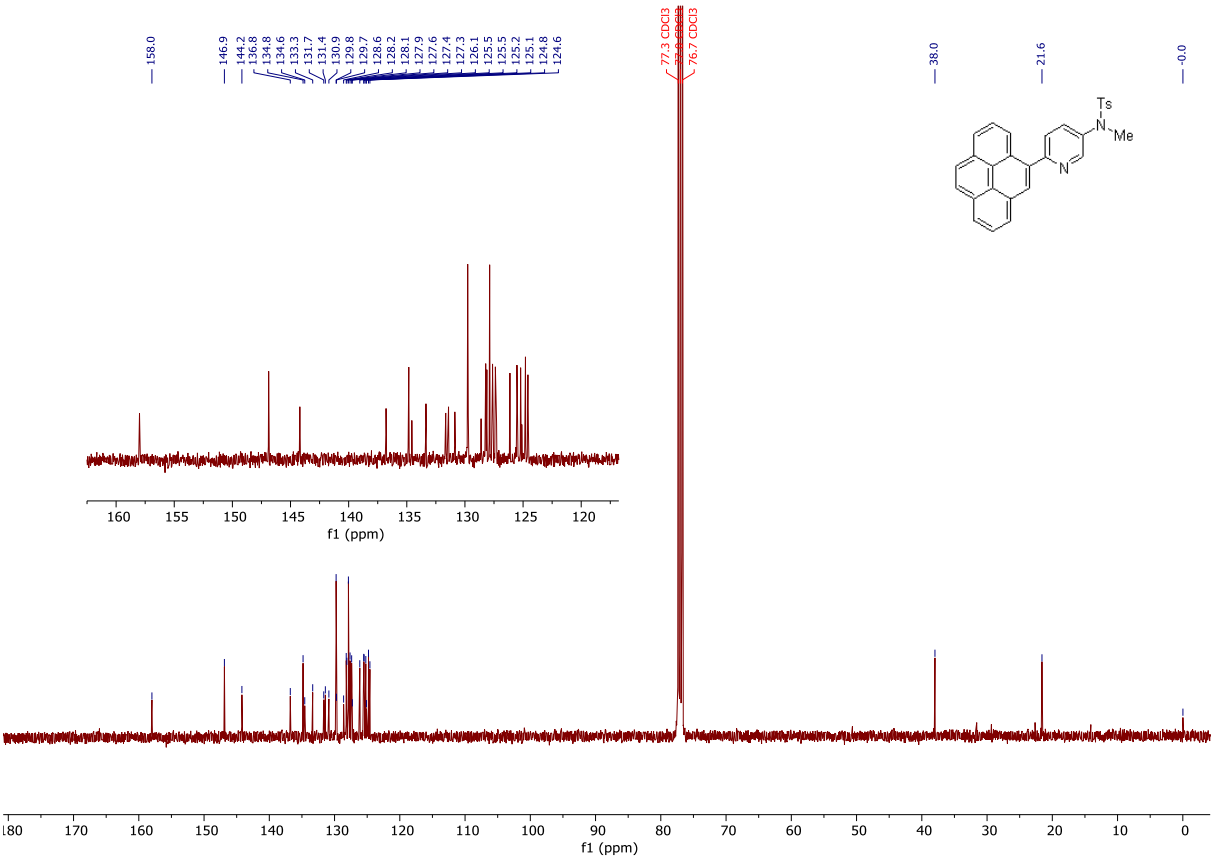

^{1}H NMR spectrum of compound 19a ($CDCl_3$, 298 K)

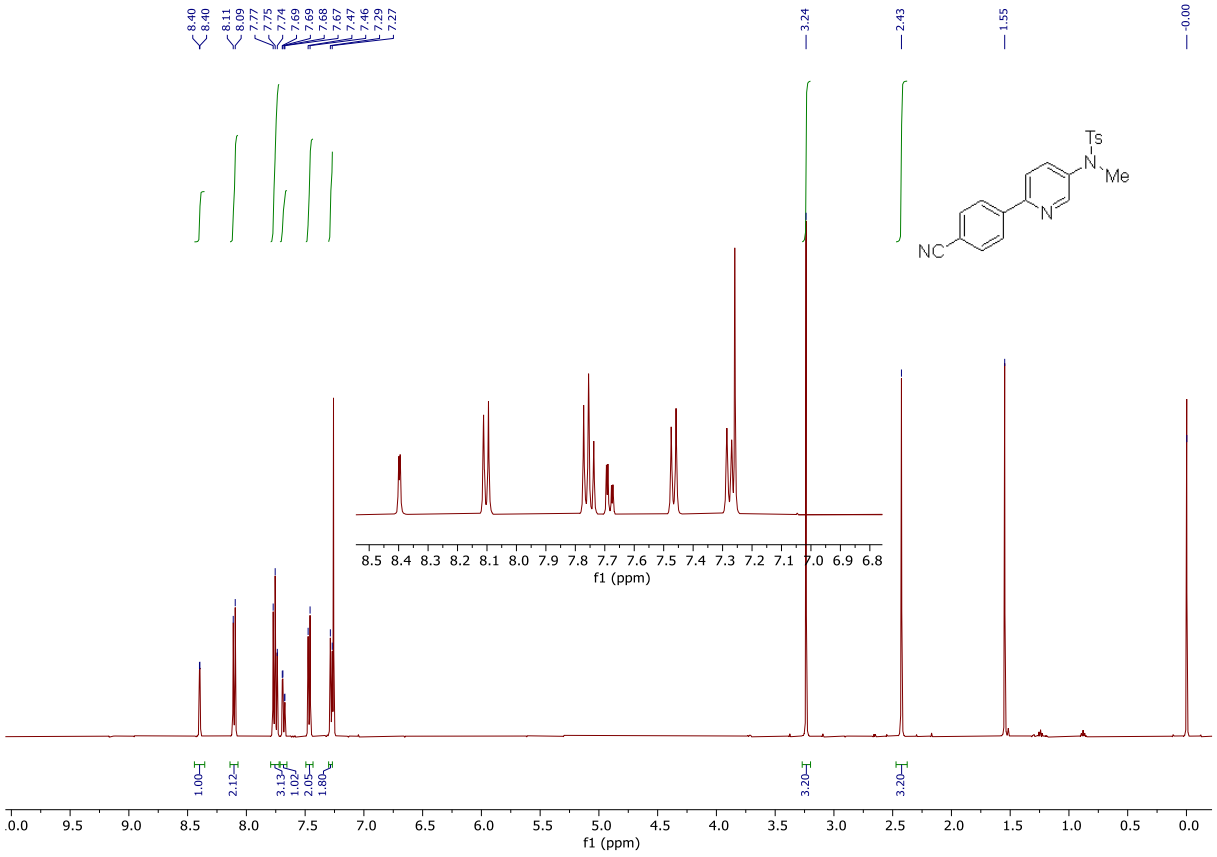

^{13}C NMR spectrum of compound 19a ($CDCl_3$, 298 K)

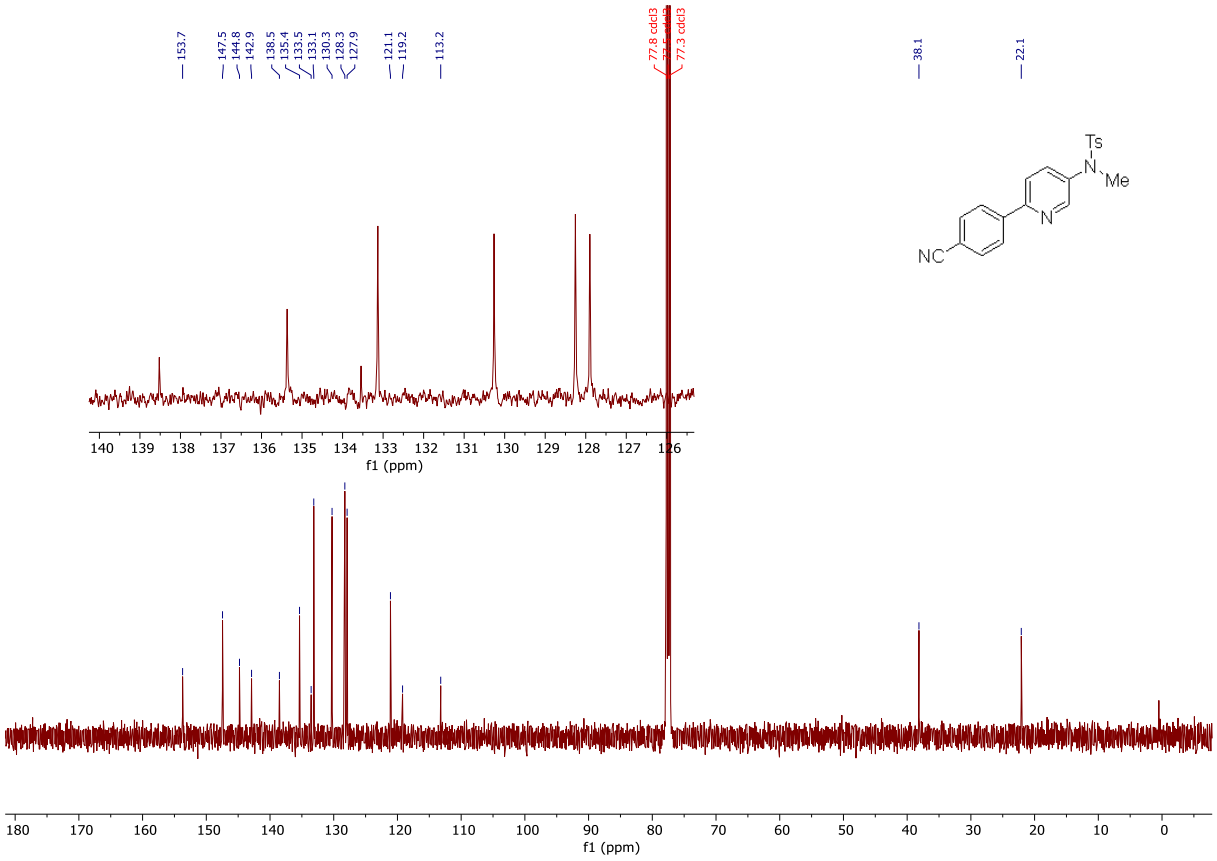

^{1}H NMR spectrum of compound 20a ($CDCl_3$, 298 K)

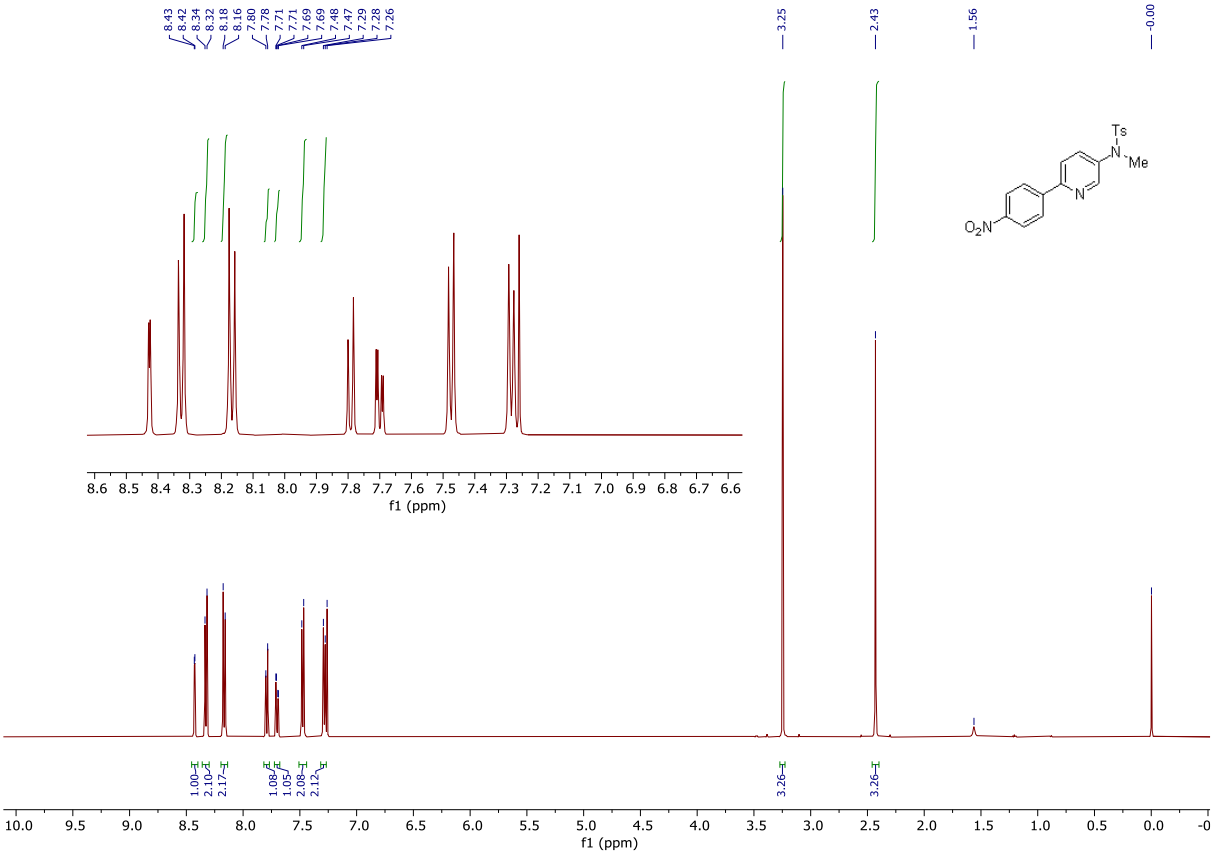

^{13}C NMR spectrum of compound 20a ($CDCl_3$, 298 K)

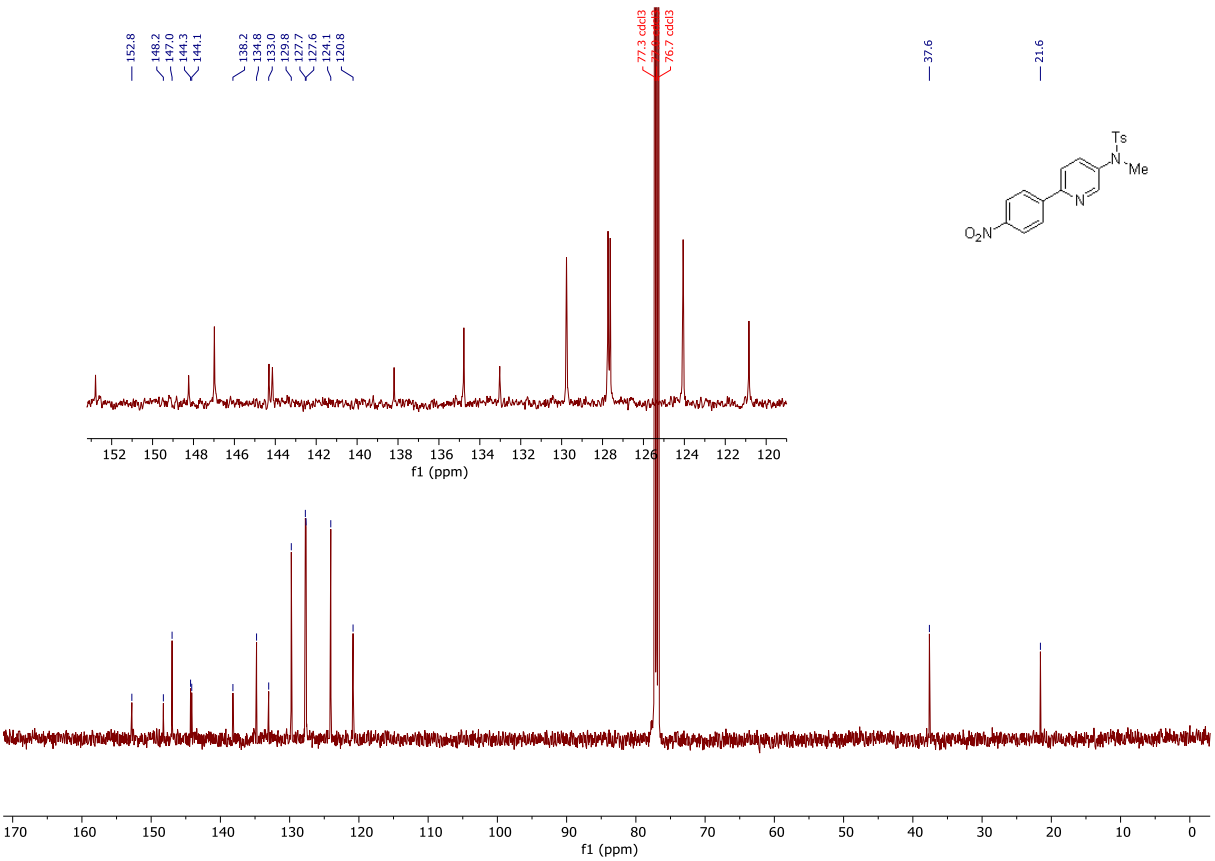

^{1}H NMR spectrum of compound 21a ($CDCl_3$, 298 K)

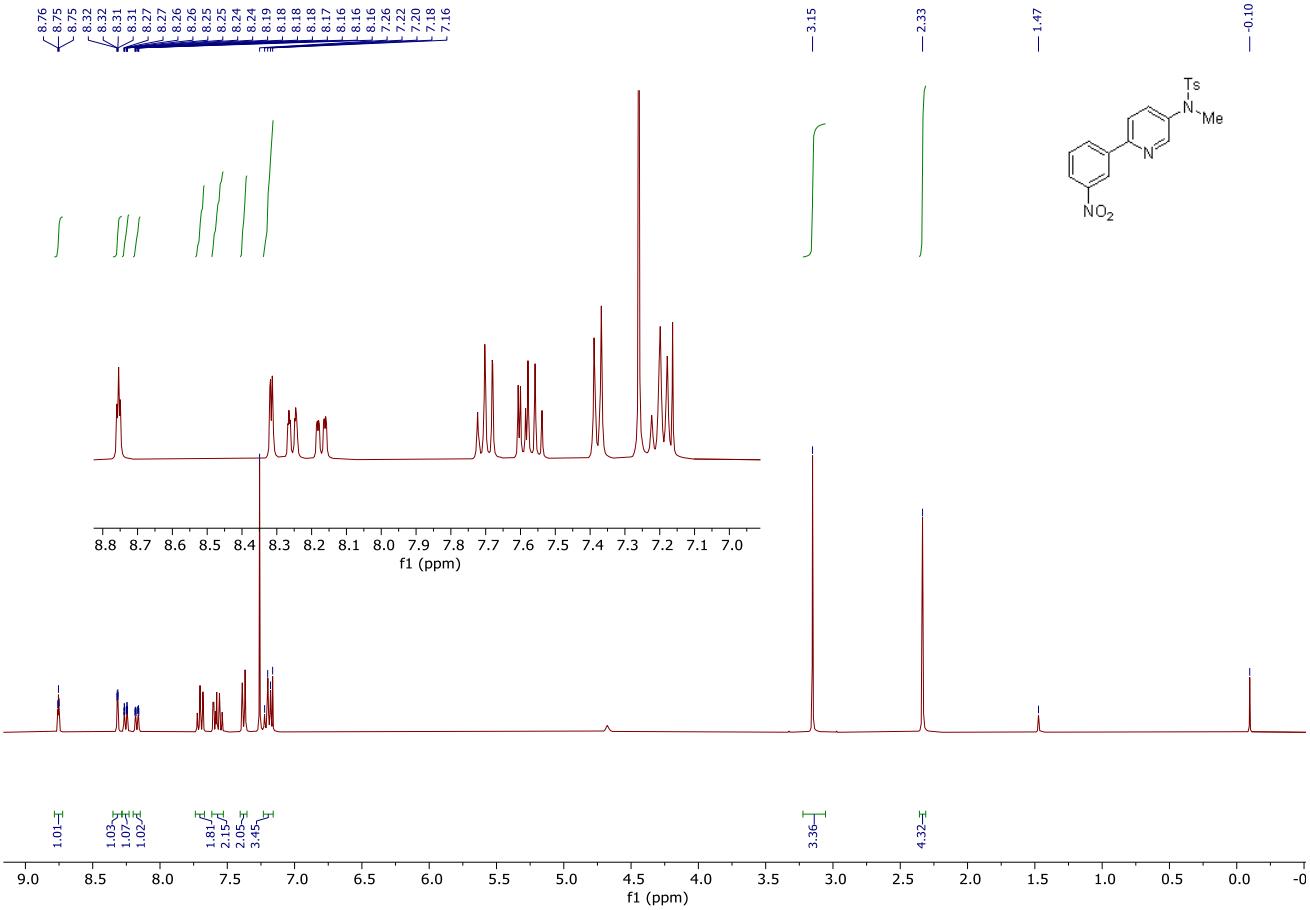

^{13}C NMR spectrum of compound 21a ($CDCl_3$, 298 K)

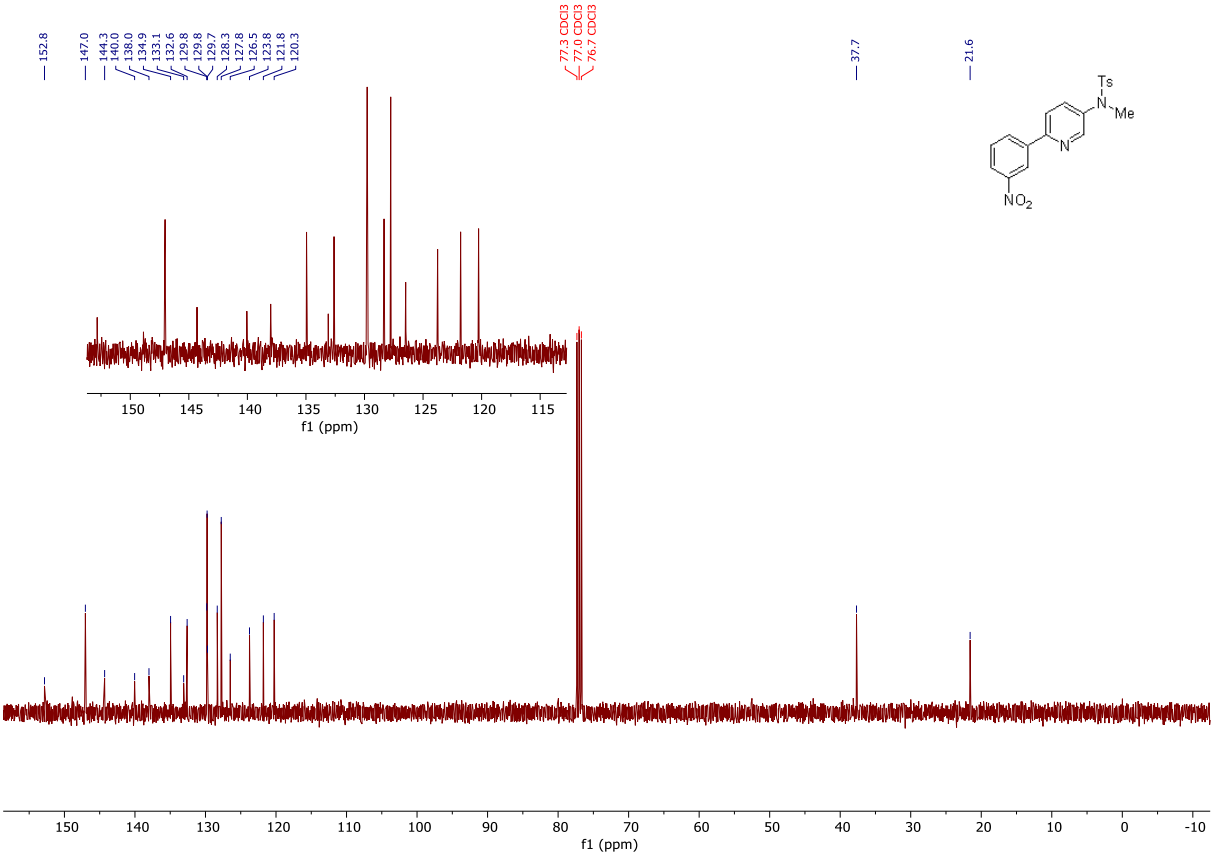

^{1}H NMR spectrum of compound 22a ($CDCl_3$, 298 K)

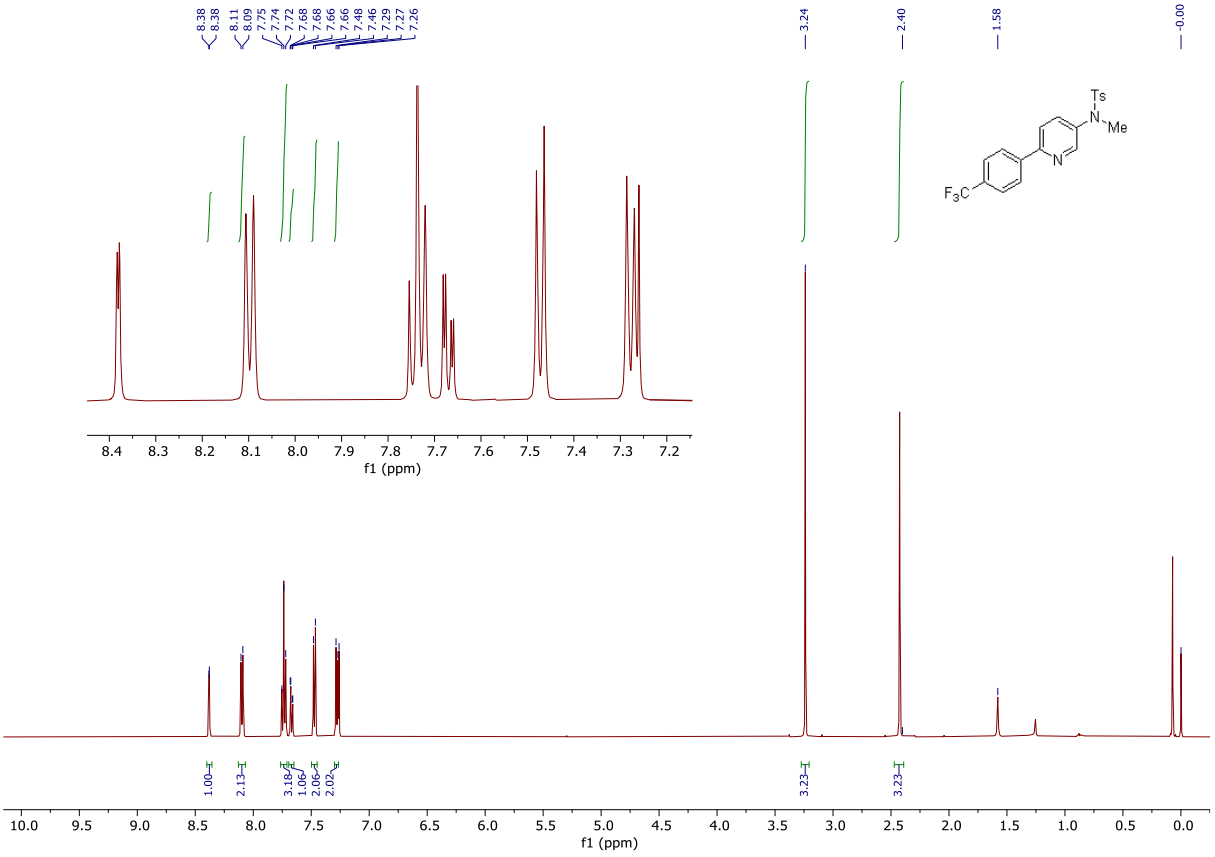

^{13}C NMR spectrum of compound 22a ($CDCl_3$, 298 K)

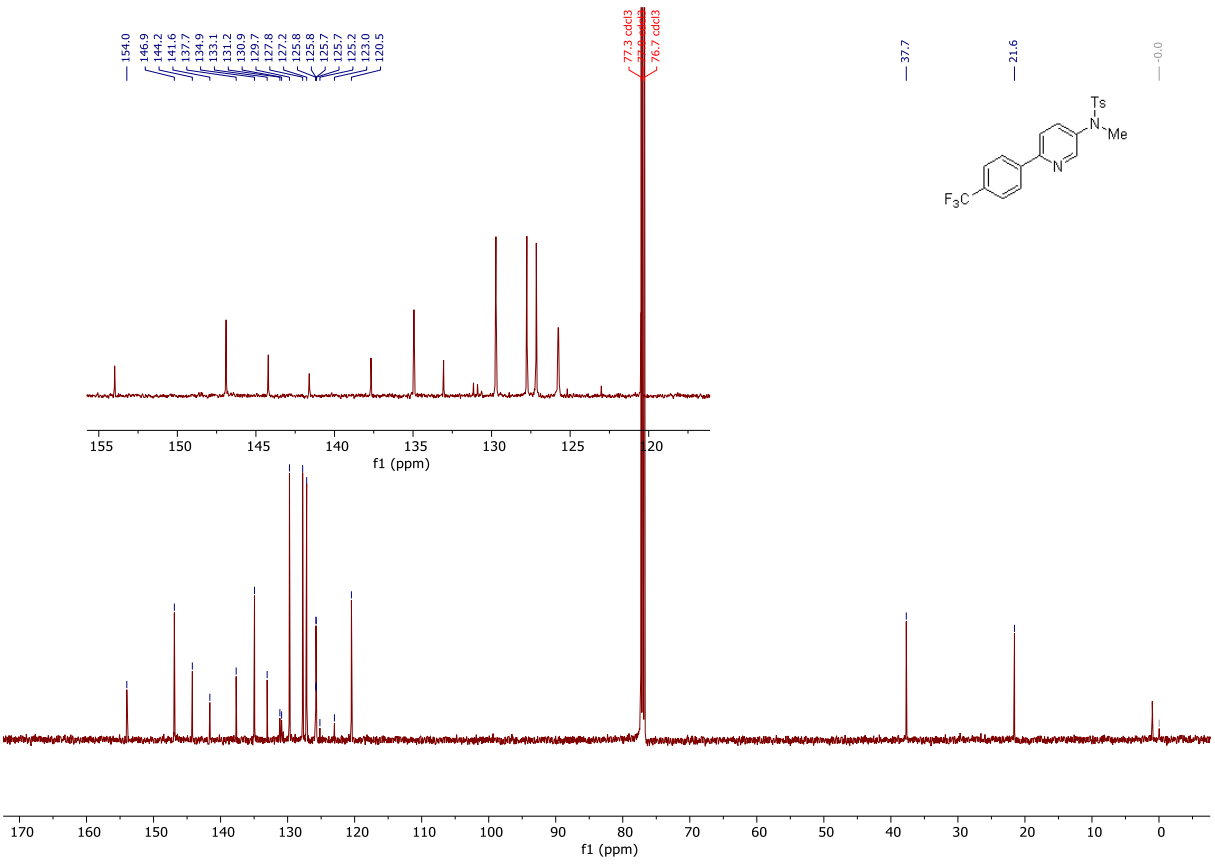

^{1}H NMR spectrum of compound 23a ($CDCl_3$, 298 K)

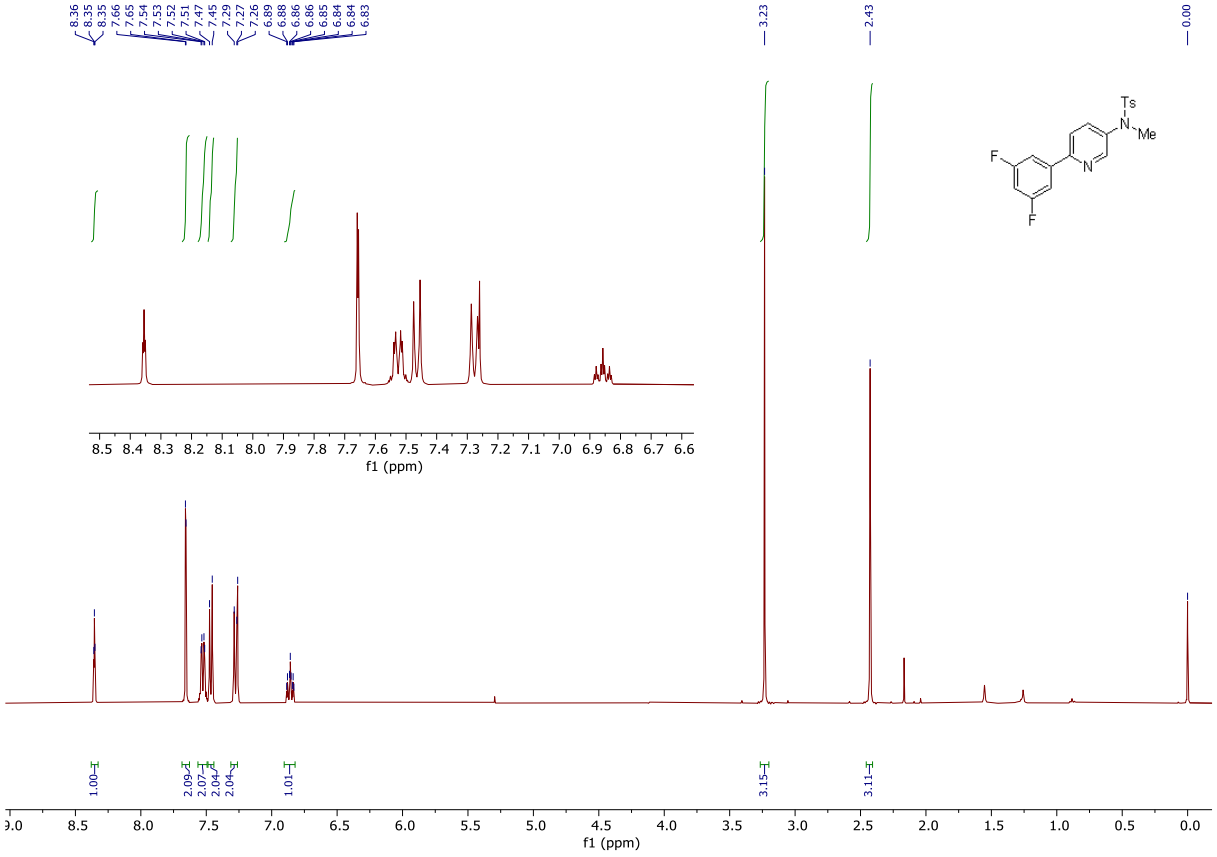

^{13}C NMR spectrum of compound 23a ($CDCl_3$, 298 K)

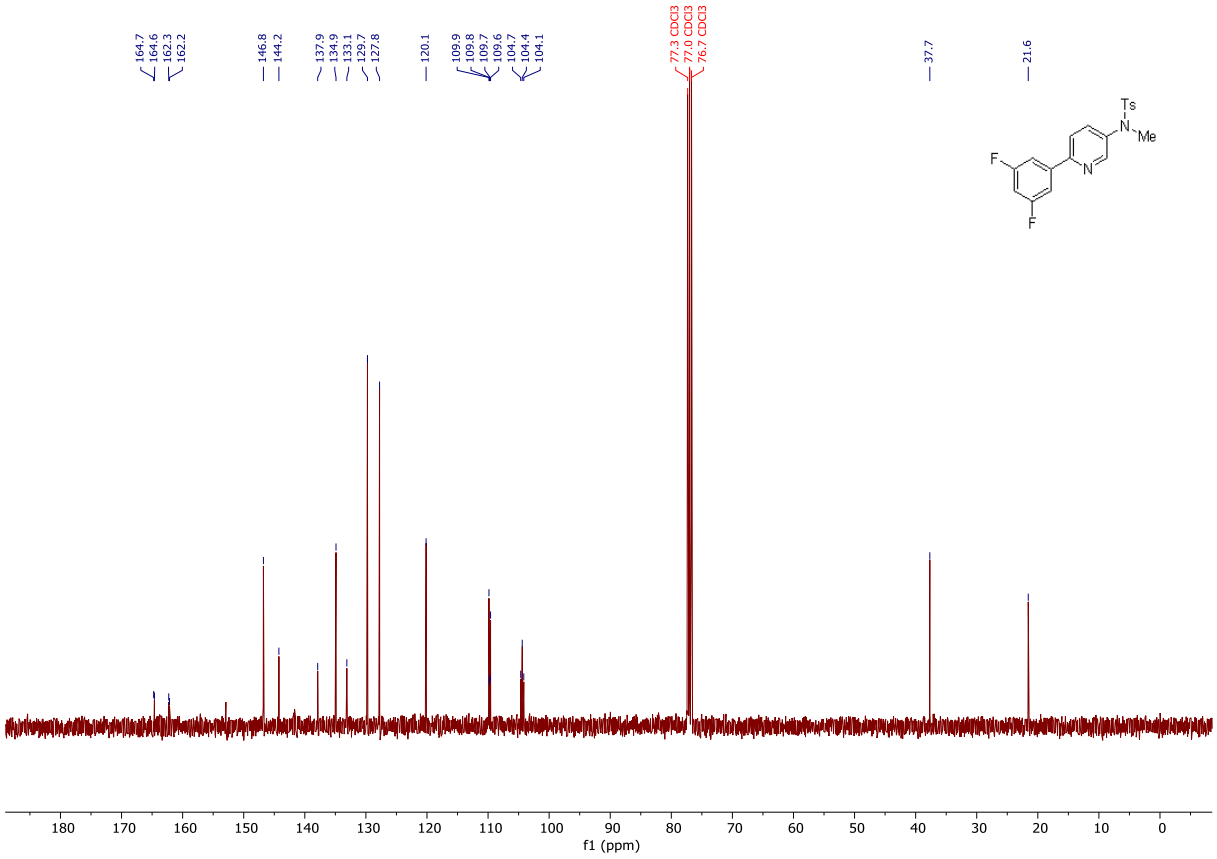

^{1}H NMR spectrum of compound 24a ($CDCl_3$, 298 K)

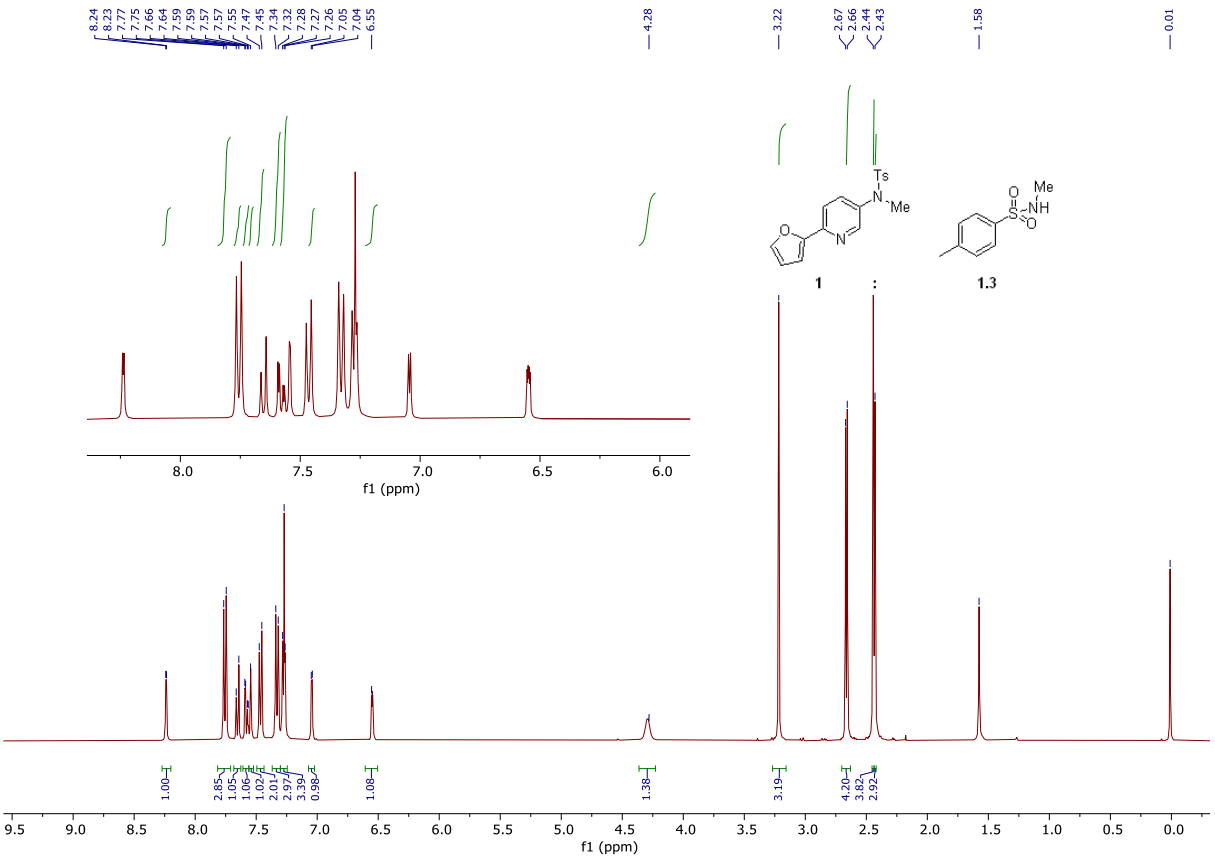

^{13}C NMR spectrum of compound 24a ($CDCl_3$, 298 K)

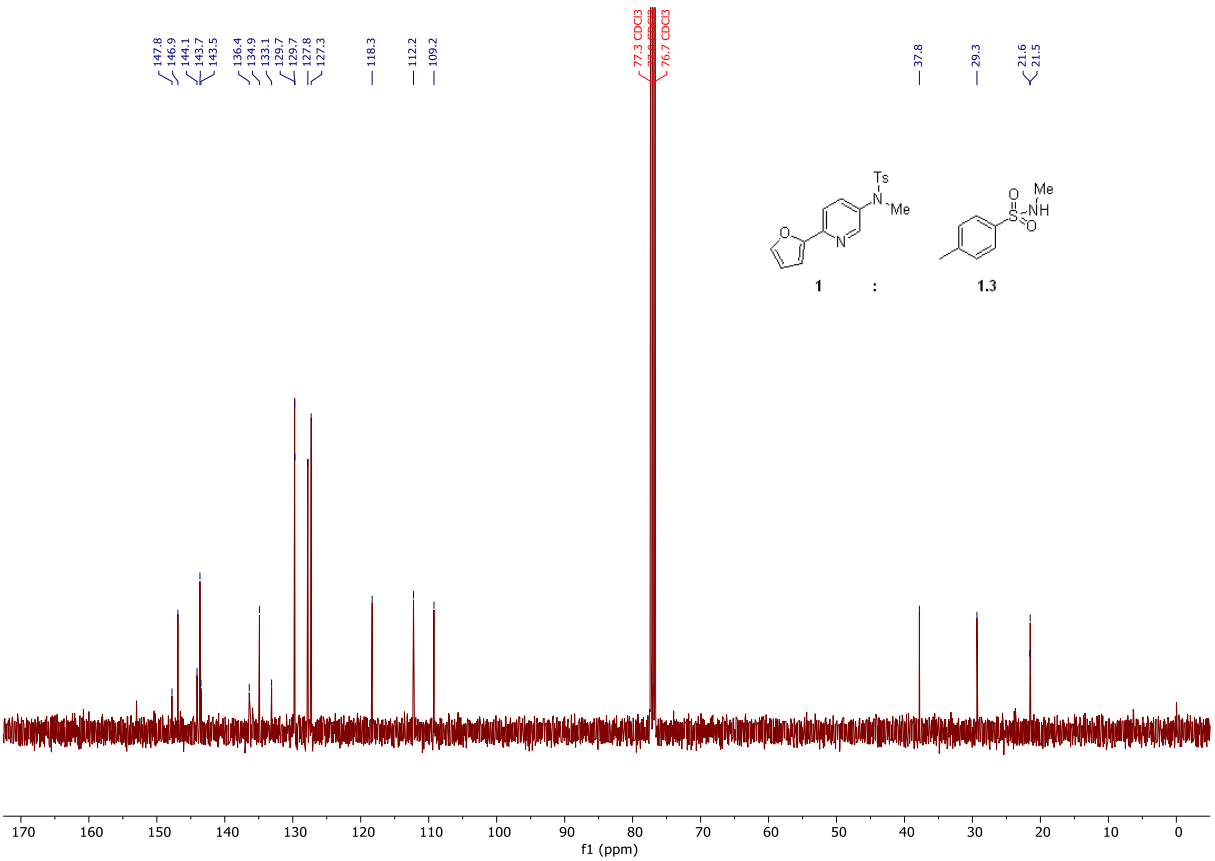

^{1}H NMR spectrum of compound 24b ($CDCl_3$, 298 K)

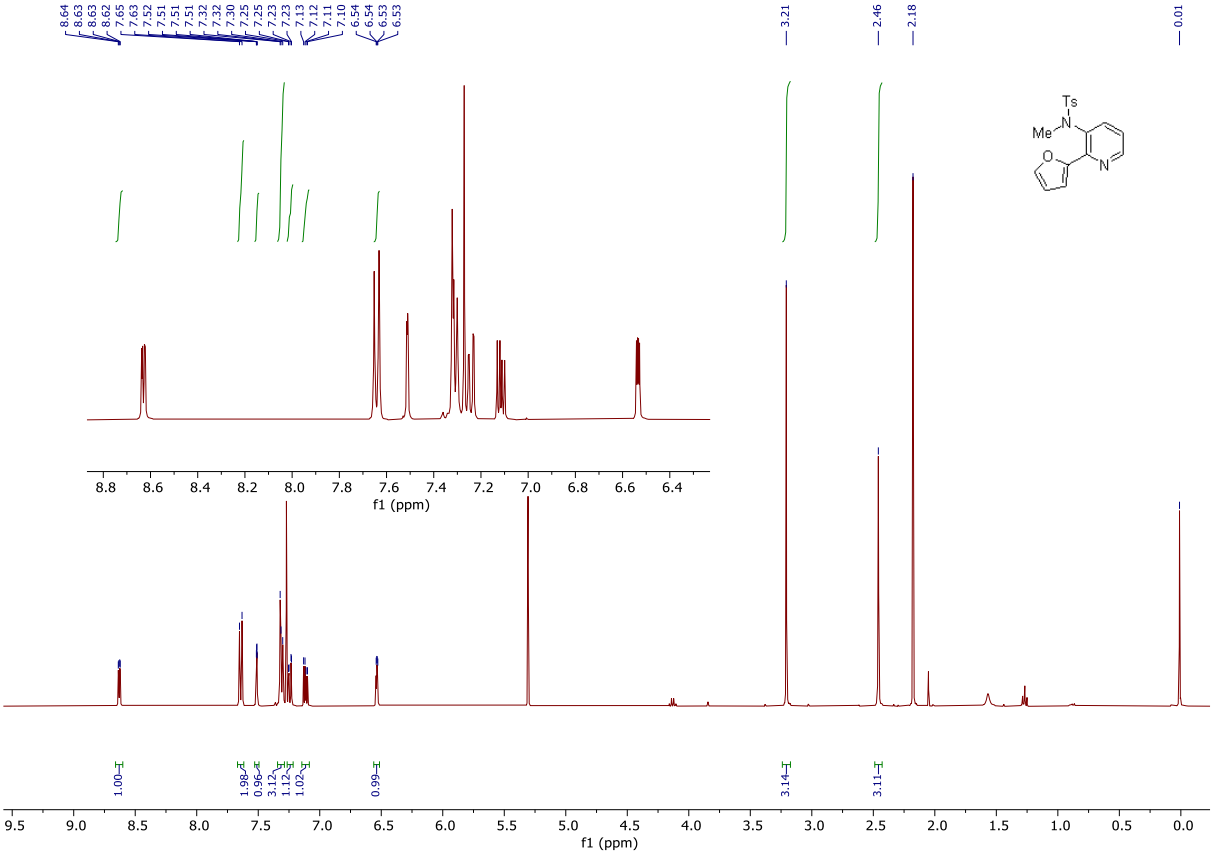

^{13}C NMR spectrum of compound 24b ($CDCl_3$, 298 K)

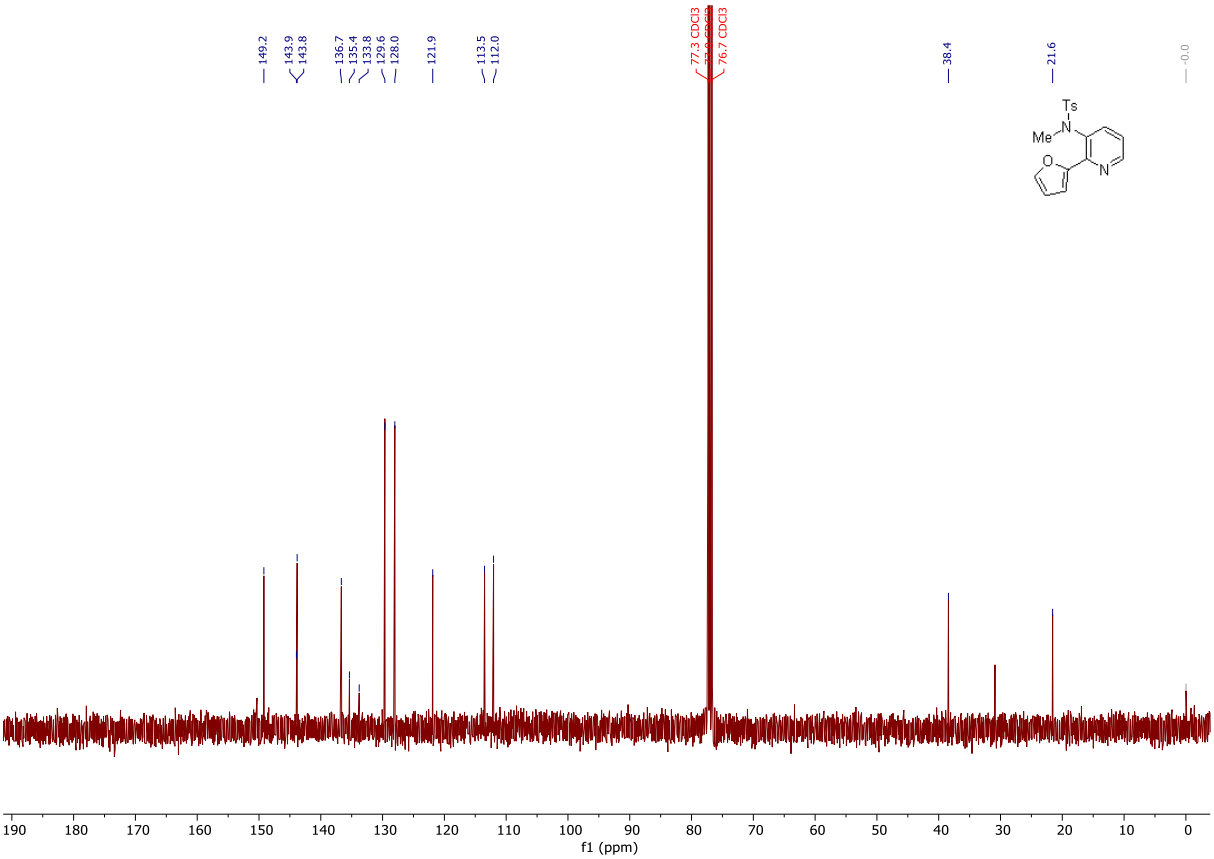

^{1}H NMR spectrum of compound 25a ($CDCl_3$, 298 K)

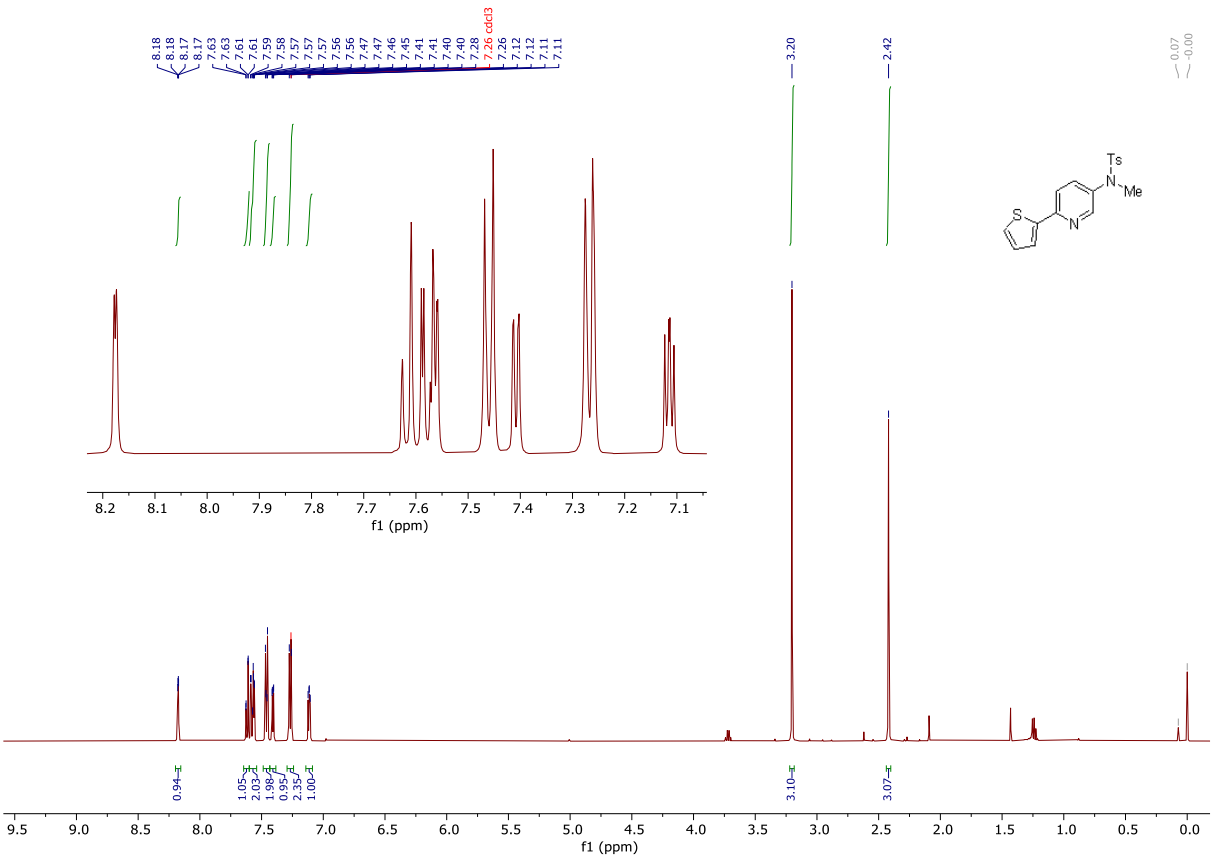

^{13}C NMR spectrum of compound 25a ($CDCl_3$, 298 K)

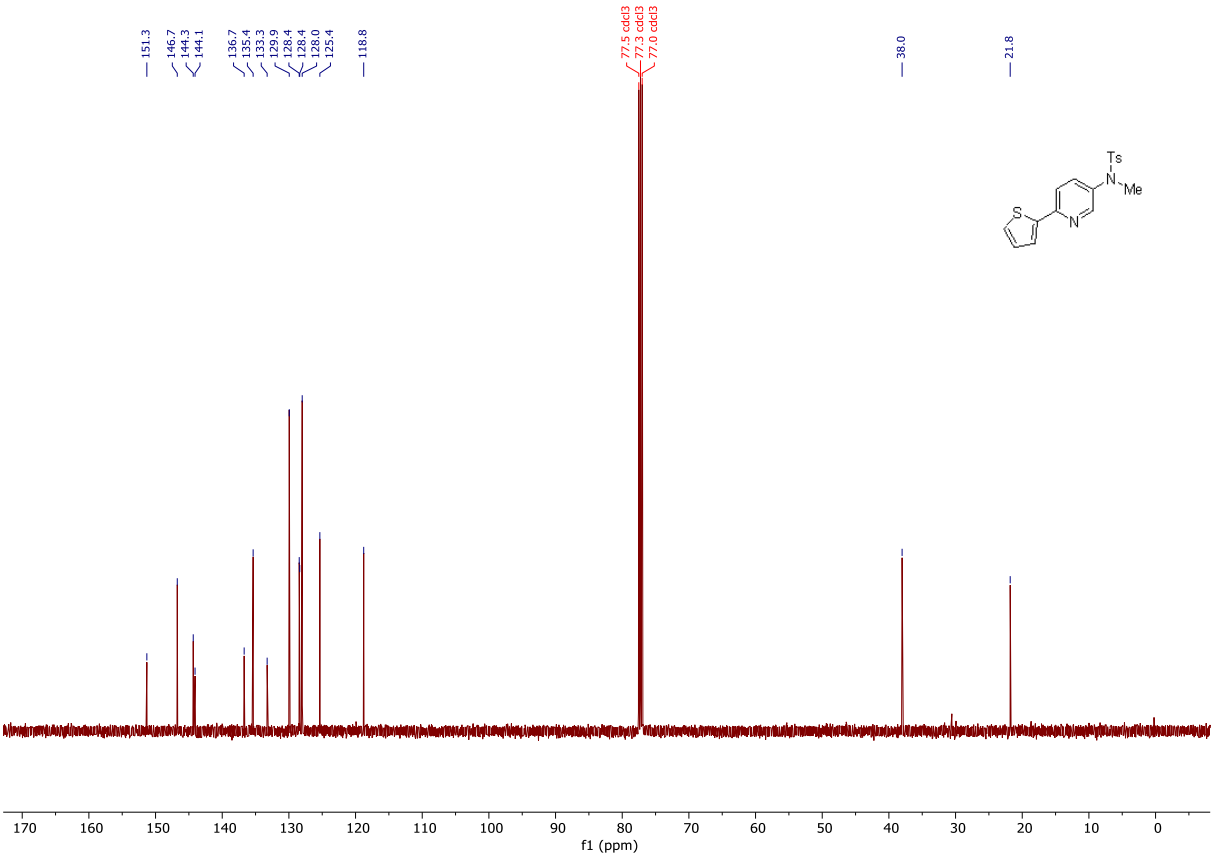

^{1}H NMR spectrum of compound 26a ($CDCl_3$, 298 K)

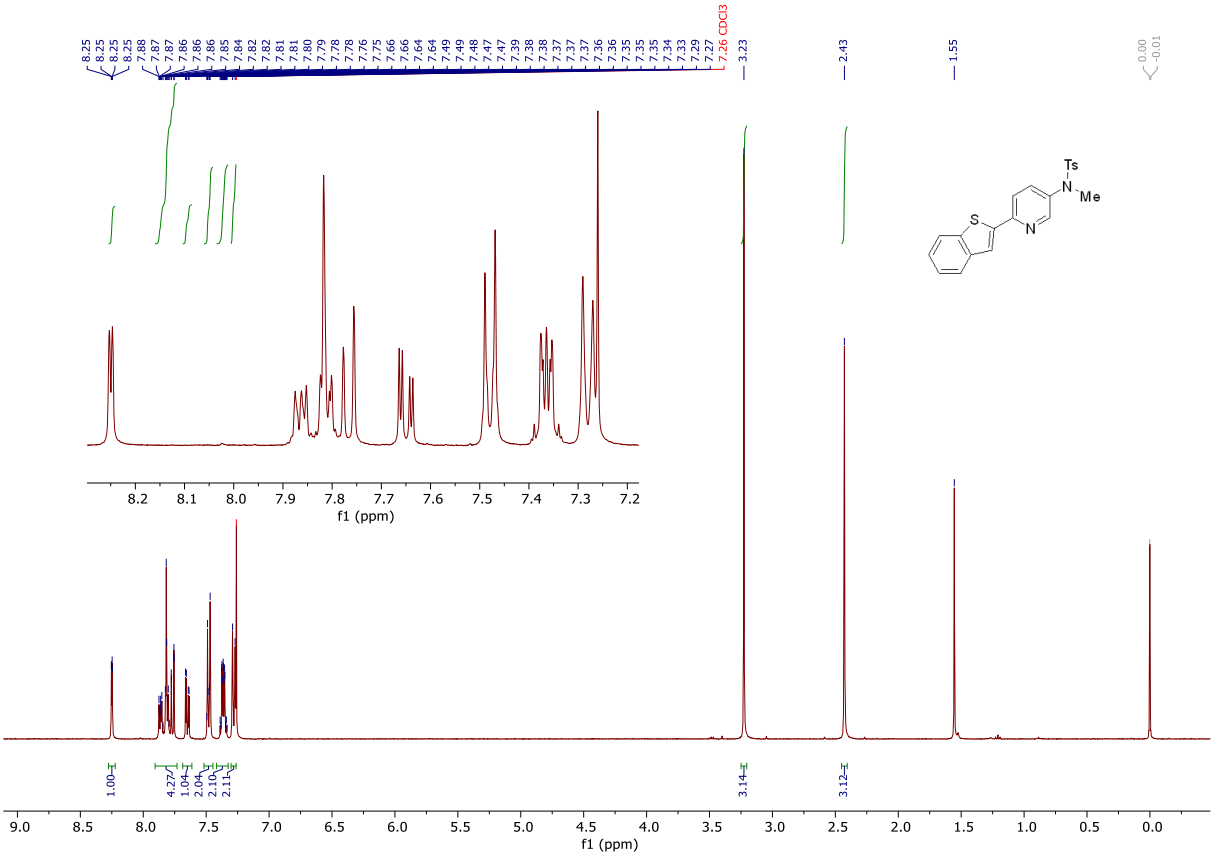

^{13}C NMR spectrum of compound 26a ($CDCl_3$, 298 K)

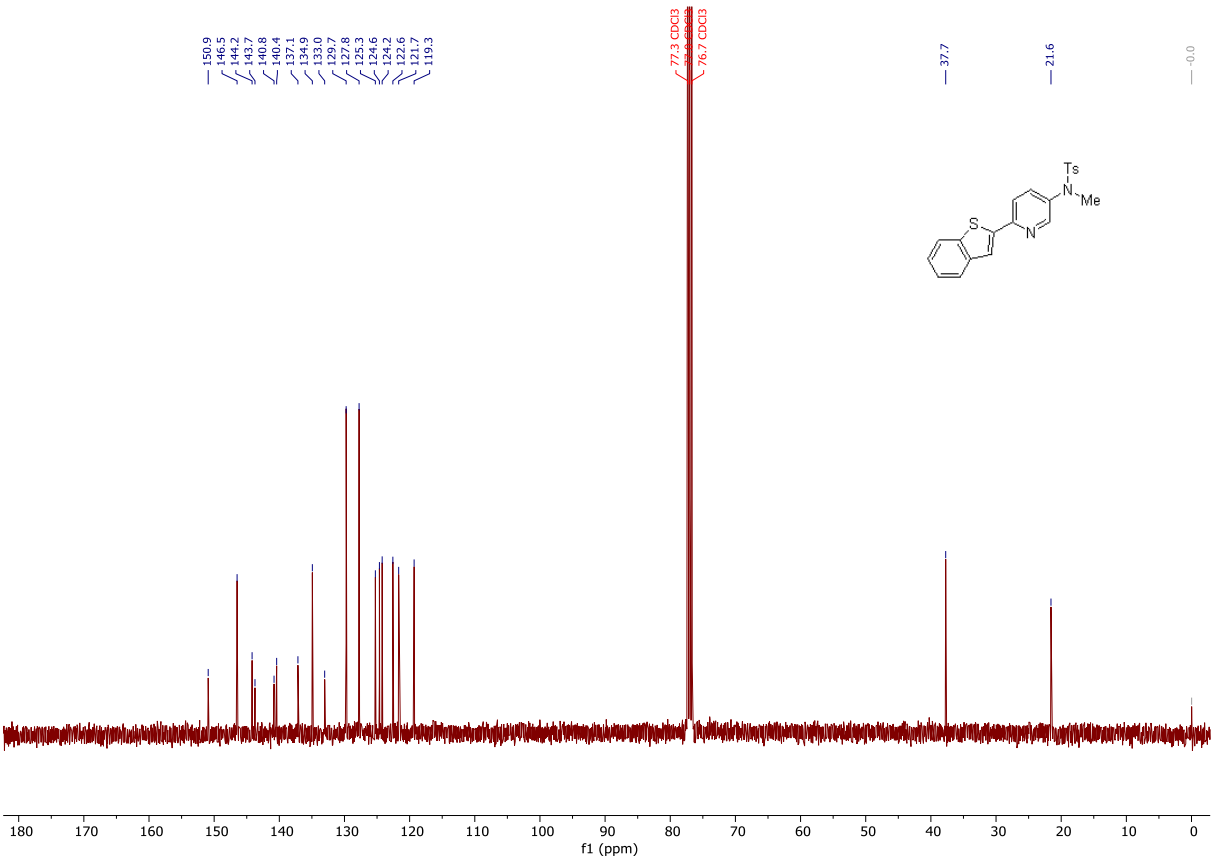

^{1}H NMR spectrum of compound 27a ($CDCl_3$, 298 K)

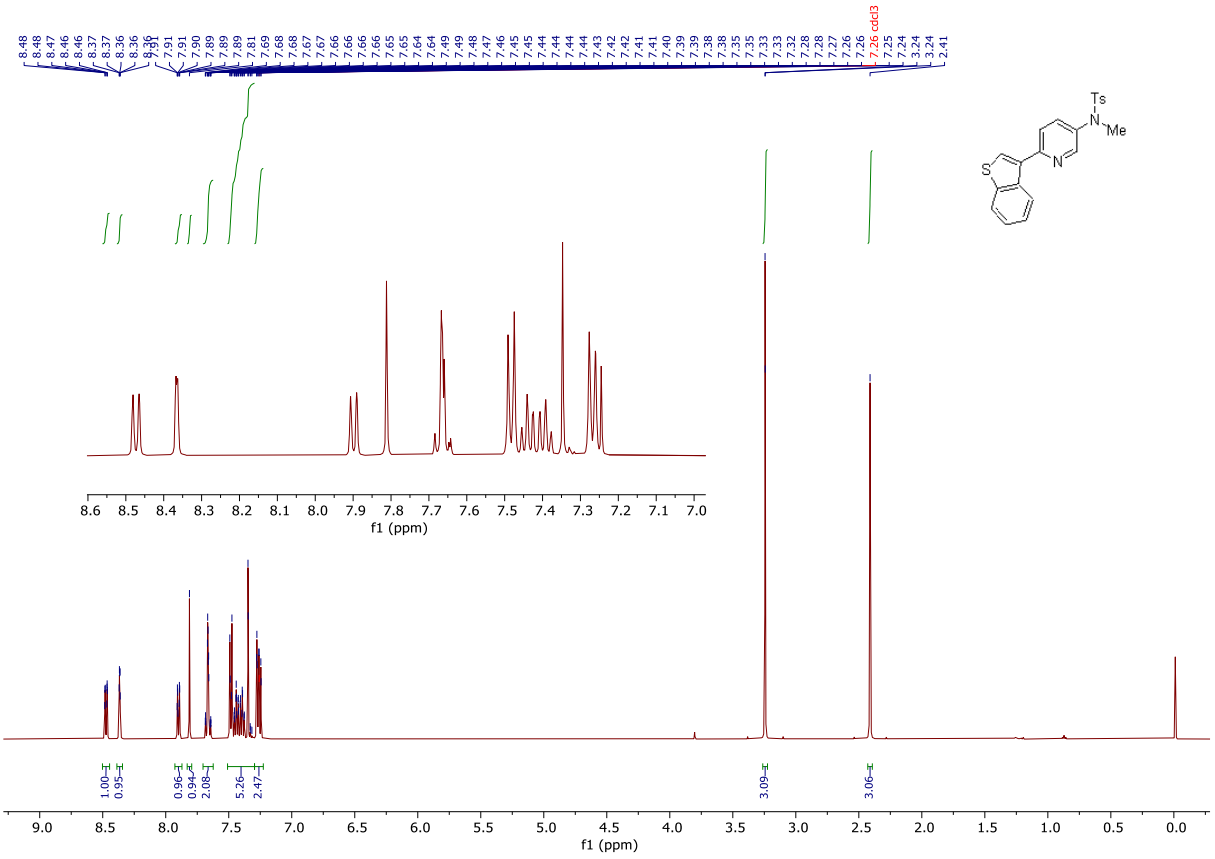

^{13}C NMR spectrum of compound 27a ($CDCl_3$, 298 K)

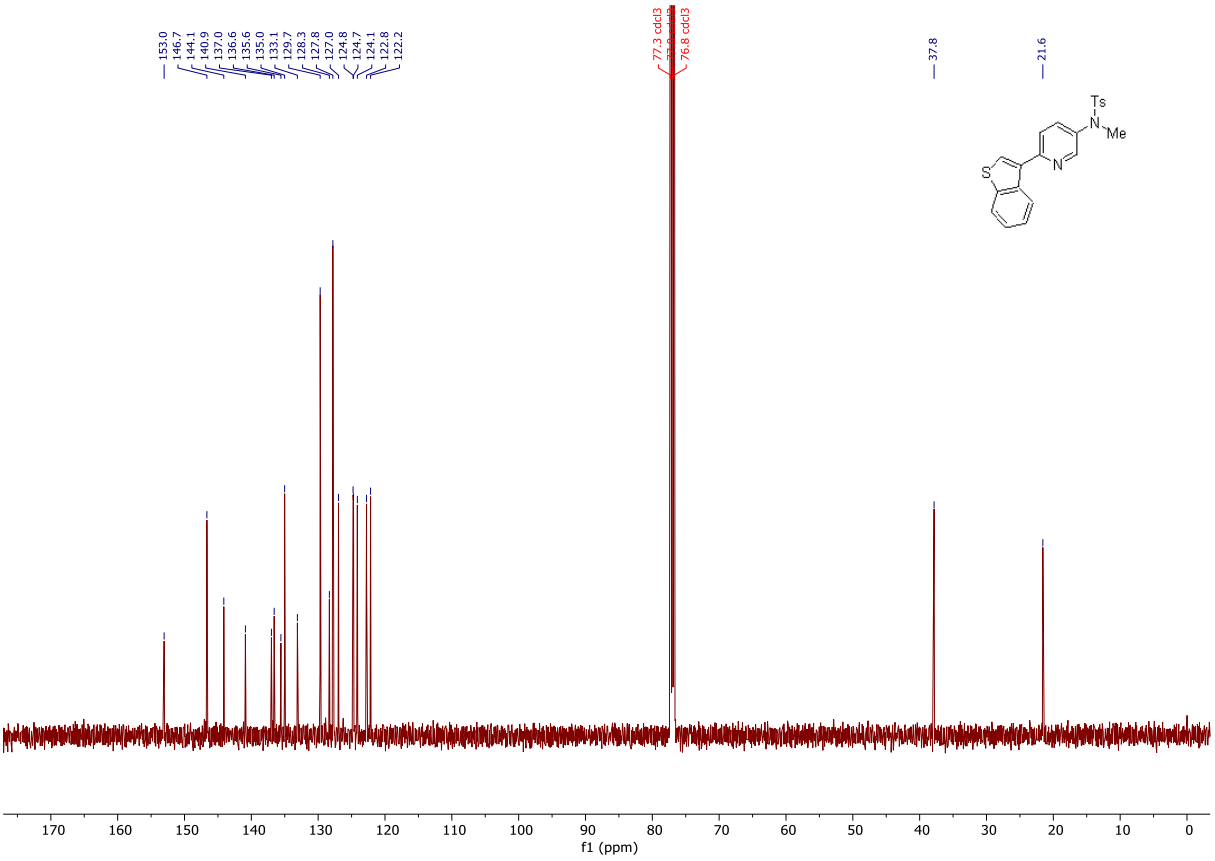

^{1}H NMR spectrum of compound 28a ($CDCl_3$, 298 K)

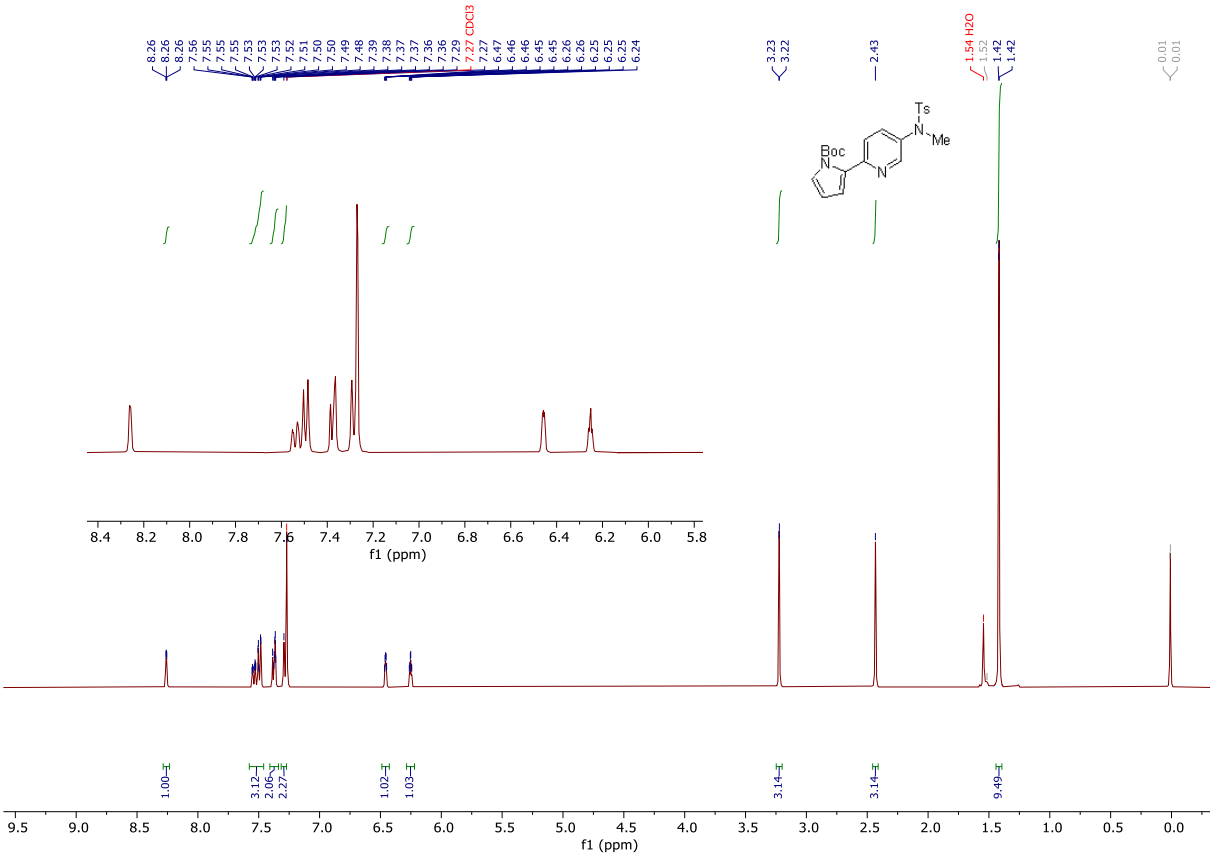

^{13}C NMR spectrum of compound 28a ($CDCl_3$, 298 K)

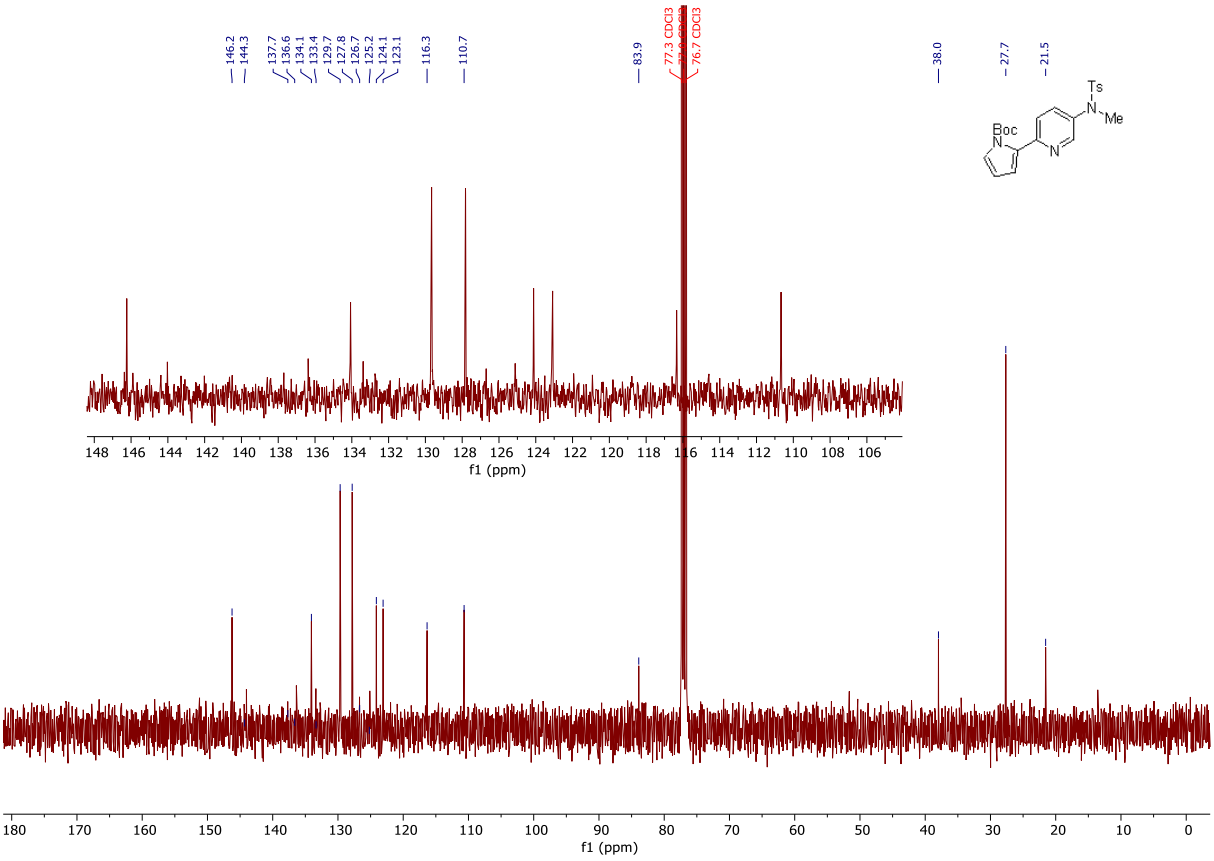

^{1}H NMR spectrum of compound 29a ($CDCl_3$, 298 K)

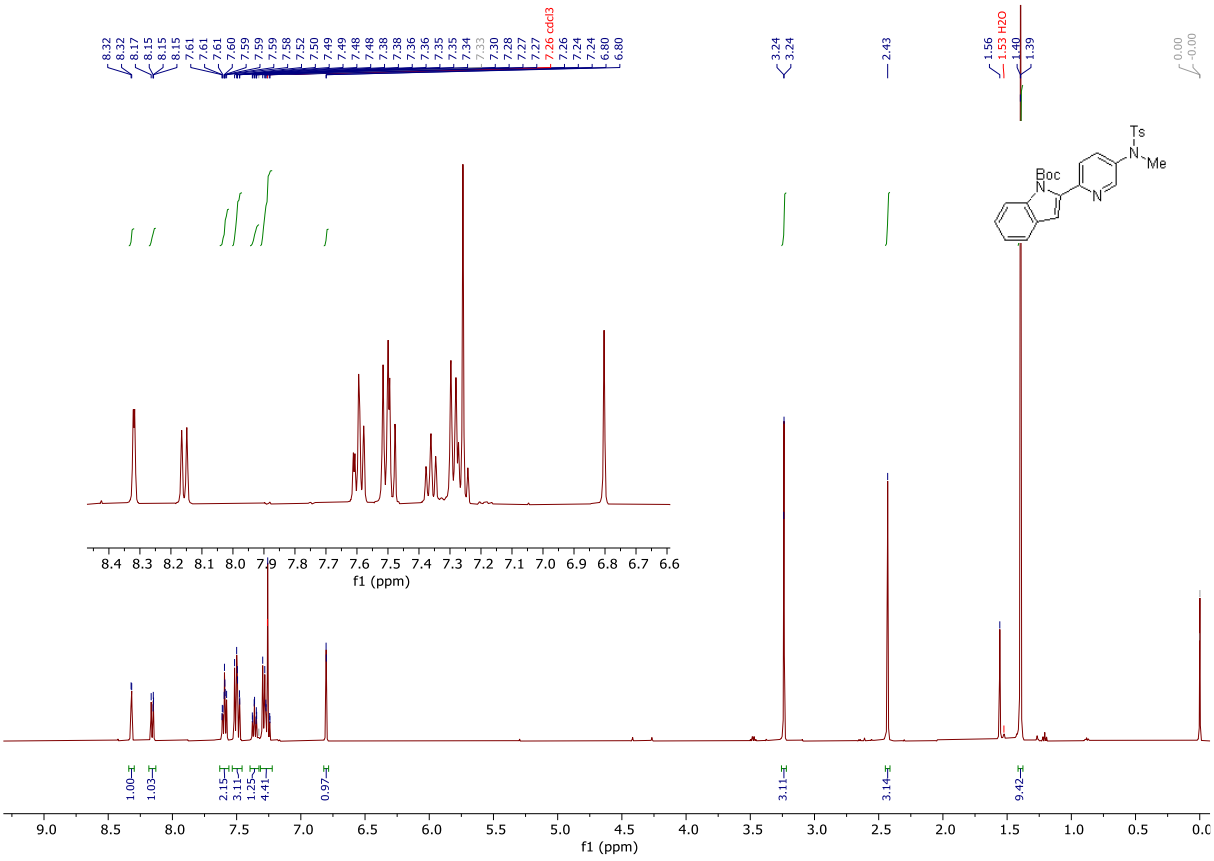

^{13}C NMR spectrum of compound 29a ($CDCl_3$, 298 K)

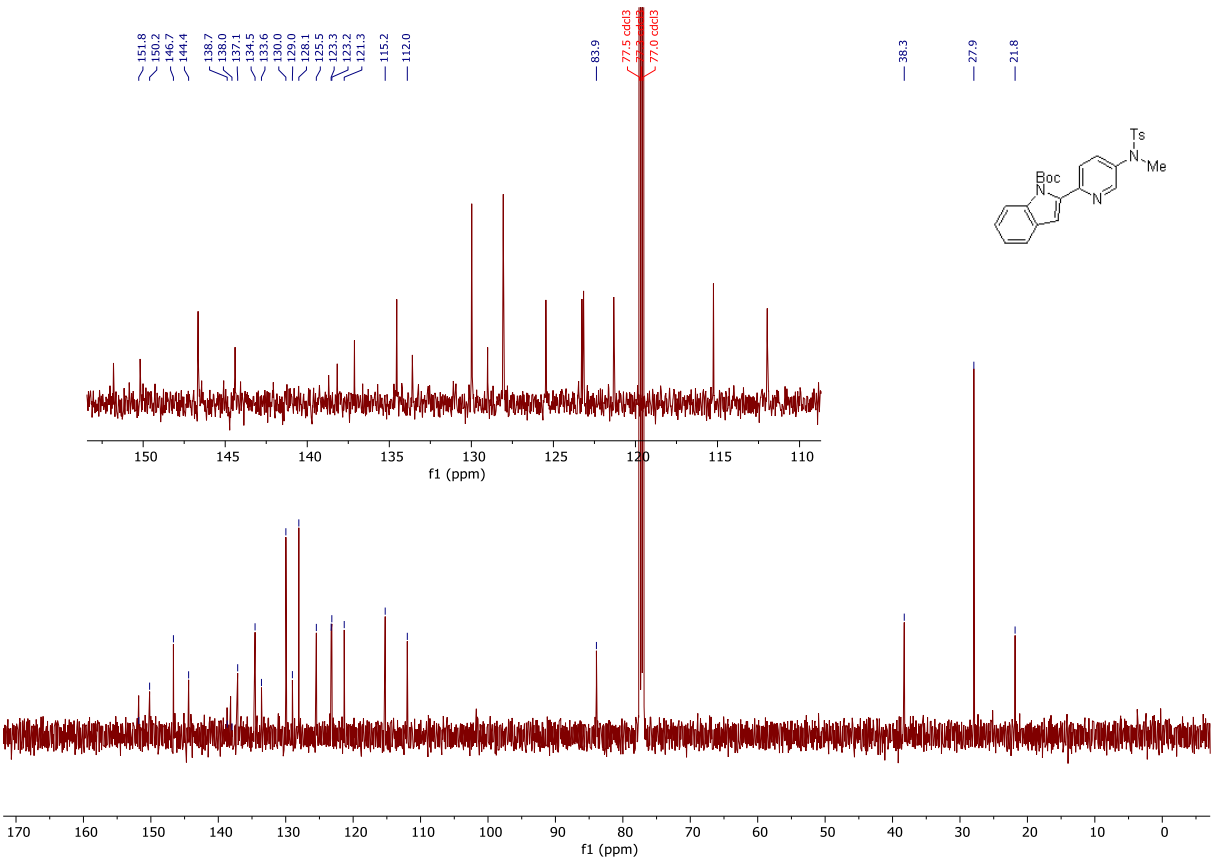

^{1}H NMR spectrum of compound 30b ($CDCl_3$, 298 K)

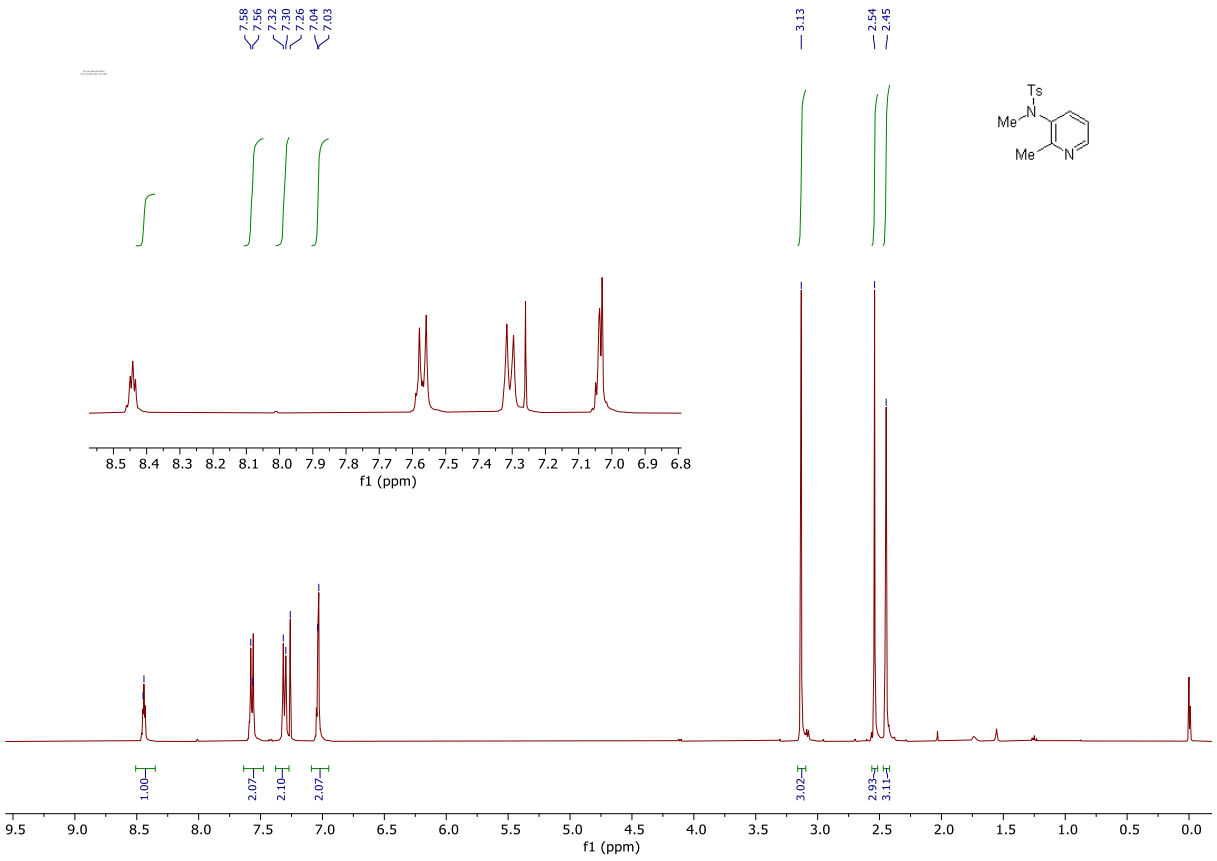

^{13}C NMR spectrum of compound 30b ($CDCl_3$, 298 K)

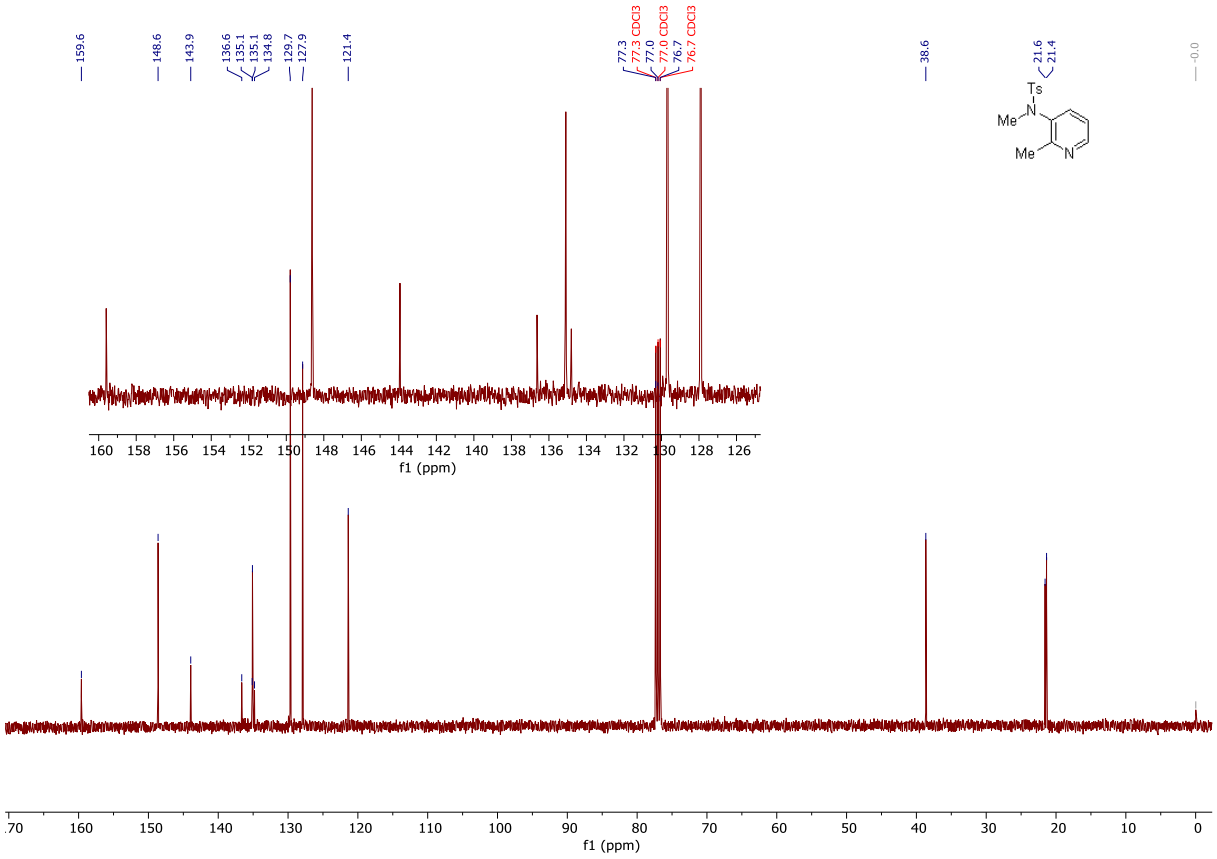

^{1}H NMR spectrum of compound 31b ($CDCl_3$, 298 K)

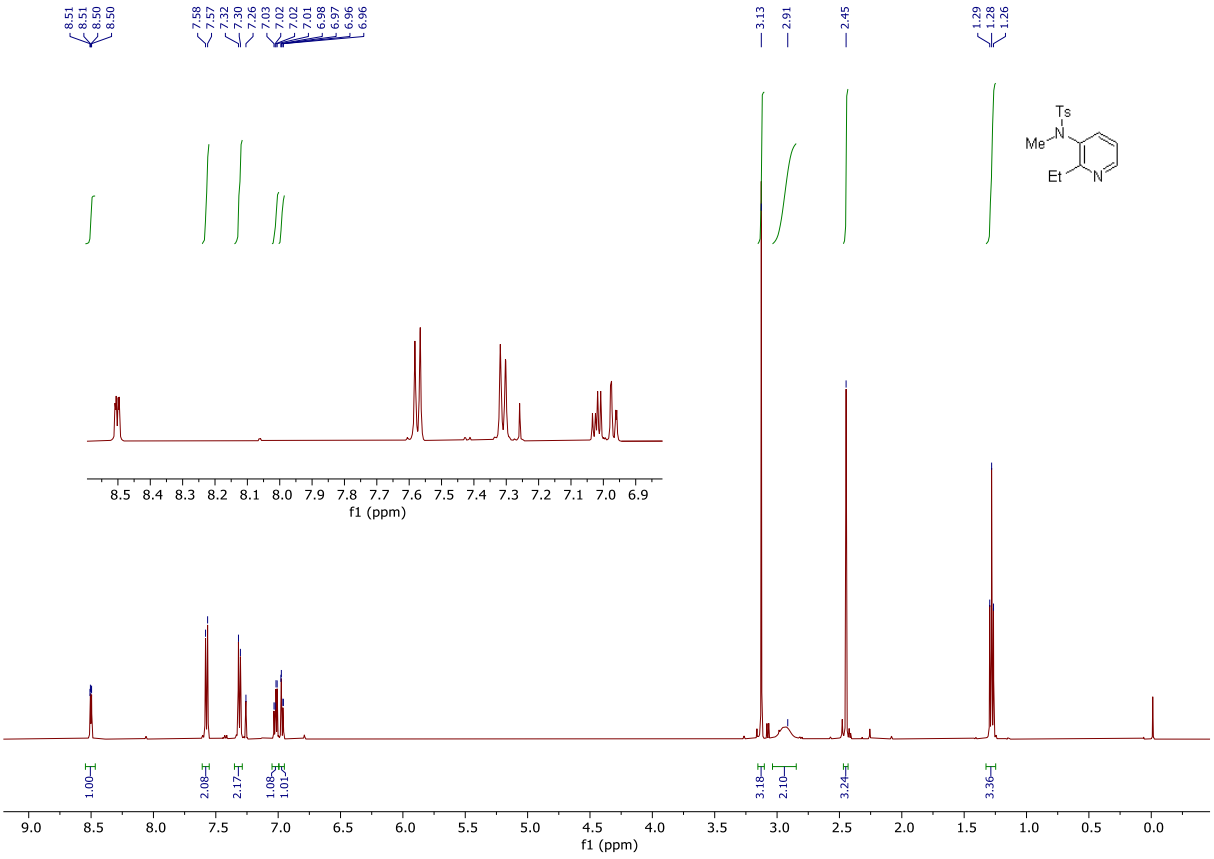

^{13}C NMR spectrum of compound 31b ($CDCl_3$, 298 K)

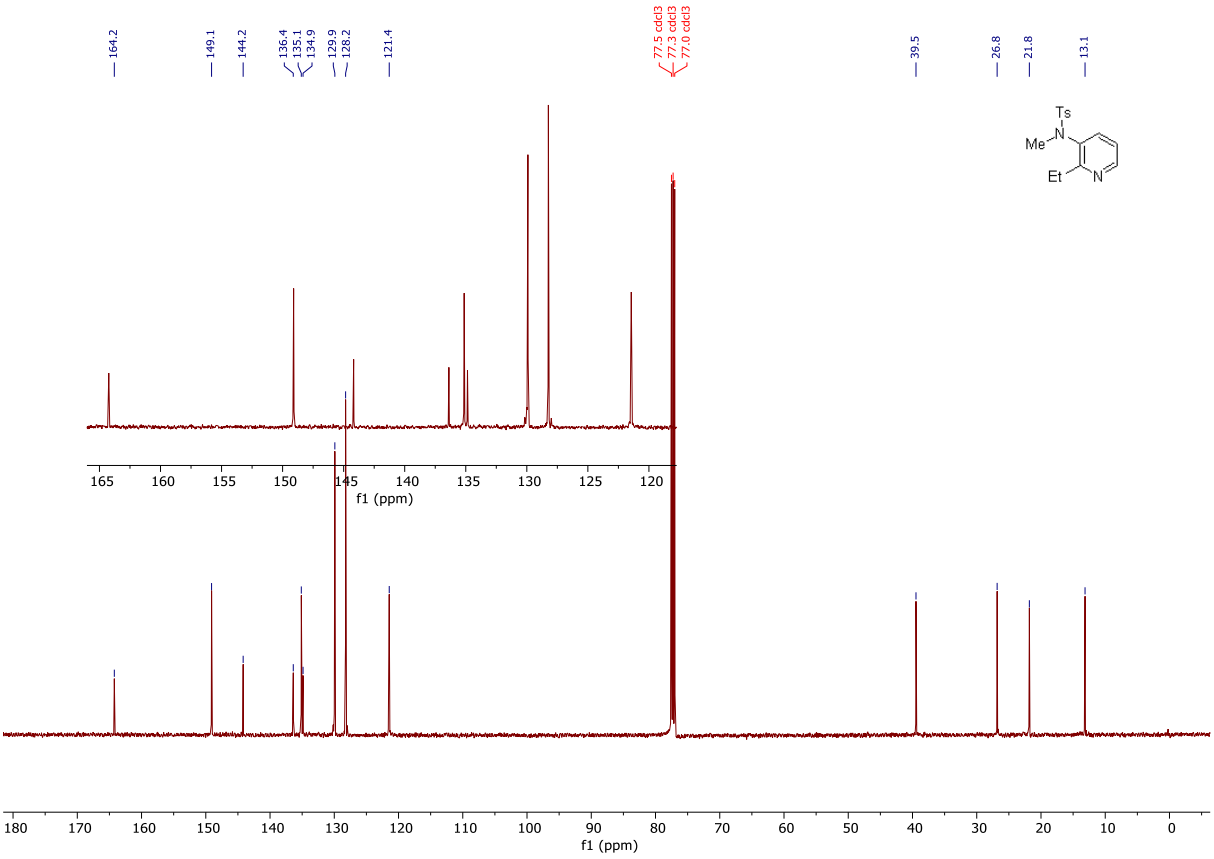

^{1}H NMR spectrum of compound 32b ($CDCl_3$, 298 K)

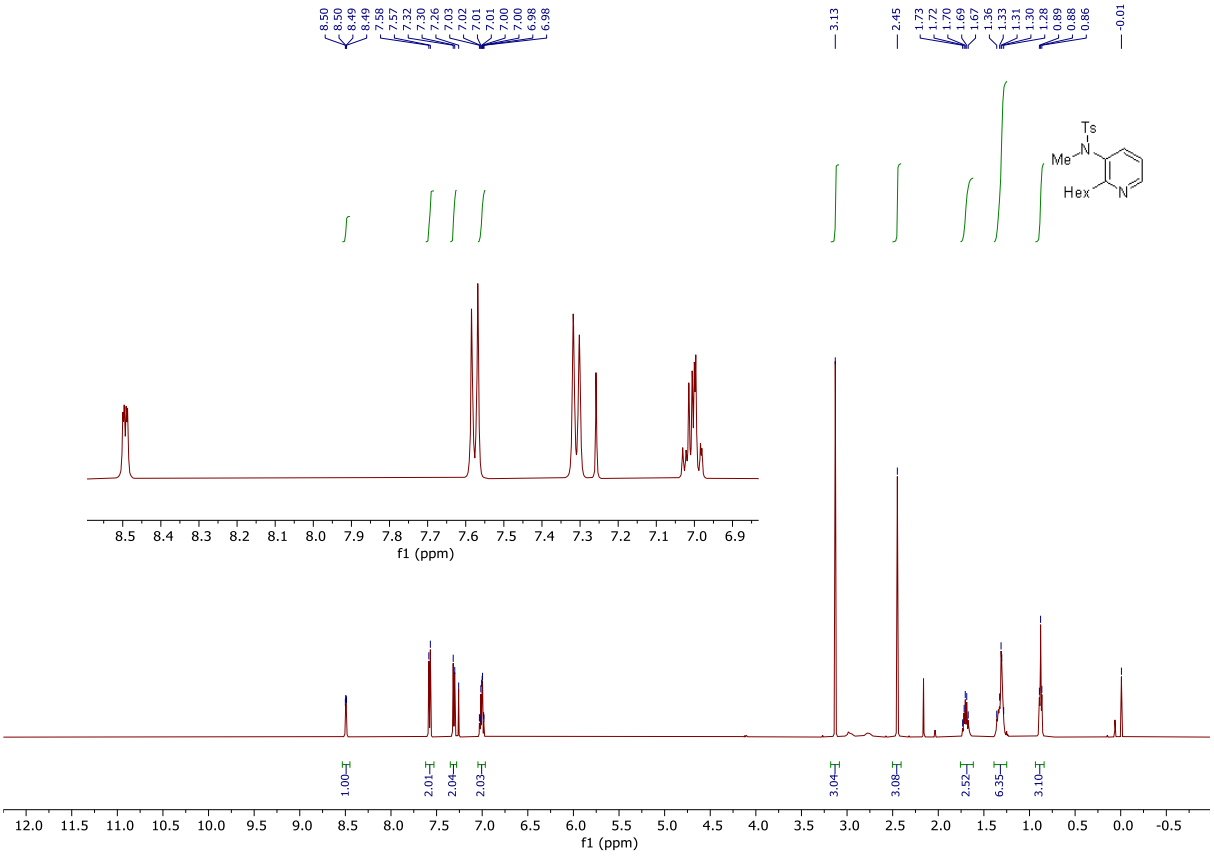

^{13}C NMR spectrum of compound 32b ($CDCl_3$, 298 K)

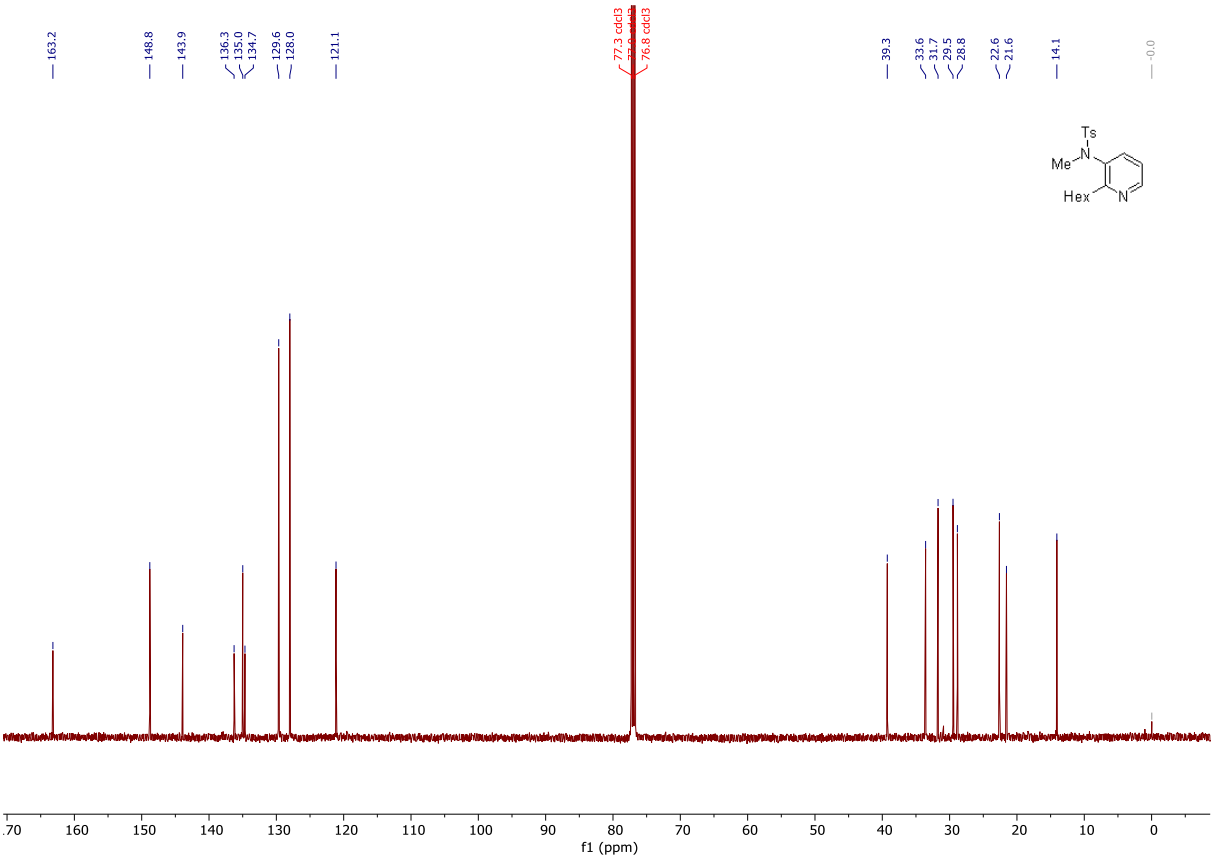

^{1}H NMR spectrum of compound 33a ($CDCl_3$, 298 K)

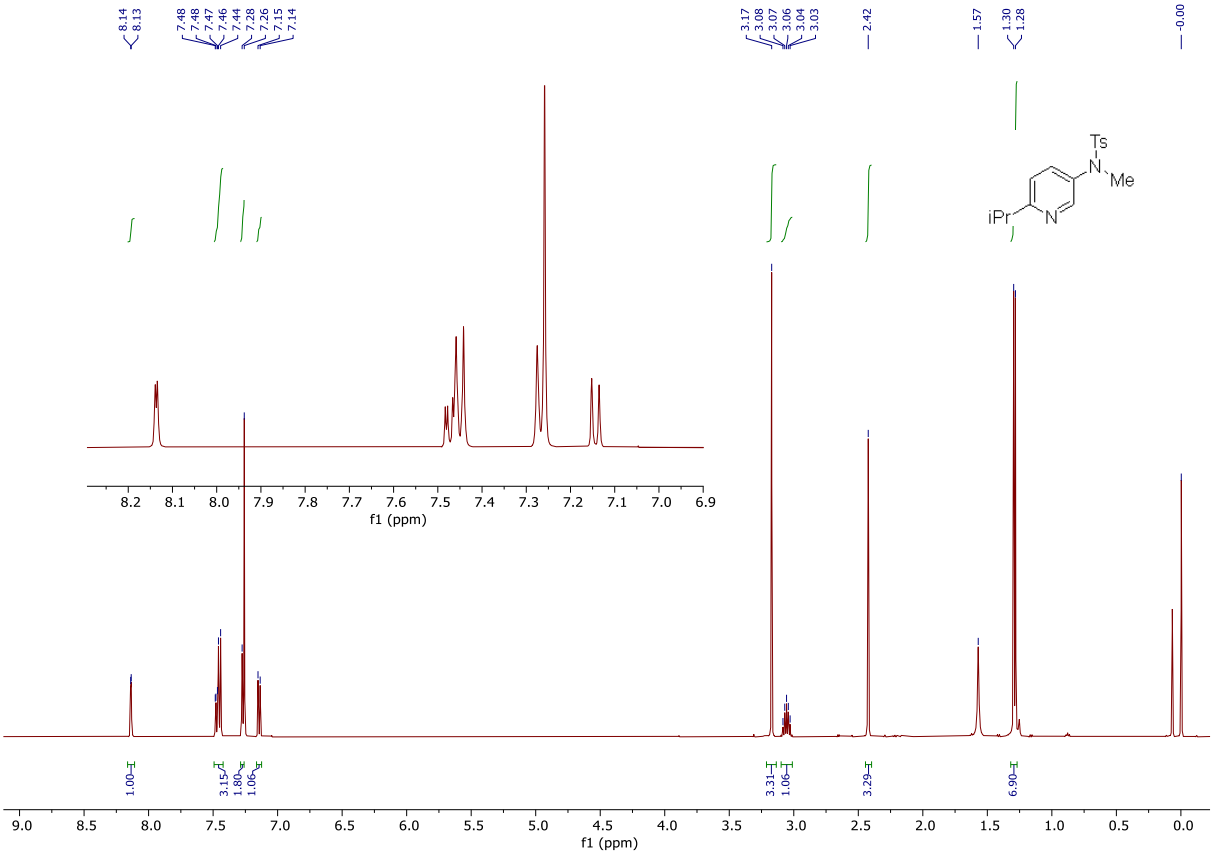

^{13}C NMR spectrum of compound 33a ($CDCl_3$, 298 K)

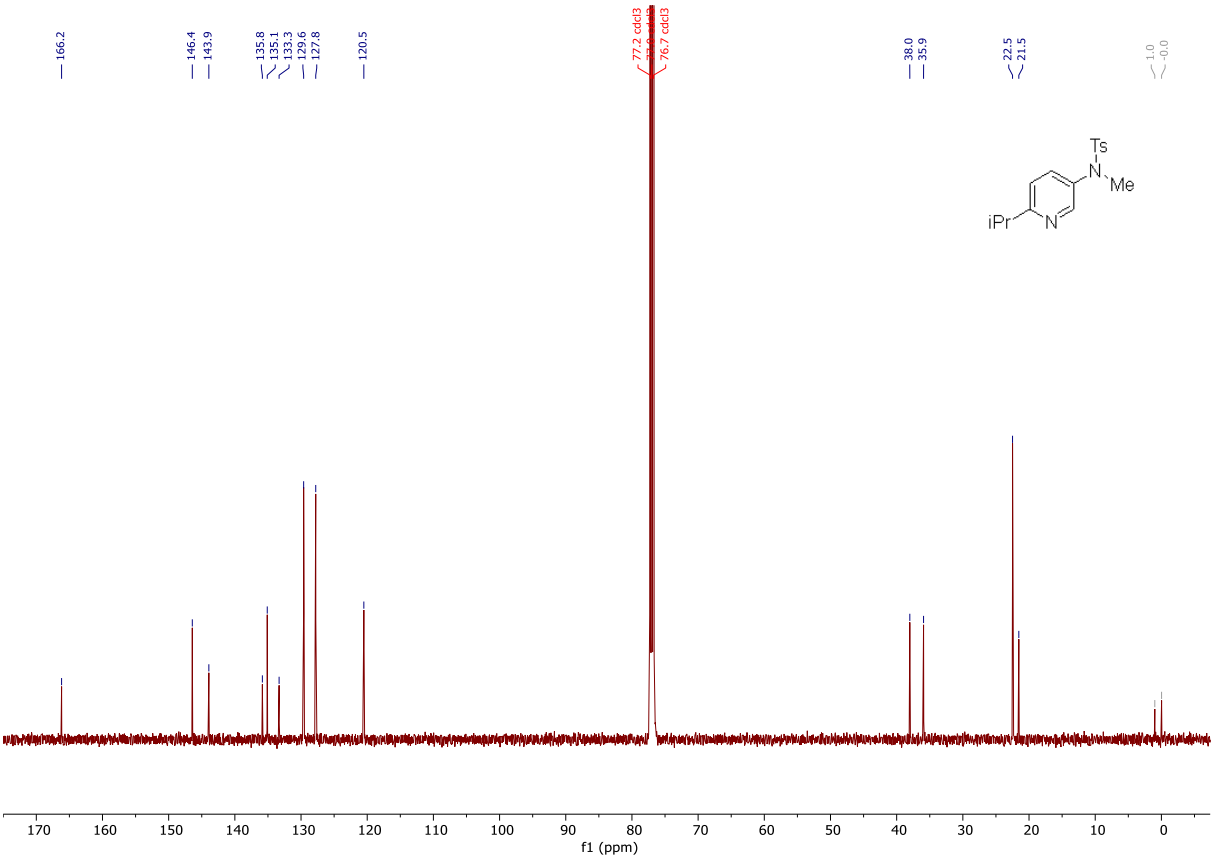

^{1}H NMR spectrum of compound 33b ($CDCl_3$, 298 K)

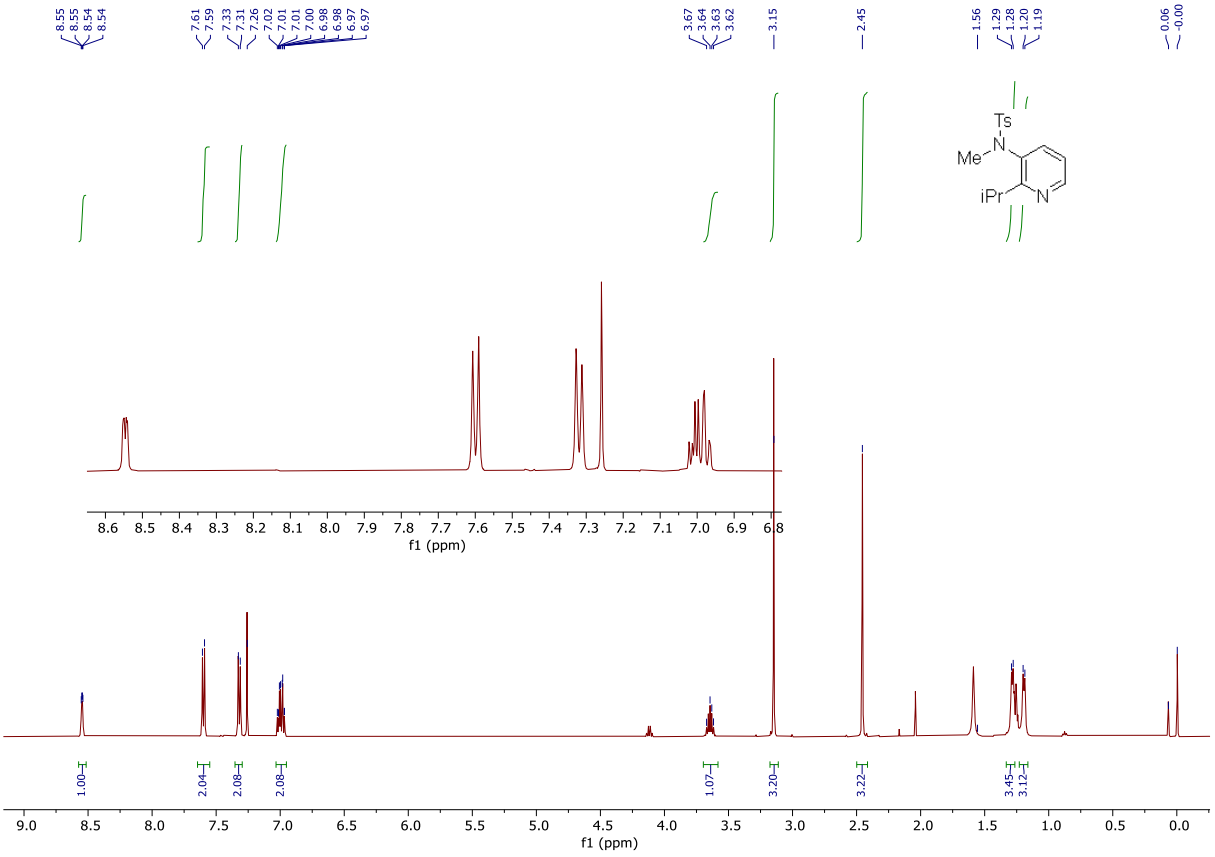

^{13}C NMR spectrum of compound 33b ($CDCl_3$, 298 K)

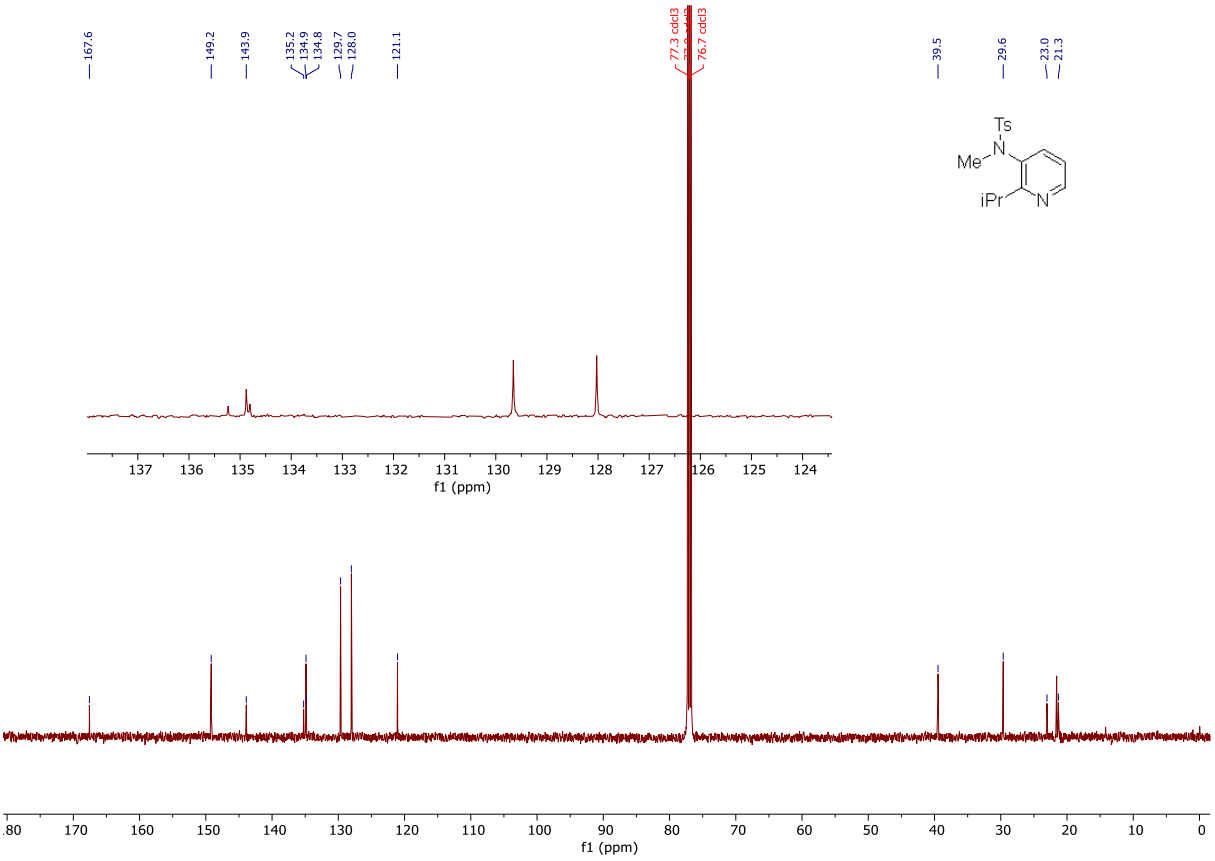

^{1}H NMR spectrum of compound 34b ($CDCl_3$, 298 K)

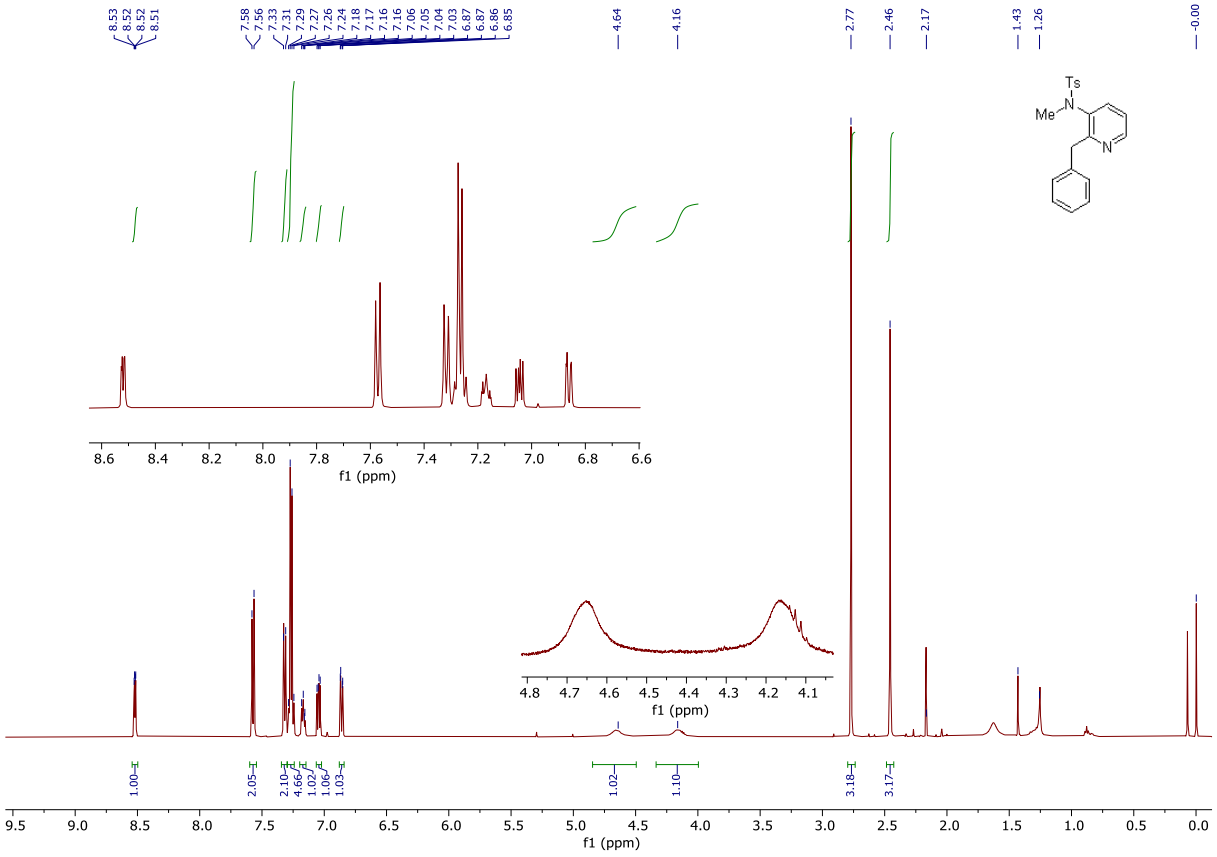

^{13}C NMR spectrum of compound 34b ($CDCl_3$, 298 K)

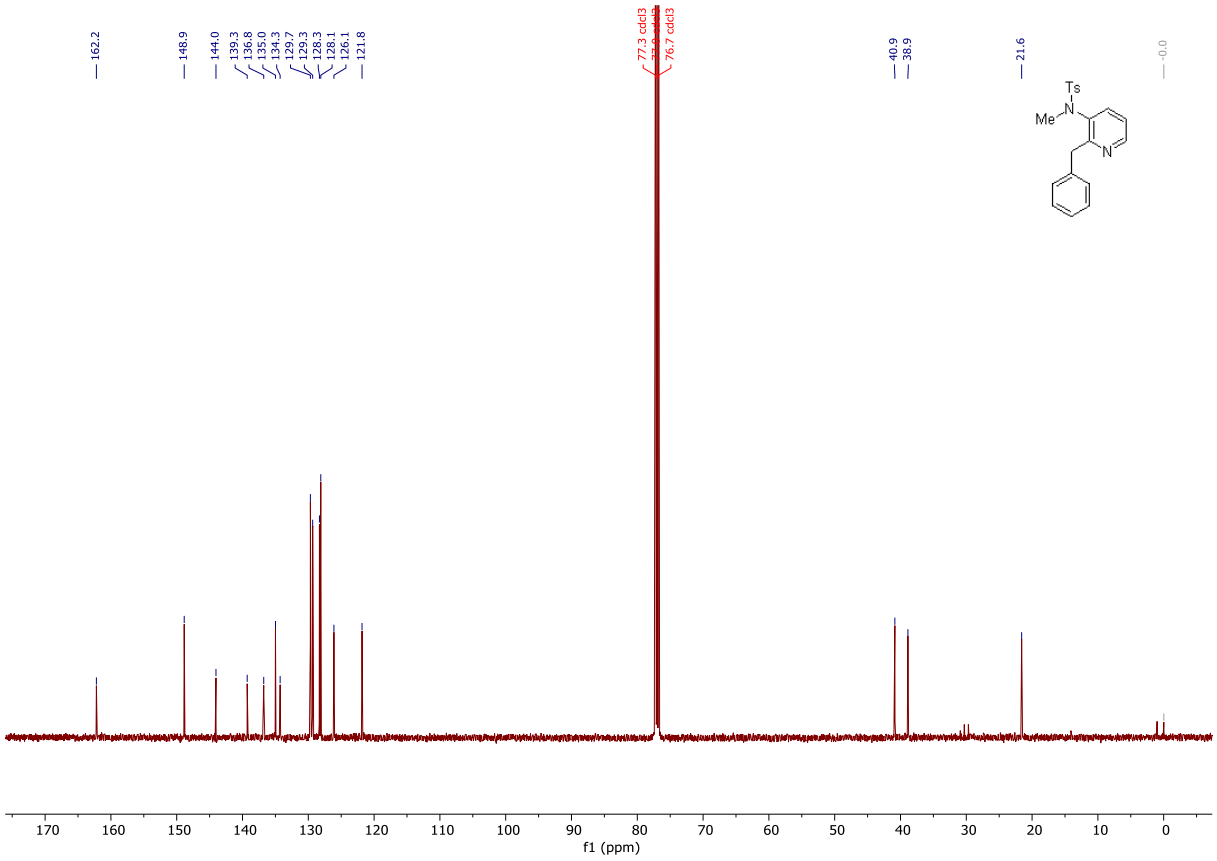

^{1}H NMR spectrum of compound 35a ($CDCl_3$, 298 K)

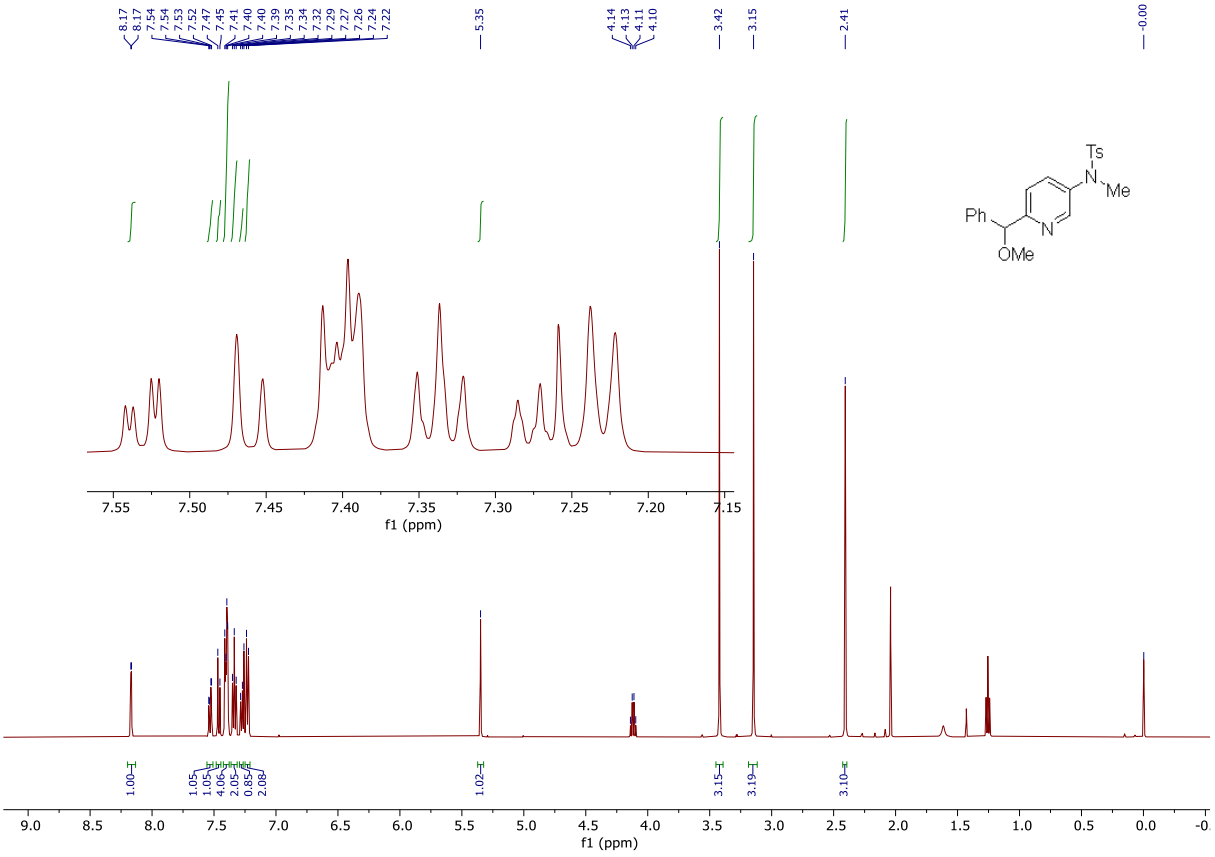

^{13}C NMR spectrum of compound 35a ($CDCl_3$, 298 K)

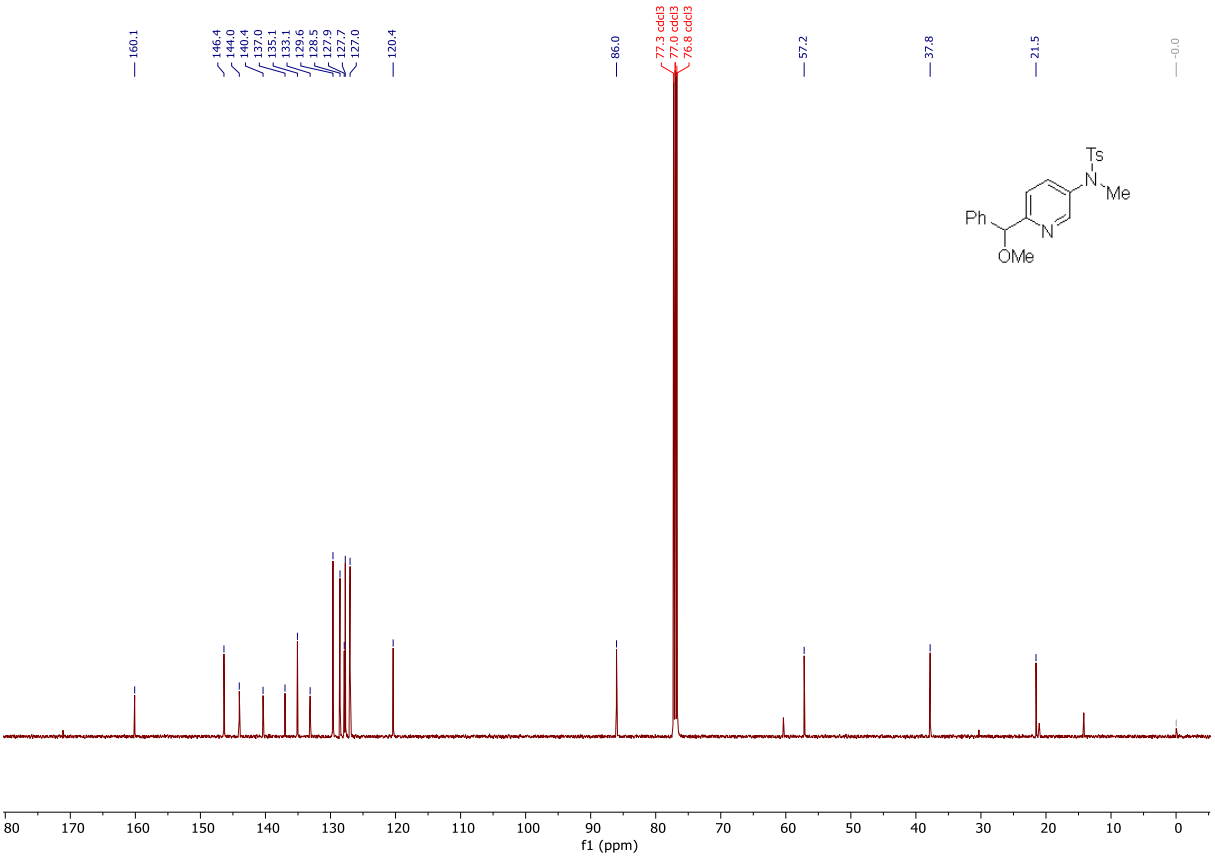

^{1}H NMR spectrum of compound 35b ($CDCl_3$, 298 K)

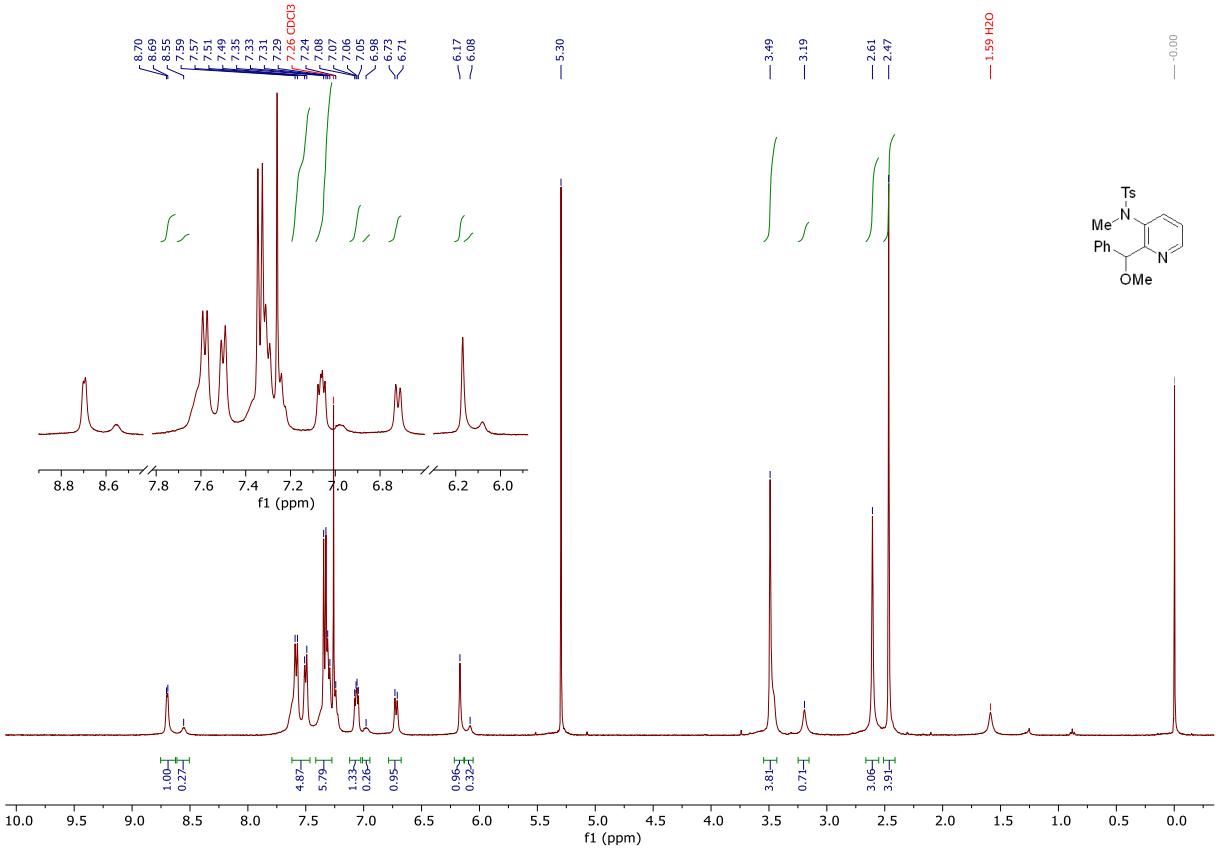

^{13}C NMR spectrum of compound 35b ($CDCl_3$, 298 K)

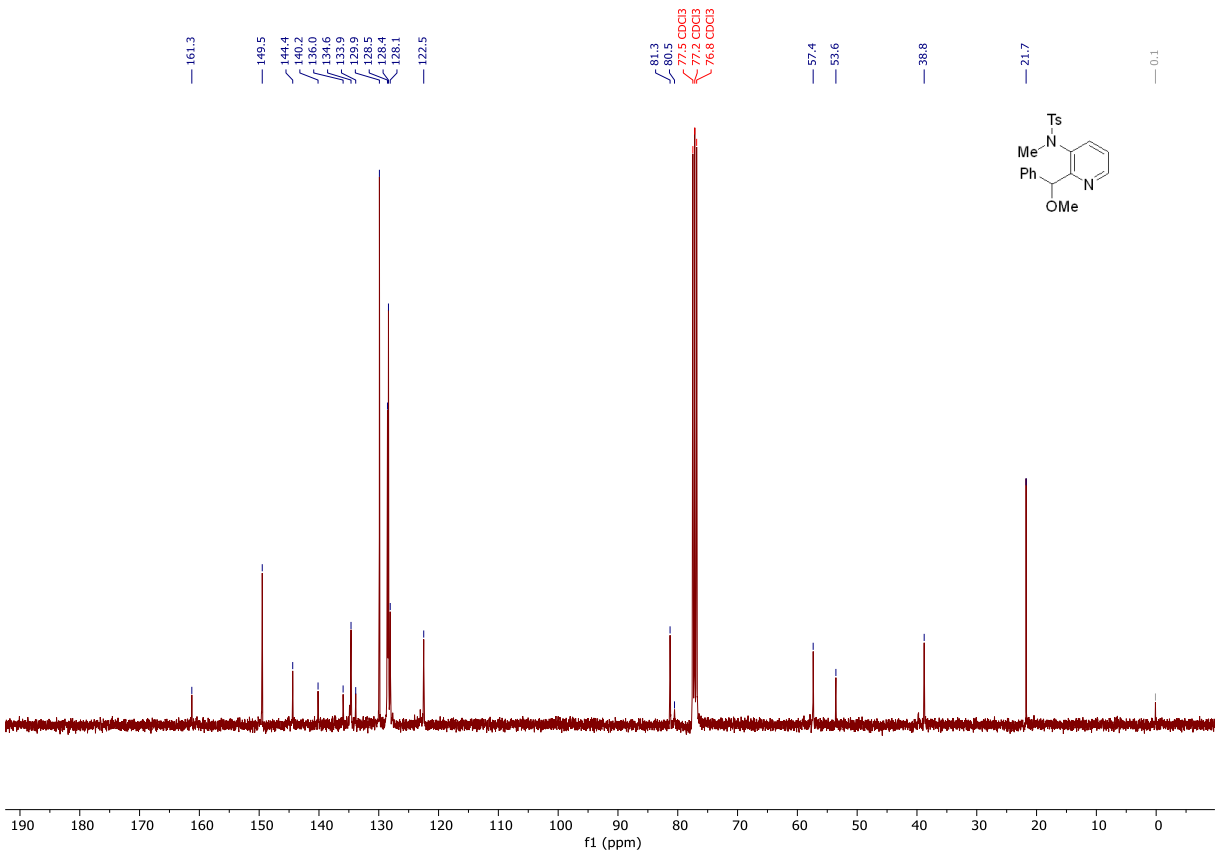

^{1}H NMR spectrum of compound 35b (CD_3OD, 298 K)

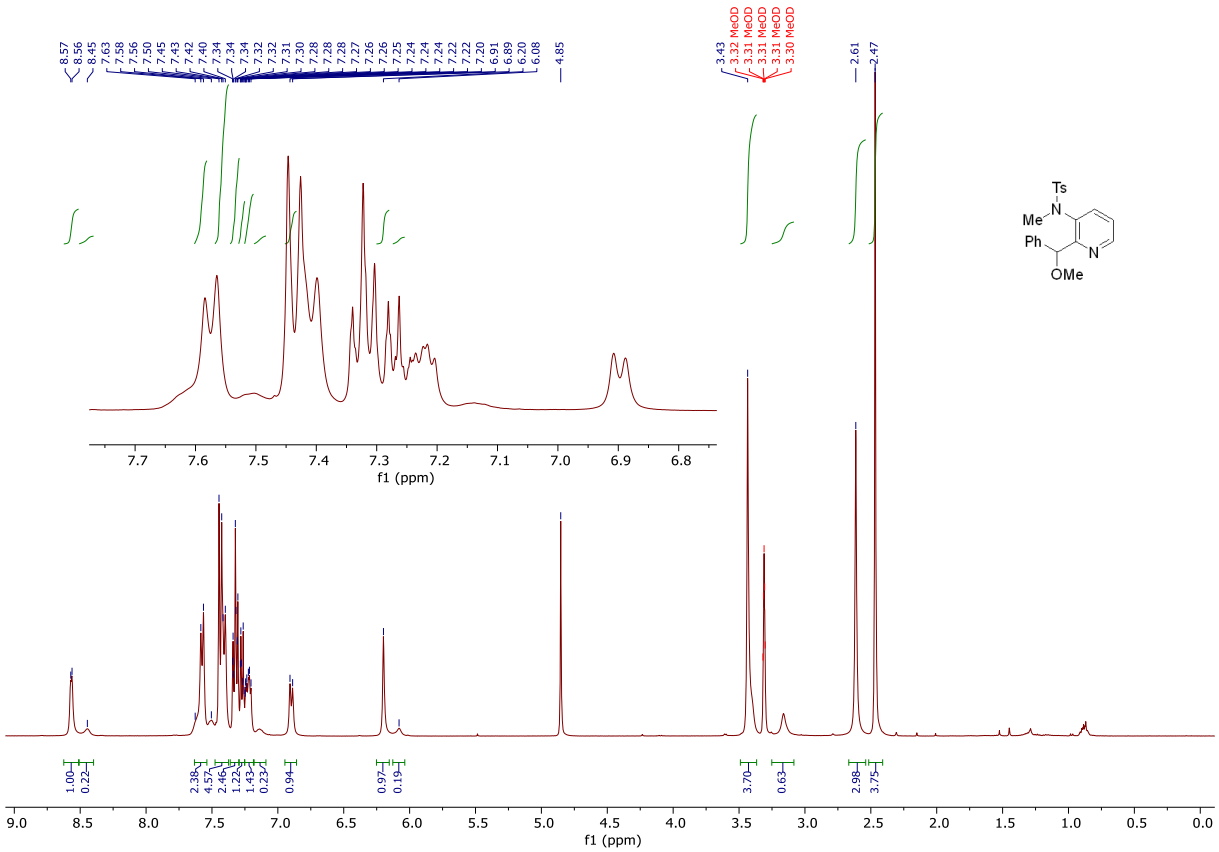

^{13}C NMR spectrum of compound 35b (CD_3OD, 298 K)

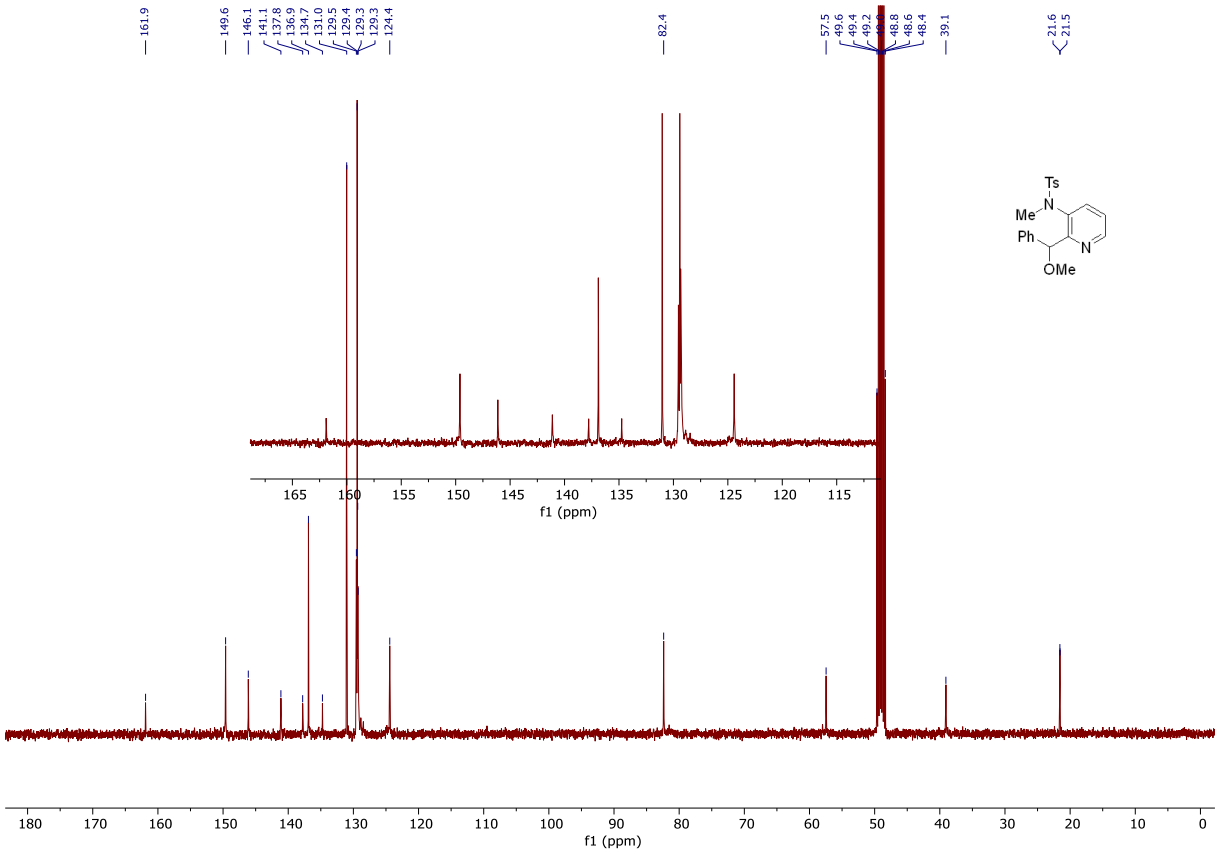

^{1}H NMR spectrum of compound 35b (DMSO-d_6, 298 K)

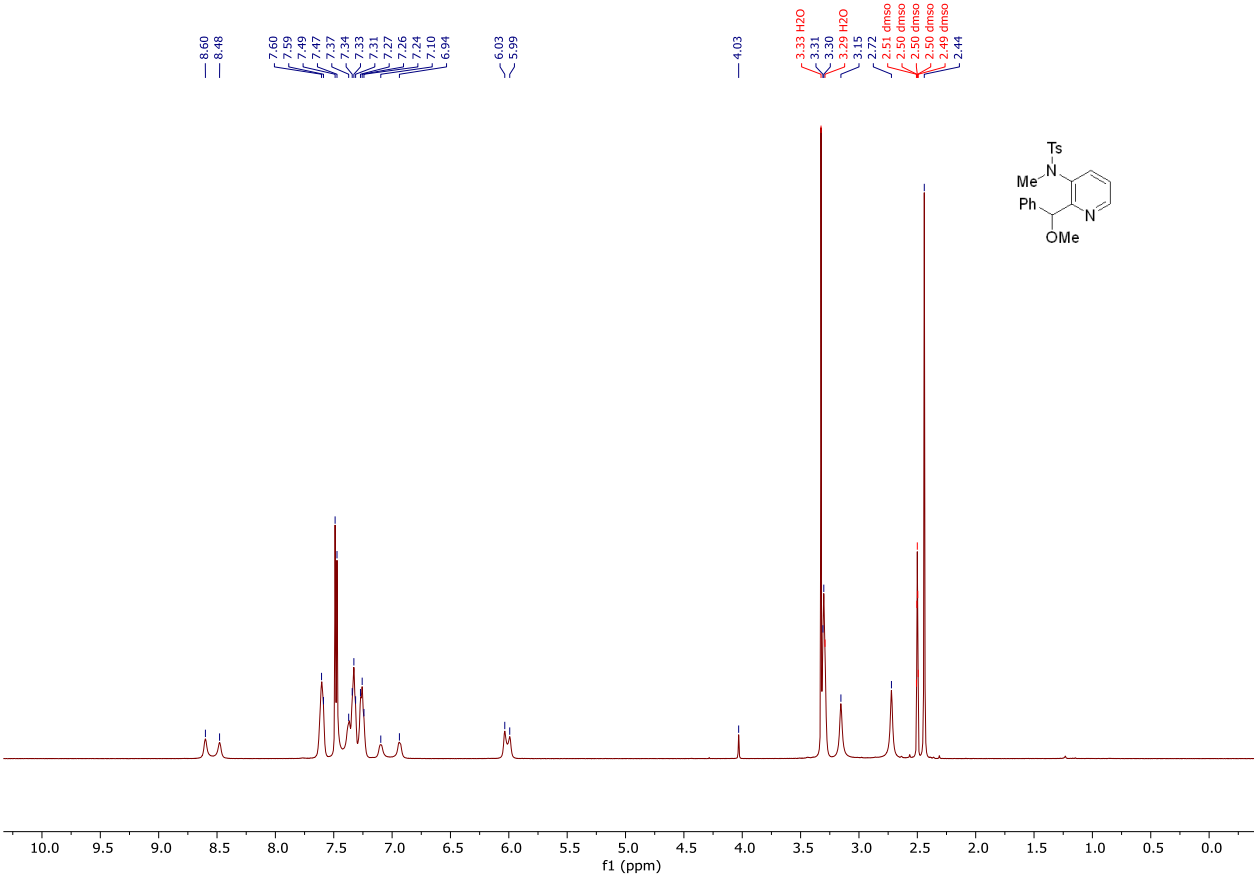

^{1}H NMR spectrum of compound 35b (DMSO-d_6, 353 K)

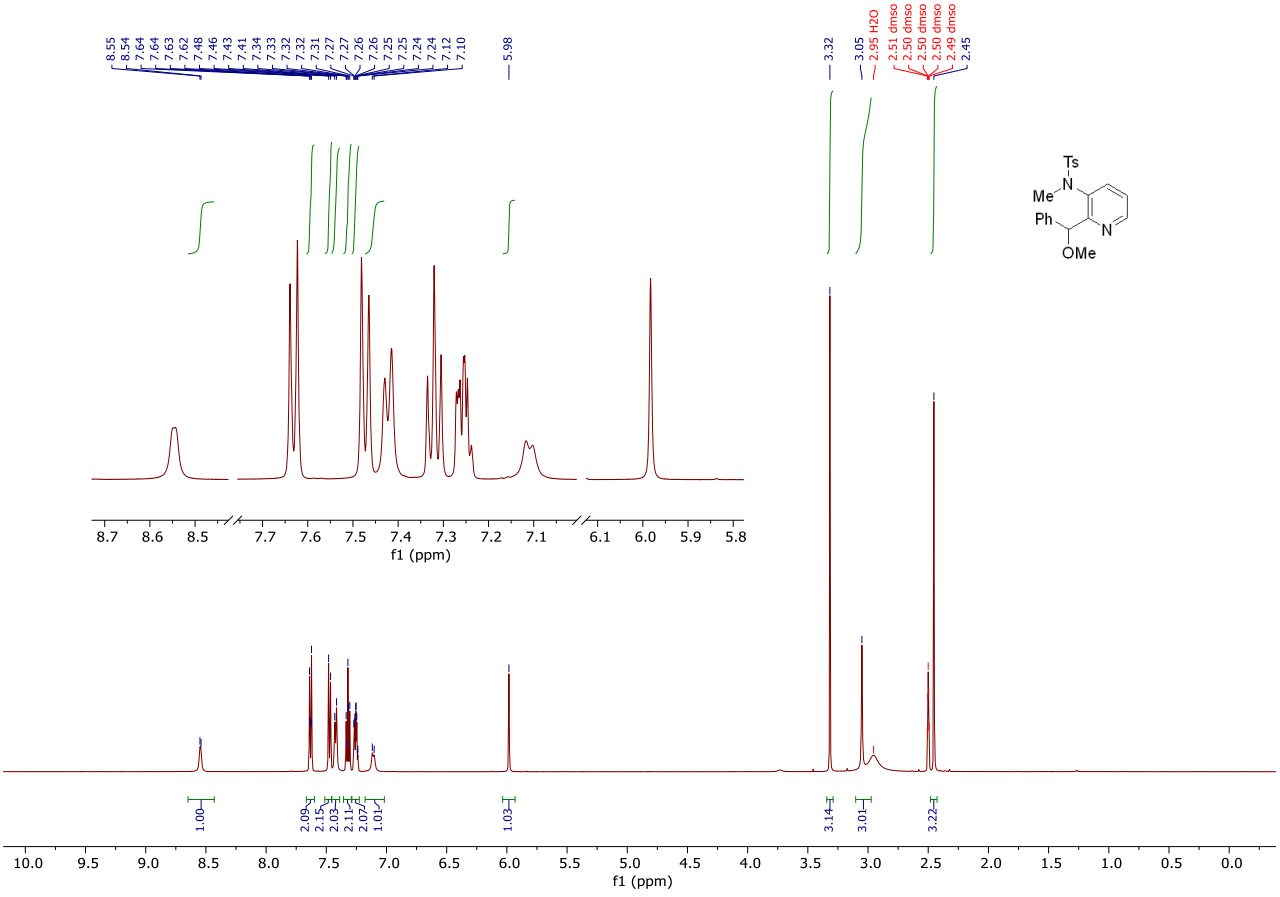

^{13}C NMR spectrum of compound 35b (DMSO-d$_6$, 353 K)

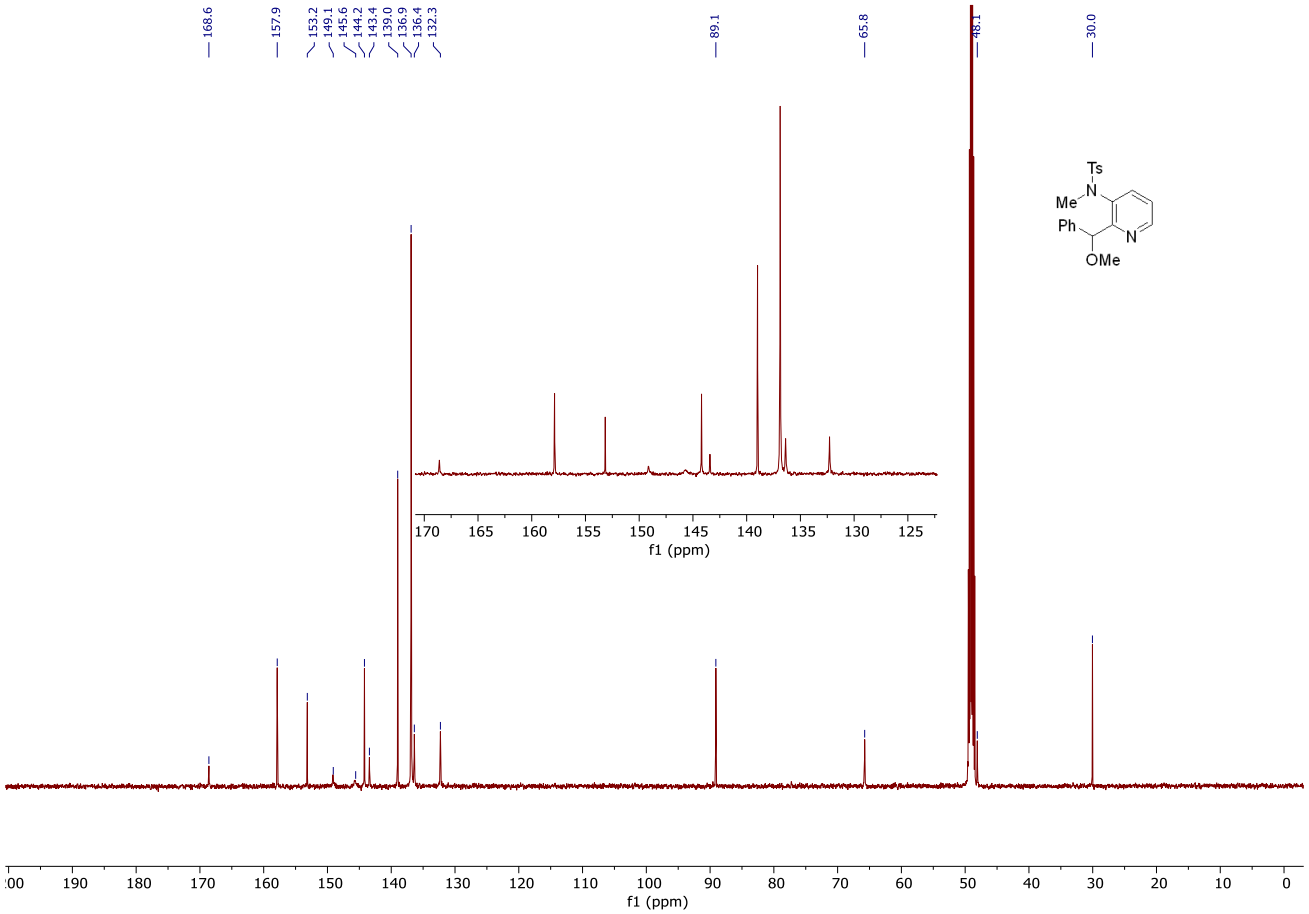

LR-MS chromatogram of compound 35b

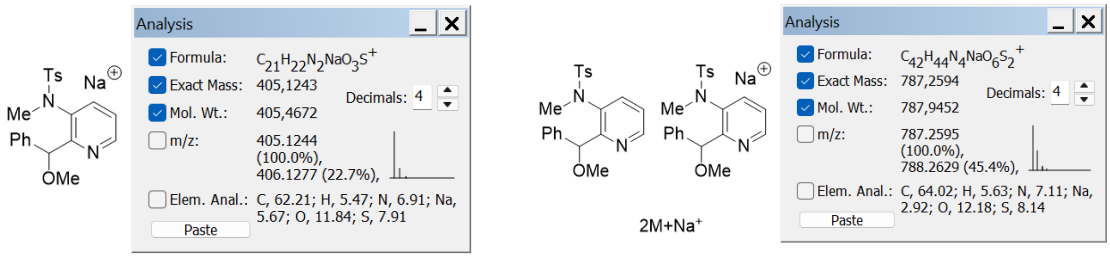

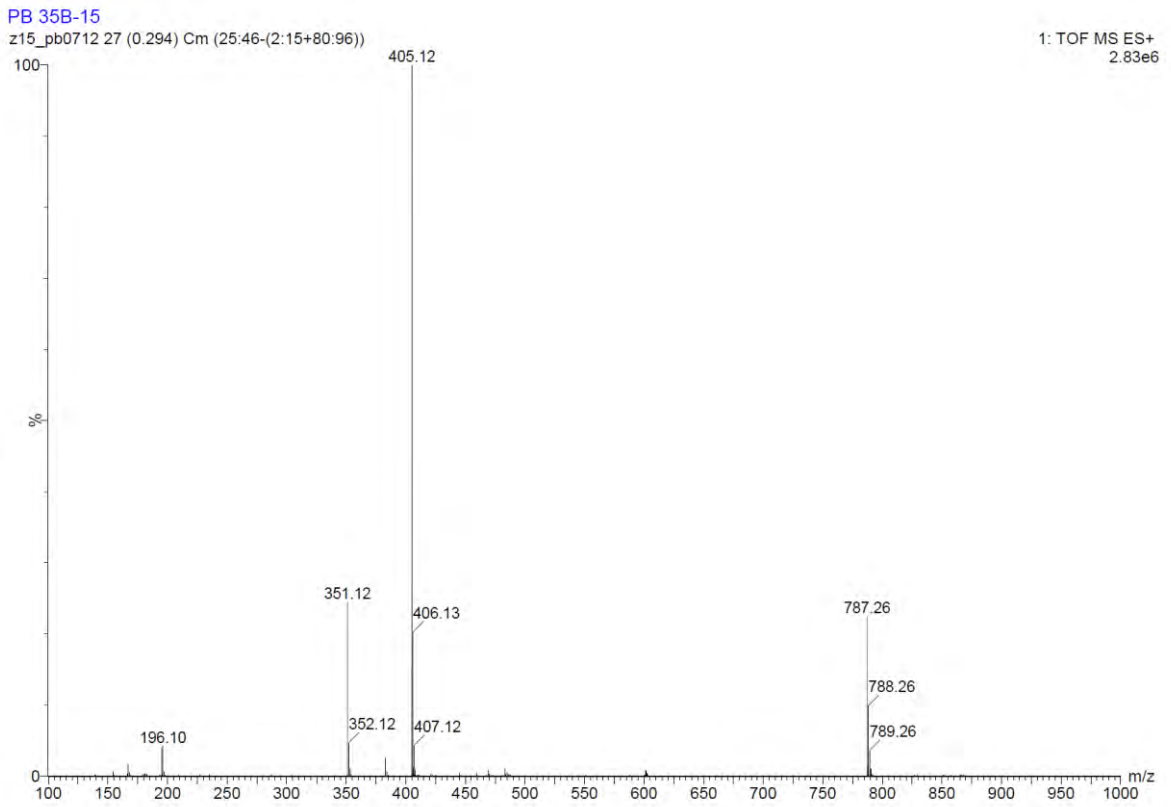

GC-FID chromatogram of compound 35b

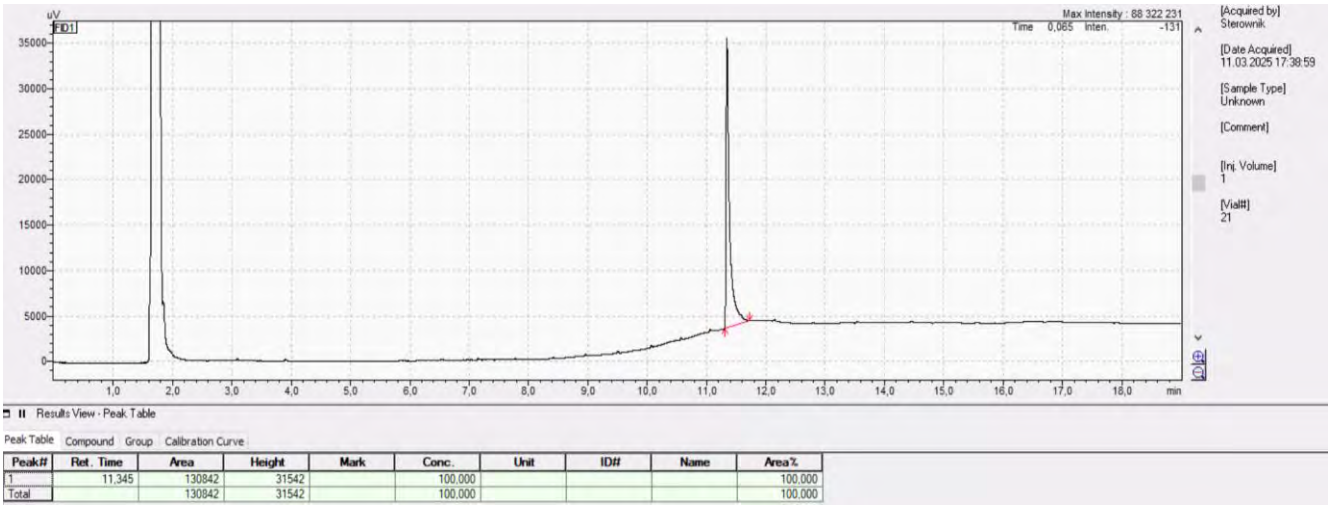

^{1}H NMR spectrum of salt Py-salt (DMSO-d_6, 298 K)

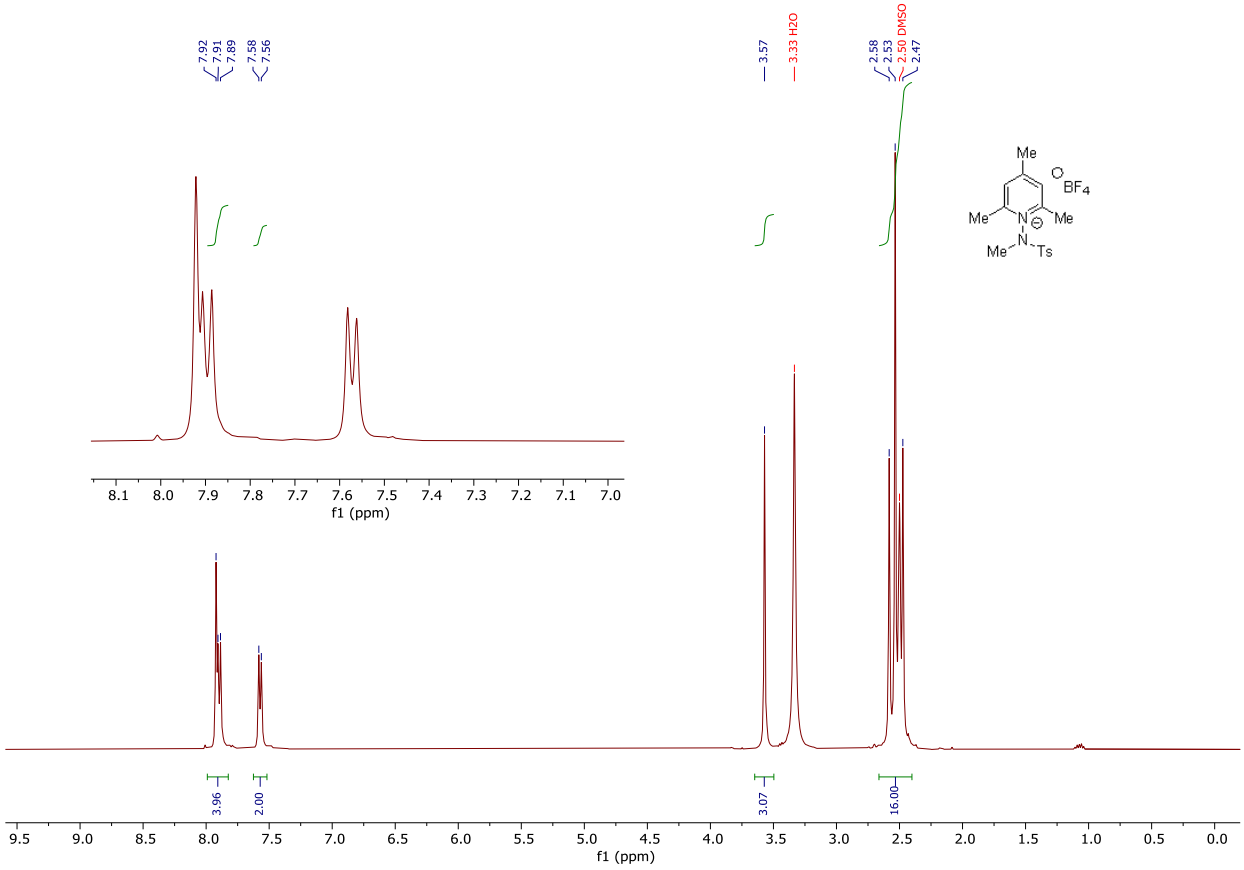

^{1}H NMR spectrum of compound 36 ($CDCl_3$, 298 K)

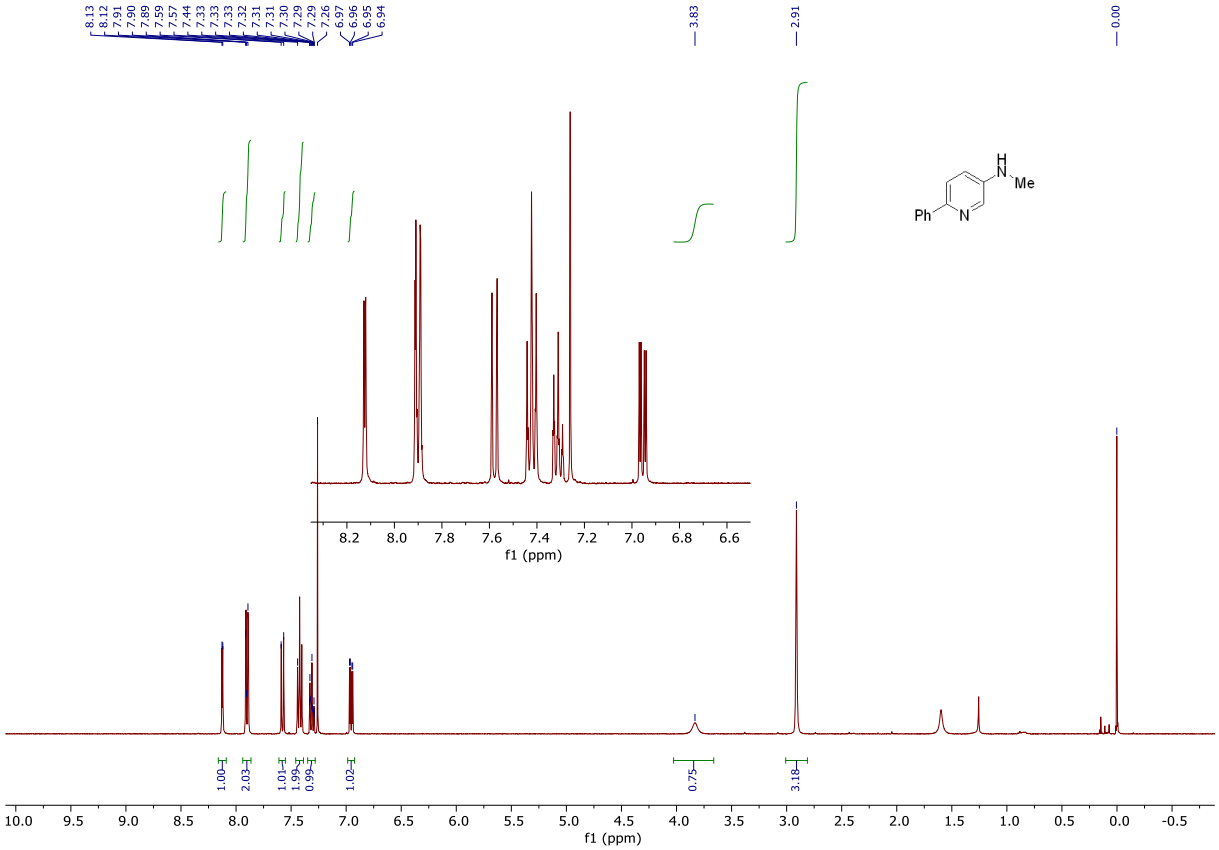

^{13}C NMR spectrum of compound 36 ($CDCl_3$, 298 K)

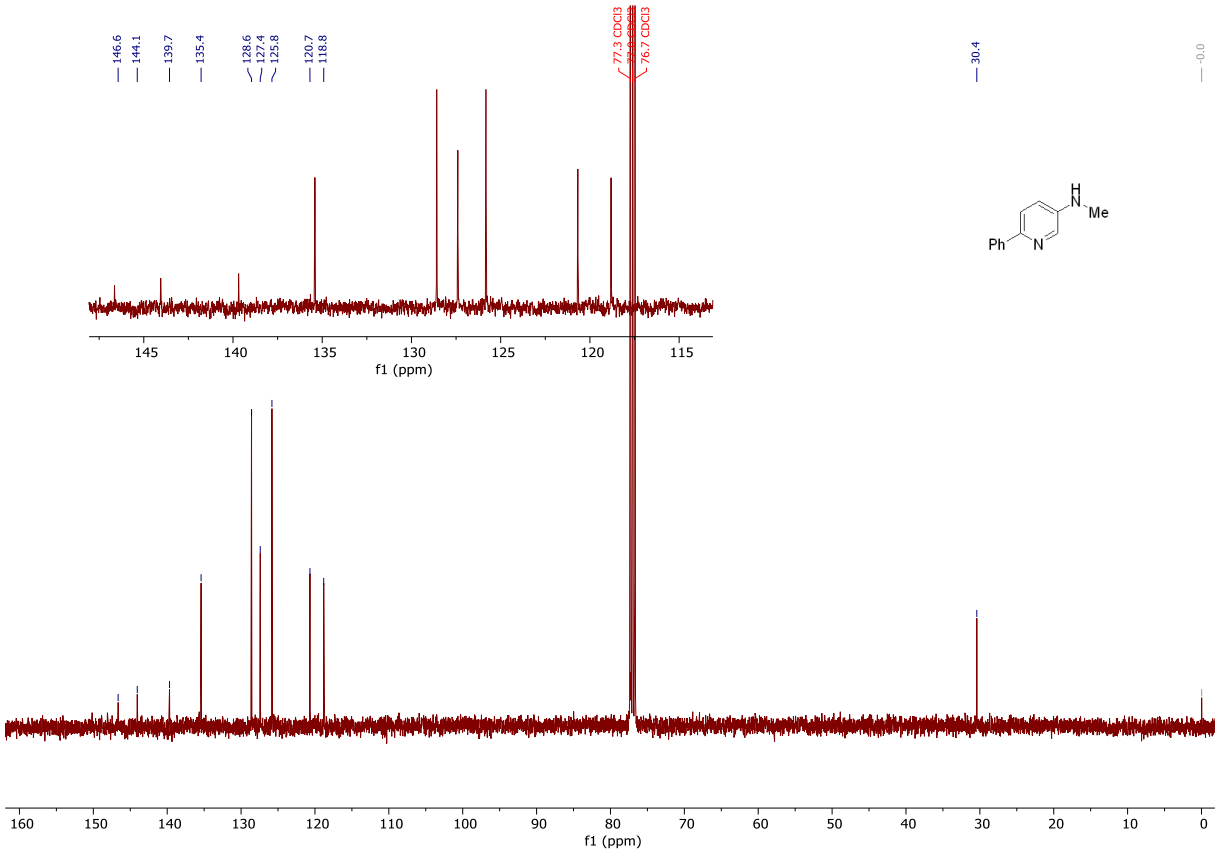

^{1}H NMR spectrum of compound 37 ($CDCl_3$, 298 K)

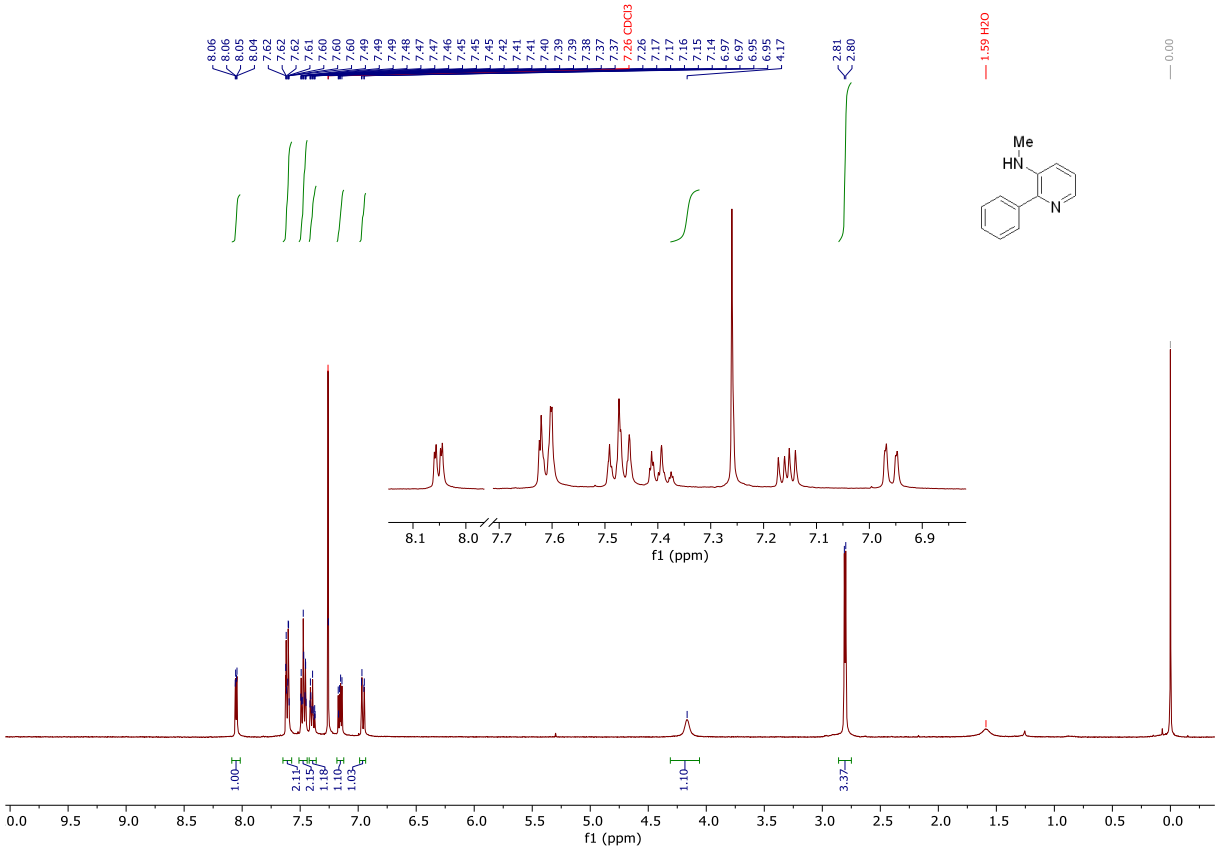

^{13}C NMR spectrum of compound 37 ($CDCl_3$, 298 K)

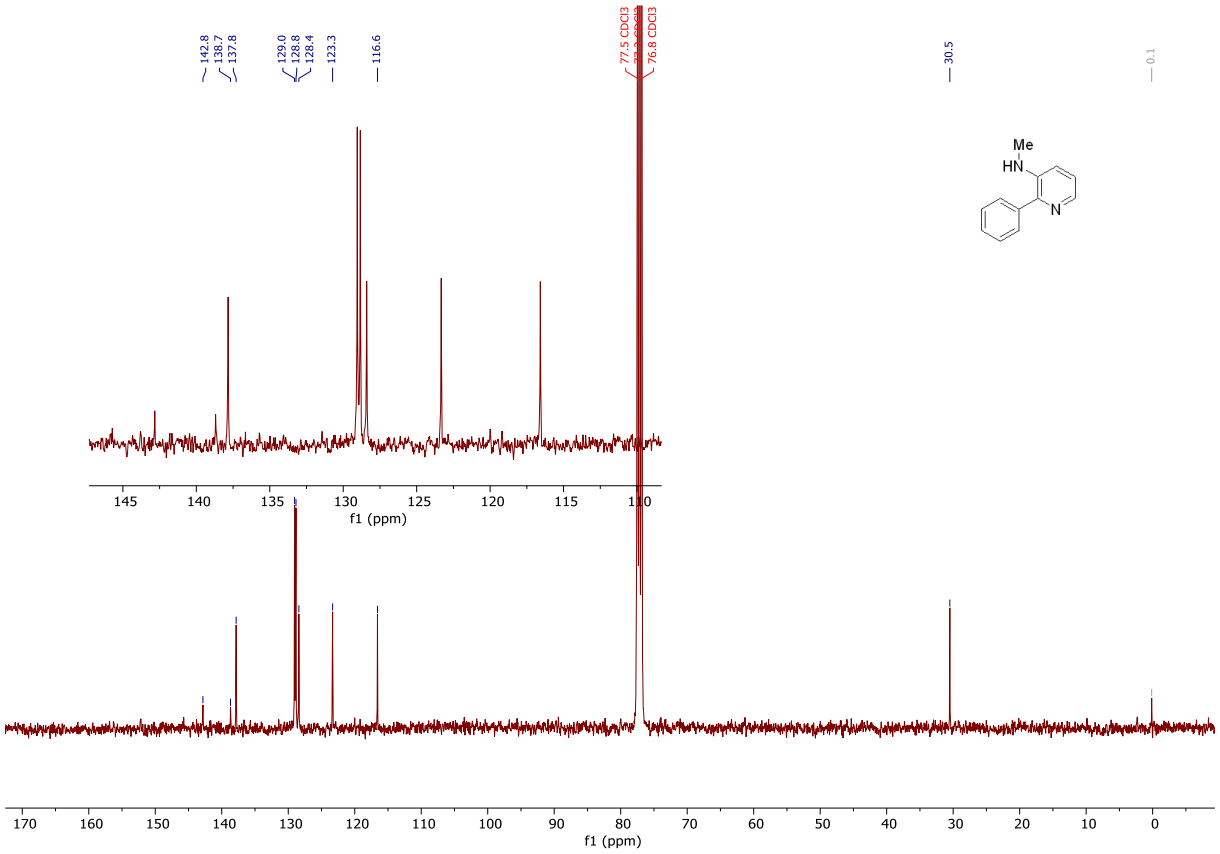

^{1}H NMR spectrum of compound 38 ($CDCl_3$, 298 K)

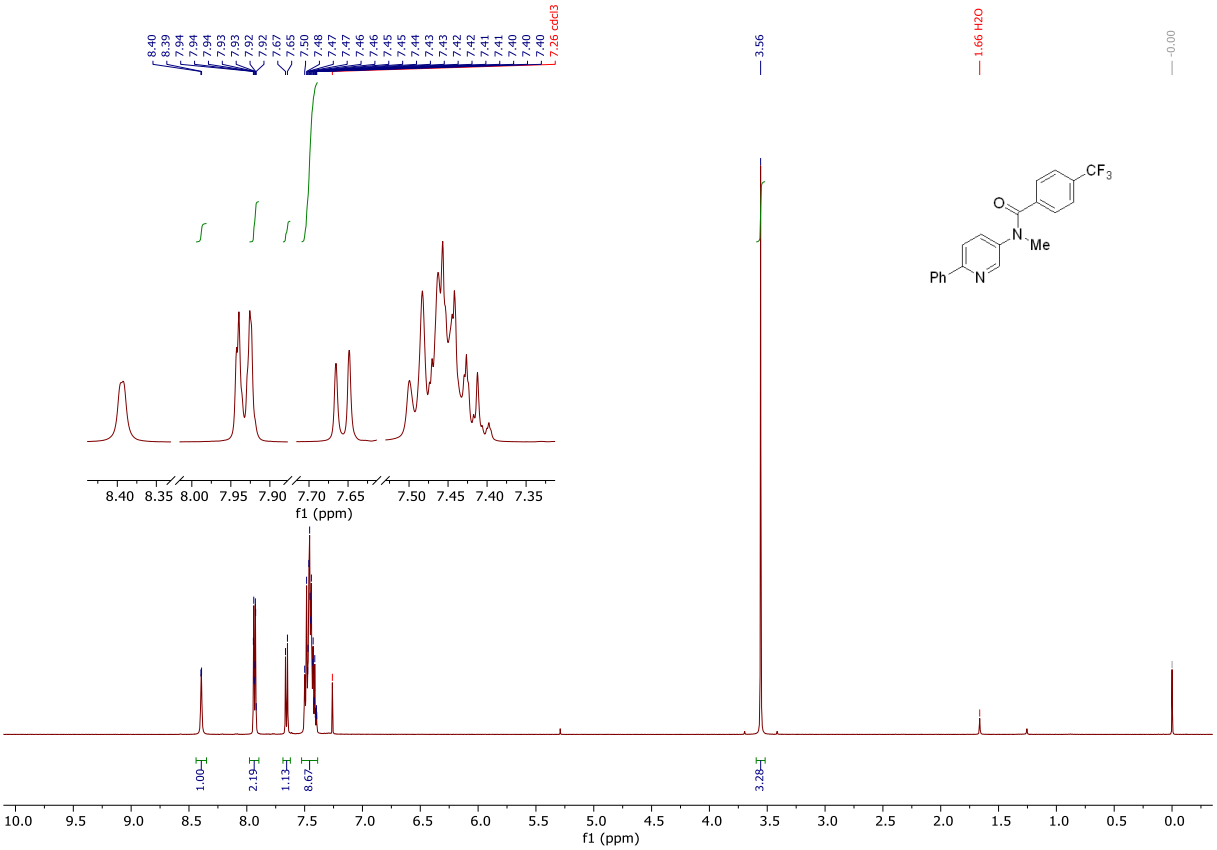

^{13}C NMR spectrum of compound 38 ($CDCl_3$, 298 K)

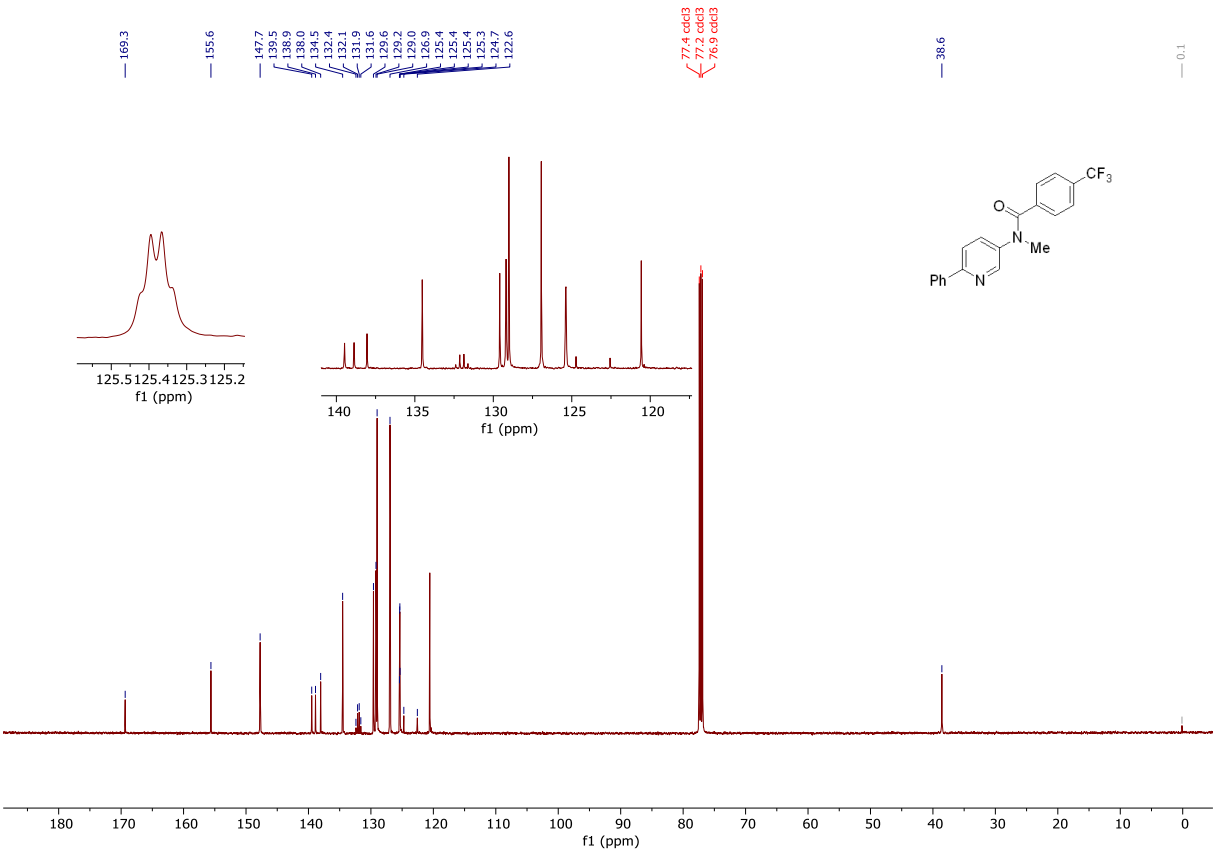

^{19}F NMR spectrum of compound 38 ($CDCl_3$, 298 K)

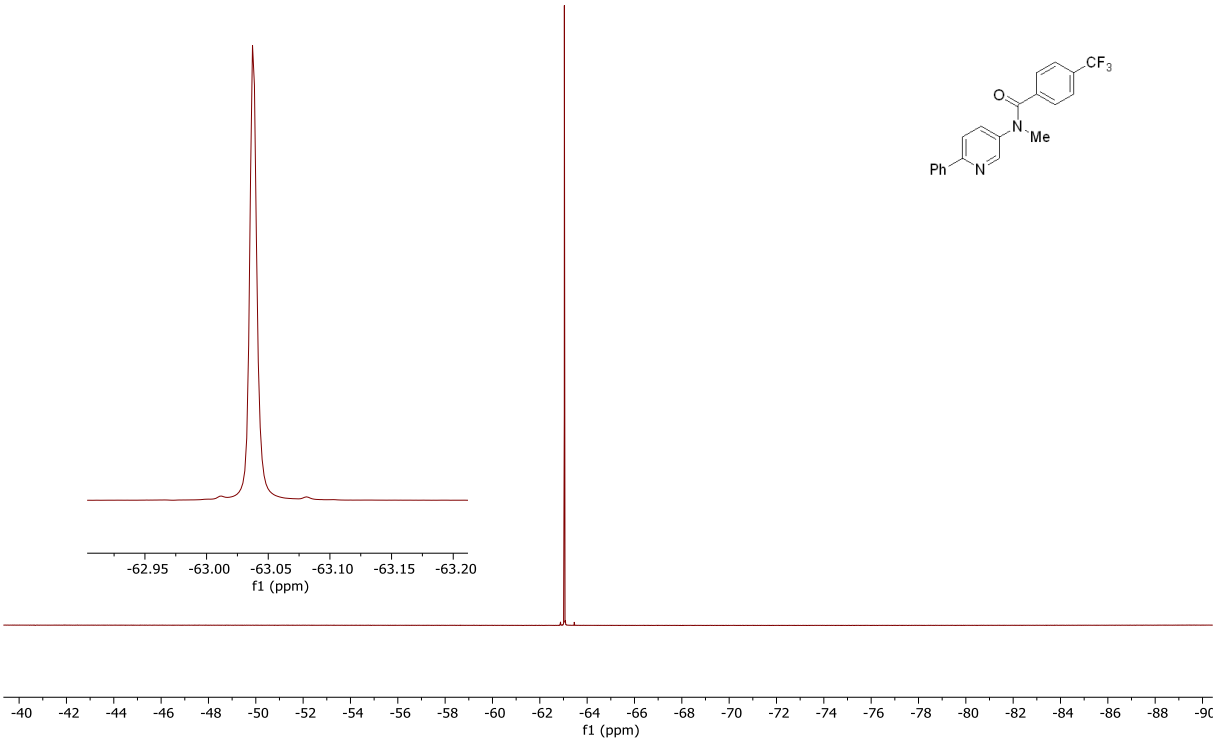

^{1}H NMR spectrum of compound 39 ($CDCl_3$, 298 K)

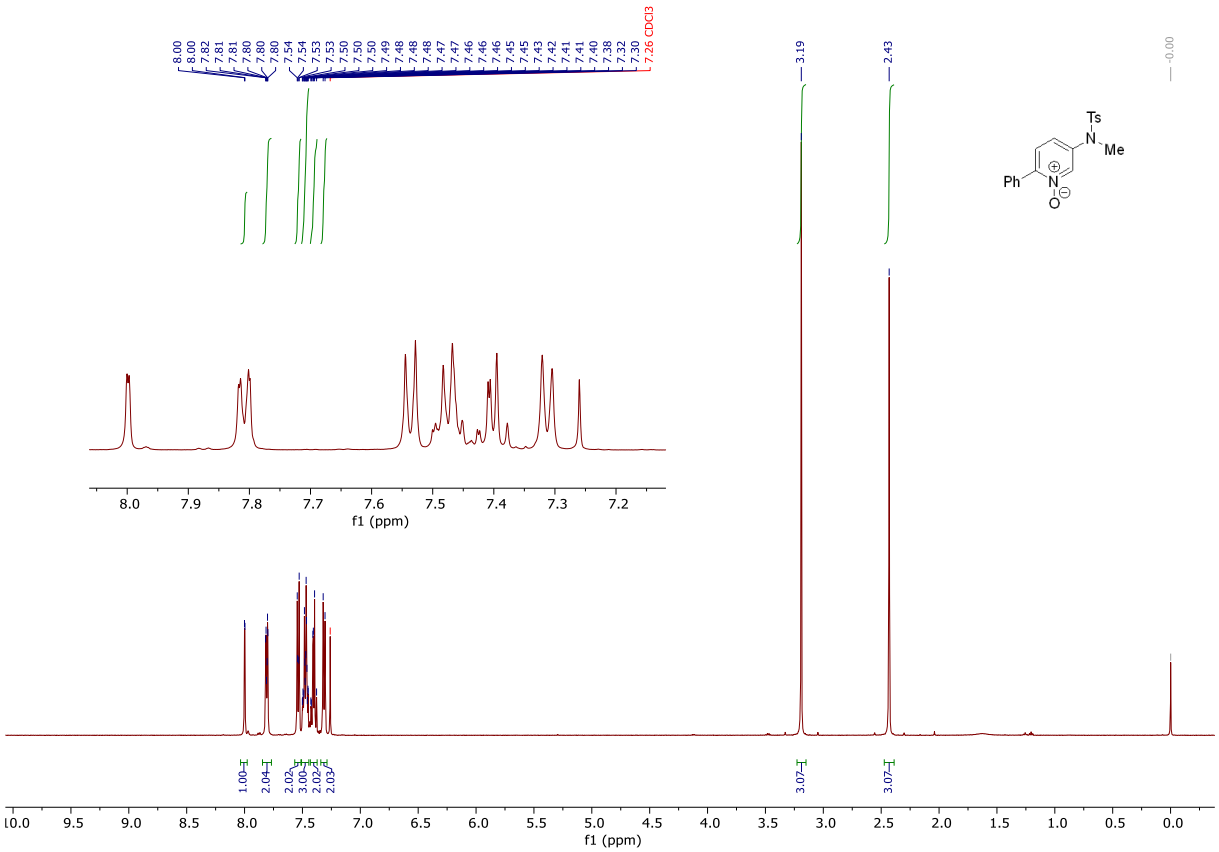

^{13}C NMR spectrum of compound 39 ($CDCl_3$, 298 K)

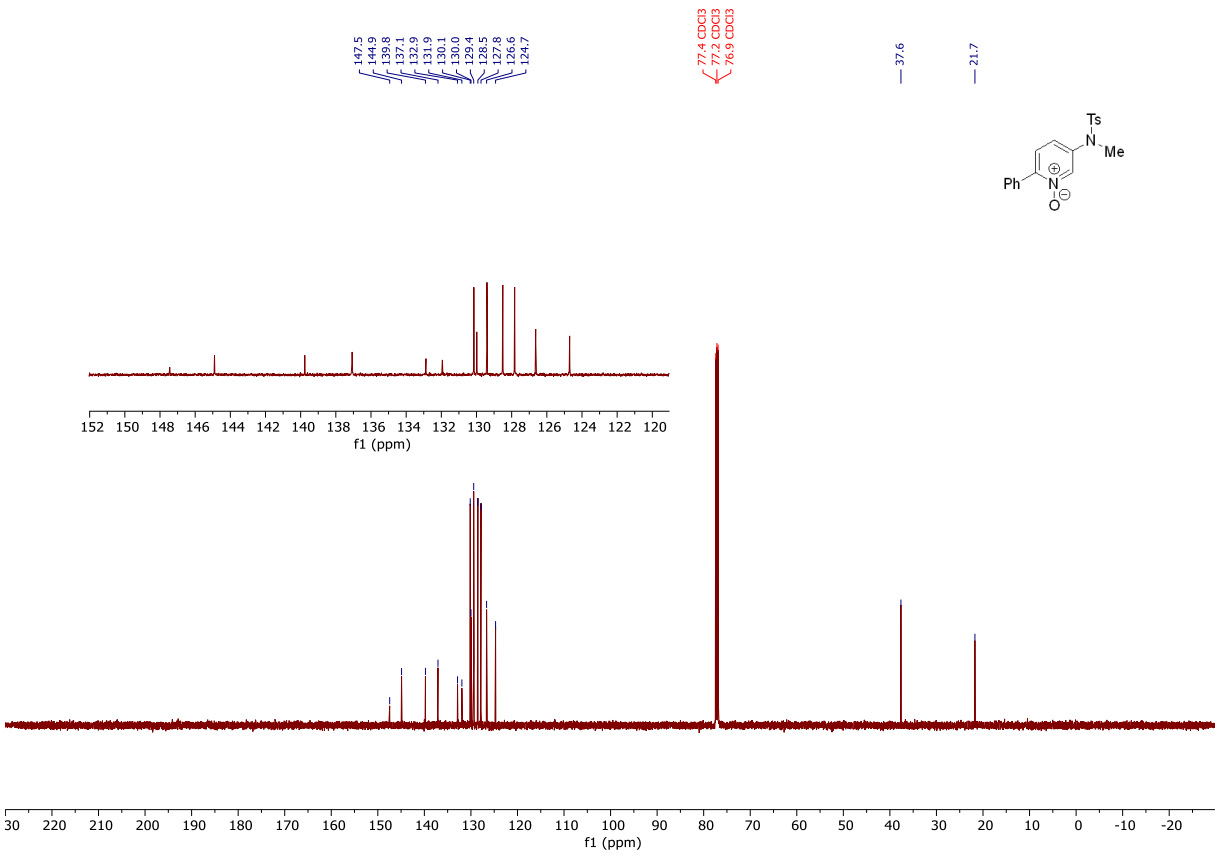

^{1}H NMR spectrum of compound 40 (DMSO-d_6, 298 K)

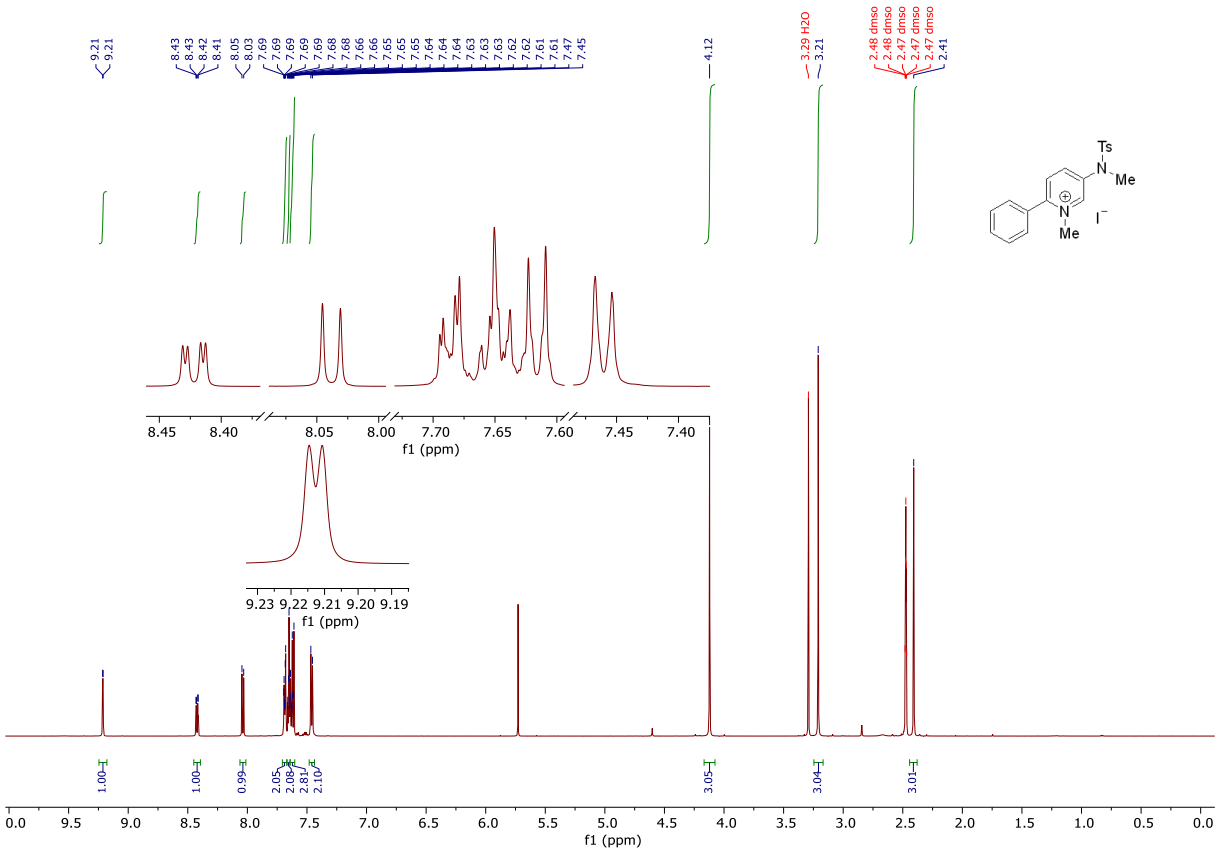

^{13}C NMR spectrum of compound 40 (DMSO-d_6, 298 K)

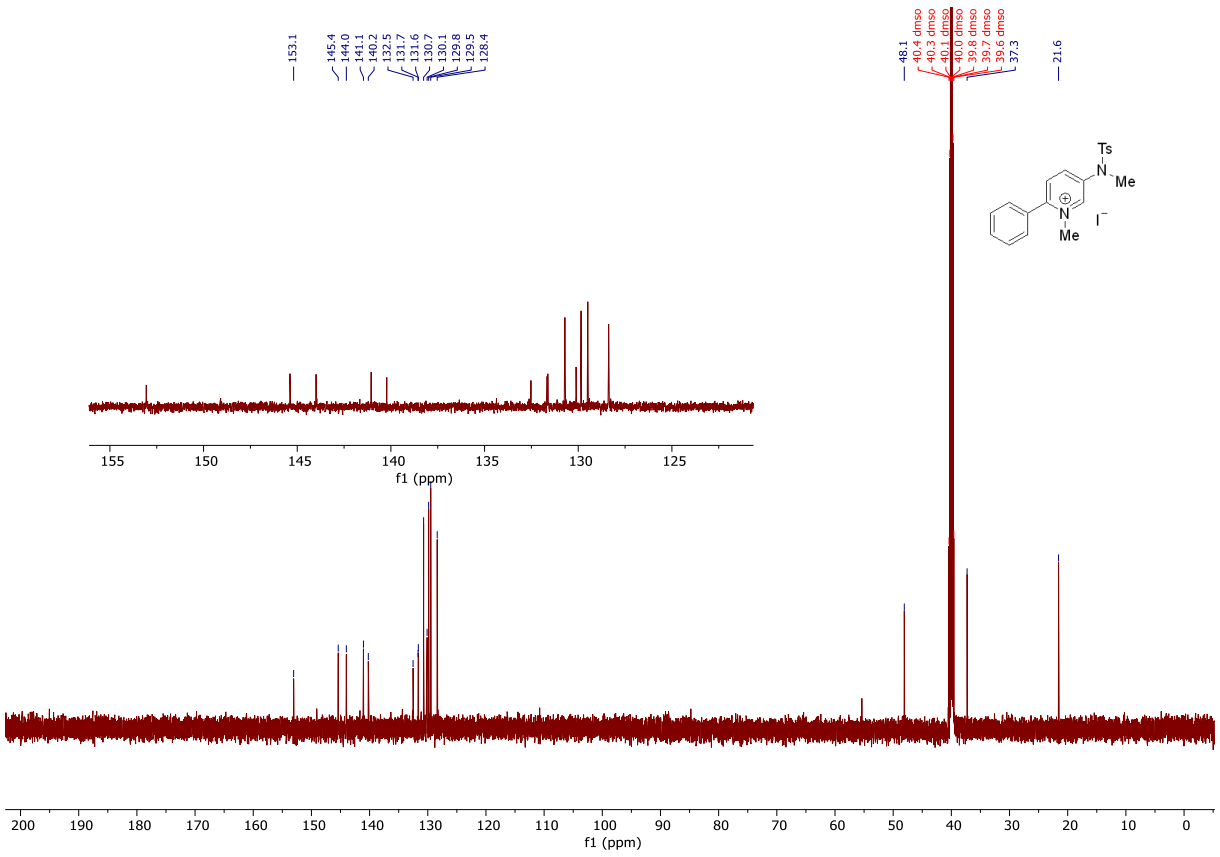

^{1}H NMR spectrum of compound 41a ($CDCl_3$, 298 K)

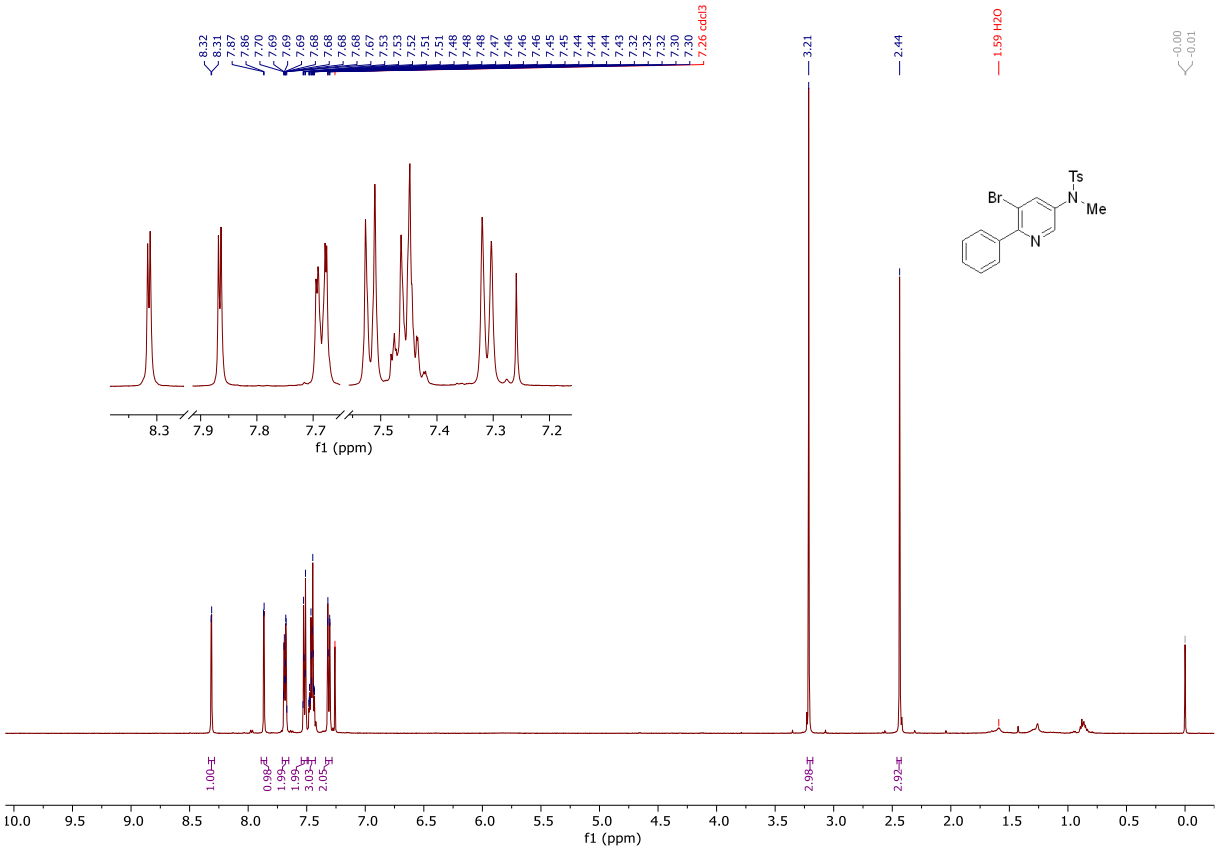

^{13}C NMR spectrum of compound 41a ($CDCl_3$, 298 K)

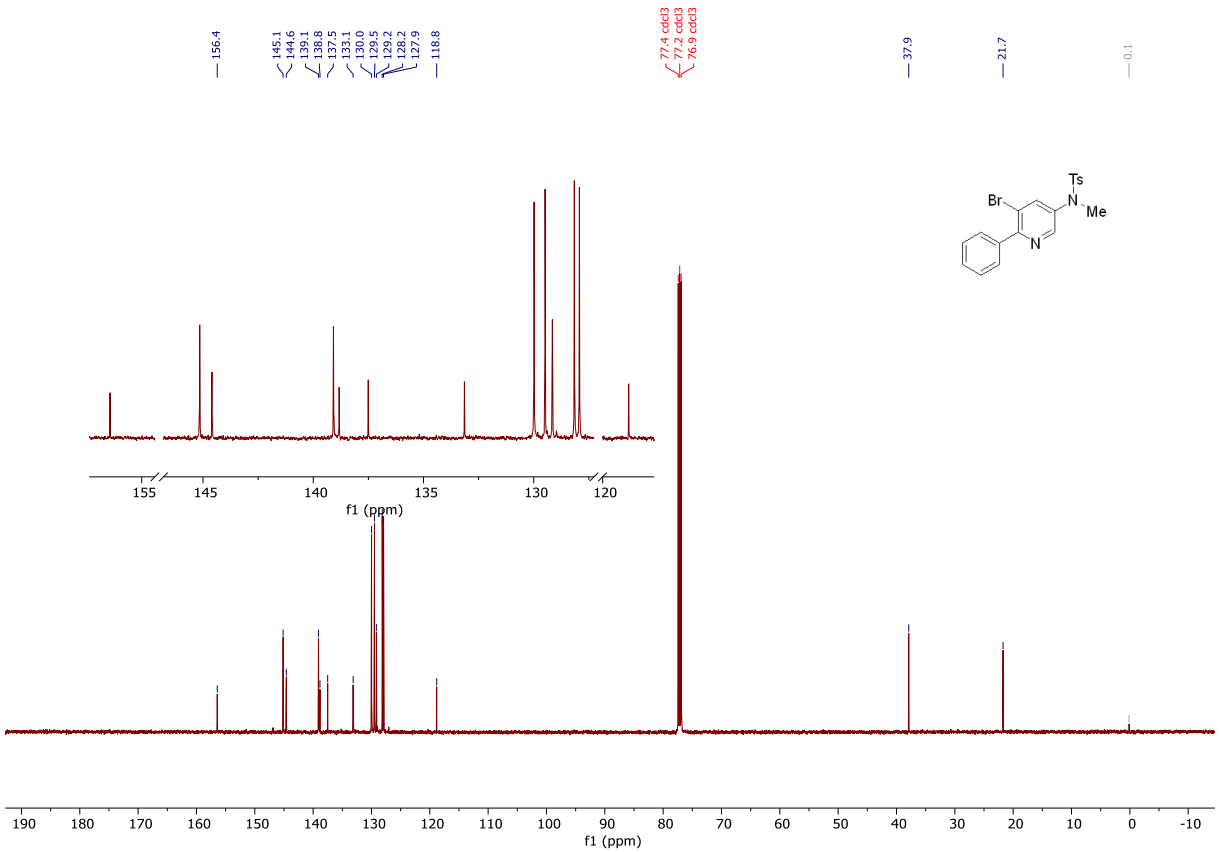

^{1}H NMR spectrum of compound 41b ($CDCl_3$, 298 K)

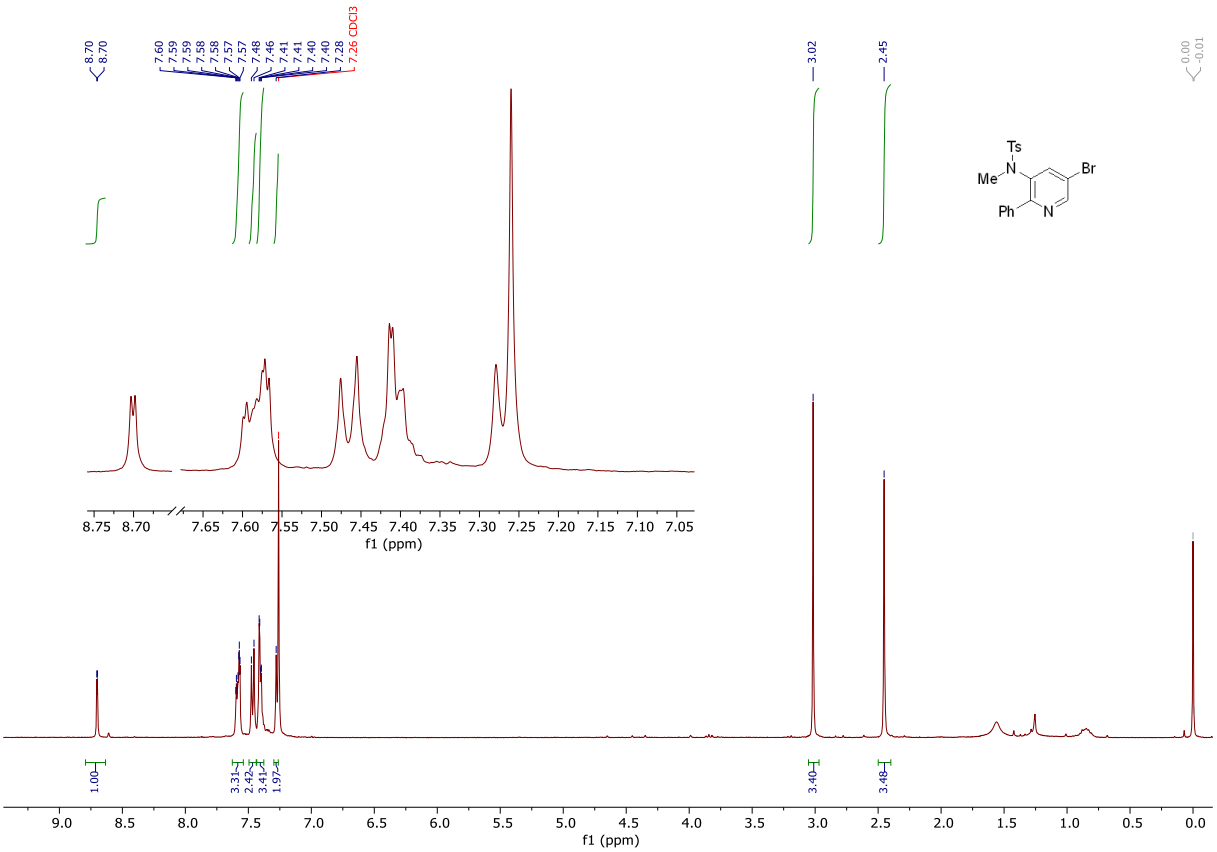

^{13}C NMR spectrum of compound 41b ($CDCl_3$, 298 K)

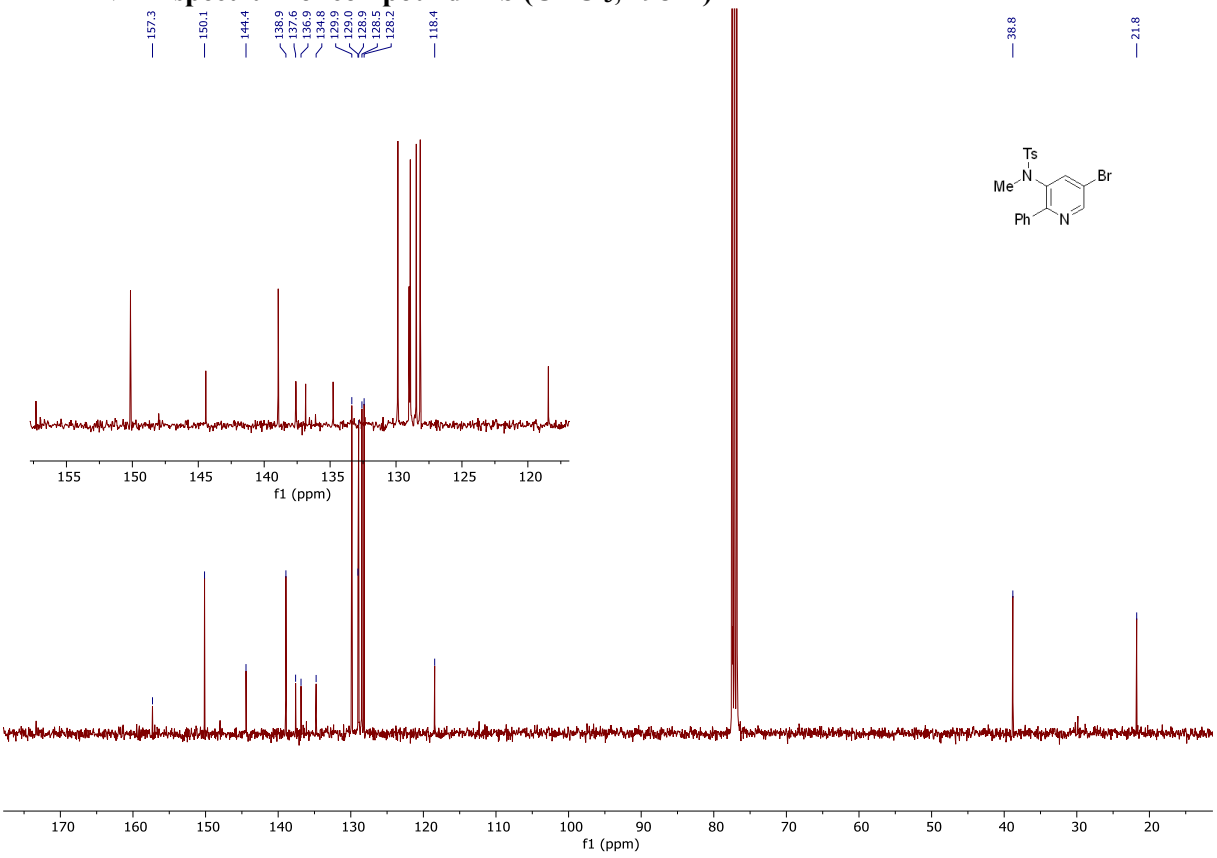

7. Crystallographic data for intermediate 2a

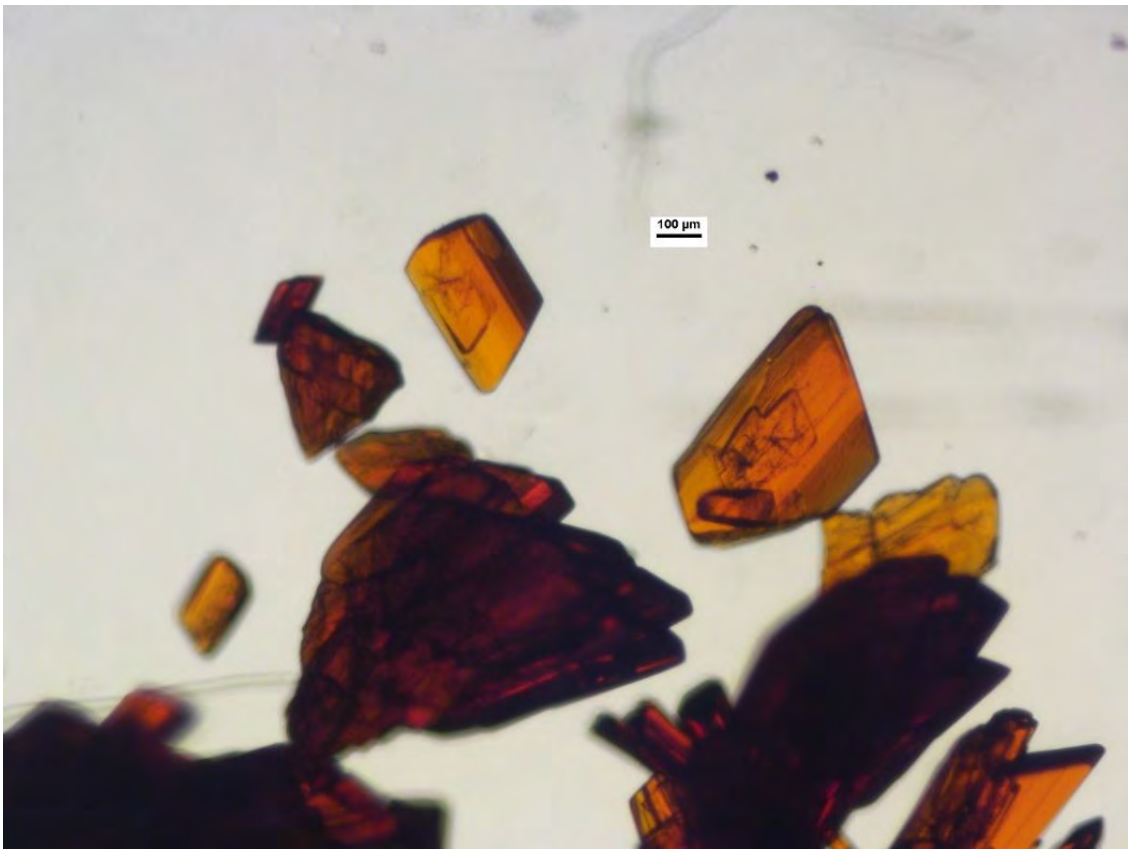

Supplementary Figure 18. Photography of a **2a** monocrystal.

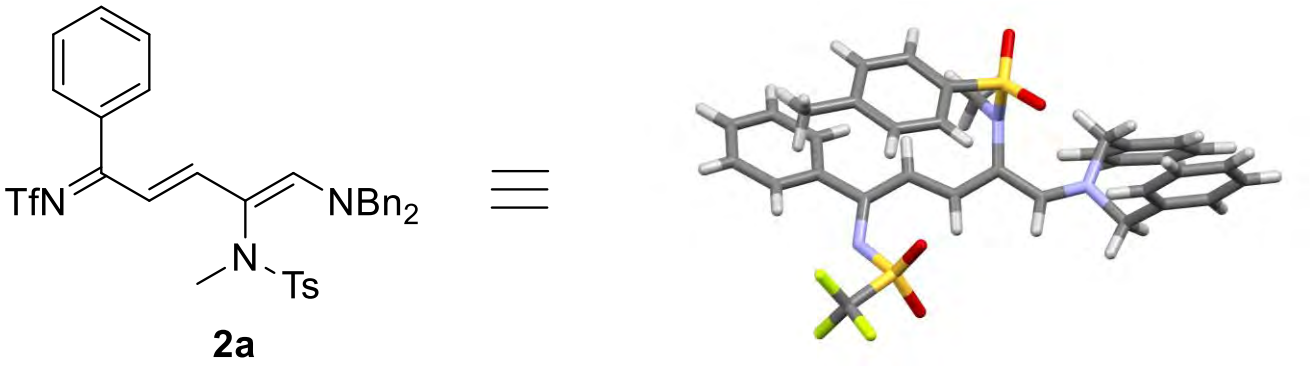

Supplementary Figure 19. Mercury drawing of **2a**.

A single crystal of $C_{34}H_{32}F_3N_3O_4S_2$ was prepared by slow evaporation of a DCM/ n-hexane solution. The suitable crystals of compounds 1-5 were mounted in paratone oil onto a nylon loop. All data were collected at 100.0(1) K, using a SuperNova Agilent, HyPix fitted with CuKα radiation (λ = 1.54184 Å). Data collection and unit cell refinement were performed using *CrysAlisPro* software.[5] The total number of data was measured in the 7.02° < 2θ < 140.112°, for compound 1, using ω scans. Data processing and absorption correction, giving minimum and maximum transmission factors (0.586, 0.754 for the compound, it was accomplished with

CrysAlisPro. All non-H atoms were refined with anisotropic displacement parameters. All hydrogen atom positions were determined by geometry and refined by a riding model.

Supplementary Table 12. Crystallographic data for the measured crystal.

Identification code	Compound ***2c-int.***
Empirical formula	$C_{34}H_{32}F_3N_3O_4S_2$
Formula weight	710.21
Crystal system	Triclinic
Space group	*P-1*
a (Å)	10.3347(3)
b (Å)	12.7875(5)
c (Å)	13.8621(5)
α (°)	113.322(4)
β (°)	95.246(3)
γ (°)	96.184(3)
Volume (Å^3)	1654.34(11)
Z	2
ρ (calc.)	1.426
λ	1.54184
Temp. (K)	100.0(1)
Crystal Size(mm)	0.220x 0.170x 0.110
Crystal Color	red
Crystal Morphology	prism
F(000)	738
μ (mm^{-1})	2.724
T_{min}, T_{max}	0.586, 0.754
$2\theta_{range}$ (°)	7.02 to 140.112
Reflections collected	15182
Independent reflections	6216 [R(int) = 0.0260]
Completeness	99.8%
Data / restraints / parameters	6216 / 0 / 444

Observed data [I > 2σ(I)]	5589
$wR(F^2$ all data)	0.0949
$R(F$ obsd data)	0.0356
Goodness-of-fit on F^2	1.008
largest diff. peak and hole (e $Å^{-3}$)	0.299 / -0.536

$$wR_2 = \{ \Sigma [w(F_o^2 - F_c^2)^2] / \Sigma [w(F_o^2)^2] \}^{1/2}$$

$$R_1 = \Sigma ||F_o| - |F_c|| / \Sigma |F_o|$$

8. Supplementary References

[1] B. T. Boyle, J. N. Levy, L. de Lescure, R. S. Paton, A. McNally, *Science* **2022**, *378*, 773–779.

[2] K. Goliszewska, K. Rybicka-Jasińska, J. Szurmak, D. Gryko, *J. Org. Chem.* **2019**, *84*, 15834–15844.

[3] K. F. Szabó, K. Goliszewska, J. Szurmak, K. Rybicka-Jasińska, D. Gryko, *Org. Lett.* **2022**, *24*, 8120–8124.

[4] J. Park, S. Chang, *Angew. Chemie Int. Ed.* **2015**, *54*, 14103–14107.

[5] S. Goggins, E. Rosevere, C. Bellini, J. C. Allen, B. J. Marsh, M. F. Mahon, C. G. Frost, *Org. Biomol. Chem.* **2014**, *12*, 47–52.

[6] S. Mo, Y. Zhu, Z. Shen, *Org. Biomol. Chem.* **2013**, *11*, 2756–2760.

[7] K. T. Hylland, I. L. Schmidtke, D. S. Wragg, A. Nova, M. Tilset, *Dalt. Trans.* **2022**, *51*, 5082–5097.

[8] L. Pignataro, M. Benaglia, R. Annunziata, M. Cinquini, F. Cozzi, *J. Org. Chem.* **2006**, *71*, 1458–1463.

[9] P. Sharma, S. Rohilla, N. Jain, *J. Org. Chem.* **2015**, *80*, 4116–4122.

[10] B. Qu, H. P. R. Mangunuru, S. Tcyrulnikov, D. Rivalti, O. V Zatolochnaya, D. Kurouski, S. Radomkit, S. Biswas, S. Karyakarte, K. R. Fandrick, J. D. Sieber, S. Rodriguez, J.-N. Desrosiers, N. Haddad, K. McKellop, S. Pennino, H. Lee, N. K. Yee, J. J. Song, M. C. Kozlowski, C. H. Senanayake, *Org. Lett.* **2018**, *20*, 1333–1337.

[11] M. S. M. Holmsen, A. Nova, K. Hylland, D. S. Wragg, S. Øien-ØDegaard, R. H. Heyn, M. Tilset,

Chem. Commun. **2018**, *54*, 11104–11107.

[12] X. Rao, C. Liu, J. Qiu, Z. Jin, *Org. Biomol. Chem.* **2012**, *10*, 7875–7883.

[13] J. L. Bolliger, C. M. Frech, *Adv. Synth. Catal.* **2010**, *352*, 1075–1080.

[14] J. Martín, E. Gómez-Bengoa, A. Genoux, C. Nevado, *Angew. Chemie - Int. Ed.* **2022**, *61*, 1–7.

[15] P. Chatelain, C. Muller, A. Sau, D. Brykczyńska, M. Bahadori, C. N. Rowley, J. Moran, *Angew. Chemie - Int. Ed.* **2021**, *60*, 25307–25312.

[16] T. Nguyen, N. German, A. M. Decker, T. L. Langston, T. F. Gamage, C. E. Farquhar, J. X. Li, J. L. Wiley, B. F. Thomas, Y. Zhang, *J. Med. Chem.* **2017**, *60*, 7410–7424.

[17] Y. Zou, G. Yue, J. Xu, J. (Steve) Zhou, *European J. Org. Chem.* **2014**, *2014*, 5901–5905.

[18] X. Chen, W. J. Li, S. Li, J. Tang, X. Du, X. L. Zheng, M. L. Yuan, H. Y. Fu, R. X. Li, H. Chen, *J. Org. Chem.* **2020**, *85*, 622–632.

[19] Y. Nishigaya, K. Umei, D. Watanabe, Y. Kohno, S. Seto, *Tetrahedron* **2016**, *72*, 1566–1572.

[20] K. K. Y. Kung, V. K. Y. Lo, H. M. Ko, G. L. Li, P. Y. Chan, K. C. Leung, Z. Zhou, M. Z. Wang, C. M. Che, M. K. Wong, *Adv. Synth. Catal.* **2013**, *355*, 2055–2070.

[21] C. V. Reddy, J. V. Kingston, J. G. Verkade, *J. Org. Chem.* **2008**, *73*, 3047–3062.

[22] S. T. Hobson, J. D. Boecker, J. H. Gifford, T. L. Nohe, C. H. Wierks, *J. Heterocycl. Chem.* **2003**, *40*, 277–282.

[23] J. D. Selingo, J. W. Greenwood, M. K. Andrews, C. Patel, A. J. Neel, B. Pio, M. Shevlin, E. M. Phillips, M. L. Maddess, A. McNally, *J. Am. Chem. Soc.* **2024**, *146*, 936–945.

[24] H. Wang, M. F. Greaney, *Angew. Chemie - Int. Ed.* **2024**, *63*, DOI 10.1002/anie.202315418.

[25] H. M. H. Nguyen, D. C. Thomas, M. A. Hart, K. R. Steenback, J. N. Levy, A. McNally, *J. Am. Chem. Soc.* **2024**, *146*, 2944–2949.

[26] M. J. Frisch, G. W. Trucks, H. B. Schlegel, G. E. Scuseria, M. A. Robb, J. R. Cheeseman, G. Scalmani, V. Barone, G. A. Petersson, H. Nakatsuji, X. Li, M. Caricato, A. V. Marenich, J. Bloino, B. G. Janesko, R. Gomperts, B. Mennucci, H. P. Hratchian, J. V. Ortiz, A. F. Izmaylov, J. L. Sonnenberg, D. Williams-Young, F. Ding, F. Lipparini, F. Egidi, J. Goings, B. Peng, A. Petrone, T. Henderson, D. Ranasinghe, V. G. Zakrzewski, J. Gao, N. Rega, G. Zheng, W. Liang, M. Hada, M. Ehara, K. Toyota, R. Fukuda, J. Hasegawa, M. Ishida, T. Nakajima, Y. Honda, O. Kitao, H. Nakai, T. Vreven, K. Throssell, J. A. Montgomery, Jr., J. E. Peralta, F. Ogliaro, M. J. Bearpark, J. J. Heyd, E. N. Brothers, K. N. Kudin, V. N. Staroverov, T. A. Keith, R. Kobayashi, J. Normand, K. Raghavachari, A.

P. Rendell, J. C. Burant, S. S. Iyengar, J. Tomasi, M. Cossi, J. M. Millam, M. Klene, C. Adamo, R. Cammi, J. W. Ochterski, R. L. Martin, K. Morokuma, O. Farkas, J. B. Foresman, D. J. Fox, *Gaussian 16, Revision C.01*, Gaussian, Inc., Wallingford CT **2016**.

[27] J.-D. Chai, M. Head-Gordon, *Phys. Chem. Chem. Phys.* **2008**, *10*, 6615–6620.

[28] F. Weigend, *Phys. Chem. Chem. Phys.* **2006**, *8*, 1057–1065.

[29] F. Weigend, R. Ahlrichs, *Phys. Chem. Chem. Phys.* **2005**, *7*, 3297–3305.

[30] A. V Marenich, C. J. Cramer, D. G. Truhlar, *J. Phys. Chem. B* **2009**, *113*, 6378–6396.

[31] C. Riplinger, F. Neese, *J. Chem. Phys.* **2013**, *138*, 34106.

[32] C. Riplinger, B. Sandhoefer, A. Hansen, F. Neese, *J. Chem. Phys.* **2013**, *139*, 134101.

[33] F. Neese, *WIREs Comput. Mol. Sci.* **2012**, *2*, 73–78.

[34] F. Neese, *WIREs Comput. Mol. Sci.* **2018**, *8*, e1327.

[35] F. Neese, F. Wennmohs, U. Becker, C. Riplinger, *J. Chem. Phys.* **2020**, *152*, 224108.

[36] F. Neese, F. Wennmohs, A. Hansen, U. Becker, *Chem. Phys.* **2009**, *356*, 98–109.

[37] C. Legault, *CYLview User Manual*, **2012**.

[38] R.I., Rodríguez, V., Corti, L. Rizzo, *et al*. *Nat Catal.,* **2004**, *7*, 1223–1231.

Photochemical C3-Amination of Pyridines via Zincke Imine Intermediates

XYZ Cartesian coordinates and energies for all the calculated structures

Kitti Franciska Szabó,[+[a]] Piotr Banachowicz,[+[a]] Antoni Powała,[[a,b]] Danijela Lunic,[[c]] Ignacio Funes Ardoiz,*[[c]] and Dorota Gryko*[[a]]

[a]*Institute of Organic Chemistry Polish Academy of Sciences; Kasprzaka 44/52, 01-224 Warsaw, Poland; correspondence: dorota.gryko@icho.edu.pl*

[b]*Department of Chemistry Warsaw University of Technology, Noakowskiego 3, 00-664 Warsaw, Poland*

[c]*Complejo Científico-Tecnológico Universidad de La Rioja, Madre de Dios, 53, 26004 Logroño, La Rioja, Spain; correspondence :ignacio.funesa@unirioja.es*

correspondence:

dorota.gryko@icho.edu.pl

ignacio.funesa@unirioja.es

XYZ Cartesian coordinates and energies for all the calculated structures

The final G energies are calculated by the sum of E(DLPNO-CCSD(T)) + E(SMD/wB97xD/Def2TZVPP) – E(gas/wB97xD/Def2TZVPP) + G_{Corr} (SMD/wB97xD/Def2SVP)

[Ir^{III}]*

E (DLPNO-CCSD(T)) =-1537.64664
E (SMD/wB97xD/Def2TZVPP) = -1540.72049
E (gas/wB97xD/Def2TZVPP) = -1540.673991
G_{Corr}= 0.421248

Ir	-0.33209600	0.23854900	-0.11266000
N	-0.21646900	2.29409100	0.10712100
C	-1.26505000	3.17329700	0.13632700
C	1.10363400	2.80189700	0.01454200
C	-1.10647900	4.52688300	0.09622400
H	-2.25902600	2.72412500	0.20461600
C	1.29245600	4.19486800	-0.03328900
C	0.22574200	5.07113500	0.01106300
H	-1.98354400	5.17525100	0.13102400
H	2.31123500	4.58176800	-0.11238800
H	0.38660900	6.15023000	-0.02585900
N	-2.51468300	0.14951600	-0.19227600
C	-3.34174600	0.11761000	0.85624600
C	-2.99817100	0.08623600	-1.45071800
C	-4.71886200	0.02800200	0.70575000
H	-2.87824300	0.16987200	1.84414500
C	-4.37463700	-0.00678900	-1.67311200
C	-5.23967000	-0.03468000	-0.58537800
H	-5.36318200	0.00702600	1.58516200
H	-4.76652100	-0.05946000	-2.68855400
H	-6.31719200	-0.10697700	-0.74615800
N	-0.17285000	0.13845600	2.13263700
C	-0.07410500	1.19681700	2.94482700
C	-0.15691500	-1.11107300	2.64218000
C	0.04218300	1.06841000	4.32106000
H	-0.09240700	2.17582400	2.46389100
C	-0.04355600	-1.31180600	4.02208400
C	0.05708000	-0.21407600	4.86656000
H	0.11872500	1.95888900	4.94574700
H	-0.03388600	-2.32164400	4.43131400
H	0.14717300	-0.35915800	5.94509600
C	-0.60630900	0.18194000	-2.07927400
C	-1.96526900	0.11822200	-2.50725000
C	0.39675300	0.20854900	-3.06869900
C	-2.27964100	0.08606300	-3.86871700
C	0.07385300	0.17039000	-4.42211700
H	1.44571200	0.25296000	-2.76938700
C	-1.26372400	0.11029100	-4.82274900
H	-3.31904200	0.04274400	-4.20003100
H	0.86768700	0.18857500	-5.17283100
H	-1.51802000	0.08231000	-5.88461200
C	1.68970400	0.43639700	-0.14229600
C	2.64732600	-0.57750400	-0.22574900
C	2.13491200	1.79325100	-0.05663700
C	4.01924800	-0.29213600	-0.23641100
H	2.32432400	-1.62062200	-0.29592100
C	3.52177800	2.06912200	-0.06280000
C	4.44930900	1.03695900	-0.15394700
H	4.74793600	-1.10407000	-0.30827500
H	3.87682900	3.10080400	0.00744500
H	5.51783000	1.26927200	-0.15810300
C	-0.36206100	-1.77730200	0.29006100
C	-0.48338700	-2.77899100	-0.68908600
C	-0.27017800	-2.18558400	1.63828400
C	-0.49963600	-4.12966100	-0.34154200
H	-0.55694200	-2.50621600	-1.74421900
C	-0.28841100	-3.54500600	1.98321100
C	-0.40159000	-4.51783300	0.99635800
H	-0.58993200	-4.88680800	-1.12509400
H	-0.21361700	-3.85249000	3.02833700
H	-0.41445300	-5.57537800	1.26892900

[Ir^{III}]

E (DLPNO-CCSD(T)) =-1537.772353
E (SMD/wB97xD/Def2TZVPP) =-1540.820225
E (gas/wB97xD/Def2TZVPP) = -1540.774413
G_{Corr}= 0.427103

Ir	-0.33929200	0.21533300	0.01050800
N	-0.17999100	2.37880600	-0.07791200
C	-1.21041900	3.23306000	-0.09266800
C	1.08990300	2.84025900	-0.13982600
C	-1.03748900	4.60699700	-0.16727700
H	-2.20792100	2.79060600	-0.04184700
C	1.33203600	4.21754700	-0.22127600
C	0.26402500	5.10440000	-0.23417200
H	-1.90559300	5.26701200	-0.17520000
H	2.35435300	4.59123200	-0.27653400
H	0.44560600	6.17943100	-0.29727400
N	-2.50782800	0.14872400	-0.09826000
C	-3.33860500	0.12588900	0.95087400
C	-2.99847000	0.11642600	-1.35843700
C	-4.71708000	0.07310200	0.80805800
H	-2.87303300	0.15191700	1.93873300
C	-4.38186300	0.05895500	-1.57037000
C	-5.24450800	0.03803800	-0.48281200
H	-5.35743200	0.05770900	1.69065600
H	-4.77947200	0.02937900	-2.58461700
H	-6.32413000	-0.00636500	-0.64111400
N	-0.22283700	0.06592400	2.17183800
C	-0.17589300	1.10088400	3.01949500
C	-0.18584900	-1.20234000	2.64067700
C	-0.09197700	0.93457300	4.39372000
H	-0.20814100	2.09654300	2.57116600
C	-0.09719700	-1.43790300	4.01865700
C	-0.05082600	-0.36513100	4.89862100
H	-0.05789500	1.80619300	5.04823700
H	-0.06392400	-2.45898600	4.39829200
H	0.01779700	-0.54166000	5.97415400
C	-0.62028600	0.18926000	-1.99226900
C	-1.97571600	0.14911200	-2.42248200
C	0.35817000	0.21889100	-3.00549000
C	-2.31283700	0.13450700	-3.78477300
C	0.02227300	0.20321900	-4.35859600
H	1.41561900	0.24938700	-2.72814100
C	-1.31759300	0.16090500	-4.75595000
H	-3.35922800	0.10328600	-4.09807400
H	0.81289900	0.22444500	-5.11434600
H	-1.58325500	0.14908200	-5.81555400
C	1.66882700	0.44909900	-0.05130400
C	2.65964200	-0.55221900	-0.02611300

C	2.13014100	1.79351700	-0.11216000
C	4.01979200	-0.24820100	-0.06532700
H	2.35855100	-1.60258400	0.01980300
C	3.49943300	2.09866400	-0.14961000
C	4.44762900	1.08145100	-0.12711600
H	4.75707500	-1.05613800	-0.04687700
H	3.83591000	3.13728200	-0.19490600
H	5.51283600	1.32217000	-0.15658000
C	-0.31995400	-1.79257400	0.25482200
C	-0.38143500	-2.78782500	-0.74054300
C	-0.24935000	-2.24784600	1.60074700
C	-0.36680000	-4.14686600	-0.42942900
H	-0.43654900	-2.49139900	-1.79178500
C	-0.23562400	-3.61597100	1.91300500
C	-0.29354600	-4.56882700	0.90153700
H	-0.41328400	-4.88793300	-1.23276400
H	-0.18051800	-3.94798000	2.95257800
H	-0.28233600	-5.63313400	1.14770900

[Ir^{IV}]

E (DLPNO-CCSD(T)) =-1537.541746
E (SMD/wB97xD/Def2TZVPP) = -1540.634042
E (gas/wB97xD/Def2TZVPP) = -1540.544763
G_{Corr}= 0.427392

Ir	-0.28057400	0.15951800	-0.03163200
N	-0.17271500	2.35263400	-0.17366000
C	-1.22488500	3.17429400	-0.27251800
C	1.08732100	2.84080900	-0.19672900
C	-1.07600800	4.54617900	-0.39815500
H	-2.21350300	2.71173900	-0.24834300
C	1.30418700	4.21665300	-0.32088600
C	0.21564000	5.07234000	-0.42316300
H	-1.95673100	5.18420600	-0.47471100
H	2.31916500	4.61260400	-0.33664200
H	0.37373400	6.14807700	-0.52235700
N	-2.47851200	0.09862700	-0.09011700
C	-3.28188700	0.03267200	0.97867700
C	-2.98782800	0.09926200	-1.34309600
C	-4.66008500	-0.03329900	0.85545500
H	-2.79615800	0.03351600	1.95658200
C	-4.37186800	0.03271600	-1.53207400
C	-5.20969700	-0.03438600	-0.42709600
H	-5.28511500	-0.08502400	1.74718000
H	-4.78789200	0.03364400	-2.53910600
H	-6.29137300	-0.08831700	-0.56537700
N	-0.13510900	0.02589500	2.14892200
C	-0.02160600	1.07047900	2.97867800
C	-0.15037000	-1.23810900	2.62691200
C	0.07817300	0.90883600	4.35109700
H	-0.01236300	2.06121100	2.51906800
C	-0.05391900	-1.46732000	4.00309300
C	0.06103800	-0.38722500	4.86773900
H	0.16787500	1.78222300	4.99742100
H	-0.07000200	-2.48508900	4.39187200
H	0.13772400	-0.55516000	5.94382800
C	-0.62792300	0.23696900	-2.02543700
C	-1.98565300	0.17792200	-2.42201400
C	0.35414600	0.34998400	-3.01969000
C	-2.33091500	0.21303800	-3.77961600
C	0.00312700	0.37453000	-4.36911200
H	1.40900100	0.40593000	-2.74045800
C	-1.33884500	0.30561400	-4.75074000
H	-3.37743700	0.16868000	-4.08784000
H	0.78352100	0.44993100	-5.13062600
H	-1.61268700	0.32803500	-5.80769500
C	1.71495100	0.47607700	0.03768300
C	2.68477600	-0.52514200	0.19981100
C	2.14388600	1.82046400	-0.07994600
C	4.04175900	-0.20594100	0.20696000
H	2.37983700	-1.56879800	0.30428300
C	3.50881500	2.13321000	-0.06013800
C	4.45504300	1.12210400	0.07677200
H	4.78435800	-1.00002700	0.31771500
H	3.84258600	3.16880900	-0.15025800
H	5.51831600	1.37099200	0.08748500
C	-0.37554200	-1.83675000	0.25422300
C	-0.53174900	-2.79671600	-0.75820500
C	-0.27500700	-2.28286800	1.59611700
C	-0.55321800	-4.15666300	-0.45353600
H	-0.62066600	-2.48099900	-1.80007700
C	-0.30923300	-3.65018500	1.89497900
C	-0.44204900	-4.58441100	0.87184800
H	-0.65901100	-4.89073600	-1.25616800
H	-0.23165700	-3.99570100	2.92777200
H	-0.46264600	-5.65022100	1.10914600

[1]Py-salt

E (DLPNO-CCSD(T)) = -1278.258639
E (SMD/wB97xD/Def2TZVPP) =-1280.389402
E (gas/wB97xD/Def2TZVPP) = -1280.29965
G_{Corr}= 0.298925

N	-1.01113100	0.82738100	-0.33849200
C	-0.85442000	-0.61463400	-0.50184300
H	-0.06966300	-0.95019400	0.18783800
H	-1.78972000	-1.11511100	-0.21509600
H	-0.58509200	-0.89597900	-1.53007400
S	-2.31743300	1.64101400	-1.05642200
O	-2.57124800	0.97445000	-2.32204900
O	-1.96422400	3.05041600	-0.99742600
N	0.06012700	1.58228100	0.09693900
C	0.96092700	2.06760400	-0.81432800
C	0.17925000	1.79244400	1.44578100
C	2.01452900	2.83134800	-0.34866300
C	1.23632600	2.55663900	1.90010200
C	2.17344700	3.10012700	1.01455800
H	2.72656700	3.22356900	-1.07549200
H	1.32557400	2.72698100	2.97366000
C	-3.69110800	1.33836600	0.01223900
C	-4.44090300	0.17329400	-0.14694600
C	-4.00974500	2.28169300	0.99120000
C	-5.51240900	-0.05652300	0.71102300
H	-4.20083600	-0.54121700	-0.93605900
C	-5.08734200	2.03490300	1.83317500
H	-3.42835400	3.20040000	1.08657500
C	-5.84974300	0.86265000	1.71351000
H	-6.10462000	-0.96682300	0.59176100
H	-5.34713400	2.77145100	2.59729500
C	-6.99204500	0.59883200	2.65271500
H	-7.68034300	-0.15601800	2.24836100
H	-6.61187200	0.22488700	3.61745600
H	-7.55699000	1.51922500	2.85989000
C	0.77587000	1.76666400	-2.26278500
H	0.63428000	0.69157900	-2.43654600
H	-0.09712500	2.30028500	-2.66405900
H	1.66253100	2.09882400	-2.81453300
C	-0.81585200	1.17125900	2.36443900
H	-1.83114700	1.53522400	2.15912500
H	-0.82401600	0.07775400	2.25011100
H	-0.55619500	1.41797600	3.39988500
C	3.32782900	3.90473600	1.51397000
H	4.15738000	3.22277200	1.76440700
H	3.68910300	4.60483200	0.74935700

H	3.06368800	4.45495100	2.42698800

col

E (DLPNO-CCSD(T)) = -365.5708833
E (SMD/wB97xD/Def2TZVPP) =-366.2657277
E (gas/wB97xD/Def2TZVPP) = -366.2538219
G_{Corr}= 0.135736

C	0.40281800	0.22975900	0.05410500
C	1.80056200	0.24216300	0.02882100
C	2.48372500	1.46070200	-0.01873100
C	1.71178100	2.62582900	-0.03484800
C	0.31693300	2.53560800	-0.00805200
N	-0.31667200	1.35782400	0.03522500
H	2.35381200	-0.70016800	0.04884300
H	2.19342000	3.60638200	-0.06634800
C	-0.54890200	3.76528700	-0.02549700
H	-1.20107800	3.78501400	0.86149900
H	0.04870700	4.68661500	-0.04293200
H	-1.20547400	3.75615200	-0.90966100
C	-0.36949300	-1.05973600	0.10836600
H	-0.99377900	-1.09186000	1.01504800
H	-1.04909800	-1.13321900	-0.75491000
H	0.29400400	-1.93499200	0.10866200
C	3.98389000	1.51544800	-0.07911600
H	4.43814200	0.65035900	0.42464400
H	4.32155600	1.50131300	-1.12845900
H	4.37092300	2.43684000	0.37887500

col-H^+

E (DLPNO-CCSD(T)) = -365.9563344
E (SMD/wB97xD/Def2TZVPP) =-366.7372187
E (gas/wB97xD/Def2TZVPP) = -366.6472544
G_{Corr}= 0.150951

C	0.43994700	0.18521200	-0.01226100
C	1.82327100	0.22953600	0.03392300
C	2.49715100	1.45815500	0.01590000
C	1.73710800	2.63457800	-0.04227500
C	0.35521700	2.57728800	-0.08748000
H	2.37825500	-0.70803700	0.08509400
H	2.22400200	3.61055800	-0.05085900
C	-0.53924800	3.76805400	-0.15041100
H	-1.22801200	3.77282200	0.70800900
H	0.05100400	4.69116100	-0.14048700
H	-1.14563900	3.74007500	-1.06855300
C	-0.36844300	-1.06759400	0.00722600
H	-1.00897500	-1.09043300	0.90220600
H	-1.02242900	-1.11393900	-0.87663300
H	0.28664400	-1.94602600	0.01545000
C	3.99141900	1.51784900	0.02912400
H	4.42637800	0.61868000	0.48486500
H	4.35865900	1.58164200	-1.00845900
H	4.34811100	2.41038300	0.56096700
N	-0.22762500	1.35811300	-0.07260100
H	-1.24843600	1.32112000	-0.10764500

^{1}1b

E (DLPNO-CCSD(T)) = -1959.220897
E (SMD/wB97xD/Def2TZVPP) = -1962.384818
E (gas/wB97xD/Def2TZVPP) = -1962.334707
G_{Corr}= 0.377928

C	1.63022400	1.20952500	-1.18897600
H	2.20727700	0.73962100	-1.98896400
C	2.12405800	2.29737700	-0.48620900
H	1.51972800	2.69023100	0.33851400
C	0.37340000	0.68124600	-0.84733100
H	-0.16117600	1.17679900	-0.02859300
N	3.26788000	2.94697600	-0.68901400
C	4.17623400	2.60693900	-1.77495600
H	3.58635200	2.18569500	-2.60244900
H	4.60821900	3.54579700	-2.14956500
C	3.69511700	4.00036400	0.23576900
H	4.08621700	4.83767600	-0.35976700
H	2.80699700	4.35457900	0.77604700
C	5.29909400	1.65710100	-1.40010900
C	6.54591900	1.79860900	-2.01774700
C	5.12728700	0.64363700	-0.45140000
C	7.60382200	0.95041400	-1.69024900
H	6.69565900	2.59440300	-2.75288700
C	6.18576400	-0.19971600	-0.11581500
H	4.16510900	0.52165400	0.05118900
C	7.42844900	-0.04892000	-0.73300500
H	8.57349200	1.08002500	-2.17708900
H	6.03840800	-0.97755700	0.63729800
H	8.25875800	-0.70678200	-0.46558500
C	4.74586700	3.51515600	1.21200100
C	6.10003600	3.78972700	1.00384700
C	4.37366900	2.71130800	2.29538700
C	7.07093800	3.25219300	1.84964400
H	6.39867000	4.41534100	0.15822500
C	5.34003200	2.17606700	3.14491300
H	3.31571200	2.49168400	2.46603200
C	6.69271200	2.44029300	2.91902600
H	8.12735200	3.46487700	1.66917800
H	5.03804300	1.54722700	3.98590000
H	7.45176800	2.01532400	3.58017500
C	-0.22015500	-0.41351800	-1.44834800
H	0.31688500	-0.95407200	-2.23319900
C	-1.48340600	-0.94068500	-1.08116800
C	-2.34616900	-0.22238500	-0.09523900
C	-2.78879700	1.08059500	-0.35427300
C	-2.72722400	-0.85893600	1.09309100
C	-3.61053100	1.73484700	0.56146200
H	-2.50029600	1.57592600	-1.28399800
C	-3.53551000	-0.19461700	2.01290600
H	-2.38573700	-1.87508900	1.30051300
C	-3.98201700	1.10038100	1.74730900
H	-3.96212100	2.74650800	0.34667300
H	-3.81898100	-0.69319900	2.94254100
H	-4.62170300	1.61675600	2.46685200
N	-1.84479000	-2.09187200	-1.62601800
S	-3.31371600	-2.74743200	-1.47181100
O	-4.43520800	-1.83381800	-1.65517800
C	-3.27069600	-3.75135200	-3.03120300
O	-3.37712500	-3.73791700	-0.40336000
F	-2.27808100	-4.62640000	-3.01133200
F	-4.41780400	-4.41101000	-3.13164700
F	-3.13563300	-2.96889600	-4.09088700

^{2}A

E (DLPNO-CCSD(T)) = -1278.425985
E (SMD/wB97xD/Def2TZVPP) = -1280.492721
E (gas/wB97xD/Def2TZVPP) = -1280.467586
G_{Corr}= 0.29446

N	-0.89747700	0.47601500	-0.93070900
C	-0.89428700	-0.97966300	-1.02341100
H	0.09823400	-1.31954400	-0.70374300

H	-1.65404800	-1.44979500	-0.37742200
H	-1.05569300	-1.29304000	-2.06244500
S	-2.21957300	1.34428200	-1.50783400
O	-2.77591700	0.53630200	-2.58474200
O	-1.75363100	2.70075200	-1.75777500
N	0.00736500	1.12489600	-0.12517700
C	0.99653500	1.91027000	-0.75839000
C	-0.24859900	1.27759200	1.26233200
C	1.57403000	2.93183900	-0.06134300
C	0.33679500	2.33070100	1.92064700
C	1.22872600	3.23001800	1.29110800
H	2.34562600	3.52003600	-0.56595600
H	0.12931100	2.43361800	2.99005800
C	-3.40576200	1.41549900	-0.19196800
C	-4.30770600	0.36533100	-0.02778200
C	-3.35978400	2.47846900	0.71154600
C	-5.16731000	0.37976000	1.06815400
H	-4.33908700	-0.45399400	-0.74829400
C	-4.22442400	2.47468200	1.79938300
H	-2.64860700	3.29320100	0.56601800
C	-5.13669700	1.42653200	1.99876100
H	-5.87614400	-0.44091300	1.20286400
H	-4.19168900	3.30266700	2.51220100
C	-6.07127100	1.44795200	3.17567600
H	-6.56749700	0.47764800	3.31448400
H	-5.53444300	1.70359200	4.10142500
H	-6.85290000	2.21147200	3.03235500
C	1.35056500	1.54168700	-2.16300900
H	1.61024300	0.47327300	-2.24162500
H	0.51073600	1.72554300	-2.85024100
H	2.20963800	2.13668000	-2.49993400
C	-1.03527000	0.20550500	1.94723000
H	-2.02181900	0.03418500	1.49144600
H	-0.49645800	-0.75730400	1.92171300
H	-1.19352800	0.47960900	2.99863000
C	1.81154000	4.41571500	2.00199100
H	2.89193200	4.51660500	1.80478300
H	1.34323600	5.36374300	1.67956600
H	1.67183000	4.33889200	3.09097900

TS-1

E (DLPNO-CCSD(T)) = -1278.201573
E (SMD/wB97xD/Def2TZVPP) =-1280.479996
E (gas/wB97xD/Def2TZVPP) =-1280.454336
G_{Corr}= 0.292835

N	-0.94308400	0.40065000	-1.14941400
C	-1.18171700	-1.02430800	-1.14270500
H	-0.23625100	-1.51177800	-0.86684700
H	-1.95708400	-1.34909600	-0.42603800
H	-1.46253200	-1.36683600	-2.14973000
S	-2.14652600	1.44468600	-1.53658900
O	-2.85742200	0.88465100	-2.68602600
O	-1.54195900	2.76840100	-1.64421200
N	0.26458900	0.89302200	-0.05003700
C	1.13272700	1.76161200	-0.66308700
C	-0.16007900	1.13539500	1.23363500
C	1.51549000	2.92694300	-0.02387200
C	0.19157400	2.31649400	1.86864700
C	1.02566700	3.25862900	1.25012400
H	2.22676000	3.58696800	-0.52703300
H	-0.16125400	2.48190300	2.89003300
C	-3.29913700	1.49553700	-0.18036100
C	-4.26001900	0.49221200	-0.05499800
C	-3.18016000	2.49625400	0.78461800
C	-5.09114900	0.48308800	1.06315100
H	-4.36109100	-0.27417700	-0.82570300
C	-4.01915600	2.47413400	1.89331200
H	-2.43068500	3.28009400	0.66634200
C	-4.98188300	1.46629100	2.05524600
H	-5.84152500	-0.30492300	1.16573800
H	-3.92554300	3.25603000	2.65161300
C	-5.89186800	1.46685900	3.25220900
H	-6.38892300	0.49541900	3.38138600
H	-5.33742200	1.70283300	4.17256700
H	-6.67582000	2.23343100	3.13917200
C	1.61823300	1.39201100	-2.02909100
H	1.86855100	0.32182200	-2.08309100
H	0.83111700	1.58522300	-2.77363200
H	2.50477700	1.98245700	-2.29669600
C	-0.95473500	0.06310400	1.91196200
H	-1.94643500	-0.06566100	1.45173900
H	-0.43514300	-0.90541400	1.84448400
H	-1.10537300	0.31057300	2.97084400
C	1.37991500	4.55724500	1.91373200
H	2.40292500	4.87115700	1.65805300
H	0.70111900	5.36212800	1.58417100
H	1.29725400	4.48524800	3.00793700

^{2}B

E (DLPNO-CCSD(T)) =-912.8687315
E (SMD/wB97xD/Def2TZVPP) = -914.24234
E (gas/wB97xD/Def2TZVPP) =-914.2250597
G_{Corr}= 0.128493

N	-1.32040000	0.44809000	0.06530400
S	-0.55708600	1.13953200	-1.26474000
O	0.21798200	0.08028500	-1.90456200
O	0.11300100	2.36329200	-0.83731200
C	-1.93216100	1.55755700	-2.29299300
C	-2.44126400	0.60121600	-3.17313800
C	-2.49178900	2.82967000	-2.19873200
C	-3.53326000	0.93378200	-3.96527100
H	-1.98498100	-0.38819000	-3.23920700
C	-3.58560500	3.14379400	-3.00167700
H	-2.07619000	3.56726400	-1.50984800
C	-4.12249800	2.20615800	-3.89304500
H	-3.93809900	0.19188900	-4.65826100
H	-4.02923800	4.14006600	-2.93433800
C	-5.29472700	2.54729700	-4.76938800
H	-4.99011900	2.57326600	-5.82778600
H	-6.08629500	1.78799500	-4.67902800
H	-5.71942700	3.52708300	-4.51192300
C	-0.42365800	0.14197700	1.14026100
H	-0.90596000	-0.57398600	1.81888900
H	0.55127700	-0.24973100	0.80106200
H	-0.22070900	1.06943000	1.71173500

C5-selectivity

TS-2

E (DLPNO-CCSD(T)) =-2872.10894
E (SMD/wB97xD/Def2TZVPP) =-2876.634886
E (gas/wB97xD/Def2TZVPP) =-2876.5724300
G_{Corr}= 0.535675

C	1.99162000	2.15551100	-1.55800800
H	1.35406700	1.91228600	-2.41078500

C	0.36181900	1.02258300	-0.19738700
H	-0.22006000	0.92095200	-1.11775200
N	3.15444600	2.69982200	-1.84736900
C	4.07879700	3.16776700	-0.81953500
H	4.55890600	4.07748500	-1.20627600
H	3.48010200	3.47829800	0.04931500
C	3.56249200	2.86732900	-3.24694100
H	2.67171400	2.72756600	-3.87246700
H	3.91175000	3.90175900	-3.37196400
C	5.14787700	2.16833300	-0.42028000
C	4.93820600	0.78681400	-0.46905000
C	6.38730400	2.64759700	0.01784000
C	5.95143900	-0.09773100	-0.09920700
H	3.98441000	0.38710900	-0.82138300
C	7.39823100	1.76526000	0.39647600
H	6.56759100	3.72572200	0.04974600
C	7.18513300	0.38768500	0.33446700
H	5.77408800	-1.17438900	-0.15556900
H	8.36195900	2.15682900	0.73088100
H	7.97987300	-0.30554600	0.61975900
C	4.64683500	1.88615900	-3.63149300
C	5.98997100	2.27086100	-3.64342100
C	4.31613500	0.55262400	-3.89620300
C	6.99206300	1.33282500	-3.89404000
H	6.25448300	3.31118000	-3.43532100
C	5.31417100	-0.38576700	-4.15065000
H	3.26654500	0.24479900	-3.88731300
C	6.65586100	0.00212300	-4.14279800
H	8.03978500	1.64239500	-3.89003600
H	5.04587700	-1.42551400	-4.35233600
H	7.43987200	-0.73439100	-4.33423500
C	-0.05747500	0.38184600	0.93628900
H	0.47339900	0.54026000	1.87861200
C	-1.21398200	-0.46708800	1.01220900
C	-1.86589400	-0.95974400	-0.23209000
C	-1.09923700	-1.56116100	-1.24041500
C	-3.24994400	-0.82897000	-0.40595000
C	-1.71165200	-2.02681700	-2.40156300
H	-0.02247000	-1.68169400	-1.10594000
C	-3.85573300	-1.28249900	-1.57403300
H	-3.85521500	-0.35634300	0.36875800
C	-3.08886800	-1.88296300	-2.57303500
H	-1.10886400	-2.50563500	-3.17626800
H	-4.93361000	-1.16420300	-1.70449400
H	-3.56656300	-2.24254900	-3.48729800
N	-1.63822300	-0.75214000	2.22280900
S	-2.80038500	-1.83022000	2.58151400
O	-2.73144400	-3.09024300	1.85549000
C	-2.19514700	-2.23379500	4.28888600
O	-4.09072700	-1.18593400	2.78703600
F	-2.19387300	-1.15907200	5.05825900
F	-3.01290500	-3.13642400	4.81163000
F	-0.97283400	-2.73756200	4.24168200
C	1.50786000	1.88639400	-0.24516600
H	2.24337600	1.75316400	0.55206400
N	1.09837200	3.66267300	0.53900100
S	0.07933700	4.59478000	-0.31440300
C	0.84175300	3.51531400	1.95441400
O	0.54118100	4.57449800	-1.70434700
O	-0.06179200	5.89355800	0.35111900
C	-1.54092400	3.83854900	-0.28671400
H	1.69599800	2.99053700	2.40913100
H	0.75941900	4.50098100	2.44064200
H	-0.07382200	2.93837000	2.18783500
C	-1.98461600	3.10573400	-1.38561000
C	-2.34091800	3.96303300	0.85151500
C	-3.23332500	2.48944400	-1.33993400
H	-1.35625900	3.02519500	-2.27429800
C	-3.58000500	3.33089000	0.88798600
H	-2.00371200	4.56015000	1.70076900
C	-4.04907100	2.58910900	-0.20561100
H	-3.58027900	1.91771200	-2.20442800
H	-4.20278600	3.42373100	1.78165200
C	-5.40668800	1.94432800	-0.15955300
H	-5.54398800	1.23226900	-0.98488600
H	-5.56215200	1.41379300	0.79208900
H	-6.19826100	2.70733200	-0.23760100

^{2}C

E (DLPNO-CCSD(T)) =-2872.109611
E (SMD/wB97xD/Def2TZVPP) =-2876.653958
E (gas/wB97xD/Def2TZVPP) =-2876.579182
G_{Corr}= 0.537752

C	2.03965900	0.22040600	0.20753600
H	1.99716500	-0.46516900	1.05546900
C	0.41124500	-0.19441300	-0.79334000
H	-0.03388200	0.75960400	-1.08205900
N	2.36425000	1.48827200	0.47442200
C	2.59442900	2.47172700	-0.57405500
H	1.73422000	2.47599000	-1.26340700
H	2.59541700	3.46048200	-0.09430200
C	2.47536000	1.92584400	1.87002300
H	1.94391300	2.88243800	1.97641100
H	1.96430100	1.18468400	2.49709000
C	3.87707100	2.30520600	-1.36796200
C	4.03638000	3.06634900	-2.53311300
C	4.90525400	1.44433100	-0.97905800
C	5.20342700	2.97422600	-3.28766700
H	3.23409800	3.73789200	-2.85173100
C	6.07059500	1.34153200	-1.74202000
H	4.80162300	0.84130800	-0.07536300
C	6.22558000	2.10704800	-2.89597000
H	5.31174200	3.57582300	-4.19338300
H	6.86142900	0.65704700	-1.42598900
H	7.13635000	2.02556600	-3.49377000
C	3.92329700	2.06520400	2.28195300
C	4.58593700	3.29134700	2.17374100
C	4.64349200	0.93523500	2.68866500
C	5.95058900	3.38516500	2.45069400
H	4.03001100	4.17962600	1.86159700
C	6.00580800	1.02673200	2.96749600
H	4.13124700	-0.02688200	2.77873400
C	6.66351200	2.25248800	2.84304100
H	6.45900000	4.34773300	2.35760700
H	6.55803000	0.13824000	3.28281100
H	7.73240900	2.32471700	3.05765000
C	-0.35500100	-1.20176900	-0.20880500
H	0.13632100	-2.14954000	0.02923500
C	-1.71223900	-1.10737700	0.13552000
C	-2.50091400	0.11094200	-0.21194900
C	-2.61369100	0.53738900	-1.54195100
C	-3.14385600	0.84044300	0.79748300
C	-3.35858900	1.67241700	-1.85635600
H	-2.12582700	-0.03475200	-2.33452500
C	-3.87938200	1.98083600	0.48115400
H	-3.06645100	0.51296900	1.83637100
C	-3.99042700	2.39841600	-0.84565600
H	-3.44891600	1.98942800	-2.89794600
H	-4.36953800	2.54647300	1.27698800
H	-4.57191300	3.28976000	-1.09283100
N	-2.24733200	-2.13089600	0.82567100
S	-3.81697300	-2.33428100	1.05137300
O	-4.67284300	-2.05726400	-0.10023500
C	-3.80501100	-4.18450600	1.17857400
O	-4.27434800	-1.89697100	2.36866700
F	-3.04935000	-4.59578000	2.18680100

F	-5.04927700	-4.60190100	1.38631300
F	-3.35827100	-4.73435900	0.05807800
C	1.85923900	-0.34279800	-1.14214700
H	2.16764500	0.35239400	-1.93673800
N	2.38206800	-1.68759700	-1.31876900
S	2.09751100	-2.33972400	-2.84212900
C	3.70945700	-1.96625400	-0.77146500
O	0.72720100	-2.00675700	-3.19974500
O	2.52509400	-3.72875100	-2.78454800
C	3.18793500	-1.45238600	-3.92834100
H	3.70395700	-1.75984700	0.30593700
H	3.93153900	-3.03103300	-0.90566600
H	4.50106400	-1.36167800	-1.24638200
C	2.73856700	-0.28198900	-4.54466300
C	4.50077400	-1.89358400	-4.09465000
C	3.62404200	0.45371300	-5.32435700
H	1.70483300	0.04499200	-4.41905400
C	5.37263500	-1.14272400	-4.87847100
H	4.83797700	-2.81642000	-3.61953300
C	4.95224000	0.03941500	-5.50139800
H	3.27766100	1.37223800	-5.80464700
H	6.40306000	-1.48285700	-5.00721400
C	5.89237500	0.84440000	-6.35316000
H	5.68643000	0.67058600	-7.42198500
H	5.76838400	1.92161400	-6.16886700
H	6.94023600	0.57277500	-6.16483600

^{1}D

E (DLPNO-CCSD(T)) = -2871.939588
E (SMD/wB97xD/Def2TZVPP) =-2876.524789
E (gas/wB97xD/Def2TZVPP) =-2876.400013
G_{Corr}= 0.546006

C	2.72840300	1.92313000	0.05069400
H	2.09118900	1.91875200	0.94203100
C	0.75242700	0.97509400	-1.11992100
H	0.18526500	1.90671500	-1.02552900
N	3.84333000	2.54619400	0.14782300
C	4.78937100	2.73756800	-0.97619500
H	4.42529300	2.18535000	-1.84763300
H	4.75276200	3.81240600	-1.20287000
C	4.22774100	3.15189600	1.44404700
H	4.76493800	4.08159600	1.21947500
H	3.29918500	3.40983200	1.96960900
C	6.19576800	2.31231900	-0.63754200
C	7.19614400	3.26757500	-0.44576200
C	6.50637700	0.95392300	-0.50604900
C	8.48987300	2.87296400	-0.10389600
H	6.95763400	4.32875400	-0.55384300
C	7.79336500	0.55999100	-0.15054800
H	5.73691400	0.20084100	-0.68794600
C	8.78663000	1.52042400	0.05625900
H	9.26583100	3.62683900	0.04694800
H	8.02459500	-0.50177900	-0.03971100
H	9.79639000	1.21071800	0.33568000
C	5.08447800	2.22083300	2.27773700
C	6.31937400	2.65807700	2.76286300
C	4.65303000	0.92536200	2.58026700
C	7.12109600	1.80749900	3.52377200
H	6.66400100	3.66820600	2.52979000
C	5.45599700	0.07177600	3.33413800
H	3.68725800	0.56430900	2.21937600
C	6.69496000	0.50970700	3.80440700
H	8.08845600	2.15946500	3.88930400
H	5.11082600	-0.94074800	3.55539300
H	7.32689000	-0.16075100	4.39140000
C	0.12849400	-0.20268000	-1.23369200
H	0.68430300	-1.14011500	-1.28645900
C	-1.32800700	-0.36471700	-1.27612600
C	-2.19419800	0.80095700	-1.58165200
C	-1.94591300	1.56030200	-2.73461200
C	-3.25718400	1.14495300	-0.73499300
C	-2.77302700	2.63458000	-3.04996700
H	-1.11769000	1.29307200	-3.39365400
C	-4.06456700	2.23595900	-1.04537700
H	-3.44360400	0.57238400	0.17478900
C	-3.82989300	2.97533800	-2.20488200
H	-2.58783100	3.21039400	-3.95909100
H	-4.88301800	2.50899400	-0.37615400
H	-4.47171200	3.82467500	-2.44959800
N	-1.74427800	-1.57197500	-1.05149500
S	-3.31549200	-2.04988000	-1.18462100
O	-3.92929100	-1.70058500	-2.45524800
C	-2.96702300	-3.87404100	-1.26592400
O	-4.04149200	-1.86592000	0.06006500
F	-2.39323700	-4.27796500	-0.14861800
F	-4.12453700	-4.49617200	-1.41417600
F	-2.18440900	-4.16156500	-2.28992100
C	2.25026400	1.15592100	-1.16674900
H	2.44510500	1.78713500	-2.05132800
N	3.04459400	-0.05085500	-1.29705700
S	3.58235600	-0.50247600	-2.81474300
C	3.08123600	-1.04502400	-0.22140900
O	4.57609000	-1.53824800	-2.58586400
O	3.93309100	0.72950100	-3.51461500
C	2.17440300	-1.20425700	-3.62281300
H	2.44549000	-0.69412900	0.60195000
H	2.68720600	-2.01843300	-0.54960500
H	4.10190000	-1.18030700	0.16163200
C	1.83346800	-2.53457900	-3.37532200
C	1.34677200	-0.37305500	-4.37826700
C	0.62521200	-3.02102200	-3.86597400
H	2.49881100	-3.18105200	-2.80001900
C	0.14918700	-0.88087300	-4.86743000
H	1.63122100	0.66254400	-4.57171700
C	-0.24133400	-2.20184700	-4.60390000
H	0.34946800	-4.05926800	-3.66895300
H	-0.50279700	-0.23535900	-5.46087100
C	-1.57562000	-2.70454300	-5.07517700
H	-1.59446300	-3.80064900	-5.14529900
H	-2.35968300	-2.39920500	-4.36379700
H	-1.83661200	-2.28114200	-6.05574700

TS-3

E (DLPNO-CCSD(T)) =-3237.518256
E (SMD/wB97xD/Def2TZVPP) = -3242.791875
E (gas/wB97xD/Def2TZVPP) = -3242.669086
G_{Corr}= 0.704826

C	6.87578500	-0.76473300	-4.76761100
H	7.60117300	-1.33109500	-4.17384000
C	5.30849600	-2.03028600	-3.44098100
H	6.19008900	-2.44971600	-2.94961200
N	7.40216700	-0.16601500	-5.78947600
C	6.71288700	0.75295600	-6.71420700
H	5.66046200	0.80195700	-6.42671700
H	7.15349200	1.74506100	-6.54105300
C	8.85453300	-0.33310300	-6.02748200
H	9.23607300	0.63035700	-6.38851300
H	9.32379800	-0.53635200	-5.05610700
C	6.88047700	0.36346100	-8.16380600
C	7.48920700	1.24908900	-9.05562000
C	6.44747900	-0.88313700	-8.63072000
C	7.66802800	0.89576100	-10.39442000

H	7.83753800	2.22135100	-8.69721300
C	6.63346500	-1.24198900	-9.96255800
H	5.98721500	-1.59030100	-7.93869600
C	7.24585700	-0.35217800	-10.84870000
H	8.14790900	1.59677300	-11.08123500
H	6.30297600	-2.22310300	-10.31122700
H	7.39412400	-0.63475900	-11.89359300
C	9.17403500	-1.43577000	-7.01395700
C	9.91519700	-1.15528500	-8.16448500
C	8.73242200	-2.74421200	-6.78966800
C	10.19261800	-2.16095000	-9.09034600
H	10.26046000	-0.13469200	-8.34781500
C	9.00389000	-3.74916300	-7.71598200
H	8.16003600	-2.98757500	-5.89025200
C	9.73073000	-3.45862300	-8.87202100
H	10.76312200	-1.92523300	-9.99171400
H	8.64615500	-4.76533100	-7.53439100
H	9.93815100	-4.24535800	-9.60109200
C	4.11793000	-2.63713400	-3.27647500
H	3.20610000	-2.24063400	-3.72087900
C	3.91445500	-3.79334700	-2.42161600
C	5.07564900	-4.47995400	-1.79709800
C	5.16065000	-4.55736000	-0.40105200
C	6.09108600	-5.02655700	-2.59164000
C	6.25788900	-5.17501200	0.19337100
H	4.37718900	-4.11845800	0.22038000
C	7.17565800	-5.66056800	-1.99032500
H	6.02164300	-4.96795700	-3.68002600
C	7.26260400	-5.73083300	-0.59925800
H	6.32746600	-5.22225100	1.28210500
H	7.95828100	-6.10035700	-2.61217200
H	8.11880200	-6.22090600	-0.13029500
N	2.67222200	-4.12295900	-2.21710200
S	2.19624800	-5.45511700	-1.38606700
O	1.83572300	-5.11252800	-0.01837600
C	0.58998900	-5.69735700	-2.29002900
O	2.95961600	-6.66141700	-1.65686200
F	0.81782300	-5.88067200	-3.57853200
F	0.00608700	-6.77529700	-1.79233300
C	5.54094300	-0.76092700	-4.17575000
H	5.89115600	0.01937500	-3.14227600
N	4.43652500	-0.29632600	-4.97953600
S	3.43467400	0.94189000	-4.47927200
C	3.93170900	-1.14672800	-6.06494200
O	2.66159400	1.31092600	-5.65567100
O	4.26072800	1.93267200	-3.80437600
C	2.34325700	0.23900300	-3.27543600
H	2.93135900	-1.55377900	-5.85159900
H	3.89330700	-0.59188400	-7.01147200
H	4.62026000	-1.99296900	-6.17955400
C	1.21722000	-0.47435500	-3.69023500
C	2.69201000	0.31746700	-1.92841300
C	0.46289500	-1.15279700	-2.73759800
H	0.93726400	-0.50593600	-4.74473400
C	1.92400900	-0.36382100	-0.99080500
H	3.56102400	0.90153600	-1.62159500
C	0.81195300	-1.12371700	-1.37948100
H	-0.41256100	-1.72318100	-3.05645200
H	2.19918700	-0.31055700	0.06547100
C	0.04404300	-1.92059800	-0.36460600
H	0.54051600	-2.89113800	-0.20443800
H	0.00697300	-1.40350200	0.60498000
H	-0.98303900	-2.12126500	-0.69924300
C	7.04055800	1.94622100	-2.21245300
C	7.42381000	2.77913200	-1.16426800
C	7.20248600	2.39863800	0.16071200
C	6.60408500	1.15574300	0.37121900
C	6.23755800	0.35310700	-0.70802300
N	6.43647300	0.76444100	-1.97588700
H	7.90015500	3.73501300	-1.39229900
H	6.41913400	0.79687700	1.38568300
C	5.64884000	-1.00409600	-0.46234800
H	6.36311500	-1.78752200	-0.75871500
H	5.42414100	-1.13835900	0.60328100
H	4.72746800	-1.15736000	-1.03545600
C	7.32948100	2.33382600	-3.63093100
H	8.16275700	1.73085900	-4.02386200
H	6.44400900	2.17776200	-4.25851600
H	7.62272000	3.38938800	-3.69145700
C	7.62419500	3.27311400	1.30318000
H	7.45827900	4.33498600	1.07220800
H	7.08622600	3.01748000	2.22615600
H	8.70196800	3.14353200	1.49419900
F	-0.21078700	-4.65906600	-2.13122900

^{1}E

E (DLPNO-CCSD(T)) = -2871.575463
E (SMD/wB97xD/Def2TZVPP) =-2876.094609
E (gas/wB97xD/Def2TZVPP) = -2876.038797
G_{Corr}= 0.533212

C	3.20023800	1.98672600	-0.89493200
H	2.44694400	2.71248500	-0.57783400
C	1.29653200	0.54455000	-0.99666000
H	0.75735700	1.42956200	-0.64530300
N	4.43260800	2.47622800	-0.88212700
C	5.63623600	1.71926600	-1.20862000
H	5.51998500	1.28674800	-2.20956900
H	6.45540300	2.44868500	-1.28209800
C	4.63500300	3.86824500	-0.44705700
H	5.33170500	4.34426200	-1.15125800
H	3.67333400	4.39016000	-0.52238400
C	6.03119300	0.64032900	-0.22382900
C	6.98706300	-0.29904000	-0.63024100
C	5.50036400	0.54655700	1.06409600
C	7.40428800	-1.30926000	0.23324400
H	7.39447200	-0.24653100	-1.64375000
C	5.91632200	-0.46632000	1.93079800
H	4.74814300	1.26222400	1.40057000
C	6.86897900	-1.39698300	1.52047000
H	8.14699900	-2.03701800	-0.10263700
H	5.48744700	-0.52583400	2.93407500
H	7.19176700	-2.19112600	2.19783100
C	5.16828600	3.94599300	0.96510200
C	6.54277000	4.01368100	1.21158300
C	4.28560500	3.86626400	2.04934600
C	7.03035800	3.98265700	2.51883900
H	7.23928600	4.08299100	0.37149600
C	4.76970300	3.83797400	3.35583700
H	3.20881100	3.81512000	1.86478900
C	6.14511600	3.88983400	3.59254200
H	8.10696800	4.03007200	2.69873800
H	4.07171300	3.77419700	4.19402300
H	6.52590700	3.86319500	4.61629900
C	0.58268300	-0.62376000	-1.14705700
H	1.08473600	-1.55158300	-1.41824800
C	-0.82060500	-0.73205400	-0.96458300
C	-1.65416900	0.48889900	-0.75862700
C	-1.68649900	1.48749800	-1.74051500
C	-2.41086300	0.64134200	0.41020000
C	-2.47915000	2.61892200	-1.56055700
H	-1.09918000	1.36514700	-2.65285700
C	-3.18759300	1.78348400	0.59278000
H	-2.38566900	-0.13074100	1.18120000
C	-3.22792900	2.77008400	-0.39293000
H	-2.51012400	3.38701400	-2.33653600
H	-3.76558300	1.90232700	1.51193600

H	-3.84407500	3.66082100	-0.24980100
N	-1.33449100	-1.95033300	-0.99727800
S	-2.91911400	-2.26786600	-0.96459900
O	-3.71619000	-1.55862700	-1.96088200
C	-2.80522400	-4.01480600	-1.58174700
O	-3.45213500	-2.40499400	0.38537300
F	-2.10643100	-4.76241800	-0.74388500
F	-4.03626900	-4.50029800	-1.66618600
F	-2.24331600	-4.07013200	-2.77932100
N	3.49269600	-0.33945700	-1.71697400
S	3.69309400	-0.44295600	-3.37284800
C	3.68072700	-1.56683200	-0.94010600
O	4.61395900	-1.54889400	-3.60058300
O	4.02293600	0.89440300	-3.85690500
C	2.10398200	-0.86328300	-4.03465100
H	3.38046900	-1.35319500	0.09260000
H	3.07156300	-2.40667500	-1.31142800
H	4.73667200	-1.86600800	-0.94148900
C	1.68781300	-2.19528300	-4.02869400
C	1.24301600	0.15878100	-4.43226600
C	0.37681600	-2.49405200	-4.38563200
H	2.37810900	-2.98892800	-3.73673700
C	-0.06087500	-0.16015900	-4.79598700
H	1.58826300	1.19356900	-4.44462500
C	-0.52242100	-1.48325800	-4.75652400
H	0.04258800	-3.53377000	-4.37077100
H	-0.73977200	0.63735700	-5.10823600
C	-1.95813000	-1.79874500	-5.06476200
H	-2.07399300	-2.82089600	-5.45133100
H	-2.56055200	-1.71901500	-4.14531000
H	-2.37428900	-1.09288100	-5.79777400
C	2.68690800	0.72700500	-1.21793200

^{1}F

E (DLPNO-CCSD(T)) =-2871.559285
E (SMD/wB97xD/Def2TZVPP) =-2876.060136
E (gas/wB97xD/Def2TZVPP) = -2876.020308
G_{Corr}= 0.532004

C	1.09225400	0.67891900	-0.82663800
C	0.06172900	1.56851300	-0.48467400
H	-0.91850800	1.09823300	-0.38673500
C	0.77943700	-0.65833200	-1.15069500
H	1.47966500	-1.10644800	-1.86817400
N	0.02469200	2.88404500	-0.36120900
C	1.18537100	3.77774200	-0.45856200
H	2.07749600	3.15725100	-0.56913200
H	1.07062200	4.37743200	-1.37417300
C	-1.28798300	3.54822400	-0.26516500
H	-1.23065100	4.46574400	-0.86711000
H	-2.02658200	2.89068600	-0.74277000
C	1.32559300	4.68259700	0.74237300
C	1.26771500	6.07053300	0.60508300
C	1.50521300	4.12775500	2.01477500
C	1.36934200	6.89748100	1.72586500
H	1.12681400	6.50968200	-0.38647200
C	1.58839300	4.94916600	3.13559200
H	1.58013700	3.04336600	2.11704300
C	1.51695600	6.33793700	2.99406100
H	1.31885900	7.98254300	1.60727200
H	1.71257800	4.50438500	4.12598700
H	1.58114400	6.98260800	3.87401100
C	-1.73365200	3.87939200	1.14324500
C	-1.89387100	5.20583400	1.55438000
C	-2.00289900	2.85205500	2.05096100
C	-2.28481700	5.50092400	2.86039200
H	-1.69566400	6.01654000	0.84902700
C	-2.38873800	3.14172600	3.35822800
H	-1.89614000	1.80963700	1.74341200
C	-2.52439000	4.46867800	3.76871700
H	-2.39496300	6.54267200	3.17130200
H	-2.57896400	2.31881800	4.05076500
H	-2.82187100	4.69873800	4.79472500
C	-0.23691700	-1.52459800	-0.75801100
C	-0.94682100	-1.57014500	0.46265000
C	-1.83650300	-2.75737800	0.65485800
C	-1.37000000	-4.05591400	0.41219000
C	-3.16453100	-2.56845900	1.06134900
C	-2.21562400	-5.14885800	0.58868300
H	-0.33297600	-4.21325000	0.10689800
C	-4.01209900	-3.66270200	1.21809900
H	-3.53986900	-1.56003000	1.24738500
C	-3.53873200	-4.95470200	0.98790500
H	-1.83775400	-6.15882800	0.41433800
H	-5.04903100	-3.50396900	1.52267200
H	-4.20257100	-5.81237100	1.11920600
N	-0.80986300	-0.63643800	1.40196600
S	-1.22537000	-0.87660800	2.94280600
O	-1.00578800	-2.22015900	3.46703700
C	0.11018500	0.12844000	3.76794900
O	-2.46490300	-0.18807800	3.29349500
F	0.31414300	1.29205600	3.18027000
F	-0.26768100	0.34303400	5.02153500
F	1.24968600	-0.54962400	3.78387200
H	-0.36279100	-2.40695500	-1.38820200
N	2.42376600	1.11861800	-1.11275100
C	2.84183900	1.23656800	-2.50544100
S	3.56679600	0.72726000	0.04806700
H	3.82637800	1.71546000	-2.55341900
H	2.88741400	0.26192900	-3.02187000
H	2.11544800	1.87931200	-3.02220900
O	3.04482600	1.20729000	1.32078800
C	3.59910100	-1.04585300	0.11386000
O	4.84835000	1.21314100	-0.44531000
C	2.80816100	-1.70280100	1.05353500
C	4.32257200	-1.75813600	-0.84534100
C	2.73259500	-3.09230300	1.02559100
H	2.23933200	-1.13106100	1.78546100
C	4.23321000	-3.14563000	-0.86015000
H	4.94476500	-1.23434600	-1.57393100
C	3.43477700	-3.83439400	0.06785000
H	2.10232900	-3.60442000	1.75710200
H	4.79292700	-3.70984100	-1.61051000
C	3.35814300	-5.33518000	0.04149100
H	4.26473800	-5.77369600	0.48954000
H	2.49204800	-5.70331000	0.60889700
H	3.29011800	-5.71169700	-0.98972800

^{1}TS^{-F}

E (DLPNO-CCSD(T)) = -2871.53695
E (SMD/wB97xD/Def2TZVPP) =-2876.031239
E (gas/wB97xD/Def2TZVPP) = -2875.990992
G_{Corr}= 0.532643

C	1.42970600	-0.10755300	-0.24460000
C	0.19324200	0.73276100	-0.12258800
H	-0.58602100	0.32859600	-0.77613200
C	1.27436700	-1.44896100	-0.22379800
H	2.11073300	-2.08547100	-0.52036300
N	0.15577700	2.07050900	-0.08758900
C	1.24930800	2.97510600	0.31810400
H	2.19582000	2.54023300	-0.01263300
H	1.09935100	3.89673600	-0.25942300

C	-0.99748000	2.71439200	-0.74312500
H	-0.64255000	3.14119900	-1.69567700
H	-1.72182800	1.92593200	-0.98399100
C	1.38340600	3.32244900	1.78584300
C	0.77431000	4.45760200	2.32971900
C	2.18298700	2.52777200	2.61199200
C	0.93416200	4.77350100	3.67836100
H	0.16418300	5.10226400	1.69336300
C	2.34146100	2.83658900	3.96177800
H	2.68392900	1.64955100	2.20061700
C	1.71296600	3.95900900	4.50144200
H	0.44852900	5.66309600	4.08773800
H	2.96075400	2.19598900	4.59481600
H	1.83726800	4.20474100	5.55924200
C	-1.68754100	3.79523800	0.05242000
C	-1.55520200	5.13757600	-0.31677500
C	-2.47935900	3.47215600	1.15949800
C	-2.18130400	6.14462800	0.41975200
H	-0.94621000	5.39812300	-1.18700600
C	-3.09931000	4.47432800	1.90191400
H	-2.58790200	2.42867300	1.45590000
C	-2.94803000	5.81424400	1.53665600
H	-2.06514800	7.18947600	0.12223700
H	-3.70523300	4.20932000	2.77174500
H	-3.43468200	6.59959100	2.12013900
C	0.04338000	-2.09912300	0.15405600
C	-0.91886600	-1.50874000	0.91365900
C	-2.14483700	-2.26173900	1.29109100
C	-2.06707100	-3.57373200	1.77167000
C	-3.40453500	-1.67663600	1.09894600
C	-3.22976000	-4.29154300	2.05309700
H	-1.08855100	-4.02788400	1.94413400
C	-4.56340500	-2.39709200	1.36999700
H	-3.46893600	-0.65054100	0.73012400
C	-4.47927800	-3.70662500	1.85040500
H	-3.15706000	-5.31179300	2.43708700
H	-5.54010100	-1.93501700	1.20773000
H	-5.39003100	-4.26902900	2.06982200
N	-0.77329700	-0.16088500	1.27929800
S	-0.98426400	0.26276200	2.82426400
O	-2.18109000	-0.28826500	3.44450500
C	0.38893500	-0.59893500	3.75326900
O	-0.72126600	1.67978100	2.96381300
F	0.48300500	-0.08169200	4.97142900
F	0.11423000	-1.89483200	3.86048800
F	1.54852900	-0.46584900	3.13807400
H	-0.10777500	-3.13067400	-0.16801700
N	2.63553600	0.50903100	-0.67300100
C	2.67833200	0.97839200	-2.05769000
S	4.10115900	0.20177300	0.06982000
H	3.53572100	1.64793600	-2.19828100
H	2.73737200	0.13601700	-2.76775800
H	1.76474700	1.55201900	-2.26732700
O	3.81663300	-0.20889800	1.43690500
C	4.84147900	-1.17195600	-0.77918700
O	4.93048900	1.37258500	-0.18457600
C	4.75565400	-2.44932200	-0.22151300
C	5.49127700	-0.96014900	-1.99468200
C	5.31391800	-3.52335200	-0.90472200
H	4.26074300	-2.59722400	0.73992200
C	6.03976300	-2.04981800	-2.66699100
H	5.57854100	0.04434800	-2.41217500
C	5.95875100	-3.34420000	-2.13831900
H	5.25118400	-4.52434600	-0.47031500
H	6.54689300	-1.88745500	-3.62115700
C	6.55700900	-4.52019800	-2.85824600
H	7.37546600	-4.96068500	-2.26720900
H	5.80548300	-5.31040400	-3.00859900
H	6.95894900	-4.23165100	-3.83905200

$^1F^+$

E (DLPNO-CCSD(T)) =-2871.929067
E (SMD/wB97xD/Def2TZVPP) =-2876.460808
E (gas/wB97xD/Def2TZVPP) = -2876.387973
G_{Corr}= 0.547401

C	1.13341000	0.66838300	1.20693400
C	0.57145800	1.86445900	0.98801200
H	0.78515400	2.69543200	1.65639500
C	1.06244600	-0.52607400	0.34062600
H	2.05159400	-0.84589200	-0.00896400
N	-0.31250700	2.16635600	-0.12552100
C	0.28561400	2.07094400	-1.50816700
H	0.69077700	1.05326100	-1.58739700
H	-0.57137100	2.13357900	-2.18994000
C	-1.16366700	3.39754800	0.12596600
H	-1.90148200	3.39744600	-0.68552500
H	-1.68871700	3.18524200	1.06502900
C	1.32839600	3.09129800	-1.89137600
C	1.20342800	3.71594100	-3.13700800
C	2.43084500	3.40599300	-1.08806400
C	2.14295600	4.65299700	-3.56401600
H	0.34769400	3.47865800	-3.77453500
C	3.35873500	4.35899200	-1.50375800
H	2.57270700	2.91992600	-0.12269700
C	3.21773500	4.98754800	-2.74171700
H	2.02445300	5.13385800	-4.53768400
H	4.20247200	4.60666700	-0.85564500
H	3.94727600	5.73336300	-3.06551400
C	-0.43429600	4.71324100	0.18944200
C	-0.37107900	5.53499100	-0.94196000
C	0.16123700	5.15430300	1.37798200
C	0.32473700	6.74074000	-0.90704700
H	-0.86510000	5.21859700	-1.86295200
C	0.86349200	6.35860000	1.41477900
H	0.06651800	4.56130000	2.29110500
C	0.95687400	7.14796600	0.26892600
H	0.37386500	7.36483700	-1.80221500
H	1.33070600	6.68525800	2.34652700
H	1.50889700	8.09035400	0.29614900
C	0.03114500	-1.32607600	0.02040400
C	-1.35547300	-1.22027300	0.48627800
C	-2.02032100	-2.51440600	0.79712100
C	-1.51942200	-3.28072400	1.85831000
C	-3.09103500	-2.98223100	0.02690000
C	-2.11887500	-4.49776600	2.16915800
H	-0.68864500	-2.89798500	2.45567200
C	-3.66752300	-4.21293100	0.33317100
H	-3.46584300	-2.39161600	-0.80931300
C	-3.19022600	-4.96500100	1.40633700
H	-1.74470200	-5.08501500	3.01027500
H	-4.49869300	-4.58324000	-0.27050300
H	-3.65435400	-5.92385400	1.64814000
N	-1.88300100	-0.04221900	0.60259000
S	-3.43965200	0.27523000	1.14437700
O	-4.44736900	-0.28806800	0.27053700
C	-3.62004800	-0.55524000	2.83561300
O	-3.44147700	1.69109000	1.45132700
F	-4.21264100	-1.72331200	2.72007300
F	-2.43858900	-0.69662800	3.40124500
F	-4.36865000	0.24322300	3.56889300
H	-1.01368900	1.38158000	-0.08557400
N	2.07927600	0.59079500	2.26404700
C	3.29912400	1.39559700	2.22593700
S	1.97166000	-0.65956500	3.37066300
H	3.83818600	1.27308900	3.17250900
H	3.95089200	1.09328700	1.39140100

H	3.04548400	2.45956900	2.12846600
O	0.59961400	-1.14254400	3.28374100
C	3.07145600	-1.93508300	2.80679500
O	2.49553400	-0.15123500	4.62754200
C	2.57185600	-3.01253700	2.07785700
C	4.43563200	-1.82936400	3.09199700
C	3.45493600	-3.98591100	1.61664600
H	1.50473700	-3.09710900	1.87073700
C	5.30161700	-2.80710700	2.61789400
H	4.81725700	-0.99713100	3.68600000
C	4.82888300	-3.89800300	1.87173000
H	3.06414300	-4.83344200	1.04850700
H	6.36932400	-2.72720700	2.83732700
C	5.78493700	-4.94495200	1.37373200
H	6.29637500	-5.43595400	2.21639600
H	5.26915900	-5.71685100	0.78663100
H	6.56481000	-4.49152500	0.74249700
H	0.25040900	-2.22982100	-0.55391300

$^1TS^{F+}$

E (DLPNO-CCSD(T)) =-2871.894013
E (SMD/wB97xD/Def2TZVPP) =-2876.426061
E (gas/wB97xD/Def2TZVPP) =-2876.351288
G_{Corr}= 0.54984

C	0.43469200	0.66861700	1.43925300
C	-0.57343000	1.53885000	1.06669600
H	-0.84601300	2.29769500	1.79928200
C	0.54935900	-0.65685300	0.96350200
H	1.50841200	-1.16797100	1.09560300
N	-0.92730300	1.99955400	-0.28586700
C	-0.39778400	1.26266700	-1.50705300
H	-0.38828100	0.19884500	-1.25595600
H	-1.18200600	1.41785100	-2.25702100
C	-0.82011100	3.53077500	-0.36549400
H	-0.86382400	3.77149900	-1.43326500
H	-1.74134400	3.88990300	0.10914400
C	0.92305300	1.71556100	-2.06793000
C	0.92670700	2.49557800	-3.23151300
C	2.14834400	1.34751200	-1.49897100
C	2.12618500	2.92671200	-3.79715100
H	-0.02304100	2.77307600	-3.69638700
C	3.34734900	1.78619900	-2.05577100
H	2.17206600	0.71700600	-0.61068600
C	3.33963500	2.58149500	-3.20261900
H	2.11108400	3.53719800	-4.70261400
H	4.29423300	1.50040900	-1.59230600
H	4.28102300	2.92378300	-3.63851200
C	0.37721800	4.15680300	0.31025800
C	1.54599700	4.45992400	-0.39819700
C	0.30477800	4.51165700	1.66586200
C	2.63156800	5.05551600	0.24211400
H	1.60856300	4.24105300	-1.46386500
C	1.39141300	5.09924300	2.30964600
H	-0.61791200	4.34173200	2.22739100
C	2.56277300	5.36411400	1.60029200
H	3.53539100	5.28084500	-0.32840800
H	1.31763300	5.35781700	3.36816100
H	3.41634000	5.82483500	2.10287500
C	-0.52425900	-1.41967600	0.54293700
C	-1.88757500	-1.08643700	0.78355900
C	-2.84291700	-2.22361500	0.87729500
C	-2.57972800	-3.30546600	1.72991500
C	-3.98338000	-2.23973500	0.06299000
C	-3.47091800	-4.37113900	1.79618200
H	-1.68596300	-3.29858100	2.35619500
C	-4.85948400	-3.32112500	0.11798300
H	-4.17839100	-1.41382000	-0.62136700
C	-4.61151500	-4.37960900	0.99076800
H	-3.27227200	-5.20136000	2.47702800
H	-5.74196500	-3.33377200	-0.52501200
H	-5.30720300	-5.22041100	1.03993700
N	-2.25643000	0.17946600	0.97097000
S	-3.66998200	0.69878700	1.69700800
O	-4.80756000	0.54767700	0.81222900
C	-4.03102400	-0.36371000	3.22368100
O	-3.34500600	2.00530300	2.23690400
F	-4.91018300	-1.29847800	2.93157400
F	-2.92748900	-0.91268900	3.68747600
F	-4.53808800	0.44193800	4.13512300
H	-1.93946900	1.82154200	-0.34857300
H	-0.33141000	-2.45714400	0.26809700
N	1.25884300	1.11548200	2.51240900
C	2.57690100	1.64755500	2.18053100
S	0.95256000	0.51725000	4.04123600
H	3.00264200	2.14079100	3.06176100
H	3.26627600	0.86013500	1.83066400
H	2.45575800	2.39573500	1.38552800
O	-0.49517300	0.53704100	4.19455600
C	1.47708000	-1.17791500	4.03337200
O	1.80504200	1.26580100	4.95273900
C	0.52396500	-2.18856200	3.94642700
C	2.84305700	-1.47170800	4.04938400
C	0.94582600	-3.51330800	3.86196900
H	-0.53786500	-1.93911900	3.93741200
C	3.24594200	-2.79867500	3.95939500
H	3.58367400	-0.67362100	4.13376200
C	2.30751100	-3.83940200	3.86179800
H	0.19990800	-4.30920400	3.79296800
H	4.31276300	-3.03606500	3.96853500
C	2.76547900	-5.26858700	3.78219100
H	3.17684200	-5.59480500	4.75100900
H	1.93834600	-5.94285400	3.52110200
H	3.56441300	-5.38651100	3.03489900

^1G

E (DLPNO-CCSD(T)) =-1986.932958
E (SMD/wB97xD/Def2TZVPP) =-1990.3227
E (gas/wB97xD/Def2TZVPP) = -1990.284398
G_{Corr}= 0.52291

C	2.03771400	1.19177400	1.52435900
C	1.03917000	2.11926200	1.65314200
H	1.11504600	2.76403900	2.53239500
C	2.19033400	0.11203300	0.54994100
H	3.19836300	0.03110900	0.12327500
N	-0.03211400	2.37364800	0.86464700
C	-0.10540600	1.98856000	-0.53268800
H	-0.23032200	0.89986300	-0.63918900
H	-1.02559000	2.43265800	-0.93898800
C	-1.03696800	3.32501400	1.35446900
H	-2.02442700	2.97647000	1.02009100
H	-1.03263800	3.28542200	2.45127800
C	1.06573300	2.42371500	-1.39433200
C	1.39905600	1.65631100	-2.51625200
C	1.80284400	3.58325900	-1.13214300
C	2.43572900	2.04224600	-3.36520500
H	0.84178200	0.73785200	-2.72241700
C	2.84650500	3.96773700	-1.97484100
H	1.56641300	4.19340000	-0.25805400
C	3.16616100	3.20039500	-3.09524500
H	2.68001000	1.42997000	-4.23677100
H	3.41277000	4.87527300	-1.75137700
H	3.98467400	3.50128200	-3.75357300

C	-0.78663800	4.73919400	0.87895900
C	-1.38364200	5.22156600	-0.29057300
C	0.12062100	5.55918700	1.56251100
C	-1.06463300	6.48842200	-0.78154000
H	-2.10308500	4.59604700	-0.82631300
C	0.43995100	6.82580200	1.07585500
H	0.58801600	5.19590300	2.48185000
C	-0.14807600	7.29088000	-0.10224900
H	-1.53509300	6.85008300	-1.69902100
H	1.15062500	7.45395800	1.61838000
H	0.10368900	8.28230100	-0.48642700
C	1.32170900	-0.84287400	0.14188400
C	-0.01695000	-1.17054100	0.67350900
C	-0.71810900	-2.33755700	0.04108400
C	-0.02123900	-3.46425800	-0.41755000
C	-2.11714100	-2.32783200	-0.04944700
C	-0.70859500	-4.55567000	-0.94941300
H	1.06701200	-3.50994100	-0.33916300
C	-2.80249100	-3.41058100	-0.59530500
H	-2.66300900	-1.45431500	0.31315000
C	-2.09967100	-4.53015100	-1.04534300
H	-0.15056900	-5.43161000	-1.28882700
H	-3.89228600	-3.38176800	-0.66952400
H	-2.63656000	-5.38187900	-1.46982200
N	-0.62278100	-0.58696900	1.64393400
H	-0.05662200	0.17656600	2.01536000
N	3.14091400	1.36185400	2.43495700
C	4.42922700	1.78363000	1.89676100
S	3.10591800	0.42384300	3.81453400
H	5.10392900	2.05030700	2.71791000
H	4.91375900	1.01151000	1.27366200
H	4.25823300	2.67671700	1.27953600
O	1.84382200	0.69012500	4.49402600
C	3.05892000	-1.26555500	3.25885700
O	4.36386200	0.65729300	4.51585400
C	1.87994100	-1.99356200	3.37452500
C	4.18162000	-1.80758600	2.62612000
C	1.81371900	-3.27161000	2.82278200
H	1.01132000	-1.55337300	3.86517200
C	4.09719900	-3.08077600	2.07736900
H	5.10896100	-1.23535200	2.55168900
C	2.91010800	-3.82877900	2.15622300
H	0.88249700	-3.83855800	2.89786900
H	4.96742500	-3.50544500	1.57022900
C	2.83238200	-5.19769900	1.53990500
H	3.47022400	-5.90814700	2.09012700
H	1.80453200	-5.58586900	1.54931400
H	3.19045600	-5.18166200	0.49924700
H	1.69166300	-1.51520900	-0.63487400

$^{1}TS^{-G}$

E (DLPNO-CCSD(T)) = -2871.575463
E (SMD/wB97xD/Def2TZVPP) =-2876.094609
E (gas/wB97xD/Def2TZVPP) = -2876.038797
G_{Corr}= 0.533212

C	1.97837400	0.87226000	1.09246900
C	0.76593200	1.60400000	1.35965400
H	0.59701200	1.89754500	2.40011300
C	2.08879800	-0.17504700	0.18896000
H	3.10490900	-0.46911500	-0.10248800
N	0.09821200	2.34151500	0.47412200
C	0.32121400	2.23186200	-0.96110500
H	0.18766200	1.18500400	-1.28186400
H	-0.46684800	2.81888600	-1.45332400
C	-1.12224700	3.02434800	0.90604900
H	-1.98169800	2.58764400	0.37382500
H	-1.26010900	2.81664100	1.97475400
C	1.66785100	2.74911000	-1.42178100
C	2.43724800	2.01023600	-2.32522100
C	2.14857000	3.98835900	-0.98278600
C	3.66780700	2.49165300	-2.77389900
H	2.07466300	1.03766600	-2.66865800
C	3.37699200	4.47255200	-1.42996100
H	1.55911000	4.57634200	-0.27542800
C	4.14348000	3.72394200	-2.32535000
H	4.26051000	1.89662500	-3.47310400
H	3.73871800	5.44051900	-1.07455000
H	5.10875400	4.10054600	-2.67217200
C	-1.04962300	4.51488200	0.67153200
C	-1.71518200	5.11545400	-0.40037900
C	-0.25653400	5.31000000	1.50950100
C	-1.58424500	6.48529500	-0.63994800
H	-2.34058400	4.50410600	-1.05702400
C	-0.12527700	6.67665400	1.27455600
H	0.27052000	4.84708000	2.34866600
C	-0.78753100	7.26716500	0.19501700
H	-2.10707300	6.94182100	-1.48378900
H	0.49638200	7.28580400	1.93513000
H	-0.68335900	8.33866200	0.00803800
C	1.04345300	-0.97242000	-0.28595200
C	-0.19112100	-1.06395300	0.42014300
C	-1.01876800	-2.30332800	0.24307800
C	-0.43064000	-3.56295700	0.05345200
C	-2.41840600	-2.21836800	0.29115500
C	-1.21990300	-4.70534800	-0.07162900
H	0.65696400	-3.65505700	0.02719000
C	-3.20833900	-3.35945900	0.15996400
H	-2.89516800	-1.24293600	0.41812900
C	-2.61108600	-4.60763000	-0.01928700
H	-0.74297700	-5.67928400	-0.20609100
H	-4.29696700	-3.27178800	0.19285200
H	-3.22899600	-5.50318200	-0.11941000
N	-0.57510300	-0.13699100	1.26474800
H	-1.32976900	-0.45345800	1.87652100
N	3.10969100	1.26401700	1.89320900
C	4.31660100	1.70581600	1.20394800
S	3.27555300	0.44953100	3.34222400
H	5.02317100	2.13474300	1.92369400
H	4.82037500	0.89350700	0.65025600
H	4.02544000	2.48701100	0.48872300
O	2.09413400	0.75271300	4.14539200
C	3.20034200	-1.28194700	2.94108600
O	4.59717600	0.76399200	3.87657700
C	2.00801100	-1.97472500	3.12960900
C	4.30470900	-1.89641600	2.34713300
C	1.91506100	-3.29619400	2.70013500
H	1.15439600	-1.47457400	3.58862200
C	4.19243500	-3.21354500	1.91636500
H	5.23959200	-1.34772900	2.21438100
C	2.99495600	-3.93008700	2.07469000
H	0.97788400	-3.84014100	2.84049100
H	5.04994600	-3.69804600	1.44211400
C	2.88010000	-5.34089400	1.56818400
H	3.64858100	-5.98651000	2.02117900
H	1.89340600	-5.76965200	1.79129400
H	3.03191300	-5.37494400	0.47773100
H	1.27745200	-1.74699300	-1.01747300

^{1}H

E (DLPNO-CCSD(T)) =-1986.961148
E (SMD/wB97xD/Def2TZVPP) =-1990.3536
E (gas/wB97xD/Def2TZVPP) = -1990.31688
G_{Corr}= 0.527143

C	1.71791500	0.71533400	1.40033600
C	0.30061700	0.71853800	1.94367600
H	0.34382700	0.56555300	3.02838400
C	2.04224800	0.05092300	0.26814900
H	3.05428500	0.13381400	-0.13595200
N	-0.36594200	1.98781400	1.76532100
C	-0.69535500	2.42311900	0.42226200
H	-0.96630300	1.55691800	-0.20815300
H	-1.60318000	3.04469000	0.48194600
C	-1.17324700	2.50287800	2.85478900
H	-2.24197100	2.55382200	2.57554800
H	-1.10299200	1.79687200	3.69663100
C	0.37586100	3.22406100	-0.29788700
C	0.88894600	2.78497600	-1.52250000
C	0.86185300	4.42471700	0.23690100
C	1.87288000	3.51498400	-2.19287200
H	0.52112000	1.84788000	-1.95041500
C	1.84018400	5.15968700	-0.43007500
H	0.47245800	4.78530200	1.19120000
C	2.35350300	4.70507600	-1.64714200
H	2.26713600	3.14918400	-3.14428700
H	2.20717700	6.09267600	0.00505100
H	3.12494000	5.27775600	-2.16770600
C	-0.72030500	3.86960600	3.32947100
C	-1.53630600	4.99516500	3.19999100
C	0.56969100	4.02841300	3.85476700
C	-1.07413700	6.25974000	3.57759700
H	-2.54265500	4.88473900	2.78530300
C	1.03459100	5.28484100	4.23173700
H	1.22197200	3.15711800	3.94527600
C	0.21307400	6.40802700	4.09075000
H	-1.72247600	7.13216000	3.46337300
H	2.04526500	5.39088700	4.63418200
H	0.57860000	7.39586300	4.38185000
C	1.08534100	-0.76329100	-0.43389200
C	-0.13491600	-0.97187400	0.14388400
C	-1.17586900	-1.84173300	-0.46017500
C	-1.35339000	-1.87487100	-1.85149600
C	-1.99483700	-2.64993900	0.34339600
C	-2.32104600	-2.69821300	-2.42352800
H	-0.73897100	-1.23608500	-2.48981600
C	-2.96255600	-3.47235000	-0.23121500
H	-1.86373000	-2.65481200	1.42830500
C	-3.12924200	-3.49978000	-1.61595700
H	-2.45029800	-2.70664800	-3.50836100
H	-3.58615800	-4.10067300	0.40905400
H	-3.88913200	-4.14335400	-2.06538700
N	-0.41632700	-0.41788100	1.36219600
H	-1.36909700	-0.51369100	1.69696100
N	2.64110800	1.58861100	2.05428300
C	3.58174600	2.34843800	1.23178300
S	3.27273700	1.06138900	3.51627000
H	3.95170500	3.21185500	1.79716800
H	4.44132000	1.74477900	0.88959400
H	3.04008100	2.70896000	0.35045500
O	2.17726000	0.49361500	4.29406700
C	4.39227200	-0.25172900	3.10302300
O	4.03757100	2.17213300	4.06763100
C	3.89292000	-1.54337200	2.91606000
C	5.74096100	0.03477100	2.89593600
C	4.76219700	-2.55106900	2.51396300
H	2.83647400	-1.75695000	3.08707200
C	6.59689100	-0.98867600	2.49553500
H	6.11872800	1.04666600	3.05279700
C	6.12435500	-2.29227800	2.29678800
H	4.37591400	-3.56271100	2.36592500
H	7.65506400	-0.76805600	2.33469100
C	7.05392000	-3.40009800	1.88650900
H	7.30775300	-4.02887200	2.75554300
H	6.58564000	-4.05489100	1.13698400
H	7.99239700	-3.00610900	1.47248300
H	1.35126500	-1.25123300	-1.37016300

^{1}I

E (DLPNO-CCSD(T)) = -1390.800294
E (SMD/wB97xD/Def2TZVPP) =-1393.061767
E (gas/wB97xD/Def2TZVPP) = -1393.036528
G_{Corr}= 0.283171

C	0.27424300	1.07848100	-0.90345500
C	-1.01002800	1.18992300	-0.35966800
H	-1.49995100	2.16773600	-0.34189900
C	0.85924800	-0.18812900	-0.93305800
H	1.85384400	-0.33589600	-1.35804100
C	0.15448300	-1.26749100	-0.41431100
C	-1.11478800	-1.05764900	0.14115300
C	-1.91810800	-2.16965800	0.72781600
C	-1.33164500	-3.38760900	1.10311600
C	-3.29770000	-2.00314800	0.92126900
C	-2.10493300	-4.41104600	1.64883700
H	-0.25716000	-3.54318300	0.98777500
C	-4.07048700	-3.02732700	1.46312300
H	-3.75835000	-1.05549200	0.63792500
C	-3.47727400	-4.23672200	1.82851400
H	-1.62840300	-5.35008400	1.94000700
H	-5.14443200	-2.88005700	1.60046600
H	-4.08241600	-5.04014400	2.25518300
N	-1.67149500	0.16168100	0.15107400
H	0.59572500	-2.26366800	-0.45066000
N	0.93118000	2.23532300	-1.40774000
C	1.71819200	2.09323400	-2.63193100
S	1.56481300	3.28228800	-0.24904100
H	1.92578200	3.08765100	-3.04314800
H	2.67191000	1.55962300	-2.47528400
H	1.11443600	1.53405900	-3.35842700
O	0.55208200	3.44414900	0.78279100
C	2.93944200	2.40529200	0.45055000
O	2.06471000	4.43934300	-0.97556700
C	2.71979900	1.53087400	1.51546000
C	4.20699300	2.54642800	-0.11744100
C	3.78721000	0.78541400	2.00829800
H	1.72707600	1.43951100	1.95985900
C	5.26106400	1.79407700	0.38998900
H	4.36732500	3.24541000	-0.94025700
C	5.06918900	0.89992400	1.45389500
H	3.62029200	0.10297700	2.84523800
H	6.25682900	1.90620900	-0.04638600
C	6.21418700	0.07419600	1.97012800
H	7.13438200	0.67235300	2.04272000
H	5.99167900	-0.35099200	2.95852500
H	6.42289300	-0.76207300	1.28304600

$^{1}NH_4^+$

E (DLPNO-CCSD(T)) = -56.81655671
E (SMD/wB97xD/Def2TZVPP) =-56.9862016
E (gas/wB97xD/Def2TZVPP) = -56.91072833
G_{Corr}= 0.029582

N	1.04156500	3.60719200	0.00000400
H	1.38392700	2.63960500	-0.00000900
H	1.38417000	4.09132400	0.83776400
H	1.38417600	4.09131200	-0.83776100
H	0.01558500	3.60721600	0.00000200

$^{1}OAc^-$

E (DLPNO-CCSD(T)) = -228.1827909
E (SMD/wB97xD/Def2TZVPP) =-228.5955088
E (gas/wB97xD/Def2TZVPP) = -228.540793
G_{Corr}= 0.021068

C	-0.00277500	1.80257900	0.04534400
O	-1.13634300	2.01213100	0.52589300
O	0.90698400	1.08407000	0.51157700
C	0.33930600	2.55562200	-1.26901200
H	0.92864400	3.45739700	-1.02659900
H	0.96122100	1.93411000	-1.93287900
H	-0.56645800	2.87972200	-1.80453800

^{1}HOAc

E (DLPNO-CCSD(T)) = -228.7574464
E (SMD/wB97xD/Def2TZVPP) =-229.1209448
E (gas/wB97xD/Def2TZVPP) = -229.1144942
G_{Corr}= 0.035021

C	-0.05391900	1.87450800	0.00769400
O	-1.14351400	1.92105400	0.52366800
O	0.95828200	1.18026900	0.53945900
C	0.33924200	2.55688700	-1.26762800
H	1.18468200	3.23531700	-1.08107500
H	0.67279700	1.80747800	-2.00058000
H	-0.51119700	3.11936700	-1.66857100
H	0.63498100	0.76144200	1.35512300

^{1}Tf-NH$_2$

E (DLPNO-CCSD(T)) =-941.1022256
E (SMD/wB97xD/Def2TZVPP) =-942.3080714
E (gas/wB97xD/Def2TZVPP) = -942.3017246
G_{Corr}=0.017983

S	-4.01032900	-0.37641800	-0.24680600
O	-5.06286400	-1.14069600	-0.88394500
C	-3.86466200	-1.09674500	1.45799800
O	-4.09644600	1.05411400	-0.03618200
F	-2.83556400	-0.55751100	2.09029600
F	-4.97276500	-0.84201300	2.13462200
F	-3.69228200	-2.40589800	1.38287400
N	-2.57954400	-0.75901300	-0.89146600
H	-2.57095300	-1.49997900	-1.58994500
H	-1.90249300	-0.00513400	-0.99585400

^{1}HNBn$_2$

E (DLPNO-CCSD(T)) =-596.1655118
E (SMD/wB97xD/Def2TZVPP) =-597.2987944
E (gas/wB97xD/Def2TZVPP) = -597.2824033
G_{Corr}= 0.217974

N	-1.80966400	-0.01736300	0.13848800
C	-1.37893800	-0.09684000	-1.24690400
H	-1.52156900	-1.13914700	-1.57762700
H	-1.99999600	0.53427800	-1.91619000
C	-1.97673700	1.33444500	0.65585900
H	-2.41502000	2.01831800	-0.09970000
H	-2.69345800	1.28195700	1.49021400
C	0.07416000	0.28268200	-1.45257000
C	0.44486100	1.16822700	-2.46814100
C	1.07293900	-0.23711500	-0.61952400
C	1.78040100	1.53793700	-2.64498400
H	-0.32506700	1.59000500	-3.12091800
C	2.40505800	0.13318100	-0.78682700
H	0.79012100	-0.91863100	0.18638800
C	2.76409700	1.02653100	-1.80022200
H	2.04963300	2.23790600	-3.44001300
H	3.16978200	-0.27268500	-0.11959400
H	3.80829500	1.32222000	-1.92811400
C	-0.68333300	1.93458100	1.17079200
C	-0.09275600	3.03903300	0.55181100
C	-0.03285800	1.35317400	2.26668500
C	1.13021700	3.54273400	1.00116800
H	-0.58635600	3.49964600	-0.30879900
C	1.18450200	1.85343600	2.72276600
H	-0.48258500	0.48374400	2.75465600
C	1.77427400	2.94864800	2.08584700
H	1.58403300	4.39894500	0.49577000
H	1.68051900	1.38553900	3.57701700
H	2.73333800	3.33760600	2.43667800
H	-2.68418100	-0.52444600	0.23901400

C2-selectivity

TS-2

E (DLPNO-CCSD(T)) = -2872.095396
E (SMD/wB97xD/Def2TZVPP) = -2876.629857
E (gas/wB97xD/Def2TZVPP) = -2876.562893
G_{Corr}= 0.536432

C	1.80990800	0.48849800	-1.04026300
H	2.36861400	-0.38530300	-1.38094400
C	0.47689200	0.34553600	-0.66138900
H	-0.07047000	1.24703300	-0.36038800
N	3.55128300	2.10302300	-1.59346600
C	4.43137800	1.14887200	-2.28639300
H	3.85804000	0.25276800	-2.54331700
H	4.74711000	1.62340400	-3.22452700
C	4.01889500	3.48913200	-1.52829400
H	4.56266700	3.69643900	-2.45863500
H	3.12839600	4.13233900	-1.52432000
C	5.62470600	0.81593100	-1.42055700
C	6.85542600	1.44166200	-1.63471500
C	5.47753500	-0.05571000	-0.33557300
C	7.92287000	1.21425900	-0.76567000
H	6.97249100	2.12751700	-2.47799400
C	6.54330700	-0.28587200	0.53169000
H	4.51537300	-0.54537100	-0.16102300
C	7.76633300	0.35492600	0.32159500
H	8.87838500	1.71575700	-0.93584500
H	6.41903400	-0.96499200	1.37834500
H	8.59963800	0.18098100	1.00645800
C	4.88904200	3.82047800	-0.33468300
C	5.84318100	4.83431100	-0.46975900
C	4.73013800	3.19882000	0.90630000
C	6.62348100	5.22385000	0.61751600
H	5.97692100	5.32302100	-1.43861700
C	5.51899600	3.57938900	1.99228300
H	3.99458500	2.40150900	1.03751700
C	6.46554100	4.59444500	1.85298400
H	7.36396100	6.01798500	0.49599900
H	5.38972800	3.07798100	2.95426700
H	7.08160500	4.89187700	2.70471000
C	-0.15467100	-0.88560900	-0.75412500
H	0.42892900	-1.77082300	-1.02323700
C	-1.56778600	-1.12462400	-0.53658700

C	-2.51355300	0.00522800	-0.35372900
C	-2.50749400	1.08524200	-1.24588300
C	-3.41739000	-0.00221800	0.72070800
C	-3.40358200	2.13689500	-1.07486100
H	-1.79334800	1.12007300	-2.07078300
C	-4.30634500	1.05379300	0.88881800
H	-3.41503700	-0.82788000	1.43487000
C	-4.30459800	2.12110300	-0.01212200
H	-3.35766300	2.98823500	-1.75617100
H	-4.99970700	1.04716800	1.73255700
H	-5.00112500	2.95143400	0.12602600
N	-1.89942000	-2.38749100	-0.51859100
S	-3.44130900	-2.95653100	-0.47253500
O	-4.36237000	-2.28561700	-1.37322800
C	-3.07492700	-4.58960700	-1.27890800
O	-3.83593000	-3.28031200	0.88818800
F	-2.20811000	-5.28149000	-0.56344100
F	-4.21129100	-5.26347900	-1.35683500
F	-2.59412900	-4.40511300	-2.49544500
C	2.40272500	1.79323400	-1.05277300
H	1.89400100	2.58196300	-0.50132100
N	0.52728400	2.97162000	-2.46318200
S	-0.22674900	4.02722100	-1.57191100
C	0.89930400	3.35287700	-3.80493500
O	-0.50942800	3.39045800	-0.26700900
O	-1.36267800	4.69374900	-2.24160200
C	0.92532700	5.35759400	-1.17425700
H	1.21175500	2.44990600	-4.35492600
H	0.07054400	3.81025000	-4.37975000
H	1.75453800	4.06062500	-3.85016800
C	1.54106000	5.38646000	0.07708500
C	1.29447700	6.28737700	-2.15116100
C	2.54817500	6.31486400	0.33722700
H	1.23578700	4.66834800	0.84031600
C	2.30960200	7.20255700	-1.88403200
H	0.79075900	6.29549900	-3.11998400
C	2.96207300	7.22513200	-0.64161300
H	3.03312500	6.32034900	1.31729900
H	2.60422400	7.91731100	-2.65767100
C	4.07497400	8.20330500	-0.38003400
H	4.88519000	8.08310100	-1.11628200
H	3.71577200	9.24146600	-0.46277500
H	4.50158900	8.06814900	0.62373100

^{2}C

E (DLPNO-CCSD(T)) = -2872.140812
E (SMD/wB97xD/Def2TZVPP) =-2876.661797
E (gas/wB97xD/Def2TZVPP) = -2876.605948
G_{Corr}= 0.535955

C	1.35888500	0.89536900	0.07883300
H	2.06215500	0.15744700	0.47540300
C	0.09823200	0.51054200	-0.29621200
H	-0.58106500	1.28299300	-0.66659000
N	3.23184400	2.43044700	-0.22735500
C	3.75936200	1.71075200	-1.38035800
H	3.00710500	0.97390900	-1.70445200
H	3.91518100	2.38371500	-2.24333300
C	3.74176600	3.78384000	-0.05182200
H	3.36372000	4.46063100	-0.84460900
H	3.34540000	4.16216700	0.90336400
C	5.04855100	0.96323200	-1.09678600
C	6.13262200	1.05137200	-1.97414000
C	5.17142900	0.15998000	0.04288400
C	7.31954400	0.36223100	-1.71598700
H	6.05474600	1.68465000	-2.86259600
C	6.35125200	-0.53382600	0.30267100
H	4.33864300	0.10123900	0.74781500
C	7.43319400	-0.43191900	-0.57535800
H	8.16159300	0.45402700	-2.40661300
H	6.43119200	-1.15297900	1.19979600
H	8.36260000	-0.96793100	-0.36799800
C	5.24878200	3.87218900	-0.02498700
C	5.94140900	4.53379600	-1.04175200
C	5.97844300	3.27329800	1.00968100
C	7.33756700	4.58255700	-1.03952700
H	5.38095900	5.00681300	-1.85322700
C	7.36977800	3.31549700	1.01483800
H	5.44441200	2.75243600	1.80873100
C	8.05469400	3.96741500	-0.01502700
H	7.86508500	5.09823200	-1.84569300
H	7.92619100	2.83502200	1.82338400
H	9.14703000	3.99698000	-0.01410300
C	-0.35158400	-0.81586100	-0.22485600
H	0.30269900	-1.59013000	0.18551500
C	-1.65466600	-1.24306500	-0.63526800
C	-2.58533000	-0.27650600	-1.28607000
C	-2.22109000	0.35388900	-2.48304100
C	-3.81692200	0.02044700	-0.68984500
C	-3.08698400	1.26543700	-3.08122500
H	-1.26111500	0.12196800	-2.94983200
C	-4.67364600	0.94291600	-1.28730500
H	-4.10104600	-0.46026800	0.24815000
C	-4.31220500	1.56364700	-2.48264500
H	-2.80185800	1.74770800	-4.01877000
H	-5.62810900	1.17947600	-0.81208400
H	-4.98670200	2.28522900	-2.94919600
N	-1.95555500	-2.49535300	-0.37745400
S	-3.34901700	-3.20495200	-0.87155700
O	-3.66783900	-2.99595500	-2.27432900
C	-2.73800500	-4.95542100	-0.76721400
O	-4.38784600	-3.10210500	0.14095000
F	-2.38011600	-5.25498300	0.46818200
F	-3.72835000	-5.75297500	-1.13725200
F	-1.71027200	-5.13705800	-1.57803900
C	1.82399300	2.32716800	0.05992400
H	1.67442000	2.70369100	1.08683000
N	0.93938900	3.15251400	-0.78488300
S	0.00761500	4.34762400	-0.12080600
C	1.06188500	3.08909200	-2.23297100
O	-0.16939700	4.01371700	1.28816700
O	-1.15914500	4.51313100	-0.97854900
C	0.97146600	5.83678500	-0.22142800
H	1.16246900	2.03952000	-2.54189000
H	0.15003200	3.48399500	-2.69647300
H	1.93388000	3.65327800	-2.60325800
C	1.62347500	6.31120700	0.91529800
C	1.13318900	6.46501400	-1.45712500
C	2.46797100	7.41147000	0.80296600
H	1.47684800	5.81755500	1.87730300
C	1.98652700	7.56029300	-1.55231300
H	0.59994800	6.10552800	-2.33922300
C	2.67538200	8.04389500	-0.43069600
H	2.98040200	7.78500100	1.69311500
H	2.11857700	8.05227500	-2.51918700
C	3.63226800	9.19705700	-0.54983000
H	3.62647600	9.81786700	0.35760800
H	4.66092000	8.82423700	-0.68595000
H	3.39222600	9.83216600	-1.41406200

^{1}D

E (DLPNO-CCSD(T)) = -2871.856724
E (SMD/wB97xD/Def2TZVPP) =-2876.449212
E (gas/wB97xD/Def2TZVPP) = -2876.32488

G_{Corr}= 0.537936

C	1.28341700	1.06486800	0.04593300
H	1.93602000	0.32140700	0.51743100
C	-0.00344100	0.69567200	-0.35207300
H	-0.66782500	1.44103200	-0.79472700
N	3.19470200	2.50280200	-0.30157900
C	3.68652700	1.78894100	-1.47856400
H	2.88741300	1.11015200	-1.82332800
H	3.87797200	2.48471400	-2.31446500
C	3.77557900	3.81987800	-0.04676200
H	3.40013400	4.56386600	-0.77577900
H	3.43390900	4.13953800	0.94911800
C	4.93059700	0.96094400	-1.22449700
C	6.01307400	1.02353300	-2.10569800
C	5.01619900	0.11547600	-0.11277100
C	7.16345600	0.26561700	-1.87866000
H	5.96347700	1.69010000	-2.97135100
C	6.16031500	-0.64543200	0.11638500
H	4.18729400	0.07303700	0.59748600
C	7.24113000	-0.57048900	-0.76551300
H	8.00553500	0.33680400	-2.57146400
H	6.21296200	-1.29666000	0.99240100
H	8.14265200	-1.15988300	-0.58175600
C	5.28351200	3.82894000	-0.08188800
C	5.96378100	4.47596600	-1.11619200
C	6.02288000	3.16375800	0.90369400
C	7.35861500	4.44497000	-1.17971200
H	5.39423100	5.00024200	-1.88869300
C	7.41293600	3.12437400	0.84092700
H	5.49775700	2.65505400	1.71638300
C	8.08500800	3.76218800	-0.20583200
H	7.87735500	4.95079700	-1.99757800
H	7.97793900	2.59216100	1.61002300
H	9.17594700	3.72841500	-0.25733000
C	-0.37281700	-0.61197400	-0.20323000
H	0.29591100	-1.32802800	0.28506000
C	-1.68426400	-1.15661600	-0.63607400
C	-2.54401700	-0.37295600	-1.54781400
C	-2.00516900	0.14684500	-2.73551300
C	-3.88736400	-0.13340100	-1.22288200
C	-2.81390300	0.87892900	-3.59844800
H	-0.96099000	-0.04100500	-2.99582600
C	-4.68170800	0.61906100	-2.08212000
H	-4.30636800	-0.51138100	-0.28868200
C	-4.14905500	1.11974700	-3.27019100
H	-2.39799400	1.26684400	-4.53026900
H	-5.72268100	0.81673000	-1.81944600
H	-4.77778800	1.70604300	-3.94388600
N	-1.93708000	-2.29827000	-0.09675500
S	-3.30186600	-3.20616600	-0.42353500
O	-3.60201800	-3.30274700	-1.83694700
C	-2.55608800	-4.84336200	0.05466300
O	-4.32338200	-2.91657800	0.56199300
F	-2.20810400	-4.83250600	1.32441100
F	-3.47495000	-5.76911800	-0.14665500
F	-1.50228400	-5.09306300	-0.69711200
C	1.79906100	2.44380900	-0.02782700
H	1.63556900	2.69104100	1.05762200
N	0.92203800	3.33952600	-0.76785800
S	0.06107400	4.52313300	0.03279600
C	1.04689400	3.40750700	-2.21771300
O	-0.06282000	4.05377700	1.40888300
O	-1.12553600	4.78599500	-0.76573400
C	1.08016200	5.97262900	0.02252600
H	1.08691000	2.38604200	-2.62215600
H	0.15773400	3.89628200	-2.63313100
H	1.94956800	3.95511100	-2.53348500
C	1.77721900	6.32443200	1.17769900
C	1.22602800	6.70019700	-1.15939100
C	2.65189400	7.40480400	1.13539500
H	1.64051700	5.75344500	2.09746900
C	2.11102300	7.77376200	-1.18369100
H	0.65834400	6.43676400	-2.05370600
C	2.84439200	8.13664600	-0.04500000
H	3.20001900	7.68429100	2.03854400
H	2.23224500	8.34457700	-2.10750400
C	3.83107300	9.26912000	-0.08887000
H	3.82618100	9.83950500	0.85118600
H	4.85193200	8.87703400	-0.22853400
H	3.62045000	9.95577100	-0.92043100

C3-selectivity

TS-2

E (DLPNO-CCSD(T)) = -2872.100425
E (SMD/wB97xD/Def2TZVPP) = -2876.635608
E (gas/wB97xD/Def2TZVPP) =-2876.570092
G_{Corr}= 0.537928

C	2.14658800	2.26620300	0.80626700
H	1.95932900	1.80458300	1.77657800
C	0.27367400	0.98032000	-0.15831400
H	-0.39713800	0.92329800	-1.02011600
N	3.05583500	3.21346000	0.80116800
C	3.50617900	3.86906300	-0.42397700
H	4.58476100	4.04811600	-0.31364900
H	3.39376600	3.14753100	-1.24628300
C	3.69761900	3.62814200	2.05598600
H	3.43596800	2.88854600	2.82276800
H	4.78499700	3.59398500	1.89965700
C	2.81183000	5.17983600	-0.74054600
C	1.49933200	5.45194400	-0.34331500
C	3.51394300	6.15169000	-1.46213800
C	0.90574500	6.67681000	-0.64904200
H	0.93460900	4.71504900	0.23272400
C	2.91914700	7.37262800	-1.77668800
H	4.54506800	5.95457400	-1.76830600
C	1.61300500	7.64180200	-1.36587100
H	-0.11625900	6.87762600	-0.31895200
H	3.48426000	8.12257400	-2.33541200
H	1.14891100	8.60260300	-1.60058800
C	3.25906800	5.01236500	2.47557600
C	4.04116200	6.13185900	2.17949100
C	2.01633500	5.19074900	3.09294700
C	3.57911400	7.41474200	2.47462800
H	5.01262700	5.99828400	1.69593300
C	1.55421300	6.47052100	3.39313300
H	1.39978000	4.31818600	3.32716600
C	2.33261900	7.58607100	3.07699200
H	4.19365400	8.28394100	2.22881200
H	0.58089100	6.59985000	3.87233000
H	1.96792400	8.59049500	3.30487900
C	-0.00962800	0.20370000	0.93445500
H	0.59283700	0.26465700	1.84350200
C	-1.07362800	-0.74836700	0.99561900
C	-1.84960900	-1.09905600	-0.22595100
C	-1.18002200	-1.52197600	-1.38241500
C	-3.24943200	-1.03045300	-0.22564700
C	-1.90146500	-1.89191900	-2.51452600
H	-0.09084400	-1.58006500	-1.38774100
C	-3.96542600	-1.38150100	-1.36760000
H	-3.78050600	-0.69441800	0.66677600
C	-3.29476400	-1.81937400	-2.51031400

H	-1.36936700	-2.23715200	-3.40384200
H	-5.05550800	-1.31383100	-1.36333800
H	-3.86034700	-2.10315900	-3.40085500
N	-1.29214900	-1.29980100	2.17439000
S	-2.28782000	-2.55105400	2.43703500
O	-2.14218900	-3.67002800	1.51422300
C	-1.50296300	-3.12869900	4.01768000
O	-3.62483600	-2.12823200	2.83171500
F	-1.56206700	-2.18823500	4.94439400
F	-2.16995000	-4.19306700	4.43971200
F	-0.23626100	-3.46721100	3.82716800
C	1.42040000	1.82679200	-0.34561600
H	1.31550900	2.55569800	-1.15195600
N	2.71497200	0.86790800	-1.45335000
S	3.62147700	-0.29334500	-0.77955400
C	2.18321000	0.63899600	-2.77892600
O	3.90341500	0.13232800	0.59481200
O	4.75632900	-0.59260100	-1.65847500
C	2.66660300	-1.80289500	-0.68242500
H	1.74827600	1.58167200	-3.14584400
H	2.98307700	0.35140800	-3.48071100
H	1.39363900	-0.13580300	-2.81763900
C	2.05774600	-2.16406000	0.51969500
C	2.51003700	-2.59657300	-1.81999300
C	1.26411700	-3.30543900	0.56942700
H	2.20712100	-1.55079300	1.40881000
C	1.71265700	-3.73784000	-1.75511400
H	3.01196400	-2.32934000	-2.75181500
C	1.06905800	-4.10424900	-0.56621700
H	0.76332700	-3.56962600	1.50250300
H	1.58198900	-4.35123500	-2.65033900
C	0.18318700	-5.31601700	-0.49290300
H	-0.75954100	-5.06723000	0.01644600
H	-0.04431000	-5.71117700	-1.49277800
H	0.66734200	-6.11855600	0.08704600

^{2}C

E (DLPNO-CCSD(T)) = -2872.140399
E (SMD/wB97xD/Def2TZVPP) =-2876.66157
E (gas/wB97xD/Def2TZVPP) =-2876.607654
G_{Corr}= 0.539553

C	1.41241800	0.47320700	-0.91722100
C	2.13504600	1.64081800	-0.70395500
H	1.69924500	2.43774300	-0.09428800
C	0.14872200	0.21598000	-0.40057600
H	-0.37623900	0.96678800	0.19589500
N	3.38579200	1.91390500	-1.18265100
C	4.10299100	0.98809200	-2.03615900
H	3.37437300	0.47540800	-2.68460200
H	4.74600200	1.57865500	-2.70643400
C	4.13739900	3.02518100	-0.61596600
H	4.75194600	3.47140300	-1.41238800
H	3.41708400	3.78732300	-0.28458000
C	4.96322400	-0.04856000	-1.33024700
C	6.21037100	-0.38352100	-1.86657800
C	4.54870800	-0.68702600	-0.15469500
C	7.02479000	-1.33502800	-1.25205500
H	6.55553500	0.11693600	-2.77565500
C	5.36180000	-1.63448800	0.46559500
H	3.58920800	-0.42969200	0.29689000
C	6.60296700	-1.96471600	-0.08167700
H	7.99738400	-1.57861700	-1.68677600
H	5.02281000	-2.11584400	1.38631500
H	7.24039500	-2.70589400	0.40628600
C	5.02295100	2.60899900	0.54297900
C	6.39660900	2.42218900	0.36453500
C	4.45749800	2.31587500	1.78983900
C	7.18904700	1.92808100	1.40155300
H	6.84794200	2.64630300	-0.60611600
C	5.24545800	1.82449300	2.82937800
H	3.38448000	2.46213100	1.94341600
C	6.61370100	1.62269200	2.63520700
H	8.25943200	1.77562000	1.24288900
H	4.79023600	1.59566100	3.79615400
H	7.23125700	1.23107400	3.44713000
C	-1.78527400	-1.27470400	0.19493600
C	-2.82491300	-0.24978800	-0.05010900
C	-3.13285800	0.14547600	-1.36033100
C	-3.47052200	0.36628600	1.03165100
C	-4.09999200	1.12134400	-1.58188700
H	-2.63706400	-0.32743400	-2.21036700
C	-4.41966300	1.35843900	0.80294400
H	-3.21630400	0.08570300	2.05581600
C	-4.74030000	1.73177300	-0.50224700
H	-4.35173500	1.41009100	-2.60439900
H	-4.91020200	1.84232000	1.64996400
H	-5.49061900	2.50558800	-0.67948600
N	-1.86683800	-2.26334500	1.00983800
N	0.44180500	-2.23095900	-0.30652500
C	1.19407700	-2.29934300	0.93725500
H	0.76168400	-3.02446800	1.64072100
H	2.24683800	-2.55889000	0.74489500
H	1.17896700	-1.30365800	1.39877200
S	0.55779100	-3.50997100	-1.34242600
O	-0.56715400	-3.42174900	-2.26813100
C	2.04774800	-3.21778300	-2.27096200
C	2.00498600	-2.35197000	-3.36649300
C	3.23923900	-3.82968100	-1.88829000
C	3.17170200	-2.10514700	-4.08000800
H	1.06632900	-1.88068300	-3.66418100
C	4.39885200	-3.57430700	-2.61885000
H	3.25801600	-4.50921900	-1.03463700
C	4.38434900	-2.71662000	-3.72465900
H	3.14097900	-1.42978800	-4.93885600
H	5.33386100	-4.05547600	-2.32177000
C	5.62331200	-2.47883400	-4.54125300
H	5.70020700	-1.42705700	-4.85286200
H	6.53111700	-2.74899500	-3.98477800
H	5.59686200	-3.08977600	-5.45872900
H	1.88937400	-0.33714300	-1.47896400
O	0.76304700	-4.71630000	-0.55180900
S	-3.22215900	-2.74340300	1.81348200
O	-4.44217200	-2.71176200	1.02731500
C	-2.74746400	-4.53771600	1.90997600
O	-3.20128600	-2.25309100	3.18047400
F	-1.62819300	-4.68784400	2.59424400
F	-3.72410000	-5.18262100	2.52732100
F	-2.59397700	-5.03505300	0.69693700
C	-0.48230800	-1.14334300	-0.58096000
H	-0.79565700	-1.26819100	-1.63461500

^{1}D

E (DLPNO-CCSD(T)) = -2871.94498
E (SMD/wB97xD/Def2TZVPP) = -2876.536166
E (gas/wB97xD/Def2TZVPP) = -2876.407642
G_{Corr}=0.543454

C	1.34940500	0.20412000	-0.92253500
C	2.02620300	1.45581600	-0.72361700
H	1.47927700	2.27602100	-0.24824800
C	0.05965800	0.06933800	-0.57196600
H	-0.50093800	0.92765700	-0.18894100
N	3.26003900	1.68679200	-1.03943800

C	4.10866800	0.70470000	-1.73383000
H	3.47108300	0.11928500	-2.40961600
H	4.79631500	1.27945000	-2.36638900
C	3.88177700	2.99416300	-0.74942900
H	4.10201700	3.46818200	-1.71637500
H	3.13889900	3.60336400	-0.22002700
C	4.89579400	-0.21691900	-0.82457200
C	6.22547300	-0.49921700	-1.15071500
C	4.32777300	-0.83991800	0.29240100
C	6.96864500	-1.40219700	-0.39102600
H	6.68645400	-0.00594800	-2.00983100
C	5.06996800	-1.74079300	1.05420400
H	3.30129300	-0.62516100	0.59488100
C	6.39136300	-2.02956600	0.71223800
H	8.00606100	-1.61109100	-0.66209500
H	4.60985400	-2.21791900	1.92255800
H	6.97200800	-2.73596200	1.30984100
C	5.14322300	2.82689500	0.06169500
C	6.39410300	3.05971900	-0.51424000
C	5.06883200	2.37286500	1.38328000
C	7.56038600	2.82730300	0.21612200
H	6.45593100	3.41202600	-1.54721700
C	6.23147800	2.13314800	2.11094300
H	4.09141200	2.18681900	1.83721600
C	7.48038300	2.35572100	1.52563100
H	8.53468700	3.00675300	-0.24418000
H	6.16521200	1.76780200	3.13827600
H	8.39280800	2.16238200	2.09461700
C	-1.92273400	-1.35206700	0.14218200
C	-2.89733700	-0.24324700	0.05092700
C	-3.24015500	0.30147800	-1.19614300
C	-3.45443000	0.29235900	1.22176200
C	-4.15336200	1.34930100	-1.26704000
H	-2.81673100	-0.10675600	-2.11614400
C	-4.35000800	1.35410800	1.14324800
H	-3.17379200	-0.10762200	2.19815600
C	-4.70493200	1.87884500	-0.09971600
H	-4.43396200	1.75584700	-2.24069500
H	-4.77243700	1.77323300	2.05859300
H	-5.41361300	2.70791200	-0.15921000
N	-2.03157400	-2.41258900	0.85229200
N	0.23799100	-2.37099800	-0.52427500
C	0.93510200	-2.59324400	0.73816200
H	0.50396000	-3.43451900	1.29621800
H	2.00741600	-2.77348300	0.56659300
H	0.84737500	-1.68670900	1.34989200
S	0.38157100	-3.53876000	-1.69571900
O	-0.62205700	-3.23661100	-2.71045100
C	1.99170800	-3.26021100	-2.39335200
C	2.12393900	-2.37369500	-3.46420400
C	3.10606600	-3.88604200	-1.83574200
C	3.39152900	-2.11343900	-3.97155900
H	1.24394800	-1.89502900	-3.89767300
C	4.36928500	-3.60572800	-2.35230400
H	2.98895900	-4.58960900	-1.00976000
C	4.53300300	-2.72112000	-3.42533400
H	3.49938600	-1.42289200	-4.81179900
H	5.24513600	-4.08844500	-1.91211300
C	5.89079700	-2.44478300	-4.00634600
H	6.01638900	-1.37559200	-4.23128700
H	6.69300900	-2.75814100	-3.32454800
H	6.01811500	-2.99378900	-4.95378900
H	1.89917400	-0.65551000	-1.30922800
O	0.39983800	-4.83580300	-1.03743400
S	-3.37573500	-2.88534100	1.68663400
O	-4.62638500	-2.69079200	0.97785600
C	-3.02314500	-4.70786600	1.58101500
O	-3.24165400	-2.53107800	3.08774800
F	-1.88248500	-4.99488600	2.17956700
F	-4.00859500	-5.34396700	2.19131100
F	-2.96969300	-5.08805400	0.31887300
C	-0.65154700	-1.25638000	-0.70274800
H	-1.03190300	-1.30183800	-1.74263600

C4-selectivity

TS-2

E (DLPNO-CCSD(T)) = -2872.097562
E (SMD/wB97xD/Def2TZVPP) =-2876.615817E
(gas/wB97xD/Def2TZVPP) = -2876.563313
G_{Corr}= 0.538517

C	2.61949500	-0.45235300	-0.07551000
H	2.88780700	-0.59394800	0.97211200
C	3.56783900	-0.01637400	-0.98532900
H	3.28047700	0.13898300	-2.02662100
N	4.84287900	0.25995600	-0.73140600
C	5.40999300	0.13893300	0.60236800
H	5.02069200	-0.77977400	1.06862200
H	6.49272400	-0.01322100	0.48954800
C	5.73183500	0.73860600	-1.79130500
H	6.59688500	0.06065000	-1.85218400
H	5.18511300	0.67262900	-2.74105200
C	5.16397500	1.31979900	1.52614800
C	5.94299600	1.43454300	2.68432500
C	4.17818900	2.27924200	1.27933200
C	5.73808800	2.48347700	3.57933900
H	6.72284200	0.69414400	2.88470400
C	3.97262400	3.33015400	2.17525500
H	3.56010700	2.22373900	0.38107800
C	4.74918500	3.43702500	3.32792600
H	6.35773300	2.55902000	4.47630200
H	3.19278300	4.06546300	1.96178200
H	4.58834100	4.26057000	4.02776500
C	6.20298200	2.15611800	-1.55017500
C	7.51082300	2.41146400	-1.13035100
C	5.31137500	3.22635900	-1.69552700
C	7.92510900	3.71604800	-0.85297000
H	8.21138100	1.57994000	-1.01229600
C	5.72322800	4.52822600	-1.42108800
H	4.27584400	3.03216300	-1.98929400
C	7.03116800	4.77609900	-0.99642600
H	8.94928200	3.90250700	-0.52096100
H	5.01766700	5.35539200	-1.53129300
H	7.35166500	5.79740300	-0.77668500
C	0.71068100	-0.62350800	-1.72563700
H	1.30573000	-0.31090000	-2.58609500
C	-0.61291800	-1.06363000	-2.02820900
C	-1.52215300	-1.55745000	-0.95597600
C	-2.70923300	-0.86787500	-0.68404000
C	-1.20135500	-2.71077900	-0.22973500
C	-3.56468500	-1.32759200	0.31519600
H	-2.95581400	0.03267900	-1.24849800
C	-2.06830000	-3.17370600	0.75670100
H	-0.27783700	-3.25188200	-0.44893500
C	-3.24809200	-2.48070100	1.03302800
H	-4.48454300	-0.78039900	0.53236100
H	-1.82055600	-4.08016600	1.31324500
H	-3.92340000	-2.84185900	1.81206400
N	-0.95960100	-0.99248400	-3.29422100
S	-2.35330700	-1.64757600	-3.86776000
O	-3.46653800	-0.71285800	-3.84631900
C	-1.81447000	-1.74464200	-5.64295600
O	-2.55745000	-3.02804700	-3.46098500
F	-0.76703400	-2.54156400	-5.75904200

F	-2.82164800	-2.24399300	-6.34231500
F	-1.50907400	-0.55063900	-6.11783400
C	1.25046600	-0.57079100	-0.40012400
H	0.62589700	-1.01306600	0.37661600
N	0.22451900	1.25395400	0.07660100
S	0.71286400	2.51421500	-0.83801600
C	0.50833300	1.36912000	1.49466800
O	2.07914100	2.37272200	-1.37660700
O	0.44010800	3.77046000	-0.12808000
C	-0.39043500	2.40916200	-2.22909400
H	1.58440600	1.32657800	1.74543800
H	0.10959800	2.31633000	1.89209100
H	-0.00115200	0.54399600	2.01424100
C	0.12249900	2.36199000	-3.51999900
C	-1.76909500	2.43935500	-2.00583300
C	-0.75755800	2.32025300	-4.60177500
H	1.20191300	2.34502700	-3.67753100
C	-2.63131800	2.39210600	-3.09204600
H	-2.16076300	2.48222700	-0.98752200
C	-2.14179200	2.32648300	-4.40718700
H	-0.35562000	2.27013200	-5.61666300
H	-3.71065800	2.39822700	-2.92129900
C	-3.09858700	2.23442000	-5.56144200
H	-3.62859200	1.27018400	-5.52588600
H	-3.85828000	3.02936900	-5.50982400
H	-2.57994600	2.30990300	-6.52700100

^{2}C

E (DLPNO-CCSD(T)) = -2872.120701
E (SMD/wB97xD/Def2TZVPP) =-2876.626834
E (gas/wB97xD/Def2TZVPP) =-2876.588279
G_{Corr}= 0.538756

C	2.20661800	0.81367600	-1.00789700
H	2.72455500	-0.13956100	-0.86890400
C	2.88463500	1.95030000	-1.27312000
H	2.33206600	2.89127000	-1.34865800
N	4.22771200	2.10512200	-1.48115300
C	5.14065300	0.98471000	-1.44772400
H	4.61169700	0.09689100	-1.83137700
H	5.95554300	1.18520300	-2.16096100
C	4.79267800	3.44672500	-1.47742100
H	5.65197400	3.46292600	-2.16500800
H	4.03478700	4.13529900	-1.87951400
C	5.75466500	0.66669200	-0.09270100
C	7.07929100	0.22341600	-0.02238800
C	5.03709700	0.82275500	1.09988600
C	7.67905600	-0.05236100	1.20749400
H	7.65763600	0.10931100	-0.94394500
C	5.63476600	0.55498200	2.33037800
H	4.00642500	1.18144700	1.06934600
C	6.95948300	0.11740000	2.38988600
H	8.71807000	-0.38956600	1.24112200
H	5.06263500	0.69560500	3.25083200
H	7.42938800	-0.08666800	3.35502500
C	5.22949700	3.91268300	-0.10165100
C	6.57419000	3.87404900	0.27799500
C	4.27214600	4.30669900	0.84106800
C	6.95605700	4.19461600	1.58141400
H	7.32971600	3.56796400	-0.45112500
C	4.64873300	4.62860100	2.14416900
H	3.21773500	4.35019800	0.55223500
C	5.99257900	4.56631300	2.51965800
H	8.00992000	4.14814600	1.86673200
H	3.89058600	4.93005500	2.87123000
H	6.28828900	4.81276800	3.54231300
C	0.08565900	-0.15258200	-1.87826200
H	0.59795400	-0.28400800	-2.83440600
C	-1.05689500	-0.96344200	-1.67523800
C	-1.82680100	-0.90519400	-0.39676300
C	-2.52750000	0.25248100	-0.03654700
C	-1.84211300	-2.02057700	0.45021400
C	-3.24454000	0.28608300	1.15713000
H	-2.50810600	1.13012500	-0.68291900
C	-2.55173100	-1.97525900	1.64889900
H	-1.29252400	-2.92244400	0.17475500
C	-3.25616400	-0.82472900	2.00199700
H	-3.79592100	1.18895800	1.42864100
H	-2.55237400	-2.84505000	2.30942300
H	-3.81545900	-0.79243700	2.93985300
N	-1.35963000	-1.76365200	-2.68228200
S	-2.70970800	-2.69801900	-2.69095000
O	-3.93669700	-1.94209500	-2.50572700
C	-2.66221200	-3.14223600	-4.49600000
O	-2.50478900	-3.95932600	-1.99776700
F	-1.48815000	-3.64822000	-4.82646900
F	-3.60220300	-4.04952100	-4.70867400
F	-2.90915500	-2.08342900	-5.24802100
C	0.71050700	0.73351700	-0.83284700
H	0.53011200	0.19378300	0.11615500
N	-0.01139100	1.99309200	-0.60624300
S	-0.42249300	3.14613600	-1.74676200
C	0.07861700	2.53409300	0.74593500
O	0.61711200	4.17261400	-1.86102200
O	-1.75977800	3.61737300	-1.39085600
C	-0.50917300	2.24817700	-3.26496400
H	1.11725100	2.77157200	1.02979100
H	-0.52994900	3.44395900	0.82512800
H	-0.32955000	1.79667200	1.45343800
C	0.61511600	2.16803900	-4.08732700
C	-1.71846600	1.65242400	-3.62635100
C	0.53385600	1.42273900	-5.25886200
H	1.54280800	2.67185200	-3.81144300
C	-1.78101400	0.91803600	-4.80270500
H	-2.59588000	1.74721400	-2.98439800
C	-0.65436800	0.77352900	-5.62579200
H	1.41224500	1.34359100	-5.90378300
H	-2.72078300	0.43753400	-5.07986400
C	-0.71276300	-0.08367900	-6.85753900
H	0.01856400	0.24277200	-7.61008700
H	-0.47931300	-1.12890400	-6.59687200
H	-1.71561300	-0.07345900	-7.30695600

^{1}D

E (DLPNO-CCSD(T)) = -2871.940957
E (SMD/wB97xD/Def2TZVPP) = -2876.527337
E (gas/wB97xD/Def2TZVPP) = -2876.406614
G_{Corr}= 0.546244

C	0.58012000	1.65405800	-1.32783200
H	1.08188300	1.47386300	-2.27723500
C	1.38905200	2.11409900	-0.21259800
H	0.91179000	2.26386400	0.76185900
N	2.65411700	2.34419500	-0.26619900
C	3.42780600	2.26497400	-1.51200300
H	2.83453900	2.74333200	-2.30334300
H	4.31627400	2.89238500	-1.36901100
C	3.40332800	2.70804500	0.95511700
H	3.90249200	3.66538000	0.75472900
H	2.67146200	2.84855900	1.75916200
C	3.84184100	0.87305700	-1.94124400
C	4.81111200	0.78273400	-2.94829100
C	3.28565000	-0.29986300	-1.42619500
C	5.21028600	-0.45801200	-3.43784900

H	5.25590900	1.69662900	-3.35086100
C	3.68900500	-1.54402400	-1.91602400
H	2.53768300	-0.27077900	-0.63133200
C	4.64757100	-1.62785700	-2.92334700
H	5.96787400	-0.51155600	-4.22307500
H	3.24578800	-2.45145100	-1.50098600
H	4.96087700	-2.60247200	-3.30437100
C	4.40179800	1.63036100	1.30093000
C	5.75718800	1.79081900	1.00063500
C	3.96107400	0.43545100	1.88091300
C	6.66379300	0.76520300	1.27069200
H	6.10411100	2.72314000	0.54738400
C	4.86717800	-0.58577400	2.15650500
H	2.90048500	0.29464800	2.10734900
C	6.21929200	-0.42398500	1.84745400
H	7.72100500	0.89704700	1.02945600
H	4.51593000	-1.51416300	2.61121200
H	6.92821400	-1.22783300	2.05937900
C	-0.57745000	0.70724600	-1.03857900
H	-0.71373600	-0.03866300	-1.82902900
C	-0.76142500	0.14142900	0.34114300
C	-1.93385100	0.55642700	1.13314600
C	-3.18131000	0.68906000	0.50418700
C	-1.80361800	0.86541300	2.49554200
C	-4.29182600	1.08419800	1.24136000
H	-3.28515200	0.45919000	-0.55726100
C	-2.91389200	1.28705000	3.22032200
H	-0.83099200	0.80691900	2.98732200
C	-4.15813300	1.38778600	2.59777200
H	-5.26519800	1.16405700	0.75346200
H	-2.80482700	1.54044600	4.27657700
H	-5.02921000	1.71246400	3.17127700
N	0.17845400	-0.66046300	0.70641200
S	0.17757200	-1.58899800	2.07360400
O	-1.09393500	-2.21508800	2.37991800
C	1.24282400	-2.95155300	1.38889800
O	0.96424400	-0.94939200	3.11556500
F	2.44822700	-2.49889700	1.09923100
F	1.33781500	-3.88614800	2.31712400
F	0.69107300	-3.46013900	0.30372400
C	-0.87332900	2.11836300	-1.38657400
H	-1.19052300	2.77143900	-0.56356800
N	-1.41796900	2.38911600	-2.67747300
S	-0.78001700	3.69393900	-3.50419600
C	-2.79670800	1.98291400	-2.92453800
O	-0.26945500	4.66813700	-2.54580000
O	-1.77578200	4.10193800	-4.48550800
C	0.61842800	3.00126600	-4.35861500
H	-2.87655400	0.89806500	-2.76715700
H	-3.50661300	2.50086000	-2.25924400
H	-3.05919500	2.20104400	-3.96506000
C	1.79711700	3.73917700	-4.42873100
C	0.51236800	1.75141000	-4.97093100
C	2.88910600	3.20693700	-5.11197300
H	1.86961800	4.70975100	-3.93512200
C	1.61419000	1.23247100	-5.64040500
H	-0.41191500	1.17378000	-4.90016200
C	2.81846700	1.94936100	-5.72345500
H	3.81988800	3.77764000	-5.15678000
H	1.54220300	0.24572500	-6.10440500
C	3.99395900	1.38178100	-6.46752000
H	4.93761600	1.84191300	-6.14306700
H	4.06458700	0.29326600	-6.32987900
H	3.88581000	1.56906300	-7.54863500

Me-substrate

^{1}1b^{Me}

E (DLPNO-CCSD(T)) = -1767.846512
E (SMD/wB97xD/Def2TZVPP) = -1770.635573
E (gas/wB97xD/Def2TZVPP) = -1770.604665
G_{Corr}= 0.327382

C	-7.12712200	-1.11364100	6.16793100
C	-6.29422000	-0.26117600	6.87670500
H	-6.64386500	0.10706600	7.84689500
C	-8.38769300	-1.43995800	6.69299100
H	-8.66444900	-0.99021500	7.65510500
N	-5.09061800	0.18072800	6.52078000
C	-4.48618700	-0.15282400	5.23878700
H	-5.29132000	-0.30365200	4.50439100
H	-3.92179300	0.72805900	4.90081600
C	-4.29261900	0.98743600	7.44829800
H	-3.87418900	1.83649500	6.88845600
H	-4.97058400	1.38732700	8.21397200
C	-3.56292200	-1.35752700	5.25325600
C	-2.46373800	-1.38068600	4.38822000
C	-3.77349700	-2.44625800	6.10542000
C	-1.58795100	-2.46604600	4.37742000
H	-2.28239500	-0.53002900	3.72515800
C	-2.89345500	-3.52822000	6.10343700
H	-4.61935300	-2.44569400	6.79645900
C	-1.79686600	-3.54194400	5.24062400
H	-0.73039400	-2.46422600	3.70016700
H	-3.06506300	-4.36440800	6.78553800
H	-1.10553300	-4.38797400	5.24330100
C	-3.18235100	0.18619400	8.09372400
C	-1.87083700	0.26583900	7.61830500
C	-3.47883600	-0.71124700	9.12576200
C	-0.87389900	-0.55473300	8.14770000
H	-1.63202900	0.96328500	6.81067000
C	-2.48527000	-1.52932700	9.65969000
H	-4.50322900	-0.77973700	9.50319400
C	-1.18074000	-1.45746900	9.16581300
H	0.14548100	-0.49151400	7.75954400
H	-2.72891300	-2.22914600	10.46265900
H	-0.40246800	-2.10398100	9.57836000
C	-10.57272700	-2.57218500	6.69657900
N	-10.89657200	-2.01100800	7.85308500
H	-6.81252200	-1.55337600	5.21828900
S	-12.30237200	-2.28571000	8.58656400
O	-12.38117500	-3.58773000	9.24157900
C	-12.07738200	-1.07148900	9.96900800
O	-13.47113200	-1.80686500	7.85496300
F	-11.94512100	0.15984800	9.50084400
F	-13.15414000	-1.12044100	10.74263200
F	-11.01475300	-1.37098900	10.69960200
C	-9.31377500	-2.28437200	6.10785700
H	-9.08382500	-2.76063100	5.15159200
C	-11.50689200	-3.49945000	5.97050200
H	-11.85255200	-4.29727500	6.64505700
H	-12.39758300	-2.94049400	5.64385300
H	-11.02876600	-3.95182900	5.09389300

C5-selectivity

TS-2^{Me}

E (DLPNO-CCSD(T)) =-2680.727133

E (SMD/wB97xD/Def2TZVPP) =-2684.871669
E (gas/wB97xD/Def2TZVPP) =-2684.831151
G_{Corr}= 0.482984

C	1.93200100	2.18244300	-1.07996700
H	1.27473600	2.08791800	-1.94901100
C	0.27727700	0.92522400	0.16608300
H	-0.32078000	0.94480400	-0.74967100
N	3.09765300	2.76799000	-1.30550000
C	4.05217200	3.05444200	-0.23809000
H	4.48371000	4.04379300	-0.44577000
H	3.49902600	3.13974100	0.70719300
C	3.49333300	3.11341100	-2.67553300
H	2.58199600	3.14210500	-3.28686900
H	3.92563300	4.12336600	-2.65607600
C	5.16752700	2.03707100	-0.09646000
C	4.94408400	0.66643500	-0.26476800
C	6.45501100	2.47660300	0.22641000
C	5.99191100	-0.24354800	-0.13131200
H	3.94830700	0.30075800	-0.52720000
C	7.50266400	1.56707200	0.37099100
H	6.64313900	3.54652200	0.35187400
C	7.27547900	0.20345100	0.18605300
H	5.80346400	-1.30951000	-0.27982800
H	8.50406900	1.92812500	0.61758600
H	8.09668800	-0.51011500	0.28662800
C	4.48437900	2.12425000	-3.25008600
C	5.84534200	2.43226000	-3.31972200
C	4.05089300	0.85589000	-3.65165600
C	6.76469400	1.48070400	-3.76268900
H	6.19093200	3.42054600	-3.00465200
C	4.96591000	-0.09562100	-4.09770900
H	2.98706200	0.60673200	-3.60031500
C	6.32691600	0.21347800	-4.14765100
H	7.82791000	1.72912500	-3.80192000
H	4.61716500	-1.08434200	-4.40527800
H	7.04607100	-0.53411500	-4.49071000
C	-0.13204000	0.19682400	1.23960700
H	0.45370500	0.22215200	2.16237200
C	-1.32027100	-0.62045700	1.28431000
N	-1.52588100	-1.24072200	2.41905700
S	-2.80611300	-2.23192300	2.64061700
O	-2.77508300	-3.41303700	1.79037800
C	-2.33315000	-2.82939500	4.33227900
O	-4.05700300	-1.50963000	2.82509300
F	-2.29195300	-1.82524000	5.18983900
F	-3.25229300	-3.69807700	4.72716400
F	-1.15626600	-3.42998300	4.30406200
C	1.46939100	1.73830200	0.18413300
H	2.20985700	1.50401800	0.95119200
N	0.99967500	3.47172100	1.09068200
S	1.27697700	3.37092800	2.69220500
C	-0.33628900	3.88114500	0.71200400
O	2.57987900	2.71185700	2.86343500
O	0.14658100	2.82744700	3.45616600
C	1.47192500	5.07595800	3.18878000
H	-0.40124000	3.86359400	-0.38685700
H	-1.13412400	3.23323600	1.11746200
H	-0.54453500	4.91764300	1.03418200
C	2.60983700	5.77883400	2.78299000
C	0.48377600	5.69653200	3.94626000
C	2.74955100	7.11188600	3.14721200
H	3.38110000	5.28530100	2.18739700
C	0.63821800	7.03668900	4.30393200
H	-0.39760100	5.13250500	4.25636100
C	1.76787500	7.76338800	3.91327900
H	3.63968500	7.66398800	2.83384200
H	-0.13764900	7.52453800	4.89960100
C	1.94725600	9.20353500	4.30727400
H	2.18916600	9.82510200	3.43166000
H	1.04253200	9.60808100	4.78164300
H	2.78145800	9.30945500	5.01932400
C	-2.21501400	-0.77351400	0.09012900
H	-2.08693800	0.03542700	-0.63645500
H	-1.97921100	-1.72735000	-0.40776000
H	-3.26943800	-0.80303100	0.39555000

C3-selectivity

TS-2^{Me} (estimation via adduct formation)

E (DLPNO-CCSD(T)) = -2680.728856
E (SMD/wB97xD/Def2TZVPP) = -2684.882689
E (gas/wB97xD/Def2TZVPP) =-2684.841634
G_{Corr}= 0.484794

C	1.91281100	0.36886900	-0.86692100
C	2.93883100	1.00493600	-0.15884700
H	2.74707900	1.27997800	0.88306200
C	0.71566300	0.08373300	-0.21416800
H	0.63974600	0.32528100	0.85139900
N	4.13773700	1.33420200	-0.61021000
C	4.59278900	0.98481500	-1.95127300
H	5.66161000	0.74029900	-1.88101200
H	4.08067100	0.06096400	-2.25260400
C	5.05351200	2.12043900	0.22552600
H	4.69465300	2.06096500	1.26107200
H	6.04462300	1.64814600	0.17753600
C	4.38850200	2.05871800	-3.00144300
C	3.26978100	2.89779400	-2.99967900
C	5.34480700	2.20906700	-4.01141800
C	3.11643300	3.87434400	-3.98354700
H	2.51698100	2.80923300	-2.21294500
C	5.18730000	3.17721700	-5.00260800
H	6.23176500	1.56965400	-4.01232000
C	4.07364700	4.01718000	-4.98862800
H	2.24295700	4.53027900	-3.96095600
H	5.94628500	3.28447500	-5.78123300
H	3.95350100	4.78466000	-5.75681900
C	5.12884000	3.56071400	-0.23166500
C	4.07845100	4.43880200	0.05778500
C	6.19720400	4.00955300	-1.01202700
C	4.08763800	5.73997700	-0.44021400
H	3.23871100	4.09393000	0.66796000
C	6.20748800	5.31096700	-1.51546600
H	7.01946400	3.32737100	-1.24423200
C	5.15029800	6.17634200	-1.23465600
H	3.26087500	6.41657500	-0.21135800
H	7.04262100	5.64780200	-2.13415000
H	5.15496100	7.19410000	-1.63202300
C	-1.63098100	-0.72625900	-0.07159700
N	-1.60641500	-0.49019200	1.21201900
N	-0.30321800	-2.75469100	-0.40936200
C	0.63466500	-2.88884500	0.67570000
H	0.74604600	-3.94747100	0.96696600
H	1.64312600	-2.48470000	0.46191300
H	0.22337500	-2.34775000	1.54260500
S	-0.00033600	-3.53931300	-1.79672100
O	-1.08040900	-3.19985700	-2.72705700
C	1.51166000	-2.92056600	-2.52866700
C	1.44470800	-2.04451400	-3.61160000
C	2.74806500	-3.34350400	-2.03689800
C	2.62137600	-1.59194300	-4.20317100
H	0.47251200	-1.73095400	-3.99584000
C	3.91689700	-2.87705400	-2.63319800
H	2.80006300	-4.04920900	-1.20559100

C	3.87418500	-2.00619800	-3.73096000
H	2.56576700	-0.90759700	-5.05380300
H	4.88408800	-3.20785400	-2.24606400
C	5.13939300	-1.54749000	-4.40137600
H	5.00908100	-0.56189500	-4.86989500
H	5.97575800	-1.49315100	-3.68985100
H	5.42900000	-2.25441700	-5.19640100
H	2.02491600	0.12333600	-1.92583000
O	0.23901300	-4.95727100	-1.50513200
S	-2.88809100	-0.77586600	2.17190900
O	-3.17743400	-2.19404400	2.33467200
C	-2.07963200	-0.26211400	3.76045500
O	-3.98275200	0.16136600	1.96954900
F	-1.03278300	-1.02806500	4.02289500
F	-1.69025400	1.00016900	3.70219600
F	-2.96604100	-0.39637800	4.73558600
C	-0.39220900	-0.51885500	-0.80700000
H	-0.43325200	-0.64272200	-1.88995800
C	-2.84804100	-1.13121300	-0.84092700
H	-3.50837700	-1.77494600	-0.24578000
H	-2.55763300	-1.66153700	-1.75519400
H	-3.40392300	-0.21783600	-1.10943700

*i*Pr-substrate

^{1}1b^{iPr}

E (DLPNO-CCSD(T)) =-1846.327895
E (SMD/wB97xD/Def2TZVPP) = -1849.269638
E (gas/wB97xD/Def2TZVPP) =-1849.23819
G_{Corr}= 0.382073

C	-7.12853700	-1.11586800	6.12270700
C	-6.30312700	-0.24922600	6.82057100
H	-6.66479500	0.14418800	7.77635300
C	-8.39886600	-1.42516000	6.63901000
H	-8.68389500	-0.95414600	7.58825200
N	-5.09282400	0.18223400	6.47052700
C	-4.47054100	-0.18640200	5.20724300
H	-5.26524800	-0.35819600	4.46603600
H	-3.90127600	0.68466400	4.85229800
C	-4.30642800	1.00886400	7.38975900
H	-3.86975300	1.83801700	6.81424800
H	-4.99599400	1.43659400	8.12974600
C	-3.54782300	-1.39007600	5.26891100
C	-2.43086000	-1.43397000	4.42791500
C	-3.77684100	-2.45840500	6.14206000
C	-1.55595200	-2.51963800	4.46072000
H	-2.23488600	-0.59927900	3.74888900
C	-2.89779800	-3.54034200	6.18389400
H	-4.63710600	-2.44090800	6.81492700
C	-1.78362300	-3.57486100	5.34435600
H	-0.68459900	-2.53398500	3.80146500
H	-3.08412800	-4.36027700	6.88169400
H	-1.09327500	-4.42090000	5.38111800
C	-3.21536500	0.21934900	8.08103800
C	-1.89314600	0.28058700	7.63352900
C	-3.53904500	-0.64860700	9.13002600
C	-0.91213600	-0.52947100	8.20705800
H	-1.63294300	0.95507700	6.81310400
C	-2.56151800	-1.45612200	9.70799900
H	-4.57171600	-0.70249400	9.48672500
C	-1.24588400	-1.40311100	9.24194400
H	0.11593500	-0.48093800	7.84030200
H	-2.82647300	-2.13281900	10.52394100
H	-0.48010400	-2.04140200	9.68921900
C	-10.58676800	-2.55184100	6.64199400
N	-10.89002500	-1.99901000	7.80508000
H	-6.80375900	-1.57940800	5.18788600
S	-12.28613200	-2.22679300	8.57188300
O	-12.47011400	-3.57388300	9.10388000
C	-11.89397500	-1.18446400	10.05372000
O	-13.42745300	-1.56658000	7.94485000
F	-11.66027900	0.07070100	9.70416900
F	-12.93998200	-1.21287100	10.86917900
F	-10.83851300	-1.65602500	10.69877700
C	-9.32261900	-2.27113000	6.05630100
H	-9.07890800	-2.75442500	5.10826500
C	-11.51414600	-3.53429300	5.93880400
H	-12.52904200	-3.36791300	6.32866900
C	-11.09746100	-4.96467700	6.30826900
H	-10.08544500	-5.18854900	5.93639200
H	-11.11341600	-5.10869900	7.39798200
H	-11.79639100	-5.68458500	5.85580100
C	-11.57931200	-3.33703200	4.42416900
H	-11.80842100	-2.29322800	4.16155000
H	-10.63915000	-3.62124300	3.92810900
H	-12.37516500	-3.97394100	4.00933100

C5-selectivity

TS-2^{iPr}

E (DLPNO-CCSD(T)) =-2759.2039
E (SMD/wB97xD/Def2TZVPP) =-2763.501842
E (gas/wB97xD/Def2TZVPP) = -2763.460726
G_{Corr}= 0.537154

C	1.92035600	2.23777500	-1.08588300
H	1.26421300	2.18598300	-1.95931400
C	0.22298600	1.00715400	0.12733200
H	-0.36859600	1.06472000	-0.79056000
N	3.10991100	2.77844900	-1.29423000
C	4.07421700	2.98683400	-0.21825200
H	4.58087500	3.94183000	-0.41632700
H	3.52365500	3.10798300	0.72544500
C	3.52275100	3.15161600	-2.65214100
H	2.61763000	3.20757700	-3.27048300
H	3.96841600	4.15505800	-2.60355100
C	5.10971600	1.88821000	-0.07236500
C	4.80702900	0.54425200	-0.31353300
C	6.40498100	2.22624600	0.33302600
C	5.78543900	-0.43902800	-0.16986300
H	3.80482000	0.25655700	-0.64060600
C	7.38219100	1.24332000	0.48715800
H	6.65507400	3.27488700	0.51636900
C	7.07682400	-0.09332500	0.22996600
H	5.53587000	-1.48270000	-0.37549800
H	8.39081500	1.52587000	0.79838000
H	7.84367900	-0.86391400	0.33848500
C	4.50590600	2.16285900	-3.23910200
C	5.87570900	2.43763100	-3.25397800
C	4.05350800	0.92346700	-3.70477600
C	6.78447600	1.48006500	-3.70568000
H	6.23582900	3.40340700	-2.88925000
C	4.95806400	-0.03356700	-4.16019300
H	2.98252200	0.70130200	-3.69625700
C	6.32736600	0.24109200	-4.15482500
H	7.85433200	1.70153000	-3.70198900
H	4.59466400	-0.99981100	-4.51801600
H	7.03814700	-0.51120000	-4.50500200

C	-0.20164800	0.26038500	1.18293100
H	0.39336600	0.25119800	2.09997500
C	-1.39960300	-0.55054100	1.22590100
N	-1.55813200	-1.18512600	2.35863800
S	-2.69615300	-2.24469800	2.81240200
O	-2.87794900	-3.38322100	1.91946100
C	-1.76096400	-2.93854700	4.25703300
O	-3.85827500	-1.59570200	3.39911500
F	-1.52692300	-2.00324300	5.16068700
F	-2.50454600	-3.88949700	4.80483600
F	-0.61252400	-3.46396600	3.86489600
C	1.43271500	1.79215200	0.16904200
H	2.15993300	1.52814600	0.93918200
N	0.98921900	3.52806700	1.07456800
S	1.28832900	3.43201900	2.67204200
C	-0.35237400	3.93865700	0.71610100
O	2.60937900	2.80527700	2.82620400
O	0.18348400	2.85696100	3.45023700
C	1.44315300	5.14157800	3.16794400
H	-0.43474500	3.91925000	-0.38149500
H	-1.14460300	3.29231000	1.13493100
H	-0.55394300	4.97586600	1.03980800
C	2.50408300	5.90336900	2.66983400
C	0.50202100	5.70429100	4.02336800
C	2.61433300	7.23697400	3.04138000
H	3.23697100	5.45666700	1.99419000
C	0.62648700	7.04584100	4.38809700
H	-0.32014100	5.09451600	4.40185800
C	1.67866400	7.83102600	3.90586600
H	3.44362300	7.83563000	2.65505200
H	-0.11211100	7.48797200	5.06170500
C	1.81975600	9.27675500	4.29483400
H	2.76977800	9.44735300	4.82538300
H	1.82735700	9.92341000	3.40352400
H	0.99851200	9.60076800	4.94880200
C	-2.29643500	-0.63950600	0.00523300
H	-2.09893400	0.26770400	-0.57962700
C	-3.79751400	-0.64164300	0.29887400
H	-4.15046800	-1.60305600	0.69382400
H	-4.07542500	0.15423400	1.00487100
H	-4.33822400	-0.46351500	-0.64241300
C	-1.86810200	-1.83944800	-0.85442000
H	-2.02681500	-2.78297500	-0.31309900
H	-2.46839600	-1.86122600	-1.77626800
H	-0.80717800	-1.76982700	-1.13670400

C3-selectivity

TS-2^{iPr}

E (DLPNO-CCSD(T)) =-2759.20611
E (SMD/wB97xD/Def2TZVPP) = -2763.512611
E (gas/wB97xD/Def2TZVPP) =-2763.471699
G_{Corr}= 0.541637

C	1.92533300	0.25013900	-0.87159900
C	2.91166600	0.92493000	-0.14462400
H	2.68326600	1.20367100	0.88895000
C	0.71454400	-0.03256800	-0.24374200
H	0.62066300	0.23187100	0.81473900
N	4.11084900	1.29506700	-0.56605900
C	4.61012700	0.95819600	-1.89276400
H	5.69213700	0.78804600	-1.80405900
H	4.16705500	-0.00349900	-2.18530800
C	4.97422600	2.11985900	0.28678100
H	4.57602300	2.07482800	1.30852300
H	5.97782500	1.67150500	0.28804400
C	4.34939100	1.99443000	-2.96852100
C	3.20570000	2.79896800	-2.97117000
C	5.28012000	2.14070000	-4.00292900
C	3.00184800	3.73626000	-3.98405900
H	2.47175900	2.71511000	-2.16657300
C	5.07285100	3.06949800	-5.02188400
H	6.18588100	1.52861700	-4.00246300
C	3.93317700	3.87428100	-5.01345200
H	2.10863700	4.36520500	-3.96464800
H	5.81282500	3.17375600	-5.81903400
H	3.77362000	4.61082100	-5.80441800
C	5.03302600	3.55073900	-0.20054900
C	3.96323600	4.41688600	0.05138900
C	6.10466500	3.99923400	-0.97675000
C	3.95708200	5.70536600	-0.47865800
H	3.12054800	4.07194900	0.65744200
C	6.09946300	5.28756900	-1.51289400
H	6.94222000	3.32629600	-1.17974600
C	5.02331700	6.14064500	-1.26892800
H	3.11551400	6.37276700	-0.27850600
H	6.93752900	5.62383100	-2.12792300
H	5.01599100	7.14815900	-1.69158700
C	-1.67315200	-0.61347400	-0.10994300
N	-1.58862600	-0.56397100	1.18807600
N	-0.25720600	-2.79169400	-0.50980100
C	0.59458100	-2.91993300	0.65140300
H	0.67165200	-3.97514900	0.96039400
H	1.62141700	-2.52999900	0.50997800
H	0.12638700	-2.36241700	1.47574500
S	0.18562100	-3.64588500	-1.82234000
O	-0.85568500	-3.48805200	-2.83796000
C	1.67371500	-2.95032500	-2.53519500
C	1.57443900	-2.09972000	-3.63492000
C	2.92470800	-3.30642200	-2.02664100
C	2.73446200	-1.61235300	-4.23418200
H	0.59218500	-1.83764400	-4.03190800
C	4.07486400	-2.80980000	-2.63264300
H	2.99933200	-3.99080400	-1.17951100
C	4.00055700	-1.97001000	-3.75399900
H	2.65422800	-0.95139300	-5.10107100
H	5.05399200	-3.09369000	-2.23787100
C	5.25467300	-1.48760600	-4.42861200
H	5.04407300	-0.67632600	-5.13878300
H	5.98917400	-1.12760000	-3.69278900
H	5.73138700	-2.31013600	-4.98617300
H	2.07152400	-0.00626000	-1.92361600
O	0.53684600	-5.00968300	-1.40568300
S	-2.87290700	-0.57395900	2.19033600
O	-3.56075200	-1.85596000	2.21987600
C	-1.90215500	-0.49986900	3.77025400
O	-3.64475400	0.66010800	2.16268800
F	-1.15109300	-1.57961800	3.91110300
F	-1.13070000	0.57362300	3.79581700
F	-2.76191300	-0.43916500	4.77544100
C	-0.40506200	-0.62672200	-0.83938900
H	-0.45174200	-0.71213900	-1.92514200
C	-2.98254100	-0.52313700	-0.86521300
H	-3.77533800	-0.87932000	-0.19053600
C	-3.04907800	-1.35758900	-2.13914800
H	-4.08152000	-1.34065200	-2.51936900
H	-2.39941200	-0.94940500	-2.92776500
H	-2.74552700	-2.39676300	-1.96716500
C	-3.23617300	0.96577900	-1.15927900
H	-2.45472100	1.37200200	-1.82034400
H	-4.20576300	1.07502300	-1.66765300
H	-3.26161900	1.55844700	-0.23434500

Supporting Information

Vitamin B_{12} and Micellar Solution Enable Regioselective Ring Opening of Epoxides and Aziridines with Electrophilic Olefins

Kitti Franciska Szabó, Tomasz Wdowik, Aleksandra Krzeszewska, Krzysztof Mazurek, Martin P. Andersson, and Dorota Gryko*

Institute of Organic Chemistry Polish Academy of Science
Kasprzaka 44/52, 01-224 Warsaw, Poland

Center for Integrative Petroleum Research, King Fahd University of Petroleum and Minerals, Dhahran 31261, Kingdom of Saudi Arabia

e-mail: dorota.gryko@icho.edu.pl

Table of Contents

1. General information

***General Procedures*.** Unless otherwise noted, reactions were performed without the exclusion of air or moisture. Photochemical reactions were performed in 10 mL glassy vials sealed with aluminum caps containing a rubber septa or glass reaction tube (inner diameter = 18 mm). Reactions were monitored by gas chromatography (GC, specification below) or thin-layer chromatography (TLC) on Merck silica gel (GF254, 0.20 mm thickness), visualizing with UV-light or ceric ammonium molybdate (CAM)/Hanessian's stain. Colum chromatography was performed using Merck silica gel 60 (230-400 mesh) or commercially available cartridges with a CombiFlash. GC yields were calibrated using dodecane or mesitylene as an internal standard.

***Materials*.** Commercial reagents and solvents were purchased from Sigma-Aldrich, Alfa Aesar, Fluorochem, and TCI, and used as received unless otherwise noted. Dry solvents: dimethyl sulfoxide (DMSO), dichloromethane (CH_2Cl_2), tetrahydrofuran (THF), acetonitrile (CH_3CN) were taken from Solvent Purification System (SPS). Deuterated solvent ($CDCl_3$) was purchased from Eurisotop. 4-(Phenylsulfonyl)-1,2-epoxybutane, and calatyst: $(CN)(H_2O)Cby(OMe)_7$ was synthesized according to literature procedures.[1]

Before the reaction, zinc was activated by the following method: a) washing with 10% HCl, b) grinding, c) washing with H_2O, EtOH, and Et_2O, d) drying in a vacuum.

***Instrumentation*.**

- **NMR Spectroscopy:** ^1H and ^{13}C NMR spectra were recorded at 25 °C on a Bruker 400 MHz, 500 MHz or Varian 600 MHz instrument with TMS as an internal standard. NMR chemical shifts are reported in ppm and referenced to the residual solvent peak of $CDCl_3$ (7.26 ppm - ^1H NMR and 77.0 ppm - ^{13}C NMR). Multiplicities are indicated by singlet (s), doublet (d), triplet (t), quartet (q), multiplet (m) and broad (br). Coupling constants (*J*) are reported in Hertz. All data analysis was performed using MestReNova software package.

- **GC/MS Chromatography:** GC-MS analyses were performed using Shimadzu GCMS-QP2010 SE gas chromatograph with FID detector and Zebron ZB 5MSi column. (length: 30.0 m; thickness: 0.25 um, diameter: 0.25 mm).
  GC program time: 12.39 min; pressure: 121.8 kPa; total flow: 30.3 mL/min; column flow: 1.30 mL/min; linear velocity: 33.1 cm/s; purge flow: 3.0 mL/min; split ratio: 20.0.

	rate	temperature [°C]	hold time
0	-	100.0	1.00
1	40.00	180.0	1.50
2	40.00	260.0	1.50
3	45.00	300.0	1.00
4	50.00	325.0	2.00

- **High Resolution Mass Spectrometry:** High-resolution mass spectra (HRMS) were recorded on a Waters AutoSpec Premier instrument using electron ionization (EI) or a Waters SYNAPT G2-S HDMS instrument using electrospray ionization (ESI) with time of flight detector (TOF).

[1] Ociepa, M.; Wierzba, A. J.; Turkowska, J.; Gryko, D. Polarity-Reversal Strategy for the Functionalization of Electrophilic Strained Molecules via Light-Driven Cobalt Catalysis. *J. Am. Chem. Soc.* **2020**, *142* (11), 5355–5361. https://doi.org/10.1021/jacs.0c00245.

- **Low Resolution Mass Spectrometry:** Low-resolution mass spectra (LRMS) were recorded on an Applied Biosystems API 365 mass spectrometer using electrospray ionization (ESI) technique.

- **CombiFlash:** Products were purified using CombiFlash NextGen 300+ system with 12-inch display, 1-300 mL/min, 300 psi (with automatic injection valve).

  Flash program: time: 30.0; column: silica 4g; flow rate: 13 mL/min; automatic peak hold: on.

entry	time [min]	hexane [%]	AcOEt [%]
1	0	100	0
2	5	100	0
3	7	92	8
4	12	92	8
5	13	90	10
6	14	90	10
7	15	80	20
8	21	80	20
9	30	0	100

2. Setup for photoreactions

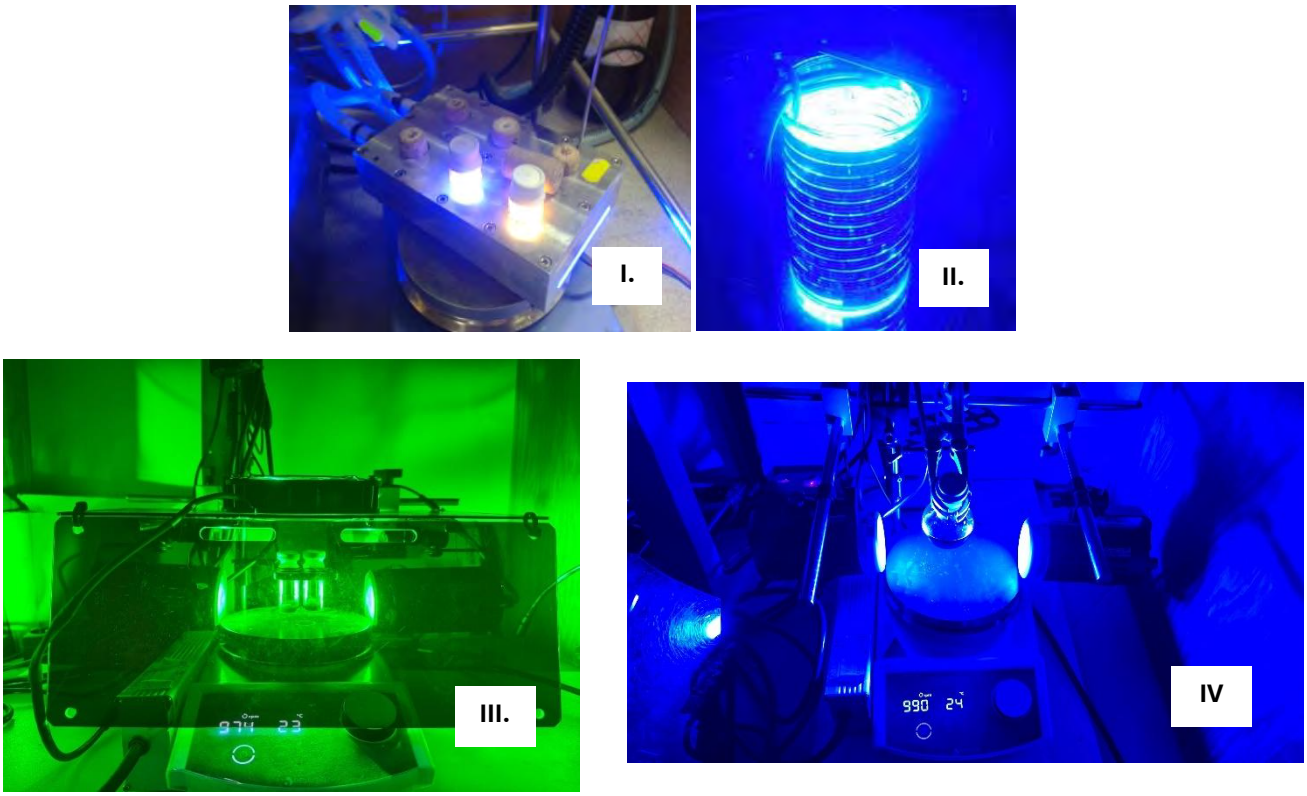

Figure 1. Photograph of photoreactors

Characteristics of photoreactors:

I. Single diode (LT-2855 royal blue, λmax: 446 nm, 3W), controlled by mini chiller set up at 25 ˚C, reactions in 10 mL vials, distance from the reaction vessel: 6 mm.

II. Reactions were carried out in homemade photoreactors made of 400 mL beakers covered on the inside with LED tape. A cooling fan with an adjustable spin rate was used to maintain ambient temperature inside the photoreactor.

Blue LED tape: 8 mm SMD3528 LED strip, 60 LED diodes/m Power consumption: 4.8 W/m blue light – λmax = 460 nm, 4.5 lm.

III and IV. Commercially available Kessil lamps were used. Blue (emission maximum at 440 nm) and green (emission maximum at 525 nm) LED light was supplied to each reaction vial using two Kessil lamps (each with a total intensity of 40 W at 100% power), placed on opposite sides with specially design cooling fan system.

Green Kessil lamps were used for the aziridine ring-opening reactions, while blue Kessil lamps were used for the 1 mmol scale-up reaction.

3. Surfactants and their abbreviations

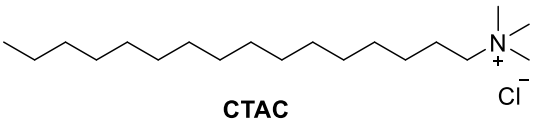

CTAC

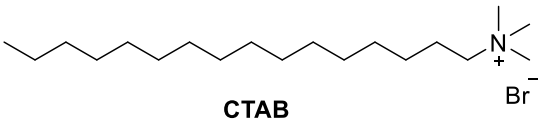

CTAB

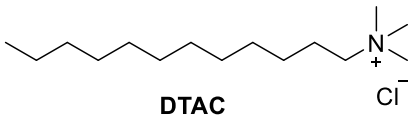

DTAC

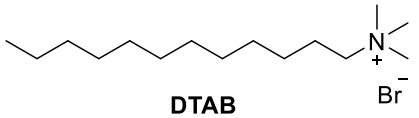

DTAB

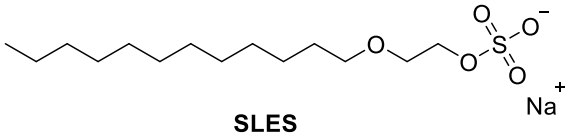

SLES

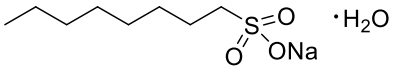

Sodium 1-octasulfonate monohydrate

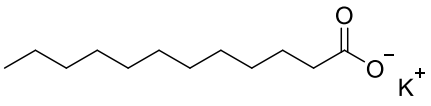

Potassium laurate

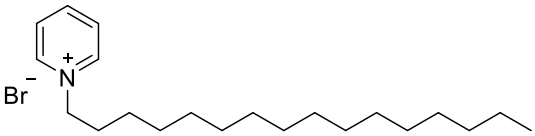

Hexadecylpyridinium bromide

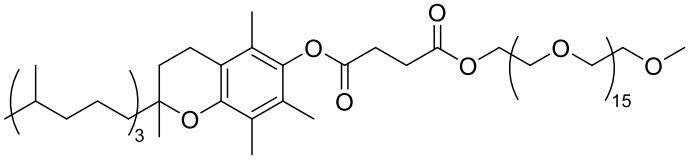

TPGS-750-M

4. Background experiments of alkyl epoxides with olefins

Model reaction:

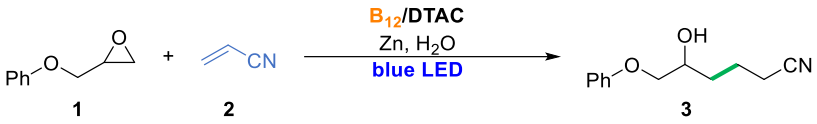

Entry	Deviation from the Standard Conditions	Yield of **3**[b] [%]
1	**none**	**85**
2	No B_{12}	0
3	No Zn	0
4	Air atmosphere	0
5	No light	0
6	No DTAC	47
7	No light, 50 °C	traces

Reaction conditions: epoxide **(1)** (0.2 mmol, 1.0 equiv.), acrylonitrile (**2**) (16 mg, 1.5 equiv.), Zn (40 mg, 3.0 equiv.), B_{12} (13.5 mg, 5.0 mol%), DTAC (264 mg, 5.0 equiv.), EtOH (0.5 ml), H_2O (4.5 mL), blue LED, 16h. [b]Yields determined by GC analysis.

5. Optimization of reactions parameters of alkyl epoxides with olefins

Procedure: Each reaction was performed in a glass vial (10 mL) sealed with an aluminum cap with a rubber septum equipped with a magnetic stirring bar. It was charged with activated Zn^0 dust (40 mg, 0.6 mmol, 3.0 equiv.), DTAC (264 mg, 5.0 equiv.) and B_{12} (5.0 mol%, 13.5 mg). Then water (4.5 mL) and ethanol (0.5 mL) were added. The resulting mixture was degassed by purging with argon with simultaneous sonication in an ultrasonic bath for 15 min. An epoxide (0.2 mmol, 1.0 equiv.) was added dropwise *via* a syringe followed by a Michael acceptor (1.5 equiv.). The resulting mixture was irradiated with blue LED light (single diode, 3 W; λ = 460 nm at room temperature) for 16 h. The resulting mixture was diluted with AcOEt (~ 3 mL) and washed with brine (20 mL). The organic phase was dried over Na_2SO_4, then filtered through the cotton wool and concentrated *in vacuo*. A crude product was purified by means of column chromatography.

Model reaction:

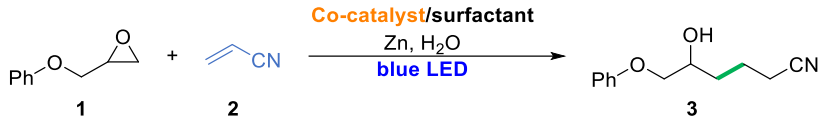

Reaction conditions: epoxide **(1)** (0.2 mmol, 1.0 equiv.), acrylonitrile (**2**) (16 mg, 1.5 equiv.), Zn (40 mg, 3.0 equiv.), Co- catalyst (5.0 mol%), DTAC (264 mg, 5.0 equiv.), EtOH (0.5 ml), H_2O (4.5 mL), blue LED, 16 h.

5.1. The influence of light

Entry	Light	Yield of **3**[b] [%]
1	White LEDs (tape)	19
2	Blue LEDs (tape)	42
3	Green LEDs (tape)	37
4	Violet LEDs (tape)	40
5	**Blue LED (single diode, 3 W)**	**43**
6	Green LED (single diode, 3 W)	14
7	Blue LED (single diode, 7 W)	24
8	Blue LED (single diode, 25 W)	39
9	Blue Kessil lamp (40 W)	<10

Reaction conditions: epoxide (**1**) (0.2 mmol, 1.0 equiv.), acrylonitrile (**2**) (16 mg, 1.5 equiv.), Zn (40 mg, 3.0 equiv.), NH_4Cl (32 mg, 3.0 equiv.), HME (12 mg, 5.0 mol%), MeCN (*c* = 0.1 M), 16 h. [b]Yields determined by GC analysis.

5.2. Screening of surfactants

A) HME-catalyzed reactions

Entry	Surfactants	Yield of **3**[b] [%]
1	CTAC	10
2	**DTAC**	**33**
3	CTAB	25
4	DOSS	15
5	SLES	25
6	Potassium laurate	10
7	TPGS-750-M	13

Reaction conditions: epoxide (**1**) (0.2 mmol, 1.0 equiv.), acrylonitrile (**2**) (16 mg, 1.5 equiv.), Zn (40 mg, 3.0 equiv.), NH_4Cl (32 mg, 3.0 equiv.), HME (12 mg, 5.0 mol%), surfactant (2.5 eq.), MeCN (*c* = 0.1 M), Blue LED (single diode 3 W), 16 h. [b]Yields determined by GC analysis.

B) B_{12}-catalyzed reactions

Entry	Surfactants	Yield of **3**[b] [%]
1	DTAC	64
2	**DTAC (without NH_4Cl)**	**59**
3	CTAB	73
4	CTAB (without NH_4Cl)	59
5	SLES	46
6	Potassium laurate	45
7	OTAI	56
8	CTAC	58
9	DTAB	47
10	1-Hexadecylpyridinium bromide	31

Reaction conditions: epoxide (**1**) (0.2 mmol, 1.0 equiv.), acrylonitrile (**2**) (16 mg, 1.5 equiv.), Zn (40 mg, 3.0 equiv.), NH_4Cl (32 mg, 3.0 equiv.), B_{12} (13.5 mg, 5.0 mol%), surfactant (2.5 eq.), H_2O (5 mL), Blue LED (single diode 3 W), 16 h. [b]Yields determined by GC analysis.

C) The amount of the surfactant

Entry	DTAC (equiv.)	Yield of **3**[b] [%]
1	1	68
2	2.5	59
3	**5**	**76**
4	7.5	64
5	10	69

Reaction conditions: epoxide (**1**) (0.2 mmol, 1.0 equiv.), acrylonitrile (**2**) (16 mg, 1.5 equiv.), Zn (40 mg, 3.0 equiv.), B_{12} (13.5 mg, 5.0 mol%), DTAC, H_2O (5 mL), Blue LED (single diode 3 W), 16 h. [b]Yields determined by GC analysis.

5.3. B_{12} – Impact of the catalyst loading

Entry	Catalyst loading [%]	Yield of **3**[b] [%]
1	2.5	66
2	**5**	**76**
3	7.5	67
4	10	58

Reaction conditions: epoxide **(1)** (0.2 mmol, 1.0 equiv.), acrylonitrile (**2**) (16 mg, 1.5 equiv.), Zn (40 mg, 3.0 equiv.), B_{12}, DTAC (264 mg, 5.0 equiv.), H_2O (5 mL), Blue LED (single diode 3 W), 16 h. [b]Yields determined by GC analysis.

5.4. Optimization of the substrates' ratio

Entry	**1** (equiv.)	**2** (equiv.)	Yield of **3**[b] [%]
1	**1**	**1.5**	**76**
2	1	2	61
3	1	3	65
4	2	1	60
5	1	1	72

Reaction conditions: epoxide **(1),** acrylonitrile (**2**), Zn (40 mg, 3.0 equiv.), B_{12} (13.5 mg, 5.0 mol%), DTAC (264 mg, 5.0 equiv.), H_2O (5 mL), Blue LED (single diode 3 W), 16 h. [b]Yields determined by GC analysis.

5.5. The influence of the amount of Zn

Entry	Zn (equiv.)	Yield of **3**[b] [%]
1	1	65
2	1.5	64
3	**3**	**76**
4	5	65

Reaction conditions: epoxide (**1**) (0.2 mmol, 1.0 equiv.), acrylonitrile (**2**) (16 mg, 1.5 equiv.), Zn, B_{12} (13.5 mg, 5.0 mol%), DTAC (264 mg, 5.0 equiv.), H_2O (5 mL), Blue LED (single diode 3 W), 16 h. [b]Yields determined by GC analysis.

5.6. Concentration of epoxide (1)

Entry	[mol/dm^3]	Yield of **3**[b] [%]
1	0.08	70
2	**0.04**	**76**
3	0.03	70

Reaction conditions: epoxide (**1**) (0.2 mmol, 1.0 equiv.), acrylonitrile (**2**) (16 mg, 1.5 equiv.), Zn (40 mg, 3.0 equiv.), B_{12} (13.5 mg, 3.0 equiv.), DTAC (264 mg, 5.0 equiv.), H_2O, Blue LED (single diode 3 W), 16 h. [b]Yields determined by GC analysis.

5.7. Screening of additives

Entry	Additives	Yield of **3**[b] [%]
1	-	76
2	MeOH	76
3	**EtOH**	**85**
4	Propanol	81
5	*i*-Propanol	80
6	Butanol	77
7	*t*-Butanol	64

Reaction conditions: epoxide (**1**) (0.2 mmol, 1.0 equiv.), acrylonitrile (**2**) (16 mg, 1.5 equiv.), Zn (40 mg, 3.0 equiv.), B_{12} (13.5 mg, 5.0 mol%), DTAC (264 mg, 5.0 equiv.), H_2O (4.5 mL), additive (0.5 mL), Blue LED (single diode 3 W), 16 h. [b]Yields determined by GC analysis.

6. Optimization of reactions parameters of aryl epoxides with olefins

Procedure: Each reaction was performed in a glass vial (10 mL) sealed with an aluminum cap with a rubber septum equipped with a magnetic stirring bar. It was charged with activated Zn^0 dust (40 mg, 0.6 mmol, 3.0 equiv.), DTAC (132 mg, 2.5 equiv.) and B_{12} (5.0 mol%, 13.5 mg). Then water (4.5 mL) and ethanol (0.5mL) were added. The resulting mixture was degassed by purging with argon with simultaneous sonication in an ultrasonic bath for 15 min. An epoxide (0.2 mmol, 1.0 equiv.) was added dropwise *via* a syringe followed by a Michael acceptor (5.0 equiv.). The resulting mixture was irradiated with blue LED light (tape, 32 W; λ = 460 nm) at room temperature for 16 h. The resulting mixture was diluted with AcOEt (~ 3 mL) and washed with brine (20 mL). The organic phase was dried over Na_2SO_4, then filtered through the cotton wool and concentrated *in vacuo*. A crude product was purified by means of column chromatography.

Model reaction:

20 **2** **7**

Reaction conditions: epoxide (**20**) (0.1 mmol, 1.0 equiv.), acrylonitrile (**2**) (16 mg, 1.5 equiv.), Zn (40 mg, 3.0 equiv.), B_{12} (13.5 mg, 5.0 mol%), DTAC (132 mg, 2.5 equiv.), EtOH (0.5 ml), H_2O (4.5 mL), Blue LED, 16h.

6.1. The influence of light

Entry	Light	Yield of **7**[b] [%]
1	**Blue LEDs (tape)**	**40**
2	Blue LED (single diode, 3 W)	27
3	Blue LED (single diode, 7 W)	20
4	Blue LED (single diode, 25 W)	35
5	Blue LED (single diode, 10 W, 1 h)	<10

Reaction conditions: epoxide (**20**) (0.2 mmol, 1.0 equiv.), acrylonitrile (**2**) (16 mg, 1.5 equiv.), Zn (40 mg, 3.0 equiv.), B_{12} (13.5 mg, 5.0 mol%), DTAC (264 mg, 5.0 equiv.), H_2O (4.5 mL), EtOH (0.5 mL), 16 h. [b]Yields determined by GC analysis.

6.2. Screening of surfactant

Entry	DTAC (equiv.)	Yield of **7**[b] [%]
1	1	35
2	**2.5**	**41**
3	5	40
4	7.5	29
5	10	35

Reaction conditions: epoxide (**20**) (0.2 mmol, 1.0 equiv.), acrylonitrile (**2**) (16 mg, 1.5 equiv.), Zn (40 mg, 3.0 equiv.), B_{12} (13.5 mg, 5.0 mol%), DTAC, H_2O (4.5 mL), EtOH (0.5 mL), Blue LED, 16 h. [b]Yields determined by GC analysis.

6.3. The influence of the amount of Zn

Entry	Zn (equiv.)	Yield of **7**[b] [%]
1	1	22
2	1.5	34
3	**3**	**41**
4	5	38

Reaction conditions: epoxide (**20**) (0.2 mmol, 1.0 equiv.), acrylonitrile (**2**) (16 mg, 1.5 equiv.), Zn, B_{12} (13.5 mg, 5.0 mol%), DTAC (132 mg, 2.5 equiv.), H_2O (4.5 mL), EtOH (0.5 mL), Blue LED, 16 h. [b]Yields determined by GC analysis.

6.4. Screening of additives

Entry	Additives	Yield of **7**[b] [%]
1	-	24
2	MeOH	26
3	**EtOH**	**41**
4	Propanol	25
5	*i*-Propanol	32
6	Butanol	31
7	*t*-Butanol	27

Reaction conditions: epoxide (**20**) (0.2 mmol, 1.0 equiv.), acrylonitrile (**2**) (16 mg, 1.5 equiv.), Zn (40 mg, 3.0 equiv.), B_{12} (13.5 mg, 5.0 mol%), DTAC (132 mg, 2.5 equiv.), H_2O (4.5 mL), additive (0.5 mL), Blue LED (single diode 3 W), 16 h. [b]Yields determined by GC analysis.

6.5. The amount of EtOH

Entry	EtOH v/v	Yield of **7**[b] [%]
1	5 %	31
2	**10 %**	**41**
3	20 %	33
4	40 %	16
5	50 %	30

Reaction conditions: epoxide (**20**) (0.2 mmol, 1.0 equiv.), acrylonitrile (**2**) (16 mg, 1.5 equiv.), Zn (40 mg, 3.0 equiv.), B_{12} (13.5 mg, 5.0 mol%), DTAC (132 mg, 2.5 equiv.), H_2O (4.5 mL), EtOH, Blue LED, 16 h. [b]Yields determined by GC analysis.

6.6. B_{12} – Impact of the catalyst loading

Entry	Catalyst loading [%]	Yield of **7**[b] [%]
1	2.5	31
2	**5**	**41**
3	10	15

Reaction conditions: epoxide (**20**) (0.2 mmol, 1.0 equiv.), acrylonitrile (**2**) (16 mg, 1.5 equiv.), Zn (40 mg, 3.0 equiv.), B_{12}, DTAC (132 mg, 2.5 equiv.), H_2O (4.5 mL), EtOH (0.5 ml), Blue LED (single diode 3 W), 16 h. [b]Yields determined by GC analysis.

6.7. Optimization of the substrates' ratio

Entry	**20** (equiv.)	**2** (equiv.)	Yield of **7**[b] [%]
1	1	1.5	41
2	1	3	35
3	**1**	**5**	**48**
4	1	10	39
5	1	1	17

Reaction conditions: epoxide (**20**), acrylonitrile (**2**), Zn (40 mg, 3.0 equiv.), B_{12} (13.5 mg, 5.0 mol%), DTAC (132 mg, 2.5 equiv.), H_2O (4.5 mL), EtOH (0.5 ml), Blue LED (single diode 3 W), 16 h. [b]Yields determined by GC analysis.

7. Background experiments for alkyl aziridine reaction with olefin

Model reaction:

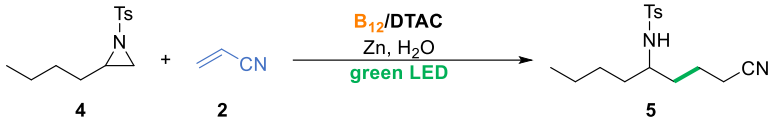

Entry	Deviation from the Standard Conditions	Yield of **5**[b] [%]
1	**none**	**83**
2	No Co-cat.	0
3	No Zn	0
4	No light	0
5	No DTAC	29

Reaction conditions: aziridine (**4**) (0.2 mmol, 1.0 equiv.), acrylonitrile (**2**) (16 mg, 1.5 equiv.), Zn (40 mg, 3.0 equiv.), B_{12} (7 mg, 2.5 mol%), DTAC (185 mg, 3.5 equiv.), *i*PrOH (0.5 ml), H_2O (4.5 mL), green LED, 24 h. [b]Yields determined by GC analysis.

8. Optimization of reactions parameters of alkyl aziridines with olefins

Procedure: Each reaction was performed in a glass vial (10 mL) sealed with an aluminum cap with a rubber septum equipped with a magnetic stirring bar. It was charged with activated Zn^0 dust (40 mg, 0.6 mmol, 3.0 equiv.), DTAC (185 mg, 3.5 equiv.) and B_{12} (2.5 mol%, 6.75 mg). Then water (4.5 mL) and isopropanol (0.5 mL) were added. The resulting mixture was degassed by purging with argon with simultaneous sonication in an ultrasonic bath for 25 min. Then, aziridine (0.2 mmol, 1.0 equiv.) was added dropwise *via* a syringe followed by a Michael acceptor (3.0 equiv.). The resulting mixture was irradiated with green LED light (Kessil, 40 W; λ = 525 nm) for 24 h at room temperature. The resulting mixture was diluted with AcOEt (~ 3 mL) and washed with brine (20 mL). The organic phase was dried over Na_2SO_4, then filtered through the cotton wool and concentrated *in vacuo*. A crude product was purified by means of column chromatography.

Model reaction:

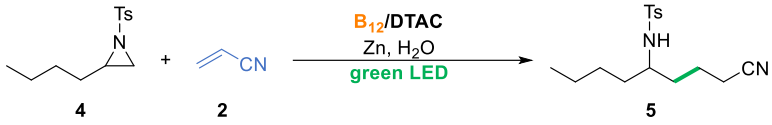

Reaction conditions: aziridine (**4**) (0.2 mmol, 1.0 equiv.), acrylonitrile (**2**) (16 mg, 1.5 equiv.), Zn (40 mg, 3.0 equiv.), B_{12} (7 mg, 2.5 mol%), DTAC (185 mg, 3.5 equiv.), *i*PrOH (0.5 ml), H_2O (4.5 mL), green LED, 24 h.

8.2. The influence of light

Entry	Light	Yield of **5**[b] [%]
1	White LEDs (tape)	31
2	Yellow LEDs (tape)	26
3	Green LEDs (tape)	37
4	Violet LEDs (tape)	43
5	**Green Kessil lamp (40 W)**	**61**
6	Blue Kessil lamp (40 W)	38
7	Green LED (23 W)	60
8	Green LED (single diode, 3 W)	56
9	Blue LED (single diode, 3 W)	57
10	Blue LED (single diode, 7 W)	51

Reaction conditions: aziridine (**4**) (0.2 mmol, 1.0 equiv.), acrylonitrile (**2**) (16 mg, 1.5 equiv.), Zn (40 mg, 3.0 equiv.), B_{12} (13.5 mg, 5.0 mol%), DTAC (264 mg, 5.0 equiv.), H_2O (5 mL), X LED, 24 h. [b]Yields determined by GC analysis.

8.3. Screening of surfactants

Entry	Surfactants	Yield of **5**[b] [%]
1	DTAB	60
2	**DTAC**	**61**
3	CTAB	43
4	CTAC	54
5	SLES	50
6	Potassium Laurate	38
7	Sodium 1-octanesulfonate monohydrate	39
8	TPGS-750-M	52
9	1-Hexadecylpyridinium bromide	49

Reaction conditions: aziridine (**4**) (0.2 mmol, 1.0 equiv.), acrylonitrile (**2**) (16 mg, 1.5 equiv.), Zn (40 mg, 3.0 equiv.), B_{12} (13.5 mg, 5.0 mol%), X (5.0 equiv.), H_2O (5 mL), Green LED, 24 h. [b]Yields determined by GC analysis.

B) The amount of the surfactant

Entry	DTAC (equiv.)	Yield of **5**[b] [%]
1	1	37
2	1.5	38
3	2.5	50
4	3	56
5	**3.5**	**57**
6	5	64
7	7	56

Reaction conditions: aziridine (**4**) (0.2 mmol, 1.0 equiv.), acrylonitrile (**2**) (16 mg, 1.5 equiv.), Zn (40 mg, 3.0 equiv.), B_{12} (13.5 mg, 5.0 mol%), DTAC (X equiv.), H_2O (5 mL), Green LED, 24 h. [b]Yields determined by GC analysis.

8.4. B_{12} – Impact of the catalyst loading

Entry	Catalyst loading [%]	Yield of **5**[b] [%]
1	**2.5**	**61**
2	5	60
3	7.5	61
4	10	63

Reaction conditions: aziridine (**4**) (0.2 mmol, 1.0 equiv.), acrylonitrile (**2**) (16 mg, 1.5 equiv.), Zn (40 mg, 3.0 equiv.), B_{12} (X mol%), DTAC (185 mg, 3.5 equiv.), H_2O (5 mL), Green LED, 24 h. [b]Yields determined by GC analysis.

8.5. Optimization of the substrates' ratio

Entry	**4** (equiv.)	**2** (equiv.)	Yield of **5**[b] [%]
1	1	1	47
2	**1**	**1.5**	**57**
3	1	2	37
4	2	1	58
5	1	2.5	36
6	1	3	38

Reaction conditions: aziridine (**4**) (X), acrylonitrile (**2**) (X), Zn (40 mg, 3.0 equiv.), B_{12} (6.75 mg, 2.5 mol%), DTAC (185 mg, 3.5 equiv.), H_2O (5 mL), Green LED, 24 h. [b]Yields determined by GC analysis.

8.6. The influence of the amount of Zn

Entry	Zn (equiv.)	Yield of **5**[b] [%]
1	1	52
2	1.5	54
3	**3**	**57**
4	5	42

Reaction conditions: aziridine (**4**) (0.2 mmol, 1.0 equiv.), acrylonitrile (**2**) (16 mg, 1.5 equiv.), Zn (X), B_{12} (7 mg, 2.5 mol%), DTAC (185 mg, 3.5 equiv.), H_2O (5 mL), Green LED, 24 h. [b]Yields determined by GC analysis.

8.7. Concentration of aziridine

Entry	[mol/dm^3]	Yield of **5**[b] [%]
1	0.02	43
2	**0.04**	**57**
3	0.06	52
4	0.08	42

Reaction conditions: aziridine (**4**) (0.2 mmol, 1.0 equiv.), acrylonitrile (**2**) (16 mg, 1.5 equiv.), Zn (40 mg, 3.0 equiv.), B_{12} (7 mg, 2.5 mol%), DTAC (185 mg, 3.5 equiv.), H_2O (X), Green LED, 24 h. [b]Yields determined by GC analysis.

8.8. Screening of additives

Entry	Additives	Yield of **5**[b] [%]
1	-	57
2	MeOH	55
3	EtOH	49
4	Propanol	64
5	***i*-Propanol**	**83**
6	Butanol	59
7	*t*-Butanol	61

Reaction conditions: aziridine (**4**) (0.2 mmol, 1.0 equiv.), acrylonitrile (**2**) (16 mg, 1.5 equiv.), Zn (40 mg, 3.0 equiv.), B_{12} (7 mg, 2.5 mol%), DTAC (185 mg, 3.5 equiv.), H_2O (4.5 ml), additive (0.5 ml), Green LED, 24 h. [b]Yields determined by GC analysis.

9. Mechanistic consideration

9.1. Proposed mechanism

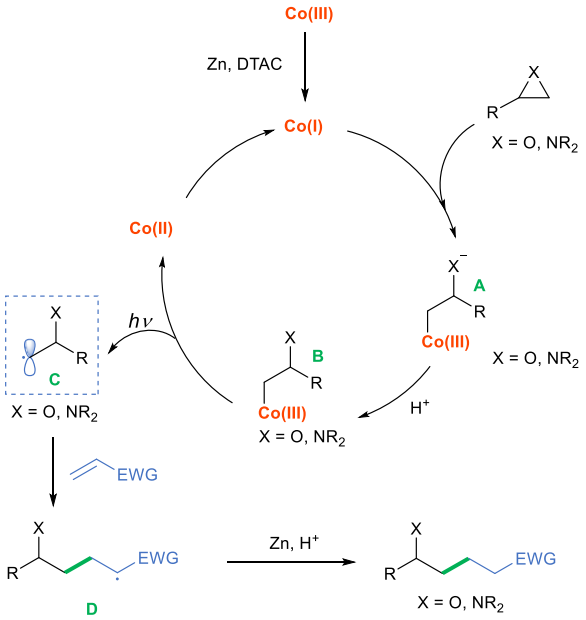

9.2. Kinetic studies of the model alkyl epoxide

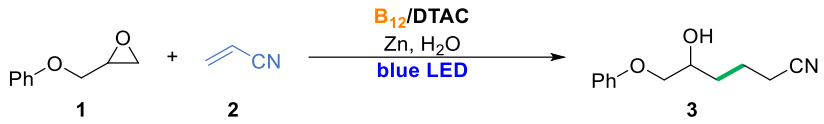

Reaction conditions: epoxide (**1**) (0.2 mmol, 1.0 equiv.), acrylonitrile (**2**) (16 mg, 1.5 equiv.), Zn (40 mg, 3.0 equiv.), B_{12} (13.5 mg, 5.0 mol%), DTAC (264 mg, 5.0 equiv.), H_2O (4.5 mL), additive (0.5 mL), Blue LED (single diode 3 W).

The reaction of the model alkyl epoxide with the olefin was set up according to the general procedure **A** on 0.2 mmol scale with the addition of dodecane as an internal standard. The reaction was monitored by GC/FID for 24 h.

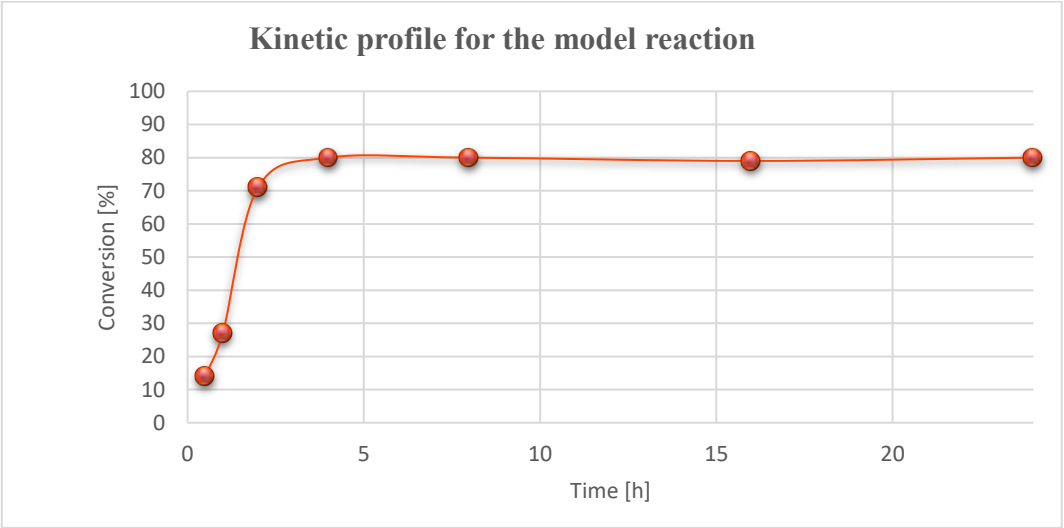

Figure 2. The rate of the conversion of 5-hydroxy-6-phenoxyhexanenitrile (**3**)

Conclusion: Kinetic studies indicated an optimal time of 4 h for product 3 formation, with no significant decomposition observed subsequent to 4 hours of reaction time.

9.3. Co(III)-alkyl complex formation

A) Epoxide

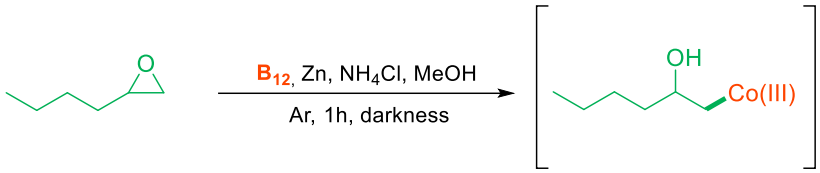

22

Reaction conditions: 2-butyloxirane (0.05 mmol, 1.0 equiv.), vitamin B_{12} (0.05 mmol, 1.0 equiv.), Zn (1.50 mmol, 30 equiv.), NH_4Cl (1.50 mmol, 30 equiv.), MeOH (1 mL), darkness, 1h.

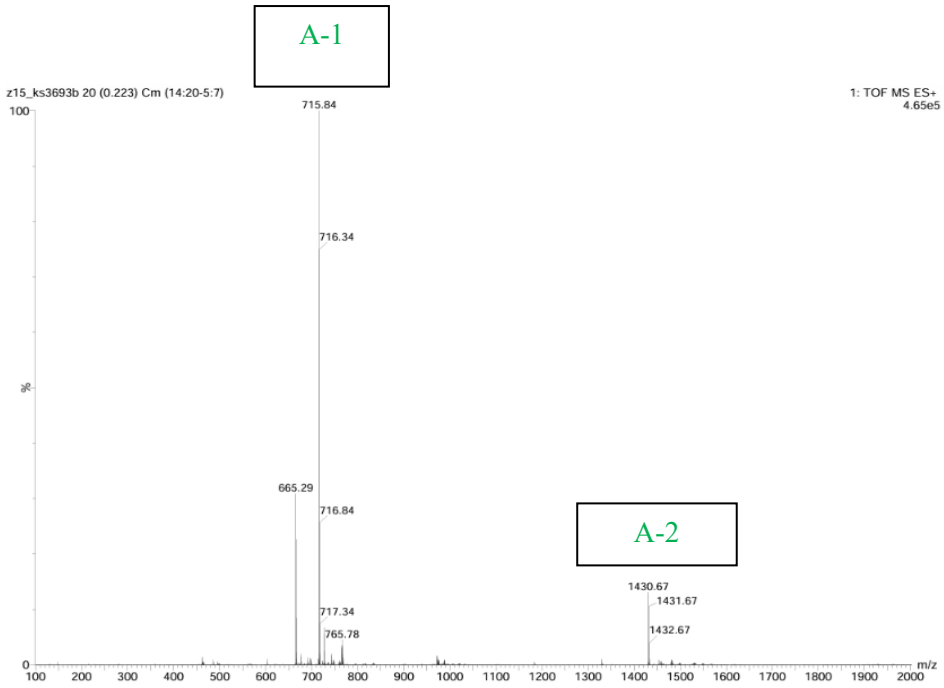

Signal A-1

$C_{63}H_{102}CoN_{13}O_{15}P^{2+}$

Calcd mass = 715,84
Found = 715,84

Signal A-2

$C_{63}H_{102}CoN_{13}O_{15}P^{+}$

Calcd mass = 1430,67
Found = 1430,67

The HRMS ESI (+) spectrum of the reaction mixture indicates the presence of two main forms of the alkylcobalamin complexes (signals A-1 and A-2). Signals A-1 and A-2 correspond to the mass of alkylcobalamin complex.

Conclusion: This experiment supports the hypothesis that the reaction involves an alkyl-cobalt complex.

B) Aziridine

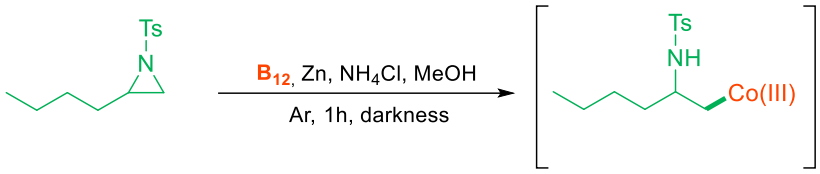

23

Reaction conditions: 2-butyl-1-tosylaziridine (0.05 mmol, 1.0 equiv.,), vitamin B_{12} (0.05 mmol, 1.0 equiv.), Zn (1.50 mmol, 30 equiv.), NH_4Cl (1.50 mmol, 30 equiv.), MeOH (1 mL), darkness, 1h.

A glass reaction tube equipped with a magnetic bar was charged with vitamin B_{12} (68 mg, 0.05 mmol, 1 equiv.) ammonium chloride (80 mg, 1.50 mmol, 30 equiv.) and activated zinc (98 mg, 1.50 mmol, 30.0 equiv.), then MeOH (1 mL) was added. Tube was sealed with a septum and the resulting mixture was degassed by purging the solution with argon for 20 minutes with simultaneous sonication in ultrasonic bath (the solution turned from pink to dark brown). Subsequently, the reaction tube was then sealed with aluminum foil, epoxide or aziridine (0.05 mmol, 1.0 equiv.) was added and the reaction was placed on a magnetic stirrer. After 60 minutes an aliquot was taken from the reaction mixture and its composition was studied by HRMS ESI(+).

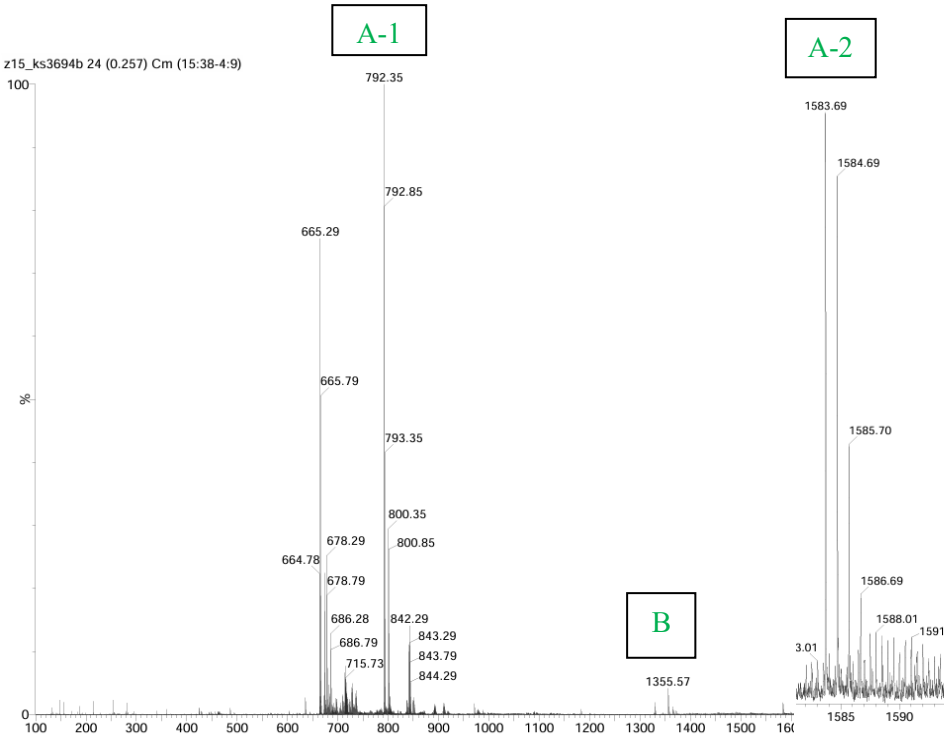

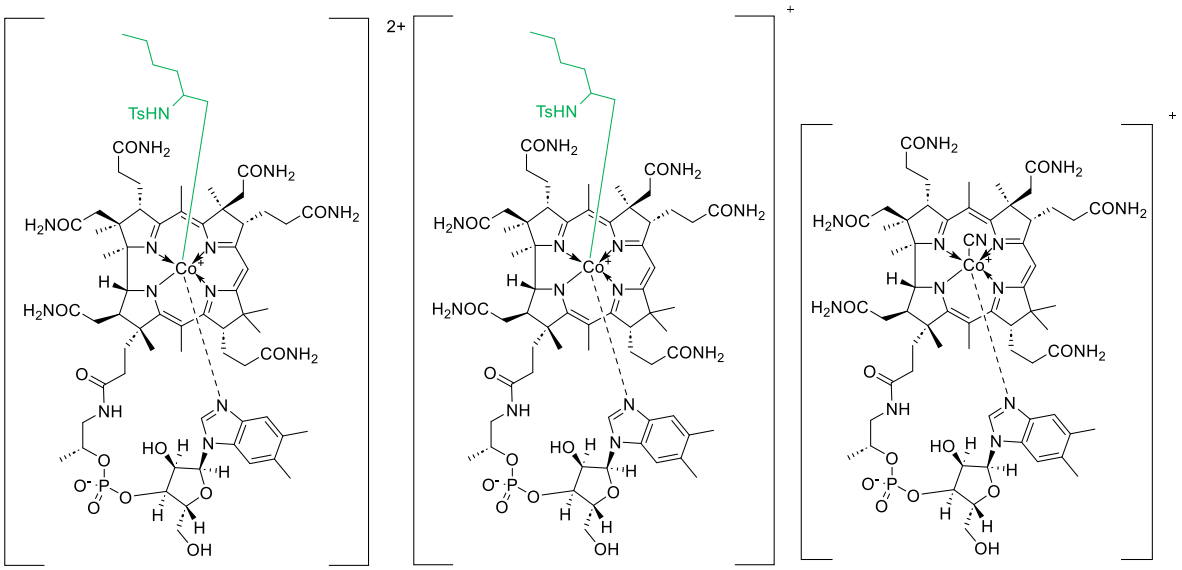

Signal A-1
$C_{75}H_{109}CoN_{14}O_{16}SP^{2+}$

Calcd mass = 792,35
Found = 792,35

Signal A-2
$C_{75}H_{109}CoN_{14}O_{16}SP^{+}$

Calcd mass = 1583,69
Found = 1583,69

Signal B
$C_{63}H_{88}CoN_{14}O_{14}P^{+}$

Calcd mass = 1355,57
Found = 1355,57

The HRMS ESI (+) spectrum of the reaction mixture indicates the presence of three main forms of alkylcobalamin complexes (signals A-1-2 and B). Signals A-1 and A-2 correspond to the mass of alkylcobalamin complex. Signal B corresponds to the mass of the catalyst.

Conclusion: This experiment supports the hypothesis that the reaction involves an alkyl-cobalt complex.

9.4. Experiment with a radical trap

A) Epoxide

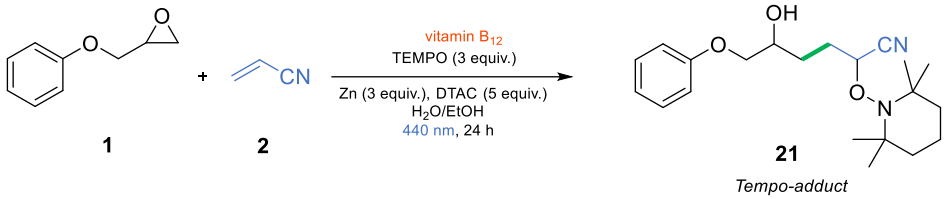

Reaction conditions: epoxide (**1**) (0.2 mmol, 1.0 equiv.), acrylonitrile (**2**) (16 mg, 1.5 equiv.), Zn (40 mg, 3.0 equiv.), B_{12} (13.5 mg, 5.0 mol%), DTAC (264 mg, 5.0 equiv.), H_2O (4.5 mL), EtOH (0.5 mL), 24 h, blue LED (single diode 3 W).

The reaction was set up following the general procedure A (in 4 mL of H_2O). Subsequently (after 30 min), TEMPO (3 equiv., 0.60 mmol in 1 mL of DTAC solution in H_2O) was added. Then the reaction was worked up as usual. HRMS ESI(+) analysis of the crude reaction mixture indicates the formation of the TEMPO adduct with the radical.

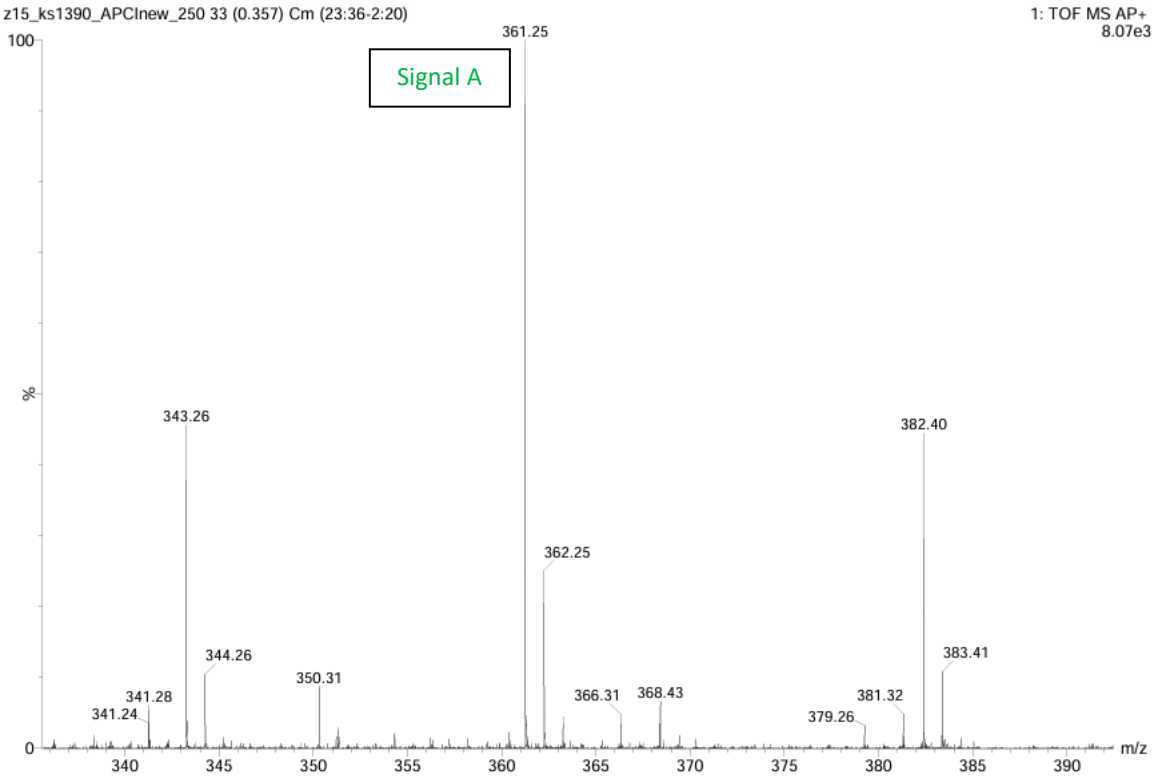

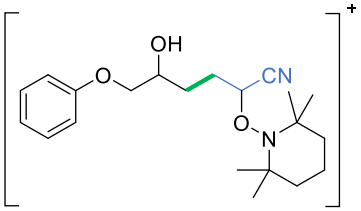

Signal A

Chemical formula: $C_{21}H_{33}N_2O_3^+$

Exact Mass: 361.2491

Found: 361.2492

The HRMS ESI (+) spectrum of the reaction mixture indicates the presence of the radical adduct (signal A). Signal A corresponds to the mass of product/TEMPO adduct **21**.

Conclusion: This experiment supports the hypothesis that the reaction involves a radical as an intermediate.

B) Aziridine

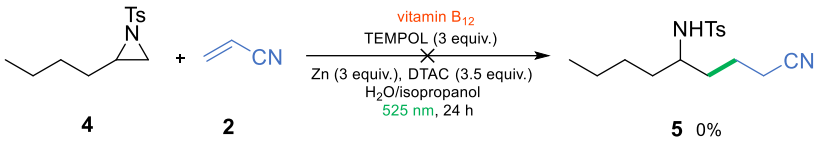

4 **2** **5** 0%

Reaction conditions: aziridine (0.2 mmol, 1.0 equiv.), acrylonitrile (0.3 mmol, 1.5 equiv.), vitamin B_{12} (0.005 mmol, 2.5 mol%), Zn (0.6 mmol, 3.0 equiv.), DTAC (0.7 mmol, 3.5 equiv.), TEMPOL (0.6 mmol, 3.0 equiv.), H_2O (4.5 mL), *i*PrOH (0.5 ml) 24 h, green Kessil LED.

The reaction was set up following the general procedure **C** with the addition of TEMPOL. Then the reaction was worked up as usual. TLC showed no conversion of the starting material, GC-FID further proved that the starting material was not converted. The reaction was halted completely by the addition of a TEMPOL.

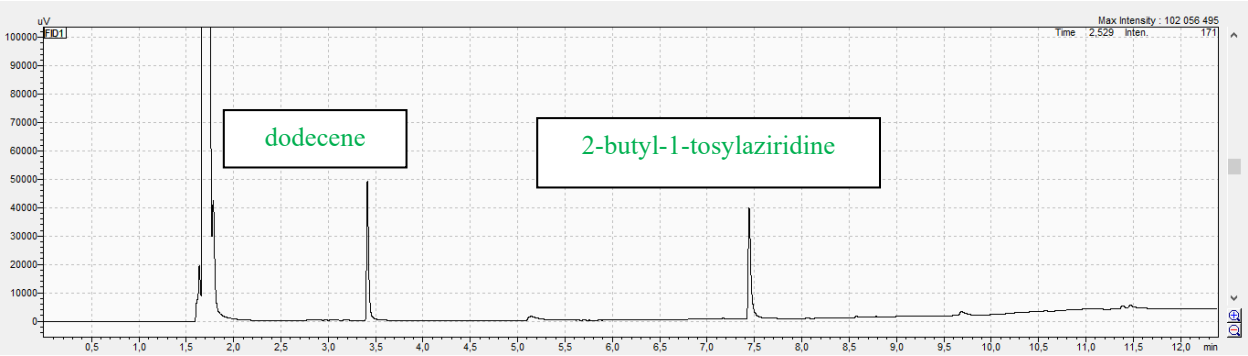

Conclusion: This experiment supports the hypothesis that a radical intermediate is involved in the reaction.

10. Preparation of starting materials (S1-S12) and characterization of new compounds

10.1. Synthesis of starting materials

Not commercially available substrates were synthesized according to the reported procedures.[2,3,4,5,6,7,8] The observed characterization data (^{1}H and ^{13}C NMR) are consistent with those previously reported.

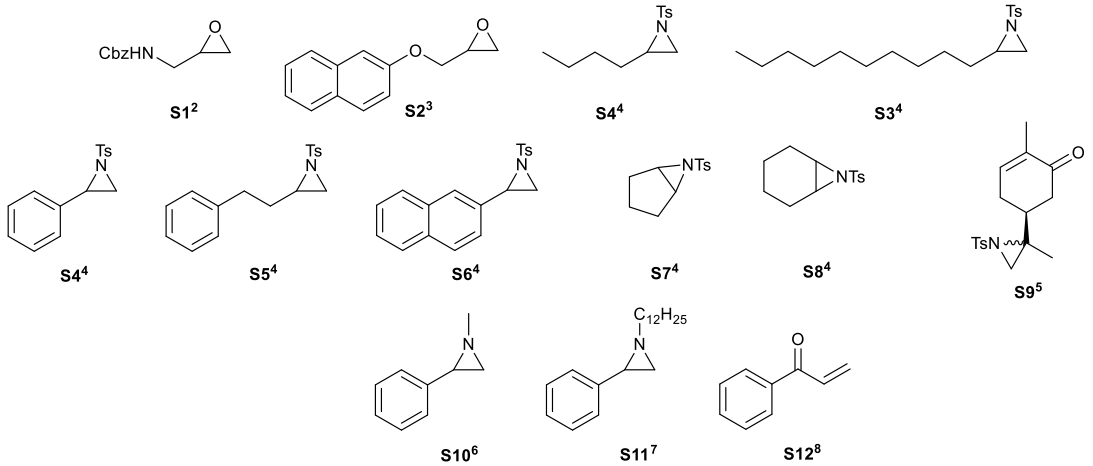

[2] Giordano, C.; Gallina, C.; Consalvi, V.; Scandurra, R. Irreversible Inactivation of Papain and Cathepsin B by Epoxidic Substrate Analogues. *Eur. J. Med. Chem.* **1990**, *25* (6), 479–487. https://doi.org/https://doi.org/10.1016/0223-5234(90)90142-P.

[3] Tacon, C.; Guantai, E. M.; Smith, P. J.; Chibale, K. Synthesis, Biological Evaluation and Mechanistic Studies of Totarol Amino Alcohol Derivatives as Potential Antimalarial Agents. *Bioorg. Med. Chem.* **2012**, *20* (2), 893–902. https://doi.org/https://doi.org/10.1016/j.bmc.2011.11.060.

[4] Park, S.; Koo, J.; Kim, W.; Lee, H. G. A Tandem Process for the Synthesis of β-Aminoboronic Acids from Aziridines with Haloamine Intermediates. *Chem. Commun.* **2022**, *58* (23), 3767–3770. https://doi.org/10.1039/D2CC00808D.

[5] Sureshkumar, D.; Koutha, S. M.; Chandrasekaran, S. Chemistry of Tetrathiomolybdate: Aziridine Ring Opening Reactions and Facile Synthesis of Interesting Sulfur Heterocycles. *J. Am. Chem. Soc.* **2005**, *127* (37), 12760–12761. https://doi.org/10.1021/ja052969z.

[6] Bresciani, G.; Bortoluzzi, M.; Pampaloni, G.; Marchetti, F. Diethylammonium Iodide as Catalyst for the Metal-Free Synthesis of 5-Aryl-2-Oxazolidinones from Aziridines and Carbon Dioxide. *Org. Biomol. Chem.* **2021**, *19* (18), 4152–4161. https://doi.org/10.1039/D1OB00458A.

[7] Depa WJ, Majumder S, Nadirova M, Cmoch P, Chaładaj W, Andersson MP, et al. CO2 utilization in a micellar system: synthesis of cyclic carbonates. ChemRxiv. 2024; doi:10.26434/chemrxiv-2024-jd8vk This content is a preprint and has not been peer-reviewed.

[8] Chanthamath, S.; Takaki, S.; Shibatomi, K.; Iwasa, S. Highly Stereoselective Cyclopropanation of α,β-Unsaturated Carbonyl Compounds with Methyl (Diazoacetoxy)Acetate Catalyzed by a Chiral Ruthenium(II) Complex. *Angew. Chemie Int. Ed.* **2013**, *52* (22), 5818–5821. https://doi.org/https://doi.org/10.1002/anie.201300468.

10.2. Scope limitation: unsuccessful starting materials

A) *Epoxides*

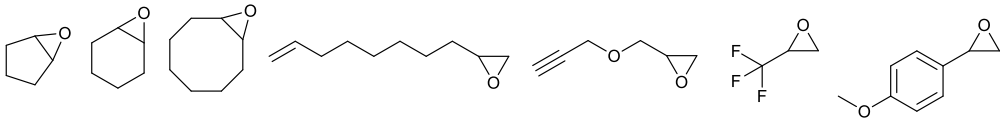

B) *Aziridines*

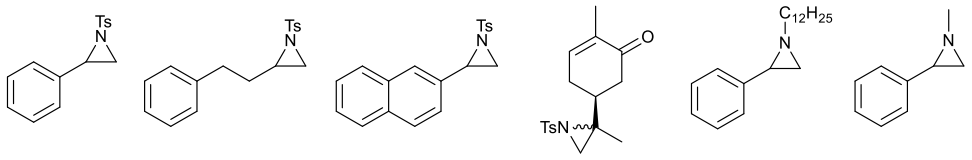

C) *Michael acceptors*

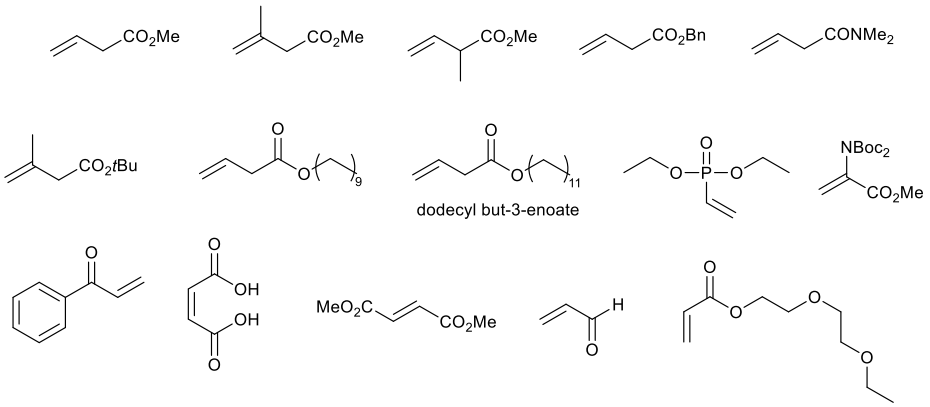

11. General Procedures

A. *General procedure for aliphatic epoxide:*

Each reaction was performed in a glass vial (10 mL) sealed with an aluminum cap with a rubber septum equipped with a magnetic stirring bar. It was charged with activated Zn^0 dust (40 mg, 0.6 mmol, 3.0 equiv.), DTAC (264 mg, 5.0 equiv.) and B_{12} (5.0 mol%, 13.5 mg). Then water (4.5 mL) and ethanol (0.5 mL) were added. The resulting mixture was degassed by purging with argon with simultaneous sonication in an ultrasonic bath for 15 min. An epoxide (0.2 mmol, 1.0 equiv.) was added dropwise *via* a syringe followed by a Michael acceptor (1.5 equiv). The resulting mixture was irradiated with blue LED light (single diode, 3 W; λ = 460 nm at room temperature) for 16 h. The resulting mixture was diluted with AcOEt (~ 3 mL) and washed with brine (20 mL). The organic phase was dried over Na_2SO_4, then filtered through the cotton wool and concentrated *in vacuo*. A crude product was purified by means of column chromatography.

B. *General procedure for aryl epoxide:*

Each reaction was performed in a glass vial (10 mL) sealed with an aluminum cap with a rubber septum equipped with a magnetic stirring bar. It was charged with activated Zn^0 dust (40 mg, 0.6 mmol, 3.0 equiv.), DTAC (132 mg, 2.5 equiv.) and B_{12} (5.0 mol%, 13.5 mg). Then water (4.5 mL) and ethanol (0.5mL) were added. The resulting mixture was degassed by purging with argon with simultaneous sonication in an ultrasonic bath for 15 min. An epoxide (0.2 mmol, 1.0 equiv.) was added dropwise *via* a syringe followed by a Michael acceptor (5.0 equiv). The resulting mixture was irradiated with blue LED light (tape, 32 W; λ = 460 nm) at room temperature for 16 h. The resulting mixture was diluted with AcOEt (~ 3 mL) and washed with brine (20 mL). The organic phase was dried over Na_2SO_4, then filtered through the cotton wool and concentrated *in vacuo*. A crude product was purified by means of column chromatography.

C. *General procedure for alkyk aziridine:*

Each reaction was performed in a glass vial (10 mL) sealed with an aluminum cap with a rubber septum equipped with a magnetic stirring bar. It was charged with activated Zn^0 dust (40 mg, 0.6 mmol, 3.0 equiv.), DTAC (185 mg, 3.5 equiv.) and B_{12} (2.5 mol%, 6.75 mg). Then water (4.5 mL) and isopropanol (0.5 mL) were added. The resulting mixture was degassed by purging with argon with simultaneous sonication in an ultrasonic bath for 25 min. Then, aziridine (0.2 mmol, 1.0 equiv.) was added dropwise *via* a syringe followed by a Michael acceptor (3.0 equiv.). The resulting mixture was irradiated with green LED light (Kessil, 40 W; λ = 525 nm) for 24 h. at room temperature. The resulting mixture was diluted with AcOEt (~ 3 mL) and washed with brine (20 mL). The organic phase was dried over Na_2SO_4, then filtered through the cotton wool and concentrated *in vacuo*. A crude product was purified by means of column chromatography.

11.1 Note:

- The reaction can be easily monitored by TLC chromatography (AcOEt/Hexane) using UV visualization or the Hanessian's stain.
- Reactions require using activated zinc (unactivated zinc gives a low yield).

11.2 Procedure for the 1 mmol scale synthesis of 5-hydroxy-6-phenoxyhexanenitrile (3)

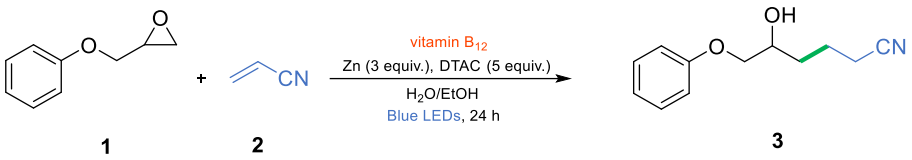

1 2 3

Reaction condition: The reaction was carried out in a 50 mL round-bottom flask sealed with a rubber septum and equipped with a magnetic stirring bar. The flask was charged with activated zinc dust (200 mg, 3 mmol, 3.0 equiv), DTAC (1.32 g, 5.0 equiv), and vitamin B_{12} (67.5 mg, 5.0 mol%). Water (22.5 mL) and ethanol (2.5 mL) were then added. The resulting mixture was degassed by purging with argon while simultaneously sonicating in an ultrasonic bath for 30 minutes. Subsequently, 2-(phenoxymethyl)oxirane **1** (150 mg, 1 mmol, 1.0 equiv) was added dropwise via syringe, followed by acrylonitrile **2** (80 mg, 1.5 mmol, 1.5 equiv). The reaction mixture was irradiated with blue LED light (Kessil lamps, 2 × 20 W, λ = 440 nm) at room temperature for 24 hours. After completion, the mixture was extracted with ethyl AcOEt and brine. The organic layer was dried over anhydrous Na_2SO_4, filtered through cotton wool, and concentrated under reduced pressure. The crude product was purified by flash column chromatography using a hexanes/AcOEt gradient to afford compound **3** (165 mg, 80%) as the final product.

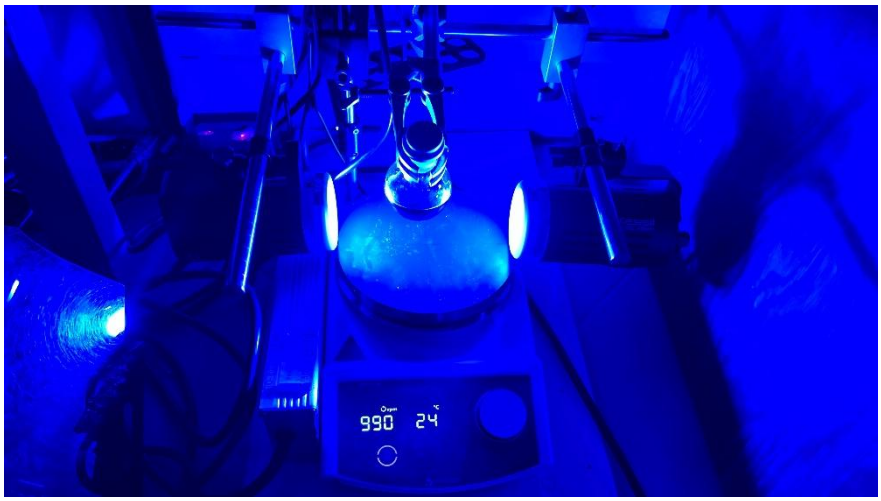

Figure 3. Set-Up for the 1 mmol-scale reaction

12. Scope and characterization of new compounds

12.1. Epoxides

5-hydroxy-6-phenoxyhexanenitrile (3)

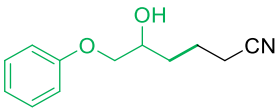

Following the general procedure **A** compound **3** was obtained from 2-(phenoxymethyl)oxirane (**1**) (30 mg, 0.20 mmol) and acrylonitrile (**2**) (16 mg, 0.30 mmol). The crude product was purified by flash chromatography (gradually from hexane to 60:40 ethyl acetate/hexane) to afford 35 mg of 5-hydroxy-6-phenoxyhexanenitrile (**3**) as colorless oil, (yield = **85%**).

^{1}H NMR (400 MHz, $CDCl_3$): δ 7.31 – 7.27 (m, 2H), 6.99 – 6.96 (m, 1H), 6.90 – 6.89 (m, 2H), 4.04 – 4.01 (m, 2H), 3.97 (dd, *J* = 9.2, 3.2 Hz, 1H), 3.84 (dd, *J* = 9.2, 7.3 Hz, 1H), 2.48 – 2.42 (m, 1H), 2.38 (d, *J* = 6 Hz, 1H), 2.00 – 1.91 (m, 1H), 1.87 – 1.78 (m, 1H), 1.77 – 1.66 (m, 2H).

^{13}C NMR (100 MHz, $CDCl_3$): δ 158.3, 129.6, 121.4, 114.5, 77.2, 71.9, 69.3, 31.7, 21.7, 17.1.

HRMS (ESI) $[M+Na]^+$ calculated for $C_{12}H_{15}NO_2Na$: 228.1000, found: 228.1001.

1-phenoxy-5-(phenylsulfonyl)pentan-2-ol (6)

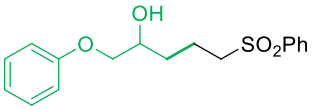

Following the general procedure **A** compound **6** was obtained from 2-(phenoxymethyl)oxirane (30 mg, 0.20 mmol) and phenyl vinyl ketone (**2**) (50 mg, 0.30 mmol). The crude product was purified by flash chromatography (gradually from hexane to 60:40 ethyl acetate/hexane) to afford 21 mg of 1-phenoxy-5-(phenylsulfonyl)pentan-2-ol (**6**) as colorless oil, (yield = **33%**).

^{1}H NMR (500 MHz, $CDCl_3$): δ 7.93 – 7.91 (m, 2H), 7.67 – 7.7.64 (m, 1H), 7.58 – 7.55 (m, 2H), 7.30 – 7.26 (m, 2H), 6.98 – 6.95 (m, 1H), 6.88 – 6.86 (m, 2H), 3.98 – 3.94 (m, 1H), 3.92 (dd, *J* = 9.2, 3.4 Hz, 1H), 3.80 (dd, *J* = 9.2, 7.2 Hz, 1H), 3.25 – 3.14 (m, 2H), 2.38 (s, 1H), 2.04 – 1.95 (m, 1H), 1.93 – 1.86 (m, 1H), 1.70 – 1.60 (m, 2H).

^{13}C NMR (125 MHz, $CDCl_3$): δ 158.3, 139.1, 133.7, 129.6, 129.3, 128.1, 121.3, 114.5, 71.8, 69.5, 56.0, 31.4, 19.2.

HRMS (ESI) $[M+Na]^+$ calculated for $C_{17}H_{20}O_4SNa$: 343.0980, found: 343.0983.

5-hydroxy-5-phenylpentanenitrile (7)

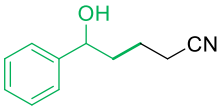

Following the general procedure **B** compound **7** was obtained from 2-phenyloxirane (24 mg, 0.20 mmol) and acrylonitrile (**2**) (16 mg, 0.30 mmol). The crude product was purified by flash chromatography (gradually from hexane to 60:40 ethyl acetate/hexane) to afford 17 mg of 5-hydroxy-5-phenylpentanenitrile (**7**) as colorless oil, (yield = **48%**).

NMR data matched those reported in the literature.[9]

^{1}H NMR (500 MHz, $CDCl_3$): δ 7.40 – 7.28 (m, 5H), 4.76 – 4.72 (m, 1H), 2.44 – 2.32 (m, 2H), 1.98 – 1.79 (m, 4H).

5-(4-fluorophenyl)-5-hydroxypentanenitrile (8)

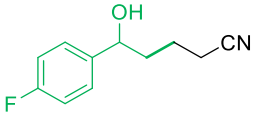

Following the general procedure **B** compound **8** was obtained from 2-(4-fluorophenyl)oxirane (28 mg, 0.20 mmol) and acrylonitrile (**2**) (16 mg, 0.30 mmol). The crude product was purified by flash chromatography (gradually from hexane to 60:40 ethyl acetate/hexane) to afford 20 mg of 5-(4-fluorophenyl)-5-hydroxypentanenitrile (**8**) as colorless oil, (yield = **53%**).

^{1}H NMR (500 MHz, $CDCl_3$): δ 7.34 – 7.29 (dd, *J* = 8.35, 5.49 Hz, 2H), 7.07 – 7.02 (t, *J* = 8.60 Hz, 2H), 4.76 – 4.69 (dd, *J* = 7.31, 4.43 Hz, 1H), 2.46 – 2.42 (m, 1H), 2.42 – 2.35 (q, *J* = 6.68 Hz, 2H), 1.92 – 1.81 (m, 4H).

^{13}C NMR (151 MHz, $CDCl_3$): δ 163.12, 161.49, 139.73, 127.37, 119.49, 118.59, 115.55, 115.41, 73.04, 37.68, 24.26, 21.79, 17.07, 16.68.

HRMS (APCI) $[M+H]^+$ calculated for $C_{11}H_{13}NOF$: 194.0981, found: 194.0982.

5-hydroxynonanenitrile (9)

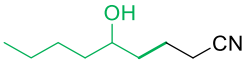

Following the general procedure **A** compound **9** was obtained from 2-butyloxirane (20 mg, 0.20 mmol) and acrylonitrile (**2**) (16 mg, 0.30 mmol). The crude product was purified by flash chromatography (gradually from hexane to 60:40 ethyl acetate/hexane) to afford 23 mg of 5-hydroxynonanenitrile (**9**) as colorless oil, (yield = **73%**).

NMR data matched those reported in the literature.[10]

^{1}H NMR (500 MHz, $CDCl_3$): δ 3.67 – 3.60 (m, 1H), 2.44 – 2.37 (m, 2H), 1.91 – 1.82 (m, 1H), 1.79 – 1.70 (m, 1H), 1.69 – 1.61 (m, 1H), 1.55 – 1.43 (m, 3H), 1.42 – 1.28 (m, 5H), 0.91 (t, *J* = 7.0 Hz, 3H).

^{13}C NMR (125 MHz, $CDCl_3$): δ 119.7, 71.1, 37.5, 35.9, 27.7, 22.6, 21.8, 17.2, 14.0.

[9] Nagaki, A.; Yamashita, H.; Hirose, K.; Tsuchihashi, Y.; Yoshida, J. Alkyllithium Compounds Bearing Electrophilic Functional Groups: A Flash Chemistry Approach. *Angew. Chem. Int. Ed.* **2019**, *58*, 4027-4030. https://doi.org/10.1002/anie.201814088.
[10] O'Shea, M. G.; Kitching, W. Organotin and -Mercury Routes to Enones, Dienones Amd Spiroacetals. *Tetrahedron* **1989**, *45* (4), 1177–1186. https://doi.org/https://doi.org/10.1016/0040-4020(89)80026-2.

5-hydroxypentadecanenitrile (10)

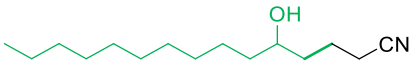

Following the general procedure **A** compound **10** was obtained from 1,2-epoxydodecane (37 mg, 0.20 mmol) and acrylonitrile (**2**) (16 mg, 0.30 mmol). The crude product was purified by flash chromatography (gradually from hexane to 60:40 ethyl acetate/hexane) to afford 19 mg of 5-hydroxypentadecanenitrile (**10**) as colorless oil, (yield = **40%**).

^{1}H NMR (500 MHz, $CDCl_3$): δ 3.65 – 3.60 (m, 1H), 2.39 (t, *J* = 7.2 Hz, 2H), 1.90 – 1.81 (m, 1H), 1.77 – 1.69 (m, 1H), 1.67 – 1.59 (m, 1H), 1.55 – 1.48 (m, 1H), 1.47 – 1.36 (m, 4H), 1.26 (m, 15H), 0.87 (t, *J* = 6.9 Hz, 3H).

^{13}C NMR (125 MHz, $CDCl_3$): δ 119.7, 71.1, 37.8, 35.9, 31.9, 29.6, 29.6, 29.3, 25.6, 22.66, 21.8, 17.2, 14.1.

HRMS (APCI) $[M+H]^+$ calculated for $C_{15}H_{30}NO$: 240.2327, found: 240.2328.

5-hydroxy-6-(naphthalen-2-yloxy)hexanenitrile (11)

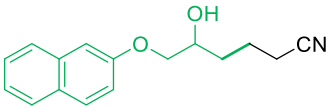

Following the general procedure **A** compound **11** was obtained from 2-((naphthalen-2-yloxy)methyl)oxirane (40 mg, 0.20 mmol) and acrylonitrile (**2**) (16 mg, 0.30 mmol). The crude product was purified by flash chromatography (gradually from hexane to 50:50 ethyl acetate/hexane) to afford 21 mg of 5-hydroxy-6-(naphthalen-2-yloxy)hexanenitrile (**11**) as colorless oil, (yield = **41%**).

^{1}H NMR (500 MHz, $CDCl_3$): δ 7.79 – 7.72 (m, 3H), 7.48 – 7.43 (m, 1H), 7.38 – 7.34 (m, 1H), 7.17 – 7.14 (m, 2H), 4.14 – 4.07 (m, 2H), 3.97 (dd, *J* = 10.0, 8.5 Hz, 1H), 2.53 – 2.40 (m, 3H), 2.00 – 1.95 (m, 1H), 1.90 – 1.85 (m, 1H), 1.82 – 1.70 (m, 2H).

^{13}C NMR (125 MHz, $CDCl_3$): δ 156.3, 134.4, 129.6, 129.2, 127.7, 126.8, 126.6, 124.0, 119.5, 118.5, 107.0, 72.0, 69.3, 31.8, 21.8, 17.2.

HRMS (ESI) $[M+Na]^+$ calculated for $C_{16}H_{17}NO_2Na$: 278.1157, found: 278.1158.

***tert*-butyl ((2S)-6-cyano-3-hydroxy-1-phenylhexan-2-yl)carbamate (12)**

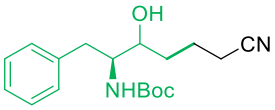

Following the general procedure **A** compound **12** was obtained from tert-butyl ((1*S*)-1-(oxiran-2-yl)-2-phenylethyl)carbamate (53 mg, 0.20 mmol) and acrylonitrile (**2**) (16 mg, 0.30 mmol). The crude product was purified by flash chromatography (gradually from hexane to 60:40 ethyl acetate/hexane) to afford 26 mg of tert-butyl ((2S)-6-cyano-3-hydroxy-1-phenylhexan-2-yl)carbamate (**12**) as a white solid, (yield = **40%**).

^{1}H NMR (500 MHz, $CDCl_3$): δ 7.32 – 7.29 (m, 2H), 7.24 – 7.22 (m, 3H), 4.58 (d, *J* = 7.4 Hz, 1H), 3.83 (br s, 1H), 3.69 – 3.68 (m, 1H), 3.32 (br s, 1H), 2.86 (dd, *J* = 14.1, 5.0 Hz, 1H), 2.82 – 2.71 (m, 1H), 2.41 (td, *J* = 7.0, 2.4 Hz, 2H), 1.98 – 1.92 (m, 1H), 1.78 – 1.73 (m, 1H), 1.61 – 1.57 (m, 2H), 1.37 (s, 9H).

^{13}C NMR (125 MHz, $CDCl_3$): δ 137.6, 129.1, 128.7, 126.7, 119.7, 80.2, 73.2, 57.2, 36.0, 31.5, 28.2, 22.1, 17.1.

HRMS (ESI) $[M+Na]^+$ calculated for $C_{18}H_{26}N_2O_3Na$: 341.1841, found: 341.1844.

benzyl (5-cyano-2-hydroxypentyl)carbamate (13)

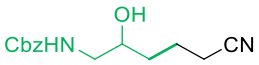

Following the general procedure **A** compound **13** was obtained from benzyl (oxiran-2-ylmethyl)carbamate (**S1**) (38 mg, 0.20 mmol) and acrylonitrile (**2**) (16 mg, 0.30 mmol). The crude product was purified by flash chromatography (gradually from hexane to 80:20 ethyl acetate/hexane) to afford 26 mg of benzyl (5-cyano-2-hydroxypentyl)carbamate (**13**) as colorless oil, (yield = **53%**).

^{1}H NMR (500 MHz, $CDCl_3$): δ 7.38 – 7.32 (m, 5H), 5.22 (br s, 1H), 5.10 (s, 2H), 3.73 (s, 1H), 3.36 – 3.29 (m, 1H), 3.17 – 3.07 (m, 1H), 2.71 (s, 1H), 2.39 – 2.36 (m, 2H), 1.89 – 1.79 (m, 1H), 1.77 – 1.71 (m, 1H), 1.56 – 1.55 (m, 1H), NH was not detected in the NMR spectrum, likely due to solvent-mediated exchange.

^{13}C NMR (125 MHz, $CDCl_3$): δ 157.4, 136.2, 128.6, 128.3, 128.1, 119.6, 70.6, 67.1, 47.1, 33.2, 21.7, 17.1.

HRMS (APCI) $[M+H]^+$ calculated for $C_{14}H_{19}N_2O_3$: 263.1396, found: 263.1398.

5-hydroxy-7-(phenylsulfonyl)heptanenitrile (14)

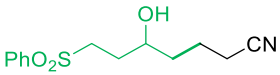

Following the general procedure **A** compound **14** was obtained from 2-(2-(phenylsulfonyl)ethyl)oxirane (42 mg, 0.20 mmol) and acrylonitrile (**2**) (16 mg, 0.30 mmol). The crude product was purified by flash chromatography (gradually from hexane to 80:20 ethyl acetate/hexane) to afford 34 mg of 5-hydroxy-7-(phenylsulfonyl)heptanenitrile (**14**) as a white solid, (yield = **63%**).

^{1}H NMR (500 MHz, $CDCl_3$): δ 7.94 – 7.89 (m, 2H), 7.69 – 7.66 (m, 1H), 7.60 – 7.57 (m, 2H), 3.84 – 3.75 (m, 1H), 3.31 – 3.22 (m, 2H), 2.39 (t, *J* = 7.0 Hz, 2H), 2.10 (d, *J* = 5.2 Hz, 1H), 2.01 – 1.92 (m, 1H), 1.89 – 1.77 (m, 2H), 1.77 – 1.67 (m, 1H), 1.64 – 1.50 (m, 2H).

^{13}C NMR (125 MHz, $CDCl_3$): δ 139.0, 133.9, 129.4, 127.9, 119.5, 69.0, 52.9, 36.0, 30.2, 21.7, 17.1.

HRMS (ESI) $[M+Na]^+$ calculated for $C_{13}H_{17}NO_3SNa$: 290.0827, found: 290.0826.

12.2. Aziridines

N-(1-cyanooctan-4-yl)-4-methylbenzenesulfonamide (5)

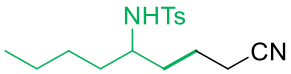

Following the general procedure **C** compound **5** was obtained from 2-butyl-1-tosylaziridine (**4**) (51 mg, 0.20 mmol) and acrylonitrile (**2**) (16 mg, 0.30 mmol). The crude product was purified by flash chromatography (gradually from hexane to 60:40 ethyl acetate/hexane) to afford 50 mg of (**5**) as *N*-(1-cyanooctan-4-yl)-4-methylbenzenesulfonamide colorless oil, (yield = **80%**).

^{1}H NMR (400 MHz, $CDCl_3$): δ = 7.74 (d, *J* = 8.3 Hz, 2H), 7.30 – 7.29 (m, 2H), 4.47 (d, *J* = 8.6 Hz, 1H), 3.23 – 3.17 (m, 1H), 2.42 (s, 3H), 2.29 (td, *J* = 6.7, 2.4 Hz, 2H), 1.74 – 1.65 (m, 1H), 1.62 (m, 2H), 1.47 – 1.39 (m, 1H), 1.34 – 1.27 (m, 1H), 1.26 – 1.20 (m, 1H), 1.15 – 1.04 (m, 3H), 1.04 – 0.96 (m, 1H), 0.73 (t, *J* = 7.1 Hz, 3H).

^{13}C NMR (100 MHz, $CDCl_3$): δ = 143.5, 138.1, 129.7, 126.9, 119.4, 53.3, 35.0, 34.1, 27.4, 22.3, 21.5, 21.4, 16.8, 13.7.

HRMS (ESI) $[M+Na]^+$ calculated for $C_{16}H_{24}N_2O_2SNa$: 331.1456, found: 331.1458.

4-methyl-*N*-(9-oxodecan-5-yl)benzenesulfonamide (15)

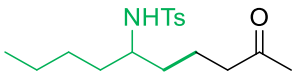

Following the general procedure **C** compound **15** was obtained from 2-butyl-1-tosylaziridine (**4**) (51 mg, 0.20 mmol) and methyl vinyl ketone (21 mg, 0.30 mmol). The crude product was purified by flash chromatography (gradually from hexane to 60:40 ethyl acetate/hexane) to afford 26 mg of (**15**) as 4-methyl-*N*-(9-oxodecan-5-yl)benzenesulfonamide colorless oil, (yield = **40%**).

^{1}H NMR (400 MHz, $CDCl_3$): δ = 7.75 (d, *J* = 8.2 Hz, 2H), 7.29 (d, *J* = 8.0 Hz, 2H), 4.35 (d, *J* = 8.3 Hz, 1H), 3.18 (h, *J* = 6.8 Hz, 1H), 2.42 (s, 3H), 2.32 (t, *J* = 7.0 Hz, 2H), 2.08 (s, 3H), 1.52 – 1.36 (m, 3H), 1.36 – 1.24 (m, 3H), 1.16-1.09 (m, 3H), 1.07 – 1.01 (m, 1H), 0.76 (t, *J* = 7.0 Hz, 3H).

^{13}C NMR (100 MHz, $CDCl_3$): δ = 208.5, 143.2, 138.3, 129.6, 127.0, 53.8, 43.1, 34.6, 34.4, 29.8, 27.4, 22.4, 21.5, 19.3, 13.8.

HRMS (APCI) $[M–H]^-$ calculated for $C_{17}H_{26}N_2O_3S$: 324.1633, found: 324.1636.

4-methyl-*N*-(1-(phenylsulfonyl)octan-4-yl)benzenesulfonamide (16)

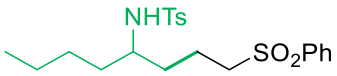

Following the general procedure **C** compound **16** was obtained from 2-butyl-1-tosylaziridine (**4**) (51 mg, 0.20 mmol) and phenyl vinyl ketone (50 mg, 0.30 mmol). The crude product was purified by flash chromatography (gradually from hexane to 60:40 ethyl acetate/hexane) to afford 14 mg of (**16**) as 4-methyl-*N*-(1-(phenylsulfonyl)octan-4-yl)benzenesulfonamide colorless oil, (yield = **17%**).

^{1}H NMR (400 MHz, $CDCl_3$): δ = 7.89 (d, *J* = 7.2 Hz, 2H), 7.71 (d, *J* = 8.2 Hz, 2H), 7.67 (t, *J* = 7.4 Hz, 1H), 7.58 (t, *J* = 7.7 Hz, 2H), 7.29 (d, *J* = 8.0 Hz, 2H), 4.27 (d, *J* = 8.4 Hz, 1H), 3.21 – 3.12 (m, 1H), 3.02 (pt, *J* = 7.9, 4.4 Hz, 2H), 2.42 (s, 3H), 1.80 – 1.64 (m, 2H), 1.49 – 1.39 (m, 1H), 1.34 – 1.16 (m, 3H), 1.14 – 1.01 (m, 3H), 1.01 – 0.92 (m, 1H), 0.73 (t, *J* = 7.1 Hz, 3H).

^{13}C NMR (100 MHz, $CDCl_3$): δ = 143.4, 139.1, 138.0, 133.7, 129.7, 129.3, 128.0, 127.0, 55.7, 53.4, 34.6, 33.7, 27.3, 22.3, 21.5, 18.7, 13.7.

HRMS (ESI) $[M+Na]^+$ calculated for $C_{21}H_{29}NO_4S_2Na$: 446.1436, found: 446.1437.

_N_-(1-cyanotetradecan-4-yl)-4-methylbenzenesulfonamide (17)

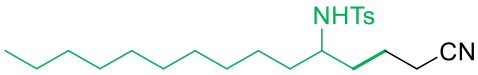

Following the general procedure **C** compound **17** was obtained from 2-decyl-1-tosylaziridine (**S3**) (68 mg, 0.20 mmol) and acrylonitrile (**2**) (16 mg, 0.30 mmol). The crude product was purified by flash chromatography (gradually from hexane to 60:40 ethyl acetate/hexane) to afford 37 mg of (**17**) as *N*-(1-cyanotetradecan-4-yl)-4-methylbenzenesulfonamide colorless oil, (yield = **47%**).

^{1}H NMR (400 MHz, $CDCl_3$): δ = 7.74 (d, *J* = 8.1 Hz, 2H), 7.31 (d, *J* = 8.1 Hz, 2H), 4.34 (d, *J* = 8.6 Hz, 1H), 3.27 – 3.16 (m, 1H), 2.43 (s, 3H), 2.31 (dt, *J* = 6.9, 3.9 Hz, 2H), 1.75 – 1.60 (m, 3H), 1.49 – 1.41 (m, 1H), 1.34 – 1.13 (m, 14H), 1.10 – 1.04 (m, 4H), 0.88 (t, *J* = 7.0 Hz, 3H).

^{13}C NMR (100 MHz, $CDCl_3$): δ = 143.5, 138.1, 129.7, 127.0, 119.4, 53.3, 35.3, 34.2, 31.9, 29.6, 29.5, 29.3, 29.3, 29.2, 25.3, 22.7, 21.5, 21.4, 16.8, 14.1.

HRMS (ESI) $[M+Na]^+$ calculated for $C_{22}H_{36}N_2O_2SNa$: 415.2395, found: 415.2399.

4-methyl-*N*-(2-oxohexadecan-6-yl)benzenesulfonamide (18)

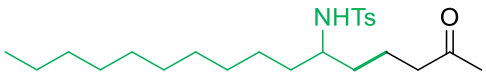

Following the general procedure **C** compound **18** was obtained from 2-decyl-1-tosylaziridine (**S3**) (68 mg, 0.20 mmol) and methyl vinyl ketone (21 mg, 0.30 mmol). The crude product was purified by flash chromatography (gradually from hexane to 60:40 ethyl acetate/hexane) to afford 33 mg of (**18**) as 4-methyl-*N*-(2-oxohexadecan-6-yl)benzenesulfonamide colorless oil, (yield = **40%**).

^{1}H NMR (400 MHz, $CDCl_3$): δ = 7.74 (d, *J* = 8.2 Hz, 2H), 7.29 (d, *J* = 8.0 Hz, 2H), 4.28 (d, *J* = 8.3 Hz, 1H), 3.18 (h, *J* = 6.7 Hz, 1H), 2.42 (s, 3H), 2.33 (t, *J* = 7.0 Hz, 2H), 2.09 (s, 3H), 1.52 – 1.38 (m, 3H), 1.37 – 1.14 (m, 15H), 1.12 – 1.09 (m, 4H), 0.88 (t, *J* = 7.0 Hz, 3H).

^{13}C NMR (100 MHz, $CDCl_3$): δ = 208.5, 143.2, 138.3, 129.6, 127.0, 53.9, 43.1, 34.9, 34.5, 31.9, 29.8, 29.6, 29.5, 29.4, 29.3, 29.3, 25.2, 22.7, 21.5, 19.3, 14.1.

HRMS (ESI) $[M\text{-}Na]^+$ calculated for $C_{23}H_{39}NO_3SNa$: 432.2548, found: 432.2553.

***N*-(cyclopent-2-en-1-yl)-4-methylbenzenesulfonamide (19)**

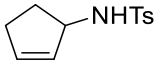

Following the general procedure **C** side product **19** was obtained from 6-tosyl-6-azabicyclo[3.1.0]hexane (**S7**) (48 mg, 0.20 mmol) and acrylonitrile (**2**) (16 mg, 0.30 mmol). The crude product was purified by flash chromatography (gradually from hexane to 60:40 ethyl acetate/hexane) to afford 29 mg of (**19**) as *N*-(cyclopent-2-en-1-yl)-4-methylbenzenesulfonamide white solid, (yield = **60%**).

NMR data matched those reported in the literature.[11]

^{1}H NMR (400 MHz, $CDCl_3$): δ = 7.77 (d, *J* = 8.3 Hz, 2H), 7.30 (d, *J* = 8.1 Hz, 2H), 5.89 – 5.81 (m, 1H), 5.44 (dt, *J* = 5.5, 2.0 Hz, 1H), 4.48 – 4.33 (m, 2H), 2.43 (s, 3H), 2.35 (m, 1H), 2.24 – 2.06 (m, 2H), 1.55 – 1.45 (m, 1H).

[11] Yamamoto, H.; Ho, E.; Sasaki, I.; Mitsutake, M.; Takagi, Y.; Imagawa, H.; Nishizawa, M. Intermolecular Amination of Allyl Alcohols with Sulfamates: Effective Utilization of Mercuric Catalyst. *European J. Org. Chem.* **2011**, *2011* (13), 2417–2420. https://doi.org/https://doi.org/10.1002/ejoc.201100054.

***N*-(cyclohex-2-en-1-yl)-4-methylbenzenesulfonamide (20)**

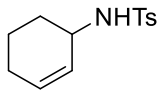

Following the general procedure **C** side product **20** was obtained from 7-tosyl-7-azabicyclo[4.1.0]heptane (**S8**) (50 mg, 0.20 mmol) and acrylonitrile (**2**) (16 mg, 0.30 mmol). The crude product was purified by flash chromatography (gradually from hexane to 60:40 ethyl acetate/hexane) to afford 35 mg of (**20**) as *N*-(cyclohex-2-en-1-yl)-4-methylbenzenesulfonamide white solid, (yield = **70%**).

NMR data matched those reported in the literature.[12]

^{1}H NMR (400 MHz, $CDCl_3$): δ = 7.77 (d, *J* = 8.3 Hz, 2H), 7.29 (d, *J* = 8.1 Hz, 2H), 5.79 – 5.74 (m, 1H), 5.37 – 5.32 (m, 1H), 4.58 (d, *J* = 8.5 Hz, 1H), 3.84 – 3.79 (m, 1H), 2.42 (s, 3H), 1.98 – 1.86 (m, 2H), 1.75 (m, 1H), 1.62 – 1.48 (m, 3H + H_2O).

[12] Wallach, D. R.; Chisholm, J. D. Alkylation of Sulfonamides with Trichloroacetimidates under Thermal Conditions. *J. Org. Chem.* **2016**, *81* (17), 8035–8042. https://doi.org/10.1021/acs.joc.6b01421.

7. Author Declarations

Institute of Organic Chemistry
Polish Academy of Sciences

Kitti Franciska Szabó

PhD Student, Group XV

kitti.szabo@icho.edu.pl

Institute of Organic Chemistry, Polish Academy of Sciences

Kasprzaka 44/52

Warsaw, 01-224, Poland

Warsaw, 28/05/2025

I declare that my contribution to the creation of the following publications included:

- Site-Selective, Photocatalytic Vinylogous Amidation of Enones, **Szabó, K. F.**; Goliszewska, K.; Szurmak, J.; Rybicka-Jasińska, K.; Gryko, D. *Org. Lett.* **2022**, *24*, 8120-8124.

Preparation of α,β-unsaturated carbonyl compounds as starting materials and completion of the scope regarding *N*-aminopyridinium salts. Additionally, contribution to the development of the scope for α,β-unsaturated carbonyl compounds and collection of all relevant data for the synthesized compounds. Conducted mechanistic experiments, prepared the supporting information, and wrote the first draft of the manuscript.

- Photochemical C3-amination of pyridines via Zincke Imine intermediates **Szabó, K. F.**; Banachowicz, P.; Powała, A.; Lunic, D.; Ardoiz, I. F.; Gryko, D. *Nat. Commun.* **2025**, accepted, doi:10.26434/chemrxiv-2024-3dj94.

Discussion of the proposed research concept, designing strategies and planning experimental work. preparation of Zincke imine derivatives and various *N*-aminopyridinium salts. Contributed to the optimization of *N*-aminopyridinium salts and the model Zincke imine derivative. Conducted several experiments related to the scope of 2-phenyl Zincke imine derivatives and carried out the purification of all 2-alkyl Zincke imine derivatives. Performed UV-Vis and cyclic voltammetry (CV) studies, as well as mechanistic investigations. Collected all relevant data required for compound synthesis. Participated in editing the supporting information and wrote the first draft of the manuscript.

- Vitamin B_{12} and Micellar Solution Enable Regioselective Ring Opening of Epoxides and Aziridines with Electrophilic Olefins, **Szabó, K. F.**; Wdowik, T.; Krzeszewska, A.; Mazurek, K.; Andersson, M. P.; Gryko, D. *Org. Lett.*, **2025**, doi.org/10.1021/acs.orglett.5c01376.

Preparation of starting materials for aziridine derivatives; investigation of the scope of aziridine derivatives as well as acrylates; performance of mechanistic studies and selected examples for the epoxide scope. Collected all relevant data for the synthesized compounds. Prepared all parts of the manuscript, including the supporting information.

I confirm that the above statements are true: Dorota Gryko Digitally signed by Dorota Gryko Date: 2025.05.30 13:41:47 +02'00' (Supervisor signature)

Kitti Franciska Szabó

KITTI FRANCISKA SZABÓ

Institute of Organic Chemistry
Polish Academy of Sciences

Prof. Dorota Gryko

Group Leader, Group XV

+48 22 343 2051

dorota.gryko@icho.edu.pl

Institute of Organic Chemistry, Polish Academy of Sciences

Kasprzaka 44/52

Warsaw, 01-224, Poland

Warsaw, 28/05/2025

I declare that my contribution to the creation of the following publications included:

- Site-Selective, Photocatalytic Vinylogous Amidation of Enones, **Szabó, K. F.**; Goliszewska, K.; Szurmak, J.; Rybicka-Jasińska, K.; Gryko, D. *Org. Lett.* **2022**, *24*, 8120-8124.

Conceptualization of the project and providing guidance and corrections during the preparation of the manuscript and Supporting Information.

- Photochemical C3-amination of pyridines via Zincke Imine intermediates, **Szabó, K. F.**; Banachowicz, P.; Powała, A.; Lunic, D.; Ardoiz, I. F.; Gryko, D. *Nat. Commun.* **2025**, accepted, doi:10.26434/chemrxiv-2024-3dj94.

Conceptualization of the project and providing guidance and corrections during the preparation of the manuscript and Supporting Information.

- Vitamin B_{12} and Micellar Solution Enable Regioselective Ring Opening of Epoxides and Aziridines with Electrophilic Olefins, **Szabó, K. F.**; Wdowik, T.; Krzeszewska, A.; Mazurek, K.; Andersson, M. P.; Gryko, D. *Org. Lett.*, **2025**, doi.org/10.1021/acs.orglett.5c01376.

Conceptualization of the project and providing guidance and corrections during the preparation of the manuscript and Supporting Information.

Dorota Gryko

Digitally signed by Dorota Gryko
Date: 2025.05.29 23:29:42 +02'00'

Institute of Organic Chemistry
Polish Academy of Sciences

Dr. Katarzyna Rybicka-Jasińska

XVb group leader

katarzyna.rybicka-jasinska@icho.edu.pl

Institute of Organic Chemistry, Polish Academy of Sciences

Kasprzaka 44/52

Warsaw, 01-224, Poland

Warsaw, 27/05/2025

I declare that my contribution to the creation of the following publications included:

- Site-Selective, Photocatalytic Vinylogous Amidation of Enones, **Szabó, K. F.**; Goliszewska, K.; Szurmak, J.; Rybicka-Jasińska, K.; Gryko, D. *Org. Lett.* **2022**, *24*, 8120-8124.

The contributions include supervising the preparation of the manuscript and Supporting Information, as well as supervising the experimental work.

Katarzyna Rybicka-Jasińska

Elektronicznie podpisany przez Katarzyna Rybicka-Jasińska
Data: 2025.05.28 12:30:32 +02'00'

.....

Institute of Organic Chemistry
Polish Academy of Sciences

Dr. Tomasz Wdowik

Team leader

tj.wdowik@uw.edu.pl

Institute of Organic Chemistry, Polish Academy of Sciences

Kasprzaka 44/52

01-224 Warsaw, Poland

Warsaw, 27/05/2025

I declare that my contribution to the creation of the following publication:

- Vitamin B_{12} and Micellar Solution Enable Regioselective Ring Opening of Epoxides and Aziridines with Electrophilic Olefins, **Szabó, K. F.**; Wdowik, T.; Krzeszewska, A.; Mazurek, K.; Andersson, M. P.; Gryko, D. *Org. Lett.*, **2025**, doi.org/10.1021/acs.orglett.5c01376.

included performing extractions and selected reactions related to the aziridine scope, as well as editing the manuscript and Supporting Information.

Institute of Organic Chemistry
Polish Academy of Sciences

Dr. Katarzyna Goliszewska
katarzyna.goliszewska@icho.edu.pl

Institute of Organic Chemistry, Polish Academy of Sciences

Kasprzaka 44/52

Warsaw, 01-224, Poland

Warsaw, 27/05/2025

I declare that my contribution to the creation of the following publications included:

- Site-Selective, Photocatalytic Vinylogous Amidation of Enones, Szabó, K. F.; Goliszewska, K.; Szurmak, J.; Rybicka-Jasińska, K.; Gryko, D. *Org. Lett.* **2022**, *24*, 8120-8124.

The contributions include conceptualization of the project, optimization of a silyl dienol ether derivative, and expansion of the scope regarding *N*-aminopyridinium salts and α,β-unsaturated carbonyl compounds.

Katarzyna Goliszewska

Institute of Organic Chemistry
Polish Academy of Sciences

Jakub Szurmak
jakub.szurmak@gmail.com

Institute of Organic Chemistry, Polish Academy of Sciences

Kasprzaka 44/52

Warsaw, 01-224, Poland

Warsaw, 27/05/2025

I declare that my contribution to the creation of the following publications included:

- Site-Selective, Photocatalytic Vinylogous Amidation of Enones, **Szabó, K. F.**; Goliszewska, K.; Szurmak, J.; Rybicka-Jasińska, K.; Gryko, D. *Org. Lett.* **2022**, *24*, 8120-8124.

The contributions included preparation of starting material.

Jakub Szurmak

Institute of Organic Chemistry
Polish Academy of Sciences

Dr. Ignacio Funes Ardoiz
ignacio.funesa@unirioja.es

Institute of Organic Chemistry, Polish Academy of Sciences

Kasprzaka 44/52

Warsaw, 01-224, Poland

Warsaw, 27/05/2025

I declare that my contribution to the creation of the following publications included:

- Photochemical C3-amination of pyridines via Zincke Imine intermediates, **Szabó, K. F.**; Banachowicz, P.; Powała, A.; Lunic, D.; Funes-Ardoiz, I.; Gryko, D. *Nat. Commun.* **2025**, accepted, doi:10.26434/chemrxiv-2024-3dj94.

The specific contributions include the planning and direction of the DFT study of the reaction mechanism, the analysis and interpretation of the obtained data and preparation of the manuscript section concerning DFT investigation of the reaction mechanism.

Dr. Ignacio Funes-Ardoiz

Institute of Organic Chemistry
Polish Academy of Sciences

Dr. Piort Banachowicz

Post doc.

piotr.banachowicz@icho.edu.pl

Institute of Organic Chemistry, Polish Academy of Sciences

Kasprzaka 44/52

Warsaw, 01-224, Poland

Warsaw, 27/05/2025

I declare that my contribution to the creation of the following publications included:

- Photochemical C3-amination of pyridines via Zincke Imine intermediates, Szabó, K. F.; Banachowicz, P.; Powała, A.; Lunic, D.; Funes Ardoiz, I.; Gryko, D. *Nat. Commun.* **2025**, accepted, doi:10.26434/chemrxiv-2024-3dj94.

The contributions include developing the methodology and performing experiments related to the synthesis and characterization of compounds, and collecting all relevant data required for compound synthesis. Furthermore, contribution to the preparation of the manuscript and supporting information.

27.05.2025 P. Banachowicz

Institute of Organic Chemistry
Polish Academy of Sciences

Antoni Powała

PhD Student

antoni.powala@icho.edu.pl

Institute of Organic Chemistry, Polish Academy of Sciences

Kasprzaka 44/52

Warsaw, 01-224, Poland

Warsaw, 27/05/2025

I declare that my contribution to the creation of the following publications included:

- Photochemical C3-amination of pyridines via Zincke Imine intermediates, **Szabó, K. F.**; Banachowicz, P.; Powała, A.; Lunic, D.; Funes Ardoiz, I.; Gryko, D. *Nat. Commun.* **2025**, accepted, doi:10.26434/chemrxiv-2024-3dj94.

The contributions include preparation of starting materials, development of the substrate scope bearing alkyl derivatives and performing one-pot protocol for *meta-meta*-difunctionalization.

Antoni Powała

Institute of Organic Chemistry
Polish Academy of Sciences

Danijela Lunic

Institute of Organic Chemistry, Polish Academy of Sciences

Kasprzaka 44/52

Warsaw, 01-224, Poland

Warsaw, 27/05/2025

I declare that my contribution to the creation of the following publications included:

- Photochemical C3-amination of pyridines via Zincke Imine intermediates, Szabó, K. F.; Banachowicz, P.; Powała, A.; Lunic, D.; Funes-Ardoiz, I.; Gryko, D. *Nat. Commun.* **2025**, accepted, doi:10.26434/chemrxiv-2024-3dj94.

The contributions include the evaluation through DFT calculations of the reaction mechanism.

.....

Institute of Organic Chemistry
Polish Academy of Sciences

Dr. Martin P. Andersson

Team leader

martin.andersson@kfupm.edu.sa

Institute of Organic Chemistry, Polish Academy of Sciences

Kasprzaka 44/52

Warsaw, 01-224, Poland

Warsaw, 27/05/2025

I declare that my contribution to the creation of the following publications included:

- Vitamin B_{12} and Micellar Solution Enable Regioselective Ring Opening of Epoxides and Aziridines with Electrophilic Olefins, **Szabó, K. F.**; Wdowik, T.; Krzeszewska, A.; Mazurek, K.; Andersson, M. P.; Gryko, D. *Org. Lett.*, **2025**, doi.org/10.1021/acs.orglett.5c01376.

The contributions include performing COSMO-RS calculations.

.....

Institute of Organic Chemistry
Polish Academy of Sciences

Krysztof Mazurek

mazurekkrzysztof34@gmail.com

Institute of Organic Chemistry, Polish Academy of Sciences

Kasprzaka 44/52

Warsaw, 01-224, Poland

Warsaw, 27/05/2025

I declare that my contribution to the creation of the following publications included:

- Vitamin B_{12} and Micellar Solution Enable Regioselective Ring Opening of Epoxides and Aziridines with Electrophilic Olefins, **Szabó, K. F.**; Wdowik, T.; Krzeszewska, A.; Mazurek, K.; Andersson, M. P.; Gryko, D. *Org. Lett.*, **2025**, doi.org/10.1021/acs.orglett.5c01376.

The contributions include preparing starting materials for the epoxide section and optimizing the model aryl epoxide derivative.

Krzysztof Mazurek

Institute of Organic Chemistry
Polish Academy of Sciences

Dr. Aleksandra Krzeszewska

Institute of Organic Chemistry, Polish Academy of Sciences

Kasprzaka 44/52

Warsaw, 01-224, Poland

Warsaw, 29/05/2025

I declare that my contribution to the creation of the following publications included:

- Vitamin B_{12} and Micellar Solution Enable Regioselective Ring Opening of Epoxides and Aziridines with Electrophilic Olefins, **Szabó, K. F.**; Wdowik, T.; Krzeszewska, A.; Mazurek, K.; Andersson, M. P.; Gryko, D. *Org. Lett.*, **2025**, doi.org/10.1021/acs.orglett.5c01376.

Co-conceptualization of the project, optimization of alkyl- and aryl epoxides, development of the scope for epoxide derivatives, and collection of data for their characterization.

Aleksandra Krzeszewska